Al-Mustansiriyah Journal of Science

ISSN 1814 - 635X

Vol. 22, No. 5, 2011

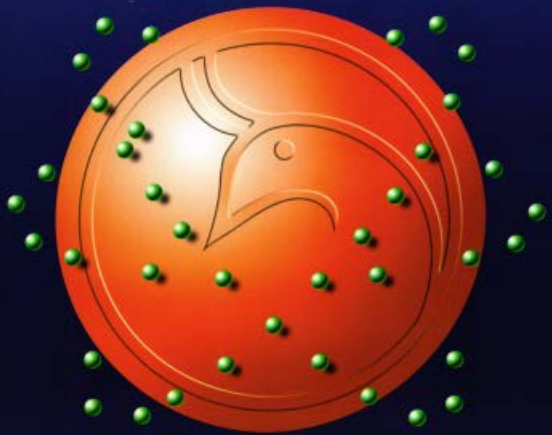

Issued by College of Science - Mustansiriyah University

Vol. 22
No. 5
2011

Al- Mustansiriyah Journal of Science

Issued by College of Science- Al- Mustansiriyah University

Special Edition
Researchs of The 7th Conference College Of Science Al-Mustansiriyah University
From 4-5 May

Mobile: 07711184399
e-mail: mustjsci@yahoo.com

CONTENTS

Evaluation of Immune Response in Patients with Chronic Hepatitis B Infection. II: Humoral Immunity

Muhammed A. Al-Dabagh
Medical Research Unit-College of Medicine-Al-Nahrain University
Received : 10/04/2011 Accepted : 29/05/2011

الخلاصة

تلعب الاستجابة المناعية الخلطية دورا اساسيا من عن طريق ازالة خمج التهاب الكبد الفايروسي ب الذي يقترن مؤقتا مع انتاج اضداد الغطاء البروتيني للفايروس . تهدف هذه الدراسة لتقييم الاستجابة المناعية الخلطية في مرضى التهاب الكبد الفايروسي ب المزمن عن طريق تخمين المستويات المصلية لكل من بين ابيضاض-4 وبين ابيضاض-6 وبين ابيضاض-10 فضلا عن تخمين المستويات المصلية لكل من الكلوبيولينات المناعية IgA و IgG و IgM.

جمعت عينات الدم الوريدي من 45 مريضا بخمج التهاب الكبد الفايروسي ب المزمن. عشرون عينة دم جمعت من اشخاص اصحاء كمجموعة سيطرة. استخدمت تقنية الاليزا لتخمين المستويات المصلية لكل من بين ابيضاض 4 وبين ابيضاض 6 وبين ابيضاض 12، كما استخدمت تقنية الانتشار المناعي المنفرد لتخمين المستويات المصلية لكل من الكلوبيولينات المناعية

اظهرت النتائج انخفاضا غيرمعنويا في المستويات المصلية لكل من بين ابيضاض4 والكلوبيولين المناعي G كما اظهرت ارتفاعا غير معنويا في المستويات المصلية لكل من بين ابيضاض 6 وكل من الكلوبيولينين المناعيين A, M بينما اظهرت المستويات المصلية لبين ابيضاض 10 ارتفاعا معنويا بالمقارنة مع مجموعة السيطرة.

ABSTRACT

The humoral immune response play an essential role during hepatitis B virus (HBV) infection .HBV clearance is associated temporally with production of anti-envelope antibodies. The aim of this study was to evaluate the humoral immune response in patient with chronic hepatitis B virus (CHBV) infection via estimation of serum level of interleukin-4 (IL-4),interleukin-6 (IL-6),interleukin-10 (IL-10) and immunoglobulis IgG IgA and IgM .Venus blood samples were collected from 45 patients with CHBV infection. Other 20 blood samples were collected from healthy individuals as

control group. Enzyme linked immune sorbent assay (ELISA) was used to estimate the serum levels of IL-4,IL-6 and IL-10.Single radial immuno-diffusion (sRID) assay was used to estimate serum levels IgG, IgA and IgM.

The results showed insignificant dropping in serum levels of IL-4 and IgG respectively while there insignificant elevation in IL-6, IgM and IgA respectively ,IL-10 levels shows significant elevation in CHBV patients group as compared with healthy control group.

INTRODUCTION

Hepatitis B virus (HBV) infect more than 400 million people worldwide and is a common cause of liver disease, HBV a member of the hepadnaviridae family , is a small DNA virus (1-4).

The chronic HBV and HCV are major causes of morbidity and mortality (5).Patients with chronic hepatitis B (CHBV) are at risk of developing sever liver disease, including cirrhosis and hepatocellular carcinoma (6-8). As HBV is currently viewed as non-cytopathic virus, HBV- associated liver damage is thought to be the consequence of long lasting cytolytic immune response against infected hepatocytes (9,10). HBV replicate in hepatocytes to produce HB_SAg particle can be taken up by antigen presenting cells, which degraded the viral proteins to peptides that are able then presented on the cell surface bound to MHC-I or MHC-II molecules (1,11).The degree of inflammatory activity did not correlate with the intensity of HB_SAg expression in hepatocytes. However, an inverse relationship between the degree of diffuse membranous HB_SAg expression and inflammatory local response in chronic hepatitis B (CHB) of minimal and mild activity was established (12). In CHBV patients, the T-cell response and circulating cytokines profile are associated with viral replication and liver function (13). The clearance of virus was clearly associated with efficient adaptive immune response (14).Activation of the virus-specific cellular immunity followed by the humoral response, which appears at last 10 to12

Weeks after HBV infection. Th_2 is able to neutralize HBV by antibodies and inhibit HBV replication through cytokines (15,16). The antibody response in patients with HBV plays a critical role viral clearance through the formation of complexes with viral particles and their removal from the circulation (17-19). Th_2 response characterized by IL-4,IL-5 IL-6 and IL-10 (20). However, recent reports on the ability of IL-4 to induce dendritic-cells-specific ICAM-

3 grabbing nonintegrin (DC-SIGN), a myeloid DC-specific lectin , suggest that IL-4 not only suppresses the monocyte and/or microphage lineage but its actively promotes the differentiation of monocytes along the DC lineage (21).Previous reports also suggest that IL-4 alone can activate accessory properties of monocytes and up-regulate MHC-I molecules, co-stimulatory molecules (22,23) and down-regulate CD14 on monocytes (22,24). A number of laboratories have reported that IL-4 inhibits the production of GM-CSF in a variety of cell including human monocytes (25-29). IL-6 is a multifunctional cytokine is critically involved in the acute phase response, T-cell proliferation ,B-cell maturation ,macrophage maturation and cytotoxic T-cell differentiation. In combination with IL-1, IL-2 and IFN-γ, IL-6 induces expression of IL-2 receptor (IL-2R), thus participating in the activation of resting T-cells (31). Furthermore, IL-6 seems to contribute to MHC-non-restricted cytotoxic activity by inducing natural killer (NK) cell proliferation (32). Interleukin-6 is considered a major source of early Th_1/Th_2 control during $CD4^+$ T-cells activation at it attributes to the promotion of Th_1 polarization. Moreover IL-6 activates the production IL-4 by $CD4^+$ T-cells and their differentiation into Th_2 effector cells. Furthermore , it inhibits Th_1 differentiation by interference with IFN-γ signaling and the development of Th_1 cells (33). Up regulation of Th_2 response, associated with cytokines IL-6 and IL-10, may occur to some degree and adversely affected the functioning of Th_1 response (34).The severity of liver injury in hepatitis is regulated by balance between aggressive and protective cytokines TNF-α , IFN-γ and IL-4 promote liver inflammation, which is attenuated by IL-6, IL-10 and IL-22 (35). Anti-inflammatory effects of IL-10 have lead to its use in hyper inflammatory status. IL-10 possesses anti-fibrotic activity and may be valuable as therapeutic cytokine for patients with liver cirrhosis (36,37). Successful clearance of the virus as well as the establishment of liver diseases largely driven by complex interaction between the virus and host immune response (38).

MATERIALS AND METHODS

Forty five (15-65 years old, mean 39.5years, 25 males and 20 females) patients with CHBV infection in Kadhmiya teaching hospital, during period from October 2008 to march 2010 were used for this study. the cause of chronic liver disease was determined using standard diagnostic criteria.

chronic hepatitis B was diagnosed by positive serological tests for serum hepatitis B surface antigen (HBsAg) for at least 6 months. Twenty (18-55 years old, mean 33.4 years, 10 males and 10 females) healthy individuals were used as control group.

Five ml of venous blood were collected from each individual in plain tube. Serum were separated , put in eppendorf tubes and stored at (deep freezing -20 C^0).

Immunological assays:

Enzyme-linked immune-sorbent assay (ELISA), (eBiosience, England) and (Biosource, Belgium) was used to estimate the serum levels of IL-4 and (IL-10,IL-6) respectively.

Single radial immunodiffusion (SRID) assay (Binding site, England) was used to estimate serum levels of IgG , IgM and IgA respectively(39).

Statistical Analysis

Statistical analysis has been performed using (SPSS, version 11.0) for windows. Continuous variables were expressed as mean ±standard error (SE). data were analysed using independent sample student`s *t* test. Significance was assigned for p values (<0.05) with 95% confident interval.

RESULTS AND DISCUSSION

Interleukin-10: Serum levels of IL-10 showed significant elevation in CHB patients group on (23.67 ± 4.68 pg/ml) as compared with healthy control group (4.29±1.08 pg/ml). Fig.1

Interleukin-6: Serum levels of IL-6 showed insignificant elevation in CHBV patients (20.57± 7.70 pg/ml) as compared with healthy control group (17.67 ± 4.88 pg/ml).Fig.1

Interleukin-4: Serum levels of IL-4 showed insignificant dropping in CHB patients group (26.36 ± 3.43 pg/ml) as compared with healthy control group (27.00 ± 354.36 pg/ml). Fig.1

Immunoglobulin G: Serum levels of IgG showed insignificant dropping in CHB patients group (9188.33±1311.64 mg/dl) as compared with healthy control (9574.44 ± 1035.47 mg/dl). Fig.2

Immunoglobulin M: Serum levels of showed insignificant elevation in CHB patients (95.67±16.52 mg/dl) as compared with healthy control group (77.42 ± 15.76 mg/dl). Fig.3

Immunoglobulin A : Serum levels of IgA showed insignificant elevation in CHB patients group

(39.50 ± 3.62 mg/dl) as compared with healthy control group (33.44 ± 4.93 mg/dl).Fig.3

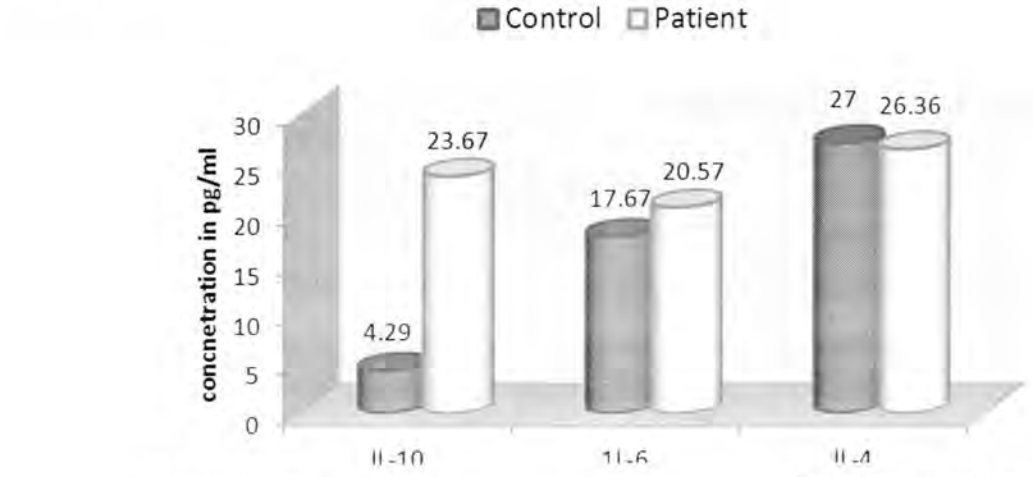

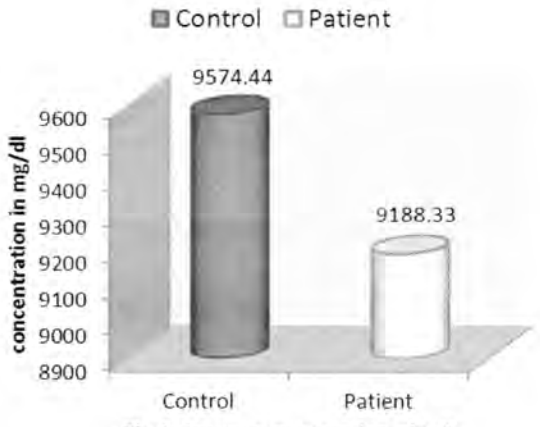

Fig.2: Serum concentration of IgG

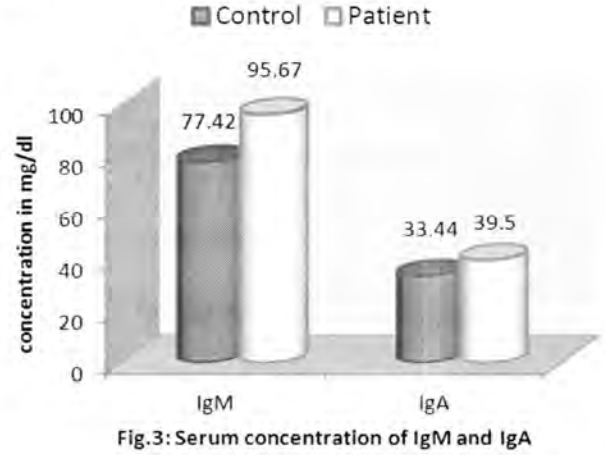

Fig.3: Serum concentration of IgM and IgA

Conventional definition of Th_1 and Th_2 cells depend strictly on the ability to secrete IFN-γ and IL-4 respectively (40,41). Th_2 response associated with cytokines IL-6 and IL-10 may occur to some degree and adversely affected the functioning of Th_1 response (34). IL-10 is an immunoregulatory cytokine and its on of the key cytokines in the Th_2 response. The decrease in serum IFN-γ levels coincides with increase in the levels of IL-10 which inhibit IFN-γ synthesis (42,43).Interleukin-10 levels were significantly increase while significant decrease in IL-4 levels were observed in patients with HBV infection (44). Both of TGF-β and IL-10 negatively regulate

production of Th_1 and Th_2 cytokines. Their over expression may impair the immune mechanisms
directed against pathogen and tumor antigen (45-47). The persistence of high IL-10 levels in the convalescent phase is important in the secretion of surface antibodies against HBV and development of immunity. Anti-HB_SAg block the adherence of viral particles to non infected cells and remove from the circulation the free antigenic particles, protecting the individual against reinfection (48). The current study showed significant elevation in serum levels of IL-10.

The significant elevation of IL-10 may contribute to its production by $CD4^+CD25^+$ regulatory cells (Tregs). Tregs are immunosuppressive T-cells that play an essential role in controlling immune responses and auto immunity (49).Recent finding suggest that Tregs also play a role in regulating immune responses to HBV infection (50). High levels of Tregs have been detected in CHB and are thought to be responsible for the chronicity of HBV infection, propably by inhibiting HBV- specific T-cell response (8).

It was shown that HBV was recognized by Kuppfer cells (KC), although the virus dose not replicate in these cells, and within hours post infection ,this recognition lead to the activation of
NF_KB and subsequently to release IL-6 and other pro-inflammatory cytokines (43,51). The current study shown insignificant elevation of serum levels of IL-6 in CHBV patients, our results
agree with other papers which revealed the elevation in serum levels of IL-6 (51). Interleukin-6
elevation may refer to Th_2 activation, in another words slightly dominant of Th_2 response.

Type 2 cytokines such as IL-4 and IL-5 may also involved in the clearance of circulating virus by promoting the production the neutralizing antibodies against the HBV surface and core antigens (51). Current study agree with Mansour et al (53), which refer to IL-4 dropping
in HBV patients. The elevation of IL-10 leads to suppression of IL-4 production in HBV patients (44), while the elevation of serum levels of IL-4 and IL-6 found in patients with autoimmune CHBV infection (54).

The elevation of IL-4 in CHBV patients with liver damage may revealed the dominant of Th_2 response (20,55) .Severity of liver injury in hepatitis

patients is TNF, IFN-γ and IL-4 promote liver inflammation ,which is attenuated by IL-6, IL-10 and IL-22 (35)

Th_2 cytokines inhibit growth of extracellular parasites and suppress phagocytosis . They augment B-cells proliferation derive antibody production switch IgG to IgE class of antibodies (41).Current study showed slightly elevation of serum levels of IgM while showed slightly dropping in each of IgG and IgA. Serum levels of immunoglobulins were ranged between normal to slightly elevation in HBV patients (56). If the host is able to clear the infection eventually the HB_SAg will become undetectable and will be followed by IgG antibodies to the HB_SAg and core antigen (57). HBV clearance is associated temporally with production of anti-envelop antibodies (58), through the formation of antivirus immunoglobulins-viral particles complex and there removal from the circulation (17-19).

REFERENCE

[1] Ali K., Ali N., Seyed M. and Mohammad Y. "Immunology of HCV and HBV in renal failure and transplantation". *Hepatitis monthly*. 7(2):93-101; (2007).

[2] Brike B., "Hepatitis B and C viruses and hepatocellular carcinoma". *Virsus*, 2: 1504-1509; (2010).

[3] Yanfang J., Wanyu L, Lei Y, and *etal*. "Enhancing the antihepatitis B virus immune response by adefovir dipivoxil and entecavir therapies". *Cellular & Mol.Immunol*, 8: 75-82, (2011).

[4] Jake L. "Hepatitis B: The Virus and Disease".*Hepatology*; 49: S13-S21, (2010).

[5] Hirofumi U., Shuji K., Yoichiro Takami and Hirohito T. "clinical proteomics for liver disease: a promising approach for discovery of novel biomarkers". *Proteome Science*. 8:70-76, (2010).

[6] Dienstag J. "Hepatitis B virus infection". *N.Engl.J.Med*.359:1486-1500, (2008).

[7] Lavanchy D. "Worldwide epidemiology of HBV infection, disease burden, and vaccine preventation". *J.Clin.Virol*. 34:S1-3, (2005).

[8] Bertoletti A, Gehring A. "The immune response during hepatitis B virus infection. *J. Gen. Virol*.87: 1439-1449: (2006).

[9] Lai C., Shouval D., Lok A. and *etal*. A comparison of entecavir versus lamivudine for patients with HBeAg-negative chronic hepatitis *B. N Engl. J.Med*. 354:1011-1020 (2010).

[10] Rehermann B. and Nascimbeni M. "Imuunology of hepatitis B virus and hepatitis C virus infection.Nat.Rev.Immunol.5:215-229, (2005).

[11] Jakobisiak M. "Presentation of antigen to T lymphocytes". *Immunology*. Warsaw: PWN ,157-175 (2002).

[12] Bozena W., Kazmierz M., Joanna J. and *etal.* "Composition of inflammatory infiltrate and its correlation with HBV/HCV antigen expression". *World of Gastroenterology*, 14(25): 4040-4046, (2008).

[13] Huang C., Lin S., Ho Y. and *etal.* "The immune response induced by hepatitis B virus principal antigens". *Cell Mol. Immunol.* 3:97-106, (2006).

[14] Wieland S.and Chisari F. Stealth and cunning: Hepatitis B and hepatitis C viruses. *J.Virol* 5:9369-9380, (2005).

[15] Guidotti L., Rochford R., Chung J and *etal.* "Virla clearance without destruction of infected cells during antiviral therapy of chronically infected ducks". J. of Virology. 68:8321-8330 (1999).

[16] Chen M., Salberg M., Sonnerberg A and *etal.* Limited humoral immunity in hepatitis C virus infection". Gastroenterology, 116:116:135-143(1999).

[17] Bocher W., Galun E., Marcus H. and *etal.* "Reduced hepatitis B virus surface antigen-specific Th1 helper cell frequency of chronic HBV carriers is associated with a failure to produce antigen-specific antibodies in the trinera mouse". *Hepatology*, 31:480-487 (2007).

[18] Chisari F. "Hepatitis B virus immune pathogenesis". *Ann.Rev.Immunol.* 13: 29-60 (1995).

[19] Chu C., Sheen I., Yeh C. and *etal.* "Serum levels of interferon-alpha and gamma in acute and chronic hepatitis B virus infection". *Dig.Dis.Sci.* 40:2107-2112 (1995).

[20] Katia F., Claudio V. Margherita D. and *etal.* "Cytokine patterns correlate with liver damage in patient with chronic hepatitis B and C". Annals of clinical and laboratory Science.36:144-150 (2006).

[21] Relloso M., Puig, Pello O. and *etal.* "DC-sign (CD209) expression is IL-4 –dependant and is negatively by IFN, TFG-B and inflammatory agent". *J.Immunol.*168:2634-2645 (2002).

[22] Ruppert J., Friedrichs, and Peters J. "IL-4 decreases the expression of the monocyte differentiation marker CD14, paralleled by an increasing accessory potency. *Immunobiol.*182:449-464 (1991).

[23] Ulanova M., Tarkowki A., Hahn-Zoric M and Hanson L. The common vaccine adjuvant aluminum hydroxide up-regulates accessory properties of

human monocytes via an interleukin-4-dependant mechanism. Infext.Immun.69:1151-1159 (2001).

[24] Lauencer R., Goyert M, Geha R. and Vercelli D. "Interleukin-4 down-regulates the expression of CD14, in normal human monocytes". *Eur.J.Immunol.* 20:2375-2381 (1990).

[25] Sato N., Sawada K., Tarumi T. and *etal.* "Recombinant human interleukin-4 inhibits the production of granulocyte-macrophage colony stimulating factor by blood mononuclear cells" *Br.J.Haematol.*86: 695-701 (1994).

[26] Dechanet j., Rissoan M., Banchereau J. and Miossee P. "Interleukin-4, but not interleukin-10, regulates the production of inflammation mediators by rheumatoid synviocytes". *Cytokine7*, 176-183 (1995).

[27] Alkashi K., Shibuya T., Harada M and *etal.* "Interleukin-4 suppresses the spontaneous growth of chronic myelomonocytic leukemiya cells". *J.Clin.Invest.* 88:223-230 (1991).

[28] Trindade M., Nakashimi Y., Lind M. and *etal.* "Interleukin-4 inhibits granulocyte-macrophage colony stimulating factor, interleukin-6, and tumor necrosis factor-alpha expression by human monocytes in response to polymethylacrylate particle challenge in vitro". *J.Orthop.Res.* 17:797-802 (1999).

[29] Sawada K., Sato N. and Koike T. "Inhibition of GM-CCSF production by recombinant human interleukin-4; negative regulator of hemostopoiesis". *Leuk.Lymphphoma.* 19:33-42 (1995).

[30] Galy A. and Spits H. "IL-1, IL-4 and IFN- gamma differentially regulate cytokine production and cell surface molecule expression in cultured human thymic epithelial cells". *J.Imuunol.* 147:3823-3830 (1991).

[31] Lauta V. "A nreview of the cytokine network in multiple myeloma: diagnostic, prognostic, and therapeutic implications". *Cancer.* 97:2440-2452 (2003).

[32] Brandu S., Riemensberger J., Jacobsen M. and *etal.* "NK cells are essential for the effective BCG immunotherapy". *Int. J. Cancer.* 92:697-702(2001).

[33] Diehl S., Rincon M. "The two faces of IL-6 on Th1/Th2 differentiation". *Mol.Immunol.* 39: 531-536 (2002).

[34] Bevers R., Kurth K., and Schanhart D. "Role of urothelial cells in BCG immunotherapy for superficial baldder cancer". *Brit. J. of Cancer.* 91:607-612 (2004).

[35] Christian W., Ursula M., Frank L. and *etal.* "IL-22-dependent attenuation of T cell-dependnet (ConA) hepatitis in herpes virus entry mediator deficiency". *J.Immunol.*182:4521-4528 (2009).

[36] Spellberg B., Edwards J. "Type1/Type2 immunity in infections diseases". *Clin. Infect. Dis.*32:76-102 (2001).

[37] Rachmawati H., Reker-Smit C. Lub-de Hooge and *etal.* "Chemical modification of interleukin-10 with mannose 6-phosphate groups yields a liver-selective cytokine". *Drug Metab Dispos.* 35:814-821 (2007).

[38] Judy J. and Sharon R. "Immuno-pathogenesis of hepatitis B virus infection immune-pathogenesis of HBV infection". *Immunology and Cell Biology.* 85:16-23 (2007).

[39] Cruse,J.M. and Lewis, R.E.Atlas of immunology, CRC Press LLC,USA,P.107-413 (2000).

[40] Annuziato F., Cosmi L. Santarlasci V. and *etal.* "Dual control of human interleukin-2 and interferon-g gene expression by histamine: activation and suppression". *Cell Immunol.* 170:149-155 (1996).

[41] Kaiko G., Horvt J., Beagley K. and Hansbro P. "Immunological decision-making :how does the immune system decode to mount a helper T-cell respose?". *Immunology.* 122:326-338 (2008).

[42] Raynor B. "Cytokines".*Adv.Obset.Gynecol.*3:27-46 (1996).

[43] Nineca R., Staecy R., Philip J. and *etal.* Induction of a stricking systemic cytokine cascade prior to peak viraemia in acute human immunodeficiency virus type1 infection, in contrast to more modest and delayed responses in acute hepatitis B and C virus infections.Am.Soc. Microbiol. (2009)

[44] Francisa M., Tania A., Jesus E. and *etal.* "Concentrations of cytokines, soluble interleukine-2 receptor and soluble CD30 in sera of patients with hepatitis B virus infection during acute and convalescent phase". *Clinical and diagnostic laboratory Immunology*, 9(6):1372-1375 (2002).

[45] Levings M., Sangregorio R., Galibiati and *etal.* "IFN-α and IL-10 induce the differentiation of human type1 T cells". *J.Immunol.*166:5530-5539 (2001).

[46] Liu H., and Leung B. "CD4+CD25+regulatory T cells in health and disease". *Clin.Exp. Pharmacol Physiol.* 33:519-524 (2006).

[47] Roncarlo M., Gregori S., Battaglia M. and *etal.* Interleukin-10-secreting type1 regulatory T cells in rodents and humans. Immunol.Rev. 212: 28-50 (2007).

[48] Machado B., Deibis L. and Toro F. "Repuesta immunologica en hepatitis viral". *Gen.*2:85-93 (1997).

[49] Billerbeck E., Bottler T. and Thimme R. "Regulatory T cells in viral hepatitis". *World J. Gastroenterol.* 13:4858-4864, (2007).

[50] Stoop J., Van der Molen R., Kuipers E. and *etal.* "Inhibition of viral replication reduces regulatory T cells and enhances the antiviral immune response in chronic hepatitis B". *Virology*, 361:141-148, (2007).

[51] Hosel M., Quuasdorff M., Wiegmann K. and *etal.* " Not interferon but interleukin-6 controls early gene expression in hepatitis B virus infection". *Hepatology*, 50:1773-1782, (2009).

[52] Milich D., Schodel F., Hughes J. and *etal.* "The hepatitis B virus core and e antigens elicit different Th cell subsets: antigen structure can affect Th cell phenotype". *J.Virol.* 71:2192-2201, (1997).

[53] Anastassakos A., Wolstencrott A., Portman P and *etal.* "Interleukin-1 and interleukin-2 activity in chronic hepatitis B virus infection". *Gastroenterology.* 94:999-10005 (1998).

[54] Al-Wabel A., Al-Janadi M., and Raziuddins. "Cytokine profile of viral and auto immune chronic active hepatitis". *J.Allergy Clin.Immunol.* 92:902-908 (1993).

[55] Xing T., Zhang L., Lu Q. and *etal.* "Th1/Th2 type cytokines in hepatitis B patients treated with interferon-α". *Chin.Med.J.* 114:921-924 (2001).

[56] Geo F., Janet S., Karen C. and Stephan A. "Medical Microbiology". Mc Graw-Hill companies. USA .24ed. P-473(2007).

[57] Zuckerman A. Hepatitis viruses. In: *Barons Medical Microbiology* (4^{th} ed.). Univ. of Texas Medical Branch.(1996).

[58] Antonio B and Carlo F. "kinetics of the immune response during HBV and HCV infection". Hepatology.38(1):4-13 (2003).

Detection of C-reactive protein (CRP), Tumor necrosis factor-alpha (TNF-α) and immunoglobulin A (IgA) serum levels in healthy smokers and nonsmokers

Nawal M. Utba Al-Okabi
Department of Biology-College of Science-University of Baghdad

Received : 03/04/2011 Accepted : 29/05/2011

الخلاصة

التدخين هو احد العوامل الرئيسية المؤثرة على صحة الانسان حيث تنشط الخلايا الالتهابية استجابة لتأثيردخان السكائر وتنتج العديد من الوسائط الالتهابية مثل TNF-α و CRP (عامل نخر الورم – الفا) وكذلك يؤثر دخان السكائر على مستويات الغلوبيولي المناعي نوع A (IgA) في مصل المدخنين. شملت الدراسة اربعين فردا من الاصحاء المدخنين (25 ذكر و 15 انثى) و 16 فردا من الاصحاء غير المدخنين (10 ذكور و 6 اناث). قسم المدخنين الى قسمين ثانويين: الاول الذين يدخنون اقل من علبة يوميا وعددهم عشرون فرد والثاني الذين يدخنون اكثر من علبة يوميا وعددهم عشرون فرد ايضا. استخدمت طريقة (ELISA) لتقييس مستويات المصلية ل CRP و TNF-α وطريقة (RID) لتقييس مستويات الغلوبيولينات المناعية نوع A لدى الاصحاء المدخنين وغير المدخنين. مستويات CRP و TNF-α و IgA كانت مرتفعة معنويا ($P< 0.05$) لدى كل المدخنين المشمولين بالدراسة مقارنة بغير المدخنين (مجموعة السيطرة) و مستويات CRP و IgA كانت مرتفعة معنويا ($P < 0.05$) لدى المدخنين لاكثر من علبة يوميا مقارنة باقل من علبة يوميا بالاضافه الى انه كانت مستويات TNF-α مرتفعة عند المدخنين لاكثر من علبة مقارنة مع الاقل من علبة يوميا ولكن الفروقات غير معنوية. ولم نجد اي تاثير للجنس ولا للعمر على مستويات CRP و TNF-α و IgA عند المدخنين ما عدا وجود تزايد لمستويات CRP مع زيادة العمر. واظهرت الدراسة وجود علاقة موجبة (طردية) بين كل من CRP و TNF-α ($r = 0.4$) وكذلك بين CRP و IgA ($r = 0.37$) وعلاقة موجبة ضعيفة بين مستويات و TNF-α و IgA ($r = 0.29$).

الزيادة المعنوية لمستويات CRP و TNF-α تشير الى عدم التوازن ما بين proinflammatory و anti inflammatory نتجة للتعرض لدخان السكائر. قياس مستويات الـ CRP و TNF-α في مصل المدخنين تعتبر من المؤشرلت الحيوية للدلالة على المدخنين الشرهين المعرضين لخطر الاصابة بامراض الناتجة عن التدخين.

ABSTRACT

Smoking is one of the major lifestyle factors influencing the health of human beings. In response to cigarette smoke, activated inflammatory cells produce a great variety of inflammatory mediators, such as CRP and TNF- α, also cigarette smoke affects the IgA levels in serum of smokers. We included in our study 40 healthy smokers (25 males and 15 females), and 16 healthy nonsmokers (10 males and 6 females) as a control group. Smokers group was classified into two subgroups: less than one pack (20 subjects) and more than one pack per day (20 subjects). The serum levels of CRP and TNF-α were assessed by Enzyme-Linked Immuno Sorbent Assay (ELISA). Otherwise IgA levels were assessed by Radial immunodiffusion (RID).

The levels of CRP, TNF-α and IgA in serum were significantly higher in smokers group than non smokers ($P< 0.05$). CRP and IgA concentrations are significantly higher ($P < 0.05$) in serum of smokers with more than one pack per day compared with those with less than one pack per day. We also noticed an increased TNF- α concentration in the serum of smokers with more than one pack per day compared with those with less than one pack per day but the result was not significant. We did not found any significant influence of gender in smokers on TNF-α, CRP and IgA levels. On the other hand, the results shown significant increased in the levels of serum CRP with age increased. There was positive correlation between the levels of TNF-α and CRP, the levels of CRP with IgA and weak positive correlation between the level of TNF-α and IgA in the serum of our smoker subjects ($r = 0.4$), ($r = 0.37$) and ($r = 0.29$) respectively. The significant increased CRP and TNF-α serum levels could induce in smokers, suggest the imbalance between proinflammatory and anti-inflammatory factors as a result of tobacco Smoke exposure. Serum levels of TNF-α and CRP might

be useful biomarkers for the selection of heavy smokers with a risk of developing smoke induced diseases.

INTRODUCTION

Smoking is one of the major lifestyle factors influencing the health of human beings. Tobacco smoking is associated with increased prevalence of various diseases, both in the respiratory tract and in distal organs. The possibility that tobacco smoke induced changes in immune and inflammatory processes may play a part in the aetiology and pathogenesis of many of these diseases (1).

In response to cigarette smoke, activated inflammatory cells produce a great variety of inflammatory mediators, first of all, acute-phase proteins (APPs) and cytokines (2). The activation of the acute phase response from infection, immune activation or injury is signaled by interleukin-6 (IL-6), which produces proteins such as fibrinogen, C-reactive protein (CRP), and serum amyloid A that lead to inflammatory reactions. CRP is a member of the class of acute-phase reactants, as its levels rise dramatically during inflammatory processes occurring in the body. This increment is due to a rise in the plasma concentration of IL-6, which is produced predominantly by hepatocytes, as well as adipocytes. Localized inflammation can induce CRP expression (3). CRP binds to phosphocholine on microbes. It is thought to assist in complement binding to foreign and damaged cells and enhances phagocytosis by macrophages (opsonin mediated phagocytosis), which express a receptor for CRP. It is also believed to play another important role in innate immunity, as an early defense system against infections (4).

Inhaled cigarette smoke can also induce tumor necrosis factor-alpha (TNF-α) production by alveolar macrophages, which in turn may enhance metalloproteinases (MMPs) production. MMPs have been involved in mediating the inflammation and lung destruction (5). TNF-α was originally described as a factor produced by the endotoxin stimulated macrophages that causes hemorrhagic necrosis of tumors (6). It is a powerful proinflammatory cytokine with pleiotropic properties and a key mediator of inflammation. TNF-α operates by binding to two structurally related cell surface receptors: p55 and p75. However, the p55 receptor seems to be responsible for mediating the majority of TNF-α function (7).

The effects of cigarette smoking on humoral immunity have been studied extensively. Several studies have found that smokers had serum immunoglobulin levels (IgA, IgG, and IgM) 10% to 20% lower than those of nonsmokers. Mili et al (8) found that IgA, IgG, and IgM levels were higher among former smokers than current smokers and increased with duration of smoking cessation. This suggests that the effect was reversible, with a return toward the immunoglobulin levels of nonsmokers (9).

The present study aimed to 1. measure the CRP, TNF-alpha, IgA serum levels in healthy smokers compare to healthy nonsmokers, determining the dose-response relationship with cigarette smoke exposure, 2. analyze the possible influence of gender and age on this variables 3. determine a possible association between this variables in healthy smokers.

MATERIALS AND METHODS

Subject: Forty healthy smokers (25 males and 15 females), their age range between 19-60 years in addition to 16 healthy nonsmokers (10 males and 6 females) age range between 20- 59 years as a control group were included in this study. Smokers group was classified into two subgroups: less than one pack (20 subjects) and more than one pack per day (20 subjects).

A clinical and paraclinical evaluation was performed in both groups, without any evidence of infection or chronic obstructive pulmonary disease (COPD).

Details of subject medical histories and smoking status were asked in the questionnaires.

Specimen collection: Blood was collected from each individual including in this study, 5 ml of blood was drawn by vein puncture using disposable syringe. The blood was placed in plastic disposable tubes to obtain serum, which were stored at -20 °C till tested.

Methods: The serum levels of CRP and TNF-α were assessed by Enzyme-Linked Immuno Sorbent Assay (ELISA) using quantitative CRP in human serum or plasma kit (IBL international, Germany), following the instructions provided by the manufacturer and Assay Max TNF -α ELISA kit (Assaypro, USA) designed for the detection of TNF-α levels in human serum or plasma, also following the instructions provided by the

manufacturer (10). On the other hand, IgA levels were assessed by Radial immunodiffusion according to the guidelines mentioned in the leaflet supplied by the manufacturer (Immuchem, Belgium) (11).

Statistical analysis:

Data are expressed as mean ± standard deviation (SD). The statistical analysis system SAS (2004) program used to study the effect of smoking and all of sex and age in TNF-α, CRP and IgA levels between study groups. The least significant difference (LSD) test was used to the significant compare between means, and SAS program was employed for the correlation coefficient calculation to evaluate the associations between variables (12).

RESULTS AND DISCUSSION

The levels of CRP and IgA in serum were significantly higher in smokers group than non smokers ($p< 0.05$). CRP and IgA concentrations in serum of smokers with more than one pack per day compared with those with less than one pack per day also significantly higher ($p < 0.05$) as it shown in table 1.

The TNF-α serum level was significantly higher in smokers group than in nonsmokers ($p<0.05$). We also noticed a non significant increased TNF- α concentration in the serum of smokers with more than one pack per day in comparison to those with less than one pack per day (table 1).

Table -1: Effect of tobacco smoking in the levels of TNF-α, CRP and IgA in the healthy smokers compared with healthy non smokers (control).

Smokers	No.	Mean ± SD		
		TNF-alpha (pg/ml)	CRP (µg/ml)	IgA (mg/dl)
Smokers more than one pack	20	43.0 ± 11.5 a	7.82 ± 0.66 a	240.82 ± 18.01 a
Smokers less than one pack	20	21.8 ± 7.0 ab	3.93 ± 0.55 b	191.13 ± 14.09 b
Non smokers	16	9.9 ± 1.6 b	3.69 ± 0.48 b	168.32 ± 17.59 b
LSD	--	0.025 *	1.702*	49.171*

(P< 0.05) *

Mean values that have different letters have significant difference between them. SD= standard deviation

Results revealed insignificant influence of gender in smokers on TNF-α, CRP and IgA levels (table 2). We did not able to show any significant differences in smokers TNF-α and IgA levels between age groups. However, table 3 illustrates higher significant ($p < 0.05$) levels of CRP in serum of third age group (more than 40 years) in expense of the second age group (31- 40 years).

Table -2: Effect of gender on smoker TNF- α, CRP and IgA levels.

Smokers	No.	Mean ± SD		
		TNF-alpha (pg/ml)	CRP (µg/ml)	IgA (mg/dl)
Male	25	31.9 ± 10.0	5.72 ± 0.063	227.53 ± 16.0
Female	15	23.5 ± 6.5	7.04 ± 1.02	205.23 ± 20.0
(P > 0.05). SD= standard deviation				

Table -3: Effect of age on smoker TNF- α, CRP and IgA levels.

Smokers age group (year)	No.	Mean ± SD		
		TNF-alpha (pg/ml)	CRP (µg/ml)	IgA (mg/dl)
Less than 30 -30	16	18.3 ± 11.4	5.86 ± 0.87 ab	222.43 ± 21.71
31- 40	9	30.7 ± 20.3	4.12 ± 0.78 b	231.83 ± 22.72
More than 41	15	36.8 ± 9.1	7.58 ± 0.88 a	211.13 ± 21.11
LSD	--	NS	2.049*	NS
(P < 0.05) * , NS : not significant. SD: standard deviation Mean values that have different letters have significant difference between them.				

There was positive correlation between the levels of TNF-α and CRP, also between the levels of CRP and IgA in the serum of smoker subjects, r = 0.4 and 0.37, respectively. Whereas there was weak positive correlation between the level of TNF-α and IgA (r = 0.29) as follows in table 4.

Table -4: Correlation coefficients between different variables.

Related Variables	Correlation coefficients (r)	Significance level
TNF-α and CRP	0.40	**
TNF- α and IgA	0.29	*
CRP and IgA	0.37	**
***(P<0.05), **(P<0.01)**		

In the present study, the levels of CRP in serum were significantly higher in smokers group than non smokers one. This increase in the CRP levels was found to be related to the number of smoked cigarette per day. These results are in agreement with Lao *et al* (13), who found that smoking is associated with increased CRP and WBC levels in older Chinese men and with Das (14), who stated that male and female smokers showed an acute phase response indicated by significantly raised serum CRP levels than non smokers. On contrary, Helmersson *et al* (15) observed that the increase in CRP levels in smokers was not statistically significant. Ohsawa *et al* (16) reported that CRP levels are elevated in smokers while the increased CRP levels unrelated to the number of cigarettes smoked per day. Lowe *et al* (17) demonstrated that a dose-dependent correlation between CRP levels and number of cigarettes per day. No significant gender – specific differences for smoking and CRP levels were noticed in our findings. Likewise, Fröhlich *et al* (18) suggested that serum CRP concentrations were significantly higher in male regular smoker than male never smoker, but no significant differences was observed in women. The increased CRP has been found to be associated with increasing age (4).

The acute inflammatory response is induced by cigarette smoking and leads to gross changes in the levels of CRP and other acute phase proteins. The primary regulators of CRP and the acute phase proteins are the cytokines interleukin (IL)-6 and IL-1β and tumor necrosis factor (TNF) - α, which are secreted by neutrophil granulocytes and macrophages at sites of injury. These cytokines bind to cell surface receptors and initiate an intracellular signaling cascade, leading to activation of several transcription factors which is directly responsible for inducing transcription of CRP (19).

Our TNF-α results are in agreement with Petrescu *et al* (5) who indicated that the serum levels of TNF-α were significantly higher in the smoker group than in the nonsmoker group and the concentration of TNF-α

is elevated in the serum of healthy heavy smokers in cigarette dose-dependent manner also with Wirtz *et al* (20) who reported a trend for higher baseline TNF- α levels among healthy smokers. On the other hand, these results are not in agreement with Diez-Pina *et al* (21) who mentioned that TNF- α levels in serum did not show either differences between smoker and non smoker groups. Dissimilarly, Gander *et al* (22) findings failed to show significant effects of smoking on TNF- α plasma levels.

The serum levels of TNF- α were also significantly higher in smoker of more one pack per day than less one pack per day are in agreement with the observations of Zoppini *et al* (23) who demonstrated a marked increase of TNF- α system activation with an increase in the number of cigarettes smoked per day. Similar results were reported by Fernandez- Real and coworkers (24).

Present work results didn't found any differences in TNF- α level in serum of two groups according to the age or gender, these results disagreed with the study of Chatila (25) which showed that tobacco smoke effects might be sex dependent. Diez-Pina *et al* (21) found higher levels of TNF- α in serum of male smokers, otherwise they have not confirmed any significant influence of age on TNF- α levels. Himmerich *et al* (26) showed a significant influence of age on the serum TNF- α levels (increasing with age) and also confirmed a mild influence of gender on the serum TNF- α levels. We were not able to verify the influence of these two factors on the serum levels of TNF- α.

The major role of TNF- α in smoke- induced lung injuries is supported by large number of studies. The components of cigarette smoke that are responsible for local and systemic inflammatory response have not fully elucidated. The bacterial endotoxin contained in tobacco can survive combustion as an active compound of tobacco smoke. Thus, it might be one of the many pathologic substances involved in cigarette smoke-induced inflammatory reaction (27).

The levels of IgA in serum were significantly higher in smokers group than non smokers. IgA concentrations in serum of smokers with more than one pack per day compared with those with less than one pack per day were also found to be significantly higher. In regard to smoker serum level of IgA, no effect of gender or age was observed. Even as Holt (28) indicated that concentration of the immunoglobulins IgG, IgM and

IgA are reduced by 10 -20% in the serum of smokers. Gonzalez – Quintela *et al* (29) also found that serum levels of IgA in smokers were not significant different from those of non smokers but agreed with him in the results show that sex- and age-related changes in immunoglobulin concentrations are smoking independent.

IgA levels increment, in response to cigarette smoke, activates inflammatory cells to produce a great variety of inflammatory mediators like circulating cytokines, one of them IL-6 which is a co-factor for immunoglobulin synthesis. Beagley *et al* (30) confirmed that there was some parallelism between IgA and IgG concentrations and serum concentration of IL-6, a marker of inflammation. Serum IL-6 levels were positively correlated with IgA and IgG concentrations.

The serum levels of TNF- α were positively correlated with CRP levels. Our findings are in agreement with Petrescu *et al* (5) who observed the same result. Also there is positively correlation between the levels of CRP and IgA in the serum of our smoker subjects; whereas there was a weak positive correlation between the level of TNF-α and IgA.

TNF-α and IL-1β are classical proinflammatory cytokines; together, they initiate a second wave of cytokines, including IL-6, whose activities include stimulating liver production of acute phase protein such as CRP (31)

Conclusions: significant increase in CRP and TNF-α serum levels could be induced in smokers, suggest the imbalance between proinflammatory and anti-inflammatory factors as a result of tobacco Smoke exposure. Serum levels of TNF-α and CRP might be useful biomarkers for the selection of heavy smokers with a risk of developing smoke induced diseases.

REFERENCES

1- Holt PG. " Immune and inflammatory function in cigarette smokers". *Thorax*; 42: 241–9. (1987).

2- Yanbaeva DG, Dentener MA, Creutzberg EC, Wesseling G, Wouters EF. "Systemic effects of smoking". *Chest*; 131: 1557–66. (2007).

3- Calabro P, Chang DW, and Willerson JT, Yeh ET. "Release of C - reactive protein in response to inflammatory cytokines by human adipocytes: linking obesity to vascular inflammation". *J Am Coll Cardiol*; 46: 1112–3. (2005).

4- Pepys MB and Hirschfield GM. "C-reactive protein: a critical update". *J Clin Invest*; 111 (12): 1805–12. (2003).

5- Petrescu F, Voican SC and Silosi I. "Tumor necrosis factor-α serum levels in healthy smokers and nonsmokers". *Int J Obes*; 5: 217-222. (2010).

6- Carswell EA, Old LJ, Kassel RL, Green S, Fiore N and Williamson B. "An endotoxin-induced serum factor that causes necrosis of tumors". *Proc Natl Acad Sci U S A.*; 72:3666–3670. (1975).

7- Vieira LQ, Goldschmidt M, Nashleanas M, Pfeffer K, Mak T and Scott P. "Mice lacking the TNF receptor p55 fail to resolve lesions caused by infection with Leishmania major, but control parasite replication". *J Immunol.*; 157:827–835.(1996)

8- Mili F, Flanders WD, Boring JR, Annest JL and Destefano F. "T he associations of race, cigarette smoking, and smoking cessation to measures of the immune system in middle-aged men". *Clin Immunol Immunopathol.*; 59:187-200. (1991)

9- Arcavi L and Benowitz N L. "Cigarette Smoking and Infection". Arch Intern Med.; 164 (20):2206-2216. (2004).

10- Van Weemen BK, Schuurs AH. "Immunoassay using antigen-enzyme conjugates." *FEBS Letters* 15 (3): 232–6. (1971).

11- Mancini, G; Carbonara, AO; Heremans, JF. "Immunochemical quantitation of antigens by single radial immunodiffusion". Immunochemistry; 2 (3): 235–254. (1965).

12- SAS. "SAS / STAT Users Guide for Personal Computers". Release 7.0. SAS Institute Inc., Cary, NC., USA. (SAS= Statistical Analysis System). (2004).

13- Lao XQ, Jiang CQ, Zhang WS, Adab P, Lam TH, Cheng KK and Thomas GN. "Smoking, smoking cessation and inflammatory markers in order Chines men: The Guangzhou Biobank Cohort Study". *Atherosclerosis*; 203(1):304-10. (2009).

14- Das I. "Raised C-reactive protein levels in serum from smokers". *Clin Chim Acta*. Nov 29; 153(1):9-13. (1985).

15- Helmersson J, Larsson A, Vessby B and Basu S. "Active smoking and a history of smoking are associated with enhanced prostaglandin F-2 alpha, interleukin-6 and F-2-isoprostane formation in elderly men". *Atherosclerosis;* 181: 201–7. (2005).

16- Ohsawa M, Okayama A, Nakamura M, Onoda T, Kato K, Itai K, Yoshida Y, Ogawa A, Kawamura K and Hiramori K. "CRP levels are elevated in smokers but unrelated to the number of cigarettes and are decreased by long-term smoking cessation in male smokers". *Prev Med;* 41: 651–6. (2005).

17- Lowe GDO, Yarnell JWG, Rumley A, Sweetnam PM, Rumley C, Bainton D and Ben-Shlomo Y. "C-reactive protein, fibrin D-dimer, and incident ischemic heart disease in the speedwell study – are inflammation and fibrin turnover linked in pathogenesis?". *Arterioscler Thromb Vasc Biol;* 21: 603–10. (2001).

18- Fröhlich M, Sund M, Lowel H, Imhof A, Hoffmeister A and Koenig W. "Independent association of various smoking characteristics with markers of systemic inflammation in men – results from a representative sample of the general population (MONICA Augsburg Survey 1994/95)". *Eur Heart J;* 24: 1365–72. (2003).

19- Black S, Kushner I and Samols D. "C-reactive protein". *J Biol Chem;* 279: 48487–90. (2004).

20- Wirtz PH, von Kanel R, Kunz-Ebrecht S, Ehlert U and Fischer JE. "Enhanced glucocorticoid sensitivity of cytokine release from circulating leukocytes stimulated with lipopolysaccharide in healthy male smokers". *Brain Behav Immun*; 18,536-543. (2004).

21- Diez-Pina JM, Fernandez-Aceñero MJ, Llorente-Alonso MJ, Diaz – Lobato S, Mayoralas S and Florez A."Tumor necrosis factor alpha as a marker of systemic and local inflammation in "healthy" smokers". *Int J Gen Med.*; 2:9–14. (2009).

22- Gander ML, Fischer JE, Maly FE and Känel RV. "Effect of the G-308A polymorphism of the tumor necrosis factor (TNF)-α gene promoter site on plasma levels of TNF-α and C-reactive protein in smokers: a cross-sectional study". *BMC Cardiovasc Disord*; 4, 17. (2004).

23- Zoppini G, Faccini G, Muggeo M, Zenari L, Falezza G and Targher G. "Elevated plasma levels of soluble receptors of TNF-α and their association with smoking and microvascular complications in young adults with type 1 diabetes". *J Clin Endocrinol Metab.*; 186:3805–3808. (2001).

24- Fernandez-Real J-M, Broch M, Vendrell J and Ricart W. "Smoking, fat mass and activation of the tumor necrosis factor-α pathway". *Int J Obes.*; 27:1552–1556. (2003).

25- Chatila WM, Wynkoop WA, Vance Criner GJ. "Smoking patterns in African Americans and whites with advanced COPD". *Chest* .; 125:15–21. (2004).

26- Himmerich H, Stephany F, Linseisen J, Seiler H, Wofram G, Himmerich S, GedrichK and Pollmächer T. "TNF –alpha, soluble TNF receptor and interleukin-6 plasma levels in the general population". *Eur Cytokine Netw.*; 17:196-201. (2006).

27- Hasday JD, Bascom R, Costa JJ, Fitzgerald T and Dubin W. "Bacterial endotoxin is an active component of cigarette smoke". *Chest.*; 115:829–835. (1999).

28- Holt PG. "Immune and inflammatory function in cigarette smokers". *Thorax*; 42:241-9. (1987).

29- Gonzalez-Quintela A, Alende R, Gude F, Campos J, Rey J, Meijide LM, Fernandez-Merino C and Vidal C. "Serum levels of immunoglobulins (IgG, IgA, IgM) in a general adult population and their relationship with alcohol consumption, smoking and common metabolic abnormalities". *Clin Exp Immunol.* 151(1):42-50. (2008).

30- Beagley KW, Eldridge JH, Lee F, Kiyono H, Everson MP, Koopman WJ, Hirano T, Kishimoto T and McGhee JR. "Interleukins and IgA synthesis. Human and murine interleukin 6 induce high rate secretion in IgA-committed B cells". *J Exp Med.*; 169:2133–48. (1989).

31- Richards C and Gauldie J. "Role of cytokines in the acute- phase response. In: Human Cytokines: Their Roles in Diseases and Therapy (Aggarwal, B.B. and Puri, R. k., eds.)", pp. 253-269. Blackwell Science, Cambridge, MA. (1995).

Studying the Anti-Adhesion Ability of S-layer Proteins and Filtrate of *Lactobacillus spp.* Against Some Pathogenic Microorganisms *In Vitro*

***Raghad A. Hassan, **Amina N. Al-Thwani, ***Faris A. Al-Ubaidi** and ******Maysaa Ch. Al-Yas**

*Department of Biology-College of Education-The Islamic University

**Genetic Engineering and Biotechnology Institute of Postgraduate Studies-Baghdad University

***Research Center and Natural History Museum-Baghdad University

****Department of Biotechnolog-College of Science-Al-Nahrain University

Received: 23/03/2011 Accepted: 29/05/2011

الخلاصة

أجريت هذه الدراسة لتقييم فعالية البروتينات السطحيه المعزوله من بكتريا حامض اللاكتيك العصويه بالمقارنة مع فعالية راشح البكتريا الخام المركز ضد بعض الاحياء المجهريه الممرضه داخل الزجاج. أستخدمت (12) عزله من بكتريا حامض اللاكتيك المعزوله من الخل و حليب البشر و حليب البقر و اللبن و المهبل للكشف عن وجود البروتينات السطحيه بطريقة Sodium Dodecyl Sulfate-Polyacrylamide gel electrophoresis (SDS-PAGE) , ثم عزلت البروتينات بواسطة قطع حزمة البروتين السطحي ومعاملتها مع guanidin hydrochloride(G-HCl) تركيز 6 عياري لاسترجاع البروتين من الهلام. قدرت الاوزان الجزيئيه للبروتينات وكانت تتراوح ما بين (37– 63 kDa) حسب اختلاف انواع بكتريا حامض اللاكتيك, كذلك حسبت تراكيز البروتينات السطحيه بأستخدام عده تعتمد في آلية عملها على طريقة البيوريت. و تم أختيار العزلتين *Lactobacillus acidophilus* و *Lactobacillus casei* أعتمادا على الوزن الجزيئي و تركيز البروتين.

أظهرت نتائج التركيز المثبط الادنى MIC لرواشح مزروع بكتريا حامض اللاكتيك المركز لثلاث مرات ان نسبتي 40% و50% من كلا نوعي بكتريا حامض اللاكتيك العصويه هما التركيزين المثبطين الدنيا ضد بكتريا *Pseudomonas aeruginosa* و *Escherichia coli* على التوالي, و أما نسبة 60% فقد كانت التركيز المثبط الادنى ضد *Salmonella typhimurium* و *Cadida albicans* بينما كانت نسبتي 50% و 60% هما التركيزان المثبطان الدنيا ضد بكتريا *Staphylococcus aureus*.

أستخدم التركيز المثبط الادنى لدراسة ظاهرة الالتصاق لبكتريا *E. coli* و *Staph. aureus* على الخلايا الطلائيه, وبينت النتائج فعالية الراشح المركز في التقليل من التصاق خلايا هاتين

الممرضتين بالخلايا الطلائية بمعدل وصل الى 5-12 و 4-9 بكتريا /خلية بدلاً من 50- 60 و 29-35 بكتريا / خلية على التوالي كما وتناقص التصاق بكتريا *E. coli* و *Staph. aureus* بالخلايا الطلائيه قد تناقص ايضا بوساطة البروتينات السطحيه بمعدل (3-9) بكتريا /خلية لكلا النوعين من البكتريا.

ABSTRACT

This project was conducted to evaluate the activity of S-layer proteins extracted from *Lactobacillus* in comparison with the activity of concentrated filtrate of *Lactobacillus* against some pathogenic microorganisms *in vitro*. Twelve isolates of *Lactobacillus spp.* obtained from, vinegar, human milk, cow milk, yoghurt and vagina, were used to detect the S-layer protein (Slp) by Sodium Dodecyl Sulfate-Polyacrylamide gel electrophoresis (SDS-PAGE) then extracted it by excised the Slp pand and treated with 6M guanidin hydrochloride (G-HCl) to eluted the protein from gel. The Molecular weights (MW) of Slps were estimated between (37-63 kDa) depending on the *Lactobacillus* species. The concentrations of Slp were estimated by using a Kit based on the Biuret method. One isolate of each of *Lactobacillus acidophilus* and *Lactobacillus casei*, were selected depending on the MW and concentrations of S-layer proteins. Minimum inhibitory concentrations (MICs) of *Lactobacillus spp.* concentrated filtrates were determined. Results showed 40% and 50% of the concentrated filtrate of both *Lactobacilli* were the MIC for *Pseudomonas aeruginosa, Escherichia coli*, respectively, where as MIC for *Salmonella typhimurium* and *Cadida albicans* it was 60%, while 60% and 50% of *L. acidophilus* and *L. casei* respectively, were MIC against *Staphylococcus aureus*. At such MIC,s of *Lb. spp.*, adhesion of *E. coli* and *Staph. aureus* to the uroepithelial cells was minimized when the average decreases recorded were (5-12) and (4-9) bacteria/cell after they were (50-60) and (29-35) bacteria/cell, respectively. Adhesion of *E. coli* and *Staph. aureus* to the uroepithelial cells was also decreased by S-layer proteins with average decreased (3-9) bacteria/cell for both tested bacteria.

INTRODUCTION

The administration of Lactic Acid Bacteria (LAB) contained in fermented foods, especially dairy products, has been found to exhibit a wide range of physiological and therapeutic effects, including enhancement of non-

specific and specific immune responses, suppression of intestinal infection and alleviation of food allergies. However, the protective and immune-enhancing effects of probiotic LAB are known not as genus- or species-specific, but as strains. Accordingly, probiotic LAB strains have become very important in the fields of nutrition, health, and food for research and commercial development. Probiotics LAB have mostly been found in animal sources, dairy products, human and animal intestines (1). An important property proposed for a probiotic bacterium is the ability to adhere and colonize host tissues, which enhances multiplication and survival of bacteria in the host and prevents colonization by pathogenic bacteria. Suppression of the growth of pathogens can also be achieved through competition for nutrients as well as by production of bactericidal components, such as bacteriocins, lactic acid or hydrogen peroxide (2).

Lactobacilli interact with the host via several distinct surface components. Adhesion to host tissues is considered to be the first step in bacterial colonization. The role of proteinaceous surface molecules in adhesion has been proposed in several studies (3). Like many other bacteria, several species of *Lactobacillus* have a surface (S-) layer as the outermost component of the cell (4). S-layers are periodic crystalline arrays that are composed of protein or glycoprotein subunits, which form a solid layer to cover the whole cell surface (5). The function of *Lactobacillus* S-layers characterized so far is involved in mediating adhesion to different host tissues. In addition to surface layer proteins (Slps) adhesive properties, the very large number of S-layer subunits present on the cell surface has prompted research aiming at the use of S-layers as a vehicle for the delivery of biologically active compounds, such as drug molecules, antibodies, enzymes and vaccine antigens (6).The members of the genus *Lactobacillus* are important residents of the gastrointestinal (GI) microbiota and have been subjects of increasing interest due to their possible role in the maintenance of GI health. Because of this putative health promoting properties, *Lactobacillus* species are widely used as probiotics. This study aimed to extraction S-layer proteins from *Lactobacillus spp.* of different sources, evaluating the activity of S-layer proteins and *Lactobacillus* concentrated filtrates to inhibit the adhesion of some pathogenic bacteria *in vitro*.

MATERIALS AND METHODS

Bacterial Isolates:

Bacterial isolates used in this study were obtained from different sources as indicated below:

Isolate	Source	Supplied by
Two isolates of *Lactobacillus acidophilus*	chicken intestine	College of Veterinary Medicine/ Baghdad University
Lactobacillus acidophilus	faeces of children	Biotechnology Research Centre /AL-Nahrain University
Lactobacillus casei		
Escherichia coli	Skin infection	Biotechnology Department/College of Science/Al-Nahrain University
Staphylococcus aureus		
Pseudomonas aeruginosa		
Salmonella typhimurium		
Candida albicans		

Isolation of *Lactobacillus* from different sources:

Two samples of vinegar, five samples (3ml) of human milk (taken from healthy women), three samples of cow milk, and four of yoghurt were collected in order to isolate *Lactobacillus*, also *Lactobacillus* isolates were isolated from the vagina of healthy premenopausal women by the gynecologist doctor in Kamal AL-Samarai hospital, Baghdad. *Lactobacillus* isolated according to the method was performed by (7).

Detection of S-layer proteins:

Lactobacillus cells grown in MRS broth were collected by centrifugation at 10,000 rpm for 10 min at 4°C and washed once with 0.5M Tris-HCl, pH 7.5. The pellet, equivalent to 1 ml of culture, was resuspended directly in 200 µl of Laemmli sample buffer and analysed by sodium dodecyl sulfate-polyacrylamide gel electrophoresis 10% (SDS-PAGE) (8).

Extraction of the S-layer protein:

The bands which located in the range between Transferrin and Trypsine was excised and cut into pieces. The protein was eluted from the gel pieces in 1.5 ml of 6 M guanidine hydrochloride-0.5 M Tris-HCl-2 mM EDTA, pH 7.5, by incubating in an end-over mixer at room temperature for 10 h. The eluate was dialyzed against 0.1M Tris-HCl, pH 8.5, at +4°C for 10 h. also analyzed by (SDS-PAGE), In order to ensure the purity of protein. This method was done according to (9).

Determination of Total Protein:

Protein concentration was estimated using specific kit depending on Biuret method.

Determining Minimum Inhibitory Concentration (MIC) and Minimum Bactericidal Concentration (MBC) of *Lactobacillus spp.* Concentrated Filtrates:

One hundred ml of filtrate of *Lactobacillus* was concentrated by oven at 40-45 °C to one- fold (50 ml), two -fold (25 ml) and three- fold (12.5 ml).

Serial dilutions (10ml) of three fold concentrated filtrate of *Lactobacillus* were made in tubes containing sterile nutrient broth. The ratios were (10, 20, 30, 40, 50, 60, 70, 80 and 90%) giving final volume of 10 ml in each tube. After each concentration was inoculated by 0.1 ml of the test organisms (*P. aeruginosa*, *E. coli*, *Staph. aureus*, *Sal. typhimurium* and *C. albicans*), it was incubated at 37 °C for 24 hr. Growth intensity of each tube was observed by inoculation on nutrient agar and Sabouraud dextrose agar (for *Candida albicans*) then incubated overnight at (37°C) Results were recorded as growth (+), and no growth (-) (10).

Bacterial Adhesion Test (11):-

Preparation of *E. coli* and *Staph. aureus*:

Ten milliliter of nutrient broth medium was inoculated with bacterial growth culture, and incubated at 37°C for 24 hr. After that, the culture of bacteria was collected by centrifugation at 1000 rpm for 20 min then, washed twice with PBS and concentrated by centrifugation at 1000 rpm for 20 min and resuspended in PBS.

Preparation of Epithelial Cells:

Uroepithelial cells were isolated from urine of some healthy females by centrifugation at 1000 rpm for 5 min then washed three times with 5ml of PBS and recentrifuged at 1000 rpm for 10 min before resuspension in 5mlof PBS.

Adhesion Test:

- A mixture of bacterial suspension, and epithelial cells suspension (0.2 ml for each) beside 0.1 ml of PBS were incubated at 37°C for 1 hr.
- Unattached bacterial cells to uroepithelial cells were removed by centrifugation in 5ml of PBS at 1000 rpm for 10 min. The filtrate was ignored.

- The pellet was resuspended in PBS. A drop of suspension was transffered to a microscopic slide, air - dried, fixed with methanol: acetic acid (3:1) and stained with methylene blue.
- The adhered bacterial cells to epithelial cells were observed by the compound light microscope.
- The control contained only epithelial cells.

Effect of Concentrated Filtrates on Adhesion Property of Tested Organisms:

The minimum inhibitory concentration of the concentrated filtrates of *Lactobacillus spp.* isolate was used to investigate its effect on adhesion property of tested organisms on uroepithelial cells *in vitro* as following:

Nutrient broth medium containing minimum inhibitory effect of concentrated filtrates was dispensed in sterile tubes and incubated with a loopfull of each liquid culture of the tested bacteria at (37°C) for (24) hr.. Adhesion test as mentioned above was reused to examine inhibitory effect of the concentrated filtrate after treatment.

Effect of S-layer proteins on Adhesion of Tested Organisms (12):

Mixtures consisted of 0.2 ml from each of the following, bacterial suspension, epithelial cells suspension and S-layer proteins isolated from *Lactobacillus spp.* were incubated at 37°C for 1 hr. Procedure was completed as mentioned above.

RESULTS AND DISCUSSION

S-layer proteins and their extraction with Guanidine HCl:

Presence of crystalline arrays of protein (that so-called S-layer) covering the cell surface has been shown in several *Lactobacillus* species (13).

Putative S-layer proteins on the bacterial cell surface can be deduced by the occurrence of a dominant protein band in the protein profile of non-lysed bacteria.

Twelve isolates of *Lactobacillus spp.* were analyzed by electrophoresis using 10% SDS-PAGE and the lane of proteins bands obtained were compared with four marker proteins (γ-globulin MW = 150 kDa, Transferrin MW = 80 kDa, Trypsine MW = 20 kDa, Lysozyme MW = 14 kDa).

To extract S-layer protein, the band which located between Transferrin and Trypsine excised and treated with 6M G-HCl from crude column.

(4) Found that *Lactobacilli* surface layer proteins are among the smallest detected with molecular masses ranging from 25 to 71 kDa. The S-layer subunits are non-covalently linked to each other and to the supporting cell envelope, and can be disintegrated into monomers by denaturing agents such as urea or guanidin HCl, metal-chelating agents or by cation substitution (14).

Results of protein profile by SDS-PAGE revealed that seven bands with MW range between 10.26-108.71 kDa were obtained after analysis of *L. acidophilus* isolate (1) which isolated from chicken intestine. Then, detected band were excised and treated with 6M guanidine hydrochloride and analysed by SDS-PAGE. Results showed that only one band was obtained with MW 47.74 KDa. It was corresponded to the original band in crud column as shown in figure (1). This came in accordance to (15) who mentioned that S-layer proteins of *lactobacilli* have molecular mass between 40 and 55 kDa.

Analysis of protein profile of *L. acidophilus* (2) isolate from chicken intestine gave eight bands with MW range between 11.50-177.74 kDa. Band with MW 50 kDa represented the S-layer protein, and treatment of this band with 6M guanidine hydrochloride gave one band with MW 48.37 kDa which corresponded to the original band in crud column (figure, 1).

-A- -B-

Fig. -1 : Protein profile analysis of *Lactobacillus* by 10% SDS-PAGE: (A) *L. acidophilus*1 and (B) *L. acidophilus*2 isolated from chicken intestine.
L1: Protein markers, L2: Crude analysis and L3: Pure S-protein analysis

Results of protein profile analysis of *L. acidophilus* from feces of children showed seven bands with MW ranged between 13.10 -147.53 kDa. Band with MW 49.46 KDa represented the S-layer protein. On the other hand, five bands were obtained from *L.casei* of children feces with MW range between 14.37- 292.50 KDa. Only band with MW 43.59 KDa represented S-layer protein.

Analysis S-layer from *L. acidophilus* and *L. casei* after treating with 6M guanidine hydrochloride gave two bands with MW 49.46 and 44.66 KDa, respectively as shown in figure (2).

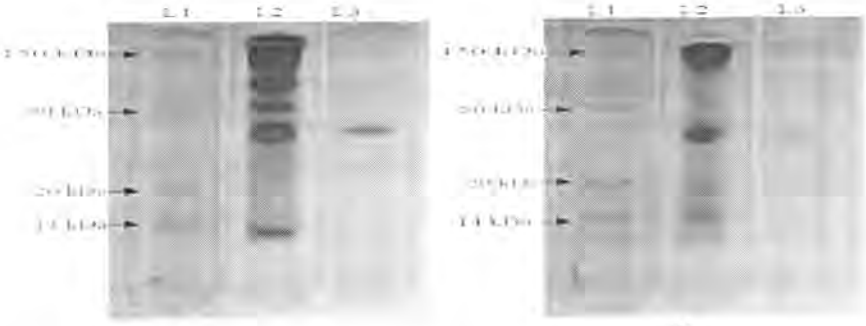

-A- -B-

Fig. -2 : Protein profile analysis of *Lactobacillus* by 10% SDS-PAGE: (A) *L. acidophilus* (B) *L. casei* isolated from faeces of children, L1: Protein markers, L2: Crude analysis and L3: Pure S-protein analysis

Results in figure (3) indicated that bands with MW 46.52 and 44.25 KDa represented the S-layer protein of *L. plantarum* and *L. acidophilus* isolated from yoghourt, respectively. Treatment of these bands with 6M guanidine hydrochloride gave bands with MW 48.69 and 43.42 kDa, respectively, which were corresponded to the original band in crud column. (16) Found that the molecular weight of surface protein was 43 kDa when extracted from *L. acidophilus* ATCC 4356 by treatment of whole cells with 4 M guanidine hydrochloride.

Analysis of protein profile of *L. gasseri* from human milk gave seven bands with MW range between 13.70 – 158.94 KDa. Band with 38.92 kDa represented S-protein; treatment of this band with 6M guanidine hydrochloride gave one band with MW 37.58 KDa was corresponded to the original band in crud column as shown in figure (4).

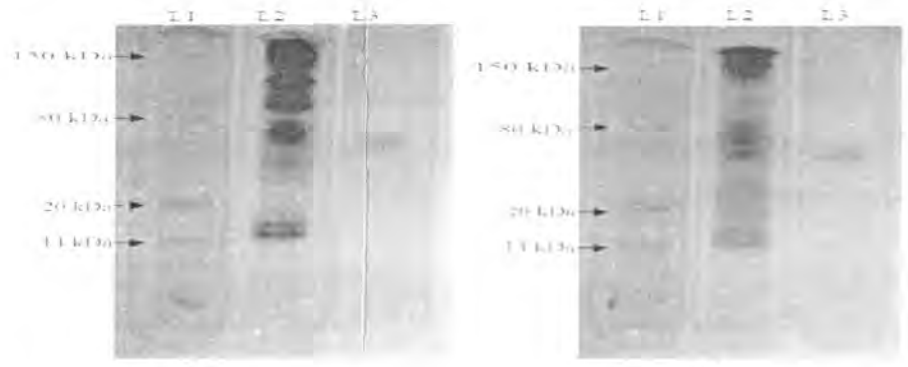

-A- -B-

Fig. -3 : Protein profile analysis of *Lactobacillus* by 10% SDS-PAGE: (A) *L. plantarum* (B)*L.acidophilus* isolated from yoghurt

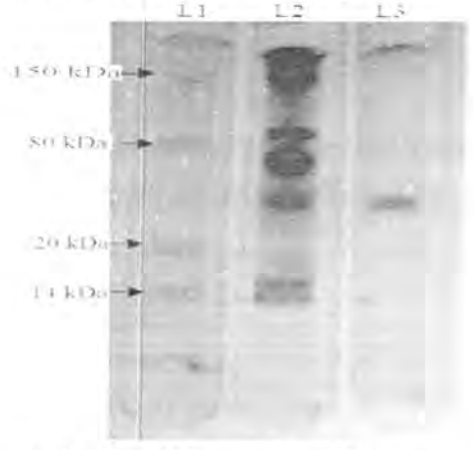

Fig. -4 : Protein profile analysis of *Lactobacillus gasseri* isolated from human milk by 10% SDS-PAGE

L1: Protein markers, L2: Crude analysis and L3: Pure S-protein analysis

S-layer proteins did not appeared in protein profile analysis of *L. fermentum* isolated from vagina (figure, 5). This result was disagreed with that of (17) who purified and characterized a 29-kDa cell surface protein from *L. fermentum*.

(18) Stated that among lactic acid bacteria, the S-layer seems to be a typical surface structure in several *Lactobacillus* species, e.g., in *L.acidophilus*, *L. helveticus*, *L. casei*, *L. brevis*, *L. buchneri*, *L.fermentum*, *L. bulgaricus* , and *L. plantarum* .

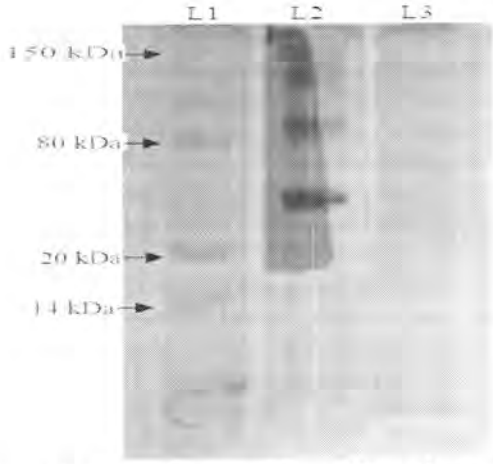

Fig. -5 : Protein profile analysis of *Lactobacillus fermentum* isolated from vagina by 10% SDS-PAGE.
L1: Protein markers, L2: Crude analysis and L3: Pure S-protein analysis

Results of analysis of protein profile of *Lactobacillus plantarum* from vinegar, showed that only one band with MW of 63.06 kDa was visible, while *Lactobacillus plantarum* from cow milk gave S-layer band with MW 51.46 kDa, as indicated in figure (6).

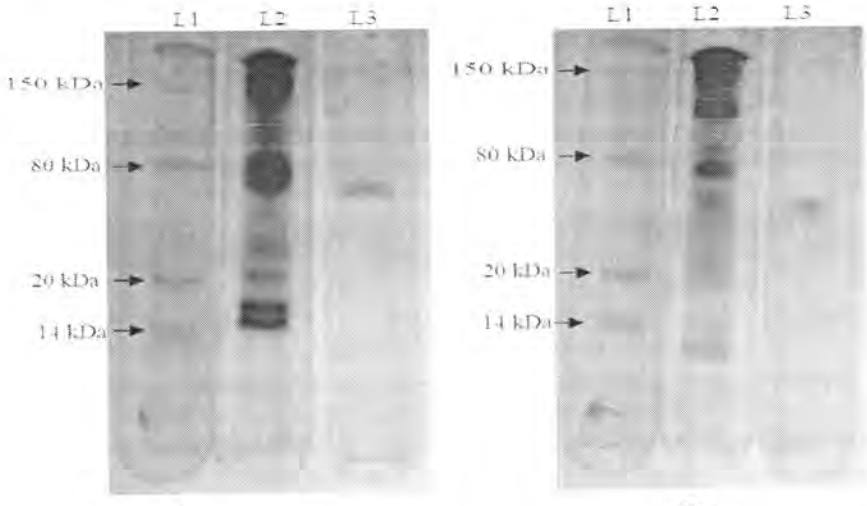

-A- **-B-**

Fig. -6 : Protein profile analysis of *Lactobacillus* by 10% SDS-PAGE (A) *L.plantarum* from vinegar (B) *L.plantarum* from cow milk.
L1: Protein markers, L2: Crude analysis and L3: Pure S-protein analysis

Protein profile analysis of *L. rhamenosus* and *L. curvatus* from cow milk showed that two bands were obtained with MWs 60.09 and 39.64 kDa, respectively, (figure, 7).

(19) Found that the molecular masses of S-layer proteins of *Lactobacillus spp.* which isolated from pig intestine ranging between 45–62 kDa.

The molecular weight of S-layer protein is varied depending on species and sources of *Lactobacillus.* Most S-layers are composed of a single protein species which greatly varies in size related to different bacterial genera (20).

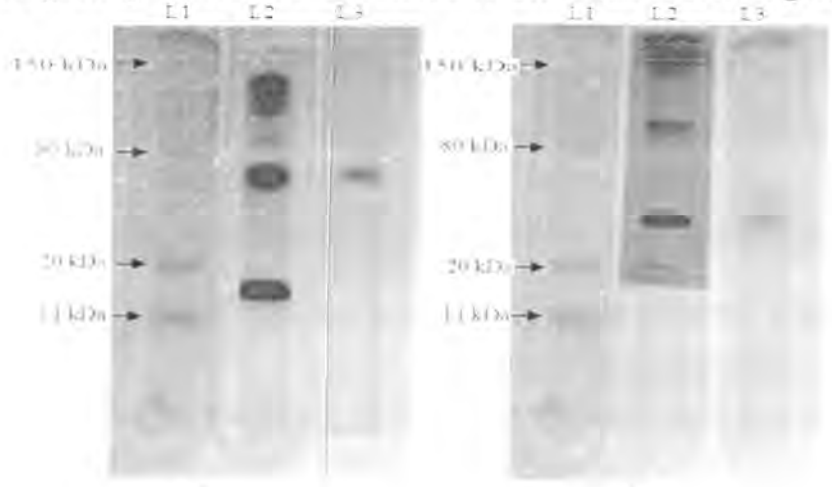

-A- -B-

Fig. -7 : protein profile analysis of *Lactobacillus* by 10% SDS-PAGE: (K) *L. rhamenosus* (L) *L. curvatus* isolated from cow milk.
L1: represents protein markers, L2: represents crude analysed cells of *Lactobacillus* and L3: is pure protein.

Concentrations of *Lactobacillus* S-layer proteins:

The concentrations of extracted S-proteins from *Lactobacillus* were determined by using Kit which depended on Biuret method.

Results of the concentrations of S-proteins showed that were ranged from 1.87 mg/ml for *L.acidophilus* (isolated from chicken intestine) to 0.13 mg/ml for *L. curvatus* (from cow milk) as shown in table (1). Under laboratory cultivation conditions, yield of the S-layer glycoprotein ranges between 0.5 and 2.0 g wet weight per litre of growth medium (21).

Table -1: Concentrations of S-layer proteins of *Lactobacillus* isolates

S-layer protein from		Concentration of protein (mg/ml)
Isolates	**sources**	
L. acidophilus1	From chicken intestine	1.87
L. acidophilus2		1.79
L. acidophilus	From feces	1.56
L. casei		1.39
L. plantarum	From yoghurt	0.83

L. acidophilus		0.32
L. gasseri	From human milk	0.55
L. plntarum	From vinegar	1.21
L. plantarum	From cow milk	0.57
L. rhamenosus		1.17
L. curvatus		0.13

Two S-layer proteins extracted from *L. acidophilus*1 and *L.casei* which their molecular weight were (47 and 44 kDa) and their concentrations were (1.87 and 1.39 mg/ml), respectively, were used in this study to evaluate the biological role of S-layer proteins.

Minimum Inhibitory Concentration (MIC) and Minimum Bactericidal Concentration (MBC) of LAB Filtrates against pathogens:

Results (table 2) indicate that concentrations 10% and 20% of both *L.a* and *L.c* filtrates had no effect on the tested microorganism when clear growth of pathogenic microorganisms was observed after (24hr) of incubation. Adversely, 40% of both filtrates led to minimized growth (MIC) of *P. aeruginosa*, while concentration 50% of both LAB filtrates was needed to inhibit growth of this bacterium completely (MBC).

At the time that a sharp decrease in growth of *E. coli* was recorded by treatment with concentration 50% of both LAB filtrates, growth was completely inhibited by 60% concentration. The concentrations of 50 % and 60 % of *L. acidophilus* and *L. casei* filtrates respectively, were considered the MIC,s against *Staph.aureus*, where as 60 % and 70 % were the MBC,s. Concentration 60% of both *L.a* and *L.c* filtrates (MIC) were sharply reduced growth of *Sal. typhimurium* and *C. albicans*, while 70 % completely inhibited their growth. (22) found that concentration 50% of LAB was the MIC for *E. coli*, while 60% for *Staph.aureus* and *P. aeruginosa*. (23) found that the MIC of *L.acidophilus* and *L. plantarum* concentrated filtrates were 50% and 60% respectively, for *Proteus mirabilis* isolates.

Table -2: Minimum Inhibitory Concentrations (MIC,s) and Minimum Bactericidal Concentrations (MBC,s) of Concentrated Filtrates of *L. acidophilus* and *L. casei* against pathogens:

	Isolates	LAB filtrate concentration (%)								
		10	20	30	40	50	60	70	80	90
L. acidophilus	***Pseudomonas aeruginosa***	+	+	+	+	-	-	-	-	-
	Escherichia coli	+	+	+	+	+	-	-	-	-
	Salmonella typhimurium	+	+	+	+	+	+	-	-	-
	Staphylococcus aureus	+	+	+	+	+	-	-	-	-
	Cadida albicans	+	+	+	+	+	+	-	-	-
L. casei	***Pseudomonas aeruginosa***	+	+	+	+	-	-	-	-	-
	Escherichia coli	+	+	+	+	+	-	-	-	-
	Salmonella typhimurium	+	+	+	+	+	+	-	-	-
	Staphylococcus aureus	+	+	+	+	+	+	-	-	-
	Cadida albicans	+	+	+	+	+	+	-	-	-

Growth = + No Growth= -

Adhesion of *Escherichia coli* and *Staphylococcus aureus* :

Adherence of pathogenic bacteria to host epithelial cells is an important step in the initiation of the infectious process (24). Bacterial adhesion is initially based on non-specific physical interaction between two surface, which then enable specific interaction between adhesion usually (proteins) and complementary receptors (25). In the current study, adherence property of *E. coli* and *Staph . aureus* as well as how this property may be affected by LAB isolate and S-proteins, was investigated.

Adherence ability of *E.coli* and *Staph. aureus* to uroepithelium (UEP) is shown in (Figure 8). Results clarified that the average number of *E. coli* adhering to UEP ranged from 50-60 bacteria/cell, whereas the number of *Staph. aureus* adhering to UEP ranged from 29-35 bacteria/cell.

Many researches confirmed that pili mediate attachment of uropathogenic *E. coli* to human urinary tract epithelium (26) while *Staph. aureus* and *streptococci pyogenes* adhere to host epithelial cells through the expression of surface proteins which bind to the host extracellular matrix proteins such as fibronectin and collagen (27).

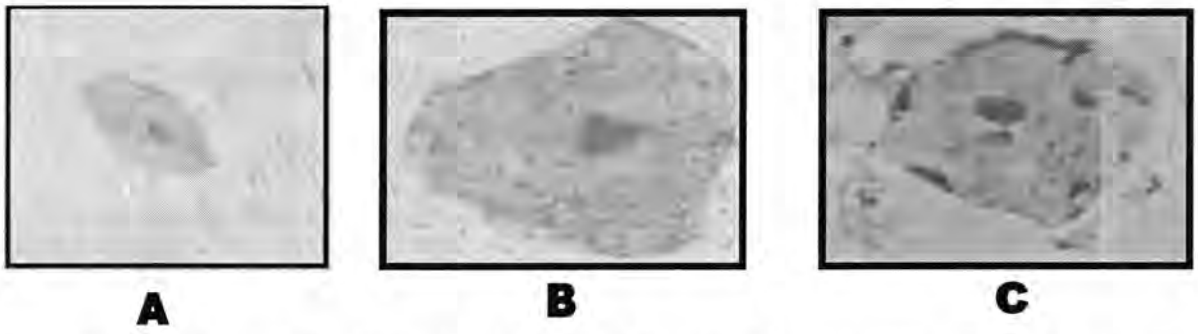

Fig. -8: Microscopical Examination of Adhesion Property of *E. coli* and *S. aureus* Ureoepithelium cell under Oil - Immersion Objective (100xs). (A) Normal Uroepithelial cell (B) *E.coli* Adhered to Ureoepithelial Cell (C) *S. aureus* adhered to Uroepithelial Cell.

Adhesion Inhibition by LAB Filtrates and S-layer protein:

The effect of concentrated filtrate of LAB and S-layer protein against adhesion property of *E. coli* and *Staph . aureus* were studied. Results showed that the three-fold concentrated filtrate of LAB (*L.acidophilus* and *L.casei*) minimized adhesion of *E. coli* to uroepethilial cell reaching an average of (5-12) bacteria / cells (fig. 9.A). In this aspect (28) found that *L. fermentum* produced a proteinaceous component detectable in spent culture fluid during growth in both complex and defined media; this component inhibited the adhesion of *E. coli* fimbriae to ileal mucus by interacting with mucus components.

The three-fold concentrated filtrates of both LAB minimized adhesion of *Staph. aureus* to the uroepethilial cell reached an average of (4-9) bacteria / cells (fig. 3-9.B). Study of (29) found that precoating of LAB strains reduced the binding of uropathogenic (*Staphylococci* and *E. coli*) to 8 bacteria /cell.

Similar reduction also observed when the S-layer protein was used and, adhesion *E. coli* and *Staph. aureus* to the uroepethilial cells reached an average of (3-9) bacteria / cells. S-layer protein has the potential to play a role in the competitive exclusion of pathogens (5). (30) who found that S-layer protein extracted from *L. helveticus* had inhibition effect on enterohaemorrhagic *E. coli* adhesion to host epithelial cells.

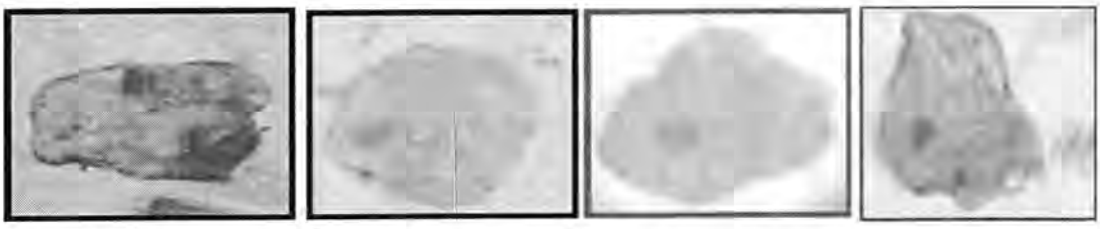

A B C D

Fig. -9: Microscopical Examination of Adherence of *E.coli* and *Staph. aureus* to the Uroepithelium Cells after Treatment with the Concentrated Filtrate of LAB and S-layer protein (100 X).

-A- After treating *E. coli* with three-fold of LAB.

-B- After treating *Staph. aureus* with three-fold of LAB.

-C- After treating *E. coli* with Slp.

-D- After treating *Staph. aureus* with Slp.

Three-fold concentrated filtrates of LAB and S-layer protein had effect on the adhesion of *E.coli* and *Staph. aureus*.

REFERENCES

1. Ishida-Fujii, K.; Sato, R.; Goto, S.; Yang, X.; Kuboki, H.; Hirano, S. and Sato, M. Prevention of Pathogenic *Escherichia coli* Infection in Mice and Stimulation of Macrophage Activation in Rats by an Oral Administration of Probiotic *Lactobacillus casei* I-5. Biosci. Biotechnol. Biochem., 71: 866-873. (2007).
2. Reid, G. and Burton, J. Use of *Lactobacillus* to prevent infection by pathogenic bacteria. Microbes Infect., 4:319-324. (2002).
3. Lorca, G.; Torino, M. I.; Font de Valdez, G. and Ljungh, A. A. *Lactobacilli* express cell surface proteins which mediate binding of immobilized collagen and fibronectin. FEMS Microbiol. Lett., 206:31-37. (2002).
4. Åvall-Jääskeläinen, S. and Palva, A. *Lactobacillus* surface layers and their applications. FEMS Microbiol. Rev., 29(3): 511-529. (2005).
5. Sara, M. and Sleytr, U. B. S-layer proteins. Bacteriol. J., 182: 859-868. (2000).
6. Sleytr, U. B.; Huber, C.; Ilk, N.; Pum, D.; Schuster, B. and Egelseer, E. M. S-layers as a tool kit for nanobiotechnological applications. FEMS Microbiol. Lett., 267:131-44. (2007).
7. Buck, L. M. and Gilliland, S. E. Comparisons of freshly isolated strains of *Lactobacillus acidophilus* of human intestinal origin for ability to assimilate cholesterol during growth. Dairy Sci. J., 77: 2925 – 2933. (1995).

8. Laemmli, U. K. Cleavage of structural proteins during the assembly of the head of bacteriophage T4. Nature (London) 227:680-685. (1970).
9. Vidgren, G.; Palva, I.; Pakkanen, R.; Lounatmaa, K. and Palva, A. S-Layer Protein Gene of *Lactobacillus brevis*: Cloning by Polymerase Chain Reaction and Determination of the Nucleotide Sequence. Bacteriology. J., 174: 7419-7427. (1992).
10. Atlas, R. M.; Brown, A. E. and Parks L. L. Laboratory Manual of Experimental Microbiology (1st Ed.). Mosby. Inc. Missouri. (1995).
11. Iwahi, T.; Abc, Y. and Tauchiya, K. Virulence of *H.pylori* in a sending urinary tract infection in mice. J. Med. Microbiol., 15: 303-316. (1982).
12. Velraeds, M. M.; van de Belt-Gritter, B.; van de Mei, H. C.; Reid, G and Busscher, H. J. Interference in initial adhesion of uropathogenic bacteria and yeasts to silicon rubber by *Lactobacillus acidophilus* bio-surfactant. Med. Microbiol. J., 47: 1081-1085. (1998)
13. Boot, H. J.; Kolen, C. P.; Pot, B.; Kersters, K. and Pouwels, P. H. The presence of two S-layer protein encoding genes is conserved among *Lactobacillus acidophilus*. Microbiol., 142: 2375-2384. (1996).
14. Sara, M. Conserved anchoring mechanisms between crystalline cell surface S-layer proteins and secondary cell wall polymers in gram-positive bacteria. Trends Microbiol., 9: 47-9. (2001).
15. Frece, J.; Kos, B.; Svetec, I. K.; Zgaga, Z.; Mrsa, V. and Suskovic, J. Importance of S-layer proteins in probiotic activity of *Lactobacillus acidophilus* M92. J. Appl. Microbiol. 98, 2: 285-292. (2005).
16. Boot, H. J.; Kolen, C. P.; van Noort, J. M. and Pouwels, P. H. S-layer protein of *Lactobacillus acidophilus* ATCC 4356: Purification, expression in *Escherichia coli*, and nucleotide sequence of the corresponding gene. Bacteriol. J., 175 (19): 6089-6096. (1993).
17. Rojas, M.; Ascencio, F. and Conway, P. L. Purification and Characterization of a Surface Protein from *Lactobacillus fermentum* 104R That Binds to Porcine Small Intestinal Mucus and Gastric Mucin. Appl. Environ. Microbiol., 68:2330-2336. (2002).
18. Kahala, M.; Savijoki, K. and Palva, A. In Vivo Expression of the *Lactobacillus brevis* S-Layer Gene. Bacteriol. J., 179: 284-286. (1997).
19. Jakava-Viljanen, M and Palva, A. Isolation of surface (S) layer protein carrying *Lactobacillus* species from porcine intestine and faeces and characterization of their adhesion properties to different host tissues. Veterinary Microbiol. J., 124: 264-273. (2007).

20. Boot, H. and Pouwels, P. Expression, secretion and antigenic variation of bacterial S-layer proteins. Mol Microbiol., 21:1117–1123. (1996).
21. Eshinimaev, B. T.; Khmelenina, V. N.; Sakharovskii, V. G.; Suzina, N. E.; and Trotsenko, Y. A. Physiological, biochemical, and cytological characteristics of a haloalkalitolerant methanotroph grown on methanol. Microbiol. (Moscow), 71: 512-518. (2002).
22. Mohamed, B. J. Evaluate the inhibitory effect of *Lactobacillus spp* isolated from different sources as probiotic on pathogenic microorganism of urogenital tract infections in women. M.Sc. Thesis institute of Genetic Engineering and Biotechnology Institute for Postgraduate Studies, Baghdad University. (2008).
23. Al-Jeboury, G. H. Probiotic effect on *Proteus mirabilis* and its adhesion property. M.Sc. Thesis. College of Science, Al-Nahrain University. (2005).
24. Finlay, B. B. and Caparon, M. Bacterial adherence to cell surfaces and extracellular matrix. In *Cellular Microbiology.* Cossart, P., Boquet, P., Normark, S., and Rappuoli, R. (eds). Washington, DC: American Society for Microbiology Press: 105–120. (2005).
25. Rojas, M. and Conway, P. L. Colonization by *lactobacilli* of piglet small intestinal mucus. J. Appl. Bacteriol., 81: 474-480. (1996).
26. Cook, S. W.; Mody, N.; Valle, J. and Hull, R. Molecular Cloning of *Proteus mirabilis* Uroepithelial Cell Adherence (*uca*) Genes. Infect. Immun. J., 63(5): 2082–2086. (1995).
27. Jost, B. H. and Billington, S. J. *Arcanobacterium pyogenes*: molecular pathogenesis of an animal opportunist. Antonie van Leeuwenhoek, 88: 87-102. (2005).
28. Blomberg, L.; Henriksson, A. and Conway, P. L. Inhibition of Adhesion of *Escherichia coli* K88 to Piglet Ileal Mucus by *Lactobacillus* spp. Appl. Environ. Microbiol. 59(1): 34-39. (1993).
29. Hawthorn, L. A. and Reid, G. Exclusion of uropathogen adhesion to polymer surfaces by *Lactobacillus acidophilus*. J. Biomed. Mater. Res. 24: 39-46. (Cited by Fergus M. C. (1999)). (1990).
30. Johnson Henry, K.C.; Hagen, K.E.; Gordonpour, M.; Tompkins, T.A. and Sherman, P.M. Surface layer protein extracts from *Lactobacillus helveticus* inhibit enterohaemorrhagic *Escherichia coli* O157:H7 adhesion to epithelial cells. Cell Microbiol., 9 (2):356-367. (2007).

Cytotoxic, Cytogenetics and Immunomodulatory Effects of Thymol from *Thymus vulgaris* on Cancer and Normal Cell Lines in Vitro and in Vivo

Reema M. Abed
Biotechnology Department, College of Science, Baghdad University

Received: 29/03/2011 Accepted: 29/05/2011

الخلاصة

أستخلص مركب الثايمول من الاوراق الجافة لنبات الزعتر *thymus vulgaris* بأستعمال هيدروكسيد الصوديوم والايثر ثنائي الاثيل, وقد تم الكشف عن وجود مركب الثايمول بطريقة كروموتوكرافيا السائل عالي الكفاءة بالاعتماد على زمن الاحتجاز لمركب الثايمول القياسي ومستخلص الزعتر. أستعملت تراكيزنصفية من مركب الثايمول المستخلص (244,122,61,30.5,15) نانوغرام/مل لدراسة فعاليتها في خطين خلويين سرطانيين للانسان (خلايا سرطان عنق الرحم البشريHeLa , خلاياسرطان الحنجرة البشري Hep), وخط خلوي طبيعي (الخلايا الطبيعية لجنين الجرذ Ref)أذ حضنت الخطوط الخلوية بدرجة 37 درجة مئوية لمدة 72 ساعة, حيث بينت النتائج أختلاف حساسية الخطوط الخلوية تجاه السمية الخلوية لمركب الثايمول الذي أظهر تأثيرا" معنويا"P<0.05 في جميع التراكيزالمستعملة تجاه الخطوط الخلوية. بينت النتائج, السمية العالية(87.25%) لمركب الثايمول تجاه سرطان العنق البشري HeLa,وسمية متوسطة (51.45%) تجاه سرطان الحنجرة البشري Hep وسمية قليلة(20.94%) تجاه الخلايا الطبيعية لجنين الجرذ Ref, أذ سجلت اعلى سمية خلوية للثايمول عند التركيز 30.5 نانوغرام /مل. بصورة عامة لوحظ ان بقاء الخطوط الخلوية الثلاثة يعتمد على جرع المادة المستخدمة . بالاضافة الى ان خلايا سرطان عنق الرحم البشريHeLa أظهرحساسية عالية تجاه مركب الثايمول مقارنة مع الخطين الخلويين الاخريين. أظهرت الدراسة أيضا"التأثير السمي الوراثي لمركب الثايمول عند حقنه داخل البريتون في الفئران المختبرية بالتراكيز (5, 2.5,1.25) ملغم/كيلوغرام من وزن الجسم متمثلا بمعامل الانقسام الخلوي (MI) ,وبينت النتائج اختلافات معنوية(P< 0.05) بين التراكيز العالية لمركب الثايمول ومعامل السيطرة ,اذ ادى مركب الثايمول انخفاضا "معنويا" في معامل الانقسام الخلوي(MI) فيالتركيز (5.0) مليغرام/كيلوغرام من وزن

الجسم مقارنة بمعامل السيطرة. بينت النتائج عدم وجود تأثير لمركب الثايمول في تحفيز كريات الدم البيضاء مقارنة مع معامل السيطرة.

ABSTRACT

Thymol was extracted from leaves of *thymus vulgaris*, by using NaOH and diethylether. High performance liquid chromatography (HPLC) carried out to identify thymol in the aliqaut extract of thymus vulgaris depended on retention time of thyme extract and standard of thymol. The cytotoxic activity of thymol against two human cancer cell lines HeLa (Human epithelial cervical cancer), Hep (Human larynx epidermoid carcinoma) and one normal cell line Ref (Rat embryonic fibroblast) were estimated in vitro. The grown cells in 96 multi well plates were treated with different concentrations of thymol (15, 30.5, and 61,122,244) ng/ml and incubated at 37c° additional period 72hr. Cancer and normal cell lines elicited **various degrees of sensitivity to the cytotoxic effect of thymol .thymol exhibited significant differences (P<0.05) at all concentrations against three human cell lines. The results showed highest toxicity (87.25%) 0f thymol on HeLa cell line, a moderate** cytotoxicity (51.45%) on Hep-2, and slight toxicity (20.94%) on normal cell line (Ref), furthermore the highest toxicity was recorded at concentration 30.5 ng/ml for all cell lines. In general, a dose-dependent decrease the survival of the three cell lines was observed, in additional to HeLa cell line was showed higher sensitivity against thymol than the other cell lines. Also the study was conducted to investigate the effect of thymol intraperitoneally administration in mice at doses of (1.25, 2.5, 5) mg/kg body weight by determining the cytogenetic analysis represented by (mitotic index). The results showed significant differences (P<0.05) between highly doses of thymol and untreated control. Thymol decreased the mitotic index (MI) in high concentrations (5.0) mg/kg when compared with control. The results a showed no effect of thymol in stimulation of leukocytes compared with the negative control.

INTRODUCTION

Thyme has a wide spectrum of pharmacological properties. In fact, it has been reported that the essential oil of *Thymus vulgaris*, the most studied species of thyme, has antibacterial, antifungal and antioxidant activities (1, 2). Additionally, dietary supplementation with thyme oil maintained significantly higher superoxide dismutase and glutathione peroxidase activities and total antioxidant status (3,4,5). At non-toxic concentrations, thyme extract was also identified as a natural antimutagen with the possibility of enhancement of error-free DNA repair (6).

Furthermore, thyme extract has been shown to induce a considerable stimulation of leucopoiesis and also an elevation of thrombocyte count in blood (7). In addition, there is evidence that thymol, a constituent of the essential oil, could be involved in the stimulation of active proliferation of pulp fibroblasts (8).

The use of medicinal plants for the treatment of diseases is as old as mankind. Essential oils and their components are becoming increasingly popular as naturally occurring bioactive agents (9). Thyme, the most popular medicinal plant in Morocco, has been used in traditional medicine for thousands of years in African and European countries, particularly in the Mediterranean basin (10).

Recent investigations suggested that thyme extracts are anti-mutagenic due to potent antioxidant properties of thymol (11). Thyme leave extracts and its phenolic compounds thymol and carvacrol contain substance induces enzymes of both phase I and phase II biotransformation of xenobiotic substance in the mice liver (12). Another study conducted by (13) showed that phenolic chemotype (thymol and carvacrol) posses stronger anti-oxidant properties than the non-phenolic linal oil in *Thymus vulgaris (*14).

Systemic therapy with cytotoxic drugs is the basis of most effective treatments of disseminated cancers. However, the tumors responses to chemotherapeutic regimens vary, and failures are frequent owing to the emergence of drug resistance. Additionally, the induction of tumor cell resistance to one drug often results in coordinate resistance to other structurally and functionally unrelated drugs, and this defines the multiple drug resistance phenotypes (15).

It is expected that drug resistance may be circumvented by the rational design of new non-cross-resistant agents, by novel delivery or

combinations of known drugs and by the development of other treatments that might increase the activity of - or reverse resistance to - known antineoplastic agents (16).

The present study was planned with the aim to evaluate the antitumor potentials of thymol from leaves of thymus vulgaris in vitro by using two cancer Hela (Human epithelial cervical cancer), Hep (Human larynx epidermoid carcinoma) and one normal Ref (Rat embryonic fibroblast)cell lines and estimate the cytogenetic analysis of mitotic index (MI) in mice bone marrow cells, furthermore its immunomodulation effect on leukocytes.

MATERIALS AND METHODS

All the chemicals were obtained from Sigma Chemical Co. (USA) and BDH abundances for each of the populations (England), and the fresh plant was obtained from Jordan.

Extraction of thymol from Thyme leaves:

Air dried leaves of thymus vulgaris were grinded ,then 15g of leaves powder were extracted with 300ml of 5% NaOH , then filtrated with wattman no. 1, the filterate mixed with diethylether(2:1)(v:v) in separating funnel to removed non phenolic constitutes and upper layer was acidified with concentrated acid (HCL)pH 5.7 , then the product obtained by cooled the solution in -20c and collected crystallized granules from internal walls of flask to use in further experiments (17).

Identification of thymol by High performance liquid chromatographic quantization (HPLC):

The thyme leaves extract and standard compound were dissolved in DMSO; both samples were analyzed by HPLC separation with column Luna 5u C_{18} (250 × 4.6) mm internal diameter (id). The mobile phase was acetonitrile (ACN) 100% with a flow rate of o.5 ml/min. Injection volume for sample and standard solution was 10 µl. The pH was adjusted to 3.5. The detection occurred at UV light at 305 nm wave length.

1- Cell growth and cytotoxcity assays:

- Cell culture:

HeLa (Human epithelial cervical cancer), Hep (Human larynx epidermoid carcinoma) and Ref (Rat embryonic fibroblast) cell lines were obtained from

Iraq Center for Cancer and Medical Genetics Research (ICCMGR)–Almustansiriya University. cells were cultured in15 ml of RPMI-1640 media containing 10% Fcs in T-25 tissue culture flask and incubated at 37c for 24-48 hr.to complete confluent monolayer by changing the media with a new fresh medium daily.

-Cytotoxcity assay:

Cells growth were detected from the surface of flask and collected by trypsin /EDTA solution.

The trypsin activity was stopped by adding fresh media, then 200µl of cell suspension seeded at required density (1x10 cell/ml) in 96 micro-plates, and incubated for 24hr. in humidified atmosphere supplement with 5% at 37c°. The cells were treated with 200µl of five concentrations (15, 30.5, 61,122,244) ng/ml prepared in DMSO: SFM of thymol for additional period 72hr. (in tripicales).

After the end incubation periods,the procedure done according to (18,19).

2- Experimental Animals:

twenty male albino mice purchased from the Biotechnology Research Center/ AL-Nahrain University, were used in this study and their ages were ranged between (8-12) weeks and weighting range from(20-25) gm,maintained in controlled animal house at 25c ,12 hr. artificial light/12hr. dark .Before carring out experiments, the animals were kept for 5 days prior to dosing inanimal house of biology department –baghdad university to allow for their acclimatization for the laboratory conditions.The were divided into 4 groups, and each group was putted in a separate plastic cage. The animals were fed with a suitable quantity of water and complete diet.

Administration of Experimental Animals:

The groups of animals used in this experiment were injected intraperitoneally (I.P) with one dose only of thymol concentrations(1.25,2.5,5)mg/kg B.W. sacrificed after 24h.

Group1: Negative control, injected with (0.25ml) of DMSO.

Group 2: Animal in this group injected I.P with (0.25 ml) of thymol (1.25mg /Kg) B.W.

Group 3: Animal in this group injected .IP with (0.25 ml) of thymol (2.5mg /Kg) B.W.

Group 4: Animal in this group injected I.P with (0.25 ml) of thymol (5mg /Kg) B.W.

Chromosomal preparation from somatic cells of the mouse bone marrow:

All this experiment was done according to (20).

3- Immunomodulating effect of thymol:

Immunization procedure:

This procedure was done according to the method described by (21)

Five animals unless control was injected with 1 mg/ml of thymol intraperitoneally, after one week, each animal was injected with the same dose. The animals were killed after one week of the last dose. Blood smear was done for each animal to study the blood picture (Lymphocyte, Monocyte, Granulocyte), after stained by Giemsa stain

The percent of leukocytes calculation:

The percent of leukocytes determined in microscopically examination for animals were compared to control group using the following formula (22), (L= leukocytes):

$$\text{Control group L \%} = \frac{\text{L ratio in experiment}}{\text{L ratio in control}} \times 100$$

Statistical Analysis:

Statistical analyses were done using SPSS (version 17) program. Mean and standard deviation were descriptive measures of quantitative data using the analysis of variance test (ANOVA) for independent samples. P-value , $p<0.05$ were considered significant test (23).

RESULTS AND DISCUSION

The HPLC was used to detect the presence of thymol in the leaves extract. The result showed a retention time of the standard was 3.309 min and 3.292 min for the sample. Figure (1-A, 1-B). the results gave a white crystals with aromatic odor.

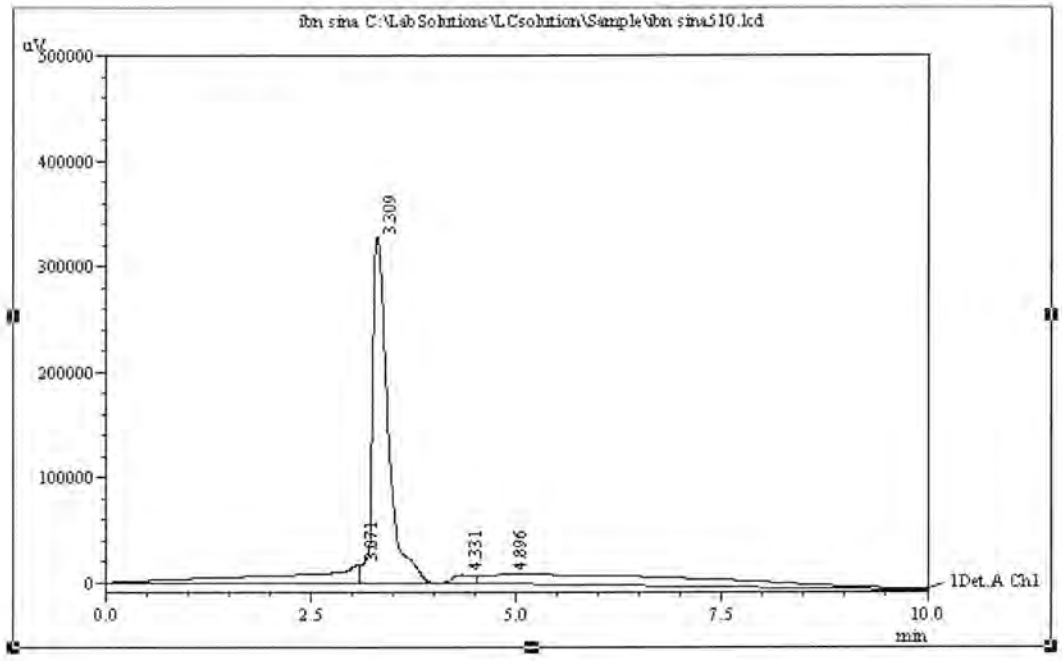

(A)

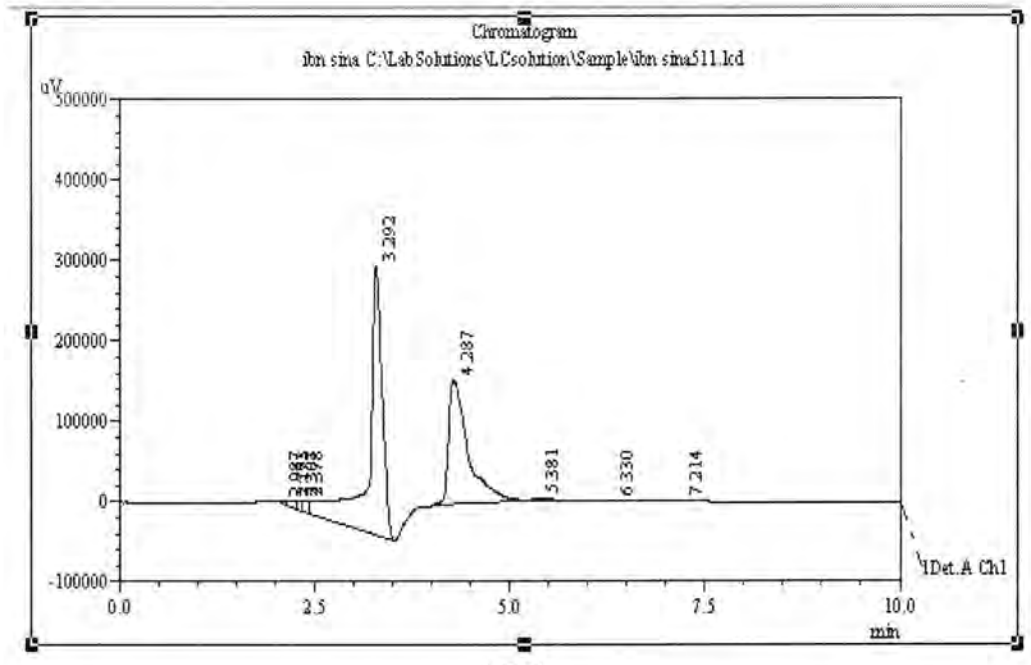

(B)

Fig. – 1: Chromatographic resolution by HPLC of thymol standard (A) and thymol extracted from leaves of thymus vulgaris (B), in column Luna 5u C_{18} by mobile phase acetonitrile (ACN) 100% with flow rate 0.5 min/ml, 305nm.

1- Cytotoxcity assays:

To investigate the effect of thymol on two cancer (HeLa, Hep) cell lines and normal cell line (Ref), HeLa, Hep and Ref, the cell cultures exposed to different concentrations of thymol.

The results showed a significant differences ($p<0.05$) in percentage of inhibition on Hela cell line dependet on concentration of thymol ,thus the percentage of inhibition ranged from(87.25-74.06)% , and the concentration renged from(30.5-244)ng/ml,the highest inhibition 87.25% recorded at concentration 30.5 ng/ml after 72hr of exposure.(figure 2)

The results showed a significant differences ($p<0.05$) in percentage of inhibition on Hep cell line dependet on concentration of thymol ,thus the percentage of inhibition ranged from(51.45-28.94)% , and the concentration renged from(30.5-244)ng/ml,the highest inhibition 51.45% recorded at concentration 30.5 ng/ml after 72hr of exposure.(figure 3)

The results showed a significant differences ($p<0.05$) in percentage of inhibition on Ref cell line dependet on concentration of thymol ,thus the percentage of inhibition ranged from(20.94-10.20)% , and the concentration renged from(30.5-244)ng/ml,the highest inhibition 20.94% recorded at concentration 30.5 ng/ml after 72hr of exposure.(figure 4)

This results deal with (24) that thymol was inhibit the growth of HeLa cell line.

In general, a dose-dependent decrease in survival of the three tumor and normal cell lines was observed. However, thymol exhibited stronger cytotoxicity at concentration 30.5 ng/ml towards three human cell lines.
The inhibition effect of thymol on Ref cell in significant manner lower than other cell line may be due to high cytotoxicity of thymol toward cancer (HeLa, Hep) cell line than normal cell line (Ref).

This results were came in agreement with (25) that thyme essential oil, which contains carvacrol and thymol, as the major components have an important *in vitro* cytotoxic activity against tumor cells .The molecular mechanism of the observed cytotoxicity is unknown, but owing to their lipophilic nature, plant volatile compounds appear to accumulate in the cell membrane and increase its permeability, resulting in leakage of enzymes and metabolites (26,27).

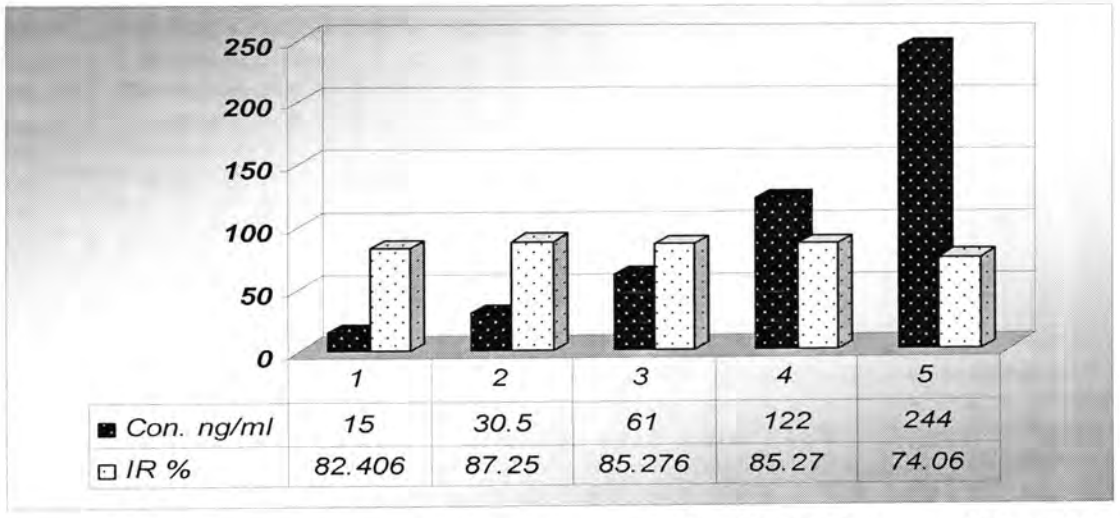

Fig. -2: Percentage of Cytotxicity represented by inhibition rate(IR) in HeLa cell line treated with different concentrations of thymol

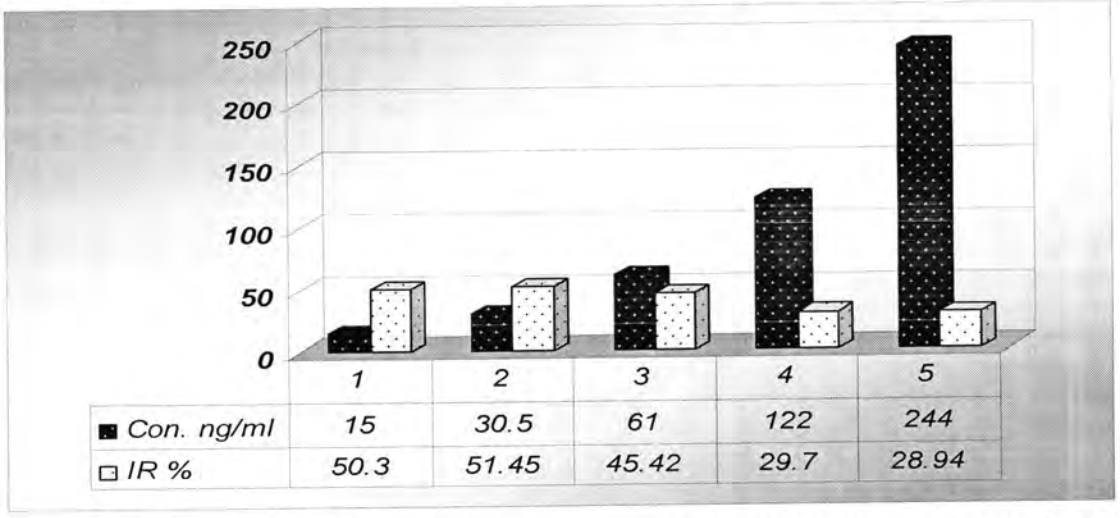

Fig. -3: Percentage of Cytotxicity represented by inhibition rate(IR) in Hep cell line treated with different concentrations of thymol

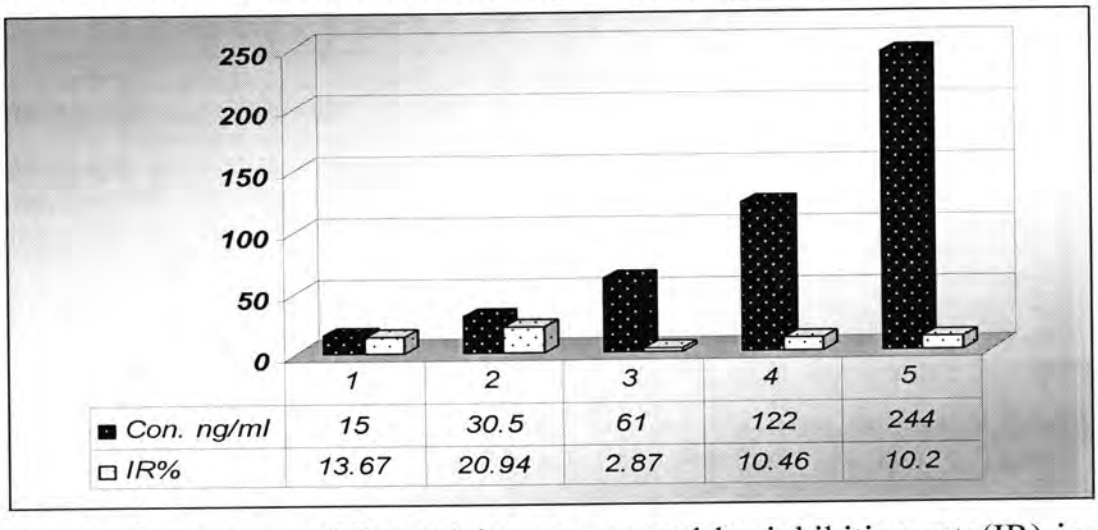

Fig. -4: Percentage of Cytotxicity represented by inhibition rate(IR) in Ref cell line treated with different concentrations of thymol.

2- Cytogenetic analysis of thymol on mitotic index:

The effect of thymol administrated (I.P) in three concentration(1.25,2.5,5)mg/kg B.W. in animal groups were studies by estimating the mitotic index in mice bone marrow cells.

In Table (1) shows significant differences ($P<0.05$) in MI of bone marrow cells between animal groups depended on doses of thymol in compression to negative control animals

Under normal experimental conditions, white mice had a mitotic index of (49.92) % in their bone marrow cells (table 1) this considered as a negative control.Table (1) was showed that low-dose of thymol don't caused a significant reduction ($p<0.05$) in MI (1.25 and 2.5) mg/kg B.W. (49.61% and48.86%) respectively , while high dose have shown significant reduction in MI (5.0) mg/kg B.W. (47.35%) in comparison with negative control These results were came in agreement with (28) that Thymol decreased the MI at the higher concentration without dose-dependent effect. The present work demonstrated the bad effect of this spice when used in large quantities, induced DNA damage (29) and inhibit cell proliferation (30) and this may be due to the poisonous effect of aromatic compound including phenolic compounds and terpene-phenolic derivatives which are poisonous .this conclusion is in consistence with those offered by (31).

Table -1: Cytogenetic effect of *thyme extract* in comparison with control (0.0) on mouse bone marrow cell.

Concentration of thyme extract mg/kg	Mitotic index (mean±Std. deviation)
0.0	49.92±0.096
1.25	49.61±0. 204
2.5	48.86±0.357
5.0	47.35±0.294

Significant different (P< 0.05) .Each value represents Mean± standard deviation

3- Immunomodulation examination:

The results in vivo procedure were showed; no effects of thyme extract were seen in stimulation of leukocytes compared with the control. These

results were came in agreement with (32) that no effects were seen in the thymus, spleen, lymph nodes, white cell counts, red cell counts, haemoglobin counts, or hematocrits following the dosing of rats with 1000 or 10000mg/kg of food grade thymol for 19 weeks administration.

It can be concluded that thymol have strong antitumar activity against HeLa cell line and decreased mitotic index at the higher concentration without dose-dependent effect; also the results showed no effect of thymol in stimulation of leukocytes compared with the negative control.

RERERENCES

1- Gottesman, M.and Pastan, I." Biochemistry of multidrug resistance mediated by the multidrug transporter", *Annu Rev Biochem*; 62: 385-427(1993).

2- Thuille, N.; Fille, M.and Nagl, M." Bactericidal activity of herbal extracts". *IntJ Hyg Environ Health*; 206: 217-221(*2003*).

3- Youdim, K.A.,and Deans, S.G." Dietary supplementation of thyme (*Thymus vulgaris* L.) essential oil during the lifetime of the rat: its effects on the antioxidant status in liver, kidney and heart tissues". *Mech Ageing Dev*; 109: 163-175(1999).

4- Tsai, P.J.; Tsai, T.H.and Yu CH, H.O." Evaluation of NO-suppressing activity of several Mediterranean culinary spices". *Food Chem Toxicol;* 45: 440-447(2007).

5- Youdim, K.A.and Deans, S.G." Effect of thyme oil and thymol dietary supplementation on the antioxidant status and fatty acid composition of the ageing rat brain". *Br J Nutr*; 83: 87-93(2000).

6- Vukovic-Gacic, B.and Simic, D." Identification of natural antimutagens with modulating effects on DNA repair". *Basic Life Sci*; 61: 269-277(1993).

7- Von Ardenne, M.and Reitnauer, P.G." The elevation of the leukocyte and thrombocyte counts produced by a thyme extract in the peripheral blood as compared to that caused by 2-cyanoethylurea". *Pharmazie*; 36: 703-705(1981).

8- Tsukamoto, Y.; Fukutani, S.; Takeuchi, S.; Okamoto, T. and Mori, M. "Some phenolic compounds stimulate the proliferation of human pulpal fibroblasts". *Shika Kiso Igakkai Zasshi*; 31: 357-362(1989).

9- Dursun, N.; Liman, N.; Ozyazgan, I.; Gunes, I. and Saraymen, R." Role of thymus oil in burn wound healing". *J Burn Care Rehabil*; 24:395-399(2003).

10- Lai, P.K.and Roy, J. "Antimicrobial and chemopreventive properties of herbs and spices". *Curr Med Chem*; 11: 1451-1460(2004).

11- Szentandrassy, N.; Szentesl, P.;Nanasi, P.P.and Cszernoch, L."Effect of thymol on kinetic properties of Ca and K currents in rat skeletal muscle". *BMC pharmacology;* 3:9:1-84(2003).

12- Sasaki, K.; Wad, K.;Yoshimura, T.and Matuoka, K."Thyme leaves and its constituents increase the activities of xenobiotic metabolizing enzymes in mouse liver". *Journal of medicinal food.* 8(2):184-189(2005).

13- Jukic, M.and Milos, M."Catalytic oxidation properties of thyme essential oils, *Thymus vulgaris .Croatica Chemica".ACTA*.78 (1)105-110(2005).

14- Esiyok, D.;Otles, S.and Akciek, E." Herbs as a food source in Turkey". *Asian Pacific J. Cancer Rev* 5:334-339(2004).

15- Pastan, I. and Gottesman, M." Multiple-drug resistance in human cancer".*N Engl J Med*; 16:1388-1393(1987).

16- Zyad, A.;Cai, Z.; Morizet, J.; Legres, L.G.; Bénard, J.and Chouaib, S." *In vivo* effect of the combination of TNF and adriamycin against a human breast cell line expressing the MDR-phenotype". *Inter J Oncology;* 7: 1067-1072(1995).

17- Peach, K.and tracy, m."Modren method of plant analysis".springer-verlage, berlin gottingen hide berg.vol.3, 412(1955).

18- Freshney, R.S."Culture of animal cells",(3rd ed.).A Manual of Basic Technique. Willy-liss, New Yourk, press.Pp:287-308(1994).

19- Chiang,L.C.;Chang,M.Y.and Lin,c.c."In vitro cytotoxic,Antiviral and Immunomodulatory effect". The American Journalof Chinese Medicine 31:252-234(2003).

20- Allen, J. W.; Shuler, C. F.; Memnders, R. W.and Olatt, S. A. "A simplified technique for in vivo analysis of sister chromatid exchange using 5-bromodeoxyuridine tablets". Cytogen. Cell Genet, 18: 231-237 (1976).

21- Kournikakis, B.and Ostroff, G."Pilot Study: Orally-Administered Yeast β1, 3-glucan Prophylactically protects Against Anthrax Infection and Cancer in Mice" .Journal of the American Nutraceutical Association. 5 (2): 1521-4524(2002).

22- us˘an, P.; Claire, B.; Andreasen, M.; Herolt, W.and Menzeld, A."Immunomodulatory effects of b-glucan on neutrophil function in fathead minnows (Pimephales promelas Rafinesque, 1820)". Developmental and Comparative Immunology. 30: 817–830(2006).

23- Al-Mohammed, N. T.; Al-Rawi K. M.; Younis M. A.and Al-Morani W. K."Principle of Statistics". J. Al-Mousl University (in Arabic) (1986).

24- Andrea, L.; Medina-Holgui, F.; Omar, H.;Sandra, m.; Sondra, g.and Simon, b. "Chemotypic variation of essential oils in the medicinal plant, *Anemopsis californica* " .Phytochemistry, 69: 919–927(2008).

25- Brek, L.; Ait Mouse, H.; Jaâfari, A.; Aboufatima, R.; Benharref, A.; Kamal, M.; Bénard. J.; El Abbadi, N.; Bensalah, M.; Gamouh, A.; Chait, A.; Dalal, A.and Zyad, A. "Cytotoxic effect of essential oil of thyme (Thymus broussonettii) on the IGR-OV1 tumor cells resistant to chemotherapy". *Braz. J. Med. Biol. Res.*, *40*, 1537–1544(2007).

26- Bard, M.; Albrecht, M.R.; Gupta, N.; Guynn, C.J.and Stillwell, W." Geraniol interferes with membrane functions in strains of *Candida* and *Saccharomyces.Lipids"*23: 534-38(1988).

27- Sikkema, J.;de Boont, J.A.and Poolman, B." Mechanisms of membrane toxicity of hydrocarbons". *Microbiol Rev*; 59: 201-222(1995).

28- Buyuleyla, M.and Rencuzogullari, E."The effects of thymol on sister chromatid exchange, chromosome aberration and micronucleus in human lymphocytes".Ecotoxicol.Environ.Saf. 72,943-947(2009).

29- Aydin, S.; Basaran, A.A.and Basaran, N. "odulating effects of thyme and its major ingredients on oxidative DNA damage in human lymphocytes"J Agric. Food Chem.53, 1299-1305(2005).

30- Stammati, A.; Bonsi, P.; Zucco, F. Moezelaar; R. Alakomi, H.L.and von Wright, A."Toxicity of selected plant vlatiles in microbial and mammalian short-term assays"Food Chem.Toxicol 37, 813-823(1999).

31- Imad, O.; Saleh, A.L.; Hasan, D.; Ibrahim, A. ; Amin, I.; Valery, M.D.and Lumi, R.O.H." A variety of volatile compounds as markers in Palestinian honey from Thymus capitatus, Thymelaea hirsuta and Tolpis virgata" Food Chemistry, 101: 1393-1397 (2007).

32- Hagan, E.C.; Hansen, W.H.; Fitzhugh, O.G.; Jenner, P.M.; Jones, W.I.; Taylor, J.M.; Long, E.L.; Nelson, A.A.and Brouwer J.B. "Food flavourings and compounds of relatedstructure. II. Subacute and Chronic Toxocity ". Fd. Cosmet. Toxicol. 5. 141-157(1967).

Evaluation of Immune Response in Patients with Chronic Hepatitis B Infection. I: Innate Immunity

[1]Muhammed A. Al-Dabagh, [2]Khalid W. Qasim and [2]Safaa I .Kader
[1]Medical Research Unit/College of Medicine/Al-Nahrain University
[2]Pathology Department/College of Medicine/Al-Nahrain University

Received: 03/04/2011 Accepted: 29/05/2011

الخلاصة

لا ينحصر دور الاستجابة المناعية المتأصلة فقط في حماية الجسم المضيف للفايروس خلال بدء فترة الحمج لكنها ايضا تحدد شكل الاستجابة المناعية المتكيفة. الهدف من هذه الدراسة هو تقييم الاستجابة المناعية المتأصلة في مرضى التهاب الكبد الفايروسي المزمن عن طريق تخمين المستويات المصلية لكل من العامل المحفز لمستعمرة الخلايا المحببة والخلايا الملتهمة الكبيرة وبين ابيضاض 1 ألفا، وبين ابيضاض 8 فضلا عن كل من المكونين الثالث والرابع من المتمم. جمعت عينات الدم الوريدي من 45 مريضا بحمج التهاب الكبد الفايروسي ب المزمن. عشرون عينة دم جمعت من اشخاص اصحاء كمجموعة سيطرة. استخدمت تقنية الاليزا لتخمين المستويات المصلية لكل من العامل المحفز لمستعمرة الخلايا المحببة والخلايا الملتهمة الكبيرة وبين ابيضاض 1 ألفا وبين ابيضاض 8 ، كما استخدمت تقنية الانتشار المناعي المنفرد لتخمين المستويات المصلية لكل من المكونين الثالث والرابع من المتمم. اظهرت النتائج انخفاضا معنويا في المستويات المصلية للعامل المحفز للخلايا المحببة والخلايا الملتهمة الكبيرة كما اظهرت انخفاضا غير معنويا في المستويات المصلية لكل من المكونين الثالث والرابع من المتمم. بينما أظهرت النتائج ارتفاعا غير معنوي في المستويات المصلية لكل من بين ابيضاض 1 ألفا وبين ابيضاض 8 بالمقارنة مع مجموعة السيطرة.

ABSTRACT

The innate immune system has role not only in protecting the host during the initial period of virus infections but also shaping the nature of adaptive immune response . The aim of this study was to evaluate the innate immune response in patients with chronic hepatitis B virus(CHBV) infection via estimation of serum levels of granulocyte macrophage colony stimulating factor (GM-CSF), interleukin-1alpha (IL-1α), interleukin-8 (IL-8) and

complement components C3 and C4. Venus blood samples were collected from 45 patients with CHBV infection. Other 20 blood samples were collected from healthy individuals as control group. Enzyme linked immune sorbent assay (ELISA) was used to estimate the serum levels GM-CSF, IL-1α and IL-8. Single radial immuno-diffusion (sRID) assay was used to estimate serum levels of C3 and C4. The results showed significant dropping in serum levels of GM-CSF and insignificant dropping in C3 and C4, respectively. While there was insignificant elevation in serum levels of IL-1α and IL-8, respectively in CHBV patients group as compared with healthy control group.

INTRODUCTION

Chronic infection with hepatitis B virus is a member of hepadnaviridae, a heterotropic non-cytopathic DNA virus is a major cause of liver disease worldwide [1,2]. More than 400 million people are persistently infected and at risk of developing chronic liver inflammation resulting in liver cirrhosis and hepatocellular carcinoma. 1 miliion death each year at directly attributable to be HBV – related liver disease [3-5]. Innate immune cell (mainly monocytes, neutrophils, and dendritic cells) and molecules play a central role in promptly controlling infections in the early phases and providing environment required for priming efficient adaptive immune response [6-11]. Both innate and adaptive arms of immune system are generally involved in responding to viral infection with innate responses being important for control of viral replication and dissemination very early after infection [12-14]. Due to the large number of immune cells present, the liver may be considered an immunological organ, with particular innate features, and therefore thought to be play an active role in the first line host defense against pathogens [15,16]. After sensing the presence of virus professional innate cells kupffer cells (KC), dendritic cells (DCs),natural killer (NK) and natural killer T cells (NKT) produce cytokines and chemokines that have antiviral properties (e.g., IFN-α, IFN-β, TNF-α, …) or that are meant to attract and stimulate adaptive immune cells (e.g., IL-2, IL-6, IL-10 …) [2,10,17].

In general, infected cells can detect the presence of viral components of PAMPs (pathogen-associated molecular patterns) via cellular sensor or PRRs (patterns recognition receptors), such as Toll-like receptors (TLRs), RIG-like helicases (RLHs), or Nod-like receptors (NLRs) [18,19], and produce antiviral type1 interferons (IFNs) ,IFNα and IFNβ as well as other pro-inflammatory cytokines (e.g., IL-1β, IL-6 ...) [20-23].

TLRs recognize microbes either at the cell surface or on lysosome/endosome membranes, while pathogens that invade the cytosol are detected by cytoplasmic PRRs such as RLHs or NLRs [18,19]. Various TLRs were expressed in parenchymal and non parenchymal cells of the liver [24]. Hepatocyte expressed mRNA for all TLRs [25,26]. Whereas KCs expressTLR4 and TLR2 [27,28]. In the case of lymphocytes T and NK cells express TLR 1,2,4,5 and 9, whereas B cells express high levels of TLR 1,6,7,9 and 10 [29].

Dendritic cells can be myeloid (mDC) or lymphoid (plasmacytoid, or pDC) origin, and represent an important component of innate immunity in the liver. Both recognize and present antigen to T cells but are distinct in their TLR expression and cytokine production profile [29-31]. Plasmacytoid DCs express TLR 7 and 9 and produce large amounts of IFN-α, whereas, mDCs express TLR 2, 3, 4 as well as 9 and produce pro-inflammatory cytokines and IFN-β but not IFN-α [29,32].

While virtually all liver cells types express RLRs [33]. The downstream effect of any IFN-α produce may be attenuated in antigen-activated cells [34,35] or modified by increase in other cytokines such as IL-1 [36] and IL-8 [37,38]. The level of IL-8 typically increase with the increase in HBV DNA, in keeping with reported ability of HBV to transactivate the IL-8 gene [39]. NK cells have been shown to express the high affinity IL-8 receptor CXCR1 and migrate in response to IL-8 [40].

MATERIALS AND METHODS

Forty five (15-65 years old, mean 39.5years, 25 males and 20 females) patients with CHBV infection in Kadhmiya teaching hospital, during period from October 2008 to march 2010 were used for this study. the cause of chronic liver disease was determined using standard diagnostic criteria.

chronic hepatitis B was diagnosed by positive serological tests for serum hepatitis B surface antigen (HBsAg) for at least 6 months. Twenty (18-55 years old, mean 33.4 years, 10 males and 10 females) healthy individuals were used as control group.

Five ml of venous blood were collected from each individual in plain tube. Serum were separated, put in eppendorf tubes and stored at (deep freezing -20°C).

Immunological assays:

Enzyme-linked immune-sorbent assay (ELISA), Immunotech, France) was used toe estimate serum levels of GM-CSF, IL-1α, and IL-8.

Single radial immunodiffusion (SRID) assay (Binding site, England) was used to estimate serum levels of C4 and C3 respectively(41).

STATISTICAL ANALYSIS

Statistical analysis has been performed using (SPSS, version 11.0) for windows. Continuous variables were expressed as mean ±standard error (SE). data were analysed using independent sample student`s *t* test. Significance was assigned for p values (<0.05) with 95% confident interval.

RESULTS AND DISCUSSION

GM-CSF: There was insignificant dropping of serum levels of GM-CSF in patients with chronic hepatitis B infection (13.00±2.74 pg/ml) as compared with healthy control group (35.5±2.57 pg/ml). Fig.-1

Interleukin-1 alpha: Serum levels of IL-1α showed insignificant elevation in CHBV patients (14.04±2.51 pg/ml) as compared with healthy control group (11.34±1.83 pg/ml).Fig.2

Interleukin-8: Serum levels of IL-8 showed insignificant elevation in CHB patients group (872.86±173.35 pg/ml) as compared with healthy control group (694.44±354.36 pg/ml). Fig.2

C3 complement: Serum levels of C3 showed insignificant droping in CHB patients group (1260.5±205.48 mg/dl) as compared with healthy control (1774.78±221.33 mg/dl). Fig.3

C4 complement: Serum levels of C4 showed insignificant dropping in CHB patients (19.91±5.1 mg/dl) as compared with healthy control group (30.91±3.63 mg/dl). Fig.4.

Macrophage activation represent one of the first events of innate resistance against intracellular infection. In response to pathogens, macrophages and other inflammatory cells. Secret cytokines IFNϒ, IL1,IL6,IL8 and TNFα. Some of these cytokines lead to activate against pathogens, activate effector cells involved in the cellular interaction that occur during inflammation and are part of acute and chronic stages of viral hepatitis [42,43].

The significant dropping of serum level of GM-CSF refer to suppression of its production by macrophages . GM-CSF paly an important role in activation , proliferation and differentiation of granulocytes monocytes and macrophages [44-49].

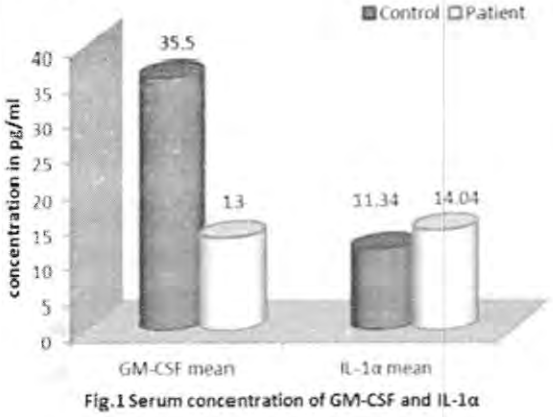

Fig.1 Serum concentration of GM-CSF and IL-1α

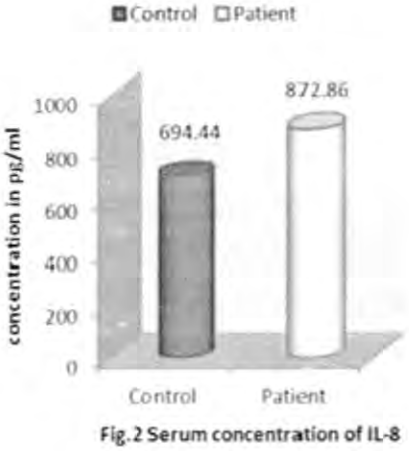

Fig.2 Serum concentration of IL-8

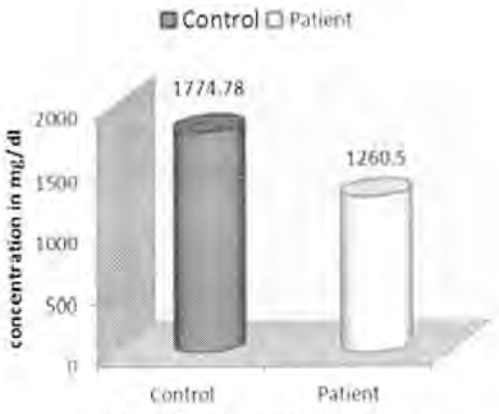

Fig.3 Serum concentration of C3

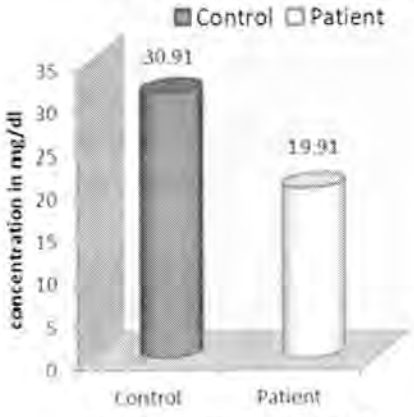

Fig.4 Serum concentration of C4

A number of laboratories have reported that IL4 inhibit the production of GM-CSF in a variety of cells including human monocytes [50-54] by down-regulation of mRNA precursor [55]. Th1/Th2 cytokines producing T cells were significantly lower in chronic HBV patients as compared to normal individuals [5]. The Th2 cytokines inhibit growth of extracellular parasites and suppress phagocytosis [56].

That's mean suppression of GM-CSF production which regulate phagocytosis function by phagocytic cells particular macrophage.

IL-1α is a main key of many of cellular responses , by regulation of GM-CSF production by macrophages [57,58].

The elevation of serum levels of IL-1α agree with Missate (59) which showed an increase of IL-1 in serum of CHB patients. HBV causes an inflammatory illness characterized by mononuclear and polymorphonuclear cellular infiltrate with evidence hepatic macrophage activation [60].

These inflammatory cells produce such cytokines as TNF-α, IFN-γ, IL-1α and IL-6, [60] which mediate the inflammatory process and which contribute to the successful clearance of virus [61].

IL-1 induce expression of IL2R, thus participating in the activation of resting T-cells [62].

So, the elevation of IL-1α in CHB patient may help in support of immune response.

Mahe [39] had showed that increase levels of IL8 associated with the increase in HBV DNA. The elevated levels of serum IL-8, IFN-α and NK cell tumor necrosis factor-related apoptosis-inducing ligand (TRAIL) to patients with HBV infection with active liver inflammation a apposed to HBV carriers or control [63]. CHB patients with liver inflammation were accompanied by increase in NK cell activation and surface TRAIL expression [3].

TRAIL pathway revealed that IL8 is capable of up-regulation a death-inducing receptor TRAIL.

The complement system plays an important role in immunological and inflammatory response. Complement deficiency may increase patients susceptibility to invasive infection. One of the causes of reduced production of complement components may be hepatic function disturbances in patients with chronic viral hepatitis [63].Our results agree with (Bussone and Mouthon)[64] and Sjoholm [65], which (revealed dropping in serum levels of C3 and C4 in patients with hepatitis B infection. Hepatic function disturbances in course of chronic viral hepatitis B and C may lead to deficiency of complement components (hypocomplementaemia) and further to the risk of invasive bacterial infection [63].

REFERENSES

1- Antonio B. and Adam J. G. The immune response during hepatitis B virus infection. *J. Gen. Virol*, 2006; 87: 1439-1449.

2- Ali K., Ali N., Seyed M. and Mohammad Y. *Hepatitis monthly*. 7(2):93-101.(2007).

3- Claire D., Maurizia B., Gary R., ."Cytokines induced during chronic hepatitis B virus infection promote a pathway for NK cell-mediated liver damage" *J.Exp. MED.*204(3):667-680.(2007).

4- Yanfang J., Wanyu L., Lei Y., " Enhancing the antihepatitis B virus immune response by adefovir dipivoxil and entecavir therapie" *Cellular & Molecular Immunology*.8:75-82.(2011).

5- Yanfang J, Zhenhua M., Guijie X., "Th1 and TH2 immune response in chronic hepatits B patients during a long–term treatment with adefovir dipivoxil". *Mediators of Inflammation.*. ID 143026, 10p.(2010).

6- Matzinger P."Tolerance, danger, and the extended family". *Annu Rev. Immunol.*12:991-1045.(1994).

7- Akira S., Uematsu S.,and Takeuchi O. "Pathogen recognition and innate immunity" *Cell.* 124:783-801.(2006).

8- Fritz J., Ferrero R. Philpott D. and Girardin S. Nod-like proteins in immunity, inflammation and disease]. *Nat.Immunol.* 7:1250-1257.(2006).

9- Petrilli V., Dostert C., Muruve D and Tschopp J."The inflammasome : a danger sensing complex triggering innate immunity" *Curr Opin. Immunol.* 19:615-622.(2007).

10- Antonio,B.and Carlo,F."kinetics of immune response during HBV and HCV infection".*Hepatology*.38(1):

11- Guidotti, L.G., Morris A., Mendez H., " Interferon-regulated pathways that control hepatitis B virus replication in transgenic mice". *J. Virol.* 76:2617-2621.(2002).

12- Biron C. and Sen G. "Innate responses to viral infections". In Fields Virology: 5th ed.; Kniepe, D.M., Howley, P.M, Eds.; Lippincott Williams & Wilkins: Philadelphia, PA, USA, 1:249-278.(2007).

13- Acaapezzato D., Francavilla V., Paroli M., " Hepatic expansion of a virus-specific regulatory CD8+ Tcell population in chronic C virus infection" *J.Clin.Invest.* 113:963-972.(2004).

14- WHO. Hepatitis B. Geneva:WHO, 2008.

15- Gao B., Jenog W. and Tian Z."Liver: an organ with predominant innate immunity" *Hepatology*. 47:729-736.(2008).

16- Racanelli V. and Rehermann B. "The liver as an immunological organ" *Hepatology*. 43:45-62.(2006)

17- Crispe I." The liver as a lymphoid organ". *Annu. Rev. Immunol.* 27:147-163.(2009).

18- Akira S., Uematsu S. and Takeuchi O. "Pathogen recognition and innate immunity". *Cell.*124: 783-801.(2006).

19- Kawai T.and Akira S."Innate immune recognition of viral infection" *Nat.Immunol.* 7: 131-137.(2006).

20- Randall R.and Goodbourn S."Interferons and viruses: an interplay between induction, signaling, antiviral responses and virus countermeasures" J.Gen.Virol.89:1-47.(2008).

21- Martinon F., Mayor A. and Tschopp J. "The inflammasomes: guardians of the body" *Annu.Rev.Immunol.* 27:229-265.(2009).

22- Samuel C." Antiviral actions of interferons" *Clin. Micrbiol.Rev.* 14:778-809.(2001).

23- Mucoca R., Philip J.,Li Q., "Induction of striking systemic cytokine cascade prior to peak viraemia in acute human immune-deficiency virus type1 infection, in contrast to more modest and delayed responses in acute hepatitis B and C virus infections" *J. Virol.* 10:1128-1132.(2009).

24- Zarember K.and Godowski P. "Tissue expression of human Toll-like receptors and differential regulation of Toll-like receptor mRNAs in leukocytes in response to microbes, their products, and cytokines" *J. Immunol.* 168:554-561.(2002).

25- Liu S., Gallo D.,Green A., "The role of Toll-like receptor in changes in gene expression and NF-kappa B activation in mouse hepatocytes stimulated with lipopolysaccharides" *Infect. Immun.* 70:3433-3442.(2002).

26- Nishimura M. Naito S."Tissue-specific mRNA expression profiles of human ATP-binding cassette and solute carrier transporter superfamilies". *Drug Metab. Pharmacokinet.* 20:452-477.(2005).

27- Ojaniemi M., Liljeros, M.,and Harju K."TLR-2 is upergulated and mobilized to the hepatocyte plasma membrane in the space of Disse And to the Kupffer cells TLR-4 dependently during acute endotoexmia in mice". *Immunol.Lett.* 102:158-168.(2006).

28- Paik Y., Schwabe R. Bataller R., "Toll-like receptor-4 mediates inflammatory 37:1043-1055.(2003).

29- Hornung V., Rothenfusser S. Britsch S, "Quantitative expression of toll-like receptor 1-10 mRNA in cellular subsets of human peripheral blood

mononuclear cells and sensitivity to CpG oligodeoxynucleotides" *J.immunol.* 168: 4531-45347.(2002).

30- Kazumasa H., Junichi E., Shigeake I., " Immune response of cytotoxic T lymphocytes and possibility of vaccine development for hepatitis C virus infection" J. *of Biomed. and Biotech.* 2010:1155-1165.(2010).

31- Albert M. Decalf J.and Pol. S." Plasmacytoid dendritic cells move down on the list of suspects: in search of the immune pathogensis of chronic hepatitis C". *J.Hepatol.* 49:1069-1078.(2008).

32- Vogel S., Fitzgerald K.and Fenton M. "TLRs: differential adapter utilization by toll-like receptors mediates TLR-specific patterns of gene expression" *Mol.Interv.* 3:466-477.(2003).

33- Malka A., Julie L., Fabien Z., "Innate antiviral immune responses to Hepatitis B virus.*Viruses.* 2:1394-1410.(2010).

34- Marrack P., Kappler J. and Mitchell. "Type I interferons keep activated T cells alive" *J.Exp.Med.* 189:521-530.(1999).

35- Dondi E., Rogge G., Lutfalla G., " Down-modulation of responses to type1 IFN upon T cell activation" *J.Immunol.* 170:749-756.(2003).

36- Tian Z., Shen X., Feng H,." IL- 1 beta attenuates IFN-alpha beta-induced antviral activity and STAT1 activation in the liver: involvement of proteasome-dependent pathway". J.Immunol. 165:3959-3965.(2000).

37- Khaber K., Al-Zoghibi F., Al-Ahdal M., "The α chemokine, interleukin8, inhibits the antiviral action of interferon α" *J. Exp .Med.* 186:1077-1085.(1997).

38- Polyak S., Khabar K., Rezeiq M.and Gretch D. "Elevated levels of interleukin-8 in serum are associated with hepatitis C virus infection and resistance to interferon therapy" *J. Virol.* 75:6209-66211(2001).

39- Mahe Y., Mukaida N., Kuno K., "Hepatitis B virus X protein trans-activates human interleukin-8 gene through acting on nuclear factor-kB and CCAAT/enhancer-binding protein-like cis-elemets" *J.Biol.Chem.* 266:13759-13763.(1991).

40- Campbell J., Qin S., Unutmaz D., "Unique subpopulations of CD56 + NK and NK-T peripheral blood lymphocytes identified by chemokine receptor expression repertoire" *J.Immunol.* 166:6477-6482.(2001).

41- Cruse,J.M. and Lewis, R.E.Atlas of immunology, CRC Press LLC,USA,P.107-413 (2000).

42- Chisari F.and Ferrari C." Hepatitis B virus immunopathogenesis" *Ann. Rev.Immunol.* 13:29-60.(1995).

43- Vento S., Ranieri S., Williams R., "A prospective study of cellular immunity to hepatitis B virus antigens from the early incubation phase of acute hepatitis B" *Lancet.* 2:119-122.(1987).

44- Cantrell M., Anderson D., Cerretti D., "Cloning sequence and expression of human granulocyte/macrophage colony stimulating factor. *Proc.Natl.Acad.Sci.* 82:6250.(1985).

45- Burdach S., "The granulocyte/macrophage-colony stimulating factor GM-CSF: basic science and clinical application" *Clin.Pediatr.* 203(4):'302-310.(1991).

46- Popisilova D., Borovikova J., Polouckova., "Generation of functional dendritic cells for treatment of acute lymphoblastic leukemia" *Cancer Immunol.* 51(2): 72-78.(2002).

47- Jasper M., Tremellen K., and Robertson S. " Primary unexplained infertilitty is associated with reduced expression of the T-regulatory cell transcription factor Foxp3 in endometrial tissue" *Mol.Hum.Repord.*(2006).

48- Peakman M., and Vergani D. "Basic and clinical immunology",Churchill Livingstone, New York, p.68.(1997).

49- Keshab C., Gautam B., Srabanti R., " IL-4 alone without the involvement of GM-CSF transforms human peripheral blood monocytes to a CD1a, CD83 myeloid dendritic cell subset" *J. of Cell Sci.* 117:3435-3445.(2004).

50- Sato N, Sawada K. Tarumi T., "Recombinant human interleukin-4 inhibits the production of granulocyte-macrophage colony stimulation factor by blood mononuclear cells. *Br.J.Haematol.* 86:695-701.(1994).

51- Dechanet J. Rissoan M., Banchereau J. and Miossee P." Interleukin-4, but not interleukin 10, regulates the production of inflammation mediators by rheumatoid synoviocytes" Cytokine. 7:176-183.(1995).

52- Akashi,K., Shibuya,T., Harada,M., "Itnerleukin 4 suppresses the spontaneous growth of meylomonocytic leukemia cells"*J. Clin. Invest.* 88:223-230.(1991).

53- Trindade,M.C., Nakashema,Y., Lind,M., "Inerleukin 4 inhibits granulocyte-macrophage colony stimulating factor, interleukin-6 and tumor necrosis factor-alpha expression by human monocytes in response to polymethylmethacrylate particle calling in vitro" *J.Orthop.Res.* 17:797-802.(1999).

54- Sawada,K., Sato,N. and Koike,T."Inhibition of GM-CSF production recombinant human iterleuki-4:negative regulator of hematopoiesis" *Leuk. Lymphoma.* 19:33-42.(1995).

55- Akahane,K.and Pluznik,D.H."Iterleukin-1 alpha induced granulocyte-macrophage colony stimulating factor gene expression in murine B lymphocyte cell line via downregulation of RNA precursor" *Blood.* 79:3188-3195.(1992).

56- Zidek,z.,Anzenbacher,P.and Kmonickova,E."Current status and challinges of cytokine pharmacology" *Br. J. Pharmacol.* 157(3):342-361.(2009).

57- Ridgway,D., Borzy,M.S. and Bagby,g.c/"Granulocyte-macrophage colony stimulating activity production by cultured human thymic non-lymphoid cells is regulated by endogenous interleukin-1"*Bood.* 72(4):1230-1236.(1988).

58- Bagby,G.C.and Jr,M.D."Inerleukin-1 and hematopoiesis" *Blood Reviews.*3(3):151-161.(1989).

59- Mieeale,G., Ferrari,C.,Fiaccadori,F."Cytokines mediators in acute inflammation and chronic course of viral hepatitis"*Ann.Ital.Med.Int.* 1:14-18.(1995).

60- Gilles,P.Fey,and Chisari,F.V."Tumor necrosis factor alpha negatively regulates hepatitis B virus gene expression in transgenic mice"*J.Virol.* 66:3955-3950.(1992).

61- Biron,C.A. "Cytokines in the generation of immune response to,and resolution of virus infection. *Curr.Opin.Immunol.* 6:530-538.(1994).

62- Bevers,R.F.,Kurth,K.H. and Schamhart,D.H.J."Role urothelial cells in BCG immunotherapy for superficial blader cancer" *British Journal of Cancer.* 91:607-612.(2004).

63- Maria,P.L., Barbara,k.m., Malgorzata,A., "Hypocomplementaemia in children with chronic viral hepatitis as a risk factor for invasive encapsulated bacterial infection" *Med. Wieku. Rozwoj.* 12(2pt2):6693-697.(2008).

64- Bussoni,G.and Mouthon,L. "Autoimmune manifestations in primary immune deficiencies" *Autoimmun. Rev.* 8(4):332-336.(2009).

65- Sjoholm,A.G.,Jonsson,G., Braconier,J.H., "Complement deficiency and disease: an update" Mol. Immunol. 43(1-2):78-85.(2006).

Absence of Menstruation(Amenorrhea)Due to Chromosomal Abnormalities

Wafaa Abdulzahra Kadhim
Department of Medical analysis-college of health and medical techniques

Received: 03/04/2011 Accepted: 29/05/2011

الخلاصة

تعتبر حالة انحباس الطمث للنساء البالغات عرض وليس مرض , يمكن ان ينتج عن عدة اسباب, ولقد اثبتت فحوصات الوراثة الخلوية ان حدوث تغيرات كروموسومية غير طبيعية من الاسباب المهمة المؤدية الى حدوث هذه الحالة لذلك فان هذه الدراسة هدفت الى اجراء اختبارات الوراثة الخلوية على حالات انحباس الطمث الاولي. ولقد تم الحصول على 55 حالة خلال فترة الدراسة وباستخدام تقنية (كمزا –تربسين –كمزا) تم تحديد التغيرات الكروموسومية غير الطبيعية والتي ادت الى ظهورحالة انحباس الطمث وكانت النتائج كالاتي:74.5%(41 حالة) كانت لا تعاني من اي تغيير في الكروموسومات وان 25.5%(14 حالة) اظهرت تغيرات عددية وتركيبية في الكروموسومات وهذه التغيرات يمكن ان تقسم الى ثلاثة اقسام :تغيرات عددية في الكروموسوم الجنسي X. في 57.14%(8 حالات) من الحالات التي اظهرت تغيرات كروموسومية .اما النوع الثاني من التغيرات التي لوحظت في هذه الدراسة هو وجود اناث تحمل الكروموسوم الذكري اي ان الهيئة الكروموسومية لهذه الاناث هي XY في 4 حالات اي 28.5% من جميع الحالات التي اظهرت تغيرات كروموسومية .والنوع الثالث والاخير من التغيرات تمثلت في تغيرات تركيبية للكروموسوم الجنسي X في حالتين فقط اي 14.2% من الحالات ذات التغيرات الوراثية الخلوية.

ABSTRACT

Absence of menstruation(amenorrhea) is not a disease but symptom that may results from several causes .Cytogenetic investigation have shown the importance of chromosomal abnormalities as a cause of amenorrhea. The present study aimed at performing chromosomal analysis in patients with primary amenorrhea .Cytogenetic investigations were carried out on 55 women with primary amenorrhea by using GTG-band analysis of metaphases from peripheral blood leukocytes .The karyotypes results revealed 74.5%

(n=41) with normal chromosome composition and 25.5% (n=14) showed chromosomal abnormalities .these abnormalities can be classified into three types ,the x chromosome abnormality (including monosomy x , pure x numerical abnormality ,and Turner mosaicism) was observed in 57.14%(n=8) of all chromosomal abnormalities , the other type of abnormal karyotype in this study is a karyotype showed pure xy female found in only 4 cases (28.5%),and the last type of abnormalities which represented in structural abnormalities of x chromosome in 2 cases (14.2%)one of theme showed marker chromosome and the other case showed deletion of x chromosome.

INTRODUCTION

Primary amenorrhea is defined as the absence of menstruation and sexual characteristics in phenotypic women aged 14 years or older or aged 16 years or older if secondary sexual characteristics are absent [1]. Patients with secondary amenorrhea have at least one spontaneous bleeding episode , followed by no menstruation for a minimum of 12 months at or before the age of 42 years old [2].The world health organization has estimated 15 % of the human population as being infertile and amenorrhea as the sixth largest major cause of female infertility among the general population, amenorrhea seemed to have affected 2-5 % of all women [3].Hormonal disorders are the main causes of primary and secondary amenorrhea, common hormonal causes of primary amenorrhea includes chronic systemic disease, hypothalamic-pituitary dysfunction and absent ovarian function [4].Secondary amenorrhea can be due to pregnancy, hypothalamic- pituitary disorders, polycystic ovarian disease, resistant ovarian syndrome, and absent or premature ovarian failure [2].Cytogenetic investigation have shown the importance of chromosomal aberration as an important cause of amenorrhea .different surveys have implicated chromosomal aberration in causing this symptoms in 16-50 % of causes [4] . also genetic or chromosomal causes are the most important as their presence affects subsequent management , for example , girls with XY gonadal dysgenesis have a high (30%) risk of gonadal malignancy and their testes should be removed as soon as possible [2].For this reason this study is undertaken to determine the frequency and types of chromosomal abnormalities that result in primary amenorrhea

MATERIAL AND METHODS

All cases were obtained from Baghdad Government and Private Hospitals. Data on family history ,clinical features ,and laboratory tests were recorded.

A total of 55 women who failed to menstruate before 18 years of age were studied between 2008-2010 , their age ranged between 18-36 years , about 1 ml of peripheral blood was collected from each patient in a heparinized container are used for cytogenetic analysis . About 6-7 drops of blood from each patient was inoculated in 8 ml of RPMI medium supplemented with 2 ml of human plasma, 0.3-0.5 ml of PHA (phytohemagglutinin) and incubated at 37 C° with frequent shaking every 24 hrs. After 71 hours of incubation colcemid (0.1 ml) was added with mild shaking and incubated for another (1) hour , the cells were then harvested by hypotonic treatment (20 minutes with 0.075 M kcl at 37 C°) , fixed and washed thrice with (Carnoys fixative) (methanol and glacial acetic acid in a ratio of 3: 1) and casted on wet, pre chilled ,grease –free slides .Multiple slides were casted for each sample , slides then stained with freshly made Giemsa stain (1 part Giemsa to 4 parts of Sorensen's buffer) for 2-3 minutes , slides then exposed to trypsin solution for banding process for 7-10 seconds at room temperature . Stained with Giemsa, air dried. For each sample, 10 metaphase were analyzed and karyotype was interpreted, whenever abnormal karyotype was obtained, a more number of metaphase (25) were analyzed.

RESULTS AND DISCUSSION

About 25.5% of the 55 cases with primary amenorrhea showed an abnormal karyoype .The type and frequency and aberrations involving the sex chromosomes are detailed in table (1). A large number of studies undertaken to ascertain in the frequency of sex chromosomal anomalies in patients presents with primary amenorrhea have shown a wide variants in the incidence of chromosomal anomalies [4,6,7,8,9,10,11,12,13].Previous estimates of the frequency of chromosomal abnormalities vary from 15.9% [7] to 63.3% [2]. The variation between the present and that of the previous studies may be due to the difference in the selection of patients include for analysis.

Table -1 : Constitution Karyotype of Patients with Primary Amenorrhea

Chromosomal abnormalities		Karyotype	No of cases
1	Normal karyotype	46,XX	41 (74.55%)
2	Numerical abnormalities		
a-	Monosomy X (pure turner)	45,X	4(7.27%)
b-	Pure X numerical abnormality	47,XXX	1(1.81%)
c-	Turner mosaicism	45,X/ 46,XX	3(5.45%)
d-	Pure XY female	46,XY	4(7.27%)
3	Structural abnormalities		
a-	Marker chromosomes	46,X,+m	
b-	Deletion of X chromosome	46,X,del(xq)	1(1.81%)

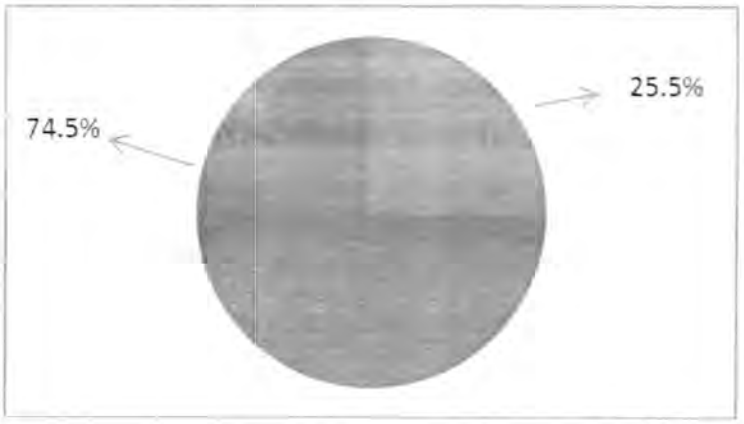

Fig. -1: The percentage of normal and abnormal karyotype in 55 patients with primary Amenorrhea.

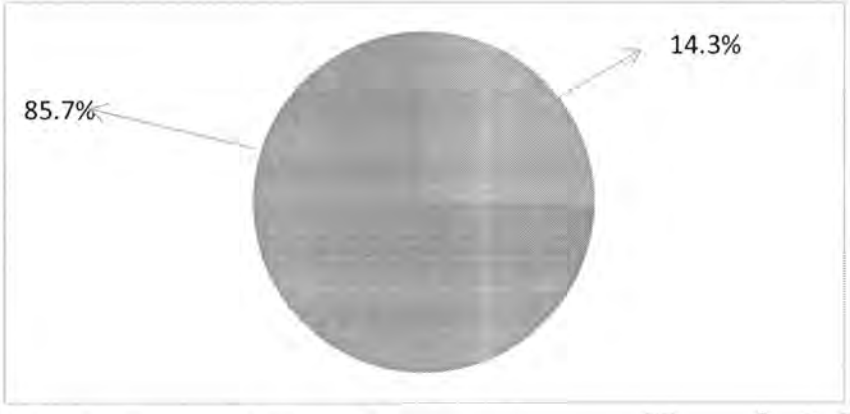

Fig. -2 : The percentage of numerical and structural abnormalities in patients with abnormal chromosomes constituents.

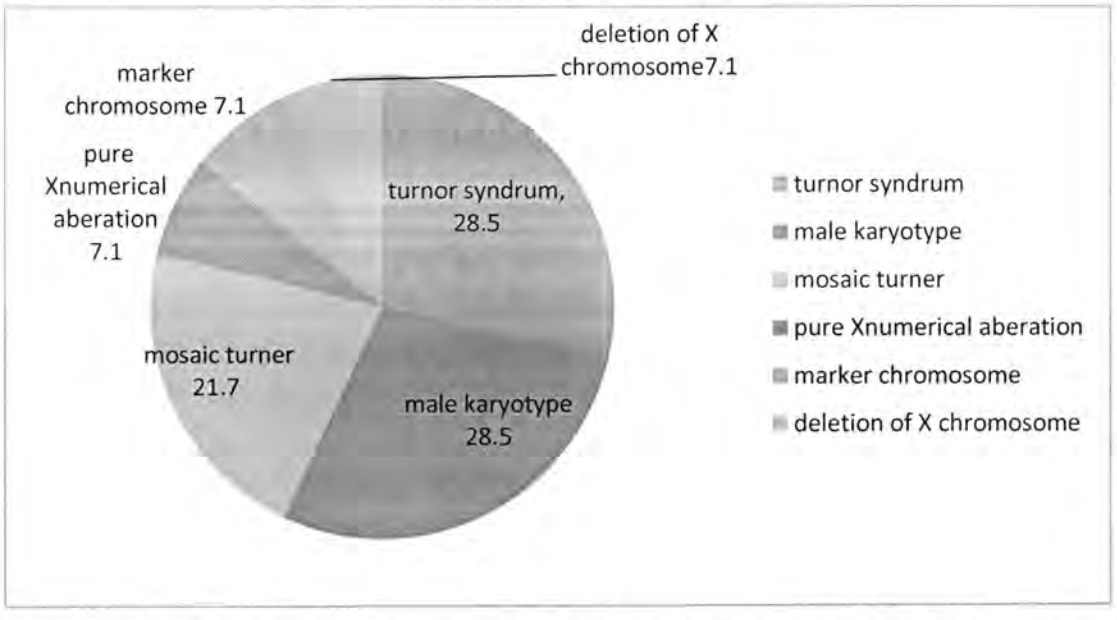

Fig. -3 : The distribution of numerical and structural aberration among the patients with chromosomal abnormalities

In patients with abnormal chromosome constituents ,85.7% (n=12) exhibit numerical aberration and 14.3%,(n=2) with structural aberration . Fig (2).

Fig (3) shows the distribution of numerical and structural aberration among the patients with abnormal chromosomal constituents. Among the different type of chromosomal abnormalities 28.5% (n=4) of them showed complete Monosomy of (X) chromosome (45, X). The Monosomy of X chromosome is the typical karyotype of Turner's syndrome [14]. The clinical spectrum of patients with abnormalities of the X chromosome is wide. In

general patients with Monosomy X showed typical Turner's stigmata while those with structural anomalies showed one or more Turner's-like features [15]. The differences in clinical manifestation are postulated that genes whose absences determine the somatic features of Turner's syndrome are distributed a long all of Xp and the middle of Xq [16].

The obtained results are in good correlation with that of previous studies as Turner's syndrome is reported to be the leading cause of primary amenorrhea, also the obtained results further strengthened the role of gene composition on the X chromosome in the normal female physiology and reproduction, for this reason this obtained results are in agreement with studies that conducted in the past. The second frequently occurring karyotype in this study is the mosaic Turner 45, X \46,XX (21.7%) (n=3).

Patients with 45,X \46,XX karyotype also manifest a wide phonotypical variability of them have shown a features of Turner's syndrome, variable gonad morphology ranging from a testis to a streak gonad [17]. Also it should be informed that women with sex chromosome anomalies, especially having X mosaicism, pregnancy cannot be ruled out [18]. Other X chromosome abnormalities in this study which pure X numerical abnormality, 47, XXX. This abnormality reported in only one case (1.81%). It has been suggested that girls with karyotype 47, XXX have a higher incidence of ovarian failure [19].Also the extra X can slow down emberyonic cell development in a special way [20].

Male karyotype 46, XY present in a significant percentage 28.5%, (n=4) of patient with abnormal karyotype.

The obtained results are in agreement with the previous studies which have reported 25% of cases with Y chromosome constitution [21].Studies have demonstrated that a female karyotype can occur in XY embryo when testes determining factor (TDF) or other genes in the testes determining pathway are lost, mutated, or compromised [22]. Generally the differential diagnosis of XY females can be classified into four types, based on clinical features, hormonal profile and histology of the gonads. The two commonest and best known are testicular feminizing syndrome (androgen insensitivity syndrome) and pure XY gonadal dysgenesis (Swyers syndrome) [23]. Pedigree studies have shown that testicular feminizing syndrome is inherited through a gene whose expression limited to the male sex [24].

The outstanding feature of this syndrome is feminizing of the patient, absence of fallopian tubes, uterus and cervix [23, 24]. On the other hand, pure XY gonadal dysgenesis is a genetically heterogeneous condition. It appears to be inherited either as a sex-linked or an autosomal- linked gene [24]. The presence of cervix or mullerian system, sexual infantilism and low-normal testosterone levels in these patients serve to differentiate XY gonadal dysgenesis from testicular feminizing syndrome [4]. The pathological significance of these two forms is that they at risk of developing malignant tumors of the gonads [14]. Early diagnosis of XY gonadal dysgenesis and testicular feminizing syndrome and removal of them as soon as possible before malignant growth develops [3].the different structural abnormalities of the X chromosome included deletion of the long arm 46,Xdel(Xq) reported in only one case (7.1%),and another case showed the presence of marker chromosome 46,X+m (7.1%).

The phenotype may be indirectly influenced as per the size and the loss \gain\ altered genetic function. In the deleted or duplicated segments in X. [25].

On the other hand a gene essential for gonadal function are located on the proximal part of XP, the long arm of X proximal to (Xq13)and\or the long arm of X distal to Xq 26 [20,26]. Large deletion of X q with break points at proximal to q13 are expected to produce gonadal dysgenesis with primary amenorrhea, half of the patients with such deletion have Turner's syndrome [27]. Also it has been reported that primary amenorrhea patients with 46, X+ mar karyotype may have usually severe phenotypes ,with mental retardation or abnormal facial features [28].

In conclusion this study confirms that chromosomal abnormalities are significant etiological factors in gonadal dysgenesis resulting in primary amenorrhea. The application of molecular cytogenetic and molecular techniques would aid in the delineation of the genetic etiology in cases of amenorrhea presenting with a normal karyotype.

REFERENCES

1- Kalavathi V., Chondra N. , Renjini G. , "chromosomal abnormalities in 979 cases of Amenorrhea" Int. j. Hum. Genetic ,.10 ,65-69,(2010).

2- Wong M., Lam S. , "cytogenetic analysis of patients with primary and secondary amenorrhea in Hong Kong : retrospective study; Hong Kong. Med j., . 11,267-272, (2005).

3- Rajangam S. , Nanjappal L. " cytogenetic studies in amenorrhea" . Saudi med. J.,.28(2),187-192,(2007.)
4- Ten SK chin YM, Noor PJ, Hassan K "cytogenetic studies in women with primary menorrhea" Singapore Med. J.,. 31,:355-359,(1990).
5- Birke beak NH, Cruger D,Hansen J, Nielsen J "Brun-petersen Turner syndrome". Genetic , 61,:.35-39,(2002).
6- Van Niekerk WA. "Chromosomes and groncologist" Am. J. Obstet Gynecol. , 130,:862-875, (1978).
7- Joseph A., Thomas IM., "cytogenetic investigation in 150 cases with complaints of sterility or primary amenorrhea" Hum. Gent. . 61, : 105-109, (1982).
8- Ko M.S "cytogenetic survey of primary amenorrhea". J. Hum. Genet. 27,:35-42,(1982).
9- Mulye V, Ambani L, Shringi M, Peter J ,Motashaw N. "Cytogenetic studies in primary amenorrhea" India J.Med.Res. 78,: 53-58. (1983).
10- Optiz O, ZollB, Hansmann I, Hinney B. "cytogenetic investigation of 103 patients with primary or secondary amenorrhea". Hum.Genet, 65,:46-47,(1983).
11- Chang SM, Lee TY, Lim SJ, Jean HH. "A chromosomal study of 864 cases of female genital abnormalities (Turner's syndrome)" J Formosan Med. Assoc., . 84, :1301-1312, (1985).
12- GHalib MA. Jyothy A, Isaac GS. Kusuma Kumari C, sujatha M, Redd, OS. "Abnormal karyotypes in female referred for sex chromosome abnormalities". In:PS Chauhan,pp Reddy (Eds). "nature of genetic variation in man", Bombay, EMSI.Bar C, : 151-156 (1988).
13- Park YS, Kang KC. "Cytogenetic study of primary amenorrhea" Korean J. Obtet Gynecol. . 42, :814-820,(1999).
14- J.Vijayalakshmi, T.Koshy , H.Kaur , F. Andrea Mary ,R.Selvi , V,Deepa , R.Bhavani , R.Vikram , P.Venkatchalam , solomon F.D. Paul "Cytogenetic analysis of patients with primary amenorrhea "Int J Hum Genet . 10(1-3) :71-76 .(2010).
15- Suri M.,Kabara M., Jain U., Sanders V.,Saxena R.,Shukla A.,Singh GV.,Verma IC. "Clinical and cytogenetic study of Turner's syndrome" Ind.pediatrics, 23 :433,(1995).

16- Wyss D.,Delozier CD, Daniell J., Engel E., "Structural anomalies of the X chromosomes :personal obserration and review of non mosaic cases". Clin.Gene.,21 :145-159 (1982).

17- Optiz O., Zoll B., Hansmann I., Hinney B., "Cytogenetic investigation of 103 patients with primary or secondary amenorrhea" Hum. Gene. .65 :46-47.(1982).

18- Spereff F., Glass RH., Kase NG., "Amenorrhea in :clinical gynecologic Endocrinology and infertility " 6^{th} ed. USA: Lippincott Williams and Wilkins :421-476 (1999).

19- Dew Hurst J. "Fertility in 47,XXX and 45,X patients" J. Med. Gene. . 15 :132-135.(1978).

20- De La Chapelle A., Schroder J., Haahtala T..,Aro P. "Deletion mappingof the human X chromosome" Heredita. .:113-120 (1975).

21- Anupam K., Surbhi M., Singh JR. "Cytogenetic analysis in cases with sex abnormalities" Int. J. Hum. Gene.. 4 :167-171 (2004).

22- Oster H., Wright G., Clyton M., Skordis N., Macgillivary MH. "Femel XX chromosomal translocation management of male psudohemophoditism: a case rport spanning twenty-one years" Paediat psycho,. 15 :699-709, (1989).

23- Madan K., Schoemaker J., "XY female with enzyme deficiencies of steroid metabolism , a brief view" Hum. Gent. ,. 53 :291- 295,(1980).

24- Sato GE "Cytogenetic of fifty patients with primary amenorrhea" J. Obstet. Gyne.col., . 119: 14-23 (1974).

25- Charles RK, Neil SR., "Pregnancy in patient with 47,XX, I (Xq) karyotype" J.Med. Genet. . 19 : 467- 468,(1980).

26- Ferguson- Smith MA. "Karyotype-phenotype in gonadal dysgenesis and their bearing or pathogenesis of malformation" Med. Genet. ,. 2: 142-156, (1965).

27- Fraccaro M., Maraschio. P., Pasquali F., Scappaticcis "Women heterozygous for deficiency of the (p21 pter) region of the X chromosome are fertile" Hum.Genet., . 39 :283-292, (1977).

28- Wolff DJ. Miller AP, Van Dyke DL, Schwarl12,5 Willard HF. "Molicular definition of break point with human Xq isochromosomes :Implications for mechanisims of formation" Am. J. Hum. Genet. , . 58, :154-160,(1996).

The Reproductive Cycle and Oocytes Development of Khishni Female *Liza abu (Heckel,1843)* from south of Iraq

Kadhim A. Muhsin
Biology Department/College of Science/Al-Mustansiriyah University

Received : 28/04/2011 Accepted : 29/05/2011

ABSTRACT

The reproductive cycle and development of oocyte diameter in 235 female, out of 2423 *Liza abu* (Heckel1843) collected from Majidia river, Northern Basra, were studied. The maturation phases of oocytes were determined and described according to the vitellogenic process. They were: Oogonia phase; Primary oocyte phase; Secondary oocyte phase; Ova phase and Atretic oocyte phase. The ovaries maturation stages were determined according to the oocytes phases and diameter development in addition to their morphological characters. They were found to be: - The resting stage (May-June), their diameters was 0.02 – 0.06 mm, with the dominance of primary oocytes , and presence of oogonia. In the Developing and Maturity stage (July- Nov.) eight new oocytes diameter groups appear in this stage reaching maximum diameter of 0.33mm. In the prespawning stage (Dec.-Jan.) four new oocytes diameter groups appear, reaching maximum oocyte diameter of (0.41mm.). The Spawning stage was in Feb. –to the end of March. The atretic oocytes appear in the spawning stage and increased in the post-spawning stage. Sex ratio was found to be 2.1female: to 1 male.

الخلاصة

درست دورة التكاثر ونمو اقطار البيوض في 235 انثى من اصل 2423 سمكةخشني *Liza abu* (Heckel1843) في نهرالماجدية شمال البصرة.وتم تحديد مراحل نضج البيوض ووصفها اعتمادا على عملية ترسب المح فيها . وهذه المراحل هي:-مرحلة سليفة البيوض Oogonia phase، مرحلة البيوض الاولية Primary oocyte phase، البيوض الثانوية Secondary oocyte phase، البيوض الناضجة Ova phase والبيوض المجهضة Atretic oocyte phase. اما مراحل نضج المبايض فقد تم تحديدها من خلال مراحل نضج البوض ونمو اقطارها وصفاتها الخارجية وكانت مرحلة الراحة The resting stage(0.02-0.06mm) والتي امتدت لشهرين، مايس وحزيران ،حيث كانت البيوض الاولية هي السائدة مع وجود سليفات البيوض.

اما بمرحلة النمو والنضج Developing and Maturity stage التي امتدت من تموز الى تشرين الثاني فقد ظهرت ثمانية مجاميع جديدة من اقطار البيوض حيث وصلت الى اقصى قطرلها (0.33mm) اما في مرحلة ما قبل التناسل the prespawning stage التي امتدت لشري كانون الاول وكانون الثاني فقد اضيفت اربعة مجاميع من اقطار البيوض حيث وصلت اعلى قطر لها (0.41mm) اما مرحلة التناسلThe Spawning stage فكانت في شباط والى نهاية اذار . اما البيوض المجهضة atretic oocytes فقد ظهرت في مرحلة التناسل وازدادت في مرحلة ما بعد التناسل the post-spawning stage . ومن خلال تشخيص الجنس في كافة الاسماك فقد وجد ان نسبة الجنس في الخشني هي 2 انثى : الى 1 ذكر

INTRODUCTION

Liza abu (Heckel 1843) an important species of the family Mugilidae, Order Perciformes, class: Osteichtheys, phylum Vertebrata, (1, 2). its distribution included Iraqi freshwater bodies especially the middle and south of Iraq and also in Euphrates in Syria (2). The total length reported of *liza abu* was 31 cm in Mhejran river south of Iraq Basra by Yusuf (3) it tolerate waters of 7.4-9.0 pH (4) and salinity of 5.8-7.34 ppt (5). The mean length of the first, second, third and fourth year of age are 136, 167, 185, and 202 mm respectively. The females grow faster than males (6; 7). The reproductive cycle is a crucial link in the life cycle of a fish and its connection with other links in the cycle insures the representation of an individual gene in the next generation. Environment has also serious effect on the reproductive cycle (8). *Liza abu* is one of the important commercial fish which represents 29% of the total catch of fish in the south of Iraq, (3).Gonad Somatic Indices GSI, eggs diameter and oocytes stages were used for the determination of the reproductive cycle of female *Liza abu.*

MATERIALS AND METHODS

A total of 2423 fish were collected using cast net from Al-Majidia River, one of the western branches of Shatt Al- Arab waterway at Harthe northern Basra, from May 1988- April1989. Total, standard length and total weight, of samples were taken. The weights of 235 ovaries were measured (using Mettler balance) during the whole period at mean of 18-20 ovaries each month. Each ovary was weighed and reserved separately in buffered

5% formalin in small plastic vales, for further analysis and histological sectioning. Gonad somatic index (GSI) was determined as:

100(ovary wet weight / total body wet weight gm.) (9; 10). Histological sections were used for each ovary. Cross sections were taken, from the middle of each ovary and the Mallory's triple stain was used for staining. The diameters of the oocytes in each section were measured, with micrometer eyepiece; using Olympus microscope (11).The micrometer eyepiece calibrated with 0.1 mm slide (100um) .Only oocytes with clear nucleus were measured. The diameter then was calibrated as follow:

Real oocyte diameter (mm.) = micrometer eyepiece reading * 4.1um/ 1000
The stage of maturation of each oocyte was determined also in each section of ovary. The percentage of each stage of maturation was calculated (primary oocytes, secondary oocytes, ova and atretic oocytes) in each section.

RESULTS AND DISCUSSION

Oocytes Stages of Maturation: stages of maturation of oocytes in the ovaries of *Liza abu* were described for the first time, depending on method used by Muhsin(11) . Fig (1) shows the monthly percentages of oocytes phase. These phases are:

1- Oogonia phase (Og): they are very small follicles in the germinal epithelium. They were grouped in small nests, which are distributed in the ovary. They can be recognized by one nucleus and only one nucleolus. Their color was dark orange with Mallory stain. Their diameter was up to 0.02 mm. they were found only in the resting stage.
2- Primary oocytes phase(P): they are bigger size than oogonia.they contain only one nucleus with many nucleolus's on the peripheral of the nucleus.the cytoplasm stain dark red, while the nucleus appear in orange color. The maximum diameter of primary oocytes was 0.14 mm. No yolk appears in their cytoplasm. They appear in all the year months, and are the most dominance in the resting stage.
3- Secondary oocytes phase(S): These are vitellogenic cells which range from 0.14 – 0.33mm. in diameter . Yolk vesicles appear first as a ring on the periphery of the oocyte, spreading inwards towards the nucleus plate (6). Then later on another type of yolk appear, yolk granules, in

orange red color. Yolk granules spread also from periphery toward the center, while yolk vesicles start to disappear,plates(7and 8). The vitellogenic deposion start at the Developing and Maturity stage during July, when oocytes reached 0.14mm.They appear in the ovary until the end of spawning season. They are the most dominant at the pre-spawning stage during December as it reach 75.05% of the total oocytes. The follicles become complete, enclosing the oocyte, and vitelline membrane, the oolema is lead down surrounding the oocyte.

4- Ova phase (O): these cells grow to a maximum diameter of 0.41mm. They are recognized by the brightly yellow-staining yolk deposits. The yolk granules are still separated. The maximum ova percentage was 63.34% of the total oocytes in the ovary, during the pre-spawning stage, before it start to decrease, due to releasing eggs until the end of the spawning season.

5- Atretic Oocytes phase (A): These oocytes are formed only from oocytes which have began vitellogenesis and laid down an oolemma. First the follicle hypertrophies, the nucleus of the oocyte becomes irregular, large number of follicular cells penetrate the broken- down oolemma appear to phagocytose the cytoplasm of the oocyte. The regular outline of the oocyte is lost, and it becomes compressed between neighboring oocytes. Atretic oocytes reached its maximum percentage at the post-spawning stage (12.4%) during April.

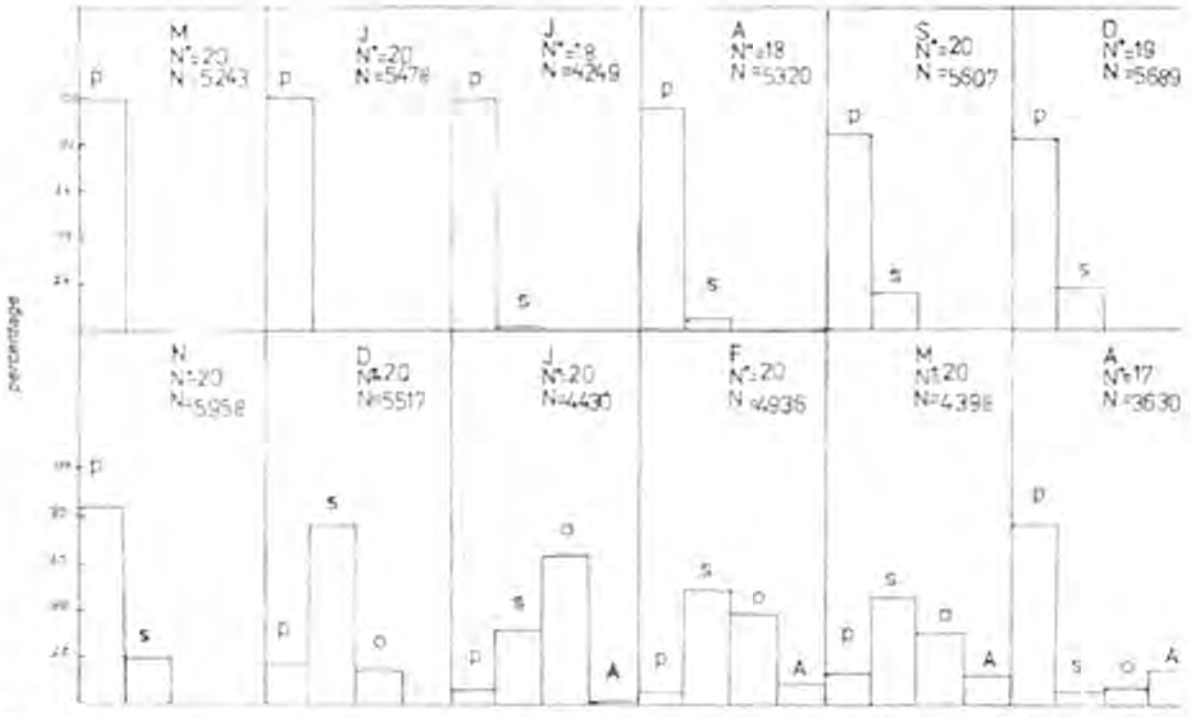

Fig.-1 : Percentage Composition of Oocyta maturational phases in the ovary of female

N* = number of sample ovaries

N = number of Oocytes counted for maturation phases.

Oocytes diameter development.

Figure (2) describes the frequency distribution of oocytes diameters for *Liza abu* during the reproductive cycle. In the resting stage: oocyte diameter range (0.02 – 0.08mm). This group of oocytes stays in the ovary even in the advance stages of maturation. in July there were a little increase in the oocytes diameters, and even some oocytes show yolk formation. New groups of bigger oocytes diameter continue to appear. In September 4 new groups of oocyte diameter were added, reaching 0,25 mm. In October 2 new oocytes diameter groups were added reaching maximum 0.29 mm. in diameter. In November a new 2 groups of oocytes diameter were added, reaching 0.33 mm. When ovaries enter the pre-spawning stage, Dec. and January, four new oocytes diameter groups were added, reaching maximum diameter of 0.41mm. The spawning season was from Feb. until the end of March. During the releasing of ova, the larger diameter groups of oocytes decreased in the ovaries, while the small size groups increased.

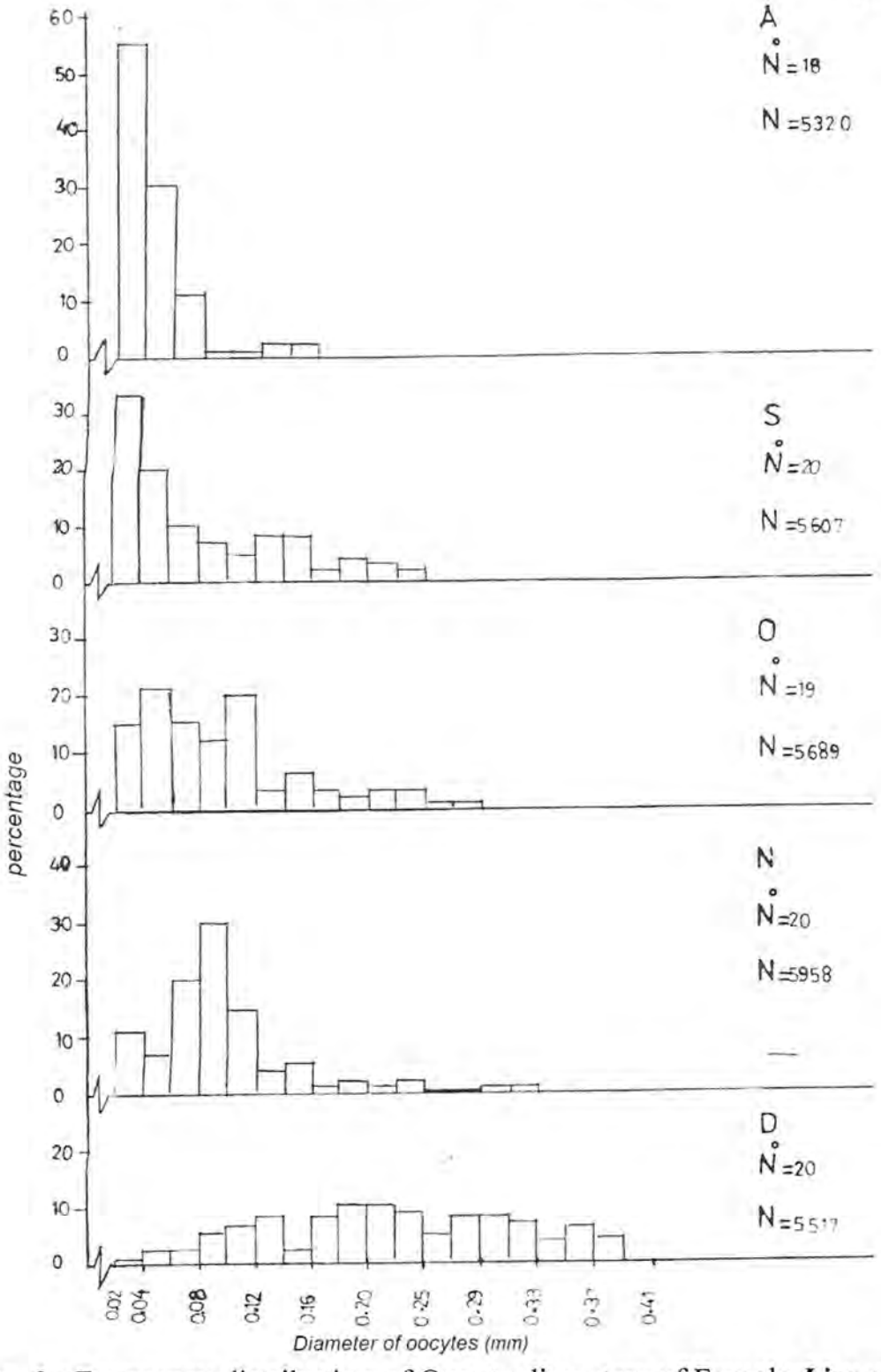

Fig.-2 : Frequency distribution of Oocyte diameters of Female ***Liza abu***

Fig. -2 Continued

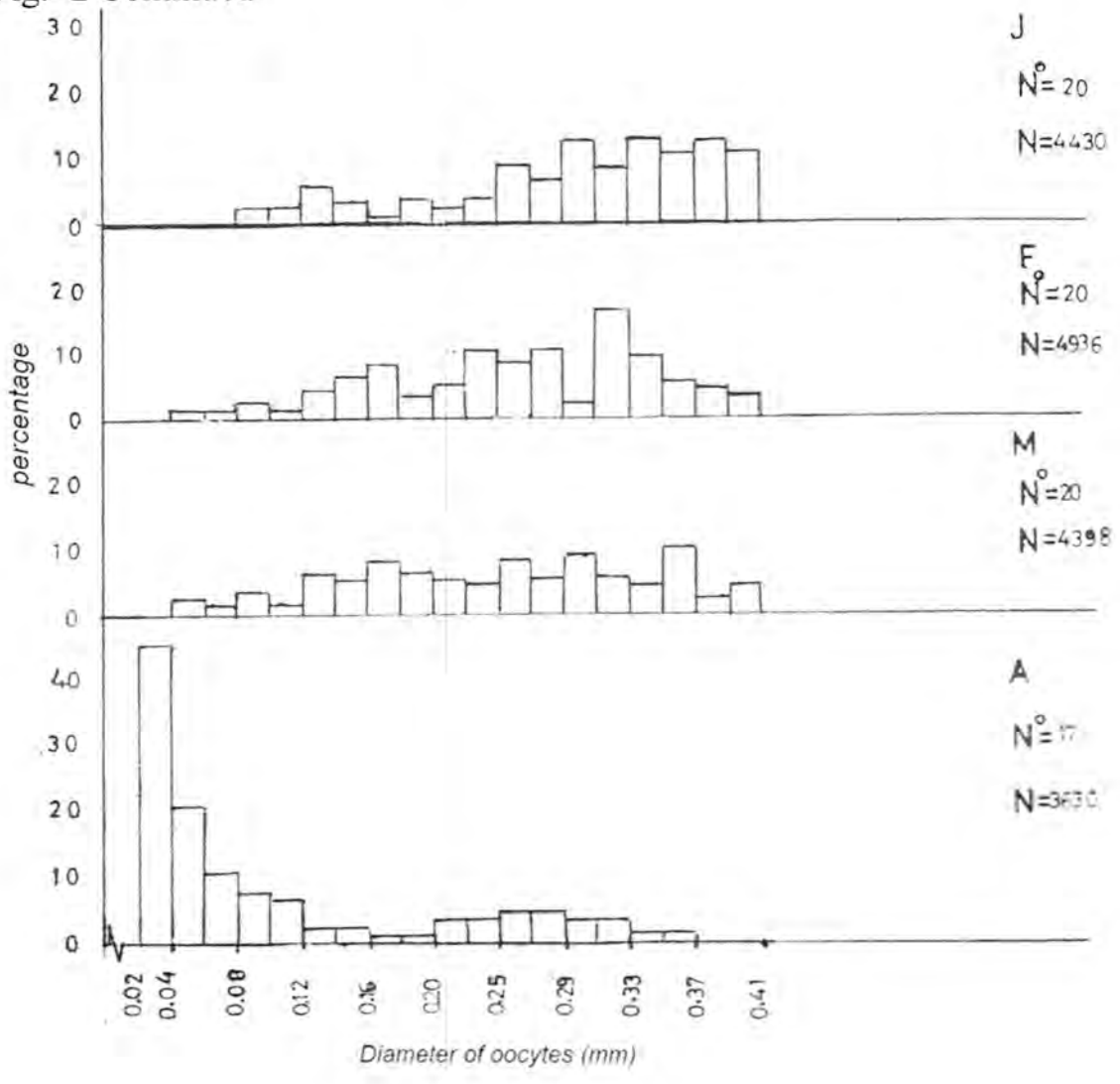

Fig. -2 Continued

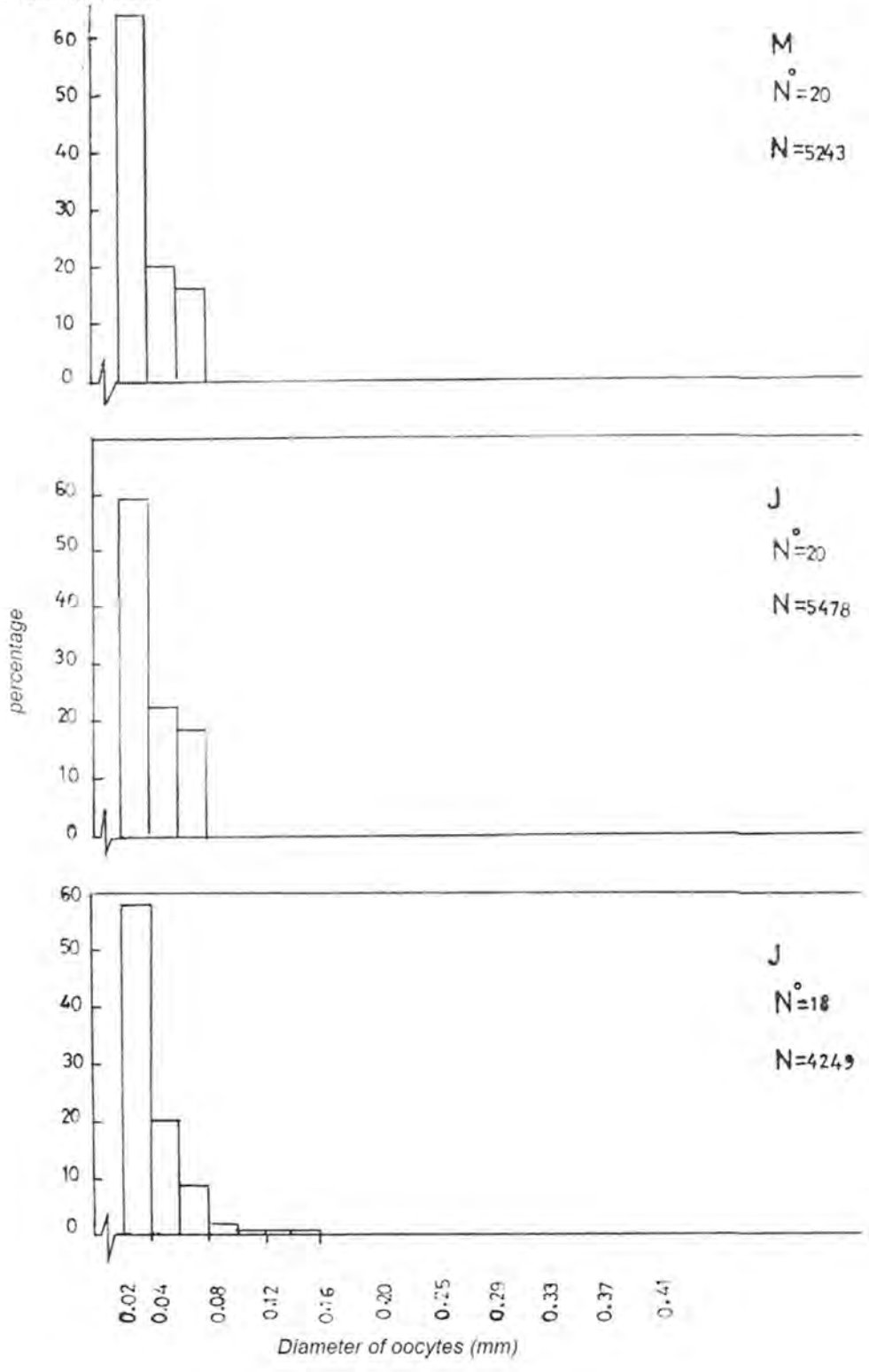

Sex ratio in *Liza abu* was found to be 2.1 female: to 1male. fig(3)shows the monthly samples percentages of females and males.

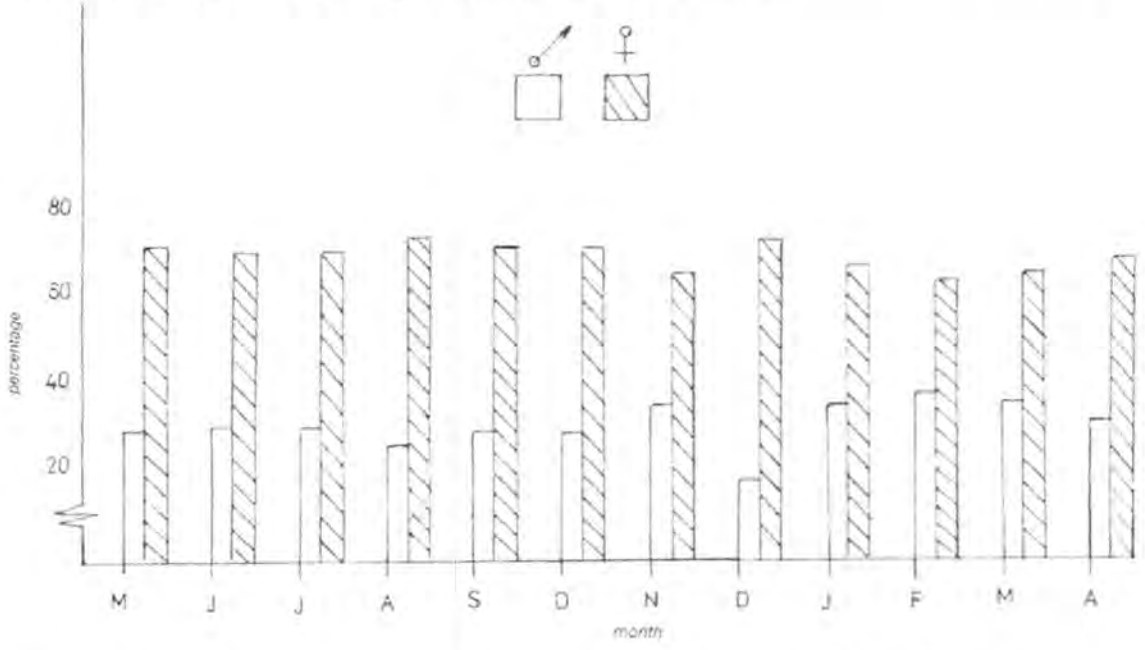

Fig.-3 : Monthly sex percentage of female and male of ***Liza abu***

Ovarian maturation: -The morphology and histology of the ovaries development cycle showed five stages and these are as follows:

1- The resting stage: the ovaries are small and filamentous in shape. Laying under the vertebrate column, and pink in color. The eggs are small. The mean GSI (0.65 – 0.68). The histological study showed the presence of oogonia, while the primary oocytes were the only oocytes in the ovary, plate (1). This stage lasted during May and June.

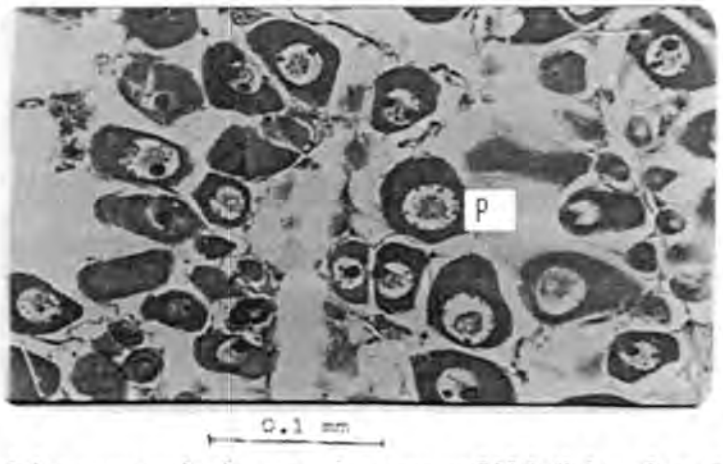

Plate -1: C.S. of the ovary during resting stage X20 (May-June) P=100%

2- The developing and maturity stage: the ovaries increased in size gradually at this stage. Their color was pink with yellow ting. The ovaries contained the primary and secondary oocytes. Plate (2). The secondary oocytes increased in numerically reaching 20% at the end of this stage. This stage started from july to the end of Nov. the mean GSI increased from 0.8 to 1.79.

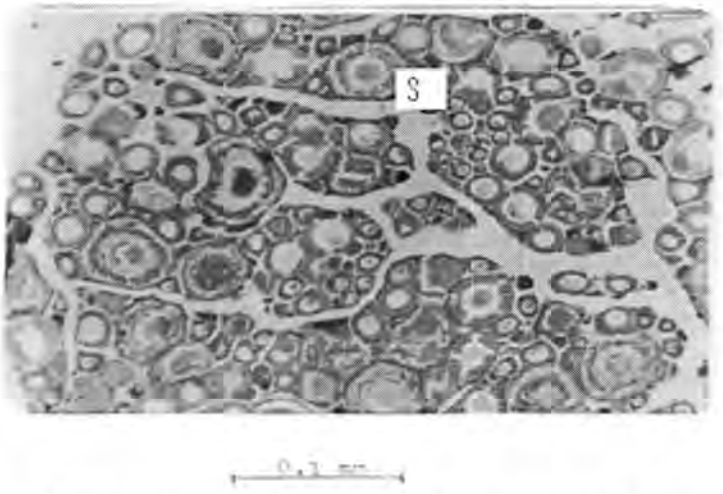

Plate -2: C.S. of ovary during developing and maturing stage. X20. (July-Nov.) P=80%, S=20%

3- The pre-spawning stage: the ovaries increased in size rapidly and occupied about two third of the body cavity. Their color was deep yellow. The surface of the ovaries appeared hyaline, plate (3). The secondary oocytes increased at the beginning of this stage reaching 75% of total egg number, while the primary oocytes decreased to 12.9%. the ova appeared for the first time reaching its higher percentage 63.3% by the end January. The mean GSI during this stage (Dec. and Jan.) was (5.83 – 10.99).

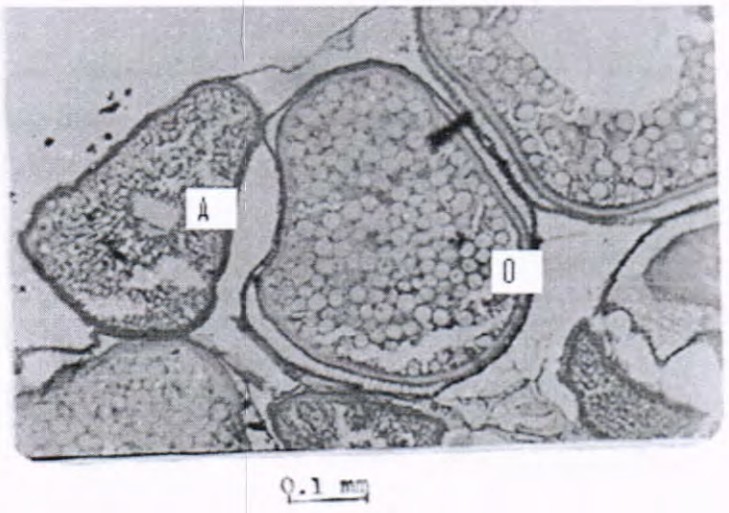

Plate -3: C. S. of the ovary during prespawning stage. X14. (Dec-Jan)
P=4.7%, S=30.8%, O=63.3%, A=1%

4- The spawning stage: the ovaries reached their highest size occupying most of the body cavity. They appeared light yellow in color. The eggs were easily released by soft massage at the abdomen. This stage continued during February and March. The ova decreased in number, while the atretic oocytes increased reaching 11.4% due to the release of eggs with the spawning activities during Feb. plate (4). The mean GSI was (9.82 – 5.11).

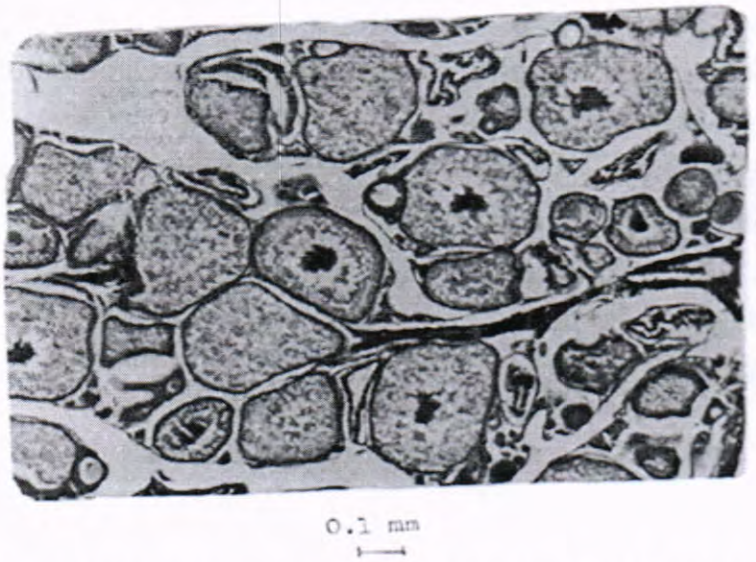

Plate -4: C. S. of the ovary during spawning stage. X6 (Feb-Mar)
P=4.4%, S=49%, O=37.4%, A=9%

5- The post-spawning stage: the ovaries were wrinkled. Irregular and red in color. It contained yellow eggs plate 5. The ovary has similar conditions to that of the spawning stage, with an increase in the

number of atretic oocytesreached 12.4 % of the total percentage, while the primary oocytes reached 77.2%.This stage continued during April. The mean GSI (1.6).

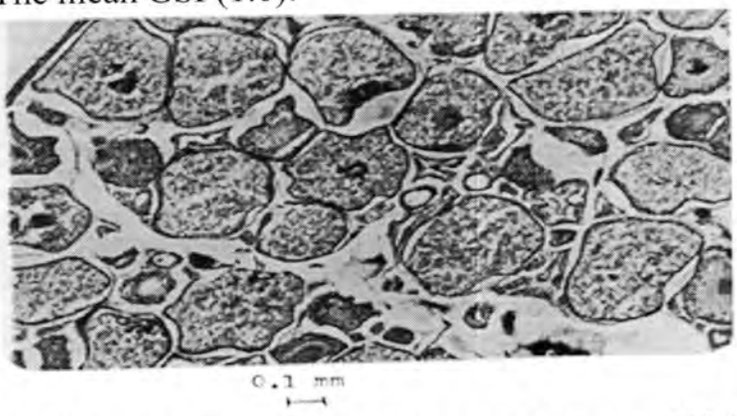

Plate-5: C. S. of the ovary during the post spawning stage X6 (Apl) P=77.2%, S=4.5%, O=6%, A=12.4%

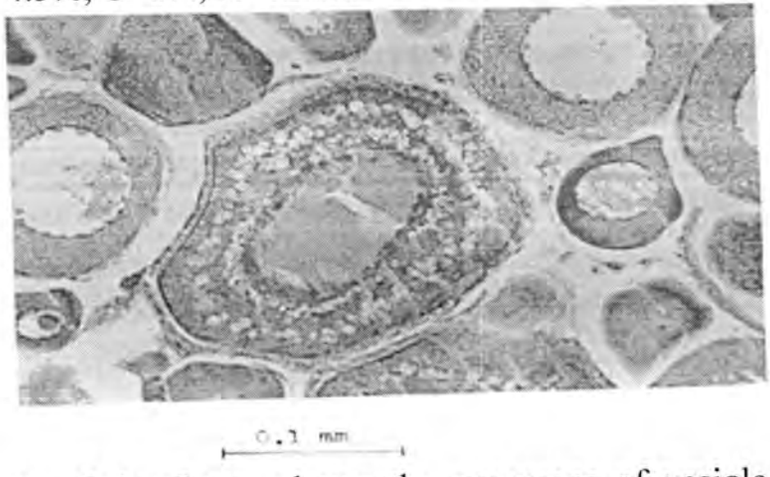

Plate -6: C. S. of the Ovary shows the appearans of vesicle yolk in the cytoplasm. X20

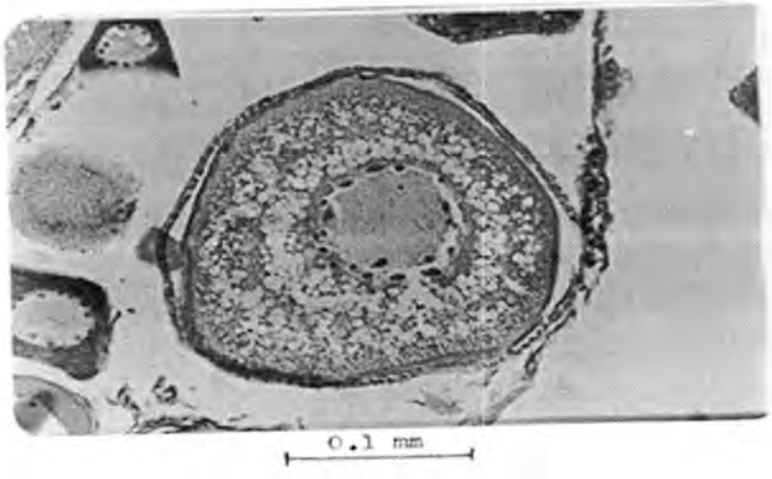

Plate -7: C. S. of the ovary shows the appearns of the yolk granules. X20

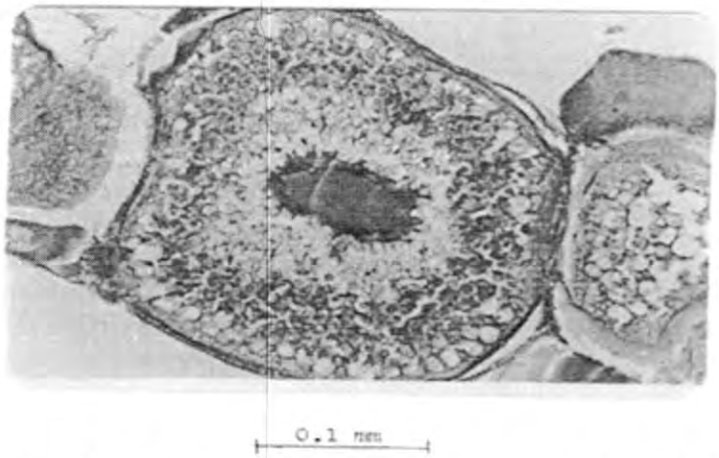

Plate -8: C. S. of the ovary shows the yolk granules distribution and the disappear of vesicles yolk. X20

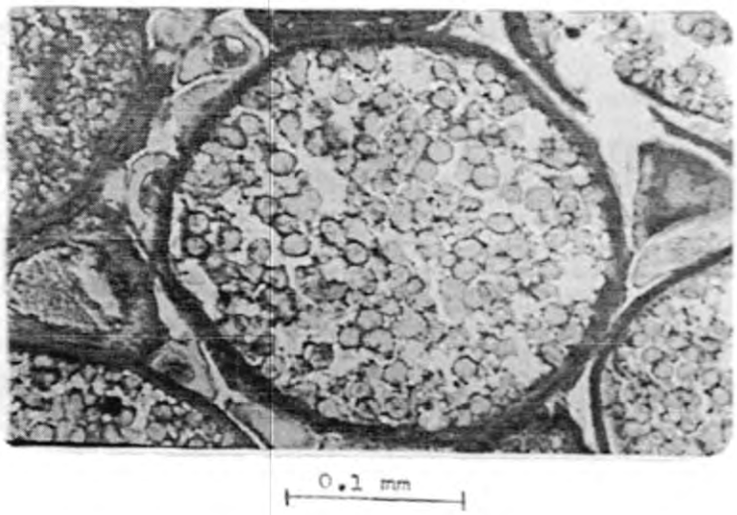

Plate -9: C. S. in the ovary with mature ova. X20

Gonad Somatic Indices (GSI) Slow growth was noticed in the ovaries in (Jul.-Nov.). Sharp increase in winter months (Dec. and Jan.). Spawning season was in (Feb.-Mar.).by the end of April GSI declined significantly to (1.6). Fig (4)

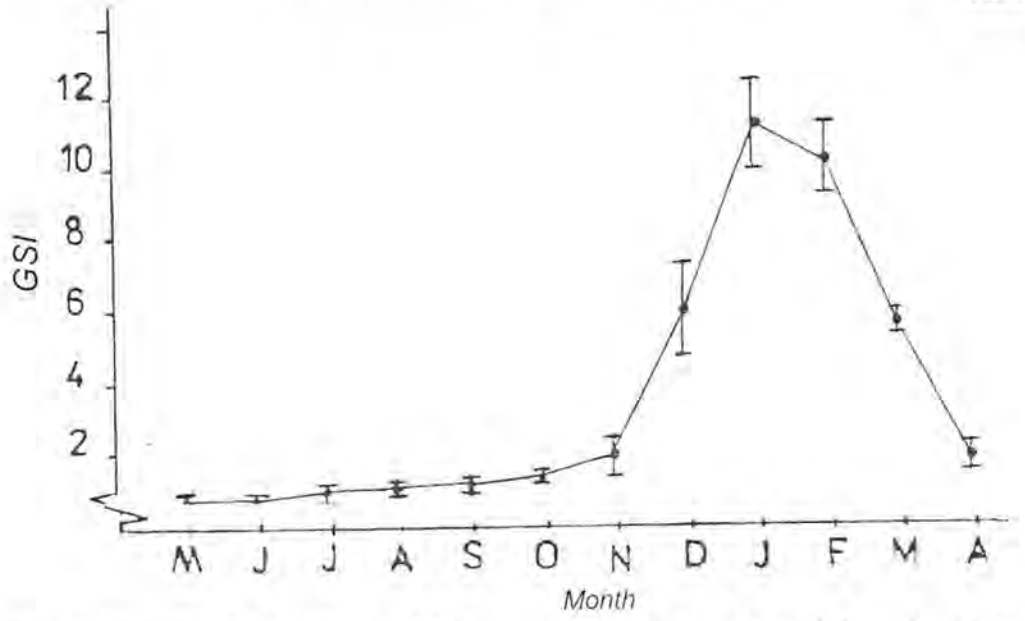

Fig. -4 : The mean GSI with 95% confidence intervals of female Liza abu during the annual cycle

In this study five maturation phases of oocytes were determined on the base of vitellogenic process. They were oogonia, primary oocytes, secondary oocyte, ovum and atretic oocyte. Reproductive cycle was divided into five stages, namely, resting stage; developing and maturity stage; pre-spawning stage; spawning stage and post-spawning stage. Others divided it into six stages (6); into seven stages (3; 4). The difference classification may be due to the criteria used for their classification. Some are using the ovaries morphological characters like ovaries color; size; or Gonad somatic index (GSI); eggs diameters, as indicators for their classification. In this study both morphological; histological and oocytes diameters of the ovaries were used in determining the ovaries stages. The vitellogenic process was use to recognize the oocytes phases in this study, which is much more precise method for such investigation. The synchronize of all these parameters (GSI;oocyte diameter; histological changes in the ovaries and oocytes vitellogenic stages) were used to define each stage in this study.

Liza abu was found to have single annual reproductive cycle each year. In the Resting stage only the primary oocytes and oogonia were presented. This was similar to the *Barbus luteus*(12), while is different with *Phoxinus phoxinus*(11), where secondary oocytes were also presented in the Resting stage. The accumulation of yolk in the oocytes is the reason behind the GSI increased in the Pre-spawning stage (13; 14; 15; 16 and 3). The presence of

atretic oocytes in the spawning and post-spawning stages was due to the failure of someova to be spawned , This was noticed in many other fishes , *Gadus merlangus; Gadus esmarkii nilsson*(17); *Cluea harengus*(18); *Limanda limanda*(19); *Phoxinus phoxinus*(11);*Tilapia nilotica*(20). Therefore a process of absorption to their yolk took place. Shortage of food intake resulted in reabsorption of yolk from eggs in the ovariesof some species, *Phoxinus phoxinus*(11); *Salmo gairdneri*(21); Gold fish (22).

Sex ratio in *liza abu*was found to be 2.1female: 1male. This was higher than others, 1.3 female: 1male (6); 1.1f:1m (3); 1.09f:1 m (4); 1.6 f: 1 m (23). It may be due to the sample size, as the size is bigger the result are more reliable. This study samples size was 1856 female while the largest size of others was 462 of Namma(6).

So, we can conclude :

1- It was found that November, Dec. and Jan. are the most critical months in the reproductive cycle of *Liza abu*. It characterize with sharp increase in GSI, oocytes diameters and yolk precipitation. This period may need much food supply to support the ovaries maturation.

2- The histological study shows that morphological characters alone are not an accurate way for studying ovaries maturation and histological sectioning is necessary to determine the oocytes phases of maturation as indicator of ovaries stage of maturation. The yolk vesicles and yolk granules precipitations in the oocytes are found to be good sign of indicting the phase of oocyte maturation.

3- The spawning season of *Liza abu* was found to be from Feb. until the end of March.

4- The effect of food supply on the reproductive cycle and ovarian maturation is needed to be investigated to find out how females response to the shortage of food supply in field on their reproductive cycle.

REFFERENCES

1- Khalaf, K. T. The marine and fresh water fishes of Iraq. Al-Rabitta press, Baghdad.164pp.(1961)

2- Beckman, W.. C. Thefresh water fishes of Syria and their general biology and managements. FAO fish. Boil.Technical Paper NO. 8, 297PP. (6).

3- Yousif, A. H. Ecologicaland Biological study of *Barbus luteus and Liza abu* from Mehejran river, South of Iraq, M. sc. Thesis Agriculture College, Basrah University 192 pp. (1983).

4- Wehab, N. Ecology and biology of three species of Mugilidea from Basrah canal.Iraq. M. Sc. Thesis agriculture Collage, Basrah University. 155pp (1986).

5- Mohamed, A. M. study of the physical and chemical characters of Saklawea drainage waters. M. Sc. Thesis Collageof Science, University of Baghdad. 128pp.(1978).

6- Naamah, A. K. Some biological aspects of two freshwater species Liza abuand Mugil dussmieri from Hor Al Hammar northof Basrah.Iraq. Thesis Collageof Science, University of Basrah.161pp.(1982).

7- Al-Nasiri,S. K.;Sarker,A. L. and Hoda, S.M.S. Feeding ecology of a mugilid fish, *Liza abu* (Heckel,1843) in Basrah Iraq. Bull.Basrah.nat. Hist. Mus. 4:27-40 (1977).

8- Maitra, S. K. Chattoraj, A. Role of photoperiod and melatonin in the regulation of ovarian functions in Indian carp *Catla catla*: basic information for future application Fish Physiol. Biochem.33:367–382. (2007).

9- Geraudie, Perrine; Gerbron, Marie ; Hill, Elisabeth and Minier, Christophe . Roach (Rutilus rutilus) reproductive cycle: a study of biochemical and histological parameters in a low contaminated site. Fish Physiol Biochem 36:767–777. (2010).

10- SImkova, Andrea; Jarkovsky´ Jiri; Koubkova, Bozena; Barus, Vlastimiand Prokes Miroslav. Associations between fish reproductive cycle and the dynamics of metazoan parasite infection. Parasitol. Res. 95: 65–72 (2005).

11- Muhsin,K.A.Some effects of food supply on the annual cycle of female *Phoxinus phoxinus*. Ph.D theses, University of Wales.U.K.(1982).

12- Al-Daham,N.K and Bhatti,M.N. Annual changes in the ovarian activity of the fresh water teleost *Barbus lutus(Heckel)* fromsouthern Iraq . J.Fish. Biol.14:381-387(1979).

13- Babikar,M.M. and Ibrahim,H. Studies on the biology of reproduction in the cichlid Tilapia *nilotica,gonadal* maturation and fecundity.J.Fish Biol. 14:434-448 (1979).

14- Shackely, S.E. and King,P.E.Thereproductive cycle and its control frequency of spawning and fecundity in *Blennius phosilis*. J.Exp. Mar.Biol. Ecol. 30: 73-83.(1977).

15- Treasure, J.W. and Holliday,F.G.T.Some reproductive biology of perch Perca fluviatilis.a histological description of reproductive cycle. J.Fish Biol. 18:359-376 (1981).

16- Guerrero,H.Y.;Cardilo,E.;Poleo,G. and Marcano,D. Reproductive biology of freshwater fishes from the Venezuelan floodplains. Fish Physiol Biochem 35:189–196 (2009).

17- Gokhale,S.V.Seasonal histological changes in the gonads of the whiting (*G.esmarkii*).Ind. J. fish. 4:92-112(1957).

18- Bowers, A.B. and Holliday,F.G.T. Histological changes in the gonad associated with the reproductive cycle of the Herrin *Clupea harengus*. Marine Res. 5 :1-16(1961).

19- Htun-Han,M.The reproductive biology of the dap *Limanda limanda* in the north sea: Seasonal changes in the ovary. J.fish Biol.13: 351-359(1978).

20- Hussein, Kh. A. Gonad maturation and fecundity of a fish with partial spawning (*Tilapia nilotica*). Arab Gulf J. Science Res. 2 (2): 683-699.(1984).

21- Scot D.P. Effect of food quantity on fecundity of rainbow trout *Salmo gairdneri*. J.Fish. Res. Bd. Can. 19:715-731 (1962).

22- Khoo, K. H.The histochemistry and endocrine control of vitellogenesis in gold fish ovaries. Can. J. Zoo. 57: 617-626. (1979).

23- Khalaf, A.N.; Al-Yamoure K.Y.; Allouse, S.B.; Al-Jafary, A. and Sadek, S.E. Age , growth, Length- weight distribution of Khishni *Liza abu(Heckel)* (Mugilidae) in a polluted habitat. JBSR, 17:63- 81.(1986).

Erythrocyte Glutathione Transferase Over-Activity and its Correlation with Plasma Homocysteine in Chronic Kidney Diseases

Kutayba F. Dawood
Department of Chemistry/College of Education for Pure Sciences/University of Anbar

Recieved : 29/03/2011 Accepted : 29/05/2011

الخلاصة

دراسة سابقه أفادت بزيادة فعاليه إنزيم كلوتاثايون ترانسفيريز كريات الدم الحمراء (eGST) للمصابين بمرض الكلى في مراحله المتأخرة المعتمدين بشكل مستمر على الغسل الكلوي (MHD)، والمستوى الفسيولوجي لهذا الإنزيم عند المصابين بأمراض الكلى المزمنة الذين هم تحت العلاج المحافظ (CKD). وحسب الدراسة السابقة تلك، فان ارتفاع مستوى الهوموسيستائين في الدم وجد عند أكثر من 90% من مرضى اليوريمي. في بحثنا هذا أردنا نحن إعادة تقييم مستويات هذا الإنزيم عند 72 مريضاً من مرضى الـ(CKD) مقسمين إلى أربع مراحل وفقاً لمبادئ التدريج لـ(K-DOQI)، 62 مريضاً من مرضى الـ(MHD) و 80 شخصاً سليماً لأجل المقارنة، وأردنا كذلك دراسة العلاقة بين تعبير هذا الإنزيم ومستوى هوموسيستائين البلازما لمرضى الغسل الكلوي. إن فعاليه هذا الإنزيم قيست باستخدام طريقه طيفيه آلية جديدة، هذه الطريقة الجديدة أكدت زيادة فعاليه هذا الإنزيم عند مرضى الغسل الكلوي بـ(10.2 ± 0.4 U/g Hb) مقارنةً بـ(5.8 ± 0.4 U/g Hb) للأشخاص السليمين. الزيادة الكبيرة المفاجئة في فعاليه الإنزيم لوحظت عند المرضى الذين هم في مرحله ما قبل الغسل الكلوي وحسب المراحل من الأولى إلى الرابعة وعلى التوالي (7.4 ± 0.5 U/g Hb، 8 ± 1 U/g Hb، 9.5 ± 0.6 U/g Hb، 12 ± 1 U/g Hb). إن العلاقة المباشرة بين الهوموسيستائين وفعالية إنزيم كلوتاثايون ترانسفيريز كريات الدم وجدت في مرضى الغسل الكلوي (MHD). إنزيم كلوتاثايون ترانسفيريز كريات الدم الحمراء يعتبر داله حيوية جديدة لكل من مرضى MHD و CKD.

ABSTRACT

Previous study reported increased expression of erythrocyte glutathione transferase (e-GST) in end-stage renal disease patients on maintenance hemodialysis (MHD), and physiological e-GST level in chronic kidney diseases

patients under conservative therapy (CKD). Hyperhomocysteinemia is present in more than 90% uremic patients. In present study we re-evaluated the e-GST levels in 72 CKD patients divided into four stages according to the Kidney Disease Outcomes Quality Initiative (K-DOQI) guidelines staging, 62 MHD patients and 80 healthy controls and studied the correlation between e-GST expression and plasma homocysteine (Hcy) levels in MHD patients. The e-GST activity was assayed using a new automated procedure. A new automated spectrophotometric procedure for e-GST activity, validated by intra-day, inter-day and recovery experiments, confirmed an increased e- GST activity in MHD patients (10.2 ± 0.4 U/g Hb) compared with controls (5.8 ± 0.4 U/g Hb). A surprising significant increase of e-GST activity was observed in predialysis patients related to K-DOQI stages (7.4 ± 0.5 U/g Hb, 8 ± 1 U/g Hb, 9.5 ± 0.6 U/g Hb, 12 ± 1 U/g Hb in stages from I to IV, respectively). A direct correlation between plasma Hcy and e-GST expression was found in MHD patients. e-GST proposes as new biomarker for MHD and CKD patients.

INTRODUCTION

Glutathione transferases (GSTs) represent a superfamily of enzymes devoted to the cell protection (1). A prominent function of these enzymes is the conjugation of glutathione (GSH) to a lot of toxic hydrophobic compounds provided of an electrophilic center (2). This reaction facilitates their inactivation and renal elimination (1). Conversely, red blood cells express almost exclusively a single GST isoenzyme (e-GST) which has been identified as GSTP1-1 (3) and represents more than 95% of the erythrocyte GST pool. Over-expression of e-GST has been found only in uremic patients under maintenance hemodialysis (MHD) (4) and in subjects affected by hyperbilirubinemia (5). e-GST expression has been proposed as possible marker to check the accumulation of uremic toxins and to probe the efficiency of dialytic procedures (4). In these previous studies e-GST levels has been checked only in a few chronic kidney disease (CKD) patients under conservative therapy and the expression of this enzyme appeared not different from the one found in the controls (4). The first aim of the present study is to develop a simple method for the determination of e-GST activity and re-evaluate the e-GST activity on a more representative number of

CKD patients divided according to K-DOQI staging (6). High-sensitive C-Reactive Protein (hs-CRP) (7), prognostic inflammatory nutritional index (PINI) (8), alpha-1 acid glycoprotein, fibrinogen, and beta-2 microglobulin (9) were also measured to check a possible correlation between e-GST over-activity versus systemic inflammation (10).

Hyperhomocysteinemia is commonly found in renal patients and attracted a lot of attention because its relation to renal dysfunction (11). In non-uremic subjects homocysteine (Hcy) metabolism is under genetic control. Increased total plasma Hcy is often caused by genetic defects of metabolic enzymes (12, 13) such as 5,10- methylenetetrahydrofolate reductase. In renal patients the total plasma Hcy is significantly increased regardless of genetic defects (12). In fact, hyperhomocysteinemia is common in uremic MHD patients (14) with > 90% of dialysis patients having increased plasma Hcy. Elevated plasma Hcy may promote endothelial dysfunction, which is probably the consequence of the oxidative inactivation of endothelium-derived nitric oxide (NO) (12). Hcy may also cause oxidative stress by inhibiting the expression or the activity of cellular antioxidant enzymes such as glutathione peroxidase-1 (GPx-1) (15). Thus a second target of this study is to verify a possible relation between the increase of plasma Hcy level and eGST activity in uremic MHD patients. The direct correlation found here discloses an interesting scenario where eGST may act as a new marker complementary or substitutive of Hcy assay for oxidative stress in MHD patients.

MATERIALS AND METHODS

Patients and Study Design

All experiments in the present study were conducted at the University of Rome "Tor Vergata", Italy. Blood samples were obtained from 72 CKD patients under conservative therapy (33 men, 39 women, mean age 54.5 years, range 24-80 years), 62 MHD patients (29 men, and 33 women, mean age 58.0 years, range 36-81 years) were on maintenance renal replacement therapy since six months at least, and 80 healthy controls (35 men, and 45 women, mean age 46.1 years, range 23-75 years) with normal renal function. K-DOQI CKD staging system was used to group pre-dialysis patients according to their estimated glomerular filtration rate (GFR). Exclusion criteria for both patients and control

subjects were a clinical history virus hepatitis B and C or serum AST and/or ALT ≥ twice the upper limit of normal values, morbid obesity, rheumatologic disorders as systemic lupus erythematosus and active malignancy. All 62 MHD patients were treated with either standard bicarbonate dialysis with 1.5 to 2.0 square-meter hollow fiber low flux polysulphone membranes (or 'on line' hemofiltration with 1.5 to 2.0 square-meter hollow fiber high flux polysulphone (B. Braun GMBH, Melsungen, Germany)) four hours, three times weekly through a well functioning native A-V fistula or a cuffed internal jugular indwelling venous catheter. The vascular access performance was satisfactory with a blood flow of at least 300 ml/min and Kt/V ratio > 1.2. Underlying disease was nephroangiosclerosis in 20 patients, chronic primary glomerulonephritis in 23 patients, chronic interstitial nephritis in 10 patients, polycystic kidney disease in 6 patients and diabetes mellitus in 3 patients.

Analytical Procedures

All the reagents in the present study were from Sigma-Aldrich (St. Louis, USA) and used without further purification. Blood samples were collected from the antecubital vein in healthy subjects and in CKD patients under conservative therapy, from the arterial site of the vascular access before dialysis in MHD patients at the end of the long interval for Hcy determinations. Blood samples were collected into K3EDTA vacutainer tubes as well, put on ice and immediately centrifuged and stored at -20°C until analysis. For e-GST activity determinations, blood drawn was collected on EDTA and stored until used at 4°C for no more than four days. One volume (20 µl) of whole blood was diluted in 20 volumes (0.5 ml) of bi-distilled water and after five minutes introduced into the Modular P800 (Roche, Switzerland) automated apparatus for GST activity determination. GST activity was assayed spectrophotometrically at 340 nm (37°C) using 20 µl of hemolyzed sample in 0.2 ml final volume containing 1 mM GSH, 1 mM 1-chloro-2,4-dinitrobenzene (CDNB) in 0.1 M potassium phosphate buffer, pH 6.5. Time run was one minute. The automated analyzer uses an optical path length of 0.5 cm and it can perform up to 800 tests per hour. Hemoglobin was determined with an automated haematology analyzer XE-2100 (Dasit, Milano, Italy). Results were expressed as enzyme units (U) per

gram of Hb. One unit represents the amount of enzyme that catalyzes the conjugation of 1 micromole of GSH to CDNB in one min at 37°C. Recombinant human GSTP1-1 expressed in *E. coli* and purified as described previously (16) was used as internal standard. All routine laboratory measurements were performed by nephelometric methods (BN IITM BNHTM nephelometer, Siemens Healthcare Diagnostics, Milano, Italy), except for fibrinogen that was quantified by phototurbimetric method (Ca 7000 Sysmex, Japan). Plasma total Hcy was assayed by a fully automated HPLC method using reversed-phase separation and fluorescence detection as reported previously (17). Cystatine C and creatinine were determined as described previously (18). prognostic inflammatory nutritional index (PINI), alpha-1 acid glycoprotein and beta-2 microglobulin were determined as described previously (8, 9).

RESULTS AND DISCUSSION

Simplified Procedure for e-GST Activity Determination

Previous studies finalized to quantify e-GST activity needed time consuming erythrocyte isolation and conspicuous blood volumes (3, 4). Our simplified procedure, adapted to an automated apparatus (Modular P800), requires only 20 µl of whole blood and no erythrocyte purification step. Actually, the amount of extra-erythrocyte GST is always negligible and no relevant spectrophotometric artifacts occur in the presence of broken erythrocytes. Furthermore GSTP1-1 represents more than 95% of all GST isoenzymes found in the red blood cells. This enzyme homogeneity makes the activity value directly related to the level of expression of GSTP1-1. Linearity and recovery experiments performed on the automated apparatus using blood samples implemented by authentic GSTP1-1 are shown in fig. 1a and b. Intra-day precision and inter-day precision were evaluated using four whole blood samples. e-GST activity was measured six times for each sample and the relative SEM was 2.9% and 3.5% for intra-day and inter-day assay, respectively. A surprising property of e-GST is represented by its strong stability in whole blood samples stored at 4°C without dilution. The loss of enzyme activity does not exceed 7% even after twelve days at 4°C (fig. 1c). Conversely, a relevant GST inactivation occurs during blood storage at -20°C or at 4°C after hemolysis. Thus, the stability of the GST activity is likely linked to erythrocyte integrity

while it is lost when GST is under dilute conditions. This behavior is consistent with the observation that GSTP1-1 under dilution, undergoes a remarkable biphasic inactivation process due to a solvatation of the active site (19).

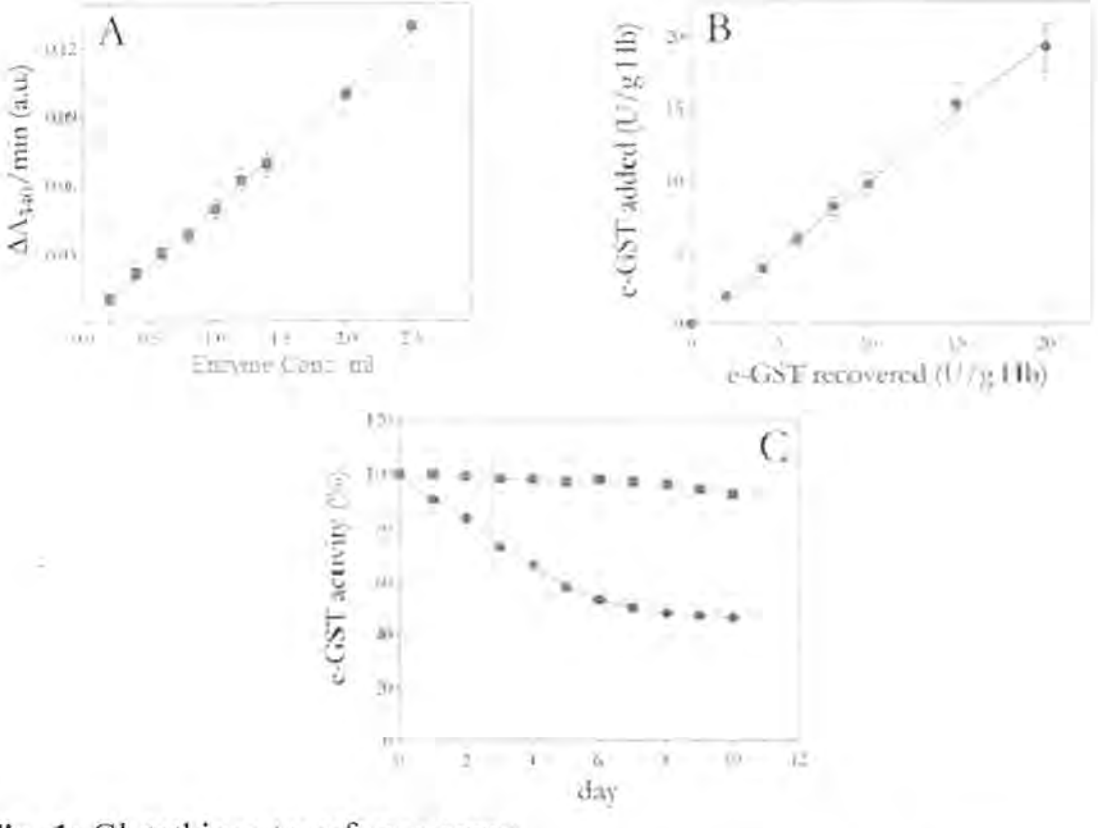

Fig.-1: Glutathione transferase assay.

(a) Linearity of the automated assay procedure. Recombinant human GSTP1-1 activity was measured on the automated Modular P800 apparatus set at 340 nm (37°C).

(b) Recovery experiments of GSTP1-1 have been performed using the standard assay procedure on the automated Modular apparatus using whole blood samples implemented by variable amounts of recombinant GSTP1-1. The unit values of the endogenous GSTP1-1 have been subtracted in each sample.

(c) Stability of e-GST in blood samples. Squares (4°C), circles (-20°C).

Evaluation of e-GST Activity in Renal Failure Patients

The aforementioned procedure was successfully employed to evaluate e-GST activity in CKD patients under conservative therapy, in MHD patients and in healthy subjects. Mean clinical features and laboratory findings of healthy subjects, MHD patients and CKD patients under conservative therapy are summarized in table 1. e- GST is highly enhanced in MHD patients, according to previous studies (5, 6). However, in disagreement to a previous report (5), we observed an increase of e-GST activity also in pre-dialysis patients, and this seems to be related to CKD stage (table 1 and fig. 2).

Table 1. Main clinical features and laboratory findings in 72 pre-dialysis patients divided into four subgroups according to K-DOQI stage (stage I to IV) CKD, 62 ESRD patients on MHD and 80 healthy subjects (control group).

	Control Group	**Stage I (CKD)**	**Stage II (CKD)**	**Stage III (CKD)**	**Stage IV (CKD)**	**ESRD on MHD**
e-GST (U/g Hb)	5.8 ± 0.4	7.4 ± 0.5	8 ± 1	9.5 ± 0.6	12 ± 1	10.2 ± 0.4
Hs-CRP (mg/l)	1.2 ± 0.7	3 ± 1	3.4 ± 0.4	4.0 ± 0.8	7 ± 2	7 ± 1
GFR (ml/min)[a]	118 ± 2	109 ± 3	77 ± 2	42 ± 2	20 ± 1	< 4.7[b]
PINI	0.5 ± 0.1	0.6 ± 0.3	1.0 ± 0.6	0.5 ± 0.1	1.3 ± 0.4	2 ± 1
alpha- 1 acid glycoprotein (g/l)	0.70 ± 0.03	0.90 ± 0.06	0.95 ± 0.04	0.92 ± 0.06	1.21 ± 0.09	1.24 ± 0.05
beta-2 microglobulin (mg/l)	0.90 ± 0.08	1.84 ± 0.09	2.2 ± 0.1	5.6 ± 0.5	12 ± 1	37 ± 2
Mean Age (years)	46.1	45.8	51.1	64.4	62.3	58.0

Data are expressed as mean ± SEM.

[a] GFR was calculated on the basis of MDRD equation.

[b] only two HMD patients showed a residual renal function while 60 were totally anuretic.

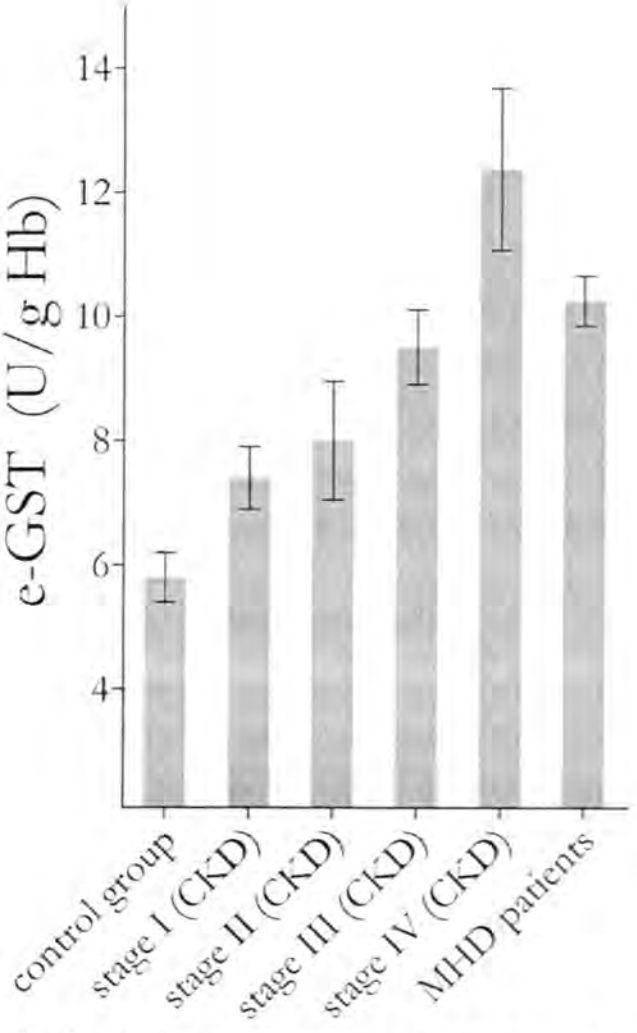

Fig.-2 : e-GST activity in healthy subjects, pre-dialysis and dialysis patients. e-GST activity is reported as U/g Hb. Healthy subjects: Control group; pre-dialysis patients: CKD stage I to IV; dialysis patients: MHD patients.

The difference is statistically significant between healthy subjects and all CKD patients ($P < 0.0001$ for groups I to IV and $P < 0.0001$ versus MHD patients). Among pre-dialysis patients the difference is significant between groups I and III ($P = 0.016$), I and IV ($P < 0.0001$), II and IV ($P = 0.015$) and III and IV ($P = 0.04$). e-GST activity is significantly higher in MHD patients than in CKD patients of groups I and II, ($P < 0.0001$ and $P = 0.016$) and in healthy

controls (P 0< 0.0001); surprisingly, it is significantly lower in MHD patients than in CKD patients of group IV (P = 0.034).

e-GST Activity Does not Correlate to Clinical Inflammation Markers

When e-GST activity was related to a few markers used to monitor the progress and gravity of the renal disease, we invariably observed a parallel increase (table 1). However, a more stringent statistical analysis demonstrated the absence of any direct correlation between e-GST activity and conventional markers of either acute phase (i.e. alpha-1 acid glycoprotein) or chronic inflammation (i.e. hs-CRP), or chronic inflammation/kidney disease (i.e. beta-2 microglobulin) and malnutritioninflammation (i.e. PINI) (table 1).

e-GST Activity Correlates to Plasma Hcy in MHD Patients

According to previous studies, almost all MHD patients display increased levels of plasma Hcy (table 2). Interestingly, we found that either mean e-GST activity and mean plasma Hcy were significantly increased in MHD patients compared to controls (10.2 ± 0.4 U/g Hb versus 5.8 ± 0.4 U/g Hb, P < 0.0001; 52 ± 4 μmol/l versus 13.6 ± 0.8 μmol/l, P < 0.0001) (table 2). Furthermore, a significant direct correlation was also found between plasma Hcy and e-GST activity (r = 0.796), as represented in fig. 3. A possible direct interaction between Hcy and e-GST has been checked. e-GST seems to be unable to use Hcy as substrate as demonstrated by the absence of transferase activity using 1 mM CDNB and 1 mM Hcy. On the other hand no detectable inhibition has been found using up to 1 mM Hcy or Hcy thiolactone in the presence of the classical GST substrates (1mM GSH and 1 mM CDNB) (not shown). Previous studies have shown a significant relationship between uremic toxins (such as Beta-2 microglobulin) and residual renal function (20). This has also been established for homocysteine (21). Therefore, residual renal function might be an important confounder for the observed relation between e-GST and plasma homocysteine. However, the multi-regression analysis that includes the residual GFR (assayed on the basis of cystatine C and creatinine) did not show any correlation between e-GST activity and these markers (r2 = 0.338 and 0.230 for cystatine C and for creatinine respectively).

Table-2: Mean e-GST activity and plasma Hcy in MHD patients versus controls

	MHD patients	Controls	*P* value
e-GST activity (U/g Hb)	10.2 ± 0.4	5.8 ± 0.4	< 0.0001
plasma Hcy (µmol/l)	52 ± 4	13.6 ± 0.8	< 0.0001

Data are expressed as mean ± SEM. $P < 0.05$ is considered statistically significant.

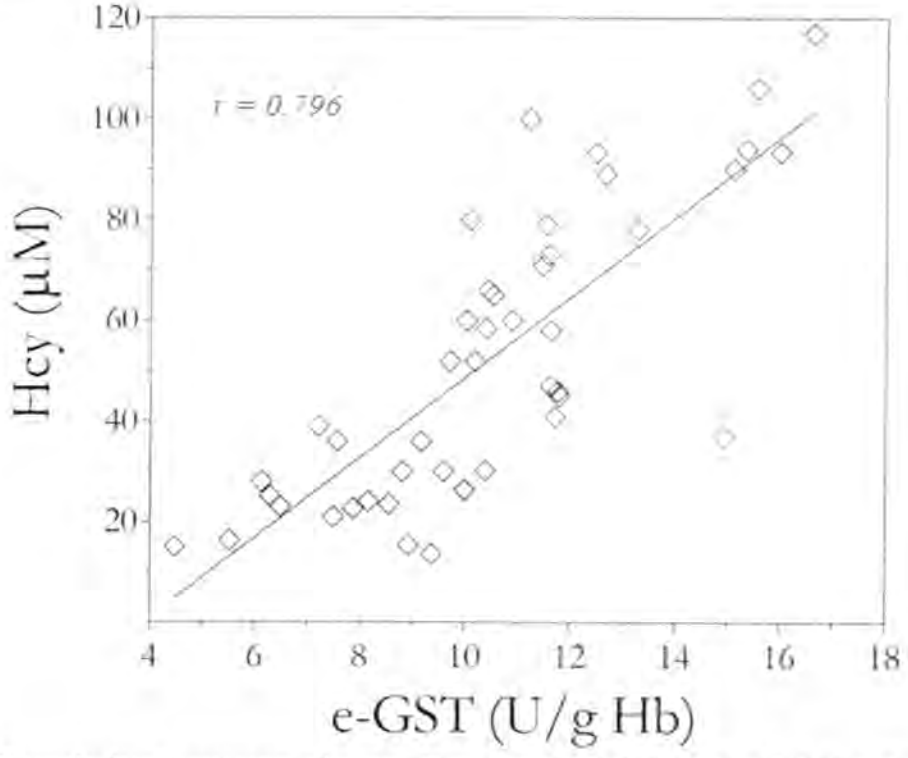

Fig. -3: Correlation between plasma Hcy levels (µM) and e-GST activity (U/g Hb).

In the previous study and before eGST activity was measured, eGST was purified from a human RBCs by affinity chromatography on Sephadex G25. This technique requires a long time and cause a loss of amount of enzyme compared with the rapid and simple method used in our study. A simple procedure to measure the activity of the e-GST on an automated spectrophotometric apparatus has been optimized and employed to evaluate e-GST activity in pre-dialysis patients under conservative therapy and in MHD

patients. The use of very small amounts of whole blood that avoids the time-consuming erythrocyte isolation represents a certain improvement over the usual procedures. This simplification is possible because the presence of extra-erythrocyte GST in the blood is always negligible, and broken erythrocyte membranes in the assay mixture do not perturb the spectrophotometric measurements. The simplified assay requires only 20 µl of whole blood which can be collected after a non-invasive pinprick. Furthermore, e-GST activity does not change appreciably during prolonged storage of the blood samples (4-6 days at 4°C) (see fig. 1a, and b). Overall, this procedure, validated by classical recovery experiments, as well as by low intra-day and inter-day variations could be of interest for routinely controls to test the efficiency of therapeutic procedures on patients with CDK. Actually, our results confirm previous reports of an enhanced e-GST activity in MHD patients (4, 5); conversely, in opposition to previous reports (4), in CKD patients under conservative therapy we observed for the first time a significant and progressive increase of e-GST activity that in likely related to the K-DOQI stage (fig. 2 and table 1). Interestingly, we also found a significantly higher activity of e-GST in pre-dialysis patients of K-DOQI stage IV compared to MHD patient. This finding is possibly explained by considering that GST expression reflects the abundance of circulating uremic toxins and that the hemodialytic procedure likely lowers the level of these toxic compounds. Both e-GST and inflammation/malnutrition markers are all significantly increased in CKD and MHD patients compared to controls (table 1). However, we did not find any significant correlation between the increased level of e-GST and all these markers. This finding is not surprising. In fact not all toxins ignite chronic or acute inflammation and GSTs are enzymes able to sweep or inactivate a lot of toxic compounds irrespectively of their inflammatory action. In this line the level of e-GST may fulfill a snapshot of the amount of circulating toxins complementary to the classical markers used to test the severity of chronic inflammation, malnutrition and kidney dysfunction. The correlation between the increased level of e-GST and plasmatic Hcy concentration in MHD patients is of particular interest. Plasma hyperhomocysteinemia is considered a cardiovascular risk factor and it is often associated to renal failure (11). The autoxidation of this sulfur-containing amino acid produces hydrogen peroxide. Moreover, high levels of Hcy reduces the

bioavailability of nitric oxide forming S-nitrosohomocysteine and inhibiting NOS. Thus, it has been proposed that high homocysteine levels are deleterious leading to endothelial dysfunctions and oxidative stress (12). In this view, homocysteine may represent the active biochemical factor that triggers these metabolic dysfunctions. However, a very different scenario is possible where Hcy is not the cause but the consequence of toxic dysmetabolisms, so Hcy could be only a marker of blood toxicity. Indeed, no effect on mortality and vascular diseases had been found in MHD patients by lowering their homocysteine level with folic acid (22). Actually, a paradoxical reverse relationship has been reported between Hcy and mortality in non-treated patients (23). The correlation found in the present study between hyperhomocysteinemia and e-GST supports the proposal that high levels of Hcy may be merely the consequence of high circulating toxins. In fact, increased levels of e-GST are certainly the effect (and not the cause) of an increased cell toxicity. In addition, our observation that the increase of e-GST in CKD patients does not correlate to inflammatory markers parallels a similar observation found for Hcy (23). The absence of any significant correlation between e-GST and cystatine C or creatinine means that the residual renal activity has no or little effect on the e-GST expression. No causative relation can be supposed for e-GST expression and plasmatic Hcy levels. It is well known that GST may bind to its active site hundred different toxic compounds but up today nobody of them is known to interact with the Hcy metabolism. In addition, we can leave out the possibility that Hcy itself or Hcy thiolactone may interact directly with e-GST because no detectable transferase activity is present using 1 mM Hcy as substrate nor relevant inhibition is caused by 1 mM Hcy or Hcy thiolactone. The possible oxidative interaction of Hcy with the essential sulfhydryl group of e-GST (Cys47) would be signaled by an inverse relation between Hcy concentration and GST activity, given that any chemical modification of this residue strongly inhibits the transferase activity (24). In conclusion, the present findings suggest that e-GST level could be a marker for toxin exposition and its determination may fulfill a useful probe to assess the efficiency of dialytic procedures. The e-GST assay may substitute or be complementary to the standard time consuming and expensive Hcy assay.

REFERENCES

1. Armstrong RN, "Structure, catalytic mechanism, and evolution of the glutathione transferases", Chem. Res. Toxicol., 10 (1): 2-18 (1997).
2. Sheehan D, Meade G, Foley VM, Dowd CA, "Structure, function and evolution of glutathione transferases: implications for classification of non-mammalian members of an ancient enzyme superfamily" Biochem. J., 360 (1): 1-16 (2001).
3. Awasthi YC, Sharma R, Singhal SS, "Human glutathione S-transferase", Int. J. Biochem., 26 (3): 295-308 (1994).
4. Galli F, Rovidati S, Benedetti S, Buoncristiani U, Covarelli C, Floridi A, Canestrai F, "Overexpression of erytrocyte glutathione-S-transferase in uremia and dialysis", Clin. Chem., 45 (10): 1781-1788 (1999).
5. Carmagnol F, Sinet PM, Rapin J, Jerome H, "Glutathione-S-transferase of human red blood cells; assay, values in normal subjects and in two pathological circumstances: hyperbilirubinemia and impaired renal function", Clin. Chem. Acta., 117 (2): 209-217 (1981).
6. "K-DOQI Clinical practice guidelines on hypertension and antihypertensive agents in chronic kidney disease", Am. J. Kidney Dis., 43, (5 Suppl 1), S1-S290 (2004).
7. Jacobs LH, van de Kerkhof JJ, Mingels AM, Passos VL, Kleijnen VW, Mazairac AH, van der Sande FM, Wodzig WK, Konings CJ, Leunissen KM, van Dieijen14 Visser MP, Kooman JP, "Inflammation, overhydration and cardiac biomarkers in haemodialysis patients: a longitudinal study", Nephrol. Dial. Transplant., 25 (1): 243- 248 (2010).
8. Dessi M, Noce A, Agnoli A, De Angelis S, Fuiano L, Tozzo C, Taccone-Gallucci M, Fuiano G, Federici G, "The usefulness of the prognostic inflammatory and nutritional index (PINI) in a haemodialysis population", Nutr. Metab. Cardiovasc. Dis., 19 (11): 811-815 (2009).
9. Bethea M, Forman DT, "Beta 2-microglobulin: its significance and clinical usefulness", Ann. Clin. Lab. Sci., 20 (3): 163-168 (1990).
10. Kendrick J, Chonchol MB, "Non traditional risk factors for cardiovascular disease in patients with chronic kidney disease", Nat. Clin. Pract. Nephrol., 4 (12): 672-681 (2008).

11. Van Guldener C, "Why is homocysteine elevated in renal failure and what can be expected from homocysteine-lowering?", Nephrol. Dial. Transplant., 21 (5): 1161-1166 (2006).
12. Welch GN, Loscalzo J, "Homocysteine and atherothrombosis", N. Engl. J. Med., 338 (15): 1042-1050 (1998).
13. Kluijtmans LA, van den Heuvel LP, Boers GH, Frosst P, Stevens EM, van Oost BA, den Heijer M, Trijbels FJ, Rozen R, Blom HJ, "Molecular genetic analysis in mild hyperhomocysteinemia: a common mutation in the methylenetatrahydrofolate reductase gene in a genetic risk factor for cardiovascular disease", Am. J. Hum. Genet., 58 (1): 35-41 (1996).
14. Bostom AG, Lathrop L, "Hyperhomocysteinemia in end-stage renal disease: prevalence, etiology, and potential relationship to arteriosclerotic outcomes", Kidney Int., 52 (1): 495-502 (1997).
15. Lubos E, Loscalzo J, Handy DE, "Homocysteine and glutathione peroxidase-1", Antioxid. Redox Signal, 9 (11): 1923-1940 (2007).
16. Lo Bello M, Battistoni A, Mazzetti AP, Board PG, Muramatsu M, Federici G, Ricci, G, "Site-directed Mutagenesis of Human Glutathione Transferase P1-1: spectral, kinetic and structural properties of Cys-47 and Lys-54 mutants", J. Biol. Chem., 270 (3): 1249-1253 (1995).
17. Pastore A, De Angelis S, Casciani S, Ruggia R, Di Giovamberardino G, Noce A, Splendiani G, Cortese C, Federici G, Dessi M, "Effects of folic acid before and after vitamin B12 on plasma homocysteine concentrations in hemodialysis patients with known MTHFR genotypes", Clin. Chem., 52 (1): 145-148 (2006).
18. Vinge E, Lindergård B, Nilsson-Ehle P, Grubb A, "Relationships among serum cystatin C, serum creatinine, lean tissue mass and glomerular filtration rate in healthy adults", Scand. J. Clin. Lab. Invest., 59 (8): 587-592 (1999).
19. Adams PA, Sikakana CN, "Factors affecting the inactivation of human placental glutathione S-transferase pi. The kinetic mechanism and pH-dependence of solvational and 1-chloro-2,4-dinitrobenzene-mediated inactivation of the enzyme", Biochem. Pharmacol., 39 (12): 1883-1889 (1990).

20. Fry AC, Singh DK, Chandna SM, Farrington K, "Relative Importance of Residual Renal Function and Convection in Determining Beta-2-Microglobulin Levels in High- Flux Haemodialysis and On-Line Haemodiafiltration", Blood Purif., 25 (3): 295-302 (2007).
21. Anwar W, Guéant JL, Abdelmouttaleb I, Adjalla C, Gérard P, Lemoel G, Erraess N, Moutabarrek A, Namour F, "Hyperhomocysteinemia is related to residual glomerular filtration and folate, but not to methylenetetrahydrofolate-reductase and methionine synthase polymorphisms, in supplemented end-stage renal disease patients undergoing hemodialysis", Clin. Chem. Lab. Med., 39 (8): 747-752 (2001).
22. Wrone EM, Hornberger JM, Zehnder JL, McCann LM, Coplon NS, Fortmann SP, "Randomized trial of folic acid for prevention of cardiovascular events in end-stage renal disease", J. Am. Soc. Nephrol., 15 (2): 420-426 (2004).
23. Kalantar-Zadeh K, Block G, Humphreys MH, McAllister CJ, Kopple JD, "A low, rather than a high, total plasma homocysteine is an indicator of poor outcome in hemodialysis patients", J. Am. Soc. Nephrol., 15 (2): 442-453 (2004).
24. Ricci G, Del Boccio G, Pennelli A, Aceto A, Whitehead EP, and Federici G, "Nonequivalence of the two subunits of horse erythrocyte glutathione transferase in their reaction with sulfhydryl reagents", J. Biol. Chem., 264 (10): 5462-5467 (1989).

Synthesis of New Compounds Derived from 2-(4-bromophenyl) -4H-1, 3-Benzodioxin-4-One

Wafaa F. Rodhan
Department of Chemistry/College of Science/Al-Mustansiriyah University

Received : 06/04/2011 Accepted: 29/05/2011

الخلاصة

يتضمن هذا البحث تحضير عدد من مشتقات المركب 2-(4-برومو)-4H- 1,3- بنزودايوكسين -4- أون (1)وبتفاعل هذا المركب مع الهيدرازين المائي تم الحصول على المشتق (2N- امينو-(4-برومو)-4H- 1,3- بنزودايوكسين -4- أون (2)ومن تفاعل المشتق (2) مع كلورواستيل كلورايد وبوجود قاعدة قوية تم الحصول على المشتق(N- كلورواستيل 2-(4-برومو)- 4H- 1,3- بنزودايوكسين -4- اون (3) . تفاعل المشتق(3) مع الثايويوريا للحصول على مشتق الايزوثايوريا (4) والذي بعد معاملتهِ مع بعض مركبات الكاربونيل اعطى المشتقات (5,6,7,8). تم الحصول على المشتق (9) من تفاعل المشتق (3) مع الهيدرازين والذي بدورهِ فوعِل مع الديهايدات اروماتية مناسبة منتجاً مشتقات جديدة لقواعد شيف (10-13)، المركبات (15,14) حضرت من خلال تفاعل المشتق (3) مع(الكواندين,اليوراسيل) بوجود كاربونات البوتاسيوم كقاعدة.

ABSTRACT

This work Involves a number synthesis of derivatives from -2-(4-bromo phenyl) -4H-1,3-benzodioxin -4- 0ne (1) ,from the reaction of compound(1) with hydrazine hydrate we got N-amino-2-(4-bromo phenyl) -4H-1,3-benzodioxin -4- 0ne(2) derivative and from the reaction of the Latest compound with chloro acetyl chloride in presence of strong base we got (N-acetyl chloride -2(4- bromo phenyl) -4H- 1,3- dioxin -4- one (3) , and from the reaction of derivative(3) with thiourea we got Isothiourea derivative (4) treatment with some carbonyl compounds to give derivatives (5-8). We got The derivative (9) from the reaction of derivative(3) with hydrazine which then reacted with suitable Aromatic Aldehydes to produced new derivatives of Schiff bases (10-13). The compounds (14,15) were synthesized from the reaction of derivative (3) with (uracil ,Gundine) in presence of potassium carbonate as base.

INTRODUCTION

The present work is conjugation with our ongoing programme on the utilizing of readily obtainable starting materials for the synthesis of hetero cyclic systems (1-3). The most important features in (4H-1,3-Benzodioxin-4-one) chemistry is their use us key starting materials for synthesizing new derivatives. The reactivity of (4H-1,3-Benzodioxnones) synthesizing from them new heterocyclic systems, potentially with the biological activity (4-7). This paper reports the synthesis of (2-(4- bromophenyl) -4H-1,3-benzodioxin -4- one) via the reaction of salicylic acid and 4-bromobenzaldehyde in presence of acetic acid as a solvent & Aluminum chloride as a catalyst and the salicylic acid is widely used in organic synthesis and function as a plant hormone it is derived from the metabolism of salicin.

MATERIALS AND METHODS

Melting points were determined in open capillary tubs on a Gallenkamp melting point apparatus and are uncorrected. The IR spectra (KBr disc were recorded with shimadzu -2N, FTIR-8400S.) UV spectra were recorded on Varian, uv-vis spectrophotometer using absolute ethanol as solvent. The "H-NMR spectra were recorded in Bruker spectrophotometer model ultra shield 300 MHZ in DMSO –d6 solution with TMS as internal standard.

Synthesis of 2-(4-bromo phenyl)-H-1,3-benzodioxin-4-one (1) (8)

A mixture of salicylic acid (0.025 mole),4-bromobenzaldyehyde (0.05 mole) and aluminum chloride (0.02 mole) in acetic acid (50 ml) was stirred for 48 hrs at 25° water (200 ml) was slowly added to the reaction mixture which was then the precipitate formed was filtered off, and recrystallized from ethanol to give compounds(1)physical properties table(1),spectral data of uv& IR table (2).

Synthesis of 3-Amino-2-(4-bromo phenyl)-2,3-dihydro-4H-1,3-benzoxazin-4-one (2) (9)

To a solution of compounds (1) (0.01 mole) in 50 ml of absolute ethanol and hydrazine hydrate (0.03 mole) was added and the reaction mixture was refluxed for 6hrs. then cooling ,the precipitate formed was filtered off and recrystallized from ethanol to give compounds(2) physical properties table(1), spectral data of uv& IR table (2).

Synthesis of (3-N-amino Acetyl chloride -2-(4-bromo phenyl) -4H-1,3-benzoxizn -4- 0ne (3) (10)

To a stirring solution of compound (2)(0.01 mole) in dry benzene , triethyl amine (0.01 mole) was added and then (0.01 mole) of chloro acetyl chloride was added dropwise , the reaction mixture was stirring at room temperature for two hours and then the solution was left to cool to produce white precipitate and then washed with sodium carbonate the (2%) precipitate filtered and recrystallized from Ethanol physical properties table(1), spectral data of uv& IR table (2).

Synthesis of (N-acetyl thio urea -2-(4-bromophenyl)-4H-1,3- benzoxine -4-one (4) (11)

To a solution of compound (3) (0.01) mole in absolute (50 ml) and (0.01) potassium carbonate, Thiourea (0.01) mol was added, and then the mixture was refluxed for (6hrs) and cooled to room temperature. The precipitate was filtered and recrystalization from ethanol. physical properties table(1), spectral data of uv& IR table (2).

Synthesis of heterocyclic carbonyl isothio derivatives (5, 6, 7, and8)(12)

To a solution of compound (4) (0.01 mol) in (25)ml a solute Ethanol Appropriate carbonyl compounds (0.01 mol) (Acetyl acetone) , (p-bromophenacyl diethyl malonate)&(Ethyl aceto acetate) was added to produce compound (5,6,7,8) after that the solution mixture was refluxed for (16 hr) the ppt was filterd & recrystalized from Ethanol physical properties table(1), spectral data of uv& IR table (3).

Synthesis of (3-N-amino Acetyl hyrazied -2-(4- bromophenyl) 2-3-dihydro -4H-1,3- benzoxiazin -4- one) (9)

To a stirring solution of compound (3) (0.01 mol) in (50ml) of a bsolute ethanol , hydrazine hydrate (0.02 mol) was added and the reaction mixture was refluxed for (12 hrs) and then the solution was left to cool, the precipitate formed and recrystallized from ethanol give compound (9) physical properties table(3) spectral data of uv& IR table (4).

Synthesis of Schiff bases (10-13) (13)

To a stirring solution of compound (9) (0.01)mole in absolute ethanol (10 ml) appropriate aldehydes (0.01)mole was added , the mixture

was refluxing for(6hrs) and cooled to room temperature . The precipitate was filtered and recrystalized from Ethanol physical properties table(4). spectral data of uv& IR table (5).

Synthesis of (N- (uracelo , Gundino) acetyl (2-4(bromo phenyl) -4H -1, 3-benzo dioxin -4- one (14, 15) (11)

To astirring solute of compound (3) (0.01 mole) in absolute Ethanol (20 ml) (0.01) potassium carbonate (0.01mole) uracil (14) Guandin (15) the mixture refluxed for (12hr) then left to cool, the precipitate was filtered and recrystalized from Ethanol physical properties table(3) spectral data of uv& IR table (4).

RESULTS AND DISCUSSION

With the aim of expanding the synthetic potential of the target compound (4H) 1,3- benzodioxinon , we have prepare new derivative compounds starting with 2-(4-bromo phenyl)-4H-1,3- benzodioxin -4-one **(1)** which were prepared from the reaction of salicylic acid with 4-bromobenzaldehyde in the presence of (ALCL3 and CH3COOH) (Table(1)) the formation of this compound was indicated by appearance in their IR spectra of carbonyl group (C=O) at 1695cm^{-1} combined with the disappearance of (O-H) stretching bands at (3237)cm^{-1}. UV spectra of compound (1) shown intense maxima at 259nm and 308nm which belonged to $\pi \rightarrow \pi^*$ and $n \rightarrow \pi^*$ transition respectively, and the Amino derivative compound (2), Table (1) that afforded from addition hydrazine hydrate to compound (1). Which then the Latest compound (2) be good choice to react with chloro acetyl chloride to give the (N-acetyl chloride) derivative so that we have prepare new derivative compounds starting with N-acetyl chloride -2(4-bromophenyl) -4H-1,3-benzodioxine -4- one)(3). The information of this compound was indicated by appearance in their IR spectra of the carbonyl group (C=O) at 1679 cm^{-1} and(C-CL)at(694)cm^{-1} combined with disappearance of the (-NH2) stretching bands. UV spectra of compound (3) mostly showed intense maxima at 308nm and 222nm which belonged to $\pi \rightarrow \pi^*$ transition respectively. The reaction between compound (3) and thio urea compound in presence of (K2CO3 –EtoH) afforded the I so- thiourea- derivative (4) in good yield. The spectrum showed the (N-H) stretching absorption near (3385-3263) cm-1 and (C-S)

at (1280) cm-1 and disappearance of (C-CL) stretching band at (694) cm-1. UV spectrum of compound (4) mostly showed intense maxima at 310nm and 225nm which belonged to $\pi \rightarrow \pi^*$ and $n \rightarrow \pi^*$ electronic transition respectively. Reaction of the Iso thiourea derivative (4) with some organic compounds that contain carbonyl group in their structure to yield new hetero cyclic derivatives (5-8) and The information of them was indicated by the presence in their IR spectra of (C=N) at (1626 -1629) cm^{-1} combined with disappearance of NH2 &NH stretching band at(3133,3430) cm-1. UV spectra of these derivatives showed intense maxima at 310nm and 221nm. And from the reaction of the Acetyl chloride derivative compound (3) with hydrazine hydrate in absolute Ethanol the (N- amino acetyl) derivative (9) obtained in good yield. The information of this compound was indicated by presence in their IR &UV spectra that show in table (3). Condensation of compound (9) with aryl aldehydes in absolute Ethanol gave the Schiff bases (10-13) that indicated by the presence in their IR spectra of Azomethine (CH=N) stretching band at (1623- 1627) cm^{-1} combined with disappearance of NH2 stretching band. UV spectra showed mainly intense maxima at 308nm and 210nm. The treatment of the Acetyl chloride derivative (3) with the uracile and Gundine compound that contain second Amine at their structure to yield new heterocyclic derivatives (14-15) and the IR spectra of these compounds showed the disappearance of (C-CL) stretching band at (694) cm-1. UV spectra of these derivatives showed intense maxima at 309nm and 223nm due to $\pi \rightarrow \pi^*$ and $n \rightarrow \pi^*$ electronic transitions respectively.

Synthesis of New Compounds Derived From 2-(4-Bromophenyl)-4H-1,3-Benzodioxin-4-one

Wafaa

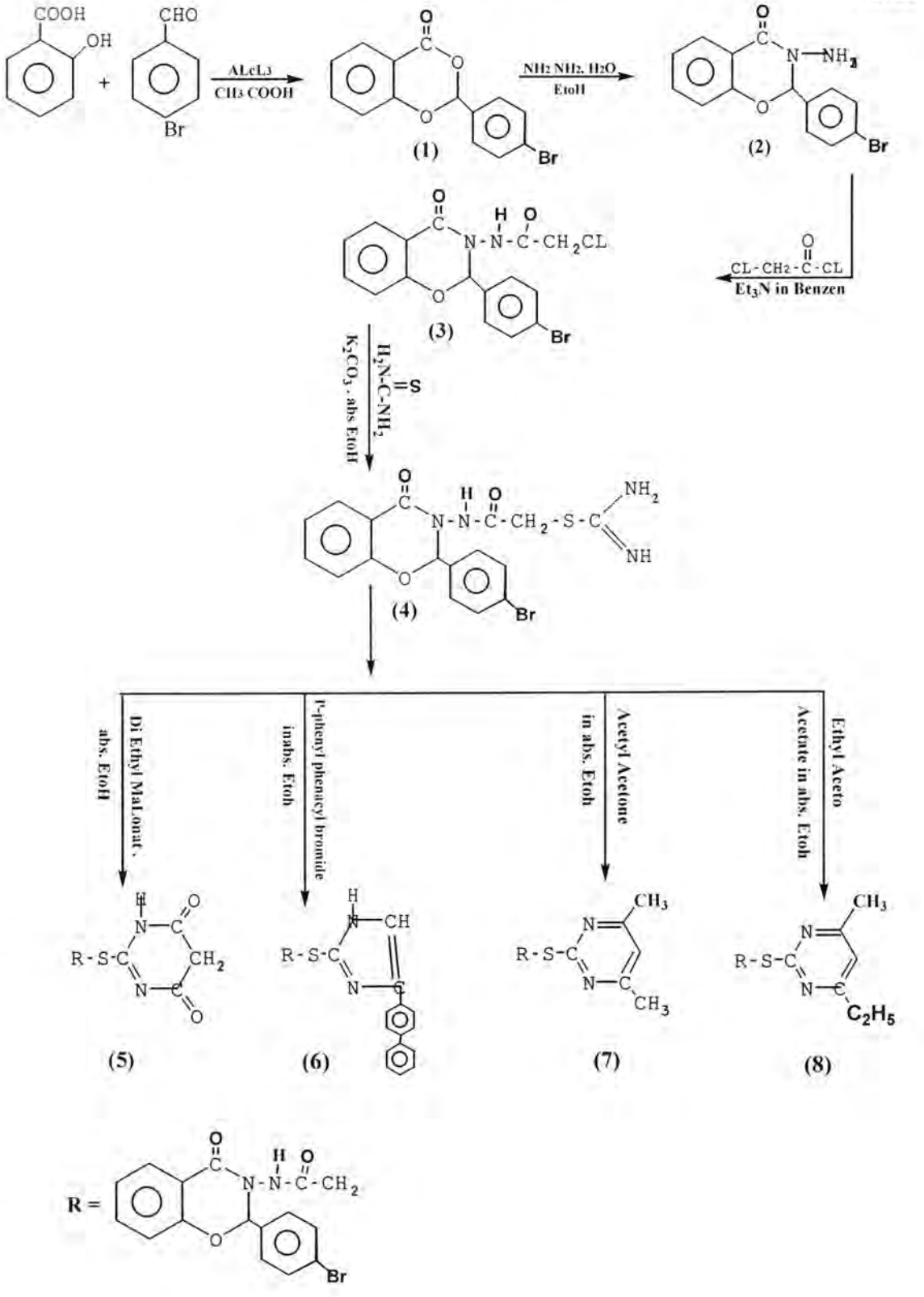

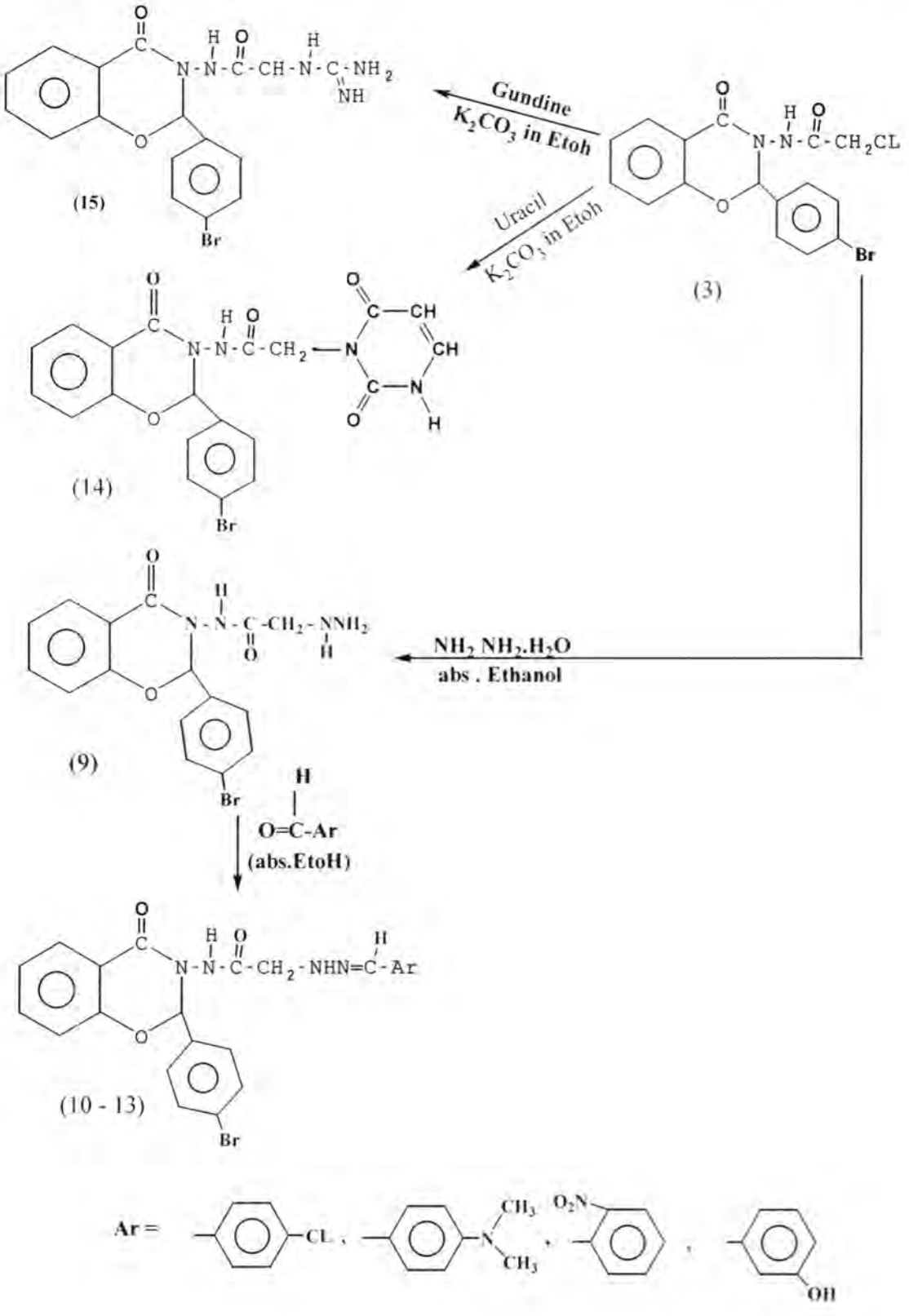
Gundine
K_2CO_3 in Etoh
Uracil
K_2CO_3 in Etoh
(15)
(3)
(14)
(9)
$NH_2NH_2.H_2O$
abs . Ethanol
O=C-Ar
(abs.EtoH)
(10 - 13)
Ar =

Table -1 : physical properties of compounds (1–15)

Comp. No.	M.P. C°	Yield %	Purification Solvent.	Molecular Formula.
1	(79 – 80)	58 %	Ethanol	C14 H9 O3 Br
2	(220 – 222)	62 %	Ethanol	C14 H11O2 Br
3	(181 – 183)	54 %	Ethanol	C16 H12 O3 N2 Br Cl
4	(212 – 214)	74 %	Ethanol	C17 H15 O3 N4 S Br
5	(218)	66 %	Ethanol	C20 H15 O5 N4 S Br
6	(190)	81 %	Ethanol	C31 H23 O3 N4 S Br
7	(202 – 204)	79 %	Ethanol	C22 H19 O3 N4 S Br
8	(143 – 145)	44 %	Ethanol	C23 H21 O3 N4 S Br
9	(206 – 208)	86 %	Ethanol	C16 H15 O3 N4 Br
10	(171- 173)	77 %	Ethanol	C23 H18O3 N4 Br Cl
11	(162 – 164)	83 %	Ethanol	C25 H24O3 N5 Br
12	(187 – 189)	69 %	Ethanol	C23 H18O5 N5 Br
13	(153 – 155)	63 %	Ethanol	C23 H19 O4 N4 Br
14	(286 – 288)	71 %	Ethanol	C20 H15O4 N4 Br
15	(227 - 229)	52 %	Ethanol	C17 H19 O3 N5 Br

Table -2: spectral data of compounds (1-4)

Comp. No.	**UV λ max (Ethanol)**	**IR Cm^{-1}**
1	308,259, 208	(C-H) ar 3082, (C=0) 1695, (C=C)ar 1585, (C-O) 1201, (C-Br) 758.
2	309,220	(N-H) 3358,3282, (C-H)ar 3039, (C=O) 1687, (C=C)ar 1591,(C-O) 1219, (C-Br) 723.
3	308 , 222	(C-H) ar 3041, (N-H) 3188, (C=C) 1589, (C-Br) 791, (C-CL) 694.
4	310 , 225	(C-H) ar 3037, (C-H) al 2941, (N-H) 3430 ,3133, (C-S) 1280, (C=N) 1626, (C-Br) 751.

Table- 3: spectral data of compounds (5-8)

Comp. No.	UV λ max (Ethanol	IR cm^{-1}
5	310,224	(C-H)ar 3100, (C-H)al .2941, (C-S) 1294,(C=N) 1624, (C=O)1652, (N-H)3286
6	310,221	(C-H) ar 3068, (C-H) al. 2941, (C=N) 1626, (C-S)1283 (C=C)1622, (N-H)3410
7	309,224	(C-H) ar 3074, (C-H) al. 2941, (C=N) 1627(C-S) 1280,
8	307,229	(C-H) ar 3063, (C-H) al. 2923, (C-CH3)al.2966, (C=N) 1629, (C-S) 1282.

Table -4: spectral data of compounds (9, 14, and 15)

Comp. No.	UV	IR cm^{-1}
9	310,225	(N-H) 3414,3360,(C-H)ar 3O47,(C-H) al. 2915 (C=N) 1627, (C=O)1663, (C-Br)715
14	309,223	(N-H) 3401, (C-H) ar 3095, (C-H) al.2941, (C=N) 1626, (C=C)1651
15	310,224	(C-H) ar 3097, (C-H) al. 2939, (N-H) 3400,3220, (C=N) 1624

Table -5: spectral data of compounds (10-13)

Comp. No.	UV	IR cm^{-1}
10	310,210	(C-H)ar 3047, (C-H) al.2939, (N-H) 3452, (C-CL) 623.
11	385,320 311,224	(C-H)ar 3046, (C-H)al. 2922,2860, (C=N) 3398.
12	309,221	(C-H)ar 3041, (C-H) al.2925, (C=N) 1623, (N-H) 3402 (-NO2) 1466.
13	308,227	(C-H) ar3041, (C-H) al.2921, (N-H) 3411, (C=N) 1627, (O-H) 3461.

Table -6: chemical shifts in HNMR Spectra of The main compound in this research.

Comp. No.	Chemical shift (S),ppm	Type of signal	No. of protons	Remarks
1	7.6-8.7	Multiplit	8H	due to aromatic protons
	7.2	singlet	1H	due to(O-CH-O) proton
2	7.2-8.0	multiplit	8H	due to aromatic protons
	7.0	singlate	1H	due to (O-CH-N)
	4.4	singlet	2H	due to (N-H)proton
3	7.6-8.2	multiplit	8H	due to aromatic protons
	4.1-4.3	duplet	2H	due to (N-H)proton
	4.6-4.8	duplet	2H	due to (C-H) aliphatic proton
9	7.4-7.9	multiplit	8H	due to aromatic protons
	4.3	singlet	2H	due to (N-H)proton
12	7.7-7.9	multiplit	12H	due to aromatic protons
	4.8-4.9	singlet	1H	due to (N-H)proton

REFERENCES

1. Jiang, J.B.; Hessen, D.p.; Dusak, B.A.; Dexter, D.L; Kang, G.J.;Hamel , E.J.Med. chem. 33, 1721,(1990).
2. Shrimali, M.; Kalsi, R.; DIxit, K.S.; Barthwal, J.P.Arzeneim Forsch., 41, 514.(1991).
3. Srivastava, M.; Mishra, B.; Nizamuddin IndJ. Chem. sec. B, 40, 342, (2001).
4. Farghaly, A.M.; Chaaban, I.; Khalil, M.A.; Bekhit, A. A. AL exandriq J. pharm. Sci., 4, 52,(1990).
5. Madkour , H.M.F.;salem , M.A.I; Adb del- Rahman , T.M.;Azab , M.E. Heterocyclic,38,57,(1994).
6. Madkour , H.M.F. Heterocyclic, 36, 947,(1993).
7. Al-Bayati ,R.I.,AL-Rawi, J.M.andAL-Naimi , K.H.,"Reaction of 2,4-dioxo- 2,4- dihydro -2H-1,3- benzoxaine with some secondary Amines," Iraqi J. of chem.., 23.2 (1997).

8. Fujita T., watanabes S.; Suga K., lsobe T. and Miura T.," The reaction of β-Hydroxy acids with al dehyde," Aust. J.chem, 33, 685-687(1980).
9. Habib J.M.,"synthesis and characterization of new nitrogen coumarin derivatives", ph.D Thesis, college of scince-) AL-Mustansirya univercity(2006).
10. Redha I.AL Bayati, Abdul – Hussain K.Sharba , Mazin J.Habid. (Synthesis of New Nitrogen coumarin Derivatives) AL-Mustansirya J.sci (2008).
11. F.A. Hussi N(Synthesis of N- substituted saccharins via Schiff's Bases) Iraqi J. of chem.. (1999).
12. Synthesis of some – Barbiturate derivatives via Schiff's Bases. Iraq.J.chem.(2000).
13. Roui I.H.," synthesis and Biological activity of some new Twin compounds containing hetero cyclic unit," AL-Mustansiriya J. sci., (2008).

Synthesis and Characterization of Hetero Cyclic Compounds Based on 1,3,4 -Thiadiazole and It's Resins

*Redha I. AL-Bayati, **Mahmood Abdul Jabar and ** Eman M.M.Hasson
*Department of Chemistry/College of Sciences/Al-Mustansiriyah University
**Department of Chemistry/College of Sciences Women/University of Baghdad

Received: 14/03/2011 Accepted: 29/05/2011

الخلاصة

تم تحضير المركب 2,2-diamino-bis-1,3,4-thiadiazole-5-disulfide methane من المركب الحلقي الغير متجانس 2-amino-5-mercapto-1,3,4-thiadiazole تم تحضير قواعد شيف الفينولية بواسطة تفاعلات التكثيف مع الباراهيدروكسي بنزالديهايد تم تحضير راتنجاتها المثيلولية والإيثيرية والإيبوكسية وتم تشخيص هذه المركبات بواسطة مطيافية الأشعة الحمراء والاشعة فوق البنفسجية والتحليل الدقيق للعناصر مع تعيين ثباتها الحراري بتقنية التحليل الحراري الوزني إضافة إلى قياس بعض خواصها الفيزيائية.

ABSTRACT

In this work, 2-amino-5-mercapto-1,3,4-thiadiazole(1) was prepared from thio semicarbized and (CS_2) in the presence of anhydrous (Na_2CO_3). The compound (2)[2,2-diamino-bis-1,3,4-thiadiazole-5-disulfide methane] was prepared from reaction compound (1) with dibromomethane and then convert into Schiff base (3) by refluxing compound with (p-hydroxy benzaldhyde, treatment of the Schiff bases (3) with formaldehyde in the presence of NaOH afforded the corresponding mthylolic phenolic resin (4) which upon treating with methanol or butanol in the presence of Conc-H_2SO_4 gave etheric resins (5-7) respectively.

The epoxy resins (8) were prepared from the corresponding etheric resins and eipychlorohydrine in the presence of NaOH. Finally Reaction of epoxy resins (8) with morpholine leads to ring open giving resin with unstitched ring (9).

INTRODUCTION

Various derivatives of 1,3,4-thiadiazole have been shown antitubercular, bactericidal, fungicidal [1] and anti-inflammatory activities [1-2], Schiff bases have also been widely reported to be biological versatile compound having antifungal and plant growth regulating activates have been

reported[3] the synthesis of some heterocyclic compounds containing 1,3,4-thiadiozole moiety was covered a wide area of applications in industry field[4].

MATERIALS AND METHODS

Melting point was determined in (Gallen Kamp) apparatus and uncorrected. The (FT-IR) spectra of the compound were recorded on (SHIMADZU) FT-IR, 8300(4000-666) cm^{-1} spectrometer as KBr-Disc, UV spectra were performed on (Cory/VARIAN) spectrophotometer in (190-900)nm using absolute ethanol as solvent, elemental analysis (C.H.N) were performed in SYRIAN ARAB REPUBLIC/ ATOMIC ENERGY COMMISSION (AECS), thermal gravimetric analysis (TGA) was performed in center of consulation/ University of Jordon.

Preparation of 2-amino-5-mercapto-1,3,4-thiadiazole (1)

This compound was prepared according to the method in the literature (10) m.p 232 -234^0 C (lit.m.p, 230-232^{0}C).

Preparation of 2,2-diamino-bis-1,3,4-thiadiazole -5-disulfide methane(2)(6)

Amixture of compound (1) (0.01 mol) with (0.04 mol) dibromomethane in (15ml) ethanolic.

Sodium hydroxide was refluxed until evolution of H_2S ceased (6h). The solid was filtered off and recrystallized from ethanol.

Preparation of 4-((E)-{[5-({[5-{[(IE)-(4-hydroxyphenyl) methylene] amino}-1,3,4-thiadiazol-2-xl) thiomethyl} thio) 1,3,4-thiadiozo1-2-YL], mine} methyl) phenol (3)

A mixture of compound (2) (0.007mole) and p-hydroxy benzaldehyde (0.014mol) in absolute ethanol was refluxed for Sh. The solid formed was recrystallized from ethanol.

Preparation of 4 ((N)-([5-[(5-((N)-3,5-bis-(hydroxymethyl)-4-hydraxy benzylidene amino)-1,3,4-thiodiazal-2-YL-thio}methyl-mio)-1,3,4-thiodiazol -2-YL], mino)methyl)-2,6-bis(hydroxyl methyl)phenol(4) (7,8)

To a mixture of an appropriate Schiff base (0.003mole) and formaldehyde solution (37-41)% (0.004mole) in tetra hydrofwean (50ml), ethanolic sodium hydroxide solution (10%) was added portion wise to keep

the PH of the reaction mixture (9-10) then heated the mixture in oil bath (50-60^{0}C) for 3h. The reaction mixture was cooled (5-10)^{0}C and neutralized with alcoholic phosphoric acid (10%), then filtered and dried. The excess solvents were distilled off and the residue recrystallized from appropriate solvent (Table1).

Preparation of Etheric Resins (5-7) (9)

General Procedure

To mixed an appropriate alcohol (CH_3OH or C_4H_9OH or Allylalcohol) (0.8mol) with concentration H_2SO_4 (0.4mol) was added gently in about 1h, then the temperature was increased gradually to the boiling point of the alcohol used. The mixture was kept at boiling alcohol for 24h then neutralized the cooled mixture using solid sodium hydroxide-the resin formed was extracted using $CHCl_3$, then dried and evaporated under vacuum, the residue was recrystallized from $CHCl_3$.

Preparation of Epoxy Resins (8) (8)

General Procedure

To amixture of an appropriate methyblic phenolic (5) (0.01mol) or etheric resin (0.12 mol) and eipychlorohydrine to 50^{0}C for 15min.was added gently sodium hydroxide (0.14mol) in two portions to keep the temperature below 65^{0}C. The stirring was continued for 2hs after first addition the aqueous layer was separated from the organic layer, then the second portion of NaOH added and stirred for 1h and left the mixture at the same temperature for 50min, and also the aqueous was separated. The organic layer were dried and excess of eipychlorohydrim and solvent distilled off under reduced pressure. The formed resins were purified by dissolving it in THF then filterazation and evaporation of excess solvent at 50^{0}C (Table1).

Preparation of Resins with Unstitched Ring (9)

A mixture of an appropriate epoxy resin (9) (0.07mol) in cooled methanol (30ml) and morpholine (0.015mol) was heated in oil bath (100-125) ^{0}C for continues 72h. After cooling, the solvent was evaporated and the residue recrystallized from methanol.

Table -1: Some Physical Properties of Compounds (1-9).

Comp. No.	Molecular formula	Yield%	Colour	Purification solvent	M.P. °C
1	$C_2H_3N_3S_2$	58	Yellow	Ethanol	230-232
2	$C_5H_6N_6S_4$	75	Yellow	Ethanol	272.274
3	$C_{19}H_{14}N_6S_4O_2$	65	Red	Ethanol	164-166
4	$C_{23}H_{22}N_6S_4O_6$	65	Red	THF	OilY
5	$C_{27}H_{30}N_6S_4O_6$	45	Red	THF	OilY
6	$C_{39}H_{50}N_6S_4O_6$	40	Brown	$CHCl_3$	OilY
7	$C_{35}H_{38}N_6S_4O_6$	45	Brown	$CHCl_3$	OilY
8	$C_{33}H_{36}N_6S_4O_8$	45	Brown	THF	OilY
9	$C_{41}H_{56}N_8S_4O_{10}$	42	Brown	methanol	OilY

THF = Tetrahydrofuran

RESULTS AND DISCUSSION

In this study summarized the performed reaction 2,2- diamino-bis-1,3,4- thiadiazole-5-disulfide methane which was prepared by condensation of 2-amino-5- mercapte-1,3,4-thiadiazole with di Bromo methan (2). The FT-IR spectrum showed the stretching bands for (NH_2) at (3407-3255) cm^{-1} and bending vibration of (C-S-C) at (617)cm^{-1} combined with disappearance of (SH) bands at (2619) cm^{-1}. UV spectrum in a maximum absorption at (335)nm, (295)nm for $n\rightarrow\pi$, $\pi\rightarrow\pi^*$ (10) respectively, another hand (C.H.N) analysis (found) [%H2.15(2.28) %C21.58(21.68)6%N30.22(30.98)] table (3). Reaction between (2) and P-hydroxy benzaldehyde gave Schiff base (3) which indicated in FT-IR spectrum stretching band of (OH) near (3295-3279)cm^{-1} and phenolic (C-O) at (1265,1212) cm^{-1}, Aromatic (C=C) at (1581,1512) cm^{-1} and (C=N) absorption bands at (1607,1597) cm^{-1} at (1265,1212) cm^{-1}, Aromatic (C=C) at (1581-1512)cm^{-1} combined with disappearance (NH_2) bands at (3407-3255). Also UV spectrum showed transitions at (365) nm and (305) nm for $n\rightarrow\pi^*$(10).

Also derivatives methylolic resin (4) prepared From reaction Schiff base (3) with for maldehyde and indicated in FT-IR spectrum of abroad peak for methylolic group at (3433-3221)cm^{-1} combined with stronge stretching bands at (2924-2985) cm^{-1} for aliphatic (CH_2). UV spectrum showed absorption at (345)nm and (288)nm due to $n\rightarrow\pi^*$,$\pi\rightarrow\pi^*$(11) transition, (C.H.N) analysis

for (4) found [%H3.63(3.89),%C45.55(45.69),%N13.86(13.98)] table (3) and study thermal stability in fig.(1)(table 4).

Compound (4) similarly reacts with (methanol, butanol or Allylalcohol) afforded esthetic resins (5-7) which indicated in FT-IR spectrum of stronge bending vibration for (C-O-C) at (1107-1058)cm^{-1}.

Compounds (5) reacted with eipy chlorohydrine afforded epoxy resins (8) in its FT-IR spectrum of peak is more sharp bands at (3414-3120) cm^{-1} combined with obtained oxirane absorption bands at (972-952)cm^{-1}, UV spectrum at (392, 310) nm for $n\rightarrow\pi^*$,at (235)nm for $\pi\rightarrow\pi^*$ transition and study thermal stability in fig (2) and table(4).

Compound (8) reacted with morpholine afforded resins (9) with unstitched ring, the FT-IR spectrum display absorption bands of oxirane in (972-952) cm^{-1} combined with increasing braading bands of (014) near (3387-3143) cm^{-1} and bending absorption of (C-O-C) at (1033-1111) cm^{-1}. Also UV spectrum at (365) nm for $n\rightarrow\pi^{*(11)}$ and at (284) nm for $\pi\rightarrow\pi^*$ transition another hand (found) (C-H-N) analysis [%H 5.91 (6-41)%c 51.90(52.60),%N 11.81 (11.99)] in table (3) and study thermal stability in fig (3) and table (4).(2)

Table -2: spectral data for compounds (1-10)

Comp. No.	UV (EtoH)	Characteristic bands of (FT-IR) spectra cm^{-1} (KBr.Disc.)					
	λ_{max} nm	$\sum_{max}$ x 10^{-3} L.$mol^{-1}cm^{-1}$	$\upsilon_{NH2, OH}$	υ_{CH2}	$\upsilon_{C=N}$	$\upsilon_{C=C}$	Others
1	310 290	1.90 2.00	3390 3275	-	1606 1597	-	υ_{NH} =3174 υ_{SH} =2619 υ_{C-S} =601-700 υ_{C-N} =1361-1320
2	335 295	1.35 1.75	3407 3317 3255	2940 2927	1627 1604	-	υ_{NH} (3247, 3168)
3	365 305	0.931 1.429	3295 3274	-	1622 1597	1580 1512	υ_{CH} out of plane (837) υ_{CH} arom (3024) υ_{C-O}(1265)
4	345 288	1.032 1.24	3433 3221 3170	2924 2985 2854	1630 1597	1522 1512	υ_{C-O}(1265)
5	314 202	0.866 1.401	3462 3180	2962 2945	1642 1622	1535 1522	υ_{C-O-C}(1056) υ_{C-O}(1209)

6	216 205 202	0.817 1.248 1.238	3360 3166	2989 2946 2916	1612 1610	1548 1538	$\upsilon_{C-O-C(1067, 1093)}$ $\upsilon_{C-O(1235,1220)}$
7	338 295	1.003 1.395	3433 3170	2924 2915	1632 1620	1550 1538	$\upsilon_{C-O-C(1107, 1058)}$ $\upsilon_{C-O(1215,1284)}$
8	392 310 235	1.420 2.500 3.10	3414 3390 3120	2958 2931	1600 1577	1512 1518	υ_{C-C} (972, 952) \ / O
9	365 284	1.421 2.725	3387 3143	2931 2850	1635 1604	1540 1535	$\upsilon_{C-O-C(1111, 1033)}$

Table -3: Some Elemental Analysis (C.H.N) of Compound (2,4,9)

Comp. No.	C.H.N Analysis % Calculated (Found)		
	% H	% C	% N
2	2.15 (2.28)	21.58 (2168)	30.22 (30.98)
4	3.63 (3.89)	45.55 (45.69)	13.86 (13.98)
9	5.91 (6.41)	51.90 (52.60)	11.8 (11.99)

Table -4: The Curing Temperature of Some Phenolic and Epoxy Shiff Bases Resins

Resins	Primary degradation	Finally degradation	%50 degradation weight	Lirnet degradation degree	Average degradation	%char. content
4	190	525	370	325	0.96	79.44
9	180	750	612	325	0.069	61.63

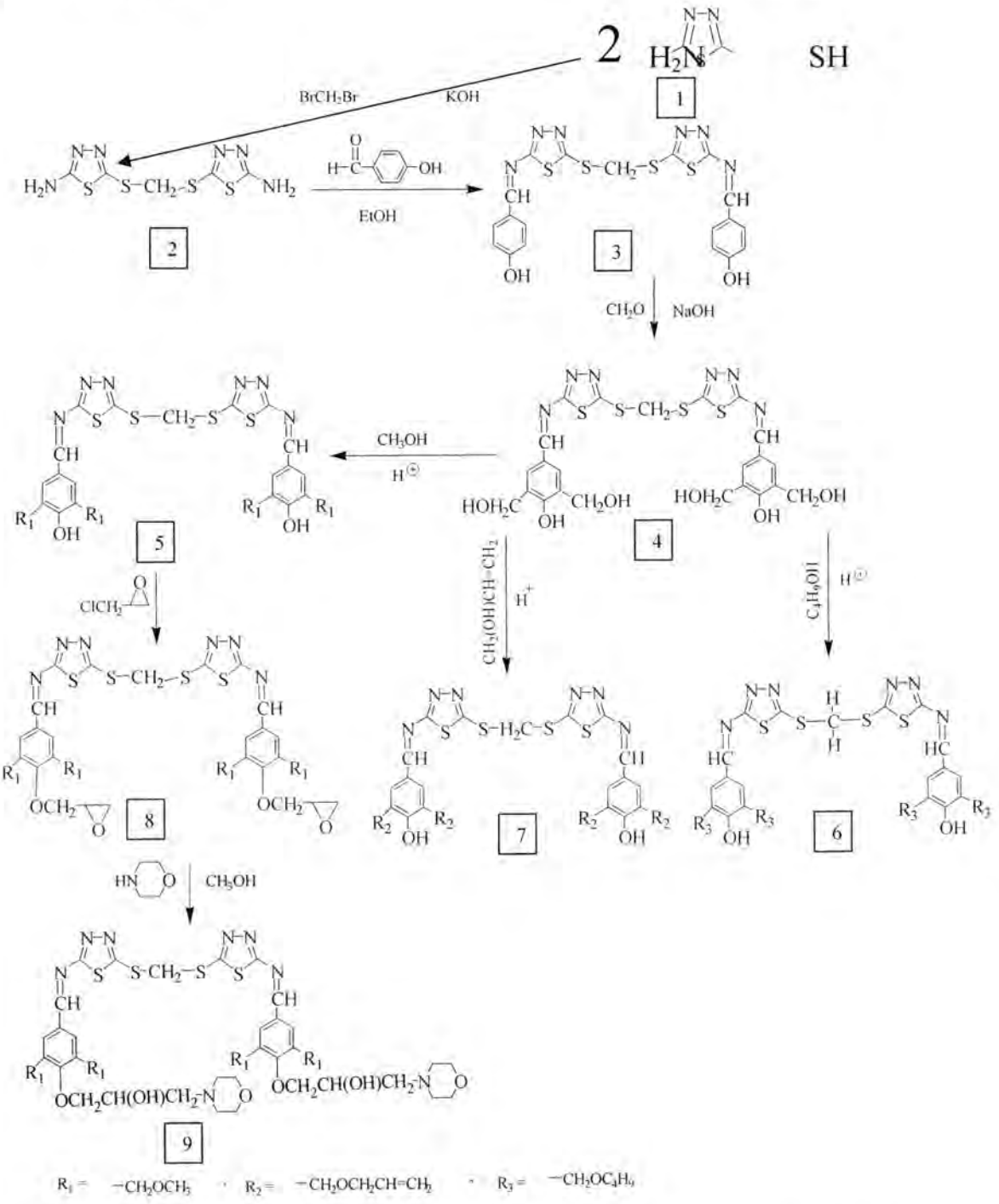

Scheme -1: Preparation of Methylolic, Etheric and Epoxy Resin for Schiff Base No. (3)

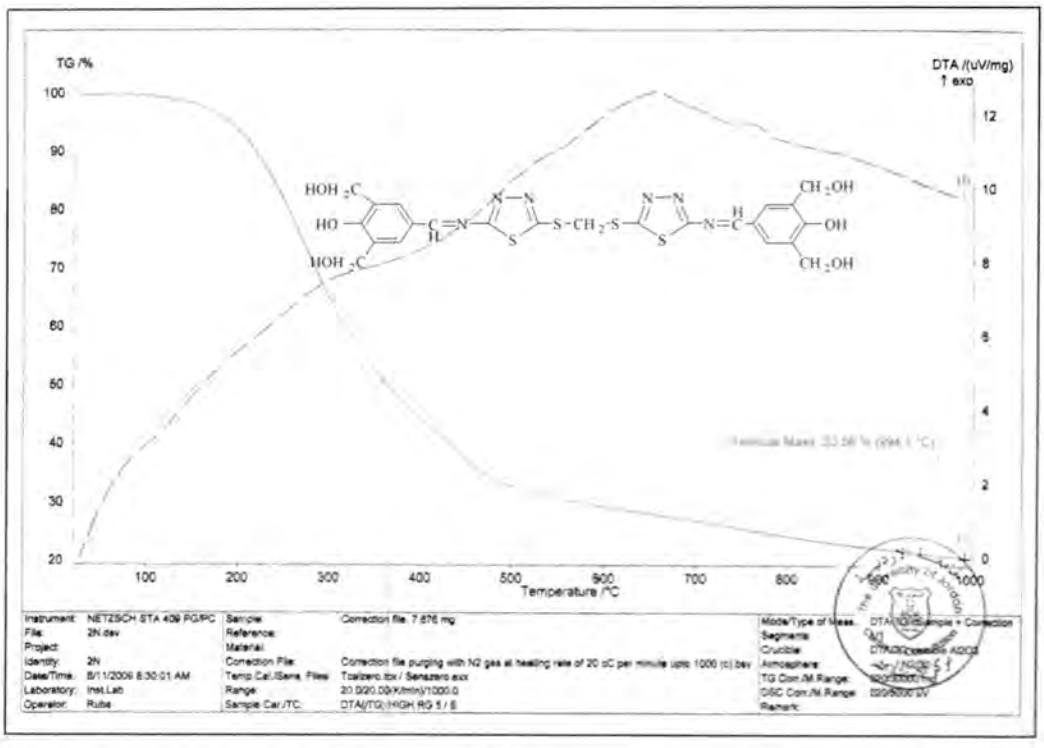

Fig. -1: Thermogram for Resin No. (4)

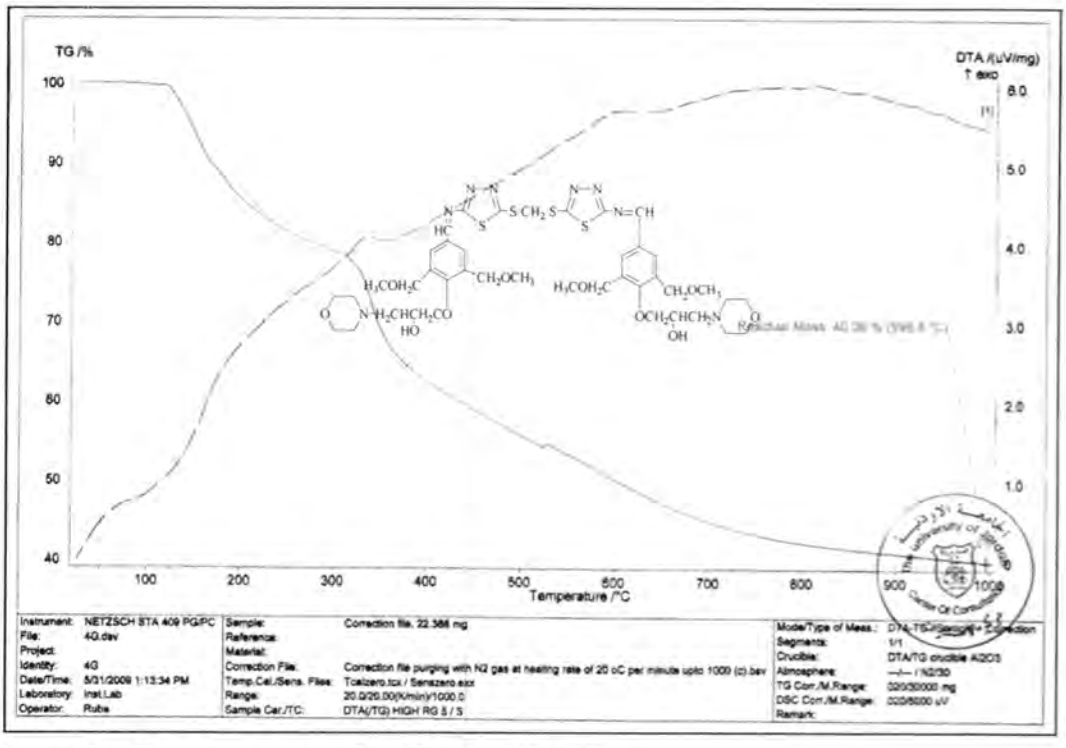

Fig. -2: Thermogram for Resin No. (9)

REFERENCES

1- Y.A.AL-Soud, N.A.AL-Masoudi;"A New class of dihaloquinolones bearing N-aldehydoglycosycarbohydrazides , mercapto-1,2,4-triazole , oxadiazoline and amino acid ester precursors: synthesis and antimicrobial activity" . Brazilian Chem. Soc; Vol (14), 790-796 (2003).

2- H.Gemma, T.Salmi,J.warn; J.Amer. Chem. Soc, Vol. (3), 131-134, (2003).

3- C. Hansong, Li.Zhengming and H.Yu Fena; " Synthesis and Fungicidal Activity against Rhizoctonia Solani of 2-Alkyl (Alkylthio)-5-Pyrazolyl-1,3,4-Oxadiazoles (Thiadiazoles) J.Agri.Food.Chem; 48, 5312-5315 (2000).

4- N.C. Robert; "Chemistry of Organic Compounds"; 3rd. Ed. Sannders Pheladelphia (1965).

5- V. Petrow, O. Stephenson; J. Amer. Chem. Soc; Vo. (1), part 1508, (1958).

6- H.Singh, L.D.S.Yadav and B.K.Bhathacharya; J.Indi.Chem.Soc, Vol (LVI), 1013-1016, (1979)

7- G.A.Adam, Iraqi, Patenr, 1846 (1986).

8- د. ذنون محمد عزيز "كيمياء اللواصق والأصباغ والأطلية البولميرية" كلية العلوم/ جامعة بغداد (77-78)، (1990)

9- J.Bouffard and T.Swager; " Fluorescent Conjugated polymers that incorporate substituted 2,1,3-Benzooxadiazole and 2,1,3-Benzothiadiazole units. Macromolecule, 41, 5559-5562 (2008).

10- R.M.Silverstein; "Spectrometric Identification of Organic Compound", 4th Ed., part 2, (1981).

Leptin and Related Biochemical Parameters in Obese Osteoarthritis

*Eman Saadi Saleh, **Suad Aziz Hassan and Mohammed H.M. Al-Osami
*Department of Clinical Laboratory Sciences-College of Pharmacy-Baghdad university
**Department of clinical laboratory sciences-college of pharmacy-Baghdad university
***Rheumatology and Rehabilitation Department-Baghdad medical city

Received : 17/03/2011 Accepted : 29/05/2011

الخلاصة

الفصال العظمي: هو علة تصيب المفاصل و يتميز بحالة تدهور تدريجي و مستمر للغضاريف المتمفصلة؛ و تعتبر السمنة واحدة من العوامل المتعددة التي تساهم في حدوث الفصال العظمي.

إن غالبية الأشخاص الذين يعانون من السمنة يكون لديهم مستوى اللبتين عالي و هذا يشير إلى وجود مايسمى بـ(Leptin Resistance) كآلية لحدوث السمنة في هذه الحالة.

تم جمع عينات من (80) مريضاً تتراوح اعمارهم بين (45-55) سنة و معدل أعمارهم (52.34 ±2.12) سنة و تم تقسيمهم الى اربع مجاميع تتألف كل مجموعة من (20) مريضا كالاتي:

المجموعة (آ): المرضى يعانون من السمنة و الفصال العظمي.

المجموعة (ب): المرضى يعانون من السمنة فقط.

المجموعة (ج): المرضى يعانون من الفصال العظمي فقط.

المجموعة (د): المرضى الاصحاء (مجموعةال control).

هناك متغيرات كيميائية حياتية بالإضافة إلى اللبتين تلعب دور مهم في حدوث السمنة و بالتالي الفصال العظمي منها: الكوليسترول الكليسيريدات الثلاثية و الدهون البروتينية مثل: (البروتين الدهني عالي الكثافة و البروتين الدهني واطئ الكثافة).

بينت هذه الدراسة وجود ارتفاع في مستوى اللبتين و البروتينات الدهنية الواطئة الكثافة في أمصال الأشخاص الين عانوا من السمنة و الفصال العظمي الذين كان مؤشر البدانة لديهم أكثر من 30كغم\م^2 .

ABSTRACT

Osteoarthritis (OA) is a joint disorder characterized by progressive deterioration of articular cartilage.

Obesity (OB) is one of many factors that participate in developing OA. Most obese (ob) subjects have high leptin (L) level suggesting "leptin resistance" as a mechanism of OB in this condition.

Other biochemical parameter in addition to L are lipid profile (LP) including cholesterol (C), triglycerides(TG), lipoprotein(Lp) such as high &low density lipoproteins (HDL,LDL) that play an important role in OB.

In this study eighty individuals were selected, divided into four groups twenty in each group.The age ranged from (45 to 55) years with mean value ± standard mean of error(52.34±2.12).

Group (A): OB+ OA.

Group (B): OB.

Group (C): OA.

Group (D): Neither OB nor OA as control (c).

This study shows an elevation in L, LP except HDL serum level in obese osteoarthritis (OOA) whose their body mass index (BMI) more than (30) measured by weight in kilograms per height square meters (Kg/m^2).

INTRODUCTION

Obesity is a growing health problem regarded as a pandemic with potentially disastrous consequences for human. In 2006 about one quarter in UK were obese; their body mass index > 30 Kg/m2 compared with 7% in 1980 &16% in 1995 (1)

Obesity is a state of excess adipose tissue mass & white adipose tissue, has been viewed as a passive depository of energy and as a protective mechanism for heat loss (2).

Adipocytes are able to produce & secrete a wide number of molecules including classical cytokines such as interleukin-one & six (IL- 1 & IL-6), tumor necrosis factor – alpha (TNF-α) in addition to noval factors adiponectin, resistin, visfatin, vaspin &Leptin ,all called adipokins(3,4,5).

Leptin is a peptide in nature, its molecular weight 16 KDa encoded by obese gene & mainly produced by adipocytes and to a lesser extent other organs (6,7).

Leptin expression is prevalently regulated by food intake, hormones and cytokines (8), also its level is directly correlated with insulin and negatively with glucocorticoides (9, 10).

The effect of Leptin on body weight are mediated through hypothalamic center that control feeding behavior and hunger, body temperature and energy expenditure (8) In essence Leptin provides the body with an index of nutritional status (11). Cholesterol(C), triglycerides(TG) blood levels are correlated positively with obesity(12)although obesity represents a strongest modifiable risk factor for osteoarthritis. Osteoarthritis (OA) is a condition characterized by a series of inflammatory processes start as synovitis which is common as an early and late face (8, 10).

Clinically OA is a disorder of diarthroidal joints leads to pain and functional limitation (8).

Radiography shows the presence of osteophytes and joint space narrawing, while histopathologic feature shows alteration in cartilage integrity, progressive loss of articular cartilage(10).

The aim of this study was to find out if there is any relation between Leptin and some Biomediacl parameteres in the blood of Obese patients and the effect of the changes in the levels of these parameters on the joints which may lead to the development of osteoarthritis and to find out if the Leptin is the link between Obesity and Osteoarthritis.

MATERIALS AND METHODS

In this study eighty individuals were selected, divided into four groups twenty in each one (25%).The age ranged from (45 to 55) years with mean value ± standard mean of error(52.34±2.12).

Group (A): OB+ OA.

Group (B): OB.

Group (C): OA.

Group (D): Neither OB nor OA as control (c).

Osteoarthritis is diagnosed by Dr. Mohammed Al-Osami a Rheumatologist in Medical City, Baghdad Teaching Hospital according to the American College of Rheumatology(ACR) (13).

Blood samples assessed in Central Public Health Laboratory in Immunological &Clinical Biochemistry Departments by using kits from SPINREACT - CC to determine TG, C, HDL& LDL calorimetrically while Leptin was analyzed by Enzyme Linked Immune Sorbent Assay

(ELISA). Body Mass Index represents the ratio of the weight of individual in Kilogram (Kg) to the height in square meters (m^2) (14).

Statistical Analysis

The data was analysed on computer statistical program SPSS version 10. The mean $\pm$ SD was also computed for comparison of the results. The comparsion of mean between the groups was tested by student's t test. Results were considered statistically significant if P value is less than 0.05, 0.02, 0.01.

RESULTS AND DISCUSSION

After collection and categorization of data taken for 60 patients who were divided into 3 groups as mentioned above and 20 control persons who mentioned as group D. Statistical analysis was done to find out the relation of Leptin with BMI and other blood parameters (TG, Cholesterol, HDL, LDL) for each group, the results revealed the following:

1- Regarding Leptin with BMI:

- There is a significant positive correlation between Leptin and BMI in group A, when mean level of Leptin (20.12$\pm$1.45) µg/ml, BMI (37.89$\pm$2.34)and P<0.05
- There is a significant negative correlation in group B, between Leptin and BMI when mean of Leptin levels (12.14$\pm$1.26) µg/ml, BMI (22.72$\pm$1.02) and P<0.05.
- There is no significant correlation in group C and D between the Leptin and BMI when means of Leptin level {(15.72$\pm$1.89), (6.44$\pm$098)} µg/ml and BMI (34.66$\pm$1.75), (22.84$\pm$2.31) .

2- Regarding Leptin with TG:

- There is no significant correlation in group A, B, and D between Leptin and TG, Leptin Level means{(20.12$\pm$1.45), (12.14$\pm$1.26), (6.44$\pm$098)}µg/ml and TG {(150.28$\pm$4.22), (133.05$\pm$6.19), (120.1$\pm$3.25)}mg/dl .
- There is positive significant correlation in group C between Leptin and TG, Leptin level means (15.72$\pm$1.89) µg/ml, TG (148.21$\pm$7.25)mg/dl and P<0.1.

3- Regarding Leptin with Cholesterol:

- There is positive significant correlation in group A, B, between Leptin and C when Leptin Level means {(20.12$\pm$1.45),

(12.14±1.26)} µg/ml, C {(218.93±9.22), (196.4±5.29)} mg/dl and P<0.1.

- There is no significant correlation in group C and D between the two mentioned parameters Leptin level mean {(15.72±1.89), (6.44±0.98)} µg/ml, C levels mean{(201.12±8.97), (183.02±7.16)}mg/dl.

4- Regarding Leptin with HDL:

- There is no significant correlation in group A, and D between Leptin and HDL, when mean level of Leptin {(20.12±1.45), (6.44±0.98)} µg/ml and mean of HDL level {(32.78±1.59), (48.98±3.53)}mg/dl.
- There is a significant positive correlation in group B Leptin level mean (12.14±1.26) µg/ml and HDL level mean (41.19±2.88)mg/dl and, P<0.001.
- There is a significant negative correlation in group C between Leptin (15.72±1.89) µg/ml, P<0.0 and HDL mean (36.55±2.11)mg/dl.

5- Regarding Leptin with LDL:

- There is a significant positive correlation between Leptin and LDL in group A, mean of Leptin (20.12±1.45) µg/ml, LDL mean level (150.78±7.11)mg/dl, and P<0.05, and group B when mean Leptin (12.14±1.26) µg/ml, LDL (125.27±8.91)mg/dl and P<0.02 .
- There is no significant correlation between Leptin and LDL in group C Leptin mean level (15.72±1.89) µg/ml and LDL(149.72±6.08) mg/dl and group D when mean level of Leptin (6.44±0.98) µg/ml and LDL (110.21±7.58)mg/dl.

Table -1 showed the level of mean ±SD for each parameter in each studied groups.

Table -1: Levels of Mean ±SD for each parameter in the four studied groups

Group / Parameters	A (OB+OA)	B (OB)	C (OA)	D (Control)
BMI Kg/m2	37.89±2.34	22.72±1.02	34.66±1.75	22.84±2.31
L µg/ml	20.12±1.45	12.14±1.26	15.72±1.89	6.44±0.98
TG mg/dl	150.28±4.22	133.05±6.19	148.21±7.25	120.1±3.25
C mg/dl	218.93±9.22	196.4±5.29	201.12±8.97	183.02±7.16
HDL mg/dl	32.78±1.59	41.19±2.88	36.55±2.11	48.98±3.53
LDL mg/dl	150.78±7.11	125.27±8.91	149.72±6.08	110.21±7.58

The figures below show the correlations:

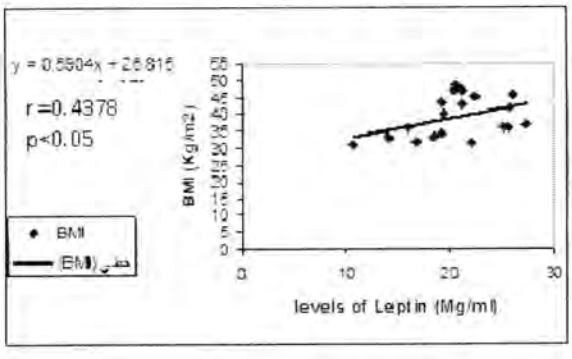

Fig -1: Leptin with BMI in group A

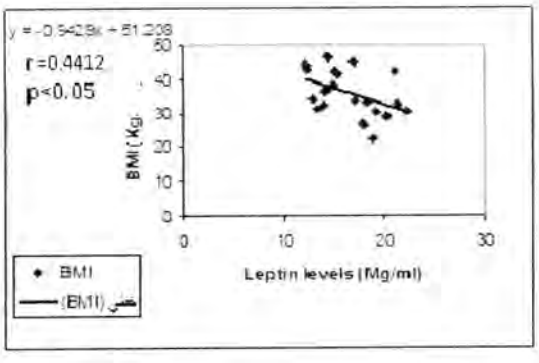

Fig -2: Leptin with BMI in group B

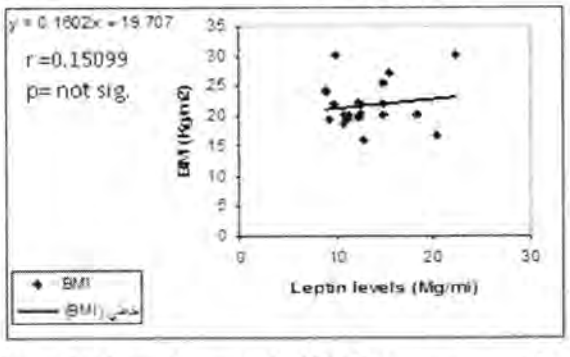

Fig-3: Leptin with BMI in group C

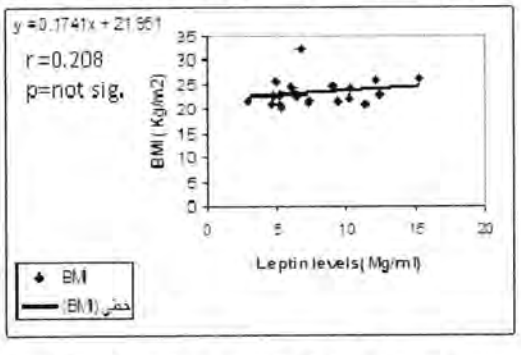

Fig-4: Leptin with BMI in group D

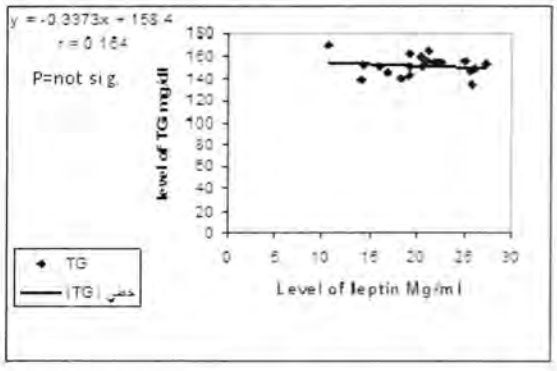

Fig-5: Leptin with TG in group A

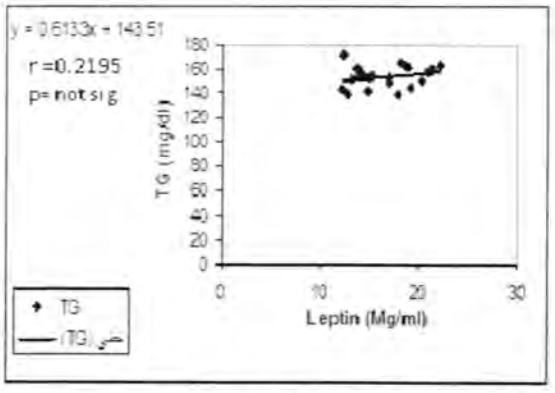

Fig-6: Leptin with TG in group B

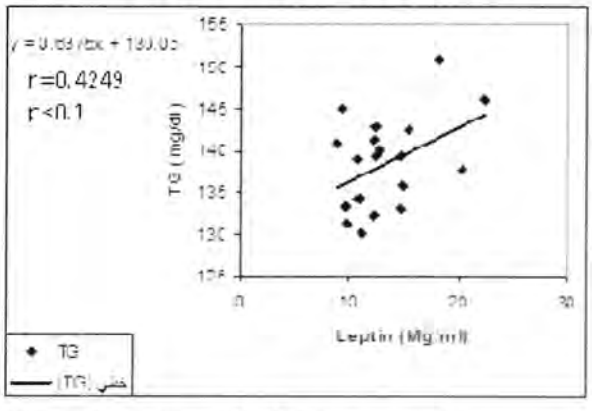

Fig-7: Leptin with TG in group C

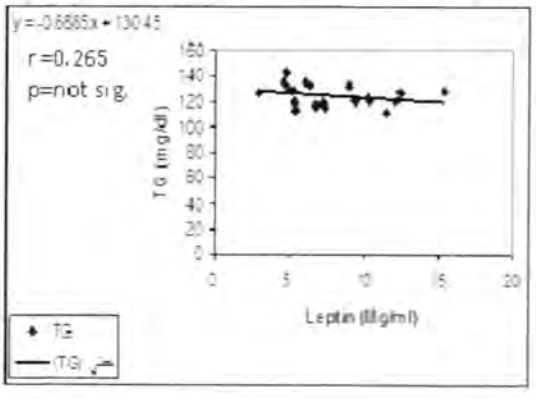

Fig -8:Leptin with TG in group D

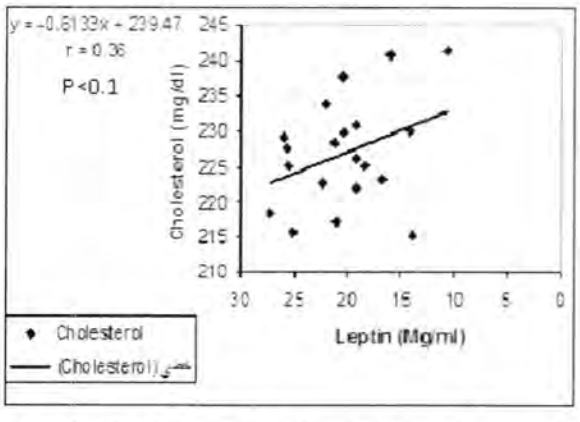

Fig -9: Leptin with Cholesterol in group A

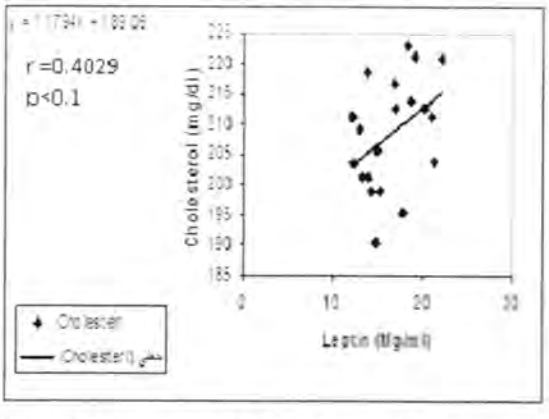

Fig-10:Leptin with Cholesterol in group B

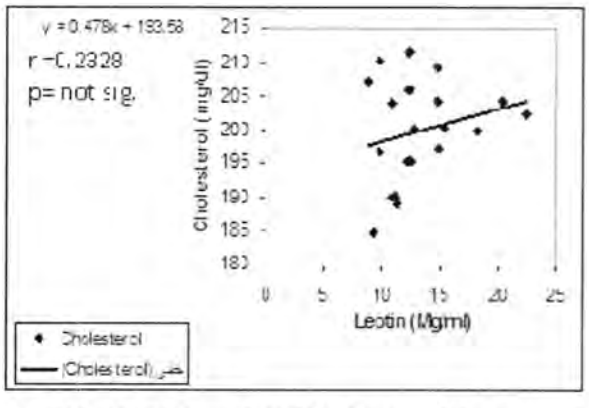

Fig-11: Leptin with Cholesterol in group C

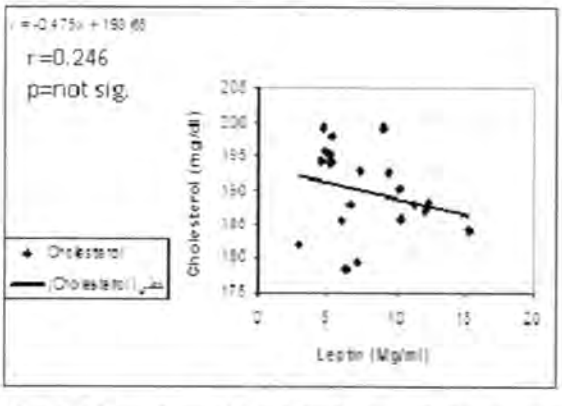

Fig-12:Leptin with Cholesterol in group D

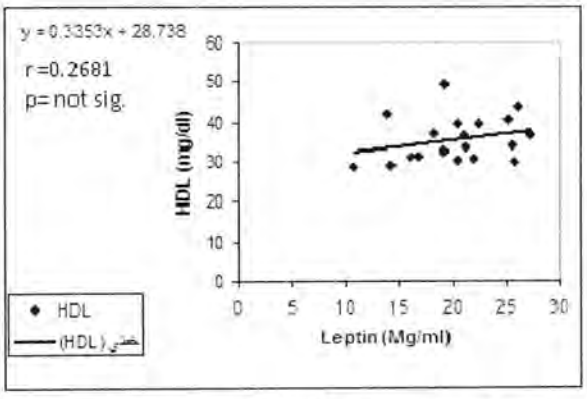

Fig-13: Leptin with HDL in group A

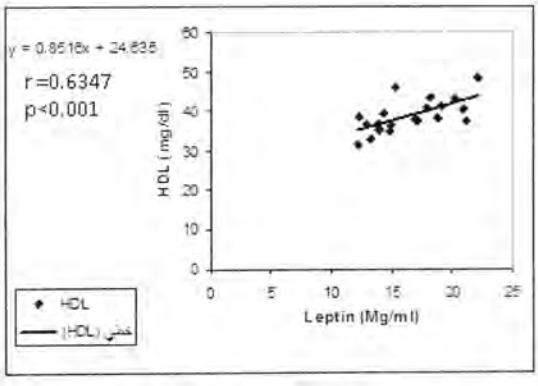

Fig-14:Leptin with HDL in group B

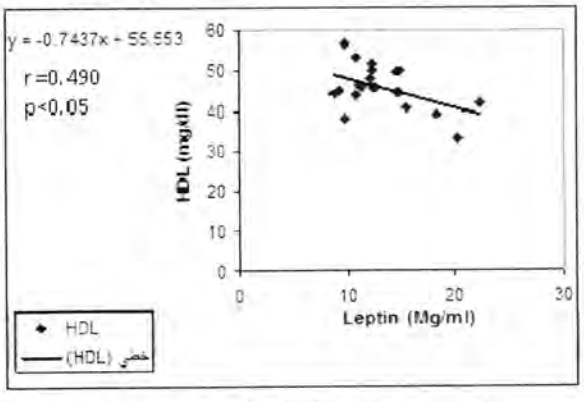

Fig-15: Leptin with HDL in group C

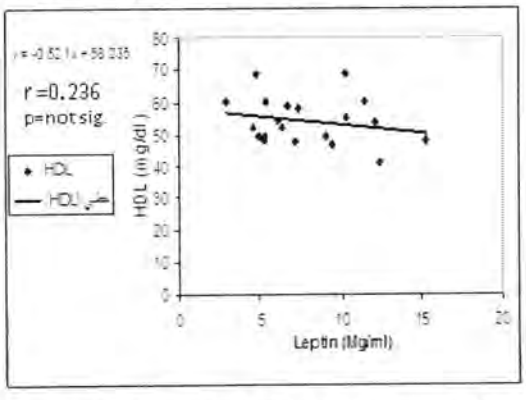

Fig-16:Leptin with HDL in group D

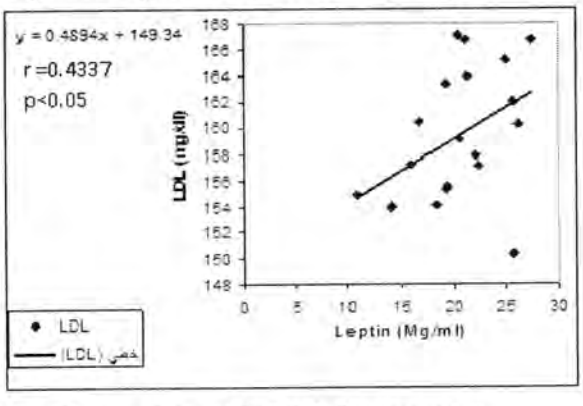

Fig-17:Leptin with LDL in group A

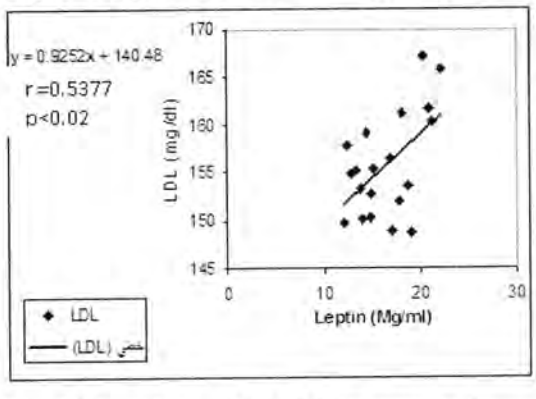

Fig-18:Leptin with LDL in group B

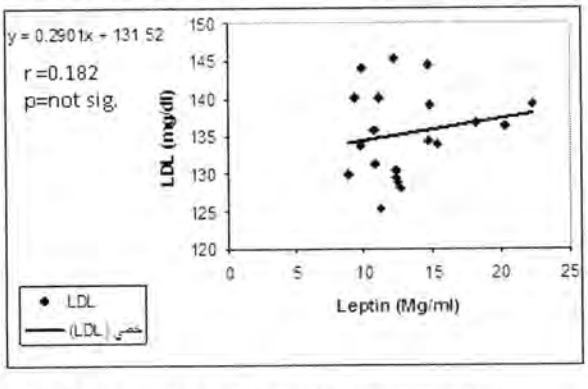

Fig-19:Leptin with LDL in group C

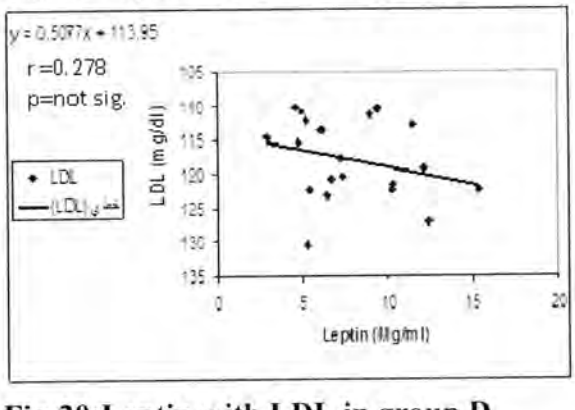

Fig-20:Leptin with LDL in group D

These results are due to: obesity as well as related metabolic diseases are the most common and detrimental illness associated with chronic inflammatory response which characterized by abnormal cytokines production, increase synthesis of acute phase reactant and activation of inflammatory signaling pathway (15).The high Leptin level explained "Leptin resistance" mechanism during OB in many subject(16,17). Previous studies showed that numerous inflammation stimuli modulate both Leptin gene expression and circulating Leptin level (18, 19, 20), although Leptin suppresses expression of hypothalamus neuropeptide Y, a potent appetite stimulating factor leading to increase the expression of melanocyte stimulating hormone(MSH) that act through melanocortin-4 receptor(MC-4R) to decrease appetite(21), thus Leptin activate series of downstream neural pathway that alter food seeking behavior and metabolism(22).Modulation of Leptin level during acute inflammatory stimuli suggest that this adipokin is participating in the development of inflammatory processes such as OA(23,24). Leptin as well as other adipokins is likely involved in the development of articular cartilage degenerative inflammatory diseases (histopathology of OA) by inducing interferon – gamma, interleukin – one level and nitric oxide production via nitric oxide synthase type II in chondrocyte(25,26). Normal chondrocyte synthesized Leptin in amount less than osteoarthritic one, Leptin expression is increased in articular rat joint injected exogenous Leptin which implies a positive feedback regulation (27). Charles EB in 2004 correlates between OB as risk factor for OA through studying mechanical processes versus metabolic one (28).

The decrement of HDL blood level in concomitant with increment of TG is due to the metabolic interaction between these two lipids (29), as well as the activation of TG synthesis rich Lp in liver latterly increase TG in lipid particle alters their metabolism and as result the hydrolysis of TG rich HDL particle enhanced leading to decline HDL level (30) on other hand the LDL level is

increased. The relationship between OA, OB and BMI was determined by others (31). From previous explanations that mentioned above show an agreement with the results that obtained from this study.

So, we can conclude that obesity is considered to be one of the greatest risk factors for osteoarthritis, a progressive musculoskeletal disorder that is characterized by loss of joint cartilage.

Leptin is a protein hormone that is produced by fat cells and responsible for regulating appetite and metabolism. The amount of Leptin in the body

increases as body fat increases with obese people having high concentrations of the hormone circulating in their bodies. The results indicate that Leptin may play an important role in pathophysiology of OA and that Leptin and BMI were independently associated with lipid and lipoprotein profiles.

REFERENCES

1- Hanlon R., Byers M.,Walker B.R. And Macdonald H.M.: Obesity In: Davidson's Principle and Practice of Medicine, 21st. Ed., Colledge N.R., Walker B.R., Ralston S.H., Churchill Livingstone Elsevier. P: 116-121, (2010).

2- Flier J.S., Maratos- Flier E.: Obesity. In: Kasper D.L., Harrison's Principle of Internal Medicine, 16th .Ed. Mc Graw- Hill Company, 64; P: 422-430, (2005)

3- Trayham P.: The biology of obesity. Proc Nutr Soc, 64; 13-18(2005).

4- Fantuzzi G.: Adipose tissue, adipokins and inflammation, J Allergy Clin Immunol.: 115; 911-920(2005).

5- Ahims R.S., Flier J.S.: Adipose tissue as endocrine organ. Trends Endocrinol Metab , 11 ;327-32(2000).

6- Zhang Y, Proenca R, Maffei M, Barone M, Leopold L, Friedman JM: Positional cloning of the mouse obese gene and its human homologue. Nature, 372; 425-32. (1994).

7- Ahims R.S., Flier J.S.: Leptin, A Metabolic Hormone That Functions Like a Proinflammatory Adipokine. Ann Rev Physiol,: 62; 413-37 (2000).

8- Ahima RS, Prabakaran D, Mantzoros C, Qu D, Lowell B, Maratos-Flier E, Flier JS.: Role of Leptin in the neuro- endocrine response to fasting. Nature, 382; 250-52(1996).

9- Kolaczynski J.W., Nyce MR, Considine RV, Boden G, Nolan JJ, Henry R: Acute and chronic effects of insulin on leptin production in human studies in vivo and in vitro. Diabetes,: 45; 699-701(1996).

10- Margetic S., Gazzola C., Pegg G.G., Hill RA.: Leptin a review of its peripheral actions and interactions. Int J Obes Relat Metab Disord.: 26; 1407- 33(2002).

11- Friedman J.M.,Halaas J.L.: Leptin and the regulation body weight in mammals . Nature,: 398; 763, (1998).

12- Rifai N., Wanick G. R.: Lipid, lipoproteins, apolipoproteins and other cardiovascular risk factor In: Burtis C.A., Ashwood E.R., Bruns D.E., Tietz Textbook of Clinical Chemistry 4th ed. vol. 3, Elsevier Saunders, 26: 903-981. (2006).

13- The American College of Rheumatology: Recommendations for Medical Managements of Osteoarthritis of hip and knee, Arthritis Rheum,: 43; 1905, (2000).

14- Bray G.A.: Definition, Measurement, Classification of the syndromes of obesity, In J Obes.; 2: 99-112. (1978)

15- Kadowaki T., Yamauchi T., Kubota N., Kazuo Hara, Kohjiro Ueki, and Kazuyuki Tobe : Adiponectin and adiponectin receptors in insulin resistance, diabetes, and the metabolic syndrome. J Clin Invest: 116(7); 1784-1792., (2006).

16- Emanuelli B, Peraldi P, Filloux C, Chavey C, Freidinger K, Hilton DJ, Hotamisligil GS, Van Obberghen E.: SOCS-3 inhibits insulin signaling and is up regulated in response to tumor necrosis factor-alpha in the adipose tissue of obese mice. J Biol Chem,276; 47944-9 (2001).

17- Gill M.S., Toogood A.A., O Neill P.A., Adams JE, Thorner MO, Shalet SM, Clayton PE: Relationship between GH status, serum leptin and body composition in healthy and GH deficient elderly subjects. Clin Endocrinol (Oxf), 47; 161-167 (1997).

18- Faggioni R., Fantuzzi G., Fuller J., Dinarello, C.A., Feingold, K.R., Grunfeld, C: IL- beta mediates leptin induction during inflammation. Am J Physiol,: 274; 8204- 8 (1998)

19- Sarraf P., Frederich R.C., Turner E.M., Ma G., Jaskowiak N.T., Rivet D.J: Multiple cytokins and acute inflammation raise mouse leptin levels potential role in inflammatory anorexia. J Exp Med, 185; 171-5(1997).

20- Gualillo O., Eiras S., Lago F., M Otero, C Dieguez, J J Gómez-Reino.: Elevated serum leptin concentrations induced by experimental acute inflammation. Life Science, 67; 2433-41(2000).

21- Blum W.F., Englaro P., Hanitsch S., Juul A, Hertel NT, Müller **J**, Skakkebaek NE, Heiman ML,: Plasma leptin levels in healthy children and adolescents dependence on body mass index, body fat mass, gender, pubertal stage and testosterone. J Clin Endocrinol Metab,: 82; 2904-10(1997).

22- Reifi C.M.: Weight loss. In: Kasper D.L. Harrison's principle of Internal Medicine, 16th ed. Mc Graw – Hill Companies,: 36; 233, (2005).

23- Sayer A.A., Poole J., Cox V., Kuh D, Hardy R: Weight from birth to 53 years: A longitudinal study of the influence on clinical hand osteoarthritis. Arthritis Rheum,: 48; 1030-3 (2003).

24- Cicuttini F.M., Baker J.R., Spector T.D.: The association of obesity with osteoarthritis of the hand and knee in women, a twin study. J Rheumatol,: 23; 1221-6 (1996)

25- Otero M., Gomez- Reino J.J., Gualillo O.: Synergistic induction of nitric oxide synthase type II: In vitro effect of leptin and interferon-gamma in human chondrocytes and ATDC5 chondrogenic cells. Arthritis Rheum: 48; 404-9(2003)

26- Otero M., Lago R., Lago F., Juan J. Gómez-Reino and Oreste Gualillo.: Signaling pathway involved in nitric oxide synthase type II activation in chondrocytes: Synergistic effect of leptin with interleukin-1. Arthritis Res Ther,:7; R (581-91), (2005).

27- Dumond H., Presle N., Terlain B., P Netter, D Mainard, and F Berenbaum: Evidence for a key role of leptin in osteoarthritis. Arthritis Rheuma , 48; 3118-29, (2003).

28- Charles E.B.: Obesity as a risk factor for osteoarthritis: Mechanical versus metabolic. Med and health RI, 87(7); 201-4. (2004).

29- Rosenson R.S.: Screening Guideline for dyslipidemia. J Up To Date, 15; 1, (2007).

30- Carr M.C., Brunzell J.D.: A bdoninal obesity and dyslipidemia in the metabolic syndrome: Importance of type 2 diabetes and familial combined hyperlipidemia in coronary artery disease risk. J Clin Endocrinol Metab, 89; 2601-2607, (2004).

31- Codero- MacIntyre Z.R., Metghalchi S., Rosen J., Peters W, Lohman TG, Fernandez ML.: Impact of weight loss on serum leptin in obese post menopausal women. J Appl Res 4; 60-67. , (2004).

Preparation and Characterization of New 1-Nitroso-2-Naphthol Derivatives

Redha H. I. Al-Bayati, Muhannad A. E. Al-Saaedy, Hiba A. M. Al-Nayar and Emad M.E. Al-Mayaa
Department of Chemistry-College of Science-Al-Mustansiriya University

Received : 07/04/2011 Accepted: 29/05/2011

الخلاصة

تم في هذا البحث تحضير مركب الأستر[H_2] من مفاعلة المركب 1-نتروزو-2-نفثول مع أثيل α-برومواستيت ومن ثم مفاعلة مركب الأستر [H_2] مع الهيدرازين المائي (99%) ليعطي المركب[H_3] الذي تم مفاعلته مع بعض الألديهايدات أو الكيتونات ليعطي مركبات الآزو ميثين [H_4-H_7] التي تم تحويلها الى المركبات [H_8-H_9]أو المركبات [H_{10}-H_{11}] وذلك بمفاعلتها مع الأستايل كلورايد أو 2,4-ثنائي نايتروبنزويل كلورايد.من جهة اخرى تم مفاعلة مشتق الهيدرازايد[H_3] مع الفنيل ايزوثايو سيانيت ليعطي مشتق الثايوسميكاربازايد [H_{12}] الذي عند أذابته في هيدروكسيد الصوديوم (2N) ومن ثم اجراء عملية التصعيد ومعادلة ناتج التصعيد بأستخدام HCl ليعطي مشتق الترايازول [H_{13}]. كما تم تحضير المركبات [H_{14}-H_{16}] من مفاعلة مشتق الترايازول [H_{13}] مع بعض الأمينات الثانوية. بالأضافة الى ذلك تم مفاعلة مشتق الثايوسميكاربازايد [H_{12}] مع الأورثو حامض الفسفوريك اللامائي ليعطي المشتق [H_{17}] .كم تم تحضير مشتق الأوكسازول [H_{18}] من مفاعلة مشتق الثايوسميكاربازايد[H_{12}] مع الفيناسيل برومايد.

ABSTRACT

In this work ester compound [H_2] has been prepared by reaction 1-Nitroso-2-Naphthol with ethyl α-bromo acetate , Then ester compound [H_2] reacted with hydrazine hydrate(98%) to gave hydrazide compound [H_3] .The treatment of hydrazide [H_3] with some aldehydes or ketones gave corresponding azo methen compound [H_4-H_7] which converted to compounds [H_8-H_9] or to [H_{10}-H_{11}] when reacted with acetyl chloride or with 2,4-dinitrobenzoyl chloride respectively . on other side , the treatment

of hydrazide [H_3] with phenyl isothio cynate gave thiosemicarbazide derivative [H_{12}] which on dissolve in solution of sodium hydroxide(2N) then neutralized with HCl gave traizole compound [H_{13}] . The reaction of triazole [H_{13}] with suitable secondary amines gave compounds [H_{14}-H_{16}] . As well as , the treatment of thiosemicarbazide [H_{12}] with anhydrous ortho phosphoric acid gave compound [H_{17}] .In addition the reaction of thio semicarbazide [H_{12}] with phynacyl bromide gave compound [H_{18}].

INTRODUCTION

Naphthalene and its derivatives were used as insecticide (1-2), a pesticide for moth ball (1-2), deodorant blocks (1-3) and as skin antiseptic(1-2).

In addition, Naphthalene and its derivatives were used as a precursor for various dyestuffs , pigments, resins, rubber processing chemicals (4-5), tanning agent (4-5) and as wetting agent that effectively disperse colloidal systems in aqueous media(5-6).

These observations promoted us to synthesize the title compounds as possible biologically active agents.

MATERIALS AND METHODES

Melting points were recorded on Gallen-Kamp MFB-Melting, Infrared spectra are obtained using a Shimadzu-2n, FTR-800 spectrophotometer as KBr discs, and the UV. Spectra were performed on Varian, UV-Visible spectrophotometer The ^{1}H-NMR spectra recorded on Brucer 60MHz NMR spectrometer (Jordan) with TMS as internal solvent.

Synthesis of 2-oxo (α-ethyl acetate)-1-nitroso naphthalene [H_2] (7-10)

To a stirring solution of compound[H_1] (0.01mole) and anhydrous potassium carbonate (0.01mole) in absolute ethanol (50ml) , α-bromo ethyl acetate(0.01mole) was added . The mixture was refluxed for (6hrs) and cooled The precipitate was filtered and recrystallized from ethanol-water. Table (1)

Synthesis of 2-oxo[α-acetic acid hydrazide]-1-nitrosonaphthalene[H_3] (7-10)

To a stirring solution of compound[H_2] (0.01mole) in absolute ethanol (30ml) , hydrazine hydrate(99%)(0.015mole) was added . The mixture was refluxed for (4hrs) and cooled . The precipitate was filtered and recrystallized from ethanol. Table (1)

Synthesis of Schiff's base [H_4-H_7] (11)

To a stirring solution of compound [H_3] (0.01mole) in absolute ethanol (15ml) , appropriate aldehyde or ketone (0.01 mole) was added , the mixture was refluxed for (4hrs) and cooled to room temperature . the precipitate was filtered and recrystallized from ethanol. Table (2)

Synthesis of 2-oxo[acetic acid-N-acetyl-N-(1-chloro-1-alkyl-1-aryl methyl)hydrazide]-1-nitroso naphthalene [H_8-H_9](12)

To a stirring solution of an appropriate Schiff bases [H_4-H_5](0.005mole) in dry benzene(15ml),acetyl chloride(0.005mole) in dry benzene(10ml) was added dropwise ,The mixture was refluxed for one hour, after cooling, colored crystals were precipitate and recrystallized from benzene. Table (3)

Synthesis of 2-oxo[acetic acid-N-(3,5-dinitrobenzoyl)-N-(1-chloro1-alkyl -1-aryl methyl)hydrazide]-1-nitroso naphthalene [H_{10}-H_{11}] (12)

To a stirring solution of an appropriate Schiff bases [H_6-H_7] (0.005 mole) in Dry benzene(15ml) , 3,5-dinitrobenzoyl chloride (0.005mole) in dry benzene (10 ml) was added dropwise ,the mixture was refluxed for one hour , after cooling, if the product was oily , The precipitate was filtered and recrystallized from benzene. Table (4)

Synthesis of 2-oxo(acetic acid-N-phenylthiosemicarbazide)-1-nitroso naphthalene [H_{12}] (13-14)

To a suspension of [H_3] (0.01 mole) in dry benzene (3o ml) , phenyl iso thio cynate (0.012 mole) was added and the reaction mixture was

refluxed for (5hr). After cooling , the solid obtained was filtered off washed with petroluim ether and recrystallized from ethanol/$CHCl_3$. Table (1)

Synthesis of 2-methoxy(2'-mercapto-1',3',4'-triazol-5'-yl)-1-nitroso naphthalene [H_{13}] (13-14)

Compound [H_{13}] (0.01 mole) was dissolved in NaOH (30ml , 2N) and heated on a water bath for (2hr) cooled and the reaction mixture filtered , and the filtrate neutralized with diluted HCl . the solid obtained was filtered off and recrystallized from ethanol. Table (6)

Reaction 0f 2- oxymethyl (2'-mercapto-1',3',4'-triazol-5'-yl)-1-nitroso naphthalene with secondary amines [H_{14}-H_{16}] (15-16)

To a stirring solution of compound [H_{13}] (0.00 mole) in dry dioxan(5ml) , a solution of suitable secondary amine (0.003 mole) in dry dioxan (5ml) was added . The mixture was refluxed for (4hrs) .After cooling the precipitate was filtered and recrystallized from methanol . Table (5)

Synthesis of 2-oxymethyl (2'-(N-phenylamino)-1',3',4'-thiadiazole-5'-yl) -1-nitroso naphthalene [H_{17}] (13-14)

The thiosemicarbazide [H_{12}](0.01mole) was added gradually with stirring to anhydrous ortho phosphoric acid(20ml) at 120°C during (30min) . The reaction mixture was heated with stirring at 120°C for another (30min) ,cooled poured onto crushed ice and the precipitate formed was filtered, washed thoroughly with water , dried and recrystallized from Ethanol-Water. Table(6)

Synthesis of 2-oxo[acetic acid-N-(3',4'-diphenyl-1',3'-oxazole-5'-yl) hydrazide] [H_{18}] (17)

A mixture of [H_{13}](0.01mole] and phenacylbromide (0.01mole) in ethanol (30ml) was refluxed for (6hr) .cooled and neutralized with ammonium hydroxide solution. The precipitate was filtered off , washed with water . dried and recrystallized from methanol giving [H17] as white solid . Table (1)

Table-1: Physical properties of compounds [H_2-H_3,H_{12},H_{18}].

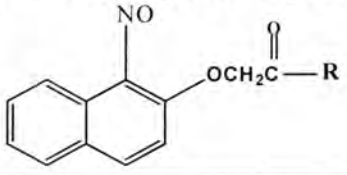

Comp.	R	M.P. C°	Yield %	Purification solvent
H_2	$-OC_2H_5$	118	73	Ethanol-Water
H_3	$-NHNH_2$	230 decomp.	94	Ethanol
H_{12}	-NHNHCSNHPH	122	80	ethanol/$CHCl_3$
H_{18}	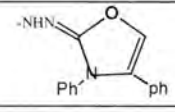	218 decomp.	72	Methanol

Table-2: Physical properties of compounds[H_4-H_7].

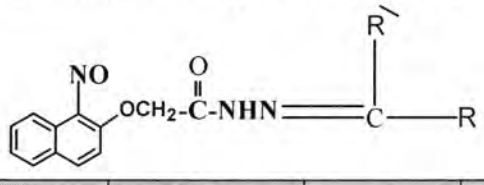

Comp.	R	R'	M.P. C°	Yield%	Purification solvent
H_4	CH_3	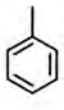	278	86	Ethanol
H_5	CH_3	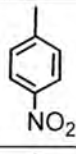	254	92	Ethanol
H_6	H	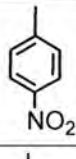	290	90	Ethanol
H_7	H	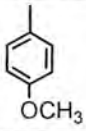	236	76	Ethanol

Table-3: Physical properties of compounds [H_8-H_9].

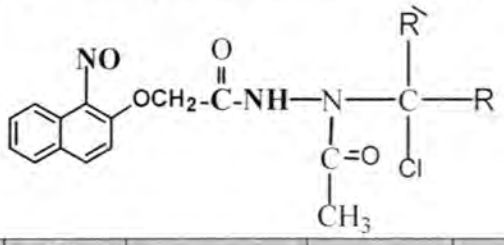

Comp.	R	R`	M.P. C°	Yield%	Purification solvent
H_8	CH_3	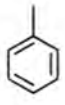	66	72	Benzene
H_9	CH_3	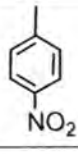	93	58	Benzene

Table-4: Physical properties of compounds[H_{10}-H_{11}].

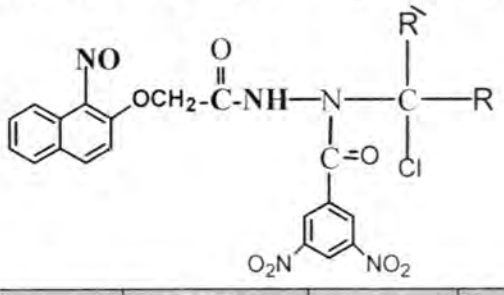

Comp.	R	R`	M.P. C°	Yield%	Purification solvent
H_{10}	H	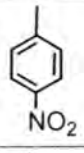	105	56	Benzene
H_{11}	H	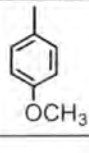	80	52	Benzene

Table-5: Physical properties of compounds[H_{14}-H_{16}].

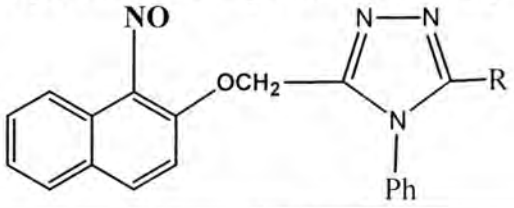

Comp.	R	M.P. C°	Yield	Purification solvent
M_{14}	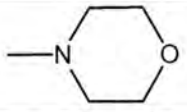	124	62	Methanol
M_{15}	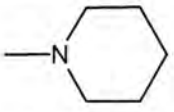	112	74	Methanol
M_{16}	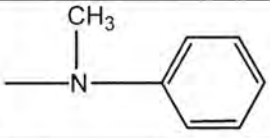	146	48	Methanol

Table-6: Physical properties of compounds[H_{13},H_{17}].

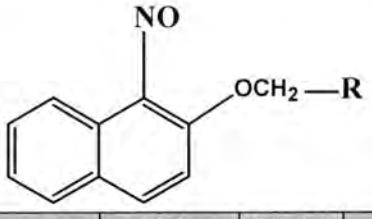

Comp.	R	M.P. C°	Yield %	Purification solvent
H_{13}	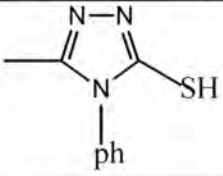	256	65	Ethanol
H_{17}	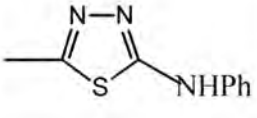	242	48	Ethanol-Water

RESULTS AND DISCUTION

The preparation of the titled compounds was carried out according to the following scheme:-

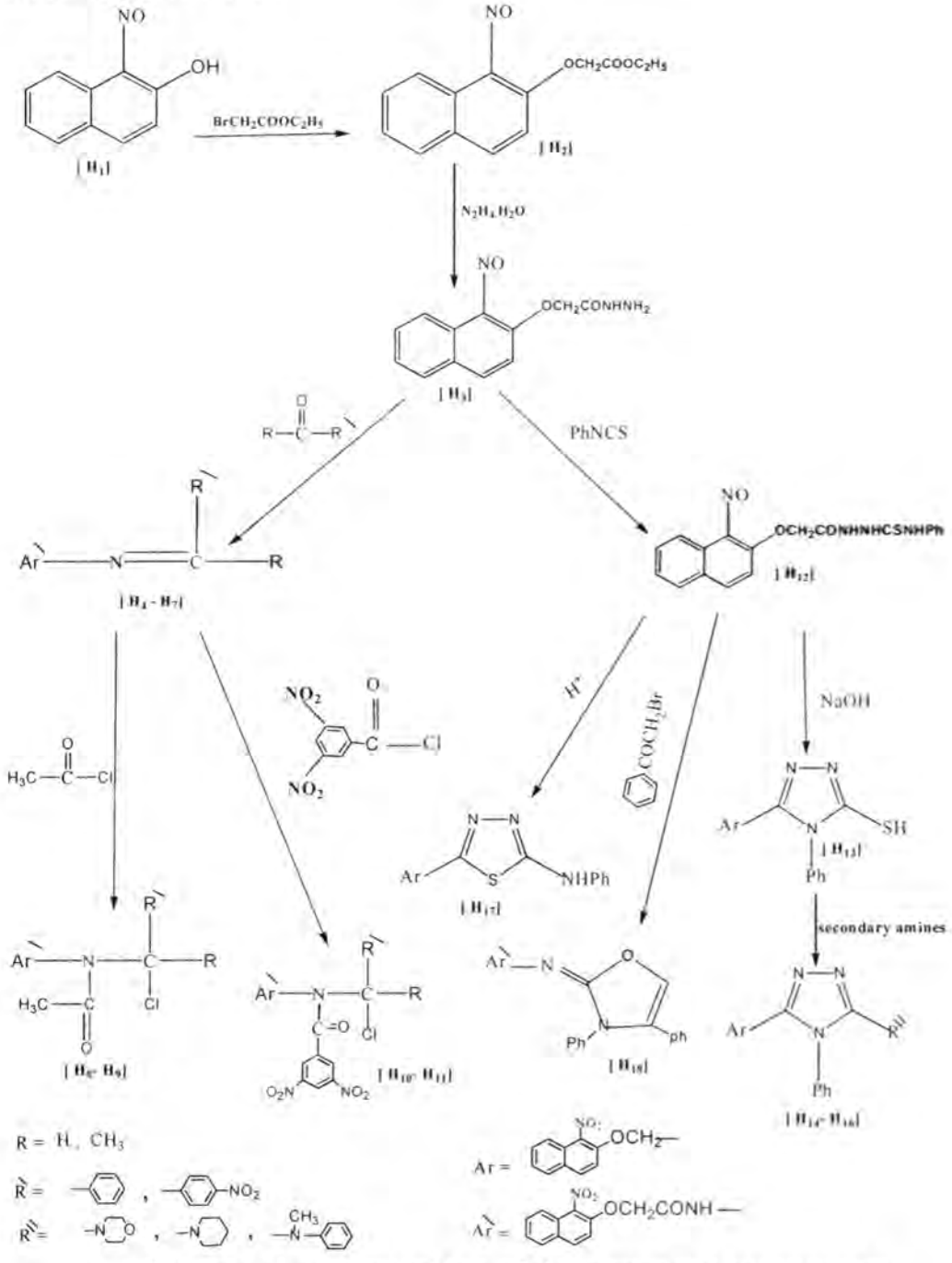

Scheme -1 : preparation of the prpeared compounds

Compound [H_1] was alkylated with ethyl α- bromo acetate in the presence of sodium bicarbonate to give ester derivative [H_2],The IR. Spectrum of compound [H_2] clearly showed the disappearance of the hydroxide (OH) vibration band of the starting material [H_1] at (3400 cm^{-1}) , combined with the appearance of vibration band at (1720 cm^{-1}) due to carbonyl group (C=O), and at(1170 cm^{-1}) due to (OC_2H_5) group as well as appearance of (C-H) aliphatic bands at (2860-2940cm^{-1}) , U.V.spectra of compounds[H_2] showed two intense maxima at (241.5-260.3nm) and (288-327.4nm) which belonged to (n-π*) and (π -π*) transitions respectively. table(7).

Then treatment of ester [H_2] with hydrazine hydrate (99%) yielded acid hydrazide [H_3]. The IR. Spectrum of compounds [H_3] showed the appearance of characteristic vibration bands near (3320 and 3180 cm^{-1}) due to the asymmetrical and symmetrical (N-H) stretching vibration , and at (1665 cm^{-1}) due to carbonyl group which appear at (1720 cm^{-1}) in ester [H_2].U.V.spectra of compounds[H_3] showed two intense maxima at (232.4-272.1nm) and (288.2-316nm) which belonged to (n-π*)and(π -π*) transitions respectively.table(7) .

The condensation of the hydrazide [H_3] with aldehyde or ketone in absolute ethanol gave the Schiff bases[H_4-H_7] were indicated by the presence in their I.R spectra of the azomethine (CH=N) stretching band at (1620cm^{-1}) combined with the disappearance of (NH_2) stretching bands.table(8). U.V.spectra of Schiff bases mostly showed two intense maxima at (240.7-279.2nm) and (286.5-334.5nm) which belonged to (n-π*)and(π-π*) transitions respectively. table(8).

Also treatment of the synthesized Schiff bases [H_4-H_7] with acid chloride gave [H_8-H_{11}](schem 1) in which the two groups (Cl and ArCO) were introduced in the same steps of the reaction.This reaction was followed by disappearance of absorption bands of (CH=N) in (1620cm^{-1}) combined with appearance vibration bands at (1710-1690cm^{-1}) and (730cm^{-1}) caused by (C=O) and (C-Cl) respectively.table(9) . U.V.spectra of compounds [H_8-H_{11}] mostly showed two intense maxima at (241.3,278.2nm) and (286-336nm) which belonged to (n-π*)and(π -π*) transitions respectively.table(9). In addition of I.R and U.V. spectra the structure of compound [H_9] have

been characterized and identified on the basis of ^{1}H-NMR spectrum (table 11),The ^{1}H-NMR spectrum of compound[H_9] show the following signals:
(S,3H) at δ(2.04ppm) that could be assigned to three protons of methyl group (CH_3).
(S,3H) at δ(2.3ppm) that could be assigned to three protons of another methyl group of ($COCH_3$).
(S,2H) at δ(4.8ppm) that could be assigned to two protons of methylene group (CH_2).
(S,1H) at δ(7ppm) that could be assigned to one proton of amide group(-CONH).
(m,10H) at δ(7.4-8.3ppm) that could be assigned to ten protons of aromatic rings.

As well as treatment the compound [H_3]with phenyl isothiocynate in dry benzene to gave a compound [H_{12}]. IR.spectra showed the carbonyl group(C=O)stretching band at 1665cm^{-1} , (N-H) stretching band at 3180,3190cm^{-1} , U.V.spectra showed intense maxima at(212.4-278.1nm) and (287.3-296.6nm) belonged to n-π* and π-π* respectively.table(7).

The treatment of compound [H_{12}] with a solution of NaOH (2N)gave [H_{13}] . I.R.spectra showed two new bands in regions 2600 and 1590 cm^{-1} which belonged to (S-H) and (C=N) respectively.U.V. spectra of compound [H_{13}] showed intense maxima at (215-278.4nm) and (288-295.6nm) due to n-π* and π-π* respectively.table(7). In addition of I.R and U.V. spectra the structure of compound [H_{13}] have been characterized and identified on the basis of ^{1}H-NMR spectrum (table 10).The ^{1}H-NMR spectrum of compound[H_{13}] show the following signals: The ^{1}H-NMR spectrum of compound[H_{13}] show the following signals:
(S,1H) at δ(4.02ppm) that could be assigned to proton of thiol group (SH).
(S,1H) at δ(5.6ppm) that could be assigned to two protons of methylene group of (CH_2).
(m,11H) at δ(7.2-7.9ppm) that could be assigned to eleven protons of aromatic rings.
On other hands the reaction of [H_{13}] with different secondary amines in dry dioxan gave compounds [H_{14}-H_{16}], IR.spectra showed the(C-N) group stretching band at (1150-1175cm^{-1}), and clearly showed the presence of

(CH_2) absorption bands at 2980cm^{-1} for asymmetrical and at 2870 for symmetrical stretching band , U.V.spectra showed intense maxima at (215-234nm) and (286.2-308nm) belonged to n-π^* and π-π^* respectively. Table (10). In addition of I.R and U.V. spectra the structure of compound [H_{16}] have been characterized and identified on the basis of ^{1}H-NMR spectrum (table 11), The ^{1}H-NMR spectrum of compound[H_{16}] show the following signals:

(S,3H) at δ(2.9ppm) that could be assigned to protons of methyl group (CH_3).

(S,1H) at δ(4.8ppm) that could be assigned to two protons of methylene group of (CH_2).

(m,16H) at δ(6.4-7.9ppm) that could be assigned to sixteen protons of aromatic rings.

The treatment of compound [H_{12}] with ortho phosphoric(20ml) gave [H_{17}].I.R.spectra showed new band in regions 1610 cm^{-1} which belonged to (C=N) , U.V.spectra showed intense maxima at (205.1-237.5nm) and(281.6-307nm) belonged to n-π^* and π-π^* respectively.table(7).

The reaction of [H_{13}] with phenacyl bromide in dry ethanol gave compound [H_{18}], IR.spectra showed the carbonyl group(C=O)stretching band at 1660cm^{-1} , (N-H) stretching band at 3180cm^{-1} , U.V.spectra showed intense maxima at (220.4-233nm) and(275.3-300.2nm) belonged to n-π^* and π-π^* respectively.table(7). In addition of I.R and U.V. spectra the structure of compound [H_{18}] have been characterized and identified on the basis of ^{1}H-NMR spectrum (table 11), The ^{1}H-NMR spectrum of compound[H_{18}] show the following signals:

(S,1H) at δ(3.6ppm) that could be assigned to proton of methylene group (CH_2).

(S,1H) at δ(4.8ppm) that could be assigned to proton of (=CH) group.

(m,2oH) at δ(6.5-8.2ppm) that could be assigned to twenty protons of aromatic rings.

(S,1H) at δ(7.2ppm) that could be assigned to two protons of (NH)group.

Table -7: Spectra data for compounds[H_2-H_3, H_{13} , H_{17}-H_{18}]

Comp No.	UV. (acetone) λ_{max} nm	Characteristic bands IR(cm^{-1},KBr disc)					
		ν(C-H) ar.	ν(C-H) aliph.	ν(-NO) ar.	ν(C=C) ar.	ν(C-O-C) ar.	ν(other) ar.
H_2	241.5,260.3, 288,327.4	3060	2940 2860	1390	1420 1540	1120	(C=O)1720 ,(O–CH_3) 1170
H_3	232.4,272.1, 288.2,316	3060	2940 2860	1390	1420 1540	1120	(C=O)1665, (N-H) 3320/3180
H_{12}	212.4,226.1, 278,287.3, 296.6	3060 3040	2940	1390	1420 1540	1120	(C=O)1665, (N-H) 3190/3180 (O-H) 3320 , (C=S)1210
H_{13}	215.0,278.4, 288,395.6	3060 3040	2940	1390	1420 1540	1120	(N-H) 3210 (S-H) 2600 , (C=S)1180
H_{17}	205.1,237.5, 281.6,307.0	3060 3040	2940	1390	1420 1540	1120	(N-H) 3290 , (C=N)1610
H_{18}	220.4,233, 275.3,300.2	3060 3040	2940	1390	1420 1540	1120	(C=O)1665, (N-H) 3180 , (C=N)1630

Table-8: Spectra data of compounds [H_4-H_7]

Comp No.	UV. (acetone) λ_{max} nm	Characteristic bands IR(cm^{-1},KBr disc)						
		ν(N–H)	ν(C–H) ar.	ν(C–H) alph.	ν(C=O)	ν(C=N)	ν(-NO)	ν(others)
H_4	243.2,278.2, 286.5,325.4	3180	3060	2960 2840	1665	1620	1390	-

H_5	244.2, 278.4,294,33 4.7	3180	3060	2960 2840	1665	1620	1390	($-NO_2$) 1560 1340
H_6	240.7,276.8, 295,334.5	3180	3060	2940	1665	1620	1390	($-NO_2$) 1560 1340
H_7	245.9,279.2, 288.0,328.6	3180	3060	2960 2840	1660	1620	1390	(OCH_3) 1200

Table -9: Spectra data for compounds[H_8-H_{11}]

Comp. No.	UV. (acetone) Λ_{Hax} nH	Characteristic bands IR(cm-1,KBr disc)					
		ν(C-H) ar.	ν(C-H) aliph.	ν(C=O)	ν(C=C) ar.	ν(-NO)	ν(other) cm^{-1}
H_8	243,278.1, 286,325.4	3080	2960 2840	1660	1410 1520	1390	(C(=O)-CH_3)1710 , (C-Cl) 730
H_9	243.7, 277.8, 288,334.7	3080	2960 2870	1660	1410 1520	1390	(C(=O)-CH_3)1710 , (C-Cl) 730 ($-NO_2$) 1560/1340
H_{10}	241.3,278.2, 287,302.5,336	3080 3040	2950	1665	1440 1560	1390	(C(=O)-Ph)1690 , (C-Cl) 730 ($-NO_2$) 1560/1340
H_{11}	244.7,278, 287.3,300,335.4	3080 3040	2960 2860	1665	1440 1560	1390	(C(=O)-Ph)1690, (C-Cl) 730 ($-NO_2$) 1560/1340 , ($-OCH_3$)1200

Table-10: Spectra data of compounds [H_{14}-H_{16}]

Comp. No.	UV. (acetone) Λ_{Hax} nH	Characteristic bands IR(cm-1,KBr disc)					
		ν(C-H) ar.	ν(C-H) aliph.	ν(C=N) ar.	ν(C-N) ar.	ν(-NO)	ν(C-O-C) ar.
H_{14}	215 230.2 304.2	3060	2960 2870	1590	1150	1390	1110
H_{15}	215.3 286.2 308	3060	2960 2870	1690	1150	1390	1110

H_{16}	215.6 234.8 296.1	3060	2960 2870	1600	1175	1390	1110

Table-11: The ^{1}H-NHR spectrum of some prepared compounds

Comp. No.	δ ppm	Type of band	No.of (H)	group
H_9	2.04 2.3 5.6 7.0 7.4-8.3	S S S S M	3 3 2 1 10	$-CH_3$ $-COCH_3$ $-OCH_2$ -CONH ar. ring
H_{13}	4.02 4.8 7.2-7.9	S S M	1 2 11	-SH $-OCH_2-$ ar. ring
H_{16}	2.9 4.8 6.4-7.9	S S M	3 2 16	$-CH_3$ $-OCH_2-$ ar. ring
H_{18}	5.6 4.8 6.5-8.2 7.2	S S M S	1 1 16 1	$-OCH_2-$ =CH ar. ring -NH

REFERENCES

1- Weintraub E. , Gandhi D. , Robinson C. , South Med Journal, 93, 427-429, (2000).

2- Chun T. , Perron J. , Osterhoudt K. , Henreetig F. " Moth ball blue: Confusion in Naphthalene Toxicities and Treatment ",Clin Toxicol , 36, 465, (1998).

3- Amoore J. and Hautala E. "Odor as an aid to chemical safety: Odor thresholds compared with threshold limit values and volatiles for 214 industrial chemicals in air and water dilution". *J. Appl Toxicology* 3 (6): 272–290, (1983).

4- "IARC Monographs on the Evaluation of Carcinogenic Risks to Humans". Monographs on The Evaluation of Carcinogenic Risks to Humans , Some Traditional Herbal Medicines, Some Mycotoxins, Naphthalene and Styrene, V. 82 , P. 367,(2007).

5- Gerd Collin, Hartmut Höke , Helmut Greim "Naphthalene and Hydronaphthalene "in Ullmann's Encyclopedia of Industrial Chemistry Wiley-VCH, Weinheim , (2003) .

6- John Kidd "Observations on Naphthalene, a peculiar substance resembling a concrete essential oil, which is apparently produced during the decomposition of coal tar, by exposure to a red heat". *Philosophical Transactions*, (1821).

7- Abu-Orabi Sultan T., Abu-Naaj Nuha A. Abu-Naaj , Al-momani Lo'ay and Ibrahim Jibril, "Synthesis of Some 1,2,4-Triazole Derivatives" , Jordan J. Chem. , 3 , 4 , 337-347 , (2008).

8- Upadhyay A.P. , Srivastava S.K. and Srivastava S.D. ,"Neat Reaction and Conventional for the Synthesis of 4-Oxo-Thiazolidines and their 5-Arylidines Derivatives and its Antimicrobial Activity" , Jordan J. Chem., 5 , 1 , 1-11, (2010).

9- Muhi-Aldeen Zuhair, Ghada Juma'a , Al-Kassi Elham and Lina Nouri,"Antimicrobial Activity of Some New Oxadiazole Derivatives", Jordan J. Chem. , 3 , 3 , 233-243 ,(2008).

10- Gadaginamath G. S. , Patil S. A. and Shyadligeri A. S.,"Synthesis and Antimicrobial Activity of 1,3,4-Oxadiazolyl/2,5-Dimethylpyrolyl/1,2,4-Triazolylmethoxybisbenzylpiperazine-2,5-diones.",Indian J. chem. , 35B , 681-684,(1996) .

11- Rajanarender E.,Kalyan E. Rao, Reddy A.Siva Rami,"A Simple Method for the Synthesis of 5-Isoxazolyl-4-thioxo-1,3,5-Benzoxadiazocines', J. Hetrocyclic Chem. , 46 ,134,(2009).

12- Hussein F.A., Ali Emad T., Najim Sabah T. and Tawfiq Maysoon T.,"Synthesis of Some Barbturate Derivatives Via Schiff's Bases", Irq. J. Chem, 26, 261-274. 2, (2000).

13- Nargund L.V., Reddy G.R., and Hariased V.,"Synthesis and Antibacterial Activity of a series 1-Aryl-2-Mercapto-5-[4-Acetamidophenoxy)methyl]-1,3,4-triazoles,Thiadiazoles and 2-[4-(Acetamidophenoxy)Carbonyl]-3,4,5-Trissubstituted Pyrazoles", Ind. J. Chem. 35B, 499-502, (1996).

14- Albar H. A., Makki M. S. I. and Faidallah H. M.,"Synthesis of Hetrocyclic Compounds form δ-unsaturated 1,3 –Diketoesters" , Ind. J. Chem. 35B, 23-29, (1996).

15- Aouad Mohamed R.,Al-Bayati Redha H. I., Sharba Husein K.,"Synthesis and Spectroscopic Study of Some New Tiosemicarbazides 1,2,4-Triazoles and Related Compounds",Iraqi J. of Chem.,28,3, , 571-581 ,(2002).

16- Al-Glennon Richarad A.,"A Convenient Synthesis of 3-Aryl-1,2,3-Triazolo[4,3-c]Quinolines,J.Hetrocyclic Chem., 27, 497-498,(1990).

17- Sayed H. El-Tanahy, Moly E. Abdel-Fattah and Ibrahim M. El-Deen,"Synthesis and Biological Activity of Some 4-Benzyl-1(2H)-Phthalazinone Derivatives", Indian Journal of Chemistry, 35B, 1067-1072, (1996).

Preparation of Poly [N- Aryl Sulfonamide Maleimide Derivatives]

Firyal M. A. Al-Salami and Lekaa H.
Al-Mustansiriyah University-College of Science-Department of Chemistry

Received : 27/03/2011 Accepted: 29/05/2011

الخلاصة

تم في هذا البحث تحضير مالي اميدات N-سلفون ايمايد وبوليمراتها المقابلة من تفاعل ملح الصوديوم الماليئمايد مع حامض كلوروسلفونيك ثم مفاعلتها مع امينات ثم بلمرتها بالجذور الحرة باستخدام ازوبيوتيرنايترايل بدرجة 70م° والدايوكسان مذيبا. درست الصفات الفيزيائية للبوليمرات المحضرة, وشخصت بواسطة الاشعة تحت الحمراء والاشعة فوق البنفسجية. ان بوليمرات السلفوناميد المحضرة والمتوقعة كمواد دوائية ومضادات حياتية ومضادات للبكتريا لاحتوائها على مجموعة السلفون امايد والايمايد معا لذا فقد قيست التحاليل الحرارية للبوليمرات المحضرة ودرجة الانتفاخ المئوية. ودرست سرع التحرر الدوائي لبولي(N-امبيسلين سلفون امايد مالي ايمايد) C_{14} PH=7.4وبدرجة حرارة 37م°.

ABSTRACT

In this work N- arylsulfonamides maleimides and their corresponding polymers were prepared from reaction of maleimide as N-sodium salt with chloro sulfonic acid, then reacted with aryl amines, the new N- sulfonamide maleimides were polymerized by free radical using Azobisisobuteronitrile at 70 °C with dioxane as a solvent.The physical properties of all prepared polymers were studied and characterized by FTIR and UV. spectroscopy. These new- sulfonamide polymers were exhibit drugs properties as antibiotics after treating bacterial infections due to containing the ($-SO_2NH$) and imide groups. Thermogravimetric analyses of the prepared polymers were measured, and swelling %was studied. and controlled release of ampicillin drug polymer was studied in{PH=7.4}at 37 ^{0}C. some of the prepared polymers are antibacterial agents to overcome shortcomings which is critically important.

INTRODUCTION

In organic chemistry, an imide is a function group consisting of two carbonyl groups bound to nitrogen. These compounds are structurally related to acid anhydrides .The relationship between esters and amide and between imides and anhydrides are analogous, the amine-derived groups are less reactive. In terms of commercial application, imdes are best known as components of high strength polymers(1).

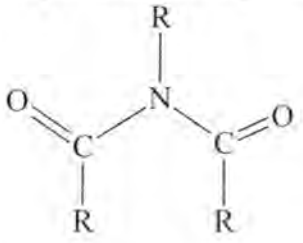

A general linear imide functional group

(Imide) refers to derivation of imide itself (NH) or organic derivation (RN). The organic functional group called an imide contains two acyl groups are attached to NHor NR.

Most imides are derived from dicarboxylic acids and their names reflect the parent acid. Examples are succinimide derived from succinic acid and phthalimide derived from phthalic acid. For imide derived from amines (vs.ammonia). the N-substituent is indicated by a prefix, e.g. N-etheylsuccinimide is derived from succinic acid and ethylamine(1).

Carbodiimides have the formula RN=C=NR, they are unrelated to imides.

The ligand in coordination chemistry known as imide has the formula NH.An imide is an intermediate in nitrogen fixation(2).

Being highly polar, imides exhibit good solubility in polar media. The N-H center for imides derived from ammonia is acidic and can participate in hydrogen bonding. Unlike the structurally related acid anhydrides, they resist hydrolysis and some can even be recrystallized from boiling water(3).

Many high strength or electrically conductive polymers contain imide subunits, i.e. the polyimides.One example is Kapton where the repeat unit consists of two imide groups derived from aromatic (4).

Tetracarboxylic acids are another example of The poly imides polyglutarimide typically made from polymethyl methacrylate (PMMA) and ammonia or a primary amine by aminolysis and cyclization of the PMMA at high temperature and pressure, typically in an extruder.This technique is called reactive extrusion. A commercial polyglutarimide product based on the methylamine derivative of PMMA, called kamax (TM), was produsedby the Rohm and Haas company. The toughness of these materials reflects the rigidity of the imide functional group(5).

Interest in the bioactivity of imide-containing compounds was sparked by the early discovery of the high bioactivity of the Cycloheximide as an inhibitor of protein biosynthesis in certain organism(4-5) Thalidomide is one unfortunate result of this research.A number of fungicides and herbicides contain the imide functionality. Examples include captan, which has been phased out because of its carcinogenic properties, and procymidone(5,6).

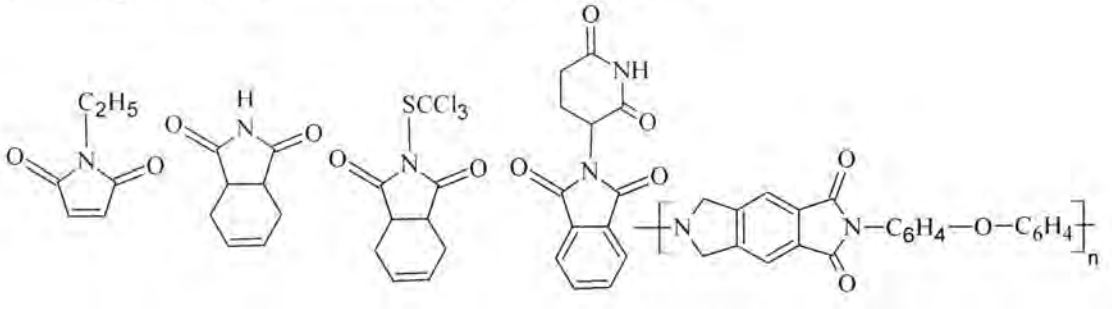

Illustrative imides, from left : N-ethylmaleimide, a biochemical reagent, phthalimide, and industrial chemical intermediate,Captan,a controversial herbicide, thalidomide, a durg that once caused many birth defects, asubunit of kaptan, a high strength polymer used to make" space suits" (5).

Most common imide are prepared by heating dicarboxylic acids or their anhydrides and ammonia or primary amines.The result is a condensation reaction :

$$(RCO)_2O + R'NH_2 \rightarrow (RCO)_2N\,R' + H_2O$$

These reactions proceed via the intermadiacy of amides.The intramolecular reactions of carboxylic acids with amides are far faster than the intramolecular reaction, which is rarely observed.

Certain imides can also be prepared in the isoimide-to-imide Mumm rearrangement (5).

For imides derived from ammonia,the N –H center is acidic. Thus,alkali metal salts are well known, a well-known example being potassium pthalimide. These salts can be alkylated to give N –alkylimides,Which in turn can be degraded to release the primary amine.Strong nucleophiles, such as potassium hydroxide or hydrazine are used in the release step.

The nitrogen in imides is not very basic, which allows it to form stable compoundes with halogens.

Treatment of imides with halogens and base gives the N-halid derivatives. Examples that are useful in organic synthesis are N-chlorosuccinimide and N-bromosuccinimide (6).

It is the responsibility of anyone who administers drugs to show animals to do so in accordance with the regulations on the drug's label.That means giving a drug to an approved animal species, for an approved indication, by one approved route of administration, and at an approved dosage as well as observing the approved with drawal times, unless specifically directed by a veterinarian within avalid veterinarian-client-patient relationship (7).

Owners of show animals would be wise to remember that sum drugs, such as sulfonamides, may be detectable in the urinelonger than the withdrawal time on the product label.It is prudent and many other imides were prepared (8-10).

MATERIALS AND METHODS

Instruments:

- Gallen-Kamp MFB-600 melting point apparatus.
- Electronic spectra measurements using Cintra-5 UV-Visible spectrophotometer.
- Infrared spectrophotometer measurements using SP3-100 Pye-Unicam (600-400 cm-1).
- Viscosity measurements using capillary viscometer type Ostward viscometer, at 30 °C.
- Thermogravimetric analysis using NETSCH Geratebau Gmbtt Model STA-409.

All chemical materials were purchased from Fluka and BDH.

Preparation of N- sodium maleimide (C1)

In a (100 ml) round bottom flask provided with a magnetic bar was placed (5 g) of maleimide which was dissolved in (10 ml) of dioxane ,the 50% of sodium hydroxide was added with vigorous stirring the precipitate was filtered ,then washed with ethanol several time, the sodium maleimide was obtained with high product.

Preparation of N-sulfonyl maleimide (C2)

Asample (5g) of the prepared sodium salt C1 was reacted with chloro sulfonic acid (2.5 ml,0.01 mol) at0 °C the mixture was stirred (1hr) .The product was cooled, and the product was washed by ether for several times.

The physical properties were measured with High yield which equalat to (90%) was obtained.

Synthesis of N-Substituted maleimides (C3-C8)

In a (100 ml) round bottom flask was added (2 g.-0.1mol) of N-Sulfonyl maleimide,dissolved in (10ml) of dry dioxane.

The stochiometric amount of primery amine such as(4- amino pyridine, 2-amino pyrimdine, 2-naphthyl amine ,2,2,6,6 tetra methyl pipridine, para amino benzoic acid,and ampicilline. The mixture was refluxed for (1hr.) the clear solution was cooled to room temperature . The precipitate of N-Sulfonamide maleimide monomers were characterized ,table (1) shows the physical properties of C3-C8.

Table- 1: Physical properties of prepared monomers C3-C8

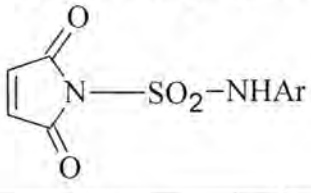

No.	-Ar	Color	Yield %	U.V absorption
C3	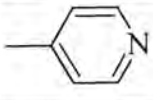 = R_1	Brown dark	80	–
C4	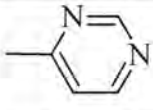 = R_2	Brown dark	90	–

C5	 = R_3	Violet	85	π −π*330
C6	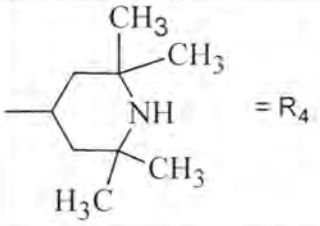 = R_4	Brown	75	π*487n-
C7	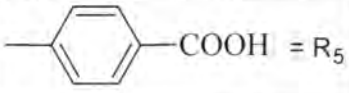 = R_5	White	87	353
C8	Ampicillin =R_6	White	80	269

Ampicillin = 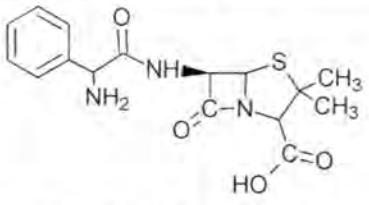

Free radical Polymerization of prepared monomers to C9-C14.

To a screw capped polymerization bottle containing (3g) of N-Sulfonamide maleimide (C3-C8) were added (0.05g) (0.25%) by weight of the monomer concentration of AIBN and 20ml of freshly distilled of dioxane . The clear solution was flashed with pure nitrogen, followed by stream nitrogen gas. The bottle was closed and incubated in water bath at (70^0C) for (2 hrs.).The mixture was cooled and the contents were poured in to a beaker. The Polymer was formed, the coagulated polymer was washed with ethanol and dried in vacuum oven , The physical properties were studied .

Table -2 : Physical properties of prepared sulfonamide maleimide polymers (C9-C14)

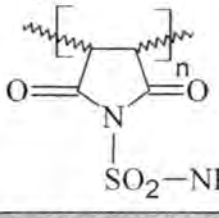

No.	-Ar	Color	CONVERSION %	dl/g.)(η	Softening point
C_9	$-R_1$	brown	80	0.41	350>
C_{10}	$-R_2$	brown	78	0.48	350>

C_{11}	$-R_3$	black	75	0.81	350>
C_{12}	$-R_4$	brown	82	0.71	350>
C_{13}	$-R_5$	yellow	87	0.61	350>
C_{14}	$-R_6$	yellow	81	0.68	350>

Controlled Release Drug Polymer (11-13)

20 mg. of prepared polymer C_{14} was placed in 20 ml of buffer solution with pH7.4 at 37 ^{0}C. At periodic intervals 3ml of solution with tested at 320 nm using UV. Spectrophotometer. The amount of released of Ampicillin was quantified using appropriate calibration curves as shown in Fig.(7).

RESULTS AND DISCUSSION

In this work, sodium maleimide salt was prepared, then converted to N-Sulfonyl maleimide according to the following reaction :-

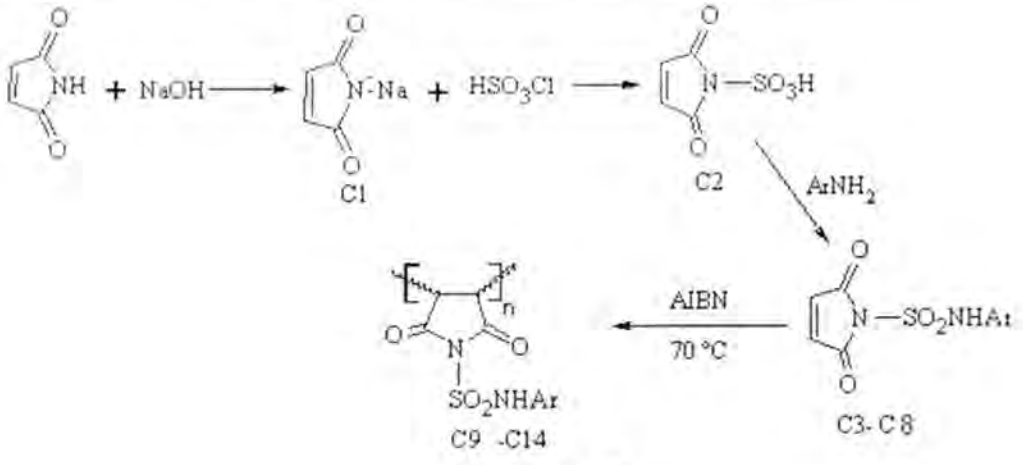

Scheme (I)

The N-Sulfonamid maleimide monomers (C3-C8) were polymerized free radically using AIBN as initiator gave different substituted sulfonoamide maleimide polymers(C9-C14), these sulfonoamide polymers contain the radical SO_2NHAr.Which exhibit as antibiotics to treat bacteria infections by interfering with a bacteriums production.

These new monomers were characterized and physical properties were listed in table (1) and their corresponding polymers were listed in table (2).

FTIR spectrum of N-Sulfonyl maleimide as shown in(Fig 1) indicated the absorption of υSO2 which appeared characteristic absorption at (1388 cm-1) asymetric SO2 and at (1122 cm-1) symmetric SO2and The broad absorption at (3404) due toOH of Sulfonic acid.

Figs.(2-5) showed the FTIR spectrum of prepared N-Substituted Sulfonamide Maleimide monomer which showed the characteristic absorption of υ–NH Sulfonamide at (3292,3335,3263m 3390cm-1) and υ-C=O at (1716-1666,1714-1626,1720-1766,1707cm-1) for maleimide monomers, υSo2 Asym. (1354, 1398, 1392, 1394), υ-So2sym.at (1192,1120,1101,1150) and their corresponding polymers which is the same absorptions with disappering of vinyl υ C=C absorption of maleimide. These prepared sulfonamide maleimide derivatives polymers exhibit outstanding thermal stability, Which are evaluated by thermogravimetric analysis (TGA) which recorder a function of temperature with loss of weight of polymer samples such as C10,C12 as shown in (Fig.8, Fig.9).

Table 3 shows thermal decomposition for typical N-Substituted Sulfonamid maleimide degradation temperature appeared at (141-339 °C) and(279-450°C) this was because high polarity of Sulfonamide group and aromatic groups which exist in polymer, that restrict the mobility of chain, therfore polymer degradated befor melting stage.

Table -3: Weight Loss Decomposition temperature for C10 and C12 poly sulfon amide malimide.

No.	Temp.^{0}C	Weight Loss%	Temp.^{0}C	Weight Loss%	Temp.^{0}C	Weight Loss%
C10	279	9.3	347	14.9	450	24.6
C12	141.1	17.3	277.8	-9.5	339	40.7

The elemental analysis values agreed quite well with the calculated values for the proposed polymer structures.

The hydrolysis of the prepared polymers in basic medium in pH 10 was illustrated as in scheme2.

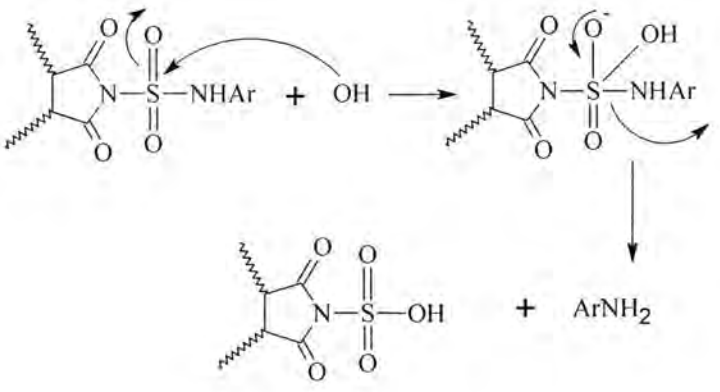

Scheme (2)

Fig.(6) Swelling curve of (C_9-C_{14}) of N-substituted sulfonamide polymers at pH7 at 37 ^{0}C shows the Swelling % through 4 days, we performed dynamic swelling studies. The S% is calculated according to the following releation ship:-

$$S\% = (M_1 - M_0)/M_0 \times 100$$

Where:- M_0 is the mass of dry polymer at time 0.

M_1 is the mass of swollen polymer at time t.

The S% for all polymers (C_9-C_{14}) were ranged between 7-15.8% .

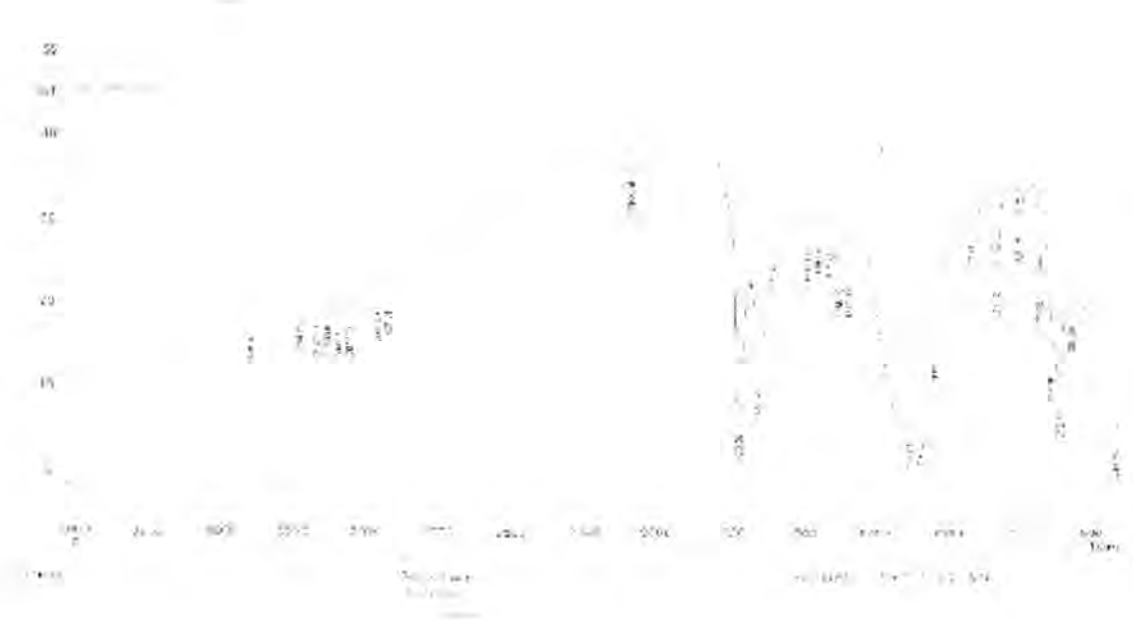

Fig.-1: FT-IR Spectrum of N-2- Sulfonyl maleimide

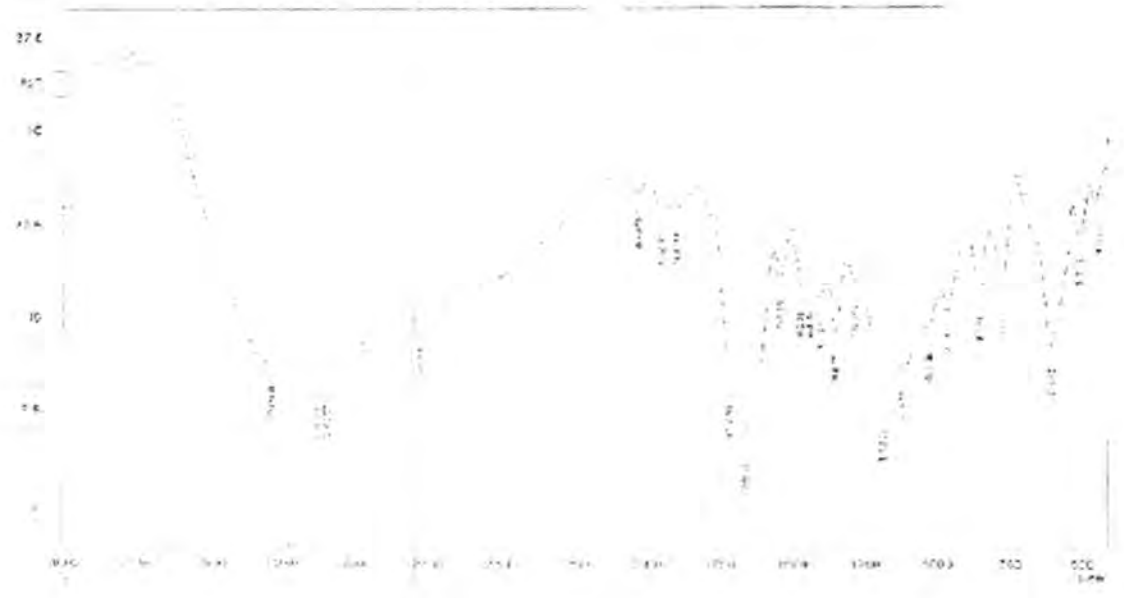

Fig. -2: FT-IR Spectrum of N-2-pyrimidyl sulfonamide maleimide

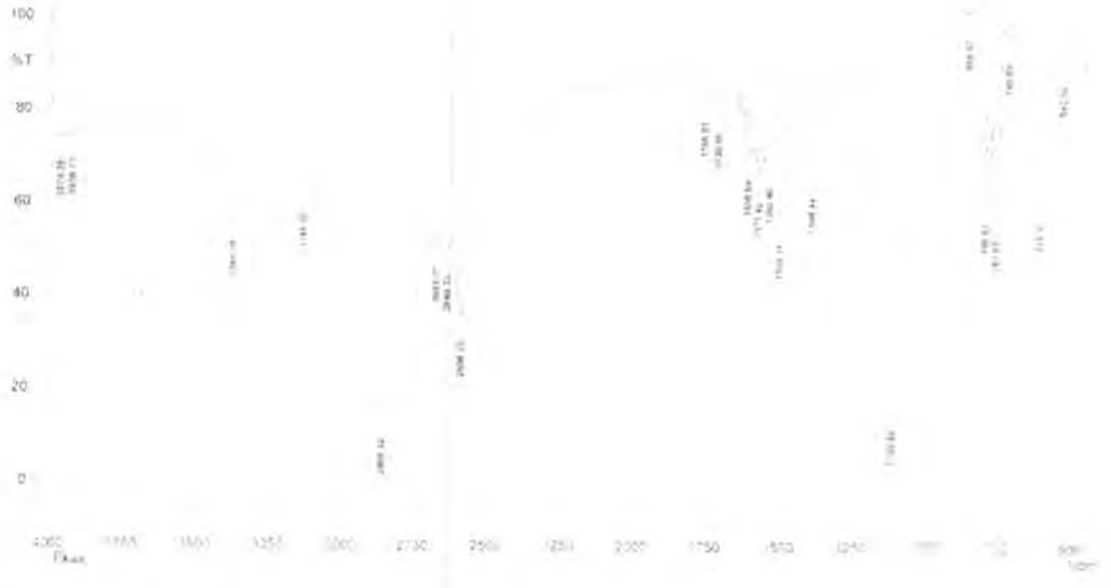

Fig. -3 : FT-IR Spectrum of N-Naphthal sulfonamide maleimide

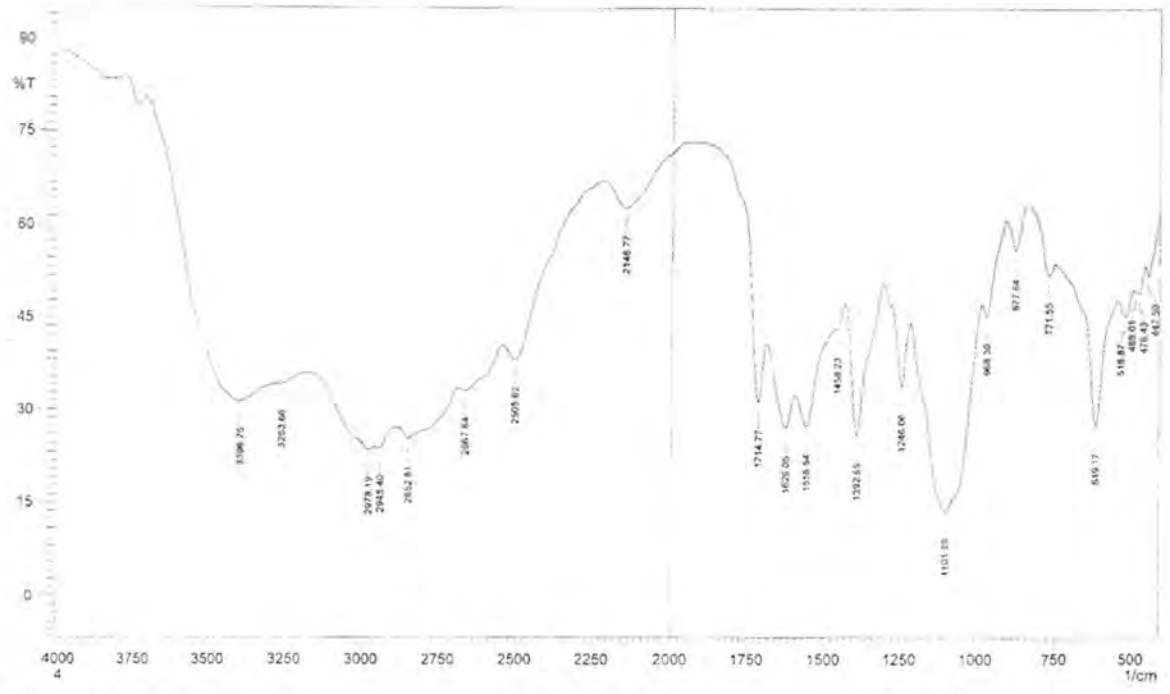

Fig.-4 :FT-IR Spectrum of N-2,2,6,6 tetra methylpipyridine sulfonamide maleimide

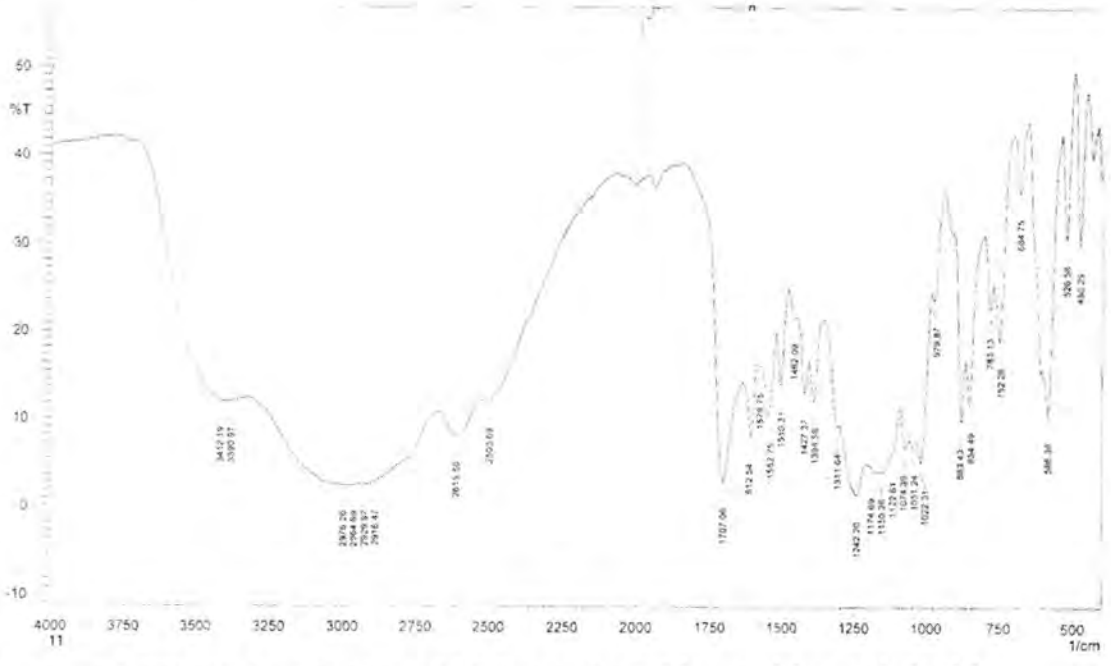

Fig. -5 : FT-IR Spectrum of N-Benzoic sulfonamide maleimide

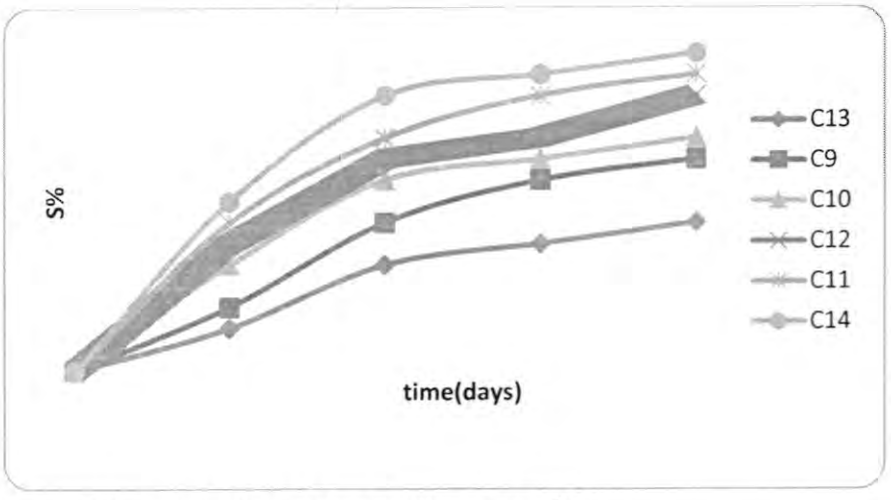

Fig. -6 : Swelling of C9-C14 at pH7 at 37 ^{0}C

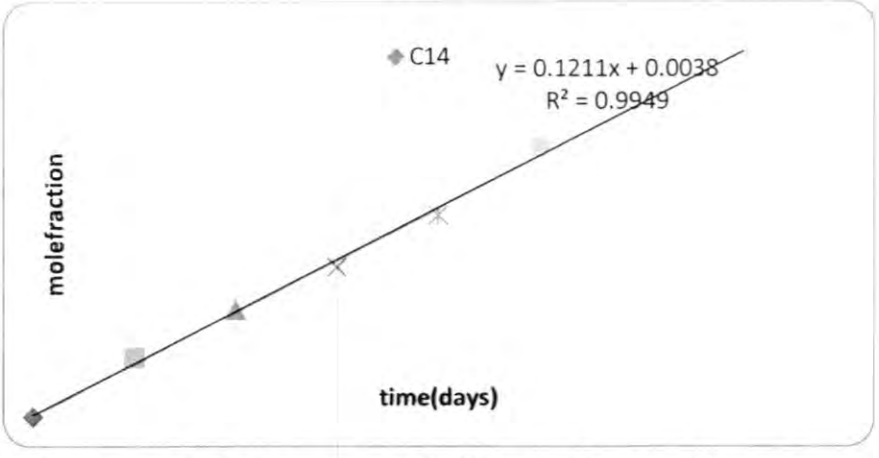

Fig. -7: Controlled Release Ampicillin Sulfonamide polymer C_{14} in pH 7.4 at 37 ^{o}C

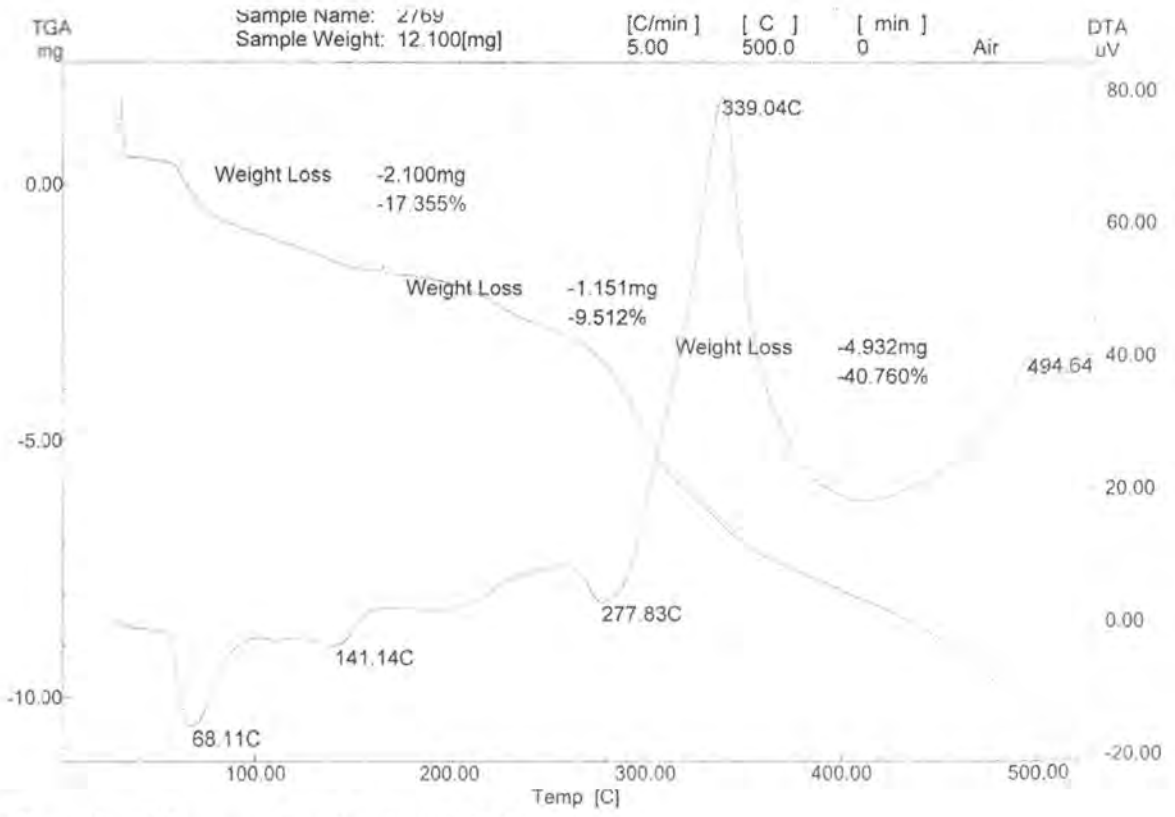

Fig. -8: Thermal analysis of C12

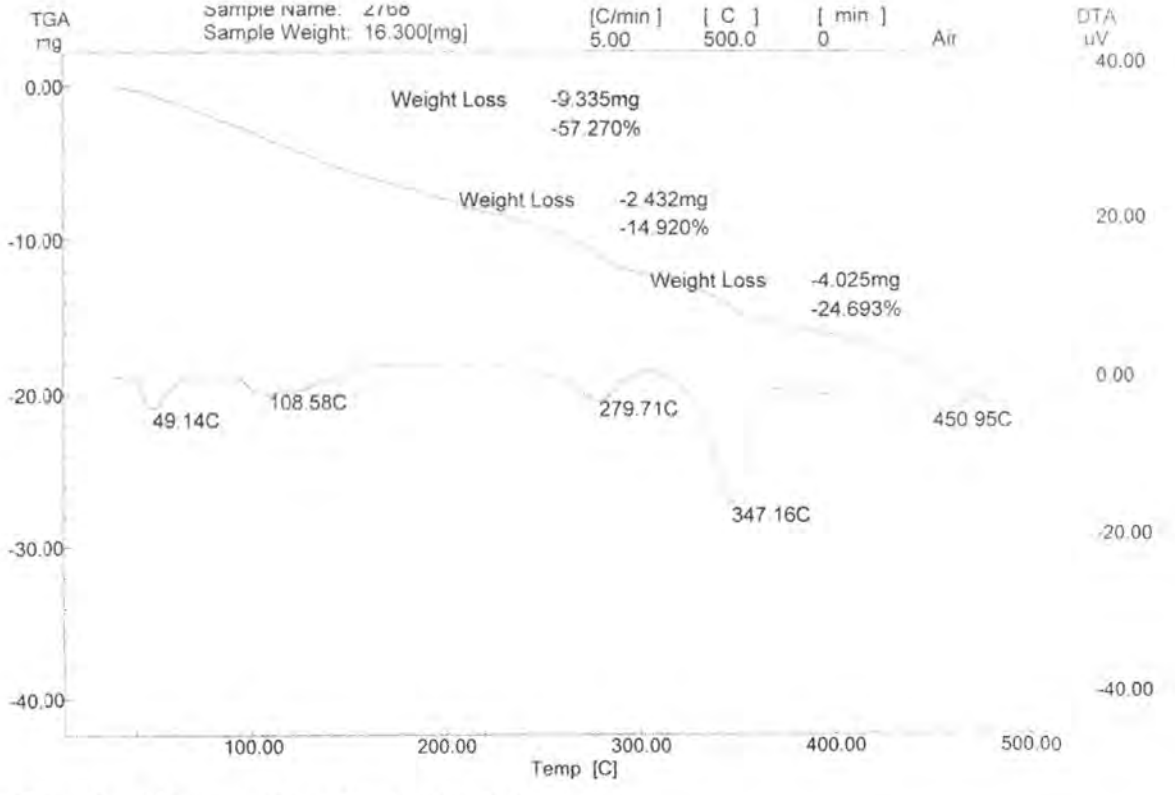

Fig. -9 : Thermal analysis of C10

REFERENCES

1. Ballentine, C."Taste of Raspberries, Taste of Death " U.S Food and Drug Administration.June 1981. FDA Consumer Magazine. Last retrieved Dec. at http://www.fda.gov/oc/history/elixir.htm.(2007).

2. U.S Food and Administration.Center for Veterinary Medicine. " Guidline for Establishing a Sfae Concentration."Last retrieved Dec. at http://www.fda.gov/cvm/Guidance/173r.htm. (2007).

3. Spoo,J. and Jim R. "Sulfonamide". Veterinary Pharmacology and Therapeutics 8 th Edition. Ed. Richard Adams.Iowa University Press(2001).

4. FDA Center for Veterinary Medicine " Sulfonamide ". Data basee of Approved Animal Drug Products.Last retrieved Dec. at http://vidbl. Vetmed.vt.edu/Nada Search/elixir.htm.(2007).

5. Sundlof F."FDAand the Veterinarian." U.S. Food and Drug Administration. Center for Veterinary Medicine. Feb.200.Last retreved Dec. at http://www.fda.gov/cvm/3047.htm.(2007).

6. Walter W. and Michael ."Polyimides" in Ullmanns´ Encyclopedia of Industrial Chemistry,Weinheim . doi:10.1002/1436007.a21-253(2002).

7. Peter A.,Paul M., Franz M. "Fungicides,Agricultural" in Ullmanns´ Encyclopedia of Industrial Chemistry,Wiley-VCH, Weinheim . doi:10.1002/1436007.a12-085(2002).

8. Firyal M. and Amin H. (Conversion of polyanhydride to poly imide) Iraq, J.Polymer.pages.2(3):,(2004).

9. Firyal M.A.(Preparation of some maleimides). J.Um-Salama Science ,pages.2(3):,(2005).

10. Firyal M. (Condensation of heterocyclic compounds with acid anhydride) J, of Education. No.(3),(2008).

11. Firyal M. A.and Abeer A.R.(polycondensation of amino acid with adipoly chloride). J. of college of education (No. 143), (2010).

12. Firyal M. A.and Abeer A.R. (modification of polyvinyl pyrrolidinone with heterocyclic or amino acids).J. of college of education, (No. 142). (2010).

13. Callahan J, Kopeckova P, Kopecek J. Intracellular trafficking and subcellular distribution of a large array of HPMA copolymers. Biomacromolecules.;10:1704–14(2009).

The Study of Antibacterial Activity of *Capparis Spinosa* Flowers

Basma M. Abd Razik
College of Pharmacy-Al-Mustansiriyah University

Received Date : 22/03/2011 Accepted: 29/05/2011

الخلاصة

ان نبات الكُبر يمتلك المركبات الفعالة التي تجعله يستخدم كمضاد لنمو الاحياء المجهرية. تم دراسة فعالية المستخلص الميثانولي والهكساني لازهار نبات الكُبر وبتراكيز تتراوح بين 125-1000mg/ml باستخدام طريقة الانتشار بالحفر ضد الانواع البكتيرية التالية.

Klebsiella sp., Pseudomonas aeruginosa, Eseherichia coli, Proteus sp., Enterococcus sp., Lactobacillus sp., Staphylococcus aureus and Streptococcus sp.

اظهرت النتائج ان المستخلص الميثانولي كان الاكثر فعالية من المستخلص الهكساني لمعظم الانواع البكتيرية المستخدمة في الاختبار. حيث حددت فعالية المستخلص بقياس قطر منطقة التثبيط حيث ابدت كل من ***Eseherichia coli, Lactobacillus sp.,*** مناطق تثبيط ***Eseherichia coli, Streptococcus sp . Staphylococcus aureus*** عند التركيز 125-1000mg./ml اما ***Klebsiella sp., Pseudomonas aeruginosa,*** ***Entero coccus sp.,*** فاعطت مناطق تثبيط عند 500-1000mg./ml في حين لم تظهر مناطق تثبيط النمو ***Proteus sp.*** لم تظهر أي مناطق تثبيط. اما المستخلص الهكساني لازهار نبات الكُبر كان اقل تأثير على نمو البكتيريا المختبرة حيث ابدت كل من ***Lactobacillus sp.*** و ***Staphylococcus aureus*** و ***Streptococcus sp.*** مناطق تثبيط عن التركيز 500-1000mg/ml بينما ابدت ***Eseherichia coli*** و ***Klebsiella sp.*** تحسسا عند تركيز 1000mg./ml في حين لم تظهر مناطق تثبيط لنمو ***Pseudomonas aeruginosa*** و ***Enterococcus sp.*** و ***Proteus sp.***

نجد من نتائج البحث ان المستخلصات المستخدمة لها دور في مجال الصناعات الدوائية وكمواد حافظة للاغذية.

ABSTRACT

Cappris spinosa has active compounds make it has antibacterial properties. Antibacterial effects of different concentrations ranging from (125-1000mg/ml) of hexane and methanol extracts of ***capparis spinosa*** flowers was determined by using agar well diffusion method in clinical strains:

Klebsiella sp., Pseudomonas aeruginosa, Eseherichia coli, Proteus sp., Entero coccus sp., Lactobacillus sp., Staphylococcus aureus *and* ***Streptococcus sp.***

Methanol extract of ***capparis spinosa*** flowers was the most active than hexane extract. The activity of ***capparis spinosa*** determined by measuring inhibition zone as following: ***Lactobacillus sp., Escherichia coli, Streptoccus sp***. and ***Staphylococcus aures*** showed inhibition zone at concentration of 125 -1000mg/ml. ***Klebsiella sp., Spedomonas arruginosa*** and ***Entero coccus sp.*** Showed inhibition zone of 500-1000mg/ ml. it was no inhibition zone for ***Proteus sp.***

Hexane extract of ***Capparis spirosa*** flowers was less active than methanol extract against tested bacteria.

Lactobacillus sp., Staphylococcus aureus **coli** and ***Streptococcus sp.*** Showed inhibition zone at concentrations 150- 1000 mg/ ml while *Eseherichia coli, aureas* and *Klebsiella sp.* Showed sensitivity at concentration 1000mg/ml. There was no inhibition zone for *Pseudomonas arruginosa, Enterococcus sp.* And *Proteus* these results support the notion that plant extracts may have a role as pharamaceutical and preservatives.

INTRODUCTION

One way to prevent antibiotic resistance of pathogenic species is by using new compounds that are not based on existing synthetic agents.

Medicinal plants might represent an alternative treatment in none sever cases of infection diseases.

They can be possible source for new potent antibiotics to which pathogenic strains are not resistant(1).

In Many part of the world medicinal plants are used for antibacterial, antifungal and antiviral. They contain numerous biologically active compounds, many of which have been shown to have antibacterial

properties. The first recorded use of *Cappairs spinosa* was for medicinal purposes in 2000 Bc by the Sumerians, the ancient Greeks and Romans also used the plant for these purposes.

The frouits and the root of the plant have been used in gout and also as diuretics, a stringents and tonics in traditional Iranian medicine.(2).

Also *Capparis spinosa* effective herbal drug for the treatment of rheumatism. (3).

Even its flower buds have some medical uses and are taken to improve liver functions or as a kidney disinfectant. Moreover, it was reported that the plant possesses significant anti – inflammatory activity against carrageenan induced edema in rats, (4) and the aqueas extract of *Capparis spinosa* exhibited anti- hyperglycemic(5) and hypolipidemic activities(6).

Other activities include antiviral, immunomodulatroy(7), anti-allergic, antihistaminic(8), anti fungal, and anti leishmania(9). Furthermore, whole extracts of the floral buttons, applied topically in cosmetic bases, are reported to possess stimulant, bioactiving, hydrating properties on dry, aged, and undernourished skin(10).

Gram positive and Gram – negative bacteria were selected as the test microorganisms based on their clinical, pharmaceutical and bromatogical importance in cases of infections and contamination of food.

The aim of the present study was to evaluate the effect of methanol and hexane extracts of the flowers against various pathogenic bacteria.

MATERIALS AND METHODS

Capparis spinosa flowers:

The flowers were collected from AL –Anbar desert in (May 2010). And was identified by Dr. Ali Al-Mosawy, Department of Biology, College of Science, Baghdad University.

BACTERIAL STRAINS

All bacterial strains used in the study are clinical strains, and kindly provided by microbiology labrotary in pharmacy college at (October to December /2010). They are *Klebsiella sp., Pseudomonas aeruginosa, Eseherichia coli, Proteus sp., Enterococcus sp., Lactobacillus sp., Staphylococcus aureus and Streptococcus sp.*

PREPARATION OF EXTRACTION:

For extraction of *capparis spinosa* flowers, methanol and hexane were used as solvents, thirty grams of the flowers were extracted with 300ml of methanol by using soxhlet apparatus for 10hr.(11) Then the extracts were filtered by using whatman No. 1 filter paper and the solvent was evaporated using rotary distillation apparatus.

In order to obtain a completing dry extract, the resultant extracts were transferred to glass dishes and were left in 40°C oven for 24hrs. Then they were left at 4°C until assessments of their antibacterial activities.

For extraction of *capparis spinosa* flowers with hexane, the same procedure was followed by using the same valume of hexane.

ANTIBACTERIAL ACTIVITY:

The residual extracts were dissolved in their extracting solvents to yield the final concentration: 1000, 500, 250 and 125 mg./ml.

The agar were diffusion method was used to determine antibacterial activity of extracts (12). The culture medium was calculated with one of tested bacteria suspended in Mueller –Hinton agar.

Six millimeter diameter wells were punched in to the agar filled with 0.1 ml of each extract. Solvents were used as negative control while antibiotic of streptomycin at the same concentration were used as positive control. By measuring the inhabitation zone diameter observed.

RESULTS AND DISCUSSION

The results showed that the methanol and hexan extracts of *Capparis spinosa* flowers had the antibacterial activity. The different concentration of hexane extract of *Cappairs spinose* flowers (table 1) produced inhibition zones against tested bacteria; *Streptoccus sp., Lactobocillus sp.* And *Staphylococcus aureus* ranging from 1000-500mg/ml., they are produced the largest inhibition zone, there was no inhibition zone for *Pseudomonas aeruginosa proteus,* and *Entero coccus sp. .Escherichia coli* and *Klebsiella sp.* Produce inhibition zone at concentration of 1000mg/ml

Eseherichia coli, Lactobocillus sp., Staphylococcus aureus and *Streptococcus sp.* showed the highest sensitivity to methanol extract of

Capparis spinosa flowers (table 2), they were sensitive to concentration ranging from 1000-125gm./ml. While *Klebsiella sp.*, *Pseudomonas aeruginosa* and *Enterococcus sp.* were sensitive to concentration of 1000-500mg./ml. *Proteus sp.* did not showed any inhibition zone to all concentration of this extract.

Hexane extract of *Capparis spinosa* was less effective than methanol extract effective against tested bacteria. Solvents (negative controls) used for preparation different concentrations showed no activity against any tested bacteria. streptomycin (positive controls) at concentration of 1000mg/ml, showed inhibition zone ranging from 40-23 mm against all tested bacteria (table -3).

Table 1: Antibacterial activities of hexane extract of *Capparis spinosa* flowers

Tested bacteria	Inhibition zone diameter (mm) concentrations of hexan extract of *Capparis spinosa* (mg/ml)			
	1000	500	250	125
Klebsiella sp.	7	-	-	-
Pseudomonas aeruginosa	-	-	-	-
Escherichia .coli	7	-	-	-
Proteus sp.	-	-	-	-
Enterococcus sp.	-	-	-	-
Lactobacillus sp.	10	8	-	-
Staphylococcus aureus	7	7	-	-
Streptococcus sp.	13	10	-	-

Table 2: Antibacterial activities of methanol extract of *Capparis spinosa* flowers

Tested bacteria	Inhibition zone diameter (mm) concentrations of methanol extract *of Capparis spinosa* (mg/ml)			
	1000	500	250	125
Klebsiella sp.	8	7	-	-
Pseudomonas aeruginosa	13	11	-	-
Escherichia coli	22	20	14	13

Proteus sp.	-	-	-	-
Enterococcus sp.	15	11	-	-
Lactobacillus sp.	20	15	7	7
Staphylococcus aureus	18	14	14	12
Streptococcus sp.	14	14	11	7

Table 3: Antibacterial activity of streptomycin 125-1000mg/ml control

Tested bacteria	**Inhibition zone diameter (mm) concentrations of *streptomycin* (mg/ml)**			
	1000	500	250	125
Klebsiella sp.	30	28	24	23
Psedomonas aeruginosa	40	39	35	35
Escherichia coli	39	35	34	32
Proteus sp.	35	33	30	30
Enterococcus sp.	20	16	-	-
Lactobacillus sp.	40	40	35	33
Staphylococcus aureus	40	40	35	30
Streptococcus sp.	35	35	34	33

The present study was designed to obtain preliminary information on the antibacterial activity of *cappairs spinosa* flowers on pathogenic bacteria.

The agar well diffusion method was preferred to be used in this study. The results showed a remarkable antibacterial activity of the methanol and hexane extracts of this plant the methanolic extracts had the best antibacterial activity than hexan extracts, the relatively high potency of the methanolic extracts may be attributed to the dissolving power of alcohol over water (13).

In literature it has been indicated that the antibacterial activity is due to different chemical agents in the extract, including alkaloids, polyprenols, flavanoids, aliphatic glycosinolates(14), and phenolic compounds derivatives play an important role in its bioactivities. (The methanolic extract of Capparis spinosa has an antioxidant effect (15, 16).

The antibacterial activity of Capparis spinosa flowers due to flavanoids, phenolic acids and glycosides (14), (17).

The results showed gram – negative bacteria were shown to be more resistant than gram positive bacteria.

The resistance of gram negative bacteria towards antibacterial substances is related to *lipopolysaccharides* in their auter membrane (18).

The activity is referred to the presence of glycosies which can get hydrolyzed to release phenolics which are toxic to microbial pathogens (19), or may be due to impairment of variety enzyme systems including those involved in energy production and structural component synthesis (20, 21).

Finally, the results of this study revealed that the flowers of *Capparis spinosa* possess some antibacterial properties as antibiotics principles, the diameters of inhibition zone of the antibacterial agents i.e. Capparis spinosa and streptomyein were different, according to the kinds, concentrations and purity, and this results obtained support the fact that more needs to be done on the purification, identification and quantification of the active of extracts components with the view of their used for in vivo studies.

REFERENCES

1. Punopas, K. E.; Griangsak, C.; Benjamart and N., Pichaya The study of antibacterial activity of some medicinal plants in Iamiaced family. Suranaree J. Scitechnol, (2003).

2. Afsharypuor, S., Jeiran, K., and Jazy, A. , A. X. First investigation of the flavour profiles of leaf, ripe fruit and root of *Capparis spinosa* var. Mucronifolia from Iran. Pharmacetutica Acta Helvetiae, 72: 307-309. (2003).

3. Fu, X.P., Aisa, H. A., Abdurahim, M., and Yill, A. Chemical constitution of *Capparis spinosa* fruits. J. Chemistry of Natural Compounds 43: 181-183, (2007).
4. Al-Said, M. S. Abdelsattar, E. A., Khalifa; S.I., and El-Feraly, F. S. Isolation and identification of an anti – inflammatory principle from *Capparis spinosa* . pharmazie, 43: 640-641, (1998).

5. Eddouks, M., Lemhadri, A. and Michel, J. B., Caraway and Caper. Potential anti – hyperglycaemic plantisn diabetic rats. J. Ethanopharmacol. 94: 143-148, (2004)

6. Eddouks, M., Lemhadri, A., and Michel, J. B., Hypolipidemic Emic activity of aqueous extract of *Capparis spinosa* L. in normal and diabebic rats. J. Ethanopharmacol. 98: 345-350, (2005),

7. Arena , A., Bisignano, G., Pavone, B., Tomaino, A., Bonina, F. P., Saija, A., Cristani, M., D'Arrigo, M., and Trombetta, D., Antiviral and Immunomodulatory effect of a hyophilized extract of *Capparis spinosa* L. buds. Phytother Res. 22: 313-317, (2008).

8. Trombetta, D., Occhinto , F., Perri D., Puglia, C., Santagati, N. A., De Pasaule, A., Saija, A., and Bonina, F., Antiallergic and antihistaminic effect of two extracts of *Capparis spinosa* L. flowering buds. Phytother. Res. 19: 29-33, (2005)

9. Jacobson, R. L and Schlein, Y., Lectins and toxins in the plant diet of phlebotomus papatas: (Diptera : Psychodidae can kill leishmania major promastigotes in the sandfly and in culture. Ann. Trop. Med. Parasitol. 93: 351-356, (1999).

10. Hemmi cena and P. Rovesti, Experimental studies and the cosmetological uses of cupparis Riv. Ital. Essenze, Profumi, Piate, off., Aromat., Syndets, Saponi, Cosmet. Aereosals, 61: 2-9, (1979).

11. Lin, J., Opoku, A. R.; Geheeb- Keller , M.; Hutchings, A. D.; Terblanche Tager, A. K. and Vanstaden, J. Preliminary screening of some traditional zulu medicinal plants for anti – inflammatory and antimicrobial activity. J. Ethanopharmacol. 68: 267-274. (1999).

12. Anesini, C. and Perez, C. Screening of plants usedin Argentine folk medicine for antimicrobial activity. J., Ethanopharmacol. 39:119-128, (1993).

13. Majorie, M. C. Plant products as antimicrobial agents cli. Microbiology Reviews, 12(4), 564-582, (1999).

14. Rodrigo M., Lazaro MJ., Alvarruiz and Giner V., (1992), Composition of Capers (*Capparis spinosa*): influence of cultivar, size and harvest date, J Food Sci., 57: 1152-1154, (1999)

15. Germano M. P, De pasquale, R. D'Angelo, V., catania, S.; Silvani, V.; and costa , C. Evaluation of extracts and isolated fraction from *capparis spinosa* L. buds as an antioxidant source. J. Agric. food chem.., 50(5): 1168-1171, (2002).

16. Yang Yu, Huiyuan Gao, Zhishu Tang, Xiaomei Song and Lijun. Wu, Several phenolic acids from the fruit of *capparis spinosa*, Asian journal of traditional Medicines, 1: 3-4, (2006).

17. Sraa' N. Muslim, Antimicrobial activity of *capparis spinosa*, L. extracts on growth of some microorganism of medical importance, M.Sc. thesis, college of sciences Al –Mustansiryah University. (2006).

18. Gao, Y., M. J. Belkun and M. Stiles.The outer membrane of Gram negative bacteria inhibits antibacterial activity of Brochacin C. Applied Enurion Microbial. 65: 4329-4333, (1999)

19. Aboaba, OO. Efuwape BM Antibacterial properties of some Nigerian spices. Bio. Res. Comm. 13: 138-188. (2001).

20. Applied and Environmental Microbiology, Feb., 47(2), 229-233, (1984).

21. Fitua, M. Aziz , The study of antibacterial activity of Juglans Regia and Thymus Vulgaris Seeds, AJPS, 7(1). (2010).

Serum and Hair Reference Levels of Zinc, Copper, and Vitamins E& A in Healthy Iraqi`s Female

Noor M. Ali, Hadeel S. Abdel Wahab and Safaa I. Kader
College of Medicine-University of Al-Nahrain

Received : 22/03/2011 Accepted: 29/05/2011

الخلاصة

إن الغرض من الدراسة هو أمكانية استخدام الشعر كمصدر لقياس العناصر النادرة والفيتامينات بدلا من مصل الدم. تمت دراسة العلاقة بين تراكيز عناصر الزنك، والنحاس، وفيتامين A و E في مصول الدم والشعر لـ49 امرأة طبيعية واللواتي تتراوح أعمارهن بين 20–45 سنة باستخدام تقنية طيف الامتصاص الذري و تقنية الفصل الكروماتوغرافي العالي الأداء. وقد كانت قيمة المتوسط الحسابي لهم في مصل الدم وفي الشعر :

(0.10µg/dl; 0.40µg/dl, 0.15 µg/dl; 0.026µg/dl, 11.18µg/dl; 6.33µg/dl and 50.92µg/dl; 27.83µg/dl على التوالي. عند تقسيم العينة لثلاثة مجاميع عمرية، تبين وجود بعض الزيادة في تراكيز النحاس و فيتامين A كدالة العمر، بينما تركيز الزنك اظهر انخفاض قليلا. عند إجراء التحليل الاحصائي كانت هناك فروق معنوية بين تراكيز الزنك، والنحاس، وفيتامين A و E بالنسبة للأعمار وكذلك حسب نوع النموذج المأخوذ (مصل الدم أو الشعر). وهذا يعني عدم أمكانية الاستعانة بتقدير تراكيز المتغيرات المذكورة أعلاه في الشعر بدلا من مصل الدم.

ABSTRACT

The aim of the study was to discover the possibility of taking a hair as a source of measuring trace elements and vitamins instead of serum. Also investigate the serum-hair reference range for Zinc (Zn), Copper (Cu), Vitamins A, and E levels in women age. Serum and hair copper, zinc, Vit.A and vit E concentrations of 49 females apparently healthy blood donors aged 20–45 years old were determined by flame atomic absorption spectrometry and HPLC. The mean zinc, copper, Vit.E and Vit. A concentrations- in serum and hair- were (0.10±0.06µg/dl; 0.40±0.27µg/dl, 0.15±0.01 µg/dl; 0.03±0.01µg/dl, 11.18±2.14µg/dl; 6.33±1.21µg/dl and 50.92±16.38µg/dl; 27.83±8.95µg/dl, respectively. When the subjects were divided into various

age groups there appeared to be some increase in copper and Vit.A concentration as a function of age, whereas zinc concentration appeared to be some decrease compared to literature data on copper and zinc levels for various countries.

There were significant variations in zinc, copper, Vit.E and Vit.A concentrations due to age and the type of sample (serum or hair). This study is the first one evaluating the serum and hair status of zinc, copper, Vit.E and Vit.A in healthy Iraqi and it has shown that they are at the highest concentration range for copper, the lowest for zinc, the highest for Vit.E and the highest for Vit.A in serum.

INTRODUCTION

Vitamins, minerals and trace elements play an important role in the prevention of many age-associated diseases [1] and in maintaining normal immune and cognitive functions [2]. Zinc (Zn) and Copper (Cu) are potent antioxidants involved in cellular defense against oxygen free radicals. The risk of deficiency in these two micro-nutrients seems also to increase in proportion to age [3]. Evidence is accumulating that most of the degenerative diseases have their origin in deleterious free radical reactions [4-6].

Copper and zinc are essential trace elements. Both are important parts of the enzymes superoxide dismutase, lysyl oxidase and ceruloplasmin, which protect cells from oxidative damage [1-3]. Apart from their role in cancer, a large number of studies have shown that copper and zinc are implicated in cardiovascular diseases, rheumatoid arthritis and other degenerative diseases [4,5]. The dietary habits and the environmental conditions may partly influence the levels of these trace elements in tissues and biological fluids as well, consequently influencing their participation in numerous biochemical mechanisms [6]. In most studies copper and zinc status have been assessed directly by measuring these elements mainly in plasma or serum. Although various studies concerning the copper and zinc levels in serum of healthy individuals have been carried out in several countries [7-10], similar studies in Iraq have not been conducted.

The aim of this study was to establish the reference range of copper and zinc concentrations in serum and scalp hair of healthy Iraqi individuals

by determining the serum level of these elements by atomic absorption spectrometry. The values obtained were compared with literature data for other countries. The effects of age were also evaluated.

MATERIALS AND METHODS

Subjects

The study was carried out on a sample group of 49 apparently healthy blood and scalp hair donors females ranging in age from 25 to 45 years. The individuals included in this study were members of an civilian population working in college of medicine, almost they are from the same socioeconomic, and residing in Baghdad-Iraq. The blood and scalp hair samples were collected during 2008–2009.

Method

This study was conducted in Medical Research Unit, College of Medicine, Al-Nahrain University, Baghdad, Iraq between 2008-2010. Serum and hair vitamins A&E were measured using High Performance Liquid Chromatography (HPLC), Shimadzu (Kyoto, Japan) which consisted of a system controller model SCL-10 AVP, a degasser model DGU-12A, two liquid delivery pumps model LC-8AVP, UV-Visible detector model SPD-10AVP, and injector model SIL-10A, equipped with 20 µl sample loop. The HPLC system has been interfaced with computer via a Shimadzu class-VP5 chromatography data system program supplied by the manufacturer; Epson LQ-300 printer model P852A (Japan) and serum and hair trace elements were measured using atomic absorption spectrophotometer AA 6200 Shimadzu (Kyoto, Japan) interfaced with computer.

Hair sample preparation

0.01 g of hair was cut off and mixed with 1.5ml of nitric acid heated at 60c° and the extracted then diluted fifty folder with deionized water.

Serum sample preparation

Five milliliter of venous blood was aspirated from each patient. In the analysis of vitamin E the samples prepared by adding 50µl of 15% 5-sulphosalsic to 400µl of serum, then mixed and centrifuge at 3000rpm for 10min. The supernated was taken and diluted ten folds with distilled water and filtrated using minipore filter paper . All samples and standard solutions of vitamin E have been chromatographically analyzed with C-18 column

using isocratic mobile phase 95% ethanol, 5% water, flow rate 1ml/min and UV-VIS detection at wavelength 229 nm in order to estimate serum.

In the analysis of trace elements the samples prepared by diluted serum ten folder with deionized water and then analyzed by atomic absorption spectrophotometer.

Collection of serum and hair samples and analytical methods

Untreated (not permed, dyed or bleached) and free (of all gels, oils and hair cream). Scalp hair samples were collected from the nape of the neck, blood samples were collected from random subjects in the college. Serum samples were obtained from the spontaneous coagulation of blood. The blood was then centrifuged at 2500 rpm for 10 min to obtain serum. Hemolyzed samples were excluded. The serum was stored at 0 C^0. All glassware and bottles used for the isolation of serum and for analysis were previously soaked in diluted nitric acid (10%) for 3 h and rinsed thoroughly with deionized water. This procedure was followed in order to exclude the possibility of contamination with zinc or copper. All samples were diluted (1:4) using water.

All analyses were performed in peak height mode to calculate absorbance rates. All samples were analyzed in triplicate.

Statistical analysis

The data were subjected to statistical evaluation, using the SPSS released version 11.0 program for Windows. The mean values obtained in the different groups classified by age were compared using t-test, assuming that there were significant differences between mean values when statistical comparison gave $P <$ 0.05.

RESULTS AND DISCUSSION

There was statistically significant zinc, copper, Vit.E and Vit.A levels in difference between serum and hair. Significant correlation was seen between age, trace elements and Vitamins levels.

Table.1 give the results of the mean values obtained in serum and hair of zinc, copper, Vit.A and Vit.E concentrations in healthy individuals group. Serum Zn level was significantly lower than hair Zn level (0.101+0.06 vs 0.402+0.26; $p<0.001$).

Table-1: Comparison of Zn, Cu, and Vit.E between serum and hair

	Group	N	Mean	Std. Deviation	p-value
Zn	serum	49	1.15	0.746	<0.001
	hair	49	0.411	0.285	
Cu	serum	49	1.36	0.537	<0.001
	hair	49	0. 278	0.117	
Vit.E	serum	49	12.79	2.873	<0.001
	hair	49	8.02	0.665	
Vit.A	serum	49	41.81	5.125	<0.001
	hair	49	23.07	2.255	

Serum Cu level was significantly higher than hair Cu level (0.149+ 0.0999 vs 0.0262+0.0117; $p<0.001$). Serum Vit.E level was significantly higher than hair Vit.E level (11.183+2.143 vs 6.332+1.213; $p<0.001$). Serum Vit.A level was significantly higher than hair Vit.A level (50.92+16.38 vs 27.83+8.95; $p<0.001$). So we cannot depend on hair level of the above mentioned variables to replace serum levels.

Serum copper levels for all studied subjects ranged between 0.049 and 0.49 µg/dl with a mean value of 0.19 µg/dl.

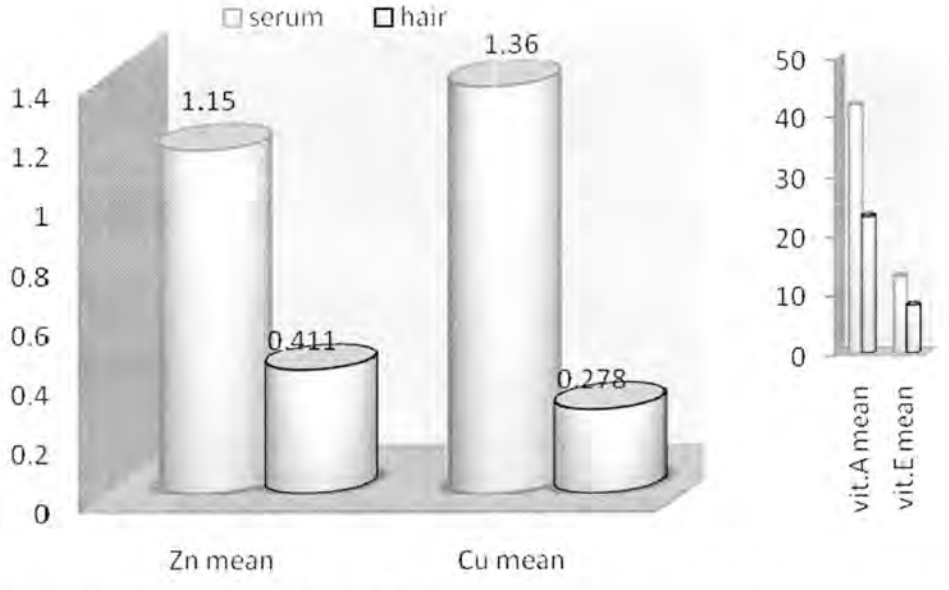

Fig.-1: Serum and hair: Zn, Cu, Vit.E and Vit.A concentration (ppm) in (n=49) at $p<0.05$

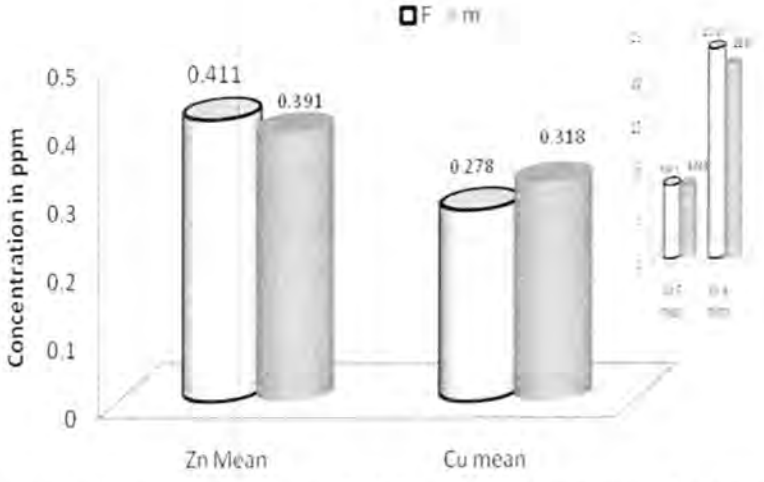

Fig. -2: Hair Zn, Cu, Vit. E. and Vit. A concentrations (ppm) as a function of gender in the (n=49) shown as mean (P<0.05)

Correlations

		CU	AGE	ZN	E	A
CU	Pearson Correlation	1	-.080	-.155	.051	-.396
	Sig. (2-tailed)	.	.631	.353	.763	.014
	N	38	38	38	38	38
AGE	Pearson Correlation	-.080	1	-.065	.183	-.054
	Sig. (2-tailed)	.631	.	.699	.271	.750
	N	38	38	38	38	38
ZN	Pearson Correlation	-.155	-.065	1	.086	.069
	Sig. (2-tailed)	.353	.699	.	.607	.680
	N	38	38	38	38	38
E	Pearson Correlation	.051	.183	.086	1	.102
	Sig. (2-tailed)	.763	.271	.607	.	.543
	N	38	38	38	38	38

	Mean	N	Std. Deviation	Maximum	Minimum
A Pearson Correlation	-.396	-.054	.069	.102	1
Sig. (2-tailed)	.014	.750	.680	.543	.
N	38	38	38	38	38

* Correlation is significant at the 0.05 level (2-tailed).

Correlations

		CU	AGE	ZN	E	A
CU	Pearson Correlation	1	-.080	-.155	.051	-.396*
	Sig. (2-tailed)	.	.631	.353	.763	.014
	N	38	38	38	38	38
AGE	Pearson Correlation	-.080	1	-.065	.183	-.054
	Sig. (2-tailed)	.631	.	.699	.271	.750
	N	38	38	38	38	38
ZN	Pearson Correlation	-.155	-.065	1	.086	.069
	Sig. (2-tailed)	.353	.699	.	.607	.680
	N	38	38	38	38	38
E	Pearson Correlation	.051	.183	.086	1	.102
	Sig. (2-tailed)	.763	.271	.607	.	.543
	N	38	38	38	38	38
A	Pearson Correlation	-.396*	-.054	.069	.102	1
	Sig. (2-tailed)	.014	.750	.680	.543	.
	N	38	38	38	38	38

*. Correlation is significant at the 0.05 level (2-tailed).

			serum	hair		serum	hair	serum	hair	serum	hair
Cu	age	GroupI	0.13	0.02	23	0.05	0.01	0.23	0.046	0.049	0.01
		GroupII	0.13	0.02	13	0.11	0.01	0.45	0.045	0.049	0.01
		GroupIII	0.19	0.03	13	0.14	0.01	0.49	0.046	0.049	0.01
Zn	age	GroupI	0.11	0.40	23	0.07	0.25	0.27	1.23	0.0010	0.21
		GroupII	0.11	0.42	13	0.07	0.37	0.27	1.23	0.077	0.21
		GroupIII	0.07	0.38	13	0.03	0.19	0.12	0.85	0.001	0.12
Vit.E	age	GroupI	10.8	6.12	23	1.38	0.78	16.50	9.35	9.65	5.46
		GroupII	12.59	7.13	13	3.38	1.91	18.1	10.25	9.29	5.26
		GroupIII	10.46	5.92	13	0.72	0.41	11.78	6.67	9.29	5.26
Vit.A	age	GroupI	46.00	25.14	23	9.71	5.31	85.51	46.72.	36.31	19.84
		GroupII	67.08	36.66	7	23.54	12.86	91.09	49.77	39.04	21.33
		GroupIII	-	-	-	-	-	-	-	-	-

Group Statistics

	GROUP	N	Mean	Std. Deviation	Std. Error Mean
ZN	SERUM	14	1.1506	.74668	.19956
	HAIR	14	.4110	.28504	.07618
CU	SERUM	14	1.3634	.53781	.14374
	HAIR	14	.2789	.11788	.03150
E	SERUM	14	12.7925	2.87311	.76787
	HAIR	14	8.0239	.66508	.17775
A	SERUM	14	41.8108	5.12513	1.36975
	HAIR	14	23.0737	2.25502	.60268

The mean copper value in females age (40 yr) and more was significantly ($p<0.001$) higher than in females (20-29yr and 30-39yr), which agrees with the findings of most authors [7-12], but contrasts with data reported by others [6,13,14] who found similar serum copper concentrations. These findings may be due to differences in diet between females or their physical condition as well as differences in copper absorption [6, 12].

Our data for serum zinc level ranged between 0.001 and 0.27 µg/dl with a mean value of 0.11 µg/dl. The mean serum zinc concentration in females (20-29yr) was significantly ($p <0.001$) higher than in females (40yr and more). This difference is smaller than the one observed for copper, which agrees with the results of various studies [9,10] which found no significant differences between the mean serum zinc concentrations for females (20-29) and females(30-39yr). However, [7] found a higher serum mean zinc concentration in females, although others found no correlation between serum zinc concentration and sex[8]. There were no significant variations in

copper and zinc levels due to occupational status and to place of residence, which has also been previously indicated by [10]. Our findings may be related to the homogeneity of the daily diet, as well as to a possible homogeneity of soil of the different areas of Iraq in copper and zinc.

Table.2

Trace elements and Vitamins in all groups

N:subject number

GroupI: females between 20-29

GroupII: females between 30-39

GroupIII: females between 40 and >

The mean copper concentration showed an increase with age in all individuals studied, which agrees with the findings of [15]. Other studies have reported inconsistent changes [11,16] or a lack of change with age [17].

Age had a weak significant effect on copper concentration in females with an increase from the youngest age group to the oldest. A similar increase has been reported by [15]. The lowest copper concentration in females was observed in females younger than 40 years, which agrees with the findings of other authors [10,18].

The mean copper concentration in serum and hair remained nearly constant in females between 20-39 years, whereas the highest concentration was observed in females older than 39 years, which is in contrast with the findings of [15] who showed an increase from the youngest age group to the oldest.

The mean zinc concentration in serum and hair did significantly change among the different age intervals considered, which is not in agreement with some authors [19-21]. Some authors have reported decreases, with [22] and without [15] statistically significant differences among groups, or decreases in females(40yr and more) but not in females (20-39yr) [23].

The zinc concentration in serum of females 20-39 years was relatively constant, which agrees with the findings of most authors [10, 15,24]. The lowest mean zinc concentration for females was observed in the interval between 20 and 29 years old.

The mean Vit.E and Vit.A concentration in serum and hair did significantly change among the different age intervals considered.

The Vit.E concentration in serum and hair of females in the interval between 20-29 years and 40 and > old years was relatively constant, The highest mean Vit.E concentration was observed in the interval between 30 and 39 years old. While highest Vit.A mean concentration of females was observed in the interval between 30-39 years old, and the lowest was in the interval between 20-29 years old.

As it can be seen from Table 2 the serum copper concentrations in the population of healthy Iraqi adults studied are similar to those reported for healthy people from most places. On the other hand, our data on zinc were lower than those for most places, but similar to the results reported for Northern Ireland [15].

In conclusion, this study is the first one evaluating the status of copper, zinc, Vit.E and Vit.A in healthy Iraqi blood and scalp hair donors and it has shown that they are at the highest concentration range for copper, the lowest for zinc, the highest for Vit.E and the highest for Vit.A in serum. When the subjects were divided into various age groups there appeared to be some increase in copper and Vit.A concentration as a function of age, whereas zinc concentration appeared to be some decrease. There were significant variations in copper, zinc, Vit.E and Vit.A concentrations due to age and type of the sample (serum and hair).

REFERENCES

1. Schmidt, K.,Zentralbl. Hyg. Umweltmed, 191, 327–329, (1991).
2. Pike, J., Chandra, R.K., Int. *J. Vitam. Nutr.* Res, 65, 117–121(1995).
3. Gilchrest, B.A., Bohr, V.A., *FASEB J*, 11, 322, (1997).
4. Florence, T.M., *Aust. NZ J. Ophthalmol*, 23(1), 3–7, (1995).
5. Harman, D., Ann. *NY Acad. Sci*, 673,126–141, (1992).
6. Mariani, E., Polidori, M.C., Cherubini, A., Mecocci, P., *J. Chromatogr. Analyt. Technol. Biomed. Life* Sci, 827, 65–75, (2005).
7. Yucel I, Arpaci F, Ozet A, Doner B, Karayilanoglu T, Sayar A, et al. *J Trace Elem Re*, 40:31– 8, (1994).
8. Zowczak M, Iskra M, Paszkowski J, Manczak M, Torlinski L, Wysocka E. *J Trace Elem Med Biol*, 15:193– 6, (2001).
9. Ho E. J Nutr Biochem, 15:572– 8, (2004).
10. Madaric A, Ginter E, Kabradova *J.Physiol Res*, 43:107– 11, (1994).

11. Silverio Amancio OM, Alves Chaud DM, Yanaguibashi G, Esteves Hilario MO. *Eur J Clin Nutr,* 57:706– 12, (2003).
12. Terre´s-Martos C, Navarro Alarcon M, Martı´n Lagos F, de la Serrana HLG, Lu¨pez Martinez MC. *Sci Total Environ*, 198:97–103, (1997).
13. Schuhmacher MS, Domingo JL, Corbella *J. Sci Total Environ*, 148:67–72, (1994).
14. Songchitsomboom S, Komindr S. *J Med Assoc Thai* 1996;79:550–7.
15. Andres JG. Nivells de seleni, course, Spain7 University of Barcelona; (1999).
16. Dı´az Romero C, Henrı´quez Sa´nchez P, Lo´pez Blanco F, Rodrı´guez E, Serra Majem L. *J Trace Med Biol*, 16:75– 81, (2002).
17. Helgeland K, Haider T, Jonsen J. *Sc and J Clin Lab Invest*, 42:35–9, (1982).
18. Johnson PE, Milne DB, Lykken GI. *Am J Clin Nutr*, 56:917– 25, (1992).
19. Lukaski HC, Klevay LM, Milne DB. *Eur J Appl Physiol*, 58:74 – 80, (1988).
20. Rukgauer M, Klein J, Kruse-Jarres JD. *J Trace Elem Med Biol*, 11:92–8, (1997).
21. McMaster D, McCrum E, Patterson CC, Kerr MF, O'Reilly D, Evans AE, et al. *Am J Clin Nutr*, 56: 440– 6, (1992).
22. Bales CW, Feeland-Graves JH, Askey S, Behmardi F, Pobocik RS, Fickel JF, et al. *Am J Clin Nutr*, 51:462–9, (1990).
23. Hinks LJ, Clayton BE, Lloyd RS. J Clin Pathol, 36:1016–21, (1983).
24. Lockitch G, Halstead AC, Quigley G, MacCallum C. *Clin Chem*, 34:1618– 21, (1988).
25. Davies IJ, Musa M, Dormandy TL. J Clin Pathol, 21:359– 63, (1968).
26. Paz de Moncada N, Chacin de Bonilla L, Villasmil JJ, Estevez J, Bonilla E. *Invest Clin*, 30:101–9, (1989).
27. Malvy DJ, Arnaud J, Burtschy B, Richard MJ, Favier A, Houot O, et al. *Eur J Epidemiol*, 9:155–61, (1993).
28. Lindeman RD, Clark MI, Colmore P. *J Gerontol* 1971;26:358– 63.
29. Rea IM. Nutr Res, 9:121– 5, (1989).
30. Versieck J, Hosie J, Barbier F, Michels H, de Rudder *J. Clin Chem*, 23:1301–5, (1977).
31. Iyengar, GV. Juelich, FRG: Report July 1975, *Nuclear Research Center*, Juelich; (1985).

Effect of Ginger on the activity of some antioxidant enzymes (Superoxide dismutase, and Catalase) of Alloxan Experimental Induced-Diabetic Rabbits

Entedhar Riffat Sarhat
College of Dentistry-University of Tikrit

Received : 13/04/2011 Accepted : 29/05/2011

الخلاصة

تعتبر حالة الإجهاد التأكسد والمرافقة بالاصابه بداء السكري واحده من العوامل المهمة التي تؤدي إلى ضعف السيطرة على مستوى الكلوكوز في الدم. لقد تم تصميم هذه الدراسة لإظهار الفوائد ألسريريه لاستخدام نبات الزنجبيل لعلاج اضطراب التأكسد. تم أجراء الدراسة على خمسون من الأرانب وبعمر (6-12) شهرا وقسمت إلى أربع مجاميع,كل مجموعة تضم 10 من الأرانب.المجموعة الأولى: مجموعه أرانب أصحاء(مجموعه سيطرة)للمجموعة الثانية . ألمجموعه ألثانيه :أحدث بها سكري وبقيت بدون علاج (مجموعه سيطر)للمجاميع الثلاث ألأخيرة .ألمجموعه ألثالثه و الرابعة أحدث بها سكري وعولجت بالزنجبيل و بتركيز 250 ملغم/كغم و 500 ملغم/كغم على التوالي من وزن الجسم جرعة مفردة يومية ولمده ستة أسابيع. اعتمدت طريقه التقييم على قياس الأنزيمات المضادة للتأكسد مصل الدم ودرجه السيطرة على مستوى الكلوكوز في الدم. أظهرت نتائج الدراسة وجود تأثيرات لنبات الزنجبيل في لعلاج اضطراب التأكسد من خلال خفض مس مستوى الكلوكوز في الدم ورفع مستوىSOD و CAT وبشكل يتناسب مع مقدار الجرعة المستخدمة وبشكل يتناسب مع مقدار الجرعة المستخدمة ويترافق هذا التأثير مع تأثير ذي قيمه معنوية واضحة في تحسين السيطرة على مستوى الكلوكوز في الدم.

ABSTRACT

Oxidative stress is considered as one of the important consequences of poor glycemic control. This study was designed to explore the possible clinical utility of ginger as a antioxidant enzymes. This study was performed on alloxan induced diabetic rabbits with age of (6,12) month's. The selected rabbits were allocated into four groups each include 10 rabbits. The first group was healthy rabbits as compared with second

group. The second diabetic without treatment as control group with the last three groups. The third and forth group diabetic treated with extract 250mg/Kg, and 500mg/Kg of body weight respectively as a single daily dose for 6 weeks. The elevation procedure was base on the measurement of the level of (Superoxide dismutase (SOD), Catalase (CAT), and blood sugar. Analysis of data revealed significant, dose dependent effects of ginger on the antioxidant enzyme, SOD, and CAT were significantly elevated, while blood glucose were significantly reduced, associated with significant improvement in glycemic control.

INTRODUCTION

Diabetes mellitus is a disorder of carbohydrate metabolism, characterized by persistent hyperglycemia, glucosuria and polyuria (1-4). Diabetes mellitus is one of the pathological conditions that are always accompanied by oxidative stress, that is, with the preponderance of oxidative reactions over the anti-oxidative protection of tissues (5-6).

The enzymes responsible for detoxifying free radicals or regenerating antioxidant molecules can provide an indication of the level of stress experienced in a cell or tissue. These enzymes are usually measured by in vitro activity assays, although changes in transcription can also provide evidence of cell stress. In long-term diabetes, Catalase, GSH reductase, GSH peroxidase, and SOD decrease in complication-prone tissue. One study reports elevated CuZn-SOD activity in the blood, although the increased activity did not correct the deficiency of antioxidant capacity or hyperglycemia induced lipid peroxidation. The study suggested that treatment with oral antidiabetic drugs was responsible for decreases in GSH peroxidase and catalase below control levels(7,8).

Ginger (Zingiber officinale L., Family Zingiberaceae) roots are commonly used as culinary spice and medicinally used for its antioxidant ,androgenic and hypoglycemic activities which were reported in animal models. The active ingredients of ginger roots and leaves such as zingerone, gingerdiol, zingibrene, gingerols and shogaols produced antioxidant activity(9-13) .

MATERIALS AND METHODS

Diabetes was induced in rabbits by injection of alloxan tetrahydrate at a dose of 180 mg/kg body weight IV in marginal ear vein(14).soon the animal were injected with 10% of glucose solution S/C.

Forty rabbits 6-12 months old and their body weight ranged 1.5-2 kg were randomly assigned to four groups. Group I of rabbits(control group)were with healthy glucose level. Group II (diabetic group) received an IV injection of alloxan tetrahydrate. Groups III and IV of diabetic rabbits treated with extract of Ginger as a single daily dose 250, 500mg/kg body weight of extraction dissolve in 1cc DW orally for 6 weeks.

Ginger ethanolic Extraction:

The officinale (Ginger) was collected from local market of Baghdad, which dried and powdered, according to Bhandari method (15). Two kilograms of air-dried rhizomes of the herb was milled into fine powder mechanically and extracted in cold percolation with 95% ethanol for 24h. The extract was recovered and 95% ethanol was further added to the ginger powder and the extraction was continued. This process was repeated three times. The three extracts were pooled together, combined, filtered and the filtrate was concentrated to dryness under reduced pressure in a rotary evaporator. The resulting ethanolic extract was air-dried, finally give 80 grams of dark brown, gelatinous extract of ginger dried rhizomes. Without any further purification, the crude ethanolic extract was used for the experiments.

Preparation of blood samples

Before taking the blood samples animals were fasted for 12 hours, and the blood samples were obtained by the heart puncture (3-5ml). The blood was centrifuged in a test tube at 2500 rpm for 15 minutes, serum was separated from plasma using a Pasteur pipette supplied with rubber bulb, and transferred to another test tube.

Biochemical analysis:

Glucose determination was carried out according to the method ofTrinder(16).

Serum CAT was determined according to Aebi method manually(17). Superoxide dismutase activity in erythrocyte was determined by using a

modified photochemical nitro-blue tetrazolium (NBT) method utilizing sodium cyanide as peroxidase inhibitors(17).

Statistical analysis

Statistical analysis was done using the ANOVA and test for comparison of data in the control group with the experimental groups. The results were expressed as mean ± S.E.M (standard error of means). P-value less than 0.05 were considered significant and are written in the parentheses.

RESULTS AND DISCUSSION

Table (1) showed that the glucose level is significantly increased in alloxan diabetic rabbits $P<0.05$ (9 ± 1.21) mmol/L compared with (3 ± 0.15) mmol/L in control rabbit. After treatment with 250 mg of ginger a significant decreased in glucose level (5 ± 0.43) mmol/L was observed compared with control group which indicated a positive correlation effect of ginger intake. The level of glucose was significantly reduced $P<0.05$ (4 ± 0.33) mmol/L in alloxan diabetic rabbits receiving 500mg of ginger compared with the level of control group.

Table (2) showed that the SOD level is significantly decreased in alloxan diabetic rabbits $P<0.05$ (29.78 ± 15.21 µ/ml compared with (150.96 ± 37.45) µ/ml in control rabbit. After treatment with 250 mg of ginger a significant decreased in SOD level (65.32 ± 17.6) µ/ml was observed compared with control group which indicated a positive correlation effect of ginger intake. The level of SOD was significantly reduced $P<0.05$ (71.3 ± 17.9) µ/ml in alloxan diabetic rabbits receiving 500mg of ginger compared with the level of control group.

Table (3) showed that the CAT level is significantly decreased in alloxan diabetic rabbits $P<0.05$ (10.14±0.23)µ/ml compared with (12.56±0.65) µ/ml in control rabbit. After treatment with 250 mg of ginger a significant decreased in CAT level (11.34±0.36) µ/ml was observed compared with control group which indicated a positive correlation effect of ginger intake. The level of CAT was significantly reduced $P<0.05$ (12±0.44) µ/ml in

alloxan diabetic rabbits receiving 500mg of ginger compared with the level of control group.

Table-1: Effect of administering ginger extract on glucose level in healthy and diabetic rabbits

Group	Glucose (mmol/L)
	Mean ±S.D.
Normal control	3 ± 0.15
Diabetic control	9 ± 1.21
Diabetic+ 250mg extract	5 ± 0.43
Diabetic+ 500mg extract	4 ± 0.33

$P<0.05$

Table-2: Effect of administering ginger extract on SOD level in healthy and diabetic rabbits

Group	SOD (μ/ml)
	Mean ±S.D.
Normal control	150.96 ± 37.45
Diabetic control	29.78 ± 15.21
Diabetic+ 250mg extract	65.32 ± 17.6
Diabetic+ 500mg extract	71.3 ± 17.9

$P<0.05$

Table-3: Effect of administering ginger extract on CAT level in healthy and diabetic rabbits

Group	CAT (μ/ml)
	Mean ±S.D.
Normal control	12.56±0.65
Diabetic control	10.14±0.23
Diabetic+ 250mg extract	11.34±0.36
Diabetic+ 500mg extract	12±0.44

$P<0.05$

Intravenous injection of alloxan rapidly damages the β cells of the islets of langerhans in pancreas. Destruction of pancreatic beta-cells by alloxan may results from reaction with glutathione or other sulfhydryl groups of proteins which would inactivate essential enzymes or coenzymes of the cell, alloxan injection may also results in generation of free radicals which cause breaking of DNA stands of beta-cells. Alloxan has also been

shown to inactivate Ca^{+2} -and calmodulin-dependent protein kinase, the activity of this enzyme was related to insulin secretion (18,19) Flavanoids, terpenoids and a host of the secondary metabolites of many plantsposses hypoglycemic effects in various experimental animal models(20,21). Many investigators reported that compounds of ginger such as 6-gingerol, tannins, polyphenolic compounds, and triterpenoids of possess hypoglycemic and other pharmacological properties (22,23).

Catalase and SOD are the two scavenging enzymes that remove toxic free radicals (24) are considered primary enzymes, since they are involved in direct elimination of reactive oxygen species (25).SOD is an important defense enzyme which catalyses the dismutation of superoxide radicals (26) and CAT is a hemoprotein which catalyzes the reduction of H2O2 and protects tissue from highly reactive OH• radicals (27).The reduced activity of SOD and CAT in the liver and the kidney observed during diabetes may be due to deleterious effect of the accumulation of superoxide anion radicals and hydrogen peroxide. Studies conducted on the chemical compounds of ginger and onion shows that they contain anti-oxidants. Ginger contains vitamins, flavonoids which their antioxidant roles have been thoroughly been proved(28,29).

In conclusion, the results of the present study showed that the ginger have blood glucose lowering effects and it also had potent antioxidant properties, which may contribute towards preventing peroxidative damage.

REFERENCES

1. Brownlee, M.. Biochemistry and molecular cell biology of diabetic complications. Nature, 414: 813-820. (2001).
2. Warkins, P.J. Diabetes mellitus, types and complications. In: P. J. Walkins (ed) ABC of Diabetes, 5th ed., BMJ Press, 5-95. (2003).
3. Baynes, J.W. and S.R. Thorpe. Role of oxidative stress in diabetic complication; a new perspective on an old paradigm. Diabetes, 48: 1-9. (1999).
4. Baynes, J.. Role of oxidative stress in development of complication diabetes, 40: 405-412. (1991).

5. Ebuehi, O.A.T., V.I. Giwa-Osagie, O.M. Ebuehi and O.F. Giwa-Osagie. Oxidative stress during the various trimesters of pregnancy in humans. Nig. Journal Health & Biomedical Sciences, 2(2): 61-64. (2003).
6. Evans, J.L., I.D. Goldfine, B.A. Maddux and G.M. Grodsky. Oxidative stress and stress--activated signaling pathways: a unifying hypothesis of type 2 diabetes. Endocr. Rev., 23: 599-622. (2002).
7. Obrosova IG, Fathallah L, Greene DA (2000) Early changes in lipid,Vincent et al. • Oxidative Stress and Diabetic Neuropathy Endocrine Reviews, 25(4):612–628 625peroxidation and antioxidative defense in diabetic rat retina: effect of DL-_-lipoic acid. Eur J Pharmacol 398:139–146. (2004).
8. Aydin A, Orhan H, Sayal A, Ozata M, Sahin G, Isimer A Oxidative stress and nitric oxide related parameters in type II diabetes mellitus: effects of glycemic control. Clin Biochem, 34:65–70. (2001)
9. Langner E, Greifenberg S, Gruenwald J. Ginger: History and use. Adv Ther;15:25-44. (1998).
10. Sekiwa, Y., Kubota K. and Kobayashi, A.: Isolation of novel glycosides from ginger and their antioxidative activity. J. Agric. Food Chem., 8: 373-379. (2000).
11. Kamtchouing, P.; Mbongue-Fandio, G.Y.; Dimo, T. and Jatsa, H.B.: Evaluation of androgenic activity of Zingiber officinale extract in male rats. Asian J. Androl., 4: 299-301. (2002).
12. Al- Amin, Z.M.; Thomson, M.; Al Qattan, K.K.; Peltonen-Shalaby, R. and Ali, M: Antidiabetic and hypolipidemic properties of ginger (Zingiber officinale) in streptozotocin - induced diabetic rats. Br. J. Nutri., 96(4): 660-664. (2006).
13. Zancan, K.C.; Marques, M.O.; Petenate, A.J. and Meireles, M.A: Extraction of ginger (Zingiber officinale Roscoe) oleoresin with CO2 and co-solvents: A study of the antioxidant action of the extracts. J. Supercri. Fluids., 24(1): 57-67. (2002).
14. Subra, A, Push, and Rajaseck, K. Effect of Artemisia Pallens wall. On blood glucose levels in normal and alloxan induced diabetic rats. J.Ethno., 50:13-17. (1996).

15. Bhandari U., Kanojia R. and Pillai K.K : Effect of ethanolic extract of Zingiber officinale on dyslipidaemia in diabetic rats. Journal of Ethnopharmacology., 97, 227–230. (2005).
16. Trinder P. Determination of glucose in blood using glucose oxidase with an alternative oxygen acceptor. Ann Clin Biochem; 6: 24-27. (1969).
17. Aebi H. Methods of Enzymatic Analysis. Academic Press.;674-84. (1974).
18. Bishop,M.; Vonlaufen,J.D. & Fody, E.P. Clinical Chemistry Principles Procedures Correlations.J.B. Lippincott Company. London, (2011).
19. Shimran, K.A. Lipid profile investigation in patients with chronic renal failure and diaetic patients undergoing renal dialysis. Diploma Thesis. College of Medical and health Technology. Commission of Technical Institutes,(2003).
20. Ross I.A : Medicinal Plants of the World –Chemical Constituents, Traditional and Modern Medicinal Uses. Humana Press Inc. New Jersey,USA, 30-45. (2001).
21. Ojewole J.A.O : Hypoglycaemic effect of Clausena anisata (Willd) Hook methanolic root extract in rats. J. Ethnopharmacol., 81, 231-237. (2002+)
22. Young H. V., Luo Y. L., Cheng H. Y., Hsieh W. C, Liao J.C., Peng W. C: Analgesic and anti-inflammatory activities of [6]-gingerol, J Ethnopharmacol, 96, 207-210. (2005).
23. Jiang H., Xie Z., Koo H.J., McLaughlin S. P.,Timmermann B. N. and Gang D.R. :Metabolic profiling and phylogenetic analysis of medicinal Zingiber species: Tools for authentication of ginger (Zingiber officinale Rosc.). Phytochemistry, 67, 232-244. (2006).
24. Wohaieb SA, Godin DV. Alterations in free radical tissue defense echanisms in streptozotocin induced diabetes in rat: effects of insulin treatment. Diabetes; 36: 169 - 173. (1987).
25. Halliwell B, Gutteridge JMC.Free radicals in biology and medicine, 2nd Cd,Oxford Clarendon Press.: 203-207. (1989).

26. Mecord JM, Keele BB, Fridovich I. An enzyme based theory of obligate anaerobiosis, the physiological functions of superoxide dismutase. P Natl Acad Sci USA; 1024-27. (1976).
27. Chance B, Greenstein DS, Roughton RJW. The mechanism of catalase action steady state analysis. Arch Biochem Biophys; 37: 301 - 39. (1952).
28. Nassiri M, Khaki A, Gharachurlu Sh,Ashteani A, Rastegarnea H, Rezazadeh Sh.Effects of Ginger on spermatogenesis in Streptozotocin-induced Diabetic Rat. J.Medicinal Plants; 31 (8): 118 – 25. (2009).
29. Khaki A, Fathiazad F, Nouri M, Khaki AA, Abassi maleki N, Ahmadi P, Jabari-kh H.Beneficial Effects of Quercetin on sperm parameters in streptozotocin -induced diabeticmale rats. Phytotherapy Res J.; (24), in press. (2010).

Resonance Tunneling Lifetime in Amorphous Si / Si_{1-x} Ge_x Quantum Wells Superlattice

*Rusul Adnan Al-Wardy, **Moafak C. Abdulrida and *Ibrahim R. Agool
*Al-Mustansiriya University, College of Science, Department of Physics
** University of Baghdad, College of Education (Ibn Al-Haitham),
Theoretical Nanoscience Optoelectronic Devices

Received : 06/04/2011 Accepted: 29/05/2011

الخلاصة

إن الغاية من هذا العمل هو تقديم دراسة نظرية حول عمر تنفق الألكترونات عبر منظومة من الشبيكة الفائقة لشبه موصل. والمنظومة التي تم أخذها بنظر الإعتبار هي a-Si/$Si_{1-x}Ge_x$ وضمن مدى الطاقة $\varepsilon <$ أرتفاع حاجز الجهد (V_o). ومن هكذا نظام عينا إعتماد عمر تنفق الألكترونات على الكسر المولي (x) وعدد الحواجز (N) و عرض منطقتي الحاجز والبئر. لقد أظهرت نتائجنا عن أحتمالية إستخدام مثل هكذا نبيطة في تطبيقات ثنائيات الليزر على المدى القريب.

ABSTRACT

The purpose of this work is to report a theoretical study for resonant tunneling lifetime (τ) of electrons tunneling through semiconductor superlattice system. The system that we have considered is a-Si/$Si_{1-x}Ge_x$ heterojunction superlattice within the energy range of $\varepsilon <$ the potential barrier height (V_o). From such system, we determined the (τ) dependency on mole fraction (x), the number of barriers, N, and the dimensions of barriers and wells width. Our results indicate that there is a possibility to use such device in laser diodes applications by near future.

INTRODUCTION

The multi-barrier potential profile needed for resonant tunneling may be realized using semiconductor by variation of doping in the same semiconductor material, but the most successful approach is to use heterojunction consisting of different types of semiconductor materials [1]. A good combination of heterojunction devices is two materials of similar lattice constants, but different in energy gap (E_g) [2]. Recently, extensive research

works have been carried out on heterojunctions between amorphous silicon (a-Si), and crystalline semiconductors, because of their use in many semiconductor devices, such as metal-amorphous silicon FET_s, solar cells. However, the physics of amorphous-crystalline heterojunctions is not clearly, understood yet [3]. On the other hand, very little work has been done on the (a-Si/SiGe) heterojunction, although (a-Si) exhibits a series of important properties (e.g. wide optical band gap, mechanical strength) and (SiGe) is the most well known semiconductor material, so that the (a-Si/SiGe) heterojunction could be very useful in many semiconductor devices. In (1969), research on quantum structures was initiated with a proposed of an "engineered "semiconductor superlattice (SL) by Esaki and Tsu [4]. The (SL) consider an alternating thin layers of two or more materials with different equilibrium lattice constants [5,6], coherent layers on nanometer thickness scale may be deposited by molecular-beam epitaxy or metal-organic vapor deposition, so thus building up a superperiodic structure on layer scale [7]. When electrons are confined within a semiconductor thin film with a thickness of the order of the de Broglie wavelength, the wave nature of the electrons becomes important [8], so that quantum phenomena such as interference, tunneling and energy quantization are exhibited in (RTD_s) [9, 10].

In classical mechanics, carriers are completely confined by the potential wells, only those carriers with excess energy higher than the barriers can escape [2]. But in quantum mechanics point of view, a particle can tunnel through a potential barrier of height higher than that of the incident particle [1]. The necessary conditions for tunneling are: (1) Occupied energy states exist on the side from the electron tunnels. (2) Unoccupied energy states exist at the same energy level on the side to which the electron can tunnel. (3) The tunneling potential barrier height is low and the barrier width is small enough that there is a finite tunneling probability, and(4) the momentum is conserved in the tunneling process [2,9]. Tunneling through a double barrier was first solved in the Wentzel-Kramers-Brillouin (WKB) approximation by David Bohm in (1951) [11], who pointed out that resonances in the transmission coefficient occurs at certain incident electron energies. The transmission coefficient is equal to one, i.e. the double barrier is very transparent for a

particle transmission. This phenomenon is called resonant tunneling [1]. It is one of the quantum vertical transport effects in nanostructures [12].

The idea of nanoelectronics has popularized in the mid (1980_s). When pioneered work on resonant tunneling and band gap engineering in low-dimensional semiconductor quantum wells and superlattices grew and championed by several groups for the exploration of new opportunities for circumventing the limit on the downscaling of conventional transistors and integrated circuits (IC's) [10]. Nanostructures are classified based on the dimensions, in which carriers are confined in one, two, or three spatial dimensions, result in quantum wells, quantum wires, and quantum dots systems. They are usually labeled as (2D), (1D), and (0D) respectively [13]. In quantum wells, i.e.in a thin layer of semiconductor with low energy gap sandwiched by two barrier layers with higher energy gap, quasi-confined states are formed at energies determined by the thickness of well (a) [8]. The resonant quasi-level lifetime, which is referred here as resonant tunneling lifetime (RTL), is one of the key issues concerning the development of the novel electronic devices based on tunneling. Furthermore, the (RTL) depends strongly on many parameters such as the height of potential barrier, the mole fraction of barrier material vis-à-vis the well material, the thickness of the barrier and well layers and the number of the barriers in the structure. Specifically, determination of the (RTL) is vital to estimate the frequency limit of high speed tunneling devices [14].

In this paper, we have considered the tunneling lifetime of ground state level and first excited state in the (MBS) as a comprehensive manner by using the energy of incident particles is less than V_o. In addition, we have examined the dependence of resonant tunneling lifetime on various factors like the mole fraction(x), the number of barriers (N) and the dimensions of barriers and wells width of the system.

Theory

It will be better, if we consider a model to understand the tunneling of electron through multi-barrier semiconductor heterojunction. In such model, we have a superlattice structure contains alternately semiconductor heterojunction of (a-Si/$Si_{1-x}Ge_x$) (for x=0.2 to 0.8). These two materials have similar band structure, but different energy gap, where the ($Si_{1-x}Ge_x$) has the small gap to form the well, and (a-Si) has the large energy gap to form the barrier. In this structure, the barriers thickness (b), thickness of well (a) and

the superlattice period (c) are related with each other $(c = a + b)$. If these systems consist of (N) barriers then one will find (N-1) wells as shown in figure (1):

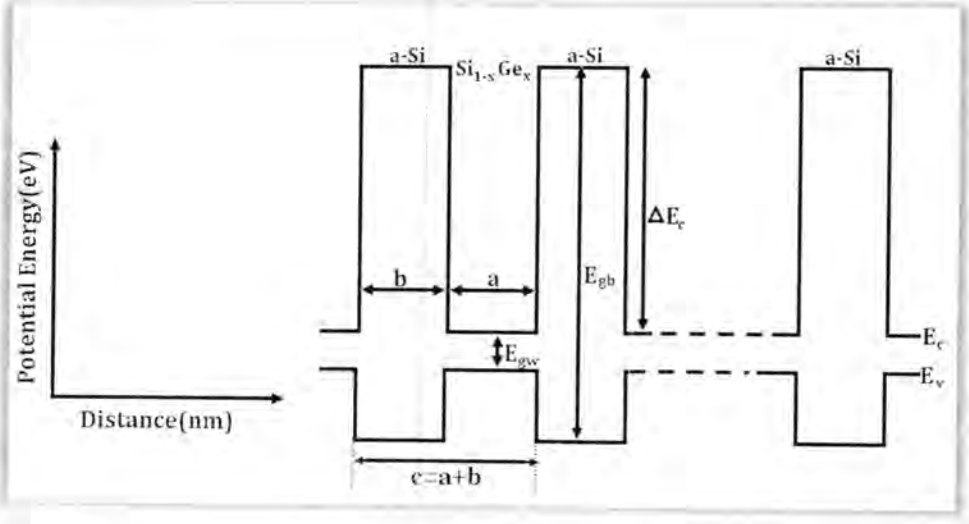

Fig. -1: Energy band diagram of stacking layer [15].

If electrons or other particles of mass (m*) and kinetic energy (E) impinge on a potential barrier of energy (V_o) and the thickness (b) in such way that ($E < V_o$), they penetrate into the barrier. If the potential barrier is thin, there is a significant chance that the particle can transmit through the barrier [16]. The derivation of (RTL) requires the knowledge of resonant transmission spectrum. The theoretical model based on the transfer matrix approach [17] has obtained the transmission coefficient T (E) for (a-Si/Si1-xGex) superlattice:

$$\boldsymbol{T(E_x)} = \frac{\mathbf{1}}{\mathbf{1} + \left| \frac{\boldsymbol{k_2^2 f^2 + k_1^2}}{\boldsymbol{2ik_1k_2f}} \boldsymbol{sinh(k_2 b)} \right|^2 . \left| \frac{\boldsymbol{sin(N\theta)}}{\boldsymbol{sin(\theta)}} \right|^2} \quad \ldots\ldots\ldots\ldots\ldots\ldots\ldots\ldots\ldots\ldots (1)$$

The resonant tunneling life time of the electrons for incident energies equal to any of the quasi-level resonant tunneling energy states in the tunneling band is given by Heisenberg's uncertainty principle[1,16];

$$\boldsymbol{\tau} = \frac{\hbar}{\boldsymbol{2\Delta E_m}} \quad \ldots\ldots\ldots\ldots\ldots\ldots\ldots\ldots\ldots\ldots\ldots\ldots\ldots\ldots\ldots\ldots\ldots\ldots\ldots\ldots\ldots\ldots\ldots\ldots\ldots\ldots\ldots\ldots (2)$$

Where

τ: is the lifetime of the quasi-bound state, which is finite (i.e. the particle or wave packet will eventually "leak out" from the potential well [1].

$\hbar = \frac{h}{2\pi}$, h: is the Planck's constant.

ΔE_m: is the half –width of the resonant peak at half-maximum of the resonant peak around the resonance energy (E_m) [14]. ΔE_m Should be inversely proportional to the lifetime of the states in the well and obtained from the curve of transmission coefficient versus incident energy by numerical computation as shown in figure (2):

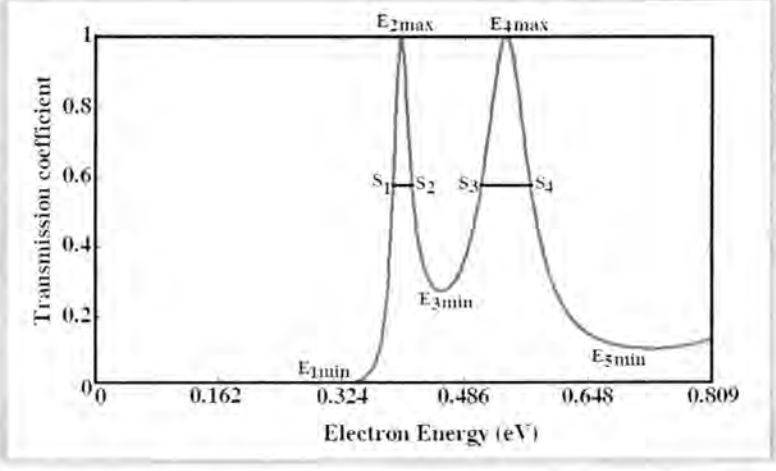

Fig. -2: Sketch of transmission coefficient versus electron energy and illustrate how to estimate the (RTL) for N=3.

$$S_1 = \frac{(E_{1min}+E_{2max})}{2},$$

$$S_2 = \frac{(E_{2max}+E_{3min})}{2} \quad \ldots\ldots\ldots\ldots\ldots\ldots\ldots\ldots\ldots\ldots\ldots\ldots\ldots\ldots (3)$$

$$\Delta E_{m1} = S_2 - S_1 \quad \ldots\ldots\ldots\ldots\ldots\ldots\ldots\ldots\ldots\ldots\ldots\ldots\ldots\ldots\ldots\ldots\ldots\ldots\ldots\ldots\ldots\ldots (4)$$

$$\tau_1 = \frac{\hbar}{2\Delta E_{m1}} \quad \ldots\ldots\ldots\ldots\ldots\ldots\ldots\ldots\ldots\ldots\ldots\ldots\ldots\ldots\ldots\ldots\ldots\ldots\ldots\ldots\ldots\ldots (5)$$

$$S_3 = \frac{(E_{3min}+E_{4max})}{2},$$

$$S_4 = \frac{(E_{4max}+E_{5min})}{2} \quad \ldots\ldots\ldots\ldots\ldots\ldots\ldots\ldots\ldots\ldots\ldots\ldots\ldots\ldots\ldots\ldots\ldots\ldots\ldots\ldots (6)$$

$$\Delta E_{m2} = S_4 - S_3 \quad \ldots\ldots\ldots\ldots\ldots\ldots\ldots\ldots\ldots\ldots\ldots\ldots\ldots\ldots\ldots\ldots\ldots\ldots\ldots\ldots\ldots\ldots (7)$$

$$\tau_2 = \frac{\hbar}{2\Delta E_{m2}} \quad \ldots\ldots\ldots\ldots\ldots\ldots\ldots\ldots\ldots\ldots\ldots\ldots\ldots\ldots\ldots\ldots\ldots\ldots\ldots\ldots\ldots\ldots (8)$$

RESULTS AND DISCUSSION

The resonant tunneling lifetime (τ) for first band states (the ground state level and first excited state, τ_0 and τ_1, respectively), can be obtained from Eq. (2). Fig (3) depicts resonant tunneling lifetime τ_0 and τ_1 versus barriers number for system, x = 0.5 as a mole fraction and a = b = 1.2 nm. The diagram clearly shows that the (τ) increase for the same values of E_m with increase in (N) in a system, see table (1) , and (τ) values for the resonant states decrease as the energy moves towards higher tunneling bands.

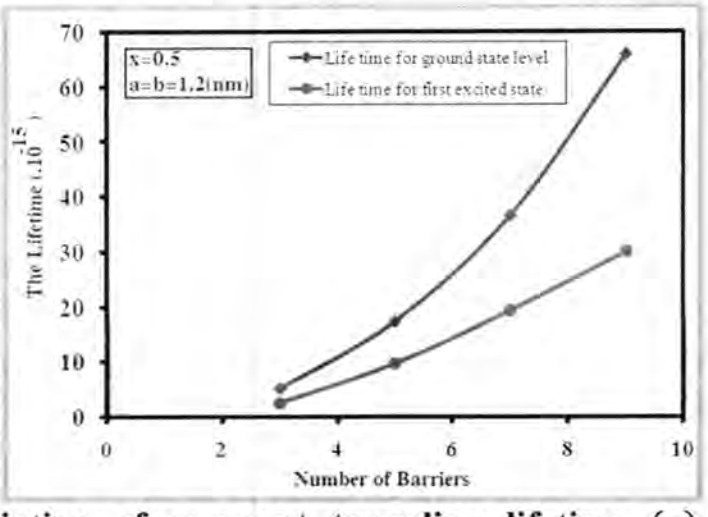

Fig. -3: Variation of resonant tunneling lifetime (τ) with different number of barriers in (a-$Si/Si_{1-x}Ge_x$) superlattice structure, where($x = 0.5, a = b = 1.2nm$).

We can see from equation (2), when (E_m) decrease conversely the lifetime increasing and when E_m becomes larger, the lifetime decreasing, and the electrons in resonant states of the higher bands can tunnel faster than they are in lower bands mainly due to their higher energy.

Table -1: The values of (RTL),τ, of (a-$Si/Si_{1-x}Ge_x$) with ($x = 0.5, a = b = 1.2nm$) for ($N = 3, 5, 7, 9$) for first band states (the ground state level (τ_0) and the first excited state (τ_1).

a-$Si/Si_{1-x}Ge_x$ Superlattice ($x = 0.5, a = b = 1.2nm$)	$N = 3$	$N = 5$	$N = 7$	$N = 9$
$\tau_o(.10^{-15}Sec)$	5.149	17.345	36.618	65.912
$\tau_1(.10^{-15}Sec)$	2.574	9.693	19.386	29.960

Figure (4a) shows the relationship between the lifetimes of ground state levels (τ_0) as a function to the well width. It is so clear, from the figure that the lifetime of ground state level increases as we increase the well width and the number of barriers in the system. Fig. (4b) shows the variation of the lifetime of ground state level (τ_0) as a function of the barrier width. It can be seen from the figure that the behavior of the lifetime of ground energy level is increasing slightly as increased barrier width. In fact, this phenomenon needs more study and more detailed to access the most appropriate explanation for this behavior.

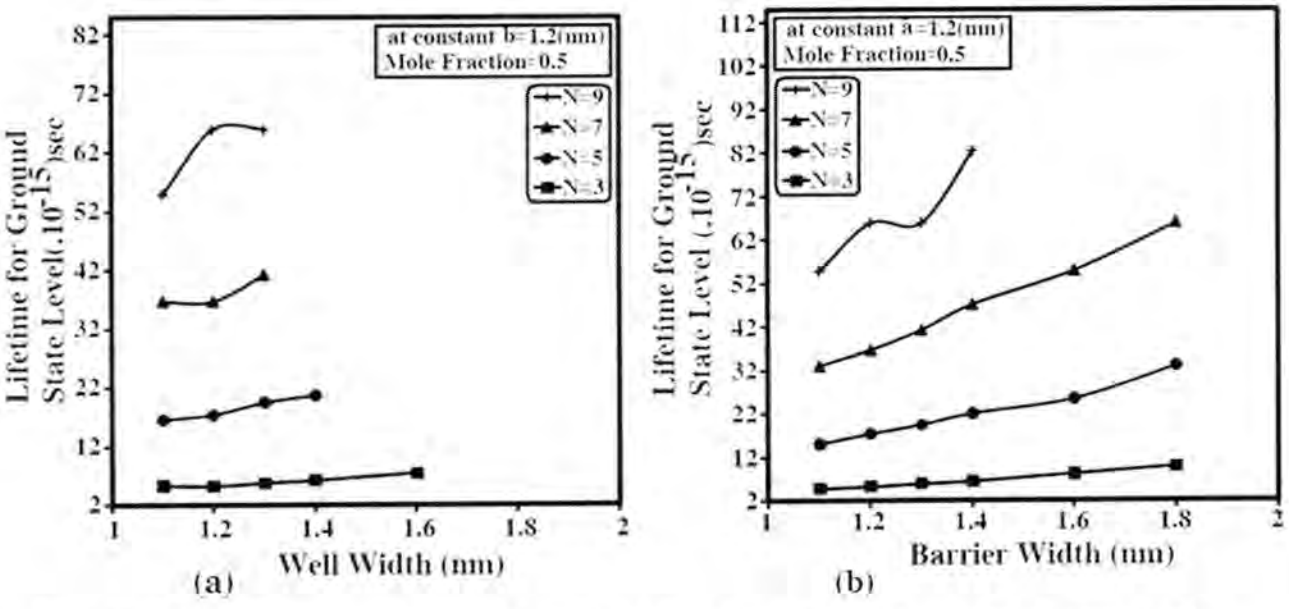

Fig.-4: The lifetime of ground state level as a function of (a) the well width and (b) the barrier width at constant mole fraction (x = 0.5).

While with regard to the lifetime of first excited level (τ_1) , it is also studied as a function of each well and barrier widths and that has been demonstrated in figure 5 (a and b) respectively. Our results had come in conformity with the practical results in terms of behavior [14], not in terms of values because we use amorphous silicon as the large energy gap of the superlattice structure and according to our knowledge such structure have not been used by others.

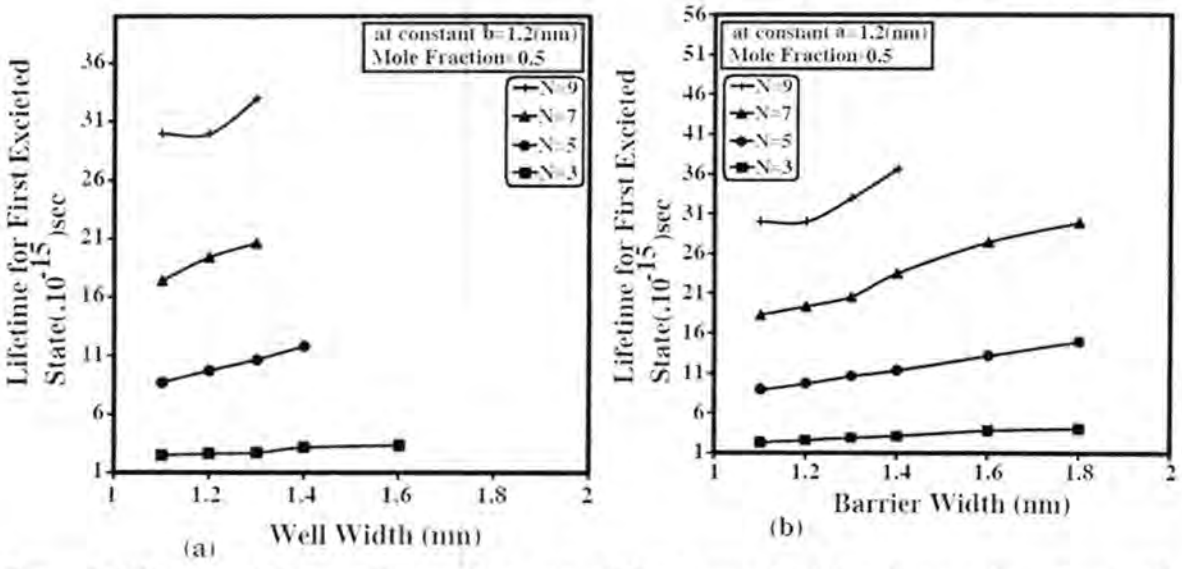

Fig. -5: The variation of the lifetime of first excited level as a function of (a) well width and (b) barrier width at constant mole fraction (x = 0.5).

We also presented the effect of mole fraction system on the value of both the lifetime of ground and first excited state (τ_0 *and* τ_1) . It is clear that both (τ_0 *and* τ_1) are independent on the mole fraction system (concentration of Ge). This is clearly illustrated in Figure 6.

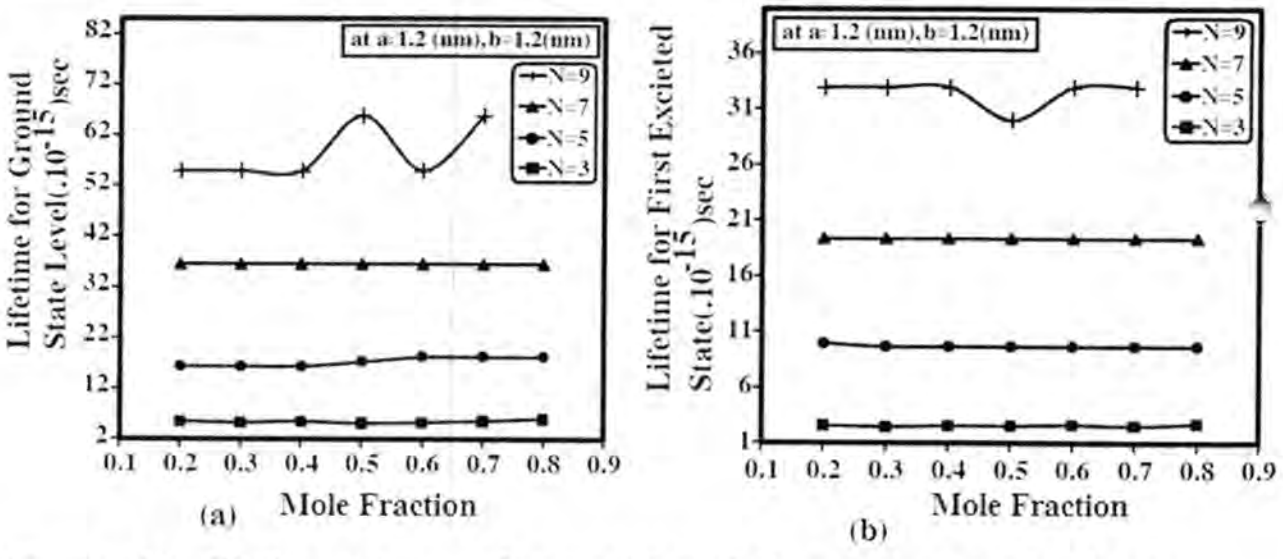

Fig. -6: The lifetime of ground state (a) and first excited state (b) as function of the mole fraction in the system for different number of barriers respectively

In this paper we have numerically determined the resonant tunneling lifetime for first band states (the ground state level and first excited state,

τ_0 and τ_1, respectively) in a-Si/Si1-xGex multi-barrier structures. We examined our structures for different parameters such as barrier and well width, number of barriers and mole fraction. The results are very sensitive to the geometry of tunneling system (barrier and well dimensions). For high well and barrier width will find high lifetime. In addition, high number of barriers shows high lifetime while the lifetime for both ground and first excited states are independent on the mole fraction of the system.

REFERENCES

1. Yu R., B.S., M.S., "Phonon-Assisted Tunneling in Silicon/Silicon Germanium Resonant Interband Tunneling Diodes", Ph.D Thesis, Ohio state university, (2007).
2. Sze S.M., and Kwok K.Ng, "Physics of semiconductor Devices", Third Edition, John Wiley& Sons., Inc.(2007).
3. Georgoulas, Magafas N. L. and Thanailakis A,"Astudy of a-Sic/c-Si (n) Isotype Heterojunctions"Active and Passive Elec.CompVol.16:P.55-64. (1993).
4. Esaki L. and Tsu R., IBMJ.Res.Develop.14, 16,(1970).
5. C.L.Roy, "Tunneling of Electrons Through Semiconductor Superlattices", Bull.Mater.Sci., Vol.25,No.6,P.469-471, (2002).
6. M.A.Herman,"Silicon-Germanium Heterostructures:Properties, Technology, and Application in Infrared Detectors", Opto-Electr.Rev.**5**,No.3, (1997).
7. Kittel C., "Introduction to Solid State Physics", 8th edition, John Wiley &Sons., Inc.,(2004).
8. Cressler J. D., "Silicon Heterostructure Devices ", Taylor&Francis Group, LLC , (2008).
9. Davis M., "Simulation and Characterization of ZnSe/BeTe Resonant Tunneling Diode on Silicon", M.SC.Thesis, the Faculty of the Graduate school of the university of Texas at Arlington,(2006).
10. Sun J.P., Haddad G. I., "Resonant Tunneling Diodes: Models and Properties", Proceeding of the IEEE, Vol.86, No.9, (1998).
11. Bohm D.,"Quantum Theory", Prentice-Hall, New York, (1951).
12. Martinez-Duart J.M., Martin -Palama R.J.,and Agullo-Rueda F.,"Nanotechnology for Microelectronics and Optoelectronics", First edition, Elsevier B.V, Great Britain,(2006).

13. Lamberit C.,"Characterization of Semiconductor Heterostructures and Nanostructures", University of Torino, Elsevier B.V, (2008).
14. Bhattacharya S.P. and Sinha S.,"Non-Relativistic Formalism of Resonant Tunneling in the Semiconductor Superlattices", Journal of Physical Science, Vol.12, 239-248, (2008).
15. Zarifkar A., Bagherabadi A.M., "Numerical Analysis of Triple-Barrier GaAs/Al_xGa_{1-x}As Resonant Tunneling Structure Using PMM Approach", IJCSNS International Journal of Computer Science and Network Security, Vol.8, No.6,(2008).
16. Levi A.F.J.,"Applied Quantum Mechanics", University of Southern California, A.Levie,(2003).
17. Al-Wardy R.A., Abdulrida M.C., .Agool I.R, "The Resonance Tunneling in Amorphous Si/$Si_{1-x}Ge_x$ Quantum Wells Superlattice", A special Issue for the Kufa's First Conference for Physics 6^{th} -7^{th} October ,(2010).

The Optical Properties of (CuInSTe) Thin Films

Bushra A. Hassan, Muthafar F. Al. Hilli, Duaa A. Umran
Department of physics, College of Science, University of Baghdad

Received : 06/04/2011 Accepted : 29/05/2011

الخلاصة

تم قياس الخواص البصرية لاغشية (CuInSTe)لاسماك مختلفة (700, 500, 300) نانومتر المحضرة تحت الفراغ بدرجة حرارة الغرفة.تم قياس طيف النفاذ للاغشية المحضرة من للمنظومة الرباعية ضمن الطول الموجي (950 - 1400) نانومتر، لوحظ زيادة معامل الانكساروالجزء الخيالي من ثابت العزل وثابت الخمود مع زيادة السمك والطول الموجي. ازداد معامل الامتصاص مع زيادة طاقة الفوتون .لقد وجد ان فجوة الطاقة البصرية لاغشية (CuInSTe) قلت ثم ازدادت مع زيادة السمك.فسرت النتائج بدلالة التغير في النفاذ مع زيادة السمك.

ABSTRACT

Optical properties of (CuInSTe) thin films with different thickness (300, 500, and 700nm) prepared under vacuum at room temperature. The optical transmission spectrums of films of quaternary thin film (CuInTeS) are measured in the wavelength range (950–1400 nm) by spectrophotometer. It is observed that refractive index (n), real dielectric constant (ε_1), extinction coefficient (k), imaginary dielectric constant (ε_2) increase with the increasing of thickness and decrease with increasing of wavelength (λ). The absorption coefficient (α) increases with photon energy ($h\nu$). It is found that the optical energy gap (Eg) of (CuInSTe) thin films decreases but then increases with increasing of sample thickness. The results are explained in terms of variation of the transmittance of the prepared samples with thickness.

INTRODUCTION

The ability to fabricate light-weight and flexible photovoltaic cells with scalable processing has initiated numerous research activities in the

solar community. Among the various materials, chalcopyrites, such as ($CuInSe_2$ (CIS)), ($CuIn(S,Se)_2$) (CISS), and ($Cu(In,Ga)Se_2$) (CIGS) have attracted considerable attention. These materials have an absorption coefficient on the order of (10^5 cm^{-1}), which translates to 90% absorption with (200 nm) thickness [1]. This property renders the chalcopyrites advantageous for weight considerations. However, the standard thickness of the chalcopyrite layer in a solar cell is presently (1.5–2 μm) [2], and a thinner absorber layer thickness is generally associated with an increase in shunt conductance. The shunting is a result of surface roughness on the same order as film thickness [3–4].In addition to decreasing the chalcopyrite thickness, replacing sodalime glass with polyimide substrates would provide further advantages in reducing the weight of the device and also the possibility of being flexible. Given that the glass-transition temperature of polyimide is approximately (773K), adopting the conventional deposition methods for (CIS), such as coevaporation or electrodeposition, has been shown to be challenging [5]. Recently, a solution processing of (CIGS) method has been demonstrated using hydrazine as a solvent [6]. The chalcopyrite layer, processed at (543K), has been shown to have a photovoltaic efficiency of 10.2%.

On the other hand copper indium diselenide (CIS) is a promising absorber material for thin film solar cells, mainly due to its appropriate band gaps, high optical absorption coefficient and proper charge densities [7]. Various techniques have been reported for the preparation of ($CuInSe_2$) films such as selenization of metallic precursor [8], elemental co-evaporation [9], spray pyrolysis [10], electro deposition [11], chemical vapor depositi [12], and chemical bath deposition [6].

In the present paper we report the optical properties measurements in glassy (CuInTeS) alloys to study the effect of thickness on the optical constants of the prepared films.

MATERIALS AND METHOD

Glassy alloys of CuInTeS are prepared by quenching technique. The exact proportions of high purity (99.999%) (Cu, In, Te and S) elements, in accordance with their atomic percentages, are weighed using an electronic balance with the least count of (10^{-4} gm). The material was

then sealed in evacuated (~10^{-5} Torr) quartz ampoule (length ~ 25 cm and internal diameter ~ 8 mm). The ampoules containing material are heated to (1100 °C) and were held at that temperature for (12 hours). The temperature of the furnace was raised slowly at a rate of (3-4 °C / minute). During heating, the ampoules are constantly rocked, by rotating a ceramic rod to which the ampoule was tucked away in the furnace. This is done to obtain homogeneous glassy alloys. After rocking for about (12 hours), the obtained melt was then rapidly quenched in to air. Thin films of glassy alloys were prepared by vacuum evaporation technique with different thickness (300,500, and 700nm), the substrates which were corning glass were subjected to several cleaning stages. In which the substrates are kept at room temperature (~25°C) at a base pressure of (10^{-5} Torr) using a molybdenum boat. The films are kept inside the deposition chamber for (24 hours) to achieve the metastable equilibrium. A double UV/VIS/NIR Computer Controlled Spectrometer (Hitachi-330) is used for measuring optical transmission of thin films as a function of wavelength of the incident light.

Basic Considerations

The fundamental absorption edge of polycrystalline or crystalline semiconductors is the region in which the electrons are excited from the valence band (V.B) to the conduction band (C.B) by absorbing the incident photons these photons should have energy equal or greater than the energy gap of semiconductors. The absorption coefficient (α) which is the decrement ratio of incident radiation relative to unit length in the direction of wave propagation inside the medium is relating with the absorbance (A) through the relation[11] :-

$$\alpha = \frac{2.303A}{t} \quad \ldots\ldots (1)$$

Where (t) is the sample thickness. Many researchers [4] put the empirical equation between the optical energy gap (Eg) and energy of the incident photon which is:-

$$(\alpha h\nu) = A(h\nu - Eg)^r \quad \ldots\ldots (2)$$

Where (A) is constant, (hν) is the energy of incident photon which can be calculated using the equation:-

$$h\nu = \frac{1240}{\lambda(nm)} \quad \ldots\ldots (3)$$

Where (r) is the order of the optical transition depending on the nature of electronic transition .The transition is called direct if the extremities of (V.B) and (C.B) lie at the same K-space ,while the transition is called indirect if the transition possible only with phonon assisted ($\Delta k \neq 0$) [7].Thus the value of (r) may be (1/2,2,3/2, and 3) corresponding to the allowed direct ,allowed indirect, forbidden direct and forbidden indirect transition recpectively.The absorption edge become wide for polycrystalline and amorphous semiconductors because of allowed localized states are found in the energy gap, the width of these localized states can be calculated using Urbach Rule[10]:-

$$\alpha = \alpha_0 e^{h\nu/Ee} \quad \ldots\ldots (4)$$

Where (α_0) is constant and (E_e) is the width of localized states.

The optical behavior of materialsutilized to determine its optical constants (refractive index (n), extinction coefficient (k), real and imaginary parts of dielectric constants (ε_1, ε_2)). Several methods were proposed to determine the optical constants, they involve spectrophotometric measurements of reflectance (R) and transmittance (T) of sample in the wavelength range the extinction coefficient (imaginary part of the refractive index) can be calculated by the relation [1]:-

$$k = \frac{\alpha\lambda}{4\pi} \quad \ldots\ldots (5)$$

Where (λ) is the wavelength, (α) is the absorption coefficient which can be obtained using equation (1).

The refractive index (n) can be measured (when the reflectance (R) and (k) are known) by using the equation [5]:-

$$n = \sqrt{\frac{4R}{(R-1)^2} - k^2} - \frac{(R+1)}{(R-1)} \quad \ldots\ldots (6)$$

The complex index ($\bar{N}$) is given by[6]:-

$$\bar{N} = n - ik = \sqrt{\varepsilon} \quad \ldots\ldots (7)$$

Where (ε) is the complex dielectric constant, given by:-

$$\varepsilon = \varepsilon_1 - i\varepsilon_2 \quad \ldots\ldots (8)$$

The parameter (ε_1) is the real part of dielectric constant, (ε_2) is the imaginary part of dielectric constant, from equations (7) and (8) one can obtain:-

$$\varepsilon_1 = n^2 - k^2 \quad \text{..... (9)}$$

$$\varepsilon_2 = 2nk \quad \text{..... (10)}$$

RESULTS AND DISCCSION

The transmittance spectra of (CuInSTe) films with different thickness are plotted in Figure (1), the figure show decreasing of transmittance (T) with increasing of thickness (t) , indeed (T) decrease from (0.830 to 0.452) when (t) increase from 300 to 700 nm. The refractive index (n) of (CuInTeS) films with different thickness were measured and plotted as function of wavelength (λ) in Figure (2).It was found that (n) decreased with (λ) in the range (950-1450 nm),on the other hand (n) at λ=1200nm which lies in middle of spectrum of the transparent region increases from (1.712 to 2.2409) with increasing thickness from (300 to 700nm) indicating that the increasing of thickness made the samples films more opaque to the incident light.

The dependence of the extinction coefficient (k) on the wavelength is shown in Figure (3). It is evident that the values of (k) were reduced, become smaller at the region beyond the absorption edge, they are relatively small with increasing of (λ).It is remarked that (k) values at at (λ=1200nm) increased from (0.0598 to 0.1094) when t increases from 300 to 700nm ,however (k) decreases with further increasing of (t) .The increasing of (k) can be attributed to the increasing of absorption coefficient, hence (k) wick be increased according to equation (5), while the decreasing of k is ascribes to eliminating of defect states responsible about the absorption processes in the band gap[3].Real and imaginary parts of dielectric constant (ε_1 and ε_2) of (CuInSTe) films deposited at room temperature with different thickness were calculated using equs.(9 and 10). The dependence of (ε_1) and (ε_2) on (λ) are shown in Figs.(4) and (5) ,it is concluded that the variation of (ε_1) mainly depend on the value of (n^2) because the smaller value of (k) comparison with (n^2) ,while the imaginary part of dielectric constant (ε_2) mainly depend on (k) values which are related to the variation of (α).

The variation of $(\alpha\ h\nu)^2$ with photon energy ($h\nu$) for direct allowed transition are plotted in Figure (6) for (CuInSTe) samples with different thickness and the optical energy gaps are determined which are listed is

Table.1. It is clear that (Eg) decreases with increasing of thickness, although (Eg) decreases with further increasing of thickness, moreover (Eg) decreases from (1.06 to 1.04 eV) when (t) increase from (300to 500 nm), while (Eg) increases from (1.04 to 1.1 eV) when (t) increase from (500to 700 nm) this can be explained on the fact that increasing of thickness approach the material structure from that of bulk material which accompanies by reduction in bonds lengths and angles which consequently decreases (Eg) values ,similar results are obtained by Z. Djebbour et al[3] , they showed that the width of (Eg) has tendency to decrease with the increasing of film thickness.While the interpretation of the increasing of (Eg) is likely to be attributed to the decrease in the amount of (Te) atoms with the increase of thickness.

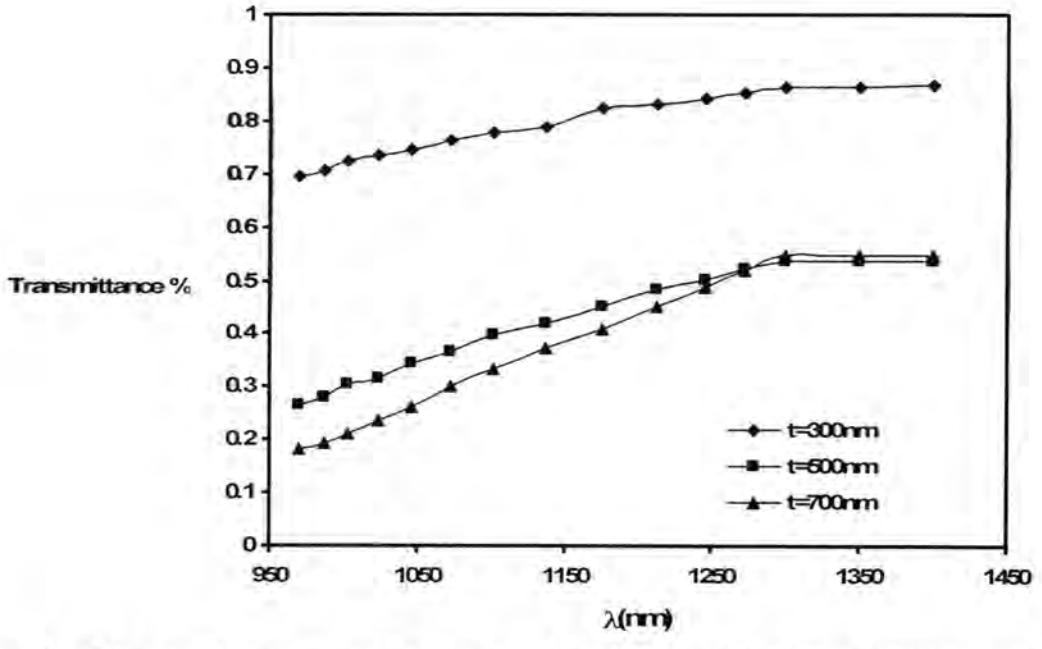

Fig.-1: Transmittance spectra of (CuInSTe) thin films deposited at room temperature

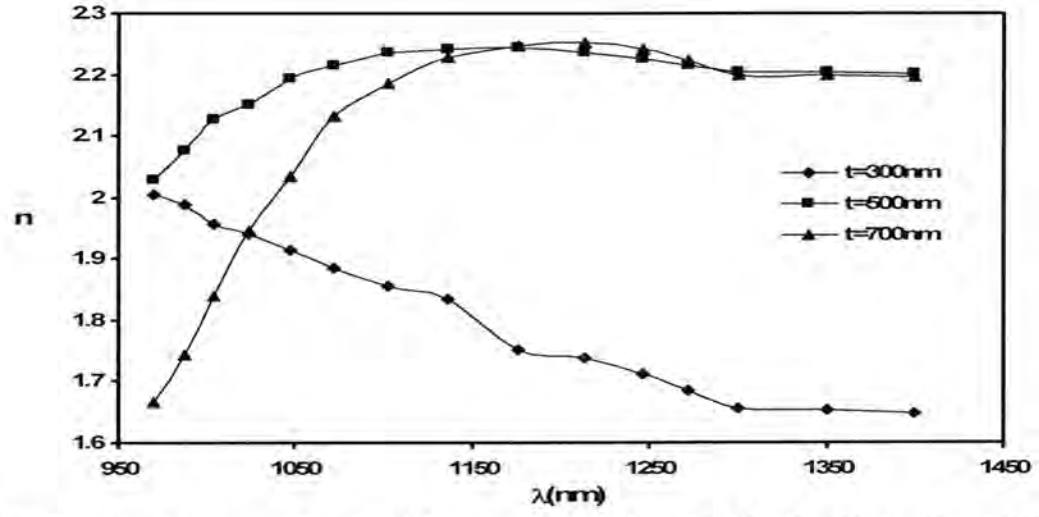

Fig.-2: Variation of n with wavelength of (CuInSTe) thin films deposited at room temperature.

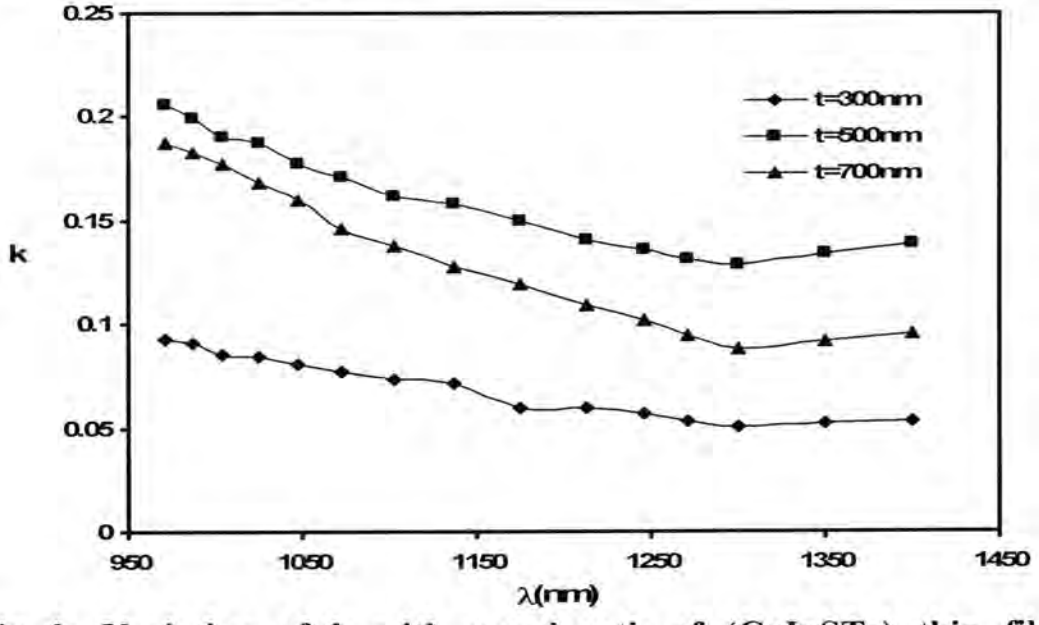

Fig.-3: Variation of k with wavelength of (CuInSTe) thin films deposited at room temperature.

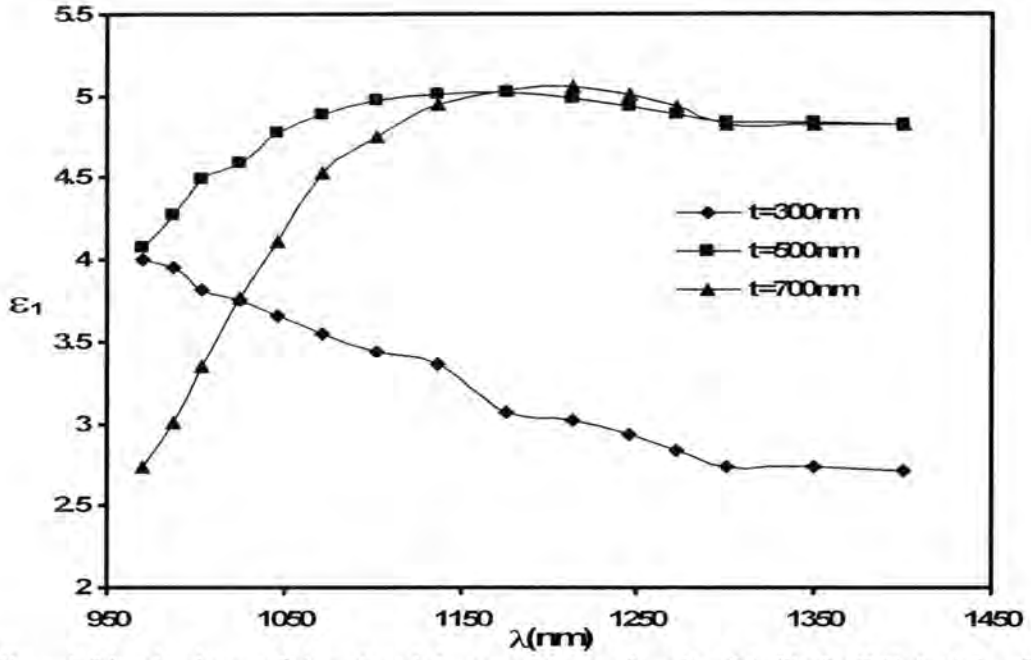

Fig.-4:Variation of (ε_1) with wavelength of of (CuInSTe) thin films deposited at room temperature

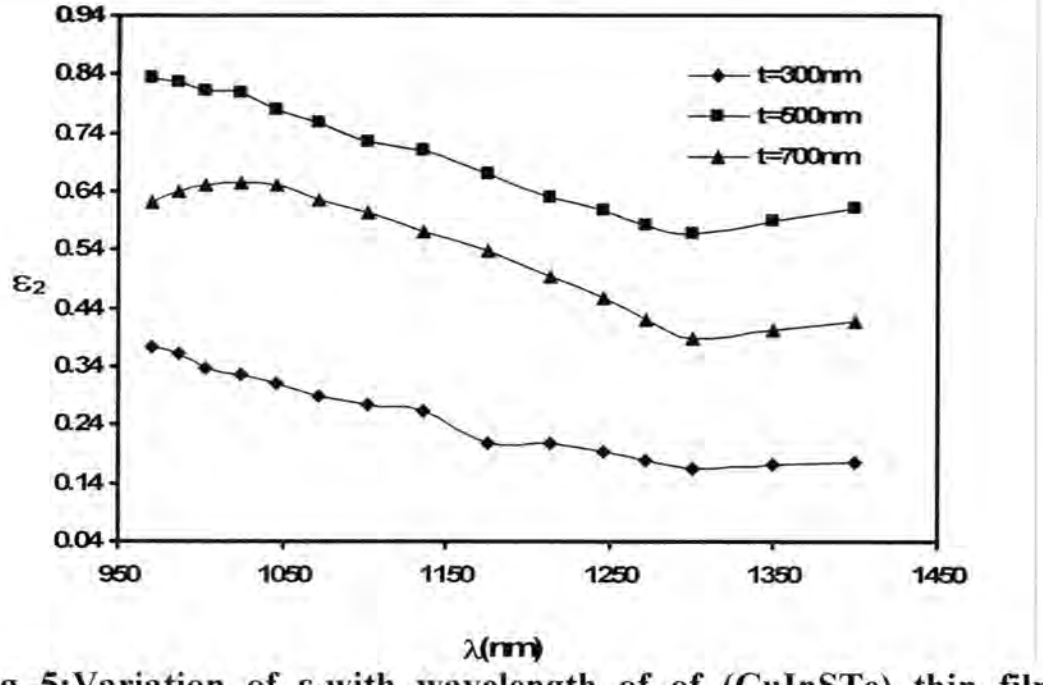

Fig.-5:Variation of $\varepsilon_2$with wavelength of of (CuInSTe) thin films deposited at room temperature.

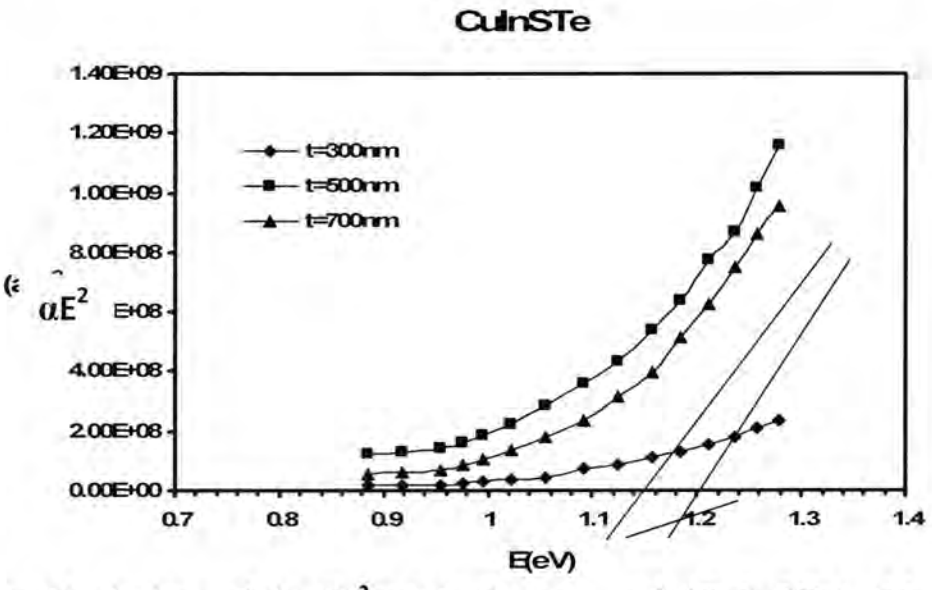

Fig.-6: Variation of $(\alpha E)^2$ with Energy of (CuInSTe) thin films deposited at room temperature

Table-1: The values of (n, k, ϵ_1, ϵ_2), and (T at λ=1200nm) for (CuInSTe) thin films.

Thickness (nm)	n	k	ϵ_1	ϵ_2	E_g (eV)	T
300	1.712	0.0598	3.0218	0.2080	1.06	0.830
500	2.226	0.1409	4.9830	0.6304	1.04	0.482
700	2.240	0.1094	5.0561	0.4929	1.10	0.452

The optical transmission spectra of amorphous thin films of (CuInSTe) thin films are measured in the wavelength range (950–1450 nm) by spectrophotometer. It is observed from optical transmission measurements that optical energy gap (Eg) decreases for low value of thickness and increases for residual thickness. It is also found that refractive index (n), real dielectric constant (ε_1), extinction coefficient (k), imaginary dielectric constant (ε_2) increase with increasing of thickness but decreasing with increasing of (λ).

REFERENCES

[1] F.O. Adurodija, J. Song, I.O. Asia, and K.H. Yoon: Formation of CuIn(S, Se) $_2$ thin film by thermal diffusion of sulfur and selenium vapors into Cu-In alloy within a closed graphite container. Sol. Energy Mater. Sol. Cells 58, 287 (1999).

[2] S. Shirakata, T. Terasako, and T. Kariya: Properties of CuIn $(S_xSe_{1-x})_2$ polycrystalline thin films prepared by chemical spray pyrolysis. J. Phys. Chem. Solids 66, 1970 (2005).

[3] Z. Djebbour, A.M. Dubios, A. Darga, D. Mencaraglia, C. Bazin, J.P. Connolly, J-F. Guillemoles, D. Lincot, B. Canava, and A. Etcheberry: Comparison of optical and electrical gap of electrodeposited $CuIn(S,Se)_2$ determined by spectral photo response and I-V-T measurements. Thin Solid Films 515, 6233 (2007).

[4] P. Peranantham, Y. L. Jeyachandran, C. Viswanathan, N. N. Praveena, P. C. Chitra, D. Mangalaraj, and K. S. Narayandass, "The Effect of Annealing on Vacuum-Evaporated Copper Selenide and Indium Telluride Thin Films", Materials Characterization, 58(2007), p. 756.

[5] H. Zhang, X. Y. Ma, and D. R. Yang, "Effects of Complexing Agent on CdS Thin Films Prepared by Chemical Bath Deposition", Materials Letters, 58(2003), p. 5.

[6] D. Mitzi, M. Yuan,W. Liu, A. Kellock, S. Chey, L. Gignac, A.G. Schrott, "Low-temperature processing of a solution-deposited CuInSSe thin-film solar cell" Thin Solid Films ,517 (2009) 2158.

[7] O. Roussel, M. Lamirand, N. Naghavi, J.F. Guillemoles, B. Canava, and A. Etcheberry: Interfacial chemistry control in thin film solar cells based on electrodeposited $CuIn(S,Se)_2$. Thin Solid Films 515, 6123 (2007).

[8] R. K. Sharma, A. C. Rastogi, and G. Singh, "Electrochemical Growth and Characterization of Manganese Telluride Thin Films", Materials Chemistry and Physics, 84, 46. (2004).

[9] Z. Djebbour, A.M. Dubios, A. Darga, D. Mencaraglia, C. Bazin, J.P. Connolly, J-F. Guillemoles, D. Lincot, B. Canava, and A. Etcheberry: Comparison of optical and electrical gap of electrodeposited $CuIn(S,Se)_2$ determined by spectral photo response and I-V-T measurements. Thin Solid Films 515, 6233 (2007).

[10] J. Cowen, L. Lucas, F. Ernst, P. Pirouz, A. Hepp, and S. Bailey. Liquidphase deposition of α- cis thin films. In Proceedings of Space Photovoltaic Research and Technology Conference (SPRAT). Ohio Aerospace Institute, (2003).

[11] Murat Kaleli, Investigation of Electrical and Optical Properties of Ag-In-Se Based Devices, PhD. Thesis in Physics Department of Middle East Technical University, (2010).

[12] Tahir Çolakoğlu, The Effect of Post-Annealing Process on The Physical Properties of Silver-Indium-Selenium Ternary Semiconductor Thin Films Deposited By Electron Beam Technique, PhD Thesis in Physics Department of Middle East Technical University, (2009).

Determination of the Maximum Quantum energy of X-ray radiation independent on the molybdenum anode using LiF & NaCl crystals

Mohammed Jassim Mohammed Ali
Department of Physics, College of Sciences, Al-Mustansiriyah University

Received : 30/03/2011 Accepted: 29/05/2011

الخلاصة

تم دراسة طيف الانبعاث للاشعة السينية من انود المولبيدنيوم باستخدام بلورتي NaCl & (LiF) لحساب الطاقة الحركية للالكترونات المعجلة بفولتية (35Kv) و الطاقة العظمى للالكترونات بعد التصادم والمنعكسة من البلورتين اضافة الى سرعة الالكترونات المغادرة من القشرة (K) الى القشرتين (L ,M). اظهرت النتائج بان الطاقة الحركية للالكترونات المنبعثة من انود المولبيديوم تقدر (56KeV) وسرعة الالكترونات (1.1 Mm/sec) وان الطاقة الكمية العظمى المنبعثة من الانود والمنعكسة من خلال بلورة (NaCl) تقدر (50.8KeV) واقصر طول موجي (0.02nm) اما في بلورة (LiF) فتقدر الطاقة (44.3KeV) واقصر طول موجي (0.014 nm).

ABSTRACT

The aim of this research is to determine X-ray emission spectrum of molybdenum anode by using LiF and NaCl Crystals to calculate the Kinetic Energy for accelerated electrons in (35KV), The maximum Energy of electron after collision and reflected from crystals and The velocity of electron which travels from the (K-shell) to the (L-M shell). The results showed that the max. Kinetic energy of electrons emitted from the anode Molybdenum estimated (50.8KeV) and the speed of electrons (1.1Mm/sec). Maximum Quantum energy of x-ray radiation energy which emitted from anode and reflected by NaCl crystal (50.8KeV) and the shortest wavelength (0.02nm) either in LiF crystal estimated energy is (44.3KeV) and the shortest wavelength (0.014nm).

INTRODUCTION

X-rays were discovered in 1895 by William Roentgen and their uses and benefits were recognized before their risks. The problems caused by X-

rays are due to their ionizing ability. This means that X-rays are capable of initiating chemical changes on the atomic level [1].

X-rays primary interact with electrons in atoms. When X-ray photons collide with electrons, some photons from the incident beam will be deflected away from the direction where they originally travel, much like billiard balls bouncing off one another. If the wavelength of these scattered x-rays did not change (meaning that X-ray photons did not lose any energy), the process is called elastic scattering (Thompson Scattering) in that only momentum has been transferred in the scattering process. These are the x-rays that we measure in diffraction experiments, as the scattered X-rays carry information about the electron distribution in materials. On the other hand, in the inelastic scattering process (Compton Scattering), x-rays transfer some of their energy to the electrons and the scattered x-rays will have different wavelength than the incident x-ray [2].

Diffracted waves from different atoms can interfere with each other and the resultant intensity distribution is strongly modulated by this interaction. If the atoms are arranged in a periodic fashion, as in crystals, the diffracted waves will consist of sharp interference maxima (peaks) with the same symmetry as in the distribution of atoms. Measuring the diffraction pattern therefore allows us to deduce the distribution of atoms in a material [3].

X-ray can be produced in two ways:

By acceleration the charged particles are usually electron-these rays are bremsstrahung as forms continuous spectrum (a mixtures of electromagnetic waves is very short and short) .or when the electron transition in the cover of atom from Avery high level. X-ray will then show a certain wavelength, and have a specific energy. Both cases above occur in the cavity X-ray, where the electrons arise from anode (fuse molybdenum) and speed by voltage to collision by the surface of cathode and then produce X-ray and heat. 99% of the electricity used appears as temperature is not helpful and only 1%of the energy converted to X-rays [4].

Theoretical part:

The difference between the energy of electron accelerated before and after the collision can be written by the flowing equation:

$$E = e\,U = 1/2\, m_e v_1^2 = E_{Ph} + 1/2\, m_e v_2^2 \qquad (1)$$

e : elementary charge of the electron ($e=1.602*10^{-19}$ C).
U : anode voltage.
m_e : electron mass.
v_1 : velocity of the electron before the collision.
v_2 : velocity of the electron after the collision
E_{ph} : energy of the photons (energy of an X-ray quantum).
The energy of radiation quantum is:

$$E_{Ph} = h \cdot f = h \frac{c}{\lambda} \qquad (2)$$

h: Planck's constant ($h = 6.625*10^{-34}$ W. sec).

c : light velocity in vacuum ($c = 2.998*10^{8}$ m . sec^{-1}).
f : frequency.
λ : Wavelength.
The bremsstrahlung has a continuous spectrum with an edge at short wavelengths. This corresponds to those electrons which transpose their whole kinetic energy into an X-ray photon (total slowdown, $v_2=0$). The photon has then a maximum energy; hence its wavelength is minimum in this case [4]:

$$E_{Ph} = eV = h \cdot f = hc/\lambda_{min} \qquad (3)$$

Wavelengths below λ_{min} can't occur at a given anode voltage because the entire kinetic energy of the electrons is already transformed in X-ray quanta. Equation (3) represented the maximum energy of electrons accelerated to the shortest wavelength.

Electron Shells:

As a simple model, an atom may be considered to be a positive charged nucleus surrounded by shells of negative charged electrons. The shells are termed K, L, M, and N (starting from the innermost, most strongly bound shell). More accurately, an atom consists of a nucleus surrounded by electrons that occupy volumes of space (orbital's) around it (Figure 1) only some of which are spherical.

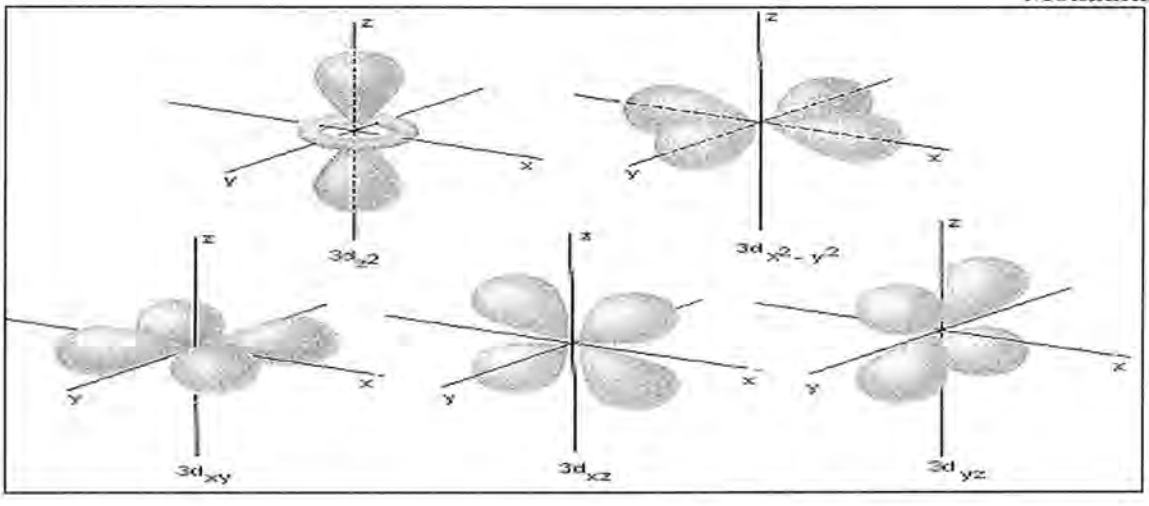

Fig.-1: Actual probability distributions for electron clouds, which are considered as shells in this discussion.

When a sample is bombarded by an electron beam, some electrons are knocked out of their shells in a process called inner-shell ionization. About 0.1% of the electrons produce K-shell vacancies; most produce heat. Outer-shell electrons fall in to fill a vacancy in a process of self-neutralization (Figure 2). The energy required to produce inner-shell ionization is termed the excitation potential or critical ionization potential (E_c) [5].

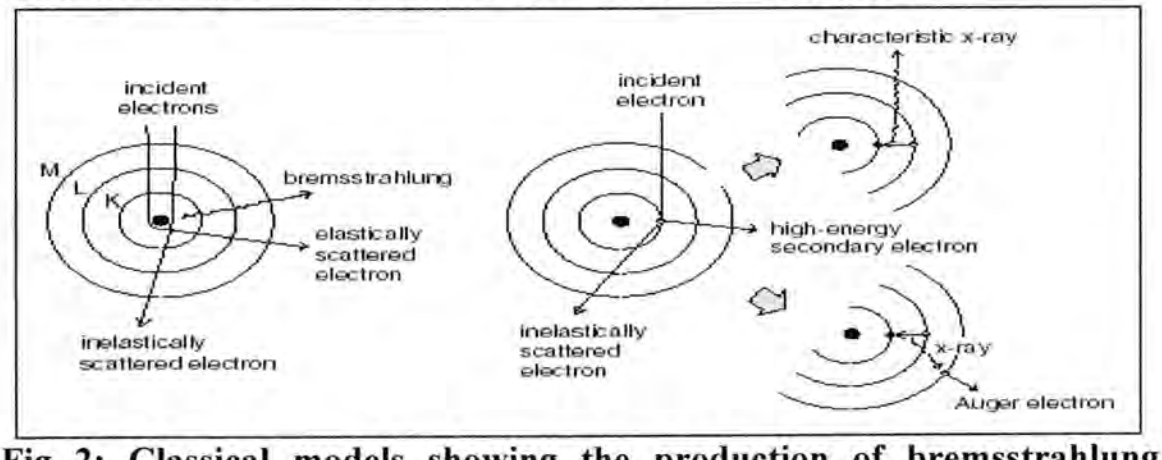

Fig.-2: Classical models showing the production of bremsstrahlung, characteristic X-rays, and Auger electrons.

(Left) Electrons are scattered elastically and in elastically by the positively charged nucleus. The in elastically scattered electron loses energy, which appears as bremsstrahlung. Elastically scattered electrons (which include backscattered electrons) are generally scattered through larger angles than are in elastically scattered electrons. (Right) An incident electron ionizes the sample atom by ejecting an electron from an inner-shell (the K shell, in

this case). De-excitation, in turn, produces characteristic X-radiation (above) or an Auger electron (below) [5].

When outer-shell electrons drop into inner shells, they emit quantized photon "characteristic of the element". The energies of the characteristic X-rays produced are only very weakly dependent on the chemical structure in which the atom is bound, indicating that the non-bonding shells of atoms are the X-ray source. An atom remains ionized for a very short time (about 10^{-14} second) and thus the incident electrons that arrive about every 10^{-12} second can repeat atom ionization. However, not all outer-shell electrons can fall in to produce X-rays [6].

From fig.2 the photons (energy quantum) which are emitted during these electron jumps are called k_α *and* k_β ,respectively. The corresponding wavelength can calculated from:

$$\lambda_{k_\alpha} = \frac{h \cdot c}{E_L - E_K} \quad and \quad \lambda_{k_\beta} = \frac{h \cdot c}{E_M - E_K} \qquad (4)$$

$E_L - E_K$ The difference in electron energy between the L and K –shell.

$E_M - E_K$ The difference in electron energy between the M and K –shell.

Because this energy difference is a characteristic of the material, the radiation is called "characteristic radiation". This radiation exhibits a line spectrum.

Bragg diffraction:

Bragg diffraction occurs when electromagnetic radiation or subatomic particle waves with wavelength comparable to atomic spacing's are incident upon a crystalline sample, scattered in a specula fashion by the atoms in the system, and undergo constructive interference in accordance to Bragg's law. For a crystalline solid, the waves are scattered from lattice planes separated by the linear distance *d*. Where the scattered waves interfere constructively; they remain in same phase since the path length of each wave is equal to an integer number of multiple of the wavelength [4, 5, 6].

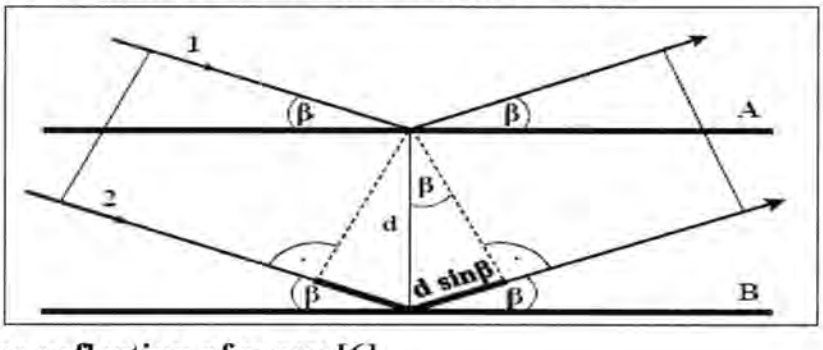

Fig.-3: Bragg reflection of x-ray [6].

The path difference between two waves undergoing constructive interference is given by $2d\sin\theta$, where θ is the scattering angle. This leads to Bragg's law which describes the condition for constructive interference from successive crystallographic planes (*h, k, l*) of the crystalline lattice [6]:

2d sin θ = n λ (5)

Where n is an integer determined by the order given, and λ is the wavelength. A diffraction pattern is obtained by measuring the intensity of scattered waves as a function of scattering angle. Very strong intensities known as Bragg peaks are obtained in the diffraction pattern when scattered waves satisfy the Bragg condition.

Selection rules and practical crystallography

Bragg's law, as stated above, can be used to obtain the lattice spacing of a particular cubic system through the following equation:

$$d = \frac{a}{\sqrt{h^2 + k^2 + l^2}} \quad (6)$$

where ***a*** is the lattice spacing of the cubic crystal, and *h*, *k*, and *l* are the Miller indices of the Bragg plane. Combining this relation with Bragg's law [6]:

$$\left(\frac{\lambda}{2a}\right)^2 = \frac{\sin^2\theta}{h^2 + k^2 + l^2}, \quad (7)$$

One can derive selection rules for the Miller indices for different cubic Bravais lattices; the selection rules for several will be given at table -1.

Table -1 : Allowed and Forbidden Reflections of Different Bravais Lattices

Bravais lattice	Allowed reflections	Forbidden reflections
Simple cubic	Any *h, k, l*	None
Body-centered cubic	*(h + k + l)* even	*(h + k + l)*odd
Face-centered cubic	*(h, k, l)*all odd or all even	*(h, k, l)* mixed odd and even
Diamond F.C.C.	all: odd, or even &(*h+k+l*) = 4n	above, or even &(*h+k+l*)≠ 4n
Triangular lattice	*l* even, $h + 2k \neq 3n$	$h + 2k = 3n$ for odd *l*

To overcome this difficulty, Niels Bohr proposed, in 1913, what is now called the *Bohr model of the atom*. He suggested that electrons could only have certain *classical* motions [11, 12]:

1. The electrons can only travel in special orbits at a certain discrete set of distances from the nucleus with specific energies.
2. The electrons do not continuously lose energy as they travel. They can only gain and lose energy by jumping from one allowed orbit to another, absorbing or emitting electromagnetic radiation with a frequency (f) determined by the energy difference of the levels according to the *Planck relation.*
3. The frequency of the radiation emitted at an orbit of period (T) is as it would be in classical mechanics; it is the reciprocal of the classical orbit period[7,9]:

$$T = \frac{1}{f} \qquad (8)$$

The particle side:

1- Description of the X-ray device with diffract meter:

The case of the X-ray device shown in figure 4 [The device is made by LD didactic company, Germany] shielded from radiation consists of three separated chambers. The largest (right-hand side) chamber is the experimental space. It contains the geometry (facility for controlling and measuring angles) that holds the LiF crystal and the detector (Geiger-Muller counter tube). The X-ray tube is placed in the middle chamber. The left chamber contains the microprocessor controlled electronics, the controls and displays. The mechanism of X-ray is excluded because the high voltage at the X-ray tube is only present when the two sliding doors of the experimental and the tube chamber are closed. The doors and windows consist of lead glass, which prevents any escape of inadmissible radiation. Lead glass is soft, be careful for not to scratch it. The same happens to the LiF crystal fixed on the geometry [8].

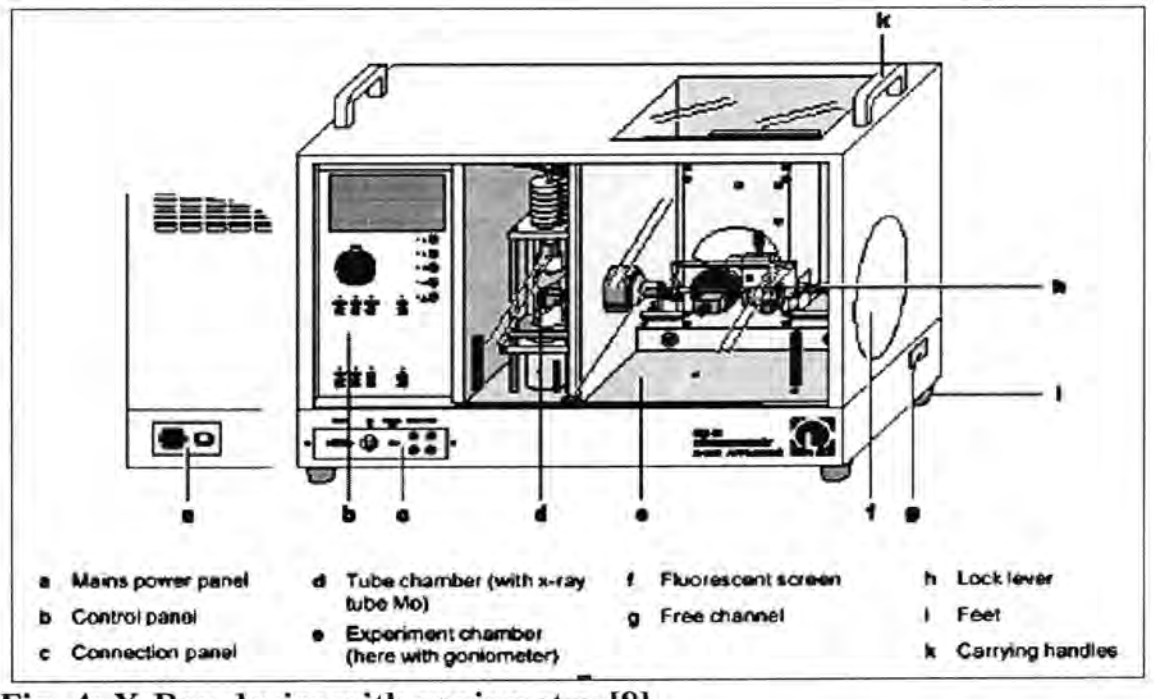

Fig.-4: X-Ray device with goniometry [8].

2- For recording the X-ray spectrum in the Bragg arrangement the following working parameters should be set up: Tube current: I = 1 mA , High voltage: U = 35 kV , Measuring time: t = 5 s , Initial angle = 5° ,Final angle max. = 40^{0}

3- Determine the wavelength and quantum energies for the characteristic lines K_{α} and K_{β} of the Mo anode for NaCl and LiF .

4- Calculate the maximal quantum energy for each experimental value of the anode voltage U from the angles belonging to the corresponding short-wave edge using equation (3). List the energies in a table and compare them with the kinetic energy E = eU of the electrons accelerated by the voltage U.

5- Calculate the $E_L - E_K$ The difference in electron energy between the L and K –shell and $E_M - E_K$ The difference in electron energy between the M and K –shell by using equation (4).

6- Using equation (1) to find the velocity and interval time of electron and the displacement between the orbits.

RESULTS AND DISSECTION

1- The kinetic energy of accelerated electrons valued before collision (56keV) and velocity (1.1Mm/sec).

2-The maximum energy for estimation after collision and reflected from NaCl crystal (50.8KeV) with wavelength (λ_{min}=0.0214nm) for first order of diffraction (k=1), $E_L - E_K$=14.16KeV i.e. λ_α =0.0876nm and $E_M - E_K$=6.53 KeV i.e. λ_β= 0.19nm.

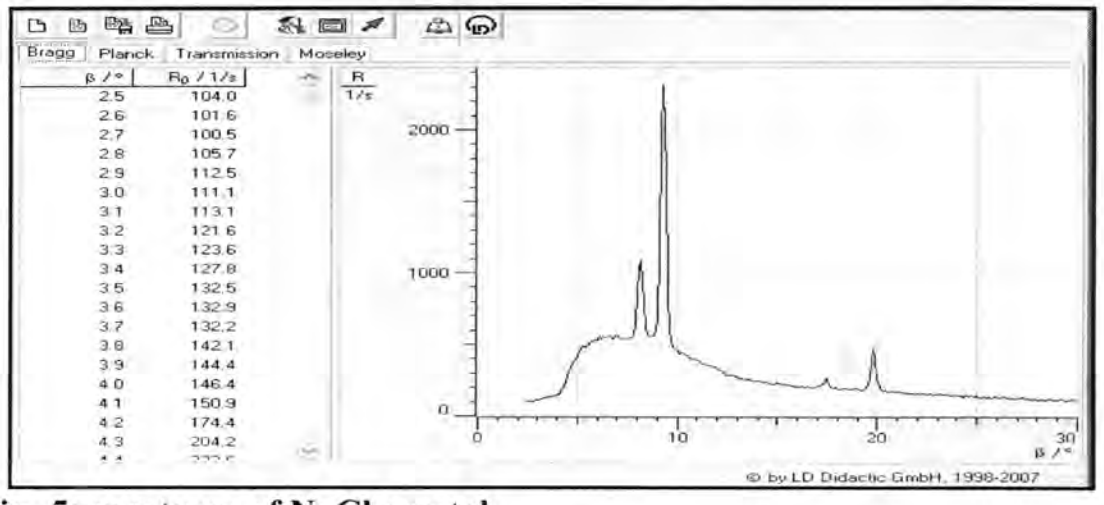

Fig.-5: spectrum of NaCl crystal

As can be seen from Figure (5) that the spectrum contains and three sharp lines which characterize the spectrum of X-ray for anode molybdenum reflected from a NaCl crystal with special angle and that can be determined theoretically from the equation (5)

The ratio (d/n) has meaning in the crystals science of to imagination surfaces. Taking into account that the linear spectrum cannot be done without voltage estimated at 35 KV and without that we will get a continuous spectrum of X-rays. But the electrons tend to have the movement of vibration energy generating heat where the electrons do not have the crust to leave (K-shall).

3-The maximum energy for estimation after collision and reflected from LiF crystal (44. 3 KeV) with wavelength (λ_{min} =0.014nm) for second order of diffraction (k=2), $E_L - E_K$=25.3KeV i.e $\lambda\alpha$ =0.04899nm and $E_M - E_K$=14.16 KeV i.e λ_β= 0.097nm.

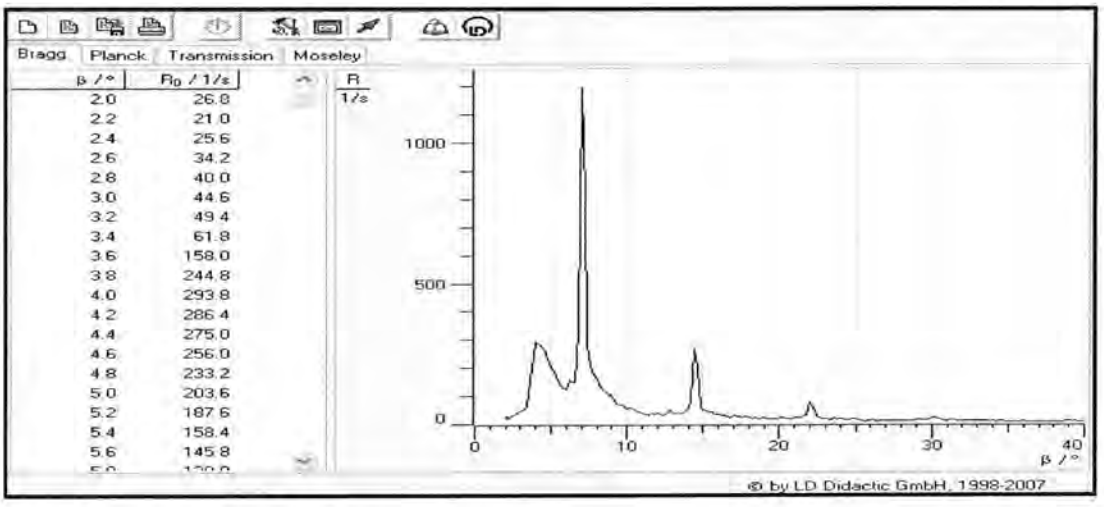

Fig.-6: spectrum of LiF crystal.

Figure (6) noted a linear spectrum and three peaks characteristic of crystal LiF. But the first peak is getting closer to the shorter wavelength compared to crystallize NaCl.

4-by using equation (1) to calculate the velocity of the electron after the collision and travel from $E_M - E_K$ represented as (v_β = 0.046Mm/sec) and $E_L - E_K$ as (v_α = 0.7Mm/sec) in NaCl crystal compare to the LiF (v_β = 0.67Mm / sec) and (v_α = 0.94Mm / sec).

Conclusions:

1- Increasing the voltage between the anode and cathode (accelerating voltage) is not the only factor that's causing the figure of the linear spectrum of X-rays but mainly depends on the type of anode material.

2- Most important features of the spectrum of linear high intensity in X-rays more than 90 times or more of the other rays that have the same wavelength.

3- X-ray radiation, especially (K- Line) plays a main rule in an important study the crystalline structure of solids.

REFERENCES

1. Ben, G. Streeman, "Solid State Electronic Devices" 2nd Edition, Prentice-Hall Inc., Englewood Cliffes, N. J.(1980).
2. Yousif, M.G., "Solid State Physics" ,(High Education Publishing, Baghdad University), 2,(1989).

3. D.D.O.Eya, A.J. Ekpunobi and C.E. Okeke, The pacific Journal of Science and Technology, 6, 2, May ,(2005).

4. مؤيد جبرائيل يوسف, "فيزياء الحالة الصلبة" , الجزء الاول, جامعة بغداد, وزارة التعليم العالي والبحث العلمي, (1980) .

5. يحي الجمال ,"فيزياء الحالة اصلبة ", وزارة التعليم العالي والبحث العلمي , جامعة الموصل, (1990).

6. Blakemore," Solid State Physics" , London, Second Edition ,(1974).

7. T.L. Tansiey and D.F. Neely ," Thin Solid Film" 121 : 95-07,(1984).

8. Lawrence,H.,Van Vlack,"Elements of Materials Science and Engineering", university of Michigan, sixth edition ,(1989).

9. James, R.," Introduction Quantitative X-Ray Diffraction Methods", EPS400-001, Introduction to X-Ray Powder Diffraction, (2010) .

10. John M. Cowley, "*Diffraction physics* ", North-Holland, Amsterdam, ISBN ,(1975).

11. H. P. Myers, Introductory Solid State Physics, Taylor & Francis, (2002).

12. Carl. R. Nave, "*Bragg's Law*", Hyper Physics, Georgia State University, http://hyperphysics.phy-astr.gsu.edu/hbase/quantum/bragg.html, retrieved, (2008).

Study of Chemical Gas Sensing and IR Detector Properties of Lead Chalcogenid

Morooj A. Abood, Abdul-Hussain K.Iltaif, Ashwaq .A. Jabor, Mohammed K. Khalaf and Karameh A. Muhmmad
Ministry of Science and Technology

Received : 31/03/2011 Accepted: 29/05/2011

الخلاصة

تم تصنيع ودراسة الخصائص الكشفية والتحسسية لأغشية PbSe,PbS المحضرة بطريقة الترسيب الكيمياوي على قواعد (سليكون- زجاج) عند سمكμm(1-1.2). رسبت هذه الأغشية عند درجة حرارة 335K,300K. فحوصات X-ray أثبتت أن الأغشية المرسبة عند درجة حرارة T_s=335K,300K متعددة التبلور ودرست الخصائص البصرية بإستخدام جهاز FTIR فأظهرت النتائج أن الفحوصات التركيبية والبصرية تعتمد على نوع ودرجة حرارة الأرضية المرسبة عليها تلك الأغشية، كذلك درست خصائص تيار- فولتية على السليكون والزجاج عند درجة حرارة الأرضية 335K,300K ودرست الأستجابية ووجدت إنها تزداد مع زيادة درجة حرارة الأرضية T_s. الأغشية المرسبة أظهرت تحسساً واضحاً لغاز CO_2 وخصوصاً تلك المرسبة على السليكون.

ABSTRACT

Fabrication and studying detecting characteristics of PbS and PbSe by chemical path deposition over Si and glass substrate at thickness (1-1.2μm). These deposition were plasticized from the degree 300K to 335K. X-Rays analyses (XRD) have illustrated that the structure of the deposition film at room temperature T_s 300K and 335K is polycrystalline. Optical properties studied by FTIR, UV/VIS/NIR absorption. The results show that the films structural and optical properties are influenced by kind and temperature of substrate. The characteristics of the current and voltage were studied on Si and glass substrate at T_s 300K and 335K. Responstivity were studied for the detector PbSe ,PbS as a function to the wavelength , and it found that is increased with T_s increment. The films exhibited as a good sensitivity to the CO_2 gas with more response-recovery characteristics.

INTRODUCTION

These sensors perform the important task of sensing chemicals analytes and also giving quantitative information of the concentration of

analyte in the environment. Today there is a great deal of interest in the development of gas sensors for application of air pollution monitoring, detection of harmful gases in mines, grading of agro-products like coffee and spices, home safety, exhaust gas monitoring, hand held breath analyzers etc. The infrared region from 1 μm to 5 m is an area of interest for both spectroscopic and thermo graphic applications. Lead sulphide (PbS) and lead selenide (PbSe) are intrinsically photoconductive materials that cover this important spectral region and have a long history of development and manufacturing[1]. They have several advantages over competing materials, but because of their nature, they also have several challenges that need to be addressed. PbS and PbSe detectors are photoconductive sensors whose resistance decreases with increasing infrared light. PbS sensors operate from 1.3 μm to 3.2 μm with a peak sensitivity near 2.2 μm, while PbSe sensors operate from 1.3 μm to 5.2 μm with a peak sensitivity near 4.2 μm[2].They can be used at room temperature or cooled with a thermoelectric cooler.Large active area devices (5mm × 5mm) are available. Both PbS and PbSe detectors are used in pyrometers for temperature measurements, as flame monitors, in gas sensors and in analytical instruments that PbS and PbSe have a long history of development and have taken advantage of advances in manufacturing techniques to continue to be important detectors for infrared sensing. chemical bath deposition involves relatively low costs and is a relatively easy technique. Substrates of various sizes and shapes may be used and no toxic gaseous precursors are needed. Moreover, the chemical bath deposition method allows the production of large volumes of powders and films for industrial applications (gas sensor for example)[3].

MATERIALS AND METHODE

1- A chemical reaction of lead acetate solution $Pb(CH_3COO)_2$ (0.1 M) with thiourae solution $(NH_2)_2CS$ (0.1 M) was done to precipitate PbS material on the bases from the degree 300K to 335K.
2- A chemical reaction of lead acetate solution $Pb(CH_3COO)_2$ (0.1 M) with selenourae solution $(NH_2)_2$ CSe (0.1 M) was done to precipitate PbSe material on the bases from the degree 300K to 335K.
3- The bases were coated with the above solutions then dried by drying oven at temperature of 333 K.

RESULTS AND DISSCUSION

1- The component characteristics are measured by using X-ray system. The best membranes are that which precipitated on the silicon are it clear in Figures 1 to 3.

2- Spectral tests were conducted using spectral analysis (spectrophotometer) . Through the study of absorption spectrum of the membranes , it can be noted a move in the absorption edge towards the short wavelengths when the temperature substrate increase , as it is appeared in fig. 4 and 5. This corresponds with what R.Dalven has got [4], and the reason is due to the expansion of the energy package not allowed transitions to Chalcogenide when increasing the temperatures substrate .

3- The energy gap is counted for direct allowed transition from drawing graphic relationship between absorption coefficient with fallen photon energy. And from the intersection of the straight line tangent to the curve as in fig.6 and 7 with the X-axis [$(\alpha h\upsilon)^2=0$] it can be noted the value of the direct energy gap(Eg), which equal to 0.29 eV, and its value increases with the increasing of the temperature substrate that it is equal to 0.32 eV for (PbSe) and Energy gap for PbS 0.43 eV, increase with the increasing of the temperature substrate equal to 0.47eV which is approach to the value reached by (heini saloniemi) [5] , that is equal (0.27 , 0.31) eV to (PbSe) , (0.41 – 0.43) eV of (pbS) .

4- Current change was measured as a bias voltage function , as it was used infrared light source (1μm -5μm) , power supplier , and sensitive measure of the current (digital electrometer keithely). The current of darkness is recorded first as a function as a voltages and then re – measured the source in the presence of light with the introduction of the current of darkness.

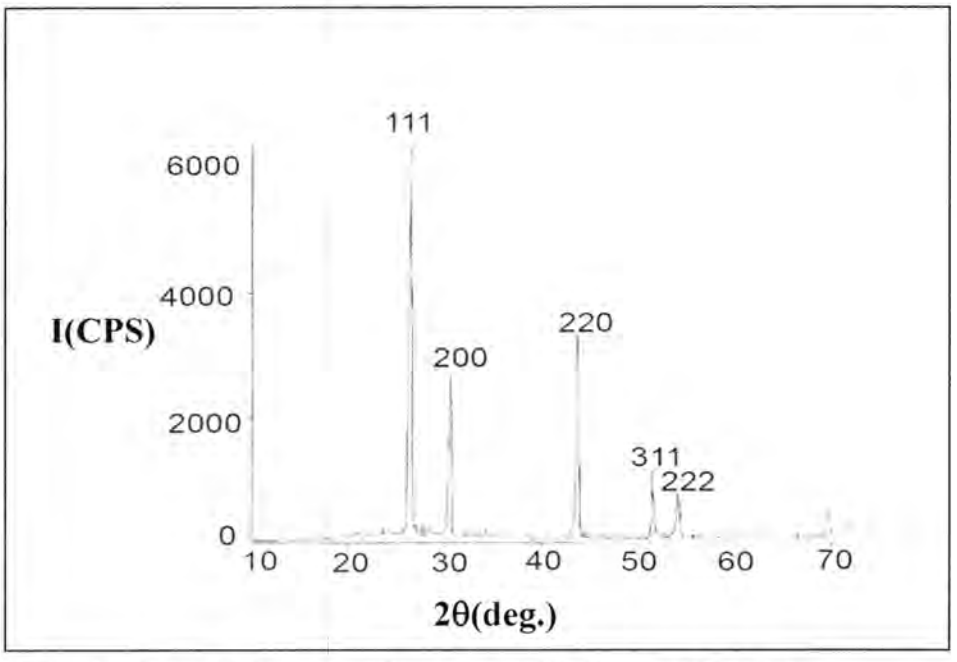

Fig.-1 : X-ray Diffraction Spectra for PbS/glass thin Film.

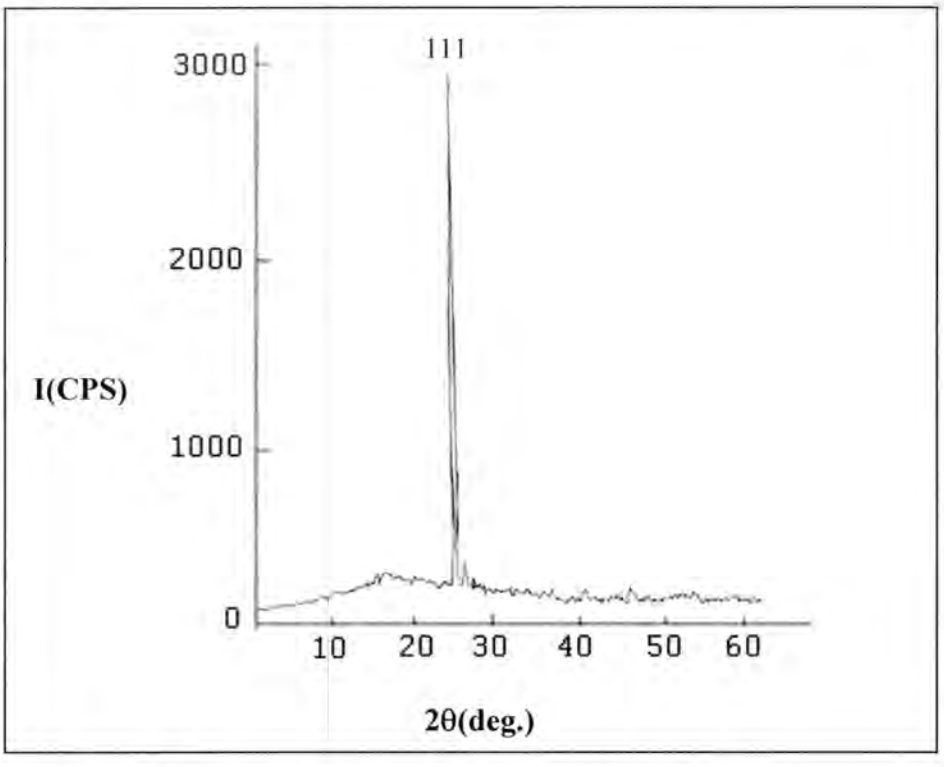

Fig.-2 : X-ray Diffraction Spectra for PbS/Si thin Film

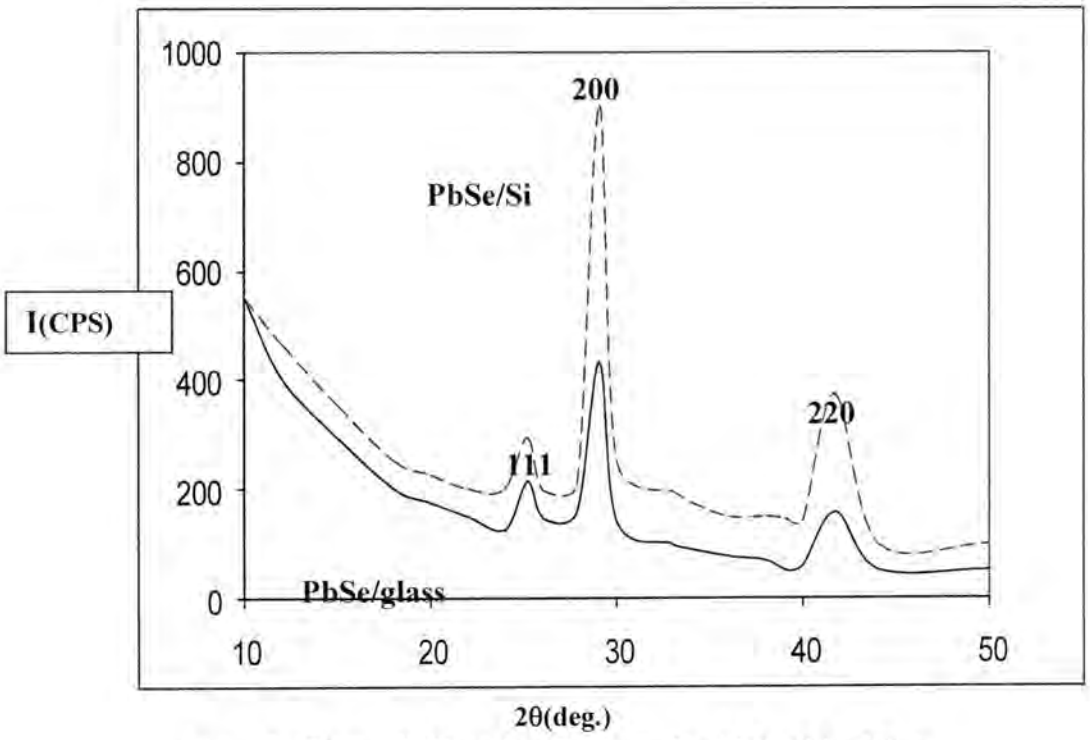

Fig. -3: X-ray Diffraction Spectra for PbSe thin Film

5- Comparison between both currents I_d and I_{ph} was done by drawing graphic voltage- current shown as in fig. 8 to 11 .The difference between I_{ph} and I_d noticed for membranes precipitated on the silicon is clear than membranes precipitated on the (glass).

6- The spectral response of the prepeared samples , which are deposited on different bases , has been studied . It can be noticed that the models deposited on glass bases no response to the IR radiation . while the models deposited on (Si) showed clear response in fig.12.

7- Graphic relation is drawn between Responstivity (R_λ) an wavelengths for manufactured detectors shown in fig.(12). The value of the top response to the PbSe membranes are equal to (0.55×10^{-1}A/w) , while the value of the top response to PbS membranes are equal to (0.39×10^{-1}A/w) by using formula (1)[6] are closed to the recorded standard ones [5].

$R_\lambda = I_{ph} / P_{in}$ or $R_\lambda = V / P_{in}$ ..... (1)

P_{in} (power of incident light)

8- The sensitivity of PbS and PbSe membranes to CO_2 gas is tested . It has showed a clear sensitivity as shown in figures 13,14, 15 and 16, used formula (2) for the reducing and oxidizing gases [3] :

$S = \Delta R / R_{air}$ ..... (2)

Where $\Delta R = R_{air} - R_{gas}$

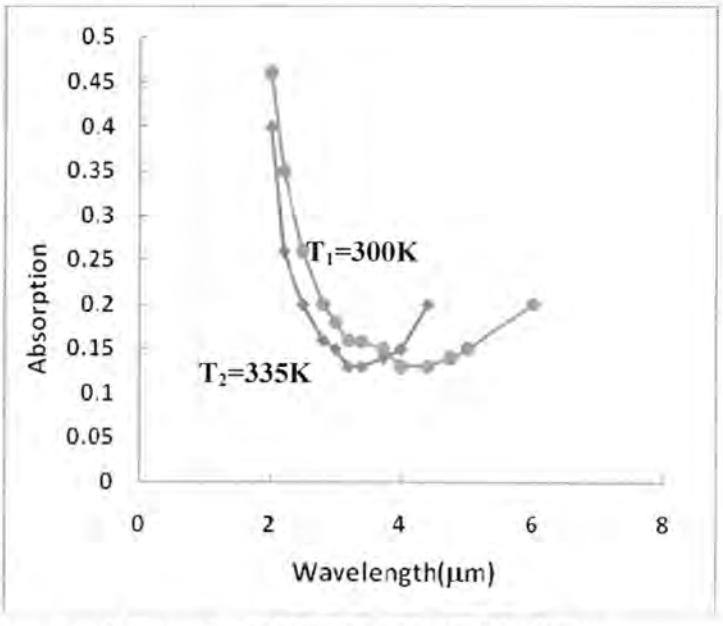

Fig. -4: Absorption Edge for PbSe thin Film

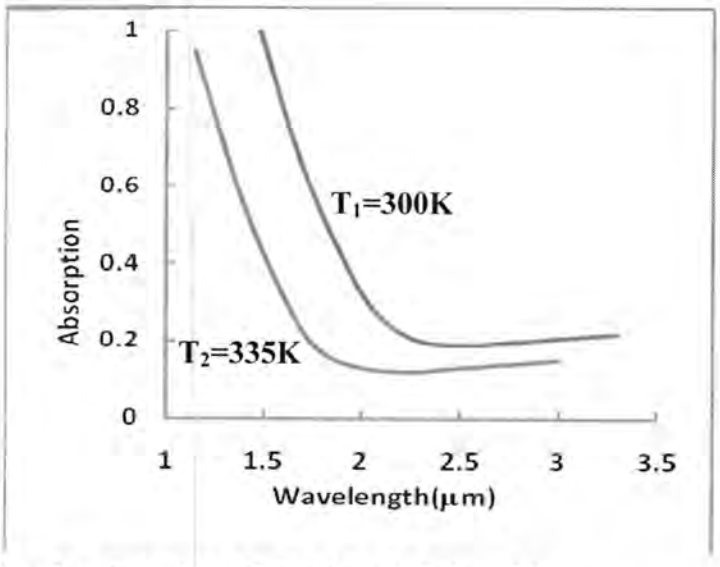

Fig.- 5: Absorption Edge for PbS thin Film

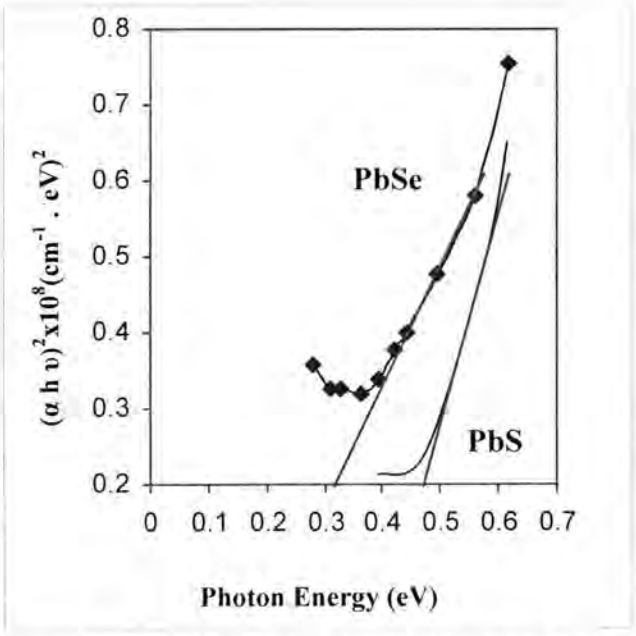

Fig.- 6: $(\alpha h\upsilon)^2$ versus photon energy at 335K

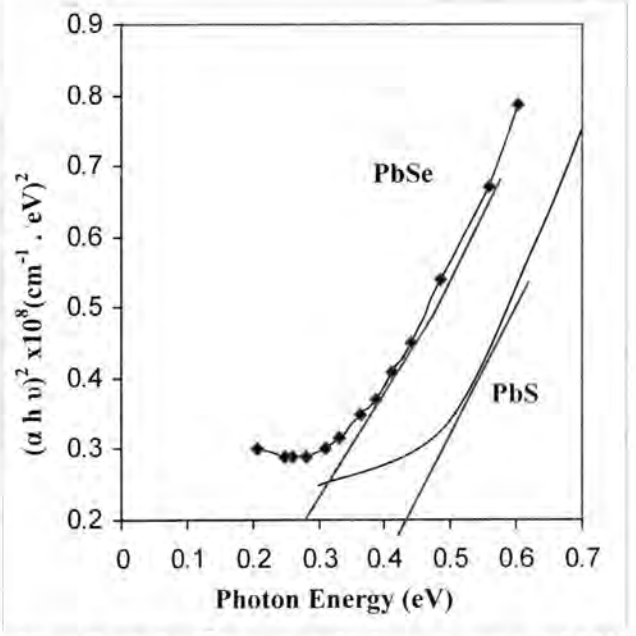

Fig. -7: $(\alpha h\upsilon)^2$ versus photon energy at 335K

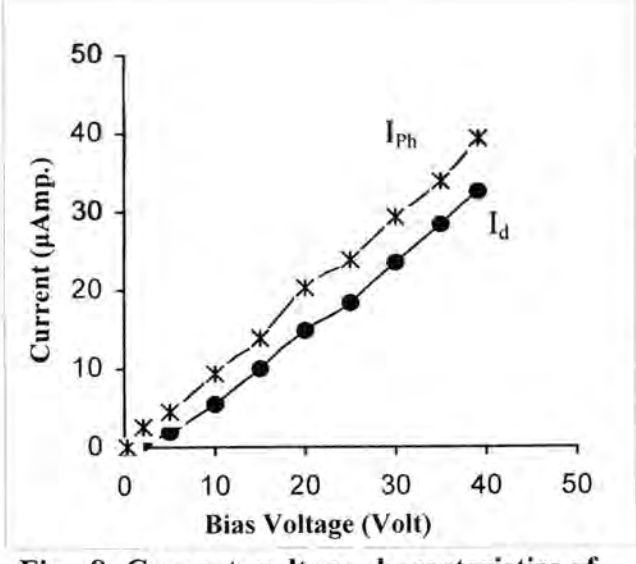

Fig. -8: Current- voltage characteristics of PbSe on glass

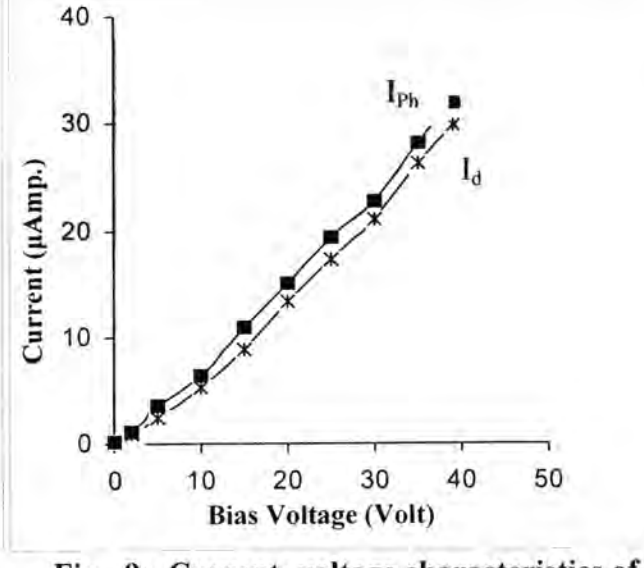

Fig. -9: Current- voltage characteristics of PbS on glass

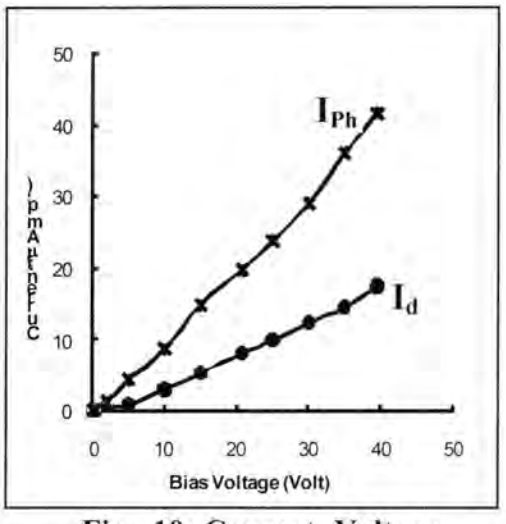

Fig. -10: Current- Voltage characteristics of PbSe on Si

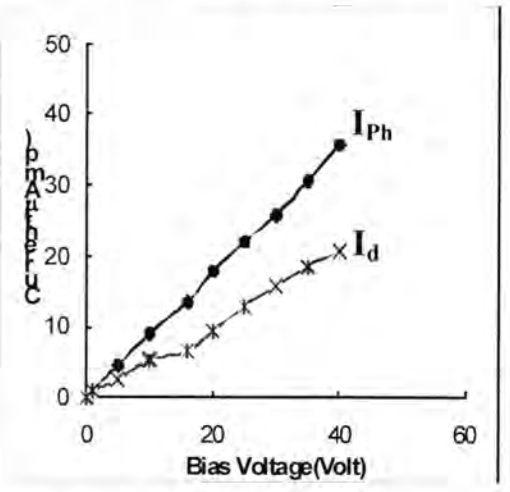

Fig. -11: Current- Voltage characteristics of PbS on Si

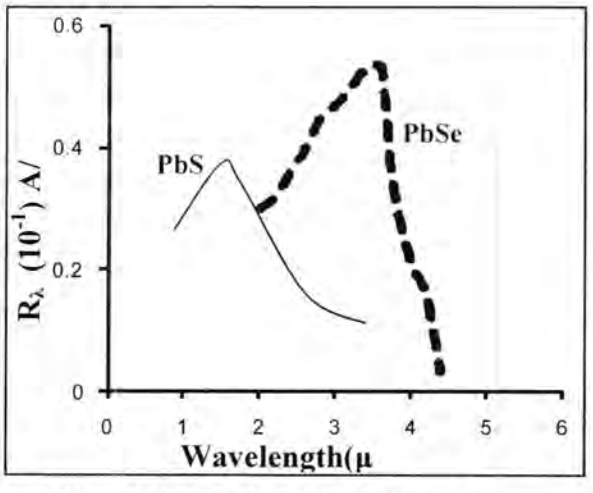

Fig.- 12: Relationship between the Responstivity & wavelength of PbSe/Si , PbS/Si

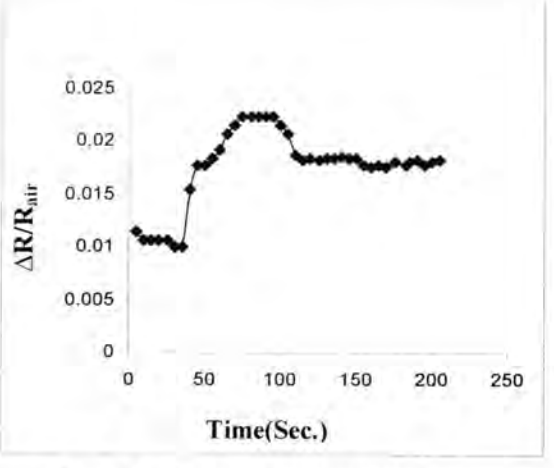

Fig.-13: Sensitivity of PbS/Si Thin Films to CO_2 gas

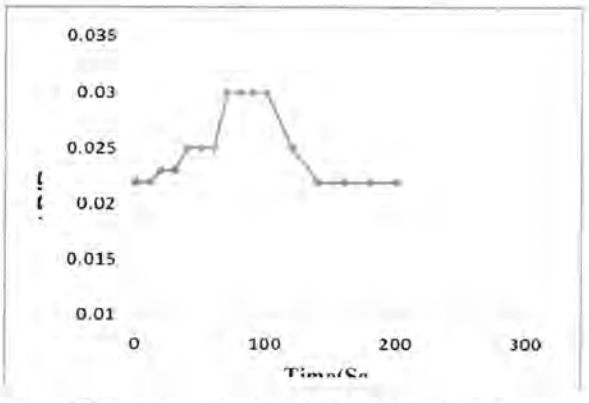

Fig.-14 Sensitivity of PbS/glass Thin Films to CO_2 gas

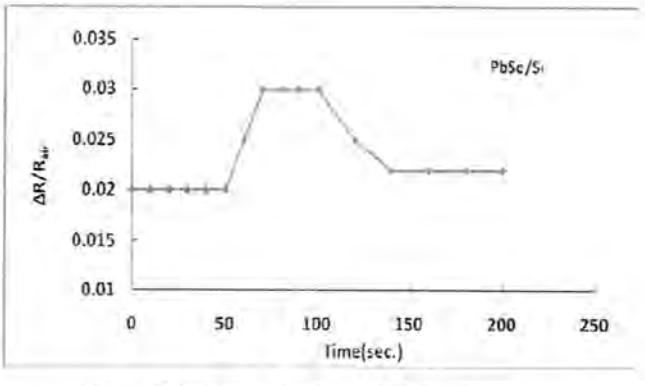

Fig. -15: Sensitivity of PbSe/Si Thin Films to CO_2 gas

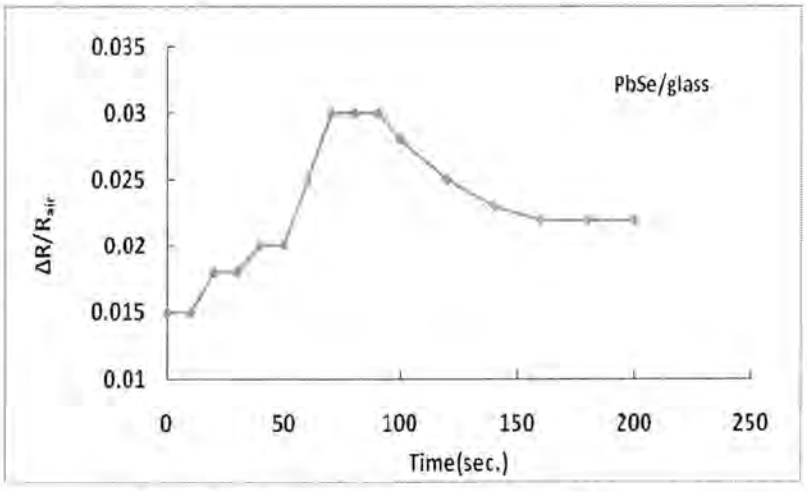

Fig. -16: Sensitivity of PbSe/glass Thin Films to CO_2 gas

So, we can conclude :

1- The peaks of reflections indicate(XRD) that films are of polycrystalline structure and the intensity of plane (111) reflection is higher than that of other planes, which means that this plan is suitable for crystal growth.

2- The peaks of reflections indicate on Si is suitable for crystal growth than glass thin film .

3- the results have shown that the best properties to the films, was at the temperature 335K , and found that energy gap value increased with T_S increase .

4- It can be e found that Ts increase will reduce of the dark current values I_d to half , which leads to the decrease of noise current (In) and good sensitivity .

5- No sensetive to IR radiation (1-5)μm for membranes precipitated on glass but membranes precipitated on Si have a good sensitivity.

6- Films deposits on Si exhibited good sensitivity to the CO_2 gas with more response-recovery characteristics than glass because crystal growth of films on Si appear more crystalline than films on glass and no effect appear when T_s increase.

REFERENCE

1. G. Bauer, H. Clemens, Semicond. Sci. Technol. 5 S122 (1990).
2. D. Beydoun, R. Amal, G. Low, S.J. McEvoy, Nanopart. Res. 1 439(1999).

3. Physics, Chemistry and Technology of SolidConstantinos Christofides, ISBN: 978-0-4 State Gas Sensor Devices Andreas Mandelis, 71-55885-9 Hardcover, 352 pages, October (1993).
4. R.Dalven,'' electronic structure of PbS, of PbSe, PbTe'' , Dep.of physically university of California Berkeley California (1975).
5. (Heini Saloniemi ,"Electrode position of PbS, PbS and PbTe thin film (2000).
6. R.J.Keyes, "Optical and Infrared Detector", ed. R.J.Keyes Springer-Verlag Berlin, Heidelberg (1980).
7. Lead chalcogenide VECSEL on Si emitting at 5 μm ,Electronic Letters 44, 25, pp. 1467-1469, (2008).

Design of Dielectric Bragg Mirror Consisting Quarter-Wave Stacks Using Transfer-Matrix Method

Amal M. A. Al-Hillou* and Elham Jasim Mohammad**
College of Engineering, Al-Mustansiriyah University
Physics Department, College of Sciences, Al-Mustansiriyah University

Received : 03/04/2011 Accepted : 29/05/2011

الخلاصة

اغلب البحوث الحالية في العراق تتعاملُ مع تكنولوجيا النانو. بينما بحثنا هذا يَتعاملُ مع تكنولوجيا الفيمتو، والذي يعد من التقنيات المتقدّمة جداً في مجالِ الألياف البصرية والليزرَ. أن تكنولوجيا النانو = 10^{-9}. بينما: تكنولوجيا الفيمتو = 10^{-15}. حيث في ليزرِ Femtosecond: تنبْعثُ نبضاتَ الليزر بمدى بين بضعة جزء من ألف مليون مليون من الثانية ومئات جزء من ألف مليون مليون من الثانيةِ.

إنّ توليد النبضات فائقة القصر، وهي تلك النبضاتُ في مدى ليزر Picoseconds و Femtosecond يَتضمّنُ عناصر بصرية مطلية ، ومثال على ذلك: - العاكسات العالية (HR) ، مرايا الخرج الضوئي (OC) و طلاءات مضادّ الإنعكاس (AR) . هذه العناصرِ البصريةِ مستندة على ظاهرةِ تداخلَ الضوءِ. وتحليلها النظري يَعتمدُ على شكليةِ مصفوفةِ التّحويل المشهورةِ والمشتقّة عموماً مِنْ معادلاتِ ماكسويل. يَعتمدُ أداءُ الليزرِ بصورة اساسية على نوعيةِ الطلاءاتِ البصريةِ Reflectance للعاكساتِ العاليةِ ويَجبُ أنْ يَقتربَ مِنْ القيمة المثالية 100 % ضمن قيمة الطولِ الموجي العملي لكي يُقلّل الخسائرَ داخل تجويفِ فجوة الليزر. وأنتاج الإزدواج يَجبُ أنْ يَشملَ قِيَمَ معيّنةَ لضمان العمليةِ المثاليةِ. هذا البحث يدرس تصميم نظري لمرآةِ براگ العازلة للحصول على انعكاسية عالية. وقد استخدمنا في تحليلاتنا Reflectivity (R), Group Delay (GD) and Group Delay Dispersion (GDD) والمواد العازلة TiO2/SiO2 رتبت بحزمة دوريةُ لتَصميم مرايا براگ واستخدمنا Fused Silica. كقاعدة. في هذا البحث اعطت مرآة براگ متعددة الطبقات انعكاسية تصل لمدى اكبر من 99.999999 % في منطقة الطول الموجي للتصميم. كما حصلنا على تذبذب منخفض لكلا من Group Delay و Group Delay Dispersion .

ABSTRACT

All recent researches in Iraq deal with Nanotechnology. Our research deals with Femtotechnology, which is very advanced in laser and fiber optics technology. Where: Nanotechnology = 10^{-9} seconds. Nevertheless:

Femtotechnology = 10^{-15} seconds. Where in femtosecond lasers: lasers emitting pulses with durations between a few femtoseconds and hundreds of femtoseconds. The generation of ultrashort pulses, that is pulses in the order of picoseconds and femtosecond lasers involves optical coatings as important functional elements, e.g. high reflectors (HR), output couplers (OC) and antireflection (AR) coatings. These optical elements are based on the interference phenomenon of light. Their theoretical analysis generally relies on the well-known scattering matrix formalism derived from the Maxwell equations. Laser performance strongly depends on the quality of optical coatings: reflectance of high reflectors should approach the ideal 100% value at the operation wavelengths in order to minimize laser inter cavity losses and output coupling has to be set to specific values to ensure optimal operation. This paper reports a theoretical design of dielectric Bragg mirror (DBM) to achieve high reflectivity and dispersion compensation over a broad bandwidth. Analytic expressions for reflectivity (R), group delay (GD) and group delay dispersion (GDD) are used. Dielectric materials TiO2/SiO2 arranged as a periodic stacks have been used to design Bragg mirrors using the Fusedsilica as a substrate. In this paper we demonstrate a dielectric multilayer mirror with a controlled reflectivity and dispersion in the wavelength range $650-900nm$, it exhibits a reflectivity of >99.999999%. These stacks have a maximum reflectivity at 800nm. The group delay and group delay dispersion also have shown a low oscillation.

INTRODUCTION

In this paper, we study the theoretical design of Dielectric Bragg Mirror (BM). In the design of dielectric mirrors, an optical transfer-matrix method can be used. The most general method of calculating the reflectance and the transmittance of a multilayer is based on a matrix formulation, of the boundary conditions at the film surfaces derived from Maxwell's equations.

A Bragg Mirror is a periodic structure composed of pairs of layers of dielectric or semiconductor materials characterized by different refractive indices. A Bragg mirror (also called distributed Bragg reflector) is a structure, which consists of an alternating sequence of layers of two different optical materials [1-3].

The most frequently used design is that of a quarter-wave mirror, where each optical layer thickness corresponding to one quarter of the wavelength for which the mirror is designed. The latter condition holds for normal incidence; if the mirror is designed for larger angles of incidence, accordingly thicker layers are needed [2].

Bragg mirrors can be fabricated with different technologies:

(a) - *Dielectric Bragg mirrors,* based on thin-film coating technology, fabricated for example with electron beam evaporation or with ion beam sputtering, are used as laser mirrors in solid-state bulk lasers. The mirror structure then consists of amorphous materials [4].

(b) - *Fiber Bragg gratings,* including long-period fiber gratings, are often used in fiber lasers and other fiber devices. They can be fabricated by irradiating a fiber with spatially patterned ultraviolet light [4]. Similarly, volume Bragg gratings like (BragGrate™ Mirror) can be made in photosensitive bulk glass. The BragGrate™ Mirror is a reflecting volume Bragg grating (RBG) recorded in a bulk of photosensitive silicate glass. BragGrate™ Mirror placed in a laser resonator enables spectral and thermal management of the laser radiation and can withstand high optical densities up to 5 J/cm^2. The laser modal structure is controlled by the longitudinal mode selection with the bandwidth down to 20 pm and the customized central wavelengths with accuracy of 0.1- 0.5 nm. BragGrate™ Mirrors have record low absorption and allow thermal laser wavelength shift reduction to 0.005 nm/K [5,6].

(c) - *Semiconductor Bragg mirrors*, can be produced with lithographic methods. They are used, for example, in laser diodes, particularly in surface-emitting lasers.

There are various types of Bragg reflectors used in other waveguides, based on, e.g., corrugated waveguide structures which can be fabricated via lithography. Such kind of gratings are used in some distributed Bragg reflector or distributed feedback laser diodes [7,8].

PRINCIPLE OF OPERATION

The principle of operation and the theory model for dielectric Bragg mirror can be understood as follows:

Each interface between the two dielectric materials contributes a Fresnel reflection [4]:

$$r_F = (n_h - n_l)/(n_h + n_l) \quad \ldots..(1)$$

Where r_f Fresnel reflectivity, n_h high refractive index and n_l low refractive index.

For the design wavelength, the optical path length difference between reflections from subsequent interfaces is half the wavelength; in addition, the reflection coefficients for the interfaces have alternating signs. Therefore, all reflected components from the interfaces interfere constructively, which results in a strong reflection. The reflectivity achieved is determined by the number of layer pairs and by the refractive index contrast between the layer materials. The reflection bandwidth is determined mainly by the index contrast [4].

Ultrashort pulse generation has advanced to a level where the bandwidth of standard Bragg mirrors, composed of SiO2 and TiO2 quarter-wave layers, limits the pulse width (Figure-1).

Fig.-1 : Standard dielectric quarter-wave Bragg mirror [5]

The limitation is two fold. First, due to the limited difference in refractive index of both materials, SiO2=1.45 and TiO2=2.4, the high-reflectivity bandwidth of a standard quarter-wave Bragg mirror at 800 nm is only about 200 nm. Second, the higher order group delay dispersion (GDD) produced by quarter-wave Bragg mirrors further limits the useful bandwidth to about 100 nm for 10-fs pulses. The effect of the dispersion from quarter-wave Bragg mirrors on short pulse generation has already been investigated with CPM-dye lasers [5].

In this paper, we present the transfer matrix method allowing solving Maxwell equations in multilayer dielectric structures. We shall consider an example of a periodical structure (Bragg mirror) and derive general equations in planar structures. In the beginning, we consider propagation of light in the normal to layer planes direction. We shall generalize the transfer matrix approach for TE and TM linear polarizations of light. By definition, TE-polarized (also referred to as s-polarized) light has the electric field vector parallel to the layer planes, TM-polarized light (also referred to as p-polarized) has the magnetic field vector parallel to the planes (see Figure-2).

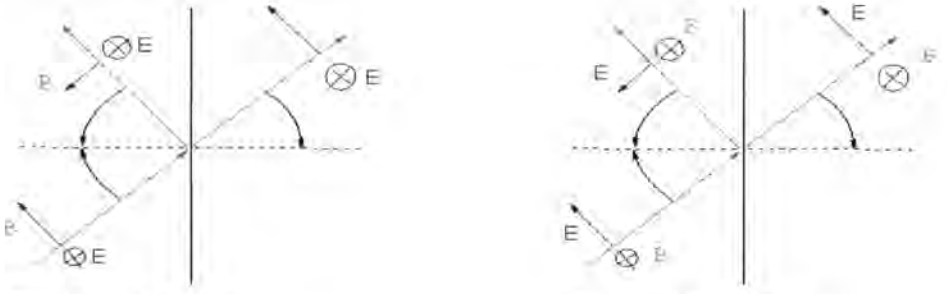

TE-polarization TM-polarization

Fig. -2: Orientation of electric and magnetic fields in TE- and TM-polarized incident on a planar boundary [9].

What happens to the electromagnetic field at the planar interface between two dielectric media with different refractive indices? The answer can be found by resolving the system of Maxwell equations independently in the two media and then matching of the solutions for electric and magnetic fields by the Maxwell boundary conditions at the interface. These conditions require continuity of the tangential components of both fields. They can be microscopically justified for any abrupt interface in the absence of free charges and free currents.

Consider a transverse light-wave propagating along the z-direction in a medium characterized by a refractive index n that is homogeneous in the xy plane but possibly z-dependent. The wave equation in this case becomes [1,9]:

$$\frac{\partial^2 E}{\partial z^2} = -k_0^2 n^2 E \qquad .....(2)$$

where k_0 is the wave-vector of light in a vacuum. The general form of the solution of Eq. (1) writes:

$$E = A^+ \exp(ikz) + A^- \exp(-ikz) \qquad .....(3)$$

where $k = k_0 n$, A^+, A^- are coefficients. Using the Maxwell equation one can easily obtain the general form of the magnetic field amplitude

$$B = A^+ n \exp(ikz) - A^- n \exp(-ikz) \qquad .....(4)$$

If we consider reflection of light incident from the left side to the boundary $(z = 0)$ between two semi-infinite media characterized by refractive indices n_1 (left) and n_2 (right), the matching of the tangential components of electric and magnetic fields would give

$$A_1^+ + A_1^- = A_2^+ \qquad .....(5)$$

$$\left(A_1^+ - A_1^-\right) n_1 = A_2^+ n_2 \qquad .....(6)$$

where A_1^+, A_1^- and A_2^+ are the amplitudes of incident, reflected and transmitted light, respectively. One can easily obtain the amplitude reflection coefficient

$$r \equiv \frac{A_1^-}{A_1^+} = \frac{n_1 - n_2}{n_1 + n_2} \qquad .....(7)$$

and the amplitude transmission coefficient

$$t \equiv \frac{A_2^+}{A_1^+} = \frac{2n_1}{n_1 + n_2} \qquad .....(8)$$

The ratio of reflected to incident energy flux (reflectivity) is given by

$$R = |r|^2 \qquad .....(9)$$

and the ratio of transmitted to incident energy flux (transmittance) is

$$T = \frac{n_2}{n_1} |t|^2 \qquad .....(10)$$

In the last formula, the factor $\frac{n_2}{n_1}$ comes from the ratio of light velocities in two media.

In multilayer structures, direct application of Maxwell boundary conditions at each interface leads to the necessity to resolve a substantial number of algebraic equations (two per interface). A convenient method allowing reducing the number of equations to be resolved to a strict minimum (four in general case) is the transfer matrix method, which we are going to describe briefly here.

Let us introduce the vector

$$\Phi(z) = \begin{bmatrix} E(z) \\ B(z) \end{bmatrix} = \begin{bmatrix} E(z) \\ -\frac{i}{k_0} \frac{\partial E(z)}{\partial z} \end{bmatrix} \qquad .....(11)$$

where *E(z), B(z)* are the amplitudes of the electric and magnetic field of any light wave propagating in the z direction in the structure under study. Note that $\vec{\Phi}(z)$ is continuous at any point in the structure due to the Maxwell's boundary conditions. In particular, it is continuous at all interfaces where n changes abruptly.

By our definition, the transfer matrix $\hat{T}_a$ across the layer of width a is such a 2×2 matrix that:

$$\hat{T}_a \vec{\Phi}\big|_{z=0} = \vec{\Phi}\big|_{z=a} \qquad .....(12)$$

It is easy to verify by substitution into Eq.(11) of the electric and magnetic amplitudes (2), (3) that if n is homogeneous across the layer,

$$\hat{T}_a = \begin{bmatrix} \cos ka & \frac{i}{n}\sin ka \\ in\sin ka & \cos ka \end{bmatrix} \quad .....(13)$$

The transfer matrix across a structure composed of m layers can be found as

$$\hat{T} = \prod_{i=m}^{i=1} \hat{T}_i \quad .....(14)$$

Where $\hat{T}_i$ is the transfer matrix across *i-th* layer. The order of multiplication in Eq. (13) is essential. The amplitude reflection and transmission coefficients (r_s *and* t_s) of a structure containing m layers, and sandwiched between two semi-infinite media with refractive indices n_{left}, n_{right} before and after the structure, respectively, can be found from the relation

$$\hat{T}\begin{bmatrix} 1+r_s \\ n_{left} - n_{left} r_s \end{bmatrix} = \begin{bmatrix} t_s \\ n_{right} t_s \end{bmatrix}. \quad .....(15)$$

One can easily obtain

$$r_s = \frac{n_{right}t_{11} + n_{left}n_{right}t_{12} - t_{21} - n_{left}t_{22}}{t_{21} - n_{left}t_{22} - n_{right}t_{11} + n_{left}n_{right}t_{12}} \quad .....(16)$$

$$t_s = 2n_{left}\frac{t_{12}t_{21} - t_{11}t_{22}}{t_{21} - n_{left}t_{22} - n_{right}t_{11} + n_{left}n_{right}t_{12}} \quad .....(17)$$

The intensities of reflected and transmitted light normalized by the intensity of the incident light are given by

$$R = |r_s|^2, \quad T = t_s^2 \frac{n_{right}}{n_{left}} \quad .....(18)$$

respectively.

In its turn, the transfer matrix across a layer can be expressed via reflection and transmission coefficients of this layer. If the reflection and transmission coefficients for light incident from the right-hand side and left-hand side of the layer are the same, and $n_{left} = n_{right} \equiv n$ (the symmetric case realized, in particular, in a quantum well embedded in a cavity), the Maxwell boundary conditions for light incident from the left and right sides of the structure yield:

$$\hat{T}\begin{bmatrix} 1+r_s \\ n - nr_s \end{bmatrix} = \begin{bmatrix} t_s \\ nt_s \end{bmatrix},$$
$$\hat{T}\begin{bmatrix} t_s \\ -nt_s \end{bmatrix} = \begin{bmatrix} 1+r_s \\ -n + nr_s \end{bmatrix}. \quad .....(19)$$

This allows the matrix $\hat{T}$ to be expressed as:

$$\hat{T} = \frac{1}{2t}\begin{bmatrix} t_s^2 - r_s^2 + 1 & -\dfrac{(1+r_s)^2 - t_s^2}{n} \\ n\left((r_s-1)^2 - t_s^2\right) & t_s^2 - r_s^2 + 1 \end{bmatrix} \quad .....(20)$$

For a quantum well, $t_s = 1 + r_s$, and Eq. (19) becomes

$$\hat{T}_{QW} = \begin{bmatrix} 1 & 0 \\ -2n\dfrac{r_s}{t_s} & 1 \end{bmatrix} \quad .....(21)$$

In the oblique incidence case, in the TE-polarization, one can use the basis $\begin{bmatrix} E_\tau(z) \\ B_\tau(z) \end{bmatrix}$, where E_τ, B_τ are the tangential (in-plane) components of the electric and magnetic fields of the light wave. In this case, the transfer matrix (4) keeps its form provided that the following substitutions are made:

$$k_z = k\cos\varphi, \quad n \to n\cos\varphi \quad .....(22)$$

where φ is the propagation angle in the corresponding medium ($\varphi = 0$ at normal incidence).

In the TM-polarization, following Born and Wolf [1] we use the basis $\begin{bmatrix} B_\tau(z) \\ E_\tau(z) \end{bmatrix}$, which still allows the transfer matrix (12) to be used provided that the substitutions are done:

$$k_z = k\cos\varphi$$

$$n \to \frac{\cos\varphi}{n} \quad .....(23)$$

Note that the transfer matrices across the interfaces are still identity matrices, and Eq. (13) for the transfer matrix across the entire structure is valid.

In the formulas for reflection and transmission coefficients (15-18) one should replace, in the TE-polarization

$$n_{left} \to n_{left}\cos\varphi_{left}, \quad n_{right} \to n_{right}\cos\varphi_{right} \quad .....(24)$$

and in the TM-polarization

$$n_{left} \to \frac{\cos\varphi_{left}}{n_{left}}, \quad n_{right} \to \frac{\cos\varphi_{right}}{n_{right}} \quad .....(25)$$

where φ_{left}, φ_{right} are the propagation angles in the first and last media, respectively. The same transformations would be applied to the transfer matrices

(19), (20). Note that any two propagation angles φ_i, φ_j in the layers with refractive indices n_i, n_j are linked by the Snell-Descartes law:

$$n_i \sin\varphi_i = n_j \sin\varphi_j \quad .....(26)$$

which is also valid in the case of complex refractive indices, when the propagation angles formally become complex as well.

The group delay is defined as the negative of the derivative of the phase response with respect to frequency, GD, also known as "Envelope Delay" [16→20]. In physics and in particular in optics, the study of waves and digital signal processing, the term group delay has the following meaning:
The rate of change of the total phase shift with respect to angular frequency [21,22]:

$$GD = -\frac{d\phi}{d\omega} \quad .....(27)$$

Through a device or transmission medium, where ϕ is the total phase shift in radians, and ω is the angular frequency in radians per unit time, equal to $2\pi f$, where f is the frequency (hertz if group delay is measured in seconds).

Group delay dispersion is a ubiquitous, and often irritating, phenomenon in ultrafast laser labs. When ultrashort pulses propagate through dispersive media, their frequency components emerge at different times due to GDD, causing the resulting pulse to be chirped and stretched and reducing the pulse's peak power [23].

$$GDD = -\frac{d^2\phi}{d\omega^2} \quad .....(28)$$

This effect can be compensated by using a pulse compressor, which can introduce negative GDD [20]. The standard method for computing the GDD is to compute complex reflection coefficients using the transfer matrix technique and then take successive finite difference over frequency [21,22]. Group-delay dispersion of optical elements is a critical parameter for the generation and control of femtosecond laser pulses. GDD can either increase or decrease then pulse duration by modulating the spectral phase of the femtosecond laser pulses. The effect of GDD becomes more significant as the laser pulse duration gets shorter. Ideally, a femtosecond dielectric mirror should not only have high reflectance but also low dispersion over a sufficiently broad spectral bandwidth [24].

RESULTS AND DISCUSSION

For the visible region and near infrared region, the most common coating materials are titanium dioxide TiO2 and the silicon dioxide SiO2. The properties of dielectric optical materials used in this paper, are shown in table-1.

Table-1: Properties of Dielectric Optical Materials in the Wavelength Range $650-900nm$

Materials Name	Materials Symbol	Materials Index of Refraction	Physical Thickness	Optical Region	Method of Deposition
Titanium Dioxide	TiO2	2.2505	88.86914	Visible	Electron beam evaporation/ Suttering
Silicon Dioxide	SiO2	1.4716	135.9065	Infrared	Electron beam evaporation/ Suttering

In this simulation, we used a quarter wave Bragg mirror. The structure of Bragg mirror design consists of 18 stack layers and in the wavelength range $650-900nm$ for normal incidence of light from air, with $n_h = 2.2505$, $n_l = 1.4716$, for the refractive indices of TiO2 and SiO2 respectively, this results in a Fresenel reflectivity $r = 0.209$ and optical thicknesses=200nm. The Bragg wavelength $\lambda_B = 800nm$ in the rang $650-900nm$.

1- Figure-3 shows the relationship between the refrative index and the wavelength for (the Fusedsilica substrate, TiO2 material and SiO2 material). This determines the dispersion properties of the structure.

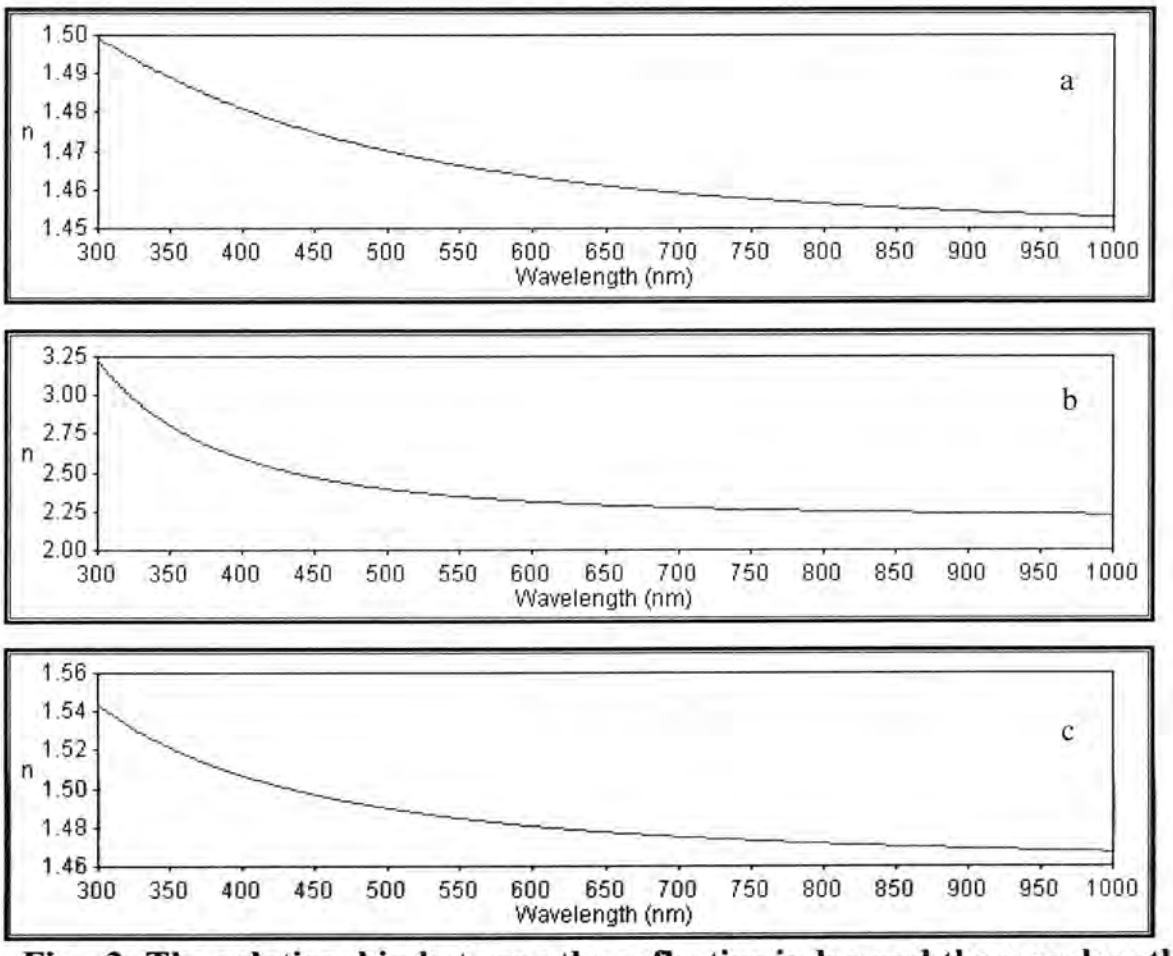

Fig. -3: The relationship between the reflective index and the wavelength for: a-(Fusedsilica) substrate. b- TiO2 material. c- SiO2 material

2- Figures-4 The relationship between the refractive index and the distance from substrate.

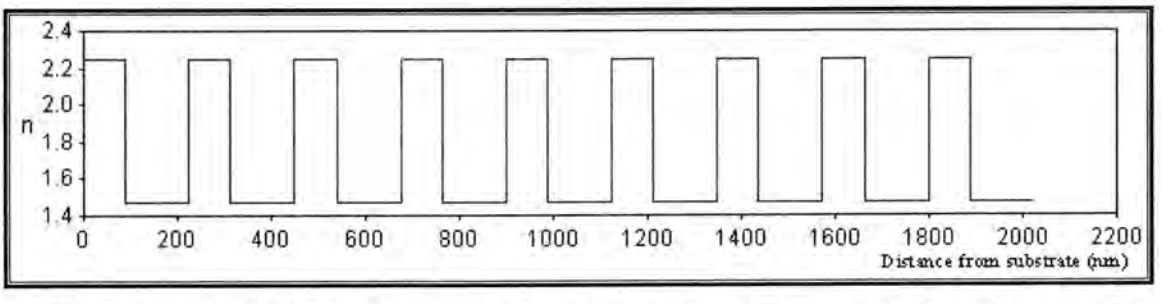

Fig.-4 : The relationship between the refractive index and the distance from substrate

3- Figure-5 the relationship between the phase and the wavelength we see the properties of phase shift in the rang between 650-900nm for DGMs.

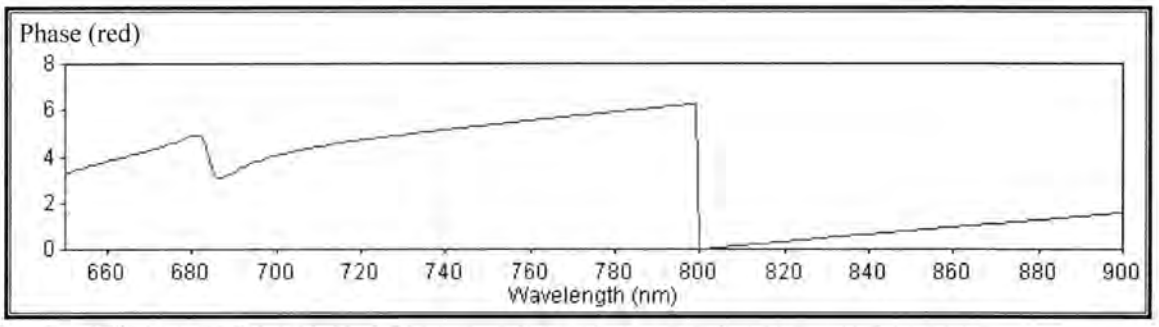

Fig.-5 : The relationship between the phase and the wavelength.

4- Results given in Figure-6 reveal almost high reflector at design wavelength ($\lambda_{\beta} = 800nm$) when the distribution Bragg mirror consist of alternating periodic quarter-wavelength stack of low and high refractive index. It exhibits a reflectivity of >99.999999%.

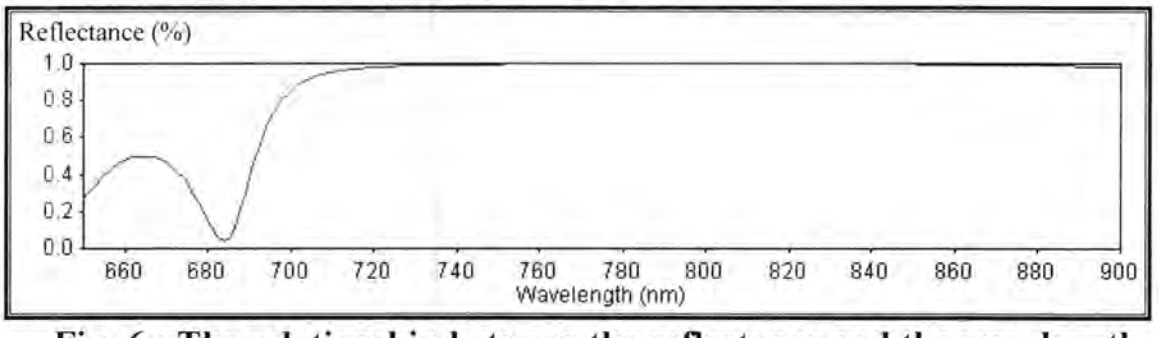

Fig.-6 : The relationship between the reflectance and the wavelength.

5- Figure-7 shows the characteristics of GD as a function of wavelength, where the group delay is nearly constant over a bandwidth of about 740-850nm.

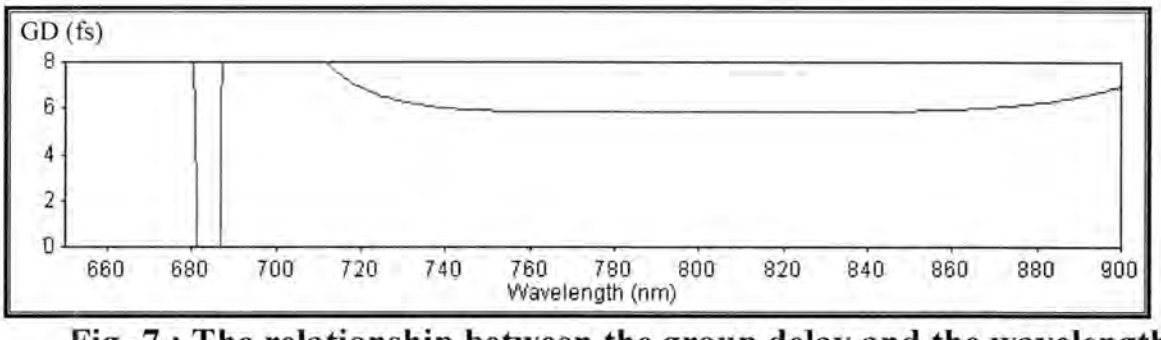

Fig.-7 : The relationship between the group delay and the wavelength

6- Figure-8 shows the dependence of GDD on the optical wavelength. It is clearly seen that the decrease of the oscillation in GDD in the rang wavelength from 770-840nm.

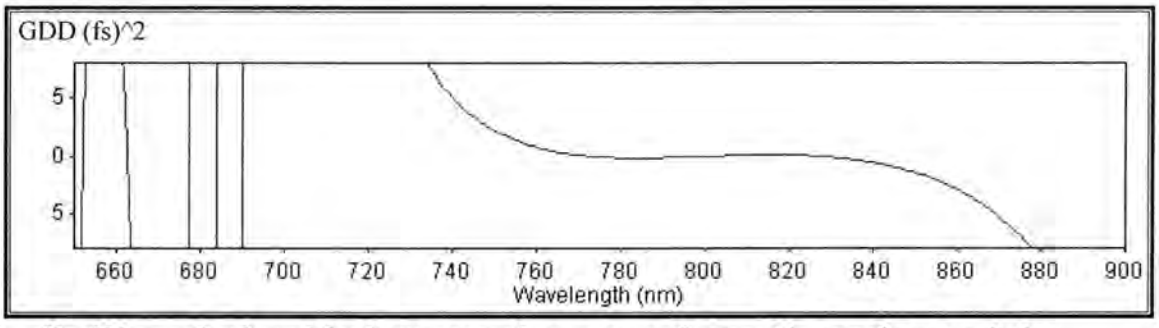

Fig.-8 : The relationship between the group delay dispersion and the wavelength

Furthermore, group delay dispersion shows monotonic behavior within wavelength range. In the case of high reflectors, a combination of materials with the highest refractive-index ratios n_h / n_l is usually preferred since the higher the ratio, the higher the theoretical reflectance and bandwidth of standard quarter wave stacks. Among its competitors, the TiO2/SiO2 pair has the highest ratio. The results obtained gives a relatively high density optical coatings of the TiO2/SiO2 material pairs with low absorption and scattering losses.
These stacks have a peak in the reflectivity at 800nm (Bragg wavelength)and the group delay, group delay dispersion have low oscillation.

REFERENCES

(1)- Kittel C., "Introduction to Solid State Physics 4", John Wiley and Sons, New York, QC176 .K5 (1971).

(2)- Giancoli D. C., "Physics Principles With Applications", 2nd edition, Printice-Hall International Editions, USA, Pag. 598, QC23.G399 (1985).

(3)- Beiser A., "Concepts of Modern Physics", 6th edition, Reprinted in India by arrangement with the TATA McGRAW-HILL Companies Inc., New York, pag. 370, (2008).

(4)- Paschotta R. , "Encyclopedia of Laser Physics and Technology", via Wiley-VCH, October (2008).

(5)- Matuschek N., K¨artner F. X., and Keller U., " Theory of Double-Chirped Mirrors", IEEE Journal of Selected Topics in Quantum Electronics, vol. 4, no. 2, pag. 197, (1998).

(6)- OptiGrate Corp, "BragGrate™ Mirror: Reflecting Bragg Grating (RBG) for laser mode selection ", Copyright ©, (2010).

(7)- Keller U., Weingarten K. J., Kärtner F. X., Kopf D., Braun B., Jung I. D., Fluck R., Hönninger C., Matuschek N., and Juerg Aus der Au, " Semiconductor Saturable Absorber Mirrors (SESAM's) for Femtosecond to Nanosecond Pulse Generation in Solid-State Lasers", IEEE LEOS newsletter, Pag. 18, (2007).

(8)- Paschotta R., "RP Coating Design of Optical Multilayer Structures", RP Photonics Consulting GmbH, (2009).

(9)- Macleod H. A., "Thin Film Optical Filters"; Printed in the UK by J W Arrowsmith Ltd, Bristol, third edition, (2001).

(10)-Ya-Ping Li(李雅萍), " Investigation of Chirped Cavity Dispersion Compensator Filter", Ph.D. Theses, Optics and Photonics, (2007).

(11)- Microwave Encyclopedia, "Group Delay", (2010).

(12)- Steinmeyer G., " Pulse generation and dispersion compensation", BIPM comb workshop, Max-Born-Institute for Nonlinear Optics and Short Time Spectroscopy, Berlin, Germany, (2003).

(13)- Kitano M., Nakanishi T. and Sugiyama K., "Negative Group Delay and Superluminal Propagation: an Electronic Circuit Approach", IEEE Journal of Selected Topics in Quantum Electronics, vol. 9, no. 1, pag. 197, (2003).

(14)- Woodley J. F. and Mojahedi M., "Negative Group Velocity and Group Delay in Left-Handed Media", American Physical Society, 70 046603-1, (2004).

(15)-Applied Radio Labs, "Group Delay Explanations and Applications", www.radiolab.com.au , (1999).

(16)- Akturk S., Gu X., Kimmel M. and Trebion, " Extremely simple single-prism ultrashort-pulse compressor ", Optics Express, vol. 14, no. 21, pag. 10101, (2006).

(17)- Jonathan R. B., Christian J. and Kärtner F. X.,"Efficient Analytic Computation of Group Delay Dispersion from Optical Interference Coatings", Optical Society of America, (2004).

(18)- Imran T., Kyung-Han H., Tae J. Yu and Chang H. N., " Measurement of the group-delay dispersion of femtosecond optics using white-light interferometry", American Institute of Physics, vol. 75, pag.. 2266-2270, (2004).

Preparation and Study the Characterization of CdO Thin Films Obtained By Rapid Thermal Oxidation (RTO)

Raad S. Sabry, Ibrahim R. Agool and Jameel I. Kadum
Department of Physics-College of Science-Al Mustansiriyah University

Received : 17/04/2011 Accepted : 29/05/2011

الخلاصة

في هذا البحث تم تحضير المفرق الهجين CdO/Si وأغشية CdO بطريقة ألأكسدة الحرارية السريعة.تم دراسة الخواص التركيبة والكهربائية والفولتائية لأسماك مختلفة (150,200, 250nm). من دراسة نتائج X-ray تم التحقق من أن أغشية CdO متعدد البلورات وبتركيب مكعب. .تم حساب حجم الحبيبات باستخدام معادلةScherer وحصلنا على القيم التالية (216.5, 144.3, 123.5 nm) لمختلف ألأسماك (150,200, 250) على التوالي للاتجاه (111). وباستخدام تقنية إلSEM تم التأكد أن جميع أغشية إلCdO ذات سطح ناعم ومتجانس ولا يحوي على تشققات. الصفات الكهربائية أظهرت إن التوصيلية الكهربائية تتغير مع زيادة درجة الحرارة. أيضا أظهرت نتائج قياس هول أن تركيز حاملات الشحنة ومعامل هول وتحركية الحاملات كانت($2.95*10^{26}cm^{-3}$) و ($2.31*10^{-8}cm^{-3}$) و ($5.629*10^{-4}cm^2/Vs$) على التوالي. تضمنت الخصائص الكهروبصرية قياس (I-V) تحت ألإضاءة والظلام, وتم إثبات أن التوصيلية الضوئية والتحسسية الضوئية تتأثر كثيرا بالسمك. أيضا تم دراسة الخصائص الفولتائية للمفرق الهجين CdO/Si التي تضمنت حساب تيار الدائرة القصيرة وكان (*530,* *498, 452μA*) وفولتية الدائرة المفتوحة وكانت (*401, 381.8, 349mV*) عند AM1.

ABSTRACT

In the present paper CdO/Si heterojunction and CdO films has been prepared by rapid thermal oxidation method. Structure, electrical and photovoltaic characteristics were studied for different thicknesses (150, 200, 250nm). The XRD study reveals that the films are polycrystalline with cubic structure, the mean X-ray grain size perpendicular to (111) direction was estimated by using Scherer's relation, the value of grain size is found to be (123.5, 144.3, 216.5 nm) for different thickness (150,200,250nm) respectively. Scanning electron microscopy (SEM) confirms that all films have a smooth and homogeneous surface morphology and all films have not cracks. The electrical characterization shows that the electrical conductivity changed with increasing temperature. Hall effect measurement study reveals that the carrier

concentration (N_d), Hall coefficients (R_H) and carrier mobility (μ_H) are of the order of ($2.95*10^{26}cm^{-3}$),($2.31*10^{-8}cm^{-3}/C$) and ($5.629*10^{-4}cm^2/Vs$) respectively. The optoelectronic characteristics include (I-V) in dark and illumination conditions, the photoconductivity and photosensitivity shows dependence with the thickness is an important effect. The photovoltaic characteristics of CdO/Si heteojunction include short circuit photocurrent (530, 498, 452μA), open circuit photovoltge (401, 381.8, 349mV) respectively was studies at (AM1) condition.

INTRODUCTION

The use of transparent conducting oxides (TCO) in optoelectronic and photovoltaic devices has stimulated research on this field in recent years. The first report of a transparent conducting oxide (TCO) was published in 1907, when Badeker reported that thin films of Cd metal deposited in a glow discharge chamber could be oxidized to become transparent while remaining electrically conducting. TCOs are essential part of technologies that require both large-area electrical contact and optical access in the visible portion of the light spectrum.

The CdO compound being one of the TCOs, is reddish brown in color and is formed by burning of Cd in air. The CdO have special features such as high conductivity, high transmission, and low band gap made it applicable in photodiodes, phototransistors [1], photovoltaics, transparent electrodes, gas sensors [2], liquid crystal displays, IR detectors [3] and antireflection coatings [4]. A variety of techniques have been reported to make CdO thin films [5].

The rapid thermal oxidation process relatively low cost comparison with other process used in preparation film having high efficiency. The reports on the physical properties of other oxide films prepared by thermal oxidation of metallic films revealed a strong dependence of these properties on the heating rate during oxidation process, However, until now, not much attention has been paid to the preparation of the CdO thin films by thermal oxidation of metallic Cd thin films [6].

Where δ (is the thickness of the oxide layer) approach a nearly constant value at short process-times because the ramping times under oxygen ambient are not negligible anymore. Since oxidation processes mainly depend on process-temperature and process-time [7].

MATERIALS AND METHODS

Cd thin films were obtained by thermal evaporation under vacuum ($1.2*10^{-5}$Torr) of metallic cadmium pellets of *(99.9%)* purity, from Thomas Baker Company. The Glass and single–crystal silicon wafers of p-type with [111] orientation it has a resistivity in the range of *(1.5–4Ω.cm)* with each of *($1\times1cm^2$)* area and one face of the wafer was polished are used as substrates during film deposition. These wafers were chemically cleaned in alcohol with ultrasonic waves in order to remove the impurities and residuals from their surfaces and Si wafers are cleaned in Ethanol alcohol with *(99.99%)* purity for *(15 min)* to remove the oil dirts, after that the wafers are rinsed with a distilled water to remove the dust on the surfaces of the samples. The samples were etched with solution consisting of (H_2O, H_2O_2, HCL) of ratios (2:1:1) will remove certain ionic and metal surface contamination *(2-4min)* clean is recommended. The wafers are put for *(5min)* in an (HF) acid solution which is diluted with distilled water ($HF:H_2O$) with a proportion of (1:10) [8], the purpose of this process is to remove the thin oxide layer SiO_2 *(1nm)* that usually covers the surfaces of silicon wafers. Such a layer grows on any silicon wafer within *(24hours)*, while thicker oxide layers of about *(3nm)* grow in long periods of time [9]. As soon as the samples are taken out of the (HF) solution, they are rinsed in Ethanol alcohol solution. This process decreases the possibility of the oxide growing again on the surfaces of the wafers. Eventually the samples are dried with a clean cloth of silk and kept to be used in time. The cleaned Si substrates were located down stream at a position where the distance to the Cd source is about *(10cm)*. The substrate temperature (T_S) during film deposition was *($373^{\circ}K$)*; the film growth rate was about *(2.5nm/sec)*. A *(150, 200, 250nm)* thick CdO thin film was grown on glass and Si by rapid thermal oxidation of deposited Cd film using a halogen lamp with power *(650W)*. The quartz tube *(3cm)* diameter with two open ends was used to ensure the flowing of air through it (source of dry oxygen) attached with halogen lamp to obtain the temperature of about *($625^{\circ}K$)* for *(45sec)* in static air. It is put parabolic reflector like half circuit under the lamp to increase the heating efficiency. The ohmic contacts of the device were made by depositing a thick film of indium (In) films thick *(200nm)* onto the front of the CdO film and the back surface of the silicon. Figure (1) shows a cross-section of CdO/Si heterojunction structure.

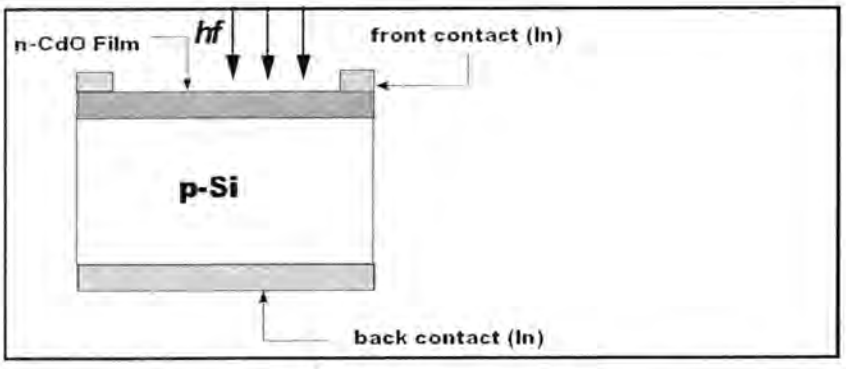

Fig.-1: Cross-sectional view of CdO/Si heterojunction.

In our work the thickness of the films were measured by using two types: cross sectional view of SEM image and the weight method. The crystalline structure of the films was confirmed by X-ray diffraction (XRD) with CuKα radiation (Rigaku Model, $\lambda=1.54059\,\mathring{A}$). The morphological properties of all films were investigated using (Zeiss Supra 50VP) scanning electron microscope (SEM, operating voltage was 20.00 kV). The electrical and photovoltaic measurements were carried out on films in our study include measure the current flow within a film in illumination and dark conditions with voltage *(0-0.4volt)*.

RESULTS AND DISCUSSION

Structural characterization:

Figure (2) shows the X-ray diffraction profiles of CdO films with different thickness. The XRD patterns obtained for the films grown on bare slides glass plates at room temperature were scanned in (2θ) range of $(20\text{-}60^{\circ})$ and is shown in this figure. It can observe that all analyzed samples are polycrystalline; for the as-deposited films the peaks associated to planes (111), (200) and (220) of the cubic structure are observed. The narrow and strong peak localized at $(2\theta=33.02^{\circ})$ of (111) plane parallel to the substrate surface for all thicknesses. The same (111) preferred orientation was found to be characteristic for the CdO films prepared by other methods such as reactive vacuum evaporation [10], and sputtering [11]. From X-ray diffraction, it can be seen that the diffraction peaks are symmetric and wide, and there is a slight shift regarding their normal position. This means that there are crystallites with compressed lattice planes and other with expanded lattice planes distributed in equal proportions (macrostrains are not apparent in our results, and therefore

they are discarded). The mean X-ray grain size perpendicular to (111) direction was estimated by using corrected Scherer's relation, the values of grain size is found to be (123.5, 144.3, 216.5nm) for different thickness respectively.

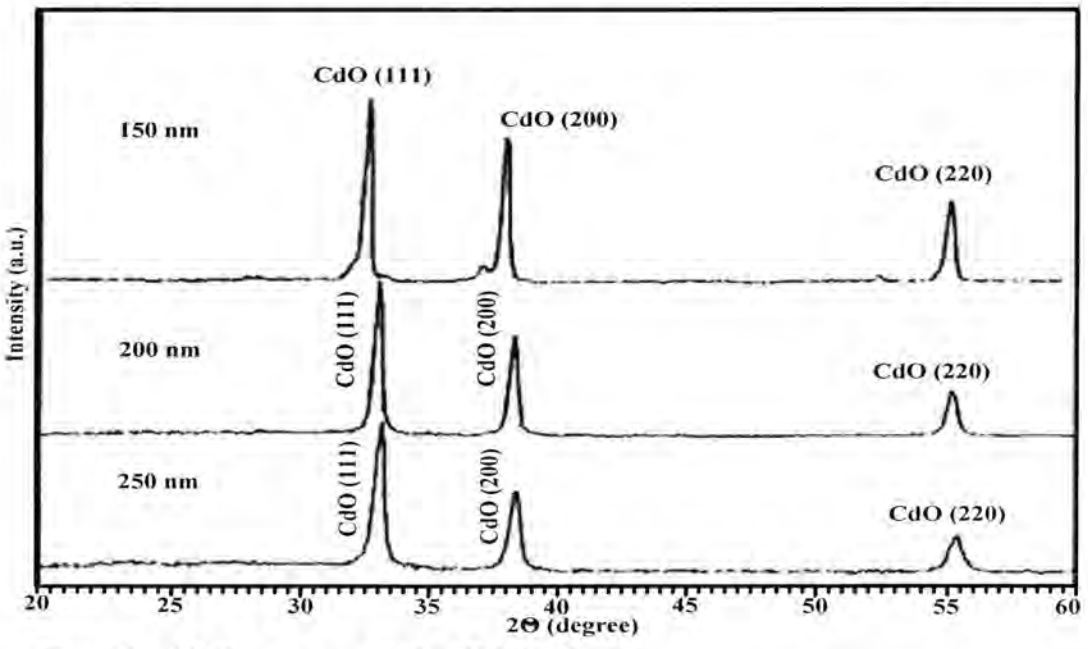

Fig. -2 : XRD pattern of a CdO films.

It is known that the surface properties of the TCO films influence their optical and electrical properties which are important factors for applications in optoelectronic devices [12]; Therefore, it is very important to investigate the surface morphology of the films. Figure (3) shows the SEM micrographs of the CdO films for different thickness. The surface properties of the CdO films appear to change significantly as a function of thickness. It can be obviously seen from this figures that well-crystallized grains in the (c) image belongs to thickness *(250 nm)*. Figure (3c) shows the SEM image of film prepared at *(250nm);* it consists of closely packed uniform shape without crack. This indicates the film is well adherent with substrate.

Also, we have found that all films have smooth and homogeneous surface morphology and all films have not cracks.

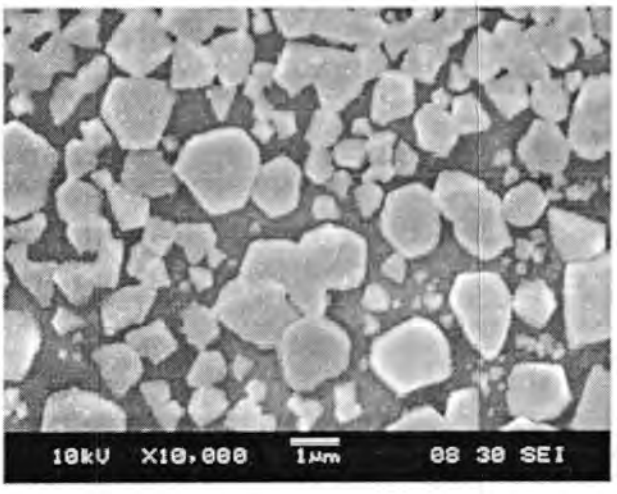

a-150 nm

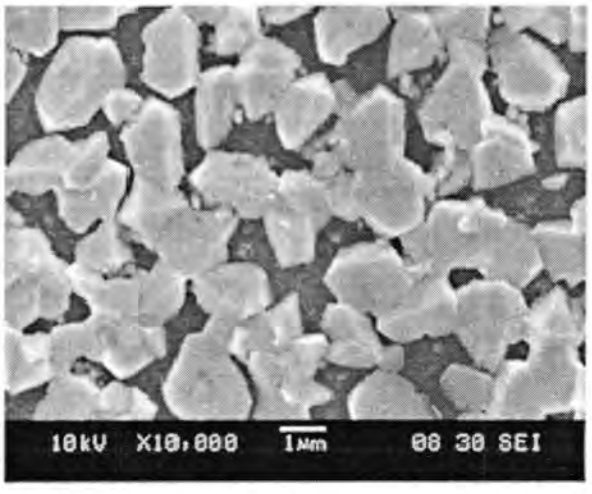

b-200 nm

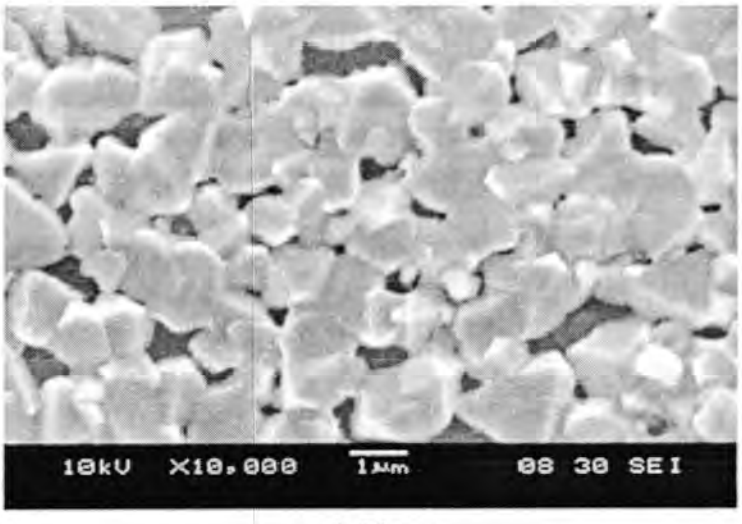

c- 250 nm

Fig. -3 : The SEM micrographs CdO of films by RTO.

Electrical Properties

One of the reasons for the application of the CdO thin films in the optoelectronic devices technology is their good electrical conductivity even without any extrinsic doping [13]. The electrical resistivity *(ρ)* of the films was studied by two-probe method in the temperature range *(300–473°K)*. The data from the electrical resistivity *(ρ)* were used to calculate the electrical conductivity $(\sigma_{d.c})$ and activation energy (E_a) for CdO films at different thickness. Figure (4) shows the relation between $(ln\sigma_{d.c})$ and temperature *(1000/T)* for (CdO) films. It can be seen from this figure that the conductivity

for all films was changed with increasing temperature as expected for semiconductor materials. The figure reveals the conductivity of CdO films increase with increasing of cadmium atoms concentration, where could be attributed to the increasing of average grain size which is accompanied by a decrease in the grain boundary scattering [12].

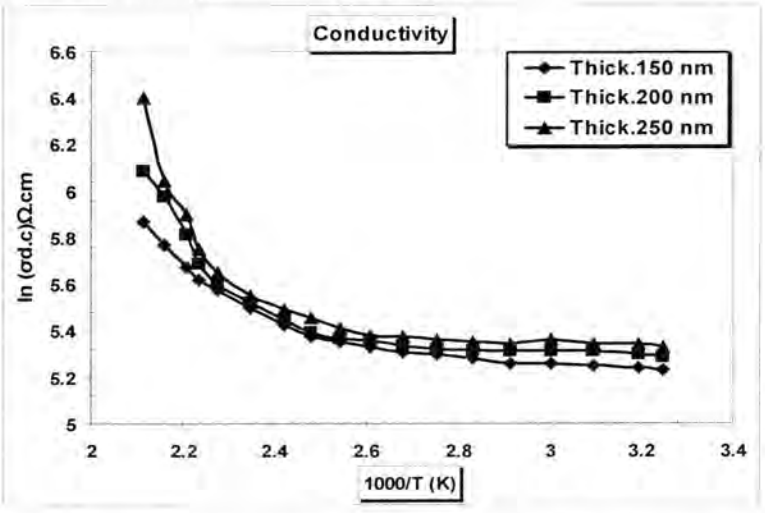

Fig. -4 : Variation in conductivity as a function for different thickness.

The (XRD) investigations of (CdO) films observed that film is polycrystalline then two activation energies it will be calculated for low and high temperatures within thermal range *(300-473°K)* [14]. Table (1) shows activation energy of CdO films.

Table -1 : The obtained results from the measure Electrical conductivity.

Thickness (nm)	*E_{a1}(eV) at low temperatures*	*E_{a2}(eV) at high temperatures*
150	*0.009377*	*0.23487*
200	*0.005001*	*0.16206*
250	*0.002593*	*0.1094214*

The data showed that the activation energy decreases slightly with the increasing of thickness. This change in magnitude of activation energy is attributed to the decreasing of energy gap with thickness.

The variation of Hall voltage *(V_H)* with current *(I)* through sample at constant magnetic field is as shown in figure (5) which indicates a linear increase in Hall voltage with increasing in current through the sample.

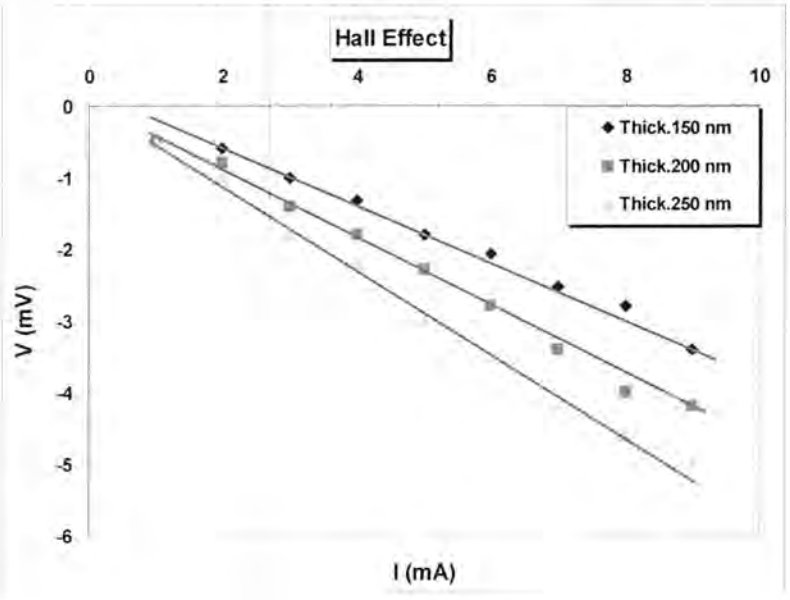

Fig. -5 : Variation of Hall voltage (V_H) with current through the CdO film constant magnetic field (B)

Table (2) shows the hall coefficient, concentration (N_D) and mobility (μ_H) of carriers charge of CdO films.

Table -2 : The obtained results from the measurements Hall Effect.

Thickness (nm)	$R_H(cm^{-3})$	$N_D\ (cm^{-3})$	$\mu_H\ (cm^2/V\ s)$	*Type of conductivity*
150	$2.31*10^{-8}$	$2.7*10^{26}$	$3*10^{-6}$	*n-type*
200	$1.92*10^{-8}$	$3.25*10^{26}$	$4*10^{-6}$	
250	$1.9*10^{-8}$	$3.28*10^{26}$	$4.2*10^{-6}$	

We have found that the carrier mobility and concentration of carriers charge increasing thickness. This behavior is attributed to the increase of the number of atoms with the increasing thickness and decreasing of energy gap (E_g) as shown in optical measurements. Also, this behavior is attributed to the increasing grain size due to partial decreases in potential barrier in the grain boundary Similar results of the Hall Effect were reported by CdO thin films prepared by C.H. Bhosale et al. [13].

I-V Characteristic

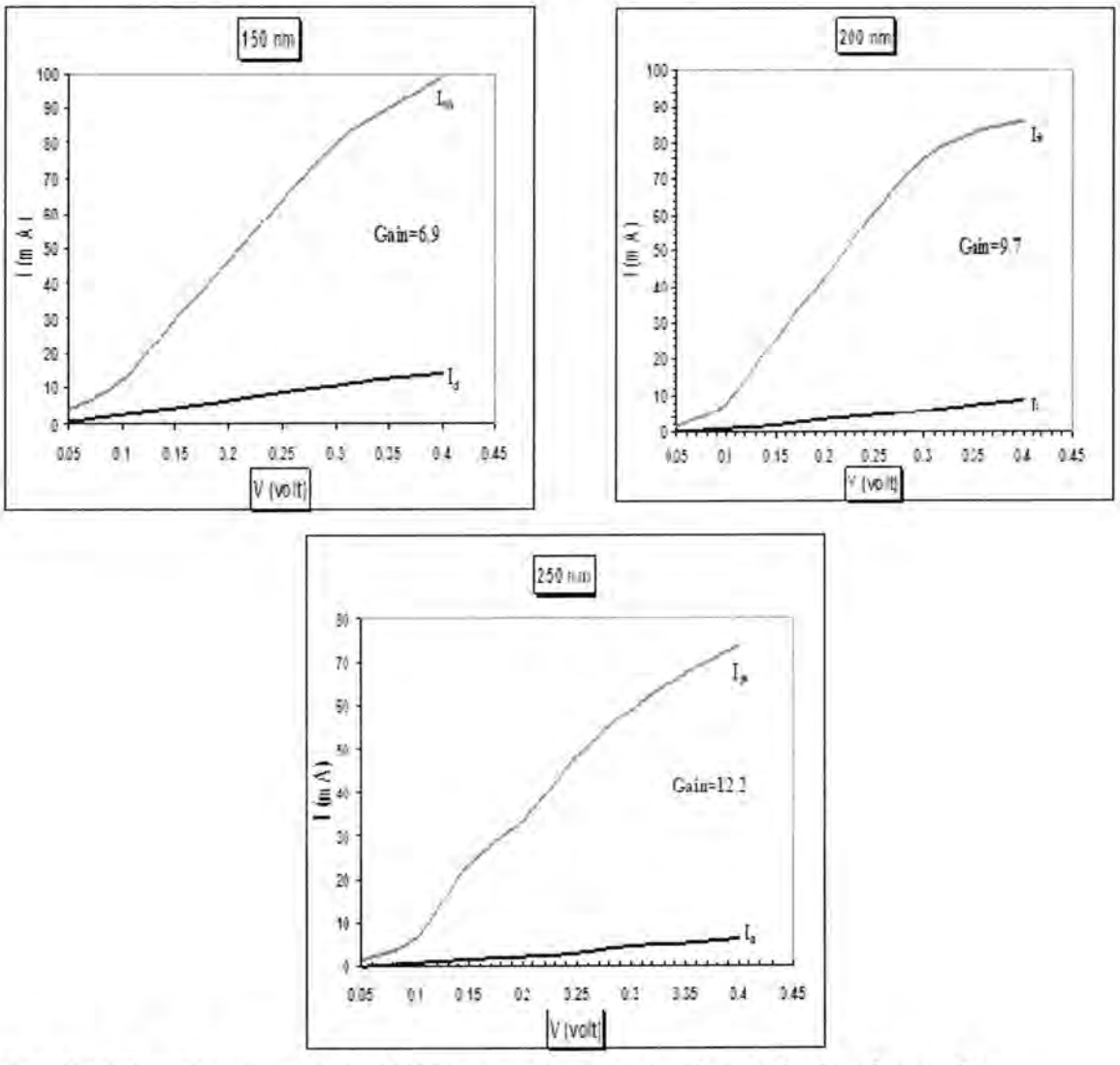

Fig.-6 : The Photoconductivity as a function of applied voltage for CdO/glass

Figure (6) shows the photoconductivity of CdO films as a function of applied voltage. From measurements of the current flow within the film in illumination *(I_{ph})* and dark *(I_d)* conditions with applied voltage *(V)* done the gain *(G)* was calculated the gain can be defined as a ratio between illumination current *(I_{ph})* to dark current [15].

Also from measuring the current flow within the film to be done calculated the photosensitivity was calculated [16]); as shows in figure (7). Also we can notice from the figures (6 & 7) that the gain and photosensitivity increase slightly with the increasing of film thickness. This behavior is attributed to the increase the number of atoms with the thickness that leads to

the increase of the number of collisions between atoms, which in turn, leads to the increase of absorptions.

Also, the photosensitivity tends to saturate at (V>0.1volt) due to the total separation of the photo-generated electron-hole pairs.

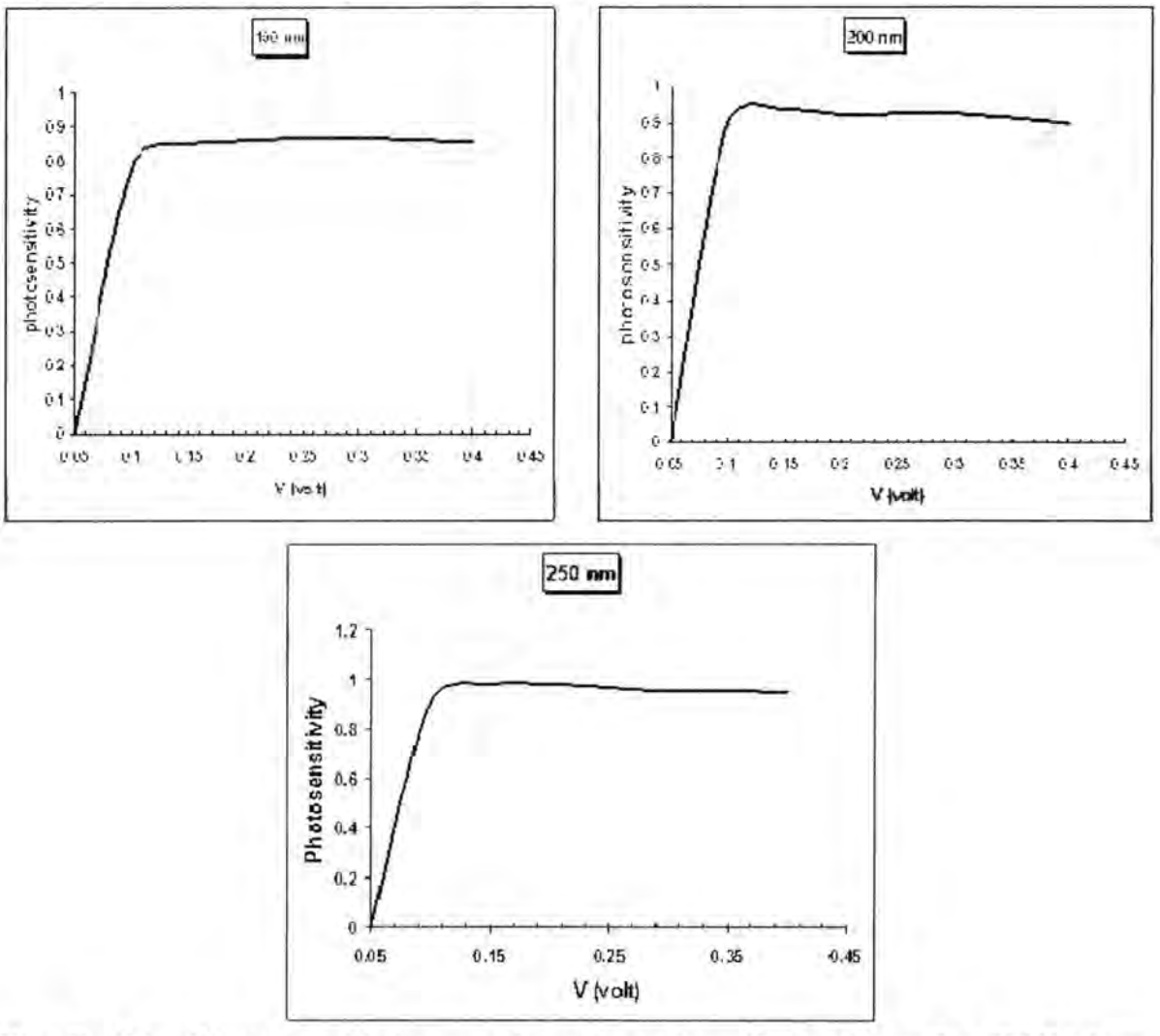

Fig.-7 : The Photosensitivity as a function of applied voltage for CdO/glass

Photovoltaic characteristics:

The two main parameters describe the photovoltalic properties are the open circuit voltage *(V_{oc})* and the short circuit current *(I_{sc})*, where may be separated of the photo-generated electron-hole pairs in depletion region by internal electrical field [17]. Figure (8) shown short circuit *(I_{sc})* current and open circuit voltage *(V_{oc})* of CdO/Si heterojunction as function of illumination power density the short circuit current increase with increase the illumination power

density then (I_{sc}) tends to saturate. From the result obtained it is observed that this is a linear relation between (I_{sc}) and the incident photo power until reach a maximum value beyond which the device tends to be saturated and become constant. This occurs due to the total separated of the electron-hole pairs.

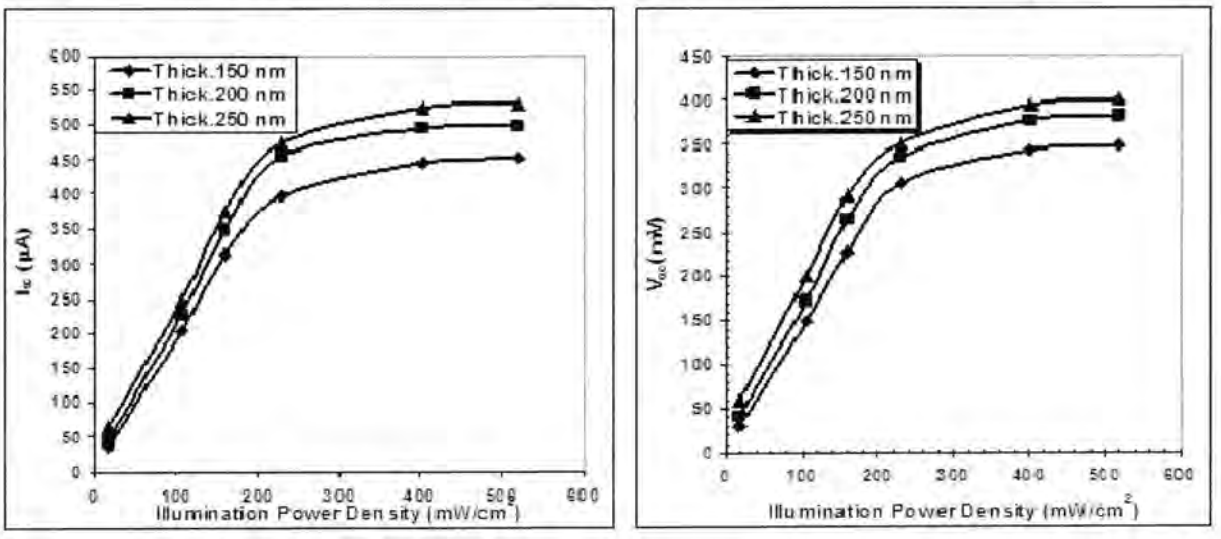

Fig.-8: I_{sc} and V_{oc} as function of illumination power density for CdO/Si

It can be concluded that the present work summarized as follows:

i. CdO films and CdO/Si heterojunction can be prepared by rapid thermal oxidation.

ii. The structure, electrical and photovoltaic characteristics are strongly dependent on the film thickness.

iii. These results confirm the fact that CdO films grown by RTO technique are very promising for different application.

REFERENCE

1. B.G. Jeyaprakash1, K. Kesavan, R. Kumar, S. Mohan & A. Amalarani," Analysis of Precursor Decomposition Temperature in the Formation of CdO Thin Films Prepared by Spray Pyrolysis Method", Department of Physics, PRIST University, Thanjavur – 614 904, Tamilnadu, India, Marsland Press, Journal of American Science 2010.

2. R.S. Mane, H.M. Pathan, C.D. Lokhande & Sung-Hwan Han," An effective use of nanocrystalline CdO thin films in dye-sensitized solar cells", Thin Film Physics Laboratory, Department of Physics, Shivaji University, Kolhapur 416 004, India, Solar Energy 80, p.p185–190, (2006).

3. A.A. Al-Qurani, C.H. Champness, in: Proceedings of the 26th IEEE Photovoltaic Specialists Conference, Anaheim, CA, p. 415, (1997).

4. X. Mathew, J. Phys. D: Appl. Phys. 33, 1565, (2000).

5. R. Ferro, J.A. Rodriguez, O. Vigil, A. Morales-Acevedo, G. Contreras-Puente, Phys. Status Solidi a 177, 477, (2000).

6. C. Dant¸us, G.G. Rusu, M. Dobromir, M. Rusu, (Preparation and characterization of CdO thin films obtained by thermal oxidation of evaporated Cd thin films), Al.I. Cuza University, Faculty of Physics, Carol I Boulevard, No. 11, 700506 Iasi, Romania. Applied Surface Science 255, 2665–2670, (2008).

7. A.Stadler, T. Sulima, J. Schulze, C. Fink, A. Kottantharayil, W. Hansch, H. Baumgartner, I. Eisele & W. Lerch " Dopant di usion during rapid thermal oxidation", University der Bundeswehr Munchen, Germany, Solid-State Electronics 44, 831-835, (2000).

8. K.L.Chopra, "Thin Film Devices Application", Plenum Press, New York, (1983).

9. K. Nishiyama, M. Arai, N.W. Watanabe, Jap.J. Appl. Phys., 19, 563 (1980).

10. K.T. Ramakrishna Reddy, C. Sravanib, R.W. Miles "Characterisation of CdO thin films deposited by activated reactive evaporation", Department of Physics, Sri Venakteswara, Journal of Crystal Growth 184/185, 1031-1034, (1998).

11. Mauricio Ortega, Guillermo Santana1, and Arturo Morales-Acevedo "Optoelectronic properties of CdO-Si heterojunctions", Permanent address: Facultad de Fisica-IMRE, Universidad de la Habana, 43100, and La Habana, Cuba. Superficies y Vacio 9, 294-295, (1999).

12. Salih Kosea, Ferhunde Atay, Vildan Bilgin, & Idris Akyuz "In doped CdO films: Electrical, optical, structural and surface properties" Canakkale Onsekiz Mart University, Department of Physics, 17100 Canakkale, Turkey, international journal of hydrogen energy 34, 5260-5266, (2009).

13. C.H. Bhosale, A.V. Kambale, A.V. Kokate, K.Y. Rajpure "Structural, optical and electrical properties of chemically sprayed CdO thin films" Department of Physics, Shivaji University, Kolhapur 416 004, India. Materials Science and Engineering B 122, 67–71, (2005).

14. R.S. RUSU & G.I. RUSU "The Hall Effect In CdO:Sn Thin Films", Al.I. Cuza University, Iasi, Romania, s.1.b.fasc.2 Fizica Starii Condensate, (2004).

15. I.Zh. Alferov "Semiconductor heterostructures physical processes and applications" Printed in RSSA, (1989).

16. D.A. Neamen,"Semiconductor Physics and Devices", Richard D. Irwin, Inc., (1992).

Tensile Strength Investigation of UPE and EP Composites Filled with Rice Husk Fibers

Harith I. Jaffer and Mohammed K. Jawad
Department of Physics, Collage of Science, University of Baghdad

Received : 11/04/2011 Accepted: 29/05/2011

الخلاصة

تم بحث متانة الشد لمتراكبات البولي استر الغيرمشبع والايبوكسي المملوء بالياف قشة الرز. استخدمت طريقة القالب المضغوط لتحضير الواح من متراكبات البولي استر غير المشبع والايبوكسي المملوء بقشة الرز. اظهرت النتائج تحسن في خواص الشد لكلا البوليمرين المتراكبين,ولكن متراكب الايبوكسي كان له متانة شد اعلى، لكون ان المادة الرابطة (الايبوكسي) تمتلك خصائص ميكانيكية افضل من البولي استرالغير مشبع كمادة رابطة. ان استخدام قشة الرز بالتسليح قد عزز خصائص الشد للمتراكبات البوليمرية.

ABSTRACT

Tensile strength for UPE&EP composites filled with Rice Husk has been investigated. A compressed mold method was used to prepare sheet of UPE&EP composites filled With Rice Husk. The results show that improving in tensile properties for the two polymer composites, but the EP composite have the higher values of tensile strength, since the matrix (EP) have better mechanical properties than UPE matrix. The filling with the Rice Husk enhanced the tensile properties of the polymers composites.

INTRODUCTION

Plant-fiber composites and hybrid laminates including plant fibers are increasingly used for semi-structural applications, as they show a better end-of-life profile, being intrinsically carbon dioxide neutral . However, the mechanical behavior of plant fibers as reinforcement is not easily predicted. In particular, plant fibers are heterogeneous, being cellular structures assembled in nature through a hierarchical procedure, and present a hollow, or lumen, of variable dimensions . [1]. The interest in natural fiber-reinforced polymer composite materials is rapidly growing both in terms of their industrial applications and fundamental research. They are renewable, cheap, completely or partially recyclable, and Biodegradable..[2]. Rice husk (RH) is one of the major agricultural residues produced as a by-product during rice processing. Usually it

has been a problem for rice farmers due to its resistance to decomposition in the ground, difficult digestion and low nutritional value for animals. According to Marti-Ferrer the lignin and hemicellulose contents of rice husk are lower than wood whereas the cellulose content is similar. For this reason RHF can be processed at higher temperatures than wood. Therefore, the use of rice husk in the manufacture of polymer composites is attracting much attention[3].The utilization of lightweight, low cost natural fibers offers the potential to replace a large segment of the glass and mineral fillers in numerous automotive interior and exterior parts.. The primary thermoset resins used today in natural-fiber composites for automotive applications are polyester, vinyl ester, and epoxy resins. Polyester resins are widely used, particularly the "unsaturated" type capable of cure from a liquid to a solid under a variety of conditions. A range of polyesters is made from different glycols (polyethylene glycol, ethylene glycol, etc.), acids (maleic, anhydride), and monomers, all having various properties .Orthophthalic polyester is the standard economic resin commonly used, and it yields highly rigid products with low heat resistance . Epoxy resins offer high performance and resistance to environmental degradation. Typically, the monomer is produced by reacting epichlorohydrin and bisphenol-A with hardeners such as amines or anhydrides common in industry. Epoxies have wide appeal in industry, although in the automotive industry epoxies have not gained broad use due to longer cure schedules and high monomer cost [4-5]. The benefits offered by lignocellulosic materials include making the final product light , decreasing the wear of the machinery used, low cost, biodegradability, and absence of residues or toxic byproducts[6]. In the present study we used a thermoset polymer (UPE&EP) as the matrix and a lignocellulosic material(rice-husk) as the reinforcing filler to prepare a filler-reinforced composite to examine the possibility of using lignocellulosic materials as reinforcing fillers and to determine testing data for the tensile strength properties of the composite according to the reinforcing filler.

MATERIALS AND METHODS

1-Raw Materials

Two type of polymers (epoxy resin and unsaturated polyester) were used to prepare sheets of composites which reinforced with rice husk.

1-1Epoxy resin

A clean disposable container was used for maxing epoxy resin type (Euxit 50) supplied by Swiss Chem company, with ratio 1:3 the content were mixed thoroughly by a fan type stirrer for(5)min.

1-2Unsaturated polyester

100g of unsaturated polyester resin type Viapad (H-265) was mixed with 0.5g accelerator (Cobalt napthenate) a 2g hardener(Methyl Ethyl Keton Peroxide) were added to the mixture and the contents again mixed thoroughly until a homogeneous state of the mixture was obtained.

1-3Rice husk

This type of natural fibers were obtained from local markets. Rice husk pass throw steps before used as a reinforced fibers:

a) Washing of rice husk

Rice husk were washed with water in order to remove dust and mud.

b) Drying of rice husk

Rice husk were dried under sunlight for 2 days at 38°C , and then in a hot air oven for 6 hours at 80°C.

1-3 Composites preparation

After prepare the required amount of the resin(epoxy or unsaturated polyester) about 75% by weight we add the rice husk to the resin which about 25% by weight and mix them thoroughly
until a homogeneous state ,then we emptying the content in the cast mold which made of iron and consist of two plates, the first one acts as a base with (300 mm × 300 mm × 10 mm) dimension. This plate should polish without any defect. The second plate used as a cover putting on the first plate to make symbols thickness uniform. This plate has dimension (200 mm × 200 mm × 10mm) fixed with Compression machine to press the symbol. The four sides of the base were made of iron that connected to the base strips. These sides were removable, so that the symbol was easy to move, when it dries. Before casting, the iron plates were cleaned to remove the dirt and dust that were presented on the surfaces .*The plates were dried in an oven, the base*
and the cover of the iron plates were coated with wax.

2- Tensile test

The test was conducted according to ASTM D638, and was performed at crosshead speeds of (2 mm/min), and temperature (25±2 °C) of relative humidity (50±5). the test were performed with Instron testing machine type Tinius Olsen, H50 KN full scale load capacity.

RESULTS AND DISCUTION

Mechanical properties are of major importance for all applications of natural-filled polymer composites .The results for UPE filled with rice husk(Rh) natural fibers fig.(1), show that an improving in tensile properties which lead to increase in the values of ultimate tensile stresses(UTS), yield stress and modulus of elasticity as shown in table(1), while for pure UPE which obtained by Farhan the UTS (33.1MPa) and modulus of elasticity(4.3GPa) [7] those values less than for UPE filled with rice husk and that indicate to the effect of the rice husk act . During the tensile deformation of composites, the applied stress was partially transferred to strong natural fibers, especially those in the direction of elongation. Generally, fiber-reinforced composites have higher tensile strength than particle-reinforced composites[8]. As the filler loading increased, thereby increasing the interfacial area, the worsening interfacial bonding between filler (hydrophilic) and matrix polymer (hydrophobic) decreased the tensile strength, which nevertheless remained within acceptable levels . Tensile modulus improved with increasing filler loading . For irregularly shape fillers, the strength of the composites decreases due to the inability of the filler to support stresses transferred from the polymer matrix [9] while poor interfacial bonding causes partially separated micro-spaces between filler and matrix polymer, which obstructs stress propagation when tensile stress is loaded and induce increased brittleness. The cell wall of a fiber consists of a number of layers: the primary wall, which is the first layer deposited during cell development, and the secondary wall, which in turn is made up of three layers, containing cellulose, hemicellulose and lignin in varying amounts. In addition, the introduction of plant fibers in a polymer matrix may generate compatibility issues, whose consequence may be a large scattering of properties in the final laminate.

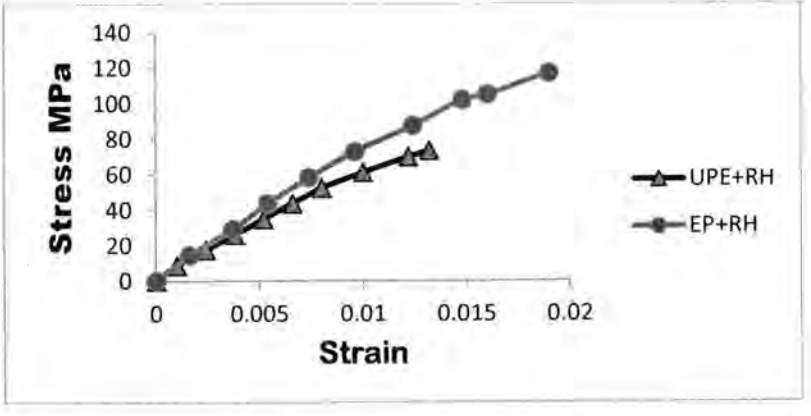

Fig.-1: Stress-strain curves for UPE and EP composites

The results for EP filled with rice husk natural fibers fig.(1) show that this type of composites have good tensile strength and better than UPE composites, and owned higher values of ultimate tensile stresses(UTS), yield stress and modulus of elasticity as shown in table(1) , also this values are higher than that for pure epoxy which obtained by Jaffer [10] , epoxies are stronger, stiffer, tougher, more durable. Also fig(2) shows the shape of the crack in the composites (A) UPE and (B) EP, the photographic pictures make clear that the adhesion between EP matrix and rice husk is better than for UPE and the rice husk, which give the EP composite more strength ,because the interfacial adhesion between the natural fiber and polymer matrix determines the composite physical properties, it is usually necessary to compatibilist or couple the blend. The increase in the Young's modulus with the addition of cellulosic depends on many factors such as the amount of fibers used, the orientation of the fibers, the interaction and adhesion between the matrix, the ration of the fiber to matrix Young's modulus, etc.[11]. The matrix acts as the load-transfer medium between fibers and, in less ideal cases, where loads are complex, the matrix may even have to partly bear loads. The matrix also serves to protect the fibers from environmental damage before, during, and after composite processing[12].This is a common behavior when rigid fillers are incorporated into softer polymer matrices. Natural lignocellulose fillers have been found as having elastic modulus higher than polymer matrix. Because of this the rigidity of its composites tends to strongly increase with addition of these fillers. Some authors have also related the increase in composites' rigidity with the reduction of polymer chains mobility in the presence of the filler[13].

Table-1: Value of ultimate tensile stresses(UTS), yield stresses(Oy) and modulus of elasticity(E) for UPE&EP composites

Sample type	UTS (MPa)	Oy (MPa)	E (GPa)
UPE	33.1	-	4.3
UPE/Rh	73.42	52.44	6
EP	60.4	44.7	2.79
EP/Rh	117.13	101.99	6.76

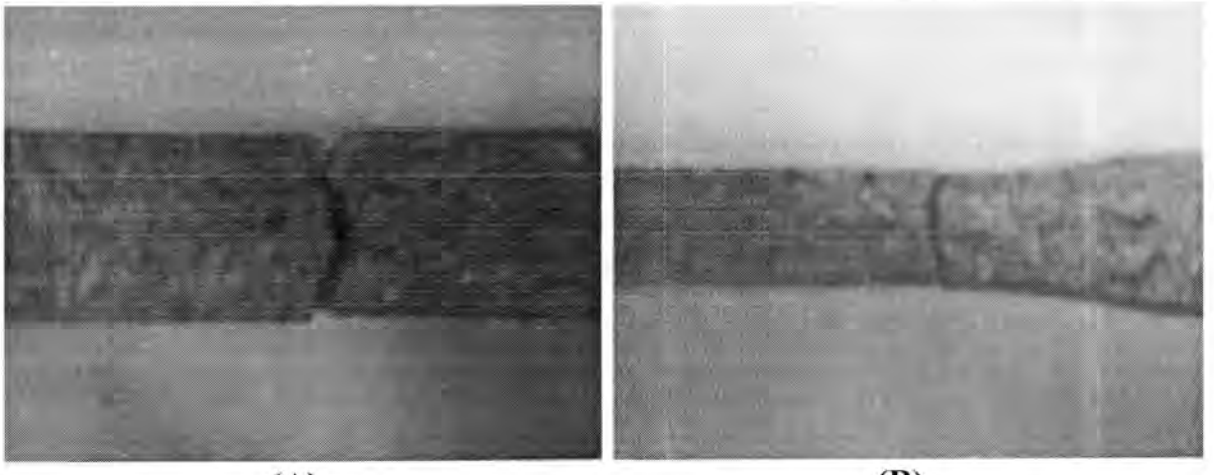

(A) **(B)**

Fig. -2: Photographic picture show the fracture surface in (A) UPE composite,(B) EP composite

The use of natural fibers (Rice Husk) improve the mechanical properties(tensile strength) of Unsaturated polyester and Epoxy polymer composites , The convenience of these composites lies in the fact that the ingredients are obtained easily from natural wastes and hence the composites can be made relatively easily. The EP composite owned good tensile properties better than UPE composite.

REFRENCES

[1] I.M. De Rosa ;C. Santulli &F. Sarasini, "Natural Fiber Composites Monitored by Acoustic Emission" Journal Acoustic Emission,Vol.26,pp.220-228,(2008).

[2] Prakash Tudu , Processing &Characterization of Natural Fiber Reinforced Polymer Composites ,Bachelor of Technology in Mechanical Engineering. Thesis Dep. of Mech. Eng . ,National Institute of Technology,Rourkela,pp.14-18,(2009).

[3] S.M. Rosa; E.F. Santos ;C.A. Ferreira &S.M. Nachtigall , "Studies on the Properties of Rice-Husk-Filled PP Composites-Effect of Maleated PP" Materials Research, Vol. 12(3) :333-338, (2009).

[4] S. Taj ;M.A. Munawar and S. Khan *Saira, "Natural fiber-Reinforced Polymer Composites", Proc. Pakistan Acad. Sci. ,Vol.44(2)*:129-144,(2007).

[5] N. Chand and B.D. Jhod, "Mechanical ,Electrical &Thermal properties of Maleik Anhydride Modified Rice Husk filled PVC Composites"BioResources,Vol.3(4):1228-1243,(2008).

[6] H.S. Yang, H.J. Kim, J. Son, H.J. Park ,B.J. Lee and T.S. Hwang "Rice-husk flour filled polypropylene composites; mechanical and morphological study" Composite Structures ,Vol. 63, ,pp. 305–312.(2004).
[7] A.J. Farhan." Investigation of Some Mechanical properties of Sawdust & Chopped Reeds/UPE Composites .Msc .Thesis . University of Baghdad . pp.53-62,(2011).
[8] G.R. Liu, "A step-by-step method of rule-of-mixture of fiber & particle reinforced composite materials ",Compos Struct,Vol.40(3-4):312-322,(1997).
[9] H. Ismail ;J.M. Nizam & A. Khalil, "The effect of compatibilizer on the mechanical properties and mass swell of white rice husk ash filled natural rubber/linear low density polyethylene blends", Polym. Testing,Vol.20(2):125-133,(2001).
[10] H. I. Jaffer. "Investigation of Interlaminar Toughness of Reinforced Polymer
Blends" PhD. Thesis University of Baghdad.pp.59-65,(2000).
[11] R. Rowell, A. Sanadi, D. Caulfield & R. Jacobson, Lignocellulosic - Plastics Composites (Utilization of Natural Fibers in Plastic Composites: Problems and Opportunities), pp23-51,(1997).
[12] A. Satapathy ;A. Kumar; S. Mantry; S. K. Singh & A. Patnaik, "Processing and Characterization of Jute–Epoxy Composites Reinforced with SiC Derived from Rice Husk ",J. Reinforced Plastic & Composites ,pp.1-10,(2009).
[13] A.K. Rana , B.C. Mandal , R. Mitra , R. Jacobson , A. Rowell and N. Banerjee, "Short jute fiber reinforced polypropylene composites: Effect of compatibilizer". *J. of Applied Polymer Science.* 69(2):329-338 , (1998).

The Effect of Cu_2O Layer on the Properties of Cu-SiC Composites Using Liquid Phase Sintering Technique

Samir B. Younis
Department of Applied science, Technology University

Received : 27/03/2011 Accepted : 29/05/2011

الخلاصة

تم تحضير عينات من النحاس المدعم بكاربيد السليكون (بنسبة حجمية 25%) وتلبيدها بالطور السائل عند درجة حرارة °C (1100,1000,900) في جو الفرن الاعتيادي . تم فحص الكثافة , المسامية. ووجد نقصان في الكثافة مصحوبة بزيادة في المسامية عند أزدياد درجة الحرارة. تم فحص العينات مجهرياً و فحص تشتيت الاشعة السينية , حيث لوحظت تكون الجزر من أوكسيد النحاس في العينات وان هذه الطبقة تزداد بزيادة درجة حرارة التلبيد , وهذا ما يقود الى تكوين متراكبات مسامية بشكل أكبر, وتباعد بين حبيبات كاربيد السليكون عن النحاس . تم فحص صلادة فيكر للعينات , اضافة الى فحص البلى عند أوزان N(5,10) , ووجد صغر في صلادة المادة المتراكبة بالاضافة الى زيادة في معدل البلى عند زيادة درجة الحرارة في كلتا حالتي الحمل.

ABSTRACT

SiC particulate-reinforced (25 vol%) copper composites were fabricated using liquid phase sintering in (900,1000,1100° C) at argon atmosphere of electric furance. Density, porosity test were performed Characterization of the composites sintered were conducted by XRD and microstructure analysis. It was found that Cu_2O islands formed on the surface of copper crystallites in the coated particles during sintering at different temperatures. The oxide layer Cu_2O was increased on copper, and this led to porous composites with flocculation of SiC grains and segregation from coagulated copper blocks when the temperature was increased. It was found that decreasing in density and increasing in porosity with temperature . Vicker microhardness, dry sliding wear tests of $Cu–SiC_p$ composites were carried out with a typical experimental plan of simultaneous variation of loads (5,10)N . Loosing in composite hardness, moreover wear rate will be increased with highest temperatures.

INTRODUCTION

Copper and copper alloys are well known for a combination of good corrosion resistance in a variety of environments, excellent workability,

high thermal and electrical conductivities, and attractive mechanical properties at low, normal and moderately elevated temperatures.

Thus they are widely used in the electronic application and bearing materials. Metal matrix composites combine the advantages of the matrix and reinforcement to obtain the required properties, to increase strength, toughness and anti-wear and heat resistance as compared with the conventional Cu alloys , The composites incorporated with particles reinforcement, owing to better isotropic behaviors, were mostly used as bearing materials[1-3].

It is very important to understand wetting phenomena of liquid metals-ceramics systems in metallurgical, welding and joining fields to obtain high quality and high performance materials. For example, to understand phenomena such as a reaction between liquid alloys and refractory, Metal-ceramics joining and a fabrication of metal matrix composites, information on wettability of solid oxide, nitride, carbide and carbon by liquid metals is indispensable[4,5].

Accordingly, many research articles concerning the wettability of solid ceramics by liquid metals have been published. However, there is a considerable difference in the contact angle between liquid metal on solid ceramics, which is one of an index of wettability[6-9].

When analyzing data on interface stability, the most discussed quantities are the work of adhesion or the wetting angle. By definition, the work of adhesion is the reversible free energy change for making free surfaces from interfaces, whereby the free surfaces are in equilibrium with the solid (or liquid) and gaseous components. For the ceramic (S)/liquid metal(L)/vapor (V) system, the Dupré equation is[10]:

$$W_{ad} = \sigma_{SV} + \sigma_{LV} - \sigma_{SL} \quad \ldots\ldots (1)$$

where σ_{SV} is the ceramic surface energy, σ_{LV} the liquid metal surface energy and σ_{SL} the interfacial ceramic-liquid metal energy. W_{ad} can be evaluated by sessile drop data (σ_{LV} and contact angle Θ of the metal on the ceramic) using the Young-Dupré equation:

$$\sigma_{SV} = \sigma_{SL} + \sigma_{LV} \cos\Theta) \ldots\ldots\ldots\ldots (2)$$

$$W_{ad} = \sigma_{LV} (1+\cos\Theta) \ldots\ldots\ldots\ldots (3)$$

It is well known that the wettability is affected by many factors such as temperature, partial oxygen pressure in an atmosphere, surface condition

of ceramics (surface roughness and surface crystal structure), thermo-dynamical stability of ceramics and metal and alloying element[11].

MATEWRIALS AND METHODS

A composite of copper powder (purity of 95%) reinforced with SiC_p (25 wt%) . The composite mixture was prepared by mixing with a ball mill for two hour to ensure a homogeneity .Gteen compacts pressed at (250MPa) a steel mold of (12mm)diameter were then sintered in different temperatures (900,1000,1100 °C) for (2) hours in atmosphere of an electric furnace , the samples were grinded and polished with SiC papers , then optical microscopy and XRD test were performed as shown in figure (1) and (2) respectively . The density of copper composites was determined according to Archimedes' method. In this technique, density is determined by measuring the difference between the specimen's weight in air and when it was suspended in distilled water at room temperature., The porosity can be determined by the equation :

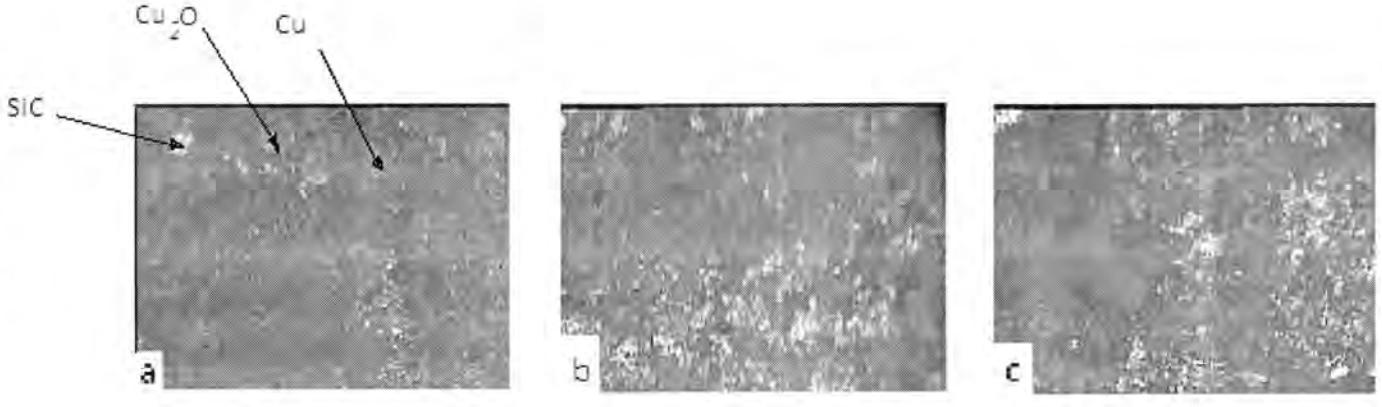

Fig. -1 : Optical microscopy for copper based composite samples (a) 900°C (b) 1000°C (c) 1100°C

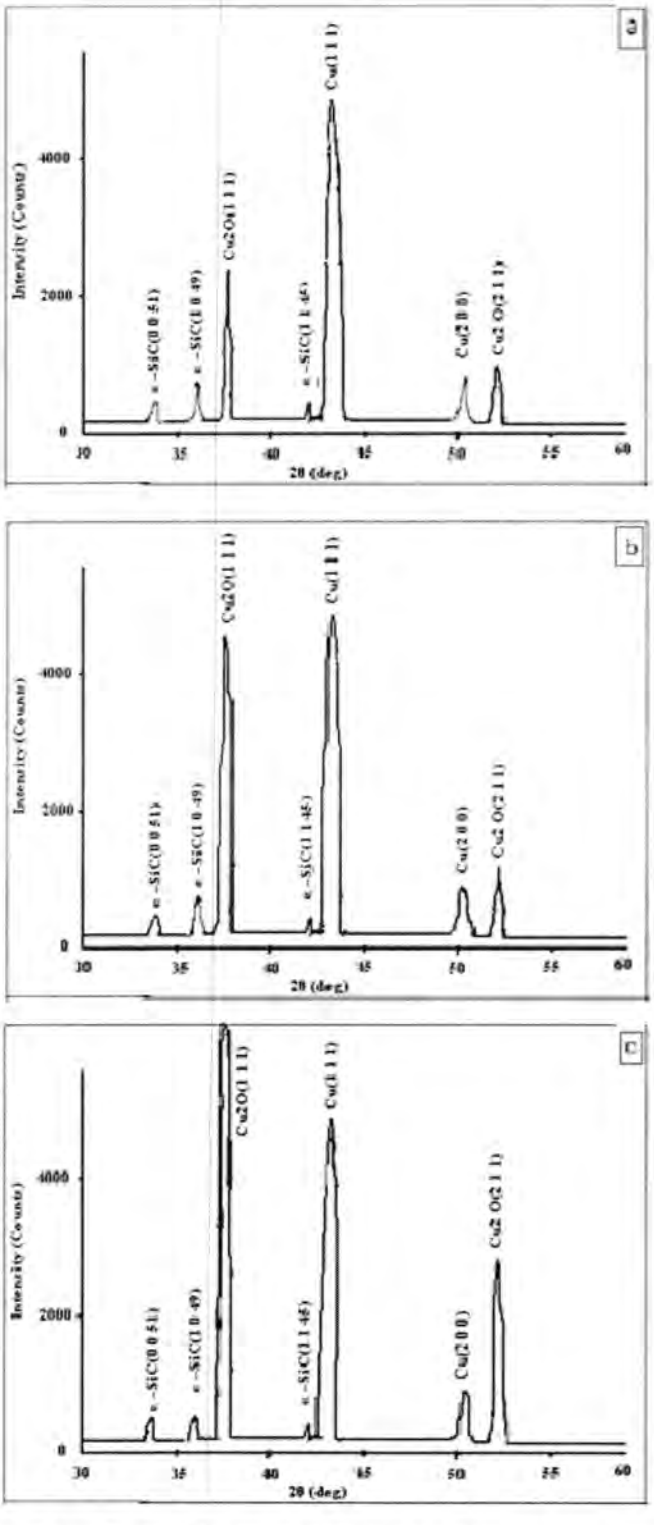

Fig.-2 : XRD test for Cu/SiC composites at temperatures (a) 900°C, (b) 1000° C, (c)1100° C

$P\% = 1 - \rho / \rho_t \times 100$

where ($P\%$) is the pore volume percentage, (ρ) is the measured density and (ρ_t) is the theoretical density. Vicker's microhardness test were then conducted for the sintered samples by (HVS- 1000) instrument . Dry sliding wear tests of Cu–SiC_p composites were carried out using pin on disc apparatus with a typical experimental plan of simultaneous variation of loads (5,10)N .the results were prepared in table (1).

Table -1: illustrate variation of composites properties with temperature.

Temp.(° C)	Density (g/cm^3)	Porosity (%)	HV (MPa)	Wear rate $(g/cm)\times10^{-7}$ at 5 N load	Wear rate $(g/cm)\times10^{-7}$ at 10 N load
900	7.34	2.71	64.4	27.9	55.2
1000	7.12	2.83	43.7	39.7	73.4
1100	6.84	2.97	39.2	45.6	103.6

RESULTS AND DISCUSSIONS

1. Increasing temperature will reduce composite density due to segregation of SiC_p from coagulated copper blocks when the temperature was increased, as shown in table (1).
2. More temperature means more Cu_2O layer on copper matrix as illustrated in figure in figure (1).
3. Composites hardness is mainly affected by temperature. The composite will be more pores with increasing temperature cause to decrease the hardness.
4. In the Cu/SiC_p composites shows higher wearing rate and penetration rate when the temperature increased due to increasing composite brittleness as shown in figure (1), b and c .
5. The wear rate of Cu/SiC_p increases with increasing loads for the two wear Tests. Many little shear dimples on it suggest severe deformation in the subsurface region.
6. XRD test shows Cu_2O layer is found previously on phase (111) in higher percentage and will increased gradually with temperature.

So, we can conclude :

1- The oxide layer Cu_2O was increased on copper, and this led to porous composites with flocculation of SiC grains and segregation from coagulated copper blocks when the temperature was increased.

2- From the microstructure tests indicate the debonding at the SiCp–matrix interface along the reinforcement. The surfaces of the composite present numerous microscopic voids and pores that increased gradually with temperature and effect on microhardness as illustrated in table (1).

3- It is well known that the wear loss is inversely proportion to the hardness of the material. The un incorporation of SiCp worse the hardness of the composite markedly and the extent of plastic deformation for composite is increased under the friction condition. In addition, a great deal of SiCp are pulled out from the matrix and trapped into the counterface during the sliding process when the load is increased.

4- Increasing temperature is one of the methods for reducing contact angle, but it is not suitable for this composite as illustrated in this paper.

REFERENCES

1. M.Taya and R.J.Arsenault: Metal Matrix Composites—Thermomechanical Behavior, Pergamom Press, Oxford. (1989).
2. Murakami, K. Matsui, Evaluation of mechanical and wear properties of potassium acid titanate whisker-reinforced copper matrix composites formed by hot isostatic pressing, Wear, 201,193, (1996).
3. K. Ichikawa, M. Achikita, Control of the reaction at the fibre–matrix interface in a Cu/SiC metal matrix composite by modifying the matrix with 2.5 wt.% Fe, Mater. Trans.,JIM 34, 718, (1993).
4. Monastyrsky GE, Odnosum V, Van Humbeeck J, and Kolomytsev VI, Powder metallurgical processing of Ni-Ti-Zr alloys undergoing martensitic transformation Part I, Intermetallatics, Vol.No10, 95-103, (2002).
5. H. Nakae and A.Gato, Reactive and nonreactive wetting, proc. Int. conf. high temperature capillarity, 29June-2July,Cracow, Poland, (1997).

6. A. Chrysanthou, G. Erbaccio, J. Fabrication of SiCw reinforced copper matrix composite by electroless copper plating, Scripta Mater. Sci. 30 .6339, (2001).
7. M.C. Payne, MP. Teter, DC. Allan , T.A. Arias and J.D Joannpoulos, Wear Transitions in Particulate Reinforced Copper Matrix Composites, Rev.Mod.Phys. 64, 1045,(1992).
8. Jianhua Zhu, Lei Liu, Bin Shen, Wenbin Hu ,Mechanical properties of Cu/SiCp composites fabricated by composite electroforming, State Key Laboratory of Metal Matrix Composites, Shanghai Jiao Tong University,China, (2003).
9. A.M. Stoneham, D.M. Dufy, J. H. Harding & P.W.Tasker, Designing Ceramic Inerfaces II: Understanding And Tailoring Interfaces for Coating, Composite and Joining Applications ed.S. D. Peteves, Committee of European Communities, Luxembourg: 573-82, (1993).
10. Yongzhong Zhan, Guoding Zhang," The effect of interfacial modifying on the mechanical and wear properties of SiCp/Cu composites", State Key Laboratory of Metal Matrix Composites", China, Materials Letters 57 ,(2003) ,4583– 4591.
11. A.R. Kennedy, A.E. Karantzalis, J.V. Wood, J.D. Ellis and J.LF.Kellie, The mechanical properties of Al-TiC metal matrix composites fabricated by a flux- casting technique, Patent applied for, Non9616640.0, (1999).

Density of states of CdTe thin films

Issam M. Ibrahim
Department of Physics, College of Science, University of Baghdad

Received : 11/04/2011 Accepted : 29/05/2011

الخلاصة

تم في هذا البحث دراسة تاثيردرجة حرارة التلدين T_a على التوصيلية الكهربائية المتناوبة وكذلك على ثابت العزل الحقيقي والخيالي $\varepsilon_r,\varepsilon_i$ وزمن الاسترخاء τ لأغشية CdTe الرقيقة والمحضرة بطريقة التبخير الحراري في الفراغ وبسمك (300nm) . تمت قياسات التوصيلية المتناوبة ضمن مدى الترددات(10^2Hz-10^5Hz) وفي مدى درجات الحرارة(303-473K) حيث وجد انها تخضع الى العلاقة $\sigma=Aw^s$ حيث تكون فيها قيمة s بين (0.3-0.95). تظهر التوصيلية المتناوبة اعتمادية على مدى التردد(100Hz-100kHz). اوضحت النتائج ان الاستقطابية تقل بينما يزداد زمن الاسترخاء بزيادة درجة الحرارة.تم قياس فجوة الطاقة وعرض الذيول ضمن مدى (200-900nm) والتي اوضحت ان الانتقال هو انتقال مباشر مسموح.واخير من خلال كل القياسات اعلاه تم اقتراح موديل لكثافة مستويات الطاقة(DOS).

ABSTRACT

The effect of annealing temperature *(T_a)* on the ac conductivity, real and imaginary part of dielectric constant *(ε_r, ε_i)*, relaxation time *(τ)* had been measured for CdTe thin films with 300nm thickness which were prepared at room temperature*(R.T)* using thermal evaporation under vacuum. Measurements of ac conductivity over frequency range *(10^2-10^5 Hz)* in temperature range *303K* to *473K*, showed that the ac conductivity obeys the formula $\sigma_{ac}=Aw^s$, where (*s*) lies between (0.3-0.95). σ_{ac} declared exponentially dependence on the frequency range. The results show that distribution parameter(Polarizibility) *(β)* decreases while microscopic relaxation time *(τ_0)* increases with the increasing annealing temperatures. Optical energy gap and tails width were measured in the range of (200-900nm) which revealed allowed direct transition. Finally we suggested an experimental model for density of states.

INTRODUCTION

Chalcogenide glasses based on sulfides, Selenide and Telluride alloys in binary and multi-component system, have evoked much interest in terms of the understanding of basic physics of crystalline and non-crystalline solids, as well as for the development of various semiconducting devices. These glasses are also promising materials for various optical and photonic applications [1].

In recent years, much attention has been shown in semiconducting II-VI compounds because of their opto-electric properties and their possible applications in switching and memory devices, photodiodes and solar cells [2].the existing examples of Cadmium Telluride application indicate the appreciable dependence of the electrical and structure properties of CdTe films on the method and technological conditions of its passivation[3-6].

Extensive studies have been made on the structural, electrical and optical properties of CdTe thin films, but Alternative current behavior are not very abundant in the scientific literature[7].with the rapid development of advanced technologies in all areas, today much attention is presently paid to binary semiconductors AB(A=Zn,Cd,B=S,Se,Te) and their alloys[8].For fabrication of the CdTe films a variety of preparation techniques have been employed such as vacuum evaporation[9-11],chemical spray pyrolysis, electro-deposition ,electrolyses deposition[9],R.F Sputtering, close-space sublimation [12] pulsed laser deposition [13].The vacuum evaporation method has some advantages such as the amount of impurities included in the growing layer will be minimized, the tendency to form oxides will be considerably reduced [14].

MATERIALS AND METHODS

Cadmium telluride thin films were prepared by thermal evaporation of a stoichiometric powder of the compound (chemical purity 99.999%) in a residual air pressure of 10^{-5} Torr ,molybdenum boat sources were used for the evaporation. glass slides were used as substrates for structural and electrical characterization. the thickness of the films used for these characterization was in the range 500-530nm.The structural observations were made on X-ray diffraction using (Philips PW 1410/20 X-ray diffractometer)operating at 40 kV by using Cu(λ=1.54A) as a target. The electrical characterization involved

the study of the variation of resistivity, capacity and frequencies with temperatures. HP-LCR meter has been used for electrical characterization, while for optical measurements we use shemadzu spectroscopy (200-900nm) wave length.

RESULTS AND DISCUSSION:

1. STRUCTURAL PROPERTIES:

The evaluation of any material for application is complete and meaningful only when its structure and compositions are precisely known. Thermally evaporation CdTe thin films were polycrystalline in nature [15]. The XRD patterns of samples as –deposited and that which annealed at 373 K, 423 K and 473 K are shown in Fig.(1).This figure shows a polycrystalline structure of all samples before and after annealing. They have a highest peaks at diffraction peaks at 2θ=23.68,23.78,23.76 and 23.82 respectively which correspond to reflection planes (111),while peaks appeared at 2 θ =39.39.39.24,39.46 and 39.59 which correspond to reflection from planes (110).The reflection from (102) at 2θ=39.19 and 32.13 are beings to disappear when the annealing increases to T_a=423 and 473K,this may be due to the layer stability of (102) planes which reflects the less relaxed bond with minimum energy, or improved the crystallinity of the structure which leads to growth in the grain size. In addition to that there is no separate Cd or Te phase form.

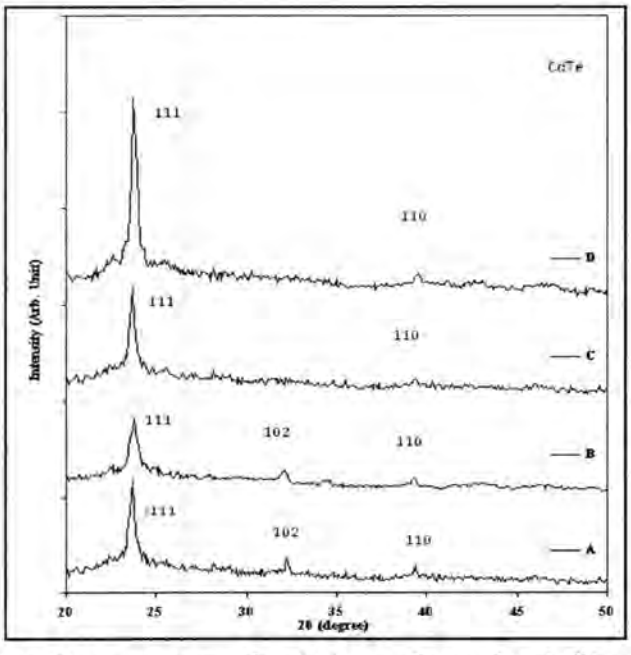

Fig.-1: X-ray diffraction pattern for(A) as-deposited film,(B) T_a=373 K (C) T_a=423 K (D)T_a=473 K

2. FREQUENCY DEPENDENCE OF CONDUCTIVITY:

Figure (2) shows the total measured conductivity as a function of frequency $\sigma_{tot}(w)$ in the frequency range *100-100kHz* at various temperatures in the range *300-423K* for *CdTe* films. The conductivity behavior can be divided according to the measured frequency (low and high frequencies). In the low frequencies region, the conductivity is constant and is taken to be the dc conductivity σ_{dc}. Theoretically, this behavior may be modeled by transport taking place through infinite random free-energy barriers [16].When the frequency increases, the conductivity is found to obey a power relation, $\sigma_{ac} \sim w^s$, where s is a function of temperature such behavior may be modeled as transport is dominated by conduction hopping through infinite clusters [16].The crossover frequency from σ_{dc} to σ_{ac} is frequency loss and increases with temperature. At higher frequencies, the conductivity tends to stability, at higher temperature; the curve of $log\sigma_{tot}$ *vs.* log f becomes nearly linear. Hence, the total conductivity is a sum of the two components dc conductivity, which is independent of frequency: and frequency dependent conductivity σ_{ac} i.e.

$$\sigma_{tot}(w)) = \sigma_{dc} + \sigma_{ac} \quad \text{.....(1)}$$

The values of σ_{dc} are obtained by extrapolating $\sigma_{tot}(w)$ to $w=0$. Values of frequency exponent (s) is plotted against temperature T for each samples of CdTe films, and shown in Figure(3) .Each curve in this figure shows decreases in the exponent s with an increase of the temperature, thus the experimental results agree with the correlated barrier hopping model*(CBH)*.For a critical test of the CBH models comes from the temperature dependence of the ac conductivity and the a frequency exponent.

For the mechanism of ac conduction, the model of correlated barrier hopping *(CBH)* of bipolarons (i.e. two-electron hopping charge defects D^+ and D^-) has been proposed. According to the Guintini model, each pair of D^+ and D^- is assumed to form a dipole with relaxation energy. This type of energy can be attributed to the existence of a potential barrier over which the carrier can hop. This observation leads to decrease in the density of states due to the conversion of some bipolaron states (D^+, D^-) states into a single polaron state (D^0) according to the relation $D^+ + D^- = 2D^0$, the theory has explained many low temperature features, particularly the temperature dependent values of the parameters A and s. However, it does not explain the high temperature

behavior so well, particularly in the low frequency range, shimakawa suggested that D^0 states are produced by thermal excitation of D^+ and /or D^- states and that single polaron hopping (i.e. one-electron hopping between D^0 and D^+ or D^-) contributed at high temperature.

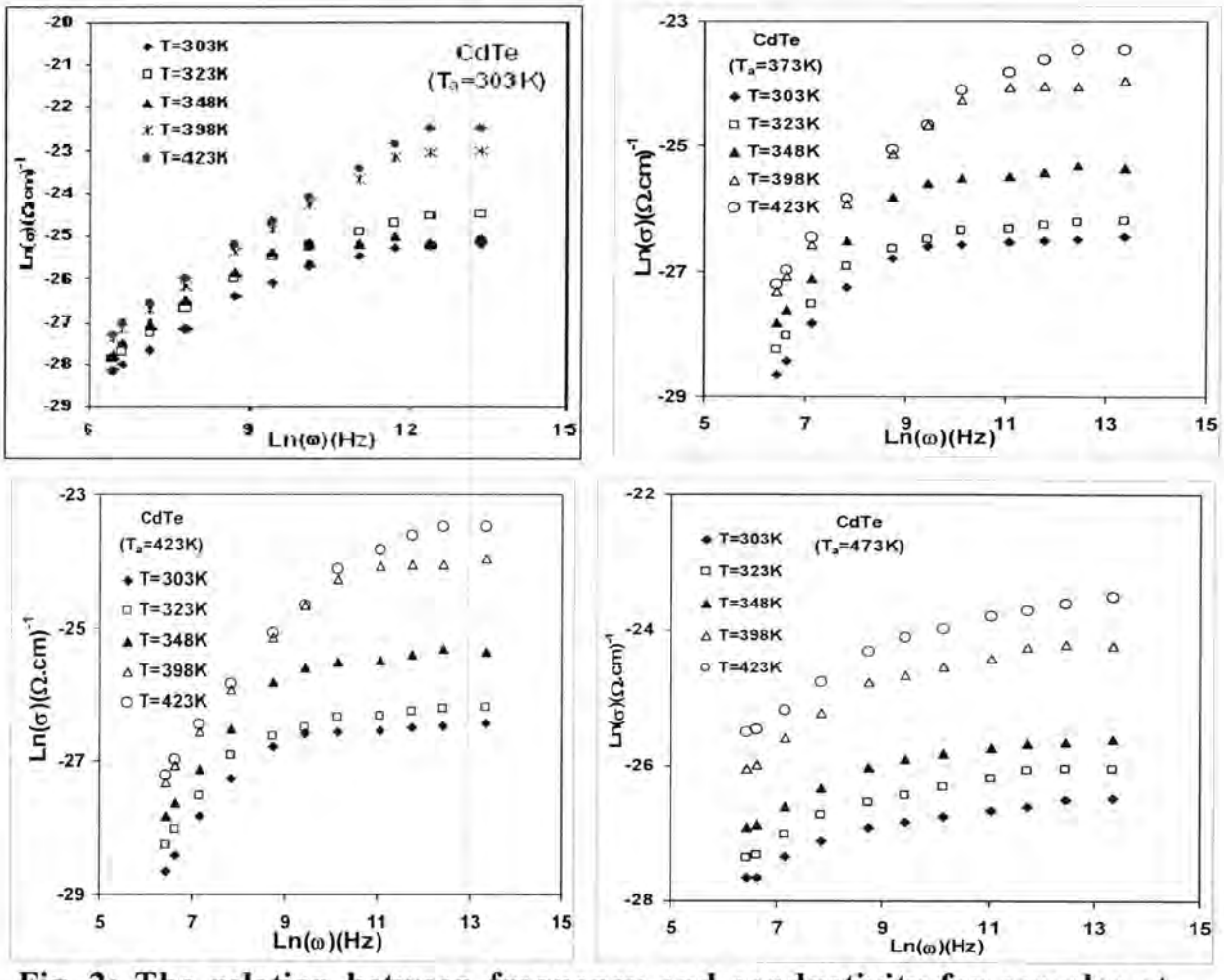

Fig.-2: The relation between frequency and conductivity for samples at T_a=303,373 ,423 and 473K annealing temperature.

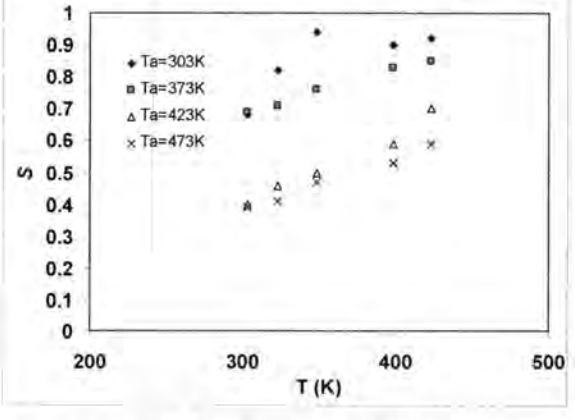

Fig.-3: The exponent s with temperatures at different annealing temperatures

Table-1: the values of exponent *s* with different annealing temperatures

	T_a=303K	T_a=373 K	T_a=423K	T_a=473K
T(K)	*s*	*s*	*s*	*s*
303	0.68	0.69	0.4	0.39
323	0.82	0.71	0.46	0.41
348	0.90	0.76	0.5	0.47
398	0.94	0.83	0.59	0.53
423	0.92	0.85	0.7	0.59

3- COLE-COLE DIAGRAM: (ANALYSIS OF DIELECTRIC DATA)

A compact and informative way of display the relation between $\varepsilon`(w)$ and $\varepsilon``(w)$ and their dependence on frequency,$w/2\pi$,was proposed by Cole and Cole [17].The method consists in plotting $\varepsilon``(w)$ as a function of $\varepsilon`(w)$ and such plot is for the Deby equation[17]

$$\varepsilon(w)=\varepsilon`(w)-i\varepsilon`(w) \quad \text{.....(2)}$$

$$=\varepsilon_\alpha+\frac{(\varepsilon_s-\varepsilon_\infty)}{1+w^2\tau_D^2}-i\frac{w\tau_D(\varepsilon_s-\varepsilon_\infty)}{1+w^2\tau_D^2} \quad \text{...(3)}$$

Where τ_D=relaxation time which verifies that locus of the points $[\varepsilon`(w),\varepsilon``(w)]$ is a semicircle with radius $(\varepsilon_s-\varepsilon_\infty)/2$ and centre on the $\varepsilon`=(\varepsilon_s-\varepsilon_\infty)/2$,that is when $w\tau_D=1$.For Debye dielectric the relaxation time τ_D can be determined by measuring the angular frequency at which
$\varepsilon`$ is maximum. *A* circular arc is also obtained for the Cole-Cole formula :

$$\varepsilon(w)=\ =\varepsilon_\alpha+\frac{(\varepsilon_s-\varepsilon_\infty)}{1+w^2\tau_D^2} \quad \text{.....}0\le\alpha\le1\ \text{.....(4)}$$

But in this case the centre lies below the horizontal axis. This is confirms the existence of distribution of τ_0 in all films. we present in Figure(3) results of temperature dependence of the real and imaginary part of dielectric constants for selected frequencies(100Hz-100kHz).In our measurements, we observe that as dielectric properties for deposited CdTe and annealed at 373,423 and 473K are relatively sensitive to change with temperature, where the losses in dielectric constant increases with increase of temperatures. The values of polarizibility(β) had been determined by measuring the angles(β=2θ/2) were listed in table(2).

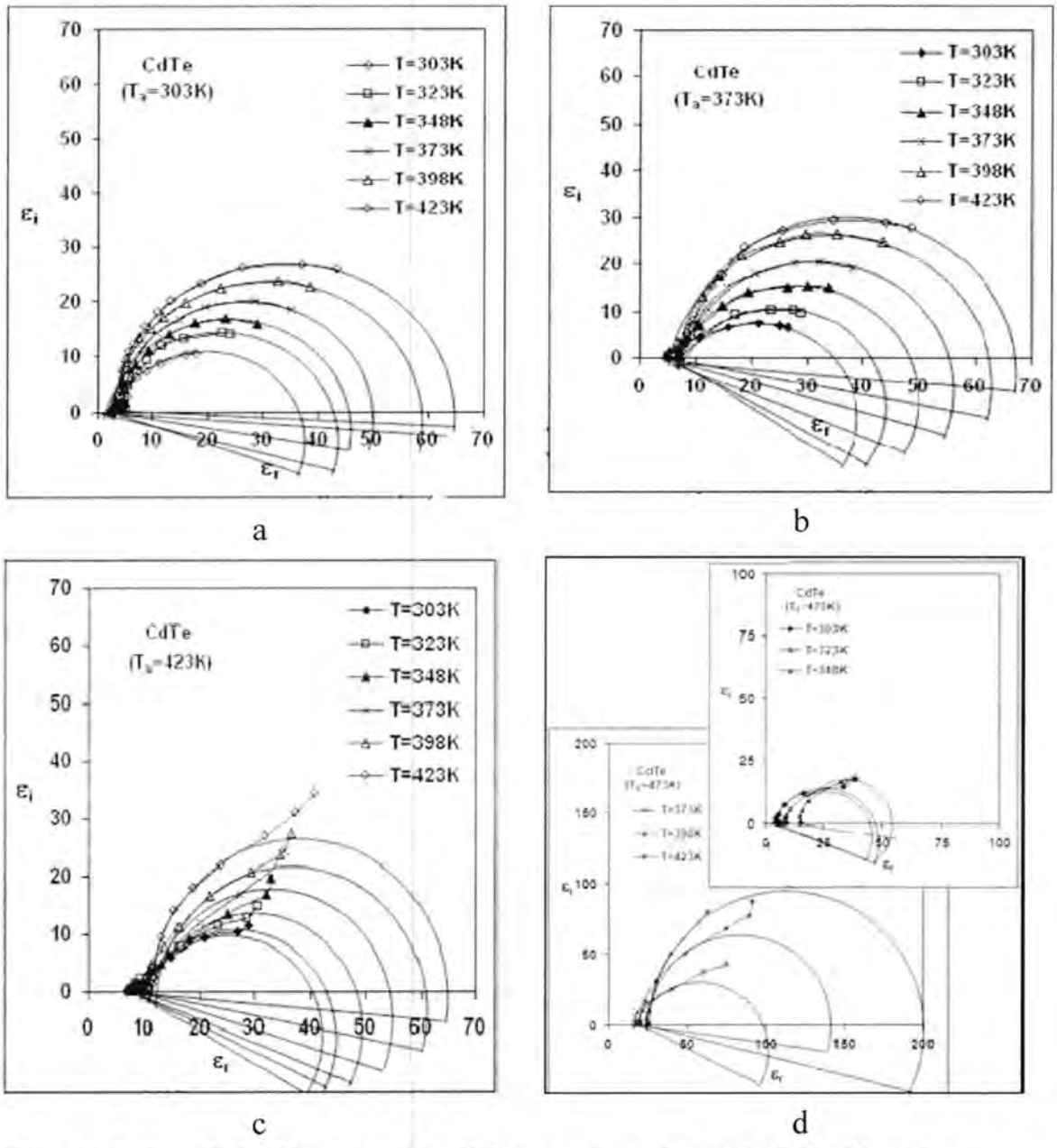

Fig.-4: Cole –Cole diagram for different samples of CdTe thin films

It is clear that τ_0 for as deposited CdTe films decreases with thermal treatments, and. The decreases with thermal measurements. The decrease of τ_0 attributed to rising of intermolecular force [18].

Table-2: Polarizibility and relaxation time at room temperature at different annealing temperature

	T_a=303K		T_a=373K		T_a=423K		T_a=473K	
T(K)	β	τ_o(ms)	β	τ_o (ms)	β	τ_o (ms)	β	τ_o(ms)
303	0.17	0.839	0.34	0.725	0.23	0.746	0.21	0.751
323	0.14	0.153	0.25	0.148	0.21	0.15	0.18	0.151

348	0.08	0.163	0.15	0.167	0.17	0.168	0.11	0.164
398	0.04	0.403	0.02	0.133	0.07	0.389	0.07	0.389
423	0.02	0.16	0.01	0.159	0.02	0.16	0.01	0.159

4- DENSITY OF STATES (DOS)

The investigation of steady state and transient is a valuable tool for the study of transport mechanism and defect states in Chalcogenide glass semiconductors. The common feature of these glasses is the presence localized states in the mobility gap as a result of the absence of long range order as well as various inherent defects.

The localized states in the mobility gap are the D^+ & D^- states, so these measurements in Chalcogenide may be helpful in understanding the recombination mechanism which in turn gives information regarding the localized states present in the mobility gap of these materials.

In our study, we obtained the optimum values for the optimum preparation conditions, as shown in table (3),we assumed a new model implying the variation of Density of states*(DOS)* with annealing temperatures. For *CdTe* films the optical energy gap is shown to be increasing from *1.45* to *2.15eV* when increasing annealing temperature to T_a=*473K*.This indicates the decreasing of defect states inside band gap ,we may deduce that the defect states decrease as T_a increase to *473K* as shown in Figure(4) we expect the density of defects decrease of reconstruct almost all the dangling bonds link to form molecular bonds on the surface, which may produce bonding states near the edge of the valence & conduction bonds.

The activation energy, which is measured from *D.C* conductivity, means that Fermi level shifted up word, or down word *C.B* or *V.B* respectively depending on the type of majority carriers. The Fermi level lay approximately at the midgap conduction in this region is expected to occur within about K_BT at the edge of E_c, therefore we can calculate the density of extended states $N(E_{ext})$ from the relation (5):[19]

$$\sigma_o(ext)=(e^2\hbar/6m)N(E_{ext}) \quad \ldots\ldots\ldots\ldots\ldots(5)$$

Where $\sigma_o(ext)$ pre-exponential factor and m is the electron mass .Table (3) shows the value of activation energy and density of extended states.

We can calculate the density of states in Fermi level according to the relation [20]:

$$\sigma_{ac}(w)=\frac{1}{3}[\pi e^2 k_B T][N(E_f)]^2\alpha^{-5}w[\ln(1/w\tau)]^4 \quad \ldots\ldots\ldots(6)$$

i.e. $\sigma(w)\ \alpha\ w^s$, where α is the decay of localized states wave function,(assuming that α=0.1 nm)which varies as w^s, s is weak function of frequency if w<<1/T.

Table (3) represents the value of Fermi level. For samples as prepared and those which annealed at 348K, 373K and 423K.

Table-3: activation energy (E_a), extended states, localized states, density of Fermi level $N(E_f)$, tails width and optical energy gap for *CdTe* films

T_a (K)	$N(E_{ext})$ (cm^{-3})	$N(E_{loc})$ (cm^{-3})	$N(E_f)$ (cm^{-3})	E_a (eV)	E_t (eV)	E_g (eV)
303	$8.92*10^{22}$	$6.1*10^{11}$	$2.83*10^{15}$	0.27	0.318	1.40
373	$1.26*10^{21}$	$1.37*10^{12}$	$2.11*10^{15}$	0.30	0.286	1.65
423	$5.35*10^{21}$	$4.59*10^{12}$	$2.31*10^{15}$	0.43	0.245	2.0
437	$7.24*10^{22}$	$6.72*10^{13}$	$1.89*10^{15}$	0.55	0.172	2.15

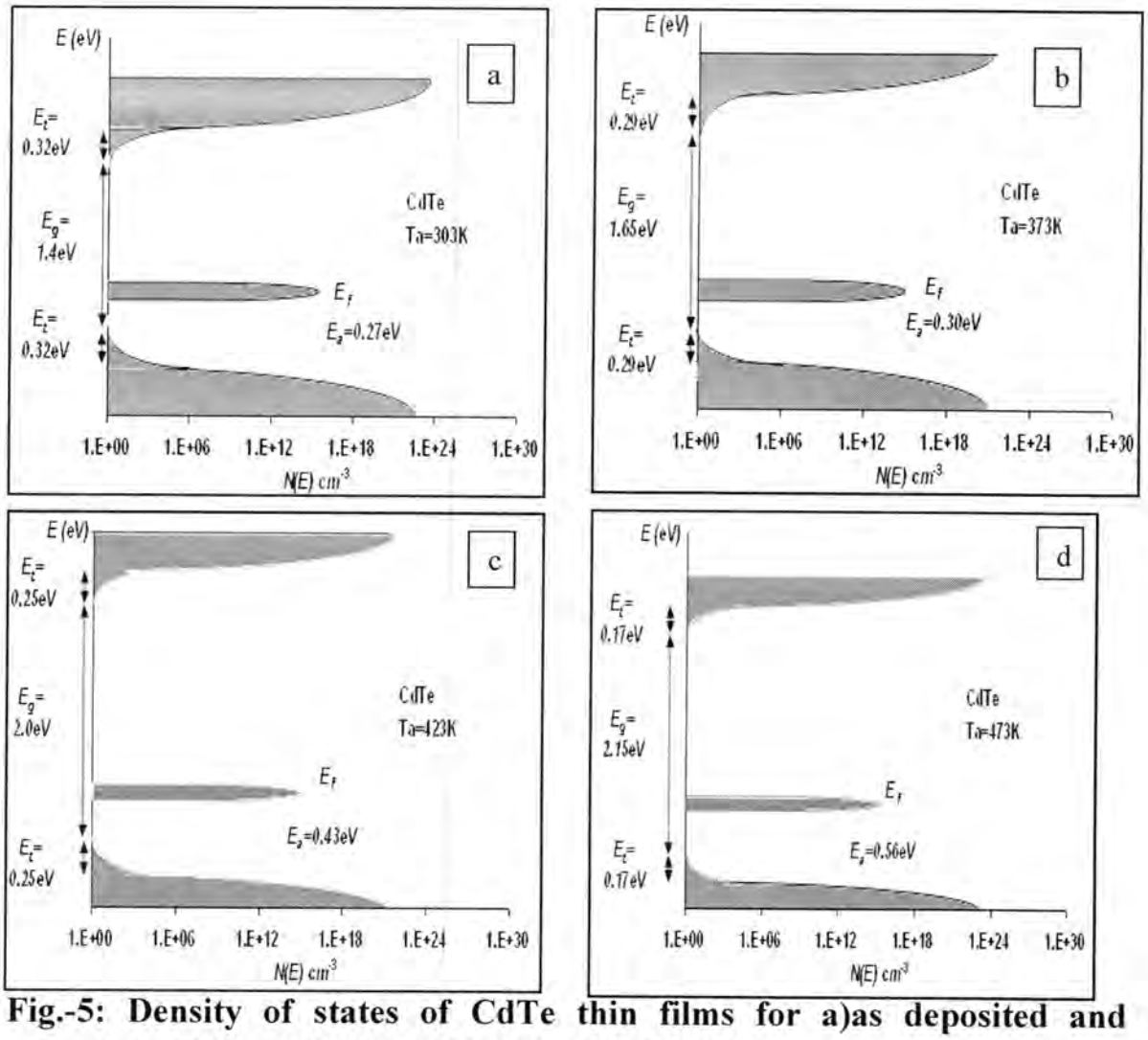

Fig.-5: Density of states of CdTe thin films for a)as deposited and annealed at b)T_a=373 c)T_a=423 d)T_a=473K.

CdTe thin films are prepared by thermal evaporation technique, the XRD-pattern appeared a polycrystalline structure of as-deposited and annealed at 373-473 K.From the variation sequence of the (s) values with temperature one can adopt the (CBH) model to explain our results of CdTe thin films. The Polarizibility and relaxation time decreases with increase of temperature. The optical energy gap increases with the increasing annealing temperatures, also the density of extended and Fermi states are decreases with increasing of annealing temperature.

From all above measurements, the density of states model was suggested which showed that Fermi level shifted to middle of energy gap with increase of annealing temperatures.

REFERENCE

1. N.choudhary,A.Kumar "Dielectric Relaxation in Glassy $Se_{100-x}Sb_x$" *Turk J.Phys*., 29:119-125.(2005).
2. K.N.Shreekanthan,Kusturi V.Bangera,G.K.Shivakumar and M.G.Molesh"Structure and properties of vacuum deposited cadmium telluride thin films",*Indian Journal of Pure &Applied Physics*,44: 705-708.(2006).
3. A.Z.Evmenova,V.A.Odarch,F.F.Sizov,M.V.Vuichyk"Absorptive CdTe films optical parameters and film thickness determination by the ellipsometric method",*J.Optica Applicata*, Vol.XXXVIII, 3 :586-600,(2008).
4. Rusu M.,Rusu G.G.,"On the optical properties of evaporated CdTe films",*J.Physics of low Dimensional structures*, No.3/4:105-15(2002).
5. Paulson P.D.,Xavier M.,"Spectroscopic ellipsometry investigation of optical and interface properties of CdTe films deposited on metal foils",*Solar energy materials and Solar cells*, 82(1-2): 279-90, (2004).
6. Kornienko K.N.,Odarych V.A., Popernko L.V.,Vuichik M.V.,"Detrmination of optical parameters of CdTe films by principle angle ellypsometry", *J.Functional materials*"13 (1): P.179-82(2006) ,.
7. M.M.Rahman,M.K.R.Khan,Y.Zaman,M.O.Hakim,M.G.Choudhury"T hermoelectric power of CdTe thin films prepared by vacuum evaporation method",*J.The nucleu,*39(3-4): 137-143(2002).
8. R.John,D.,S.pushpalatatha"Theoritical investigation on II-VI binary semiconductors",*Chalcogenide letters*, 7(4) :277-288(2010).

9. B.T.Kolomieto,"Vitreous Semiconductors(II)",*Phys.Status Solidi*, Vol.7,no.3:713-731 (1964).
10. S.H.Moustafa "Effect of Layer Sequence on Formation of CdTe thin film prepared by Stacked elemental layers"*Egypt.J.Solids*,31(1):1-10(2008).
11. B.Roling and K.Funke"Polaronic Transport in Vanadium phosphate Glasses",*J.Non-Cryst .Solids*"212:1-10(1997).
12. J.R.Macdonald,"Analysis of dispered,conductivity-system frequency-response data",*J.Non-Cryst. Solids*" 197: 83-110(1996).
13. S.R.Elliot,"Atheory of a.c. conduction in Chalcogenide glasses" ,*Phil.Mag.*, B46: 123 (1982).
14. Dr.Muslm Fadhel Al-Zubadi, Waseem Najeeb Ibrahim"Increasing the conductivity of cadmium Telluride films, *Eng. &Tech. Journal*, 27(14), (2009).
15. S.Deivanayayaki,P.Jayamurgan,R.Marippan"Optical and structural characterization of CdTe thin films by chemical bath deposition technique",*Chalcogenide letters*, 7(3), :159-163(2010).
16. Fathy Salman"AC conductivity and Dielectric study of Chalcogenide glasses of Se-Te-Ge system",*Turk J.Phs*.28:41-48 (2004).
17. B.K.P.Scaife"*Principle of Dielectrics*" Oxford Science Puplications.P.67(1998).
18. Raad M.S. Al-haddad,"A.C. conductivity of gold doped Germanium films",*J.Fondazione Giorgio Ronchi*, LIV(4) :571-578 (2009).
19. Issam M.Ibrahim,Izzat M.Al-Essa,Raad M.Al-Haddad"Density of States of Se-Te-Ge thin films",*Iraqi J.of Physics*" 5(7), 120-128 (2008).
20. A.Khelfa,N.Benramanet,J.P.Guesdon and C.Julien "Ac conductivity of amorphous Indium-Selenium films", J. Semicond. Sci. Technol. 9: 2263-2266,(1994).

Self-Absorption Effect on the Spectral Properties of 2-Methylnaphthalene in Different Solvent

Abdulla Ahmed Rasheed, Waleed Salah Abdul Whaab and Nasma Adnan Jabr
Physics Department, Sciences College, Al- Mustansiriyah University

Received : 05/04/2011 Accepted : 29/05/2011

الخلاصة

تم دراسة و قياس طيف الفلورة لمحلول (2-مثيل نفثالين) المذاب في المذيبات (الهكسان, الايثانول و البراقين) كدالة للتركيز المولاري و بطول موجي مهيج(λ_{ex}= 270nm). لقد تم حساب الكفاءة الكمية (q_{FM})، زمن الفلورة الإشعاعي (τ_{FM})، معدل العمليات لإشعاعية (K_{FM}) و اللا إشعاعية(K_{IM}) حيث وجد أن الكفاءة الكمية لمحلول (2-مثيل نفثالين) في الهكسان والايثانول عند التركيز [10^{-4}M] تكون مساوية إلى (q_{FM} =0.20) و (q_{FM} =0.15) على التوالي. إما عند حساب الكفاءة الكمية لمحلول (2-مثيل نفثالين) في البراقين فأنها تساوي (q_{FM} =0.24) أن هذا الاختلاف في قيم الكفاءة الكمية يكون بسبب اختلاف قطبية المذيب و لزوجة المحاليل. كما وجد أن زيادة التركيز المولاري يؤدي إلى نقصان شدة طيف الفلورة و بالتالي نقصان الكفاءة الكمية و ثابت العمليات الإشعاعية و ذلك بسبب ظاهرة الامتصاص-الذاتي. لقد تم حساب الكفاءة الكمية نسبة إلى مركب النفثالين بكفاءة مقدارها (q_{FM} =0.14) كمركب قياسي عند نفس الطول الموجي المهيج. أن جميع القياسات أجريت بدرجة حرارة الغرفة.

ABSTRACT

The fluorescence spectra for 2-Methylnaphthalene solution which dissolved in hexane, ethanol and paraffin as a function of concentration at excitation wavelength (λ_{ex}= 270nm) was measured and investigated the quantum efficiency (q_{FM}), the radiative fluorescence lifetime (τ_{FM}), rate parameter of radiative (K_{FM}) and non-radiative (K_{IM}) processes were calculated. Where the quantum efficiency is equal to (q_{FM} =0.20) and (q_{FM} =0.15) for 2-methylnaphthalene solution dissolved in hexane and ethanol at concentration [10^{-4}M], respectively. But the quantum efficiency of 2-methylnaphthalene in paraffin is equal to (q_{FM} =0.24) at same concentration. This different in the values of quantum efficiency refers to different in polar solvent and viscosity of solutions. It's found that the increase in molar concentration led to decrease the intensity of

spectrum, quantum efficiency and rate parameter of radiative process (K_{FM}) because of the effect of self-absorption phenomena. In additional, the quantum efficiency measurement was calculated relative to standard compound of naphthalene with quantum efficiency (q_{FM} =0.14) at same excitation wavelength. All measurement were carried at room-temperature.

Theory

Luminescence is the emission of light from any substance and occurs from electronically excited states. Luminescence formally divided into two categories: fluorescence and phosphorescence depending on the nature of the excited state (1). Fluorescence is a radiative process when molecules transition between states of the same multiplicity ($S_1 \rightarrow S_0$). But when molecules transition between states of different multiplicity is described as phosphorescence ($T_1 \rightarrow S_0$). Symbols (S- Singlet, T- Triplet) refers to singlet and triplet electronic states respectively. While non-radiative processes occur when molecules transition between isoenergetic vibrational levels of different electronic states. Such transitions are normally preceded by radiationless thermal activation of the initial electronic state and followed by radiationless de-activation of the final electronic state. A radiationless transition between states of the same multiplicity is described as internal conversion (2). One between states of different multiplicity is described as intersystem crossing as shown in figure [1].

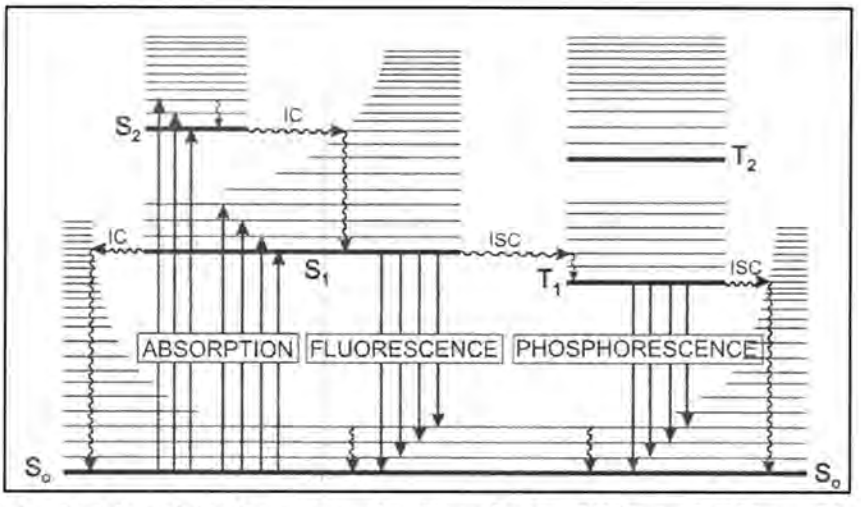

Fig.-1: Jablonski diagram the Symbols (ISC and IC) refers to intersystem crossing and internal conversation(3).

That each processes a rate constant determines probability occurrence that process. The molecular fluorescence quantum efficiency (q_{FM}) which is defined the ratio of the number of fluorescence photons emitted by a system of molecules in dilute solution to the number of molecules excited into S_1 (the number of absorbed photons) is equal to:

$$q_{FM} = \frac{K_{FM}}{K_{FM} + K_{IM}} = \frac{\tau_M}{\tau_{FM}} \quad \ldots\ldots\ldots\ldots (1)$$

Where K_{FM} and K_{IM} the rate constant of radiative emission (fluorescence) and radiationless processes by internal quenching.

τ_M: the molecular fluorescence lifetime of the excited state which is defined the average time that molecule spends in the excited state prior to return to the ground state and is equal to:

$$\tau_M = \frac{1}{K_{FM} + K_{IM}} \quad \ldots\ldots\ldots\ldots (2)$$

The lifetime of the fluorescence in the absence of non-radiative processes is called the intrinsic or natural lifetime, which is defined as the reciprocal of the radiative transition probability K_{FM} (in Sec^{-1}), is given by (3):

$$\tau_{FM} = \frac{1}{K_{FM}} \quad \ldots\ldots\ldots\ldots (3)$$

The intensity of fluorescence can be described by a wide verily of processes such decreases in intensity are called quenching. Quenching can occur by different mechanisms. Collision quenching occurs when the excited state of fluorophore is deactivated upon contact with some other molecule in solutions, other type of quenching is radiative migration (4). There is commonly an overlap of the 0-0 bands of the fluorescence and absorption spectra, the spectral overlap may be considerable and lead to self-absorption of the fluorescence emission. If (a) is the probability of self-absorption of an emitted photon, so that (1– a) is the photon escape probability. Photons which are absorbed are re-emitted with quantum efficiency (q_{FM}) and lifetime (τ_M). The phenomena of self- absorption is reduced through the use of solutions with a low concentration or by the correction to the value of quantum yield (Φ_{FM}) and molecular lifetime (τ) were equal to the following:

$$\Phi_{FM} = \frac{q_{FM\,(1-a)}}{1 - a\, q_{FM}} \quad \ldots\ldots\ldots\ldots (4)$$

$$\tau = \frac{1}{(1-a)K_{FM}+K_{IM}} = \frac{\tau_M}{1-aq_{FM}} \quad \text{..... (5)}$$

Practically, the probability of self-absorption (a) is calculated from the following equation:

$$a = 1 - \frac{A_m^T}{A_m} \quad \text{..... (6)}$$

Where A_m^T and A_m represent the area under the fluorescence spectrum of the concentrated and diluted solution, respectively. Normalized in the low-energy region.

Because of the many problems associated with absolute quantum yield measurements, several simple relative methods have been devised which substitute a compound of "known" quantum yield in place of standard scatter as a reference. Relative measurement full conveniently into two classes: optically dense and optically dilute methods (5).

The determination of quantum yields using optically dilute solutions is the most common method currently employed. The optically dilute measurement rests on Beer's law:

$$I_a = I_0 B = I_0 (1 - 10^{-Ad}) \quad \text{..... (7)}$$

Where

B: is the fraction of light absorbed by the sample.

I_0: is the intensity of the incident light (quanta/sec).

I_a: is the intensity of the absorbed light (quanta/sec).

A: is the absorbance/cm.

d: is the path length (cm).

If the luminescence intensity for each compound is proportional to I_0B, then the expression for the quantum yield becomes (6):

$$\Phi_{FM} = \Phi_{FR} \left(\frac{B_r}{B_x}\right) \left(\frac{I(\lambda r)}{I(\lambda x)}\right) \left(\frac{n_x^2}{n_r^2}\right) \left(\frac{D_x}{D_r}\right) \quad \text{..... (8)}$$

Where

$I(\lambda)$: is the relative intensity of the exciting light at wavelength λ.

n: is the average refractive index of the solution to the luminescence.

D: is the integrated area under the corrected emission spectrum. Subscripts x and r refer to the unknown and reference solution.

A more commonly used relation is obtained by expanding the exponential of eq. (7) in a power series of (*Ad*) and truncating the result:

$$\mathbf{B = (1- 10^{-Ad}) = 1- [\ 1- 2.303Ad + (2.303Ad)^2 /2 + ...]} \quad \ldots\ldots\ldots (9)$$

At low concentration or in optically dilute solution

$$\mathbf{B = 2.303\ A\ d} \quad \ldots\ldots\ldots (10)$$

Substitution of the approximate expression for B in eq. (8) yield the working equation commonly employed by investigators using calibrated spectrometers

$$\boldsymbol{\Phi_{FM} = \Phi_{FR}} \left(\frac{A_r}{A_x}\right) \left(\frac{I(\lambda r)}{I(\lambda x)}\right) \left(\frac{n_x^2}{n_r^2}\right) \left(\frac{D_x}{D_r}\right) \quad \ldots\ldots\ldots (11)$$

Many assumptions are inherent in eq. (8) and (11). For both unknown and reference it is assumed that:

1- The integrated luminescence intensity is proportional to the fraction of light absorbed.
2- All geometrical factors are identical.
3- The excitation beams are monochromatic.
4- Reflection losses are the same internal reflection effects are equal.
5- Re-absorption and reemission are negligible.
6- All light emanating from the cuvette is isotropic.

If any one of these conditions does not hold, serious error can be introduced into the final value. The approximate *eq*. (9) introduces ≈ 5% systematic error for Ad = 0.043 if the detector views either symmetrically around the centre or the entire cuvette. If this error is unacceptable, the exact form of the equation or lower optical densities must be used (7).

Alternatively, both the standard and the unknown solution can be made up to have equal absorbencies at their respective exciting wavelengths and the need for any correction factor is eliminated. Even if the two experimental optical densities are not exactly the same, *eq*. (11) may be used for relatively high optical densities if the two absorbencies are comparable. Equations (8) and (11) do not correct for re-absorption and re-emission. Fortunately, the real beauty of the optically dilute method is that these corrections are rarely necessary unless the material happens to

be excited in an absorption minimum and there is substantial overlap between the absorption & the emission.

Many of researchers used this method such as *J.B. Birks and J.B. Aladekoman* (8), to determination of quantum efficiency for aromatic compound like *naphthalene* and its derivatives such as (2-*methylnaphthalene),(2,6-dimethylnaphthalene) and (2-ethylnaphthalene)*. In 1972, *A.W. Jackson* (9), calculate quantum yield and lifetime of (*2,3-pentanedione*) at various temperature. In 1984 (10) study the fluorescence quantum yield and free rotor effect and found the fluorescence quantum yield (Φ_{FM}) for *dyestuff(1)* approaches unity in *ethanol-ether (1:1)* glass at 98k°.

Fluorescence and phosphorescence properties of naphthalene in aqueous *D-Glucose* solutions containing (*6-Deoxy-6-iodo-β-cyclodextrin*) at room temperature has been observed by Sanyo Hamai in 1997(11), the fluorescence quantum yield of naphthalene in aqueous solution was evaluated to be (q_{FM}= *0.086*). *T.S. Ahn*(12) *and et al.* in 2007, study self-absorption correction for solid-state photoluminescence quantum yield obtained from integrating sphere measurements. In 2008 (13) study the measurement of the fluorescence quantum yield using a spectrometer with an integrating sphere detector. *Ryszard Misiak* (14) *and et al.*, in 2011 study self-absorption correction and efficiency calibration for radioactivity measurement of environmental samples by *gamma-ray* spectrometry.

MATERIALS AND METHODS

The solution of 2-Methylnaphthalene in hexane, ethanol, paraffin prepared at room temperature with concentration [10^{-4}, 10^{-3}, 10^{-2}, 5×10^{-2} M]. *2-Methylnaphthalene* purchased from *Uma* Company imported from *India.* Fluorescence spectra were recorded on a (*JASCO- model-FP-770*) spectrofluorometer; samples were mounted in cubic cell of quartz dimensions ($1\times1\times5$) cm^3 at right angle 90° with incident beam. This optical geometry was chosen to eliminate the effect of scattered incident radiation and reduce the phenomenon of self-absorption. The fluorometry has dedicated computer which control instrumental operating (excitation and emission wavelength, monochromator slit width, detector parameter).

In this research we use exciting wavelength (λ_{ex}= *270nm)* in the measurements. When measured the concentration [10^{-4}, 10^{-3} M] we used slit width of excitation (S_{ex}=*1.5 nm*) and same value to slit width of emission (S_{em}= *1.5 nm*), but in concentration [10^{-2}, 5×10^{-2} M] the slit width of excitation (S_{ex}=*3 nm*) and slit width of emission (S_{em}= *5 nm*), the measurements were made in the same sensitivity of photomultiplier where the oxygen was expelled by evacuation prior to sealing the specimen cell. Naphthalene use as a standard compound dissolved in hexane, ethanol and paraffin with concentration [10^{-4}M] and quantum efficiency equal to (q_{FM} =0.14), at room temperature.

RESULTS AND DISCUSSION

In this research, we study fluorescence spectra of naphthalene solution dissolved in hexane, ethanol and paraffin with concentration [10^{-4} M] and then study the solutions of (2MN) is one of the naphthalene derivatives, is naphthalene molecule with added *methyl* group (CH_3) as shown in figure [2], with concentration [10^{-4}, 10^{-3}, 10^{-2} & 5×10^{-2} M] and observation the effect of increasing concentration in the form of the fluorescence spectrum as well as calculation of quantum efficiency.

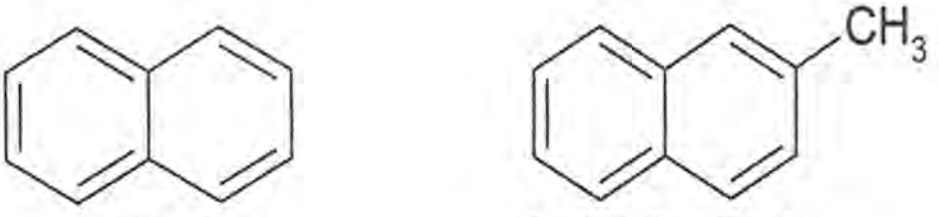

Naphthalene $C_{10}H_8$ *2-Methylnaphthalene* $C_{11}H_{10}$

Fig.-2: Chemical formula of compounds

Figure [3-a] shows the fluorescence spectrum of naphthalene dissolved in hexane at concentration [10^{-4} M] at exciting wavelength (λ_{ex}=270 nm), where it appears in the shape of spectrum is structure consists of two peaks located at wave numbers (29.673 x 10^3cm^{-1})(28.409 x 10^3cm^{-1}) which are found the same values of fluorescence spectrum of naphthalene solutions in ethanol and paraffin as in figure [3- b, c]:

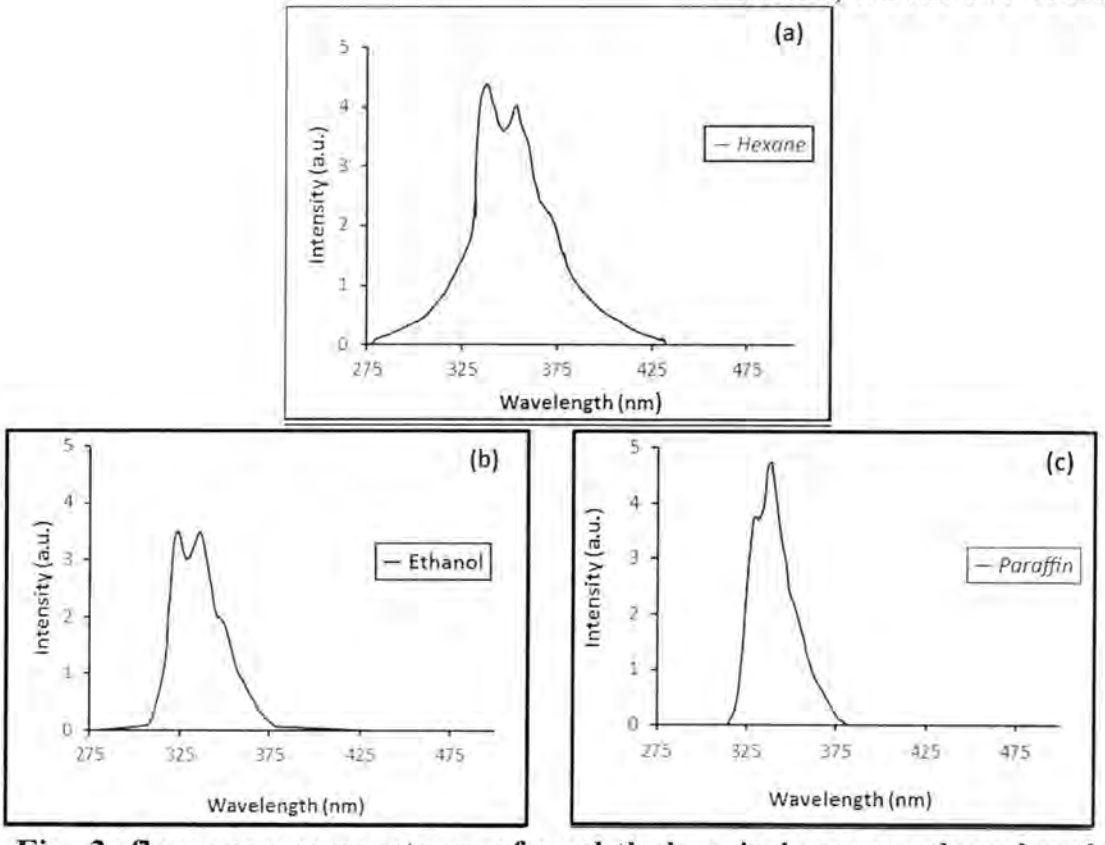

Fig.-3: fluorescence spectrum of naphthalene in hexane, ethanol and paraffin at concentration [10^{-4}] M, λ_{ex}= 270nm.

The fluorescence spectrum of *2-Methylnaphthalene* solutions has been measured at different concentrations are [10^{-4}, 10^{-3}, 10^{-2}, 5×10^{-2} M] in the solvents mentioned previously, at exciting wavelength (λ_{ex}= *270 nm*). We have found that the fluorescence spectrum of *2-Methylnaphthalene* in hexane at concentration [10^{-4}M] be structure into three peaks located at wave numbers (31.4×10^{3} cm^{-1}), (30.66×10^{3} cm^{-1}) and (29.93×10^{3} cm^{-1}) as in figure [4]. We found the value of quantum efficiency is equal to (q_{FM} = *0.20*), notes the increase in the value of quantum efficiency comparison with the quantum efficiency of naphthalene, the reason is due to the influence of *methyl* group substitutes to increase the rate of radiative processes.

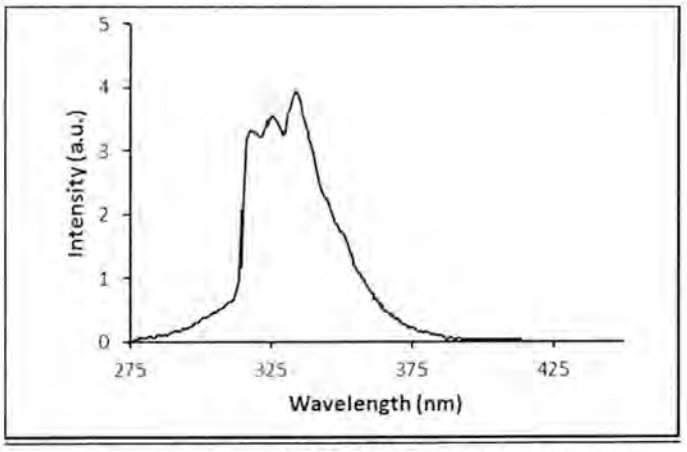

Fig. -4: fluorescence spectra of 2MN in hexan at concentration =10^{-4} M, λex= 270 nm

At concentration [10^{-3} M] noted decrease in the relative fluorescence intensity and disappear the first peak, where the spectrum shows two peaks located at wave number (30 ×10^3 cm^{-1}) and (29.26×10^3 cm^{-1}), figure-5.

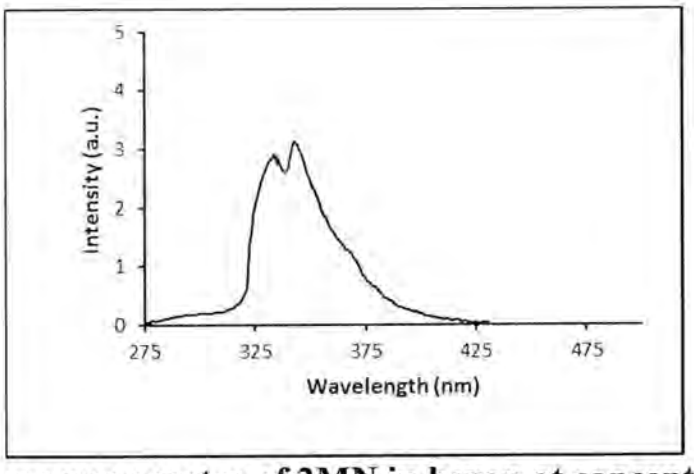

Fig.-5: fluorescence spectra of 2MN in hexan at concentration =10^{-3} M, λex= 270 nm

But when the concentration equal to [10^{-2}, 5×10^{-2} M] the second peak disappear because of self-absorption was increase and the fluorescence spectra is structureless as shown in figure [6]:

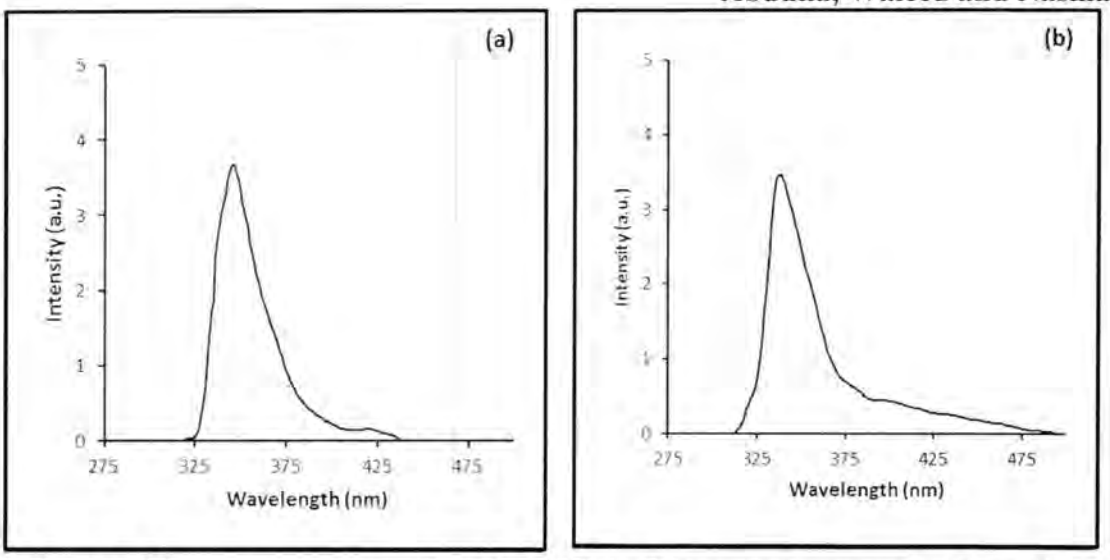

Fig.-6: fluorescence spectra of 2MN in Hexan at concentration (a) [10^{-2}] M, (b) [5×10^{-2}] M, λex=270 nm

In addition, for the fluorescence spectrum of *2-Methylnaphthalene* in ethanol and paraffin at same concentrations shown in figure (7), (8). The quantum efficiency of 2-Methylnaphthalene in ethanol is equal to (q_{FM}= *0.16)*, this difference in the value of a quantum efficiency due to the different type of solvent. The decrease in the intensity of the peaks with increased of concentration is caused by the phenomenon of *self-absorption* where *re-absorption* of emitted photons before leaving the solution by the molecules in the ground state leading to decrease of quantum efficiency by (2%) or (3%), respectively, for the value at the concentration [10^{-4} M] and using the necessary correction, according to the relation (4), (6) was reached approached value.

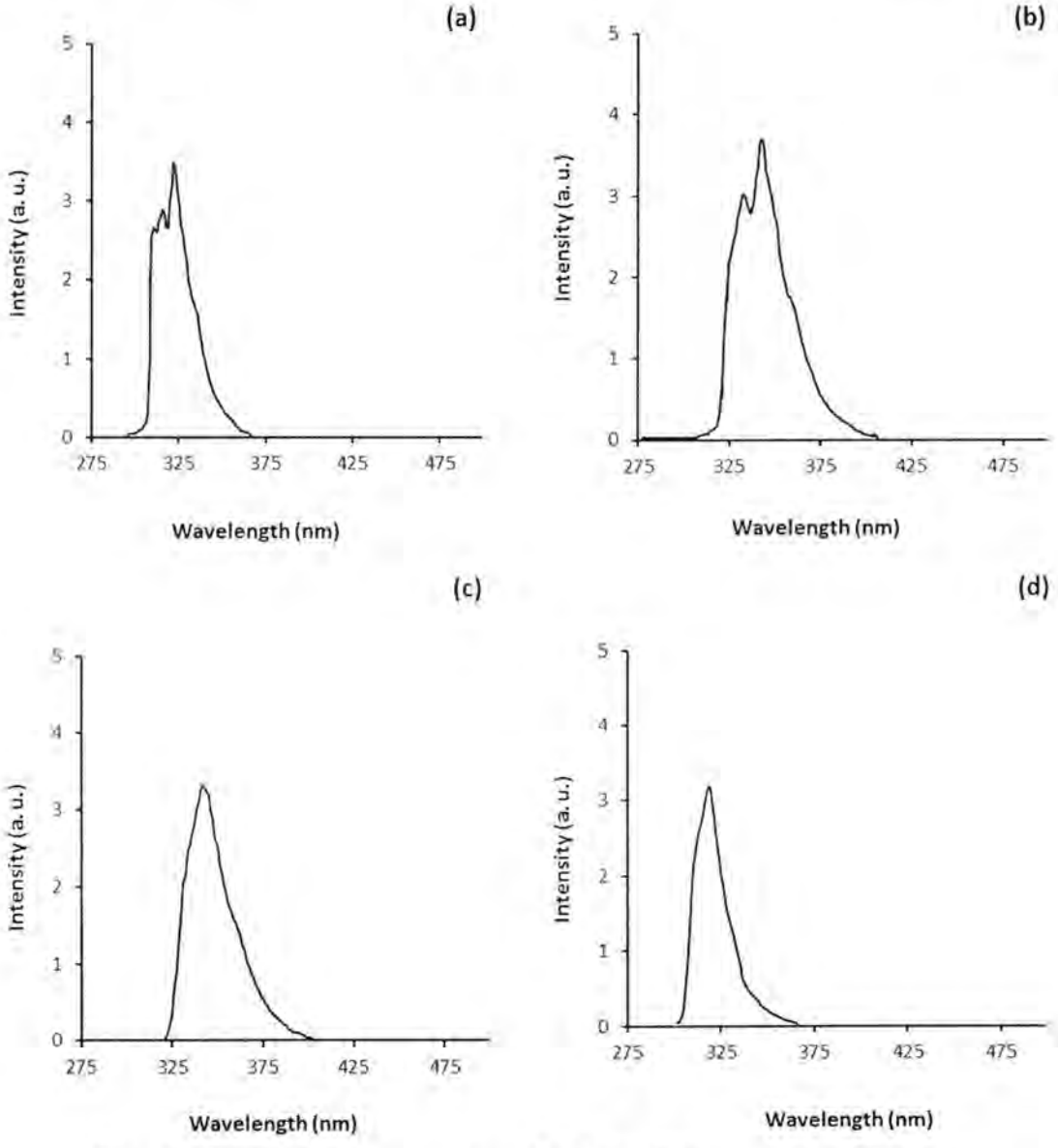

Fig.-7: fluorescence spectra 2MN in Ethanol, λ_{ex}=270 nm, (a) [10^{-4} M], (b) [10^{-3}M], (c) [10^{-2} M] (d) [5× 10^{-2} M]

That decrease in the value of quantum yield will be accompanied by an increase in the fluorescence lifetime (τ_{FM}) and thus a decrease in the rate parameter of radiation processes and increase the rate parameter of radiationless processes.

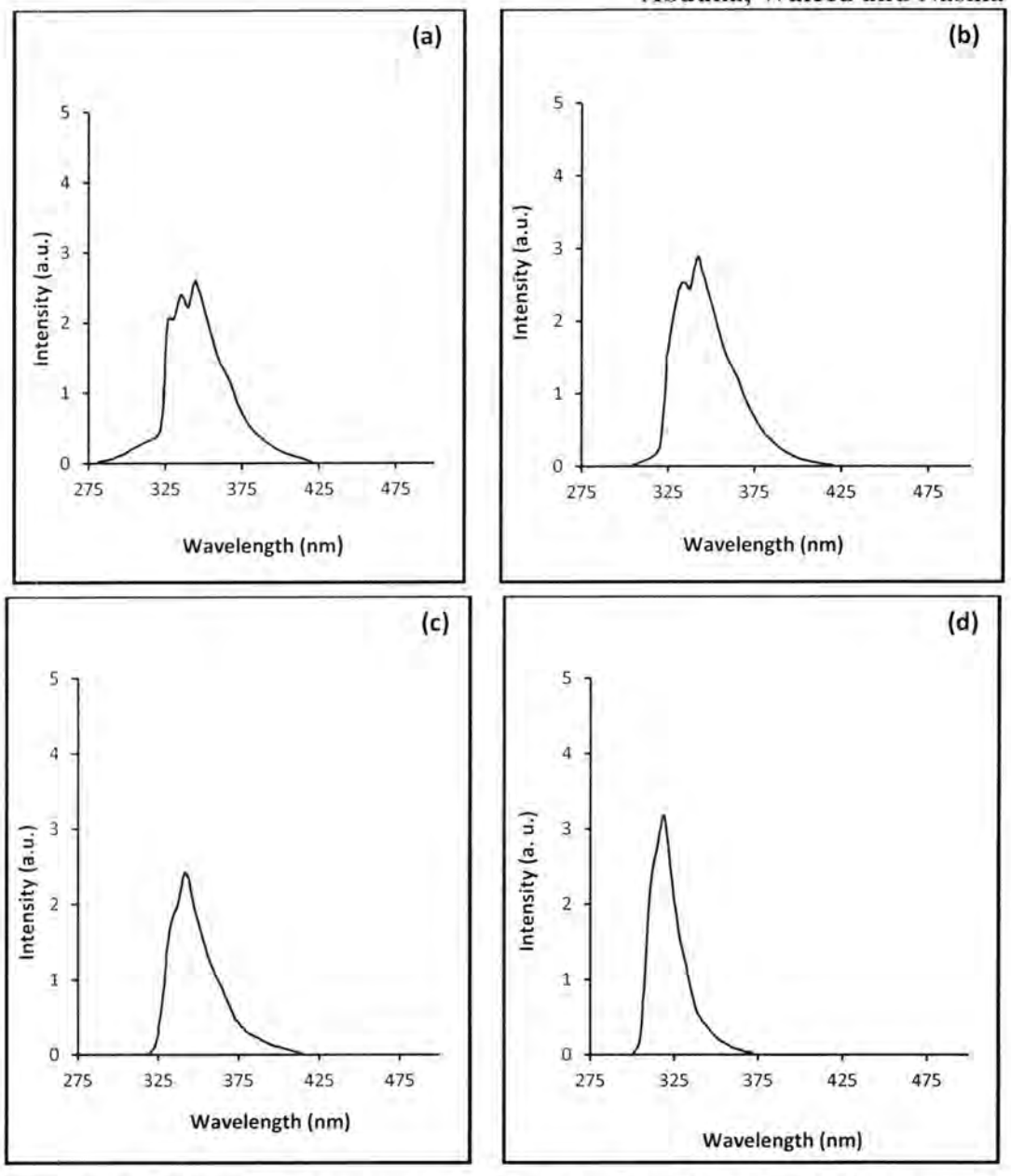

Fig.-8: fluorescence spectra 2MN in Paraffin, λ_{ex}=270 nm, (a) [10^{-4} M], (b) [10^{-3} M], (c) [10^{-2} M] (d) [5×10^{-2} M]

Where increasing rate of non-radiative transition (internal conversion). The tables [1], [2] and [3] describe the values of quantum efficiency, rate parameter of radiative and non-radiative processes depending on previous relationships.

Table -1: the quantum efficiency, rate of radiative and non-radiative processes of 2MN solutions in Hexane.

$[M]$ mol	Φ_{FM}	τ_M nsec	τ_{FM} nsec	$K_{FM} \times 10^6$ sec^{-1}	$K_{IM} \times 10^6$ sec^{-1}	$(K_{FM})_0 \times 10^6$ sec^{-1}
10^{-4}	0.20	59	295	3.4	13.2	1.7
10^{-3}	0.17	60	352	2.8	13.7	1.5
10^{-2}	0.14	60.8	434	2.3	14	1.2
5×10^{-2}	0.12	61	469	2.1	14.13	1.11

Table -2: the quantum efficiency, rate of radiative and non-radiative processes of 2MN solutions in Ethanol.

$[M]$ mol	Φ_{FM}	τ_M nsec	τ_{FM} nsec	$K_{FM} \times 10^6$ sec^{-1}	$K_{IM} \times 10^6$ sec^{-1}	$(K_{FM})_0 \times 10^6$ sec^{-1}
10^{-4}	0.15	47	313	3.15	18.1	1.7
10^{-3}	0.13	47.5	365	2.7	18.5	0.97
10^{-2}	0.12	47.8	398	2.5	19.1	0.9
5×10^{-2}	0.11	48	436	2.3	19.5	0.8

Table-3: the quantum yields of 2-MN solutions in Paraffin

$[M]$ mol	Φ_{FM}
10^{-4}	0.24
10^{-3}	0.19
10^{-2}	0.17
5×10^{-2}	0.14

Reduced intensity of fluorescence spectrum and the quantum efficiency with increased an molar concentration for 2-Methylnaphthalene because of the phenomenon of self-absorption of emitted photons before leaving the solution by the molecules as a result that increase in radiationless processes and decrease radiation processes. So effect methyl group (CH_3) substation in naphthalene molecule, an increase the rate of radiative transition and quantum efficiency compared with naphthalene compound.

REFERENCES

1. J.B. Birks, "Photophysics Aromatic molecules", Wiley and Sons, London, (1970).
2. I.B. Berlman, "Handbook of fluorescence spectrum of Aromatic molecules", Academic press, New York, 1st edition (1965), 2nd edition (1971).
3. B. Valeur, "Molecular fluorescence: principles and applications", Wiley-VcH Verlag GmbH, (2001).
4. J.R. Lakowics, "Principles of fluorescence spectroscopy", Springer science and Business media LLC, 3rd edition (2002).
5. T.S. Peter, "fluorescence spectrophotometry", Macmillan publishers Ltd, Nature, Nature publishing group, (2002).
6. C.A. Parker, " photoluminescence of solution", Elsever publishing company, New York, (1968).
7. M.D. Lumbin, "Luminescence spectroscopy", Academic Press, London, (1978).
8. J.B. Aladekomo and J.B. Birks, "Spectral Studies of Naphthalene and Its Derivatives", Pros. R. Soc., Lond. A, 284, 551-565, (1965).
9. A.W. Jackson and A.J. Yarwood, "Fluorescence and Phosphorescence of 2,3-Pentanedione", J. Chem., 50, 1331, (1972).
10. M.S. Abdel-Mottaleb, "Fluorescence Quantum Yield and Free Rotor Effect", Laser chem., 4, 305-310, (1984).
11. S. Hamai, "Fluorescence and Phosphorescence Properties of Naphthalene in Aqueous D-Glucose Solutions Containing 6-Deoxy-6-iodo-β-cyclodextrin at Room Temperature", chem. Soc. Jpn., 71, 1549-1554, (1998).
12. T.S. Ahn, "self-absorption correction for solid-state photoluminescence quantum yields obtained from integrating sphere measurements" Rev. Sci. Instrum., 78, 086105, (2007).
13. A.K. Gaigalas and L. Wang, "Measurement of the Fluorescence Quantum Yield Using a Spectrometer With an Integrating Sphere Detector", J. Res. Natl. Inst. Stand. Technol. 113, 17-28, (2008).
14. R. Misiak, "self-absorption correction and efficiency calibration for radioactivity measurement of environmental samples by gamma-ray spectrometry", Nukleonika, 56(1), 23-28, (2011).

Effect Optimized Thickness on the Performance of Multilayer Antireflection Coatings for VIS and IR (3-5) μm Bands

Adnan H. Mohammed
Department of Physics, College of Education, Al-Mustansiryah University

Received : 07/04/2011 Accepted : 29/05/2011

الخلاصة

تم التركيزفي البحث على تصميم طلاء مضاد للانعكاس للسقوط العمودي في المنطقة المرئية والمنطقة تحت الحمراء ضمن المدى (**3-5**) مايكرون لتقليل الانعكاسية لسطوح الزجاج والجرمانيوم والسليكون وسلينايد الزنك , المهمة الاولى للبحث كانت بناء برنامج لتصميم ومحاكاة الاداء لطلاء متعدد الطبقات اما المهمة الثانية فكانت التحقيق لنتائج البرنامج المنشئ مع عدد من البحوث المنشورة , وبعد ذلك تم تحسين اداء الطلاء ذو الثلاث طبقات ليكون قريبا من اداء الطلاء ذو الاربع طبقات عن طريق تغيير السمك ,بينت نتائج التحليل بان العملية المفروضة (تغيير السمك) كانت فعالة في المناطق المدروسة.

ABSTRACT

The work devoted to the design multilayer antireflection coatings for normal incidence in **VIS** and IR (3-5) μm bands to reduce reflectance from glass, germanium(Ge),silicon(Si) and zinc selenide (ZnSe) .the first task was development a software programme to design and simulate the performance of multilayer coatings and secondly, the programme verification to match published researches. After these tasks the designed layers are optimized for their performance by varying their thickness to get performance for three layers is very close to four layers .the analysis has shown that the proposed process was effective in some studied regions.

INTRODUCTION

The antireflection (AR) coating is the most used optical coating in all the optical systems, in order to reduce the losses Thus, to achieve a high quality (AR) coating is a need in the optical systems in some applications

antireflection coatings are required for the reduction of surface reflections. In other not only reflection is reduced but also transmittance is increased considerably (that means that absorption coefficient k ≈0) [**1, 2**].

The theory of antireflection coating is examined by many authors [**3, 4**] for determining the optimum thickness and materials to be used as ARCs on polished or textured silicon. The matrix formula [**1**, **5**] is usually employed for calculation of reflection coefficient. In this paper, we present the result of calculations obtained by our computer programme of three and four-layers ARCs on different substrate.

THEORY

These basic equations for designing and simulating the performance of multilayer coatings

are based on boundary conditions for Maxwell's equations at m^{th} interface and are given as these equations as .

$$E_{m-1}^{-t} = 1/2\left(1+\frac{n_m}{n_{m-1}}\right)E_m^{-t}e^{j\varphi_m} + 1/2\left(1-\frac{n_m}{n_{m-1}}\right)E_m^{-t}e^{-i\varphi_m} \qquad (1)$$

$$E_{m-1}^{-r} = 1/2\left(1+\frac{n_m}{n_{m-1}}\right)E_m^{-t}e^{i\varphi_m} + 1/2\left(1-\frac{n_m}{n_{m-1}}\right)E_m^{-t}e^{i\varphi_m} \qquad (2)$$

Equations (1& 2) may be formed as Matrix formula, is used to evaluate the reflectance a multilayer system on glass.Si, Ge and ZnSe substrates. Matrix formula of N layers interlocked between two semi-infinite mediums is given in Ref. [5]

$$\begin{vmatrix} E_{m-1}^{-t} \\ E_{m-1}^{-r} \end{vmatrix} = 1/2 \begin{vmatrix} \left(1+\frac{n_m}{n_{m-1}}\right)e^{i\varphi_m} & \left(1-\frac{n_m}{n_{m-1}}\right)e^{-i\varphi_m} \\ \left(1-\frac{n_m}{n_{m-1}}\right)e^{i\varphi_m} & \left(1+\frac{n_m}{n_{m-1}}\right)e^{i\varphi_m} \end{vmatrix} \begin{vmatrix} E_m^{+t} \\ E_m^{+r} \end{vmatrix}$$

Where i^2 =-1, n_m is the real refractive index of m^{th} layer, ϕ_m is the phase thickness of m^{th} layer, $\varphi = 2\pi n_m d_m / \lambda$ with d_m as physical film thickness and λ (400-700nm, 3-5μm) inthis work.

The system shown in Fig.1 is characterized by matrix formula which relates the amplitudes of electromagnetic field components at (m-1) interface with the incident electromagnetic field components at m interface thus, the consideration requires that the last layer (substrate) completely defined , at the last layer then electromagnetic wave travels in infinite thickness medium (that is means φ_m equal to zero and there is no reflected wave therefore ($E_m^{+r}=0$, $E_m^{+l}=1$) .

$$\begin{vmatrix} E_{m-1}^{-l} \\ E_{m-1}^{-r} \end{vmatrix} = \frac{1}{2} \begin{vmatrix} \left(1+\frac{n_m}{n_{m-1}}\right)e^{i\varphi_m} & \left(1-\frac{n_m}{n_{m-1}}\right)e^{-i\varphi_m} \\ \left(1-\frac{n_m}{n_{m-1}}\right)e^{i\varphi_m} & \left(1+\frac{n_m}{n_{m-1}}\right)e^{i\varphi_m} \end{vmatrix} \begin{vmatrix} 1 \\ 0 \end{vmatrix}$$

the reflectance of each layer is gradually included to reach to the incidence medium (almost air), the reflectance and transmittance are given as

$$R = \left(\frac{E_0^{-r}}{E_0^{-l}}\right)^2 \qquad (3)$$

$$T = \frac{n_{m-1}}{n_0}\left(\frac{E_m^{-l}}{E_0^{-r}}\right)^2 \qquad (4)$$

The reflectance, transmittance and absorptance are then related by R + T + A = 1. The solution of this matrix formula is a laborious job for multilayer coatings. Based on the matrix formula, we have developed a software program to design and simulate the performance of multilayer coatings .

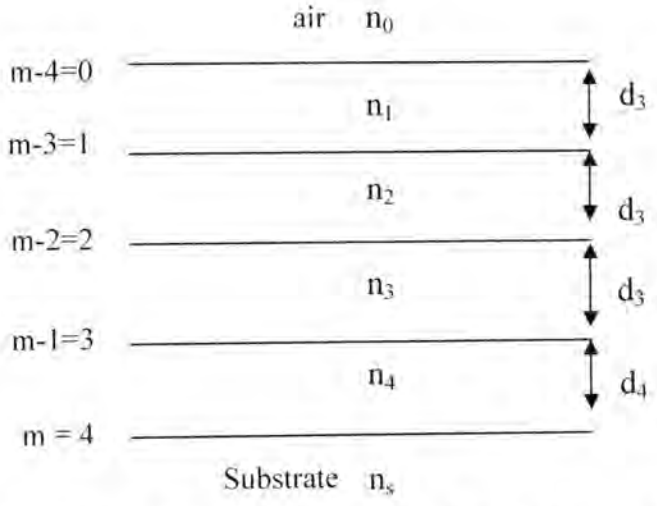

Fig.-1:A multilayer stack scheme of 4-layers on a semi-infinite substrate n_s

The +, - sign of E_{m-1}^{-r}, E_{m-1}^{-r}, E_m^{+l} and E_m^{+r} represent what take place upper and lower m^{th} interface (up and down interface are denoted by symbol (-) and (+)respectively.

MODELING AND ANALYSIS

Thin film materials are required to have certain characteristics to become a potential candidate for multilayer structures. This includes high transparency, homogeneity, high packing density, good adhesion, low stress, hardness and ability to survive in different environmental and deposition conditions [1]. These materials are then used to reduce reflection from the surfaces, which are basically caused by the sharp variation of the refractive index at the incident medium-substrate interface. Multilayer coating structures based on those materials have wide band of applications in electronics, optoelectronics, optics and optoelectronics equipments.

(A) Visible Region: The reflectance profile of three and four -layer coatings comprising of one layer and two layers are almost more effective **[1, 8]**. We have modeled such coatings on glass substrate at a design wavelength of 550 nm. The performance of the three layer
Air/MgF2/CeO2/SiO/Glass coating is further improved by the addition of forth layer. The reflectance is further reduced by four-layer design comprising

Air/MgF2/ZnS/CeO2/SiO/Glass), but the important feature of this design is the zero reflectance at two spectral points and the maximum and average reflectance has appreciably reduced to 0.039% and 0.4 %, respectively. The combined reflectance plot of the four layers configurations is shown in Fig. 1. This application of multiple encourages the use of multi-layers to achieve wide transmission bands By increasing number of layers .The optimization of thickness of the three layers coatings shown in the figure 1 reduces reflectance in some regions (525-625) nm to reach at 575 nm to 0.097% without optimization of thickness while the reflectance at the same

Table-1: Design data and reflectance values for all configurations on glass

No. of layers	Mat.	Refr. index(n)	Thickness (d nm)				Rp%	Rave
			d1(nm)	d2	d3	d4		
Three layers	MgF2 CeO2 SiO	1.38 2.2 1.8	99.6 125 78.5	97 122.5 76.9	101 127.5 80	103 130 82	**1.2,0.8 7, 1.67, 2.5** *	**0.321,0.3 31,0.236 ,0.336***
Four-layers	MgF2 ZnS CeO2 SiO2	1.38 2.36 2.2 1.8	99.6 58.25 62.5 78.5				**0.95** *	**0.08** *

*** calculated within the band (450-700) nm**

Wavelength was 0.167% for four layers design, these results are very clear in the associated figure . However, the magnitude of reduction in reflectance with the optimizing thicknesses
of three layers showed in the Figure 1 shift the reflectance curve for d2 ,d3 , and d4 thicknesses towards the left and right respectively with respect (d1) where, d1 represents the thickness without use optimizing thicknesses .
The Optimization of thickness of three layers is used for obtaining the performance is close to the four layers ,but the effect of this process was very small comparison with four layer coating within the studied bands. This may suggest that the performance requirements are not very stringent. The reduction

in reflectance with the addition fourth layer was pretty for obtaining ARC within VIS band

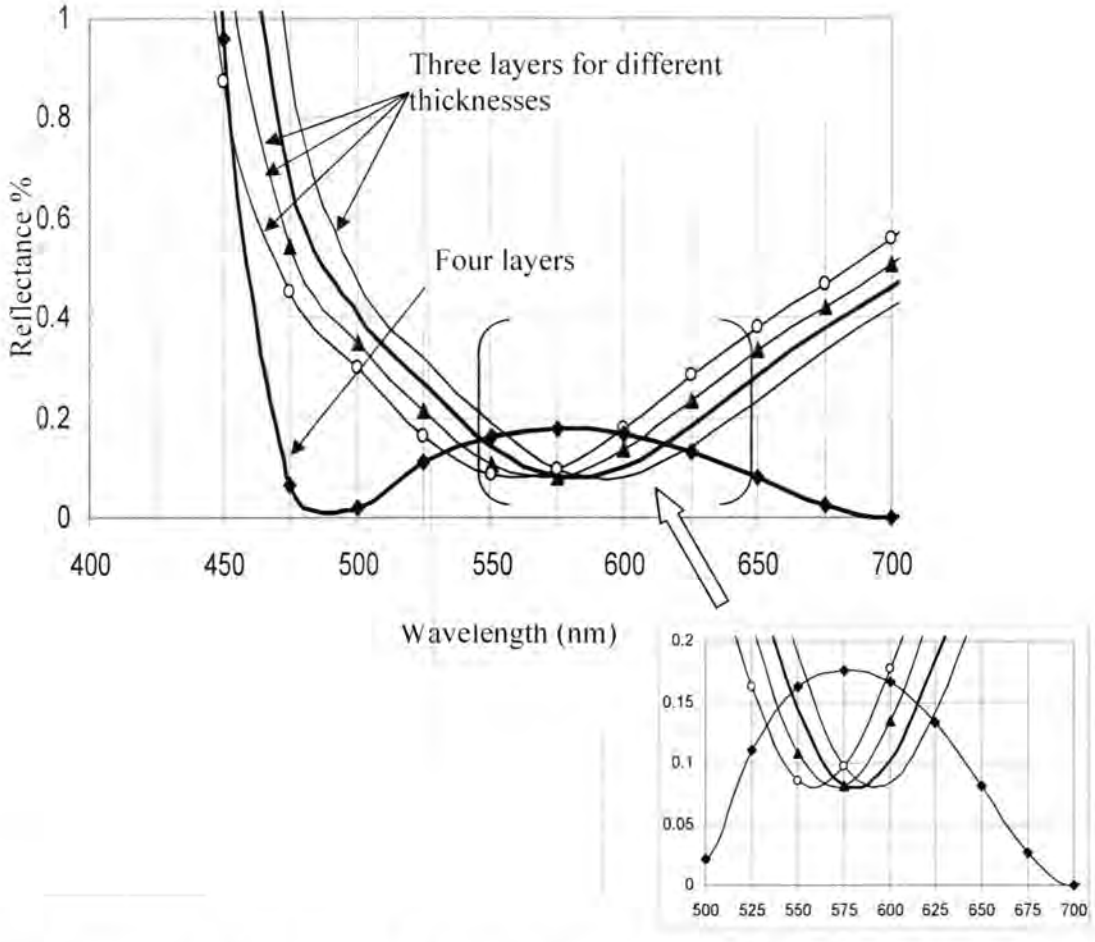

Fig. -2: Simulated reflectance for confi- guration on glass showed in table 1. The associated figure to show the indicated features of main figure.

(B) Infrared region: Ge, Si and ZnSe have been used as substrates material as they are commonly used in 3-5μm band for many optical and electro-optical applications [1]. All these substrates exhibit a very high reflectance value in the

said spectrum. In most of the applications, this high value of reflectance is not acceptable as it reduces the total energy reaching the detector surface with every increasing optical component in the system or device. Therefore, it is necessary to reduce their surface reflectance by applying ARC.s. The materials used as film layers are ZrO2, Si, CdTe, BaF2, Y2O3 and ZnS, MgF_2. All these materials are suitable for antireflection films in the desired region of wavelength [**1, 8**] .The reflectance of bare germanium substrate in 3.5mm is 36%. Multilayer coatings can be used to reduce this value to an appreciably low level [12]. We have modeled such coatings on germanium substrate at a design wavelength of 4mm. The process starts from a three layers model, and a layer are increased to reduce the value of maximum and average reflectance over the desired band. The single and two layers are not effect for obtaining ARC.s. as in three and four layers [1]. Table 2 shows the model data and calculated values of maximum and average reflectance over the entire band for a three layers modal. The data shows that the maximum and average value of reflectance has decreased form 0.57% and 0.4% respectively while of the four layers the values were 2.9% and 0.7% respectively. The maximum and average value of reflectance for three layers were smaller than four layers but the performance for four layers within the range 3.4-4.6μm were 0.5% and 0.15% respectively for the said values. Optimization of thickness for three and four layers shows that the maximum and average value of reflectance were 1.16%, 0.42% and 2.02%, 0.68% respectively. The combined reflectance plot of the two designs is shown in Fig. 2.We note that three layers with optimization of thickness verify the goal of the work.

Table-2: Design data and reflectance values for all configurations on germanium

No. of layers	Material	Refractive index(n)	Thickness (d nm)		Maximum ref. (Rp %)		Ref. average Rave %	
			d1 (μm)	d2 (μm)	Rp(d1)%	Rp(d2) %	Rave (d1) %	Rave (d1) %
Three layers	Si ZnS MgF2	3.42 2.24 1.38	0.29 0.44 0.72	0.203 0.308 0.532	0.57	1.16	0.4	0.42

Four layers	Si	3.42	0.29	0.278	2.9	2.02	0.7	0.68
	CdTe	2.24	0.44	0.425				
	ZrO2	2.05	0.48	0.461				
	MgF2	1.38	0.72	0.69				

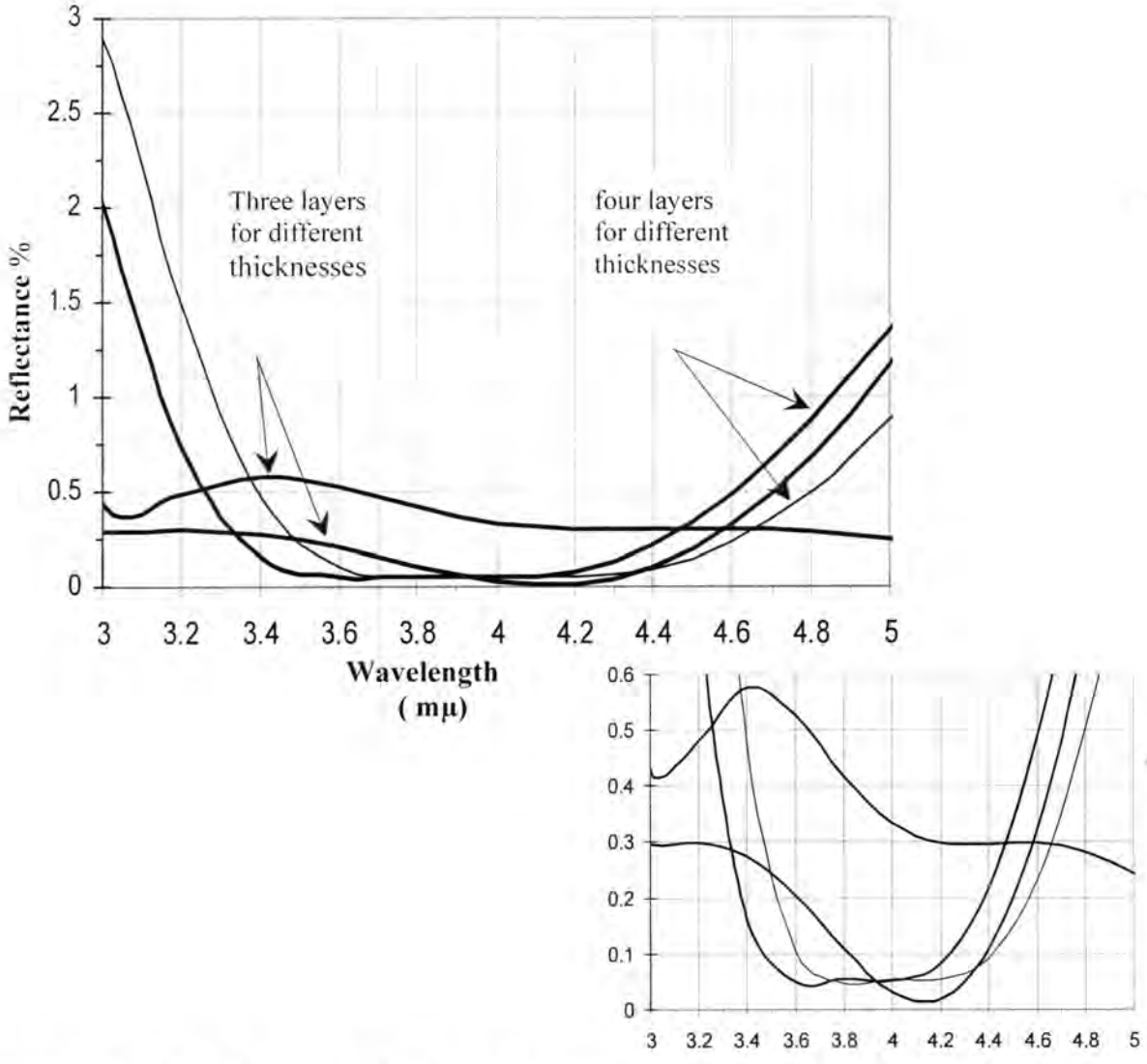

Fig.-3: Simulated reflectance for configuration germanium showed in table 2. The associated figure show the indicated feature of main figure

The reflectance from bare silicon substrate surface is 30% [**1**]. This value is lower as compared to the germanium, as it has got a lower refractive index in

the given spectrum. Similar procedure of layer addition has been employed to model and analyze multilayer structures for reducing reflectance from the substrate. Table 3 shows the model data with maximum and average values of reflectance for two configurations. Fig. 3 shows the combined plots for three and four layer configurations. However, in this case the performance for three layers configurations is even better and the design curve with Optimization of thickness is more flatland comparatively closer to the horizontal axis. Only two materials are used in four layers configuration. This shows that proper optimization not only helps in getting good performances but also tend to reduce unnecessary variety of materials which is very critical in manufacturing process. In the figure 3, shifting to the right side (upper wavelength values) is obtained. The associated of the main figure shows the effect of optimization of thickness of four layers in it notes that the curve was more flat than the other designs, it is closer to the horizontal axis. The maximum and average reflectance do not show in this work, it is clearly the performance ARC.s. was good agreement with the work goal within (4-7.5) μm

Table-3: Design data and reflectance values for all configurations on silicon

No. of layers	Material	Refractive index(n)	Thickness (d nm)		Maximum refractance (Rp %)		Reflectance average Rave %	
			d1 (μm)	d2 (μm)	Rp(d1) %	Rp(d2) %	Rave (d1) %	Rave (d1) %
Three layers	CdTe ZrO2 MgF2	2.64 2.05 1.38	0.38 0.48 0.72	0.39 0.49 0.735	2.4	2.46	1.4	1.4
Four layers	ZnS MgF2 ZnS MgF2	2.24 1.38 2.24 1.38	0.41 1.44 0.88 0.72	0.525 1.84 1.12 0.92	1.68	------	0.74	-----

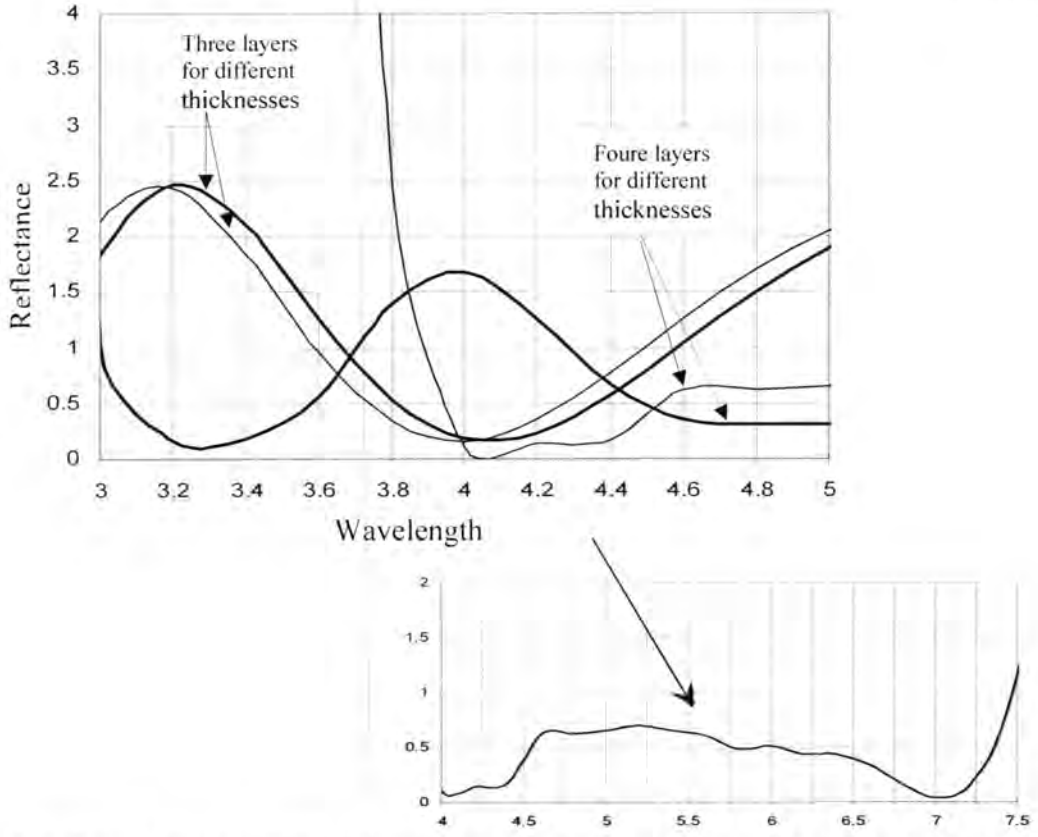

Fig.-4: Simulated reflectance for configurations on silicon showed in table 1. The associated figure shows the indicated features of main figure

Table -4: Design data and reflectance values for all configurations on zinc selenide

No. of layers	Material	Refractive index(n)	Thickness (d nm)		Maximum ref. (Rp %)		Ref. average Rave %	
			d1 (μm)	d2 (μm)	Rp(d1) %	Rp(d2) %	Rave (d1) %	Rave (d1) %
Three layers	ZrO_2 Y2O3 BaF2	2.05 1.73 1.3	0.48 0.58 0.77	0.49 0.59 0.785	1.13	4.62 **1.29***	0.68	1.16 **0.53 ***
Four layers	ZrO_2 Y2O3 ZrO_2 MgF2		0.48 0.58 0.48 0.72	0.39 0.475 0.39 0.59	1.73	2.1	0.54	0.98

*** calculated within the band (3.4-5) μm**

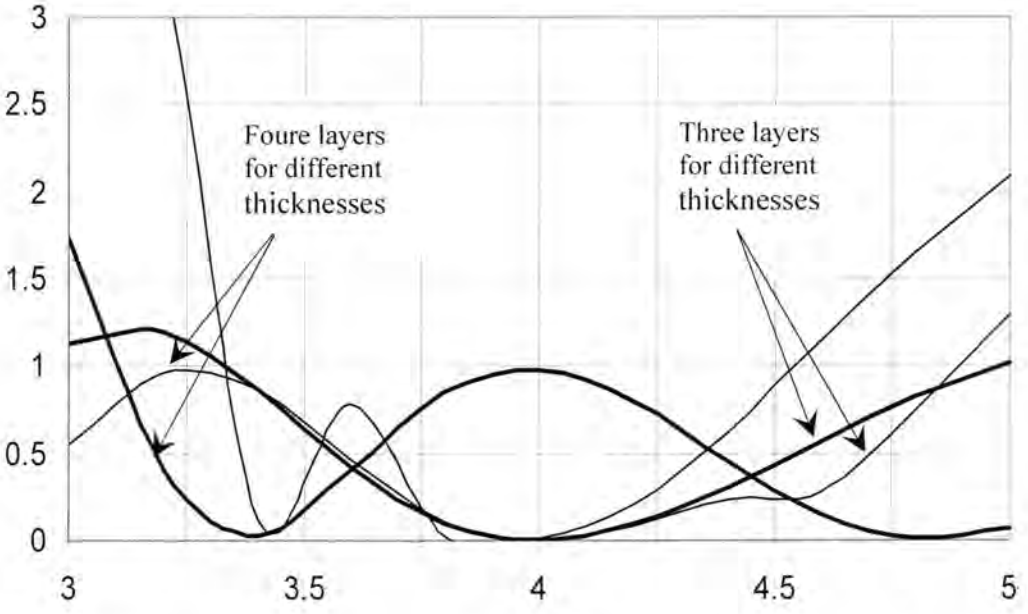

Fig.-4: Simulated reflectance for configurations on zinc selenide showed in table 4. The associated figure to show the indicated features of main figure

The reflectance of bare ZnSe substrate is 16.81% [**1**]. Multilayer antireflection coatings are employed on the substrate to drastically lower this value. Table 4 shows the model data and calculated values of maximum and average reflectance for three and four layer structures to reduce the reflectance from the substrate. Figure 4 shows the combined plots of the configurations. The sharp fall in the reflectance values at the lower side is observed. The showed values of maximum and average value of reflectance for three layers were smaller than four layers within the band (3.4-5) μm .thus, three layers ARC.s. with optimization of thickness may be verified the goal of this work and the performance may be developed by increasing run of design programme

Multilayer antireflection coatings for normal incidence in VIS and IR (3.5mm) band have been modeled for three and four layers configuration. The performance of three layers configuration has been optimized for obtaining performance of three layers to be close from the performance for four layers . The analysis of these designs reveal that three layers ARC.s. with optimization

of thickness was effective in some studied bands and the performance may be developed by increasing run of design programme.

REFERENCES

1. M.H.Asghar, M.B. Khan, and S. Naseem, "Modeling high performance multi-layers antireflection coating for VIS and IR (3-5) μm bands ", Vol. 6, No. 4, P. 508-513, 2003.
2. Gh.Honcicinc and Gh. Singurel," antireflection coating for the spectral range 400-700,400-900 and 800-1600 nm", Vol. 6, No. 4, P. 1199-1205, December 2004.
3. H. George and Rudolf E. Than "physics of thin film ", Vol.2, Academic press, New York, p.224, 1964.
4. P.H.Berning,"Theory of optical thin film ", in: physics of thin film collec. Vol.1, Academic press, New York, p.69, 1963.
5. D.Bouhaf and et al," Design and simulation of antireflection coatings system for Optoelectronic device", Vol.52, p.79-98, 1998.
6. G.Hass and Rudolf E. Than "physics of thin film ", Vol.1, Academic press, New York, p.69, 1966.
7. H.A. Macleod,"thin film optical filter ", IOP, institude of physics publishing, and Philadelphia, 2001.
8. H.K.pulker, "charectaristicization of optical thin film ", applied optics, Vol.12, p. 1969-1977, 1979.

New Forms of KC and LC Spaces

Haider G. Ali and Anmar Hashim Al-Sheikhly
Mathematics Department, College of Science, Al-Mustansiriyah University

Received : 31/03/2011 Accepted : 29/05/2011

الخلاصة

كرس هذا البحث لتقديم مفاهيم جديده هي الفضاءات $K(s^*gc)$, s^*gK_2 و$L(s^*gc)$. مبرهنات عديده ومتنوعه حول هذه المفاهيم قد برهنت. فضلا عن ذكر خصائصها وكذلك تحري العلاقات بين هذه المفاهيم والفضاءات LC.

ABSTRACT

This paper is devoted to introduce new concepts which are called $K(s^*gc)$, s^*gK_2 and $L(s^*gc)$ spaces. Several various theorems about these concepts are proved. Further properties are stated as well as the relationships between these concepts and LC-spaces are investigated.

INTRODUCTION

It is known that compact subset of a Hausdorff space is closed, this motivates the author [1] to introduce the concept of KC-space, these are the spaces in which every compact subset is closed. Lindelof spaces have always played a highly expressive role in topology. They were introduced by Alexandroff and Urysohn back in 1929. In 1979 the authors [2] introduce a new concept namely LC-spaces, these are the spaces whose lindelof sets are closed. The aim of this paper is to continue the study of KC-spaces and LC-spaces.

Preliminaries: The basic definitions that needed in this work are recalled. In this work, spaces always mean topological spaces on which no separation axioms are assumed unless explicitly stated, a topological space is denoted by (X, τ) (or simply by X). For a subset A of X, the closure of A in X is denoted by $\bar{A}$. We use the symbol s*g-closed (s*g-open) instead of s* closed (s* open) which is introduced in [3].

Definition 2.1.[4].A set A in a topological space X is semi open (written S.O) if there exists an open set O such that $O \subseteq A \subseteq \overline{O}$.

Definition 2.2.[3].A set A in a topological space X is

(i) s*g-closed if the closure of A is a subspace of all semi open set U which contains A.

(ii) s*g-open set if the complement of A in X is s*g-closed.

So every closed set in a topological space X is s*g-closed but the converse may not be valid.

Theorem 2.3 [3]: Let A⊆Y⊆X, Y is open in X. If A is s*g-closed in X, then A is s*g-closed in Y.

Definition 2.4.[5]. A topological space X is said to be s*g -T_1 space if for any two distinct points x and y of X, there are an s*g -open set U of x which does not contain y and s*g -open set V of y which does not contain x . That is, $x \in U, y \notin U$ and $x \notin V, y \in V$.

Theorem 2.5.[5]. A topological space X is an s*g -T_1 space if every singleton set is s*g -closed but the converse may not be valid.

Definition 2.6.[5]. A topological space X is said to be an s*g-regular space if given any closed subset F of X and any point x of X which is not in F, there are s*g-open sets U and V such that $x \in U, F \subset V$,and $U \cap V = \phi$.

Definition 2.7.[5]. The intersection of all s*g-closed sets containing A is called the s*g-closure of A .It is denoted by $\overline{A}^{s^*g}$.

Remark 2.8.[5]. Let X be a topological space such that $A \subset X$, then $\overline{A}^{s^*g}$ is contained in every s*g-closed set containing A.

Theorem2.9.[5]. Let X be a topological space and $A \subseteq X$,then A is an s*g-closed set if and only if $\overline{A}^{s^*g}$ = A.

Theorem2.10.[3]. Let f be a homeomorphism function from a space X in to a space Y. If B is an s*g-closed set in X, then f(B) is an an s*g-closed set in Y.

Definition 2.11. Let X be a topological space and $A \subset X$. A point $x \in A$ is said to be an s*g-interior point of A if there exists an s*g-open set U in X such that $x \in U \subset A$. The set of all s*g-interior points of A is said to be the s*g-interior of A and is denoted by s*g-int(A).

Strong forms of KC-spaces:

The author in [1] introduced the concept of KC-spaces; while in the present paper we introduce a new of KC-spaces namely K(s*gc) and s*gK_2, also we study the properties and fact about these concepts and the relationships between these concepts and KC-spaces.

Definition 3.1. A space X is said to be K(s*gc)-space if every compact set in X is s*g-closed. So every KC-space is K(s*gc), but the converse is not true in general.

Example 3.2. Let $X \neq \phi$ and Γ be the indiscrete topology on X. Then (X, Γ) is K(s*gc) but not KC-space. Since if B is a nonempty proper set in X, then clearly B is compact which is not closed. Also it is s*g-closed, since the only semi open set which contains B is the whole space and cl(B) = X.

Definition 3.3. A space X is said to be s*gK_2 if $\overline{A}^{s^*g}$ is compact, whenever A is a compact set in X.

Theorem 3.4. Every K(s*gc)-space is s*gK_2.

Proof: Let A be a compact set in K(s*gc)-space X.
Then A is s*g-closed.
By 2.9 we get that $\overline{A}^{s^*g}$ = A, which implies that $\overline{A}^{s^*g}$ is also compact.

Theorem 3.5. Every K(s*gc)-space is s*g-T_1.

Proof: Let $x \in X$, since {x} is finite, then it is compact in X, which is K(s*gc)-space, then it is s*g-closed. So by 2.5 X is s*g-T_1.

Definition 3.6. A set M in a topological space X is said to be s*g-neighbourhood of a point $x \in X$ if there exists an s*g-open set U such that $x \in$

$U \subset M$. Clearly every neighbourhood is s*g-neighbourhood but the converse may be not true.

Example 3.7: Let $X \neq \phi$ and Γ be the indiscrete topology on X. Then in (X, Γ) the set $\{x\}$ is an s*g-neighbourhood of x but it is not neighbourhood of x .

Theorem 3.8 The following statements are equivalent for a space X:

1) X is s*g-regular

2) If U is open in X and $x \in X$ with $x \in U$, then there is an s*g-open set V containing x such that $\overline{V}^{s^*g} \subset U$.

3) Each $x \in X$ has an s*g-neighbourhood base consisting of s*g-closed sets.

Proof: (1)→ (2) Suppose that X is s*g-regular, U is an open set in X and $x \in U$.

Then X-U is a closed set in X which is not containing x.

Since X is s*g-regular ,then disjoint s*g-open sets V and W can be found with $x \in V$ and $X-U \subset W$.

Then X-W is an s*g-closed such that $V \subset X-W$.

So by 2.8 we get that $\overline{V}^{s^*g} \subset X-W$.

But $X-W \subset U$ which leads to $\overline{V}^{s^*g} \subset U$.

(2) →(3) if (2) applies, then every open set U containing x contains an s*g-closed neighbourhood (namely $\overline{V}^{s^*g}$) of X.

So the s*g-closed neighbourhoods of x form a neighbourhood base.

(3) →(1) suppose (3) applies and A is a closed set in X which is not containing x.

Then X-A is a neighbourhood of x which leads that X-A is s*g-neighbourhood of x .

So by (2), there is an s*g-closed neighbourhood B of x with $B \subset X-A$.

Then s*g-Int(B) and X-B are disjoint s*g-open sets containing x and A respectively. Thus X is an s*g-regular space.

Definition 3.9. A function f from a space X into a space Y is s*g-closed if f(F) is an s*g-closed set in Y for each closed set F in X.

Theorem 3.10. Every continuous function from a compact space X into a K(s*gc) space Y is an s*g-closed function.

Proof: Let A be closed set in X, which is compact, then A is compact. But f is continuous, then f(A) is compact in Y, which is K(s*gc)-space, then f(A) is s*g-closed. Therefore f is an s*g-closed function.

Theorem 3.11: The property of a space being K(s*gc) is a hereditary on an open set.

Proof:

Let Y be an open subspace of a K(s*gc) space X and A be any compact subset of Y. Then A is compact in X which is K(s*gc).

So A is an s*g-closed set in X. By 2.3 we get that A is an s*g-closed set in Y. Hence Y is a K(s*gc) space.

Theorem 3.12: The property of a space being K(s*gc) is a topological property.

Proof:

Let f be a homeomorphism function from a K(s*gc) space X in to a space Y and B be compact in Y. Then $f^{-1}(B)$ is compact in X ,which is K(s*gc).

Then $f^{-1}(B)$ is s*g-closed. By 2.10, we get that $f(f^{-1}(B))=B$ is s*g-closed in Y.

Farther type of LC-spaces:

In 1979 the authors [2] introduce a new concept namely LC-spaces, these are the spaces in which every lindelof sets are closed. In the present paper we introduce a new concept namely L(s*gc)-spaces .

Definition 4.1. A space X is said to be L(s*gc)-space if every lindelof set is s*g-closed.

So every LC-space is L(s*gc) but the converse is not true in general.

Example 4.2. Let R with the indiscrete topology Γ. Clearly (R,Γ) is L(s*gc), since for every Lindelof set difference from R and ϕ is s*g-closed but not closed.

Theorem 4.3. Every L(s*gc) space is s*g-T_1.

Proof: Let X be L(s*gc)-space and $x \in X$.

Since {x} is lindelof set in X which is L(s*gc), then it is s*g-closed and by 2.5 we get that X is s*g-T_1.

Theorem 4.4. The property of a space being L(s*gc) is a hereditary on an open set.

Proof:

Let Y be an open subspace of an L(s*gc) space X and A be any lindelof subset of Y. Then A is lindelof in X which is L(s*gc).

So A is an s*g-closed set in X. By 2.3 we get that A is an s*g-closed set in Y.

Hence Y is an L(s*gc) space.

Theorem 4.5. The property of a space being L(s*gc) is a topological property.

Proof:

Let f be a homeomorphism function from an L(s*gc) space X into a space Y and B be lindelof in Y. Then $f^{-1}(B)$ is lindelof in X ,which is L(s*gc).

Then $f^{-1}(B)$ is s*g-closed. By 2.10, we get that $f(f^{-1}(B))=B$ is s*g-closed in Y.

Definition 4.6. A space X is said to be s*-$T_{1/2}$ space if every s*g-closed set is closed.

Theorem 4.7: If X is L(s*gc) and s*-$T_{\frac{1}{2}}$ -space, then every compact set in X is finite.

Proof: Let A be compact set in X. If A is finite, then the proof is finished, if A is infinite, then either A is countable or uncountable. Suppose A is countable and U is any set in A, then U is countable, so U is lindelof in A, which implies it is lindelof in X, which is L(s*gc), then U is s*g-closed in X. But X is s*-$T_{\frac{1}{2}}$, and then U is closed in X. But $U \cap A=U$, then U is closed in A, that is, A is discrete but A is compact, then A is finite, which is a contradiction. If A is uncountable, then there exists a subset K of A is countable and so K is lindelof in A, so it is lindelof in X, which is L(s*gc) and s*-$T_{\frac{1}{2}}$ space, then K is closed. Put $K=\{a_1, a_2 \ldots\}$. Let $U_1=K^c$, now $a_1 \in U_2=A-\{a_2, a_3,\ldots\}$ and $a_2 \in A-\{a_3, a_4\ldots\}\ldots$, then $\{U_i\}_{i=1}^{\infty}$ is an open cover of A, which has no finite subcover, which is a contradiction. Then A is finite.

REFERENCES

1. Wilansky A.," Between T_1 and T_2 " , Amer. Math. Monthly 74(1967) 261-266.
2. T. K. Mukherji and M. Sarkar, On a class of almost discrete spaces, Mat. Vesnik 3(16) (31) (1979), 459-474.
3. Al-meklafi S.A.,"New Types of Separation Axioms";Thesis submitted to the col, of education Al-Mustansirya univ.,(2002)
4. Levin,N.;"Semi Open Sets And Semi Continuity in Topological spaces";The Amer.Math.Monthly,70(1963)36-41.
5. Al-Sheikhly Anmar H.,and Arkan J.," Spotlight On Separation Axioms", Journal of college of education, Al-Mustansiryah uni, 2011.

On *-Derivation Pairs Of Prime And Simeprime *-Ring

A. H. Majeed and A. A. ALTAY
Department of Mathematics, College of Science, University of Baghdad

Received : 20/03/2011 Accepted : 29/05/2011

الخلاصة

لتكن R حلقة-*, في هذا البحث سنبرهن النتائج الآتية: (1) لتكن R حلقة-* أولية غير ابدلية طليقة الألتواء من النمط 6 فان R تكون سوية اذا وفقط اذا وجدت دالة مشتقات-*جوردان المزدوجة الغير الصفرية الابدالية. (2) لتكن R حلقة-* شبه أولية طليقة الألتواء من النمط 2 ولتكن (d,g) دالة مشتقات-* المزدوجة وتحقق الشرط الاتي: $d(xy+yx)=g(xy+yx)=0$ لكل x,y في R فان d=g=0. (3) لتكن R حلقة-* شبه أولية طليقة الألتواء من النمط 2 فانه لاتوجد (d,g) دالة مشتقات-* المزدوجة وتحقق الشرط الاتي: $d(xy+yx)=g(xy+yx)=xy+yx$ لكل x,y في R.

ABSTRACT

Let R be a *-ring, The purpose of this paper is to prove the following result: (1) Let R be a non-commutative prime *-ring with an identity element which is 6- torsion free. Then R is normal if and only if there exists a non-zero commuting Jordan *- derivation pair. (2) Let R be a 2-torsion free semiprime *-ring, and let (d,g) be a *-derivation pair satisfies $d(xy+yx)=g(xy+yx)=0$ for all $x,y \in R$, then d=g=0. (3) Let R be a 2-torsion free semiprime *-ring, then there is no *-derivation pair (d,g) satisfies $g(xy+yx)= d(xy+yx)=xy+yx$ for all $x, y \in R$.

INTRODUCTION

Throughout, R will represent an associative ring with center Z(R). A ring R is n-torsion free, if $nx = 0$, $x \in R$ implies $x = 0$, where n is a positive integer. Recall that R is prime if $aRb = (0)$ implies $a = 0$ or $b = 0$, and semiprime if $aRa = (0)$ implies $a = 0$. An additive mapping $x \rightarrow x^*$ on a ring R is called an involution if $(xy)^* = y^* x^*$ and $(x)^{**} = x$ for all $x, y \in R$. A ring equipped with an involution is called *-ring (see [1]). An element x in a *-ring R is said to be hermitian if $x^* = x$ and skew-hermitian if $x^* = -x$. The sets of all hermitian and skew-hermitian elements of R will be denoted by $H(R)$ and $S(R)$, respectively[1]. Recall that an element x is normal if $xx^*=x^*x$, and if all

the elements of R are normal then R is called a normal *-ring, for example on anormal *-ring the ring of quaternions. A description of normal rings can be found in [2].An additive mapping d: R→R is called a derivation if $d(xy) = d(x)y + xd(y)$ holds for all pairs $x,y \in R$, and is called a Jordan derivation in case $d(x^2) = d(x)x + xd(x)$ is fulfilled for all $x \in R$(see [3]). Every derivation is a Jordan derivation, but the converse is in general not true. A classical result of Herstein [4] asserts that every Jordan derivation on a prime ring of characteristic different from 2 is a derivation. Cusack [5] generalized Herstein's theorem to 2-torsion free semiprime ring. An additive mapping D:R →R, such that R is a *-ring, is called a *- derivation if $D(xy)=D(x)y^*+xD(y)$ holds for all pairs $x,y \in R$, and is called a Jordan *-Derivation in case $D(x^2) = D(x)\, x^* + x\, D(x)$ holds for all $x \in R$. The concepts of *-derivation and Jordan*-derivation were first mentioned in [6]. The study of Jordan *-derivation has been motivated by the problem of the represented quadratic form by bilinear forms. If d, g: R→R are additive mappings such that

$$d(x^3) = d(x)\, x^{*2} + xg(x)\, x^* + x^2 d(x) \quad \text{for all } x \in R. \qquad (1.1)$$

$$g(x^3) = g(x)\, x^{*2} + xd(x)\, x^* + x^2 g(x) \quad \text{for all } x \in R. \qquad (1.2)$$

Then (d, g) is called a Jordan*-derivation pair. The notion of a Jordan*-derivation pair first appeared in [7] and [8]. Hence we define a *-derivation pair$(d, g)$of an additive mapping $d, g : R \to R$ as follows, an additive pair (d,g) is called a *-derivation pair if satisfy the system of the equations

$$d(xyx) = d(x)\, y^* x^* + xg(y)\, x^* + xyd(x) \quad \text{for all } x, y \in R. \qquad (1.3)$$

$$g(xyx) = g(x)\, y^* x^* + xd(y)\, x^* + xyg(x) \quad \text{for all } x, y \in R. \qquad (1.4)$$

A *-derivation pair (d, g) is called inner if $d(x)=ax^*-xb$, and $g(x)=bx^*-xa$, holds for all $x \in R$ and a fixed elements $a, b \in R$. Let us recall a left (right) centralizer of R is an additive mapping T: R→R which satisfies $T(xy) = T(x)y$ ($T(xy) = xT(y)$) for all $x, y \in R$. A centralizer of R is an additive mapping which is both left and right centralizer. A left (right) Jordan centralizer of R is an additive mapping T: R→R which satisfies $T(x^2) = T(x)x$ ($T(x^2)= xT(x)$) for all $x \in R$. A Jordan centralizer of R is an additive mapping which is both left and right Jordan centralizer (see [9,10,11, and 12]). Every centralizer is a Jordan centralizer. B. Zalar [12] proved the converse when R is 2- torsion free semiprime ring . A pair (T, S), where T, S: R→ R, is called a double centralizer if T is a left centralizer, and S is a right centralizer, and

they satisfy a balanced condition $xT(y) = S(x)y$ for all $x, y \in R$. The typical example for *-derivation pair is the following. Let (T_1, S_1) and (T_2, S_2) be double centralizers. Then the mappings $d, g : R \to R$ defined by $d(x) = T_1(x^*) + S_2(x)$, $g(x) = -(T_2(x^*) + S_1(x))$ for all $x \in R$, form a *-derivation pairs. Every *-derivation pair is a Jordan *-derivation pair but the converse is in general not true. Majeed and Altay[13] giving a condition on a *-ring R to get the converse. A Jordan *-derivation pairs (d, g) is called commuting on *-ring R if both d and g are commuting mapping, i.e. $[g(x),x]=[d(x),x]=0$ for all $x \in R$. in this paper we will give relation between normal *-ring and commuting *-derivation, and some result on a *-derivation pair.

RESULTS AND DISCUSSION

M. Breŝar and J. Vukman In [6] proved that, if R be a non-commutative prime *-ring of characteristic different from 2, then R is normal ring if and only if there exists a nonzero commuting Jordan *-derivation. In this section, we will give a result similar to the result of M. Breŝar and J. Vukman [6], but in case Jordan *-derivation, And we'll give some results on normal *-ring and *-derivation pair of a semiprime *-ring.

Theorem 2.1. Let R be a non-commutative prime *-ring with an identity element which is 6- torsion free. Then R is normal if, and only if, there exists a non-zero commuting Jordan *- derivation pair.

To proof the above theorem we need the following lemmas have easy proving

Lemma 2.2. Let R be a 6-torsion free with an identity element, and (d,g) is a Jordan *-derivation pair then

$$(d\text{-}g)(x)=ax^*+xa \qquad \text{for all } x \in R.$$
$$(g\text{-}d)(y)=by^*+yb \qquad \text{for all } y \in R.$$

Where $a=d(1)$, and $b=g(1)$.

Lemma 2.3. Let R be a 2-torsion free ring with an identity element, and let d: R→R be an additive mapping satisfies

$$d(xyx)= d(x)y^*x^*+xd(y)x^*+xyd(x) \qquad \text{for all } x \in R.$$

Then d is a Jordan *-derivation.

Proof of theorem2.1: If R is a normal *-ring, then let we define

d: R→R by

$$d(x)=2x^*-x \quad \text{for all } x \in R. \tag{2.1}$$

g: R→R by

$$g(x)= x^*-2x \quad \text{for all } x \in R. \tag{2.2}$$

Since,

$$d(x)x^{*2}+xg(x)x^{*}+x^{2}d(x)=(2x^{*}-x)x^{*2}+x(x^{*}-2x)x^{*}+x^{2}(2x^{*}-x)$$
$$=2x^{*3}-xx^{*2}+xx^{*2}-2x^{2}x^{*}+2x^{2}x^{*}-x^{3}=2x^{*3}-x^{3}=d(x^{3}) \quad (2.3)$$

And,

$$g(x)x^{*2}+xd(x)x^{*}+x^{2}g(x)=(x^{*}-2x)x^{*2}+x(2x^{*}-x)\,x^{*}+x^{2}\,(x^{*}-2x)$$
$$=x^{*3}-2xx^{*2}-x^{2}x^{*}+2xx^{*2}+x^{2}x^{*}-2x^{3}=x^{*3}-2x^{3}=g(x^{3}) \quad (2.4)$$

Also,

$$[d(x),x]=[2x^{*}-x,x]=2[x^{*},x]=0=[x^{*}-2x,x]=[g(x),x] \quad \text{for all } x\in R. \quad (2.5)$$

Since R is a 6-torsion free, then we get (d,g) is a non-zero commuting Jordan *-derivation pair.

To show the converse, let (d,g) be a nonzero commuting Jordan*-derivation pair, then by using Lemma2.2, we get

$$(d-g)(x)=ax^{*}+xa \qquad \text{for all } x\in R. \quad (2.6)$$

Where $a=d(1)$, since (d,g) commuting mapping then (d-g) is a commuting mapping, therefore

$$[(d-g)(x),x]=[ax^{*}+xa,x]=0 \qquad \text{for all } x\in R. \quad (2.7)$$

Linearization the relation (2.7), we get

$$[ax^{*}+xa,y]=[x,ay^{*}+ya] \qquad \text{for all } x,y\in R. \quad (2.8)$$

Replace y by 1 in (2.8) we get, $2[x,a]=0$ for all $x\in R$, since R be a 6-torsion free we get $a\in Z(R)$, then from (2.8) we get

$$a\,[x^{*},y]=a\,[x,y^{*}] \qquad \text{for all } x,y\in R. \quad (2.9)$$

Setting $x=y$ in (2.9) we get

$$a\,[x,x^{*}]=0 \qquad \text{for all } x\in R. \quad (2.10)$$

Left multiplication by y we get

$$a\,y\,[x,x^{*}]=0 \qquad \text{for all } x\in R. \quad (2.11)$$

By primness of a *-ring R we get either R is normal *-ring, or $a=0$, hence d=g, then by Lemma 2.3, we get d is a Jordan*-derivation hence by the second result of M. Breŝar and J. Vukman [6] , we get R is a normal *-ring.

In the following theorem we will give an important relation to a *-derivation pair (d,g) on semiprime *-ring.

Theorem 2.4. Let R be a 2-torsion free semiprime *-ring, and let (d,g) be a *-derivation pair satisfies $d(xy+yx)=g(xy+yx)=0$ for all $x,y\in R$, then d=g=0.

Proof: We have, since R is a 2-torsion free

$$d(x)y^{*}x^{*}+xg(y)x^{*}+xyd(x)=0 \qquad \text{for all } x,y\in R. \quad (2.12)$$

And,

$g(x)y^*x^*+xd(y)x^*+xyg(x)=0$ for all $x,y \in R$. (2.13)

Replace y by $(zy+yz)$, in (2.12) we obtain

$$d(x)(yz+zy)^* x^*+x(yz+zy)d(x)=0 \quad \text{for all } x,y,z \in R. \quad (2.14)$$

If we replace x by $(yz+zy)$, and y by y_1 in (2.13), we obtain

$$(yz+zy)\, d(y_1)\, (yz+zy)^*=0 \quad \text{for all } x,y,z \in R. \quad (2.15)$$

Setting $x=y_1$ in the relation (2.15) we get

$$(yz+zy)\, d(x)\, (yz+zy)^*=0 \quad \text{for all } x,y,z \in R. \quad (2.16)$$

Left multiplication the relation (2.14) by $(zy+yz)$, and using (2.16) we get

$$(zy+yz)x(zy+yz)d(x)=0 \quad \text{for all } x,y,z \in R. \quad (2.17)$$

Linearization the relation (2.17) we get

$$(zy+yz)x(zy+yz)d(w)+ (zy+yz)w(zy+yz)d(x)=0 \quad \text{for all } x,y,z,w \in R. \quad (2.18)$$

Replace w by $(ab+ba)$ in (2.18), we get

$$(zy+yz)(ab+ba)(zy+yz)d(x)=0 \text{ for all } x,y,z,a,b \in R. \quad (2.19)$$

Putting $(ab+ba)$ for a in (2.19) we get

$$(zy+yz)(bab)(zy+yz)d(x)=0 \quad \text{for all } a,b \in R. \quad (2.20)$$

Hence,

$$(zy+yz)\, b_1\, a\, b_2\, (zy+yz)\, d(x)=0 \quad \text{for all } a,b_1,b_2 \in R. \quad (2.21)$$

Replace b_1 by $d(x)$ in (2.21) we get

$$(zy+yz)\, d(x)\, a\, b_2\, (zy+yz)\, d(x)=0 \quad \text{for all } a,b_2 \in R. \quad (2.22)$$

Left multiplication the relation (2.22) by b_2 we get

$$b_2(zy+yz)\, d(x)\, a\, b_2\, (zy+yz)\, d(x)=0 \quad \text{for all } a,b_2 \in R. \quad (2.23)$$

Since R is *-semiprime ring, then from the relation (3.23) we obtain

$$b_2(zy+yz)\, d(x)=0 \quad \text{for all } x,y,z,b_2 \in R. \quad (2.24)$$

Left multiplication the relation (2.24) by $(zy+yz)\, d(x)$,we get

$$(zy+yz)\, d(x)\, b_2(zy+yz)\, d(x)=0 \quad \text{for all } x,y,z,b_2 \in R. \quad (2.25)$$

Therefore,

$$(zy+yz)\, d(x)=0 \quad \text{for all } x,y,z \in R. \quad (2.26)$$

Replace z by $(zy+yz)$ we get, $yzyd(x)=0$ for all $x,y,z \in R$. Putting $d(x)z$ for z we get, $yd(x)zyd(x)=0$ for all $x,y,z \in R$, hence $yd(x)=0$ for all $x,y \in R$. Left multiplication by $d(x)$, we obtain, $d(x)\ y\ d(x)=0$ for all $x \in R$. By semiprimness of R we get, $d=0$.

Similar way we can show $g(x)=0$ for all $x \in R$.

The following proposition proved there is no *-derivation pair (d,g) satisfies $g(xy+yx)=d(xy+yx)=xy+yx$ for all $x, y \in R$, on a semiprime *-ring R.

Proposition 2.5. Let R be a 2-torsion free semiprime *-ring, then there is no *-derivation pair (d,g) satisfies $g(xy+yx)= d(xy+yx)=xy+yx$ for all $x, y \in R$.

To proof above proposition we need the following lemma:

Lemma 2.6. Let R be a semiprime *-ring, if there exist an element $h \in H(R)$ which satisfy $h\, H(R)\, h=0$, then $h=0$.

Proof: We have, $h\, x\, h=0$ for all $x \in H(R)$, Since $(y+y^*) \in H(R)$, for all $y \in R$, then $h\, y\, h=- h\, y^*\, h$ for all $y \in R$. Also since $(yhy^*) \in H(R)$, therefore $h\, y\, h\, y^*\, h=- h\, y\, h\, y\, h=0$ for all $y \in R$. Linearization we get, $h\, y\, h\, z\, h+ h\, zh\, y\, h=0$ for all $z,y \in R$. Left multiplication by $y\, h$ we obtain $h\, y\, h\, z\, h\, y\, h=0$ for all $z,y \in R$. By the semiprimeness of R, we get $h=0$.

Proof of proposition 2.5: Assume d=g=0 then we get, $xy+yx=0$ for all $x, y \in R$, Replace x by $xy+yx$, we have $x\, R\, x=0$, since R is a semiprime *-ring we get contradiction.

Hence assume that (d,g) be a non-zero *-derivation pair, we have

$$d(xy+yx)= xy+yx \quad \text{for all } x, y \in R. \tag{2.27}$$

Replace y by $xy+yx$ in (2.27) we get

$$d(x^2y+yx^2)+2d(xyx)= x^2y+yx^2+2(xyx) \quad \text{for all } x, y \in R. \tag{2.28}$$

Since R is a 2-torsion free, we get from (2.27) and (2.28)

$$d(xyx)=d(x)y^*x^*+xg(y)x^*+xyd(x)=xyx \text{ for all } x, y \in R. \tag{2.29}$$

Setting $y=h\, h_1\, h$, $x=d\, d_1\, d$ where $h,h_1,d,d_1 \in H(R)$, then from (2.29) we get

$$x\, h\, h_1\, h\, x=0 \quad \text{for all } h,h_1 \in H(R), \tag{2.30}$$

Left and right multiplying by h, we get

$$h\, x\, h\, h_1\, h\, x\, h=0 \quad \text{for all } h,h_1 \in H(R), \tag{2.31}$$

hence by lemma 2.6 we get

$$h\, d\, d_1\, d\, h=0 \quad \text{for all } h,d,d_1 \in H(R), \tag{2.32}$$

Left and right multiplying by d in relation (2.32) we get

$$d\, h\, d\, d_1\, d\, h\, d=0 \quad \text{for all } h,d,d_1 \in H(R), \tag{2.33}$$

Then by using Lemma2.6 we get $H(R) =0$, therefore $x=-x^*$ for all $x \in R$, hence R=0. This is contradiction.

REFERENCES

1. I. N. Herstein: Topics in ring theory, University of Chicago Press, (1969).
2. I.N. Herstein: Rings with involution. University of Chicago Press, Chicago, (1976).

3. E.C .Posner : Derivations in prime rings, Proc. Amer. Math. Soc. 8:1093-1100. (1957).
4. I. N. Herstein: Jordan derivations in prime rings, Proc. Amer. Math. Soc. 8 :1104-1110. (1957).
5. J. Cusack: Jordan derivations on rings, Proc. Amer. Math. Soc. 53 : 321-324. (1975).
6. M.Brešar, and J.Vukman, On some additive mappings in rings with involution, Aequations Math., 38:178-185. (1989).
7. B.Zalar: Jordan-von Neumann theorem for Saworotnow's generalized Hilbert space, Acta Math. Hungar. 69:301–325. (1995).
8. B.Zalar: Jordan *-derivation pairs and quadratic functionals on modules over *-ring, Aequationes Math. 54 :31-43. (1997).
9. J. Vukman: An identity related to centralizers in semiprime rings, Comment. Math. Univ. Carolinae 40: 447-456. (1999).
10. J. Vukman: Centralizers on semiprime rings, Comment. Math. Univ. Carolinae 42: 237-245. (2001).
11. J. Vukman and I. Kosi-Ulbl: On centralizers of semiprime rings, Aequationes Math. 66, 3 :277 - 283. (2003).
12. B. Zalar: On centralizers of semiprime rings, Comment. Math. Univ. Carolinae 32 :609-614. (1991).
13. A.H .Majeed and A.A.Altay Additive mappings on prime and semiprime ring with involution. Baghdad University (Iraq). Msc. thesis. Advisor: A.H. Majeed, (2009).

The Degree of Best Approximation of unbounded Functions by Bernstein operators

Saheb K. Al – Saidy and Lekaa A. Husain
Department of Mathematics, College of Science, Al-Mustansiriyah University

Received : 11/04/2011 Accepted : 29/05/2011

الخلاصة

الغرض من هذا العمل هو ايجاد درجة التقارب لدالة f ∋ B(α) بواسطة متعددة حدود برنشتاين في الفضاء $L_{p,\alpha}$ ($1 \le p \le \infty$) وبأستخدام مقياس النعومة $\omega_r^{\phi}(f, x, \delta)_{p,\alpha}$

ABSTRACT

The purpose of this work is to find the degree of the approximation of a function $f \in B(\alpha)$ by Bernstein polynomial in $L_{p,\alpha}$ -space ,$1 \le p \le \infty$, by using the modulus of smoothness $\omega_r^{\phi}(f, x, \delta)_{p,\alpha}$

INTRODUCTION

Let X=[0,1] , we denote by $L_\infty(X)$ the set of all bounded measurable functions with usual sup-norm ([1]) .

$$\|f\|_\infty = \sup \{|f(x)| : x \in X\}$$

For $1 \le p < \infty$, let $L_p = \{f$: f is a bounded measurable function for which $\|f\|_p < \infty\}$

where

$$\|f\|_p = \left[\int_X |f(x)|^p \, dx \right]^{1/p} \qquad \ldots(1)$$

The family of semi-norms (locally global norms) for $\delta > 0$ and $(1 < p < \infty)$ is defined by ([2]):

$$\|f\|_{\delta,p} = \|f_\delta(.)\|_p = \left[\int_X \left(\sup\{|f(y)| : y \in \left[x - \frac{\delta}{2}, x + \frac{\delta}{2} \right] \right)^p dy \right]^{1/p} \qquad \ldots(2)$$

The $L_{\delta,p}$ is the space of all bounded measurable function, such that $\|f\|_{\delta,p} < \infty$.

The discrete norm is defined by ([1]) :

$$\| f \|_{L_p^n(X)} = \left[\frac{1}{n+1} \sum_{k=0}^{n} | f(x_{k,n}) |^p \right]^{1/p} < \infty \qquad \ldots(3)$$

Where $x_{k,n} = \frac{2k\pi}{n+1}$, k = 0, 1, …, n.

The $L_p^n(X)$ space is defined by

$L_p^n(X) = \{ f : X \longrightarrow \square$, such that $\| f \|_{L_p^n(X)} < \infty \}$

The degree of best approximations of a function $f \in L_p(X)$ with trigonometric polynomials or with algebraic polynomials in the metric of the space L_p are given by ([3]):

$E_n(f)_p = \inf \{ \|f - Q\|_p : Q \in P_n \}$ …(4)

Where P_n denotes the set of all trigonometric polynomials or algebraic polynomials of degree at most n.

The k^{th} locally modulus of smoothness for $f \in L_\infty$ is defined by ([3]) :

$$\omega_k(f, x, \delta) = \sup_{|h| \le \delta} \{ | \Delta_h^k f(t) | : t, t + kh \in [x - \frac{k\delta}{2}, x + \frac{k\delta}{2}] \cap X \} \qquad \ldots(5)$$

and the k^{th} difference is defined by ([3]):

$$\Delta_h^k f(x) = \begin{cases} \sum_{m=0}^{k} (-1)^{m+k} \binom{k}{m} f(x + mh), & x, x + mh \in X \\ 0, & \text{otherwise} \end{cases} \qquad \ldots(6)$$

The k^{th} average modulus of smoothness for $f \in L_p$ is defined by ([3]):

$$\tau_k(f, \delta)_p = \| \omega_k(f, ., \delta) \|_p \qquad \ldots(7)$$

Where $\omega_k(f, ., \delta)$ is defined by (5)

Let α be any positive number and $w(\alpha, x)$ be a positive function on X depends on α. Consider the set of all function f defined on X, such that $|f(x)| \le Mw(\alpha, x)$, where M is a positive constant. $w(\alpha, x)$ may be tend to infinity and suppose that the function $f(x)/w(\alpha, x)$ is integrable, then denote this set by:

$B(\alpha) = \{ f : X \longrightarrow R : |f(x)| \le Mw(\alpha, x) \text{ and } \int_X f(x) / w(\alpha, x) dx < \infty \}$

The locally modulus of smoothness of the function $f \in B(\alpha)$, is defined by:

$$\omega_r(f, x, \delta)_\alpha = \sup|\Delta_h^r f(t)/w(\alpha, t)| : r \in N, \delta \geq 0, t, t + rh \in [x - r\frac{h}{2}, x + r\frac{h}{2}] \cap X \ldots(8)$$

Where:

$$\Delta_h^r f(x) = \begin{cases} \sum_{i=0}^{r} (-1)^{r+i} \binom{r}{i} f(x + ih), & x + rh \in X \\ 0, & \text{otherwise} \end{cases} \quad \ldots(9)$$

the following semi-norm is defined by:

$$\|f\|_{p,\alpha} = \left[\int_X | f(x) / w(\alpha, x) |^p \, dx \right]^{1/p}, \quad 1 \leq p < \infty \quad \ldots(10)$$

The set $B(\alpha)$ with norm $\|f\|_{p,\alpha}$ is a linear normed space and is denoted by $L_{p,\alpha}(X)$-space. That is:

$$L_{p,\alpha}(X) = \{f : X \longrightarrow R, \text{ such that } \|f\|_{p,\alpha} < \infty\}$$

If f is integrable, then:

$$\|f\|_p = \|f\|_{p,\alpha}$$

which means that if f is integrable, then we take $\alpha = 0$ ($w(\alpha,x) = 1$).

For $f \in B(\alpha)$, we define f', such that $f' = \left(\frac{f}{w}\right)'$ and we say that f has the second derivative in $B(\alpha)$ if $\left(\frac{f}{w}\right)''$ exists.

Let us define the average integral modulus of $f \in B(\alpha)$, such that:

$$\tau_k(f, \delta)_{p,\alpha} = \|\omega_k(f, ., \delta)_\alpha\|_p$$

$$= \| \sup_{|h| \leq \delta} | \Delta_h^k f(t)| \|_{p,\alpha} \quad \ldots(11)$$

The degree of best approximation to a given function $f \in B(\alpha)$ with trigonometric polynomials or with algebraic polynomials on the interval X is given by:

$$E_n(f)_{p,\alpha} = \inf \{\|f - Q\|_{p,\alpha} : Q \in P_n\} \quad \ldots(12)$$

Where P_n denotes the set of all trigonometric polynomials or algebraic polynomials of degree at most n .

Bernstein polynomial of $f \in B(\alpha)$ is defined by:

$$B_n(f, x) = \sum_{k=0}^{n} f\left(\frac{k}{n}\right) P_{n,k}(x) \qquad \ldots(13)$$

$$P_{n,k}(x) = C_k^n x^k (1-x)^{n-k}$$

for $x \in [0, 1]$, let us define:

$$\Delta(x, \delta) = \delta\Phi(x) + \delta^2, \ \Phi(x) = \sqrt{x(1-x)} \qquad \ldots(14)$$

$$\Delta(x) = \frac{\sqrt{\phi(x)}}{\sqrt{n} + \frac{1}{2n}}, \ \phi(x) = 1 - \frac{x^2}{2} \qquad \ldots(15)$$

The ordinary Ditzian-Totik modulus of smoothness for $f \in B(\alpha)$, is defined as follows:

$$\omega_r^{\phi}(f, x, \delta)_{p,\alpha} = \sup_{0 \le h \le \delta} \| \Delta_{h\phi}^r f(.) \|_{p,\alpha} \qquad \ldots(16)$$

where:

$$\Delta_{h\phi(.)}^r f(x) = \begin{cases} \sum_{i=0}^{r} (-1)^{i+r} C_i^r f(x + i\phi h), & x + i\phi h \in [0,1] \\ 0, & x + i\phi h \notin [0,1] \end{cases}$$

The locally Ditzian-Totik modulus of smoothness for $f \in B(\alpha)$ is defined as follows:

$$\omega_r^{\phi}(f,x,\delta)_{\alpha} = \sup_{0 \le h \le \delta} \{ | \Delta_{h\phi(.)}^r \frac{f(t)}{w(\alpha,t)} | : t, t+r\phi h \in [x - \frac{r\delta}{2}, x + \frac{r\delta}{2}] \cap X \} \qquad \ldots(17)$$

The average Ditzian-Totik modulus of smoothness for $f \in B(\alpha)$ is given by:

$$\tau_r^{\phi}(f, \delta)_{p,\alpha} = \| \omega_r^{\phi}(f, . , \delta)_{\alpha} \|_p \qquad \ldots(18)$$

Let $w_p^r[a,b]$ be the set of all functions f on [a, b], such that $f^{(r-1)}$ are absolutely continuous and $f^{(r)} \in L_p$ and $w_{p,\alpha}^r[a,b]$ be the set of all functions f on [a, b], such that $\left(\frac{f}{w}\right)^{(r-1)}$ are absolutely continuous and $\left(\frac{f}{w}\right)^{(r)}$ exists and integrable.

Consider now (see [4]):

$$S_u(x) = \begin{cases} u(x-1), & 0 \le u \le x \le 1 \\ x(u-1), & 0 \le x \le u \le 1 \end{cases} \quad \ldots(19)$$

Some theorems and lemmas needed in this work are listed as follows:

Theorem (A), [5]:

If $f, g \in L_p$, $1 \le p \le \infty$, then:

$$\|f+g\|_p \le \|f\|_p + \|g\|_p \quad \ldots(20)$$

$$\left(\int_X |fg|^p \, dx\right)^{1/p} \le \left(\int_X |f|^p \, dx\right)^{1/p} \left(\int_X |g|^q \, dx\right)^{1/q}, \frac{1}{p}+\frac{1}{q}=1, (1\le q\le\infty) \ldots(21)$$

Theorem (B), [6]:

If f is a bounded measurable function on [a, b], $a, b \in \square$; then:

$$\int_a^b f(x)dx \approx \frac{b-a}{n}\sum_{i=1}^{n} f(x_i) \quad \ldots(22)$$

where $x_i = a + \dfrac{(b-a)(2i-1)}{2n}$.

Lemma (1):

Let $f, g \in B(\alpha)$, $(1 \le p \le \infty)$, $\delta > 0$ then:

$$\tau_k(f,\delta)_{p,\alpha} \le \tau_k((f-g),\delta)_{p,\alpha} + \tau_k(g,\delta)_{p,\alpha} \quad \ldots(23)$$

Proof:

$$\tau_k(f,\delta)_{p,\alpha} = \|\omega_k(f,.,\delta)_\alpha\|_p$$

$$= \left\| \sup_{|h|\le\delta} \left\{ \left| \Delta_h^k \frac{f(t)}{w(\alpha,t)} \right| : t, t+kh \in \left[x-k\frac{h}{2}, x+k\frac{h}{2} \right] \cap X \right\} \right\|_p$$

Then:

$$\tau_k(f,\delta)_{p,\alpha} = \tau_k(((f-g)+g,\delta)_{p,\alpha}$$

$$= \left\| \omega_k(((f-g)+g),.,\delta)_\alpha \right\|_p$$

$$= \left\| \sup_{|h|\le\delta} \left\{ \left| \Delta_h^k \frac{((f-g)+g)(t)}{w(\alpha,t)} \right| : t, t+kh \in \left[x-k\frac{h}{2}, x+k\frac{h}{2} \right] \cap X \right\} \right\|_p$$

$$= \left\| \sup_{|h|\le\delta} \left\{ \left| \sum_{i=0}^{k} (-1)^{k+i} C_i^k \left(\frac{((f-g)(t+ih)+g(t+ih))}{w(\alpha,t+ih)} \right) \right| \right\} \right\|_p$$

$$\leq \left\| \sup_{|h|\leq\delta} \left\{ \left| \sum_{i=0}^{k} (-1)^{k+i} C_i^k \frac{(f-g)(t+ih)}{w(\alpha,t+ih)} \right| + \left| \sum_{i=0}^{k} (-1)^{k+i} C_i^k \frac{g(t+ih)}{w(\alpha,t+ih)} \right| \right\} \right\|_p$$

$$= \left\| \sup_{|h|\leq\delta} \left| \sum_{i=0}^{k} (-1)^{k+i} C_i^k \frac{(f-g)(t+ih)}{w(\alpha,t+ih)} \right| + \sup_{|h|\leq\delta} \left| \sum_{i=0}^{k} (-1)^{k+i} C_i^k \frac{g(t+ih)}{w(\alpha,t+ih)} \right| \right\|_p$$

$$\leq \left\| \sup_{|h|\leq\delta} \left\{ \left| \sum_{i=0}^{k} (-1)^{k+i} C_i^k \frac{(f-g)(t+ih)}{w(\alpha,t+ih)} \right| \right\} \right\|_p + \left\| \sup_{|h|\leq\delta} \left\{ \left| \sum_{i=0}^{k} (-1)^{k+i} C_i^k \frac{g(t+ih)}{w(\alpha,t+ih)} \right| \right\} \right\|_p$$

$$= \left\| \sup_{|h|\leq\delta} \left| \Delta_h^k \frac{(f-g)(t)}{w(\alpha,t)} \right| \right\|_p + \left\| \sup_{|h|\leq\delta} \left| \Delta_h^k \frac{g(t)}{w(\alpha,t)} \right| \right\|_p$$

$$= \|\omega_k((f-g), ., \delta)_\alpha\|_p + \|\omega_k(g, ., \delta)_\alpha\|_p$$

$$= \tau_k((f-g), \delta)_{p,\alpha} + \tau_k(g, \delta)_{p,\alpha}. \quad \blacksquare$$

Lemma (2):

Let $f \in B(\alpha)$, $(1 \leq p \leq \infty)$, then:

$$\tau_k(f, \delta)_{p,\alpha} \leq c\|f\|_{p,\alpha} \ , \qquad c, \delta > 0 \qquad \ldots(24)$$

Proof:

$$\tau_k(f, \delta)_{p,\alpha} = \|\omega_k(f, ., \delta)_\alpha\|_p$$

$$= \left\| \sup_{|h|\leq\delta} \left\{ \left| \Delta_h^k \frac{f(t)}{w(\alpha,t)} \right| : t, t+kh \in \left[x - k\frac{h}{2}, x + k\frac{h}{2} \right] \cap X \right\} \right\|_p$$

$$= \left\| \sup_{|h|\leq\delta} \left\{ \left| \sum_{i=0}^{k} (-1)^{k+i} C_i^k \frac{f(t+ih)}{w(\alpha,t+ih)} \right| : t, t+kh \in \left[x - k\frac{h}{2}, x + k\frac{h}{2} \right] \cap X \right\} \right\|_p$$

$$\leq 2^k \left\| \frac{f(.)}{w(\alpha,.)} \right\|_p \qquad \text{(see [3])}$$

$$= c\|f\|_{p,\alpha}. \quad \blacksquare$$

Lemma (3):

If $f \in L_p$, $(1 \leq p \leq \infty)$, then:

$$\|f\|_{\delta,p} \leq c(p)\|f\|_p \qquad \ldots(25)$$

Where $c(p)$ is a positive constant dependes on p

Proof:

From the definition of $\|f\|_{\delta,p}$ and (22) and (3), we have:

$$\|f\|_{\delta,p} = \left[\int_X \left(\sup \left\{ |f(y)| : y \in \left[x - \frac{\delta}{2}, x + \frac{\delta}{2} \right] \right\} \right)^p dy \right]^{1/p}$$

$$\leq \left[\frac{b-a}{n} \sum_{i=0}^{n} |\sup f(x_i)|^p \right]^{1/p}$$

$$= \left[\frac{c}{n} \sum_{i=0}^{n} |f(x_i)|^p \right]^{1/p}$$

$$\leq c(p)\, \|f\|_{L_p^n(X)}$$

$$\leq c(p)\, \|f\|_p. \quad \blacksquare$$

Lemma (4):

If $f, g \in B(\alpha)$, $1 \leq p \leq \infty$, then:

$$\|f + g\|_{p,\alpha} \leq \|f\|_{p,\alpha} + \|g\|_{p,\alpha} \qquad \ldots(26)$$

$$\|fg\|_{p,\alpha} \leq \|f\|_{p,\alpha}\|g\|_{q,\alpha}, \quad \frac{1}{p} + \frac{1}{q} = 1,\ 1 \leq q \leq \infty, \qquad \ldots(27)$$

Proof:

Since $f, g \in B(\alpha)$, then $f(x)/w(\alpha, x)$ and $g(x)/w(\alpha, x)$ are bounded. Let:

$$H(x) = f/w(\alpha, x)$$

$$G(x) = g/w(\alpha, x)$$

$$\|f + g\|_{p,\alpha} = \|f(.)/w(\alpha, .) + g(.)/w(\alpha, .)\|_p$$

$$= \|H + G\|_p$$

by using (20), we get:

$$\|f + g\|_{p,\alpha} \le \|H\|_p + \|G\|_p$$
$$= \|f/w(\alpha, .)\|_p + \|g/w(\alpha, x)\|_p$$
$$= \|f\|_{p,\alpha} + \|g\|_{p,\alpha}$$

which prove (26).

Now, to prove (27)

$$\|fg\|_{p,\alpha} = \|(f(.)/w(\alpha, .)) \cdot (g(.)/w(\alpha, .))\|_p$$
$$= \|HG\|_p$$

By using (21), we get:

$$\|fg\|_{p,\alpha} \le \|H\|_p \|G\|_q, \quad \frac{1}{p} + \frac{1}{q} = 1$$
$$= \|f(.)/w(\alpha, .)\|_p \, \|g(.)/w(\alpha, .)\|_q$$
$$= \|f\|_{p,\alpha} \, \|g\|_{q,\alpha}$$

That is:

$$\|fg\|_{p,\alpha} \le \|f\|_{p,\alpha} \, \|g\|_{q,\alpha}, \quad \frac{1}{p} + \frac{1}{q} = 1. \quad \blacksquare$$

Lemma (5), [5]:

S_u has the following properties:

$$(B_n(S_u, x) - S_u(x)) \ge 0 \qquad \ldots(28)$$

$$\int_0^1 (B_n(S_u, x) - S_u(x))\, dx \le n^{-1}\phi(u) \qquad \ldots(29)$$

Lemma (6), [4]:

Let $n \in N$ and $g \in w_p^2[0, 1]$, then:

$$B_n(g, x) - g(x) = \int_0^1 (B_n(S_u, x) - S_u(x))g''\, du, \; 0 \le x \le 1 \qquad \ldots(30)$$

MAIN RESULTS

We attempt to prove a direct and inverse theorems in $L_{p,\alpha}[0,1]$, $1 \le p \le \infty$; for Bernstein operator $B_n(f)$ in terms of Ditzian modulus of smoothness.

Theorem (I) (Direct Inequality):

If $f \in B(\alpha),(1 \le p \le \infty)$, then:

$$\|f(.) - B_n(f,.)\|_{p,\alpha} \le c\,\omega_2^{\phi}(f, x, \delta)_{p,\alpha} + \tau_2^{\phi}(f, \delta)_{p,\alpha}$$

Where c is a positive constant

Theorem (II) (Inverse Inequality):

If $f \in B(\alpha),(1 \le p \le \infty)$, then:

$$\tau_2^{\phi}\left(f, \Delta\left(., \frac{1}{n}\right)\right)_{p,\alpha} \le \frac{1}{n}\sum_{k=0}^{n} \|f - B_k(f)\|_{p,\alpha}$$

The following lemmas are needed to prove our theorems:

Lemma (7):

Let $n \in N$ and $g \in w_p^r[a, b]$, $1 \le p \le \infty$, then:

$$\|B_n(g) - g\|_p \le \frac{1}{n}\|\phi g''\|_p \qquad \ldots(31)$$

Proof:

Consider the linear operator:

$$T\left(\frac{f}{w}\right) = \int_0^1 (B_n(S_u, x) - S_u(x))\frac{1}{\phi(u)}\frac{f(u)}{w(\alpha, u)}\,du$$

Let $G = \dfrac{f}{w}$

Then:

$$\|T(G)\|_p = \left\|\int_0^1 (B_n(S_u,.) - S_u(.))\frac{1}{\phi(u)}G(u)\,du\right\|_p$$

$$= \left[\int_0^1 \left|\int_0^1 (B_n(S_u, x) - S_u(x))\frac{1}{\phi(u)}G(u)\,du\right|^p dx\right]^{1/p}$$

By using (29) and Holder inequality, we get:

$$\|T(G)\|_p \le \left[\int_0^1 \left|n^{-1}\phi(u)\frac{1}{\phi(u)}G(u)\right|^p du\right]^{1/p}$$

$$\leq \frac{1}{n}\left[\int_0^1 |G|^p \, du\right]^{1/p}$$

$$= \frac{1}{n} \|G\|_p$$

Let $G = \phi g''$

By using (30), we obtain:

$$\|T(\phi g'')\|_p = \left\| \int_0^1 (B_n(S_u,.) - S_u(.)) \frac{1}{\phi(u)} \phi(u) g''(u) \, du \right\|_p$$

$$= \|B_n(g) - g\|_p$$

So that:

$$\|B_n(g) - g)\|_p = \|T(\phi g'')\|_p$$

$$\leq \frac{1}{n} \|\phi g''\|_p. \quad \blacksquare$$

Lemma (8):

Let $F \in w_p^2[a, b]$, $1 \leq p \leq \infty$, then:

$$\|(\Delta)^2 F''\|_p \leq \frac{c}{n^p} \omega_2^{\phi}(f, x, \delta)_{p,\alpha} \qquad \ldots(32)$$

Proof:

Setting:

$$F(x) = \frac{1}{n^{1+p}} \sum_{i=1,2} (-1)^{3-i} C_i^2 \left(\frac{2}{\phi ih}\right)^2 \int_0^{\frac{\phi ih}{2}} \int_0^{\frac{\phi ih}{2}} \frac{\phi^{-1}(x) f(x + u_1 + u_2)}{w(\alpha, x)} \, du_1 du_2$$

where $h = \frac{1}{n}$

$$F''(x) = \frac{\phi^{-1}}{n^{1+p}} \sum_{i=1,2} (-1)^{3-i} C_i^2 \left(\frac{2}{\phi ih}\right)^2 \Delta_{\frac{\phi ih}{2}}^2 \frac{f(x)}{w(\alpha, x)}$$

From (15), we have:

$$\|(\Delta)^2.F''\|_p = \left\| \left(\frac{\sqrt{\phi(.)}}{\sqrt{n} + \frac{1}{2n}} \right)^2 .F'' \right\|_p$$

$$\leq \left\| \frac{\phi}{n} \frac{\phi^{-1}}{n^{1+p}} \sum_{i=1,2} (-1)^{3-i} C_i^2 \left(\frac{2}{\phi i h} \right)^2 \Delta^2_{\frac{\phi i h}{2}} \frac{f(.)}{w(\alpha,.)} \right\|_p$$

$$\leq \frac{1}{n^{2+p}} \left\| 8\Delta^2_{\frac{\phi h}{2}} \frac{f(.)}{w(\alpha,.)} - \Delta^2_{\phi h} \frac{f(.)}{w(\alpha,.)} \right\|_p$$

$$\leq \frac{c}{n^{2+p}} \left(\left\| \Delta^2_{\frac{\phi h}{2}} \frac{f(.)}{w(\alpha,.)} \right\|_p + \left\| \Delta^2_{\phi h} \frac{f(.)}{w(\alpha,.)} \right\|_p \right)$$

$$\leq \frac{c}{n^{2+p}} \left(\sup_{h \leq \delta} \left\| \Delta^2_{\frac{\phi h}{2}} \frac{f(.)}{w(\alpha,.)} \right\|_p + \sup_{h \leq \delta} \left\| \Delta^2_{\phi h} \frac{f(.)}{w(\alpha,.)} \right\|_p \right)$$

$$\leq \frac{c}{n^{2+p}} \omega_2^{\phi} (f, x, \delta)_{p,\alpha}$$

$$\leq \frac{c}{n^{p}} \omega_2^{\phi} (f, x, \delta)_{p,\alpha}. \quad \blacksquare$$

Lemma (9):

If $f \in B(\alpha)$, $1 \leq p < \infty$, then:

$$\left| F(x) - \frac{f(x)}{w(\alpha, x)} \right| \leq 2\ \omega_2^{\phi}(f, x + \phi h, \phi h)_{\alpha}. \qquad \ldots(33)$$

Proof:

$$\left| F(x) - \frac{f(x)}{w(\alpha, x)} \right| = \left| \frac{\phi^{-1}(x)}{n^{1+p}} \sum_{r=1,2} (-1)^{3-r} C_r^2 \left(\frac{2}{r h \phi} \right)^2 \int_0^{\frac{r h \phi}{2}} \int_0^{\frac{r h \phi}{2}} \frac{f(x + u_1 + u_2)}{w(\alpha, x)} du_1 du_2 - \frac{f(x)}{w(\alpha, x)} \right|, \ h = 1/n$$

$$\leq \left| \sum_{r=1,2} (-1)^{2-r} C_r^2 (\phi h)^{-2} \int_0^{\phi h}\int_0^{\phi h} \frac{f\left(x + r\left(\frac{t_1+t_2}{2}\right)\right)}{w(\alpha,x)}\, dt_1 dt_2 + \frac{f(x)}{w(\alpha,x)} \right|$$

$$\leq \left| (\phi h)^{-2} \int_0^{\phi h}\int_0^{\phi h} \sum_{r=0}^{2} (-1)^{2-r} C_r^2 \frac{f\left(x + r\left(\frac{t_1+t_2}{2}\right)\right)}{w(\alpha,x)}\, dt_1 dt_2 \right|$$

$$\leq (\phi h)^{-2} \int_0^{\phi h}\int_0^{\phi h} \left| \Delta^2_{\frac{t_1+t_2}{2}} \frac{f(x)}{w(\alpha,x)} \right| dt_1 dt_2$$

Let $t_1 = 2u_1 - u_2$ and $t_2 = u_2$, we obtain:

$$\left| F(x) - \frac{f(x)}{w(\alpha,x)} \right| \leq 2(\phi h)^{-2} \int_0^{\phi h}\int_0^{\phi h} \left| \Delta^2_{u_1} \frac{f(x)}{w(\alpha,x)} \right| du_1 du_2$$

$$\leq 2(\phi h)^{-1} \int_0^{\phi h} \left| \Delta^2_{u} \frac{f(x)}{w(\alpha,x)} \right| du$$

$$\leq 2(\phi h)^{-1} \int_0^{\phi h} \sup_{0\leq u\leq \phi h} \left| \Delta^2_{u} \frac{f(x)}{w(\alpha,x)} \right| du$$

$$= 2\,\omega_2^{\phi}(f, x + \phi h, \phi h)_{\alpha}. \quad \blacksquare$$

Lemma (10):

If $f \in B(\alpha)$, $(1 \leq p \leq \infty)$, $n \geq 2$, then:

$$\| B_n(F,.) - B_n(f,.)/w(\alpha,.) \|_p \leq c\ \tau_2^{\phi}(f, \delta)_{p,\alpha} \qquad \ldots(34)$$

Proof:

$$\| B_n(F) - B_n(f)/w(\alpha,.) \|_p = \left[\int_0^1 \left| \sum_{k=0}^{n} \left(F\left(\frac{k}{n}\right) - \frac{f\left(\frac{k}{n}\right)}{w\left(\alpha, \frac{k}{n}\right)} \right) p_{n,k}(x) \right|^p dx \right]^{1/p}$$

By using (33), we get:

$$\|B_n(F) - B_n(f)/w(\alpha,.)\|_p \le \left[c\int_0^1 \left| \sum_{k=0}^{n} \omega_2^{\phi}\left(f, \frac{k+\phi}{n}, \delta \right)_{\alpha} p_{n,k}(x) \right|^p dx \right]^{1/p}$$

$$\le c_p \left(\sum_{k=0}^{n} \int_0^1 \left| \omega_2^{\phi}\left(f, \frac{k+\phi}{n}, \delta \right)_{\alpha} \right|^p dx \right)^{1/p}$$

$$\left(\int_0^1 \left(p_{n,k}(x) \right)^q dx \right)^{1/q}, \quad \ni \frac{1}{p} + \frac{1}{q} = 1$$

$$= M_1 M_2,\ M_2 = c$$

$$M_1 \le c_p \left(\sum_{k=0}^{n} \int_{k/n}^{(k+1)/n} \left| \omega_2^{\phi}(f, x+\phi h, \delta)_{\alpha} \right|^p dx \right)^{1/p}, \quad h = \frac{1}{n}$$

$$\le c_p \left(\int_0^{1+h} \left| \omega_2^{\phi}(f, x+\phi h, \delta)_{\alpha} \right|^p dx \right)^{1/p}$$

$$= \tau_2^{\phi}(f, \delta)_{p,\alpha}. \quad \blacksquare$$

Lemma (11):

Let $n \in N$ and $F \in w_p^2[a, b]$, $1 \le p < \infty$, then:

$$\|F - B_n(F)\|_p \le c\ \omega_2^{\phi}(f, x, \delta)_{p,\alpha} \qquad \ldots(35)$$

Proof:

From (31) and (32), we obtain:

$$\|F - B_n(F)\|_p \le \frac{1}{n} \|\phi F''\|_p$$

$$\le \frac{1}{n} \|(\Delta)^2 F''\|_p$$

$$\le c\ \omega_2^{\phi}(f, x, \delta)_{p,\alpha}. \quad \blacksquare$$

Lemma (12), [2]:

If $1 \le p, p' \le \infty$, $g \in w_p^k[0, 1]$, then:

$$\tau_k(g, \Delta(\delta))_p \le c_k \|\Delta(\delta)^k g^{(k)}\|_{p'} \qquad \ldots(36)$$

Lemma (13), [2]:

If $f \in R$, $g \in w_p^2[0, 1]$, then:

$$\|\Phi^2 B_n''(f)\|_p \le cn\|f\|_{\frac{1}{n},p} \quad \ldots(37)$$

$$\|B_n''(f)\|_p \le cn^2\|f\|_{\frac{1}{n},p} \quad \ldots(38)$$

$$\|\Phi^2 B_n''(g)\|_p \le \left\|\left(\Phi^2 + \frac{1}{n}\right)g''\right\|_p \quad \ldots(39)$$

$$\|B_n''(g)\|_p \le \|g''\|_p \quad \ldots(40)$$

Lemma (14):

If $g \in w_{p,\alpha}^k[0, 1]$, $1 \le p \le \infty$, then:

$$\tau_k(g, \Delta(\delta))_{p,\alpha} \le c_k\|\Delta(\delta)^k g^{(k)}\|_{p,\alpha} \quad \ldots(41)$$

Proof:

$$\tau_k(g, \Delta(\delta))_{p,\alpha} = \|\omega_k(g, ., \Delta(\delta))_\alpha\|_p$$
$$= \|\omega_k(G, ., \Delta(\delta))\|_p$$

where $G = \dfrac{g(.)}{w(\alpha,.)}$

$\therefore \tau_k(g, \Delta(\delta))_{p,\alpha} = \tau_k(G, \Delta(\delta))_p$

by using (36), we get:

$$\tau_k(g, \Delta(\delta))_{p,\alpha} \le c_k|\Delta(\delta)^k G^{(k)}\|_p$$
$$= c_k\|\Delta(\delta)^k g^{(k)}\|_{p,\alpha}. \quad \blacksquare$$

Lemma (15):

If $f \in B(\alpha)$, $n \in \square$, then:

$$\left\|\Delta\left(.,\frac{1}{n}\right)^2 B_n''(f)\right\|_{p,\alpha} \le c\left(n^{-1}\|\Phi^2(.)B_n''(f)\|_{p,\alpha} + n^{-2}\|B_n''(f)\|_{p,\alpha}\right) \quad \ldots(42)$$

Proof:

By using the definition of $\Delta\left(.,\frac{1}{n}\right)$, we get (42). $\blacksquare$

Lemma (16):

If $f \in B(\alpha)$, $g \in w^2_{p,\alpha}[0, 1]$, then:

$$\|\Phi^2 B_n''(f)\|_{p,\alpha} \le cn\|f\|_{p,\alpha} \quad \ldots(43)$$

$$\|B_n''(f)\|_{p,\alpha} \le cn^2\|f\|_{p,\alpha} \quad \ldots(44)$$

$$\|\Phi^2 B_n''(g)\|_{p,\alpha} \le \left\|\left(\Phi^2 + \frac{1}{n}\right)g''\right\|_{p,\alpha} \quad \ldots(45)$$

$$\|B_n''(g)\|_{p,\alpha} \le \|g''\|_{p,\alpha} \quad \ldots(46)$$

Proof:

To prove (43):

$$\|\Phi^2 B_n''(f)\|_{p,\alpha} = \quad = \left[\int_0^1 \left|\Phi^2 \frac{B_n''(f,x)}{w(\alpha,x)}\right|^p dx\right]^{1/p}$$

Let $G(x) = \dfrac{f(x)}{w(\alpha,x)}$, then:

$$\|\Phi^2 B_n''(f)\|_{p,\alpha} = \|\Phi^2 B_n''(G)\|_p$$

By using (37), we get:

$$\|\Phi^2 B_n''(f)\|_{p,\alpha} \le cn\|G\|_{\frac{1}{n},p}$$

From (25), we obtain:

$$\|\Phi^2 B_n''(f)\|_{p,\alpha} \le c'n\|G\|_p$$

$$= c'n\|f\|_{p,\alpha}$$

Analogously, we get (44).

To prove (45), we have the identity (see [7]):

$$\Phi^2 B_n'' f(x) = n^2 \sum_{k=1}^{n-1} \Delta^2_{\frac{1}{n}} f\left(\frac{k-1}{n}\right)\Phi^2\left(\frac{k}{n}\right)p_{k,n}(x)$$

for $f = \dfrac{g}{w}$, we get:

$$\Phi^2 B_n''\left(\frac{g}{w}\right)(x) = n^2 \sum_{k=1}^{n-1} \Delta^2_{\frac{1}{n}}\left(\frac{g}{w}\right)\left(\frac{k-1}{n}\right)\Phi^2\left(\frac{k}{n}\right)p_{k,n}(x)$$

Note that $\Phi^2(y) \le \Phi^2(z) + \dfrac{1}{n}$, if $|y - z| \le \dfrac{1}{n}$

So for $g \in B(\alpha)$, such that $\left(\frac{g}{w}\right)''$ exists and belong to $w_p^2[0, 1]$ we get :

$$\left|\Delta_{\frac{1}{n}}^2\left(\frac{g}{w}\right)\left(\frac{k-1}{n}\right)\right|\Phi^2\left(\frac{k}{n}\right) \le \Phi^2\left(\frac{k}{n}\right)\int_{-\frac{1}{2n}}^{\frac{1}{2n}}\int_{-\frac{1}{2n}}^{\frac{1}{2n}}\left|\left(\frac{g}{w}\right)''\left(\frac{k}{n}+s+t\right)\right|dsdt$$

$$\le \int_{-\frac{1}{2n}}^{\frac{1}{2n}}\int_{\frac{k}{n}+t-\frac{1}{2n}}^{\frac{k}{n}+t+\frac{1}{2n}}\left(\Phi^2(v)+\frac{1}{n}\right)\left|\left(\frac{g}{w}\right)''(v)\right|dvdt \quad ...(47)$$

From (47) and by using Jensen inequality and Holder inequality two times, we get:

$$\left\|\Phi^2 B_n''\frac{g}{w}\right\|_p^p = n^{2p}\int_0^1\left|\sum_{k=1}^{n-1}\Delta_{\frac{1}{n}}^2\left(\frac{g}{w}\right)\left(\frac{k-1}{n}\right)\Phi^2\left(\frac{k}{n}\right)p_{k,n}(x)\right|^p dx$$

$$\le n^{2p}\sum_{k=1}^{n-1}\left|\Delta_{\frac{1}{n}}^2\left(\frac{g}{w}\right)\left(\frac{k-1}{n}\right)\Phi^2\left(\frac{k}{n}\right)\right|^p\int_0^1 p_{k,n}(x)dx$$

$$\le n^{2p-1}\sum_{k=1}^{n-1}\left(\int_{-\frac{1}{2n}}^{\frac{1}{2n}}\int_{\frac{k}{n}+t-\frac{1}{2n}}^{\frac{k}{n}+t+\frac{1}{2n}}\left(\Phi^2(v)+\frac{1}{n}\right)\left|\left(\frac{g}{w}\right)''(v)\right|dvdt\right)^p$$

$$\le n^{2p-1}\sum_{k=1}^{n-1}\int_{-\frac{1}{2n}}^{\frac{1}{2n}}\left(\int_{\frac{k}{n}+t-\frac{1}{2n}}^{\frac{k}{n}+t+\frac{1}{2n}}\left(\Phi^2(v)+\frac{1}{n}\right)\left|\left(\frac{g}{w}\right)''(v)\right|dv\right)^p dt\left(\frac{1}{n}\right)^{p-1}$$

$$\le n^p\sum_{k=1}^{n-1}\int_{-\frac{1}{2n}}^{\frac{1}{2n}}\int_{\frac{k}{n}+t-\frac{1}{2n}}^{\frac{k}{n}+t+\frac{1}{2n}}\left(\Phi^2(v)+\frac{1}{n}\right)^p\left|\left(\frac{g}{w}\right)''(v)\right|^p dv\left(\frac{1}{n}\right)^{p-1}dt$$

$$\le n\int_{-\frac{1}{2n}}^{\frac{1}{2n}}\left(\sum_{k=1}^{n-1}\int_{\frac{k}{n}+t-\frac{1}{2n}}^{\frac{k}{n}+t+\frac{1}{2n}}\left(\Phi^2(v)+\frac{1}{n}\right)^p\left|\left(\frac{g}{w}\right)''(v)\right|^p dv\right)dt$$

$$= n\int_{-\frac{1}{2n}}^{\frac{1}{2n}}\int_{t+\frac{1}{2n}}^{1+t-\frac{1}{2n}}\left(\Phi^2(v)+\frac{1}{n}\right)^p\left|\left(\frac{g}{w}\right)''(v)\right|^p dvdt$$

$$\leq n \int_{-\frac{1}{2n}}^{\frac{1}{2n}} \int_{0}^{1} \left(\Phi^2(v) + \frac{1}{n} \right)^p \left| \left(\frac{g}{w} \right)'' (v) \right|^p dv\,dt$$

$$= \left\| \left(\Phi^2(.) + \frac{1}{n} \right) \left(\frac{g}{w} \right)'' (.) \right\|_p^p$$

Then:

$$\left\| \Phi^2 B_n'' \frac{g}{w} \right\|_p \leq \left\| \left(\Phi^2(.) + \frac{1}{n} \right) \left(\frac{g}{w} \right)'' (.) \right\|_p$$

This implies that:

$$\left\| \Phi^2 B_n'' g \right\|_{p,\alpha} \leq \left\| \left(\Phi^2 + \frac{1}{n} \right) g'' \right\|_{p,\alpha}$$

Now, to prove (46) using that (see [2])

$$\sum_{k=1}^{n-1} \Phi^{-2}(x) \Phi^2 \left(\frac{k}{n} \right) p_{k,n}(x) = \frac{n-1}{n}, \; x \in [0, 1]$$

and

$$\int_0^1 \Phi^{-2}(x) \Phi^2 \left(\frac{k}{n} \right) p_{k,n}(x)\, dx \leq \frac{1}{n}$$

we get:

$$\left\| B_n'' \frac{g}{w} \right\|_p^p = n^{2p} \left\| \sum_{k=1}^{n-1} \Phi^{-2}(x) \Phi^2 \left(\frac{k}{n} \right) p_{k,n}(x) \Delta_{\frac{1}{n}}^2 \left(\frac{g}{w} \right) \left(\frac{k-1}{n} \right) \right\|_p^p$$

$$\leq n^{2p} \left(\frac{n-1}{n} \right)^{p-1} \sum_{k=1}^{n-1} \left| \Delta_{\frac{1}{n}}^2 \left(\frac{g}{w} \right) \left(\frac{k-1}{n} \right) \right|^p \int_0^1 \Phi^{-2}(x) \Phi^2 \left(\frac{k}{n} \right) p_{k,n}(x)\, dx$$

$$\leq n^{2p-1} \sum_{k=1}^{n-1} \left| \Delta_{\frac{1}{n}}^2 \left(\frac{g}{w} \right) \left(\frac{k-1}{n} \right) \right|^p$$

$$\leq n^{2p-1} \sum_{k=1}^{n-1} \left(\int_{-\frac{1}{2n}}^{\frac{1}{2n}} \int_{\frac{k}{n}+t-\frac{1}{2n}}^{\frac{k}{n}+t+\frac{1}{2n}} \left| \left(\frac{g}{w} \right)'' (v) \right| dv\,dt \right)^p$$

$$\leq n^{2p-1}\sum_{k=1}^{n-1}\int_{-\frac{1}{2n}}^{\frac{1}{2n}}\left(\int_{\frac{k}{n}+t-\frac{1}{2n}}^{\frac{k}{n}+t+\frac{1}{2n}}\left|\left(\frac{g}{w}\right)''(v)\right|dv\right)^{p}dt\left(\frac{1}{n}\right)^{p-1}$$

$$\leq n^{p}\sum_{k=1}^{n-1}\int_{-\frac{1}{2n}}^{\frac{1}{2n}}\int_{\frac{k}{n}+t-\frac{1}{2n}}^{\frac{k}{n}+t+\frac{1}{2n}}\left|\left(\frac{g}{w}\right)''(v)\right|^{p}dv\left(\frac{1}{n}\right)^{p-1}dt$$

$$= n\int_{-\frac{1}{2n}}^{\frac{1}{2n}}\int_{t-\frac{1}{2n}}^{1+t-\frac{1}{2n}}\left|\left(\frac{g}{w}\right)''(v)\right|^{p}dv\,dt$$

$$\leq \left\|\left(\frac{g}{w}\right)''\right\|_{p}^{p}$$

Then:

$$\left\|B_n''\frac{g}{w}\right\|_{p} \leq \left\|\left(\frac{g}{w}\right)''\right\|_{p}$$

This implies that:

$$\|B_n''g\|_{p,\alpha} \leq \|g''\|_{p,\alpha}. \quad \blacksquare$$

Proof of Theorem (I):

$$\|f - B_n(f)\|_{p,\alpha} = \left\|\frac{f(.)-B_n(f,.)}{w(\alpha,.)}\right\|_{p}$$

$$= \left\|\frac{f(.)}{w(\alpha,.)} - F + F - B_n(F) + B_n(F) - \frac{B_n(f,.)}{w(\alpha,.)}\right\|_{p}$$

$$\leq \left\|\frac{f(.)}{w(\alpha,.)} - F\right\|_{p} + \left\|F - B_n(F)\right\|_{p} + \left\|B_n(F) - \frac{B_n(f,.)}{w(\alpha,.)}\right\|_{p}$$

By using (33), (35) and (34), we get:

$$\|f - B_n(f)\|_{p,\alpha} \leq 2\,\omega_2^{\phi}(f, x+\phi h, \phi h)_{\alpha} + c\;\omega_2^{\phi}(f, x, \delta)_{p,\alpha} + \tau_2^{\phi}(f, \delta)_{p,\alpha}$$

$$\leq c\;\omega_2^{\phi}(f, x, \delta)_{p,\alpha} + \tau_2^{\phi}(f, \delta)_{p,\alpha}. \quad \blacksquare$$

Proof of Theorem (II):

We will use the lemma in [8] to prove our theorem namely if μ_n, ν_n, $\psi_n \geq 0$, with $\mu_1 = \nu_1 = 0$ satisfying $(1 \leq k \leq n)$:

$$\mu_n \leq \left(\frac{k}{n}\right)\mu_k + \nu_k + \psi_k \qquad \ldots(48)$$

$$\nu_n \leq \left(\frac{k}{n}\right)^2 \nu_k + \psi_k \qquad \ldots(49)$$

Then it follows that:

$$\mu_n \leq \left(\frac{c'}{n}\right)\sum_{k=1}^{n}\psi_k \qquad \ldots(50)$$

Setting:

$$\mu_n = n^{-1}\|\Phi^2(.)B_n''(f)\|_{p,\alpha} + n^{-2}\|B_n''(f)\|_{p,\alpha}$$

$$\nu_n = n^{-2}\|B_n''(f)\|_{p,\alpha}$$

$$\psi_n = c''\|B_n(f) - f\|_{p,\alpha}$$

Then:

$$\mu_n \leq n^{-1}\|\Phi^2(.)B_n''(B_k(f))\|_{p,\alpha} + n^{-2}\|B_n''(B_k(f))\|_{p,\alpha} + n^{-1}\|\Phi^2(.)B_n''(B_k(f) - f)\|_{p,\alpha} + n^{-2}\|B_n''(B_k(f) - f)\|_{p,\alpha}$$

Now, by using (45), (46), (43) and (44) in lemma (16), we get:

$$\mu_n \leq n^{-1}\|(\Phi^2(.) + \frac{1}{n})B_k''(f))\|_{p,\alpha} + n^{-2}\|B_k''(f)\|_{p,\alpha} + n^{-1}[c_1 n\|B_k(f) - f\|_{p,\alpha}] + n^{-2}[c_2 n^2\|B_k(f) - f\|_{p,\alpha}]$$

$$\leq n^{-1}\|\Phi^2 B_k''(f)\|_{p,\alpha} + n^{-1}\|\frac{1}{n}B_k''(f)\|_{p,\alpha} + n^{-2}\|B_k''(f)\|_{p,\alpha} + c_1\|B_k(f) - f\|_{p,\alpha} + c_2\|B_k(f) - f\|_{p,\alpha}$$

$$= n^{-1}\|\Phi^2 B_k''(f)\|_{p,\alpha} + n^{-2}\|B_k''(f)\|_{p,\alpha} + n^{-2}\|B_k''(f)\|_{p,\alpha} + c_3\|B_k(f) - f\|_{p,\alpha}$$

$$= (n^{-1}k/k)\|\Phi^2 B_k''(f)\|_{p,\alpha} + (n^{-2}k^2/k^2)\|B_k''(f)\|_{p,\alpha} + (n^{-2}k^2/k^2)\|B_k''(f)\|_{p,\alpha} + c_3\|B_k(f) - f\|_{p,\alpha}$$

$$= (n^{-1}k)[k^{-1}\|\Phi^2 B_k''(f)\|_{p,\alpha} + (n^{-1}k^{-2}k)\|B_k''(f)\|_{p,\alpha}] + n^{-2}k^2\nu_k + \psi_k$$

$$\leq (n^{-1}k)[k^{-1}\|\Phi^2 B_k''(f)\|_{p,\alpha} + k^{-2}\|B_k''(f)\|_{p,\alpha}] + n^{-2}k^2\nu_k + \psi_k$$

$$= (n^{-1}k)\mu_k + (n^{-2}k^2)v_k + \psi_k$$

which prove (48)

Now, to prove (49), we get the following:

$$v_n \le n^{-2}\| B_n''(B_k(f))\|_{p,\alpha} + n^{-2}\| B_n''(B_k(f) - f)\|_{p,\alpha}$$

Then, by using (46) and (44) in lemma (16), we get:

$$v_n \le n^{-2}\| B_k''(f)\|_{p,\alpha} + n^{-2}(c_4n^2)\|B_k(f) - f\|_{p,\alpha}$$

$$= n^{-2}\| B_k''(f)\|_{p,\alpha} + c_4\|B_k(f) - f\|_{p,\alpha}$$

$$= (n^{-2}k^2/k^2)\,\| B_k''(f)\|_{p,\alpha} + \psi_k$$

$$\le (k/n)^2 v_k + \psi_k$$

From (48) and (49), we get (50)

Now, let m, n $\in$ N with $(n/2) \le m \le n$, such that:

$$\|B_m(f) - f\|_{p,\alpha} \le \|B_k(f) - f\|_{p,\alpha}, \text{ for any } (n/2) \le k \le n$$

By using (2.13) and (2.14), we obtain:

$$\tau_2\left(f, \Delta\left(.,\frac{1}{n}\right)\right)_{p,\alpha} \le \tau_2\left(f - B_m(f), \Delta\left(.,\frac{1}{m}\right)\right)_{p,\alpha} + \tau_2\left(B_m(f), \Delta\left(.,\frac{1}{m}\right)\right)_{p,\alpha}$$

$$\le c_5\|B_m(f) - f\|_{p,\alpha} + \tau_2\left(B_m(f), \Delta\left(.,\frac{1}{m}\right)\right)_{p,\alpha}$$

By using (41) and (42), we have:

$$\tau_2\left(f, \Delta\left(.,\frac{1}{n}\right)\right)_{p,\alpha} \le c_5\|B_m(f) - f\|_{p,\alpha} + c_6\|\Delta(., \frac{1}{m})^2 B_m''(f)\|_{p,\alpha}$$

$$\le c_5\|B_m(f) - f\|_{p,\alpha} + c_6c_7[m^{-1}\|\Phi^2 B_m(f)\|_{p,\alpha} + m^{-2}\| B_m''(f)\|_{p,\alpha}]$$

$$\le c_5\|B_m(f) - f\|_{p,\alpha} + c_8\mu_m$$

$$\le c_5\|B_k(f) - f\|_{p,\alpha} + c_8(c'/m)\sum_{k=1}^{m}\psi_k$$

$$\le c_5\|B_k(f) - f\|_{p,\alpha} + (c''/m)\sum_{k=1}^{m}\|B_k(f) - f\|_{p,\alpha}$$

$$\leq (c/n)\sum_{k=1}^{n} \|B_k(f) - f\|_{p,\alpha}$$

Since $\tau_2^{\phi}\left(f,\Delta\left(.,\frac{1}{n}\right)\right)_{p,\alpha} \leq \tau_2\left(f,\Delta\left(.,\frac{1}{n}\right)\right)_{p,\alpha}$, so that:

$$\tau_2^{\phi}\left(f,\Delta\left(.,\frac{1}{n}\right)\right)_{p,\alpha} \leq \frac{c}{n}\sum_{k=1}^{n} \|B_k(f) - f\|_{p,\alpha}. \quad \blacksquare$$

We found an equivalence between the degree of best approximation of a function $f \in B(\alpha)$ with respect to Bernstein polynomial and the average Ditzian – Totic modulus of smoothness

REFERENCES

1. Powell M. J., "Approximation theory and methods", Cambridge University (1981)
2. Jassim S. K., "On Bernstein Polynomials for Riemann Integrable Functions", Serdica Bulgarica Mathematics Publication,17,: 59-66, (1991).
3. Popov V. A. , Sendov B., "The Average Moduli of Smoothness", Wiley and Sons,(1988).
4. Bhaya E. S. ,"A Study on Approximation of Bounded Measurable Function with Some Discrete Series in L_p –Spaces ($0 < p \leq 1$) ", M.Sc. Thesis ,Baghdad University ,Department of Mathematics ,College of Education Ibn Al-Haitham,(1999).
5. Zygmund A. "Trigonometric Series ",Vol.I,II, Cambridge,(1958)
6. Sendov B. , popov V. A. ,"Average Modulus of Smoothness",Sofia, (1983).
7. Berens H. , Lorentz G. G., "Inverse Theorems for Bernstein Polynomials", Indiana Univ. Math. J.,21,: 693-708, (1972).
8. Ivanov K. G. ,"Approximation by Bernstein Polynomials in L_p-Metric ,$1 \leq p < \infty$ ", Constructive theory of Functions, 48, Buly ,Acad of Sci,: 421-429,(1984).

Relation between Earliness and Tardiness Problems

Tariq S. Abdul-Razaq and Manal G. Ahmed Al-Ayoubi
Mathematic Depatment, College of science, Al- Mustansiriyah University

Received : 13/04/2011 Accepted : 29/05/2011

الخلاصة

في هذا البحث تناولنا مسألة جدولةn من الاعمال على ماكنة واحده لمناقشة العلاقة بين مسألة التبكير والتأخير .وبما ان هاتين المسألتين من النوع الصعب , برهنا إن قاعدة EDD والتي فيها $E_i \leq P_i$ تعطي حل امثل للمسألة $1/C_i \leq d_i / \Sigma E_i$ وكانت النتيجة جيدة.وكذلك برهنا ان E_{max} و T_{max} مسألتان متكافئتان .خواص هاتان المسألتان اعطيت مع بعض الامثلة.

ABSTRACT

In this paper we consider the problem of scheduling n jobs on a single machine to discuss the relationship between earliness and tardiness problems (i.e., the problems $1/c_i \leq d_i/\sum E_i$ and $1/C_j \geq d_j/\sum T_j$). These two problems are NP-hard ,for special case we proved a good result that EDD rule with $E_i \leq P_i$ is optimal for $1/c_i \leq d_i/\sum E_i$ problem .

Also we proved that E_{max} and T_{max} are equivalent for $1/C_i \leq d_i/ E_{max}$ problem and $1/C_j \geq d_j/ T_{max}$ problem. The properties between earliness and tardiness problems are given with some examples.

INTRODUCTION

The two objectives $\sum E_i$ and $\sum T_i$ that are important in practice as well. The $1/ / \sum T_i$ problem has received an enormous amount of attention in the literature [1] ,[2],[3] .It is well know that the problems $1/ / \sum E_i$ and $1/ / \sum T_i$ and their generalizations $\sum W_i E_i$ and $\sum W_i T_i$ are NP-hard problems. Since the earliness objectives are non regular functions, hence there is a few studies to earliness problems.

The scheduling problem under consideration can be described as follows: there are n jobs to be scheduled on a single machine, which can handle one job at a time , each job i has a positive integer processing time P_i and a positive integer due date d_i .Job i (i=1,2,…..,n) becomes available for processing at time zero . The main object of this paper to prove the equivalence of the following problems :

$1/C_i \le d_i/\sum E_i$ and $1/C_i \ge d_i/\sum T_i$, $1/C_i \le d_i/E_{max}$ and $1/C_i \ge d_i/T_{max}$ where

$E_{max} = Max\{E_i\} = Max\{d_i\_c_i, 0\}$ and $T_{max} = Max\{T_i\} = Max\{C_i\_d_i, 0\}$.

In this paper in section one, we proved that $1/c_i \le d_i/E_{max}$ is equivalent to $1/c_j \ge d_j/T_{max}$. and we proved that EDD schedule with $E_i \le P_i$ is optimal for $1/c_i \le d_i/\sum E_i$ .In section two we showed the properties between earliness and tardiness problems with some examples for each case is given. In section three we showed the conclusion and future work.

The following lemma shows that the total earliness problem is equivalent to the total tardiness problem.

Lemma (1) [4]

The following measures are equivalent:

$$1\text{-}\sum_{i=1}^{n} E_i, \quad 2\text{-}\sum_{j=1}^{n} T_j.$$

Proof: Let $C=\sum_{j=1}^{n} p_j$, consider an instance of the total tardiness ($\sum_{j=1}^{n} T_j$) problem where $P_j = P_i$ and $d_j = C - d_i + P_i$ for j = 1, 2,…,n. Suppose that S is an optimal schedule for this instance. Define a new schedule S' as follows: If a job j is the k-th job scheduled in S, then i is the (n-k+1)th job scheduled in S',where S and S' are scheduled for the tardy and early jobs respectively.

Clearly, we have $C_j = C - C_i + P_i$ and hence

$T_j = \max\{C_j - d_j, 0\} = \max\{(C - C_i + P_i) - (C - d_i + P_i), 0\}$

$= \max\{d_i - C_i, 0\} = E_i$.

Therefore, the minimum total earliness is the same as the minimum total tardiness. Hence, as we know that the total tardiness problem on one machine is NP-hard [5], then the total earliness must also NP-hard.

It should be noted that in our problem $1/c_i \le d_i/\sum_{i=1}^{n} E_i$ every job i is either early or on time, but in the total tardiness problem $1/c_j \ge d_j/\sum_{j=1}^{n} T_j$, every job j is either tardy or on time.

Lemma (2)

E_{max} is equivalent to T_{max}

Proof:

Let $C=\sum_{j=1}^{n} p_j$, consider an instance of the total tardiness ($\sum_{j=1}^{n} T_j$) problem where $P_j = P_i$ and $d_j = C - d_i + P_i$ for j = 1, 2,…,n. Suppose S is an optimal schedule for this instance. Define a new schedule S' as follows:

If a job j is the k-th job scheduled in S, then i is the (n-k+1)th job scheduled in S'. Clearly, we have $C_j = C - C_i + P_i$ and hence

$T_{max} = \max\{T_j\} = \max\{\max\{ C_j - d_j, 0 \} \} = \max \{\max(C - C_i + P_i) - (C - d_i + P_i), 0 \} = \max \{ \max\{d_i - C_i, 0 \}\} = E_{max}$.

Theorem (1) If the EDD schedule with $T_j \le P_j$ for each job j is optimal for $1/c_j \ge d_j/\sum_{j=1}^{n} T_j$, then the EDD schedule with $d_i = C - d_j + P_j$ and with $E_i \le P_i$ is optimal for $1/c_i \le d_i/\sum_{i=1}^{n} E_i$ problem.

Proof:

Let S be the optimal schedule for $1/c_j \ge d_j/\Sigma T_j$ problem obtained by EDD rule for the due date d_i and with $Tj \le P_j$ for each j.

Now construct a schedule S' by EDD rule for $d_i = C - d_j + P_j$, where $C = \sum_{j=1}^{n} P_j$ and the completion time for each job i is given by $C_i = C - C_j + P_j$.

From lemma (1) the measures $\sum_{i=1}^{n} E_i$ and $\sum_{j=1}^{n} T_j$ are equivalent.

For the optimal schedule S, we have $T_j \le P_j$. Hence $C_j - d_j \le P_j$, using the definition of d_i and C_i in the schedule S' we have for each job i

$T_j = C_j - d_j = (C + P_j - C_i) - (C + P_j - d_i) = d_i - C_i = E_i \le P_j$ and $P_i = P_j$

Then $E_i \le P_i$.

Hence the EDD schedule with $E_i \le P_i$ for each job i is optimal for $1/c_i \le d_i/\sum_{i=1}^{n} E_i$.

Now we will give some examples to show some of the important properties between the earliness and tardiness problem which is given in the above results.

Example (1) Consider the earliness problem with six job.

We now show that the earliness and tardiness are equivalent with the following six-job, for which the processing times and due dates are shown in the following table (1). The jobs are already numbered in EDD order.

Table -1 : data for 1 /$c_i \le d_i$/ ΣE_i problem

EDD	1	2	3	4	5	6
P_i	6	5	3	4	2	1
d_i	10	14	15	18	21	22
C_i	6	11	14	18	20	21
E_i	4	3	1	0	1	1

is clear from table(1) that C = 21 and the minimum $\sum_{i=1}^{6} E_i = 10$ and $E_i \le P_i$ for each i , $E_{max} = 4$.

Table -2: data for 1/$c_j \ge d_j$/ ΣT_j problem

EDD	6	5	4	3	2	1
P_j	1	2	4	3	5	6
D_j	0	2	7	9	12	17
C_j	1	3	7	10	15	21
T_j	1	1	0	1	3	4

It is clear from table(2) that minimum $\sum_{j=1}^{6} T_j = 10$ and $T_j \le P_j$ for each j , $T_{max} = 4$.

Example (2) shows that, if the EDD rule is optimal for 1 /$c_i \le d_i$/ ΣE_i problem, but there exists a job i with $E_i > P_i$, then there exists an optimal schedule for 1 /$c_j \ge d_j$/ ΣT_j problem with $\Sigma E_i = \Sigma T_j$ and with same job j with $T_j > P_j$.

Table -3: data for 1 /$c_i \le d_i$/ ΣE_i problem

EDD	1	2	3	4
P_i	4	3	6	2
d_i	8	12	13	16
C_i	4	7	13	15
E_i	4	5	0	1

It is clear from table (3) that EDD rule is optimal with $E_2 = 5 > P_2 = 3$,

C= 15, $\sum_{i=1}^{4} E_i = 10$.

Table -4 : data for 1 /$c_j \geq d_j$/ ΣT_j problem

J	4	3	2	1
P_j	2	6	3	4
d_j	1	8	6	11
C_j	2	8	11	15
T_j	1	0	5	4

It is clear from table(4) that the schedule(4,3,2,1) is optimal, but it is not EDD schedule, and $\Sigma T_j = \Sigma E_i = 10$ and $T_2 = 5 > P_2 = 3$.

Properties

(1) If SPT rule gives maximum value for 1 /$c_i \leq d_i$/ ΣE_i problem, then LPT rule gives maximum value for 1 /$c_j \geq d_j$/ ΣT_j problem.

Example (3) Shows that SPT rule is maximum for 1 /$c_i \leq d_i$/ ΣE_i and LPT rule is maximum for 1 /$c_j \geq d_j$/ ΣT_j.

Table -5: data for the example (3) for 1 /$c_i \leq d_i$/ ΣE_i problem

SPT	1	2	3	4	5
P_i	2	3	4	5	6
d_i	6	5	12	20	22
C_i	2	5	9	14	20
E_i	4	0	3	6	2

It is clear from table (5) that C = 20, and $\sum_{i=1}^{5} E_i = 15$ (maximum)

Table -6: data for 1 /$c_j \geq d_j$/ ΣT_j problem

LPT	5	4	3	2	1
P_j	6	5	4	3	2
d_j	4	5	12	18	16
C_j	6	11	15	18	20
T_j	2	6	3	0	4

It is clear from table (6) that $\sum_{j=1}^{5} T_j = 15$ (maxinun).

The other feasible schedules for $1/c_j \geq d_j/\Sigma T_j$ are:
(5,4,3,1,2) with $\Sigma T_j = 14$, (4,5,3,2,1) with $\Sigma T_j = 14$,(4,5,3,1,2) with $\Sigma T_j = 13$.

It is clear from theorem(1) and property(1) above, if LPT rule gives minimum value for $1 / c_i \leq d_i / \Sigma E_i$ problem, then SPT rule gives minimum value for $1/c_j \geq d_j/\Sigma T_j$ problem, see property (2).

(2) If for each job i $\mathbf{d_i = d} = \sum_{j=1}^{n} P_j$, then LPT rule is optimal for $1/c_i \leq d_i/\Sigma E_i$ problem, and the optimal schedule for $1/c_j \geq d_j/\Sigma T_j$ problem is obtained directly by setting $d_j = P_j$ for each job j.

Example(4) Shows that if $\mathbf{d_i = d} = \sum_{j=1}^{n} P_j$ for each job i for the $1/c_i \leq d_i = d/\Sigma E_i$ problem and LPT schedule is optimal and if $\mathbf{d_j = P_j}$ for each job j, then SPT schedule is optimal for the $1/c_j \geq d_j/\Sigma T_j$ problem.

Table -7: data for $1/c_i \leq d_i/\Sigma E_i$ problem

I	1	2	3	4	5
P_i	5	4	3	2	1
d_i	15	15	15	15	15
C_i	5	9	12	14	15
E_i	10	6	3	1	0

It is clear that $C = 15$, and $\sum_{i=1}^{5} E_i = 20$.

Table -8: data for $1/c_j \geq d_j/\Sigma T_j$ problem

J	5	4	3	2	1
P_j	1	2	3	4	5
d_j	1	2	3	4	5
C_j	1	3	6	10	15
T_j	0	1	3	6	10

It is clear from table (8) that $d_j = P_j$, and $\sum_{j=1}^{5} T_j = 20$.

(3) If for each job i $\mathbf{P_i = P}$, then all the feasible solutions for the $1 / c_i \le d_i / \Sigma E_i$ and for $1 / c_j \ge d_j / \Sigma T_j$ problems are constant and equal to the optimal one.

Example (5) Shows that if $\mathbf{P_i = P}$ for each job i for $1 / c_i \le d_i / \Sigma E_i$ problem and $\mathbf{P_j = P}$ for $1 / c_j \ge d_j / \Sigma T_j$ problem then $\Sigma E_i = \Sigma T_j$ = constant for all feasible schedules.

Table -9: data for $1 / c_i \le d_i / \Sigma E_i$ problem

I	1	2	3	4	5
P_i	2	2	2	2	2
d_i	5	8	7	10	12
C_i	2	4	6	8	10
E_i	3	4	1	2	2

It is clear that C= 10, and $\sum_{i=1}^{5} E_i = 12$.

The other feasible schedules are:

(1,3,2,4,5),(2,1,3,5,4),(2,1,3,4,5),(3,1,2,4,5),(3,1,2,5,4) with $\sum_{i=1}^{5} E_i = 12$.

Table -10: data for $1 / c_j \ge d_j / \Sigma T_j$ problem

j	5	4	3	2	1
P_j	2	2	2	2	2
d_j	0	2	5	4	7
C_j	2	4	6	8	10
T_j	2	2	1	4	3

It is clear from table (10) that $\sum_{j=1}^{5} T_j = 12$.

The other feasible schedules are:

(4,5,3,2,1),(5,4,2,3,1),(5,4,2,1,3),(4,5,3,1,2) with $\sum_{j=1}^{5} T_j = 12$.

(4) If in the optimal solution for $1/c_i \le d_i/\Sigma E_i$ problem, all the jobs completed on times (i.e., $C_i = d_i$ the ideal solution) then the optimal solution for $1/c_j \ge d_j/\Sigma T_j$ problem all the jobs completed on times.

Example (6) Shows that all jobs completed on their due dates(ideally solution) for $1/c_i \le d_i/\Sigma E_i$ and $1/c_j \ge d_j/\Sigma T_j$ problems.

Table -11: data for $1/c_i \le d_i/\Sigma E_i$ problem

I	1	2	3	4	5
P_i	4	3	1	2	5
d_i	4	7	8	10	15
C_i	4	7	8	10	15
E_i	0	0	0	0	0

Hence it is clear that C =15, and $\sum_{i=1}^{5} E_i = 0$.

Table -12: data for $1/c_j \ge d_j/\Sigma T_j$ problem

J	5	4	3	2	1
P_j	5	2	1	3	4
d_j	5	7	8	11	15
C_j	5	7	8	11	15
T_j	0	0	0	0	0

Hence it is clear that $\sum_{j=1}^{5} T_j = 0$.

Conclusions and Future Work

In This study we discussed the relationship between earliness and tardiness problems. These two problems are NP-hard , and we found a very good result that the EDD rule with $E_i \le P_i$ is optimal for $1/c_i \le d_i/\Sigma E_i$ problem.

An interesting future research topic would involve experimentation discuss the relationship between

$1/C_i \le d_i/\sum W_i E_i$ and $1/C_i \ge d_i/\sum W_i T_i$

REFERENCES

1. Pinedo M. L Scheduling , Theory , algorithms and systems . Spring (2008).
2. Abdul - Razaq T. S., Potts C. N. and Van wassenhove L.N A survey of algorithms for single machine total weighted tardiness scheduling problem ,Discrete Applied mathematics 26 : 235-253. (1990)
3. Su ,L. H and Chen, C.J., Minimizing total tardiness on a single machine with un equal release date .European Journal of operation Research 186, 2: 496-503 . (2008)
4. Batzewicz J., Ecker K.H., Pesch E., Schmidt G. and Weglarz J. "Scheduling Computer and Manufacturing Process" Springer - verlay Berlin. Heidelberg (1996).
5. Du J. and Leung, Minimizing total tardiness on one processor is NP-hard, Mathematics of Operations Research 15: 483-495. (1990).

Common Fixed Points for Nonexpansive Mapping by Iteration

Salwa Salman Abd and Eman Mohmmed Nemah
Department of Mathematics, College of Education (Ibn Al-Haitham), University of Baghdad

Received : 27/03/2011 Accepted : 29/05/2011

الخلاصة

خلال هذا البحث سيتم مناقشة تقارب التكرارات ويشمل تقارب التكرارات القوي وتقارب التكرارات الضعيف نحو النقاط الصامدة المشتركة لمجموعة منتهية من التطبيقات الأنكماشية.

ABSTRACT

The purpose of this paper is to present convergence iteration scheme which converges strongly in one case and converges weakly in other cases to a common fixed point of a finite set of nonexpansive mappings.

INTRODUCTION AND PRELIMINARIES

There are a number of fixed point theorems that guarantee the existence of a fixed point of iterated sequence (Picard sequence) including the Banach 's fixed point theorem [1], for a contraction mapping defined on a complete metric space.

And then the (Browder- Gohde- Krik) theorem 1965 states that any nonexpansive mapping T on a nonempty closed bounded and convex subset of M an uniformly convex Banach space has at least one fixed point in M, unlike in the case of the Banach 's fixed point theorem, trivial example show that the Picard sequence for nonexpansive mapping T even with a unique fixed point may fail to converge to the fixed point. It suffices, for example, to take T a rotation of unit ball in the plane around the origin of coordinates [2, p.475]. However in this example one can obtain a convergent Picard sequence if instead of T. One take the nonexpansive mapping $\frac{1}{2}(I+T)$, when I denote the identity mapping of the plane, i.e. if the Picard iteration is defined for x_o in M by

$$x_{n+1} = \frac{1}{2}(x_n + Tx_n), \quad n \geq 0 \qquad \ldots (1.1)$$

Instead by the usual Picard iteration. It is easy to see that the mappings T and $\frac{1}{2}(I+T)$, have the same fixed points, so the limit of convergent sequence by (1.1) is necessary a fixed point of T.

More generally, if X is a normed linear space and M is a convex subset of X a generalization of (1.1) which has percent successful in the approximation of fixed points of nonexpansive mapping T:M→M, is the following scheme [2, p.481],

$x_0 \in M, \quad x_{n+1}=(1-\alpha)x_n+\alpha T(x_n), \quad n \geq 0, \alpha \in [0,1].$ .... (1.2)

However, the most general iterative

$x_0 \in M, \quad x_{n+1}=(1-\alpha_n)x_n+\alpha_n T(x_n), \quad n \geq 0,$ .... (1.3)

when $\{\alpha_n\} \subset [0,1]$ is a real sequence satisfying appropriate conditions. The sequence $\{x_n\}$ in (1.3) is called Mann iteration [3].

Definition 1.1 [2, p.473] X be a normed space and M be a nonempty subset of X A mapping T:M→X is called nonexpansive if:

$\|Tx-Ty\| \leq \|x-y\|$ *for all* $x, y \in M$ ..... (1.4)

Definition 1.2 [4] Let X be a Banach space, M be a nonempty convex subset of X. Suppose $\{T_i: i=1,2,...,k\}$ is a family of nonexpansive self-mappings of M. Define the following iteration scheme:

$U_0=I$, I the identity map,

$U_1=(1-\alpha)I+\alpha(T_1 o U_0)$, $\alpha \in (0,1)$,

$U_2=(1-\alpha)I+\alpha(T_2 o U_1)$,

... ...

$U_k=(1-\alpha)I+\alpha(T_k o U_{k-1})$,. .... (1.5)

$x_0 \in M, \; x_{n+1}=(1-\alpha)x_n+\alpha(T_k o U_{k-1})(x_n), \quad n \geq 0,$ .... (1.6)

Define $F=\bigcap_{i=1}^{k} F(T_i)$, where $F(T_i)$ denotes the fixed point set of T_i.

Remark 1.3 [4] : Observe that for k=1, the sequence (1.6) becomes

$x_{n+1}=(1-\alpha)x_n+\alpha T_1(x_n)$, ... (1.7)

which converges to a fixed point of T_1 see [5]

Definition 1.4 [6] A normed linear space X is said to be strictly convex when

$$\|x+y\| = \|x\| + \|y\| \quad \textit{iff } y = ax \textit{ for all } x, y \in X \textit{ and } a \geq 0.$$

Definition 1.5 [7] Let X be a Banach space, M is a nonempty subset of X, T a mapping of M into X. Then T is said to be semi contractive if there exists a mapping V of M×M into X such that T(u)=V(u, u) for u in M ,while:

i. For each fixed v in M, V (.,v) is nonexpansive from M to X.

ii.For each fixed u ∈ M, V (u,.) is completely continuous from M to X, uniformly for u in bounded subset of M (i.e. if v_j converges weakly to v in M and $\{u_j\}$is a bounded sequence in M, then V (u_j, v_j) – V(u_j, v)→0, strongly in M).

Lemma 1.6 [8] Let X be a uniformly convex Banach space, M be a nonempty closed bounded convex subset of X and T is a semi contractive mapping of M into X. Then:

i. (I – T) is demi closed and

ii. (I – T) M is closed in X.

Definition 1.7 [2, p.474] A Banach space X is said to be a uniformly convex if and only if for any

$x, y, \in X$, $R > 0$ *and* $\varepsilon \in [0,2]$, *there exists a* $\delta(\varepsilon) \in [0,1]$, *such that if* $\|x\| \leq R$, $\|y\| \leq R$ *and* $\|x-y\| \geq \varepsilon R$, *then* $\left\|\frac{1}{2}(x+y)\right\| \leq (1-\delta(\varepsilon))R$.

Lemma 1.8 [9] Let M a subset of a Banach space X and let T be a nonexpansive mapping from M into X. if there exist x_1 and $\{\alpha_n\}$ that satisfy condition A and the Mann iteration scheme (1.7) is bounded, then x_n-T(x_n) converges to zero as n→∞.

Kuhfittig [4], show that Kuhfittting's iteration (1.6) converges strongly to a common fixed point of the family. His second result is that, if X is uniformly convex an satisfies Opail's condition and M is closed convex, then (1.6) converges weakly to a fixed point in F.

Rhoades [10], show that if X is an uniformly convex and M is closed convex then Kuhfittting's iteration (1.6) converges weakly to a fixed point in F.

In this paper, we recall a particular iteration which is Kuhfittting's iteration (1.6) and give all details of two results. The first one due to Kuhfittting who prove that this iteration scheme converges strongly to family of nonexpansive mappings defined on convex compact subset of strictly convex Banach space. The second is Rhoades's results who prove that Kuhfittting's iteration (1.6) converges weakly to a fixed point of a commutative finite of nonexpansive mappings which defined on closed convex subset of uniformly convex Banach space.

MAIN RESULT

In order to prove our main theorems we need the following important propositions:

Also Kuhfittig mention to the following without proof

Proposition 2.1 [4] Let X be a Banach space and M be a nonempty convex subset of X. Suppose $\{T_i: i=1,2,\ldots,k\}$ is a family of nonexpansive self –mappings on M. Then the mappings U_i and $T_iU_i : M\to M$ $i=1,2,\ldots,k$ are nonexpansive mappings.

Proof :

$U_0=I$, I identity map and $U_0(x)=x$ for all $x\in M$ and $U_i=(1-\alpha)I+\alpha(T_iU_{i-1})$, then for all $x, y\in M$

$$\begin{aligned}\|U_1(x)-U_1(y)\| &= \|(1-\alpha)x+\alpha(T_1U_0)(x)-(1-\alpha)y+\alpha(T_1U_0)(y)\|\\ &=(1-\alpha)x+\alpha T_1(x)-(1-\alpha)y+\alpha T_1(y)\|\\ &\le(1-\alpha)\|x-y\|+\alpha\|T_1(x)-T_1(y)\|\\ &\le(1-\alpha)\|x-y\|+\alpha\|x-y\|\\ &=\|x-y\|\end{aligned}$$

Thus U_1 is nonexpansive mapping

Suppose that it is true when $i=k-1$(i.e., $\|U_{k-1}(x)-U_{k-1}(y)\|\le\|x-y\|$).

To show that when $i=k$ (i.e., to prove $\|U_k(x)-U_k(y)\|\le\|x-y\|$).

$$\begin{aligned}\|U_k(x)-U_k(y)\| &= \|(1-\alpha)x+\alpha(T_kU_{k-1})(x)-(1-\alpha)y+\alpha(T_kU_{k-1})(y)\|\\ &=\|(1-\alpha)(x-y)+\alpha(T_k(U_{k-1}(x))-T_k(U_{k-1}(y)))\|\\ &\le(1-\alpha)\|x-y\|+\alpha\|T_k(U_{k-1}(x))-T_k(U_{k-1}(y))\|\end{aligned}$$

$$\leq (1-\alpha)\|x-y\|+\alpha\|U_{k-1}(x)-U_{k-1}(y)\|$$
$$\leq (1-\alpha)\|x-y\|+\alpha\|x-y\|$$
$$=\|x-y\|$$

Also, then U_i is nonexpansive mapping for all i.

Now, for all x, y $\in$M

$$\|(T_ioU_i)(x)-(T_ioU_i)(y)\|=\|T_i(U_i(x))-T_i(U_i(y))\|$$
$$\leq\|U_i(x)-U_i(y)\|$$
$$\leq\|x-y\|$$

Thus, then T_ioU_i is nonexpansive for all i.

Demarr [10] proved the following proposition for a commutative family of contractive mappings here we present it with proof for nonexpansive mappings:-

Proposition 2.2 Let X be a Banach space, M be a nonempty compact convex subset of X. If E is a nonempty family of commutative nonexpansive mappings on M, then the family E has a common fixed point.

For the proved of this proposition we will need the following lemma:

Lemma 2.3 [11] Let M_o be a nonempty convex subset of a Banach space X and f is a nonexpansive mapping of Mo into itself. If there is a compact set $K \subseteq M_o$ such that K =f(K) and K has at least two points, then there exists a nonempty closed convex set K_1 such that f $(K_1 \cap M_o) \subseteq K_1 \cap M_o$ and $K \cap K_1^* \neq \emptyset$ (K_1^* is the complement of K_1).

Proof of the proposition :

One may show by Zorn's lemma, that there exists a minimal nonempty compact convex set $M_o \subset M$ such that Mo is invariant under each f$\in$E. If M_o consists of a single point, then f(M_o)= M_o for each f$\in$E, implies $\bigcap_{f\in E} f(M_o)=M_o$, then the proposition is proved. We shall now show if M_o consist of more than one point then we obtain a contradiction.

We may use Zorn's lemma again to show that there exists a minimal nonempty compact (but not necessarily convex) set $N \subset Mo$ such that N is invariant under each $f \in E$ (i.e., $f(N) \subset N$), We will now show that $N=\{f(x):x \in N\}$ for each $f \in E$. Since each $f \in E$ is continuous and N is compact, f(N) must also be compact. For all $f \in E$, we have $f(N) \subset N$. Let us assume that for some $g \in E$ we have $g(N) = W \neq N$; therefore for any $x \in W$, there exists $y \in N$ such that $x=g(y)$ because all functions in E is commutative, we have for all $f \in E$, $f(x)=f(g(y))=g(f(y)) \in W$, $f(x) \in W$.

Thus, we have $f(W) \subset W \subset N$ for each $f \in E$. But W is nonempty compact subset of M_o, $f(W) \subset W$ and $W \subset N$ ($W \neq N$). We have contradicted the

minimally of N. Consequently, our assumption that $N \neq W$ is false. We may assume that N has at least two points; otherwise, the theorem is proved.

We may now apply lemma (2.3) to each $f \in E$. Referring to the notation of lemma (1.5), we see that the set $K_1 \cap M_o$ is invariant under each $f \in E$. Since K_1 is closed, we see that $K_1 \cap M_o$ be a nonempty compact convex subset of M_o. Since $M_o \cap K_1^* \supset N \cap K_1^* \neq \emptyset$, we see that $K_1 \cap M_o \neq M_o$. Thus, we see that if M_o has more than one point, then we obtain a contradiction to the minimality of M_o.

Proposition 2.4 Let X be a Banach space and M a convex subset of X If $\{T_i:i=1,2,\ldots k\}$ is a family of commutative nonexpansive mappings of M. Then families $\{T_1, T_2,\ldots,T_k\}$ and $\{U_1, U_2,\ldots,U_k\}$ in (1.5) have the same set of common fixed point

Proof:

Let $y \in \bigcap_{i=1}^{k} F(T_i)$, then $y \in F(T_i)$ (i.e., $y= T_i (y)$) for all i, $U_0(y)=y$

$$U_1(y) = (1 - \alpha)\, y + \alpha T_1(y) = (1 - \alpha)\, y + \alpha y = y$$

Suppose that it is true when $i=k-1$ (i.e., $U_{k-1}(y)=y$). To prove that when i=k

(i.e., to prove $U_k (y)=y$).

$$\begin{aligned} U_k(y) &= (1 - \alpha)\, y + \alpha(T_k o\, U_{k-1})\, (y) \\ &= (1 - \alpha)\, y + \alpha T_k\, (U_{k-1}\, (y)) \\ &= (1 - \alpha)\, y + \alpha\, T_k\, (y\,) \end{aligned}$$

$$=(1-\alpha)\,y+\alpha\,y=y$$

Thus, $y=U_i(y)$ for all $i=1,2,\ldots,k$.

Here, the finite family of commutative nonexpansive mappings have common fixed points; so, we reform [4, Th. 1] for strongly converges and Rhoades' theorem for nonexpansive with commutative condition on $\{T_i:i=1,2,\ldots,k\}$.

Theorem 2.5 Let M be a nonempty convex compact subset of a strictly convex Banach space X and $\{T_i:i=1,2,\ldots,k\}$ is a family of commutative nonexpansive self-mappings on M. Then the Mann iterates scheme in (1.6) converges strongly to a common fixed point of $\{T_i: i=1,2,\ldots,k\}$.

Proof :

By proposition (2.1) the mappings U_i and T_iU_{i-1}, $i=1,2,\ldots,k$ are nonexpansive mappings of M into itself. By proposition (2.4) the families $\{T_1, T_2,\ldots,T_k\}$ and $\{U_1, U_2,\ldots,U_k\}$ have the same set of common fixed point.

Since the sequence (1.6) has the same form as (1.7), $\{U_kx_n\}$ converges to a fixed point y of T_kU_{k-1} by Edelstein's theorem [3]. We wish to show next that y is a common fixed point of T_k and U_{k-1} ($k\geq2$). To this end we first show that $(T_{k-1}oU_{k-1})(y)=y$ ($k\geq2$). Suppose not; then the closed line segment $[y, (T_{k-1}oU_{k-2})(y)]$ has positive length. Now let

$$z=U_{k-1}(y)=(1-\alpha)\,y+\alpha\,(T_{k-1}oU_{k-2})(y).$$

By hypothesis there exists a point w such that $T_1(w)=T_2(w)=\ldots=T_k(w)=w$. Since $\{T_i\}$ and $\{U_i\}$ have the same common fixed point, it follows that

$(T_{k-1}oU_{k-2})(w)=w$. By nonexpansiveness

$$\|(T_{k-1}oU_{k-2})(y)-w\|\leq\|y-w\| \qquad \ldots. (2.1)$$

and

$$\|T_k(z)-w\|\leq\|z-w\|.$$

So w is at least as close to $T_k(z)$ as to z. But $T_k(z)=(T_kU_{k-1})(y)=y$, so that w is a least as close to y as to $z=(1-\alpha)y+\alpha(T_{k-1}oU_{k-2})(y)$. Since X is strictly convex, we conclude that

$$\|y-w\|<\|(T_{k-1}oU_{k-2})(y)-w\|.$$

This contradicts (2.5.4), so that $(T_{k-1}oU_{k-2})(y)=y$. From

$$U_{k-1}=(1-\alpha)\,I+\alpha(T_{k-1}oU_{k-2}),$$

follows that $U_{k-1}(y)=(1-\alpha)y+\alpha y=y$ and $y=(T_k o U_{k-1})(y)=T_k(y)$. Consequently, y is a common fixed point of T_k and U_{k-1}.

Since $(T_{k-1} o U_{k-2})(y) = y$, we may repeat the argument to show that $(T_{k-2} o U_{k-3})(y)=y$ and that y must therefore be a common fixed point of T_{k-1} and U_{k-2}. Continuing in this manner, we conclude that $(T_1 o U_0)(y)=y$ and that y is a common fixed point of T_2 and U_1. Thus, y is a common fixed point of $\{T_i: i=1,2,\ldots,k\}$.

Theorem 2.6 Let X be a uniformly convex Banach space, M be a nonempty closed convex subset of X and $\{T_i: i=1,2,\ldots,k\}$ is a family of commutative nonexpansive self- maps on M. Then Mann iteration scheme in (1.6) converges weakly to a common fixed point of {Ti: i=1,2,…,k}.

Proof:

By proposition (2.1) the mappings U_i and T_i o U_{i-1}, i=1,2,…,k are nonexpansive mappings of M into itself. By proposition (2.4) the families $\{T_1, T_2,\ldots,T_k\}$ and $\{U_1,U_2,\ldots,U_k\}$ have the same set of common fixed points. Let $p\in F$, set $S=T_k$ o U_{k-1}. For any $x\in M$ and $p\in F(T)$, define

$E=\{u\in X: \|u-p\|\le r\}\cap M$, where $r=\|x-p\|$.

Then E is a nonempty bounded convex subset of M which is invariant under the U_i, and Ti and contains $x_0=x$. Thus, without loss of generality we may assume that M is bounded.

Since S is nonexpansive (1.2),

$$\begin{aligned}\|x_{n+1}-p\| &= \|(1-\alpha)x_n+\alpha S(x_n)\| \\ &\le (1-\alpha)\|x_n-p\|+\alpha\|S(x_n)-p\| \\ &\le (1-\alpha)\|x_n-p\|+\alpha\|x_n-p\| = \|x_n-p\|\end{aligned}$$

Therefore $\lim_{n\to\infty}\|x_n-p\|$ exists, which implies that $\{x_n\}$ is bounded.

From lemma (1.8), $\lim_{n\to\infty}\|x_n-S(x_n)\|=0$. The assumption that X is uniformly convex implies that it is reflexive. The boundedness of $\{x_n\}$ implies that there is a subsequence $\{x_{ni}\}$ of $\{x_n\}$ which converges weakly to a point $q\in M$. Since S is nonexpansive, if one define V by $V(u,v)=S(u)+v$, then V is semi contractive and from lemma (1.6), S is demi closed. That is, if $\{x_{ni}\}$ converges weakly to a point q, since $\lim_{i\to\infty}\|(I-S)(x_{ni})\|=0$, $(I-S)q=q$; so that, q

is a fixed point of S. A uniformly convex space is strictly convex, so one can use the argument of theorem (2.5), which we now do, to show that $q \in F(T)$

Suppose that q is not a common fixed point of T_{k-1} and U_{k-2}.Then the closed line segment $[q, (T_{k-1} \circ U_{k-2})q]$ has positive length. Define

$$z = U_{k-1}(q) = (1-\alpha)\, q + \alpha\, (T_{k-1} \circ U_{k-2})\, (q).$$

By hypothesis there exists a point w such that $T_1(w) = T_2(w) = \ldots = T_k(w) = w$. Since $\{T_i\}$ and $\{U_i\}$ have the same common fixed point, it follows that

$(T_{k-1} \circ U_{k-2})\,(w) = w$. Since $\{T_i\}$ and $\{U_i\}$ are nonexpansive

$$\| (T_{k-1} \circ U_{k-2})\,(q) - w \| \le \| q - w \| \qquad \ldots. (2.2)$$

$$\| T_k(z) - w \| \le \| z - w \| .$$

Therefore w is at least as close to $T_k(z)$ as to z.But $T_k(z) = (T_k \circ U_{k-1})\,(q) = q$,so that w is a least as close to q as to $z = (1-\alpha)q + \alpha(T_{k-1} \circ U_{k-2})\,(q)$. Since X is strictly convex, it follows that

$$\| q - w \| < \| (T_{k-1} \circ U_{k-2})\,(q) - w \| .$$

This contradicts (2.2), so that $(T_{k-1} \circ U_{k-2}(q) = q$. It now follows from $U_{k-1} = (1-\alpha)I + \alpha(T_{k-1} \circ U_{k-2})$ that $U_{k-1}(q) = (1-\alpha)q + \alpha q = q$ and $q = (T_k \circ U_{k-1})\,(q) = T_k(q)$. Therefore, q is a common fixed point of T_k and U_{k-1}.

Since $(T_{k-1} \circ U_{k-2})\,(q) = q$, we may repeat the above argument to show that $(T_{k-2} \circ U_{k-3})\,(q) = q$ and that q must therefore be a common fixed point of T_{k-1} and U_{k-2}.Continuing in this manner, we conclude that $(T_1 \circ U_0)\,(q) = q$ and that q is a common fixed point of T_2 and U_1. Thus, q is a common fixed point of $\{T_i : i = 1,2,\ldots,k\}$.

Corollary 2.7 [4, Th.3] If X is a uniformly convex Banach space satisfying Opial's condition, M is a nonempty closed convex subset of X and if the family of mappings $\{T_i : i = 1,2,..,k\}$ satisfies (1.2), then for any $x \in M$, the sequence $\{x_n\}$ converges weakly to a common fixed point .

Proof:

It is clear.

REFERENCES

1- Khamsi M. A. and Kirk W.A., "An Tntroduction to Metric Fixed Point Theorem", Wiley, New York, (2001).

2- Zeilder F., "Nonlinear Functional Analysis and Applications (Fixed Point Theorem)" Springer Verlag New Yory Ine,(1986).

3- Rhoades B.E. and Saliga, " Some Fixed Point Iteration Procedures -∏", Non-linear Analysis Forum, Vol. 6, No.1, pp.193-217,(2001).

4- Kuhfittig P. K. F., "Common Fixed of Nonexpansive Mappings by Iteration", Pacific J. Math.,Vol.97, pp.137-139, (1998).

5- Edelstein M., "A Remark on a Theorem of M.A. Krasnoselskii", Amer. Math. Monthy,Vol.74, , pp.509-510, (1966).

6- Narici L. and Bekenstein E., "Topological Vector Space", Marcel Dekker and INC., New York, (1985).

7- Kirk W.A. and Sims B.," An Ultrafilter Approach to Loally Almost Nonexpansive Maps", Nonlinear Anal.,Vol.63, pp. 1241-1251, (2005).

8- Browder F.E., "Some Contractive and semiaccretive Nonlinear /mapping in Banach space", Bull. Amer. Math. Soc., Vol. 74, pp. 660-665, (1968).

9- Ishikawa S., "Fixed Points and Iteration of a Nonexpansive Mapping a Banach Space", Amer. Math. Soc., Vol.59, pp.65-71, (1976).

10-Rhoades B.E., "Finding Common Fixed Points of Nonexpansive Mapping by Iteration", Bull. Austal. Math. Soc., Vol.62, pp.307-310, (2000).

11-Demarr R., "Common Fixed Points for Commuting Contraction Mappings", Pacific J. Math., Vol. 73, pp. 1139-1141, (1963).

Stability analysis in a discrete-time predator-prey model with allee effect

Alaa H. Lafta
Department of Mathematics, College of Science, University of Baghdad

Received : 04/04/2011 Accepted : 29/05/2011

الخلاصة

في هذا البحث, تم بحث نموذج المفترس- الفريسة في الحالة المتقطعة والذي يتضمن تأثير إلي(ظاهرة طبيعية تشير الى العلاقة بين التوازن في المجتمع وحجمه). تم تنفيذ و دراسة الوجود والاستقرارية المحلية لجميع النقاط الصامدة الممكنة .تبين إن, تأثير ألي يكون نظاما مميزا وذلك عند إدخال تأثير ألي في مجتمع المفترس.

ABSTRACT

In this paper, a discrete-time predator-prey model involving allee effect is investigated. The existence and local stability of all possible fixed points are carried out. It is observed that, the allee effect (phenomenon in biology refer to the positive relationship between aspects of fitness and population size) made very interesting system when it imposed in predator population.

INTRODUCTION

The dynamical relationship between predator and its prey is continuing to be one of the dominant themes in both ecology and mathematical ecology due to its universal existence and importance [1]. There are plenty of papers about the dynamics on the predator-prey system with and without different kinds of functional responses, so it is worth mentioning that the consequences of hiding behavior of prey on the dynamics of predator-prey interactions can be recognized significant [2].

In fact, the Allee effect is a phenomenon in biology named after allee [3] who brought an attention to the possibility of a positive relationship between aspects of fitness and population size over fifty years ago [4]. In the other words, for smaller population, the reproduction and survival of individuals decrease. This effect usually saturates or disappears as populations get larger. For more details see [5-11] and the reference within.

Merdan and Duman[12] presented the stability of the discrete-time model involving predation and allee effect in general and showed that an allee

effect has stabilizing role in there model. Furthermore, Celik et al [13] studied a discrete-time predator-prey with and without allee effect; they imposed the effect of Allee on the prey population and exhibit the impact of allee effect on stability.

Throughout this paper, we consider the discrete-time model with allee effect in the closed first quadrant R_+^2 of the **(x,y)** plane. Also, we discuss the existence of fixed points and studied the stability of it by calculating eigenvalues for the variation matrix at each fixed point. Furthermore, the predator population occurs with absence of prey population so it is fixed point found and studied too.

The aim of the present work is to propose the discrete-time predator-prey model involving allee effect in predator population. It is organized as follow: in the section 2, the discrete-time predator-prey model with allee effect is formulated. In section 3, the existence and local stability conditions of each fixed points are investigated. In section 4, some numerical simulations are presented. Finally, in section 5, the discussion and remarks are drawn.

The model:

The discrete-time predator-prey model is described by difference equations be in the following form:

$$\begin{cases} X_{n+1} = X_n + aX_n(1 - X_n) - bX_nY_n \\ \\ Y_{n+1} = Y_n + bY_n(X_n - Y_n) \end{cases} \quad (1)$$

Where $a, b > 0$ such that a is the parameter of the increases of the prey population in the absence of predator and b is the parameter of the decrease due to predation. While X_n and Y_n represent the densities of the prey and predator populations at the iteration $n (n = 0,1,...,)$, respectively.

Now, consider the system (1) as a subject to an allee effect on predator population. Then we get the following system:

$$\begin{cases} X_{n+1} = X_n + aX_n(1-X_n) - bX_nY_n \\ Y_{n+1} = Y_n(1-bY_n)\dfrac{Y_n}{\varepsilon+Y_n} + bX_nY_n \end{cases}$$

(2)

Where we take $\frac{Y_n}{\varepsilon+Y_n}$ as an allee function and ε as an allee constant that satisfying the assumption:

$$\frac{(ab-b^2\varepsilon)\pm\sqrt{(ab-b^2\varepsilon)^2-(ab+b^2)(a\varepsilon-ab\varepsilon)}}{2(ab+b^2)}>0 \qquad (3)$$

Remark 2.1:

If the predator density disappears in the systems (1) and (2), then the prey population satisfies the logistic equation and vise versa. While if $\varepsilon=0$ in the system (2), then there is no allee effect on the predator population.

The existence and stability of fixed points:

In this section, we first determine the existence of the fixed points of the system (2), and then investigate their stability by calculating the eigenvalues for the variation matrix of the system (2) at each fixed point.

By solving the following nonlinear algebraic equations

$$\begin{cases} X(a(1-X)-bY)=0 \\ Y\left(\dfrac{Y}{\varepsilon+Y}(1-bY)+bX-1\right)=0 \end{cases}$$

(4)

We get the fixed points $(0,0)$, $(1,0)$, $(0,\frac{1}{b})$ and (X^*,Y^*) where $X^*=\frac{a-bY^*}{a}$ and $Y^*=\frac{(ab-b^2\varepsilon)\pm\sqrt{(ab-b^2\varepsilon)^2-(ab+b^2)(a\varepsilon-ab\varepsilon)}}{2(ab+b^2)}$, obviously $(0,\frac{1}{b})$ exist if $b>0$ and (X^*,Y^*) are the only positive fixed points which exist if $a>bY^*$ and Y^* have positive real values.

To study the stability of the fixed points of our modification model, we first recall the useful lemma, which can be easily proved by the relation between roots and coefficients of a quadratic equation [14].

Lemma 3.1 [14]:

Let $F(\lambda)=\lambda^2-B\lambda+C$. Suppose that $F(1)>0$ then the two roots λ_1 and λ_2 of $F(\lambda)=0$ satisfy the following:

(i) $|\lambda_1|<1$ and $|\lambda_2|<1$ if and only if $F(-1)>0$ and $C<1$;

(ii) $|\lambda_1|>1$ and $|\lambda_2|>1$ if and only if $F(-1)>0$ and $C>1$;

(iii) $|\lambda_1|<1$ and $|\lambda_2|>1$ (or $|\lambda_1|>1$ and $|\lambda_2|<1$) if and only if $F(-1)<0$;

(iv) $\lambda_1=-1$ and $|\lambda_2|\neq 1$ if and only if $F(-1)=0$ and $B\neq 0,2$;

(v) λ_1 and λ_2 are complex and $|\lambda_1|=|\lambda_2|=1$ if and only if $B^2-4C<0$ and $C=1$.

Now, let λ_1 and λ_2 be the two eigenvalues of the fixed point (x,y). We recall some definitions of topological types for a fixed point (x,y). A fixed point **(x,y)** is called a sink if $|\lambda_1|<1$ and $|\lambda_2|<1$, so the sink is locally asymptotically stable. **(x,y)** is called a source if $|\lambda_1|>1$ and $|\lambda_2|>1$, so the source is locally unstable. (x,y) is called a saddle if $|\lambda_1|<1$ and $|\lambda_2|>1$ (or $|\lambda_1|>1$ and $|\lambda_2|<1$). And (x,y) is called non-hyperbolic if either $|\lambda_1|=1$ or $|\lambda_2|=1$.

Substituting the coordinates of the fixed point $(0,0)$ for (X,Y) of the system (2) and computing the eigenvalues of the fixed point $(0,0)$, so we obtained the following proposition.

Proposition 3.2: The origin fixed point $(0,0)$ of the system (2) is a saddle.

Proof:

The Jacobian matrix of the system (2) at the fixed point $(0,0)$ is given as follow

$$J_0=\begin{bmatrix} 1+a & 0 \\ 0 & 0 \end{bmatrix} \qquad (5)$$

and the corresponding characteristic equation can be written as

$$\lambda^2-(trJ_0)\lambda+\det(J_0)=0 \qquad (6)$$

Where trJ_0 is the trace and $\det(J_0)$ is the determinant of the Jacobian matrix J_0. Hence the two eigenvalues of the Jacobian matrix J_0 are $\lambda_1=1+a>1$ and $\lambda_2=0<1$. According to the lemma 1, we obtained that there is only one topological type of the origin fixed point $(0,0)$ for all parameters values, which means it is a saddle fixed point.

Proposition 3.3: The axial fixed point (1,0) has at least four different topological types, that means (1,0) is:

i. Sink if $a < 2$ and $b < 1$;
ii. Source if $a > 2$ and $b > 1$;
iii. Non-hyperbolic if $a = 2$ or $b = 1$;
iv. Saddle other wise.

From the condition *(iii)* of the proposition 3.3, it is easy to see that one of the eigenvalues of the fixed point $(1,0)$ is -1 and the other eigenvalue is neither 1 nor -1 and then it also implies that all the parameters locate in the following set:

$H_{(1,0)} = \{(a,b) : a \neq 2, b = 1\}$.

The fixed point (1,0) can undergo flip bifurcation when parameters vary in the small neighborhood of $H_{(1,0)}$, since when parameters are in $H_{(1,0)}$ [15]. In this case, the predator becomes extinction and the prey pass through the period-doubling bifurcation to chaos in the sence of Li-Yorke by choosing bifurcation.

Proposition 3.4: if $b > 0$, then the fixed $(0, \frac{1}{b})$ satisfying the following topological types for all permissible values of parameters.

i. Sink if $a < 1$ and $b\varepsilon > 0$,
ii. Non-hyperbolic if $a = 1$ or $b\varepsilon = 0$

The eigenvalues of the matrix J_2, are $\lambda_1 = a$ and $\lambda_2 = -\frac{1}{1+b\varepsilon}$ .So, from the existence condition of the fixed point $(0, \frac{1}{b})$ we have that $b > 0$ then we can say that the second eigenvalue depend on the allee constant and the fixed point $(0, \frac{1}{b})$ is non-hyperbolic if there is no allee effect or $a = 1$.

Now, we recall the well known condition [16] and are sufficient for the local stability of the positive fixed point. The fixed point (X^*, Y^*) is stable if it satisfies the following conditions:

$$\begin{cases} 1+Tr(J_2)+Det(J_2)>0 \\ 1-Tr(J_2)+Det(J_2)>0 \\ 1-Det(J_2)>0 \end{cases} \quad (10)$$

Proposition 3.5: By assumption(3), the positive fixed point (X^*,Y^*) of the system (2) is asymptotically stable if the following conditions are satisfied:

i. $\gamma > 1$

ii. $\dfrac{(a-bY^*)(a+a\beta-b^2Y^*)}{a(\beta+1)} < 2$ and $\beta \neq -1$

iii. $\dfrac{(a-bY^*)(a\beta-b^2Y^*)}{a(\beta-1)} > 1$ and $\beta \neq 1$

.where $\beta = \dfrac{b(a-bY^*)}{a} + \dfrac{\varepsilon Y^*(1-bY^*)}{(\varepsilon+Y^*)^2} + \dfrac{Y^*(1-2bY^*)}{\varepsilon+Y^*}$,

$\gamma = \dfrac{(\varepsilon+Y^*)^2(a-ab+2b^2Y^*)}{aY^*[2\varepsilon+(1-3\varepsilon)Y^*-2bY^{*2}]}$.

.such that $2\varepsilon+(1-3\varepsilon)Y^*-2bY^{*2} \neq 0$.

Proof:

After some calculation, the Jacobian matrix of the system (2) at the fixed point (X^*,Y^*) is:

$$J_3 = \begin{bmatrix} 1-a+bY^* & -\dfrac{b(a-bY^*)}{a} \\ bY^* & \beta \end{bmatrix} \quad (11)$$

So the characteristic equation is:

$$\lambda^2-(1-a+bY^*+\beta)\lambda+\beta(1-a+bY^*)+\frac{b^2Y^*(a-bY^*)}{a}=0 \quad (12)$$

Where

$$Tr(J_3)=1-a+bY^*+\beta \quad (13)$$

and

$$Det(J_3)=\beta(1-a+bY^*)+\frac{b^2Y^*(a-bY^*)}{a} \quad (14)$$

From the conditions (9), we obtained that the modulus of two roots of the equation (11) are in the unit circle if and only if $F(1)>0$, $F(-1)>0$ and $Det(J_3)<1$.

Now, according to lemma 1, we observed that $F(1)>0$ holds if and only $\gamma>1$. Then we investigate the conditions $F(-1)>0$ and $Det(J_3)<1$ when $\gamma>1$. It implies that $F(-1)>0$ holds if and only if $\frac{(a-b\gamma^*)(a+a\beta-b^2\gamma^*)}{a(\beta+1)}<2$ holds, and $Det(J_3)<1$ holds if and only if $\frac{(a-b\gamma^*)(a\beta-b^2\gamma^*)}{a(\beta-1)}>1$ holds, so the proof is complete.

Numerical simulation:

In this section, we give the numerical simulations to verify our theoretical results proved in the previous sections. Mainly, we present the graph of the solutions X_n versus Y_n for the prey-predator model with and without allee effect (systems (1) and (2), respectively) and show the impact of the allee effect on the phase portrait of the solutions.

Likely, çelik et al [13] fixed parameter values satisfying the existence conditions of the positive fixed point. So, we used it in our numerical simulations.

When we analyze the phase portrait of the solutions around the positive fixed point for both systems, we can easily see the stabilizing effect of allee function that we imposed on predator population by system (2).

In figure (1) we illustrate the phase portrait of prey and predator densities in systems (1) and (2) by taking $b=2$ and the initial values $x_0=0.3, y_0=0.2$. We used $a=1.4$ in figures 1 (a) and 1 (c) while $a=2.2$ in figures 1 (b) and 1 (d). Here (a) and (b) show the phase portrait of prey and predator densities in system (1), however (c) and (d) correspond to system (2) taking the same parameters as in (a) and (b).

We see from figures 1 (a) and 1 (c) that in system (1), the local stability of fixed point and trajectory of the solution approximates to the corresponding fixed point much faster than system (2). Furthermore, figures 1 (b) and 1 (d) presents that the corresponding fixed point move from priod-4 to chaotic under the allee effect. Here we take the allee effect function as $\frac{Y_n}{\varepsilon+Y_n}$ and take the allee constant as $\varepsilon=0.09$.

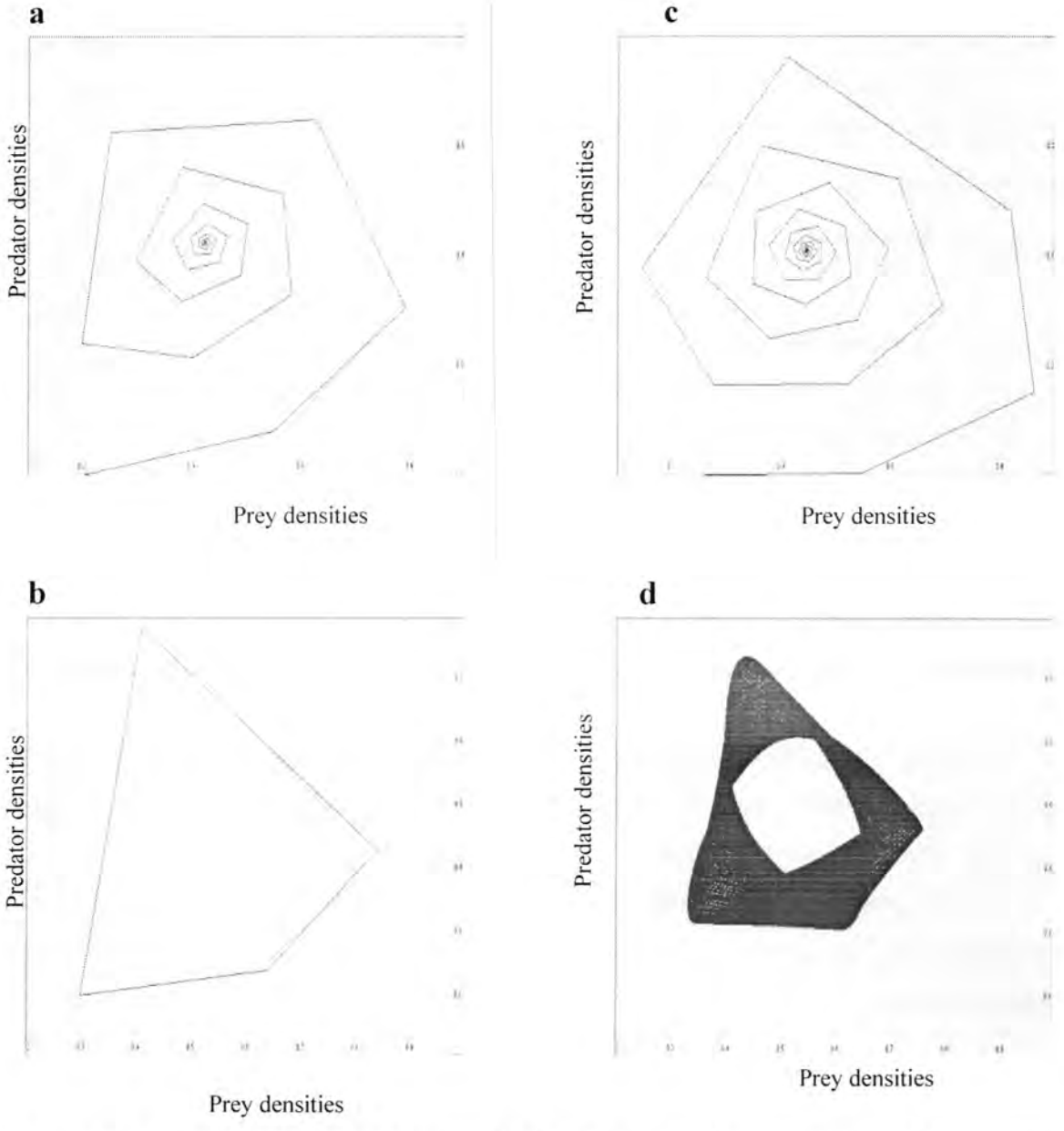

Fig.-1: The graph in (a) (resp. (b)) indicates the solution of system (1) with a=1.4(resp. a=2.2), however, the graph in (c)(resp. (d)) corresponds to system (2) with ε=0.09.

Figure (2) shows the bifurcation diagrams of prey and predator densities of systems (1) and (2) with the initial values $x_0 = 0.3, y_0 = 0.2$ as above and the parameter values $b = 2$, $\varepsilon = 0.09$ and a in the $[1.9,3]$ with step size=0.01.

In figure(*2*), we can see that the stability region in figures 2 (a) and 2 (b) are as same as in figures 2 (c) and 2 (d) while the instability region gives rich dynamic and interesting one when the predator densities is subject to the allee effect with allee constant as $\varepsilon = 0.09$.

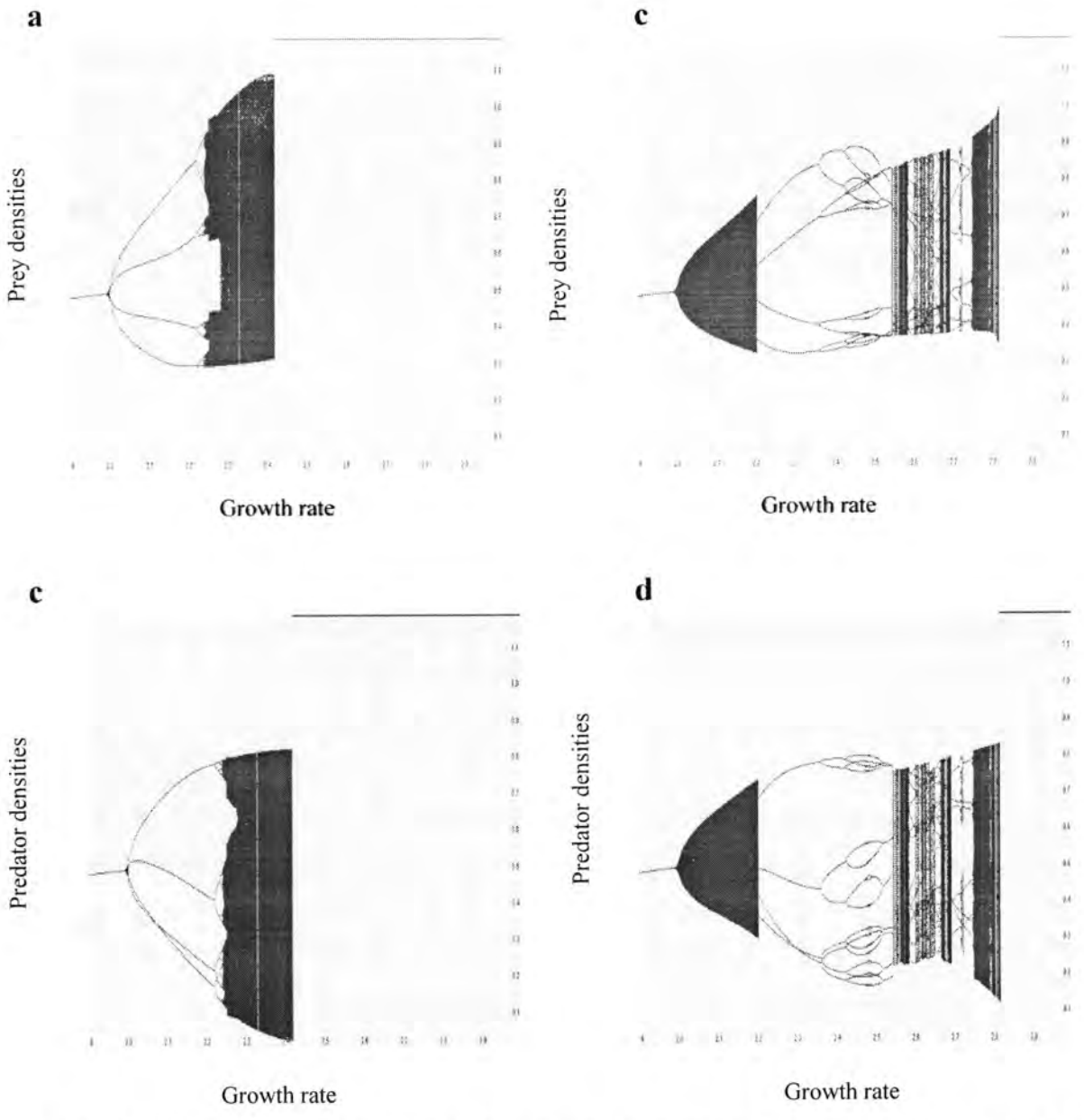

Fig.-2: Bifurcation diagrams of prey and predator densities with growth rate in systems (1) and (2)

Discussion:

In this paper, the discrete –time prey model with an allee effect was proposed. Existence and stability of fixed points were investigated by

mathematical analysis; we have shown the stability of the positive fixed point. However, it may be very complicated structure when our system delayed both prey and predator populations as subject to an allee effect. Thus it would be very interesting to improve such structure in the future.

REFERENCES

1) Song Y., Yuan S., Zhang J., "Bifurcation analysis in the delayed Leslie-Gower predator-prey system". Appl. Math. Modeling 33, 4049-4061, (2009).
2) Zhuang K., Wen Z., "Dynamical behaviors in a discrete predator-prey model with a prey refuge", Int. J. comp. Math. Sci. 5,4, 195-197, (2011).
3) Allee Wc., Animal aggretions, University of Chicago press, Checago, (1931).
4) Stephns P. A., Sutherland W. J., Freckleton R. P.," What is the allee effect", 87,1, 185-190, (1999).
5) Fowler M. S., Ruxton G. D.," Population dynamic consequences of allee effect", J. Theo. Biol. 215, 39-46, (2002).
6) William Z., Lidicker Jr., "The allee effect: Its history and future importance", Open Eco. J. 3,71-82, (2010).
7) Morozov A., Peterskii S., Li B.," Bifurcation and chaos in prey-predatoer system with allee effect", Proc. R. Soc. Lond. B271, 1407-1414, (2004).
8) Hadjiavgousti D., Ichtiarolou S.," Allee effect in a predator-prey", Chaos, Solitons and Fractals 36,2, 334-342, (2008).
9) Schenring I., "Allee effect increases the dynamical stability of population", J. Theor. Biol., 199, 407-414, (1999).
10) Merdan H., Duman O., Akin Ö., çelik C.," Allee effects on population dynamics in continuous (overlapping) case", Chaos, Solitons and Fractals 39, 1994-2001, (2009).
11) Duman O., Merdan H., "Stability analysis of continuous population model involving predation and allee effect", Chaos, Solitons and Fractals 41, 1218-1222, (2009).
12) Merdan H., Duman O., "On the stability analysis of general discrete-time population model involving predation and allee effect", Chaos, Solitons and Fractals 40, 1169-1175, (2009).

13) Çelik C., Duman O.," Allee effect in a discrete-time predator-prey system", 40, 1956-1962, (2009).
14) Liu X., Xiao D., "Complex dynamic behaviors of a discrete-time predator-prey system". Chaos, Solitons and Fractals 32, 80-94, (2007).
15) Murray J. D., "Mathematical Biology", Springer-verlag, Berlin(1998).
16) Elaydi S. N., "An introduction to difference equations", Springer-Verlag publishers, (1996).

Applying & Evaluation Cryptography Files Using Symmetric Cryptography Algorithms of Block Cipher Type

Haifaa Abd Al-Zahra Atee
Foundation of Technical Education

Received : 15/03/2011 Accepted: 29/05/2011

الخلاصة

ان عملية نقل وتبادل ملفات البيانات المهمة من مكان الى اخر او عبر شبكة الانترنت يتطلب حماية وسرية عالية لابعادها عن السرقة والعبث . لذلك فان هناك العديد من الخوارزميات التي وضعت لتشفير الملفات وتوفير البيئة الامنة لافضل نقل للبيانات من مكان لاخر او عبر الشبكة. في هذا البحث تم تطبيق وتقييم خوارزميات التشفير المتناظر من نوع تشفير المقاطع (Block Cipher) لتشفير وفك تشفير ملفات ذات احجام مختلفة باستخدام اربع خوارزميات من نوع خوارزميات التشفير المتناظر. وقد وجد ان هناك فروقاً في الوقت المستغرق لتشفير وفك تشفير نفس الملفات باستخدام خوارزميات التشفير المختلفة. كذلك وجد بان خوارزمية AES هي الاسرع في التشفير وفك التشفير ، اما خوارزمية 3-DES فقد كانت الابطا .وكذلك وجد بان الوقت المستغرق للتشفير اقل من الوقت المستغرق لفك التشفير في جميع الخوارزميات التي استخدمت في البحث. تم التشفير وفك التشفير باستخدام اربع خوارزميات هي :AES(Rijndeal) , Triple DES , Towfish و Blowfish .

ABSTRACT

The process of transfer and exchange of important data files from one place to another or over the Internet requires high protection and confidentiality to keep it away from theft and tampering. Therefore, there are many algorithms that are designed to encrypt files and provide a safe environment for better transfer of data from one place to another or over the network. In this research, implementation and evaluation of a symmetric cryptography algorithms of block cipher type is used to encrypt and decrypt files with different sizes, four algorithms of symmetric encryption block cipher type are used, It was found that there are differences in the time takes to encrypt and decrypt same files which using different encryption algorithms .So found that the AES algorithm is the fastest in the encryption and decryption, either 3-DES algorithm was the slowest. Also found that the time takes to encrypt the files was less

than the time it takes to decode the files in all algorithms used in this research. Four algorithms are used to encryption and decryption files ,these are: AES (Rijndeal) , Triple DES , Towfish ,and Blowfish.

INTRODUCTION

Nowadays when more and more sensitive information is stored on computers and transmitted over the internet, we need to ensure information security and safety.

One of the most uses of encryption is encrypting files to provide secret transition from location to another or over the internet. It doesn't depend on if the files send via public or private networks. Files may be opened by anyone along the way – so anybody , ISP, boss, etc.. Even if computer connected to server and send files via secret FTP protocols , it only means that the files can't be seen while transmitting between the computer and server .When the files reaches to server, it can be seen by FTP server provider. Then the server usually sends the files to the recipient in an unsecured way and files can also be easily seen by anyone.

According to all the above , really, there is only one sure way to protect the files security and privacy – using cryptography .

In this research, different sizes of files are used to implement and evaluate the encryption and decryption operation. four symmetric cryptograph algorithms of block cipher type are used ,these are: Towfish , AES (Rijndeal) , Triple DES , and Blowfish. It was found that there are differences in time that takes to encrypt and decrypt same files which using different encryption algorithms . Also found that the time it takes to encrypt the files was less than the time it takes to decode the encryption in all algorithms used in this research.

The experimental part of all selected block cipher algorithms has been implemented using Visual Basic programming language. Visual Basic is a high-performance language for technical computing(1). AES and Towfish has block size of 128 bits, but 3-DES and Blowfish has 64 bits as a block size.

What is Cryptography?

Cryptography is the science of using mathematics to encrypt and decrypt data, or more exactly is the art of achieving security by encoding information to make them non-readable (2).

In modern times cryptography is considered a branch of both mathematics and computer science and is affiliated closely with information theory, computer security and engineering.

Cryptography enables to store sensitive information or transmit it across insecure networks (like the internet) so that it can't be read by anyone except the intended recipient (2). The origin of the word cryptography comes from Greek, where "crypto" meant "hidden" and "grafik" meant "writing" (1).

There are two basic types of cryptography: Symmetric Key and Asymmetric Key. Symmetric key algorithms are the quickest and most commonly used type of encryption. A single key is used for both encryption and decryption(2).

There are two types of symmetric algorithms : Stream ciphers and Block ciphers. A stream cipher operates on a stream of plaintext bit by bit, while a block cipher operates on a stream of plaintext block by block. That is a stream cipher encrypts plaintext individually, and an encryption key is used for one bit only in a stream cipher. A block cipher divided a stream of plaintext into blocks, and an encryption key is used for all bits in one block in a block cipher. figure(1) illustrate the cryptography techniques (2).

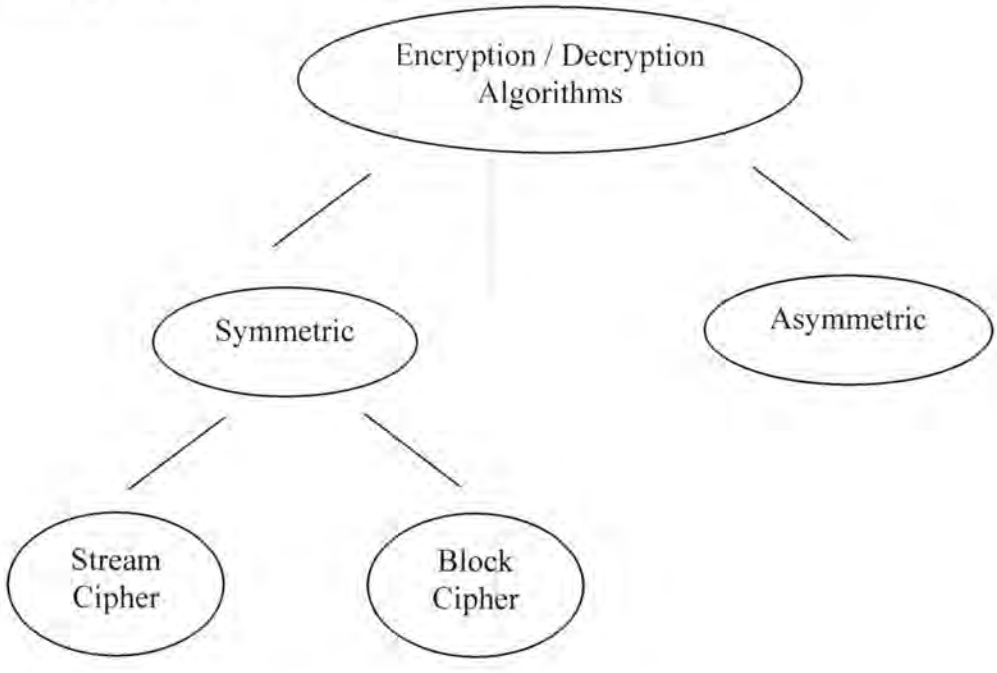

Fig.-1: Cryptography Techniques

Symmetric & Asymmetric Key Cryptography

Symmetric Key Cryptography

In symmetric key cryptography, a single key is used for both encryption and decryption. The sender uses the key (or some set of rules) to encrypt the plaintext and sends the cipher text to the receiver. The receiver applies the same key to decrypt the message and recover the plaintext(2,3).

They are usually related and it is easy to derive the decryption key once one knows the encryption key. In most cases, they are identical. A Secret key should be shared (or agreed) both the communicating parties(4).

Symmetric key cryptography schemes are generally categorized as being either stream ciphers or block ciphers. Stream ciphers operate on a single bit (byte or computer word) at a time, and implement some form of feedback mechanism so that the key is constantly changing(5).

A block cipher is a scheme to encrypts one block of data at a time using the same key on each block. In general, the same plaintext block will always encrypt to the same cipher text when using the same key in a block cipher whereas the same plaintext will encrypt to different cipher text in a stream cipher (2,6).

Asymmetric Key Cryptography

Asymmetric key cryptography involves the use of key pairs: one private key and one public key. Both are required to encrypt and decrypt a message or transmission. The private key is not to be shared with anyone. The owner of the key is responsible for securing it in such a manner that it will not be lost or compromised. Public key cryptography intends for public keys to be accessible to all users(2,6).

Block Ciphers

Block cipher is a symmetric cipher which encrypts information by breaking it down into blocks and encrypting data in each block. A block cipher encrypts data in fixed blocks (commonly of 64 bits). Some example of a symmetric encryption algorithms of block cipher type are : AES(Rijndeal), Blowfish, CAST5, DES, Triple DES, IDEA, RC2, RC5, RC6, Gost, Serpent, and Twofish(7,8). Figure(2) illustrates the encryption and decryption operation for block cipher.

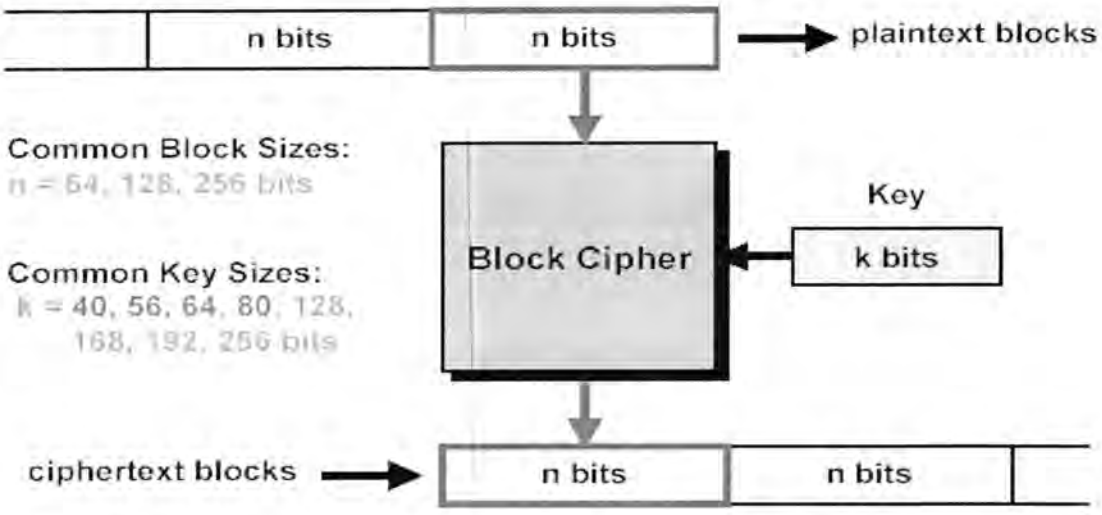

Fig. -2: Encryption & Decryption Operation for Block Cipher Algorithms

In this research, randomly selected four symmetric cryptography algorithms of block cipher type , all selected algorithms are explained in below section.

AES Block Cipher (Rijndael Block Cipher)

Rijndael is a block cipher, designed by Joan Daemen and Vincent Rijmen as a candidate algorithm for the AES. AES stands for Advanced Encryption Standard. AES is a symmetric key encryption technique which will replace the commonly used Data Encryption Standard (DES). The Advanced Encryption Standard algorithm approved by NIST in December 2001 uses 128-bit blocks(9).

The block cipher currently supports key lengths of 128, 192, and 256 bits. Each encryption key size causes the algorithm to behave slightly differently, so the increasing key sizes not only offer a larger number of bits with which can scramble the data, but also increase the complexity of the cipher algorithm(7).

Triple DES

Triple DES is a variation of Data Encryption Standard (DES). It uses a 64-bit key consisting of 56 effective key bits and 8 parity bits. The size of the block for Triple-DES is 64 bit. The idea behind Triple DES is to improve the security of DES by applying DES encryption three times

using three different keys. Triple DES algorithm is very secure (major banks use it to protect valuable transactions), but it is also very slow(7,10).

Blowfish Block Cipher

Blowfish is a symmetric encryption algorithm designed in 1993 by Bruce Schneier as an alternative to existing encryption algorithms. Blowfish has a 64-bit block size and a variable key length - from 32 bits to 448 bits. It is a 6-round Feistel cipher and uses large key-dependent S-boxes.

Blowfish is similar in structure to CAST-128, which uses fixed S-boxes(7,10).

Twofish Block Cipher

Twofish is a symmetric block cipher. Twofish has a block size of 128 bits and accepts keys of any length up to 256 bits. Twofish has key dependent S-boxes like Blowfish(11).

Twofish encryption algorithm was designed by Bruce Schneier, John Kelsey, Chris Hall, Niels Ferguson, David Wagner and Doug Whiting. The National Institute of Standards and Technology (NIST) investigated Twofish as one of the candidates for the replacement of the DES encryption algorithm(12).

Related Works

There are various studies and researches about the performance evaluation of block ciphers on low-cost microcontrollers. For example, Law et al. (2006) evaluated the performance of RC5, RC6, AES, MISTY1, KASUMI, and Camellia block ciphers for 16-bit RISC microcontroller MSP430F149. Rinne et al. (2007) measured the performance of DESL, Hight, SEA, and TEA / XTEA algorithms for 8-bit ATMEL microcontroller. Isenbarth et al. (2007) measured the performance of ES, Hight, Clefia, Crypton, DES, DESXL algorithms. In another study, Cakiroglu et al. (2010) implemented and evaluated the SEA, RC6, AES block ciphers for 8-bit TMEL microcontroller, and Murat Çakiroglu (2010) Software implementation and performance comparison of popular block ciphers on 8-bit low-cost microcontroller.

There is many researches about performance evaluation of block cipher type in term of time and other factors. For example El-Fishawy N., El-danaf T., and Abo Zaid Osama (2002) A modification of Rc6 block cipher algorithm for data security. AJ Elbirt and B.Chelwynd (2000) An FPGA implementation and performance evaluation of AES block cipher candidate algorithm finalists.

In this research, four different cryptography algorithms used to measure the efficiency of cryptograph in terms of time it takes to encrypt and decrypt different sizes files using symmetric encryption algorithms of block cipher type.

Hardware & Software Specification

One of the most important performance criteria of the encryption algorithms is execution time .Execution time related to many parameters such as structure of the algorithm, number of round, size of file, and the selected target device.[101]

The encryption and decryption algorithms were implemented by the following hardware and software specifications:

1- Intel(R) Celeron(R) D CPU 3.06 GHZ.
2- 1 GB RAM.
3- Asrock 945GCM-S Mother Board.
4- Windows XP professional ver.2002, service pack 2.
5- Hard disk 320 GB with 80GB free in C partition (C partition used as a target device).
6- All selected algorithm are tested with 16 round except AES, it tested with 12 round.
7- 128 bit data block used for AES & Twofish, the Blowfish & 3-DES used 64bit as a data block.
8- 128 bit used as a key size in both AES ,Blowfish, and Twofish, but 56 bit used in 3_DES.

The main steps used to encrypt and decrypt the files is represent in figure(3) as show below:

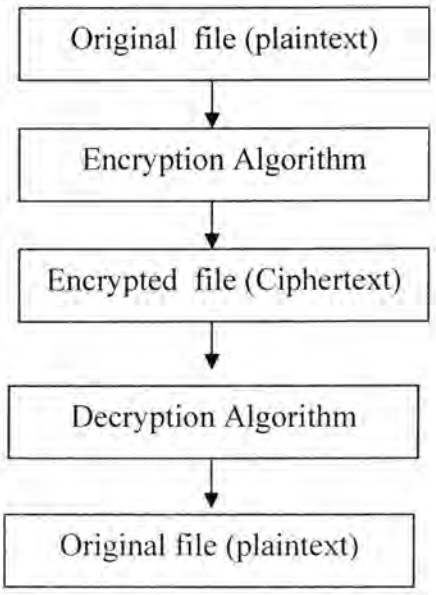

Fig. - 3: Main Steps for Encryption & Decryption the Files

EXPERIMENTAL RESULTS

Performance Comparison Of The Selected Block Cipher

Two parameters are used as a factors to measuring the efficiency of four selected algorithms that are: size of files and the time required for encryption and decryption the files. The size of files is related with the time consuming to encrypt or decrypt the file. AES and Towfish has block size of 128 bits, but 3-DES and Blowfish has 64 bits as a block size. Among all the selected block cipher algorithms the AES algorithm was the fastest because it can perform the encryption and decryption process within shorter time than the others, but the 3-DES algorithm was the slowest (because it used 3 round of encryption (each round have 16 subround) with different key to improve the security), it takes longest time than the other algorithms . While the Twofish and Blowfish comes sequentially after AES and before 3-DES in terms of speed and efficiency.

Encryption and decryption time for AES, Twofish, Blowfish, and 3-DES algorithms with size 50Mb, 100Mb, 150Mb, 200Mb, and 250 Mb are illustrated in table(1).

Table-1 : The experimental results for selected algorithms

Algorithm / Size	AES		Towfish		Blowfish		3-DES	
	T.Enc	T.Dec.	T.Enc.	T.Dec.	T.Enc.	T.Dec.	T.Enc.	T.Dec.
50	2:30	3:10	2:70	4:17	3:83	5:50	5:22	7:01
100	4:11	6:12	5:73	8:11	6:92	11:44	9:80	13:04
150	6:08	9:20	9:34	13:02	10:09	16:02	14:84	19:27
200	8:25	15:08	13:55	19:23	17:43	22:97	17:39	28:02
250	10:10	16:90	15:17	23:40	23:60	37:38	23:16	35:15

T.Enc. : Encryption time ; T.Dec. :Decryption time
The time is measured by second and millisecond

The execution time for the each one of selected block cipher algorithms are shown in the figure(4), figure(5), figure(6), and figure(7).

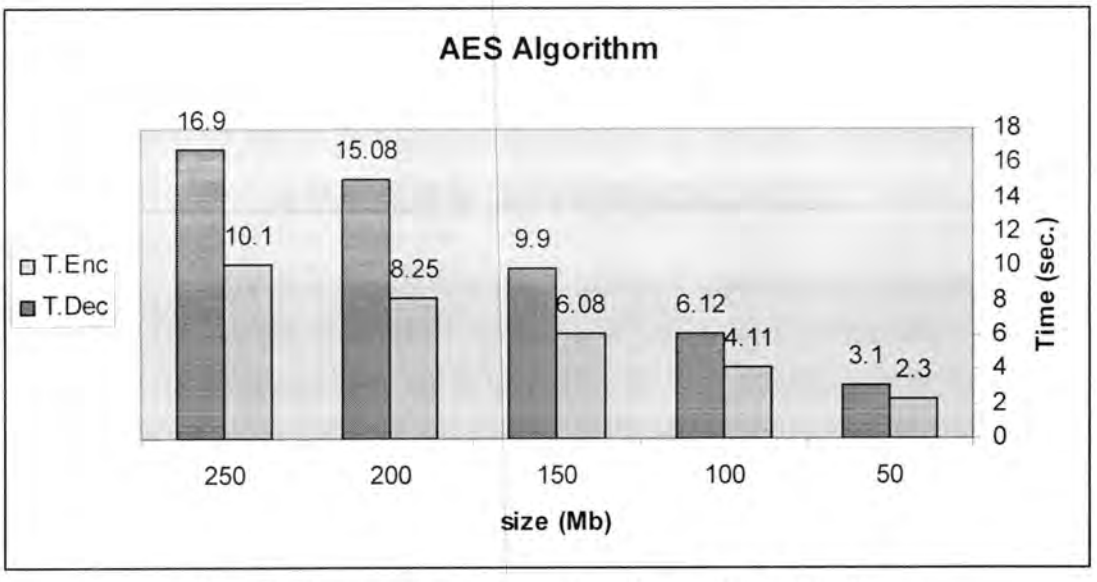

Fig.- 4: Execution Time for the AES Algorithm

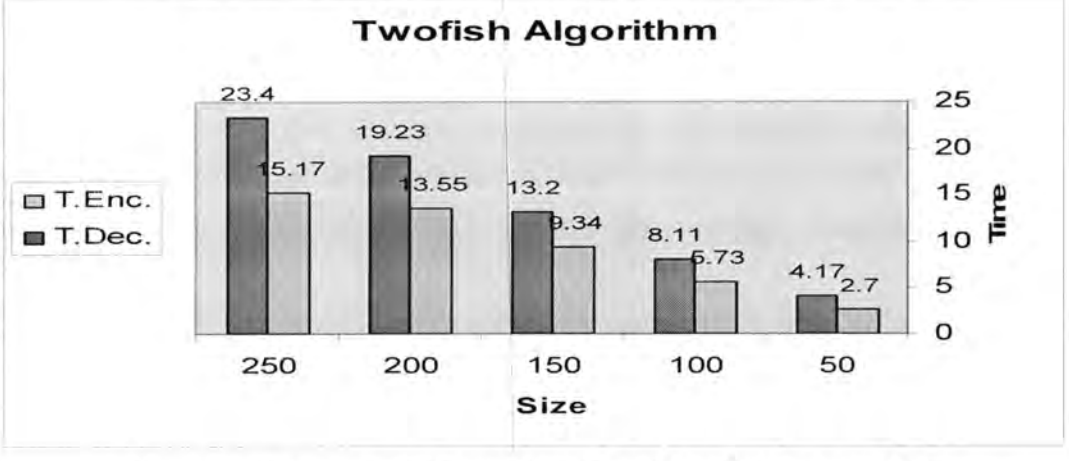

Fig.- 5: Execution Time for The Twofish Algorithm

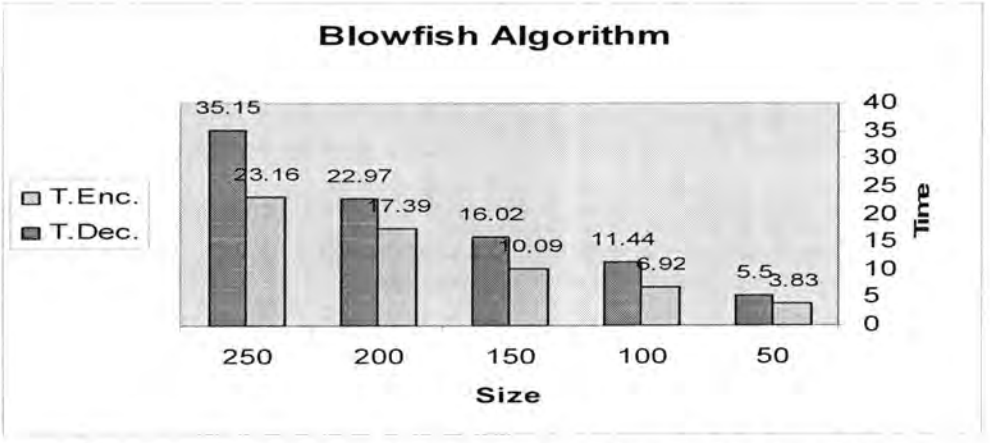

Fig. - 6: Execution Time for The Blowfish Algorithm

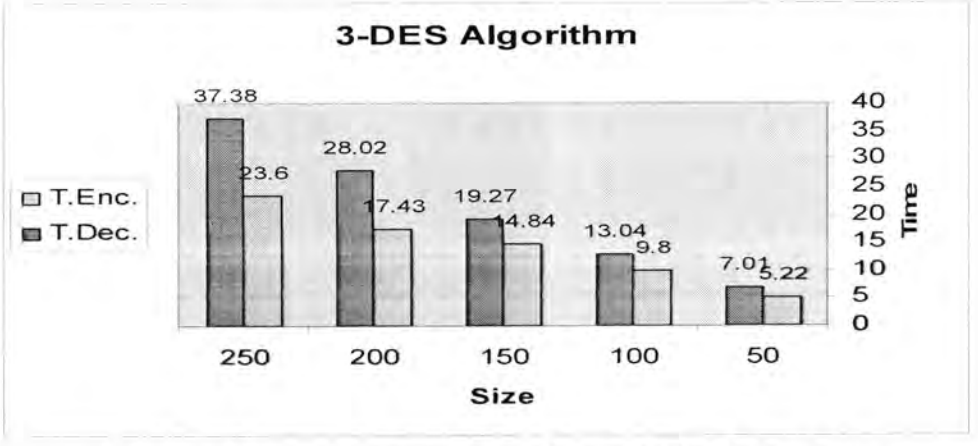

Fig.- 7: Execution Time for the 3-DES Algorithm

Figure(8),figure(9), figure(10), and figure(11) show the execution time of encryption and decryption operation for all selected block cipher algorithms.

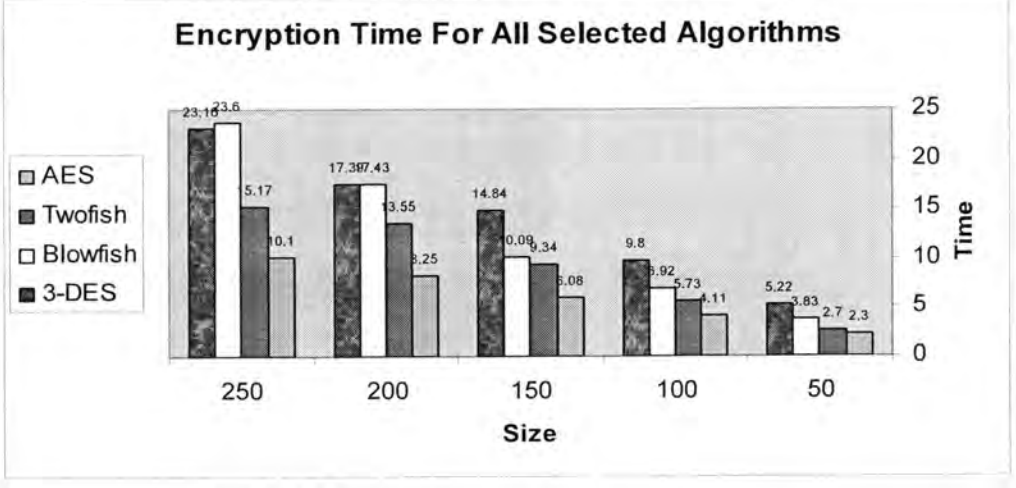

Fig.-8: Execution Time of Encryption operation for all selected algorithm

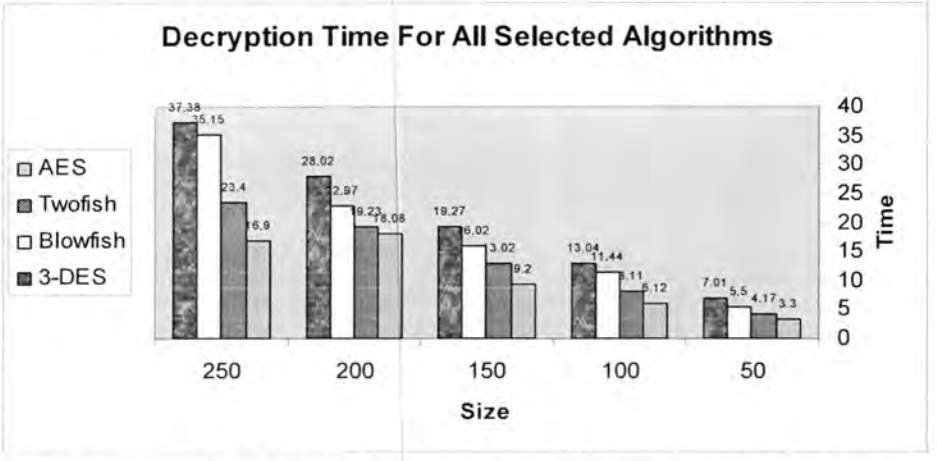

Fig.-9: Execution Time of Decryption operation for all selected algorithm

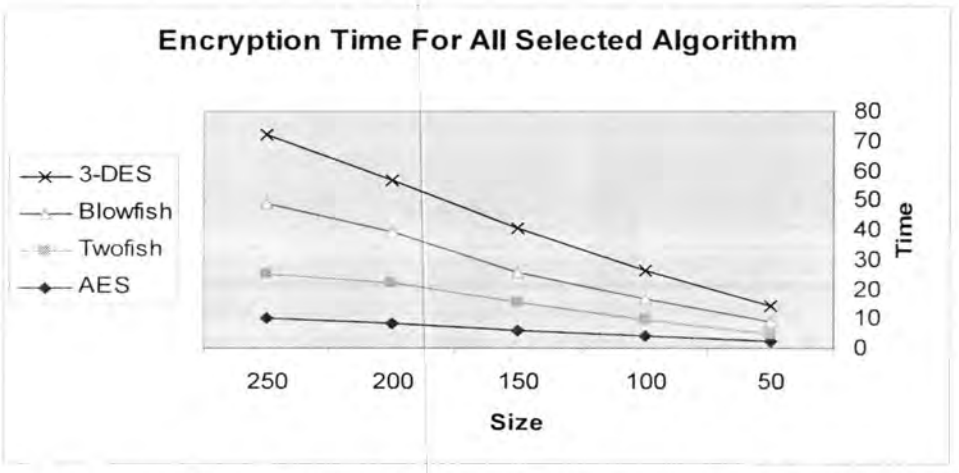

Fig.-10 : Execution Time of Encryption operation for all selected algorithm

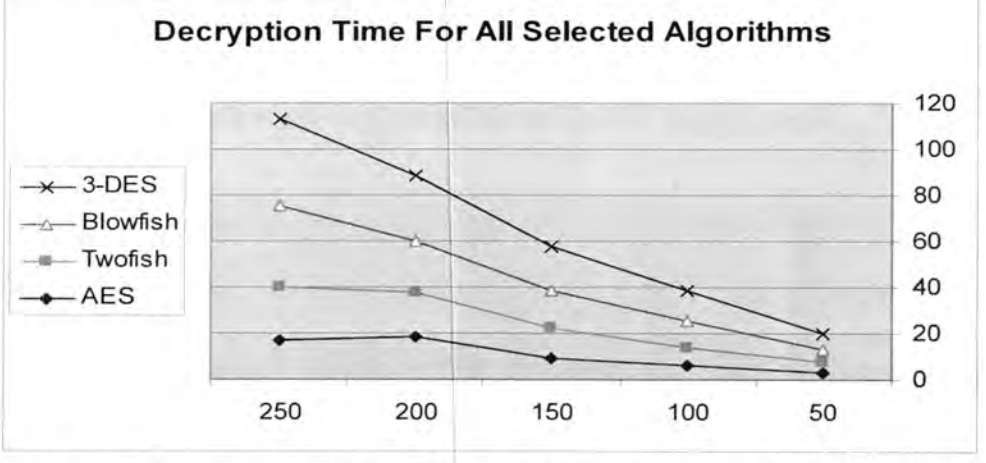

Fig.-11: Execution Time of Decryption operation for all selected algorithm

Figure(12) show the encryption & decryption time for all selected algorithms. With all the above figures, it is clear that the AES algorithm have the best performance to encrypt and decrypt the files ,the Towfish and Blowfish below the AES, the 3-Des algorithm is the slowest one among all the selected algorithm, it takes the longest time to encrypt and decrypt the same size of files.

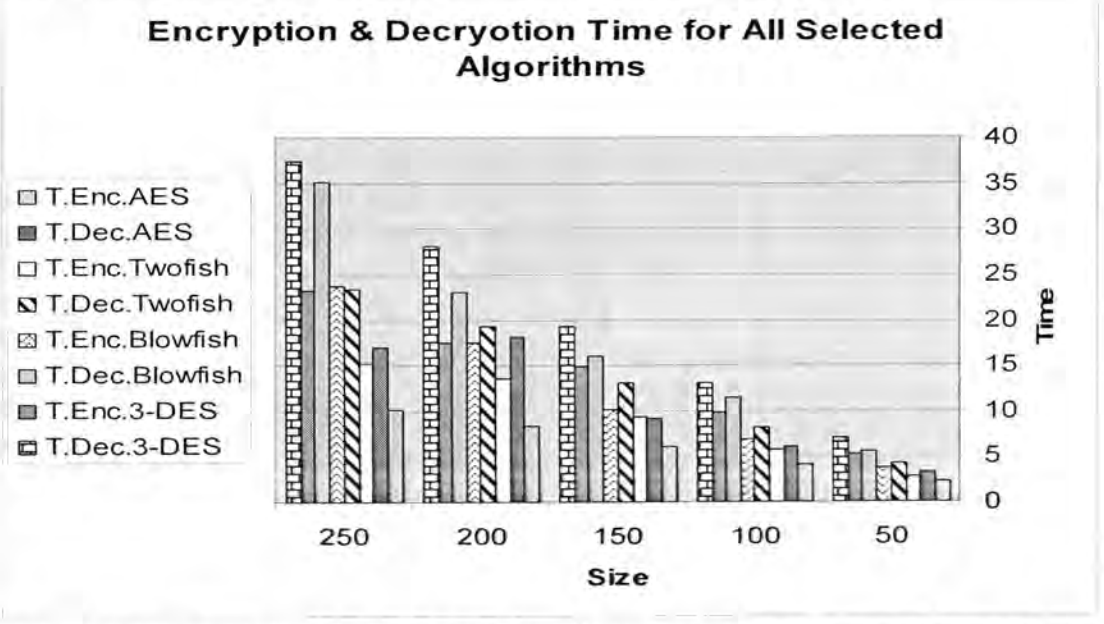

Fig.-12: Encryption & Decryption Time For All Selected Algorithms

T.Enc.AES : Time Encryption for AES algorithm.
T.Dec. AES: Time Decryption for AES algorithm.
T.Enc. Twofish: Time Encryption for Twofish algorithm.
T.Dec. Twofish: Time Decryption for Twofish algorithm.
T.Enc. Blowfish: Time Encryption for Blowfish algorithm.
T.Dec. Blowfish: Time Decryption for Blowfish algorithm.
T.Enc. 3-DES : Time Encryption for 3-DES algorithm.
T.Dec. 3-DES: Time Decryption for 3-DES algorithm.

Cryptography is used to achieve many goals like confidentiality, data integrity, authentication, safety transfer of date etc. In order to achieve these goals various cryptographic algorithm are designed.

Randomly selected four cryptograph algorithms, these are AES, Twofish, Blowfish, and 3-DES, in term of specification parameters, it found that :

1. When increase the file's size, the time taken to encrypt or decrypt the files also increase.
2. In general, the time taken to encrypt files less than the time taken to decrypt the files.
3. AES algorithm is the fastest between all selected algorithm, twofish and Blowfish below the AES, the 3-DES is the slowest one among all the selected algorithms (it takes longest execution time to encrypt or decrypt same file).

REFERENCES

1. A.I.Khamg ,"Implementation and Evaluation of New Cryptography Algorithm For E-mail Application",Msc.Dept. of Computer and communication System Engineering–University Putra, Malaysia,(2002).
2. A.R.Ayushi , "A Symmetric Key Cryptographic Algorithm" , International Journal of Computer Applications , pp15,(2010).
3. K.Jonathan and L.Yehuda,"Introduction to Modern Cryptography", Chapman and Hall,CRC press,pp(47-54), (2007).
4. G.Ratan, "cryptography", School of computer Science, University of Central Florida, Orland,(2004).
5. N.R.Wagner, "The Laws of Cryptography: Conventional Block Cipher" (2002).
6. S.William," Cryptography and Network Security :Principles and Practice, Prentice Hall, 2nd edition,pp23-50,(1999).
7. P.H.Jason, "Cryptography and Encryption Methods :How Secure are We in Our Daily Lives?",Msc.Dept. Management Information Systems, Bowie State University Maryland in Europe,pp6-13,(2008).
8. D.Morris , "Recommendation for Block Cipher Modes of Operation :Methods & Techniques, NIST Special Publication 800-38A,(2001).

9. M.Cakirglu, "Software Implementation and Performance comparison of Popular Block Cipher on 8-bit Low Cost Microcontroller", International Journal of the Physical Science,Vol.5(9) Dept of Computer Science, University of Sakarya, Turkey,pp1338-1343,(2010),
10. M.Amogh and D.Rajballav, "Data Encryption and Decryption by Using Hill Cipher Technique and Self Repetitive Matrix", Dept. of Electronics and Instrumentation engineering, National Institutes of Technology, Rourkela, pp10-28,(2007).
11. W.Doug and S.Bruce, "improver Twofish implementation", (1998).
12. S.Bruce, K.John, W.Doug, W.David, and H.Chris, "Twofish :A 128 bit Block Cipher", (1998).

Image Encryption Using Permutation and Hill Cipher

Ghassan Muslim Hassan
Computer Department, College of Sciences, Al-Mustansiriyah University

Received: 27/04/2011 Accepted : 29/05/2011

الخلاصة

يستخدم التشفير لغرض نقل البيانات بصورة امنة في شبكات الحاسوب. وتختلف خوارزميات التشفير باختلاف نوع البيانات (نص، صورة، صوت) لما لكل نوع من البيانات خواصه المختلفة. في هذا البحث تم اقتراح طريقة جديدة لتشفير الصور تتلخص باستخدام صورتين، احدهما تستخدم كمفتاح وتكون موجودة لدى المرسل والمستلم والاخرى هي الصورة المراد ارسالها يتم اضافة الصورتين باستخدام (XOR) بعدها يتم تجزئة الصورة الى أجزاء بحجم(n x n) جزء وتمرر هذه الاجزاء الى خوارزمية التشفير (Hill cipher) ويتم بعثرة هذه الاجزاء حسب جدول يتم توليدة.

ABSTRACT

Encryption is used to securely transmit data in open networks. Each type of data has its own features; therefore different techniques should be used to protect confidential image data from unauthorized access. This paper, has been proposed new encryption algorithm using two different images, one is cover image which acts as key image which is shared by both sender and receiver and other is Informative image. As first step, XOR cover image with informative image to obtain resultant image. The resultant image is decomposed into (n x n) blocks which passed to the Hill Cipher algorithm to form encrypted blocks. The encrypted blocks are transformed into new locations using permutation table.

INTRODUCTION

The rapid growth of computer networks allowed large files, such as text, audio, and image, to be easily transmitted over the internet and it is important to protect the confidentiality of image data from unauthorized access [1]. Cryptography is the science of using mathematics to encrypt and decrypt data, and thus it provides a secure way to store sensitive information or transmit it across insecure networks such as the internet, so that it cannot be read by anyone except the intended recipient [2]. In general, conventional textual cryptography algorithms such as Data Encryption Standard (DES), Triple-DES,

Data Encryption Standard (AES) and Rivest, Shamir and Adleman (RSA) cannot be used to encrypt images directly. Images are different from texts in many aspects such as high correlation among pixels and high redundancy. Thus, a variety of new image encryption schemes have been proposed [3].

Although the traditional encryption algorithms used to encrypt images directly, it is not a good idea for two reasons. The **first** is the image size is often larger than text. Consequently, the traditional encryption algorithms need longer time to directly encrypt the image data, the **second**, is the decrypted text must be equal to the original text, but this requirement is not necessary for image data. Due to the characteristic of human perception, a decrypted image containing small distortion is usually acceptable [4].

Literature Survey

Most of the algorithms specifically designed to encrypt digital images are proposed in the mid-1990s. There are two major groups of image encryption algorithms: (a) nonchaos selective methods and (b) Chaos-based selective or non-selective methods. Most of these algorithms are designed for a specific image format compressed or uncompressed, and some of them are even format compliant. The methods that offer light encryption (degradation), while others offer strong form of encryption. Some of the algorithms are scalable and have different modes ranging from degradation to strong encryption [5].

Shujun Li et al. [6] have pointed out that all permutation only image ciphers were insecure against known/chosen plaintext attacks. In conclusion, they suggested that secret permutations have to be combined with other encryption techniques to design highly secured images. Mitra A et al.[2] have proposed a random combinational image encryption approach with bit, pixel and block permutations. Zhi-Hong Guan et al. [7] have presented a new image encryption scheme, in which shuffling the positions and changing the grey values of image pixels are combined to confuse the relationship between the cipher image and the plain image. Sinha A. and Singh K. [8] proposed an image encryption by using Fractional Fourier Transform (FRFT) and JigSaw Transform (JST) in image bit planes. Maniccam S.S. and Bourbakis N G. [5] proposed image and video encryption using SCAN patterns. The image encryption is performed by SCAN based permutation of pixels and a substitution rule which together form an iterated product cipher. Ozturk I. and Sogukpinar I. [9] proposed new schemes which add compression capability to

the mirror-like image encryption MIE and Visual Cryptography VC algorithms to improve these algorithms. Maniccam S.S., Nikolaos G. and Bourbakis. [10] have presented a new methodology, which performs both lossless compression and encryption of binary and gray-scale images. The compression and encryption schemes are based on SCAN patterns generated by the SCAN methodology. Droogenbroeck M.V. and Benedett R. [11] were proposed two methods for the encryption of an image; selective encryption and multiple selective encryption. The proposed process divides the image into number of blocks with predefined maximum and minimum number of pixels (4 × 4) pixels blocks, resulting in a stronger encryption and a decreased correlation

Encryption Algorithm

In this paper, we implemented Hill Cipher and permutation techniques. The proposed algorithm uses two different images with same size, one is used cover image which act as key image and is shared by both sender and receiver, the other one is used a plain image, the algorithm of the proposed system is shown in algorithm (1);

Algorithm (1);

At the sender

Step1: XOR cover image and informative image (which are the same size) to obtained resultant image.

Step2: The resultant image from step 1 can be decomposed into blocks; each one contains a specific number of pixels (4 × 4) pixels blocks. Increasing the number of blocks by using smaller block sizes resulted in a lower correlation and higher entropy [5,8].

Step3: The blocks are passed to the Hill Cipher algorithm to form encrypted blocks.

Step4: The encrypted blocks transformed into new locations using **permutation table**.

At the receiver

Step 1: The encrypted image after receiving by receiver transformed to new location by using **permutation table** .

Step 2: Apply Hill cipher to those new locations of encrypted image by using K^{-1} (key inverse of Hill cipher), to obtain merged image.

Step 3: The merged image (XOR) with the same key image (which is shared by sender and receiver) to obtained informative image (plain image)

We can summarized the process of encryption technique in figure 1;

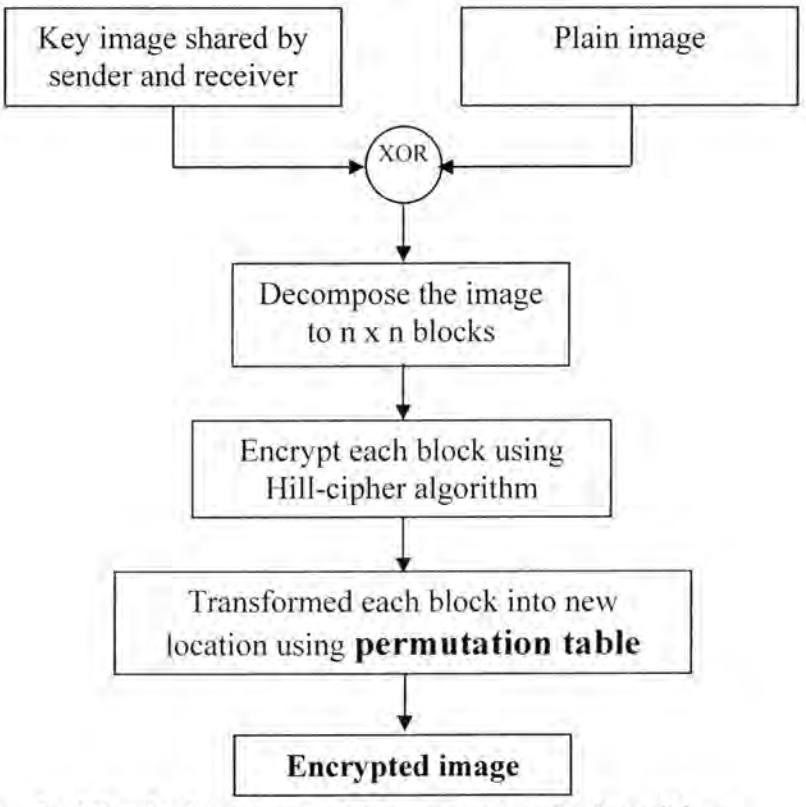

Fig. -1: Block diagram of the proposed algorithm

Hill Ciphering

The Hill cipher works on groups of letters in a somewhat different manner. The Hill cipher works by viewing a group of letters as a vector, and encryption is done by matrix multiplication [12]. Each letter is first encoded as a number. Often the simplest scheme is used: A = 0, B =1, ..., Z=25, but this is not an essential feature of the cipher. A block of *n* letters is then considered as a vector of n dimensions, and multiplied by an (n × n) matrix, modulo 26. The whole matrix is considered the cipher key, and should be random provided that the matrix is invertible (to ensure decryption is possible). A Hill cipher is another way of working out the equation of a matrix [13].

If a message 'ACT' (for example), and the key below (or GYBNQKURP in letters):

$$\begin{pmatrix} 6 & 24 & 1 \\ 13 & 16 & 10 \\ 20 & 17 & 15 \end{pmatrix}$$

Since 'A' is 0, 'C' is 2 and 'T' is 19, the message is the vector:

$$\begin{pmatrix} 0 \\ 2 \\ 19 \end{pmatrix}$$

Thus the enciphered vector is given by:

$$\begin{pmatrix} 6 & 24 & 1 \\ 13 & 16 & 10 \\ 20 & 17 & 15 \end{pmatrix} \begin{pmatrix} 0 \\ 2 \\ 19 \end{pmatrix} = \begin{pmatrix} 67 \\ 222 \\ 319 \end{pmatrix} \equiv \begin{pmatrix} 15 \\ 14 \\ 7 \end{pmatrix} \pmod{26}$$

which corresponds to a cipher-text of 'POH', every letter has changed.[13]

Algorithm-Create-Permutation-Table

The encrypted image (plain image XOR with key) is based on the combination of encrypted block (Hill-cipher) followed by permutation process. In this case, combination of Hill-cipher followed by permutation process use the original image (see Fig.2(a) and Fig.2(b)) to produce Fig.(c),(d) respectively. In this paper standard randomness measures was used to test the permutation complexity as followed ;

Statistical Tests for Randomness

The blocks was transformed to binary form to get $\mathbf{s} = \mathbf{s_0}, \mathbf{s_1}, \mathbf{s_2}, \ldots, \mathbf{s_{n-1}}$ be a binary sequence of length n. This subsection presents four statistical tests that are commonly used for determining whether the binary sequence s possesses some specific characteristics that a truly random sequence would be likely to exhibit. If a sequence passes all four tests, there is no guarantee that it was indeed produced by a random bit generator.

Frequency Test (Mono-Bit Test)

The purpose of this test is to determine whether the number of 0's and 1's in s are approximately the same, as would be expected for a random sequence. Let n_0 and n_1 denote the number of 0's and 1's in s, respectively. The statistic used is

$$X_2 = \frac{(n_0 - n_1)^2}{n} \quad \ldots\ldots (1)$$

Serial Test (Two-Bit Test)

The purpose of this test is to determine whether the number of occurrences of 00, 01, 10, and 11 as subsequences of s are approximately the same, as would be expected for a random sequence. Let n_0 and n_1 denote the number of 0's and 1's in s, respectively, and let n_{00}, n_{01}, n_{10}, and n_{11} are denote the number of occurrences of 00, 01, 10, 11 in s, respectively. Note that

$n_{00}+n_{01}+n_{10}+n_{11}=(n-1)$, since the subsequences are allowed to overlap. The statistic used is

$$X_2 = \frac{4}{n-1}\sum_{i=0}^{1}\sum_{j=0}^{1} n_{ij}^2 - \frac{2}{n}\sum_{i=0}^{1} n_i^2 + 1$$
$$= \frac{4}{n-1}\left(n_{00}^2 + n_{01}^2 - n_{10}^2 - n_{11}^2\right) - \frac{2}{n}\left(n_0^2 + n_1^2\right) - 1 \quad \ldots\ldots (2)$$

Poker Test

Let m be a positive integer such that

$$\left\lfloor \frac{n}{m} \right\rfloor \geq 5 \cdot 2^m, \text{ and let } k = \left\lfloor \frac{n}{m} \right\rfloor$$

Divide the sequence s into k non-overlapping parts each of length m, and let n_i be the number of occurrences of the i^{th} type of sequence of length m, $1 \leq i \leq 2^m$. The poker test determines whether the sequences of length m each appear approximately the same number of times in s, as would be expected for a random sequence. The statistic used is

$$X_3 = \frac{2^m}{k}\left(\sum_{i=1}^{2^m} n_i^2\right) - k \quad \ldots\ldots (3)$$

Runs Test

The purpose of the runs test is to determine whether the number of runs (of either zeros or ones) of various lengths in the sequence s is as expected for a random sequence. The expected number of gaps (or blocks) of length i in a random sequence of length n is :

$e_i=(n-i+3)/2^{i+2}$

Let k be equal to the largest integer i for which $e_i \geq 5$. Let B_i, G_i be the number of blocks and gaps, respectively, of length i in s for each i, $1 \leq i \leq K$

The statistic used

$$X_4 = \sum_{i=1}^{k}\frac{(B_i - e_i)^2}{e_i} + \sum_{i=1}^{k}\frac{(G_i - e_i)^2}{e_i}$$

The main algorithm

1: Load the plain Image
2: Input secret key
3: Get the Width and Height of the image
4.1: Lower Horizontal Number of Blocks = Integer (Image Width / 4)
4.2: Lower Vertical Number of Blocks = Integer (Image Height /4)
5: Number of Blocks = Horizontal Number of Blocks × Vertical Number of Blocks
6: Seed = | Hash value (Key) |
7: Counter of Good Keys = 0
8: For I = 0 to Number of Blocks -1
    8.1: Get the New Location of Block .
    8.2: By Using all Tests (eq.(1), eq.(2), eq.(3), and eq.(4)) , the Good Key was Chosen.
    8.3: Save the Good Key in a Table.
    8.4: Increase the Counter of Good Keys by One.
9: By Using Pseudo Random Generator, the Desired Key was Chosen From a Permutation Table
10: Set block in its new Location
END PERFORM_PERMUTATION
Input: plain Image (BMP image file) and permutation table
Output: permuted Image.
The proposed combinational scheme along with individual permutations has been implemented in the **Matlab** with several test images.

Security Analysis and Test Results

In this section, the performance of the proposed image encryption scheme is analyzed in detail. The discussion was made of security analysis of the proposed image encryption scheme including some important ones like statistical sensitivity, key sensitivity analysis, key space analysis etc. to prove the proposed cryptosystem is secure against the most common attacks.

Visual Testing

A number of images are encrypted by the proposed method, and visual test is performed. Two examples are shown in Fig. 2 (a) and Fig. 2 (b), where each image is in 24-bit color with 300x200 pixels. By comparing the original and the encrypted images in Fig. 2, there is no visual information observed in the

encrypted image, and the encrypted images are visual indistinguishable even with a big difference in the color tone found in the original images.

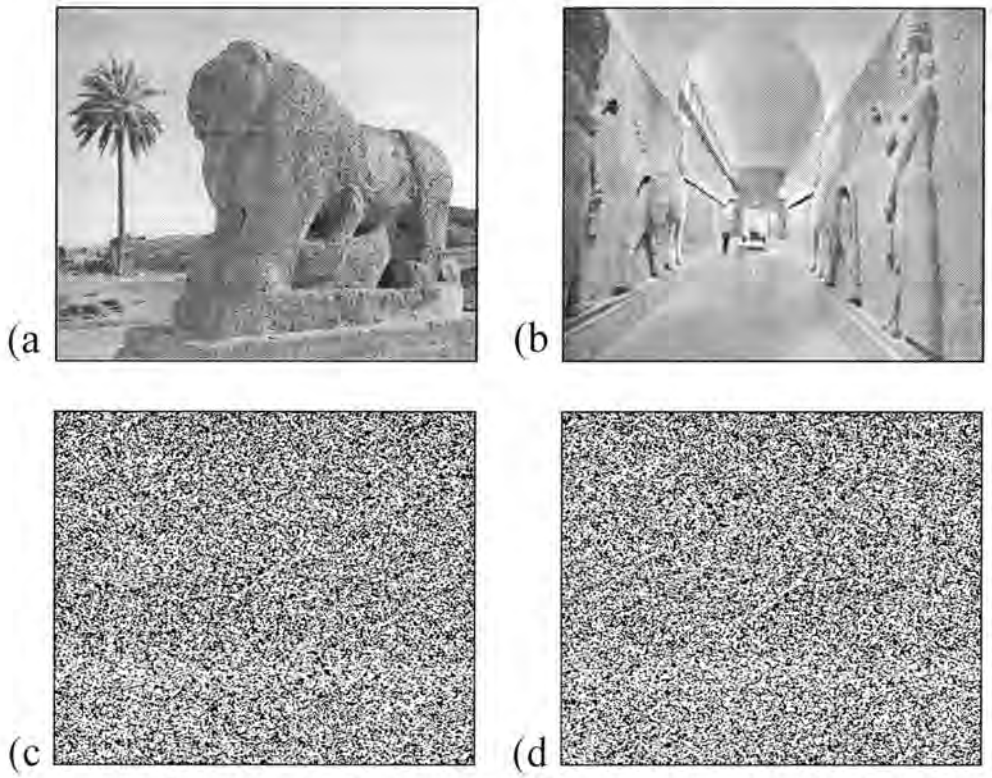

Fig. -2: show the proposed encrypted system, (a) and (b) the original images of Babylon lion and Iraqi museum, (c) and (d) the encrypted images of the plain images

Histogram Analysis

To prevent the leakage of information to attackers, it is important to ensure that encrypted and original images do not have any statistical similarities. The histogram analysis clarifies that, how the pixel values of image are distributed. Fig. (3) shows histogram analysis on test image using the proposed algorithm.

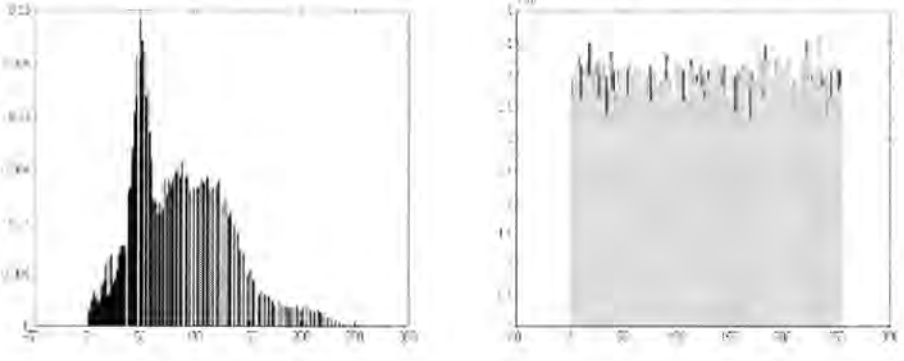

Fig.-3: shows the histograms analysis a)red channel of the plain Babylon lion image , and b)red channel of the encrypted Babylon lion image

From figure (3) we can see the histogram do not show any similarities between an original and encrypted image.

We can conclude that Image data has visual information observed in each image. However, it is very important to disturb these information among image pixels to increase the security level of the encrypted images, if the encryption will done on each image. To make a secure image system, the proposed technique divides an image into blocks of n x n size and then perform double encryption process. In this paper the proposed algorithm uses two different images, one is cover image which act as key image which is shared by both sender and receiver and the other is plain image first we XOR the plain image and cover image and pass the resultant image to hill cipher algorithm then transformed the image using permutation table. Experimental results showed the histogram analysis of red channel for both plain and encrypted image. The histogram does not show any similarities for both images. From the results, it is observed that combined method achieved the advantages all individual permutation techniques.

REFERENCE

1. W. Lee, T. Chen and C. Chieh Lee, "Improvement of an encryption scheme for binary images," *Pakistan Journal of* Information *and Technology*. 2(2), 191-200. http://www.ansinet.org., (2003).
2. G. C. Kessler, "An Overview of Cryptography," published by Auerbach, 1998' (22 Desember 2007).
3. K. Wang , Pei , Z. Liuhua ,S. Aiguo Song, H. Zhenya, "On the security of 3D Cat map based symmetric image encryption scheme," Elsevier, Physics Letters A, 343, 432–439, Issue 6, (2005).
4. S. Han, and S. Yang, "An Asymmetric Image Encryption Based on Matrix Transformat ion," e c t I transactions on computer and information technology 1(2), (2010).
5. S.S. Maniccam, N.G. Bourbakis, "Image and video encryption using SCAN patterns," Journal of Pattern Recognition Society, 37(4), 725–737, (2004).
6. Li. Shujun, X. Zheng "Cryptanalysis of a chaotic image encryption method," Inst. of Image Process. Xi'an Jiaotong Univ., Shaanxi, This paper appears in: Circuits and Systems, ISCAS 2002. IEEE International Symposium on Publication Date: 2009, 2, 2002, 708,711, (2009).

7. G. Zhi-Hong, H. Fangjun, and G.Wenjie , "Chaos - based image encryption algorithm," Department of Electrical and computer Engineering, University of Waterloo, ON N2L 3G1, Canada. Published by: Elsevier, 153-157, (2009).
8. A. Sinha, K. Singh, "Image encrypt ion by using fractional Fourier trans form and Jigsaw transform in image bit planes," Source: optical engineering, spie-int society optical engineering, 44(5), 15-18, (2005).
9. I. Ozturk, and I.Sogukpinar, "Analysis and comparison of image encryption algorithm," International Journal of Information Technology, 1(2), 64-67. http://www.waset.org , (2005).
10. S . S . Manic c am. , G . Nikolaos , and Bourbakis, "Lossless image compression and encryption using SCAN," Journal of: Pattern Recognition, 34(6), 1229– 1245, (2001).
11. M. Van Droogenbroeck and R. Benedett, "Techniques for a selective encryption of uncompressed and compressed images," In ACIVS'02, Ghent, Belgium, Proceedings of Advanced Concepts for Intelligent Vision Systems, (2007).
12. Scott Sutherland, "An Introduction to Cryptography", October 14, (2005).
13. Lester S. Hill, Concerning Certain Linear Transformation Apparatus of Cryptography, The American Mathematical Monthly 38, 135–154, (1931).

Topographic Images Classification Considering Color Information

Sundos A. Hameed Al-Azawi and Esraa Jaffar Baker
Computer Sciences Department, College of Sciences, Al-Mustainsiriyah University

Received : 29/03/2011 Accepted : 29/05/2011

الخلاصة

أثبتت المعلومات اللونية في تصنيف الصور دقة التصنيف لخصائص اللون. اعتمد النظام المقترح, في تصنيف صور التضاريس الرقمية على الخصائص الناتجة من المعلومات اللونية للصورة المدخلة في خوارزمية التصنيف. لذلك, تم اقتراح طريقة لتصنيف هذا النوع من الصور , هذه الطريقة تتضمن ثلاث مستويات رئيسية, المستوى الأول يعتمد على المعلومات اللونية والتي تتمثل بشكل رئيسي قيم RGB, المستوى الثاني يتمثل بإدخال المعلومات اللونية إلى مصفوفة التشتت لإيجاد خصائص الصور الجغرافية (التضاريس) المدخلة حسب المعلومات اللونية لكل صنف. وأخيرا, المستوى الثالث يستخدم هذه الخصائص (التي تخزن في نظام قاعدة بيانات) في تصنيف الصور الرقمية الجغرافية المدخلة وتعريف الصنف الذي تعود له تلك الصور الجغرافية.طبق نظام التصنيف على العديد من الصور الرقمية الملونة الجغرافية(التضاريس) والذي اثبت نجاحه بشكل مرضي, حيث نجحت 73 صورة من اصل 90 صوره مدخله للنظام.

ABSTRACT

In image classification, color information improves the classification accuracy of the colored features. In this proposed system, Digital Topographic Image Classification (DTIC) in this research depending on the features produce from color information for entry image for classification algorithm. Therefore, Proposed a method to classified topographic image, this method including three levels, first level it to relied on the information of color that represent RGB values basically , second level is an introduced into the Covariance Matrix to find the properties of images of geography (Topographic) entered and to which they belong such color information for each class , and finally, third level use these properties (it will be store in database system)in the classification of entered test images digital geographic and identification of its class that Image of geography. Classification system was performed on many digital color images of geography(Topographic) and that have proved successful in patients, were, 73 images was success from 90 images entered into system.

INTRODUCTION

Image analysis is the extraction of useful information from images, mainly from digital image processing techniques. An optical image capture from camera or other detector can be digitized, converted to digital form, and stored in the memory of computer, the image is stored as integers representing of intensity level of picture elements (pixels). Image analysis is used in both computer vision and image processing applications. [1, 2]

One of the most important tasks of an image analysis system is image classification , digital image was taken of color geographical areas on the surface of the earth can be classified by using image analysis techniques of coloring, digitizing and depending on the features of such images from color and texture. Image classification is the process of assigning thematic labels to each image pixel. This is a frequently used methodology to produce land cover maps from arial images or satellite images. Image classification is usually performed on RGB color space models[3, 4], The use of RGB space for representing image data is very general in image processing techniques. This is because of the availability of data produced by the camera apparatus [5].

The biggest motivation for using color is that it provides additional features at each pixel in an image to be used by a pattern classification system. Whilst gray information provides the basic representation for image features, color is a more powerful means for many applications, color was treated as a generic feature along with others such as shape or texture measures [6, 7].

Many image classification techniques and more applications on it have been proposed during the past years, In the leatrtue survey began from A. Marcal and T. Mendonca(2007) were they used black and white air photographs for the production of historic land cover maps can be done by image classification with evaluate the ability of texture[3], Imran S. Bajwa and M. Shahid Naweed (2009) they uses the principal features of an image to identify different cloud image types with better accuracy (PCA) is a feature based classification[9], P. Jeyanthi1 and V. Jawahar in(2010) the proposed they use K-means clustering for the classification of feature set obtained from the histogram refinement method[8]. In this research implemented method to classified color topographic images including (Water planes, green land, and Desert) that by using conference matrix considering color information computed from each of the three RGB planes, then found the features of

photographic images using Digital Topographic Image Classification System (DTIC).

Image Classification

Image classification is an important task for many aspects of global change studies and environmental applications[10]. Classification is the labeling of a pixel or a group of pixels based on its grey value[11, 12], it is one of the most often used methods of information extraction. In Classification, usually multiple features are used for a set of pixels i.e., many images of a particular object are needed. In Remote Sensing area, this procedure assumes that the imagery of a specific geographic area is collected in multiple regions of the electromagnetic spectrum and that the images are in good registration. Most of the information extraction techniques rely on analysis of the spectral reflectance properties of such imagery and employ special algorithms designed to perform various types of spectral analysis [4, 13].

Covariance Matrix

The covariance matrix is symmetric and positive semi definite. Consider a population of random vectors of the image is given by Eq.(1) as[14]:

$$X = \begin{pmatrix} X_1 \\ . \\ . \\ X_n \end{pmatrix} \qquad \ldots\ldots (1)$$

The mean vector of the population is given by Eq.(2)as :

$$m_x = E\{x\} \qquad \ldots\ldots(2)$$

where $E\{x\}$ is the expected value of the argument, and the subscript denotes that m is associated with the population of x vectors.

The covariance matrix (C) of the vector population is defined in eq(3) as :

$$C_x = E((x - m_x)(x - m_x)^T) \qquad \ldots\ldots(3)$$

Where *T* indicates vector transposition.

From N vector samples from a random population, the mean vector and covariance matrix can be approximated from the samples equations (1,2,and 3) by[14,15]:

$$M = \frac{1}{N^2}\sum_{i=1}^{N^2} X_i \quad \text{.....(4)}$$

$$C = \frac{1}{N^2}\sum_{i=1}^{N^2}(X_i - M)(X_i - M)^T \quad \text{.....(5)}$$

where: X_i =data sample, M=mean of the set data, (X_i-M)=distance measure from mean M to the sample data X_i, and N=number of sample vector.

Digital Topographic Images Classification

When looking at nature, there was different types of images of the geographical nature (Topographic) and in various varieties, in this research uses three types of Topographic images, first type images for an aqueous such as water parts, seas, rivers, second type images there are nature green land such as agricultural land, forests and gardens rich, and third type images for the nature of the desert and other manifestations of nature geography.

In this research, Digital topographic Image Classification system(DTIC) can be divided into two main approaches, Color Features Extraction(CFE) and Topographic Classification(TC) steps.

RGB color information are used to represent ten features for one topographic image including in one class, for represented color information we used RGB (Red, Green, and Blue) plans for each pixel in the entry topography color image.

For the purpose of determining the quality of images and classified, we can use a number of ways and means for the purpose of identification and classification of those images, based on the properties of each class, so uses the covariance matrix (Eq. 5) for the purpose of finding a set of values as properties, that is the average for each class based on values of covariance matrix of this class of images with geography (Topographic), and therefore we will defind each class of these images values by extracted the features for each image.

The matrix (3*3) is used to produce covariance matrix for digital topographic image entry, Table (1) show how can compute the values for each features in sample image by (3*3), for this sample matrix is given a nine values uses to produce the features from covariance matrix.

The result from table (1), find the average values for all images in one class, that mean we have at last just 10 values for each class, that values and its average for each class are saved in our database system to uses it in

classification stage for this system, that mean we have three classes in the database system, each class for one type topographic image, all steps for this system are explain in Color Feature Extraction Algorithm (CFE).

Table -1 : All features value for sample image

No. of pixel	X_i	M	$(X_i - M)^T$	Val=$(X_i - M) * (X_i - M)^T$	$C=\frac{1}{H*H}\sum_{n=1}^{H*H} Val$
1	3 R 7 G 2 B	4 3 4	-1 4 -2	1 -4 2 -4 16 -8 2 -8 4	$c=\frac{1}{9}\begin{pmatrix} 30 & -3 & 15 \\ -1 & 44 & 6 \\ 15 & 6 & 36 \end{pmatrix}$
2	4 R 4 G 4 B	4 3 4	0 1 0	0 0 0 0 1 0 0 0 0	
3	2 R 2 G 1 B	4 3 4	-2 -1 -3	4 2 6 2 1 3 6 3 9	
4	5 R 7 G 7 B	4 3 4	1 4 3	1 4 3 4 16 12 3 12 9	
5	6 R 2 G 2 B	4 3 4	2 -1 -2	4 -2 -4 -2 1 2 -4 2 4	
6	1 R 1 G 3 B	4 3 4	-3 -2 -1	9 6 3 6 4 -8 3 2 1	$C=\begin{pmatrix} 3.33 & -0.33 & 1.66 \\ -0.11 & 4.88 & 0.66 \\ 1.66 & 0.66 & 4 \end{pmatrix}$
7	3 R 3 G 6 B	4 3 4	-1 0 2	1 0 -2 0 0 0 -2 0 4	
8	5 R 2 G 5 B	4 3 4	1 -1 1	1 -1 1 -1 1 -1 1 -1 1	
9	7 R 1 G 6 B	4 3 4	3 -2 2	19 -6 6 -6 4 -4 6 -4 4	
Sum of : Red Comp. = 36 Green Comp. = 27 Blue Comp. = 36					

Algorithm -1:Color Feature Extraction (CFE)

Input: read color image (24 bits) and dimensions (N*N), for each class.
Output: Saved the average covariance values (features) for each class in database system.

Step 1: Find the average values by using the equation (4).
Step 2: find covariance matrix value from the (equation5).
where: C= covariance matrix, n=number of samples image, T=transpose operation
The result of this matrix N*N, by using transpose for this matrix we have a new classify matrix value:

.....(6)

$$C = \frac{1}{H^2}\begin{vmatrix} V11 & V12 & V13 \\ V21 & V22 & V23 \\ V31 & V32 & V33 \end{vmatrix}$$

Where V is a vector, and $V11, V12, ..., V33$ are the address of matrix.
Step 3: Compute The ten Features values, 3*3 and the ten value is the average of nine features value from 3*3 matrix in (eq. 6) from step 2, that we have ten covariance values (features)for each input digital topographic image.
Step 4: Compute the average values from step 3, for each image in one class, we have at last just ten values for each class, that values are saved in our database system and uses to classified the images be using Algorithm(2).

The proposed classification algorithm , Topographic Classification (TC) was applied to the values of the average of varieties resulting from the Color Feature Extraction algorithm(CFE) using to classified entry topographic image with the DTIC systems, see algorithm(2).

Algorithm -2: Topographic Classification (TC)

Input: read new digital topographic image.
Output: classified entry image belong one of three classes in DB.

Step1: applied Algorithm (1) on input image, to extract 10 Features for new digital topographic image input

Step 2: Compare the 10 Features from step 1 within each 10 Features for each class from our database show in table(2), [15]:

$$F = \sum_{i=1}^{10} \left(\frac{Fi\,t}{Fi\,db} \right) \qquad \ldots\ldots(7)$$

Where: F is the summation of ((F_i t / F_i db) * 10) , 10 is the average of (100/10) for 10 features, (F_i t) is the feature of test new Topographic digital image, (F_i DB) is any feature gets it from our database.

Step 3: Get the rate of $F \geq 85\%$, to say what one features from database is same of features get it newly from new topographic digital image input to classified it.

Step 4: If the result is more than one Topographic digital image features have same rate value ($F \geq 85\%$), the maximum value is the nearest features back in to test topographic digital image.

EXPERIMENTAL RESULTS

The system DTIC presented in this work classified topographic images using its color features. that by the designed classifier system using Color feature Extraction (CFE)algorithm and Topography Classification(TC)algorithm.

Features Extraction

Ten Average Values results from Algorithm(1) (CFE) in this work is the task to calculate the ten features of topography images for three classes stored in database. Database system have saved three feature types, Table(2) show the average feature values for each class by applied steps in algorithm(1) from 1 through 4.

Table -2: The Average Features for each class stored in database System

	Image	F1	F2	F3	F4	F5	F6	F7	F8	F9	F10
Class1		4259	4129	4071	4129	4020	4014	4071	4014	3900	4067
Class2		3934	3517	2863	3518	3235	2756	2863	2759	2785	3136

Class3		2312	2551	1676	2351	2956	2384	1676	2384	1759	2227

Where

Class1 : Water bodies, , seas, and rivers, Class2 : Forest, and green land, and Class3 : Desert, deserts, and sandy soil.

F1,F2...,F10 : are the ten average features.

Topographic Image Classification

Topographic images is classified by using feature values from Eq. (5) in different color channels for RGB color Space. From CFE algorithm steps , the data will be compared with the specification of the topography image and what had been extracted based on the methods that was represented and described of the part of Algorithm(1), considering the features that was stored in images database.

The experiment is calculated under the following conditions:

1. Only the Digital Topography image (BMP type) get from Personal Camera is analyzer throughout this system.
2. Some of test images are cutting from photograph image .
3. All of the test images have same size.

In this study, the application system (DTIC) on three varieties of digital topography images. Table(3), shown a sample test image and its features was extracted.

Table -3: One test topographic image and its features.

Test Image	F1	F2	F3	F4	F5	F6	F7	F8	F9	F10
	2312	2551	1676	2351	2956	2384	1676	2384	1759	2227.67

From the feature of test image shown in table(3)and features of three classes shown in Table(2), we finding the rate (F) by applying Eq.(7),the test image nearest from class1 at rate 98% , from class2 at rate 69.8%, and from class3 at rate 53.9%, that mean the test image classified belong class1. The

relation between test image features and three classes features in Database shown in Figure(1) and Table(4).

Table-4: Test Image Rate (F) of three Classes for Classification steps

$W = F_i\ t / F_i\ db$											$\sum W$	F=w*100
Class1	0.99	0.98	0.98	0.98	0.98	0.99	0.98	0.99	0.94	0.99	9.8	98%
Class2	0.93	0.86	0.69	0.86	0.81	0.68	0.69	0.68	0.67	0.76	7.63	69.8%
Class3	0.54	0.62	0.4	0.57	0.74	0.58	0.4	0.58	0.42	0.54	5.39	53.9%

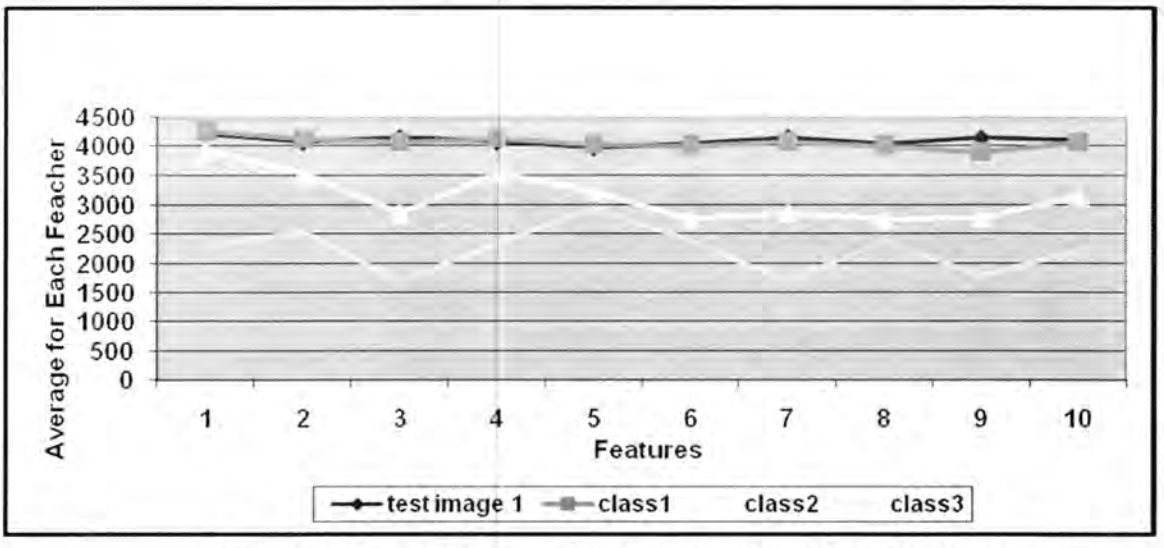

Fig. -1 : Test topographic Image classified to class1

Were tested 30 images for each class and, from Class1 succeeded 22 images out of 30 images at a rate of success of 73.3%, Class2 succeeded 24 images out of 30 images at a rate of 80%, and Class3 succeeded 27 images out of the 30 images at a rate of 90% . Figure(2) shown relation between samples entry topographic images and three classes features in classification stage.

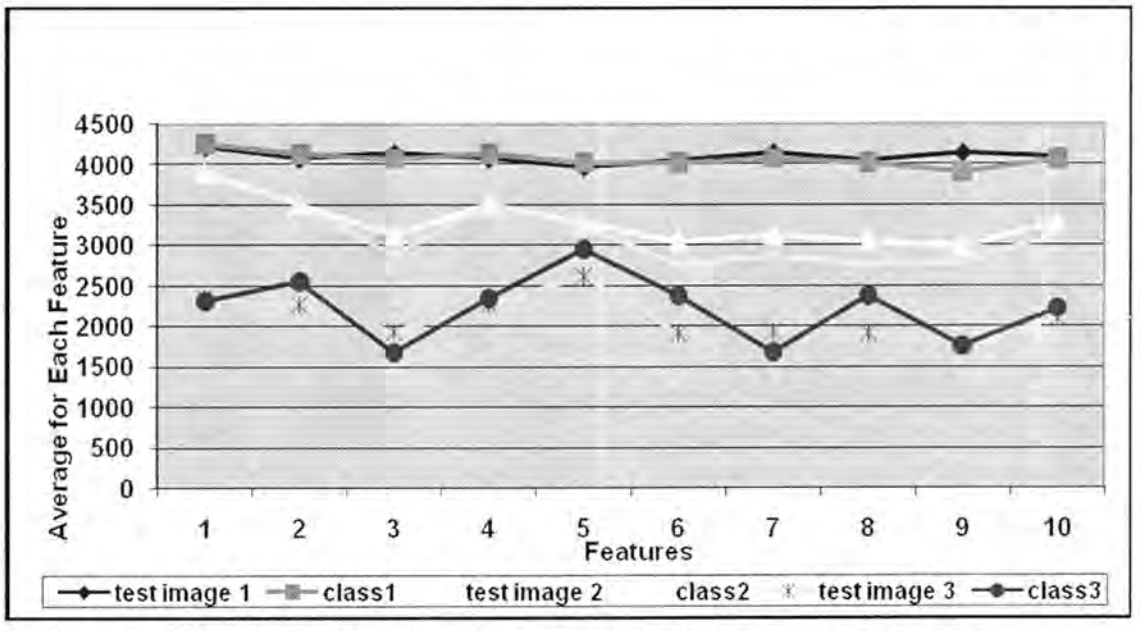

Fig. -2: Classified Relation between test image and three classes

Conclusions and Suggestion Work

The higher order of Covariance matrix give even more detailed color features of the digital topography image, the major disadvantage of Covariance matrix in general is that they are global features rather than local.

In the our proposition for Digital Topography Image with DTIC, firstly CFE method is using to extract the features based on RGB color information, One of the ways to do that Image Classification by comparing input test topography Image features entry with three classes features saved in database. From TC method result, the (rate value) more than one of the features will be seen in database, therefore the Class has Maximum rate value is the Class that test image entry related it. In this paper uses color information to classified images , it possible to merge the texture features with color information for new classification method, and used the method to the experience of other types of images.

REFRENCES

1. Umbaugh S.E., "Computer Vision and Image Processing", Prentice-Hall, (1998).
2. Young I.T., Gerbrands J.J., and . van Vliet L.J," Image Processing Fundamentals", Netherlands Organization for Scientific Research (NWO) Grant 900-538-040, (1998).
3. Marcal A.R.S,and Mendonca T., "The use of texture for image classification of black & white air-photographs", New Developments and

Challenges in Remote Sensing, Z. Bochenek (ed.), Millpress, Rotterdam, ISBN 978-90-5966-053-3, (2007).

4. Farouk E. , "Remote Sensing: Generating Knowledge about Groundwater", Special study, (2006).
5. Al Huwayzi R. S., "Design of image filtering system based on color model", Higher Studies Institute for Computer & Information, M. Sc. Thesis,(2002).
6. Luo X. Y., "Color Image Analysis For Cereal Grain Classification", University of Manitoba, Canada, Ph.D. thesis, (1997).
7. Low B. K., and Hjelmxas E., "Face Detection : A Survey", Academic Press, computer vision and Image Understanding, 83, pp. 236–274, (2001).
8. Imran S., and Shahid M., M. Nadim Asifl, and S. Irfan Hyder," Feature Based Image Classification by using Principal Component Analysis", ICGST-GVIP Journal, ISSN 1687-398X, Issue (II), (2009).
9. Jeyanthi1P., and Jawahar V., " Image Classification by K-means Clustering", Advances in Computational Sciences and Technology ISSN 0973-6107 , pp. 1–8,(2010).
10. Seetha M., " Comparison of Advanced Techniques of Image Classification", GIS Development, (2000).
11. Zhao B., "Color Space", Electrical Engineering,SUNY,NY, www.ece.sunysb.edu., (2002)
12. Baogang W., Dongming L., Yunhe P., and Wenhua X., "Interactive Image Segmentation Using Multiple Color Spaces And Its Application in Ancient Art Preservation", Artificial Intelligence Institute, Zhejiang University, Hangzhou, China P. R. 310027, (2000).
13. Rao K.M.M., " OVERVIEW OF IMAGE PROCESSING", National Remote Sensing Agency, Hyderabad, India, (2003).
14. Gonzalez R. C. and Woods E. , "Digital image processing", Addison-Wesley Publishing Company, (2004).
15. Hogg R. V., and Tanis E. A., "Probability and Statistical Inference", Pearson Education, Inc. Prentice Hall, (2006).

Large Scale Network Using Bluetooth Technology

Basim Jamil Ali
Computer Sciences Department, College of Sciences, Al-Mustainsiriyah University

Received : 27/04/2011 Accepted : 29/05/2011

الخلاصة

المعيار الاسبق للشبكات اللاسلكية ذات النطاق الشخصي (WPAN) استخدم تقنية البلوتوث في الهاتف الخلوي، السماعة، السيارة ...الخ، ان بناء شبكة ذات نطاق واسع باستخدام تقنية البلوتوث تقدم تحدي حقيقي كأساس نظام القفز الترددي. هذا البحث يستكشف هذه المشكلة ويقوم بوضع عدة حلول عملية لها. ويستكشف هذا الاقتراح الصعوبات المختلفة وتضع الحلول لبناء شبكة واسعة باستخدام تقنية البلوتوث. وتستعرض طريقة مقترحة لتسهيل تشكيل وصيانة الشبكة حسب معرفتنا، الاقتراح واحدة من الدراسات الشاملة لبناء شبكة واسعة تعتمد نظام القفز الترددي.

ABSTRACT

The earliest standard for Wireless Personal Area Networks (WPAN), Bluetooth has been widely used in cell phone, headset, car, GPS, etc. As a frequency hopping based system, however, constructing a large scale network using Bluetooth technology presents a real challenge. This proposal explores this problem and presents several feasible solutions. As the Bluetooth based frequency hopping technology is the major technology employed as in WPAN space, this proposal explores various associated difficulties and presents solutions to build a large scale network using Bluetooth technology. A new method to facilitate network formation and maintenance in a large Bluetooth network is introduced. To the best of our knowledge, the proposal is one of the first extensive studies on building large scale frequency hopping networks.

INTRODUCTION

The difficulty of using frequency hopping technology to construct a large scale wireless network lies in several areas: Firstly, explicit link establishment or network formation is difficult. Unlike other kinds of wireless networks such as WLAN, where devices can talk to each other once they are within the radio range of each other, in a frequency hopping system, devices

need to synchronize to each other first so that they can hop along the same hopping sequence. The needed explicit device discovery and link setup phases add complexity to the network formation problem. Secondly, network synchronization is not easy. Unless all the devices in the same network hop in the same hopping sequence, which is impractical in any large network, communication in one frequency hopping channel to another may be difficult. Some type of time division multiplexing may be used for bridge devices to communicate in multiple frequency hopping channels and relay data among them. This may require complex scheduling algorithms [1,2].

The major technology operating in Personal Operation Space (POS) (usually 10 meters), is Bluetooth, which employs a Master/Slave control structure to lower power consumption while a relatively fast frequency hopping scheme is used to provide robust short range communications[3]. Although frequency hopping technology has also been defined in IEEE 802.11 standard, it is never used widely in WLAN space where direct sequence spread spectrum (DSSS) technology is the dominant scheme.

Problem Domain

Bluetooth presents significant challenges in building up a large network, as the basic unit of Bluetooth network is a piconet, consisting of a master and up to 7 active slaves. A large scatternet is needed for a wireless sensor network.

Bluetooth for sensor network is restricted because of :

1. Network formation problem.
2. Difficultly of network synchronization problem.

The aim of this proposal is to present significant challenges to use on Bluetooth for
sensor network, and to present simulation results to show that Bluetooth could be a vital choice for a sensor network .

Review

The low duty cycle of Bluetooth devices could be pushed forward to make it small enough to be useful for energy constrained sensors and actuators. It has already caught attention of the IEEE 1451.5 standard committee which is considering it as one of the candidates for wireless interface in smart sensors [6].

Although recently released IEEE 802.15.4 standard has defined specifications which are more suitable for certain classes of sensor applications [6]. In 2003 its acceptance in the market is yet to be seen [7].

In 2003 some early work using Bluetooth to build sensor network has been reported, such as [8].

In 2004 a technique called "wake up" scheduling presents a great challenge in wireless sensor network [9, 10].

Background

Bluetooth Fundamentals

Bluetooth technology was originally introduced as a cable replacement technology. It has a quite complex protocol stack (Figure 1) which has many layers. In view of the popular ISO OSI 7-layer reference model, the whole Bluetooth stack can also be viewed as a new MAC/PHY which occupies the lower two layers of the OSI stack. A Bluetooth Network Encapsulation Protocol (BNEP) layer provides a consistent interface to Logical Link (LL) sub layer of OSI data link layer [4].

An interface layer Host Controller Interface (HCI) partitions the protocol stack into two parts: higher stack and lower stack. The former is usually implemented on the host computer including L2CAP (Logical Link Control and Adaptation Protocol) layer and above, the latter is implemented in the device including Baseband and LMP (Link Management Protocol) layers.

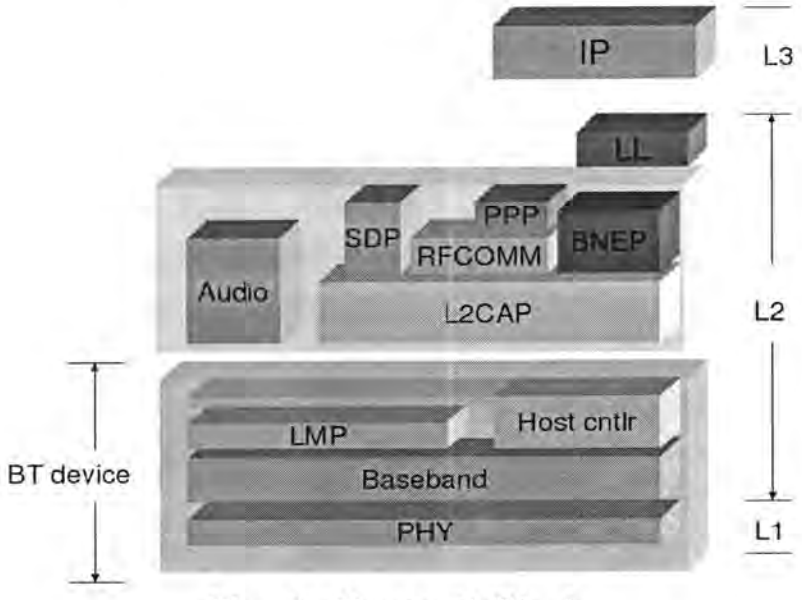

Fig. -1: Bluetooth Stack.

Baseband handles the frequency hopping kernel, transmission and receiving, etc. While LMP handles link setup and tearing down, QoS negotiation and other duties such as managing the low power modes of Hold, Sniff and Parked state. LMP also handles data encryption/decryption. At the host part, L2CAP handles data fragmentation, multiplexing data between different higher layer protocols, etc[8].

The Personal Area Network (PAN) profile basically defines a minimum bridge interface in IEEE 802 family. A star topology is specified with each device having a link to the Group Network (GN) or Network Access Point (NAP) which serves as the coordinator.

Although the media is broadcast in nature, the BNEP broadcasting is specified as GN/NAP sending the broadcast packets to all members of the PAN, one by one by unicast.

At the baseband Layer, a broadcast packet can be sent once to all slaves, using the broadcast address. There are two types of baseband broadcasting: active broadcasting can beconducted any time the master desires, while piconet broadcasting is performed during the beacon period in Parked state to parked slaves as we discuss later. Only the master is allowed to send broadcast packets.

Discovery, Connectivity and Service Discovery

Bluetooth specification defines the Bluetooth network as an ad hoc network, that is, no fixed infrastructure is assumed. Devices discovering each other, set up and tear down a connection on their own [3].

Before a connection can be set up, the initiating device needs to know something about the other party, especially the device address. A knowledge of the clock of the other end also helps and is obtained by the discovery process achieved by Inquiry and Inquiry Scan procedures. A device wishing to be discovered, enters Inquiry Scan state periodically, listening to short ID packets, hopping at a very slow pace (1 hop every 1.28s) on the predefined 32 frequencies. The device wishing to discover others in the neighborhood enters Inquiry state, sends out short ID packets, hopping at a very fast pace (3200 hops every second). Different pace of the hopping sequence makes them finally to meet to enable the discovering device to obtain the device address and clock of the discovered device[3].

After acquiring the device address and clock of another device, a device can initialize the connection setup process by entering the Page state,

sending out short ID packets at a fast pace. If the other is in the Page Scan state, it may capture one of the ID packets so that two parties meet at the correct frequency and finally hop together, to exchange further information to set up a link. After a link has been set up, devices can inquire further information of each other using Service Discovery Protocol (SDP).

It may be noted that before a link is set up by the Page/Page Scan procedures, no substantial information can be exchanged between any two devices. This is different from other types of wireless networks, where devices can talk to each other once they are within the radio range of each other. By Inquiry and Inquiry Scan of the discovery phase, limited asymmetrical information exchange is feasible, that is, only the device in Inquiry state knows the device address of the device in Inquiry Scan state, but not vice versa. The requirement that two devices need to be in complementary states makes the device discovery and connection set up processes time consuming, and could last up to several or tens of seconds[3,4,7].

Channel Characteristics

Bluetooth employs unlicensed 2.4GHz ISM band and a relatively fast frequency hopping scheme. A Bluetooth channel is defined by 3 factors:

1. The frequency hopping sequence determined by the master's clock and device address.
2. The access code prefixing each transmitting packet derived from the master's device address.
3. The timing of the slot determined by the master's clock.

A slave needs to synchronize to the channel for receiving a packet successfully. A slave turns on its receiver for 20μs, on the calculated frequency, at the right timing (slot beginning), waiting for the access code. Only if all the 3 elements (the timing, the frequency and the access code) match, can a packet be received for further processing[6].

In the active mode, the Bluetooth device clock has an accuracy of ±20ppm (parts per million), which implies that a slave device should synchronize to the channel at least every 400 slots or 250ms. If for some reasons, a device has lost contact with the master for more than 400 slots, a different synchronization process needs to be used. The synchronization windows need to be enlarged to offset maximum possible drift.

There are two types of Bluetooth physical links: Asynchronous Connection-oriented Link (ACL) and Synchronous Connection-Oriented (SCO) link. Regularly spaced slots may be reserved for SCO links to fulfill tight QoS requirement, especially for voice communication. The rest slots can be used to carry ACL traffic and channel access is controlled by the master using a polling scheme. A slave in a ACL link is allowed to send only if it is addressed successfully in the previous master-to-slave slot.

An adapted Frequency Hopping (AFH) scheme handles better coexistence issue with 802.11 networks by instructing the devices to skip over noisy channels and improve the performance.

Basic Unit of Bluetooth Network

The basic unit of Bluetooth network is a piconet which consists of a master and up to 7 active slaves. This constraint is imposed by the fact that the Logical Transport Address (LT ADDR) in a baseband packet is only 3 bits to identify 7 devices (LT ADDR 0 is used for broadcast purpose) totally. A piconet has a star like topology (Figure 2)[4,5].

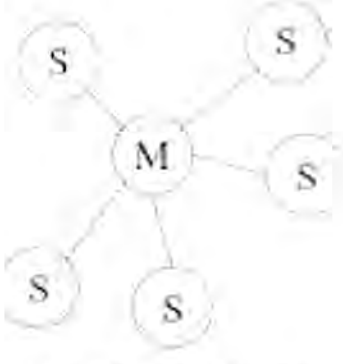

Fig. -2: A piconet

Bluetooth for Sensor Network

In our proposal, the bridging function is implemented using the Sniff mode. Because the duty cycle of a device is very small, it has plenty of time to participate in another piconet without having much effects. The bridge scheduling algorithm is implemented at the LMP layer because piconet switch and bridge scheduling need to have access to the device internal state and the exact timing control. However, message forwarding function is handled at a much higher layer, and each bridge acts as a router[9,10].

To make a large scatternet to be glued by numerous bridge nodes and make it easily manageable, we specify the following constraints on the network topology and the node's duty cycle.

1. A bridge node is a S/S bridge. That is, it serves as a slave in every piconet it participates in.
2. A bridge node is allowed to participate in at most 2 piconets.
3. A bridge node has a duty cycle at most 25% at each piconet it is participating.

It is well-known that a transceiver consumes significantly large amount of energy just for being active. There is no significant difference whether it is transmitting, receiving or being idle. However, the power consumption is 3 orders lower when it is turned off or goes in deep sleep. When calculating energy consumption, we do not differentiate between the state of the transceiver either as transmitter, receiver, or being idle. In our simulation work, we record the total time when the radio is active (Tactive) and the number of times the radio is turned on (Nwarm−up), since for turning on each time, a warm up period (Twarm−up) is needed and the energy is consumed. The warm up period is set to 200 μsec. We did not simulate the clock drift explicitly. However, for the slave, whenever it wakes up at the RP slot, an average of (500/1000000)Tsniff is added to the active time, so as to compensate for the channel synchronization time. The devices we simulated behave close to the current specification. If the beacon packet is used, the master will have slightly increased energy consumption, up to 4/Tsniff . As for a slave, the effect is minimum because when the beacon packet is used, a slave is going to spend one or two slots for receiving the beacon. While the beacon packet is not used, it has to sniff at every master to slave slot so as to decode the header and see if the packet is addressed to itself. One may offset the other. From these considerations, the average duty cycle (d) of a device over a period of t is set to:

$$d = (Tactive + Twarm-up \times Nwarm-up) / t \quad \ldots\ldots\ldots\ldots (1)$$

The scatternet is assumed to have been formed by some scatternet formation algorithm. A static routing for each pair of source and sink is generated in a breadth first search manner. This generates a shortest path for each flow, however it may not be optimized in terms of load balancing. We feel that this is acceptable since the data rate is supposed to be very low for a

typical sensor network application. The radio channel is assumed to be error free. However, if both ends of a link do not have any thing to send, the link is immediately put into the sleep mode[8,9].

Topology

An area of 50×40 m^2 which is divided into 80 small cells (Figure 3). The radio range is assumed to be 11.2 meters and each cell has the area of 5×5 m^2 so that the nodes in adjacent cells are within the radio range of each other. This enables every node to potentially become a bridge. Each cell has 6 nodes which constitute a piconet. Each piconet also gets one node from its left and one from its above neighbor cells, respectively, as bridges. Most piconets have 4 bridges to connect the 4 neighboring piconets, resulting in a mesh structured scatternet. In total, there are 80 piconets with 480 nodes. There are ten unicast flows from one side of the area to the other and each flow takes 17 to 35 hops (2 hops for traveling through each cell). The sources and sinks are randomly generated in each run. Large packets can be generated at the sources to simulate burst, because it may be segmented into a group of small baseband packets.

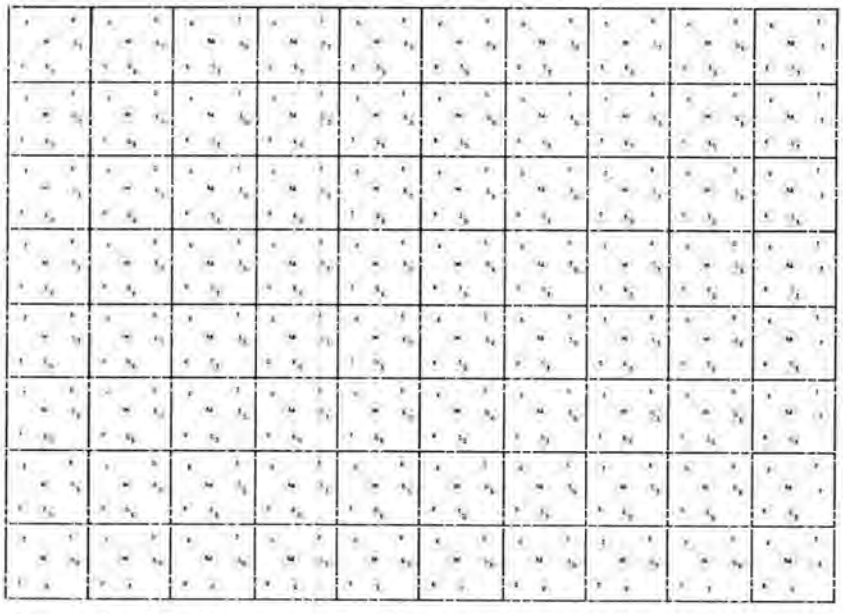

Fig. -3: Mesh structured scatternet with 480 nodes.

Packet delivery Ratio

Bluetooth baseband employs a robust ARQ scheme to ensure packet delivery at the link layer. The packet loss are due to the buffer overflow at the intermediate master and bridge nodes. If the data rate is low, the packet

delivery ratio is almost 100%. However, if the network is congested, significant packet loss may be observed[8].

Delay Vs. Superframe Size

If the network is not congested, the message delay is predictable. For a message to pass through a piconet or a bridge, a pass of superframe is needed; therefore the average delay per hop is expected to be close to half of the superframe. Again, if the network is congested, the queuing will increase the delay. In case of medium and light loads, the observed per hop delay is very close to the theoretical expectation which is half of the superframe[8,10].

Energy Consumption

Energy consumption in terms of ratio of active time over total measured time for different type of nodes (masters, bridges, and slaves), different superframe size and traffic loads. If the traffic is very light, the duty cycle is close to 1 / 1000 , provided the superframe is large enough[10].

Delay versus Energy Consumption

One of the very nice properties of Bluetooth system is that the delay is bounded if the load is not very high. If a delay of 2.5 - 5 seconds per hop is tolerable (as anticipated for a lot of sensor applications), the superframe of 8192 (5.12 seconds) – 16384 (10.24 seconds) provides a good trade off. It should also be noted that heavy loaded is relative as per baseband packet type used and allowed RW size. If most packets are larger than 27 bytes, a multi-slot packet is more efficient for increased network capacity. Also, Rendezvous Window (RW) can be set to a larger value and can be made adaptive as per the traffic loads without having much adverse effect on the energy consumption of the networks. If no useful packets are exchanged, the nodes can go to sleep, even earlier than the RW ends [10].

As the one of the first extensive research on building large scale networks using a frequency hopping system, this proposal demonstrates that:

1. frequency hopping technology is a vital choice for large scale PAN technology, as the network can be operated efficiently and it avoids many problems in multi-hop system.

2. Bluetooth wireless technology is an inexpensive, short-range radio technology that eliminates the need for proprietary cabling between devises.
3. There are three power saving modes for idle devises. these modes are: Park, Hold, and Sniff.
4. Piconets can be interconnected into larger multiple-Piconet environment known as a Scatternet.
5. Scatternet communications tackes place between the Piconet masters.

REFERENCES

1. D. Agrawal and Q. Zeng, Introduction to Wireless and Mobile Systems, 2nd ed. Brooks/Cole Pulishing, (2006).
2. C. Cordeiro and D. Agrawal, Ad Hoc & Sensor Networks, Theory and Applications. World Scientific, (2006).
3. J. Haartsen, "Bluetooth: a new radio interface providing ubiquitous connectivity," in IEEE VTC, 107–111(2000).
4. Bluetooth SIG, Specification of the Bluetooth System - Version 2.0 + EDR, Nov. (2004)
5. IEEE Std 802.15.4, Wireless medium access control (MAC) and physical layer (PHY) specifications for low-rate wireless personal area networks (LR-WPANs),(2003).
6. IEEE P1451.5 Project. [Online]. Available: http://grouper.ieee.org/groups/1451/5/].
7. C. Evans-Pughe, "Bzzzz zzz [zigbee wireless standard]," IEE Review, 49(3), March (2003).
8. M. Leopold, M. B. Dydensborg, and P. Bonnet, "Bluetooth and sensor networks: a reality check," in Proceedings of the first international conference on Embedded networked sensor systems. ACM Press, (2003).
9. R. Zheng, J. C. Hou, and L. Sha, "Asynchronous wakeup for ad hoc networks," in Proceedings of the 4th ACM international symposium on Mobile ad hoc networking & computing. ACM Press, 35–45(2003).
10. X. Yang and N. Vaidya, "A wakeup scheme for sensor networks: Achieving balance between energy saving and end-to-end delay," in 10th IEEE Real-Time and Embedded Technology and Applications Symposium (RTAS 2004), May (2004).

Computer Vision Based on Statistical Analysis for the Captured Images Using Different Camera Apertures

Anwar Hassan Mahdy, Muna Abul Hussain Radhi and Basher Khalid Mustafa
Computer Science Department, College of Science, Al Mustansiryha University

Received : 14/04/2011 Accepted : 29/05/2011

الخلاصة

إن جودة الصور محددة بعدة معاملات داخلية (معاملات منظومة التصوير) وخارجية (معاملات المحيط). هذه المعاملات مهمة جدا في عملية الرؤية الحاسوبية وتحليل الصورة. لذلك توجهنا لدراسة هذه المعاملات بالإعتماد على الخصائص الإحصائية لنقاط الحافات في الصورة الرقمية؛ إذ تم دراسة خصائص الصور الملتقطة تحت شروط إضاءة مختلفة وأقطار فتحة كاميرا مختلفة. إن الخصائص الإحصائية المعتمدة هي المعدل والإنحراف المعياري والتباين للحزم اللونية الثلاثة (الحمراء والخضراء والزرقاء) ومركبة الإضاءة للصور الملتقطة. أظهرت النتائج أن التغيرات العالية في إحصائيات الصورة من ناحية التجانس والحدة (التباين) تحدث مع تغير شدة الإضاءة وتغير قطر فتحة الكاميرا.

ABSTRACT

Image qualities limited by several parameters internal (optical systems parameters), and external (environment parameters). These parameters are very important for computer vision and image analysis. Therefore an attempt has been made to study these parameters based on computing the statistical properties of the edge points of captured images. Where we are studied the characteristics of the images that captured under different lightness conditions and used different camera apertures. The statistical properties of image edge points (mean μ, standard deviation σ, and contrast ct) of the RGB-color bands and L-component computed for all the captured images. The results show that the high statistical variations in image quality in homogeneity and sharpness (contrast) when changing the lightness and camera aperture diameter.

INTRODUCTION

A computer vision system processes images acquired from an electronic camera, which is like the human vision system where the brain processes images derived from the eyes. Computer vision is a rich and rewarding topic for study and research for electronic engineers, computer

scientists and many others. Increasingly, it has a commercial future. Computer vision, the art of processing images stored within a computer, has seen a considerable amount of research by highly qualified people and the volume of research would appear to have increased in recent years. That means a lot of new techniques have been developed, and many of the more recent approaches have yet to migrate to textbooks. The technology itself continues to advance. This means that there is new hardware, new programming languages and new programming environments. In particular for computer vision, the advance of technology means that computing power and memory are now relatively cheap. The deformity which attacks the image often affects the information's data existing in it and weakness its sharpness and reduces its contrast, then it cause interface between the details for the different regions, so lessen image clarity(1). Many former studies concerned with the luminance and contrast effect on the image quality:

- Eli Peli et.al (2) conducted a study on 1996 for contrast enhancement through the changes in luminance intensity and spatial frequency. The study adopted contrast sensing over the threshold by using contrast analogy.

- William B. et.al (3) suggested on 2003 an algorithm to enhance image in night scenes by a technique of making the images taken in the day light as if they were taken in night images through decreasing the contrast and brightness for all of the image, adding a distortion to the image and present the night image characterized with high noise, loss in optical acuity along with distortion size taking place in it.

Computer Interfaces

The basic computer *interface* needs to convert an analogue signal from a camera into a set of digital numbers. The interface system is called a *framegrabber* since it grabs frames of data from a *video sequence*, and is illustrated in Figure **1**. Note that intelligent cameras which provide digital information do not need this particular interface, just one which allows storage of their data. However, a conventional camera signal is *continuous*

and is transformed into *digital* (discrete) format using an Analogue to Digital (ADC) converter (1).

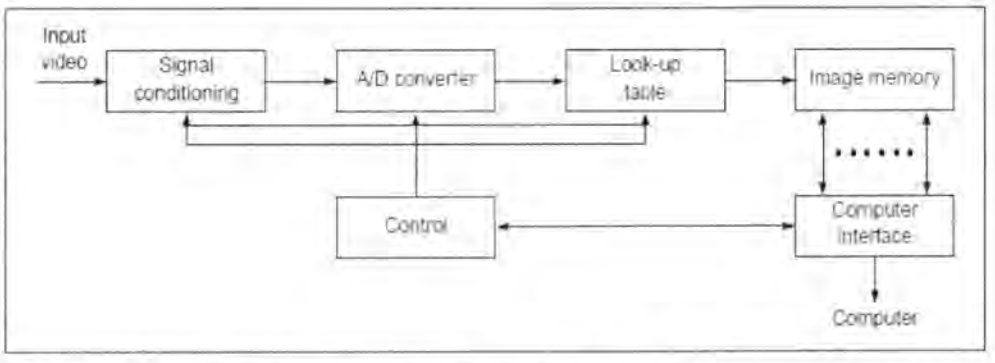

Fig. -1: A computer interface-the framegrabber (1)

The (computer) images comprise a set of points or *picture elements* (usually concatenated to *pixels*) stored as an *array of numbers* in a *computer*. Given the progress in computer technology, computer vision hardware is now relatively inexpensive; a basic computer vision system requires a camera, a camera interface and a computer. These days, some personal computers offer the capability for a basic vision system, by including a camera and its interface within the system (4).

Cameras

A *camera* is the *basic sensing element*. In simple terms, most cameras rely on the property of light to cause hole/electron pairs (the charge carriers in electronics) in a conducting material. When a potential is applied (to attract the charge carriers), this charge can be sensed as current. By Ohm's law, the voltage across a resistance is proportional to the current through it, so the current can be turned into a voltage by passing it through a resistor. The number of hole/electron pairs is proportional to the amount of incident light. Accordingly, greater charge (and hence greater voltage and current) is caused by an increase in brightness. In this manner cameras can provide as output, a voltage which is proportional to the brightness of the points imaged by the camera. Cameras are usually arranged to supply video according to a specified standard. Most image processing and computer vision techniques are implemented in computer *software*. Often, only the simplest techniques migrate to hardware; though coding techniques to maximize efficiency in image transmission are of sufficient

commercial interest that they have warranted extensive, and very sophisticated, hardware development(5).

Sobel Edge Detection Operator

Edge detection is one of the fundamental operations in image processing. Detecting edges is a basic operation in image processing. The edges of items in an image hold much of the information in the image. The edges tell us where items are, their size, shape, and something about their texture (2).

An edge is where the gray level of the image moves from an area of low values to high values or vice versa. The edge itself is at the center of this transition. The detected edge gives a bright spot at the edge and dark areas everywhere else. Convolution of the image with masks is the most often used technique of doing this. The idea is to take a 3 × 3 array of numbers and multiply it point by point with a 3 × 3 section of the image, then sum the products and place the result in the center point of the image (1, 2).

There are many edge detection techniques; in this work Sobel Operator will be used with different thresholds, where *Sobel edge detection operator* consists of two masks to determine the edge in vector form. The Sobel operator was the most popular edge detection operator. It proved popular because it gave a better performance than other edge detection operators. The coefficients of smoothing within the Sobel operator, Figure **2**, are those for a window size of 3×3 (1).

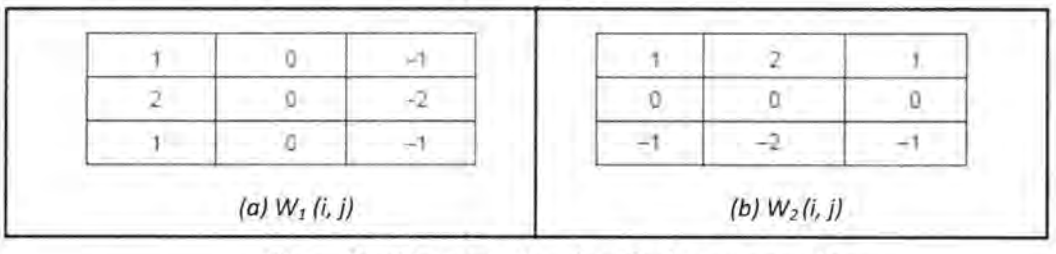

Fig. -2 : Templates for Sobel operator

Edge values above a threshold value were set to 255 and all others were set to zero. This gives a clear picture of edges and no edges (3).

Algorithm (1):Sobel Edge Detection Algorithm (6)

Input: the input of the algorithm is a color image $Img(i,j)$ RGB of sized (r×c) with color pixel values between 0 and 255.

Output: the output of the algorithm is an edge image *eImg* (i,j) of sized (r×c) with pixel values either 0 or 255.

Step 1: two square windows each of size (3×3) as in figure 2 are used to scan across the entire image, the first from left to right and the second from top to bottom. In each scan the filter output associated with center of the window is denoted as y (which is representing the output of the algorithm).

Step 2: Calculates the weighted inputs sum_1, sum_2 as follow:-

$$sum_1 = \sum_{i=1}^{3} \sum_{j=1}^{3} W_1(i,j) * Img(i,j)$$

$$sum_2 = \sum_{i=1}^{3} \sum_{j=1}^{3} W_2(i,j) * Img(i,j)$$

where *Img*(i,j) denote the input image, and $W_1(i,j)$, $W_2(i,j)$ as shown in figure 2.

Step 3: $sum_1 = abs\ (sum_1)\ /4$

$sum_2 = abs\ (sum_2)\ /4$

Step 4: Evaluate the value of y:

$y = max\ (sum_1, sum_2)$

Step 5: The output y (which represents edge point in the output edge image eImg (i,j)), can be determined using the following condition:-

If $y > th$ *then* $y = 255$

else $y = 0$

Where (th) is represent the threshold value, and different values of threshold were be used.

(th = 30 , 70 , 130 , 170 , 210).

Step 6: End.

Statistical Digital Image Properties

There are several image properties can be calculated from image data, the most imported properties (mean μ, standard deviation σ, and contrast ct) of the image or image regions (7).

The Mean (μ)

Image mean brightness is known as the mean brightness for the image elements and it determined from the following relationship (8):-

$$\mu = \frac{1}{MN} \sum \sum f(x,y) \quad \ldots\ldots\ldots\ldots\ldots\ldots (1)$$

Where M and N denotes the high and the width of the image, the multiplication of them equals the number of image elements.

The Standard Deviation (σ)

The standard deviation represent the mean of variations of the element values with respect to its mean and it determined from the following relationship (9):-

$$\sigma = \sqrt{\frac{1}{MN}\sum_{(x,y)\epsilon MN}(f(x,y)-\mu)^2} \quad \text{.....(2)}$$

The Image Contrast (ct)

Contrast is the relation between the object brightness and background brightness, and it determined from the following relationship: - $ct_e = \sigma_e/\mu_e$. Where μ_e *and* σ_e represent the mean and standard deviation of the image edge points respectively (10).

Algorithm (2): Evaluations μ_e, σ_e, ct_e Algorithm:

Input: The input of the algorithm is the color image *Img*(i,j) and edge image *eImg (i,j)* after applying sobel operator , where the values of *Img* are between 0 and 255,otherwise the values of edge image *eImg* are either 0 or 255.

Output: The outputs of the algorithm are μ_e the mean of edge image values, std_e the standard deviation of values, and ct_e the contrast of edge image values.

Step 1: calculate μ_e,σ_e,ct as follow:-

If eImg (i,j) =255 then
ne = ne+1
se = se+Img (i,j)
sse = sse+Img(i,j)^2
end if

$$\mu_e = s_e/ne$$
$$\mu_{se} = ss_e/ne$$
$$std_e = \sqrt{\mu_{se} - {\mu_e}^2}$$
$$ct_e = std_e/\mu_e$$

Step 2: end.

Where ne = number of edge points.

se = summation for edge image values (*Img(i,j)*).

sse = summation for square edge image values (*Img(i,j)^2*).

μ_e = mean of edge image values.
μ_{se} = mean of square edge image values.
std_e = standard deviation of values.
ct_e= contrast of edge image values.

RESULTS AND DISCUSSION

The captured images under different lightness conditions (low lightness using one lamp L1, medium lightness using two lamps L2 and high lightness using three lamps L3), and varying camera aperture diameter (D = 23.3 mm) by (D + ΔD), where ΔD changed from -2 mm to 2mm, where ΔD represent the variations in camera aperture diameter D, when using fixed distance between the camera and the object (d=1m). The resulted images shown in Figure **3**, from this Figure can be noted the decreasing of ΔD make the images of low lightness i.e. that look alike dark image these for all lightness conditions (L1,L2,and L3). Also, can be estimate that the increasing of lightness (from L1 to L3) gives bright images. The characteristics of these images which were studied are mean and contrast of the edge image points, as a function of Sobel operator threshold values (Th=30, 70, 130, 170, 210) by applying algorithm(1) and algorithm(2).

From Figure **4**, it can be observed that the relation between mean μ_e of RGBL image edge with the Sobel operator threshold (th) always constant except for the case of using ΔD= -2, where the relation gives increasing in μ_e with increasing (th) for low lightness L1, while for medium and high lightness (L2 and L3 respectively), the relation approximately constant. For the low lightness get low separation between the mean of RGBL-curve for all ΔD's, i.e. the image edge look alike gray. In figure **4**, also can be note that RGBL- image edge means are stationary for long range of Sobel operator thresholds, the B-band has a high stationary in mean values, because RGB-color in these images are approximately equal (three balloons red, green and blue), these three balloons with a white background, where the white background has equal contribution of RGB-color.

Image edge contrast for different lightness and ΔD's, also shown in Figure **4**, where can be noted that for all ΔD's the contrast ct_e for RGBL-image edge points decreases with increases (th), for L1, L2 and L3. The statistical contrast for the all images is approximately in the same range

values. For low ΔD, the contrast ct_e for RGBL-image edge points has low separation at low lightness L1, while for L2 and L3 for all ΔD's get high contrast separations for the RGB-bands and L-band. There are decreasing in edge image point contrast (statistical contrast) with increasing Sobel operator threshold values, because the images have high homogenously in the regions around the edges, there are no large contrast among the different color image regions. Also can be note that the contrast is stationary and constant in a large region of Sobel thresholds. The contrast of B-band higher than that of R-band and G-band, this due to the contribution of the B-band in the color image model, where the B-band has the lowest contribution in the color image model, so the effect of noise appear in B-band higher than that of RG-bands, this noise play important role in increasing the contrast in B-band (false contrast).

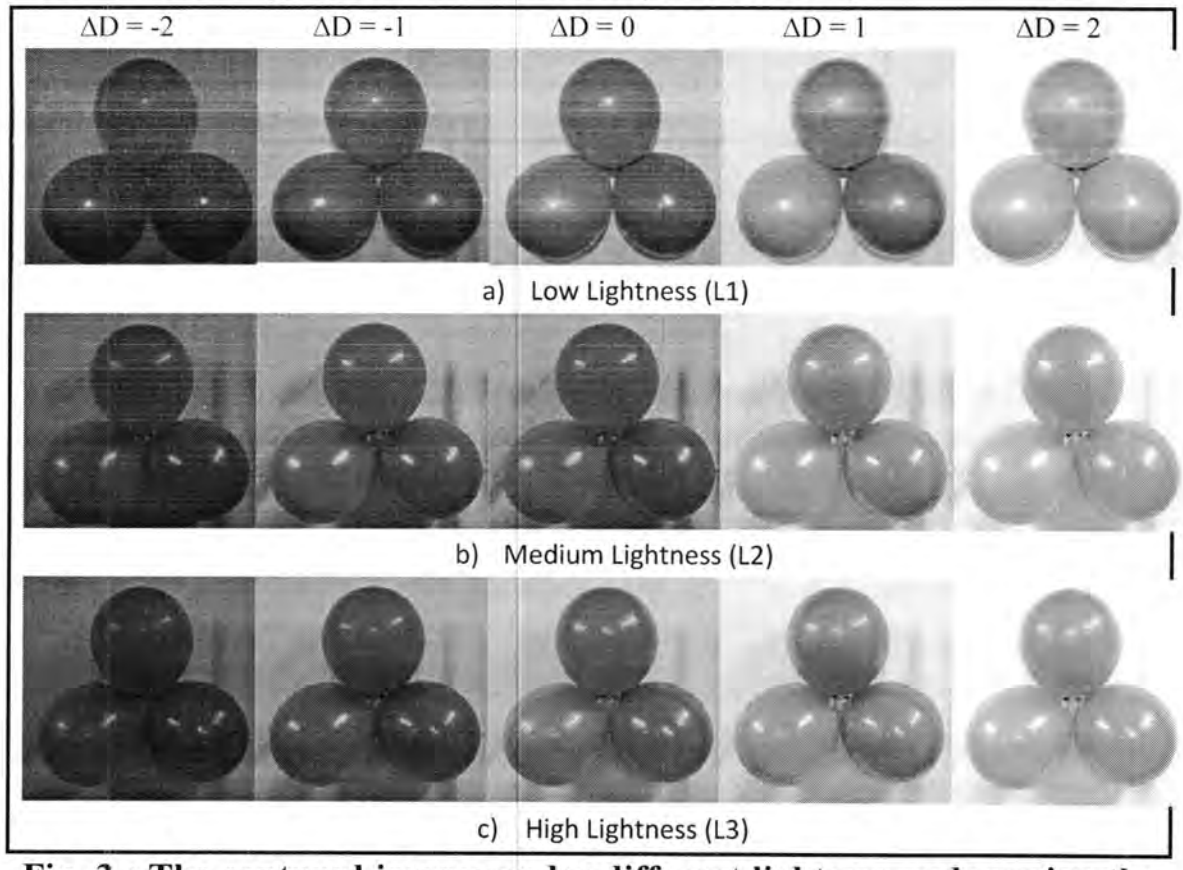

Fig.-3 : The captured images under different lightness and varying the aperture lens of the camera from ΔD = -2mm to ΔD = 2mm

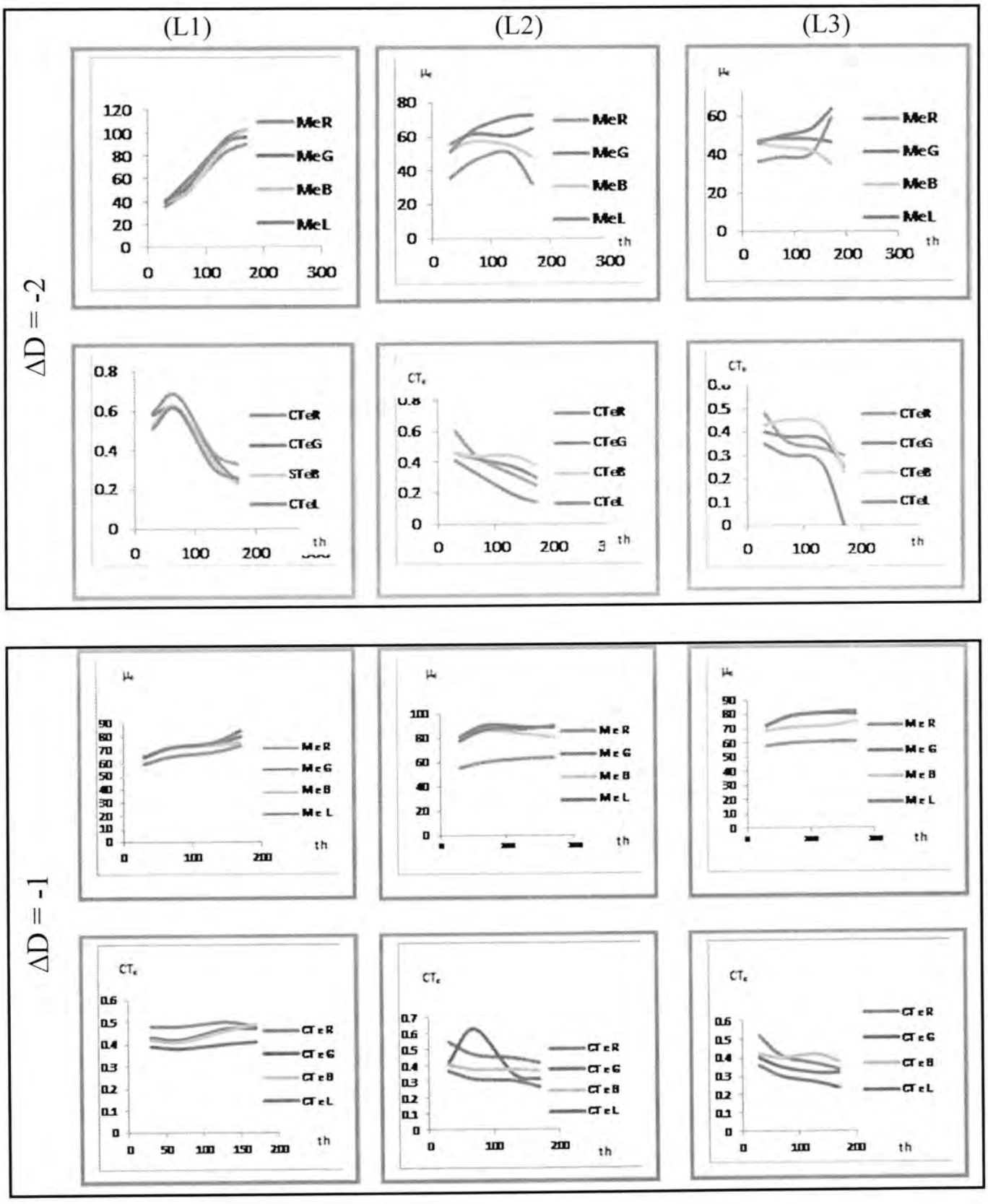
(L1)
(L2)
(L3)
ΔD = -2
ΔD = -1
MeR
MeG
MeB
MeL
CTeR
CTeG
CTeB
CTeL
th

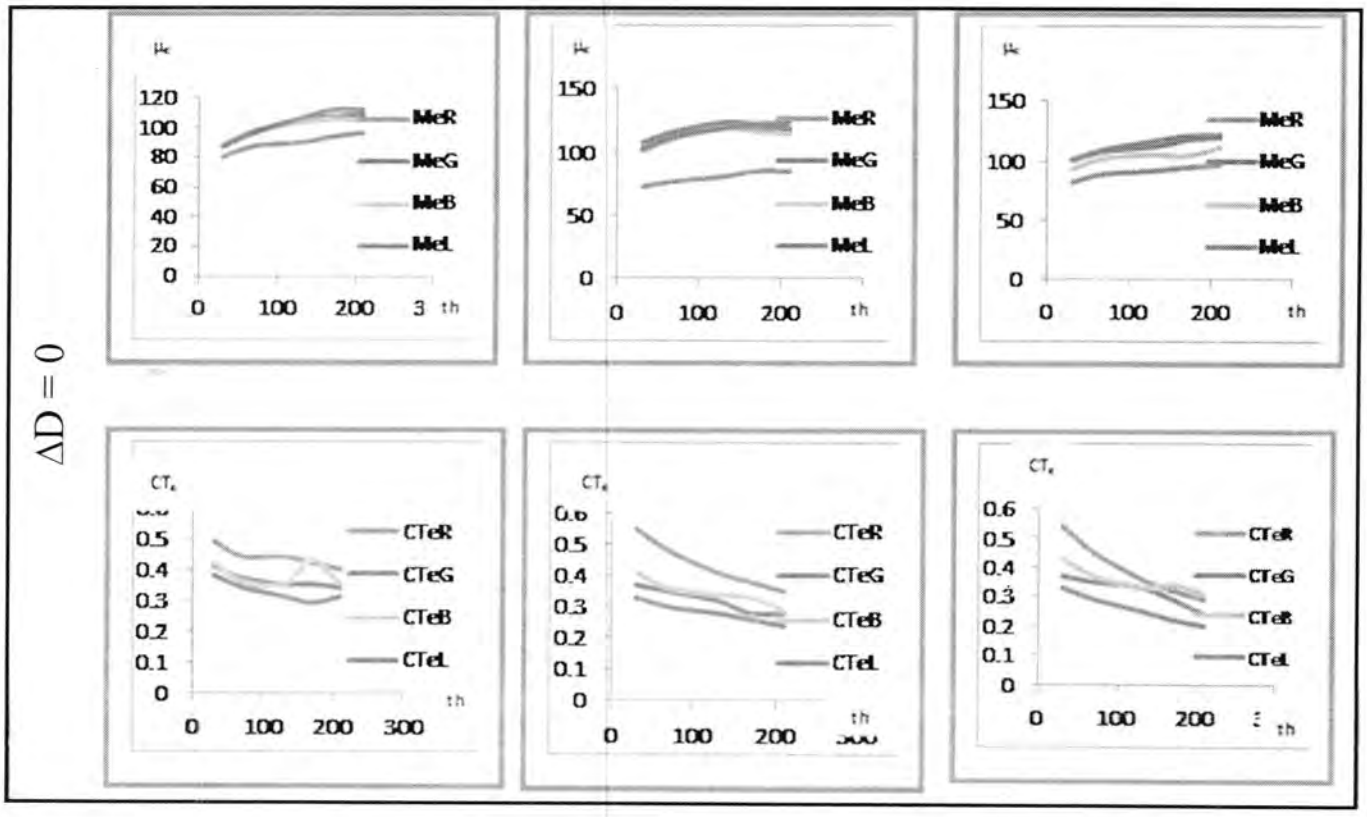
ΔD = 0
MeR
MeG
MeB
MeL
CTeR
CTeG
CTeB
CTeL
th

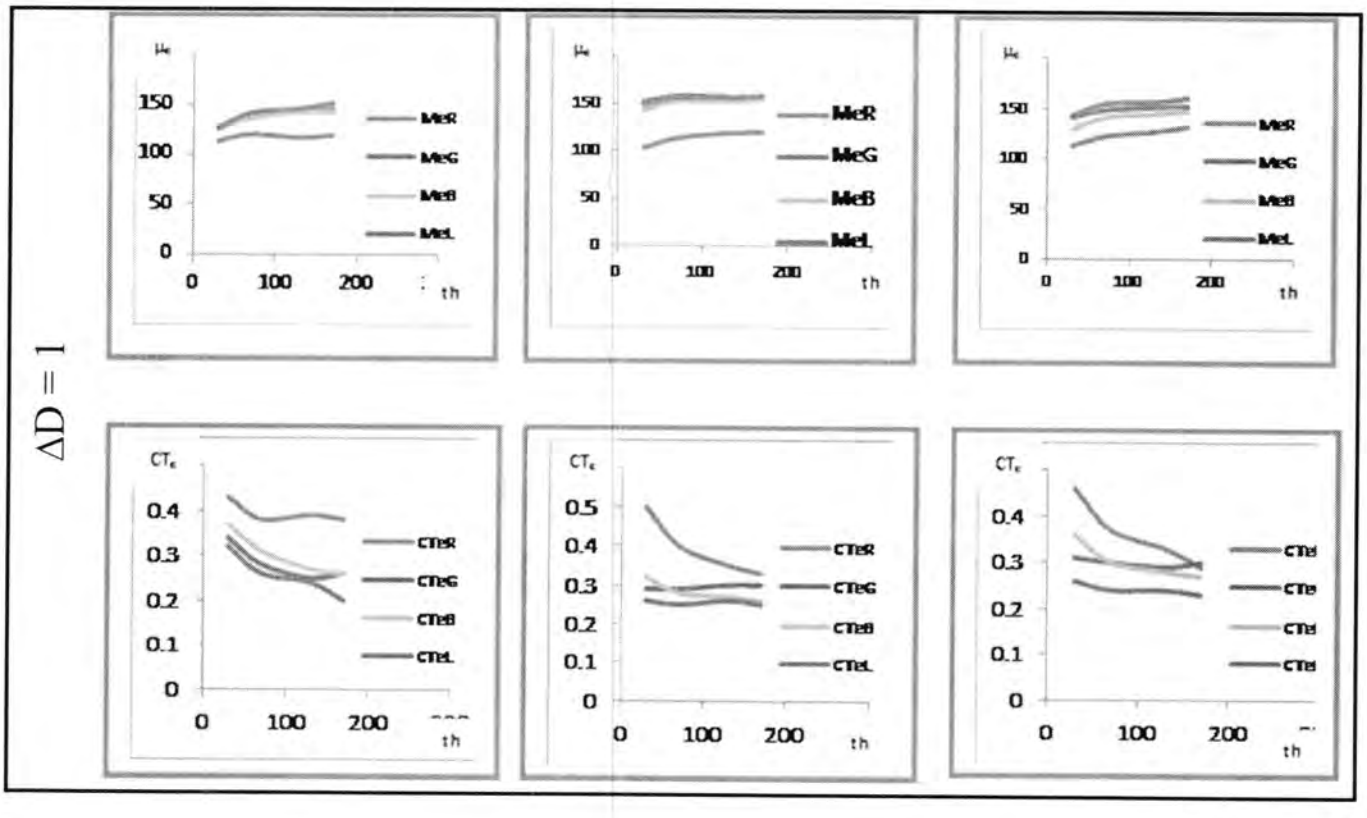
ΔD = 1
MeR
MeG
MeB
MeL
CTeR
CTeG
CTeB
CTeL
th

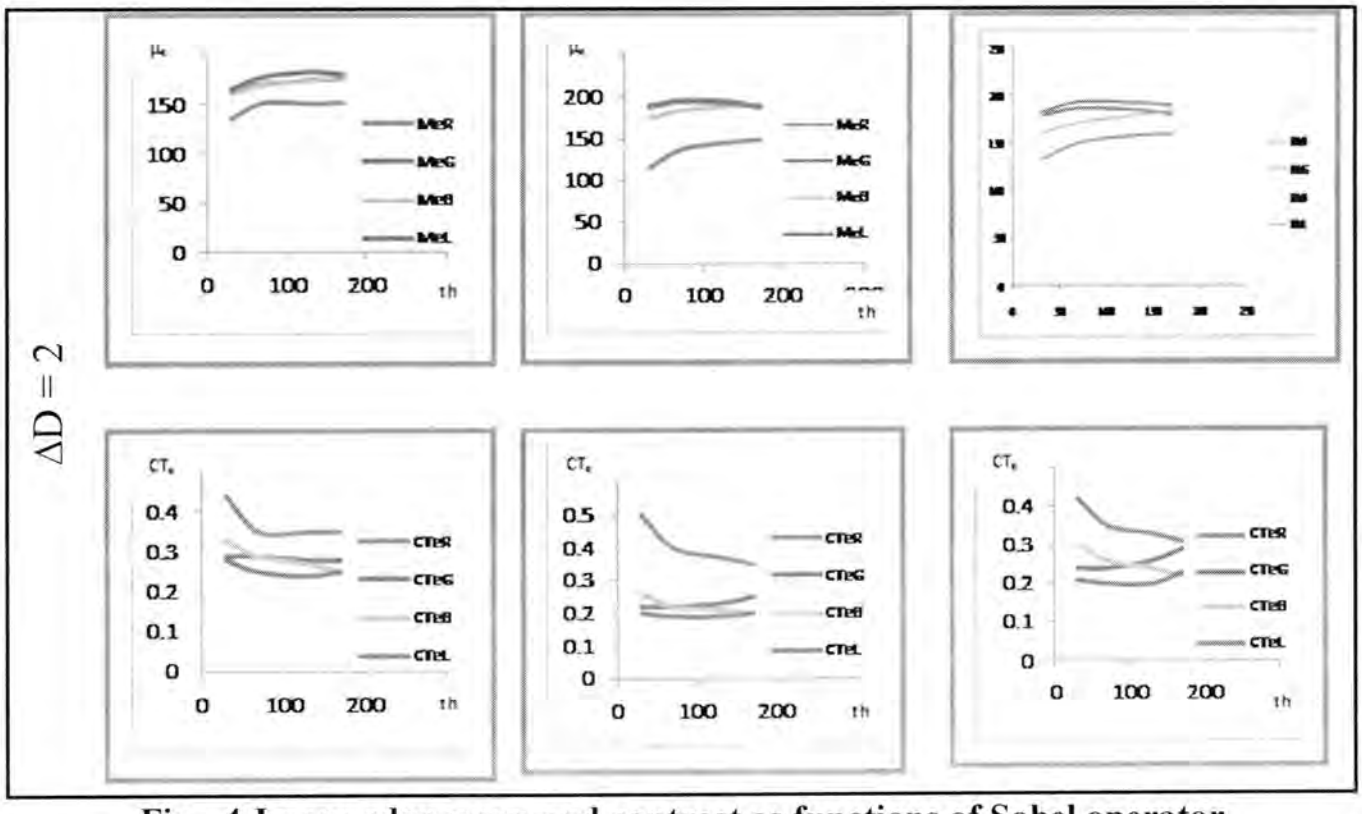

Fig. -4:Image edge mean and contrast as functions of Sobel operator thresholds

From the results can be conclude that

1. The captured image under different lightness and using different ΔD, gives constant mean for image edge points with along range of Sobel operator thresholds.
2. For low lightness the separations among the μ_e values of RGBL are low, this make the images look alike gray image.
3. The contrast of image edge points decreases with increases Sobel threshold.
4. The contrast (false contrast) of B-band higher than the other RG-bands, where the noise in B-band is so high.

REFERENCES

1. Mark S. Nixon, Alberto S. Aguado, "Feature Extraction and Image Processing", Typeset at Replika Press Pvt Ltd, Delhi 110 040, India Printed and bound in Great Britain, pages(1-111), First edition (2002).

2. Peli E . , Arend L. , Labiance T. , " Contrast Perception a Cross Changes in Luminance and Spatial Frequency " , Opt.Soc.Am.A , vol.13, no.10/October 1996/J.Opt.Soc.Am.A (1996) .
3. William B.and Shirly P.and Ferwerda J.,"A spatial Post Processing algorithm for Images of Night Scenes " Author Address : University . of Utah and Cornell University (2003).
4. Dwayne Phillips, "Image Processing in C", Copyright by Dwayne Phillips. Dwayne Phillips wns the electronic rights of this text, pages(47-50) Second Edition, (2000).
5. AL Bovik , "Handbook of Image video Processing" , Department of Electrical and Computer Engineering the University of Texas at Austin, Texas Academic, This book is printed on acid-free paper, pp 97-98,(2000).
6. Scott E Umbaugh, "Computer Vision and Image Processing", Prentice Hall PTR. Upper Saddle River, NJ07458. (1998).
7. Ali A. al-Zuky, "Examining Contrast by Change of Lightness and Spatial Frequency", Al Mustansiryha J. Sci, V20,n6,pp.16-26,(2010)
8. Ali A. al-Zuky, Salma S.S. Zuheri, and Kathem J. AL-Shujari, "Assessment Techniques for the contrast of Images have Different Illumination", Al Mustansiryha J. Sci. 21(6): 1-9, (2010).
9. Hala N. Kadom, Ali A. al-Zuky, and Kathem J. AL-Shujari, "A Study on Nokia 7610 Cell-Phone Camera Statistics Properties in Different Lightness", Al Mustansiryha J. Sci., 21(6):38-46,(2010).
10. اسماء محمد رووف ، فرح جواد كاظم ، شيماء حسين عبد مسلم ،علي عبد داود الزكي ،"دراسة الخصائص الاحصائية للشدات المسجلة بواسطة متحسسات الويب كاميرا enet لصورة اختبارية بيضاء "، مجلة علوم المستنصرية، المجلد 21، العدد 6،ص (9-16)، (2010).

Resistance Watermarks in Colored JPG Images

[1]Bashar M. Nema, [2]Ayman J. Al-Nesoor and [1]Azhar Hasan Nsaif
[1&3] Department of Computers Sceince, College of Science, Al-Mustansiriyah University
[2] College of Science and Information Technology, Al-Israa Private University, Jordan

Received Date : 14/04/2011 Accepted Date : 29/05/2011

الخلاصة

أصبحت التقنيات التي تأخذ على عاتقها احتواء العلامات المائية الرقمية، تستخدم بكثرة في مجموعة من التطبيقات الصوتية والفيديوية وكذلك في ملفات الصور الرقمية بكثرة. التحدي الأكبر في كل تلك التطبيقات هو كيفية احتواء تلك العلامة المائية الرقمية على معلومات سرية تشكل مصدر قوة وصمود ومقاومة لتلك العلامة أمام مجموعة من التهديدات التي تواجه الصور. يقترح البحث طريقة لحماية العلامة المائية الرقمية للصور ذات الألوان (RGB) من خلال مفهوم يسمى (Layer Images) والتي يتم الحصول عليها من تطبيق (DWT) مما جعل الطريقة المقترحة الأكثر صمودا أمام مجموعة من الاختبارات المعتمدة والتي تم استعراضها في البحث. مجموعة من النتائج والتوصيات والمقترحات تم تثبيتها قد تعتبر أساسا للتقييم والعمل المستقبلي في مجال البحث المقترح. عمليات الأختبار والبرمجة والفحص للبحث المقترح تمت من خلال الحزمة البرمجية MatLab2008 واضهرت النتائج التي تم التطرق لها في نهاية البحث صمود العلامة المائية للطريقة المقترحة امام الكثير من التهديدات.

ABSTRACT

Become a process of protecting intellectual property rights for multimedia files take a great deal of attention of researchers. And made the interest of research on the style in which to maintain the watermark generating digital images and meet the challenges that can be exposed.

Most common examples of the watermark is the presence of certain patterns in digital files that can be seen only when you highlight and logos in the background document of the printed text. Techniques watermarks to prevent counterfeiting and unauthorized repetition of material.

This paper proposes a means of protecting copyright color JPG images in the settlement of the situation. The proposed scheme encodes the layers of the image jpg watermark before integration and the promotion of tolerance in order to improve the attacks. This differs from traditional systems and watermarks on the supply of water directly to include images host.

The proposed uses layers of secrecy with the functionality of the host image by wavelet transform to separate image layers to produce extracts. Testing, programming and testing of the proposed research was carried out through the package code and MatLab2008 and results that have been addressed in the steadfastness of the end of the research proposed the idea in front of a lot of threats.

INTRODUCTION:

Digital watermark as physical material things, but that technology is used for water content rather than material things. In digital signal energy saving water gradually embedded in another signal. Called the signal energy-saving water and imagine some metadata such as security or information about rights to the main signal. Signal Coverage is generally a static image, audio, video sequence or text in the document in digital form. Classification techniques can turn the digital information system and water can be summarized as in **Fig.** (1) and **Fig.** (2), respectively [**1.2**].

Watermark is a technique for digital intellectual property protection of digital information. Signature, called a watermark embedded in the form of the host. When piracy happens, the author may not extract the watermark to prove ownership. Generally speaking, a good watermarking scheme should be robust enough to resist attacks; meanwhile, it should be imperceptibility so that human eyes cannot distinguish the difference between the watermarked image and the host image. In other words, the watermark embedded in the host image cannot be removed easily and destroy the host image quality too much **[3].**

A watermark can be embedded in either the spatial domain or the frequency domain. Generally speaking, a watermark embedded in the frequency domain is more robust than that in the spatial domain **[4].**

Several researchers have proposed various watermarking schemes in the frequency domain. The researcher in **[5]** transformed a host image to the YCbCr color space, and then the watermark to the frequency domain using discrete cosine transform (DCT). Next, the luminance Y was transformed to the frequency domain using the discrete wavelet transform (DWT). Then, the transformed watermark was embedded in the frequency coefficients of the luminance. The Researcher in **[6]** transformed a host image to the DCT domain, and then embedded a randomly scattered watermark into the

transformed domain. Nonetheless, one problem with the scaling factors is that they are adjusted manually, which is time-consuming, if not infeasible.

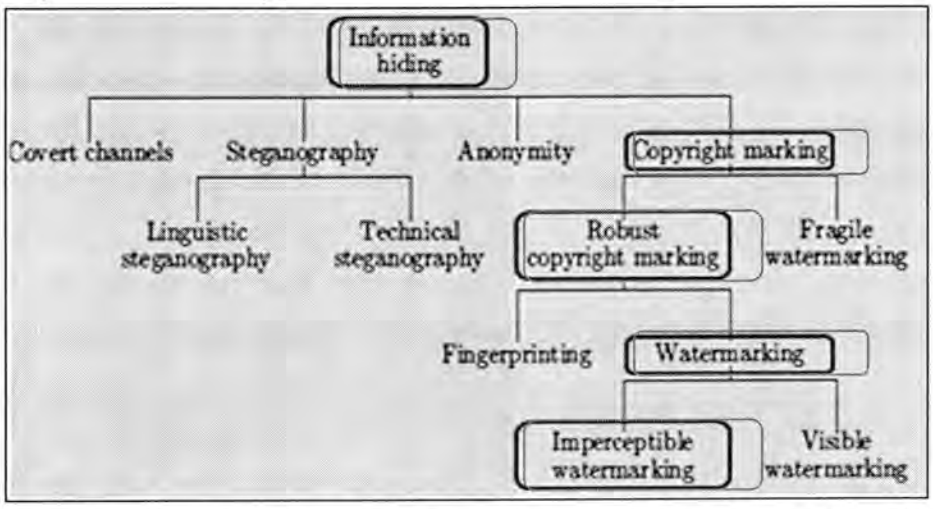

Fig. -1: Classification of Information hiding techniques [1].

The structure of this paper can be described as follow: After the introduction, the concepts and main topics of watermarking are introduced also the proposed method backgrounds described in **Section 2**.The proposed system explained in **Section 3**. Testing and experimental results for the proposed method are shown in **Section 4**. Finally, the conclusions and recommendations for the future works are explained in the last section.

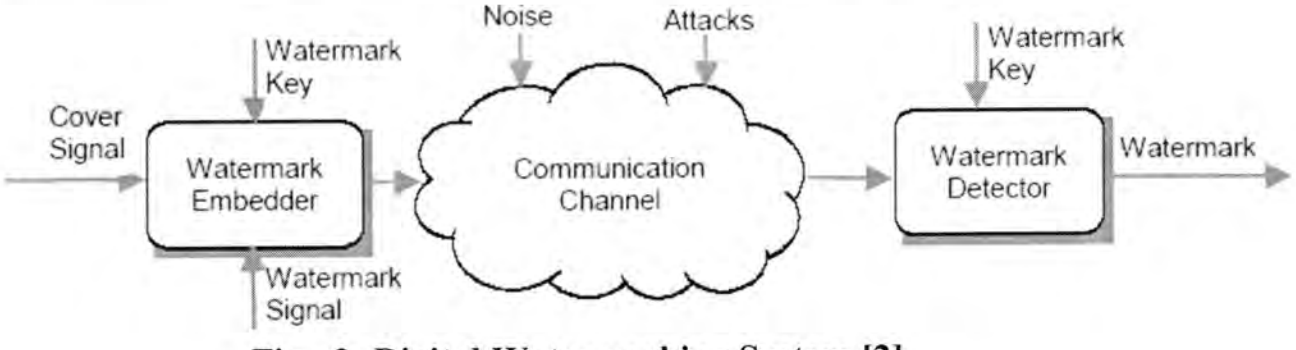

Fig. -2: Digital Watermarking System [2].

CONCEPTS & RELATED BACKGROUND:

In this section the description of watermarking attacks will be illustrate, which may be affect on the copyright of the true color images, then researcher will describe the proposed method related background.

WATERMARKING ATTACKS: [7]

First of all, have to distinguish two purposes for an attack against a watermark image:

- Hostile or malicious attacks, which are an attempt to weaken, remove or alter the watermark, and
- Coincidental attacks, which can occur during common image processing and are not aimed at tampering with the watermark.

Lossy image compression is considered the most common form of attack a watermarking scheme has to with stand. The harsh term "attack" can be easily justified: an efficient image compression has to suppress or discard perceptually irrelevant information the invisible watermark. A wide range of attacks has been described in the literature **[8]**. The following four large categories of attacks can be invoked to penetrate a watermarking system:

a) Removal attacks **b)** Geometrical attacks
c) Cryptographic attacks **d)** Protocol attacks

Removal (simple) attacks attempt to separate and remove the watermark. If somebody tries to remove the watermark from the data, this is called a removal attack. The goal is to add distortion to the host image in order to render the watermark undetectable or unreadable **[9].** The attack is successful if the watermark cannot be detected anymore, but the image is still intelligible and can be used for a particular determined purpose. Many such attack operations have been proposed:Lossy image compression (JPEG, JPEG 2000), Addition of Gaussian noise, Denoising, Filtering, Median filtering and blurring, and Signal enhancement **[10].**

Geometrical attacks, these attacks are not aimed at removing the watermark, but try to either destroy it or disable its detection. They attempt to break the correlation detection between the extracted and the original watermark sequence, where the image is subjected to translation, rotation, scaling and/or cropping. This can be accomplished by "shuffing" the pixels. The values of corresponding pixels in the attacked and the original image are the same. However, their location has changed.

Cryptographic attacks aim at cracking the security methods in watermarking schemes and thus finding a way to remove the embedded watermark information or to embed misleading watermarks. One such technique is brute-force search for the embedded secret information.

Protocol attacks neither aim at destroying the embedded information nor at disabling the detection of the embedded information (deactivation of the watermark). Rather, they take advantage of semantic deficits of the watermark's implementation. The protocol attacks aim at attracting the concept of the watermarking application. The first protocol attack was proposed by Craveret in **[11].**

SUGGESTED METHOD RELATED BACKGROUND: [12]

The techniques that have been used by the proposed method described briefly in this section, including the color image sampling, the discrete wavelet transform, the Torus-automorphism transform, and the secret sharing scheme.

A) Color Image Sampling

The proposed scheme uses the traditional 4:1:1 sampling for color images. The original RGB image is converted to the YCbCr color space before sampling. The Y component represents the luminance while the Cb and Cr components represent the chrominance. **Fig. 3** show graphically the structure of the 4:1:1 sampling. Only two lines and four pixels per line are shown in the figure.

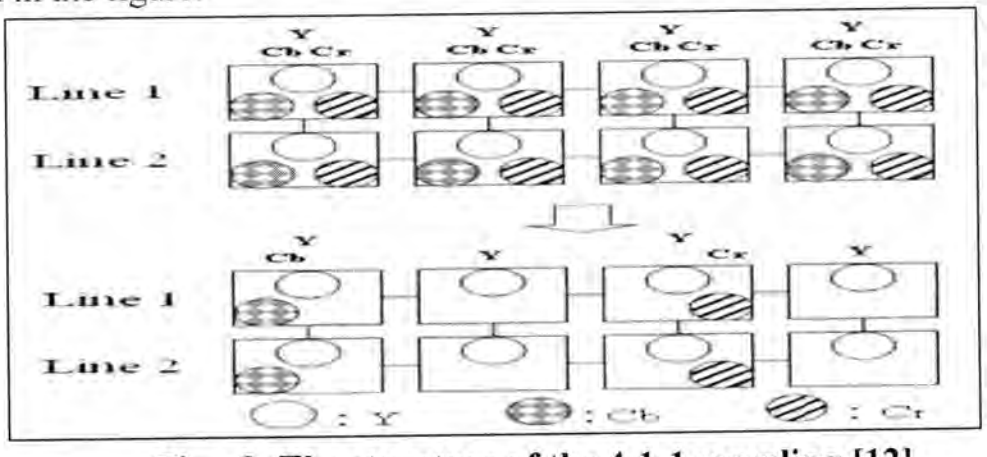

Fig. -3: The structure of the 4:1:1 sampling [12].

B) Discrete Wavelet Transform

The discrete wavelet transform (DWT) is identical to a hierarchical system and each sub-band of the system represents a section of the frequency domain of an image. The basic idea of the DWT for an image is that an image is first decomposed into four sub-bands LL1, LH1, HL1, and HH1. The LL1 sub-band can be further decomposed until there is only one coefficient in the LL sub-band. **Fig. 4** shows the image "Lenna" and the result after the two level DWT decomposition.

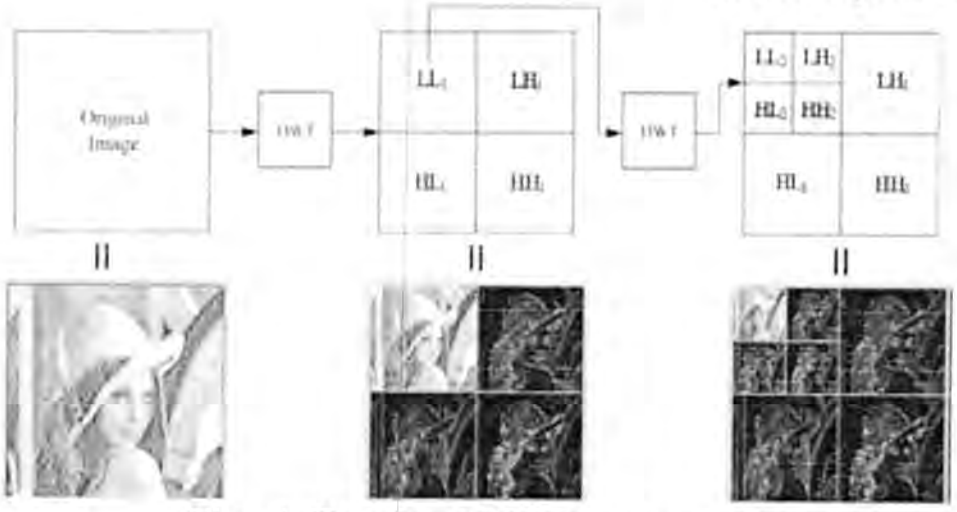

Fig. -4: Two-level DWT decomposition [12].

C) *Torus-automorphism transform*

A two-dimensional Torus-automorphism is considered to be a spatial transformation of planar regions **[13, 14].** It is used to scramble the content of the image, resulting in a chaotic mixing image.

D) *Secret Sharing*

The proposed idea applies (2, 2) secret layer **[15, 16]** to generate the layered image for embedding. The secret layering scheme splits an image into two different layers, which can later be used to restore the content of the image by stacking them together. The size of the restored image is expanded because each pixel is mapped into a block consisting of several sub pixels. The effect is called *pixel-expansion*. **Fig. 5** shows an example of (2, 2) secret sharing scheme. **Fig. 5 (a)** is the original image. **Fig. 5 (b)** is the layer image produced from the original one. **Fig. 5 (c)** is the restored image, which contains the information that can be recognized visually with the human eyes. Note, the restored image is four times larger than the original one and contains noise because of *pixel-expansion*.

(a) (b) (c)

Fig. -5: An example of (2, 2) secret layering scheme; (a) the original image; (b) the layer image; (c) The restored image

THE PROPOSED IDEA:

The proposed Idea contains the following two main parts:

- ***watermark embedding***
- ***watermark extraction.***

The details description algorithms of the embedding operation and the extraction operation, respectively can be as follow:

WATERMARK EMBEDDING ALGORITHM:

The algorithm first generates the layer image and then embeds it to the host image for copyright protection, which is described in detail as follows:

Algorithm (1): Watermark Embedding Operation:

Input: The color host image H ($N \times N$), a watermark W ($M \times M$) and a secret key.

Output: The watermarked host image.

Step0. Apply the 3-level DWT for the Host Image.

Step1. Use Torus-automorphism and the secret key to scramble the watermark W into W'.

Step2. Extract the features as well as the feature type n and the average M from the host.

Step3. For each block, generate the principal layer block (shared which is $S(k)$).

Step4. Collect $S(k)$ to form the principal layer image Wp for embedding.

Step5. Calculate the JND value from the Y plane of the host image.

Step6. Embed the principal layer image depending on the shared computed layer (**this is the strong of the method**).

Step7. Apply the three-level inverse DWT to obtain the watermarked image (**this by using Packet WT**).

The watermarked image and the secret key are then saved for the *watermark extraction* phase. The result for Embedding operation can be illustrated as in **Fig. 6** below:

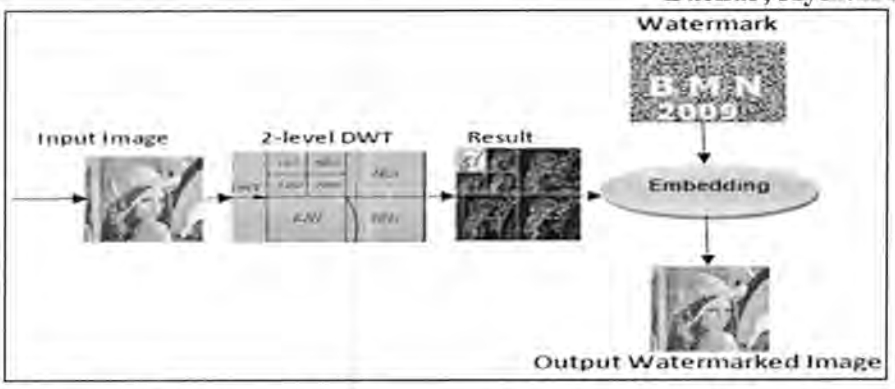

Fig. -6: Suggested Watermark Embedding Operation.

WATERMARK EXTRACTION ALGORITHM:

The extraction algorithm extracts the embedded principal layer and then reconstructs the watermark for copyright verification. The detailed algorithm is listed as follows:

Algorithm (2): Watermark Extraction Operation:

Input: The suspect color image $H'(N \times N)$ and the secret key for unscrambling.

Output: The reconstructed watermark WR $(M \times M)$.

Step1. Apply the three-level DWT on the R and B planes of the suspect color image H'.

Step2. Extract the embedded principal layer.

Step3. Extract the features as well as the feature type n and the average M.

Step4. For each block, generate the complement layer block.

Step5. Apply the *XOR* operation on each complement layer block and the corresponding principal layer block to produce the scrambled watermark W'.

Step6. Use Torus-automorphism and the secret key to unscramble the watermark W'.

Step7. Use *correction* as to obtain the corrected watermark.

Step8. Apply *reduction* to the corrected watermark to obtain the reconstructed watermark WR.

The result for Extraction operation can be illustrated as in **Fig. 7** below:

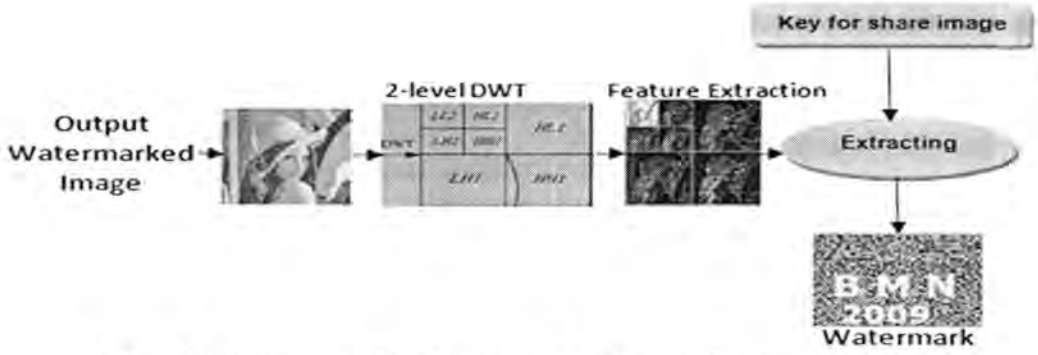

Fig. -7: Suggested Watermark Extraction operation.

TESTING & EXPERIMENTAL RESULTS:

In order to evaluate the proposed digital watermark algorithm, we first took the "Lenna" common test image of **Fig. 8 (a)** and produced the watermarked version of **Fig. 8 (b).**

a) **(b)**

Fig. -8: (a) before watermarking, and (b) after watermarking.

EXPERIMENT #1: UNIQUENESS OF WATERMARK

Fig. 9 shows the response of the watermark detector to 74 randomly generated watermarks of which only one matches the watermark present in **Fig. 8 (b)**. The positive response due to the correct watermark is very much stronger that the response to incorrect watermarks, suggesting that the algorithm has very low false positives (and false negative) response rates.

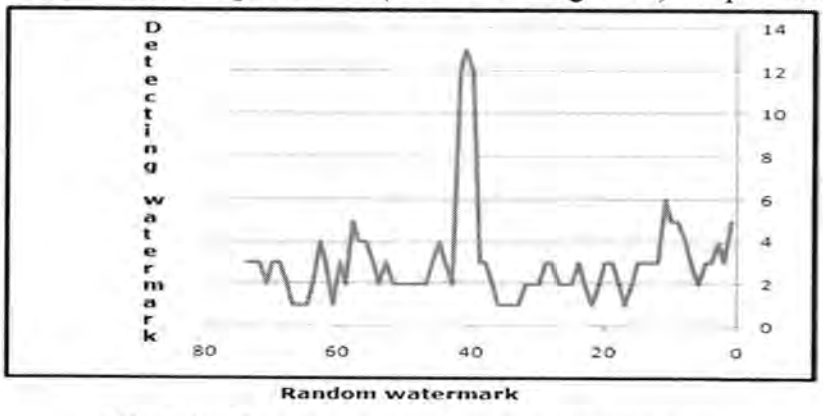

Fig.- 9: Watermark detector response.

EXPERIMENT #2: IMAGE SCALING

The watermarked image was scaled to half its original size, **Fig. 10(a).** In order to recover the watermark, the quarter-sized image was re-scaled to its original dimensions, as shown in **Fig. 10(b)**, in which it is clear that considerable fine detail has been lost in the scaling process. This is to be expected since subsambling of the image requires a low pass spatial filtering operation.

The response of the watermark detector to the original watermarked image was **32.0** to **Fig. 8(b)**, Which compare to a response of **13.4** for the rescaled version of **Fig. 10(b)**. While the detector response is down by over 50%, the response is still well above random chance level suggesting that the watermark is robust to geometric distortion. Moreover, it should be noted that 75% of the original data is missing from scaled down image of **Fig. 10(a).**

Fig. -10: (a) 0.5 scaled In watermarked Lenna image, (b) re-scaled Out Lenna image.

EXPERIMENT #3: JPEG IMAGE CODING

For the "Lenna" common image JPEG encoding version shows that the response of the watermark detector is 22.8, again suggesting that the algorithm is robust to common encoding distortions. The response of the watermark detector in this case still well above random.

EXPERIMENT #4: IMAGE CLIPPING

Fig. 11 (a) shows a clipped version of the watermarked image of "Lenna" in **Fig. 8(b)** in which only the central quarter of the image remains. In order to extract the watermark from this image, the missing portions of the image were replaced with portions from the original un watermarked image, as shown in **Fig. 11 (b).** In this case, the response of the watermark is 14.6. Once again, this is well above random even though 75% of the data has been removed

(a) (b)

Fig. -11: (a) Clipped, (b) Restored image depends on Portion of un watermarked original image.

EXPERIMENT #5: ATTACK BY COLLUSION

In a similar experiment, researcher took five separately watermarked images and averaged them in order to simulate a simple collusion attack. As before, the test shows the response of the detector to 1000 randomly generated watermarks, which include the five watermarks present in the image. Once again, five spikes clearly indicate the presence of the five watermarks and demonstrate that simple collusion based on averaging a few images is ineffective.

A need for electronic watermarking is developing as electronic distribution of copyright material becomes more prevalent. Previously, paper outlined the necessary characteristics of such a watermark.

In this paper a details description of the proposed method was given. Many looked at a range of applications and tried to place the various techniques in historical context in order to elucidate the relationships between them, and proposed. The proposed is a new watermarking idea for watermarking of JPG color images. The proposed idea satisfies the requirement of imperceptibility and robustness for a feasible watermarking scheme.

The experimental results showed that the proposed scheme can resist several attacks including clipping, scaling, and **JPEG** compression, etc. Furthermore, the unique identification experiment also demonstrated that the scheme is capable of extracting unique features from different images, which is an important requirement for feature extraction.

In watermarking, security measures the ability to resist hostile attacks. In steganography, there are three types of attacks: passive, active, and

malicious. Most current watermarking methods are designed for the resist any change which does not interfere with the Work in any way.

REFERENCES

1. R. J. Anderson, ed., *"Information hiding", 1st international workshop*, vol. 1174 of *Lecture Notes in Computer Science*, Isaac Newton Institute, Cambridge, England, Springer-Verlag, Berlin, Germany, ISBN 3-540-61996-8, (1996).
2. B. P_tzmann, "*Information hiding terminology*" , ISBN 3-540-61996-8, results of an informal plenary meeting and additional proposals, 347-350, (1996).
3. Fabien A. P. Petitcolas and others, "*Information Hiding - A Survey*", *Proceedings of the IEEE*, special issue on protection of multimedia content, 87(7):1062{1078, July (1999).
4. J. H. Kim, H. J. Kim, and K. R. Kwon, *"Multiwavelet image watermarking using perceptually tuned model"*, *Pattern Recognition Letters*, 6(12), 233-238, (2006).
5. Jung S. Cho, and others *"Enhancement of Robustness of Image Watermarks Image Watermark into Colored Image Based on WT and DCT,"*, Proceedings of International Conference on Information Technology Coding and Computing, 483 - 488, Mar. (2000).
6. Chiou-Ting Hsu and Ja-Ling Wu, *"Hidden Digital Watermarks in Images"* , Proceedings of the IEEE Transactions on Image Processing, 8(1), 58 –68, Jan. (1999).
7. Andreja Sam and J´an Tur´an, *"Attacks On Digital Wavelet Image Watermarks"* ,Journal of ELECTRICAL ENGINEERING, 59(3), 131–138, (2008).
8. BOJKOVI´C, Z, " *XXXVII International Scientific Conference on Information, Communication and Energy Systems and Technologies"*, ICEST 2002, 1, 131–134, Ni˘s, Yugoslavia, 1–4 October (2002).
9. BOJKOVI´C, Z., and others, *"Coding, Streaming and Watermarking – some Principles in Multimedia Signal Processing*", Acta Electrotechnica et Informatica, 3, 13–20, (2004).
10. TZOVARAS, and others," *Robust Image Watermarking in the Subband or DCT Domain*", EUSIPCO'98, IV, 2285–2288,Rhodes, Greece, 8–11 September (1998).

11. CRAVER, S., *"Copyright Protection Protocols based on Asymmetric Watermarking: the Ticket Concept, in Communications and Multimedia Security Issues of the New Century"*, Kluwer Academic Publishers, 159–170, (2001).
12. Shang-Lin Hsieh and others, *"Protecting Copyrights of Color Images using a Watermarking Scheme Based on Secret Sharing and Wavelet Transform "*, JOURNAL OF MULTIMEDIA, 3(4), Tatung University, Taipei, Taiwan, OCTOBER (2008).
13. Chin-Chen Chang, and others, *"An Image Copyright Protection Scheme Based on Torus Automorphisms "*, First International Symposium on Cyber Worlds (CW'02), 217 - 224, Nov. (2002).
14. G. Voyatzis and I. Pitas, *"Applications of torus automorphisms in image watermarking"*, Int. Conf. Image Processing (ICIP), Lausanne, Switzerland, 3, 237–240, Sep. (1996).
15. Lukac, R. and Plataniotis, K.N., *"A Secret Sharing Scheme for Image Encryption"* , Proceedings of IEEE Conference on Electronics in Marine, pp. 549 - 554, June (2004).
16. M. Naor and A. Shamir, *"Visual Cryptography," Advances in Cryptology"*, Eurocrypt '94, LNCS, 950, 1-12, (1995).

Image Authentication based on DCT transform watermarking

Musaab R. Abdulrazzaq
Computer Department, Collage of Science, University of Al-Mustansiriyah

Received : 12/04/2011 Accepted : 29/05/2011

الخلاصة

اصبحت حماية البيانات المرسلة على شبكة الانترنت من العبث والتزوير المتعمد من المواضيع المهمة التي تشغل الباحثين في السنوات الاخيرة. في هذا البحث تم اقتراح خوارزمية لاخفاء علامة مائية في صورة لغرض حمايتها من العبث والتزوير وتتلخص بتقسيم الصورة الى مجموعة من الاجزاء غير المتراكبة وادخال كل جزء الى تحويلة (DCT). يتم اخفاء كل بت من العلامة المائية في احد معاملات الجزء الذي يتم اختياره حسب دالة توليد ارقام عشوائية لاخفاء بت من العلامة المائية نستخدم دالة coefficient-binary-mapping. اظهرت هذه الخوارزمية كفاءة في تحديد مواقع التلاعب مع الحفاظ على نوعية الصورة .

ABSTRACT

Digital image can easily be tampered and destroyed by some people with malice. Therefore, the protection of digital information transmitted on a network has become an important research topic in recent years. The major goal of image authentication is to detect the tampered regions to achieve the authenticity and integrity. In this paper one watermark bit will be embedded in each DCT block by shifting a randomly selected coefficient to have a mapped value, in a coefficient-binary-mapping function that is identical to the watermark bit. The method was tested under different attacks and was found to provide good detection performance while maintaining the quality of the watermarked image.

INTRODUCTION

Digital image watermarking has received increasing attention in the few last years due to rapid growth in the internet traffic. It is gaining popularity due its significance in content authentication and copyright protection for digital multimedia data [1].

Watermarking applications include copyright protection, authentication, embedded and hidden information. Firstly, watermarking systems that are intended for copyright protection require a very high degree of robustness while watermarking process for authentication belongs to the fragile class of schemes. Slightest change in the image completely destroys the watermark.

Finally watermarking for embedding information requires resistance against moderate level of modification due to routine image processing such as compression or cropping [2]. Two types of authentication exist: Exact authentication and selective authentication. Exact authentication is accomplished by fragile watermark, embedded signatures and erasable watermarks. On the other hand, selective authentication is accomplished by semi-fragile watermarks, embedding semi-fragile signatures [3]. For traditional data authentication, the security requirement is to reject any message that has been altered to the slightest degree which called exact authentication. Some real applications need exact authentication and do not accept any alteration in the image at all. Consider for example an image for crime, changing any thing in the image such as a car number plate may be caused suspecting a person other than the actual criminal. On the other hand, some real applications do not need exact authentication they only need to verify some selective places in the work in order to be authenticated [1,2]. Those needed selective authentication distinguish between malicious and non-malicious attacks (i.e. it distinguishes between legal distortion such as digital signal processing operation and illegal distortions such as changing a person in image). Image authentication systems have applicability in: law, commerce, defense, and journalism. Since digital images are easy to modify, a secure authentication is useful in showing that no tampering has occurred during situations where the credibility of an image may be questioned [4,5].

The Discrete Cosine Transform (DCT)

The DCT is a very popular transform function used in signal processing. It transforms a signal from spatial domain to frequency domain. Due to good performance, it has been used in JPEG standard for image compression. DCT has been applied in many fields such as data compression, pattern recognition, image processing, and so on. The DCT transform and its inverse manner can be expressed as follows:

$$F(u,v)=\frac{4C(u)C(v)}{n^2}\sum_{j=0}^{n-1}\sum_{k=0}^{n-1}f(j,k)\cos[\frac{(2j+1)u\pi}{2n}]\cos[\frac{(2k+1)v\pi}{2n}]. \quad (1)$$

$$f(j,k)=\sum_{u=0}^{n-1}\sum_{v=0}^{n-1}C(u)C(v)F(u,v)\cos[\frac{(2j+1)u\pi}{2n}]\cos[\frac{(2k+1)v\pi}{2n}]. \quad (2)$$

DCT transform was used by many researchers in watermark embedding: Cox et al. [5] uses spread spectrum to embed watermark in the discrete cosine transform (DCT) domain. To improve Cox's method, Lu et al. [6] uses cocktail watermark to improve the robustness and used human visual system (HVS) to maintain high fidelity of the watermarked image. Hsu et al. [7],[8] embeds watermark bits by modifying the polarity of DCT and discrete wavelet transform (DWT) coefficients and uses a meaningful logo image as the watermark. Huang et al. [9] embeds a watermark pattern by modifying the DC components.

Watermark Embedding Process

In this paper the watermark is embedded in three bands (red, green, and blue). The embedding process is based on shifting the selected coefficient C_{si}, to have a mapped value in the coefficient binary mapping function $Q(c_{si})$ eq. 2, that is identical to the watermark bit W_i .

Step1: Load the image (O) to be watermarked.

Step2: Load the watermark (W) .

Step3: Segment the image into non-overlapping blocks (B_i) of size NxN pixels, and apply forward DCT to each block (B_i) to produce corresponding block (C_i) of DCT Coefficients.

Step4: A user key k is used to generate a random coefficient-selection ($1 \le k \le N^2$), denotes the index of the coefficient to be watermarked in block C_i.

Step5: let w_i be the watermark bit to be embedded in coefficient c_{si} of block (C_i). The watermarked coefficient c'_{si} is given by:

$$c'_{si} = \begin{cases} c_{si} & \text{if } Q(c_{si}) = w_i \\ c_{si} + \Delta & \text{if } Q(c_{si}) \neq w_i \quad \text{and } c_{si} \le 0 \\ c_{si} - \Delta & \text{if } Q(c_{si}) \neq w_i \quad \text{and } c_{si} > 0 \end{cases} \quad \ldots(1)$$

Where Δ is called the quantization parameter, and Q(.) is a coefficient binary mapping function given by:

$$Q(c) = \begin{cases} 0 & \text{if (round (c) / } \Delta) \text{ is even} \\ 1 & \text{if (round (c) / } \Delta) \text{ is odd} \end{cases} \quad \ldots (2)$$

Step6: once all watermark bits are embedded in the DCT blocks, the inverse DCT is applied to obtain the watermarked image O'.

Extraction

In the extraction process, the received, and possibly tampered with, image O" is the first divided into *B* blocks each of size N×N .The DCT is applied to each block B''$_i$ to produce a corresponding block C" $_i$ of DCT coefficient. The same user key *k* (hidden in the image file header) that was used at the transmitter is available also at the receiver and is used to generate the same random coefficient-selection vector S= $\{S_1,\ldots,S_B\}$. This vector is used to locate the watermark coefficient c"$_{Si}$ in each block C"$_i$ .The extracted watermark bit w"$_i$ is obtains as follows : **W"$_i$=Q (c"$_{Si}$).**

The extracted watermark bit W''$_i$ is compared to the original watermark bit W_i. If they are identical then the corresponding block B"$_i$ is authentic, otherwise it is inauthentic (i.e. tampered with).

RESULT AND DISCUSSION

For testing the performance of this algorithm, the experiments are simulated with the software **MATLAB**. We select bitmap color image of size (256 x 256) that represent the host image, and a binary image of size (128 x 128) represent the embedded watermark. An important parameter that needs to be set is the block size N. Larger block sizes result in less degradation to the quality of the watermarked image since less number of bit is embedded. On the other hand, smaller block size provide better localization of tampering area. In this paper, the block size is set to 2x2 (i.e N=2). Another major reason for selecting this block size is that it simplifies the selection of the parameter Δ.

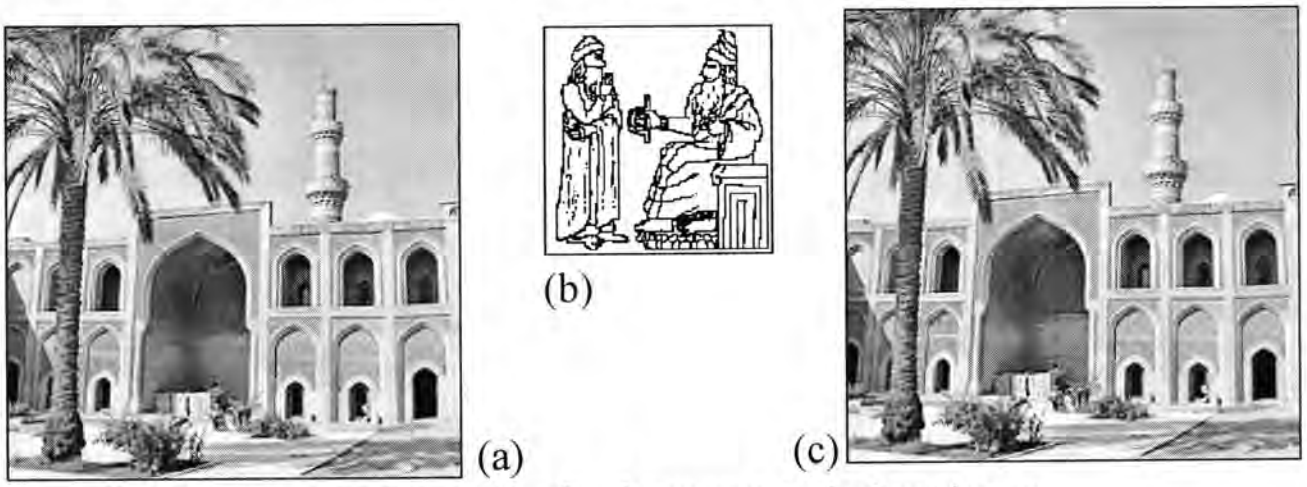

Fig.-1: a) Al- Mustansria school represents the host image
b) King Hamorabi represents the watermark.
c) The watermarked image.

To compute the value for Δ for best performance, the proposed algorithm simulate for different values of Δ ranging from (1-8) on (50) images and compute the PSNR for each value and image the results shown in the table (1) and Fig. (2):

Table-1: PSNR valus for different images and Δ

	Δ=1	Δ=2	Δ=3	Δ=4	Δ=5	Δ=6	Δ=7	Δ=8
image 1	51.017	51.099	50.506	45.339	43.976	40.742	35.760	30.756
image 2	51.160	51.120	49.905	43.968	42.987	41.836	34.873	29.98
image 3	51.067	51.591	49.942	44.987	42.238	40.671	34.989	31.78
image 4	51.271	51.966	50.643	44.781	43.987	41.892	34.975	29.567
Images (5-50) (av)	51.109	51.602	49.567	44.845	43.276	40.767	34.867	29.954
Average	51.110	51.589	49.621	44.839	43.277	40.808	34.889	29.999

From table (1) it is clear that the best performance is achieved when Δ=2. This value used in all subsequent results.

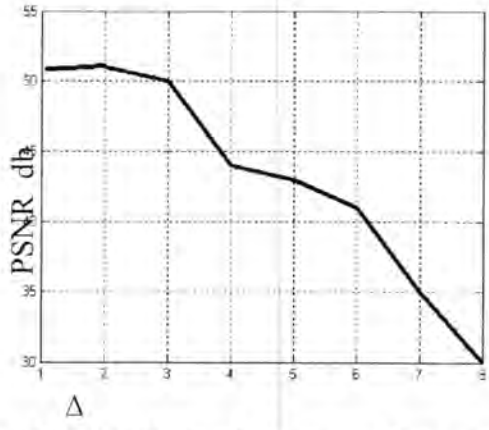

Fig.-2: PSNR performance for various values of Δ

In order to evaluate the effect of the proposed method on the quality of the watermarked image, the PSNR measure is calculate. Different approaches exist for computing the PSNR of a color image. Because the human eye is most sensitive to luma information, compute the PSNR for color images by converting the image to a color space that separates the intensity (luma) channel, such as YCbCr. The Y (luma), in YCbCr represents a weighted average of R, G, and B. G is given the most weight, again because the human eye perceives it most easily.

$$\begin{vmatrix} Y \\ Cb \\ Cr \end{vmatrix} = \begin{vmatrix} 0.229 & 0.587 & 0.114 \\ -0.168 & -0.331 & 0.500 \\ 0.500 & -0.418 & -0.081 \end{vmatrix} \begin{vmatrix} R \\ G \\ B \end{vmatrix}$$

With this consideration, compute the PSNR only on the luma channel.

$$PSNR = 10 \log_{10} \frac{255^2}{\frac{1}{N \times N} \sum_{i=0}^{N-1} \sum_{j=0}^{N-1} (x_{i,j} - \hat{x})^2}$$

Where $(x_{i,j})$, $(\hat{x}_{i,j})$, are the luma Y channel values of host and watermarked images and N x N is the size of image respectively.

Fig.-3: **a) Extracted watermark from red band**
b) Extracted watermark from blue band
c) Extracted watermark from green band
d) or (red, green, blue) to reduce noise if found

(a) (b) (c) (d)

Fig.-4: some type of intentional attacks:
a. Original image b. tampered image
c. distinguishes tampering area using proposed algorithm
d. recovered watermark

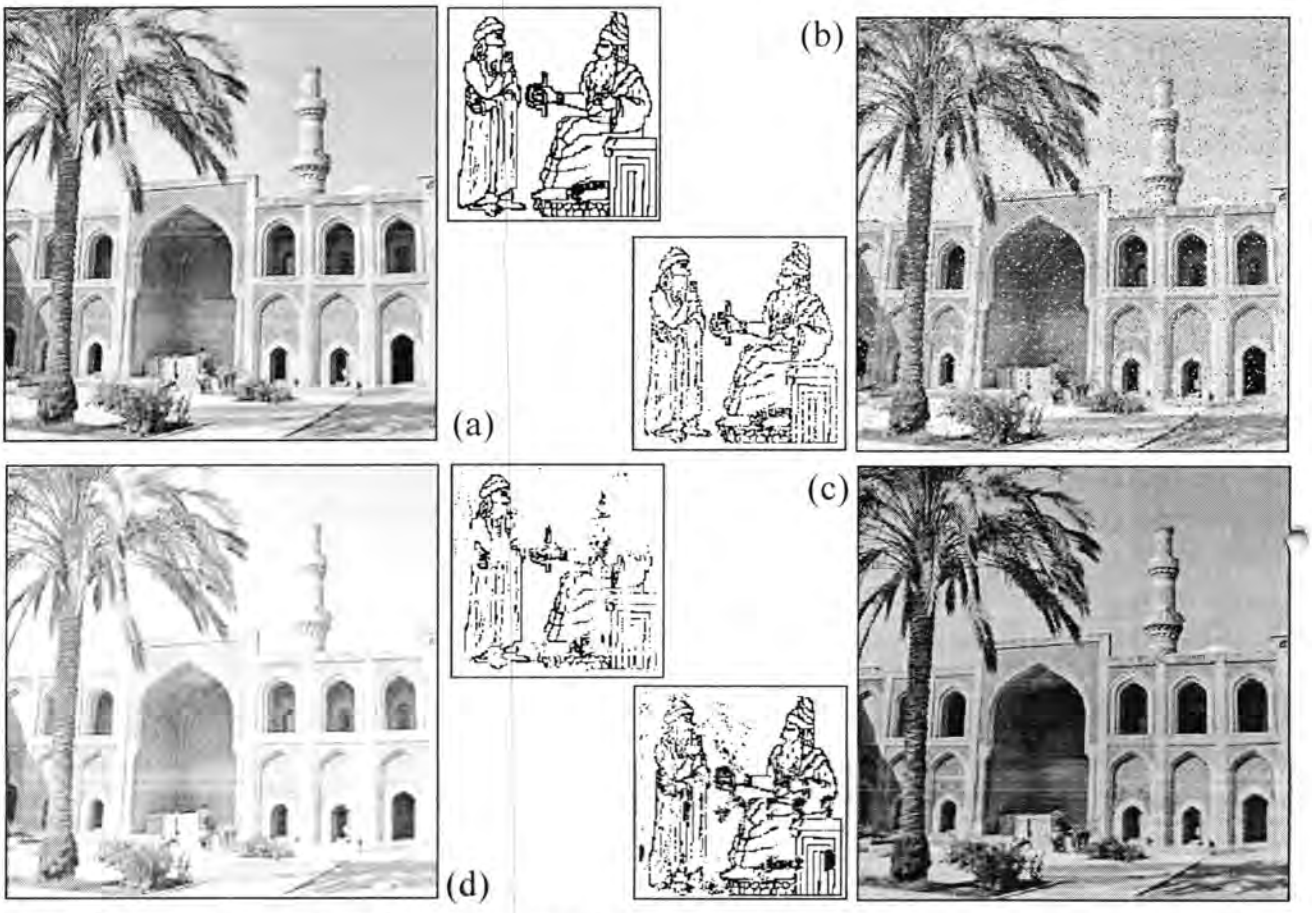

Fig.-5 : some type of accidental attacks:
a. Original image and watermark.
b. Noisy image and recover watermark
c. Darken image and recover watermark.
d. Lightened image and recover watermark

A DCT based watermark methods for image authentication has been developed. In this method a watermark in the form of a visually meaningful binary pattern is embedded for the purpose of tamper detection. The method embeds one watermark bit in each DCT block by shifting a randomly selected coefficient-binary-mapping function that is identical to the watermark bit. It can be seen from the algorithm that the PSNR decreases as Δ is increased. This is expected since a large Δ means that the watermarked coefficient are shifted by a large amount from there original values. Note that when Δ is less than 1, no watermarking is achieved, hence the infinite PSNR. The method was tested under different attacks and was found to provide good detection performance while maintaining the quality of the watermarked image. Depending on the type of attack, the method may provide exact authentication, selective authentication, or localization.

REFERENCES

1. B. Mohan and S. Kumar, "A robust image watermarking scheme using singular value decomposition" *J. Multimedia*, 3(1), 356-364, May (2010).
2. G. Lo-varco, W. Puech, and M. Dumas, "Content Based watermarking for securing color images", J. Imaging Science & Technology, 49(6), 623-629, Jan.(2006).
3. G. Voyatzis and I. Pitas, "The use of watermarks in the protection of digital multimedia products", IEEE Proceedings, 87(7), 1197-1207, July (2009).
4. Lin ET, Christine I, Podilchuk B, Delp EJ "Detection of image alterations using semi-fragile watermarks". In: Proceedings of the SPIE international conference on security and watermarking of multimedia contents II, 3971, San Jose, CA, USA(2000)
5. I. J. Cox, J. Kilian, T. Leighton, and T. Shamoon, "Secure spread spectrum watermarking for multimedia", IEEE Trans. Image Processing, 6, 1673–1687, Dec. (1997).
6. C. S. Lu, S. K. Huang, C. J. Sze, and H. Y. M. Liao, "Cocktail watermarking for digital image protection," IEEE Trans. Multimedia, 2, 209–224, Dec. (2000).
7. C. T. Hsu and J. L. Wu, "Multiresolution watermarking for digital images," IEEE Trans. Circuits Syst. II, 45, 206–216, Aug. (1998).
8. G. Miller "Hidden digital watermarks in images" , IEEE Trans. Image Processing, 8, 55–68, Jan. (1999).
9. J. Huang, Y. Q. Shi, and Y. Shi, "Embedding image watermarks in DC components," IEEE Trans. Circuits Syst. Video Technol., 10, 974–979, Sept. (2000).

Field Study into the Influence of Polluted Urban Environment on Aerosol Number Concentrations in Al-Ramadi City of Iraq

Anmar Dhirar K.*, Mohammad Taha Y.*, Jasim Hameed K.**
*Dept. of Physics, College of Education for Pure Science, Al-Anbar University
**Dept. of Meteorology, College of Science, Al-Mustansiriyah University

Received : 17/04/2011 Accepted : 29/05/2011

الخلاصة

مدى عريض لحجوم أعداد تراكيز جسيمات الهباء الجوي من 0.3 µm الى 25 µm تم رصده بإستخدام عداد الجسيمات الليزري في موقعين أولهما مأهول بالسكان ذو شوارع ضيقة مزدحمة وأسواق تجارية ومصانع قديمة ضخمة والآخر ماهول بالسكان ذو كثافة مرورية قليلة وليس ذو طبيعة تجارية ولايحوي مصانع للفترة من 4/11 الى 23/12/2010 بمعدل قراءات 17 عينة مقاسة باليوم الواحد و 34 عينة مقاسة في الساعة الواحدة من مجموع أيام القياس. التغير اليومي لتراكيز أعداد جسيمات الهباء الجوي في الموقع الملوث أشر إرتفاعا مهما في تراكيز الجسيمات الصغيرة خلال الليل والصباح وانخفاضا عند الظهيرة بينما تراكيز الجسيمات الكبيرة تنخفض في الليل وتزداد في النهار . معدل تراكيز أعداد جسيمات الهباء الجوي المقاسة لستة مديات حجمية (0.3 و 0.5 و 1.0 و 5.0 و 10.0 و 25.0 مايكرون) كانت 65378961 و 23316310 و 8242311 و 604482 و 105690 و 4912 جسيم بالمتر المكعب على التوالي. وإن معدل الزيادة في تراكيز أعداد جسيمات الهباء الجوي في البيئة الملوثة للمدن كانت 71 و 44 و 56 و 93 و 66 و 56 % فوق الطبيعي للمديات الحجمية الستة على الترتيب.

ABSTRACT

The size-separated number concentrations of aerosols ranging from 0.3 to 25 µm were observed by laser particle counter in two sites one in a residential and commercial area with narrow Streets and heavy vehicular traffic and with huge old Factories, and the other in a residential area with lower traffic density and without Industries or commercial areas for the period from 4/11 to 23/12/2010 at a rate of 17 sample/day and 34 sample/ hour of total measured days. Daily variation of aerosol number concentrations in urban area indicate a high significant for fine particles at night/morning of day and lowerly at afternoon while for coarse particles are decrease at night time and increase at day time. The measured mean of aerosol number concentration for six size channels (0.3, 0.5, 1.0, 5.0, 10.0 and 25.0 µm) was

65378961, 23316310, 8242311, 604482, 105690 and 4912 particle/m3 respectively. The increase's ratio of aerosol number concentrations in urban polluted environment was 71, 44, 56, 93, 66 and 56 % up-normal for the six size channels respectively.

INTRODUCTION

Particles in ambient air have size spanning from few nanometers to 100 μm [1]. These particles of various sizes are generated by different sources in atmosphere and rapid process of recombination; nucleation, etc. take place in atmosphere. There are two types of particles in atmosphere: (i) primary aerosols, which are directly produced in atmosphere by wind-blown dust, soil erosion, bubble bursts, volcano eruptions and human activities; (ii) secondary aerosols, which are produced by nucleation of low volatile gases and are mainly produced by industrial activities, forest fires and vehicular emission, etc. [2-4].

The particles of size > 1 μm called coarse or super micron particles are mostly generated by dust resulting from excavation, blowing wind, etc. [5]. The particles >2.5 μm are generally remove by upper respiratory tract, called respirable suspended particulate matter and are not much harmful to health [6]. The suspended particles of size less than 1 μm are called fine or submicron particles [7], they are further classified as accumulation mode (1-0.1 μm) and fine particles of this range are dangerous as they penetrate in to lungs and produce respiratory problems [8].

The Earth's climate is also influenced greatly by the physical and chemical properties exhibited by atmospheric aerosols, which alter cloud properties and the Earth's radiative balance [9-11].

Therefore, Particle number concentration in the troposphere is an important parameter controlling the climate and health impacts of atmospheric aerosols not only in the visibly affected mega-cities of the developing world, but also at the relatively low concentrations found in the air of the more developed world too [12, 13].

The objectives of this study are to determine the aerosol number concentration in Al-Ramadi city for six sizes channels by leaser particles counter and to identify the influence of polluted urban environment on aerosol number concentrations in this city.

METHODS AND TECHNIQUES

Two sites were chosen for measuring aerosol number concentrations both of them are located in Al-Anbar, Iraq. The first site was located in Al-Ramadi City Metropolitan Area In a residential and commercial area with narrow Streets and heavy vehicular traffic from 7:00 am to l0:00 pm, so it was expected to have heavy vehicular emissions. The second site was a residential area with lower traffic density and without Industrial or commercial areas called Al-Doar city away 35 km from the first site.

The ground-based measurements are the most accurate and low-cost tools for studying polluted urban environment effects, some attempts to distinguish the properties of urban aerosols were previously done [14].

In this study, Aerosol number concentrations ANC was accounted within six size-ranges (0.3, 0.5, 1.0, 5.0, 10.0 and 25.0 μm) by laser particle counter (model: Climet CI-500) to the rate of flow (28.3 liter/ Minute) and to Highest concentrations (1000000 particle/ft^3). Temperatures in the accuracy (± 0.4°C) and relative humidity with accuracy (± 2%) were also measured in the same place and time of sampling and by using the same device [15].

The samples were recorded in 48 days during the period from 4/11 to 23/12/2010 in Al-Ramadi city, at a rate of 17 sample/day and 34 sample/ hour of total measured days also recorded samples in 3 days, two of them in November and one in December for 24 hours in Al-Doar city. Sampling process was at an altitude of 1m above ground surface and for 0.01 m^3 as a sample size in the both sites.

The great efforts have been made to neutralize the effects of some factors that are not in the objectives of this study, such as wind speed or direction and the impacts in small scale, which may effect on the fact of ANC. Also the samples have been neglected in a rainy and dusty days. In addition to other processes, such as measurement of ANC, temperature and relative humidity inside and outside the fitting room to make sure that similar internal and external environment.

RESULTS AND DISCUSSION

Variation of ANC in Al-Ramadi city

The Daily behavior of Aerosol number concentrations are varied with different size of particles. Fine particles of size less than 1.0 μm have dissimilarity behavior from that of coarse particles of size greater than 2.5 μm while that for respirable suspended particulate (2.5 μm > p < 1.0 μm) is

oscillating inclined towards the dominant size-ranges of one of fine or coarse particles, as shown in Table 1.

Table -1: Hourly mean variation of aerosol number concentration in Al-Ramadi city

Time (hour)	Aerosol number concentrations (particle/m^3)					
	0.3 μm	0.5 μm	1.0 μm	5.0 μm	10.0 μm	25.0 μm
00	70803690.8	22889551	6326037	279187.9	37284.85	1506.475
01	70913483.7	25799028.1	9780126.3	279550.6	54822.88	1156.412
02	73079267.4	25230226.9	8906412.3	237442.7	55154.03	1016.103
03	72952233.9	21543539	6083130.6	192509.6	40743.7	790.1852
04	70048420	21477491	3417724.7	193862	54881.13	1135.217
05	69726500.6	17411875.6	3492773.5	189163.2	31413.03	1102.034
06	66315943.4	16473970.3	4057809.6	294578.7	46891.13	1733.833
07	64929754.9	18124980.9	5040503.5	321241.5	66416.69	2438.057
08	65776373.7	20907256.6	6970057.8	493281.7	96952.87	4813.308
09	66119693.7	20300151.7	6607492.4	578685.6	127717.2	4701.563
10	65330259.3	18777137.5	6068015.2	507640.4	114297.3	6080.889
11	62871150.2	21095717.9	7875699.7	669617.2	114319.2	7212.421
12	62633401.1	23577053.6	9840045.7	888137.1	149028.5	10470.89
13	58550106.5	19971458.7	8694783	844382.4	155705.4	12686.42
14	56776394.3	18942573.4	8145634.8	692548.4	168565.8	9477.73
15	56202153.1	17039490.3	7083998.2	717683.9	142817.6	7819.167
16	57070989.7	21089057.3	10133153	994911.3	187273.4	10564.39
17	59633109.4	30346654.8	14270594	1415341	207024.9	9058.833
18	63280238.2	33516831.1	14303004	1178958	166398.1	5959.541
19	66110705.5	34479387.8	13824623	1050848	172162.9	6018.919
20	66082944.9	30073620.2	10725955	826496.3	108346.6	3836.806
21	66515398.7	30088724	10489988	746542.6	119433.4	3744.868
22	67634772	26528240.8	8999945.4	574907.8	74221.44	2532.923
23	69738100.4	23907429.4	6677964.4	340061.1	44691.92	2036

Aerosol number concentrations for fine particles are increase at night and morning of day while decreasing at the afternoon and reached in its highest value for the three size channels (0.3, 0.5 and 1.0 μm) 73079267, 34479387 and 14303004 particle/m^3 respectively while reached in its lowest value 56202153, 16473970 and 3417724 particle/m^3 respectively. Also the daily variation of Aerosol number concentrations for coarse particles of size channels (5.0, 10.0 and 25.0μm) are decrease at night time reached 189163, 31413 and 790

particle/m^3 respectively, and increase at the day time reached 1415341, 207024 and 12686 particle/m^3 respectively. therefor the mean ANC for all six channels is 65378961, 23316310, 8242311, 604482, 105690 and 4912 particle/m^3, as shown in Table 2.

Desert nature surrounding Al-Ramadi city and its dusty wind-blown cause the up-normal ANC of coarse particles, as well as a little decrease in ANC of fine particles by compared measured data with other measured data at Baghdad [16].

Table -2: aerosol number concentration (Max., Mean, Min.) for six size channels in Al-Ramadi city and it's increasing and decreasing at day time.

Particles size channels	Day time		Aerosol number concentrations		
	ANC Increasing time	ANC Decreasing time	Max.	Mean	Min.
P > 0.3 μm	19 pm – 11 am	12 am – 18 pm	73079267	65378961	56202153
P > 0.5 μm	17 pm – 4 am 11 am -13 pm	4 am – 10 am 14 pm – 16 pm	34479387	23316310	16473970
P > 1.0 μm	16 pm – 2 am 11 am – 13 pm	3 am – 10 am 14 pm – 15 pm	14303004	8242311	3417724
P > 5.0 μm	10 am – 17 pm	18 pm – 9 am	1415341	604482	189163
P > 10.0 μm	9 am – 21 pm	22 pm – 8 am	207024	105690	31413
P > 25.0 μm	8 am – 21 pm	22 pm – 7 am	12686	4912	790

Polluted urban versus clear desert ANC.

The traffic jams areas [17, 18], large commercial areas, factories and power stations [13] inside cities cause air pollution and an increase in ANC. For assessment that pollution was chosen unpolluted city to compare with polluted city after measured aerosol number concentrations in the same field conditions.

As is evident in Figure (1) Aerosol number concentrations indicate a significant increase for all size-ranges. That increase's ratio shown in table 3 was 71, 44, 56, 93, 66 and 56 % for the six size channels 0.3, 0.5, 1.0, 5.0, 10.0 and 25.0 μm respectively.

Table-3: Increase's ratio of ANC in polluted urban environment for six particle size channels

ANC mean (no./m^3)	Particle size channels (μm)					
	0.3	0.5	1.0	5.0	10.0	25.0
1st site	65378961	23316310	8242311	604482	105690	4912
2nd site	27180653	7193773	2979692	292380	42065	1764
Increase's ANC	38198308	16122537	5262619	312101	63624	3148
Increase's ratio (%)	71	44	56	93	66	56

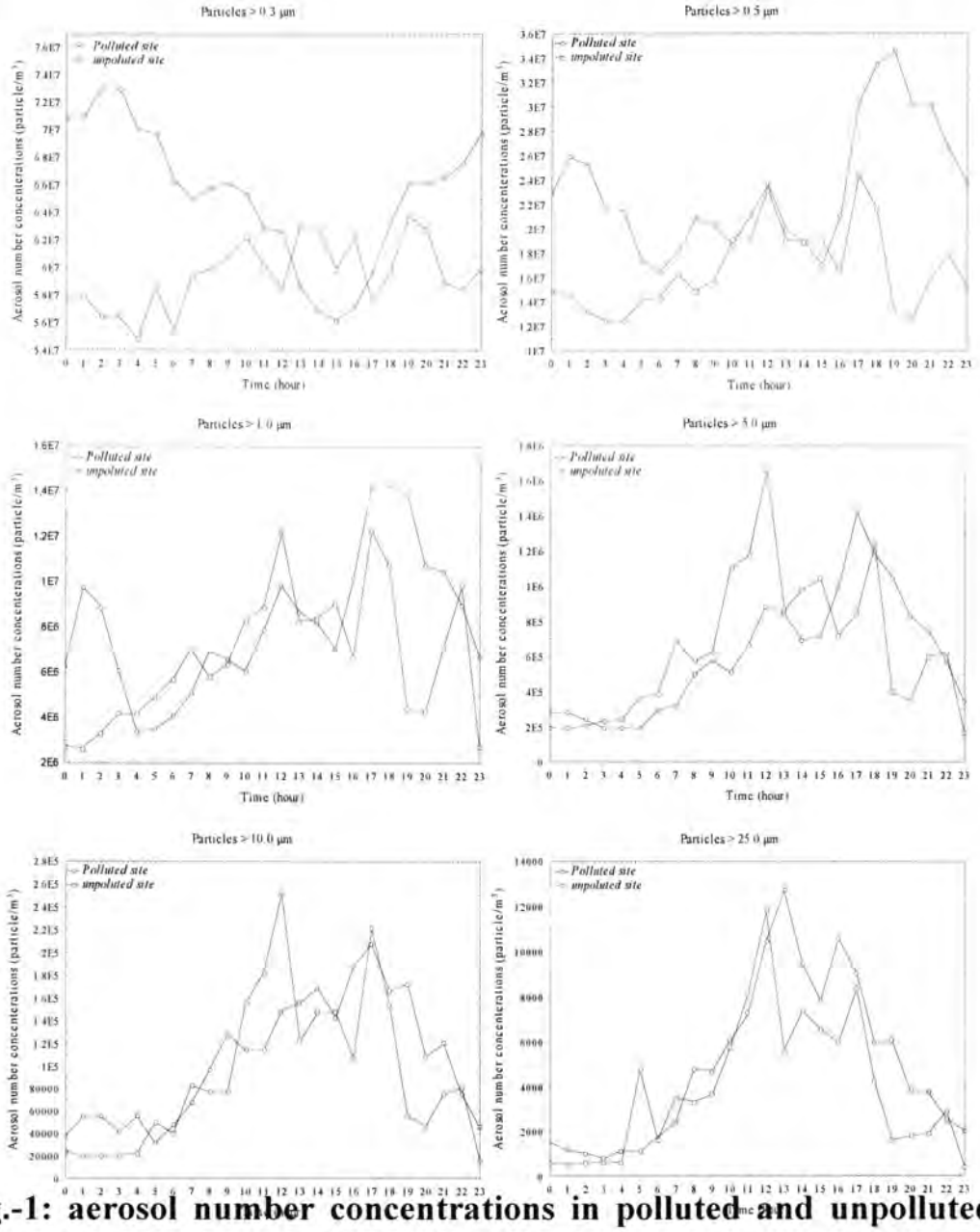

Fig.-1: aerosol number concentrations in polluted and unpolluted site for size-ranges 0.3, 0.5, 1.0, 5.0, 10.0 and 25.0 μm.

The main objective of this study was to determine the aerosol number concentration in Al-Ramadi city and to identify the influence of polluted urban environment on aerosol number concentrations. Aerosol number concentrations was accounted within six size-ranges (0.3, 0.5, 1.0, 5.0, 10.0, 25.0 μm) by laser particle counter for 48 days during the period from 4/11 to 23/12/2010 in Al-Ramadi city and 3 days in Al-Doar city.

This study showed that in Al-Ramadi city:

1) Aerosol number concentrations for fine particles are increase at night and early of day while decreasing at the afternoon while for coarse particles are decrease at night time and increase at the day time.
2) The highest value of aerosol number concentration in for the six size channels (0.3, 0.5, 1.0, 5.0, 10.0 and 25.0 μm) was 73079267, 34479387, 14303004, 1415341, 207024 and 12686 particle/m^3 respectively, and the lowest value was 56202153, 16473970, 3417724, 189163, 31413 and 790 particle/m^3 respectively.
3) The mean aerosol number concentration for the six channels was 65378961, 23316310, 8242311, 604482, 105690 and 4912 particle/m^3.
4) The increase's ratio of aerosol number concentrations in urban polluted environment was 71, 44, 56, 93, 66 and 56 % up-normal for the six size channels respectively.

REFERENCES

1. WMO/GAW; Aerosol measurement procedures guidelines and recommendations.. WMO TD No. 1178. (2003).
2. Gomac B.M.: Introduction to Aerosols. Orleans Univ., France. (1993).
3. P.Murugvel and D.M. Chate : Generation and growth of aerosols over Pune, India. Atmo. Enviro. 43(4), 820-828. (2009)
4. [4] Fangqun Yu and Gan Luo,: Spatial distributions of particle number concentrations

in the global troposphere: Simulations, observations, And implications for nucleation mechanisms. Jour. Of Geophysical research, 115; D17205. (2010)

5. Tiantao Cheng and Daren Lu.: Physical characteristics of dust aerosol over Hunshan Dake sandland in Northern China. Atmo. Enviro. 39(7), 1237-1243. (2005).

6. I. D. Longley and M. W. Gallagher.: A case study of aerosol (4.6 nm < D_p < 10 μm) number and mass size distribution measurement in a busy street canyon in Manchester, UK. Atmo. Enviro. 37(12), 1563-1571. (3003).
7. Michael P. Tolocka and Derek A. Lake.: number concentration of fine and ultrafine particles containing metals. Atmo. Enviro. 37(20), 3263-3273. (2004).
8. JON G. AYRES.: Air pollution and Health. IEH report. (2009).
9. N. Y. Chubarova and M. A. Sviridenkov.: Assessments of urban aerosol pollution in Moscow and its radiative effects. Atmos. Meas. Tech., 4, 367–378. (2011).
10. Suresh Tiwari and Swagata Payra.: Visibility degradation during foggy period due to anthropogenic urban aerosol at Delhi, India. Atmospheric Pollution Research 2, 116-120. (2011).
11. A. Weigelt and M. Hermann.: Influence of clouds on aerosol particle number concentrations in the upper troposphere. Jour. Of Geophysical research, 114; D01204. (2009).
12. Yang Zhao and Andre J. A. Aarnink.: Evaluation of an impaction and a cyclone pre-separator for sampling high PM10 and PM2.5 concentrations in livestock houses. Aerosol Science, 40, 868 – 878. (2009).
13. R. García and R. Belmont : Determination of inorganic ions and trace elements in total suspended particles at three urban zones in the Mexico City Metropolitan Area and one rural site. Atmospheric Research, 94, 313–319. (2009).
14. Gorge Pey : Variation of urban aerosols in western Mediterranea. Atmo. Enviro. 42(40), 9052-9062. (2008).
15. CI-500 Innovation Laser particle counter, operation manual 1.0 CFM. (2002).
16. Anmar Dhirar K. : Time changes in aerosols concentrations at Baghdad. Ph.D. thesis. (2007).
17. Daninius M. : Traffic-related $PM_{2.5}$ aerosols in residential houses located near major highways: Indoor versus outdoor. Atmo. Enviro. 42(27), 6575-6585. (2008).
18. A.W.Strawa and T.W.Kirchstetter : Optical and physical properties of primary on-road vehicle particle emissions and their implications for climate change. Journal of Aerosol Science, 41, 36–50. (2010).

المجلد 22
العدد 5
2011

مجلة علوم المستنصرية

تصدر عن كلية العلوم الجامعة المستنصرية

عدد خاص
ببحوث المؤتمر العلمي السابع
لكلية العلوم - الجامعة المستنصرية
للفترة 4-5 أيار لسنة 2011

Mobile: 07711184399
e-mail: mustjsci@yahoo.com

المـــحتـــويـات

تأثير نبات القرفة *(Cinnamon zylanicum)* وعقار الأنسولين في تخفيض مستوى سكر الدم لإناث الفئران البيض المستحث فيها داء السكري بمادة الالوكزان

*م.م نضال طالب شهيب و *م.م وسن حمزة مزعل و *م.م جواد كاظم عيسى و ** خالد سعد الله وردي

*جامعة واسط / كلية العلوم- قسم علوم الحياة

**دبلوم عالي/ طبيب / مستشفى الكرامة التعليمي

تاريخ تقديم البحث : 2011/ 3/29 تاريخ قبول البحث : 2011/ 5/29

الخلاصة

أجريت هذه الدراسة على 30 فأرة من إناث الفئران البيض قسمت إلى مجموعتين المجموعة الأولى تمثل مجموعة السيطرة وتضم 10 فئران أما المجموعة الثانية فتضم 20 فأرة حقنت بمادة الالوكزان ثم قسمت هذه المجموعة إلى مجموعتين ثانويتين احدهما جرعت بمستخلص كحولي لنبات القرفة والأخرى حقنت بعقار الأنسولين. أن الهدف من البحث دراسة تأثير المستخلص الكحولي الايثانولي الخام البارد لنبات القرفة (الدارسين) ودواء الأنسولين الصافي على إناث الفئران البيض المستحث فيها داء السكري عن طريق الحقن بالالوكزان alloxan monohydrate (5%w/v) بجرعة (150mg/kg) مذابة في المحلول الفسيولوجي في حجم (0.1ml) من وزن الجسم . تم إعطاء المستخلص الكحولي لنبات القرفة عن طريق الفم يوميا وبجرعة (200mg/kg) من وزن الجسم . وتم الحقن بعقار الأنسولين بجرعة (0.02 unit/mg/kg) من وزن الجسم . اثبت نتائج الدراسة وجود فروق معنوية بمستوى ($p< 0.05$) في كل المجاميع مقارنة مع مجموعة السيطرة وتبين إن المستخلص الكحولي لنبات القرفة له التأثير الأكبر بالمقارنة مع مجموعة الأنسولين في خفض مستوى سكر الدم في الفئران المستحث فيها داء السكري بالالوكزان .

ABSTRACT

This study involved 30 female albino mice were divided into two groups ,the first represent control group , involve 10 mice , the second involve 20 mice were injected by alloxan and them divide into two sub group the first given orally by alcohol extract of *Cinnamon zylanicum* plant , the second were injected by insulin drug . The objective aim from this research is to study the plant extract effect (*C. zylanicum)* & soluble insulin were induced diabetic them by alloxan monohydrated where dose (5%w/v) with (150mg/kg) of body weight, alcohol extract for Cinnamon plant have been given orally daily with (200mg /kg)dose of body

weight . insulin drug have been injected with (0.02unit /mg/kg) dose of bodyweight . In all tests were conducted it have been demonstrated study result existence significant differences ($p<0.05$) was in all groups compare with control group.(*Cinnamomum zylancium* showed have high effect(lower blood sugar) comparison with insulin group.

المقدمة

أن مرض السكري هو اضطراب في التمثيل الغذائي ويتصف بنقص في إنتاج أو فعالية للأنسولين insulin .حيث أن الأنسولين هو الهرمون الوحيد الذي يعمل على خفض نسبة الكلوكوزفي الدم وينتج هذا الهرمون في خلايا بيتا التي تكون جزءا من جزيرات لانكرهانز في النسيج البنكرياسي والأنسولين يساعد في تحويل الكلوكوز إلى كلايكوجين وتسمى العملية Glycogensis والى مواد دهنية وتسمى Lipogenesis في الأنسجة الدهنية(1). إن وجود الأنسولين في الجسم بكميات كافية مناسبة ضروري وأساسي لتمثيل الكلوكوز طبيعيا داخل الخلايا . لان هذا الهرمون يفرز من البنكرياس ليلامس المستقبلات على سطح الخلية وفوق ذلك يخبر الخلية بأنه يوجد بعض الكلوكوزفي الدم وبعد أعلام المستقبلات يسمح الكلوكوز بالدخول خلال غشاء الخلية لتغذيتها . كما إن النقص في كمية الأنسولين ينتج عنه ضعف وإعاقة تحطيم الكلوكوز داخل الخلايا وعرقلة تحويله إلى كلايكوجين glycogen أو إلى دهن ونتيجة لذلك يتراكم الكلوكوز في الدم ويسبب Hyperglycemia ويظهر كذلك في إفرازات البول Glycosurea (3) . يحتل نبات القرفة (الدارسين) مكانة مهمة في قائمة النباتات الامينة لعلاج العديد من الإمراض في العالم ومنها داء السكري والتهاب اللثة وسرطان الجلد والسعال نظرا لما يحتويه من مركبات فعال مثل Cinnamaldeehyde ,Benzaldehyde & Cuminaldhedyde phenols & methyl eugenol & Caryophllene chydro carbons وتستخدم في علاج مرض السكر لاحتوائه على على مركبات فعالة مثل Methlhdroxy chalcone polymer (MHCP)(2) حيث تتمتع بعض أنواع النباتات بخواص تشبه خواص الأدوية تساعد على معالجة السكر في المواد الغذائية السكرية حيث تساعد على تنبيه نشاط الأنسولين الذي يعني أن الجسم يمكنه أن يعالج السكر بفعالية اكبر ولذلك تكون حاجته للأنسولين اقل حيث أن نبات القرفة يساعد على زيادة ايض الكلوكوز ونقله عبر الخلايا كما يساعد على تخليق الكلايكوجين و يساعد على تنشيط مستقبلات خلايا بيتا β- cell في البنكرياس وإعادة تنظيمها لإفراز هرمون الأنسولين الذي يعمل على تنظيم مستوى السكر في الدم (4).

المواد وطرائق العمل

تحضير المستخلص النباتي الخام :- تم تحضير المستخلص الخام لنبات القرفة وفقا (5) .

المستخلص الكحولي الايثانولي :- وزن 50غم من مسحوق العينة النباتية الجاف ووضعت في الكشتبان (Thambel) ثم وضع في جهاز السكسوليت (Soxhlet) بعد آن أضيف إليه 250 مل من الكحول الايثانولي المطلق (95%) وترك لمدة ثمان ساعات ثم رشح بورق الترشيح وركز المستخلص بجهاز المبخر الدوار الى حين الحصول على سائل كثيف تم حفظه في عبوات زجاجية معقمة بدرجة (-4 م) الى حين الاستعمال .

طريقة ومدة التجريع :- أعطيت الجرعة عن طريق الفم يوميا بأستخدام الماصة الدقيقة Micro pipetteبجرعة (200 mg/k) من وزن الجسم ولمدة 30 يوما . (6).

استحداث مرضى السكر :- تم استحداث المرض عن الطريق الحقن بواسطة مادة الالوكزان Alloxan monohydrated (5% w/v) مذابة في المحلول الفسيولوجي بجرعة (150mg/kg) من وزن الجسم في حجم (0.1ml) . (6) .

الحقن بعقار الأنسولين :- تم الحقن بعقار الأنسولين بجرعة (0.02 unit/mg/kg) من وزن الجسم .(6).

جمع النماذج لقياس مستوى سكر الدم :- خدرت الحيوانات بواساطة الايثر وتم سحب الدم من القلب مباشرة ووضع الدم في أنابيب ابندروف Eppendrof tube ثم في جهاز الطرد المركزي لمدة (15) دقيقة لفصل مصل الدم ثم حفظ الى حين استخدامه لغرض قياس سكر الدم .

التحليل الإحصائي :- تم تحليل البيانات بأستخدام البرنامج التحليل الجاهز (SPSS). وتم اختبار المتوسطات وفق تحليل ANOVA (اختبار F) ومقارنة الفروق المعنوية بين المتوسطات المدروسة باستعمال اختبار Duncan متعدد الحدود على مستوى احتمالية ($P<0.05$) . (7) .

النتائج والمناقشة

اثبت نتائج الدراسة حصول انخفاض معنوي $p < 0.05$ في مستوى سكر الدم عند الفئران المجرعة بالمستخلص الكحولي الايثانولي الخام لنبات القرفة مقارنة مع مجموعة السيطرة ومجموعة الأنسولين كما هو موضح في جدول رقم (1) .

Table1:-Serum glucose level in control, alloxan diabetic mice, *Cinnamomum* and insulin group

Group	Glucose mg/dl (mean±se)
Control	A163.20 ±9.05
Treated with alloxan	A238.80±25.09
Treated with of *Cinnamomum zeylancium* extract 200mg/kg for 30days after alloxan treatment	B110.16±3.04
Treated with insulin	A153.13±8.07

Difference A,B are significant ($p< 0.05$) to compression rows

كما اثبت نتائج الدراسة أن نقص الأنسولين وارتفاع مستوى السكر في الدم يحدث عند أعطاء مادة alloxan monohydrate إذ تعمل هذه المادة على رفع مستوى السكر عن طريق تغير ايض الكاربوهيدرات وتثبيط خلايا بيتا وبالتالي يقلل نسبة الأنسولين في الدم. في هذه الدراسة لاحظنا إن المستخلص الكحولي لنبات القرفة له تأثير معاكس لاحتوائه على مركب فعال يسمى Methylhydroxy chalcone polymer(MHCP) يحفز إفراز الأنسولين من خلايا β- cells في البنكرياس وبنفس الوقت يبرمج نقل السكر إلى الأنسجة المحيطة (8).

كما يقلل (MHCP) من مستوى السكر في الدم وذلك بتحفيز الخلايا للتحسس لمستوى الأنسولين في الدم ويقلل من امتصاص الكاربوهيدرات في المعدة والأمعاء كما له عمل مشابه لعمل الأنسولين. اثبت الدراسة أيضا عند مقارنة المستخلص الكحولي لنبات القرفة ومجموعة السيطرة بأن القرفة أكثر فعالية من الأنسولين حتى بدون استخدام العقار .

حيث اثبت نتائج الدراسة إن هذه المركب يحفز استهلاك الأنسولين وتصنيع الكلايكوجين بمستوى مشابه لعمل الأنسولين (9) .كما يثبط تنشيط الإنزيمات المصنعة للكلايكوجين الزائد عن حاجة

الجسم الطبيعية (10) حيث تتحول كميات صغيره من الكلوكوز إلى كلايكوجين حيث يتم خزنه في الكبد أو في العضلات إن سعه الكبد والعضلات لخزن الكلايكوجين صغيره جدا فلذا نجد ما يتوفر من الكلايكوجين في إي وقت من الأوقات يستنفذ بسرعة وبعد توفير ما يحتاجه الجسم من الطاقة وبعد خزن قليل من الكلوكوز على شكل كلايكوجين فان الفائض منه يحول إلى انسجه دهنيه ويخزن على شكل دهون ويظهر إن ليس هنالك حدود لما يمكن أن يخزنه الجسم من الدهون وبالتالي فان الدارسين (القرفه) يضبط عمليه تصنيع الكلايكوجين ويقلل من عمليه تحويل الكلكوز غالى الانسجه الدهنيه التي تؤدي إلى السمنة والتي تجعل خلايا الجسم غير حساسة لما بالجسم من أنسولين وبذا تعجز عن سحب كلوكوز الدم إلى داخلها فترتفع نسبه الكلكوز في الدم مسببه البول السكري (10).

المصادر

1- ألنوري ,فاروق فاضل و الطالبني , لامعة جمال , 1981تغذية الإنسان , دار الكتب للطباعة والنشر الموصل , وزارة التعليم العالي والبحث العلمي .

2- عيسى جواد كاظم , 2003عالج نفسك بالغذاء من الكولسترول ,تصلب الشرايين وضغط الدم , السكري . الطبعة الأولى دار عالم الثقافة للنشر والتوزيع عمان – الأردن .

3- Furuse M, kumara C, Mabel RT , Takashi J. Dietary sorbs prevents & improves hyperglycemia genetically in diabetic mice .J Nutria 123:59-65.(1993).

4- Verspohl E *et al* .Ant diabetic effect of *Cinnamomum cassia* & *Cinnamomum zeylanicum* in vivo & in vitro phototherapy. 19:203-206.(2005).

5- Harborne ,J.B. photochemical methods science paper able active , Chapman &Hall pub (1973).

6- Benedict SR. The detection & estimation of glucose in blood .J.Am.Med.Assoc 57:1193-1196.(2006).

7- Duncan , Multiple range & Multiple F-test Biometrics, 11:1-42.(1955).

8- Khan A,*et al* .Cinnamon improves glucose & lipids of people with type 2 diabetes. Diabetes care. 26:3215-3218.(2009).

9- Jarvill- Taylor K,et al .A hydroxchalcone derived from cinnamon function as a mimetic for insulin in 3T3-L1 adipocytes.Jam Coll Nutr. 20 : 327- 336.(2001).

10- Mang B.Effect of cinnamon extract on plasma glucose ,HbA & serum lipids in diabetes mellitus type 2. Eur J Clin Invest . 36: 34-44.(2006).

دور الفسفور والزنك وتداخلهما في الحالة الغذائية لنبات الحنطة *Triticum aestivum L.*

حسن عبد الرزاق علي السعدي
الجامعة المستنصرية-كلية العلوم-قسم علوم الحياة

تاريخ تقديم البحث : 3 /3 /2011 تاريخ قبول البحث : 5/29 /2011

الخلاصة

أجريت التجربة في البيت الزجاجي التابع لقسم علوم الحياة، كلية العلوم، الجامعة المستنصرية لموسم 2009-2010، باستعمال أصص بلاستيكية ذات سعة 4000 غم من التربة، تضمنت التجربة دراسة تاثير ثلاثة مستويات من سماد فوسفات الامونيوم الثنائية (0 ، 150، 300 كغم / هـ) والتي رمز لها (P_2، P_1، P_0) على التوالي مع ثلاثة مستويات من سماد كبريتات الزنك (0 ، 5، 10 كغم / هـ) والتي رمز لها (Zn_2،Zn_1،Zn_0) على التوالي وتداخلهما في محتوى عناصر Ca،K،P،N في الجذور والجزء الخضري ومعدل امتصاص ونقل هذه العناصر حسب معادلة William، وقد تم تصميم التجربة حسب طريقة RCBD وبواقع ثلاثة مكررات لكل معاملة. أوضحت النتائج ان زيادة مستويات السمادين المذكورين اعلاه ادى الى زيادة معنوية في محتوى ومعدل امتصاص ونقل العناصر المدروسة. اما فيما يخص التداخل بين عاملي الدراسة فقد كان معنويا هو الاخر، وقد اعطت المعاملة (Zn_1+P_2) اعلى القيم للصفات اعلاه مقارنة بالمعاملات الاخرى، حيث اعطت محتوى عنصر N في الجذور ولكلا الفترتين (5.45، 9.44 ملغم / غم وزن جاف) على التوالي ، وفي الجزء الخضري (21.79، 63.37 ملغم / غم وزن جاف) على التوالي، ومعدل امتصاص ونقل هذا العنصر(869.67، 793.22 مايكروغرام / غرام وزن طري جذور / يوم) على التوالي.

ABSTRACT

This experiment was carried out in the green house of Biology Department, Collage of Science, AL- Mustansiriyia University, during the growing season of 2009-2010, by using plastic pots with capacity of 4000 gm of soil. The effect of three levels of di- ammonium phosphate (0, 150, 300 Kg/ha.) that symbolize as (P_0, P_1, P_2) respectively, three levels of zinc sulfate fertilizer (0, 5, 10 Kg/ha.) that symbolize as (Zn_0, Zn_1, Zn_2) respectively and their interaction on elements content (N, P, K, and Ca) in root and shoot and absorption and transport rate of element above according William equation.

The experiment designed according to RCBD method with three replicates for each treatment. Data showed that significant effect of two fertilizers mentioned above on content and absorption and transport rate of studied elements. The interaction between two factors studied was significant and treatment (P_2+ Zn_1) was superior to all other treatment, such as N content in root from two harvests(5.45, 9.44 mg/ g d.w.) respectively, in shoot (21.97,

63.37 mg/ g d.w.) respectively, and absorption and transport rate (869.67, 793.22 mg/g. fresh root/d.) respectively.

المقدمة

يعد نبات الحنطة ***Triticum aestivum* L.** المحصول الاستراتجيي الاول في العراق والعالم اذ تحتوي حبوبه على 63% كربوهيدرات و 17% بروتين و 17% ماء و 1.5% دهون و 1.5 % عناصر (1)، وان هذه النسب تتأثر بجاهزية العناصر في التربة ومحتواها في النبات، حيث وجدت زيادة معنوية في محتوى عنصري N، P لنبات الحنطة عند المستوى السماد الفوسفاتي 160 كغم /هـ(2) كذلك لوحظ زيادة معنوية اخرى في محتوى العناصر N ، P، K، Ca لنبات الذرة الصفراء عند المستوى السماد الفوسفاتي 40 كغم/ هـ(3)، بينما وجدت فروق معنوية في محتوى العناصر اعلاه لنبات العدس المسمد بمستويات من السماد DAP(0، 160، 320 كغم/ هـ)(4)، وحول الموضوع نفسه وجدت زيادة معنوية في عنصري N، K لنبات الرز المسمد بمستويات من سماد كبريتات الزنك (0، 10 ،20 كغم/ هـ)(5) ولنبات الحنطة المسمد أيضا بمستويات السماد اعلاه (0 ، 4، 8 كغم / هـ)(6)، في حين وجدت فروق معنوية في معدل امتصاص عناصر N ، K،P لنبات الشعير المرشوش بالمستويات (0 ، 15، 30 ملغم Zn / هـ).(7)

ونظرا لقلة الدراسات حول تداخل عنصري الفسفور والزنك في العراق ، لذا جاءت خطة البحث لدراسة تأثير عنصري اعلاه وتداخلهما في الحالة الغذائية لنبات الحنطة صنف اباء 97.

المواد وطرائق العمل

اجريت هذه الدراسة في البيت الزجاجي التابع لقسم علوم الحياة، كلية العلوم، الجامعة المستنصرية للعام 2009-2010، استعمل في هذه التجربة اصص بلاستيكية معبأة بـ 4000 غم من التربة لغرض دراسة تأثير نوعين من الاسمدة هما سماد فوسفات الامونيوم الثنائية (DAP) كمصدر لعنصر الفسفور (P% 22) وسماد كبريتات الزنك كمصدر للزنك (Zn% 21) وتداخلهما في الحالة الغذائية لنبات الحنطة صنف اباء 97.

لقد تم تصميم التجربة حسب تصميم القطاعات العشوائية الكاملة (RCBD) متضمنة ثلاثة مستويات من سماد فوسفات الامونيوم الثنائية (0 ، 150، 300 كغم / هـ) ورمز لها (P_2، P_1، P_0) على التوالي وثلاث مستويات من كبريتات الزنك (0 ، 5، 10 كغم / هـ) ورمز لها (Zn_2،Zn_1،Zn_0) على التوالي وبثلاث مكررات.تم إضافة الأسمدة أعلاه الى أصص التجربة قبل الزراعة،وتم زراعة بذور الصنف المدروس بتاريخ 9\12\2009 وبواقع 20 بذرة لكل اصيص وبعد مرور أسبوعين من تاريخ الزراعة خفت الى12 نبات فيكل اصيص، ورويت الأصص بالماء الى 75% من السعة

الحقلية على أساس الوزن، وبعد مرور 46 يوم من تاريخ الزراعة (الفترة الأولى) أخذت ستة نباتات وبعد 81 يوم تاريخ الزراعة (الفترة الثانية) أخذت أيضا ستة نباتات أخرى وتم فصل الجذور عن الجزء الخضري وتسجيل الوزن الطري لهما، بعد ذلك جففت في مجفف على درجة حرارة 75 م لمدة 48 ساعة وتسجيل الوزن الجاف لهما. أعقب ذلك طحنها بمطحنة كهربائية صغيرة واخذ وزن 0.2 غم من الوزن الجاف ليتم هضمه بإضافة 5 مل H_2SO_4 المركز (98%) وبمساعدة H_2O_2 لتقدير تركيز العناصر المدروسة: (N %) بواسطة جهاز مايكروكلدال microkjeldahl(8) و (P%) بواسطة جهاز الطيف الضوئي Spectrophotometer(9) و (K %) و (Ca%) بواسطة جهاز قياس اللهب Flame photometer (10) ، بعد ذلك تم حساب محتوى العناصر المدروسة استنادا الى المعادلة الآتية :-

محتوى العنصر (ملغم / غم وزن جاف)= تركيز العنصر (%) × الوزن الجاف (غم)× 10.

تم تقدير معدل الامتصاص حسب المعادلة الآتية(11) والتي طورت من قبل (12):-

$$\mathrm{Im} = \frac{Lnw_2 - Lnw_1}{T_2 - T_1} \times \frac{m_2 - m_1}{w_2 - w_1}$$

حيث يمثل:

Im: - معدل الامتصاص العنصر خلال الفترة ما بين T_1 الى T_2 (مايكروغرام / غرام وزن طري في جذور / يوم).

W_1، W_2 :- وزن الجذور الطرية (غم) عند الفترة الاولى والثانية على التوالي.

m_1 ، m_2:- محتوى العنصر (مايكروغرام/ غم وزن جاف) في الجذور والجزء الخضري عند الفترة الاولى والثانية على التوالي.

T_1 ، T_2: - عمر النبات (يوم) عند الفترة الاولى والثانية على التوالي.

اما معدل النقل فقد تم حسابه من المعادلة أعلاه:-

$$\bar{V} = \frac{Lnw_2 - Lnw_1}{T_2 - T_1} \times \frac{m_2 - m_1}{w_2 - w_1}$$

$\bar{V}$: معدل النقل العنصر خلال الفترة ما بين T_1 الى T_2 (مايكروغرام / غرام وزن طري في جذور / يوم).

m_1 ، m_2:- محتوى العنصر (مايكروغرام/ غم وزن جاف) في الجزء الخضري فقط عند الفترة الاولى والثانية على التوالي.

لقد تم تحليل النتائج حسب التصميم المذكور أعلاه وبموجب اختبار اقل فرق معنوي (LSD) عند مستوى احتمالية 5 %(13).

النتائج والمناقشة

تشير النتائج في الجدول (1) الى وجود زيادة معنوية في محتوى العناصر المدروسة في الجذور بزيادة مستويات التسميد الفوسفاتي، وقد اعطى المستوى P_2 افضل معدل لمحتوى العناصر N، P، K، Ca في الجذور للفترة الاولى (4.74، 0.99، 3.53، 3.87 ملغم / غم وزن جاف) على التوالي، وللفترة الثانية (6.63، 2.61، 4.76، 6.03 ملغم / غم وزن جاف) على التوالي.إما بالخصوص تأثيرالزنك فقد كان معنوياً في محتوى العناصر اعلاه وقد اعطى المستوى Zn_1 افضل معدل المحتوى العناصر N، P، K في الجذور للفترة الاولى (3.86، 0.73، 2.95 ملغم/ غم وزن جاف) على التوالي ، وللفترة الثانية (6.19 ، 2.09، 3.90 ملغم / غم وزن جاف) على التوالي، بينما اعطى المستوى Zn_2 افضل معدل لمحتوى Ca في الجذور ولكلا الفترتين (2.97 ، 6.39 ملغم / غم وزن جاف) على التوالي.

إما بالنسبة للتداخل فقد كان معنويا في محتوى العناصر المدروسة ولكلا الفترتين وأعطت المعاملة ($Zn+P_2$) أفضل قيمة لمحتوى العناصر المدروسة ولكلا الفترتين واختلفت معنوياً عن بقية المعاملات الأخرى باستثناء محتوى الفسفور في الفترة الأولى ومحتوى الكالسيوم في الفترة الثانية.

كذلك تشير النتائج في الجدول (1) أيضا ان زيادة مستويات الزنك(المعاملة $Zn_2+ P_2$) أثرت بشكل معنوي في انخفاض محتوى العناصر في الجذور مقارنة بالمعاملة ($Zn_1+ P_2$)، حيث كانت نسبة الانخفاض لمحتوى العناصر (N، P، K، Ca) للفترة الأولى (30.64، 35.78، 68.92 ، 6.95 %) على التوالي وللفترة الثانية (48.09 ، 45.90 ، 34.59، 42.14 %) على التوالي.

جدول -1: تأثير مستويات متزايدة من الفسفور والزنك (كغم/هـ) وتداخلهما في محتوى العناصر (N، P، K ، Ca ملغم / غم وزن جاف) في الجذور نبات الحنطة.

محتوى العناصر في الفترة الاولى					محتوى العناصر في الفترة الثانية				
P / Zn	P_0	P_1	P_2	المعدل	P_0	P_1	P_2	المعدل
	النتروجين				النتروجين			
Zn_0	2.00	2.78	5.00	3.26	2.63	4.76	5.55	4.31
Zn_1	2.39	3.73	5.45	3.86	4.09	5.04	9.55	6.19
Zn_2	2.76	3.65	3.78	3.40	5.59	7.11	4.90	5.87
المعدل	2.38	3.39	4.74		4.10	5.64	6.63	
LSD	0.18=P	0.18= Zn	0.31=ZnXP		0.15=P	0.15= Zn	0.26=ZnXP	
	الفسفور				الفسفور			
Zn_0	0.27	0.67	1.19	0.71	0.52	1.70	2.20	1.47
Zn_1	0.37	0.73	1.09	0.73	0.87	1.75	3.66	2.09

Zn_2	0.46	0.68	0.70	0.61	0.99	1.97	2.61	1.92
المعدل	0.37	069	0.99		0.90	1.97	2.61	
LSD	0.12=P	n.s.= Zn	0.20=ZnXP		0.15=P	0.15= Zn	0.26=ZnXP	
البوتاسيوم					البوتاسيوم			
Zn_0	0.50	1.17	2.23	1.30	0.99	2.91	2.89	2.26
Zn_1	0.81	1.67	6.37	2.95	1.61	3.22	6.88	3.90
Zn_2	1.63	2.25	1.98	1.95	1.94	4.74	4.50	3.73
المعدل	0.98	1.75	3.53		1.51	3.62	4.76	
LSD	0.14=P	0.14= Zn	0.24=ZnXP		0.19=P	0.19= Zn	0.26=ZnXP	
الكالسيوم					الكالسيوم			
Zn_0	1.03	1.56	3.82	2.14	1.97	4.53	4.94	3.75
Zn_1	1.73	2.67	a\	`	4.76	5.25	8.33	6.11
Zn_2	2.11	3.05	3.75	2.97	5.91	8.45	4.82	6.39
المعدل	1.62	2.43	3.87		4.21	6.01	6.03	
LSD	0.15=P	0.15= Zn	0.26=ZnXP		0.15=P	0.15= Zn	0.26=ZnXP	

كذلك سلك محتوى هذه العناصر السلوك نفسه في الجزء الخضري حيث تشير النتائج في الجدول(2) ازدياد معدل محتوى العناصر N، P، K، Ca وبشكل معنوي ولكلا الفترتين بزيادة مستويات التسميد الفوسفاتي، وقد اعطى المستوى P_2 ايضا أفضل معدل لمحتوى العناصر أعلاه وبلغ (18.34 ،4.43، 16.96، 11.91 ملغم /غم وزن جاف)للفترة الاولى على التوالي(48.95، 17.16، 50.85، 36.69، ملغم /غم وزن جاف) الثانية على التوالي، كذلك اثر التسميد بالزنك بشكل معنوي في معدل محتوى العناصر المدروسة للجزء الخضري، حيث اعطى المستوى Zn_1 أفضل معدل لمحتوى عنصر N ولكلا الفترتين (13.18، 44.86 ملغم / غم وزن جاف) على التوالي واعلى معدل لمحتوى عنصر P للفترة الثانية بلغ 13.03 ملغم / غم وزن جاف، بينما كان اعلى معدل لمحتوى عنصر P للفترة الاولى في المستوى Zn_0 بلغ 3.33 ملغم / غم وزن جاف، فيما سجل اعلى معدل لمحتوى عنصر K و Caعند المستوى Zn_2 للفترة الاولى (12.95، 9.01 ملغم/ غم وزن جاف) على التوالي، وللفترة الثانية (48.24، 34.58 ملغم / غم وزن جاف) على التوالي.

إما فيما يخص التداخل فقد كان معنوياً هو الاخر وقد تفوقت المعاملة (Zn_0+ P_2) في الفترة الاولى معنويا عن بقية المعاملات في محتوى العناصر P، K، Ca (6.16، 20.30، 14.93 ملغم / غم وزن جاف) على التوالي، بينما تفوقت المعاملة (Zn_1+P_2) في الفترة الثانية معنوياً عن بقية المعاملات وبشكل معنوي لمحتوى العناصر N، P، K، Ca(63.37، 21.59، 61.24، 44.25 ملغم / غم وزن جاف) على التوالي، كذلك يلاحظ من نتائج جدول (2) ايضا ان المستويات العالية

من الزنك (المعاملة $Zn2+ P_2$) سببت انخفاضاً معنوياً في محتوى العناصر المدروسة ولكلا الفترتين مقارنة بالمعاملتين المذكورتين انفاً.

ان ازدياد محتوى العناصر في النبات (الجذور والجزء الخضري) نتيجة لدور الذي يلعبه الفسفور في السماد في تشجيع على تكوين مجموع جذري قوي ومتشعب ومتغلغل في اعماق التربة والذي يؤدي الى زيادة الكفاء الامتصاصية ومن ثم زيادة محتوى هذه العناصر في النبات كذلك اشتراكة في بناء البروتينات والكاربوهيدرات والاحماض النووية ومركبات الطاقة والمرافقات الانزيمية وهذا ما يتطلب امتصاص العناصر من التربة(14)، ومن جهة اخرى احتواء السماد على نسبة عالية من الفسفور(22%) والنتروجين (18%) مما يساهم في زيادة جاهزيتها وامتصاصهما من قبل النبات.

اما بالنسبة للزنك الذي يلعب دوراً مهما في تنشيط العديد من الانزيمات منها Tryptophan synthetase المحفز لتكوين هرمون IAA المسؤول عن نمو النبات وانزيم DNA polymerase و Pyridine nucleotide dehydrogenase المسؤولة عن بناء الأحماض النووية و إنزيم Starch synthetase المسؤول عن تكوين النشا، كذلك يعد ضروري لعملية الفسفرة وتكوين الكلكوز والكلوروفيل وهذه العمليات تتطلب امتصاص العديد من المغذيات منها المدروسة(15).

إما بالنسبة للتداخل فقد أعطت المعاملة (Zn_1+P_2) أفضل القيم لمحتوى العناصر المدروسة ويرجع السبب ربما الى حصول اتزان بين العنصرين مما ساهم في خلق بيئة جيدة لنمو النبات وزيادة محصوله وهذا يتطلب امتصاص هذه العناصر بصورة كبيرة وسريعة، ولكن عند زيادة مستويات الزنك (المعاملة Zn_2+P_2) أدى الى انخفاض محتوى هذه العناصر الناتج ربما الى اختلال في الموازنة أعلاه واضطراب المسارات الايضية وعمل العضيات الخلوية وإبطال الفعالية الإنزيمية مما اثر بشكل سلبي في نمو النبات لاسيما عند الجذور مختزلاً بذلك المساحة الامتصاصية ومن ثم انخفاض محتوى هذه العناصر في النبات(16).

كذلك يلاحظ من النتائج جدولي (1، 2) بان هناك تفاوت بين محتوى العناصر المدروسة في الجذور والجزء الخضري يرجع ذلك الى عدة أسباب منها:- جاهزية العنصر في التربة ومدى تداخله مع بقية العناصر ودرجة تأثيره بعوامل التربة أخرى، الجزء النباتي الأكثر صلاحية للتحليل، وقت اخذ عينة (عمر النبات) والعوامل البيئة(17). هذه النتائج كانت على اتفاق مع نتائج كل من (2، 3، 5، 6) إثناء دراستهم على نباتات مختلفة.

جدول -2: تأثير مستويات متزايدة من الفسفور والزنك (كغم/هـ) وتداخلهما في محتوى العناصر (N، P، K، Ca ملغم / غم وزن جاف) في الجزء الخضري لنبات الحنطة.

محتوى العناصر في الفترة الاولى				محتوى العناصر في الفترة الثانية			
P / Zn	P_0	P_1	P_2	المعدل	P_0	P_1	P_2	المعدل
النتروجين				النتروجين				
Zn_0	5.85	10.08	21.65	12.53	12.34	32.39	43.84	29.52
Zn_1	6.67	10.89	21.97	13.18	29.04	42.16	63.37	44.86
Zn_2	7.94	17.89	11.54	12.37	43.15	48.29	39.63	43.69
المعدل	6.82	12.86	18.34		28.18	40.95	48.95	
LSD	0.18=P	0.18= Zn	0.31=ZnXP		0.15=P	0.15= Zn	0.26=ZnXP	
الفسفور				الفسفور				
Zn_0	0.91	2.91	6.16	3.33	3.03	9.44	18.27	10.25
Zn_1	1.05	3.25	4.49	2.93	5.04	12.45	21.59	13.03
Zn_2	1.05	3.76	2.63	2.48	5.51	15.98	11.62	11.04
المعدل	1.00	3.31	4.43		4.33	12.62	17.16	
LSD	0.12=P	n.s.= Zn	0.20=ZnXP		0.15=P	0.15= Zn	0.26=ZnXP	
البوتاسيوم				البوتاسيوم				
Zn_0	6.04	11.03	20.30	12.46	12.58	33.66	42.43	29.56
Zn_1	7.14	12.93	17.4	12.50	27.60	38.86	61.24	42.57
Zn_2	8.06	17.62	13.16	12.95	38.56	57.28	48.87	48.24
المعدل	7.08	13.86	16.96		26.25	43.27	50.85	
LSD	0.14=P	0.14= Zn	0.24=ZnXP		0.19=P	0.19= Zn	0.26=ZnXP	
الكالسيوم				الكالسيوم				
Zn_0	3.34	8.01	14.93	8.76	8.71	26.27	35.69	23.56
Zn_1	4.33	8.31	11.18	7.94	22.32	30.23	44.25	32.27
Zn_2	5.59	11.81	9.63	9.01	33.66	42.96	27.12	34.58
المعدل	4.42	9.38	11.91		21.56	33.15	35.69	
LSD	0.15=P	0.15= Zn	0.26=ZnXP		0.15=P	0.15= Zn	0.26=ZnXP	

يستخدم بعض الباحثين بعض المعادلات الرياضية لاجل الجمع بين المتغيرات وربطها بعامل الزمن ومنها معادلة William لحساب معدلي الامتصاص والنقل العنصر الغذائي خلال فترة معينة والتي تعتمد بالاساس على الوزن الطري باعتباره الحاله الواقعية للنبات، حيث تشير النتائج في الجدول (3) الى وجود زيادة خطية في معدلي الامتصاص والنقل للعناصر المدروسة بزيادة مستويات التسميد الفوسفاتي، فعند رفع مستوى السماد الفوسفاتي من (P_0 الى P_2) ازداد معدلي الامتصاص والنقل للعناصر N، P، K، Ca وبنسبة زيادة معنوية (26.4، 24.09 %) و(203.37، 208.22 %)

و(55.74، 56.81 %) و(20.08، 22.10 %) على التوالي، وبغض النظرعن مستويات الزنك، وهذا يتماشى مع محتوى هذه العناصر في الجذور (راجع جدول 1) وفي الجزء الخضري (راجع جدول2). تعزى هذه الزيادة ربما الى حدوث زيادة في كفاءة النبات في عملية البناء الضوئي وانتاج المواد المصنعة من كاربوهيدرات التي تعد مصدرا للطاقة المهمة في عملية الامتصاص الحيوي للعناصر لاسيما عنصر الفسفور عن طريق الجذور، اضافة الى زيادة جاهزيته في التربة مما يساعد بذلك على زيادة امتصاصه ونقله عن بقية العناصر الاخرى.

اما بالنسبة لتاثير الزنك في الصفات اعلاه، فقد كان معنوياً وقد اعطى المستوى Zn_1 اعلى معدل امتصاص ونقل عنصر N وبنسبة زيادة (88.22، 86.55 %) على التوالي واعلى معدل امتصاص ونقل عنصر P وبنسبة زيادة (46.03، 42.86 %) على التوالي مقارنة بالمستوى Zn_0 ، فيما اعطى المستوى Zn_2 اعلى معدل امتصاص ونقل عنصر K وبنسبة زيادة (99.99، 101.28 %) على التوالي، واعلى معدل امتصاص ونقل عنصر Ca وبنسبة زيادة (77.69، 68.31 %) على التوالي مقارنة بالمستوى Zn_0. هذه النتائج تتفق مع (7) اثناء دراستهم على نبات الشعير.

اما فيما يخص التداخل بين عاملي الدراسة في الصفتي اعلاه فقد كان معنوياً هو الاخر واعطت المعاملة (Zn_1+ P_2) اعلى معدل امتصاص ونقل عنصر N بلغ (869.67، 793.22 مايكرغرام / غرام وزن طري جذور / يوم) على التوالي واعلى معدل امتصاص ونقل P بلغ (376.88، 327.64 مايكروغرام/ غرام وزن طري جذور / يوم) على التوالي ، وهذا السلوك لهذين العنصرين مشابهه لمحتواهما في الجذور والجزء الخضري (راجع جدول 1 ،2)، وكذلك تماشى معدل امتصاصهما مع معدل نقلهما ومن هنا نستدل ان معدلي امتصاص ونقل داله على جاهزية العناصر في التربة ومحتواها في النبات وهذه نتيجة كانت مطابقة عند(4) اثناء دراستهم على نبات العدس.

اما بخصوص معدل امتصاص عنصر K فقد كان معنوياً، واعطت المعاملة (Zn_1+ P_2) اعلى قيمة واختلفت معنوياً عن بقية المعاملات باستثناء المعاملة (Zn_1+ P_2) بينما ظهر المعنوي بين المعاملتين المذكورتين اعلاه حيث سجلت المعاملة (Zn_1+ P_2) اعلى معدل نقل لعنصر K، وهذا يدل على ان المعاملة الاخيرة هي افضل النبات لانها اعطت اعلى معدل نقل لعنصر K الذي ينشط اكبر عدد من الانظمة الانزيمية عن بقية العناصر الاخرى وكذلك تميزه بالحركة السريعة في انسجة النبات، كما ان الدور الذي يلعبه عنصرين السابقين (N، P) في بناء البروتينات الذائبة وتراكمها يتطلب الى زيادة في معدل امتصاص ونقل K لنقل هذه المواد الى امكان خزنها وهذا ما يدعى بالامتصاص التحفيزي Syngrasim Absorption والذي يعرف على انه امتصاص عنصر معين يساعد او يحفز على امتصاص عنصر اخر(17) .

اما بخصوص عنصر Ca فقد سجلت المعاملة (Zn_2+ P_1) افضل معدل امتصاص بلغ 744.16 مايكروغرام / غرام وزن طري جذور / يوم واختلفت معنويا عن بقية المعاملات الاخرى، ولكن عند حساب معدل النقل لم تختلف هذه المعاملة التي اعطت معدل نقل مقداره 634.21 مايكروغرام / غرام وزن طري جذور/ يوم عن المعاملة (Zn_1+ P_2) التي اعطت معدل نقل مقداره 633.62 مايكروغرام/ غرام وزن طري جذور/ يوم، ومن هنا نستنتج ان المعاملة (Zn_1+ P_2) هي افضل للنبات بصورة عامة وذلك لاعطائها قيماً جيدة لمعاملات الامتصاص والنقل على وجه الخصوص وهذا يتماشى ايضا مع محتوى هذه العناصر في الجذور والجزء الخضري عند هذه المعاملة (راجع جدول 1، 2).

جدول -3 : تأثير مستويات متزايدة من الفسفور والزنك (كغم/هـ) في معدلي امتصاص ونقل العناصر N، P، K، Ca(مايكروغرام / غرام وزن طري جذور / يوم) في نبات الحنطة.

معدل امتصاص العناصر					معدل نقل العناصر				
P / Zn	P_0	P_1	P_2	المعدل	P_0	P_1	P_2	المعدل
النتروجين					النتروجين				
Zn_0	191.10	490.90	459.35	380.45	174.19	450.89	448.24	357.77
Zn_1	595.01	683.53	869.67	716.07	552.99	656.04	793.22	667.42
Zn_2	774.49	694.89	607.57	692.42	716.88	624.44	584.27	641.86
المعدل	520.20	623.11	645.53		481.35	577.12	608.58	
LSD	18.87=ZnXP 10.89= Zn 10.89=P				18.31=ZnXP 10.57= Zn 10.57=P			
الفسفور					الفسفور				
Zn_0	63.11	152.79	265.02	160.31	56.90	131.97	244.62	144.50
Zn_1	110.99	214.42	376.88	234.10	98.63	193.02	327.64	206.43
Zn_2	107.91	285.24	213.62	202.26	90.81	248.80	186.99	175.53
المعدل	94.00	217.48	285.17		82.11	191.26	253.08	
LSD	17.16=ZnXP 9.90.= Zn 9.90=P				16.89=ZnXP 9.75= Zn 9.75=P			
البوتاسيوم					البوتاسيوم				
Zn_0	188.69	492.52	459.15	380.12	175.53	457.35	445.81	359.56
Zn_1	525.55	576.53	849.36	650.48	505.77	544.01	839.59	629.79
Zn_2	627.29	858.17	795.18	760.21	620.98	807.48	742.77	723.74
المعدل	447.18	642.41	701.23		434.09	602.95	676.06	
LSD	15.69=ZnXP 9.06 = Zn 9.06 =p				12.43=ZnXP 7.18= Zn 7.18=P			
الكالسيوم					الكالسيوم				
Zn_0	169.36	425.02	441.98	345.45	144.13	369.03	419.35	310.84
Zn_1	519.61	514.01	716.01	592.21	444.71	459.88	633.62	512.74

Zn_2	648.87	744.16	448.45	613.83	571.50	634.21	363.79	523.17
المعدل	445.95	561.06	535.48		386.78	487.71	472.25	
LSD	11.16=P 11.16= Zn 19.33=ZnXP				6.93=P 6.93= Zn 12.00=ZnXP			

يلاحظ أيضا من النتائج في الجدول (3) ان زيادة مستويات الزنك اثرت سلباً في معدلي الامتصاص والنقل العناصر المدورسة لاسيما عنصر الفسفور، حيث اعطت المعاملة (Zn_2+P_2) معدل امتصاص للعناصر N، P، K، Ca (607.57، 213.62، 795.18، 448.45 مايكروغرام/ غرام وزن طري جذور / يوم) على التوالي، ومعدل نقل لعناصر اعلاه(584.27، 186.99، 742.77، 363.79 مايكروغرام/ غرام وزن طري جذور / يوم) على التوالي ويرجع السبب في ذلك الى زيادة الزنك تمنع امتصاص المغذيات نتيجة لحدوث اعاقة في طبقة البشرة او الخلايا السطحية لانسجة الخشب في الجذور او حدوث معقد غير ذائب يمنع انتقال العناصر المدروسة الى الجزء الخضري لاسيما عنصر الفسفور بشكل فوسفات الزنك المترسب في التربة او في جذور النبات، او ربما حدوث نمو غزير من قبل الزنك سيساهم في تخفيف العناصر المدروسة في النبات والتي لايظهر لها اي صور نقص العناصر في الجزء الخضري على وجه الخصوص الا انها تسبب خسارة في الحاصل وهذه الظاهرة تسمى بالجوع الخفي Hidden Hunger (18)، وهذه النتائج مطابقة لما وجدتها قبع (19) إثناء دراستها على معدل امتصاص ونقل عنصر الفسفور تحت المستويات من كبريتات الزنك (0 ، 5، 10 جزء بالمليون/ اصيص) لنبات الحنطة.

نستنتج من هذه الدراسة ان زيادة كل من الفسفور والزنك ساهمت في تحسين الحالة الغذائية لنبات الحنطة وجاء التداخل بين العنصرين اعلاه ليحسن بصورة اكبر وصولاً الى المعاملة (Zn_1+P_2) التي اعطت اعلى القيم لمحتوى ومعدلي امتصاص ونقل العناصر المدروسة ، وعليه نوصي باجراء دراسات اخرى على محاصيل حبوب غير الحنطة ضمن هذه المعاملات ودراسة ايضا لحركة العناصر الصغرى في هذا المحصول.

المصادر

1- اليونس ، عبد الحميد احمد ; محمد ، محفوظ عبد القادر وعبد الياس ، زكي. محاصيل الحبوب ، جامعة الموصل ، وزارة التعليم العالي والبحث العلمي ،55-62 ,(1987).

2- المعموري ، عبد الباقي داود سلمان . تاثير السماد الفوسفاتي ونسجة التربة ومصدر ماء الري في بعض صفات الكيميائية والخصوبية ونمو نبات الحنطة . رسالة ماجستير . كلية الزراعة ، جامعة بغداد،83-86, (2004).

3- Hussaini,M.A.; Ogunlela, V.B.; Ramalan, A.A. and Falaki, A.M. Mineral composition of dry season mize in response to varing levels of nitrogen, phosphorus and irrigation at kadawa, Nigeria. World J. Agric. Sci., 4(6): 775-780. (2008)

4- Al-Darkazli, M.K; Al-Saedy, A. J. and Al- Saadi, H, A. A. The influence of interaction between the phosphorus fertilizer and GA_3 on elements content of lentil crop, (2010). In press.

5- Ranjha, A.M.; Ahmed, I.; Qbab, M.I. and Ahmed, M. J. Rice response to applied phosphorus, zinc and farmyard manure. Inter .J. of Agric. Biol., 3(2): 197-198.(2001)

6- عباس، رياض سلمان . تاثير مستوى ومصدر وطريقة اضافة الزنك في نمو وحاصل صنفين من الحنطة . رسالة ماجستير، كلية الزراعة، جامعة بغداد ،77-83,(2005).

7- Abd –El-Hady, B.A. Effect of zinc application on growth and nutrient uptake of barley plant irrigated with saline water. J. appli. Sci.Res. 3(6): 431-436, (2007).

8- Schaffalen, A.C.; Miller, A. and Van Schouwenbury, J. C. H. Quick test for soil and plant analysis used by small lab. Neth. J. Agric. Sci., 9: 2-16, (1961).

9- Matt, K. J. Colorimetric determination of phosphorus in soil and plant materials with ascorbic acid, Soil Sci., 109:214-220, (1970).

10- Page, A. L.; Miller, R.H. and Kenney, D.R. Methods of Soil Analysis. Part (2) 2nd ASA. INC. Madison Wisconsin. USA.111-120 (1982).

11-Williams, R. F. The effect of phosphorus supply on the rates of intake of phosphorus and nitrogen upon certain aspects of phosphorus metabolism in gramineous plants. Aust. J. Sci: Res. Ser. Bl. 333-361, (1948).

12-Al-Samerri, I.K. The effect of nitrogen supply on zinc nutrition of wheat. Ph. D. Thesis Western Australia University, Australia, (1984).

13-Little, T. M. and Hills, F.J. Agricultural Experimentation Design and Analysis. John Wiley and Sons , New York ,64-71 (1978)

14- النعيمي ، سعد الله نجم عبد الله. علاقة التربة بالماء والنبات . مؤسسة دار الكتب للطباعة والنشر، جامعة الموصل ، وزارة التعليم العالي والبحث العلمي ،53-59, (1990).

15-Hopkins, W. G. and Huner, N. P. A. Introduction to plant Nutrition 3rd edition, Wiley international edition. USA. ,127-134 (2004).

16-Verma. S. K. and Verma, M. Text book of Plant Physiology, Biochemistry and Biotechnology 9th edition, India,148-159 (2008).

17-Marschner. H. Mineral Nutrition of Higher Plants. Academic press. INC. London, 49-56(1986).

18-Loneragan, J.F.; Grunes, D.L.; Welch, R. M.; Aducy, E. A.;Tengah, A; Lazar, V. A. and Cray, E. E. Response accumulation and toxicity in leaves in relation to zinc supply . Soil sci. Soc. Amer .J. 46:345-351, (1982).

19- قبع، عامرة محمد علي. التداخل بين الفسفور والزنك في نباتات الحنطة، رسالة ماجستير، كلية الزراعة والغابات، جامعة الموصل,49-58, (1988).

تأثير عديد سكرايد بعض الضروب المصلية لبكتريا *Pseudomonas aeruginosa* على خلايا السائل البريتوني للفأر الأبيض

خضر حسن علي الجوراني ورواء عبد الأمير عبد الجبار
الجامعة المستنصرية / كلية العلوم / قسم علوم الحياة

تاريخ تقديم البحث : 2011/ 4/11 تاريخ قبول البحث : 2011/ 5/29

ABSTRACT

The findings presented in this thesis indicated that there were a heterogeneous stimulation of different ***Pseudomonas aeruginosa*** serotypes for mouse peritoneal immune cells. Polysaccharide extracted from different times. Serotype O3 gave a clear increase in the percentages of Large Lymphocytes dependent on dose and time of stimulation. This serotype stimulated Foam cells starting at day one after stimulation. Serotype O6 was incapable of stimulating Foam cells. However, it stimulated Mast cells .Serotype O9 was similar to O6. On the other hand however , O11 serotype was highly efficient in its stimulating to Large Lymphocytes and Foam cells , The stimulation was dependent on dose and time. the percentages of large lymphocytes at 50 Mg/ml (41.867±4.277) compared to the control (11.867±0.611). Serotype O16 was potent in stimulation Mast cells . In the first day , the percentages at 20 Mg/ml and at 50 Mg/ml were (20.067±1.405) , (20.533±0757) respectively , compared to the control (1.400±0.346) , While in the third day the percentages of Mast cells at 50 Mg/ml Polysaccharide of this serotype was (23.267±1.102) compared to the control (1.667±0.643). The findings were discussed based on the available data concerning *Pseudomonas aeruginosa's* polysaccharide effect on peritoneal exudates cells and the importance of this bacterial moiety in the immune response and pathogenesis.

الخلاصة

أظهرت عديد سكرايد الزائفة الزنجارية ***Pseudomonas aeruginosa*** تأثيرا متباينا على الخلايا المناعية لجوف الفأر السويسري. استخلص عديد السكرايد من ضروب مصلية مختلفة للزائفة الزنجارية وتم حقنه داخل الجوف البطني للفئران بجرع مختلفة وبفترات مختلفة. فقد كان تأثير الضرب المصلي O3 واضحا في تحفيزه للخلايا اللمفاوية الكبيرة Large Lymphocytes اعتمادا على الجرعة والوقت ، وكان هذا الضرب متميزا في تحفيزه للخلايا الرغوية Foam cell أيضا ابتداءا من اليوم الثاني للتحفيز. كان الضرب O6 غير قادرا على تحفيز الخلايا الرغوية Foam cells ، إلا إنه تميز في حثه للخلايا البدينة Mast cells . أما الضرب O9 فقد كان محفزا جيدا للخلايا اللمفاوية الكبيرة ومتماثلا مع الضرب O6 في عدم تحفيزه للخلايا الرغوية ، في حين كان الضرب O11 قويا في تحفيزه للخلايا اللمفاوية الكبيرة والخلايا الرغوية ومعتمدا على الجرعة والوقت ، إذ بلغ معدل أعداد

اللمفاويات الكبيرة بجرعة 50 مايكروغرام/ مل (41.867 ±4.277) مقارنة بالسيطرة (11.867±0.611). تميز الضرب O16 في تحفيزه الكبير للخلايا البدينة فقد كانت أعدادها النسبية في اليوم الأول وبجرعة 20 مايكروغرام/ مل وبجرعة 50 مايكروغرام/ مل فقد بلغت (20.067±1.405) ، (20.533±0.757) على التوالي مقارنة بالسيطرة (1.400±0.346) ، و في اليوم الثالث بلغ تحفيز الجرعة 50 مايكروغرام/ مل من عديد سكرايد هذا الضرب (23.267±1.102) مقارنة بالسيطرة (1.667±0.643).

المقدمة

تمتلك الزائفة الزنجارية العديد من عوامل الأمراضية التي تستطيع من خلالها إصابة المضيف إذ تراوحت عوامل الضراوة من العوامل المرتبطة بجسم البكتريا كالأسواط (1)، والأهداب Pilli (2) وعديد السكرايد الدهني LipopolySaccharide (3) إلى تلك التي تفرز خارج الجسم الخلية البكتيرية مثل إنتاجها السموم الخارجية مثل السم الخارجي Exotoxin A (A) الذي ينتج من حوالي 90% من سلالات الزائفة (4) كما ينتج عدد من الأنزيمات كالأنزيمات الحالة للبروتين **Protease** والحالة للدم Haemolysin اللذان يعملان على إحداث أضرار موضعية للنسيج حيث يعملان على تحطيم الأنسجة الجسمية (5). تمتلك الزائفة الزنجارية عديد السكرايد الدهني **Lipopolysaccharide** الذي له أهمية في زيادة مقاومة هذه البكتريا (Labischinski *et al.*,1985) ، إذ يساعدها في الالتصاق بخلايا قرنية العين ولاسيما في حالة استخدام العدسات اللاصقة الملوثة ويسبب التهاب القرنية والذي يؤدي إلى فقدان الرؤيا (6). وكما إن الزائفة الزنجارية تستعمل عديد السكرايد الذي له دور في التصاقها على خلايا الرئة كما هو الحال في مرض التليف الحويصلي Cystic fibrosis (7)، إذ تعد الزائفة الزنجارية من الممرضات الانتهازية في الأشخاص المصابين بالتليف الحويصلي (8). نظرا لتنوع عديد السكرايد Polysaccharide المؤسس للأنواع المصلية Serotypes ، فقد ارتأت الدراسة تأثير تلك الجزيئات العيانية Macromolecules من أنواع البكتريا المصلية المختلفة على الخلايا المناعية لجوف الفأر الأبيض لاستنباط ما قد يحدث من تأثير تلك الجزيئات لهذه الخلايا ، وهي مرحلة من استجابة مناعية محددة المكان (الجوف البطني).

يهدف البحث دراسة تأثير عديد السكرايد على تحفيز او تثبيط الخلايا المناعية في الجوف البطني للفئران .

المواد وطرائق العمل

1-العزلات البكترية

استعملت عزلات بكتيرية من الزائفة الزنجارية مشخصة في قسم علوم الحياة / كلية العلوم/ الجامعة المستنصرية ، وثم نمطت مصليا من قبل مختبر الصحة المركزي التابع لوزارة الصحة. يبين الجدول (1) الأنواع المصلية Serotypes المستعملة ومصادرها المرضية.

جدول -1 : الأنواع المصلية Serotypes المستعملة ومصادرها المرضية

النوع المصلي	المصدر المرضي
3	التهاب مجاري بولية
6	الجروح Wounds
9	الجروح Wounds
11	الجروحWounds
16	الجروح Wounds

2- الحيوانات Animals

استعملت الفئران السويسرية البيضاء بعمر شهرين ومن كلا الجنسين والتي تم الحصول عليها من المركز العراقي لأبحاث السرطان والوراثة التابع لوزارة التعليم العالي والبحث العلمي ، وتم تربية الفئران في أقفاص خاصة Cages وتركت فترة للتأقلم ، وكان غذاءها من عليقة جاهزة تم الحصول عليها من نفس المصدر المجهز للفئران.

❖ **تحضير المحاليل والصبغات**

تم تحضير المحاليل المستخدمة في الدراسة ، وعقم المطلوب منها باستخدام الموصدة Autoclave في درجة 121مْ ولمدة 15 دقيقة وبضغط 15 باوند /انج^2.

❖ **تحضير الوسط الزرعي**

استخدم وسط الآكار المغذي لتنمية عزلات بكتريا Pseudomonas aeruginosa

حسب تعليمات الشركة المجهزة المثبتة على العبوة ، إذ تم إذابة 2.8 غم من مسحوق الآكار المغذي في 100 مل من الماء المقطر وعقم بجهاز الموصدة Autoclave .

❖ **استخلاص عديد السكرايد من بكتريا الزائفة الزنجارية:-**

تم تنمية بكتريا Pseudomonas aeruginosa

على وسط الآكار المغذي لمدة 18 ساعة بدرجة 37مْ ، ومن ثم تم حصاد النمو وذلك بإضافة 5 مل من المحلول الملحي الوظيفي وجمع العالق البكتيري في أنابيب ابندروف (1مل لكل أنبوبة) وتم استخلاص عديد السكرايد حسب طريقة (9).

❖ **تقدير كمية عديد السكرايد:-**

تم تقدير كمية عديد السكرايد بإضافة 0.5 مل من محلول الفينول تركيز 5% و 2.5 مل من حامض الكبريتيك المركز إلى 0.5 مل من محلول عديد السكرايد المراد تقدير كميته ، وتمت القراءة اللونية باستخدام جهاز المطياف الضوئي وقورنت مع المنحني القياسي وحسب طريقة (10).

❖ **محلول** Plasma

تم استخدام محلول plasma من صنف AB بتركيز 100% (الذي حصل عليه من المركز الوطني للتبرع بالدم).

❖ **اختبار تأثير عديد السكرايد على الخلايا المناعية لجوف الفأر :-**

▪ **مجاميع التجربة**

1- الاختبار

أعدت ست مجاميع من الفئران ، كل مجموعة تتكون من ثلاثة فئران ، خمس مجاميع للفحص Test ومجموعة للسيطرة Control. تم تحضير التراكيز (1،5،10،20،50) ميكروغرام / مل وحقنت كل مجموعة بتركيز معين من عديد السكرايد المخفف بالمحلول الملحي الوظيفي داخل الجوف البطني باستخدام محاقن نبيذة سعة 1 مل ، حقنت مجموعة للسيطرة داخل الجوف بواحد مل من حامض الخليك (محلول استخلاص عديد السكرايد) وباستخدام محاقن نبيذة سعة 1 مل، وتركت مجاميع الفئران السابقة يوم كامل.

❖ **حصد السائل الجوفي من الفئران المحقونة**

تم حصد السائل الجوفي وذلك بتخدير كل فأرة باستخدام الكلورفورم لفترة قصيرة ثم حقنت بواحد مل من محلول plasma من صنف AB وبعدها قتلت الفأرة بطريقة Cervical dislocation وعمل مساج لبطن الفأر لغرض نشر السائل المحقون بين أحشائه وعلى جدران الجوف البطني ثم أزيل الجلد المغطي للبطن ثم علق الفأر بطريقة تتدلى فيها البطن ، ثم ثقب الجزء المتدلي بمقص طبي وجمع السائل الجوفي في أنبوبة اختبار بلاستيكية بولي بربولنية Polypropylene tube يمثل السائل مصدر الخلايا المراد دراسة تأثير عديد السكرايد عليها.

❖ **تحضير الشرائح الزجاجية من السائل الجوفي للفأر**

تم عمل شريحة للسائل الجوفي من الفأر.جففت بسرعة ثم ثبتت بالميثانول Methanol تركيزه 98% ولمدة 5 دقائق لتصبح جاهزة للتصبيغ.

❖ تصبيغ الشرائح الزجاجية

1- تحضير صبغة كمزا Giemsa stain

تم تحضير صبغة كمزا و تحضير محلول دارئ الفوسفات Phosphate bufferحسب طريقة (11) واستعمل الاخير لتخفيف الصبغة.

2- تصبيغ الشرائح Slides Staining

صبغت الشرائح المثبتة بالميثانول بتمريرها بمحلول صبغة Giemsa stain المخفف لمدة 20 دقيقة وذلك باستخدام علب التصبيغ Staining jars وجففت حافة الشريحة بورق الترشيح لإزالة الصبغة الزائدة بعد الصبغ ثم مررت الشريحة بمحلول دارئ الفوسفات ثلاث مرات متتالية وبسرعة حتى تزال الصبغة الزائدة.

تركت الشرائح شاقوليا لتجف ثم فحصت باستخدام المجهر الضوئي. تم تعداد 500 خلية وصنفت الخلايا إلى وحيدات النوى Monocytes ، اللمفاويات الكبيرة Large lymphocytes ، اللمفاويات الحبيبية الكبيرة Large Granular Lymphocyte (LGL)، اللمفاويات الصغيرة Small Lymphocytes، الخلايا البدينةMast cell ، الخلايا الرغوية Foam cells ، العدلات Neutrophiles.

ثم استخراج النسب المئوية للعد التفريقي أعلاه واستخراج معدل العد التفريقي من الفئران الثلاثة للمجموعة الواحدة وكذلك الانحراف القياسي.

استخرجت نسبة الخلايا وحيدات النوى إلى الخلايا الرغوية بتقسيم أعدادها على أعداد الخلايا الرغوية.

❖ التحليل الإحصائي Statistical Analysis

تم تحليل نتائج العد التفريقي لخلايا الجوف البطني للمعاملة ومقارنتها بالسيطرة باستخدام فحص ANOVA tes و فحص Least Square Differences (LSD) (12).

النتائج والمناقشة

استخلاص عديد السكرايد للضروب المختلفة

يظهر الجدول رقم (2) استخلاص عديد السكرايد للضروب المختلفة:

جدول-2: كميات عديد السكرايد المستخلص من الضروب المصلية المختلفة.

الضرب المصلي	عديد السكرايد مايكروغرام /مل
3	330
6	420
9	400
11	285
16	500

❖ تأثير عديد السكرايد الضروب المصلية

تضمنت الدراسة تأثير عديد السكرايد الضروب المصلية Serotypes للزائفة الزنجارية على الخلايا المناعية للجوف البطني للفأر الأبيض واستعملت جرع مختلفة من عديد السكرايد وبواقع تأثير زمني من يوم الى ثلاثة ايام. ولكن تم عرض نتائج الضرب المصلي O3 في هذا البحث .

❖ العزلة المصلية O3

بينت نتائج تأثير عديد سكرايد الزائفة الزنجارية للضرب المصلي O3 إن هناك تأثيرا واضحا على زيادة طفيفة لأعداد معظم الخلايا مقارنة بالسيطرة. فقد كانت الأعداد النسبية لوحيدات النوى تزداد بزيادة الجرع فقد بلغت أعدادها بجرعة 1 مايكروغرام/ مل (1.533 ± 0.416) وبجرعة5 مايكروغرام/مل بلغت (2.533± 0.611) وبجرعة 10مايكروغرام/ مل (2.733 ±0.503) وبجرعة20 مايكروغرام/ مل (3.80± 1.562) وبجرعة 50 مايكروغرام/ مل (3.80 ±1.217) مقارنة بالسيطرة (1.467 ±0.306) ، واظهر التحليل الإحصائي ارتفاعا معنويا عاليا بجرعة 20 مايكروغرام /مل وبجرعة 50 فقد بلغت فيه الاحتمالية Probability إلى 0.008 باستخدام اختبار L.S.D.(F test) الإحصائي المرفق بجدول (3).

أما الخلايا اللمفاوية الكبيرة فقد ازدادت أعدادها النسبية أيضا بزيادة الجرع إذ بلغت أعدادها وبجرعة 50 مايكروغرام/مل (11.40± 1.833) مقارنة بالسيطرة (10.533± 0.416)، وأشارت النتائج في الجدول (3) إلى زيادة إعداد اللمفاويات الكبيرة زيادة ليست معنوية لجميع الجرع ، وباستخدام اختبار L.S.D.(F test) الإحصائي.

كما إن الخلايا اللمفاوية الحبيبية الكبيرة تزداد أعدادها النسبية بزيادة الجرع أيضا، إذ كانت الزيادة معنوية عالية كما موضح في الجدول (3).

أظهرت النتائج في الجدول (3) ارتفاعا مضطردا لأعداد الخلايا البدينة بزيادة الجرع إذ بلغت بجرعة 50 مايكروغرام/ مل (3.533 ±1.007) مقارنة بالسيطرة (1.40± 0.346)، ومن التحليل الإحصائي تبين ارتفاعا معنويا عاليا بجرعة (50،20،10) مايكروغرام/مل إذ بلغت الاحتمالية Probabilityإلى 0.045 و0.038 و0.021 على التوالي باستخدام الاختبار السابق نفسه وصورة رقم (1) تبين ازالة تحبب الخلية البدينة المحفزة بعديد السكرايد. لم يبين اليوم الأول ظهورا للخلايا الرغوية Foam cells، وكانت العدلات مشابهة تقريبا للسيطرة كما في الجدول (3).

وفي اليوم الثاني كانت النتائج متميزة تؤشر ازديادا في معدل أعداد وحيدات النوى إذ بلغت بجرعة 1 مايكروغرام/ مل (2.133±0.231) وبجرعة 5 مايكروغرام/ مل (2.800±0.872) وبجرعة 10 مايكروغرام/ مل (3.00±0.529) وبجرعة 20 مايكروغرام/ مل (4.133±0.611) وبجرعة 50 مايكروغرام/ مل (4.667 ± 1.332) مقارنة بالسيطرة (1.733± 0.416).

أظهرت النتائج ازديادا معنويا عاليا في الأعداد النسبية للمفاويات الحبيبية الكبيرة كما في صورة رقم(3) إذ بلغ عددها بجرعة 50 مايكروغرام/ مل (5.533± 0.945) مقارنة بالسيطرة ، إذ كانت (1.867±0.231) وبلغت الاحتمالية Probability لنفس الجرعة إلى 0.00 باستخدام اختبار (F test) L.S.D. الإحصائي المرفق بالجدول (4).

في حين إن اللمفاويات الصغيرة فقد أظهرت انخفاضا بزيادة الجرع إذ بلغ معدل أعدادها النسبية بجرعة1 مايكروغرام/مل (83.000±1.058) وبجرعة 5 مايكروغرام/مل (78.600±1.217) وبجرعة 10 مايكروغرام/ مل (75.000±0.529) وبجرعة 20 مايكروغرام/ مل (71.267±2.386) وبجرعة 50 مايكروغرام/ مل (69.800±1.587) مقارنة بالسيطرة (82.933±0.702)، وأشارت النتائج في الجدول (4) نقصان معنوي عالي في أعداد اللمفاويات الصغيرة إذ بلغت فيه Probability إلى 0.00 باستخدام الاختبار السابق نفسه.

وبالنسبة للعدلات إذ ازدادت أعدادها النسبية زيادة معنوية عالية بزيادة الجرع كما نلاحظ بالجدول(4).

تميزت نتائج اليوم الثاني بظهور الخلايا الرغوية Foam Cells كما في صورة رقم (3) إذ ازدادت أعدادها النسبية بزيادة الجرع ، إذ بلغ عددها بجرعة 50 مايكروغرام/ مل (3.333 ±0.643) مقارنة بالسيطرة إذ لم يتم ظهور تلك الخلايا فيها، وفي اليوم الثالث بينت النتائج ازدياد معنويا في الأعداد النسبية لوحيدات النوى فقد بلغت أعدادها النسبية بجرعة 50 مايكروغرام/ مل (6.600± 0.721) مقارنة بالسيطرة (1.800±0.400).

أشارت النتائج إلى ازدياد اللمفاويات الكبيرة بالجرع (20 ، 50) مايكروغرام/ مل إذ بلغت أعدادها النسبية (12.000±2.946) ، (16.53±3.921) على التوالي ، مقارنة بالسيطرة (11.867±0.611)، ومن التحليل الإحصائي تبين ازدياد معنوي عالي لأعدادها النسبية إذ بلغت قيمة الاحتمالية Probability إلى 0.028 عند المعاملة بجرعة 50 مايكروغرام/مل كما في الجدول (5).

وبالنسبة للمفاويات الحبيبية الكبيرة إذ تزداد بزيادة الجرع ، إذ بلغ عددها بجرعة 1 مايكروغرام/ مل (3.333 ±0.611) وبجرعة 5 مايكروغرام/ مل (4.733±0.503) في حين إن اللمفاويات الصغيرة انخفضت أعدادها النسبية انخفاضا معنويا عاليا، إذ بلغت قيمة الاحتمالية إلى 0.00 عند المعاملة بالجرع (10،20،50) مايكروغرام/ مل باستخدام اختبار L.S.D. (F test) الإحصائي المرفق بالجدول (5).

بينت النتائج ازديادا معنويا عاليا للأعداد النسبية للخلايا البدينة إذ بلغت إعدادها بجرعة 20 مايكروغرام/ مل (5.600±0.721) وبجرعة 50 مايكروغرام/ مل (5.667±0.757) مقارنة بالسيطرة (1.667 ±0.643)، وباستخدام اختبار L.S.D.(F test) كانت قيمة الاحتمالية إلى 0.00 كما في الجدول (5).

وبالنسبة للعدلات إذ ازدادت إعدادها بزيادة الجرع ، وكانت الزيادة معنوية عالية إذ بلغت قيمة الاحتمالية بجرعة (20،50) مايكروغرام/ مل إلى 0.00 باستخدام نفس الاختبار السابق المرفق بالجدول (5).

تستنتج الدراسة الحالية مايلي:-

1- ان الضروب المصلية للزائفة الزنجارية لها قدرة مختلفة على تحفيزها للخلايا المناعية.

2- يعتمد هذا التغاير في التحفيز على الضرب المصلي Serotype الذي يتأسس على تركيب عديد السكرايد الذي استعمل في هذه الدراسة.

3- لنوع عديد السكرايد للضرب المصلي المعني دورا في الاستجابة المناعية.

4- تحفز بعض الضروب المصلية دون غيرها استجابة مناعية ترتبط بظهور الخلايا الرغوية Foam cells المهمة في تصلب الشرايين.

5- هنالك تباين في ظهور الخلايا البدينة Mast cells المحفزة ببعض الضروب بقوة مما يؤشر دور بعض الضروب في انشاء الحساسية Allergy.

جدول -3: توزيع خلايا الجوف البطني (الاعداد التفريقية) بعد مرور يوم واحد على حقن الفئران داخل الجوف البطني بجرعات مختلفة من عديد السكرايد المستخلص من عزلةO3 .

نوع الخلية	المعاملة	الجرعة مايكروغرام/مل	العدد	المتوسط الحسابي	الانحراف المعياري	الخطأ المعياري	المقارنة المعنوية (C.S) P-value	
							LSD (F-test)	ANOVA (F-test)
وحيدة النواة	السيطره	---	3	1.467	0.306	0.176	--	0.023 S
	الفحص	1	3	1.533	0.416	0.240	0.929	
		5	3	2.533	0.611	0.353	0.170	
		10	3	2.733	0.503	0.291	0.109	
		20	3	3.80	1.562	0.902	0.008	
		50	3	3.80	1.217	0.702	0.008	
	Total		18					
اللمفاوية الكبيرة	السيطره	---	3	10.533	0.416	0.240	--	0.719 NS
	الفحص	1	3	8.533	1.474	0.851	0.381	
		5	3	8.533	3.177	1.834	0.381	
		10	3	9.067	4.277	2.469	0.518	
		20	3	10.20	3.079	1.778	0.882	
		50	3	11.40	1.833	1.058	0.701	
	Total		18					
	السيطره	---	3	1.667	0.416	0.240	--	
		1	3	1.533	0.611	0.353	0.862	

0.001 HS	0.040	0.416	0.721	3.40	3	5	الفحص	اللمفاوية الحبيبية الكبيرة
	0.001	0.721	1.249	5.20	3	10		
	0.002	0.406	0.702	4.733	3	20		
	0.001	0.808	1.40	4.80	3	50		
					18	Total		
0.006 HS	--	0.240	0.416	83.267	3	---	السيطره	اللمفاوية الصغيرة
	0.590	1.286	2.227	84.60	3	1	الفحص	
	0.393	2.198	3.807	81.133	3	5		
	0.049	2.873	4.976	78.0	3	10		
	0.011	1.239	2.145	76.047	3	20		
	0.003	1.048	1.815	74.267	3	50		
					18	Total		
0.171 NS	--	0.200	0.346	1.40	3	---	السيطره	الخلية البدينة
	0.237	0.529	0.917	2.40	3	1	الفحص	
	0.093	0.371	0.643	2.867	3	5		
	0.045	0.808	1.40	3.20	3	10		
	0.038	0.696	1.206	3.267	3	20		
	0.021	0.581	1.007	3.533	3	50		
					18	Total		
0.586 NS	--	0.176	0.306	1.667	3	---	السيطره	العدلات
	0.578	0.231	0.40	1.40	3	1	الفحص	
	0.780	0.240	0.416	1.533	3	5		
	0.780	0.306	0.529	1.80	3	10		
	0.551	0.495	0.857	1.953	3	20		
	0.276	0.416	0.721	2.20	3	50		
					18	Total		

N.S.:None Significant:P>0.05, S: Significant:P<0.05,H.S.:Highly Significant:P<0.01

جدول -4 : توزيع خلايا الجوف البطني (الاعداد التفريقية) بعد مرور يومين على حقن الفئران داخل الجوف البطني بجرعات مختلفة من عديد السكرايد المستخلص من عزلةO3 .

المقارنة المعنوية (C.S) P-value		الخطأ المعياري	الانحراف المعياري	المتوسط الحسابي	العدد	الجرعة مايكروغرام/مل	المعاملة	نوع الخلية
ANOVA (F-test)	LSD (F-test)							
0.003 HS	--	0.240	0.416	1.733	3	---	السيطره	وحيدة النواة
	0.528	0.133	0.231	2.133	3	1	الفحص	
	0.109	0.503	0.872	2.800	3	5		
	0.062	0.306	0.529	3.000	3	10		
	0.002	0.353	0.611	4.133	3	20		
	0.00	0.769	1.332	4.667	3	50		
					18	Total		
	--	0.400	0.693	10.600	3	---	السيطره	

تأثير عديد سكرايد بعض الضروب المصلية لبكتريا *Pseudomonas aeruginosa* على خلايا السائل البريتوني للفأر الأبيض

خضر ورواء

اللمفاوية الكبيرة	الفحص	1	3	7.333	0.611	0.353	0.002	0.005 HS
		5	3	7.667	0.757	0.437	0.004	
		10	3	9.400	0.721	0.416	0.169	
		20	3	10.333	1.553	0.897	0.751	
		50	3	10.133	1.301	0.751	0.580	
	Total		18					
اللمفاوية الحبيبية الكبيرة	السيطره	---	3	1.867	0.231	0.133	--	0.00 HS
	الفحص	1	3	2.533	0.306	0.176	0.101	
		5	3	3.400	0.346	0.200	0.002	
		10	3	3.933	0.306	0.176	0.00	
		20	3	4.733	0.115	0.066	0.00	
		50	3	5.533	0.945	0.546	0.00	
	Total		18					
اللمفاوية الصغيرة	السيطره	---	3	82.933	0.702	0.406	--	0.00 HS
	الفحص	1	3	83.000	1.058	0.611	0.954	
		5	3	78.600	1.217	0.702	0.002	
		10	3	75.000	0.529	0.306	0.00	
		20	3	71.267	2.386	1.378	0.00	
		50	3	69.800	1.587	0.917	0.00	
	Total		18					
الخلية البدينة	السيطره	---	3	1.467	0.503	0.291	--	0.003 HS
	الفحص	1	3	1.933	0.306	0.176	0.244	
		5	3	2.400	0.529	0.306	0.031	
		10	3	3.067	0.462	0.267	0.001	
		20	3	3.067	0.643	0.371	0.001	
		50	3	3.133	0.231	0.133	0.001	
	Total		18					
العدلات	السيطره	---	3	1.400	0.346	0.200	--	0.001 HS
	الفحص	1	3	1.467	0.306	0.176	0.872	
		5	3	2.600	0.529	0.306	0.012	
		10	3	2.800	0.800	0.462	0.005	
		20	3	3.267	0.416	0.240	0.001	
		50	3	3.400	0.400	0.231	0.00	
	Total		18					

جدول -5 : توزيع خلايا الجوف البطني (الاعداد التفريقية) بعد مرور ثلاثة ايام على حقن الفئران داخل الجوف البطني بجرعات مختلفة من عديد السكرايد المستخلص من عزلةO3 .

نوع الخلية	المعاملة	الجرعة مايكروغرام/مل	العدد	المتوسط الحسابي	الانحراف المعياري	الخطأ المعياري	المقارنة المعنوية (C.S) P-value	
							LSD (F-test)	ANOVA (F-test)

	--	0.231	0.400	1.800	3	---	السيطره	وحيدة النواة
	0.051	0.416	0.721	3.000	3	1	الفحص	
	0.00	0.353	0.611	4.667	3	5		
0.00 HS	0.00	0.353	0.611	5.333	3	10		
	0.00	0.521	0.902	5.467	3	20		
	0.00	0.416	0.721	6.600	3	50		
					18	Total		
	--	0.353	0.611	11.867	3	---	السيطره	اللمفاوية الكبيرة
	0.038	0.570	0.987	7.533	3	1	الفحص	
	0.053	1.168	2.023	7.867	3	5		
0.004 HS	0.289	0.757	1.311	9.800	3	10		
	0.944	1.701	2.946	12.000	3	20		
	0.028	2.264	3.921	16.533	3	50		
					18	Total		
	--	0.176	0.306	1.933	3	---	السيطره	اللمفاوية الحبيبية الكبيرة
	0.003	0.353	0.611	3.333	3	1	الفحص	
	0.00	0.291	0.503	4.733	3	5		
0.00 HS	0.00	0.353	0.611	6.067	3	10		
	0.00	0.176	0.306	6.533	3	20		
	0.00	0.133	0.231	6.867	3	50		
					18	Total		
	--	0.291	0.503	80.933	3	---	السيطره	اللمفاوية الصغيرة
	0.270	0.835	1.447	78.867	3	1	الفحص	
	0.001	0.533	0.924	73.067	3	5		
0.00 HS	0.00	0.982	1.701	67.933	3	10		
	0.00	2.310	4.002	63.533	3	20		
	0.00	1.489	2.579	58.067	3	50		
					18	Total		
	--	0.371	0.643	1.667	3	---	السيطره	الخلية البدينة
	0.004	0.306	0.529	3.400	3	1	الفحص	
	0.00	0.115	0.200	4.000	3	5		
0.00 HS	0.00	0.291	0.503	4.667	3	10		
	0.00	0.416	0.721	5.600	3	20		
	0.00	0.437	0.757	5.667	3	50		
					18	Total		
	--	0.231	0.400	1.80	3	---	السيطره	العدلات
	0.337	0.133	0.231	2.067	3	1	الفحص	
	0.002	0.176	0.306	2.867	3	5		
0.00 HS	0.001	0.115	0.200	3.000	3	10		
	0.00	0.115	0.200	3.200	3	20		

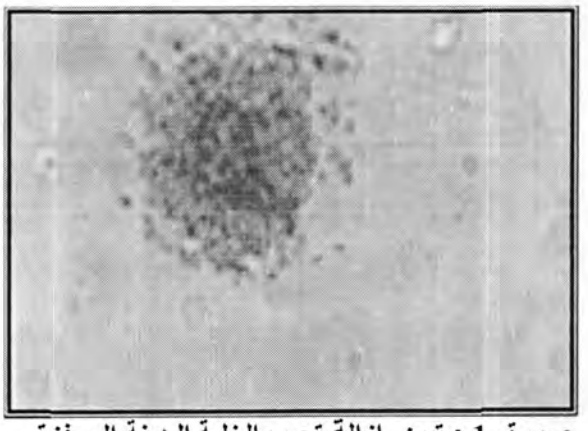

صورة -1 : تبين إزالة تحبب الخلية البدينة المحفزة بتأثير عديد سكرايد الضرب المصلي بجرعة 50 مايكروغرام / مل

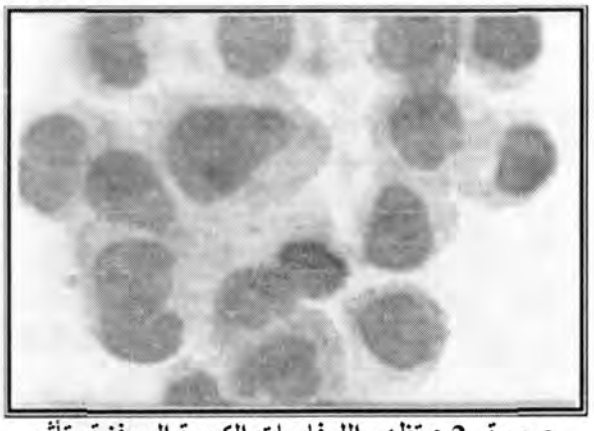

صورة -2 : تظهر اللمفاويات الكبيرة المحفزة بتأثير عديد سكرايد الضرب المصلي بجرعة 50 مايكروغرام/ مل

صورة -3 : الخلايا الرغوية المحفزة بتأثير عديد سكرايد الضرب المصلي بجرعة 50 مايكروغرام/ مل

المصادر

1. Holt, J. G. ; Krieg, N. R. ; Sneath ,P. H. ;Staley, J .T.and Williams, S.TBergey's Manual of Determination Bacteriology.9th ed. Willimas and Wilkins.93-94, (1994).

2. Cotter ,C.S.; Avidano,M.A.;Stringer,S,P. and Schultz, G.S. Inhibition of protease in Pseudomonas otitis media in chinchillas. Otolaryngology Head and Neck Surgery. 115: 42-51, (1996).

3. Labi,H. ;Barnikel, G.;Bradaczek, H. ;Nam A. D.; Reitschell, E.T. and Gresbrecht, D. High state of order of isolated bacterial lipopolysccharide

and its possible Contribution to the Permeation Barrier Properrtyb of the Outer Membranes.J Bacterial.162:9-20, (1985).

4. Lesieur, j.C. Vecesey-Semjen, B.;Abrami, L.; Fivaz, M. and Gisou, F. Membrane insertion:the strategies of toxins (Review). Mol. Mem.Biol.,14:45-64, (1997).

5. Doring, G.; Obrnessed, H.; Botzenhart, K.; Flemming, B.; Hoiby, N. and Hofman, H.Proteases of *Pseudomonas aeruginosa* in patient with cystic fibrosis.J.Infect.Dis.174(4): 44-50, (1983).

6. Robertson, D.M.; Petroll, W.M.; Jester, J.V. and Cavanagh, H.D. Current concepts: Contact lens related Pseudomonas keratitis. Cont .Lens. Anterior Eye,2, (2006).

7. Nivens, D.E; Ohman, D.E; Willimas, J. and Franklin, M.J.Role of Alginate and its O acetylation information of *Pseudomonas aeruginosa* microcolonies and biofilms. J.Bacteriol; 183: 47-57, (2007).

8. Berlutti,F.;Morea,C.;Battistoni,A.,Sarli,S.;Cipriani,P.;Superti,F.; Ammendolia, M.G.and Valenti,P.Iron availability influence aggregation ,biofilm,adhesion and invasion of *Pseudomonas aeruginosa* and *Burkholderi cenocepacia*.J.Immunopathol.Pharmacol;18 : 61-70, (2005).

9. Horton, D.; Riley, D. A ; Samveth , S. and Schweitzer, M.G. Lipopolysacchride antigens of *Pseudomonas aeruginosa* :In "Bacterial lipopolysacchride antigens of *Pseudomonas aeruginosa*: In' Bactrial lipopolysacchrides"Andersen, L.and.Eds.American chemical society. Washington,21, (1983).

10. Dubios ,M.;Gilles,A.; Hamilton,J.H.;Roberts, B.A. and Smith, F. Colourimtric method of determination of sugar and related compounds. Anal. Chem .,28:35, (1956).

11. Bancroft, J. and Stevens, A. Theory and practice of histological techniques 2nd .churchill livingstone,London, 624:635, (1982).

12. Sorlie , D.E. Medical biostatistics and epidemiology : Examination and board review Firsted. Nor walk , Connecticut , Appleton and Lange : 47-88, (1995).

تلازم بعض مجاميع الدم البشرية وأضدادها مع مرض الذبحة الصدرية غير المستقرة

خضرحسن الجوراني وعلي مرتضى حسن
قسم علوم الحياة – كلية العلوم – الجامعة المستنصرية

تاريخ تقديم البحث : 2011/ 4/10 تاريخ قبول البحث : 2011/ 5/29

ABSTRACT

A total of 150 unstable angina patients and 100 age and gender comparable healthy controls were investigated. The study dealt with finding the frequency distribution of ABO, Lewis and MNS blood groups .The findings indicated that there was an increase in the frequency of B blood groups (patients 33.3% versus 29% in control, P<0.05). On the other hand however, there was no significant difference in the patients compared to control. O blood group frequency gave a decreased frequency in patients compared to controls,(24.7% in patients vs. 31% in healthy controls , P<0.05).A noticeable increase in the frequency of Le(a-b-) was seen in patients (30.7% in patients vs. 18% in controls, P<0.05), However, Le(a-b+) demonstrated a relatively decreased frequency in patients compared to controls, While Le(a+b-) showed no differences in frequency, In MNS blood groups, NN frequency gave a statistically significant difference ,with a frequency of 19.2% in patients vs 11% in healthy controls .The aim of the study is to find a relation between unstable angina and some human blood groups .

الخلاصة

تم دراسة 150 أنموذجا لمرضى الذبحة الصدرية Unstable angina و 100 أنموذج للأصحاء ظاهريا والمضاهين الجنس والأعمار مع المرضى , واهتمت الدراسة في إيجاد ترددات مجاميع الدم ABO و Lewis ومجموعة الدم MNS, فقد سجلت النتائج إن تردد المجموعة B كان 33.3% في المرضى, و 29% في الأصحاء, و كان التحليل الإحصائي معنوي (P< 0.05, أما تردد المجموعة A فلم يعط فرقا بين المرضى والأصحاء, في حين قل تردد المجموعة O في المرضى عنه في الأصحاء, فقد بلغ في المرضى24.7% , و 31% في الأصحاء وكان التحليل الإحصائي معنوي (P< 0.05), في حين كان تردد مجموعة الدم AB في المرضى 12.0 % وفي الأصحاء بلغ 10% أيضا كان التحليل الإحصائي معنوي (P< 0.05) و برز دور المجموعة Le ($a^- b^-$) في القابلية للإصابة بالمرض , وقد سجل هذا النمط ترددا بلغ 30.7% في المرضى و 18% في الأصحاء, وكان التحليل الإحصائي مشيرا إلى معنوية هذا الفرق (P< 0.05, أما المجموعة Le(a+ b-) فقد سجلت ترددا بلغ في المرضى 15.5% وفي الأصحاء

26% والمجموعة Le(a-b+) كان ترددها 55% في المرضى و 18% في الأصحاء وكانت نتائج التحليل الإحصائي معنوية ($P< 0.05$). إن مجموعة الدم MNS أعطت مؤشرا إلى دورها في المرض و خصوصا دور المجموعة NN إذ بلغ ترددها 19.2% للمرضى مقارنة بتردد 11% للأصحاء وكانت نتائج التحليل الإحصائي معنوية ($P< 0.05$). كانت الأنماط B , AB , Le(a$^-$b$^-$) والنمط الوراثي NN أكثر خطورة نسبية للمرض .الهدف من هذه الدراسة إيجاد علاقة بين الذبحة الصدرية الغير مستقرة وبعض مجاميع الدم , وقد نوقشت النتائج في ضوء المعلومات العلمية المتوافرة للموضوع.

المقدمة

اكتشفت مجاميع الدم الثلاثة A,B,O من قبل العالم النمساوي Landsteiner في عام 1901 فقد قام بأخذ عينات من مصل الدم وكريات الدم الحمر له ولبعض زملائه, وتوصل بنهاية الأمر إلى اكتشاف المجاميع الدموية ABO , ثم تم اكتشاف الصنف AB من قبل العالمين Sturle و Von Descatello في سنة 1902 (1) . ترتبط مستضدات الدم ABO مع العديد من الأمراض كسرطان المعدة, إذ توجد علاقة بين مجموعة الدم A مع الإصابة بسرطان المعدة Stomach Cancer (2) , في حين توجد علاقة بين مجموعة الدم B مع الإصابة بسرطان البنكرياس Pancreatic Cancer مقارنة مع الأصحاء (3).وقد تبين من الدراسات إن هنالك علاقة بين مجموعة الدم O والإصابة بسرطان المثانة Bladder Cancer (4) , وأشار الباحث Guleria الى العلاقة بين مجموعة الدم B والإصابة بسرطان المرئ Esophageal Cancer (5).

إن مجموعة دم لويس تعد مجموعة مميزة, إذ إنها المجموعة الوحيدة التي لا تنتج من قبل كريات الدم الحمر , وإنما تصنع المستضدات من قبل الخلايا النسيجية, وتفرز بعدها إلى سوائل الجسم وهي بذلك توجد مبدئيا في البلازما تنتقل لتلتصق على سطح كريات الدم الحمر (6).إن المسؤول عن هذه المستضدات هو مورث لويس Le, وهو لا يشفر لها مباشرة وإنما يشفر لإنتاج إنزيم متخصص ناقل لسكر الفيوكوز Fucosyltranseferase حيث يقوم بإضافة سكر الفيوكوز إلى المادة الأساس (7) .يمتلك حوالي 90% من الإفراد مورث لويس Le الذي يوجد بتركيبين وراثيين هما LeLe و Lele (8) . يشفر مورث Le لصناعة إنزيم ناقل للفيوكوز , والذي يقوم بنقل السكر من (GTP–Fuc) Guanosine-Triphosphate Fucose الى سلسلة السكر النوع 1 الموجودة في سلسلة البروتين المسكر أو الدهون السكرية Glycolipids فيتكون المستضد Le^a (9) .توجد مستضدات لويس في سوائل الجسم النسيجية كالحليب, واللعاب, والغدد العرقية

تحت الابطية وسائل الكلية, وسائل المعدة, وتكون هذه المستضدات بشكل بروتين سكري Glycoprotien في الأماكن انفة الذكر, في حين أنها تكون دهون مسكرة Glycolipid على سطح الكرية الحمراء (10) .يتداخل نوعان من الإنزيمات الناقلة لسكر الفيوكوز Fucose في عملية تصنيع مستضدات لويس ويشفر لهذين الأنزيمين مورث Se أو FUT 2, ومورث Le أو FUT 3, فالمورث Se يشفر لإنزيم ناقل لسكر الفيوكوز من واهبه (Fucose (GTP – Fuc Guanosine – Triphosphate إلى المادة الأساس مكونا الآصرة α1-2 , والمورث الأخر Le أو FUT3 يشفر لإنزيم ناقل لسكر الفيوكوز بوساطة الأصرتين α1-3 أو α1-4 وان هذا الأنزيم قادر على إضافة السكر للسلاسل من النوع 1 و 2 , لذلك يطلق على هذا الإنزيم أحيانا تسمية (α 3/4 – FucT) (11). يتكون المستضد الذائب Le^a بإضافة سكر الفيوكوز إلى المركب N-acetylglucosamine (GLNAC) بآصرة α 1-4 الموجودة في سلسلة المادة الأساس(12) , والذي ينتقل بوساطة البلازما ليلتصق على سطح الغشاء الخارجي لكريات الدم والخلايا اللمفاوية Lymphocytes والأقراص الدموية Platelets ويكون هذا المستضد لدى حاملين نمط ($Le(a^+ b^-$) غير الفارزين لمستضدات ABO (13) .

ينتج المستضد Le^b من تداخل فعالية الأنزيمين FucT2 و FucT3 إذ إن إنزيم FucT2 يقوم بإضافة فيوكوز إلى سكر الكالكتوز الطرفي في سلسلة المادة الأساس 1 وبآصرة α 1-2 لينتج المستضد H والذي يعد المادة الأساس لعمل الإنزيم FucT3 إذ يقوم هذا الأخير بإضافة سكر فيوكوز إضافي لمركب N-acetylglucosamine بآصرة α 1-4 ليتكون المستضد b وهو المستضد الشائع لدى أصحاب النمط ($Le(a^- b^+$) الفارزين لمستضدات ABO (14) .

اكتشفت مجموعة الدم MNS من قبل العالمين Landsteiner و Levine عام 1927 (15) وهي من الأنظمة المعقدة وتتكون من أكثر من 40 مستضدا أهمها M و N و S و s و U (1) . إن مستضدات M و N تتكون من بروتين سكري كبير يسمى MN-Sailoglycoprotein أو يطلق عليه Glycophorin A (GPA) ويكون عدد هذه المستضدات 10^6 على سطح الكرية الحمراء, وتظهر هذه المستضدات بعد تسعة أسابيع من عمر الجنين (16) . يبلغ الوزن الجزيئي لـ (GPA) حوالي 36 كيلو دالتون ويتكون من 131 حامض أميني منها 72 حامضا أمينيا خارج الخلية تنتهي بالطرف الاميني, في حين يكون 36 حامضا أمينيا داخل الخلية تنتهي بالطرف الكربوكسيلي (17) , ويختلف مستضد M عن N أن الأول يحتوي على الحامضين الامينيين glycine و Serine في الموقعين 1 و 5 على التوالي في سلسلة (GPA), بينما يحتوي مستضد N على الحامضين Glutamic acid و Leucine في الموقعين 1 و 5 في سلسلة (GPA) (1) , يطلق على مستضد S و s Glycophorin B (GPB) ، ويكون

عددها 10^5x2 على سطح كرية الدم الحمراء الواحدة (18) . الهدف من الدراسة هوتبين أن لمجاميع الدم ABO , Lewis و MNSs دورا للقابلية للإصابة بالذبحة الصدرية غير المستقرة.

المواد و طرائق العمل

جمع العينات

تضمنت الدراسة جمع 150 عينة دم من المصابين بالذبحة الصدرية غير المستقرة Unstable angina ذكورا وإناثا للمراجعين والراقدين في مستشفى الجراحات التخصصية / وزارة الصحة ومستشفى بغداد التعليمي / وزارة الصحة للفترة من 2008/10/1 لغاية 2009/2/1 وتم جمع 100 عينة دم من أشخاص أصحاء ذكورا وإناثا من مستشفى بغداد التعليمي / وزارة الصحة ومن المتبرعين بالدم في المركز الوطني لنقل الدم للفترة من 2009/2/2 إلى 2009/3/1.

طريقة العمل

بعد جمع عينات الدم من المرضى والأصحاء بأنابيب EDTA تم فصل الكريات عن البلازما بوساطة جهاز الطرد المركزي بسرعة 3000 دورة / دقيقة لمدة 5 دقائق وأهمل الطافي وعلقت الكريات بالمحلول الملحي الوظيفي, وأعيد نبذها بسرعة 3000 دورة / دقيقة ولمدة 2 دقيقة ،وأعيدت الخطوة السابقة مرتين ، أهمل الجزء الطافي وعلقت كريات الدم المضغوطة Packed red cellبالمحلول الملحي الوظيفي تركيز 0.09% للحصول على عالق نهائي 5% .تم تنميط مجاميع الدم Blood grouping بأتباع الطرائق الواردة في (19). بطريقة الأنابيب المختبرية Tube test method وهي كالاتي:

*** تنميط مجموعة الدم ABO و مجموعة الدم Lewis ومجموعة الدم MNSs**

1- وضعت قطرة من Anti-A في أنبوبة اختبار نظيفة .

2- وضعت قطرة من Anti-B في أنبوبة اختبار نظيفة .

3- أضيفت لكل أنبوبة قطرة واحدة من عالق كريات الدم المحضر.

4- تركت الأنابيب بدرجة حرارة الغرفة لمدة 5 دقائق .

5- وضعت الأنابيب بجهاز الطرد المركزي لمدة 30 ثانية وبسرعة 3000 دورة/دقيقة ثم مزجت محتويات كل أنبوبة برقة وسجلت نتائج التلازن Agglutination .

وبنفس الطريقة تم تنميط مجموعة الدم Lewis ومجموعة الدم MNSs بطريقة الأنابيب المختبرية.

النتائج و المناقشة

بينت نتائج الدراسة إن تردد مجموعة الدم ABO في مرضى الذبحة الصدرية غير المستقرة والأصحاء ان صنف الدم A 30% مقارنة بالأصحاء 30% , ويبين التحليل الإحصائي عدم وجود فروق معنوية بين الترددين. ويشير الجدول(1) إلى زيادة في نسبة تردد صنف الدم B مقارنة بالأصحاء, فقد بلغت نسبة تردد صنف الدم B لمرضى الذبحة الصدرية غير المستقرة 33.3% مقارنة بالأصحاء 29 % ($X^2 = 4.581$,$P<0.05$) .أما نسبة تردد صنف الدم O للمرضى فقد بلغت 24.7 % مقارنة 31% للأصحاء($X^2 = 5.430$,$P<0.05$) , إن ذلك يعطي مؤشرا أن حاملي هذا الصنف من الممكن أن تكون لديهم مقاومة ضد المرض, لكن لا نعرف الأساس لهذا النوع من المقاومة .أما الصنف AB فكانت نسبته 12% للمرضى مقارنة بـ 10% للأصحاء, ويشير التحليل الإحصائي إلى أن هنالك فرقا معنويا بين حاملي هذا الصنف للمرضى والأصحاء ($X^2 = 4.452$,$P <0.05$), كما في الشكل(1).

جدول- 1: تردد مجموعة الدم ABO في مرضى الذبحة الصدرية غير المستقرة والأصحاء

مجموعة الدم	المرضى			الأصحاء			قيمة مربع كاي (Qi-square)
	العدد	النسبة المئوية	المجموع	العدد	النسبة المئوية	المجموع	
A	45	30.0	150	30	30	100	ns 3.00
B	50	33.3		29	29		* 4.581
O	37	24.7		31	31		* 5.430
AB	18	12.0		10	10		* 4.452
قيمة مربع كاي (Qi-square)	–	4.826 *	–	–	4.881 *	–	---

• (P<0.05).

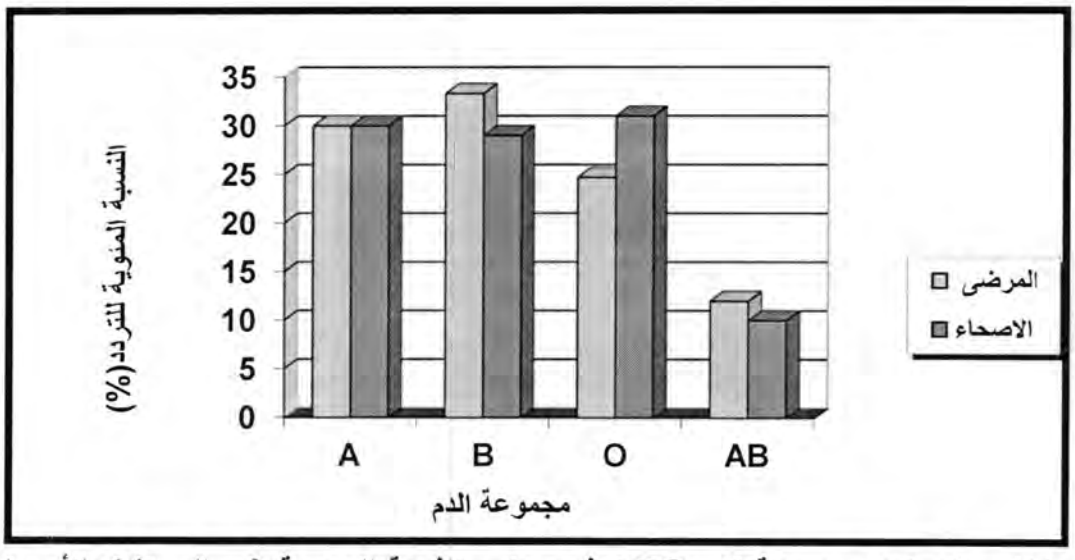

شكل -1: تردد مجموعة الدم ABO في مرضى الذبحة الصدرية غير المستقرة والأصحاء

بينت نتائج الدراسة إن نسبة تردد النمط المظهري ($Le(a^- b^-)$ الأكثر ازديادا عند مرضى الذبحة الصدرية غير المستقرة مقارنة بالأنماط المظهرية الأخرى لمجموعة الدم Lewis , فقد بلغت نسبة التردد للنمط المظهري ($Le(a^- b^-)$ 30.7% للمرضى مقارنة بالأصحاء 18%, وقد كانت نتائج التحليل الإحصائي مشيرة إلى معنوية هذه الفروقات ($X^2 = 6.236$, $p<0.05$) ,في حين انخفضت نسبة تردد الأنماط المظهرية ($Le(a^+ b^-)$ و $Le(a^- b^+)$ للمرضى مقارنة بالأصحاء فقد بلغت النسبة 15.3% و 51.7% بالمرضى مقارنة بنسبة التردد 26% و 56% للأصحاء على التوالي كما موضح في الجدول 2 والشكل 2 .

جدول- 2 : تردد مجموعة دم Lewis في مرضى الذبحة الصدرية غير المستقرة والأصحاء

مجموعة الدم	المرضى			الأصحاء			قيمة مربع كاي (Qi-square)
	العدد	المجموع	النسبة المئوية	العدد	المجموع	النسبة المئوية	
Le ($a^+ b^-$)	23	150	15.3	26	100	26	* 4.421
Le ($a^- b^+$)	82		51.7	56		56	ns 3.355
Le ($a^- b^-$)	46		30.7	18		18	* 6.236
قيمة مربع كاي (Qi-square)	–	–	* 6.452	–	–	6.645 *	---

(P<0.05): معنوي، ns: غير معنوي.

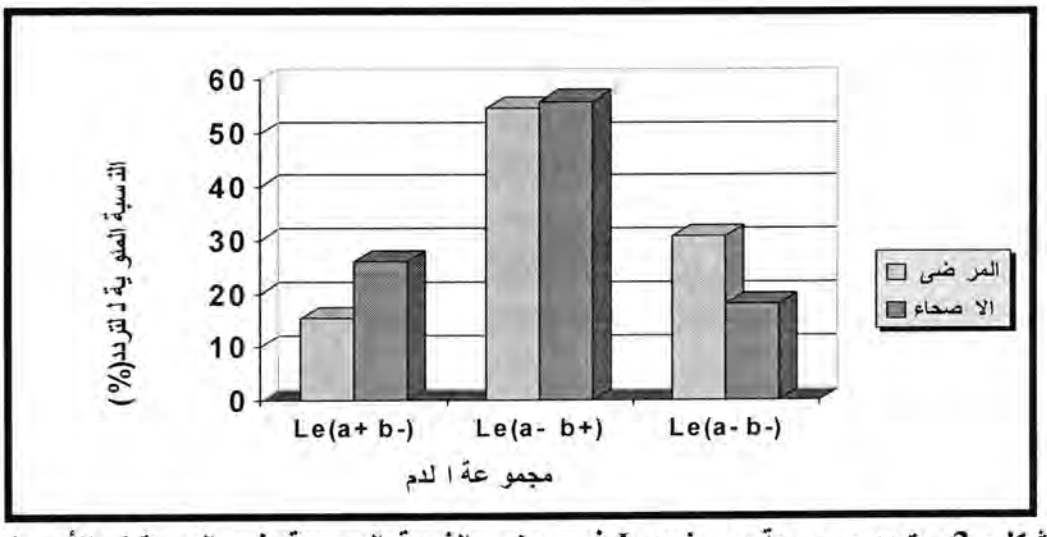

شكل- 2: تردد مجموعة دم Lewis في مرضى الذبحة الصدرية غير المستقرة والأصحاء

لقد بينت تحاليل مربع كاي أن هناك فرقا معنويا بين المرضى والأصحاء في النمط المظهري $Le(a^+ b^-)$ $(X^2= 4.421 ,P <0.05)$, في حين لم تكن هناك فروق معنوية بين المرضى والأصحاء فيما يخص النمط المظهري $Le(a^- b^+)$, إن الأساس لقابلية الإصابة أو المقاومة يمكن أن ترتبط ببناء هذه الجزيئات , إن عملية إضافة سكر الفيوكوز Fucosylation تتم بوساطة الإنزيم FucT3 إذ يقوم هذا الأنزيم بإضافة سكر الفيوكوز إلى المركب N-acetylglucosamine بآصرة α1-4 الموجودة في سلسلة المادة الأساس النوع 1 على سطح خلايا الأنسجة الذي يؤدي إلى تكوين المستضد الذائب Le a (20) ، والذي ينتقل بوساطة البلازما ليلتصق على سطح الغشاء الخارجي لكريات الدم والخلايا اللمفاوية والأقراص الدموية، ويكون هو المستضد الشائع لدى الحاملين للنمط $Le(a^+ b^-)$ غير الفارزين لمستضدات ABH(13) .أما عملية تكوين المستضد Le^b فناتجة من فعالية الأنزيمين FucT2 و FucT3 إذ يقوم الأنزيم FucT2 بإضافة فيوكوز إلى سكر الكالكتوز الطرفي في سلسلة المادة الأساس 1 وبآصرة α1-2 لينتج المستضد H الذي يستخدم كمادة أساس لعمل الأنزيم FucT3 الذي يقوم بإضافة سكر فيوكوز إضافي لمركب N-acetylglucosamine بآصرة α1-4 ليتكون المستضد Le^b وهو المستضد الشائع لدى الحاملين للنمط $Le(a^- b^+)$ الفارزين لمستضدات ABH .ولقد أشارت الدراسات إلى أن مجموعة الدم لويس تعد كعوامل التصاق للعديد من الخلايا أو واسمات للإمراض السرطانية (21) ، وكما لها علاقة بأمراض القلب والكلية (22)تؤدي هذه الجزيئات دورا في التصاق الممرضات التي يمكن أن تؤسس لاستجابة مناعية تجاه الذات. تبين أن لمجاميع الدم ABO و Lewis دورا للقابلية للإصابة بالذبحة الصدرية غير المستقرةوازداد تكرار مجموعة دم B عند مرضى الذبحة الصدرية غير المستقرة وكانت النتائج الإحصائية تشير إلى فروق معنوية عن

تلك التي في الأصحاء, أما صنف الدم O فقد قل تكراره في المرضى عنه في الأصحاء لذا من المحتمل أن يكون هذا الصنف مقاوما للمرض, ويمكن تفسير هذه النتائج بناء على ضوء التركيب البنائي لهاتين المجموعتين , أما في مجموعة دم لويس فقد ارتفع تردد المجموعة Le(a-b-) وقاومت المجموعة Le^b المرض وسجلت مجموعة الدم AB أعلى خطورة نسبية تلتها مجموعة دم B و في مجموعة دم لويس أعطى النمط المظهري Le(a-b-) أعلى خطورة نسبية.

تبين من الدراسة أن حاملي النمط الوراثي NN كانوا أكثر عرضة للإصابة بالذبحة الصدرية غير المستقرة, إذ أشارت النتائج إلى زيادة نسبة تردد النمط الوراثي NN لهؤلاء المرضى فقد بلغت19.2% مقارنة بنسبة 11% للأصحاء, وقد أكد التحليل الإحصائي إن هنالك فروقا معنوية ($X^2 = 4.790$, $P<0.05$) , الجدول 3 والشكل 3 , وتشير النتائج إلى زيادة نسبة النمط الوراثي Ss إذ بلغت 49.3% للمرضى مقارنة بـ 42% للأصحاء, وكانت الفروق معنوية إحصائيا ($X^2 = 6.549$, $P < 0.05$) في حين كان النمط الوراثي (MM) مقاوما للذبحة فقد بلغت النسبة 26.2 للمرضى مقارنة بـ 41 للأصحاء, واظهر التحليل الإحصائي وجود فروقا معنوية ($X^2 = 6.549$, $P< 0.05$).

جدول-3:تردد الأنماط الوراثية لمجموعة الدم MNS لمرضى الذبحة الصدرية غير المستقرة والأصحاء

النمط الوراثي	المرضى			الأصحاء			قيمة مربع كاي (Qi-square)
	العدد	المجموع	النسبة المئوية	العدد	المجموع	النسبة المئوية	
MM	38	146	26.2	41	100	41	* 6.549
MN	80		54.8	48		48	ns 3.535
NN	28		19.2	11		11	* 4.790
SS	20		13.7	15		15	ns 1.581
Ss	72		49.3	42		42	* 6.549
Ss	54		36.9	41		41	* 5.581
قيمة مربع كاي Qi-) (square	–	–	10.415 **	–	–	10.131 **	---

*(P<0.05)، ** (P<0.01).

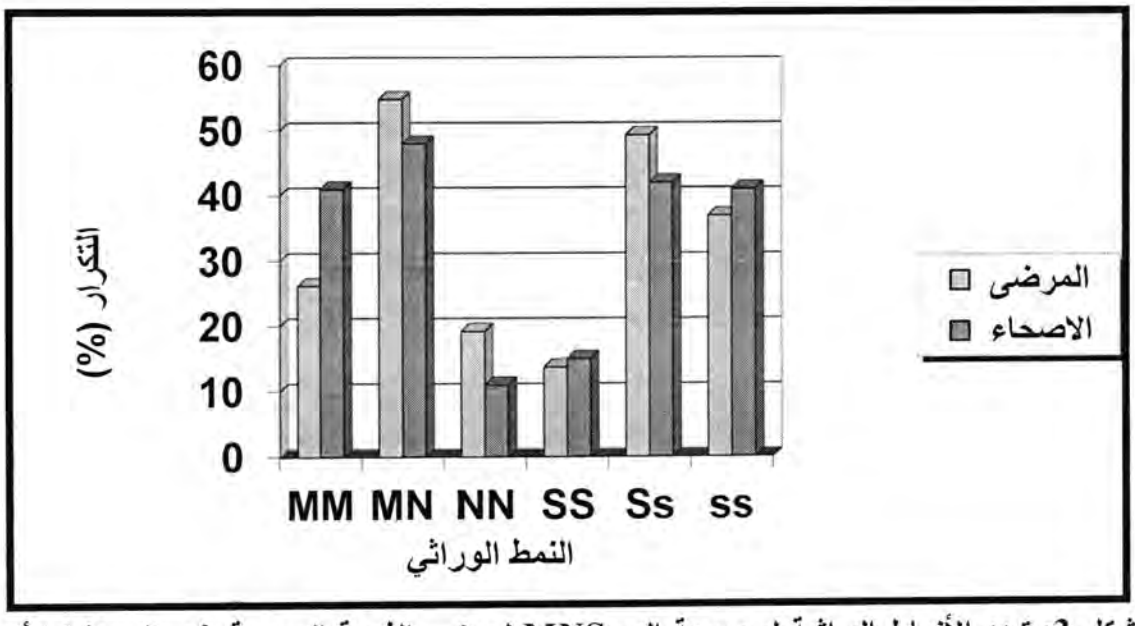

شكل-3: تردد الأنماط الوراثية لمجموعة الدم MNS لمرضى الذبحة الصدرية غير المستقرة الأصحاء

ان مستضدات MNS تعمل كمستقبلات لالتصاق الحركيات الخلوية Cytokines (23) , وتبين من الدراسات ان هناك علاقة بين الاصابة بالربو عند الأطفال والنمط M+N- (24).أما بالنسبة إلى النمط المظهري ss فبلغت نسبته 36.9% للمرضى مقارنة بـ 41 %للأصحاء (X^2 =5.581 , $P < 0.05$) و النمط المظهري MN بلغت نسبته 54.8% للمرضى مقارنة بالأصحاء 48 % , أما النمط المظهري SS بلغت نسبته 13.7 % للمرضى مقارنة بـ 15 % للأصحاء.

الخطورة النسبية Relative Risk

أبدت مجموعة الدم AB أعلى خطورة نسبية في مجاميع الدم ABO الجدول 3-11 , إذ بلغت الخطورة النسبية لمجموعة الدم AB (1.2) وتليها مجموعة الدم B , فقد بلغت الخطورة النسبية لهذه المجموعة (1.1) , في حين إن الخطورة النسبية لمجموعة الدم A و O هي (1) و (0.8) على التوالي .وأظهر النمط المظهري $Le(a^- b^-)$ أعلى خطورة مقارنة بالأنماط المظهرية الأخرى لهذه المجموعة ,إذ بلغت الخطورة النسبية لهذا النمط (1.7) في حين كان النمط المظهري $Le(a^+b^-)$ ذا خطورة بلغت (0.6), أما النمط المظهري $Le(a^-b^+)$ فقد سجل خطورة نسبية (0.97) .

جدول -4: مجاميع الدم ABO و Lewis كأساس للخطورة النسبية

مجموعة الدم	الخطورة النسبية	قيمة T-test (LSD)
ABO		
A	1	
B	1.1	

* 0.297	0.8	O
	1.2	AB
		Lewis
* 0.365	0.6	Le (a^+ b^-)
	0.97	Le (a^- b^+)
	1.7	Le (a^- b^-)

أما فيما يخص دور مجموعة الدم MNS وعلاقتها بالخطورة النسبية لمرضى الذبحة الصدرية غير المستقرة, فقد أظهرت مجموعة الدم MNS بالنمط الوراثي NN أعلى خطورة نسبية إذ بلغت (1.7) مقارنة بالأنماط الأخرى وتلاه النمط الوراثي MN , إذ بلغت الخطورة النسبية له (1.1) أما الأنماط الوراثية (MM, SS, Ss , ss) فقد كانت نسب خطورتها هي (0.6, 0.9 , 1.2, 0.9) على التوالي كما موضح في جدول 3-12 .

جدول -5: مجاميع الدم MNS كأساس للخطورة النسبية

المجموعة	الخطورة النسبية
MM	0.6
MN	1.1
NN	1.7
SS	0.9
Ss	1.2
Ss	0.9
قيمة T-test (LSD)	* 0.281

(P<0.05) *

المصادر

1- Harmening, D.M.Modern blood banking and transfusion practices. 4th ed. *F.A.Davis Company, Philadelphia, USA*. p.p. 161-169. (1999).

2- Lee, H.H. Epidemiologic characteristics and multiple risk factors of stomach cancer in Taiwan. *Anticancer Research* .10 (87): 5-82. (1990).

3- Annese,V.; Minervini, M.; Gabbriell, A.; Gambassi, G. and Manna, R. ABO blood groups and cancer of the pancreas. *Int. J. Pancreatol* .6(2):81-88. (1990).

4- Nakatas, A.Epidemiologic studies of risk factors for bladder cancer. *ACTA Urologica Japonica*. 41(12): 969-77 (1995).

5- Guleria, K.; Pal Singh, H.; Kaur, H. and Sambyal, H.ABO blood groups in gastrointestinal tract and breast carcinoma patients. *Anthropologist.* 7(3): 189-192. (2005).

6- Hein, H.O.; Sorensen, H. and Suadicani, P.The Lewis blood group a new genetic marker of ischaemic heart disease. *J. Intern. Med.* 232:481–487. (1992).

7- Harmening, D.M. and Taghizadeh, M.The Lewis System. In: Harmening, D.M : Modern Blood Banking and Transfusion Practices. *FA Davis Company Philadelphia, USA.* p.p. 133-145 (1994).

8- Henry, S.; Oriol, R. and Samuelsson, B.E.Lewis histo-blood group system and associated secretory phenotypes. *Vox Sang*. 69:166 (1995).

9- Johnson, P.H. and Watkins, W.M. Purification of the Lewis blood-group gene associated alpha-3/4- fucosyltransferase from human milk: an enzyme transferring fucose primarily to type 1 and lactose-based oligosaccharide chains. *Glycoconj.J.* 9(5):241–249. (1992).

10- Oriol, R. Genetics of ABO,H, Lewis, X and related antigens. *Vox Sang.* 51:161. (1986).

11- Koda, Y, Kimura, H. and Mekada, E. Analysis of Lewis fucosyltransferaseenes from the human gastric mucosa of Lewis-positive and -negative individuals. *Blood*, 82:2915-2919. (1993).

12- Henry, S.; Mollicone, R.; Fernandez, P.; Samuelsson, B.; Oriol, R. and Larson, G.Molecular basis for erythrocyte Le(a+b+) and salivary ABH partial-secretor phenotypes: expression of a FUT2 secretor allele with an A,T mutation at nucleotide 385 correlates with reduced α(1,2) fucosyltransferase activity. *Glycoconj. J.* 13: 985-993. (1996).

13- Johnson, P.H. and Watkins, W.M. Purification of the Lewis blood-group gene associated alpha-3/4- fucosyltransferase from human milk: an enzyme transferring fucose primarily to type 1 and lactose-based ligosaccharide chains. *Glycoconj. J.* 9(5):241–249. (1992).

14- Kyprianou, P.; Betteridge, A.; Donald, A.R. and Watkins,W.M. Purification of the blood group H gene-associated α-2-L-fucosyltransferase from human plasma. *Glycoconj.J.* 7:573-588 . (1990).

15- Landsteiner, K and Levine, P.Further observation on individual differences of human blood. *Proc. Soc. Exp. Biol.* 24:941.(1927).

16- Reid, M.E. and Lomas-Francis, CThe blood group antigen facts book, Academic Press, *San Diego*. p.210-215.(1997).

17- Rolih, S. Biochemistry of MN antigens. In Unger, P.J. and Lairdfryer, B.: Blood group systems MN. American Association of Blood Banks. Arlington,VA.USA.p.371. (1989).

18- Lutz, P. and Dzik,W.H. Molecular biology of red cell blood group genes. *Transfusion.* 32:467-470. (1992)

19- Daniels, G. Human blood groups .Oxford. Blackwell Science Publications .UK.p.77. .(1995).

20- Henry, S.; Mollicone, R.; Fernandez, P.; Samuelsson, B.; Oriol, R. and Larson, G. Molecular basis for erythrocyte Le(a+b+) and salivary ABH partial-secretor phenotypes: expression of a FUT2 secretor allele with an A,T mutation at nucleotide 385 correlates with reduced α(1,2) fucosyltransferase activity. *Glycoconj. J.* 13: 985-993. (1996).

21- Itai, S., Nishikata, J.; Yoneda, T.; Ohmori, K.; Tsunekawa,S.; Hiraiwa, N.; Yamabe, H., Arii, S.; Tobe, T. and Kannagi, R. Tissue distribution of sialyl 2-3 and 2-6 Lewis a antigens and the significance of serum 2-3/2-6 sialyl Lewis a antigen ratio for the differential diagnosis of malignant and benign disorders of the digestive tract. *Cancer*. 67: 1576- 1587. (1991).

22- Silberstein, L.E. Molecular and functional aspects of blood group antigens. American Association of Blood Banks, USA.p.p.181-182. (1995)

23- Hassoun, H.; Hanada, T.; Lutchman, M.; Sahr, K.E.; Palek, J.; Hanspal, M.; Chishti, A.H.Complete deficiency of glycophorin A in red blood cells from mice with targeted inactivation of the band 3 (AE1) gene. *Blood.* 91(6):2146- 2151.(1998).

24- Bottini, N.; Ronchetti, F.; Gloria-Bottini, F.; Stefanini, L.; Bottini, E. and Lucarini, N. Atopic and nonatopic asthma in children. *J .Asthma.* 42(2):25-8.(2005).

التوازن الهرموني ودليل كتلة الجسم في عقم النساء

سوزان عبد الرحمن إبراهيم وإقبال خضر الجوفي
قسم علوم الحياة / كلية العلوم / الجامعة المستنصرية

تاريخ تقديم البحث : 2011/ 3/30 تاريخ قبول البحث : 2011/ 5/29

ABSTRACT

The cases of infertility have increased in women lately, the current study has been conducted in order to obtain some indicators about the hormone changes and their relationship with body mass index and shedding light on the Recurrent Spontaneous Abortion which is may be one of the factors that lead to infertility. The study included 100 infertile women. In addition 30 healthy volunteers represented the control cases. The study period was from November 2007 to May 2008.

This study reached the following results:

The frequencies of infertile women within the age group (25-35) year, the duration of infertility (1-4) year & Body Mass Index were significantly increased increased in infertile women. The level of hormones was measured in the serum by using Mini-VIDIS device automatically , The level of FSH, LH , T3 in the serum of infertile women were significantly decreased ($p<0.05$) in general in comparison with control group , while the level of Prolactin increased significantly ($p<0.05$) in women with secondary infertility accompanying pervious abortion in comparison with women with primary & secondary infertility not accompanying pervious abortion & significant decrease ($p<0.05$) in the level of the T4 in women with secondary infertility accompanying pervious abortion as compared with control group.

الخلاصة

ازداد شيوع حالات العقم لدى النساء في الآونة الأخيرة, وقد أجريت الدراسة الحالية بهدف الحصول على مزيد من الإيضاحات حول التغيرات الهرمونية وعلاقتها مع دليل كتلة الجسم ، و كذلك تسليط الضوء على الإجهاض العفوي المتكرر الذي قد يعد من العوامل المؤدية إلى العقم.

شملت الدراسة الحالية 100 مريضة تعاني العقم و 30 متطوعة من السويات اللاتي يمثلن مجموعة السيطرة ، للفترة من تشرين الثاني 2007م الى ايار 2008م .

توصلت الدراسة الى النتائج الاتية :

ارتفاع تكرار النساء العقيمات ضمن الفئة العمرية (25–35) سنة ,تكرار مدة العقم (1–4) سنة ، دليل كتلة الجسم لدى مجاميع النساء العقيمات مقارنة مع السيطرة وبفروق معنوية.تم قياس

مستوى الهرمونات في مصل الدم باستخدام جهاز الـ Mini-VIDIS إذ تم حسابها آليا وكانت النتائج كالأتي:انخفاض معنوي ($P<0.05$) لمستوى الهرمون المحفز للجريبة (FSH)، و الهرمون اللوتيني (LH) و لمستوى هرمون الثايرونين ثلاثي اليود(T3) في مصل الدم للنساء العقيمات مقارنة بالسيطرة , ارتفاع مستوى هرمون البرولاكتين (Prolactin) لدى النساء ذوات العقم الثانوي المترافق مع حدوث حالات إجهاض سابقة وبفروق معنوية($P<0.05$) مقارنة مع ذوات العقم الأولي و الثانوي غير المترافق مع حدوث حالات إجهاض سابقة و انخفاض معنوي ($P<0.05$) لمستوى هرمون الثايرونين رباعي اليود (T4) لدى النساء ذوات العقم الثانوي المترافق مع حدوث حالات إجهاض سابقة مقارنة بالسيطرة .

المقدمة

العقم Infertility هو حالة طبية تشمل مضامين صحية وأخرى مرتبطة بالشخص السليم أو القويم ذات تأثير على الشخص نفسه والمجتمع(1)

يصيب العقم الجهاز التكاثري Reproductive system مؤدياً إلى أضعاف واحدة من أهم وظائفه وهي الإنجاب أو الحمل الذي يحتاج إلى أنتاج بيوض سليمة صحياً من المرأة وعدم انسداد في أنبوب فالوب ليسمح للنطفة السليمة والصحية من الرجل بأن تصل إلى البيضة وتخصبها لكي تنغرس في جدار الرحم، ويعد الزواج غير مثمر بعد مرور عام على الاتصال الجنسي المستمر وبدون استخدام موانع الحمل (2) .

تكون المرأة مسؤولة عن حوالي 40% من حالات العقم بشكل عام، إذ تشترك بثلث حالات العقم التي تعزى إلى عوامل خاصة بالأنثى فقط Female factors ، أما الثلث الأخر فيعزى إلى عوامل خاصة بالرجل Male factors ، في حين أن الزوجين يشتركان في الثلث الأخير الذي ينتج من مشاكل خاصة بالرجل و المرأة في أحداث العقم ، فضلاً عن كون 15% من الحالات تكون غير مفسرة Unexplained (3).

من الأسباب الشائعة في حدوث العقم عند النساء هي:

- فشل حدوث الاباضة Ovulation failure (40%) ويمكن أن يعزى السبب إلى العمر Age، أو اختلالات هرمونية في الغدد الصماء كما في متلازمة المبيض المتعدد الكيسات Polycystic Ovary Syndrome (PCOS) أو أمراض وراثية مثل متلازمة الفشل ألمبيضي المبكر Premature Ovarian Failure Syndrome (POFS) .
- العوامل الأنبوبية Tubal Factors (30%) وسببها ممكن أن يعود إلى أمراض الحوض الالتهابية Pelvic Inflammatory Diseases (PID) أو الجراحة Surgery

- عوامل خاصة بالرحم / المخاط العنقي Uterine / Cervical mucus Factors (3%) تعزى إلى اختلال المخاط العنقي cervical mucus نوعياً وكمياً بسبب الإصابة Infection أو التدخين Smoking ، أو وجود الأورام الليفية Fibroids .
- انتباذ بطانة الرحم Endometrioses (15%), فيما تعزى 10% من حالات العقم إلى عوامل أخرى (5,4)

تلعب السيطرة الهرمونية على وظيفة المبايض Ovaries بوساطة منبه القند Gonadotropin الدور الرئيس في العمليات الفسيولوجية فيما يتعلق بنمو الجريبة Follicle وتمايزها Differentiation ولذلك فأن التقييم الوظيفي لمحور تحت المهاد – النخامية – المبايض Hypothalamic – Pituitary – Ovarian Axis (HPOA) يتم من خلال معايرة الهرمونات الآتية : الهرمون المحفز للجريبة Follicle Stimulating Hormone ، الهرمون اللوتيني Luteinizing Hormone ، هرمون الحليب Prolactin ، الاستراديول Estradiol و البروجستيرون Progesterone إذ تعد هذه الهرمونات أساسية في تشخيص أي خلل في HPOA (7,6). ويمكن أن تؤدي الإصابة ببعض الأمراض إلى العقم مثل أمراض الدرقية Thyroid diseases التي تؤثر في الخصوبة و على الوظيفة الجنسية وعلى النمو وفي وظائف العضلات والغدد الصم إضافة إلى ارتفاع الكوليسترول ،يتم ذلك من خلال افراز الغدة الدرقية لهرمون الثايرونين الرباعي T4 وهرمون الثايرونين T3 بالاضافة الى الهرمون المحفز للدرقية الذي يقوم بتنظيم الفعالية الافرازية للغدة الدرقية (8) . ومن الممكن أن تؤدي العديد من عوامل الخطورة Risk factors إلى حدوث العقم عند النساء ومنها: العمر Age، التدخين Smoking، دليل كتلة الجسم Body Mass Index وغيرها (9)

و يعد الإجهاض العفوي المتكرر Recurrent Spontaneous Abortion (RSA) ويسمى كذلك الإجهاض المعتاد Habitual abortion من أهم أو اخطر أنواع العقم ويعرف على أنه فقدان الحمل أو الجنين لثلاث مرات أو أكثر قبل الأسبوع العشرين من الحمل (10) و تشير إحصائيات منظمة الصحة العالمية WHO إلى أن 25 % من حالات الحمل يمكن أن تنتهي بالإجهاض خصوصاً في دول العالم الثالث (11) تعاني 3 % من النساء من مشكلة الإجهاض العفوي المتكرر وتزداد مع زيادة العمر أو بسبب خلل في الكروموسومات ، أو بسبب عوامل مناعية أو اضطرابات هرمونية أو مرض ذاتي أو بسبب الخمج (12)

المواد وطرائق العمل

1- مجاميع المرضى

- **مجموعة المرضى**

شملت هذه الدراسة مائة مريضة بالعقم والمراجعات لمستشفى كمال السامرائي (مركز العقم وأطفال الأنابيب) للفترة من تشرين الثاني 2007م ولغاية شهر أيار 2008م.. وقد تضمنت العينة مجموعتين، الأولى تضم 61 مريضة مصابة بالعقم الأولي Primary infertilityالذي يعرف بانه عدم حصول الحمل لدى الزوجة مطلقاً، والمجموعة الثانية تضم 39 مريضة مصابة بالعقم الثانوي Secondary infertilityويطلق عندما يكون لدى الزوجة حالة حمل سابقة التي بدورها ضمت 23 مريضة مصابة بالعقم الثانوي مترافق مع حدوث حالات إجهاض سابقة و 16 مريضة مصابة بالعقم الثانوي غير مترافق مع حدوث حالات إجهاض سابقة.

- **مجموعة السيطرة Control group**

تضمنت هذه المجموعة ثلاثين امرأة من المتطوعات السليمات أو الخصبات وليس لديهن تاريخ إصابة أو دلائل سريرية على إصابة محتملة بالعقم، أو أي حالة مرضية أخرى مطابقات عمرياً مع مجموعة المرضى.

2- جمع عينات الدم

تم سحب 5مل من الدم الوريدي للذراع لجميع النساء موضع الدراسة في حالة الصيام ونقل الدم المسحوب مباشرة إلى أنابيب اختبار بلاستيكية، تركت هذه الأنابيب لمدة 30 دقيقة في درجة حرارة الغرفة لحين تكون الخثرة ثم فصل المصل باستعمال جهاز النبذ المركزي Centrifuge بسرعة 3000 دورة / الدقيقة ولمدة 5 دقائق، ثم وزع المصل على ستة أنابيب ابندروف صغيرة وخزن بدرجة – 20°م لحين الاستعمال.

3- حساب دليل كتلة الجسم Body Mass Index (BMI)

تم حساب BMI عن طريق قسمة وزن الجسم Body weight مقيساً بوحدة الكيلو غرام على الطول hight بوحدة المتر مربع (كغم / م^2) ، **ومقارنة النتائج مع ثلاثة مجاميع هي : الاولى** BMI اقل من(24.9) كغم /م ^{2} والمجموعة الثانية (25 – 29.9) كغم /م ^{2} والمجموعة الثالثة أعلى من أو يساوي (30) كغم /م ^{2} **(13)**.

4- التحري عن الدلائل الهرمونية

تم قياس مستوى الهرمونات (FSH , LH , Prolactin , TSH ,T3,T4) في مصل الدم لـ 50 مريضة و 20 امراة سليمة كسيطرة ،و بطريقة اوتوماتيكية باستخدام جهاز الـ- Mini VIDAS.

5- التحليل الاحصائي

تم تحليل البيانات إحصائيا باستخدام البرنامج الإحصائي الجاهز (SPSS) Statistical Package for Social Science . و استخدام قانون مربع كاي (Chi – Square) لتحليل بعض نتائج الدراسة و اعتمد اختبار اقل فرق معنوي Least- Significant differences (LSD) على مستوى احتمالية 0.05 وذلك لتقييم الفروق بين المجاميع المختلفة ، كما تم استخدام اختبار T-test للمقارنة بين معدلات العينات المستقلة T-test for Independent Samples .

النتائج والمناقشة

1 - توزيع النساء العقيمات وفقاً لنوع العقم

يوضح الشكل 1 أن من بين 100 عينة من النساء العقيمات 61% يعانين من العقم الأولي فيما كان 39% يعانين من العقم الثانوي موزعة بين 23% مترافق مع حدوث حالات إجهاض سابقة و 16% غير مترافق مع حدوث حالات إجهاض سابقة وبفروق معنوية عالية ($P < 0.05$) .

وقد يعود هذا الارتفاع في نسبة العقم الأولي إلى بعض الأسباب المناعية والو راثية غير الظاهرة، أو الإصابة ببعض الأمراض مثل مرض السكري وبالأخص Type II ، أو الإصابة بقصور الدرقية الأولي Primary Hypothyroidism غير المشخص ، أو قد يعود السبب إلى نمط الغذائي المتبع (14)، وربما هنالك أسباب أخرى مثل ارتفاع تكاليف العلاج وفترات المتابعة الطويلة التي تحتاجها برامج علاج العقم وهذا ما يقلل حماس مريضات العقم الثانوي لطلب العلاج والاكتفاء بما لديهن من أطفال على الأخص اللاتي أنجبن ذكوراً ومن المتوقع أن تكون أكثر الإصابات بالعقم الثانوي تعود إلى اخماج المسلك التناسلي ببعض المسببات الجرثومية التي تقلل فرصة الإخصاب (15) .

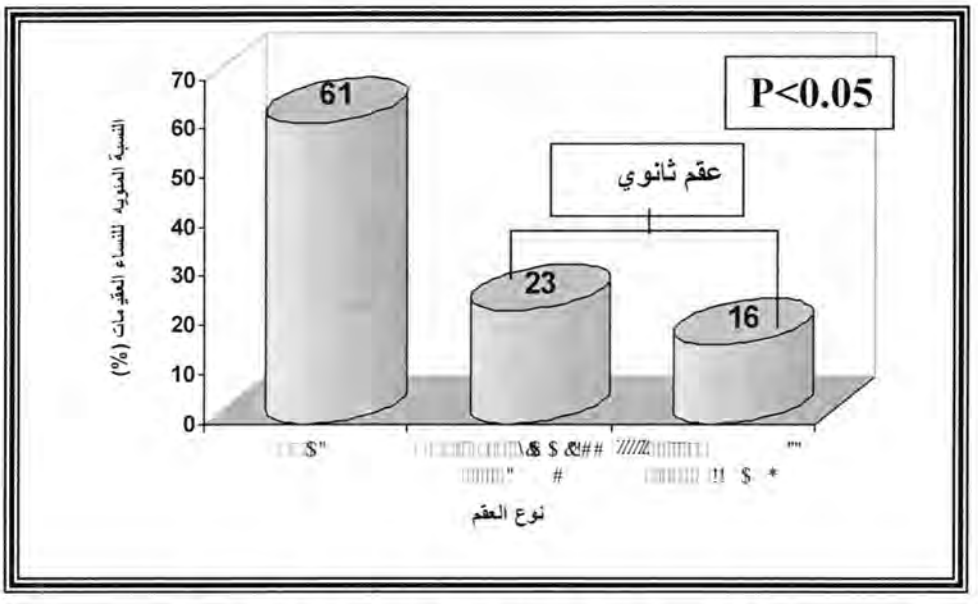

شكل – 1: توزيع النساء العقيمات وفقا لنوع العقم

2- توزيع النساء العقيمات وفقا للفئات العمرية

يبين الجدول 2 توزيع النساء العقيمات حسب الفئات العمرية إذ أظهرت نتائج الدراسة أن أعلى نسبة (55%) تقع ضمن الفئة العمرية (25-35) سنة ، ثم الفئة العمرية (15-25) سنة (26 %) ، تليها الفئة العمرية 35 سنة فأكثر(19%) . وعند مقارنة الفئات العمرية للنساء العقيمات ذوات العقم الأولي والثانوي المترافق وغير المترافق مع حدوث حالات إجهاض سابقة كان الاختلاف ذا دلالة إحصائية (X^2 = 7.967 ، درجات الحرية = 4 ، P< 0.05) يعود هذا التباين إلى ارتفاع نسبة تكرار العقم الأولي 80.8% ضمن الفئة العمرية 15-25 سنة ، والعقم الثانوي المترافق مع حدوث حالات إجهاض سابقة 36.8% ضمن الفئة العمرية 35 سنة فأكثر والعقم الثانوي غير المترافق مع حدوث حالات إجهاض سابقة 21.8% ضمن الفئة العمرية (25-35) سنة ، كما موضح في الجدول 1 .

هذه النتائج لم تأتِ متوافقة مع ما أورده الكثير من الباحثين (18,17,16) , فقد أكدوا أن تقدم العمر لأكثر من 35 سنة يلعب دوراً كبيراً في انخفاض معدلات الخصوبة وزيادة نسبة حالات الإجهاض ، إذ تقل استجابة المبايض Ovaries إلى الهرمونات المغذية للمناسل مما يؤدي إلى توقف أنتاج وتكوين البيوض والهرمونات الجنسية الأنثوية ، وبتقدم العمر يزداد أنتاج بيوض ذات كروموسومات غير طبيعية .

جدول – 1 : الأعداد والنسب المئوية للفئات العمرية الملاحظة للنساء العقيمات

الفئات العمرية (سنة)	النساء العقيمات/ نوع العقم			المجموع
	عقم أولي	عقم ثانوي مترافق مع حدوث حالات إجهاض سابقة	عقم ثانوي غير مترافق حدوث حالات إجهاض سابقة	
	العدد (%)	العدد (%)	العدد (%)	العدد (%)
25-15	21 (80.8)	3 (11.5)	2 (7.7)	26 (100)
35-25	30 (54.6)	13 (23.6)	12 (21.8)	55 (100)
35 فأكثر	10 (52.6)	7 (36.8)	2 (10.6)	19 (100)
المجموع	61 (61.0)	23 (23.0)	16 (16.0)	100 (100)

X^2 = 7.967 ، درجات الحرية = 4 ، الاحتمالية (P<0.05)

3- توزيع النساء العقيمات وفقاً لمدة العقم.

يوضح الشكل 3-3 توزيع النساء العقيمات وفقاً لمدة العقم وكانت النسبة الأعلى للمدة (1-4) سنة إذ بلغت 65% ، تليها المدة(5-8) سنة بنسبة 29% ، والمدة (9-12) سنة بنسبة 4% وأخيرا المدة (13-16) سنة بنسبة 2% .

أن ارتفاع نسبة مراجعات النساء العقيمات في بداية زواجهن لمعرفة أسباب عدم القدرة على الإنجاب ومحاولة المعالجة قد تكون وراء ارتفاع هذه النسبة بين العقيمات للفترة (1-4) سنة، وان انخفاض النسبة مع امتداد فترة العقم قد يعود إلى تقدم المرأة بالعمر إذ أظهرت النتائج (جدول2) حصول ارتفاع في مدة العقم (13-16) سنة بنسبة 50% عند زيادة عمر العقيمات إلى 35 سنة فأكثر مقارنة مع المدة (5-8) سنة بنسبة 41.4% والمدة (1-4) سنة بنسبة 12.3% وبفروق معنوية عند مستوى احتمالية < 0.05 .

جاءت هذه النتائج متوافقة مع كل من (20,19) فقد أكدوا أن زيادة عمر المرأة يترافق مع قلة الخصوبة وعدم حصول الحمل إذ تزداد أرجحية الإجهاض العفوي ونسبة أنتاج بيوض ذات كروموسومات غير طبيعية مع زيادة العمر وبذلك تقل نسبة الخصوبة وعند زيادة العمر إلى أكثر من 35 سنة فأنه غالباً ما يفسر على انه حالة عقم غير مفسرة

جدول – 2 : توزيع النساء العقيمات وفقا للفئات العمرية ومدة العقم

مدة العقم (سنة)	الفئات العمرية / سنة			المجموع
	25 – 15	35 – 25	35 فأكثر	
	العدد (%)	العدد (%)	العدد (%)	العدد (%)
4 – 1	24 (36.9)	33 (50.8)	8 (12.3)	65 (100)

8 – 5	(13.8) 4	(44.8) 13	(42.4) 12	(100) 29
12 -9	(0.0) 0	(100.0) 4	(0.0) 0	(100) 4
16 -13	(0.0) 0	(50.0) 1	(50.0) 1	(100) 2
المجموع	(28.0) 28	(51.0) 51	(21.0) 21	(100) 100

X^2= 17.22 ، درجات الحرية = 6 ، الاحتمالية (P<0.05)

4- دليل كتلة الجسم BMI

يوضح الجدول 3 الاعداد والنسب المئوية لل BMI الملاحظة لدى النساء العقيمات وطبقا لهذا التوزيع أظهرت النتائج وجود فروقاً معنوية (p<0.01) لدى مجاميع الدراسة ، و جاءت هذه النتائج متوافقة مع ذكره الكثير من الباحثين (23,22,21) الذين أشاروا أن الانحراف عن وزن الجسم الطبيعي سواء كان بالزيادة في الوزن Over weight أو بالنقصان Under weight يضعف فعالية الجهاز التكاثري بسبب تغير أو تبديل مستوى الهرمونات مؤدياً إلى اضطراب الدورة الحيضية وعسر الاباضة والإصابة ببعض الأمراض وبالتالي العقم عند النساء، إذ أن السمنة تكون مترافقة مع خطورة الإصابة بمرض السكري والقلب وأنواع السرطان.

جدول- 3: الأعداد والنسب المئوية لـ BMI الملاحظة في النساء العقيمات والسيطرة

مجاميع النساء	مجاميع BMI كغم /م ^{2}			المجموع
	< 24.9	29.9 – 25	>= 30	
	العدد (%)	العدد (%)	العدد (%)	العدد (%)
السيطرة	(76.6) 23	(20) 6	(3.3) 1	(100) 30
عقم أولي	(16.4)10	(60.7) 37	(23.0)14	(100) 61
عقم ثانوي مترافق مع حدوث حالات إجهاض سابقة	(39.1) 9	(47.8) 11	(13.0) 3	(100) 23
عقم ثانوي غير مترافق مع حدوث حالات إجهاض سابقة	(6.3) 1	(50) 8	(43.8) 7	(100) 16
المجموع	(33.1) 43	(47.7) 62	(19.2) 25	(100) 130

X^2 = 42.951 ، درجات الحرية = 6 ، الاحتمالية (P<0.01)

5- الهرمونات

- الهرمون المحفز للجريبة FSH

بينت النتائج انخفاض في معدل هرمون FSH لدى النساء العقيمات إذ بلغ معدله لديهن (4.440 ± 3.588) ملي وحدة عالمية/ مل مقارنة مع مستواه لدى مجموعة السيطرة إذ بلغ معدله (7.075 ± 1.458)) ملي وحدة عالمية/ مل وقد كان هذا الانخفاض لدى النساء ذوات العقم

الثانوي الغير مترافق مع حدوث حالات إجهاض سابقة اكبر من ذوات العقم الأولي والثانوي المترافق مع حدوث حالات إجهاض سابقة مقارنة مع مستواه لدى مجموعة السيطرة ، وقد اكتسب هذا الانخفاض دلاله معنوية ($p < 0.05$) ، كما موضح في الجدول 4. وعند المقارنة الإحصائية بين المجاميع المدروسة باستخدام اختبار اقل فرق معنوي L.S.D اظهر التحليل الإحصائي انخفاضاً معنويا ($p<0.05$) لدى النساء ذوات العقم الأولي والثانوي المترافق مع حدوث حالات إجهاض سابقة والثانوي غير المترافق مع حدوث حالات إجهاض سابقة مقارنة بالسيطرة .

جاءت هذه النتائج متوافقة مع (25,24) إذ أشاروا إلى انخفاض هرمون FSH لدى النساء العقيمات أدى إلى فشل حدوث الاباضة ، إذ أن انخفاض FSH ينتج عنه فشل في وظيفة الغدد التناسلية مؤدياً إلى انقطاع الدورة الحيضية وبالتالي العقم وقد ذكر الباحثون (27,26) أهمية هرمون FSH إذ يكون مسؤولاً عن تحفيز نمو جريبه كراف Graffian Follicle وتمايزها وبالتالي إنضاج الجريبة وتحفيزها لإنتاج الاستروجين ، أما انخفاض FSH فيلاحظ في حاله زيادة مستوى هرمون البرولاكتين في الدم ونقص منبهات القند ومتلازمة كالمان Kallmann syndrome وهذا ما أثبته المعلى (2006) (28) بدراسة أجريت على الفئران البيض إذ وجد أن الزيادة المستحثة في مستوى هرمون FSH بوساطة مستخلص عرق السوس أدى إلى زيادة العدد الكلي للجريبات المبيضية وبالتالي نموها وتمايزها وتحفيزها لإنتاج الاستروجين Estrogen وبالتالي حصول الاباضة .

جدول – 4 : معدل مستوى هرمون FSH (ملي وحدة عالمية/ مل) في مصل الدم لمجاميع الدراسة

المجموعة		العدد	مستوى هرمون FSH (ملي وحدة عالمية/ مل) في مصل الدم		
			الوسط الحسابي ± الانحراف المعياري	أعلى قيمة	اقل قيمة
السيطرة		20	α 1.458 ± 7.075	10.2	5.2
النساء العقيمات/ نوع العقم	الكلي	50	b 3.588 ± 4.440	16.6	0.1
	أولي	33	b 3.484 ± 4.429	16.6	0.1
	ثانوي مترافق مع حدوث حالات إجهاض سابقة	12	b 4.609 ± 4.712	16.6	0.8
	ثانوي غير مترافق مع حدوث حالات إجهاض سابقة	5	b 1.217 ±3.860	5.0	2.1

الحروف المتشابهة تعني عدم وجود فروق معنوية والحروف المختلفة تعني وجود فروق معنوية عند مستوى احتمالية($P<0.05$) .

N.V. : Follicular phase : 3.9 – 12 , Mid cycle peak : 6.3 – 24 , Luteal phase : 1.5 – 7 (MIu/ml)

- الهرمون اللويتني LH

أظهرت النتائج انخفاضاً كبيراً في معدل هرمون LH لدى النساء العقيمات عموما إذ بلغ معدله لديهن (1.847 ± 2.437) ملي وحدة عالمية/ مل وقد كان الانخفاض في معدل هرمون LH لدى النساء ذوات العقم الأولي اكبر مما هو عليه لدى ذوات العقم الثانوي غير المترافق مع حدوث حالات إجهاض سابقة وذوات العقم الثانوي المترافق مع حدوث حالات إجهاض سابقة مقارنه مع مجموعة السيطرة (5.020 ± 1.708) ملي وحدة عالمية/ مل وقد اكتسب هذا الانخفاض في معدل مستوى هرمون LH دلاله معنوية جداً ($P < 0.05$) ، كما موضح في الجدول 5.

وعند المقارنة الإحصائية بين المجاميع المدروسة باستخدام اختبار اقل فرق معنوي L.S.D اظهر التحليل الإحصائي انخفاضاً معنويا ($p<0.05$) لدى النساء ذوات العقم الأولي والثانوي المترافق مع حدوث حالات إجهاض سابقة والثانوي غير المترافق مع حدوث حالات إجهاض سابقة مقارنة بالسيطرة .

جاءت هذه النتائج متوافقة مع الكعبي (2005) (29) التي أشارت إلى أن انخفاض LH لدى النساء العقيمات أدى إلى فشل حدوث الاباضة ، إذ أن انخفاض LH ينتج عنه فشل وظيفة الغدد التناسلية مؤدياً إلى أنحباس الطمث Amenorrhea وبالتالي العقم . وقد أشار الباحثون (31,30)إلى الدور المهم لهرمون LH في حدوث الاباضة إذ يكون مسؤول عن أكمال النضج النهائي للجريبة وبالتالي تفجيرها محدثاً الاباضة وكذلك لوتنه الخلايا الحبيبية وخلايا القراب وتكوين الجسم الأصفر وإفراز البروجيستيرون ، أما انخفاض هرمون LH فيلاحظ في حاله ارتفاع مستوى البرولاكتين في الدم ومتلازمة كالمان Kallmann Syndrome ونقص منبهات القند. وهذا ما أثبته المعلى (2006) بدراسة أجريت على الفئران البيض إذ وجد أن الزيادة المستحثة في مستوى هرمون LH بوساطة مستخلص عرق السوس أدى إلى النمو النهائي للجريبة وبالتالي حصول الاباضة وتكوين الجسم الأصفر وإفراز البروجيستيرون.

جدول – 5 : معدل مستوى هرمون LH (ملي وحدة عالمية/ مل)في مصل الدم لمجاميع الدراسة

المجموعة		العدد	مستوى هرمون LH (ملي وحدة عالمية /مل) في مصل الدم			
			الوسط الحسابي ± الانحراف المعياري		أعلى قيمة	اقل قيمة
السيطرة		20	1.708 ± 5.020	a	7.2	1.6
النساء العقيمات /نوع العقم	الكلي	50	2.437 ± 1.847	b	14.6	0.1
	أولي	33	1.801 ± 1.630	b	6.5	0.1
	ثانوي مترافق مع حدوث حالات إجهاض سابقة	12	3.969 ± 2.341	b	14.6	0.2

	ثانوي غير مترافق مع حدوث حالات إجهاض سابقة	5	1.503 ±2.100	b	4.7	1.0

الحروف المتشابهة تعني عدم وجود فروق معنوية والحروف المختلفة تعني وجود فروق معنوية عند مستوى احتمالية ($P<0.05$) .

N.V. : Follicular phase : 1.5 – 8, Mid cycle peak : 9.6 – 80,Luteal phase : 0.2 – 6.5(MIu/ml)

- **هرمون البرولاكتين (هرمون الحليب) PRL**

أظهرت الدراسة الحالية أنخفاض في معدل مستوى هرمون البرولاكتين لدى النساء العقيمات عموما إذ بلغ معدله لديهن (10.194±16.553) نانوغرام/مل وقد كان هذا الانخفاض لدى نساء العقم الثانوي غير المترافق مع حدوث حالات إجهاض سابقة اكبر مما هو علية لدى ذوات العقم الأولي و ذوات العقم الثانوي المترافق مع حدوث حالات إجهاض سابقة مقارنة مع مجموعة السيطرة(18.130 ± 3.437) نانوغرام/مل ألا أن هذا الانخفاض لم ينل دلاله معنوية ($p>0.05$) .

وعند المقارنة الإحصائية بين المجاميع المدروسة باستخدام اختبار اقل فرق معنوي L.S.D اظهر التحليل الإحصائي ارتفاعاً وبفرق معنوي ($P < 0.05$) لدى النساء ذوات العقم الثانوي المترافق مع حدوث حالات إجهاض سابقة مقارنة مع ذوات العقم الثانوي غير المترافق مع حدوث حالات إجهاض سابقة وذوات العقم الأولي ، كما موضح في الجدول 6 .

جدول – 6 : معدل مستوى هرمون PRL (نانوغرام/مل) في مصل الدم لمجاميع الدراسة

المجموعة		العدد	مستوى هرمون PRL (نانوغرام/مل) في مصل الدم			
			الوسط الحسابي ± الانحراف المعياري		أعلى قيمة	اقل قيمة
السيطرة		20	18.130 ± 3.437	a	22.3	11.8
النساء العقيمات /نوع العقم	الكلي	50	16.553 ± 10.194	a	41.6	0.4
	أولي	33	14.910 ± 9.526	b	37.5	0.4
	ثانوي مترافق مع حدوث حالات إجهاض سابقة	12	22.400 ± 11.549	a	41.6	6.8
	ثانوي غير مترافق مع حدوث حالات إجهاض سابقة	5	13.360 ±6.537	b	20.0	5.7

الحروف المتشابهة تعني عدم وجود فروق معنوية والحروف المختلفة تعني وجود فروق معنوية عند مستوى احتمالية ($P<0.05$).

N.V : 1.3 – 25(ng/ml)

- الهرمون المحفز للدرقية TSH

أظهرت النتائج ارتفاعاً في معدل مستوى الهرمون المحفز للدرقية لدى النساء العقيمات إذ بلغ معدله لديهن (2.732 ± 1.662) ملي وحدة عالمية/ مل وقد كان هذا الارتفاع لدى النساء ذوات العقم الثانوي غير المترافق مع حدوث حالات إجهاض سابقة اكبر مما هو عليه لدى النساء ذوات العقم الأولي و ذوات العقم الثانوي المترافق مع حدوث حالات إجهاض سابقة مقارنة مع مجموعة السيطرة(2.230 ± 0.572) ملي وحدة عالمية/ مل ألا أن هذا الارتفاع لم يكتسب دلالة معنوية ($p> 0.05$) .وعند المقارنة الإحصائية بين المجاميع المدروسة باستخدام اقل فرق معنوي L.S.D لم تظهر فروق معنوية ذات دلاله إحصائية على الرغم من الزيادة البسيطة في مستوى الهرمون المحفز للدرقية TSH لدى المجاميع الثلاث للعقم ، كما موضح في الجدول 7.

أن TSH هو المنظم الفسيولوجي الأكثر أهمية في أفعال الدرقية إذ انه يحفز نمو وتميز خلايا الجريبات عن طريق تأثيره في كل خطوة من خطوات بناء وصنع وإفراز هرمونات الدرقية ، ويعمل على زيادة قنص اليود Iodide Trapping وغيرها من العمليات الوظيفية ضمن الغدة الدرقية و يعد قياس تركيز TSH الاختبار الأفضل لتحديد الخلل في وظيفة الدرقية (32).

ولكن هذا التباين لم يرقى إلى درجة الدلالة المعنوية ($P > 0.05$) والسبب قد يرجع إلى خصوصية وحجم العينة المأخوذة .

جدول-7:معدل مستوى هرمون TSH (ملي وحدة عالمية/مل) في مصل الدم لمجاميع الدراسة

المجموعة		العدد	مستوى هرمون TSH(ملي وحدة عالمية/ مل) في مصل الدم		
			الوسط الحسابي ± الانحراف المعياري	أعلى قيمة	اقل قيمة
السيطرة		20	α 0.572 ± 2.230	3.4	1.1
النساء العقيمات/نوع العقم	الكلي	50	α 1.662 ± 2.732	8.8	0.5
	أولي	33	α 1.738 ± 2.827	8.8	0.5
	ثانوي مترافق مع حدوث حالات إجهاض سابقة	12	α 1.400 ± 2.391	5.8	1.0
	ثانوي غير مترافق مع حدوث حالات إجهاض سابقة	5	α 1.957 ±2.920	6.0	0.8

الحروف المتشابهة تعني عدم وجود فروق معنوية ($P >0.05$)

N.V :0.2 – 4.0(MIu/ml)

- الثايرونين ثلاثي اليود T3

أظهرت النتائج أن هنالك انخفاضاً ملحوظاً في معدل مستوى هرمون T3 لدى النساء العقيمات عموما إذ بلغ معدله لديهن (1.764 ± 0.197) ملي مول/لتر وقد كان هذا الانخفاض لدى النساء ذوات العقم الثانوي المترافق مع حدوث حالات إجهاض سابقة ا كبر مما هو علية لدى النساء ذوات العقم الثانوي غير المترافق مع حدوث حالات إجهاض سابقة وذوات العقم الأولي (1.793 ± 0.176) مقارنة مع مجموعة السيطرة (1.910 ± 0.251) ملي مول/لتر وقد اكتسب هذا الانخفاض في معدل مستوى T3 دلاله معنوية ($P < 0.05$) .

وعند المقارنة الإحصائية بين المجاميع المدروسة باستخدام اقل فرق معنوي L.S.D اظهر التحليل الإحصائي انخفاضاً معنوياً ($P < 0.05$) لدى النساء ذوات العقم الثانوي المترافق مع حدوث حالات إجهاض سابقة مقارنة مع مجموعة السيطرة ولم تشكل المقارنات الأخرى أي فروق معنوية ، كما موضح في الجدول 8.

جاءت هذه النتائج متفقة مع جلاب(2007) (33) أن مرضى قصور الدرقية يعانون من انخفاض في مستوى هرمون T3 , كذلك اتفقت مع ما ذكره عدد من الباحثين ومنهم عبد الحسين (2006) (34)الذين أشاروا إلى أن التغيرات في مستويات هرمونات الدرقية وخصوصاً هرمون T3 تؤدي إلى دورات حيضية مضطربة وخلل في الخصوبة ويؤثر في النخامية وإفراز هرمونات الغند Gonadotropin ، وذلك أن هرمونات الدرقية وخصوصاً هرمون T3 يعمل بصورة متنازرة مع هرمون FSH في التأثير المباشر والمحفز للخلايا الحبيبية ومن ضمن هذه التأثيرات المحفزة هي زيادة عدد مستقبلات هرمون LH مؤدياً إلى تحفيز تكوين الهرمونات الستيرويدية .

جدول – 8 : معدل مستوى هرمون T3 (ملي مول/لتر) في مصل الدم لمجاميع الدراسة

المجموعة		العدد	مستوى هرمون T3 (ملي مول/لتر) في مصل الدم		
			الوسط الحسابي ± الانحراف المعياري	أعلى قيمة	اقل قيمة
السيطرة		20	α 0.251 ± 1.910	2.4	1.4
النساء العقيمات/نوع العقم	الكلي	50	b 0.197 ± 1.764	2.4	1.1
	أولي	33	α 0.176 ± 1.793	2.4	1.6
	ثانوي مترافق مع حدوث حالات إجهاض سابقة	12	c 0.245 ± 1.675	1.9	1.1
	ثانوي غير مترافق مع حدوث حالات إجهاض سابقة	5	α 0.178 ±1.780	2.0	1.6

الحروف المتشابهة تعني عدم وجود فروق معنوية والحروف المختلفة تعني وجود فروق معنوية عند احتمالية ($P<0.05$).

N.V.: 6 - 120(mmol/L)

- هرمون الثايرونين رباعي اليود T4

أظهرت النتائج وجود انخفاض طفيف في معدل مستوى هرمون الثايرونين رباعي اليود T4 لدى النساء العقيمات عموما إذ بلغ معدله لديهن (82.126 ± 16.828) ملي مول/لتر وقد كان هذا الانخفاض لدى النساء ذوات العقم الثانوي المترافق مع حدوث حالات إجهاض سابقة اكبر مما هو عليه لدى النساء ذوات العقم الأولي و ذوات العقم الثانوي غير المترافق مع حدوث حالات إجهاض سابقة الا أن هذا الانخفاض لم يكتسب دلالة إحصائية ($P > 0.05$) .

وعند المقارنة الاحصائية بين المجاميع المدروسة باستخدام اختبار اقل فرق معنوي L.S.D اظهر التحليل الإحصائي انحفاضا معنوياً ($P < 0.05$) لدى النساء ذوات العقم الثانوي المترافق مع حدوث حالات إجهاض سابقة فقط مقارنة مع مجموعة السيطرة ، ولم تشكل المقارنات الأخرى أي دلاله معنوية .

على الرغم من أن الانخفاض بسيط في معدل مستوى هرمون T4 لدى المجاميع الثلاث للعقم فأن النتائج تتفق مع العديد من الدراسات ، إذ يعد انخفاض هرمون T4 مؤشر على الإصابة بمرض قصور الدرقية Hypothyroidism وهذا يفسر الانخفاض في مستواه مقارنة بمجموعة السيطرة ، ولكن دون أن يرقى هذا التباين إلى الدلالة المعنوية ، والسبب قد يرجع إلى أن هرمون T4 المتحرر غير فعال وان حوالي 70-80 % من هذا الهرمون يتحول إلى الشكل الفعال T3 بوجود أنزيم deiodinase (35) أو إلى خصوصية وحجم العينة المأخوذة ، كما موضح في الجدول 9 .

جدول - 9 : معدل مستوى هرمون T4 (ملي مول/لتر) في مصل الدم لمجاميع الدراسة

المجموعة		العدد	مستوى هرمون T4(ملي مول/لتر) في مصل الدم		
			الوسط الحسابي ± الانحراف المعياري	أعلى قيمة	اقل قيمة
السيطرة		20	a 11.974 ± 89.320	110.0	63.6
النساء العقيمات/نوع العقم	الكلي	50	a 16.828 ± 82.126	116.1	48.9
	أولي	33	a 17.132 ± 84.330	116.1	52.0
	ثانوي مترافق مع حدوث حالات إجهاض سابقة	12	b 10.529 ± 74.566	89.0	53.1
	ثانوي غير مترافق مع حدوث حالات إجهاض سابقة	5	a 24.254 ±85.720	110.0	48.9

الحروف المتشابهة تعني عدم وجود فروق معنوية والحروف المختلفة تعني وجود فروق معنوية عند احتمالية ($P<0.05$).

N.V.: 0.95 – 2.5(mmol/L)

6- العلاقة بين BMI للنساء العقيمات و المعدل المصلي للهرمونات

أظهرت نتائج قياس مستوى الهرمونات الجنسية المتمثلة بـ Follicle stimulating hormone , Leutinizing hormone في مصل دم النساء العقيمات انخفاضا معنويا ($P<0.05$) في معدل تركيز هذة الهرمونات بزيادة الـ BMI مقارنة مع مجموعة السيطرة , في حين لم تظهر نتائج قياس مستوى كل من الـ Prolactin , T3, T4 وجود خلل في تركيز هذة الهرمونات بزيادة الـ BMI مقارنة مع مجموعة السيطرة لذلك لم يظهر التحليل الإحصائي وجود فروق معنوية ($P>0.05$) في معدل تركيز هذة الهرمونات كما موضح في الجدول 10 . وهذا ما يقوي دور السمنة وزيادة Body mass index كعامل مؤثر في قلة الخصوبة , إذ تؤثر السمنة الزائدة على افراز GnRH من تحت المهاد حيث يؤثر هذا الهرمون على إفراز كل من FSH و LH من النخامية مؤديا إلى فشل حدوث الاباضة وعدم انتظام الدورة الحيضية و بالتالي العقم لدى النساء (37,36) .

جدول – 10 : العلاقة بين BMI للنساء العقيمات و المعدل المصلي للهرمونات

معامل كتلة الجسم BMI	مستوى الهرمونات (الوسط الحسابي ± الانحراف المعياري)				
	FSH	*LH*	*Prolactin*	*T3*	*T4*
السيطرة	1.458±7.075 a	1.708 ±5.020 a	3.437 ±18.130 a	0.251±1.910 a	11.974 ±89.320 a
25.9-25	2.755±5.572 a	4.877 ±5.114 a	4.272 ±17.000 a	0.160 ±1.828 a	9.724 ±78.685 a
26.9-26	3.853±6.522 a	2.343 ±2.966 a	9.163 ±17.282 a	0.185±1.822 a	15.483 ±85.244 a
27.9-27	1.975±3.630 b	1.114 ±1.230 b	12.851 ±18.870 a	a0.330 ± 1.730	17.888 ±79.430 a
28.9-28	0.070±4.55 a	0.028 ±1.220 b	6.151 ±14.850 a	0.070 ± 1.850 a	15.627 ±91.400 a
29.9-29	0.614±0.912 b	0.500 ±0.650 b	17.041 ±16.750 a	0.141 ±1.800 a	22.500 ± 81.250 a
>=30	2.709±4.486 a	1.410 ±1.553 b	9.354 ±13.777 a	0.152±1.780 a	16.411 ±78.940 a

N.V. : FSH : 3.9-12 , LH : 1.5-8 , PRO : 1.3-25 ,T3 : 0.95-2.5 , T4 :6-120

الحروف المتشابهة تعني عدم وجود فروق معنوية والحروف المختلفة تعني وجود فروق معنوية عند مستوى احتمالية ($P<0.05$)

نستنتج من الدراسة الحالية :-

- الاصابة بالعقم الاولي اعلى من الاصابة بالعقم الثانوي.
- الفئة العمرية (25-35)سنة هي اكثر تكرارا لدى النساء العقيمات.
- مدة (1-4)سنة كانت هي الاكثر تكرار لدى النساء العقيمات.
- ارتفاع دليل كتلة الجسم لدى النساء العقيمات.
- اضطراب مستوى الهرمونات لدى النساء العقيمات
- انخفاض مستوى هرمونات الخصوبة بزيادة BMI

المصادر

1. Butler, P. "What constitutes sexual health? Progress in Reproductive Health Research" 67:3-4. (2004) .

2. البرنوطي ,رمزي" المني البشري والعقم" نشر الشركة الوطنية للتوزيع والنشر , شركة الاعتدال للطباعة الفنية المحدودة بغداد ، الطبعة الأولى. (1993).

3. FAQ(American Society for Reproductive Medicine) "Frequently Asked Questions About Infertility "(2006).

4. Rowe , P. J ., Comhaire , F.H. , Hargreave , T.B.& Mahmoud , A.M.A." WHO Manual for the Standardized Investigation, Diagnosis and Management of the Infertile Male" Cambridge University . (2000).

5. Adamson, G .D.& Baker, V.L." Subfertility: causes, treatment and outcome" Best Pract . Res. Clin. Obstet. Gynecol., 17:169-85. (2003).

6. Demers ,L.M. " General endocrinology. In: Clinical Chemistry " Kaplen ,L.A. ,Peesce,A.J. & Kozmierczak,C.S. (eds.) . Mosby .London : 809-826. (2003) .

7. Nye, E. " The gonads. In : Clinical Chemistry " Kaplen ,L.A. ,Peesce, A.J. & Kozmierczak, C.S. (eds.) . Mosby .London : 849-875. (2003).

8. Jose, A. & Boyden ,M.D. "Infertility " American Family Physician , 75(6):849-856. (2007) .

9. Hill, J. A. "Sporadic and recurrent spontaneous abortion " In: Kistner , R.W. ed. Kistners Gynecology : Principles and Practice . Mosby –Year Book. London . 6th ed. : 330-365. (1995) .

10. Berer,M." Making abortion safe : a matter of good public health policy and practice" Bulletin of WHO ., 78(5):580-592. (2000).

11. Cunningham ,R.G. , MacDonald ,P.C. ,Gant ,N.F. , Leveno ,K.J. ,Gilstrap , L.C. & Hankins ,C. William á s " Obstetrics" Appleton &Lange .U.S.A. 20th ed. , (1997).

12. Haslett ,C. ,Chilvers ,E.R. ,Boon ,N.A. & Colledge ,N.R. "The thyroid gland , Principles and Practice of Medicine " India . 19th ed., : 689-693,298. (2002).

13. Homan ,G.F. , Davies, M. & Norman ,R. "The impact of life style factors on reproductive performance in the general population and those undergoing infertility treatment: a review " Human Reproduction Update, 13(3) :209–223. (2007).

14. Muhammad , W.J." Some microbiological and immunological studies of female genital tract infections " Ms.D. College of Medicine. University of Baghdad. (2007).

15. Leridon , H. "Can assisted reproduction technology compensate for the natural decline in fertility with age? A model assessment" Human Reproduction , 19(7): 1548-1553. (2004).

16. Baird ,D.T. ,Collins .J. , Egozcue , J. ,Evers ,L.H. , Gianaroli ,L., Leridon ,H. ,Sunde ,A. ,Templeton ,A.,Van Steirteghem ,A., Cohen, J., Crosignani, P.G., Devroey, P.,Diedrich, K., Fauser ,B.C., Fraser, L., Glasier ,A., Liebaers, I., Mautone, G., Penney, G.& Tarlatzis, B.. "Fertility and ageing " Hum. Reprod .Update , 11(3):261-276. (2005).

17. Kaplan ,B. ,Nahum ,R. ,Yairi ,Y. ,Hirsch ,M. ,Pardo ,J.,Yogev ,Y. & Orvieto,R. " Use of various contraceptive methods and time of conception in acommunity-based population " Eur.J.Obstet .Gynecol.Reprod .Biol. , 123:72-76. (2005).

18. Hassan ,M.A. & Killick ,S.R. "Effect of male infertility : evidence fort the decline in male fertility with increasing age " Fertil .Steril. , 79(3):1520 -1527. (2003).

19. Lampic, C. , Svanberg, A.S. , Karlstrom, P. & Tyden, T. "Fertility awareness, intention sconcerning childbearing, and attitudes toward

sparent hood among female and male academics " Hum. Reprod. , 21: 558–564. (2006).

20. Rich-Edwards , J. W. , Spiegelman, D. , Garland, M. , Hertzmark, E. , Hunter ,D.J., Colditz, G.A., Willett ,W. C.W. & HandManson, J.E. "Physical activity, body mass index, and ovulatory disorder infertility" Epidemiology , 13: 184–190. (2002) .

21. Pasquali, R., Pelusi , C. , Genghini ,S . , Cacciari, M. & Gambineri, A. "Obesity and reproductive disorders in women" Hum . Reprod . Update , 9: 359–372. (2003) .

22. Fedorcsak ,P. ,Dale ,P.O. ,Storeng ,R. ,Ertzeid ,G. ,Bjercke ,S. ,Oldereid ,N. ,Omland ,A.K. , Abyholm ,T. & Tanbo ,T. "Impact of over weigth and under weight on assisted reproduction treatment " Hum.Reprod . , 19:2523-2528. .(2004).

23. Jose –Miller ,A. & Boyden ,M.D. "Infertility " American Family Physician , 75(6):849-856. (2007) .

24. Richards ,J.S. , Ireland ,J.J. , Rao ,M.C. , Bernath ,G.A.,Midgley, A.R. & Reichert, L.E."Ovarian follicular development in the rat : hormone receptor regulation by estradiol , follicle stimulating hormone and luteinizing hormone" Endocrinology , 99:1562. (1976).

25. Brown ,J.B. & Gronow ,M. "Endocrinology of ovulation prediction, In: Clinical Reproductive Endocrinology" Sherman, Churchill Livingstone Edinburgh ,R.P.(ed.),U.K.:164-185. .(1985).

26. Balasch, J., Miro, F.& Burzaco, I. "The role of Luteinizing hormone in human follicle development and Oocyte fertility " Am. J. Puplic. Health, 82 : 67-82. (1990).

27. Yanagimachi ,R. , Okada ,A. & Tung ,K.S. "Sperm auto antigenes and fertilization .Effects of anti –guinea pig serum antibodies on sperm – ovum interaction " Bio. Reprod . , 24:512. (1981) .

28. المعلى, اشراق كاظم عباس " تأثير مستخلص عرق السوس على تحفيز الاباضة في إناث الفئران غير البالغة" رسالة دبلوم عالي في التقنيات المختبرية المساعدة على الإنجاب ، معهد أبحاث الأجنة وعلاج العقم , جامعة النهرين . (2006).

29. ألكعبي , ميسون عبد الجليل " التغيرات المرافقة لتحفيز الاباضة عند النساء العقيمات" رسالة دبلوم عالي في التقنيات المختبرية المساعدة على الإنجاب ، معهد أبحاث الأجنة وعلاج العقم ، جامعة بغداد . (2005).

30. Sadler ,T.W. "Longmans Medical Embryology " Lippincott Williams & Wilkins , Philadelphia , 9th ed., : 3-49. (2004) .

31. Goldman , M.D. & Bennett , C. "Ovaries and development , menstrual cycle and infertility (women's health). In: Cecial text book of medicine" W.B. Saunders ,Philadelphia, 21th ed . : 1490 - 1509. (2004).

32. Park , H.S. , Kim , J.y. , Park , K.y. , Gong. G. & Hong , S.J. "Expression of human iodide sodium symporter mRNA in primary and meta static papillary thyroid carcinoma" Thyroid, 10(3): 211-7. (2000).

33. جلاب ،راوية فوزي "فقر الدم بعوز الحديد وبعض المؤشرات الكيمياء الحياتية لدى مرضى قصور الدرقية العراقين ومدى الاستجابة للعلاج بالثيروكسين " رسالة ماجستير ،كلية التقنيات الصحية والطبية (2007).

34. عبد الحسين, ذكرى عبد الأمير صاحب " تأثير قلف نبات الدارسين *Cinnamomum zeylanicum* في فعالية الغدة الدرقية وعلاقتها بالمبيض في إناث الجرذ " رسالة ماجستير ، كلية العلوم للبنات، جامعة بغداد (2006) .

35. Kirkegaard , C .& Faber, J. "The role of thyroid hormones in depression" Eur. J .Endocrinol ., 138 (1): 1-9. (1998).

36. Mitchell, M., Armstrong, D.T. , Robker, R.L.& Norman,R.J. "Adipokines:implications for female fertility and obesity" Reproduction.,130:583-597. (2005).

37. Norman, R.J., Noakes, M.W., Davies, M.J., Moran, L.& Wang, J.X. " Improving reproductive performance in over weight obese women with effective weight management" Hum . Reprod . Update , 10: 267–280. (2004).

دراسة الخواص التنموية لعزلات بكتريا حامض اللاكتيك المحلية لأستخدامها كمعززات حيوية (Probiotics)

جيهان عبد الستار سلمان[1] وعبد الواحد باقر[2] وسمير فتح الله سمعان [3]
(1 و 3) قسم علوم الحياة / كلية العلوم / الجامعة المستنصرية
(2) كلية العلوم / جامعة النهرين

تاريخ تقديم البحث : 2011/ 3/27 تاريخ قبول البحث : 2011/ 5/29

ABSTRACT

Resistance of the Four Lactic acid bacteria (LAB) isolates *(Lactobacillus gasseri , Lb.fermentum,Lb . plantarum, Lactococcus lactis)* to various levels of pH (1,2,3,4,5,6) and bile salts (0.05 , 0.15, 0.30)% for different periods of times(2,4,6,24) h. was studied along with viability of such isolates during freezing for (3) months, as well as, testing their susceptibility to antibiotics. The results showed that the isolates of LAB resist high acidity even with pH 1 for (24)h. Also the isolates resist bile salts reaching to concentration (0.30 %) for the same period. Isolates show good ability to survive during freezing for (3) months. All the isolates of LAB resisted Streptomycin, Cefalexin, Rifampicin Gentamicin and all of them were sensitive to Chloramphenicol, but they were different in sensitivity for other antibiotics.

المقدمة

تعد المقاومة للمؤثرات الهاضمة واحدة من اهم العوامل التي تحدد استخدام الاحياء المجهرية كمعززات حيوية حية ، ويمكن ان تعزى قدرة البكتريا على تحمل الظروف القاسية الى المقاومة الداخلية او الاستجابة للتطبع والذي يتضمن العديد من التحويرات الفسلجية والتركيبية للبكتريا ، ونظراً لاستخدام المعززات الحيوية بشكل رئيسي لعلاج الاضطرابات المعوية ، لذا لابد ان تعرض البكتريا المستخدمة في هذا المجال الى العديد من المؤثرات الكيميائية والفيزيائية قبل استخدامها من قبل الانسان (1). من المزايا المستخدمة في انتخاب البكتريا لاستخدامها كمعززات حيوية هي مقاومتها للحموضة واملاح الصفراء والتي تمثل المواد المثبطة للاحياء المجهرية في اعلى القناة الهضمية ، اذ يدل عدم قدرة السلالات على البقاء اثناء العبور خلال المعدة واعالي الامعاء على عدم توفر اعداد كافية من هذه البكتريا لتمكنها من اظهار التأثير المفيد . كما ووجد ان الاغذية الحاملة لتلك البكتريا ولا سيما منتجات الالبان تحفز على بقاءها

في القناة الهضمية من خلال معادلة الاس الهيدروجيني وعملها كمادة واقية للبكتريا (2) و(3). أشار (4) الى قدرة البكتريا على البقاء واستعمار القناة الهضمية عندما تتمتع بمقاومة عالية للحموضة واملاح الصفراء فضلاً عن قدرتها على الالتصاق بسطح الامعاء . واكد (5)ان هناك عدة امور يجب ان تؤخذ بنظر الاعتبار عند تحديد مدى امكانية بقاء وعبور بكتريا المعززات الحيوية خلال اعلى القناة الهضمية والتي اهمها حموضة المعدة و مدة تعرضها للحامض و تركيز املاح الصفراء وطول مدة التعرض لها .

أكدت الدراسات قدرة بكتريا حامض اللاكتيك على البقاء والعبور خلال القناة الهضمية ، كما وبينت ان بكتريا *Lb.plantarum* احتفظت بقدرتها الجيدة على البقاء حية مقارنة ببقية سلالات بكتريا حامض اللاكتيك التي اختبرت مواصفاتها الدوائية في القناة الهضمية (3) . ونظرا لقلة الدراسات المحلية لأنتقاء عزلات من بكتريا حامض اللاكتيك المعزولة من مصادر مختلفة تمتلك مواصفات المعززات الحيوية فقد هدفت الدراسة الى أختبار قابلية العزلات المحلية لهذه البكتريا على مقاومة الظروف البيئية التي تؤهلها للاستخدام كمعززات حيوية.

المواد وطرائق العمل

عزلات بكتريا حامض اللاكتيك :

أنتخبت أربع عزلات من مجموع 75 عزلة تعود لبكتريا حامض اللاكتيك والتي عزلت من مصادر مختلفة شملت براز الأطفال الرضع ومهبل النساء الصحيحات والأغذية ، وشخصت بأتباع الفحوصات الكيمو حيوية الواردة في (6) و (7) لغرض دراسة خواصها المزرعية ، وشملت هذه العزلات :

Lactobacillus gasseri و ***Lb.fermentum*** و ***Lb.plantarum*** و ***Lactococcus lactis***

قابلية بكتريا حامض اللاكتيك على مقاومة الحموضة :

حضر وسط De-Man Regosa Sharpe (MRS) السائل بست قيم من الأس الهيدروجيني(1 و2 و3 و4 و5 و 6). لقحت أنابيب الأختبار الحاوي كل منها على (10) ملليتر من الأوساط المذكورة ب(0.1) ملليتر من مزارع بكتريا حامض اللاكتيك بعمر (18-24) ساعة ، وحضنت بحرارة (37) م^{o} لفترات (2 و4 و6) ساعة ، فضلا عن (24) ساعة للتأكد من قابلية العزلات على النمو في تلك القيم من الاس الهيدروجيني لفترة طويلة . لوحظ

النمو في كل أنبوبة ولكل فترة من فترات الحضن فضلاً عن وقت الصفر من خلال قياس الكثافة الضوئية على الطول الموجي 620 نانوميتر (8) و (9).

تم تقييم مقاومة عزلات بكتريا حامض اللاكتيك للحموضة حسب ما ذكره (9) ووفقاً للسلم الآتي:

- مقاومة ممتازة [في حالة زيادة النمو في جميع قيم الأس الهيدروجيني المستخدمة ولجميع فترات الحضن وصولاً إلى (24) ساعة] .
- مقاومة جيدة جداً [في حالة زيادة النمو في ثلاثة من قيم الأس الهيدروجيني ولجميع فترات الحضن وصولاً إلى (24) ساعة] .
- مقاومة جيدة [زيادة النمو في واحد او اثنين من قيم الأس الهيدروجيني ولجميع فترات الحضن المستخدمة ، او زيادة النمو في جميع قيم الأس الهيدروجيني ولفترة حضن (4) ساعات فقط] .
- مقاومة مقبولة [زيادة النمو في أس هيدروجيني واحد ولجميع فترات الحضن وصولاً إلى (24) ساعة أو لاثنين من قيم الاس الهيدروجيني ولغاية فترة الحضن (4) ساعات] .
- حساسة [عدم حصول زيادة في النمو لأي من قيم الأس الهيدروجيني المذكورة ولجميع فترات الحضن]

قابلية بكتريا حامض اللاكتيك على مقاومة أملاح الصفراء :

حضر وسط MRS السائل وأضيف له (كلا على انفراد) (0.05 و 0.15 و 0.30) %من املاح الصفراء(30%)المعقم مسبقاً، فضلا عن وسط MRS السائل الخالي من أملاح الصفراء كمعاملة سيطرة . لقحت أنابيب الإختبار الحاوي كل منها على (10) ملليتر من الأوساط آنفة الذكر ب(0.1) ملليتر من مزارع بكتريا حامض اللاكتيك ، وحضنت الأنابيب بحرارة (37) م^{o} لفترات (2 و 4 و 6) ساعة. فضلا عن (24) ساعة للتأكد من قابلية العزلات على النمو في تراكيز املاح الصفراء المذكورة لفترة طويلة. لوحظ النمو في كل أنبوبة ولكل فترة من فترات الحضن من خلال قياس الكثافة الضوئية على الطول الموجي 660 نانوميتر (9).

حساسية عزلات بكتريا حامض اللاكتيك للمضادات الحيوية :

أختبرت حساسية بكتريا حامض اللاكتيك لـ(13) نوع من أنواع المضادات الحيوية هي : Streptomycin و Cefalexin و Rifampicin و Gentamicin و Lincomycin و Chloramphenicol و Ampicillin و Erythromycin و Neomycin و Co-trimoxazole و Ceftriaxon و Tetracyclin و Trimethoprime

وبإستخدام طريقة الأقراص التي وصفها (10) و(11) .

عيوشية عزلات بكتريا حامض اللاكتيك عند الخزن بالتجميد :

لقح وسط MRS السائل الحاوي على (10%) كليسيرول بمزارع بكتريا حامض اللاكتيك بعمر (24) ساعة ، وبعد فترة حضن (24) ساعة تم خزن البكتريا بالتجميد . قدر العدد الحي لبكتريا حامض اللاكتيك قبل الخزن وبعد (3) أشهر من الخزن بطريقة عد الأطباق على وسط MRS الصلب (9) .

النتائج والمناقشة

قابلية عزلات بكتريا حامض اللاكتيك على مقاومة الحموضة

تعد مقاومة الحموضة من الأمور الواجب مراعاتها عند إنتخاب بكتريا المعززات الحيوية ، وللتأكد من التأثير المفيد لتلك البكتريا في القناة الهضمية يجب أن تكون البكتريا المستخدمة لها القدرة على البقاء أثناء المرور خلال المعدة والتي تتميز بإنخفاض الأس الهيدروجيني ووقت العبور فيها قصير ، ويعد بقاء البكتريا عند أس هيدروجيني واطئ لمدة ساعتين قياسياً لمقاومة بكتريا المعززات الحيوية للحموضة (12)و(13) . ولذا فقد أختبرت قابلية عزلات بكتريا *Lb.gasseri* و *Lb.fermentum* و *Lb.plantarum* و *Lc.lactis* على النمو في الظروف الحامضية والتي تمثلت بقيم الأس الهيدروجيني (1 و 2 و 3 و 4 و5 و 6) ولفترات الحضن (0 و 2 و 4 و 6) ساعة فضلاً عن (24) ساعة للتأكد من قابلية البكتريا على تحمل الأس الهيدروجيني الواطئ لفترة طويلة .

تبين النتائج في الجدول (1) قدرة عزلات بكتريا حامض اللاكتيك على النمو في الظروف الحامضية وللفترات الزمنية المستخدمة ، إذ لوحظ زيادة كثافة النمو بزيادة فترة الحضن لكل قيم الأس الهيدروجيني ، في الوقت نفسه إنخفضت كثافة النمو بإنخفاض الأس الهيدروجيني للوسط .

أعطت العزلات الأربعة قيد الدراسة أعلى كثافة نمو عند الأس الهيدروجيني (6). وتمكنت العزلات أعلاه من النمو في الأس الهيدروجيني (5 و 4 و 3) مع حدوث إنخفاض في كثافة النمو مقارنة بالأس الهيدروجيني (6) ،ويدى الإنخفاض في كثافة نمو العزلات أكثر وضوحاً عند الأس الهيدروجيني الواطئ (2 و 1) ، وكانت أقل كثافة نمو لها عند الأس الهيدروجيني الأخير . ولدى ملاحظة كثافة النمو للعزلات لفترة الحضن (24) ساعة أمكن التأكد من قابليتها على تحمل الحموضة ولفترة زمنية طويلة . وقد بينت النتائج أعلاه ان بكتريا *Lb.fermentum* أكثر العزلات تحملاً للأس الهيدروجيني الواطئ ، إذ أعطت كثافة نمو أعلى

من بقية العزلات عند الأس الهيدروجيني (2 و 1) . كما إن كثافة نموها عند الأس الهيدروجيني (1) كانت أعلى مما هو عليه للعزلات الثلاثة عند الأس الهيدروجيني (2) . فيما أعطت العزلة *Lc.lactis* أعلى كثافة نمو عند قيم الأس الهيدروجيني (6 و 5 و 4 و 3) مقارنة ببقية العزلات ، وكانت هذه العزلة أقل العزلات تحملاً للأس الهيدروجيني (2 و 1) . مع كل ذلك كانت عزلات بكتريا حامض اللاكتيك قيد الدراسة قادرة على مقاومة الحموضة ، إذ تمكنت من النمو في كل قيم الأس الهيدروجيني ولاسيما في أقسى الظروف الحامضية والمتمثلة بالأس الهيدروجين (1) ولفترة طويلة بلغت (24) ساعة . ووفقاً لذلك يمكن إعتبار تلك العزلات ممتازة من حيث مقاومتها للحموضة إستناداً إلى التقسيم الذي وضعه(9) . ونظراً لمقاومة العزلات *Lb.gasseri* و *Lb.fermentum* و *Lb.plantarum* و *Lc.lactis* للحموضة يمكن ضمان قابلية تلك العزلات على العبور عبر المعدة وصولاً إلى الأمعاء ، إذ إن الأس الهيدروجيني للمعدة يتراوح بين (5) عند تناول الطعام ويصل إلى (1.8) بعد مرور (80) دقيقة من تناول الطعام (5) .

جدول -1 : قابلية عزلات بكتريا حامض اللاكتيك على النمو في قيم أس هيدروجيني مختلفة

العزلة	فترة الحضانة (ساعة)	الكثافة الضوئية (OD) عند pH					
		6	5	4	3	2	1
Lb. Gasseri	0	0.0276	0.0241	0.0239	0.0230	0.0229	0.0217
	2	0.1305	0.0660	0.0636	0.0612	0.0458	0.0245
	4	0.2456	0.0995	0.0890	0.0776	0.0652	0.0301
	6	0.5251	0.4208	0.3545	0.2691	0.0676	0.0344
	24	1.7037	1.5070	1.2656	0.9248	0.0862	0.0615
Lb. fermentum	0	0.0282	0.0232	0.0261	0.0250	0.0247	0.0235
	2	0.2340	0.0895	0.0792	0.0540	0.0452	0.0355
	4	0.6318	0.0946	0.0936	0.0860	0.0811	0.0749
	6	0.7167	0.4695	0.4162	0.3501	0.0899	0.0792
	24	1.9731	1.6813	1.2343	1.0243	0.1236	0.1029
Lb. plantarum	0	0.0288	0.0287	0.0265	0.0257	0.0231	0.0218
	2	0.1156	0.0330	0.0274	0.0270	0.0267	0.0266
	4	0.1709	0.0817	0.0759	0.0479	0.0410	0.0380
	6	0.5449	0.4784	0.3826	0.1984	0.0557	0.0393
	24	1.8646	1.8111	1.4288	1.0510	0.0916	0.0589
Lc. Lactis	0	0.0281	0.0260	0.0241	0.0222	0.0233	0.0247
	2	0.0801	0.0850	0.0624	0.0561	0.0271	0.0261
	4	0.1249	0.0930	0.0770	0.0622	0.0365	0.0290
	6	0.5639	0.5164	0.4289	0.3161	0.0408	0.0305
	24	2.0227	1.8619	1.5523	1.1116	0.0775	0.0439

تعزى مقاومة عزلات بكتريا حامض اللاكتيك للحموضة إلى إمتلاكها نظام تحمل الحموضة (Acid tolerant System) ، اذ تتمكن البكتريا من حفظ التغير في الأس الهيدروجيني من خلال خفض الأس الهيدروجيني الداخلي للخلايا (Intracellular pH) والذي بدوره يمنع تراكم وتجمع الفائض من أدينوسين ثلاثي الفوسفات (ATP) والآيونات السالبة الشحنة داخل الخلايا والتي تعد من العوامل السامة للبكتريا (14) .

لاحظ (13) إن لبكتريا *Lb.fermentum* المعزولة من الإنسان القابلية على البقاء في الأس الهيدروجيني (2) لمدة ساعتين , فيما أشار(15) إلى قابلية بكتريا *Lb.fermentum* و *Lb.plantarum* على البقاء في الأس الهيدروجيني (3 و 2.3) وبذلك تتمكن تلك العزلات من البقاء والمرور خلال المعدة إلى الأمعاء كما تمكن(9) من الحصول على عزلات تعود لبكتريا حامض اللاكتيك إتصفت بمقاومتها للحموضة عند نموها في قيم الأس الهيدروجيني (2 و 4 و 5).

قابلية عزلات بكتريا حامض اللاكتيك على مقاومة أملاح الصفراء

تعد المقاومة لأملاح الصفراء واحدة من الشروط الواجب توفرها في البكتريا عند إستخدامها كمعزز حيوي (12) . ولذا فقد تم إختبار قابلية عزلات بكتريا حامض اللاكتيك على النمو بوجود تراكيز مختلفة من أملاح الصفراء . يوضح الجدول (2) قدرة بكتريا *Lb.gasseri* و *Lb.fermentum* و *Lb.plantarum* و *Lc.lactis* على تحمل تراكيز أملاح الصفراء المستخدمة ، فقد تمكنت بكتريا *Lb.gasseri* من النمو بوجود أملاح الصفراء بتركيز (0.05 و 0.15 و 0.30)% ، ومع كون الزيادة في النمو كانت بطيئة عند تنميتها لمدة (2 و 4) ساعات ، إلاّ إنها أصبحت بارزة بعد (6) ساعات وكثيفة بعد (24) ساعة .

جدول -2 : قابلية عزلات بكتريا حامض اللاكتيك على النمو في تراكيز مختلفة من أملاح الصفراء(30%)

العزلة	فترة الحضانة (ساعة)	الكثافة الضوئية (OD)			
		تركيز املاح الصفراء (%)			
		*السيطرة	0.05	0.15	0.30
Lb. Gasseri	0	0.0210	0.0219	0.0248	0.0281
	2	0.0542	0.0275	0.0273	0.0296
	4	0.0825	0.0475	0.0460	0.0436
	6	0.3864	0.1521	0.1220	0.1000
	24	2.0751	1.8730	1.8692	1.6731

Lb. fermentum	0	0.0322	0.0352	0.0366	0.0396
	2	0.0734	0.0644	0.0600	0.0595
	4	0.1944	0.1772	0.1266	0.0856
	6	0.8074	0.7651	0.5990	0.4450
	24	2.1773	2.1220	1.9901	1.8861
Lb. plantarum	0	0.0349	0.0353	0.0374	0.0378
	2	0.0644	0.0621	0.0613	0.0611
	4	0.8780	0.7987	0.6852	0.5807
	6	1.1982	1.1532	1.1498	1.1103
	24	1.8962	1.8951	1.7733	1.7054
Lc. Lactis	0	0.0344	0.0359	0.0366	0.0369
	2	0.0838	0.0778	0.0750	0.0626
	4	0.8524	0.6357	0.5730	0.4016
	6	1.3942	0.9800	0.9221	0.8783
	24	2.0457	1.7932	1.6362	1.6024

* : بدون املاح الصفراء

أما بكتريا *Lb.fermentum* فقد تقارب نموها في معاملة السيطرة وفي الوسط الحاوي على (0.05%) أملاح الصفراء (جدول 2).

وكان الحال متشابهاً مع بكتريا *Lb.plantarum* التي بدى نموها متقارباً عند تنميتها في معاملة السيطرة وتركيز (0.05%) أملاح الصفراء ، ولوحظ إنخفاض بسيط في النمو عند زيادة تركيز أملاح الصفراء إلى (0.15 و 0.30)% مقارنة مع معاملة السيطرة .وإمتلكت بكتريا *Lc.lactis* أيضاً القدرة على النمو بوجود تراكيز من أملاح الصفراء ، فقد إزدادت كثافة النمو بزيادة فترة الحضن لدى تنميتها بوجود (0.05 و 0.15 و 0.30)% أملاح الصفراء (جدول 2).

لدى المقارنة بين قابلية العزلات الأربعة على تحمل تراكيز أملاح الصفراء لوحظ إن العزلة *Lb.fermentum* كانت أكثر تحملاً من العزلات الثلاثة الأخرى ، عندما كانت كثافة نموها أعلى من بقية العزلات عند التراكيز (0.05 و 0.15 و 0.30)% من أملاح الصفراء كما كانت كثافة نموها عند التركيز (0.30%) أعلى من كثافة نمو العزلات الأخرى عند التركيز الأقل من ذلك (0.15%) .

يتوضح من النتائج هذه قدرة العزلات *Lb.gasseri* و *Lb.fermentum* و *Lb.plantarum* و *Lc.lactis* على مقاومة تراكيز أملاح الصفراء للفترات الزمنية (2 و 4 و 6) ساعة ، فضلاً عن تأكيد مقاومتها هذه لفترة أطول لدى تنميتها لمدة (24) ساعة ، والتي قد تعطي أملاً في قدرة تلك العزلات على البقاء لفترة طويلة في التجويف المعوي للإنسان على الرغم من وجود أملاح الصفراء التي تعد عاملاً مثبطاً للعديد من الأحياء المجهرية الداخلة إلى الجهاز الهضمي. ويمكن أن تعزى قدرة العزلات على مقاومة أملاح الصفراء إلى طبيعة

بروتينات الجدار الخلوي (Surface Layer Protein-SLP) للبكتريا ، إذ وجد إن (30%) من الأحماض الأمينية المكونة لبروتينات هذه الطبقة تكون من الأنواع الكارهة للماء مما يؤدي إلى كره وإبتعاد هذا الغشاء عن الماء ، فضلاً عن وجود أواصر هيدروجينية تربط طبقات (SLP) من طبقات الجدار الخلوي للبكتريا مما يعطيها قدرة على مقاومة تراكيز أملاح الصفراء في بيئتها (16) . وكان (8) و(17) قد أشاروا إلى قدرة سلالات بكتريا حامض اللاكتيك على النمو في البيئات الحاوية على أملاح الصفراء بتركيز (0.30%) ، فيما تمكن (9) من الحصول على عزلات من بكتريا حامض اللاكتيك تتصف بقدرتها على النمو بوجود تراكيز (0.05 و 0.15 و 0.30)% من أملاح الصفراء .

أما الدراسات الجينية حول مقاومة بكتريا حامض اللاكتيك المعزولة من الإنسان لأملاح الصفراء فقد أشارت إلى وجود جينات مشفرة للأنزيمات المحللة لأملاح الصفراء يطلق عليها (Bile Salthydrolase (*bsh*) gens) والتي تلعب دوراً في زيادة المقاومة للمستويات السامة من أملاح الصفراء في القناة المعوية . ووصفت تلك الجينات في بكتريا *Lb.plantarum* و *Lb.johnsonii* و *Bifidobacterium longum* التي اخضعت لتلك الدراسة (3) .

حساسية عزلات بكتريا حامض اللاكتيك للمضادات الحيوية

أخضعت العزلات *Lb.gasseri* و *Lb.fermentum* و *Lb.plantarum* و *Lc.lactis* لفحص الحساسية لعدد من المضادات الحيوية . ويلاحظ من الجدول (3) إن جميع العزلات هذه كانت مقاومة للمضادات (Streptomycin و Cefalexin و Rifampicin و Gentamicin) ، كما وكانت مقاومة أيضاً لمضاد (Trimethoprime) بإستثناء العزلة *Lb.gasseri* عندما أدى المضاد هذا إلى تثبيط نموها بقطر بلغ (24) ملميتر ، كذلك قاومت العزلات مضاد (Ampicillin) بإستثناء العزلة *Lc.lactis* التي كان تأثرها به ضعيفاً عندما بلغ قطر منطقة تثبيطها (10) ملميتر .

تباين تأثر العزلات ببقية المضادات المستخدمة ، إذ قاومت جميع العزلات مضاد (Neomycin) بإستثناء العزلة *Lb.gasseri* التي كان تأثرها ضعيفاً له ، إذ بلغ قطر منطقة التثبيط (12) ملميتر . وكان تحسس بكتريا *Lc.lactis* ضعيفاً لمضاد (Erythromycin) حين بلغ قطر منطقة التثبيط (11) ملميتر ، في حين كانت مقاومة لمضاد (Tetracyclin) . فيما كان تأثر العزلات *Lb.gasseri* و *Lb.fermentum* و *Lb.plantarum* أكبر عندما بلغت أقطار منطقة التثبيط على التوالي (20 و 20 و 15) ملميتر لمضاد (Tetracyclin)

(23 و 18 و 15) ملميتر على التوالي لمضاد (Erythromycin) . أما بالنسبة لبقية المضادات فكانت العزلة *Lb.gasseri* مقاومة لمضادات (Lincomycin و Cefalexin و Rifampicin) في الوقت الذي كانت فيه حساسة لمضاد (Co-trimoxazole) عندما بلغ قطر التثبيط (29) ملميتر ، وكان تأثرها بسيطاً **لمضاد** (Ceftriaxon) حيث بلغ قطر التثبيط (12) ملميتر . وفي الوقت الذي أظهرت فيه بكتريا *Lb.fermentum* مقاومة للمضادات المذكورة أعلاه ، فقد تباين تأثر العزلتين *Lb.plantarum* و *Lc.lactis* بتلك المضادات وذلك عندما قاومت مضادات (Cefalexin و Ceftriaxon) في الوقت الذي كان تأثرها ضعيفاً بمضاد (Lincomycin) بقطر تثبيط بلغ لكليهما (11) ملميتر . وبدى تأثر *Lc.lactis* ضعيفاً بمضاد (Co-trimoxazole) عندما بلغ قطر منطقة التثبيط (10) ملميتر . وكانت جميع العزلات حساسة لمضاد (Chloramphenicol) عندما تراوحت أقطار مناطق التثبيط من (20–30) ملميتر .

أشار (18) إلى مقاومة بكتريا *Lb.plantarum* لمضاد (Streptomycin) . أما (19) فقد لاحظوا مقاومة *Lb.plantarum* لمضاد (Ampicillin) بتركيز (10) مايكروغرام و(6) مايكروغرام لمضاد (Erythromycin) .في حين بلغ التركيز الذي تقاومه *Lc.lactis* (5) مايكروغرام لكل من مضادي (Ampicillin و Erythromycin) . وعلى الرغم من اهمية دراسة مقاومة بكتريا حامض اللاكتيك للمضادات الحيوية ولاسيما عند انتخابها كمعززات حيوية الا إن الدراسات حول هذا الموضوع قليلة ، ونتائجها متباينة أيضاً ، إذ لم يتم التوصل إلى إتفاق مشترك حول طبيعة المقاومة للمضادات الحيوية في بكتريا حامض اللاكتيك .

عيوشية عزلات بكتريا حامض اللاكتيك عند الخزن بالتجميد

إختبرت عيوشية عزلات بكتريا حامض اللاكتيك عند الخزن بالتجميد لمدة (3) أشهر للتأكد من قدرة تلك العزلات على البقاء خلال الخزن لدى إستخدامها في النواحي التطبيقية .

يوضح الجدول (4) قابلية العزلات على البقاء عند الخزن بالتجميد بوجود الكليسيرول لمدة (3) أشهر ، فقد لوحظ حدوث إنخفاض بسيط في أعداد بكتريا *Lb.fermentum* و *Lb.plantarum* و *Lc.lactis* بعد الخزن وذلك عندما بلغت أعداد الخلايا الحية بعد الخزن على التوالي (3×10^8 و 2×10^8 و 2.9×10^8 خلية/ملليتر ، في الوقت الذي كانت فيه قبل الخزن (9×10^8 و 8×10^8 و 6×10^8 خلية/ملليتر. وكان الإنخفاض في أعداد بكتريا *Lb.gasseri* أكبر مما هو في العزلات أعلاه ، إذ لوحظ إنخفاض أعداد الخلايا الحية من (7.7×10^8 خلية/ملليتر قبل الخزن إلى (1×10^7 خلية/ملليتر بعد الخزن ، أي ما يقارب دورة لوغارتمية واحدة.

مما تقدم يتوضح إن لعزلات بكتريا حامض اللاكتيك قيد الدراسة القابلية على تحمل البقاء حية خلال الخزن بالتجميد ، وتعد قابلية عزلات بكتريا حامض اللاكتيك على تحمل الخزن من الخواص المهمة الواجب توفرها عند إنتخاب العزلات لإستخدامها كمعززات حيوية (Probiotics)، إذ يتم إستبعاد العزلات التي تقل فترة بقائها عن (2–3) أشهر من الخزن (20). وبهذا الخصوص فقد ذكر(21) إن بكتريا حامض اللاكتيك تمتلك القدرة على تحمل الخزن بالتجميد (– 20) ^{o}م أو أقل فضلاً عن إحتفاضها بحيويتها خلال ذلك . فيما أكد (9)على قابلية عزلات بكتريا حامض اللاكتيك للبقاء حية عند الخزن بالتجميد بوجود الكليسيرول لمدة تزيد عن (3) أشهر.

جدول –3 :حساسية عزلات بكتريا حامض اللاكتيك للمضادات الحيوية المستخدمة

العزلة	قطر منطقة التثبيط (ملميتر)											
	Streptomycin	Trimethoprime	Ampicillin	Neomycin	Tetracycli	Erythromycin	Chloramphenicol	Linkomycin	Cefalexin	Ceftriaxon	Co-trimoxazole	Rifampicin	Gentamicin
Lb. gasseri	R	24	R	12	20	23	30	R	R	12	29	R	R
Lb. fermentum	R	R	R	R	20	18	29	R	R	R	R	R	R
Lb. plantarum	R	R	R	R	15	15	24	11	R	R	R	R	R
Lc. Lactis	R	R	10	R	R	11	20	11	R	R	10	R	R

جدول –4 : تأثير الخزن بالتجميد لمدة (3) أشهر على عيوشية عزلات بكتريا حامض اللاكتيك (خلية / 1 ملليتر)

العزلة	قبل الخزن	بعد الخزن
Lb. gasseri	7.7×10^{8}	1×10^{7}

10×3^{8}	10×9^{8}	*Lb. fermentum*
10×2^{8}	10×8^{8}	*Lb. plantarum*
10×2.9^{8}	10×6^{8}	*Lc. Lactis*

المصادر

1. Leverrier ,P.; Dimova , D ; Pichereau, V.; Auffary ,Y. ; Boyaval, P and Jan, G. Susceptibility and adaptive response to Bile salts in *propionibacterium freudenreichii* and proteomic analysis. Appl . Environ . Microb.,69 (7) : 3809 – 18, (2003).

2. Reid , G. ; Zalai , C. and Gardiner , G. Urogenital Lactobacilli probiotics , reliability and regulatory issues . J.Dairy. Sci ., 84 : 164 – 9, (2001).

3. Vaughan , E.E. ; devries , M.C. ; Zoetendal , E.G. ; Ben – Amor, K. ; Akkermans , A.D. and Devos , W.M.. The intestinal LABs . Antonie Van Leeuwenhoek ., 82 :341 – 52, (2002).

4. Jacobson ,C.N.; Nielsen, V.R.; Hayford ,A.E.; Muller, P.L.M.; Michalesn, A.P.; Sandstr , B. and Jakobsoen, M. Screening of Probiotic activities of forty-seven strains of *Lactobcillus spp* . by *In Vitro* techniques and Evalution of the colonization ability of five selected strains in humans . Appl . Environ. Micrbiol ., 65(11) : 4949 – 56, (1999).

5. Bezkorovainy , A.. Probiotics : determinants of survival and growth in the gut . Am . J. Clin . Nutr ., 73 : 399 S – 405 **S.** (2001).

6. Hammes ,W.P. and Vogel , R.F.. The Genus *Lactobacillus* . In : The Genera of lactic Acid Bacteria . Edited by Wood , B.J. and Holzapfel , W.H, (1995).

7. Teuber , M. The Genus *Lactococcus* . In : The Genera of lactic Acid Bacteria . Edited by Wood , B.J. and Holzapfel , W.H,(1995).

8. Dunne , C. ; Murphy , L. ; Flynn , S. ; O'mahony , L. ; Morrisey, D. ; Thornton , G. ; Quigley , E.M.M. and Collins , J.K.. Probiotics :

from myth to reality . demonstration of functionality in animal models of disease and in human clinical trials. Antonie Van leeuwenhoek ., 76 : 279 – 92, (1999).

9. Brashears , M.M. ; Jaroni , D. and Trimble , J.. Isolation, Selection , and characteriztion of lactic acid bacteria for a competitive exclusion product to reduce shedding of *E.coli*_O157:H7 in cattle .J. Food . Protection ., 66(3) : 355 – 63, (2003).

10. Huys , G. ; D'Haene , K. and Swings , J.. Influnce of the culture medium on antibiotics susceptibility testing of food – associated lactic acid bacteria with agar overlay disc diffusion method . Lett . Appl . Microbiol ., 34(6) : 402 – 6, (2002).

11. Gevers , D. ; Danielsen , M. ; Itys , G. and Swings , J.. Molecular Characterization of *tet* M genes in *Lactobacillus* isolates from different types of fermented dry sausage . Appl . Environ . Microbiol ., 69(2) : 1270 – 75, (2003).

12. Dunne , C.; Mahony , L.O. ; Murphy , L.; Thornton , G.;Morrissey , D.; Halloran , S.; Feeney , M.; Flynn , S.; Fitzgerald , G.; Daly C.; Kiely , B.; Sullivan , G.C.; Shanahan , F. and Collins , K. *In Vitro* selection criteria for probiotic bacteria of human origin : correlation with *in vivo* findings . Am J-Clin-Nutr., 73:386S-92S, (2001).

13. Pereira , D.I.A. and Gibson , G.R.. Cholesterol assimilation by lactic acid bacteria and *Bifidobacteria* isolated from the human gut . Appl . Environ . Microbiol ., 68 (9) : 4689 – 4693, (2002).

14. Ogawa , M. ; Shimizu , K. ; Nomoto , K. ; Tanaka , R. ; Yamasaki, S. ; Takeada , T. and Takeda , Y. . Inhibition of *In vitro* growth of Shiga toxin – producing *E.coli* O157 : H7 by probiotic *Lactobacillus* strains due to production of lactic acid . Intern . J. Food . Microbiol ., 68 : 135 – 40, (2001).

15. Park , Y.S. ; Lee , J.Y. ; Kim , Y.S. and Shin , D.H.. Isolation and characterization of lactic acid bacteria from feces of newborn baby and from dongchimi . J. Agric. Food . Chem ., 50 (9): 2531–6, (2002).

16. Roos , S. Adhesion and autoaggregation of *Lactobacillus reuter* and description of new *Lactobacillus* species with mucus binding properties , ph D. thesis Swedish University of Agriculture Science , Appsala , Swede, (1999).

17. Banach , W. ; Bucholc , B. and Wojcik , B.. Characterstic of *Lactobacillus* strains contained in pharmaceutical.Med. Dose. Mikrobiol ., 53(2) :143–9, (2001).

18. Suskovic , J.;Brick , B.; Matosic , S. and Maric , V. *Lactobacillus acidophilus* M92 as potential probiotics strain . J. Milchwissen Schaft ., 52(8) : 430 – 35, (1997).

19. Flynn , S., Sinderen , D.V. ; Thornton , G.M.; Holo , H. and Collins , J.K.. Characterization of the genetic locus responsible for the production of ABP –118 , a novel bacteriocin Produced by the probiotic bacterium *Lactobacillus salivarius* sub sp. Salivarius UCC118 . Microbiology ., 148:973 –84, (2002).

20. Havenaar , R. ; Brink , B. and Huisin'tveld , J.H.J.. Selection of strains for probioticl use . In : Probiotics , the scientific basis , Fuller , R., Ed . Chapman and Hall , London, (1992).

21. Naidu , A.S. ; Bidlack , W.R. and Clemens , R,A.. Probiotic spectra of lactic acid bacteria (LAB) In : Critial Reviews in food science and nutrition ., 39(1), (1999).

تأثير فلافونويدات بعض النباتات على الفعل التطفيري لسم افلا B1

سجال الركابي* وبتول زينل علي** وشذى علي شفيق*

* قسم علوم الحياة – كلية العلوم – الجامعة المستنصرية

** قسم علوم الحياة – كلية التربية ابن الهيثم – جامعة بغداد

تاريخ تقديم البحث : 2011/ 4/14 تاريخ قبول البحث : 2011/ 5/29

ABSTRACT

The aim of the study is to investigate the inhibitory effect of some natural compounds there are Flavonoids extracted from the dried calax leaves of fruit roselle (*Hibiscus subdariffa L.*) , dried leaves of Rosemary (*Rosmarinus officinalis L.*) and dried leaves of sage (*Salvia officinalis L.*) towards the toxic and mutagenic effects of Aflatoxin B1 extracted from an isolate of the fungus *A. flavus.* Albino male mice (*Mus musculs*)were employed as a biological system , to achieve such aim ; two types of short term assays were employed .The first , included cytogenetic analyses (Mitotic index of bone marrow and Chromosomal aberrations and sperm head abnormality assays. To assess the cytotoxity and mutagenicity of each extracted flavonoids. gradual concentrations were prepared which proved no cytotoxic or mutagenic effects , one concentration was selected to examine the antimutagenic effect of each plant, an interaction was made between the extracted flavonoids (4) mg / kg and Aflatoxin B1 (0.1) p.p.b/ mouse given orally or with contaminated diet using two kinds of treatment ,(before and after) given mutagen to determine the antimutagenic efficiency of extracted flavonoids .

The following results were obtained :-

1- The natural compounds , extracted flavonoids from three plant showed no cytotoxic or mutagenic effects.
2- The mutagenic effect of Aflatoxin B1 was increased with increasing concentrations therefore the dose (0.1) p.p.b/mouse was used as acute dose in the later experiments. The toxic and mutagenic effects of AFB1 caused increasing in mitotic index of bone marrow and chromosomal aberration.
3- The ideal does of extracted flavonoids showed good protective activity, This was depicted by reducing the mitotic activity, chromosomal aberration and sperm head abnormalities.

However the inhibition effiency depended on the type of plant and type of treatment, Roselle came in the first order, followed by Rosemary and Sage.

الخلاصة

استهدفت الدراسة الحالية على معرفة الدور التثبيطي للمركبات الطبيعية الفلافونويدات Flavonoids المستخلصة من الاوراق الكأسية لثمار الكجرات *Hibisicus sabdariffa L.* وأوراق نباتي أكليل الجبل *Rosemarinus officinalis* L. والمرامية *Salvia officinalis L.* تجاه التأثيرات السمية والتطفيرية لسم الافلا B1 المعزول من محاصيل حقلية وبأستعمال نظام الفأر الابيض بوصفه نظاما" اختباريا" وبالاعتماد على جانبين من الاختبارات , الجانب الاول : اختبارات التحليلات الوراثية الخلوية ممثلة بأختبار معامل الانقسام الخيطي لخلايا نقي العظم , التغيرات الكروموسومية والتشوهات في رؤوس النطف . وبعد التأكد من عدم وجود تأثير سمي وراثي للفلافونويدات المستخلصة وبناءا" على الاختبارات السمية تم انتخاب جرعة واحدة من كل نبات وأجري التداخل ما بين الجرعة المثلى لفلافونويدات النباتات المستخدمة (4) ملغم / كغم وسم الافلا B1 بتركيز (0.1) جزء بالبليون لكل فأر والعليقة الملوثة بالسم وبشكل معاملتين (قبل) و(بعد) وذلك لاختبار فعالية هذه المركبات في منع أو تحوير أو تقليل فعل السم والآلية التي تعمل بها تلك المركبات وقد توصلت الدراسة الى النتائج الاتية :-

1. عدم وجود تأثير مطفر للمركبات الطبيعية الفلافونويدات المستخلصة من النباتات الثلاثة عند تجريعها الى الحيوانات المختبرية.
2. أزداد التأثير التطفيري والسمي لسم الافلا B1 بزيادة تركيز الجرعة المستخدمة وكانت الجرعة الحادة غير المميتة (0.1) جزء بالبليون لكل فأر، وقد تمثلت التأثيرات السمية والتطفيرية لسم الافلا B1 في رفع معامل الانقسام الخيطي لخلايا نقي العظم ورفع النسبة المئوية للتغيرات الكروموسومية.
3. أوضحت النتائج ان الجرعة المثلى(4ملغم/كغم) من الفلافونويدات المستخلصة من النباتات المذكورة تمتلك كفاءة عالية في خفض النسبة المئوية لمعامل الانقسام الخيطي والنسبة المئوية للتغيرات الكروموسومية بالاضافة الى خفض النسبة المئوية للتشوهات في رؤوس النطف عند اجراء التداخل، وقد أعتمدت الكفاءة التثبيطية على نوع النبات ونوعية المعاملة فقد أحتلت فلافونويدات الكجرات المرتبة الاولى تليها أكليل الجبل ثم المرمية .

المقدمة

السموم الفطرية Mycotoxins هي تلك المواد الكيمياوية الموجودة والمنتشرة في الطبيعة وتمثل نواتج الايض الثانوي Secondary metabolites للعديد من الفطريات إذ تتلوث بها المنتجات الزراعية والمواد المصنعة منها عند تعرضها للاصابة بهذه الفطريات . كما تمتلك

السموم الفطرية تأثيرات سامة معقدة للأنظمة الحيوية عند التعرض لها) وامتلاك السموم الفطرية القابلية التطفيرية في الأنظمة البايولوجية المختلفة إذ لوحظ امتلاك سم الافلا (B1) _ Aflatoxin B1القابلية العالية على احداث الطفرة الوراثية في بكتريا *Salmonella typhimurium* (1) كما انه يؤدي الى استحثاث التغيرات الكروموسومية في خلايا اللبائن خارج الجسم الحي ***In vitro*** (2) , إما داخل الجسم الحي ***In vivo*** فأنه يؤدي الى حدوث تغيرات كروموسومية في خلايا الحيوانات المختبرية والتأثير في خلاياها الجنسية (3) لذلك تعد سموم الافلا مركبات شديدة السمية للحيوان والانسان عند تناولها بجرع كبيرة وتؤدي الجرعة القليلة والمستمرة من هذه المواد الى إحداث سرطان الكبد Liver cancer (4).

وأظهرت الدراسات الحديثة علاقة الطفرات الوراثية التي تحدثها سموم الافلا بإحداث الأورام السرطانية (5) .انتشر استعمال النباتات الطبية وبشكل واسع في الوقت الحاضر وذلك لتحاشي الإعراض الجانبية التي تسببها الأدوية الكيمياوية وترجع الخاصية العلاجية للنباتات الطبية إلى وجود بعض المركبات الكيمياوية في أنسجة النباتات والتي لها تأثير معين في جسم الإنسان أو الحيوان وهذه المركبات قد تكون قلويدات أو زيوت عطرية او فلافونويدات وغيرها . تمثل هذه المركبات نواتج ايض ثانوية لأنها غير ضرورية لإدامة حياة النبات أو معظم أجزاءه ,وتعرف بالمركبات الفعالة Bioactive components لامتلاكها فعالية بايولوجية في جسم الإنسان .

لذلك هدفت الدراسة الحالية إلى الكشف عن قابلية المركبات الفلافونويدية الخام المستخلصة من الأوراق الكاسية لثمار *الكجرات* *Hibiscus sabdariffa* L. وأوراق نباتي المرامية *Salvia officinalis L.* واكليل الجبل *Rosmarinus officinalis* L. في تثبيط التأثيرات السمية الوراثية لسم الافلا B1 المستخلصة من عزلة منتجة للافلا B1 بعد التأكد من خلو تلك المركبات الفلافونويدية من أي أثار سلبية على الكائن الحي باستخدام نظام اللبائن (الفأر الابيض) وبالاعتماد على الفحوصات الاتية :-

1. اختبار معامل الانقسام الخيطي لخلايا نقي العظم
2. اختبار التغيرات الكروموسومية
3. اختبار تشوهات رؤوس النطف

المواد وطرائق العمل

تم الحصول على سموم الافلا B1 من الفطر *A. flavus* المعزول من حبوب الرز والذرة الصفراء التالفة (6) واتبعت طريقة الكوري(7) في استخلاص المركبات الفلافونويدية من الاوراق الكأسية لثمار الكجرات *Hibisicus sabdariffa L.* وأوراق نباتي أكليل الجبل.L *Rosemarinus officinalis* والمرامية *Salvia officinalis L.*)

الفار الابيض

استخدمت في هذه الدراسة الحيوانات المختبرية وهي ذكور الفئران المختبرية البيض من نوع *Musculus mus* بمعدل عمر تراوح بين (12-14) اسبوعاً وبوزن (25-30) غم والتي جهزت من قبل معهد العقم/ وزارة الصحة حيث وزعت في اقفاص لدائنية بهيئة مجاميع وحسب حاجة التجربة. وقد تم اعطاء الحيوانات الماء والعليقة المتكاملة والمصنعة محلياً في معهد العقم

1- طريقة اختيار الجرع وكيفية التجريع

اختبرت ثلاث جرع من المركبات الفلافونويدية الثلاثة والمستخلصة من النباتات (الكجرات، اكليل الجبل، المرمية) وهي (4، 40، 400) ملغم/ كغم من وزن الجسم اذ تم التجريع عن طريق الفم Orally وباستخدام محقنة خاصة سعة (1) مل وذات إبرة محورة Modified Needle تم تعقيمها في الموصدة.

2- دراسة القابلية المضادة لتطفير الفلافونويدات المستخلصة

تم تهيئة (9) فئران لكل مستخلص نباتي وبمعدل ثلاثة فئران لكل جرعة من الجرع الثلاث إذ جرع كل فأر بحجم (0.25) مل يومياً من كل من الفلافونويدات المستخلصة الثلاثة ولمدة سبعة ايام متتالية وفي الوقت نفسه جرعت ثلاثة فئران بحجم(0.25) مل من PBS لمدة سبعة ايام وعدت كسيطرة سالبة فيما تم تجريع ثلاثة فئران اخرى بحجم (0.25) مل من المطفر MTX بتركيز (2) ملغم/كغم شرحت الحيوانات بعد مرور (24) ساعة (8) وعدت كسيطرة موجبة.

3- دراسة القابلية التطفيرية لسم الافلاB1

بعد التقدير الكمي لسم الافلا B1 باستخدام جهاز Scanner densitometer تم اذابته في الكحول الاثيلي بتركيز 50% وعملت تراكيز مختلفة منه تمثلت (0.1، 0.3، 0.5، 1) جزء بالبليون وجرع كل فأر بحجم (0.1) مل حضرت (3) فئران لكل تركيز وجرعت لمدة (5) ايام كما خصصت (3) فئران جرعت بحجم (0.1) مل لكل فأر من الكحول الاثيلي بتركيز 50% وعدت كسيطرة موجبة لمدة خمسة ايام. وشرحت بعد ذلك جرعت (3) فئران اخرى بالـ PBS لمدة خمسة ايام وعدت كسيطرة سالبة.

4- دراسة التداخل بين الفلافونويدات المستخلصة الثلاثة وسم الافلا B1

استخدم في هذه التجربة تركيز واحد من سم الافلا B1 واعتبر التركيز (0.1) جزء بالبليون/فأر الجرعة الحادة التي تؤثر على الفأر دون إن تقتله وفقاً للنتائج التي تم الحصول عليها من اختبارات CA%,MI%

5- التداخل بين الفلافونويدات الثلاثة وسم الافلا B1(قبل المعاملة)

خصص لكل نبات (3) فئران، حيث جرع كل فأر بـ(0.25) مل يومياً من كل من الفلافونويدات المستخلصة الثلاثة ولمدة عشرة أيام متتالية وفي اليوم الحادي عشر جرعت الفئران بحجم (0.1) مل من سم الافلاB1 لمدة خمسة أيام متتالية. وشرحت بعد ذلك كما خصص (3) فئران أخرى جرعت بحجم (0.25) مل من PBS لمدة (15) يوم وعدت كسيطرة سالبة فيما تم تجريع (3) فئران أخرى بـ(0.25) مل من PBS لمدة عشرة أيام وفي اليوم الحادي عشر جرعت بـ(0.1) مل من سم الافلا B1 لمدة خمسة أيام متتالية واعتبرت سيطرة موجبة .

6- التداخل بين الفلافونويدات الثلاثة وسم الافلا B1(بعد المعاملة)

خصص لهذه التجربة (12) فأراً جرعت بـ (0.1) مل من سم الافلا B1 ولمدة خمسة أيام متتالية وجرعت بعد ذلك كل (3) فئران بـ(0.25) مل لكل من الفلافونويدات المستخلصة الثلاثة لمدة عشرة أيام متتالية. إما الفئران الثلاثة الباقية فقد جرعت بـ(0.25) مل من PBS ولمدة خمسة أيام وفي اليوم السادس جرعت ب0.1مل من سم الافلا B1لمدة خمسة ايام متتالية واعتبرت كسيطرة موجبة إما السيطرة السالبة فقد خصص لها ثلاثة فئران جرعت بـ(0.25) مل من PBS ولمدة (15) يوماً وشرحت بعد ذلك.

الاختبارات الوراثية الخلوية

- طريقة تحضير كروموسومات خلايا نقي العظم

اجريت الاختبارات الوراثية باستخدام طريقة (8) في حساب معامل الانقسام الخيطي% MI والتشوهات الكروموسومية CA% .

- فحص تشوهات رؤوس النطف

استخدمت طريقة Wyrobek & bruce, (9) . تم فحص الشرائح بعد ان جفت في المجهر الضوئي وباستخدام العدسة الزيتية اذ تم حساب النسبة المئوية لتشوهات رؤوس النطف من خلال فحص (1000) نطفة ومقارنة اشكال تلك النطف مع الشكل الطبيعي لرأس النطفة لفأر من الضرب Balb/C .

- التحليل الإحصائي

تم تحليل البيانات وفق التصميم العشوائي الكامل Complete Random Designer (CRD) لدراسة تأثير المعاملات المختلفة في الصفات المدروسة , و قورنت الفروق المعنوية بين المتوسطات بأختبار أقل فرق معنوي (L.S.D) Least Significant Difference واستعمل البرنامج Statistical Packages For Social Sciences SPSS في التحليل الإحصائي .

النتائج والمناقشة

اختبار سمية الفلافونويدات المستخلصة الثلاثة.

يتضح من نتأتج الدراسة الحالية الموضحة في الأشكال (1) و(2) و (3) مسبقا" ان الفلافونويدات المستخلصة من نباتات الكجرات , أكليل الجبل والمرمية خالية من التاثيرات السمية بالجرع المستخدمة (400,40,4) ملغم / كغم وهذا ماستنبط من نتائج معامل الانقسام الخيطي لخلايا نقي العظم لذكور الفئران البيض إذ لوحظ إن زيادة تركيز الجرعة من الفلافونويدات المستخلصة لاسيما الكجرات والمرمية تؤدي إلى زيادة معامل الانقسام . وهذه النتيجة تتفق مع ما توصلت اليه(10) من إن المستخلص المائي للكجرات يؤدي الى زيادة معامل الانقسام الخيطي وان الزيادة كانت مقترنة بزيادة الجرعة وفي السياق نفسه لاحظ (11) ان المستخلصات المائية والكحولية لحبة البركة ونومي بصرة أدت الى زيادة معامل الانقسام الخيطي لخلايا نقي العظم والخلايا الجنسية بزيادة الجرعة كذلك وجد (12) زيادة في معامل الانقسام الخيطي عند تجريع الفئران بجرع مختلفة من المركبات الفلافونويدية المستخلصة من بذور حبة البركة .. وربما يعزى تاثيرالفلافونويدات لتباين في زيادة معامل الانقسام في خلايا نقي العظم الى ان المركبات الفلافونويدية لها قابلية تحفيزية للخلايا على الانقسام الخلوي من خلال التأثير على نفاذية غشاء خلايا الدم البيضاء White blood cells (WBC) فتحفزها على الانقسام الخلوي بصورة غير مباشرة أو التأثير المباشر مثل حثة على تحديد النشاط والحيوية للخلايا اللمفاوية اوحثة لعملية تضاعف الـ DNA كما تشير نتائج الاختبارات الخلوية الوراثية المتعلقة بالكشف عن سمية الوراثية الى ان المركبات الفلافونويدية للنباتات المستخدمة الكجرات ,أكليل الجبل والمرمية خالية من التأثيرات السمية الوراثية . فقد ادت الجرع المستخدمة لفلافونويدات المستخلصة من الكجرات واكليل الجبل الى خفض التردد التلقائي للتغيرات الكروموسومية (CA)% في خلايا نقي العظم التي قد تحدث نتيجة التغيرات الحيوية داخل الجسم اما على مستوى الخلايا الجنسية فلم تظهر مستخلصات النباتات الثلاثة تأثيرات مطفرة في المادة الورثية للخلايا الجنسية الذكرية , حيث

لم يلحظ زيادة معنوية في نسبة تشوهات رؤوس النطف بعد سبعة أيام من تجريع الحيوانات بتلك المركبات الفلافونويدية مقارنة مع اليسطرة الموجبة المتمثلة بعقار ال MTX وقد أشار (9) إلى أن المواد المطفرة تؤدي إلى استحثاث التشوهات في رؤوس النطف في حين لم تستحث المواد الكيميائية غير المطفرة مثل هذه التشوهات أذ يعد هذا الاختبار حساسا" للكشف عن المواد المطفرة.

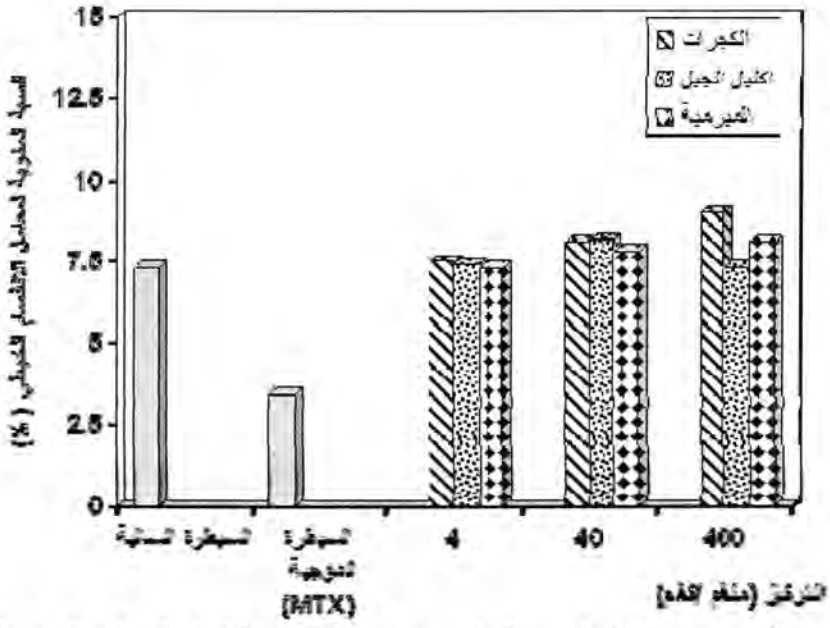

شكل –1 : تأثير جرع مختلفة من فلافونويدات (الكجرات،أكليل الجبل والمرمية) في نسب معامل الانقسام الخيطي في خلايا نقي العظم

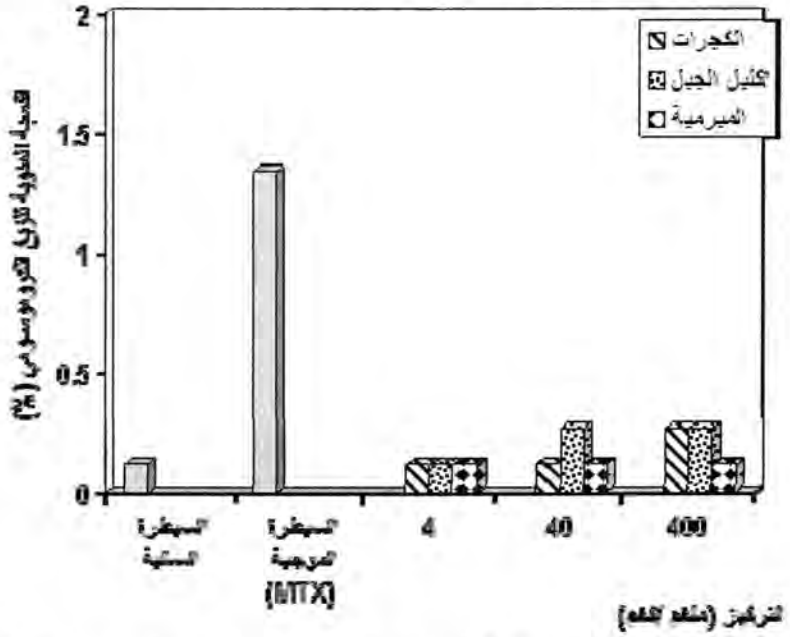

شكل –2 : تأثير جرع المختلفة من فلافونويدات (الكجرات ، اكليل الجبل ، المرمية) في النسب المئوية للتغيرات الكروموسومية التلقائية في خلايا نقي العظم

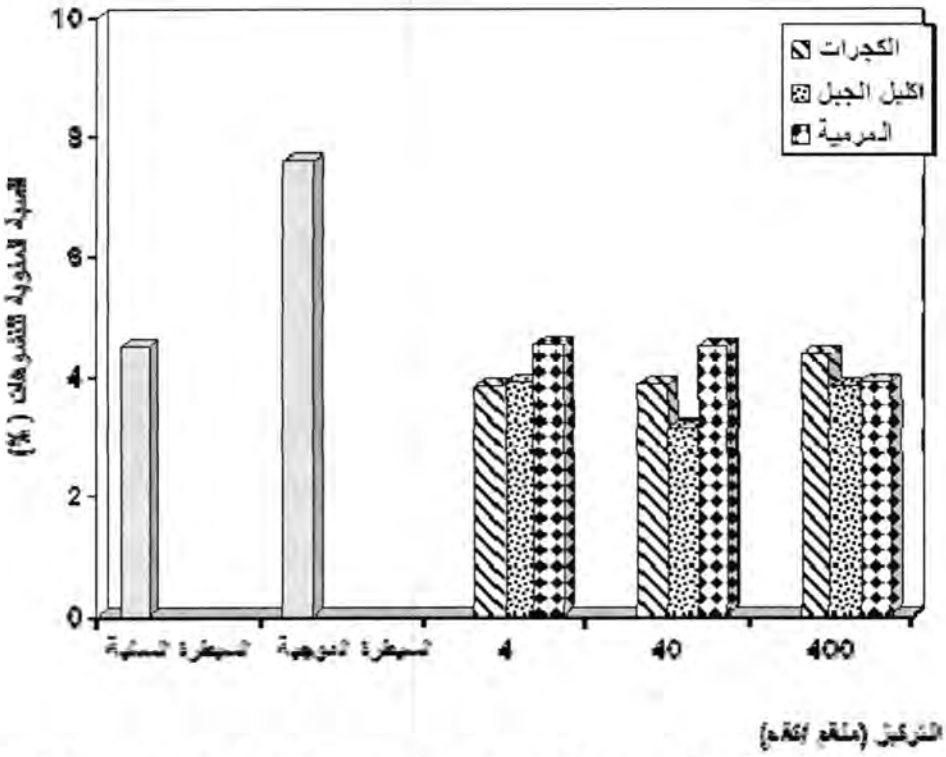

شكل –3 : تأثير جرع المختلفة من فلافونويدات (الكجرات واكليل الجبل والمرمية) في النسبة المئوية للتشوهات في رؤوس نطف ذكور الفئران

التأثيرات السمية والتطفيرية لسم الافلا B1

يبين الجدول (1) الجرع التي أستخدمت في انتخاب الجرعة غير المميتة ذات التأثير السمي والتطفيري وهي (1,0.5,0.3,0.1) جزء بالبليون لكل فأر . إذ أظهرت الجرعة (0.1) جزء بالبليون لكل فأر من سم الافلا B1 الجرعة الحادة غير المميتة مقارنة بالجرع الاخرى وتم مراقبة بعض الأعراض التي ظهرت على الحيوان أثناء التجريع تمثلت بسلوك غير طبيعي للحيوان , مثل قلة الحركة , تنفس سريع , زيادة عدد ضربات القلب , تساقط الشعر وشلل الاطراف الخلفية . وازدادت الأعراض بزيادة التركيز

جدول –1 : يبين استجابة الفئران الى التجريع الفموي لجرع مختلفة من سم الافلا B1

الجرعة (جزءبالبليون لكل فأر)	الملاحظات
1	موت الفئران مباشرة بعد التجريع مع نزيف دموي من الانف والفم
0.5	موت الحيوان بعد (6) ساعات من التجريع
0.3	موت الحيوان في الجرعة الثالثة
0.1	الجرعة الحادة غير المميتة

بينما تظهر النتائج الموضحة في الجدول (2) وجود اختلاف معنوي عالي في مؤشرات الفعالية الوراثية الخلوية المتمثلة بمعامل الانقسام الخيطي والتغيرات الكرموسومية عند مقارنة هذه النتائج مع السيطرة السالبة ولاسيما عند التركيز (0.1) جزء بالبليون لكل فأر من سم الافلا B1 (AFB1) .وهذا يكشف ان لسم (AFB1) تأثير كاسر للكروموسوم Clastogenic عن طريق أحداث ضرر كروموسومي من خلال تحرير الجذور الحرة الاوكسجينية ذات الطبيعة السامة والتي تولدها المركبات الكيميائية والارتباط بشكل نشط مع الجزيئات DNA , RNA والبروتين مكونا" نواتج أضافية كيميائية adducts بعد التنشيط الايضي للسم بفعل انزيمات (cyt P-450) الى المركب الفعال AFB1-8,9 epoxide (13) وتوافق ذلك مع ما أشار اليه (14) من امتلاك سم الافلا B1 فعالية تطفيرية تجعله أكثر تطفيرا" وتسرطنا" من الانواع الاخرى من سموم الافلا بسبب الفعالية التركيبية له كما أظهر (15) بعض التغيرات الكروموسومية التي تحدث نتيجة التسمم بسم الافلا B1 مثل فجوة وانكسار الكروموسوم , فجوة وانكسار الكروماتيد, كروموسوم ثنائي المركز , كروموسوم فاقد للمركز والكروموسوم الحلقي على خلايا الطحال ونقي العظم للفئران وكريات الدم اللمفاوية في الانسان وتزداد هذه التغيرات بزيادة الجرعة .

جدول -2 : تأثير الجرع المختلفة من سم الافلا B1 في النسب المئوية لمعامل الانقسام الخيطي والتغيرات الكروموسومية

نوع الاختبار / الجرع	MI %	Total CA %
السيطرة السالبة (PBS)	7.5±0.05 c	0.13±0.02 e
السيطرة الموجبة ايثانول (50%)	7.8±0.2 c	0.31±0.0 d
0.01 PPb/Mouse	7.9±0.1 cb	1.73±0.02 b
0.05 PPb/Mouse	8.3±0.3 b	2.10±0.06 b
0.1 PPb/Mouse	9.7±0.4 a	2.56±0.07 a

التداخل بين الفلافونويدات الثلاثة وسم افلا B1

بعد ان تم التاكد من أنعدام التأثيرات السمية والتطفيرية للتراكيز المثلى المنتخبة من المركبات الفلافونويدية المستخلصة من النباتات الثلاثة (الكجرات , أكليل الجبل و المرمية) من خلال المعايير المستخدمة في هذه الدراسة . أجريت عملية التداخل بين فلافونويدات النباتات

الثلاثة وسم افلا B1 في نظام اللبائن وعلى شكل معاملتين (قبل) و (بعد) لتحقيق الهدف من هذه الدراسة حيث يمكن معرفة الالية التي تعمل بها المثبطات للمواد المطفرة من خلال اختلاف المعاملة بين المادة المطفرة والمادة المثبطة .

وبشكل عام فأن المواد المضادة للتطفير والمطفرات التي تكون فعالة (قبل) المعاملة بالمطفر Pre-treatment قد تعمل كمثبطات مباشرة للمطفر Desmutagens من خلال تثبيط عمل المطفر كيميائيا" بتكوين معقد مع المادة المطفرة او احد متايضاتها . وبذلك يمنع وصوله الى الخلية او ربما تتفاعل المادة المضادة مع المواقع المستهدفه بفعل المطفر من خلال عملها بوصفها مادة غالقة Blocking agent تمنع المطفر من الوصول الى المواقع المستهدفة في الـ DNA او التفاعل معها مما يؤدي الى منع تأثيرات المطفر او من خلال تثبيط عمل المطفر انزيميا وذلك بتثبيط انزيمات التنشيط الايضي للمطفرات وبصورة غير مباشرة او من خلال زيادة انزيمات ازالة السمية المتواجدة بصورة طبيعية في الجسم (16)اما المثبطات التي تكون فعالة بعد اعطاء المطفر Post-treatment فتسمى مثبطات حيوية Bio-antimutagens اذ تعمل على اصلاح التلف بعد حدوثه من خلال زيادة دقة عملية تضاعف الـ DNA(DNA_Replication) وزيادة انظمة الاصلاح عن طريق زيادة الاصلاح الخالي من الخطأ والتقليل من الاصلاح القابل للخطأ (17) .

وعند أجراء التداخل مابين الجرعة الحادة غير المميتة (0.1) جزء بالبليون من سم الافلا B1 لكل فأر (السيطرة الموجبة) والفلافونويدات المستخدمة الاشكال (4) (5) ,(6). أظهرت الفلافونويدات المستخلصة من الكجرات , أكليل الجبل و المرمية فعالية مضادة لتأثيرات السم(AFB1) وهذه الفعالية أختلفت باختلاف النبات ونوع المعاملة في أثناء تطبيق الاختبارات المستخدمة في الدراسة. فيما يخص أختبار معامل الانقسام الخيطي اظهرت فلافونويدات النباتات الثلاثة و بالجرعة المستخدمة كفاءة عالية في خفض معامل الانقسام الخيطي لخلايا نقي العظم والمحفز انقسامها بفعل سم (AFB1) وبفرق ذي دلالة معنوية عند مستوى (P <0.05) .عند مقابلتها بالسيطرة الموجبة المعاملة بالسم فقط وبمعنى أدق ان المعاملة بالمركبات الفلافونويدية للنباتات الثلاثة (قبل) معاملة وفرت نسبة حماية عالية من تأثير المطفر سم الـ(AFB1) في معامل الانقسام الخيطي تصل الى(81.8, 72.7, 66.6) % (قبل) المعاملة بالمقارنة مع نسب الحماية (57.5 , 48.4 , 51.5) % (بعد)المعاملة بفلافونويدات الكجرات , أكليل الجبل و المرمية على التوالي .ومن هنا فأن المعاملة (قبل) عملت على الحد من تاثير سم (AFB1) في معامل الانقسام الخيطي ربما تكون من خلال تغير نفاذية الغشاء الخلوي لخلايا نقي العظم بحيث تمنع وصول المطفر الى داخل الخلية أو إن الفلافونويدات

عمدت على الارتباط بالمطفر ومنعه من الدخول إلى الخلية وهي بهذه الآليتين تمنع وصول السم الى الخلايا (15) وفيما يخص اختبارات التغيرات الكروموسومية والتشوهات في رؤوس النطف فقد أظهرت فلافونويدات النباتات الثلاثة المستخدمة (قبل) المعاملة كفاءة عالية في خفض النسبة المئوية للتغيرات الكروموسومية بنوعيها التغيرات التركيبية والعددية بالإضافة الى خفض النسبة المئوية لتشوهات في رؤوس النطف المستحثة بفعل سم (AFB1) وان نسبة الانخفاض كانت ذات دلالة معنوية عند مستوى ($P < 0.05$) عند الموازنة مع السيطرة الموجبة المعاملة بالسم فقط .وهذا يعني ان التاثيرات الواقية لتلك المركبات تكون على الخلايا الجذعية الجنسية Spermatogonia (امهات النطف) وهي أول مرحلة من مراحل التكوين إذ تعد هذه المرحلة أكثر حساسية لتاثير المواد المطفرة نظرا" لنشاطها الانقسامي العالي تليها مرحلة تكوين النطف Spermatogensis وهي المرحلة التي تتحول فيها اروماتِ النطف Spermatid الى النطف Sperm وقد يرجع سبب تأثر النطف بالسم في أثناء هذه المرحلة لان السم يتداخل مع تكوين النطف عند هذه المرحلة أذ تكون النطف في أثناء هذه المرحلة غير مكتملة التكوين مما يؤدي الى تأثرها بالمادة المطفرة (18) .

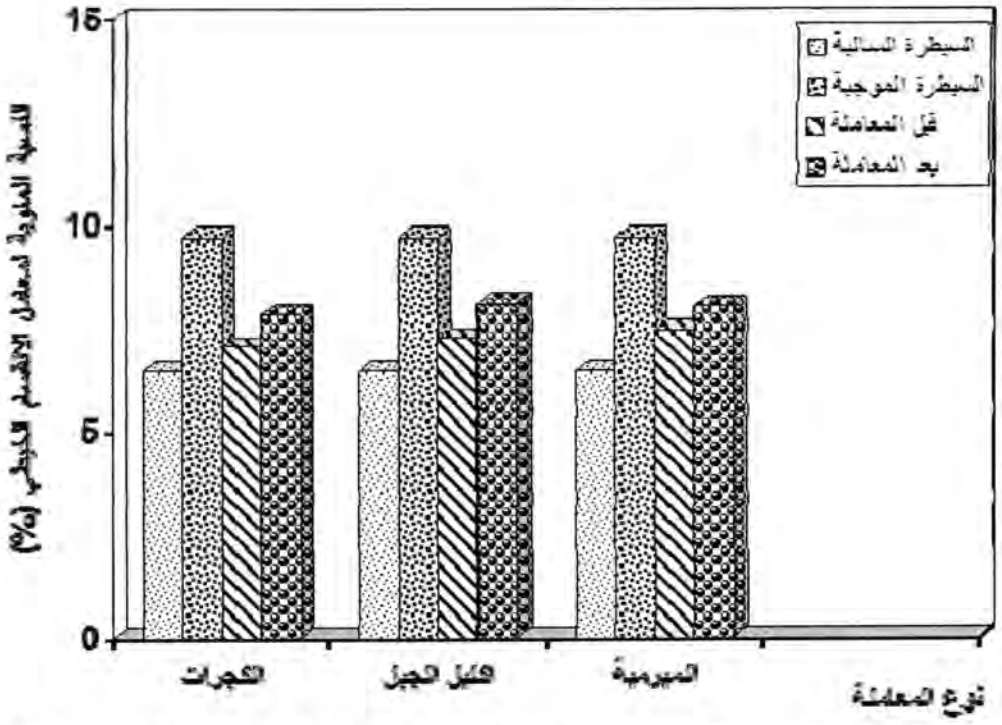

شكل-4: تأثير التداخل بين الفلافونويدات (الكجرات ، اكليل الجبل ، المرمية) وسم الافلا B1 في نسب معامل الانقسام الخيطي

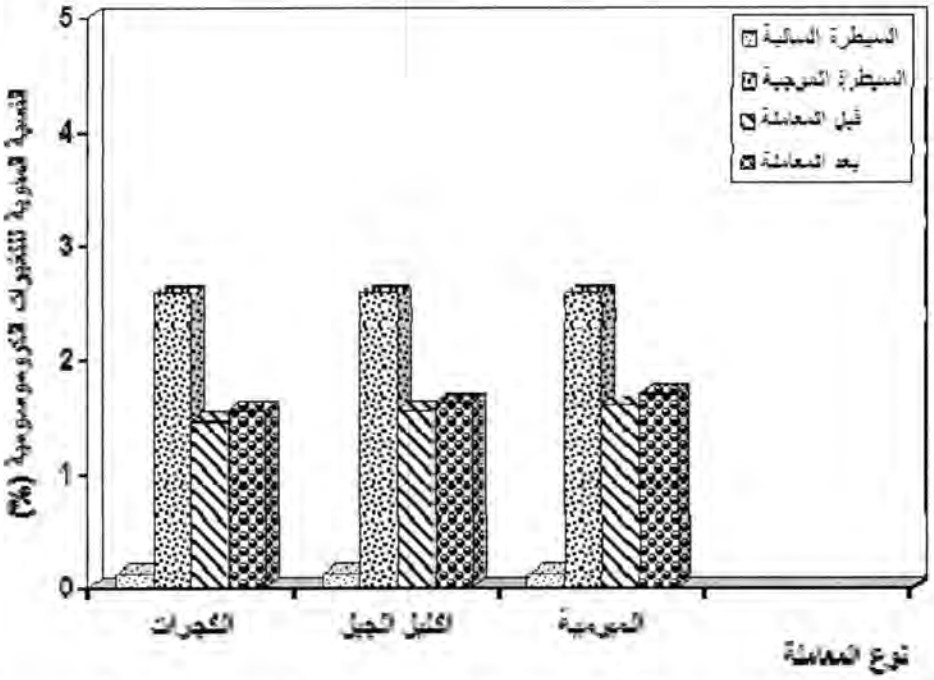

شكل –5 : تأثير التداخل بين الفلافونويدات (الكجرات ، اكليل الجبل ، المرمية) وسم الافلا B1 في النسبة المئوية للتغيرات الكروموسومية

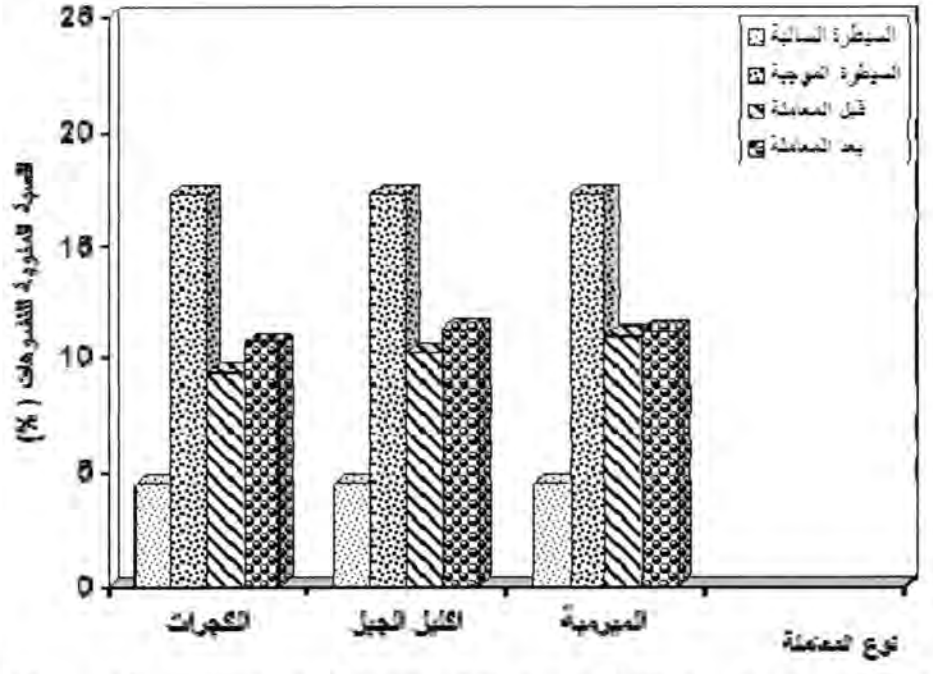

شكل –6 : تأثير التداخل بين الفلافونويدات (الكجرات وإكليل الجبل والميرمية) وسم الافلا B1 في النسبة المئوية في رؤوس نطف ذكور الفئران

المصادر

1. Sharma , N.; Trikha , P .; Athar , M .; Raisuddin , S., In vitro inhibition of carcinogen induced mutagenicity byCassia occidentalis and Emblica officinalis , Drug . Chem .Toxical . 23(3): 477-84 (2000).

2. Prasad , A. B .; Prasad , .J .S .; Shrivastav , R. R. Genotoxic capacity of extracts from naturally occurring mycotoxin producing Fungi. Lntl .Bot. congress . N(2121), (1999).

3. Mcgregor ,D.B .; Rice , J.M. and Venitt, S., The use of short and Medium term tests for Carcinogens and data on Genetic effects in Carcinogenic Hazard evalution . Printed in France : 203-25. (1999).

4. Li, H.; Lu ,Y., Effect of bicyclol on Aflatoxin B1 metabolism and hepatotoxicity in rats .Acta . Pharmacol .Sin .23(10): 942-50 . (2002) .

5. Mcglynn ,K.A,. Human ,K.; Levoyer ,.T.; Roush ,.J.; Wise,P.; michielli ,R.a.; Shen ,.F.M.; Evns ,.A.A. ,.London, W.T.; and buetow ,K.H., Susceptibility .to Aflatoxin B1 –releated primary .Hepatocellular carcinoma in Mice and Humans .Cancer Res., 63(15)4694-4601. (2003).

6. الكوري , طلال عبد الرزاق علي. استخلاص بعض المركبات الفلاقونويدات من اوراق نبات السدر واستعملها كمواد مضادة للاكسدة ومفيدة للمعادن في زيت زهرة الشمس – إطروحة دكتوراه .كلية الزراعة /جامعة بغداد. (2000).

7. Al-Kadumi, D., Enzymatic .cytogenetic study on the effect of methotrexate drug inside the living body .,M.sc. thesis Biology collage of Education for women,univ.of Baghdad. (1999).

8. Allen, J.W.;Shuler, C.F.;Mendes ,R.W.and Latt ,S.A. Asimplified technique for in *vivo* analysis of sister chromatid exchanges using 5-bromo-deoxyuridine tablets . Cytogenet. Cell Genet .,18:231-37. (1977).

9. Wyrobek , A. J and Bruce , W.R. Chemical induction of sperm abnormalities in mice . Pro. Nat . Acad . sci . U.S.A . 972: 4425-4429. (1975).

10. الخياط , بشرى محمد امين. دراسة القابلية التطفيرية والمضادة للتطفر لبعض النباتات الطبية العراقية . اطروحة دكتوراه – جامعة بغداد. (1999).

11. حسن , مفيد قائد احمد. استخدام بعض المستخلصات النباتية لتثبيط الاثر السمي الوراثي لبعض العقاقير المضادة للسرطان في الفار . إطروحة دكتوراه/كلية العلوم /جامعة بابل. (2002).

12. الجنابي , ازهار محمود حليم. دراسة تأثير بعض المستخلصات النباتية في الخلايا اللمفاوية لمرضى ابيضاض الدم النخاعيني المزمن . إطروحة دكتوراة/ كلية العلوم/الجامعة المستنصرية. (2004) .

13. Huennekens, F.M., The methotrexate story:A paradigm for development of cancer chemotherapeutic agents. , Adv . Enzyme Regul.,34:397-419. (1994).

14. Larsson , P. ; Persson, E. ; Tyden , E ., cell specific activation of Aflatoxin B1 correlates with presence of some cytochrome P450 enzymes in alfactory and respiratory tissue In horse . Res –Vet –Sci ,74 (3) : 227-33. (2003).

15. El–Zawahri , M . M., Morad , M.M. and Khishin, A.F., Mutagenic effect of aflatoxin G1 in comparision with aflatoxin B1,J.Environ.Path.Toxicol.oncol.,10(1-2) : 45-51. (1990).

16. Al-O'baidy,A.M. Study of some chromosomal Variation caused by aflatoxin B1 contamination . MSC .thesis .Biotechnology Department, Collage of Sciences, AL-Nahrain University , Iraq. (2003).

17. Kuroda, Y . ; Hara ,Y. Antimutagenecity of tea polyphenols . Mutat .Res. 436:69-97. (1999).

18. Sakr, S. A. ; el- Mofty, M . M. Aflatoxin -B1 inhibition of spermato-genesis in the toad Bufo regularis.,Folia.Morpho.38(4):3315. (1990) .

دراسة تشريحية مقارنة لبعض أنواع أجناس العائلة القرعية *Cucurbitaceae* في العراق

*شيماء محي حسون و **عبد الكريم خضير البيرماني

*كلية العلوم / جامعة بابل

**كلية العلوم للبنات / جامعة بابل

تاريخ تقديم البحث : 2011/04/04 تاريخ قبول البحث : 2011/ 5/29

ABSTRACT

The present study includes comparative anatomical study of leaf epidermis and cross section of stem , petiole , and blades in some genera speices the family Cucurbitaceae in Iraq . The present study included the species *Citrullus lanatus* (Thumb.) Matsum ., *Cucumis melo L.*, *Cucumis melo . var . flexuosus Naudn.* , *Cucumis sativus L.*, *Cucurbita maxima* Duchesne ., *Cucurbita moschata* (Duchesne) Poir. , *Cucurbita pepo L.* , and the specie *Luffa cylindrica(L.)* . Anatomical study of stems , petioles and blades showed taxonomic value to differentiate the species from other under study, such as the straight of cells walls on adaxial surface to the leaf of *Luffa* sp., the variation in number of biocollateral vascular bundle in petiole of *Cucurbita pepo* and the variation of biocollateral vascular bundle in the midrib leaf of *Cucurbita maxima.*, and other character.

الخلاصة

تضمن البحث الحالي دراسة تشريحية مقارنة تضم دراسة بشرة الأوراق والمقاطع المستعرضة لكل من السيقان والسويقات ونصول الأوراق لبعض أنواع أجناس العائلة Cucurbitaceae في العراق . فقط تضمنت الأنواع *Citrullus lanatus* (Thumb.) Matsum . و *Cucumis melo L.* و *Cucumis melo . var . flexuosus* Naudin و *Cucurbita maxima* Duchesne و *Cucurbita moschata* (Duchesne) poir و *Cucurbita pepo L.* والنوع *Luffa Cylindrica L.* . وأتضح إن للصفات التشريحية للسيقان والأوراق والسويقات أهمية تصنيفيه لعزل الأنواع قيد الدراسة عن بعضها البعض . كصفة جدران الخلايا المستقيمة على السطح العلوي للنوع *Luffa* sp. وعدد الحزم الوعائية لسويق ورقة النوع

Cucurbita pepo ويمكن استخدام عدد الحزم الوعائية في منطقة العرق الوسطي لوريقة النوع *Cucurbita maxima* إضافة إلى صفات أخرى .

المقدمة

تعد العائلة القثائية أو القرعية (Cucurbitaceae) من العوائل النباتية الكبيرة وقد عوملت هذه العائلة وحسب ما أشار إليه عدة باحثين أمثال [1] حيث ذكر أن [2] قسم العائلة القثائية إلى خمس عوئيلات هي :

(Fevilleae , Melothrieae , Cucurbitae , Sicyoideae and Cyclanthereae)

وأشار أن العويئلة الأولى Fevilleae تقسم إلى 4 عشائر والعويئلة الثانية تضم (5) عشائر والثالثة وهي العويئلة Cucurbitae تضم (4) عشائر . كما وأوضح [1] أن هذه العائلة تضمن (100) جنس و (850) نوعا موزعة في المناطق الاستوائية وشبه الاستوائية من العالم . أما [3] أكد أن نظام هجسنون يعد العائلة القرعية من اكبر العوائل النباتية الأربعة العائدة لرتبة أل Cucurbitales اذ تضم (100) جنس وما يقارب (650) نوعا ، منها حوالي (7) أجناس تنمو في العراق . كما أشار [4] إنها من العوائل الكبيرة تضم (90) جنسا وحوالي (700) نوعا ، تتمثل بريا في العراق بثلاثة أجناس فقط إضافة للأنواع المستزرعة . أما [5] و[6] قسموا العائلة إلى عويئلتين هما Subfamilies : Zanoniodeae, Cucurbitoideae وأشار [5] أن العوئيلة الأولى تضم عشيرة واحدة فيها (18) جنس وحوالي (80) نوعا ، في حين العويئلة الثانية Cucurbitoideae قسمت إلى (7) عشائر تضم (100) جنسا وحوالي (775) نوعا . كما وذكر [6] أن العائلة القثائية كبيرة تضم (120) جنسا وما يقارب (825) نوعا .

وفيما يخص الأجناس المدروسة، الجنس *Citrullus* Forsk. اشتق اسمه من الاسم المصغر للجنس *Citrus* وذلك نظرا إلى ترابط شكل ولون الثمار [7] . ومن تسميات النوع C.lanatus بالانكليزية يسمى بـ (Watermelon) في مناطق الجزيرة العربية باسم الحبحب وفي بلاد الشام باسم (الجبس) وفي دول الخليج العربي والعراق باسم الرقي أو الركي RAGGI or RQQI وفي تركيا باسم قربوز QARPUZ ,أما في مناطق كردستان العراق يسمى بـ شوتي SHUTI وشمسي SHAMSI في الموصل [8] و [7] .

أما الجنس ***Cucumis*** L. فقد أشار كل من [3] و [7] إن الاسم *Cucumis* اسم لاتيني قديم (An old Latin name). الأنواع المدروسة حاليا هي ***Cucumis sativus*** L. المعروف باسم Cucumber بمعنى الخيار بـ (الفارسية) أو القثد على لسان العرب لابن المنظور [9] . أصل زراعته في المناطق الهندية Indian region ويسمى بالعربية بخيار ماء في العراق وفي الانكليزية ("Water cucumber") [7] . أما النوع الثاني المستزرع في العراق هو ***Cucumis melo*** **L.** أشار إليه [3] و[7] باسم بطيخ BATAIKH بالعربية و في الانكليزية (Musk Melon , Melon (Sweet Melon تعني شمام آو بطيخ Sweet تعني حلو , أما Musk Melon البطيخ الأصفر . . وقد ذكر [10] أن هناك (25) ضرب Varieties وأشكال في العراق وأكثر انتشارا في مناطق الموصل وسامراء والبصرة. إلا أن العدد الكبير من الضروب تنمو في سامراء . له عدة تسميات منها في بغداد يسمى أل *Cucumis melo* بـ بطوش او بطوش العرب BATUSH or BATUSH AL-ARAB وقد شاع اسم البطيخ في العراق والدول العربية . أما الضرب ***Cucumis melo* . var. *flexuosus*** يسمى في الانكليزية بـ Snake Snake Cucumber تعني حية ، أي الثمرة تنمو على نحو ثعباني . وبالعربية بـ خيار تعروزي Khiyar Tarouzi . بخصوص الجنس L. ***Cucurbita*** فهو اسم لاتيني قديم بمعنى (Gourd , Pumpkin , Squash) تعني قرع . يضم (3) أنواع مستزرعة في العراق وهي الأنواع قيد الدراسة [3] [7] . فالنوع.L ***Cucurbita pepo*** أشارااليه [3] بعدة أسماء منها SHIJAR القرعة الحلو في العراق وفي مناطق كردستان سمي بـ كندق KUNDUQ وكولكه KULAKA . إما النوع ***C.moshata* (Duchesne)Poir.** يسمى بالعربية بـ القرع الحلو QHRA HELU إما اسمه اللاتيني فهو " Sweet gourd" [3] و[10] أشارا إلى نوعين منه تنمو في عدة مناطق هما Naples Squash و Long Neapolitan Squash القرع النابولي الطويل إذ يمتاز بعنق طويل منحني يتصل بالحامل والذي يسمى في مناطق وسط وجنوب العراق بـ شجر أبو ركبة . بينما النوع ***C.maxima* Duchesne** يسمى بالعربية BOBAR وفي الانجليزية Red gourd , squash ، ينمو يسمى في العراق بـ شجر اسلكه SHIJAR ASKALA وفي كردستان بـ قرعة الجبل QAR'A AL-JABAL [3]و[7] و[11] . أصل نموه في جنوب أمريكا [9] . أما الجنس **Mill.** ***Luff*** الليف في العربية ، في الانجليزية الخضار الأسفنجية Dish Cloth

Gourd , Vegetable sponge قماشة الصحون . الاسم *Luffa* اخذ من لف Luffa او Wrap يلف أو envelop يلف يسمى بالأمريكية ب، Lofah و Towel gourd .

المواد وطرائق العمل

1:تحضير البشرة Epidermis

أخذ جزء من ورقة كاملة النمو وركز على مكان ثابت (منتصف الورقة) تقريبا بحيث يشتمل على العرق الوسطي وجزء من النصل والحافة واستعملت طريقة التقشير Peeling أو السلخ Stripping off للحصول على البشرتين العليا والسفلى وذلك باستعمال شفرة تشريح وملقط ذي نهايتين دقيقتين Forceps بعدها نقلت البشرة المحضرة إلى طبق بتري Petri Dish نظيف يحتوي على ماء للإزالة المواد المتبقية وبقايا النسيج العالقة على البشرة . نقلت البشرة المنزوعة إلى صبغة السفرانين بتركيز (1%) المحضرة في كحول أ ثيلي(70%) وموضوعة في طبق بتري لمدة (2-5) دقيقة ، بعدها نقلت إلى أطباق بتري تحوي كحول أثيلي (70%) لعدة مرات لتخلص من الصبغة الزائدة بعد ذلك نقلت البشرة إلى الشريحة زجاجية تحتوي على قطرة من الكليسيرين وفرشت البشرة وغطيت بغطاء الشريحة وأصبحت عندئذ جاهزة للفحص والدراسة .

2- تحضير المقاطع المستعرضة Preparation of Transverse Sections:-

1- استخدمت في هذه الدراسة عينات نباتية طرية جمعت من المناطق القريبة بين محافظتي بابل وكربلاء وثبتت العينات بمحلول F.A.A. لمدة 24 ساعة ثم غسلت بكحول 70% وحفظت بنفس التركيز في الثلاجة لحين الاستعمال قطعت النماذج إلى قطع صغيرة حوالي 2ملم ومررت في سلسلة تصاعدية من كحول الأثيلي 80% - 90% - 95% لمدة ساعتين في كل تركيز وبعدها في كحول اثيلي مطلق لمدة ساعة كاملة. وبعدها مررت القطع في مزيج من كحول أثيلي مطلق وزايلين بنسب حجميه (3:1،1:1،1:3) بالتتابع ثم بالزايلين النقي لمدة ساعتين لكل معاملة [12] .

2- سكب الزايلين وأضيف بدلا منه شمع البارافين السائل في فرن بدرجة 60م ولمدة 48 ساعة كي يحل البارافين محل الزايلين المتبخر ، بعدها سكب البارافين وأضيف بدلا عنة بارافين نقي وتركت الأوعية بالفرن لمدة 72 ساعة لإزالة أثار الزايلين ، بعدها سكب البارافين ووضع بدله البارافين نقي وترك في الفرن لمدة ساعتين ، كررت هذه العملية 6 مرات وفي الأخيرة تركت في الفرن ليلة كاملة .

3- تم صب القوالب البلاستيكية بشمع المنصهر بعد وضع نموذج معين في كل قالب ، ثبت القوالب الشمعية الحاوية على النماذج على حوامل خشبية خاصة بعد أن شذبت القوالب بشكل متوازي مستطيلات يتوسطه النموذج ليكون جاهز للقطع بالمشرح الدوار Rotary Microtome .

4- قطعت النماذج بسمك 10-12 مايكروميتر ، ثم فرشت المقاطع بشكل أشرطة Ribbon على شرائح زجاجية نظيفة مطلية بطبقة من ألبومين - كليسرين وفوقها من الماء المقطر ، وبعدها وضعت الشرائح على صفيحة ساخنة 40-45م . تمت إزالة الشمع من المقاطع وتصبيغها كما جاء في [12] و ,[13] ثم فحصت الشرائح الجيدة للسيقان والأوراق والسويقات تحت المجهر وتم تصويرها.

النتائج والمناقشة

- خلايا البشرة الاعتيادية للورقة **Ordinary Epidermal cell of leaf**

اتضح من خلال الفحص ألمجهري أن الجدران العمودية Anticlinal cell walls لخلايا البشرة الاعتيادية في أنواع الأجناس قيد الدراسة متغايرة في أشكالها وأحجامها بتباين الأنواع ، كذلك بين السطحين العلوي والسفلي للورقة في نوع واحد . مما يجعله ذو صفة معتمدة في التشخيص بوضعها على شكل مجاميع (جدول 1) فقد كانت خلايا الجدران في البشرة السفلى مستقيمة - منحنية straight curved في النوع *Cucurbita pepo* ومنحنية في النوع *Citrullus lanalus* ومتموجة في النوعين *Luffa cylindrica* و *Cucumis melo* وشديدة التموج Sinuateفي بقية الأنواع المدروسة . أما بالنسبة للسطح العلوي فقد امتازت بطبيعة مقارنة لما في السطح السفلي، فقد كانت مستقيمة في النوع *Luffa cylindrica* ، في حين كانت منحنية في النوعين *Cucumis melo* و *Cucurbita pepo* ومستقيمة ومنحنية قليلا في بقية الأنواع قيد الدراسة (لوحة 1،2). كما تبين انه ليس أشكال خلايا البشرة وحدها متباينة ، إنما يتعدى ذلك إلى أبعاد الخلايا، إذ كان معدل أبعاد خلايا البشرة على السطح السفلي يتراوح بين (32,5 × 22,5) مايكروميتر في النوع *Cucurbita maxima* و (63,3 × 37,5) مايكروميتر في النوع *Cucumis sativus* ، بينما كان معدل أبعاد الخلايا على سطح العلوي بين (25 × 18,5) مايكروميتر و(53 × 32,5) مايكروميتر للنوعين *Cucurbita pepo* و *Citrullus lanatus* على التوالي. في حين كانت بقية الأنواع متداخلة بين تلك المعادلات وعلى كلا

السطحين السفلي والعلوي. أما بشرة العرق الوسطي فقد امتازت الخلايا بشكلها المستطيل ذو الجدران المستقيمة Straight ولجميع الأنواع .

- الثغور في الأوراق Stomata of leaves

تميزت أوراق أنواع الأجناس المدروسة بأنها من النوع Amphistomatic leaf إذ توجد الثغور على السطحين العلوي والسفلي. أما من ناحية المعقدات الثغرية فقد امتازت الأنواع المدروسة بالطراز الثغري الشاذ Anomocytic type وهذا يتفق مع ماذكراه [14] و [15] حينما أشاروا إلى أن الثغور في أوراق أنواع أجناس العائلة Cucurbitaceae متواجدة على السطح السفلي فقط آو في كلا السطحين وهي من الطراز الشاذ. إلا انه لوحظ الطراز نصف المتعامد Hemiparacytic إضافة إلى الطراز الشاذ في النوع *Citrullus lanatus* وبشكل اقل في النوع *Cucumis sativus* وهكذا ماكده [16].

وبخصوص كثافة الثغور وانتشارها على سطحي الورقة فقد اختلفت بين الأنواع غير إنها بصورة عامة تكون أكثر كثافة على السطح السفلي مما عليه على السطح العلوي في جميع الأنواع باستثناء النوع *Cucurbita pepo* إذ وجد عدد الثغور في السطح العلوي أكثر مما في لسطح السفلي ، وبذلك يمكن تقسيم الأنواع إلى مجموعتين حسب دليل الثغور في السطح السفلي وهما :

- **المجموعة الأولى:** كان دليل ثغور فيها محصورا بين (11.4-20.6) وتضم النوع *Cucurbita moschata* و *Cucurbita pepo* و *luffa cylindrica* .
- **المجموعة الثانية:** تراوح دليل الثغور فيه بين (21.6-30.2) وضمت بقية الأنواع المدروسة.

في حين أن دليل الثغور على السطح العلوي قسم الأنواع إلى مجموعتين هما:

- **المجموعة الأولى:** شملت أنواع الجنس *Cucurbita* مع النوع *Luffa cylindrica* إذ كان دليل الثغور فيها محصورا بين (9.1-13.7).
- **المجموعة الثانية:** شملت بقية الأنواع المدروسة والتي تراوح دليل الثغور في أوراقها بين (16.3-24.6). وقد يكون هذا التباين في كثافة الثغور حسب ماأشار إليه [17] عائد إلى أن زيادة الثغور ربما استجابة لظروف البيئة آو زيادة تعرضها لأشعة الشمس ، آو ربما

يعود للعدد الكروموسومي . وهذا مايشير إليه عدة باحثين [18] و [19].ومن ملاحظة جدول (1) يلاحظ أن هنالك تغاير قليل في أبعاد الثغور ، فقد تراوحت معدلات الأبعاد على السطح السفلي بين (14.4-19.8) مايكروميتر للنوع *Cucurbita maxima* كحد أدنى و (17.5×27.5) مايكروميتر للنوع *Luffa cylindrical* كحد أعلى. أما معدل أبعاد الثغور على السطح العلوي تراوحت بين (17.5) مايكروميتر كمعدل طول الثغر في النوع *Cucurbita pepo* و(12.5) مايكروميتر كمعدل عرض الثغر في النوع *Cucumis sativns* كحد أدنى . في حين تراوح معدل أبعاد الثغر بين (19.1×25) مايكروميتر كحد أعلى في النوع *Citrullus lanatus*، أما باقي القياسات للأنواع الأخرى فكانت متداخلة بين حدود تلك المعادلات وكلا السطحين العلوي والسفلي .

- المقطع المستعرض لنصل الورقة Cross section of blade

أتضح من نتائج الدراسة الحالية آن نمط النسيج المتوسط Mesophyll لأنواع الأجناس قيد الدراسة كان من النوع Dorsiventral إذ يتواجد النسيج ألعمادي على جانب واحد من الورقة فقط تحت البشرة العليا مباشرة ولجميع الأنواع المدروسة . وهذا يتفق مع ما أشار إليه [14] و[15] في أن صفة Dorsiventral سائدة في جميع أو اغلب أجناس العائلة القرعية Cucurbitaceae. من الناحية الأخرى فقد أظهرت الأوراق تغايرا ملحوظا في شكل المقطع العام لنصول الوريقات خصوصا عند منطقة العرق الوسطي. فقد أمكن تميز النوع *cucurbita pepo* بكون المقطع مستوي من الأعلى ومحدب من الأسفل وبهذا أمكن تميزه عن بقية الأنواع (لوحة 4). بينما كانت مستوية –معقدة أو شبه مقعرة من الأعلى – ومحدبة من الأسفل في الأنواع *Cucumis sativus* و *Cucumis* و *Cucurbita moschata* أما بقية الأنواع قيد الدراسة فقد تميز مقطع نصولها بأنه مقعر– شبه مستوي من الأعلى ومحدب من الأسفل (لوحه 3 و4). وبذلك تتفق النتائج مع ماذكراه [14] بان طبقة الميزوفيل لنصول وريقات أنواع العائلة القرعية متغايرة في الشكل والحجم . أما فيما يخص سمك النصل فقد أظهرت تغايرا واضحا باختلاف الأنواع، فمن ملاحظة (جدول 2) نلاحظ أن سمك نصل الورقة Lamina تراوح بين (150- 245) مايكروميتر و (257.5- 375.5) مايكروميتر للنوعين *Cucurbita moschata* و *ucumis 89 C* .var.flexuosus

melo على التوالي وبقية الأنواع تقع بين تلك المديات . **أما البشرة** فقد تميزت أجناس العائلة القرعية Cucurbitaceae بان السطح العلوي والسفلي لنصل الورقة حاو على خلايا كبيرة الحجم كقواعد للشعيرات والتي تبدوا واضحة أكثر في النوع *Citrullus lanatus* (لوحه 5) وهذا ماأكده [14] ، والبشرة كانت عبارة عن صف من الخلايا شبه دائرية أو المتطاولة الشكل ، وكان معدل سمكها على السطح العلوي يتراوح (18) مايكروميتر *Cucurbita pepo* و (35.5) مايكروميتر للنوع *Luffa cylindrica* . أما معدل سمكها على السطح السفلي فتراوح بين (12.1) مايكروميتر للنوع *Cucurbita maxima* و (31) مايكروميتر في النوع *Luffa culindrica* وبصورة عامة كانت معدلات سمك البشرة على السطح العلوي أعلى قليلا مما هو عليه في السطح السفلي . وعلى العموم غطت سطح البشرتين بطبقة من الأدمة Cuticle التي تختلف في مقدار سمكها باختلاف الأنواع أيضا فقد تراوحت بين (1.9) مايكروميتر و (4.7) مايكروميتر للنوعين *Cucurbita moschata* و *Citrullus lanatus* على التوالي وبقية الأنواع كانت ضمن تلك المديات .

وبخصوص طبقة الميزوفيل فتمثلت بالطبقة العمادية والطبقة الأسفنجية في جميع الأنواع المدروسة إذ تمثلت الطبقة العمادية بالنسيج الكلورنكيمي Chlorenchyma الواضح (لوحه 3و 4) وهذا يتفق مع ما أشار إليه [20] بان طبقة ميزوفيل الورقة لأنواع الجنس *Cucurbita* تضم النسيج الكلورنكيمي . إما عدد صفوف الخلايا العمادية فقد بلغ (2) صف في الأنواع *Citrullus Lanatus* و *Cucurbita maxima* و *Cucurbita pepo*, في حيث تراوح عددها بين (2-1) صف في بقية الأنواع المدروسة وعلى الأكثر (1) صف في النوع *Cucurbita moschata* وبذلك يمكن استخدامها في فصل النوع الأخير عن بقية أنواع الجنس *Cucurbita*. وكما تختلف الطبقة العمادية بأطوالها فالأطول يكون تحت البشرة يليه الأصغر . أما بالنسبة لمعدل سمكها فتراوح بين (74.6) مايكروميتر للنوع *Cucurbita moschata* و (150) مايكروميتر للنوع *Cucumis* , أما في بقية الأنواع فقد كان معدل سمك الخلايا العمادية متداخلا. إما الطبقة الثانية من الميزوفيل والمتمثلة بالخلايا الأسفنجية والتي غالبا ماتكون خلايا دائرية مفصصة ومفككة يتراوح سمكها بين (61.4) مايكروميتر للنوع *Cucurbita pepo* و (130.8) مايكروميترللنوع *Cucumis melo* . **أما عن الحزم الوعائية** فهي ذات أهمية تصنيفية معتمدة في

عزل بعض الأنواع قيد الدراسة حيث أمكن استخدام صفة عدد الحزم الوعائية في منطقة العرق الوسطي في عزل الأنواع وهذا ماأكده [14] .

وبذلك تم تقسيم الأنواع قيد الدراسة إلى ثلاث مجاميع :

- **المجموعة الأولى** : اتصفت بكون منطقة العرق حاوية على أربعة حزم وعائية ، الكبيرة منها وسطية الموقع وثلاث متوسطة الحجم ، أثنتان جانبيتان ، وثالثة صغيرة تقابل الحزمة الكبيرة لوحظت في نوعين للجنس *Cucurbita* هما *C.moschata* و *C.pepo*.
- **المجموعة الثانية:** امتازت بكون العرق الوسطي حاو على ثلاث حزم وعائية، وسطية كبيرة واثنتان صغيرة جانبيتان وقد لوحظت في النوع *Luffa cylindrica* فقط.
- **المجموعة الثالثة:** كان العرق فيها حاو على حزمتين الكبيرة في الأسفل تقابلها حزمة واحدة صغيرة وقد لوحظت بقية الأنواع القيد الدراسة.

وبذلك وباستخدام هذه الصفة أمكن عزل نوع *Luffa cylmdrica* عن بقية الأنواع المدروسة وكذلك فصل النوع *Cucurbita maxima* عن أنواع الجنس *Cucurbita* . فضلا عن ذلك، توجد حزمة جانبية تتدرج بالصغر باتجاه حافة النصل المتمثلة بالعرقيات الثانوية والثلاثية إما أشكالها فكانت على الأغلب بيضوية الشكل تحيطها الألياف السكلرنكيمية المحتشدة المتمثلة بألياف قبعة الحزمة ولجميع الأنواع المدروسة.

* فمن النتائج المحصل عليها من خلال دراسة صفات الورقة أمكن استخدامها في فصل بعض أنواع الأجناس قيد الدراسة ، وهذا يؤكد أن الصفات التشريحية للورقة ذات أهمية تصنيفية كبيرة وهذا ماأشار إليه [20] في أن بناء الورقة يعتمد عليها كأداة ضرورية في الحقل التصنيفي وقد نالت اهتمام خاص من قبل عدة باحثين أمثال [21] و[22].

- المقطع المستعرض لسويقات نصول الأوراق Cross section of petioles

امتازت أنواع الأجناس المدروسة بكونها سويقية الأوراق . إما المقاطع المستعرضة لسويقات الأنواع فقد أبدت تغايرا في الشكل المقطع وسمك منطقة القشرة وعدد وسعة الحزم الوعائية وصفات أخرى. فقد أوضحت الدراسة التشريحية لسويقات الأنواع المدروسة بان شكل المقطع العام للسويق يأخذ الشكل النصف دائري من الأسفل ومقعر من الجهة العليا لتكون زوائد جانبية باستثناء النوع

Cucurbita maxima فقد كان الشكل العام للمقطع دائري لايحوي تقعر . بهذا أمكن استخدام هذه الصفة في عزل هذا النوع عن بقية أنواع الجنس *Cucurbita* .

إما تشريحيا من الخارج إلى الداخل فقد لوحظ صف واحد من الخلايا البشرة المكعبة أو البيضوية – المستطيلة الشكل يغطيها من الأعلى طبقة من الأدمة وتراوح معدل سمك البشرة بين (16.9) مايكروميتر و (33.58) مايكروميتر للنوعين *Cucurbita moschata* و *Cucumis sativus* على التوالي تلي طبقة البشرة طبقة القشرة Cortex المتمثلة بطبقات من الخلايا الكولنكيمية وهي من النوع الكولنكيما الزاوية Angular Collenchyma ، إذ لوحظ تغاير في عدد طبقات وسمك الخلايا الكولنكيمية . تراوح عدد طبقاتها بين (2–6) طبقات كحد أدنى في النوع *Cucumis sativus* و (7–11) طبقات كحد أعلى في النوع *Cucurbita moschata*. إما معدل سمكها فتراوح بين (112.5) مايكروميتر في النوع *Cucurbita pepo* و (278.1) مايكروميتر كحد أعلى في النوع *Cucumis melo*, إما بقية الأنواع فكانت محصور بين تلك المديات ، بذلك استخدمت هذه الصفة في فصل بعض الأنواع عن بعضها كما موضح (جدول 3) (لوحه 7و 8). ومن الجدير بالذكر أن طبقة الكولنكيما الزاوية يزداد عدد طبقاتها في مناطق المقابلة للحزم الوعائية ، إما الاسطوانة الوعائية والتي كما أشار إليها [14] و [20] بأنها حزم وعائية ثنائية الجانب Bicollateral ثنائية اللحاء منفصلة عن بعضها البعض بواسطة شريط عريض من الأنسجة الأساسية ومرتبة بهيئة حلقتين 2-ring ,إلا إن أنواع الأجناس المدروسة كانت الحزم الوعائية فيها مرتبة بهيئة حلقة واحدة 1-ring (لوحة 7و 8). ويغطي تلك الحزم مجموعة من الألياف المحتشدة مع بعضها لتكون ألياف قبعة الحزمة Bund cup fiber وقد لوحظ تغاير في عدد وطول الحزم الوعائية بحيث أمكن استخدامها كصفة تصنيفية مهمة في عزل أو فصل الأنواع الأجناس قيد الدراسة كما موضح (جدول 3). اقل عدد للحزم كان في النوع *Luffa cylindrica* وبلغ (7) حزم، في حين وصل عددها (15)حزمة وعائية في النوع *Cucurbita pepo* إذ تميز هذا النوع بوجود حزمة وعائية صغيرة جدا أسفل منطقة التقعر لم تلاحظ في بقية الأنواع المدروسة , وبذلك أمكن استخدام هذه الصفة في عزل هذا النوع عن بقية أنواع الجنس *Cucurbita*. إما معدل طول الحزم الوعائية فتراوح بين (357.5) مايكروميتر و (1280.7) مايكروميتر للنوعين *Luffa cylindrica* و *Cucurbita moschata* على التوالي (لوحة 7,8). إما منطقة الخشب فقد

تميزت بوجود الوحدات الوعائية المرتبة على شكل صفوف قطرية وقد تداخلت أعداد تلك الصفوف بين أنواع الأجناس المدروسة, بلغ أدنى حد لعددها (2)صف في النوعين *Cucumis sativus* و *Cucurbita pepo* وأعلى حد كان في النوع *Cucurbita moschata* جدول (7و8). إما معدل قطر تلك الوحدات فقد تراوح بين (25.86) مايكروميتر و(44,7) مايكروميتر للنوعين *Luffa cylindrica* و *Cucurbita pepo* وقد استخدمت هذه الصفة في عزل بعض الأنواع المدروسة عن بعضها . (جدول 3) (لوحة 7و8) . مما تقدم من الخصائص التشريعية لسويقات أنواع الأجناس قيد الدراسة ، يمكن استخدم أيضا صفة كثافة انتشار الشعيرات ونوعها على بشرة السويق (جدول 3).

- ***المقطع المستعرض للساق Cross Section of stem***

- أوضحت الدراسة التشريحية لسيقان أنواع الأجناس المدروسة بان شكل المقطع العام لم يكن ذو قيمة تصنيفية عالية، فقد تميزت جميع الأنواع بأنها ذات شكل مضلع (خماسي الأضلاع).. إلا أن هناك تغاير في شكل قمة الأضلاع عند بعض الأنواع المدروسة. فكانت ذا شكل مثلث حاد الزاوية في النوع *Luffa cylindrica* , في حين كانت ذا شكل دائري في ساق النوع *Cucurbita moschata* , وبذلك استخدمت هذه الصفة في عزل هذين النوعين عن بقية الأنواع المدروسة . أما بقية الأنواع فكانت قمة الضلع ذا شكل شبه دائري – مثلث (لوحة 9و10). إما تشريحيا من الخارج إلى الداخل فقد لوحظ صف واحد من خلايا البشرة البيضوية او المتطاولة – المكعبة الشكل يغطيها من الأعلى طبقة من الأدمة Cuticle . وتراوح معدل سمك البشرة بين (10) مايكروميتر و (23.3) مايكروميتر للنوعين *Luffa cylindrica* ، *Cucumis sativus* على التوالي . **أما القشرة** فقد تمثلت بالخلايا الكولنكيمية والتي أشار إليها [14] بأنها طبقة واسعة Abundant وغالبا ما تحتل مساحة كبيرة من الساق بالأخص عند الأضلاع (in the ribs) ، وكانت من نوع الكولنكيميا الزاوية . إذ تراوح عدد طبقاتها بين (5-2) طبقات في النوع *Cucumis melo* و(10-6) طبقات في النوع *Cucurbita maxima*. أما معدل سمكها فتراوح بين (76.8) مايكروميتر و (165.2) مايكروميتر للنوعين *Cucumis sativus* و *Cucurbita maxima* على

التوالي. بقية الأنواع كانت محصورة ضمن تلك المديات . بعد هذه الطبقة تأتي طبقة الخلايا البرنكيمية الكبيرة الحجم والحاوية على مسافات بينية ، إذ تتراوح عدد طبقاتها بين (2) طبقة في النوع *Cucurbita moschata* , أما بقية الأنواع المدروسة تراوحت بين (4-1) . أما معدل سمكها بلغ (39.4) مايكروميتر في النوع *Luffa cylindrica* و (94.25) مايكروميتر في النوع *Cucumis sativus* وبذلك أمكن استخدام هذه الصفة في عزل هذين النوعين عن بقية الأنواع المدروسة. بعدها تأتي حلقة مفتوحة من الخلايا السكلرنكيمية في السيقان الفتية ثم تصبح حلقة مستمرة تحيط بالحزم الوعائية والتي يطلق عليها بـ Per vascularbundle fiber [14] وهذا يتفق مع نتائج الدراسة الحالية . إذ كانت عدد طبقاتها متداخلا بين (7-2) إذ لوحظ الحد الأدنى (2) طبقة في النوع *Cucumis sativus* و (7) طبقة الحد الأعلى في النوعين *Cucurbita moschata* و *Luffa cylindrica* . أما سمك طبقة الدائرة المحيطة السكلرنكيمية فتراوح بين (35.90) مايكروميتر و (138.1) مايكروميتر للنوعين *Cucurbita pepo* و *Cucurbita moschata* , بذلك استخدمت هذه الصفة في فصل أنواع الجنس *Cucurbita* فضلا عن عزل الأنواع الأخرى للأجناس قيد الدراسة (جدول 4) . بعد طبقة الدائرة المحيطة السكلرنكيمية تأتي طبقة من الخلايا البرنكيمية والتي يتراوح معدل سمكها بين (275.5) مايكروميتر في النوع *Citurullus lanatus* كحد أدنى و (584) مايكروميتر كحد أعلى في النوع *Cucurbita maxima* . **أما منطقة الاسطوانة الوعائية** فقد اتفقت نتائج الدراسة الحالية مع ما أشار إليه [14] بان الحزم الوعائية منفصلة عن بعضها بواسطة شريط عريض من الأنسجة الأساسية ، وثنائية الجانب (ثنائية اللحاء) Bicollatoral ومرتبة بحلقتين 2-rings أو أكثر أو اقل . كما ذكر أن الحزم الداخلية تقابل مركز الساق . فمن نتائج الدراسة الحالية لوحظ أن الحزم الوعائية للأنواع قيد الدراسة مرتبة بحلقتين الخارجية والداخلية , ففي الحلقة الخارجية كانت جميع مقاطع سيقان الأنواع المدروسة مكونة من (5) حزم وعائية حزمة في كل ضلع ، أما الحلقة الداخلية فقد كان هناك تغاير في عدد وترتيب الحزم كما موضح في (جدول 4) . إذ أمكن استخدام هذه الصفة في عزل أنواع الأجناس المدروسة عن بعضها تشريحيا . كما ذكر [14] أن عدد الحزم الوعائية في السيقان الناضجة صفة تصنيفية مهمة

في عزل أنواع أجناس العائلة القرعية ، وهذا يتفق مع نتائج الدراسة الحالية ويتعارض مع ما توصلا إليه [20] أن صفة عدد الحزم الوعائية متداخلة بين أنواع الجنس *Cucubita* ، **أما** من نتائج الدراسة الحالية فقد أمكن تقسيم الأنواع المدروسة استنادا لهذه الصفة إلى خمس مجاميع موضحة في جدول (4). **أما طول الحزم الوعائية** فتراوح بين (799.16) مايكروميتر في النوع *Cucumis sativus* كحد أدنى و (1089. 5) مايكروميتر في النوع *Cucumis sativus*. أما منطقة الخشب فقد كانت الوحدات الوعائية مرتبة على شكل صفوف تداخلت أعدادها بين أنواع الأجناس المدروسة، فقد تراوحت أعدادها بين (5-2) صف كحد أدنى في النوع *Cucurbita pepo* و (11-6) صف في النوع *Cucurbita moschata* كحد أعلى . أما معدل قطر تلك الوحدات فقد تراوح بين (29.37) مايكروميتر في النوع *Cucurbita pepo* و (90.8) مايكروميتر في النوع *Citurullus lanatus* . **أما منطقة الـ pith** فقد امتاز ساق النوع *Luffa cylindrica* انه صلد solid مكون من خلايا برنكيمية, في حين امتازت سيقان بقية الأنواع المدروسة بكونها مجوفة Hollow .

ومما سبق نستنتج ما يأتي:

1. الطراز الثغري النصف المتعامد Hemiparacytic سائد في النوع *Citrullus lanatus* إضافة للطراز الشاذ, وبذلك أمكن استخدام هذه الصفة في عزل النوع عن بقية الأنواع المدروسة.
2. أمكن عزل النوع *Cucurbita pepo* باستخدام صفة كثافة انتشار الثغور على السطح العلوي أكثر من السطح السفلي و بكون مقطع نصل الوريقة مستوي من الأعلى ومحدب من الأسفل مقارنة ببقية الأنواع .
3. امتازت منطقة ميزوفيل الورقة في النوع *Cucurbita moschata* بكونها مؤلفة على الأغلب من صف واحد من الخلايا العمادية مقارنة لبقية أنواع الجنس *Cucurbita* .
4. أمكن استخدام صفة عدد الحزم الوعائية في منطقة العرق الوسطي للورقة في فصل بعض الأنواع .

5. أمكن أيضا فصل النوع Cucurbita maxima عن بقية أنواع الجنس Cucurbita بكون المقطع العام للسويق دائري مقارنة لبقية أنواع الجنس Cucurbita . هذا فضلا عن صفات تصنيفية أخرى.

- مما تقدم نجد أن الخصائص التشريحية لأنواع الأجناس قيد الدراسة ساعدت على عزل وتشخيص الأنواع بعضها عن بعض استنادا إلى اختلافها في بعض الصفات أو من معرفة مدى تشابه وتقارب الأنواع في صفات أخرى ، وبذلك يمكن استخدام تلك الخصائص التشريحية مقرونة مع الخصائص الأخرى كدراسة الكساء السطحي للأجزاء الخضرية أو دراسة حبوب اللقاح فضلا عن الصفات المظهرية المعروفة مسبقا في تشخيص وعزل تلك الأنواع بصورة صحيحة .

جدول-1: التغايرات الكمية والنوعية في طبيعة خلايا بشرة الورقة والمعقد الثغري لأنواع الأجناس المدروسة (مقاسة بالمايكروميتر)

ت	الأنواع	السطح السفلي				السطح العلوي				طبيعة جدران خلايا البشرة		أنواع المعقدات الثغرية
		أبعاد الثغر		دليل الثغور	معدل طول × عرض خلايا البشرة	أبعاد الثغر		دليل الثغور	معدل طول × عرض خلايا البشرة			
		طول	عرض			طول	عرض					
1	*Citrullus lanatus*	22.5-15 (20)	17.5-12.5 (17.5)	21.6	27.5×47.5	30-20 (25)	20-17.5 (19.1)	18.3	32.5×53	منحنية	مستقيمة – منحنية	النصف متوازي + الطراز الشاذ
2	*Cucumis melo*	22.5-17.5 (20)	15.5-12.5 (15)	18.6	22.5×40	27.5-17.5 (22.5)	17.5-12.5 (13.75)	18.8	27.5×47.5	متموجة	مستقيمة – منحنية قليلا	الشاذ
3	*Cucumis melo.var. flexuosus*	30-17.5 (22.5)	17.5-10 (15)	30.2	26.25×34.8	30-17.5 (22.5)	17.5-12.5 (15)	24.6	22.5×37.5	متموجة – شديدة التموج	منحنية	الشاذ
4	*Cucumis sativus*	27.5-14 (25)	20-15 (17.5)	29	37.5×63.3	27.5-15 (22.5)	17.5-10 (12.5)	16.3	22.5×40	شديدة التموج	مستقيمة – منحنية قليلا	الشاذ + القليل من النصف المتوازي

الشاذ	مستقيمة – منحنية قليلا	شديدة التموج	25×50	10.6	17.5–12.5 (15)	25–17.5 (22.5)	22.5×32.5	23.3	17.5–12.5 (14.4)	22.5–15 (19.8)	***Cucurbita maxima***	**5**
الشاذ	مستقيمة – منحنية	شديدة التموج	26.1×46.7	9.1	20–15 (17.2)	30–22.5 (25)	38.7×59.1	19.9	20–15 (17.5)	30–19.5 (25)	***Cucurbita moschata***	**6**
الشاذ	منحنية	مستقيمة منحنية قليلا	18.5×25	13.7	–11.25 17.5 (15)	30–12.5 (17.5)	25×37.5	11.4	20–12.5 (16.25)	27.5–17.5 (23)	***Cucurbita pepo***	**7**
الشاذ	مستقيمة	متموجة	27.5×40	12.2	20–15 (20)	27.5–20 (22.5)	32.5×60	20.6	22.5–15 (17.5)	32.5–20 (27.5)	***Luffa cylindrica***	**8**

- **الأرقام خارج الأقواس تمثل الحدين الأدنى والأعلى وبداخلها تمثل المعدل .**

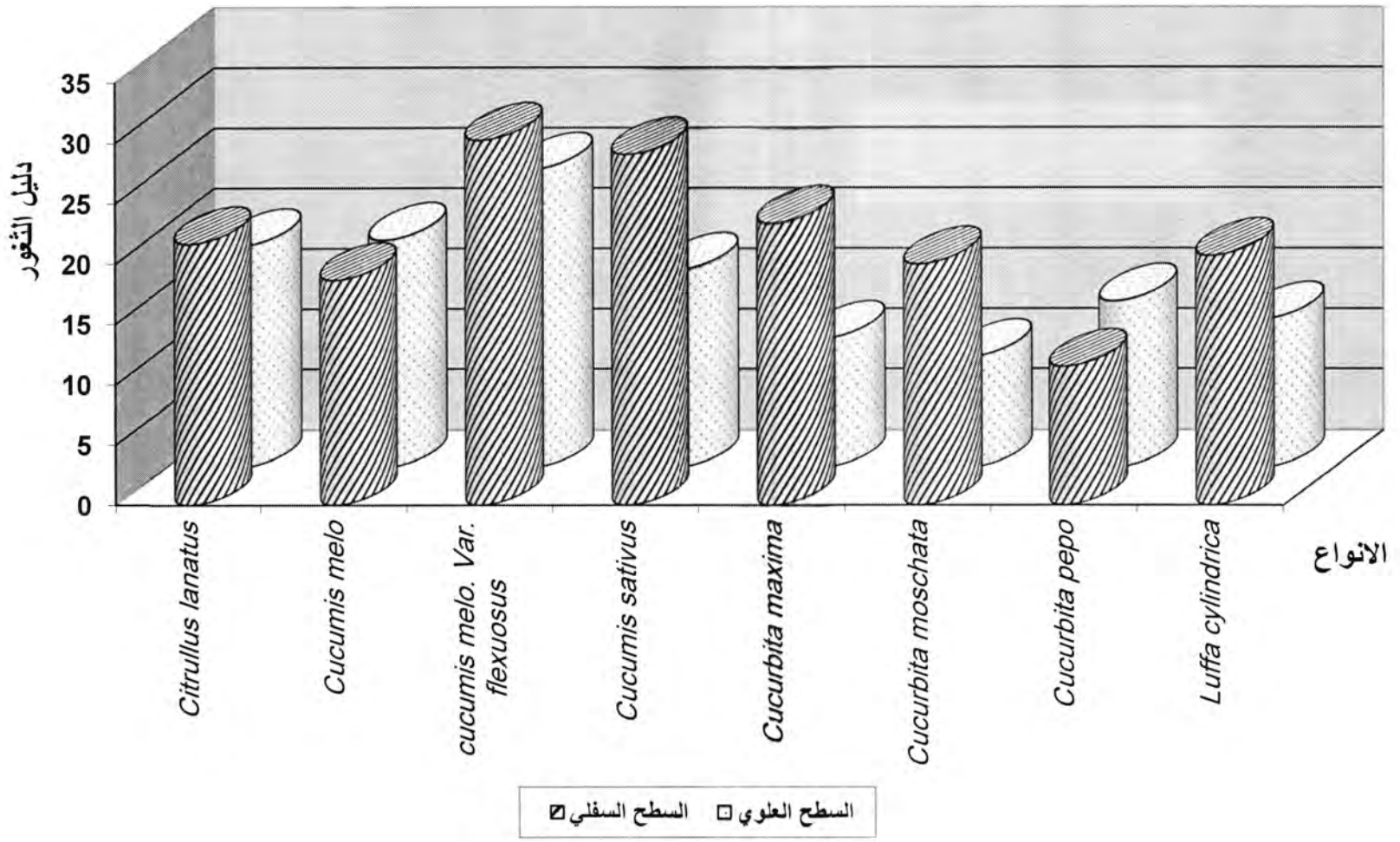

شكل –1: التغاير في دليل الثغور للسطحين العلوي والسفلي في أنواع الأجناس المدروسة

جدول -2: التغايرات في أبعاد وقياسات المقاطع المستعرضة لنصول وريقات أنواع الأجناس المدروسة مقاسه بـ (المايكروميتر)

ت	اسم النوع	سمك الكيوتكل	سمك الورقة	سمك البشرة العليا	سمك البشرة السفلى	عدد طبقات الخلايا العمادية	سمك الطبقة العمادية	سمك الطبقة الاسفنجية	الملاحظات
1	*Citrullus lanatus*	6.25-2.5 (4.7)	262.5-0.167.0 (251.4)	27.5-12.5 (18.9)	32.5-15.0 (26.7)	2 متراصة	142.5-80.0 (112.5)	110.0-70.0 (83.8)	السطح السفلي والعلوي يحوي خلايا كبيرة كقواعد للشعيرات.
2	*Cucumis melo*	2.5	375.0- 155 (306.8)	35.5-17.5 (25.9)	250-12.5 (17.5)	2-1	175.0-100.0 (150.0)	152.5-72.5 (109.7)	مستو ومقعر من الأعلى- محدب من الأسفل. العرق حاو حزمتين كبيرة وصغيرة.
3	*Cucumis melo .var. flexuosus*	2.5	375.5-257.5 (280.0)	30.0-15.0 (21.3)	17.5-10.0 (14.0)	2-1 متطاولة ومتراصة	117.5-100.0 (107.9)	150.0-112.5 (130.8)	مقعر-شبه مستو من الأعلى-محدب من الأسفل. العرق حاو حزمتين إحداهما كبيرة وأخرى صغيرة .
4	*Cucumis sativus*	2.5	275-187.5 (235.3)	47.5-22.5 (33.8)	27.5-10.0 (15.9)	2-1	120.0-95.0 (109.1)	117.5-45.0 (84.4)	مستوي-مقعر من الأعلى-محدب من الأسفل.العرق حاو حزمتين.
5	*Cucurbita maxima*	2.5	262.5-187.5 (213.6)	30.0-12.5 (20.0)	15.0-7.5 (14.1)	2 متراصة جدا	117.5-87.5 (103.9)	137.5-55.0 (78.2)	مقعرة من الأعلى-محدبة من الأسفل .العرق حاو حزمتين جانبيتين الكبيرة في الأسفل..
6	*Cucurbita moschata*	2.5-1.25 (1.9)	245.0-150.0 (172.8)	27.5-15.0 (21.4)	25.0-7.5 (13.0)	2-1	92.5-50.0 (74.6)	87.5-50.0 (66.8)	مستو- شبه مقعر من الأعلى ومحدب من الأسفل. العرق حاو حزمة كبيرة وسطية و 3 متوسطة الحجم.

7	*Cucurbita pepo*	2.5	270–155.5 (237.5)	40.0–17.5 (18.0)	32.5–12.5 (20.3)	2 غير متراصة مع بعضها	137.5–113.5 (127.5)	75–50 (61.4)	مستوية من الأعلى–محدب من الأسفل العرق فيه حزمة كبيرة من الأسفل و3 متوسطة الحجم.
8	*Luffa cylindrica*	5–2.5 (3.8)	315.0–205.0 (277.5)	42.5–27.5 (35.5)	50.0–20.0 (31.0)	2–1	160.0–72.5 (118.1)	135.0–75.0 (99.4)	مقعر –شبه مستو من الأعلى – ومحدب من الأسفل. العرق حاو على 3 حزم وعائية الوسطية كبيرة و2 صغيرتان.

- **الأرقام خارج الأقواس تمثل الحدين الأدنى والأعلى وبداخلها تمثل المعدل .**

جدول -3: التغايرات في أبعاد وقياسات المقاطع المستعرضة لسويقات أنواع الأجناس قيد الدراسة (مقاسه بالمايكروميتر)

ت	الأنواع	سمك البشرة	الكولنكيماالزاوية		الحزم الوعائية			
			عدد طبقاتها	السمك	عدد الحزم	طول الحزم	عدد صفوف الوحدات الوعائية	قطر الوحدات الوعائية
1	*Cucumis melo*	00-17.5 (30.79)	6-4	225-125 (172.9)	9	1450-950 (1140)	6-5	47.5-20 (31.33)
2	*Cucumis melo var. flexuosus*	62.5-7.5 (26.4)	7-5	325 -225 (278.1)	9+(1) صغيرة جدا	1350-600 (1050.9)	6-4	70-12.5 (41.28)
3	*Cucumis sativus*	65-10 (33.58)	6-2	200-42.5 (120.36)	7+2صغيرة	310-125 (866.9)	5-2	55-20 (35.28)
4	*Cucurbita maxima*	35-10 (20.2)	9-2	275-62.5 (196.5)	14	750-400 (608)	5-3	50-12.5 (27.5)
5	*Cucurbita moschta*	30-10 (16.9)	11-7	320-162.5 (240.7)	11	2000-850 (1280.7)	7-5	67.5-17.5 (39.04)
6	*Cucurbita pepo*	27.5-12.5 (19.8)	6-3	137.5-62.5 (112.5)	12رئيسة+3ثانوي =15حزمة	700-150 (441.1)	5-2	70-15 (44.7)
7	*luffa cylindrica*	27.5-12.5 (18.57)	8-4	200-100 (145.4)	7	400-312.5 (357.5)	5-3	42.5-10 (25.86)

- الأرقام خارج الأقواس تمثل الحدين الأدنى والأعلى وبداخلها يمثل المعدل. * لايتوفر مقطع جيد للنوع *C. lanatus*

جدول -4: التغايرات في أبعاد وقياسات المقاطع المستعرضة لسيقان أنواع الأجناس قيد الدراسة (مقاسه بالمايكروميتر) .

ت	الأنواع	سمك البشرة	القشرة				عدد طبقات السكلرنكيما	سمك طبقة الدائرة المحيطية السكلرنكيمية	سمك طبقة البارنكيميا	عدد الحزم الوعائية	طول الحزم الوعائية	شكلها	عدد صفوف الوحدات الوعائية	قطر الوحدات الوعائية
			عدد طبقات الكولنكيما	سمك طبقة الكولنكيما الزاوية	عدد طبقات البارنكيميا	سمك طبقة البارنكيميا								
1	*Citrullus lanatus*	22.5-7.5 (14.7)	7-2	170-32.5 (93.5)	4-2	125-30 (64.66)	4-3	107.5-57.5 (77.5)	520-150 (77.5)	11	1100-480 (799.16)		5-2	230-17.5 (90.8)
2	*Cucumis melo*	32.5-7.5 (18.12)	5-2	112.5-37.5 (78.75)	4-3	250-62.5 (63.66)	6-3	167.5 -80.0 (128.3)	750-150 (384.28)	12-10 (11)	2150-550 (1390)		7-5	-17.5 112.5 (62.25)
3	*Cucumis melo var. flexuosus*	30-5 (14.8)	6-2	145-52.5 (94.2)	3-2	120-50 (87.27)	4-3	112.5-62.5 (80.89)	700-50 (302.5)	-9 التغايرات10	1900-600 (1291.5)		5-3	275-27.5 (144.25)
4	*Cucumis sativus*	40-10 (23.3)	7-1	162.5-17.5 (76.8)	4-2	137.5-15 (94.25)	6-2	142.5-57.5 (100)	570-150 (362.5)	9	2150-1000 (1589.5)		6-3	205-20 (66.2)
5	*Cucurbita maxima*	27.5-7.5 (16.9)	10-6	237.5-67.5 (165.2)	3-1	95-37.5 (70.86)	5-3	112.5-57.5 (78.69)	820-350 (584)	11	1450-850 (986)		7-3	145-7.5 (66.90)
6	*Cucurbita moschata*	20-7.5 (13.3)	8-2	200-37.5 (133.6)	2	75-42.5 (54.5)	7-6	157.5-112.5 (138.1)	600-450 (498.75)	12	1450-850 (1077.3)		11-6	-17.5 212.5 (68.9)
7	*Cucurbita pepo*	22.5-7.5 (16)	10-2	200-375.5 (132.29)	4-2	100-52.5 (78.40)	4-3	40-52.5 (35.90)	650-350 (508.8)	10	1200-350 (1000)		8-4	50-17.5 (29.37)
8	*Luffa cylindrica*	15-5 (10)	9-2	175-20 (77.5)	3-1	70-17.5 (39.4)	7-3	92.5-.40 (68.5)	330-280 (3 .303)	8			5-3	130-7.5 (43.70)

- الأرقام خارج الأقواس تمثل الحدين الأدنى والأعلى وبداخلها يمثل المعدل.

تكملة جدول –4: التغايرات في أبعاد وقياسات المقاطع المستعرضة لسيقان أنواع الأجناس قيد الدراسة (مقاسه بالمايكروميتر).

ت	الانواع	ترتيب الحزم الوعائية	
		الخارجية	الداخلية
1	*Citrullus lanatus*	(5) حزم متوسطة الحجم واحدة في كل ضلع	(3) حزم رئيسية كبيرة بينها (3) حزم صغيره
2	*Cucumis melo*	(5) حزم متوسطة الحجم واحدة في كل ضلع	(3) حزم كبيرة بينها صغيرة ومتوسطة
3	*Cucumis melo var. flexuosus*	(5) حزم متوسطة الحجم واحدة في كل ضلع	(5) حزم كبيرة
4	*Cucumis sativus*	(5) حزم متوسطة الحجم واحدة في كل ضلع	(4) حزم كبيرة
5	*Cucurbita maxima*	(5) حزم متوسطة الحجم واحدة في كل ضلع	(6) حزم كبيرة
6	*Cucurbita moschata*	(5) حزم متوسطة الحجم واحدة في كل ضلع	(7) كبيرة وصغيرة الحجم
7	*Cucurbita pepo*	(5) حزم متوسطة الحجم واحدة في كل ضلع	(5) متوسطة
8	*Luffa cylindrica*	(5) حزم متوسطة كبيرة الحجم واحدة في كل ضلع	(3) متوسطة الحجم

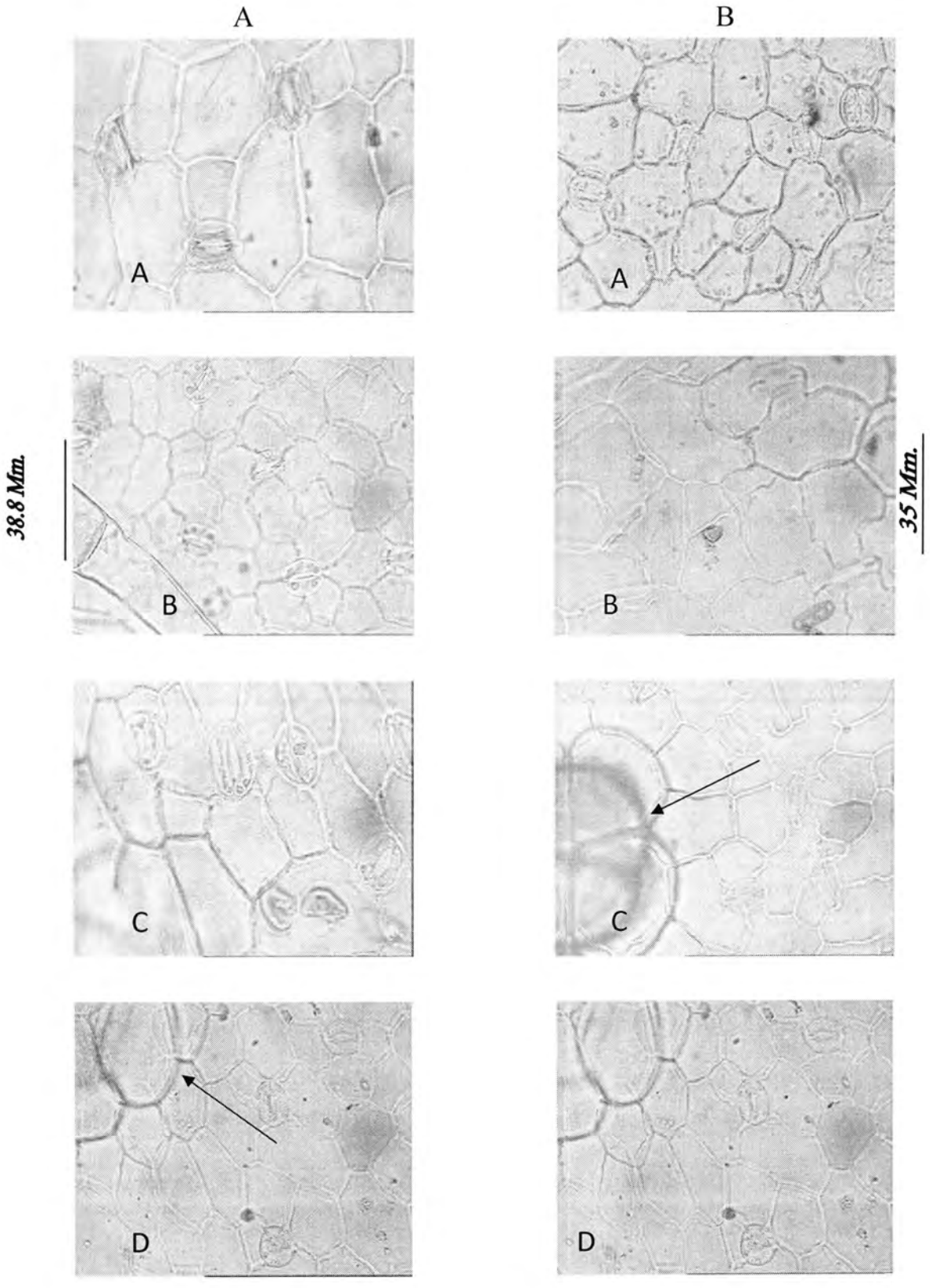

لوحة-1: التغايرات في صفات خلايا بشرة الورقة لبعض الانواع المدروسة

A: Citrullus lanatus *C : cucumis melo . var. flexuosus*

B : Cucumis melo *D: Cucumis sativus*

A : بشرة عليا *B : بشرة سفلى* ← *موقع شعيره*

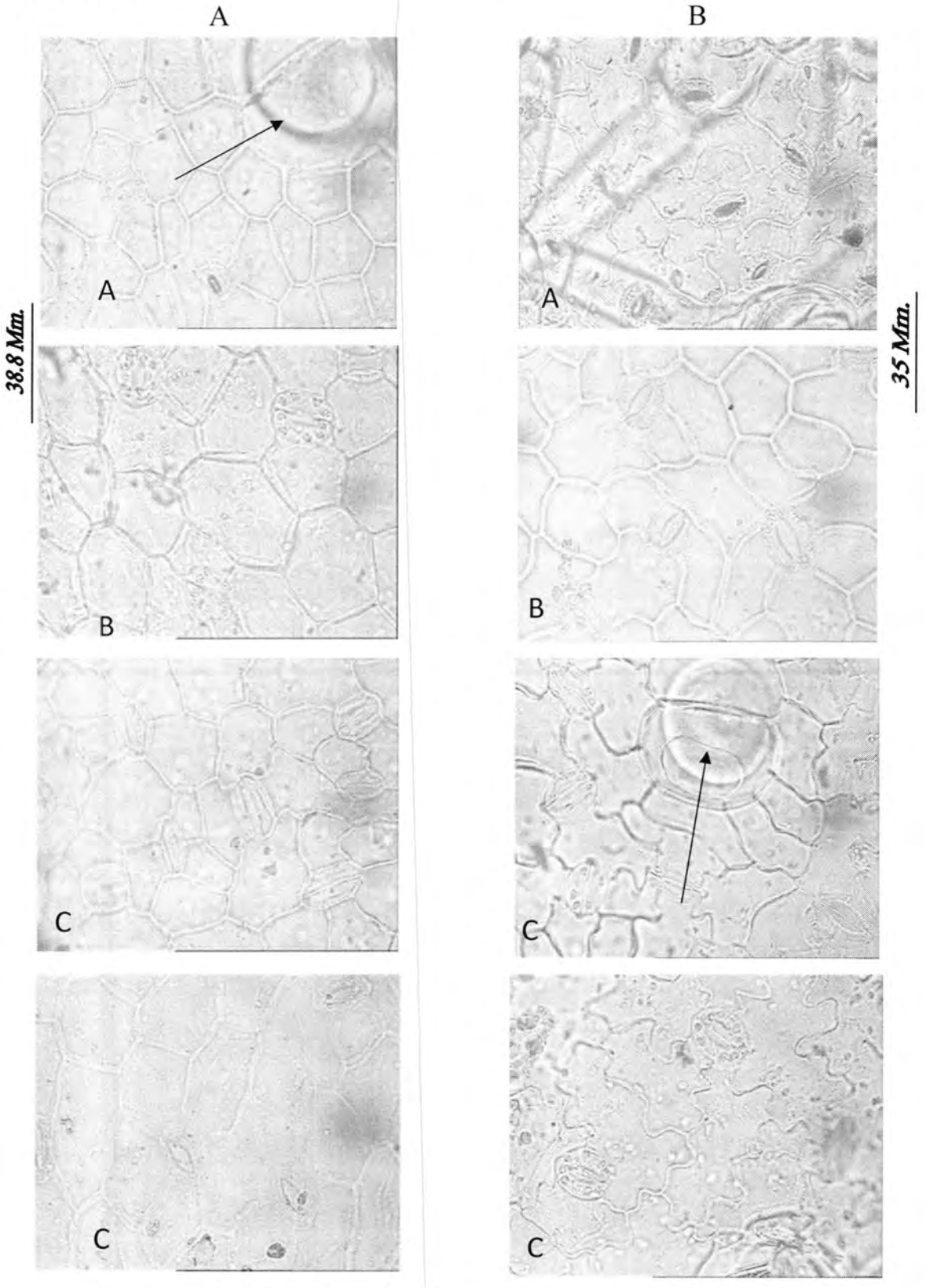

لوحة -2: التغايرات في صفات خلايا بشرة الورقة لبعض الانواع المدروسة

A: Cucurbita maxima
B : Cucurbita moschata
C : Cucurbita pepo
D : Luffa cylindrica

A : بشرة عليا *B : بشرة سفلى* ← *موقع شعيره*

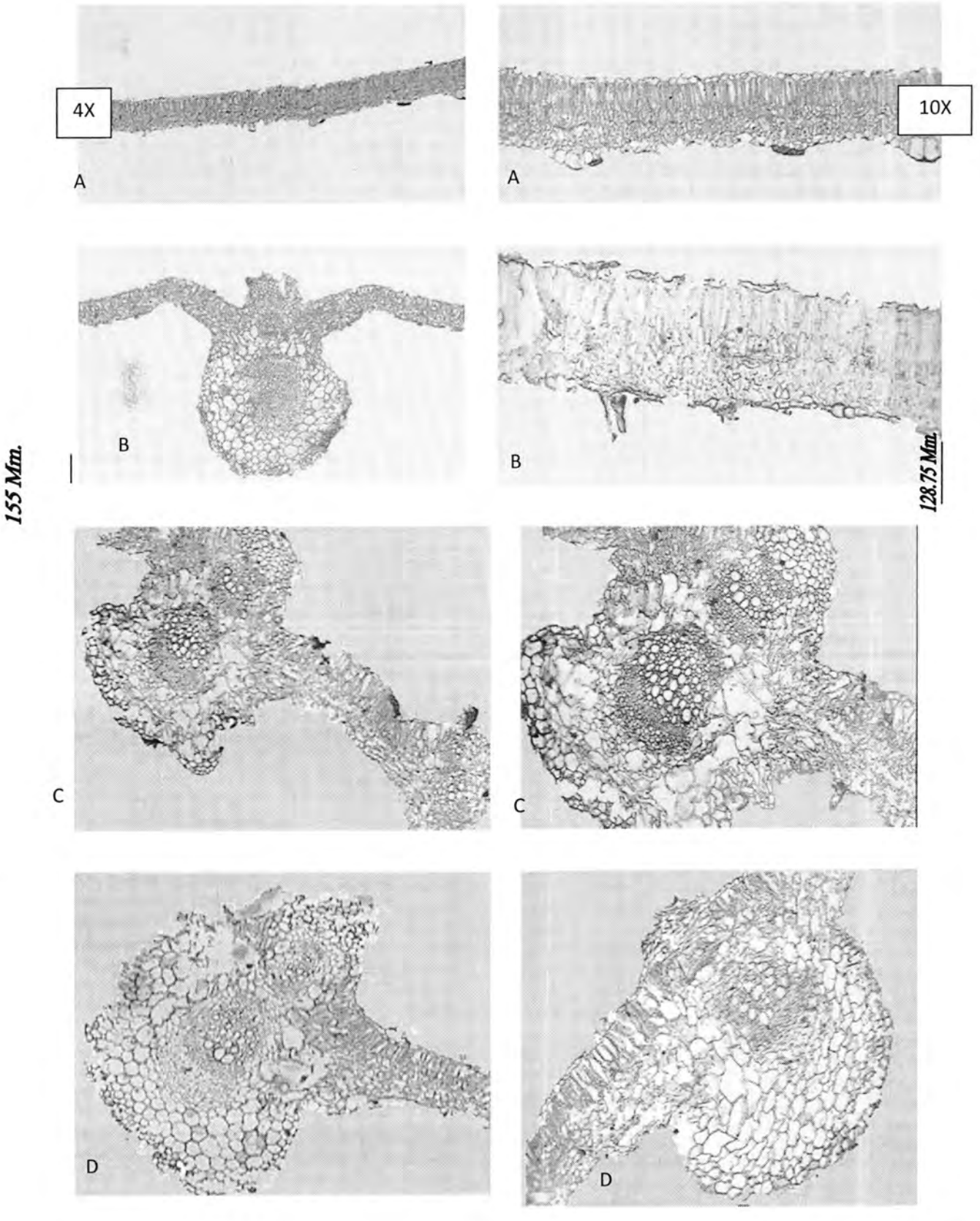

لوحة -3: التغايرات في أشكال وأبعاد نصول الأوراق لأنواع الأجناس المدروسة

A: Citrullus Lanatus
B : Cucumis melo
C : Cucumis melo. var. flexuosus
D : Cucumis sativus

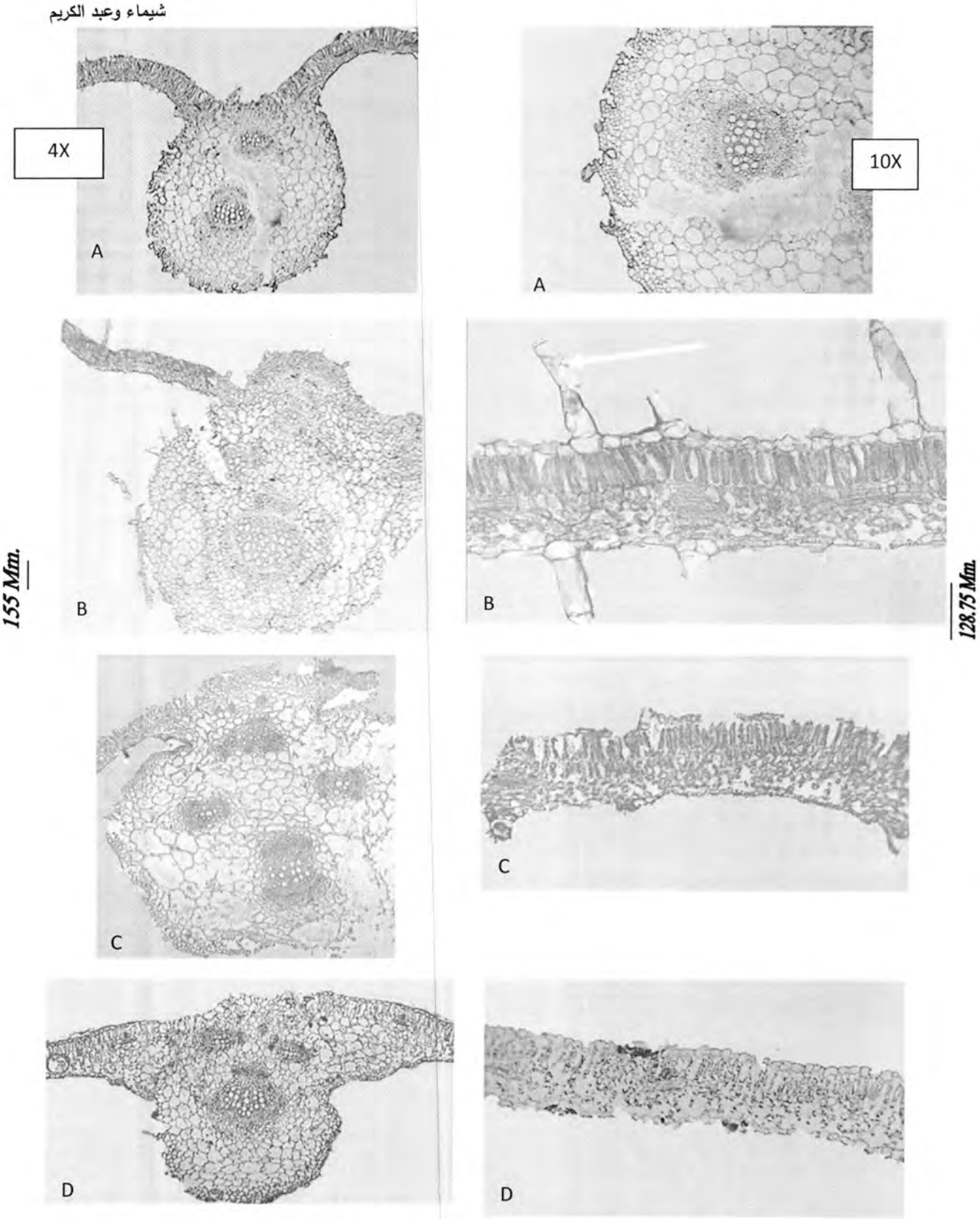

لوحة -4: التغايرات في أشكال وأبعاد نصول الأوراق لأنواع الأجناس المدروسة

A: Cucurbita maxima
B : Cucurbita moschata
C : Cucubita pepo
D : Luffa cylindrica

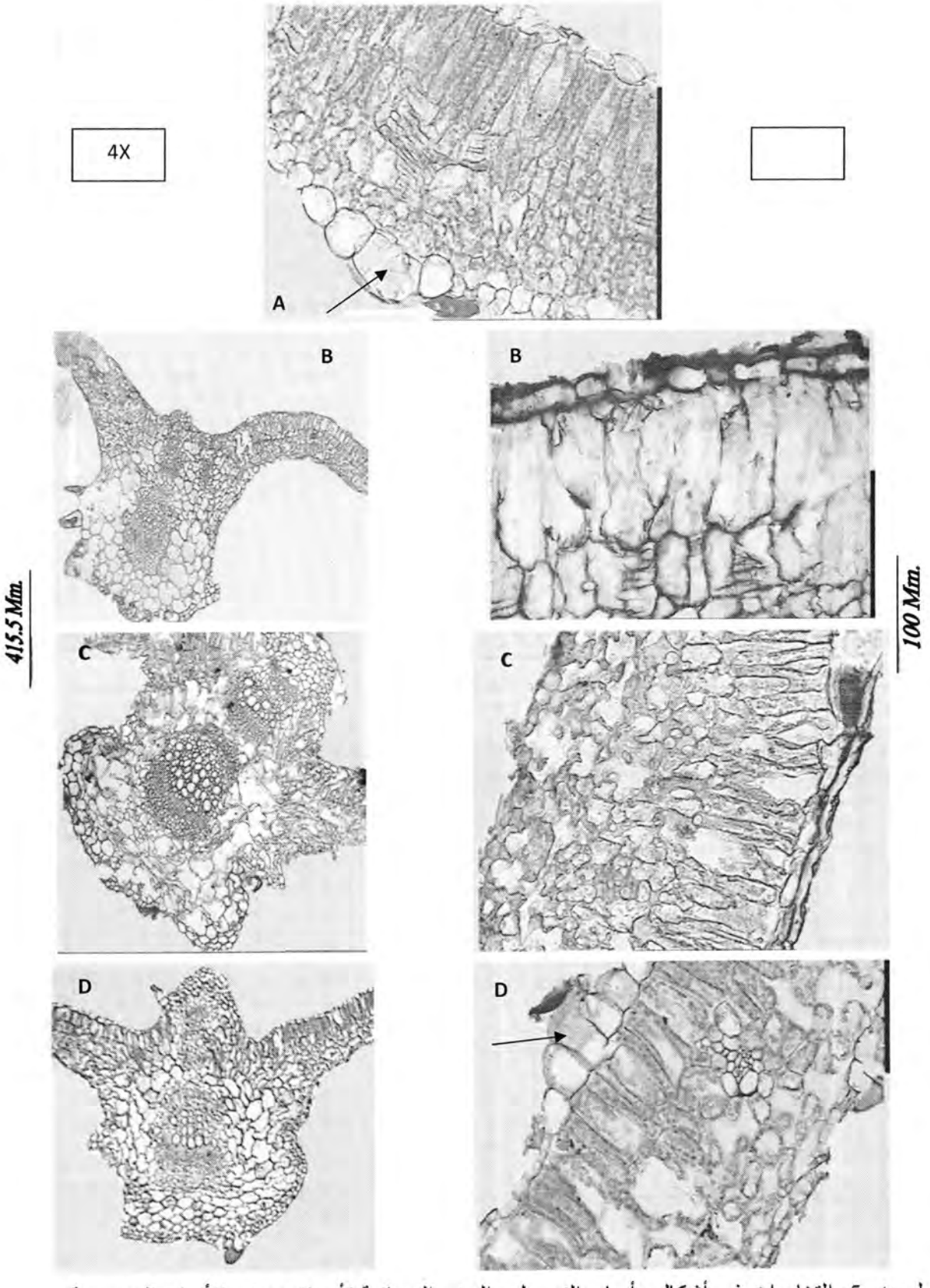

لوحه -5: التغايرات في أشكال وأبعاد النصول والحزم الوعائية لأوراق بعض الأنواع المدروسة

A : Citrullus lanatus

B : Cucumis melo

C : Cucumis melo. var.flexuosus

D : Cucmis sativus

شعيره موقع شعيره ⟶

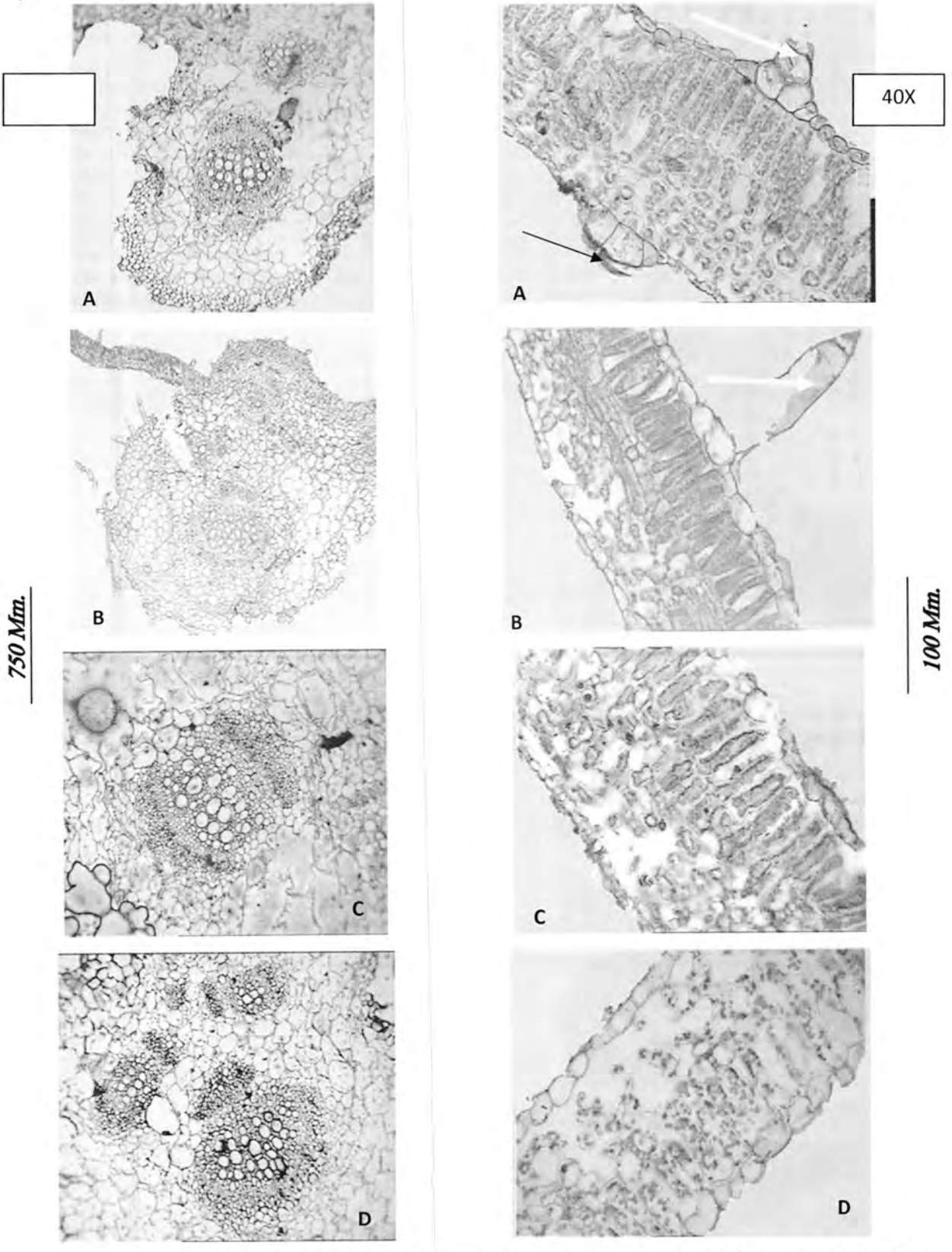

لوحة -6: التغايرات في أشكال وأبعاد النصول والحزم الوعائية لأوراق بعض الأنواع المدروسة

A : Cucurbita maxima
B : Cucurbita moschata
C : Cucurbita pepo
D : Luffa cylindrica

شعيره
موقع شعيره ⟶

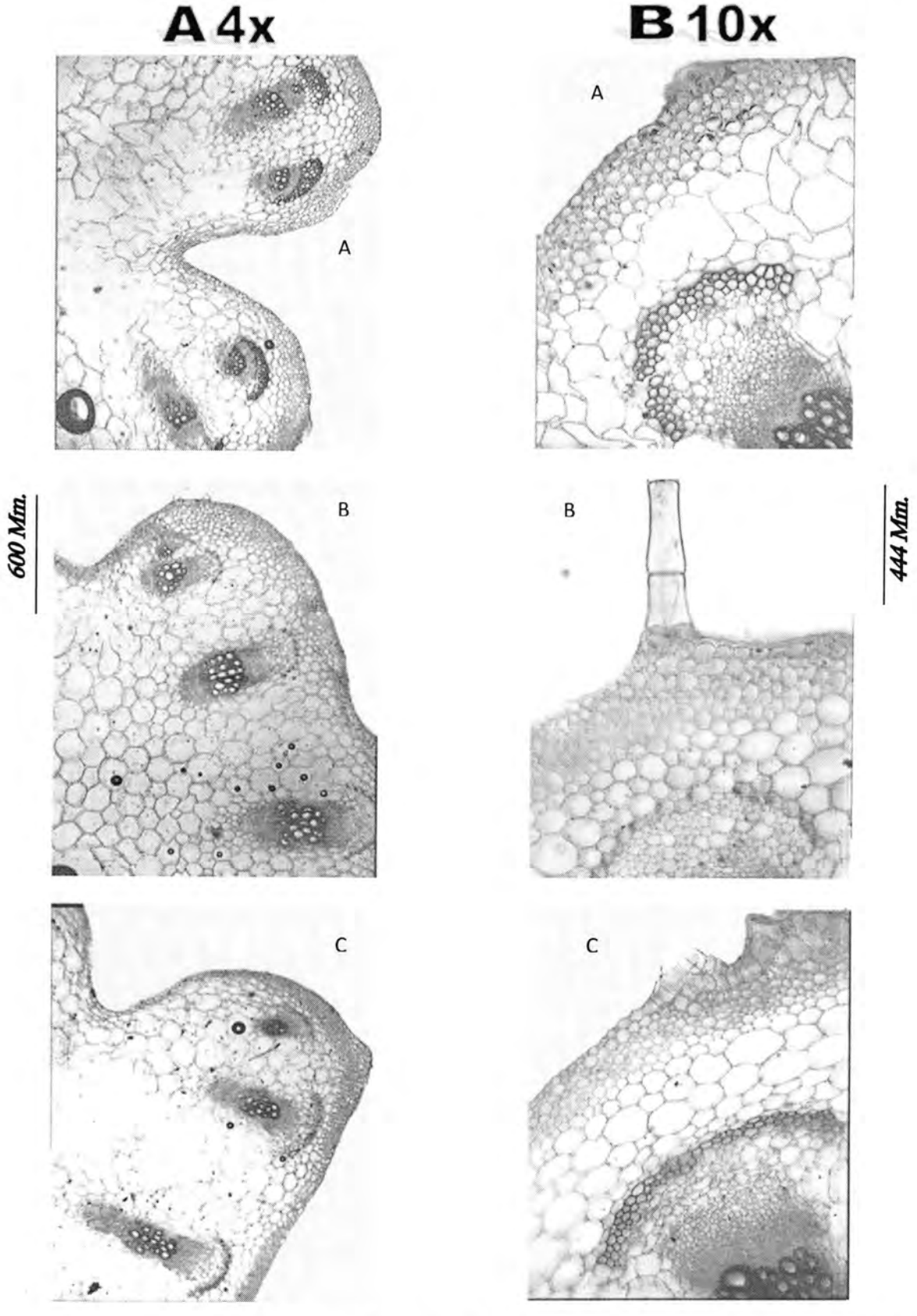

لوحة -7: التغايرات في أشكال وأبعاد سويقات نصول الوريقات لبعض الأنواع المدروسة

A: ***Cucumis melo***

B: ***Cucumis melo. Var. flexuosus*** C: ***Cucumis sativus***

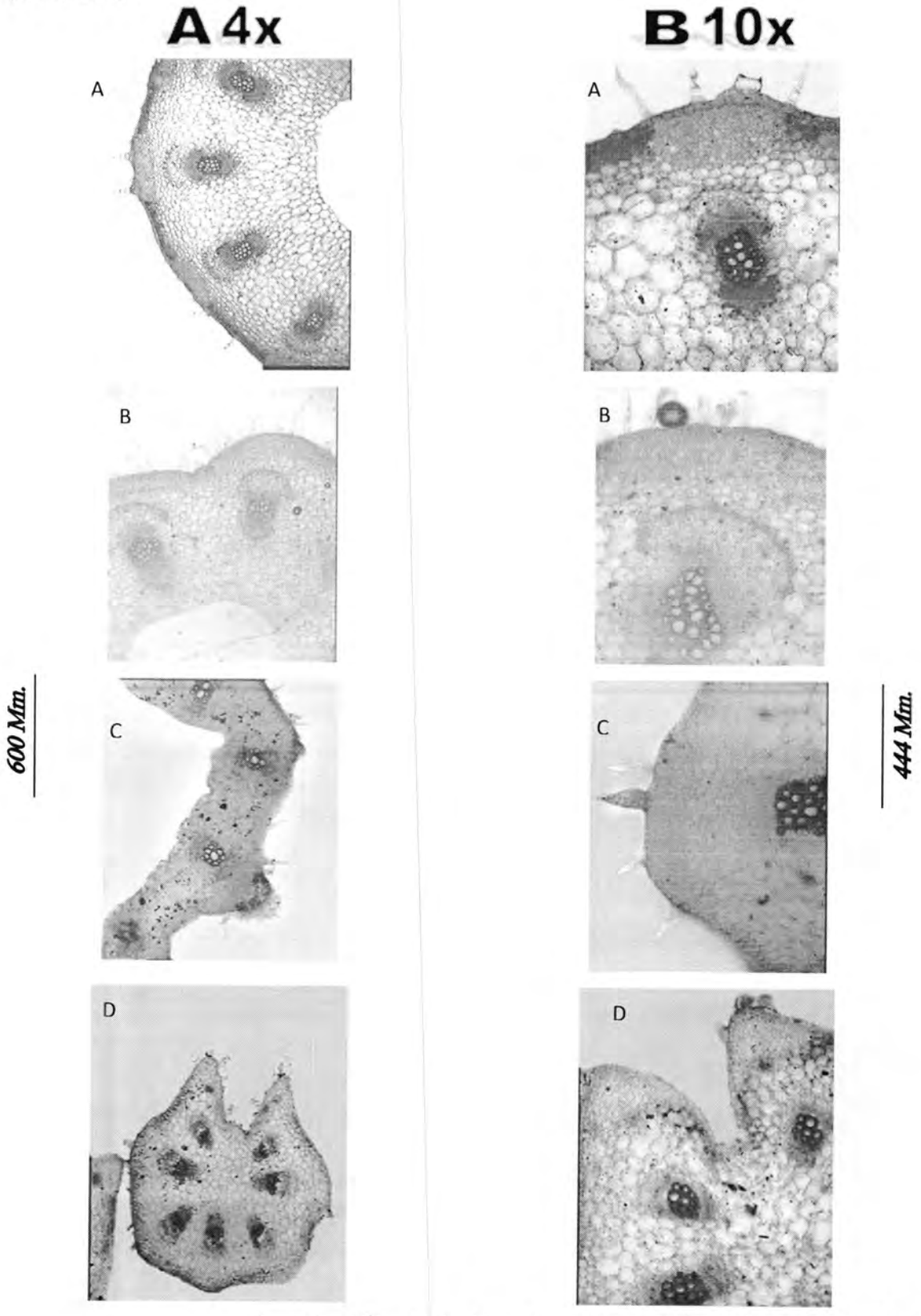

لوحة –8 : التغايرات في أشكال وأبعاد سويقات نصول الوريقات لبعض الأنواع المدروسة

A : ***Cucurbita maxima***
B : ***Cucurbita moschata***
C : ***Cucurbita pepo***
D : ***Luffa cylindrica***

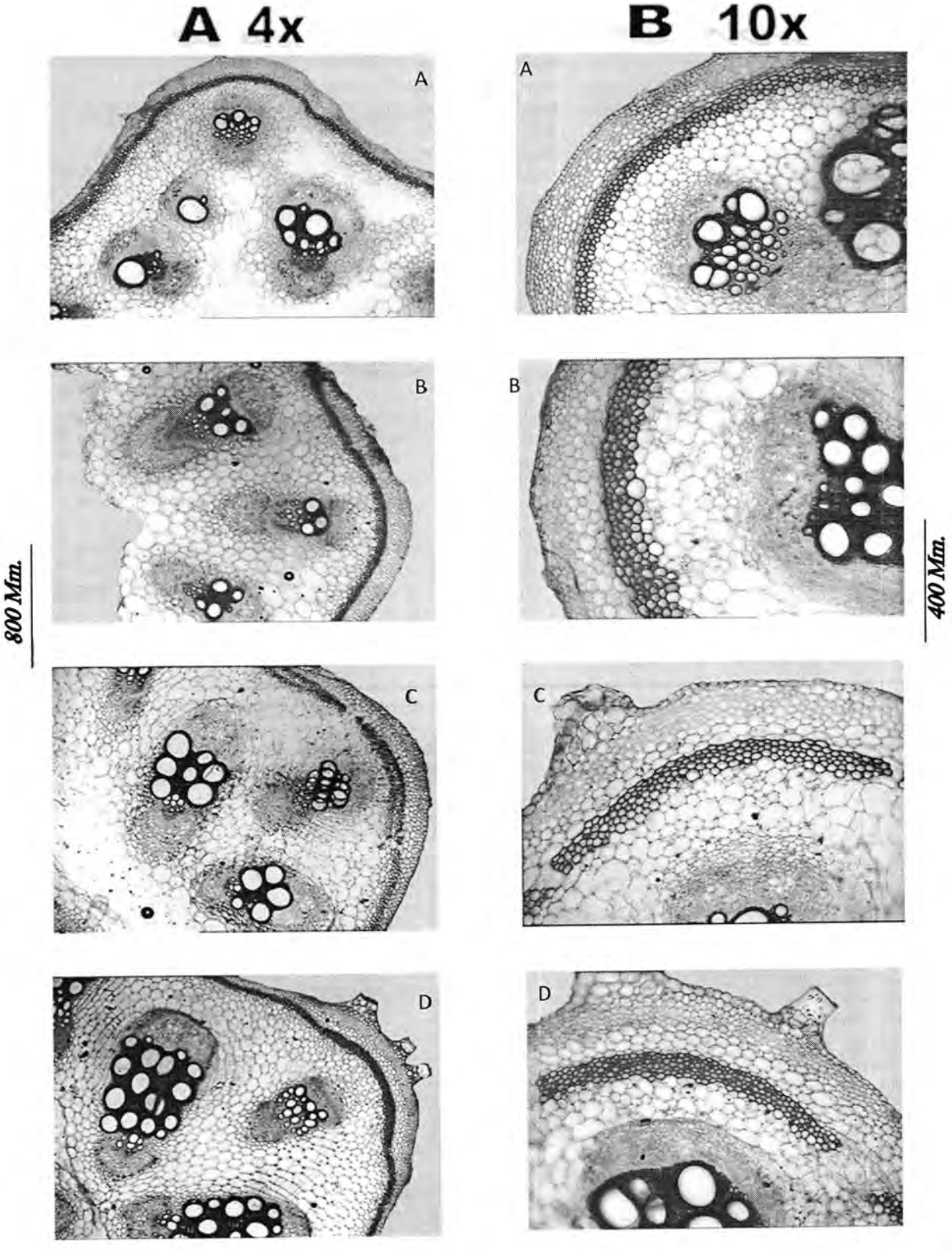

لوحة –9 : التغايرات في أِكال وأبعاد سيقان بعض الأنواع المدروسة

A : ***Citrullus lanatus*** C : ***Cucumis melo. Var. flexuosus***

B : ***Cucumis melo*** D : ***Cucumis sativus***

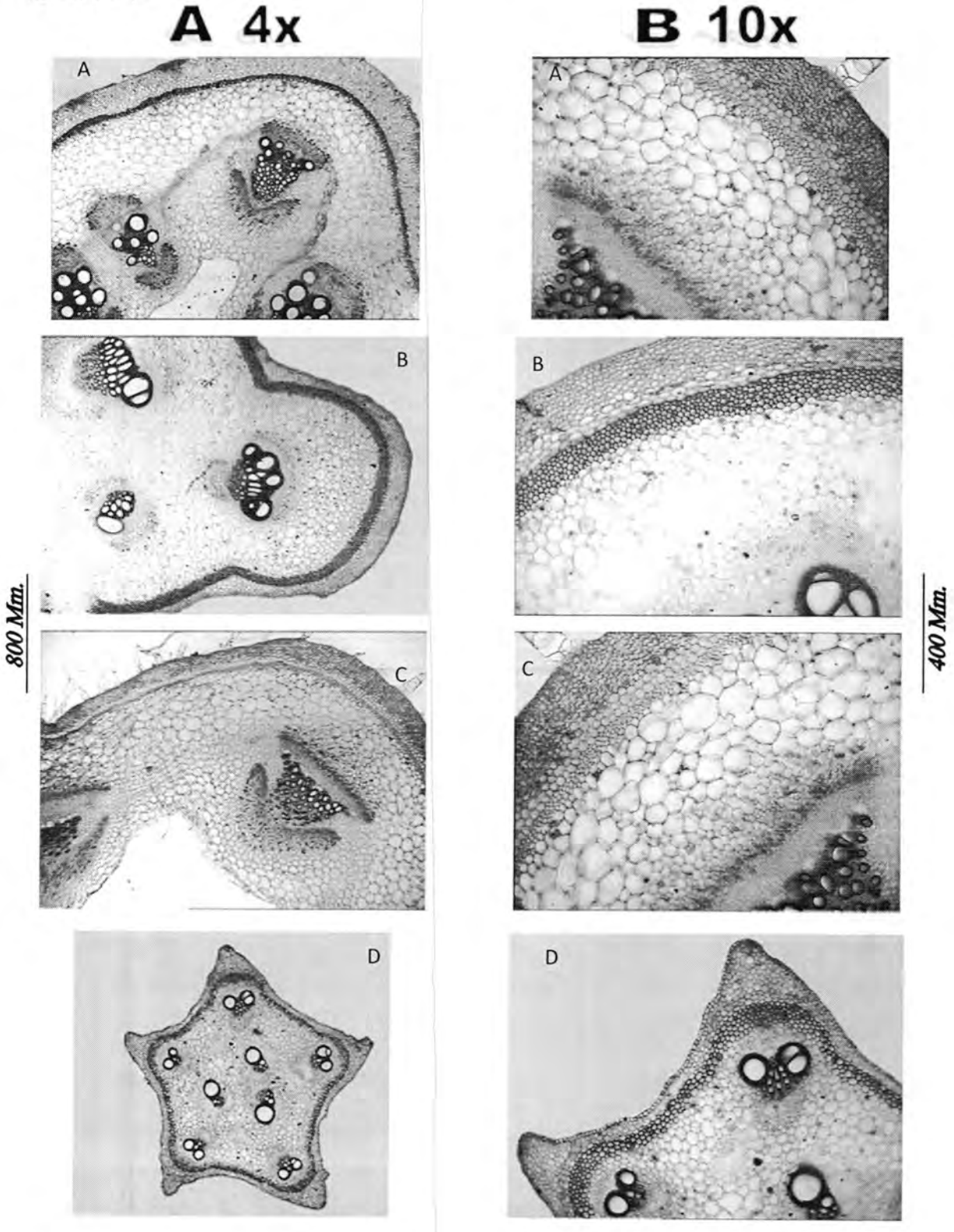

لوحة –10 : التغايرات في أشكال وأبعاد سيقان بعض الأنواع المدروسة

A : ***Cucurbita maxima*** C : ***Cucurbita pepo***

B : ***Cucurbita moschata*** D : ***Luffa cylindrica***

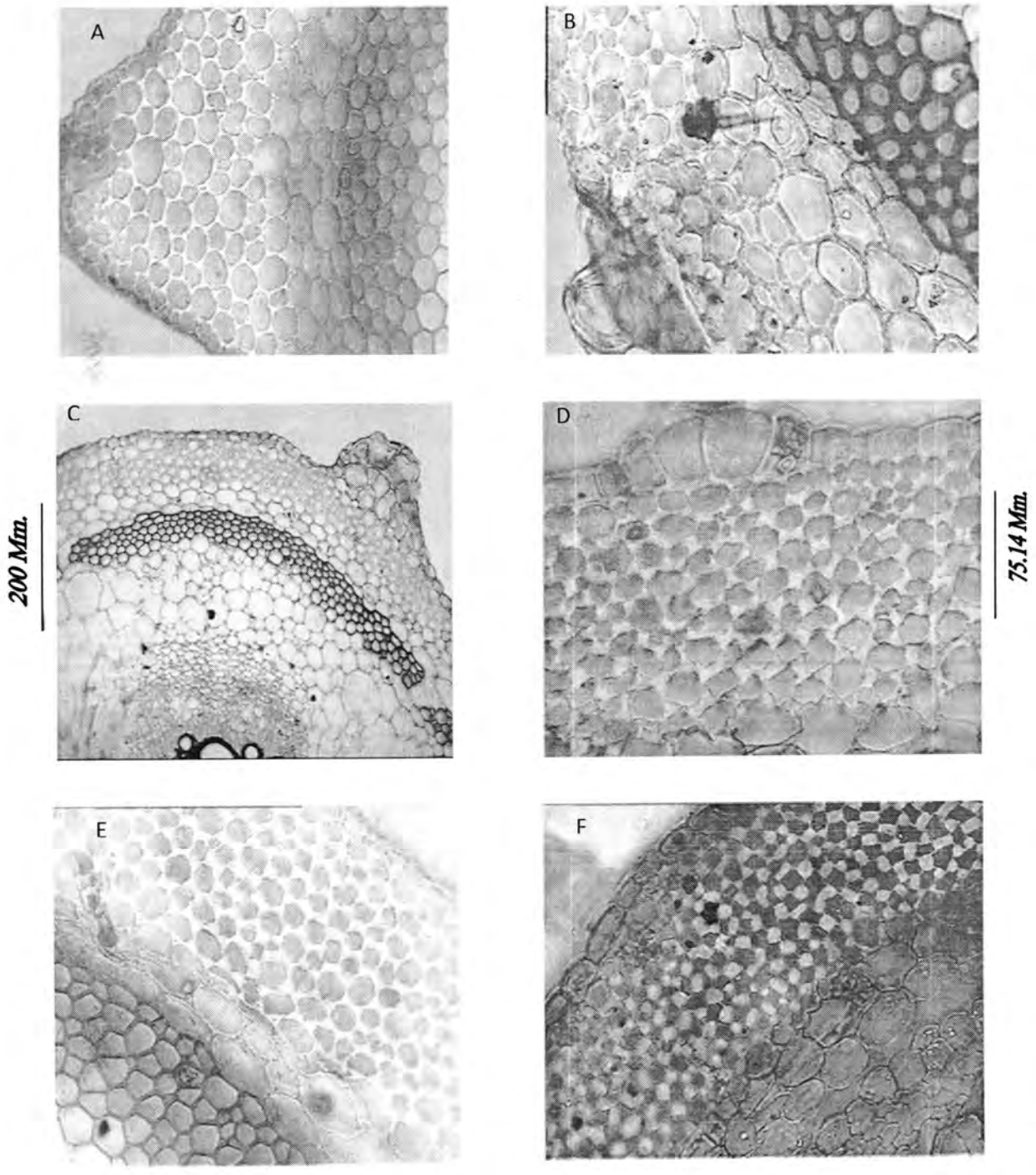

لوحة –11 : التغايرات في أشكال وأبعاد قشرة سيقان بعض الأنواع المدروسة

A : ***Citrullus lanatus***
B : ***Cucumis melo***
C : ***Cucumis melo. Var. flexuosus***
D : ***Cucurbita maxima***
E : ***Cucurbita moschata***
F : ***Cucurbita pepo***

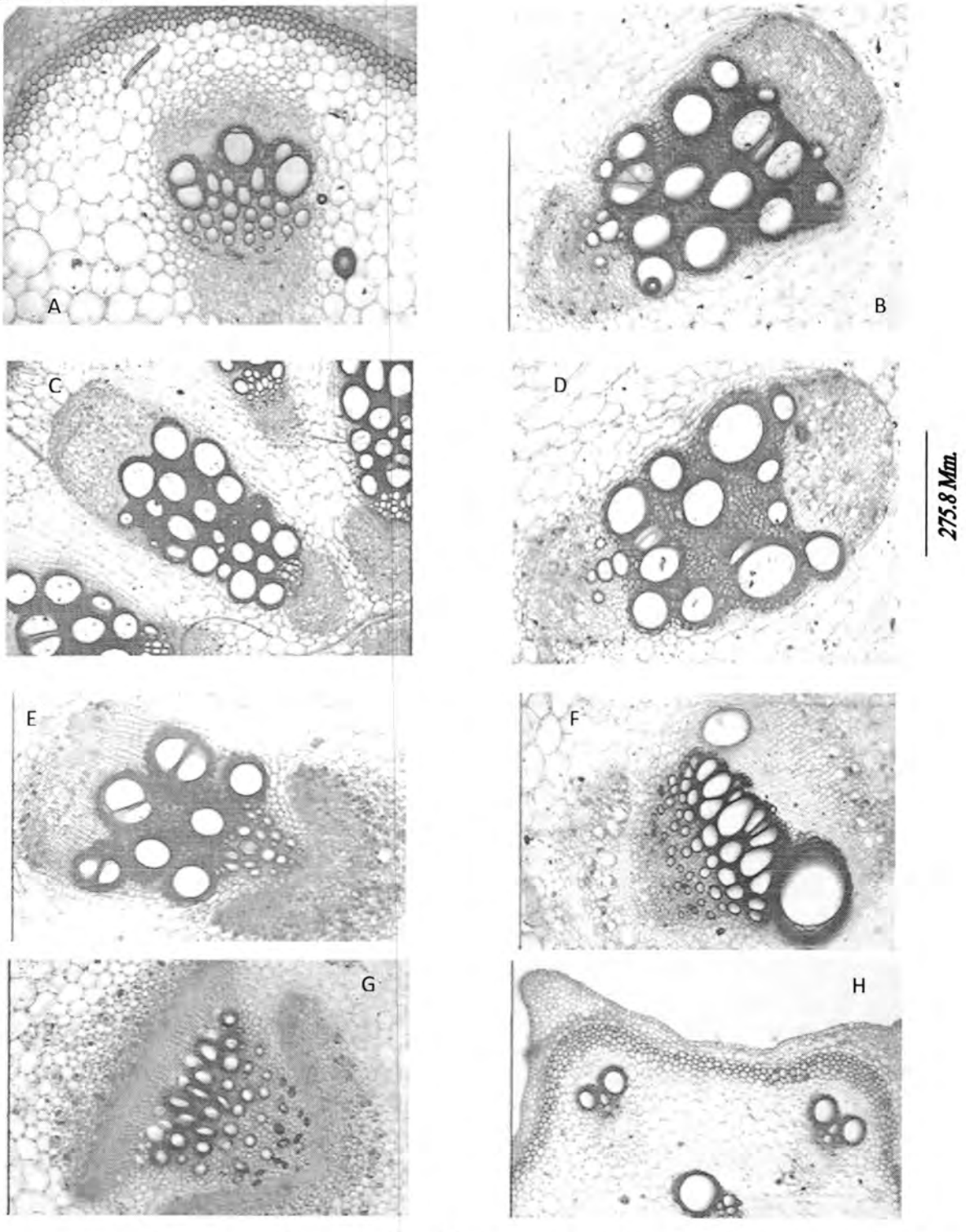

لوحة –12 : التغايرات في أشكال وأبعاد الحزم الوعائية لسيقان بعض الأنواع المدروسة

A : ***Citrullus lanatus***
B : ***Cucumis melo***
C : ***Cucumis melo. Var. flexuosus***
D : ***Cucumis sativus***
E : ***Cucurbita maxima***
F : ***Cucurbita moschata***
G : ***Cucurbita pepo***
H : ***Luffa cylindrica***

المصادر

1- Lawrence, G.H.M. Taxonomy of Vascular plants . The Macmillan Co., New York, 717-720. (1971) .

2- Pax, F. In H.M. Lawrence , Taxononmy of vasculsr plants . The Macmillan coi , New York , 719 . (1988) .

3- Townsend , C.C. and E. Guest . Flora of Iraq. Ministry of Agriculture and Agrarian Reform of the Republic of Iraq. (1974) .

4- الموسوي ، علي حسني ، علم تصنيف النبات ، وزارة التعليم العالي والبحث العلمي ، جامعة بغداد، العراق . ص . (1987).

5- Jeffery ,C. Append ix:an outline classification of the Cucurbitaceae. pages 449-463 In Bates , D.M.,R.W. Robinson &C.Jeffery , eds.Biology and Utilization of the Cucurbitaceae . I thaca , New York : Cornel Univ. Press. (1990) .

6- Austin , D. and ' 08B. O' Malley '08 . Cucrbitaceae College Seminar 235 Food for Thought ; The science , Culture , and folitics of food. Spring. (2008) .

7- Chakravarty . Plant wealth of Iraq .Vol.1. Baghdad. Botany directorate, Ministry of Agriclture and Agrarian Reform , Iraq. 131-174 . (1976) .

8- Al-Rawi,A. Wild Plants of Iraq with their distribution. Tech .Bull.14,Dir 86-87. (1964).

9- " Cucurbitaceae " . Wikipedia : the Free Encyclopedia. Wikimedia Foundation. Inc. (2011) .

10- Chakravarty , H.L.: Monograph of Cucurbitaceae of Iraq . In H.L. Chakravarty (1976) . Plant wealth of Iraq. 168 .(1966) .

11- Lira,R. Cucurbits (Cucrbita spp.), National Herb arinm of Maxico. (1994).

12- Sass, J.E. Botanical Micro technique . 3rd ed. The Lowa state Unvirsity press. 228 . (1968) .

13- Sharma , A.X. and A. Sharma. Chromosome Techniques theory and prachice . 2nd . ed . Butterworths , London. Pp.575. (1972) .

14- Metcalf , C.R.and L. Chalk . Ana tomy of the Dicot ledon leaves, stem and wood in Relation toTaxonomy. Oxford clearendon press. vol.II:Pp.648-691.(1950) .

15- Watson , L. and M.J. Dallwitz . The Families of Flowering plants : http://detta-intkey.com/0. (2007) .

16- Green Blessing . O and Horsefall . U. Taxonomic and Biosystematic studies in Certain Members of family Cucrbita ceae in Niger Delta. European Journal of Scien tific Research . ISSN 1450-216x vol.20 No.1 (2008) , Pp.6-13. (2008) .

17- Amran,Z.K. Asystematic study of the genus *Teucrium* L. (Labiatae) in Iraq . M.Sc. Thesis , Unvi. Of Basrah . (In Arabic). (1988).

18- Speckmann , G.J ; J. post and H. Dijktra. the lenth of stomata as an indicator for polyploidy in rye-grasses , Euphytica , 14:225-230. (1965) .

19- Stebbins, G.L. Chromosome Evolution in Higher plants . Edrawd Arnold , London, 216. (1971) .

20- Agbagwa, I.O. and B.C. Ndukwu. The value of morpho-anatomical features in systematics of *Cucurbita* L. (Cucurbitaceae) species in vol.3 (10), 541-546 . (2004).

21- Davies PD., Heywood VH. Principles of Angio sperm Taxonomy . Oliver and Boyd, Edinburgh. In Agbagwa , I.O. and B.C. Ndukwu. (2004). The value of morpho-anatomical features in systematics of *Cucurbita* L. (Cucurbitaceae) species in 3(10), 541-546. (1973) .

22- Metcalf C.R., Chalkl . Anatomy of Dicotyledons. 2nd , Vol. 1 : Systematic anatomy of leaf and stem , with a brief history of the subiect . In (Agbagwa , I.O. and B.C. Ndukwu. (2004) . The value of morpho-anatomical features in systematics of *Cucurbita* L. (Cucurbitaceae) species in 3(10), 541-546 . (1979) .

دراسة نسجية للسقف البصري Optic tectum في سمكة الحمري العراقية *Barbus luteus* (Heckel)

نهلة عبد الرضا البكري – أزهار رحيم حسين

جامعة بغداد – كلية التربية (ابن الهيثم) – قسم علوم الحياة

تاريخ تقديم البحث : 2011/ 3/30 تاريخ قبول البحث : 2011/ 5/29

ABSTRACT

The ceiling of the midbrain has a couple of optic lobes which are prominent and used as an optic center that reflex what it receives from eye retina fibers. The histology of optic tectum has been studied in Iraqi fish *Barbus luteus* (Heckel) . It was found that the number of optic tectum were six main strata organized from the outside to the inside as follows : the stratum marginal (SM), the stratum opticum (SO), the stratum fibrosum et griseum superficialis (SFGS), the stratum griseum central (SGC), the stratum album central (SAC), the stratum periventricular (SPV), . the tow last strata consider deep layers on the optic tectum. It was noticed that the superficial strata was the first (SM), while the thickest strata was the four (SGC), which is (80-100)μ m. it was found that the optic fibers that come from eye retina enter the optic tectum through the second stratum which is the (SO) . so these fibers go out from optic tectum through the five stratum which is the (SAC).

الخلاصة

يمتلك السقف Tectum للدماغ المتوسط Mesencephalon زوجا من الفصوص البصرية optic lobes البارزة ويعد مركزا انعكاسيا بصريا optic center reflex تستلم اليافا من شبكية العين eye retina. يتألف السقف البصري optic tectum نسجيا في سمكة الحمري العراقية *Barbus_ luteus*(Heckel) من ست طبقات رئيسة فقط مرتبة من الداخل إلى الخارج وكما ياتي : الطبقة الحافية The Stratum Marginal (SM) ، الطبقة البصرية The Stratum Opticum (SO)، الطبقة الليفية السنجابية السطحية The Stratum Fibrosum et Griseum Superfieialis (SFGS)، الطبقة السنجابية المركزية The Stratum

Griseum Centrail (SGC)، الطبقة الالبومية المركزية The Stratum Album Central (SAC)، الطبقة حول البطينية The Stratum Periventicular(SPV).

وتمثل الطبقتين الأخيرتين الطبقات العميقة Deep layers للسقف البصري سمكة الحمري العراقية . وتعد الطبقة الأولى وهي الطبقة الحافية (SM) طبقة سطحية .أما الطبقة الأكثر سمكا فهي الطبقة الرابعة وهي الطبقة السنجابية المركزي (SGC) إذ بلغ سمكها(80-100) µm .

تدخل الألياف البصريoptic fibers القادمة من شبكية العين عن طريق الطبقة الثانية وهي الطبقة البصرية (SO) في حين تخرج هذه الألياف من السقف عن طريق الطبقة الخامسة وهي الطبقة الالبومية المركزية (SAC) .

المقدمة

الأسماك من الفقريات التي لها أثر واضح في حياة الإنسان وذلك لأهميتها الاقتصادية ويعد جنس البني من أوسع أجناس أسماك المياه العذبة العراقية انتشاراً لاسيما في مياه وسط وجنوب العراق (1).ولسمكة الحمري رأس صغير نسبياً ويستدق من مقدمته وتقع العيون في نصفه الأمامي ويكون عمق الجسم Depth of body أكبر من طول الرأس (2).

لقد درس الجهاز العصبي والدماغ منذ أمد طويل لكونه من الأجهزة المعقدة جداً والمهمة لاسيما سقف الدماغ المتوسط (السقف البصري Optic tectum) الذي يلعب دوراً بارزاً في تكامل المعلومات البصرية والحسية لسلوك الكائن الطبيعي فهو المسؤول عن استلام السيلات العصبية الواردة Afferent nerve impulse (3). يختلف حجم السقف البصري وعدد طبقاته وتركيبه النسجي في الفقريات المختلفة ويعتمد على النوع (4). فهو يتكون في الأسماك من ست طبقات رئيسة فقط (5)،(6) . أما سمكة الكهف العمياء *Astyanax hubbsi* فتكون عيونها أثرية غير متطورة ولا تمتلك أي استجابة لدور النظام البصري مقارنةً مع اسماك المياه الاعتيادية (7). وفي البرمائيات فان السقف البصري يتكون من تسع طبقات فقط (8). وفي الزواحف ذكر Halpern (9) إن السقف البصري في الأفاعي العمياء Typholops يكون صغير وتركيبه الخلوي اقل تطوراً من الأفاعي الأخرى.كما وذكرحسين (10) إن عدد طبقات السقف البصري في الزاحف وزغة (أبو بريص) نصفية الأصابع *Hemidactylus flaviviridis* يتكون من أربعة عشر طبقة . ولزيادة

حاسة البصر عند الطيور نجد إن دماغها المتوسط يتميز بكبر حجم فصوصه البصرية وتركيبه ألصفائحي أكثر تطوراً وتعقيداً من الفقريات الأخرى (11) وانه يتكون من ست طبقات رئيسة(12)،(13).وفي اللبائن لاتوجد فصوص بصرية وانما لكيمات عليا Superior colliculus وبذلك ويكون المسؤول عن استلام الايعازات البصرية وتحليلها هي القشرة الأبصارية Visual cortex في الدماغ (14) ،(15) .ودرس Olivier *et al.*, (16) توزيع وانتشار الخلايا العصبية السقفية في لكيمات القرد والقطة والتي تتكون من سبع طبقات فقط .

صممت الدراسة الحالية لتسليط الضوء على سقف الدماغ المتوسط لسمكة الحمري العراقية والتعرف على عدد طبقاته والتركيب النسجي لكل طبقة من الطبقات وتعد هذه الدراسة الأولى في مجال دراسة التركيب النسجي للدماغ المتوسط في الأسماك العراقية .

المواد وطرائق العمل

أجريت الدراسة على 11 سمكة نوع حمري *Barbus luteus* (Heckel) شرحت واستخرج الدماغ الذي أجريت علية خطوات تحضير المقاطع النسجية اعتمادا على (17) ولونت الشرائح بملون Cresyl Fast Violet Stain لتوضيح التركيب الخلوي لطبقات السقف البصري ويسمى أيضا بملون نسل Nissl stain (18) كما استخدم ملون Bieschowskys Stain والذي يسمى بملون نترات الفضة لتوضيح المحاوير الاسطوانية وتغصنات الخلايا العصبية، أما ملون ازرق المثلين Methylene Blue Stain فاستخدم لتوضيح الخلايا النجمية بشكل جيد . ثم التقطت الصور الفوتوغرافية للمقاطع النسجية المنتخبة لتوضيح نتائج الدراسة الحالية . كما وأخذت القياسات باستخدام المجهر المركب (19) .

الوصف المظهري لدماغ سمكة الحمري

The Morphological Description of the Brain in The *Barbus luteus* (Heckel)

يظهر دماغ سمكة الحمري *Barbus luteus* (Heckel) عريضاً وقصيراً إذ يبلغ طوله (14) ملم ويتألف من ثلاثة أقسام رئيسة هي دماغ أمامي ووسطي وخلفي، يتكون الدماغ الأمامي من مقدم الدماغ وسرير الدماغ Diencephalon، يكون مقدم الدماغ نصفي كرة المخ Cerebral hemisphere اللذان يكونا بشكل حوصلتين جانبيتين مفصولتين عن بعضهما

بأخدود وسطي ويعلوهما من الأمام الفصان الشميان Olfactory lobes الذي يتصل كل منهما بالعصب الشميOlfactory nerve.يمثل الدماغ البيني منطقة صغيرة تقع بين نصفي كرة المخ ويغطى ظهرياً بالدماغ المتوسط. يكون الدماغ المتوسط الجزء الأكبر من الدماغ ويمثل جزؤه الظهري السقف البصري الذي يبدو بشكل فصان بصريان بيضويان كبيران Optic lobes.

أما الدماغ الخلفي فانه يتألف من المخيخ Cerebellum الذي يكون معيني الشكل وكبير الحجم ويظهر من جهته الخلفية وكأنه ينطوي على نفسه ، ويتألف أيضا من النخاع المستطيل Medulla oblongata الذي يكون بهيئة فصوص عريضة ومتصلة من الخلف بالحبل ألشوكي Spinal cord من الجهة الخلفية شكل (1)

الوصف النسجي للسقف البصري في دماغ سمكة الحمري

The Histological Description of the Optic Tectum in the *Barbus luteus* (Heckel) Brain

أن السمك الكلي للسقف البصري Optic tectum لدماغ سمكة الحمري بلغ 525-550 µm، وانه يتكون من ست طبقات رئيسة وهي كالأتي ابتداءً من ألام الحنون Pia matter في الخارج ووصولاً إلى البطين البصري Optic ventricle : الاشكال(3) و(4) و(12)

1- الطبقة الحافية The Stratum Marginal (SM)

وهي الطبقة الرئيسة الأولى من طبقات السقف البصري وتمثل الطبقة الخارجية للسقف حيث تقع بين سطح ألام الحنون والطبقة الثانية من طبقات السقف البصري، وتشكل هذه الطبقة جزء سميك من السقف إذ يبلغ سمكها بحدود 30-45 µm .

تتميز هذه الطبقة بفقدانها لأجسام الخلايا العصبية Lack of cell bodies إذ تحتوي على ألياف غير مغمدة Unmylinated fibers تسير لمسافة في اتجاه موازي لسطح السقف الاشكال (3,4) وتغصنات شوكية Dendrites spines ممتده من أجساد الخلايا العصبية الهرمية Pyramidal neurons الموجودة في الطبقة الثالثة من طبقات السقف البصري.

2- الطبقة البصرية The Stratum Opticum (SO)

وهي الطبقة الرئيسة الثانية من طبقات السقف البصري ويبلغ سمكها 40-60 µm وتمثل الطبقة الرئيسة للألياف الشبكية الواردة Afferents retinal fibers كما تحتوي هذه الطبقة على

ألياف عديدة تمتد من الطبقات العميقة للسقف باتجاه الطبقة الحافية (SM) في الأعلى وتتجمع هذه الألياف مع بعضها مكونة حزيمات Fascicles تحصر هذه الحزيمات فيما بينها مساحات تحتوي على ألياف مفردة Single fascicles قليلة مكونة فسح عريضة Gaps الأشكال (4,3). وتقسم هذه الطبقة إلى جزأين ، جزء سطحي Pars superficialis (Sos) وجزء عميق Pars profunda (Sop) الخلايا العصبية لهذه الطبقة تكون ذات أجساد كروية Spherical somata وكذلك ذات شكل كمثري مقلوب Inverted- pear shape يبلغ سمكها 6-5 µm ،كما ويوجد أيضا خلايا عصبية ممتدة أفقيا Horizontal oriented وخلايا دبقية صغيرة الحجم Small glial cells منتشرة بين الخلايا العصبية الأخرى.

3- الطبقة الليفية السنجابية السطحية
The Stratum Fibrosum et Griseum Superficial (SFGS)

تلي الطبقة السابقة وتمثل الطبقة الرئيسة الثالثة من طبقات السقف البصري، تشكل طبقة عريضة يبلغ سمكها 85-70 µm تقسم هذه الطبقة إلى ثلاثة أشرطة أفقية Horizontal streak تظهر في المقاطع المصبوغة بملون نسل Nissl stain الشكل (4). تمثل الأشرطة السطحية موقع رئيس لبروزات سقف الشبكية Tectal retino projection الأشرطة الأكثر عمقاً قد تندمج مع الطبقة التي تليها في الأسفل منها. أما بالنسبة للمكونات الخلوية Cellular component فتعد هذه الطبقة واحدة من أكثر الطبقات الخلوية عدداً في خلاياها وتتكون نسجياً من خلايا هرمية Pyramidal cells كبيرة الحجم ثنائية القطب Bipolar cells يتراوح قطرها 12-10 µm فضلاً عن عدد من الخلايا الكروية والبيضوية Spherical and oval shape وتمتلك كل خلية من هذه الخلايا نواة Nucleus كروية الشكل تظهر بشكل واضح عند استخدام ملون ازرق المثلين الشكل (5). ويبرز محوار الخلية الهرمية من القطب القاعدي Basal pole لجسم الخلية من أحد التغصنات القاعدية شكل (6). كما وتمتلك تغصنات رئيسة Chief dendrites تنزل باتجاه الأسفل.

4- الطبقة السنجابية المركزية The Stratum Griseum Central (SGC)

وهي الطبقة الرئيسة الرابعة من طبقات السقف البصري، وتمثل اسمك طبقاته إذ يتراوح سمكها 100-80 µm ، حيث تشغل المنطقة الوسطية للفص البصري وتضم طبقات خلوية ظفيرية الشكل Cellular and plexiform layers إذ تتكون هذه الطبقة مظهرياً من طبقتين خلويتين ،

ويقع أسفل الطبقة الليفية السنجابية السطحية (SFGS) شريط ليفي Fibrous streak كثيف جداً تمتد منه شبكة من البروزات الدقيقة Fine processes في الجزء العلوي من هذه الطبقة مكونة الطبقة الظفيرية الداخلية Inner Plexiform Layer (IPL) وهي من المعالم البارزة لهذه الطبقة ولاسيما المقاطع الملونة بنترات الفضة Nitrate silver stain حيث تظهر بلون داكن الاشكال (7,2). يعد الشكل المغزلي Fusiform هو الشكل المميز فيها لأجساد الخلايا العصبية إضافة إلى عدد من الخلايا الكمثرية الشكل Piriform neuron وخلايا دبقية Glial cells صغيرة الحجم وبلغ قطرها 2-4 µm ،أما الخلايا المغزلية والكمثرية فقد بلغ قطرهما بحدود 10-12 µm. ينشا المحوار المعقوف الشبيه بعصا الراعي Shepherds crook axon من القطب القمي apical pole لجسد الخلية المغزلية أو من جذع التغصنات الصاعدة الاشكال (8و9). وينشا من القطب القاعدي لجسد الخلية الكمثرية فروع تغصنية أفقية Horizontal dendritic branches . كما وترسل الخلايا الكمثرية محاوير صاعدة Ascending axons إلى الطبقة الحافية(SM) الاشكال(4, 9).

الطبقة الالبومية المركزية The Stratum Album Central (SAC)

وهي الطبقة الرئيسة الخامسة من طبقات السقف البصري تكون هذه الطبقة ضيقة نسبياً يتراوح سمكها 25-40 µm وهي طبقة ليفية Fibrous layer لكثرة الألياف النخاعينية Mylinated fibers فيها، والتي يتخللها عدد قليل من الخلايا العصبية، كما أنها تمثل الطبقة الرئيسة للألياف الصادرة Efferents fibers التي تكون مرتبة بشكل حزم ظهرية الموقع Dorsal region في الجزء الخطمي للفص البصري شكل (10). وصف في هذه الطبقة نوعين من الخلايا العصبية هي خلايا عصبية ذات أجساد كمثرية الشكل Pyriform soma وتكون صغيرة الحجم بلغ قطرها 4-6 µm وخلايا متعددة الأقطاب Multipolar soma كبيرة الحجم بلغ قطرها µm 14-16 شكل(11). وينبثق المحوار Axon من جذع قمي Apical shaft أو من واحد من تفرعاته ويسير باتجاه الطبقات الأكثر سطحية الاشكال (10و12) وأحيانًا ما ينبثق المحوار من القطب القاعدي لجسد الخلية. ترسل الخلايا متعددة الأقطاب الكبيرة فروعاً تمتد بصورة ملتوية لتنحرف إلى المستويات الأفقية ويمكن ان تمتد شاقولياً Vertically oriented باتجاه الطبقات العلوية وقد لا تتفرع خلال عدد من الطبقات من ضمنها الطبقة البصرية (SO).

5- الطبقة حول البطينية The Stratum Periventricular (SPV)

وهي الطبقة الرئيسة السادسة والأخيرة من طبقات السقف البصري وتشغل مساحة كبيرة إذ يبلغ سمكها 75-90 µm وتظهر كطبقة خلوية كثيفة Dense cellular layer حيث تظهر بلون داكن عند استخدام الملونات الأربعة، ويحد هذه الطبقة من الأسفل في المقاطع العرضية Cross sections من الجزء الخطمي للفص البصري نسيج الصمام المخيخي Valvula cerbelli وتحيط بالبطين البصري Optic ventricle في الجزء الخلفي من الفص البصري شكل (12) وفي المقاطع الطولية Sagittal sections فان هذه الطبقة يجاورها من الأسفل البطين البصري حيث تكون هذه الطبقة متداخلة مع طبقة البطانة العصبية Ependymal layer شكل (2). الخلايا العصبية الموجودة في هذه الطبقة هي خلايا كمثرية Pyriform cells ، وخلايا كروية Spheroid cells، وخلايا دبقية Glial cells ، وتكون أجسادها ذات أحجام متوسطة يبلغ قطرها 8-6 µm والقليل منها تكون ذو حجم كبير، تمتلك هذه الخلايا العصبية تغصنات صاعدة تتفرع إلى المستويات المختلفة من السقف شكل(13). تمثل الطبقات الثلاث الأخيرة الطبقات العميقة Deep layers من السقف البصري في سمكة الحمري.

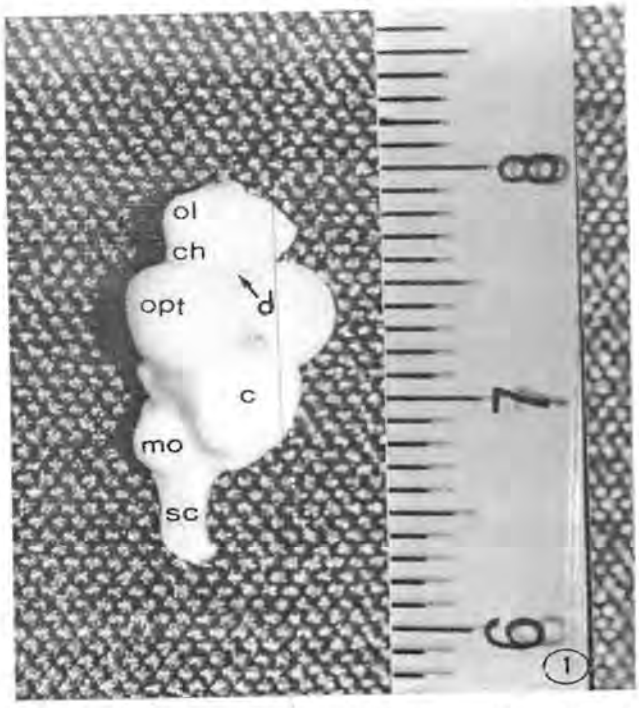

شكل -1: منظر ظهري لدماغ سمكة ألحمري ويوضح أجزاء الدماغ

c مخيخ ، ch نصفي كرة المخ ، d دماغ بيني ، mo نخاع مستطيل ، ol فص شمي ، opt فص بصري، sc حبل شوكي.

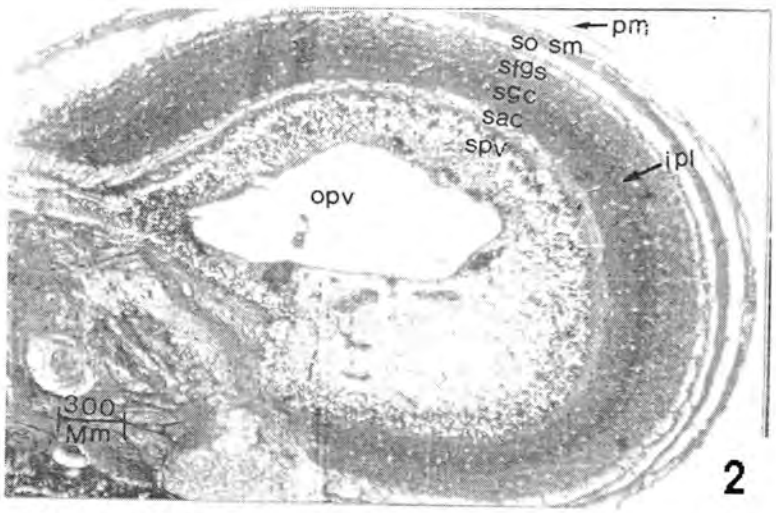

شكل – 2 : مقطع مستعرض يمر خلال الفص البصري لدماغ مكة ألحمري يوضح جميع طبقات السقف البصري ملون نترات الفضة

ipl طبقة ظفيرية داخلية ، opv بطين بصري ، pm ألام الحنون ، sac الطبقة الالبومية المركزية ، sfgs الطبقة الليفية السنجابية السطحية ، sgc الطبقة السنجابية المركزية ، sm الطبقة الحافية ، so الطبقة البصرية ، spv الطبقة حول البطينية ، vc صمام مخيخي.

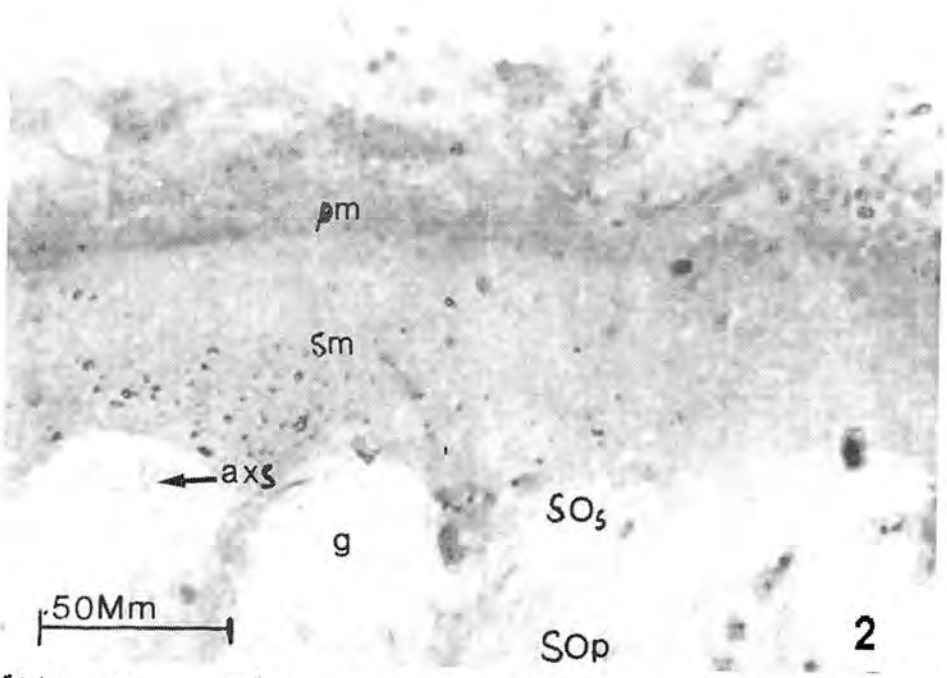

شكل–3 : مقطع مستعرض يمر خلال الفص البصري لدماغ سمكة الحمري يوضح الطبقة الاولى والفجوة واقسام الطبقة البصرية . ملون ازرق المثلين

axs المحاوير، g فجوة ، pm ألام الحنون ، sm الطبقة الحافية،so الطبقة البصرية ، sop الجزء العميق للطبقة البصرية ، sos الجزء السطحي للطبقة البصرية ، spv الطبقة حول البطينية.

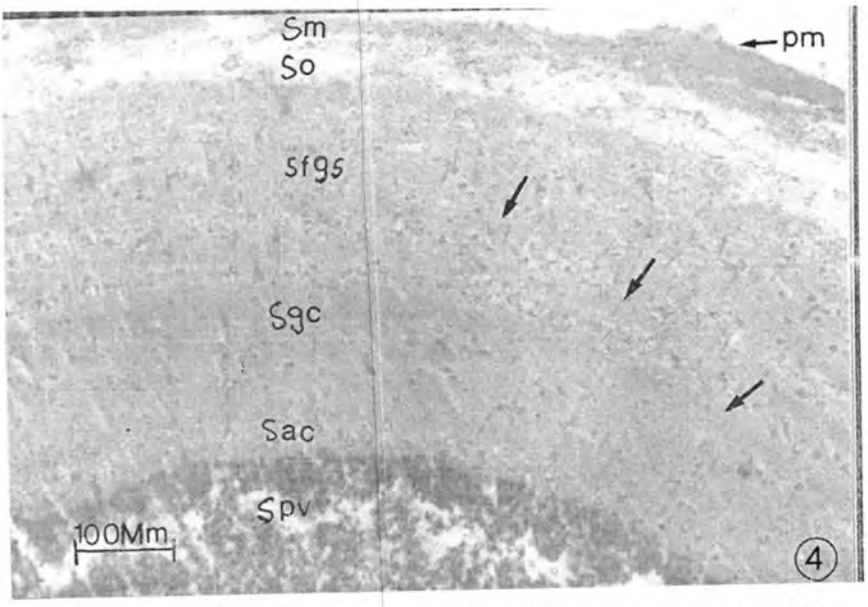

شكل – 4 : مقطع مستعرض يمر خلال الفص البصري لدماغ سمكة ألحمري يوضح جميع طبقات السقف البصري كما يوضح الأشرطة الأفقية المؤشرة بالأسهم التابعة للطبقة الثالثة والرابعة . ملون الكريسل فابوليت

pm ألام الحنون ، sac الطبقة الالبومية المركزية ، sfgs الطبقة الليفية السنجابية السطحية ، sgc الطبقة السنجابية المركزية ، sm الطبقة الحافية ، so الطبقة البصرية ، spv الطبقة حول البطينية .

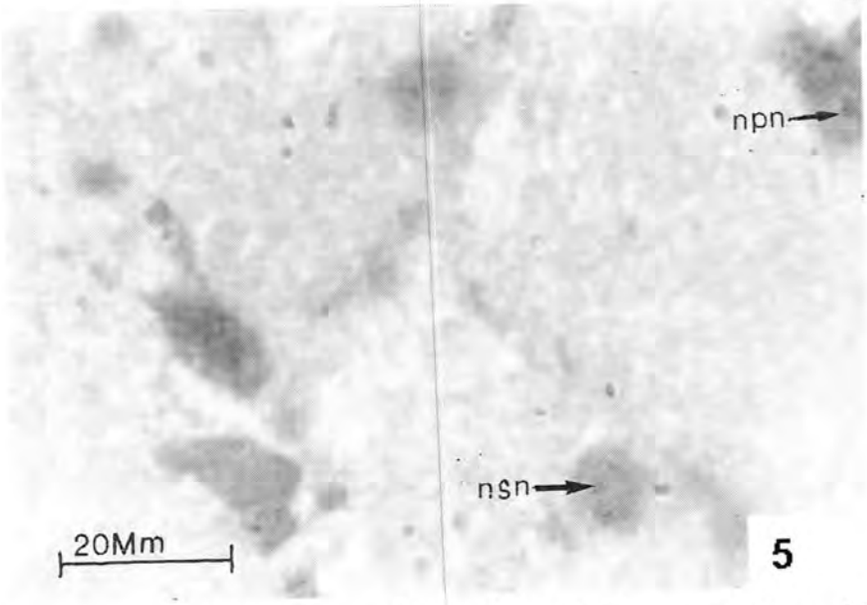

شكل – 5 : مقطع مستعرض يمر خلال الطبقة الليفية السنجابية السطحية يوضح انوية الخلايا الهرمية ، وانوية الخلايا الكروية . ملون ازرق المثلين

npn نوى الخلايا الهرمية ، nsn ونوى الخلايا الكروية .

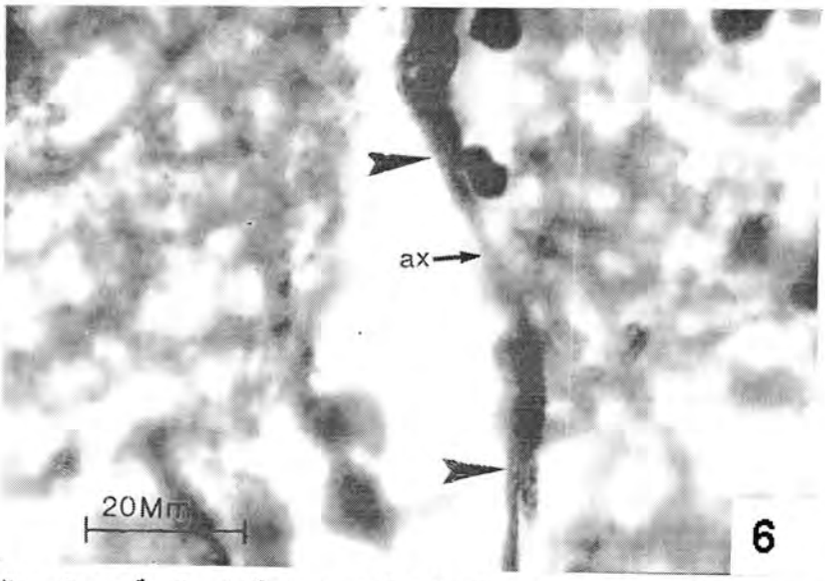

شكل – 6 :مقطع مستعرض يمر خلال الطبقة الليفية السنجابية السطحية ويوضح التغصنات القاعدية . ملون نترات الفضة

ax المحوار .

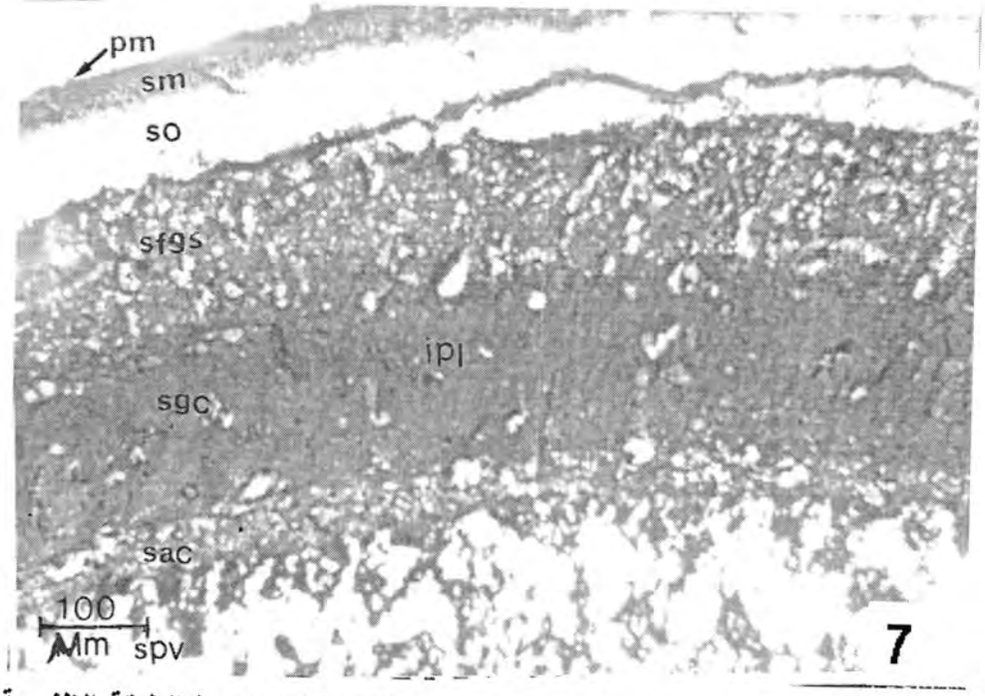

شكل–7:مقطع مستعرض يمر خلال الفص البصري يوضح طبقاته لاحظ الطبقة الظفيرية الداخلية ipl . ملون نترات الفضة

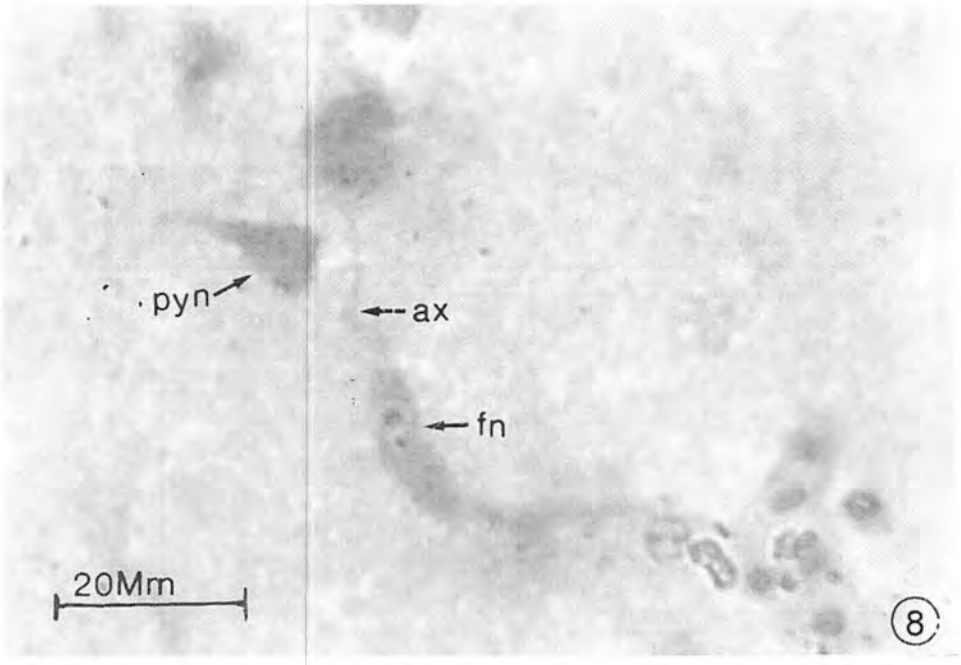

شكل – 8 : مقطع مستعرض يمر خلال الطبقة السنجابية المركزية يوضح إشكال الخلايا العصبية. ملون ازرق المثلين

axالمحوار ، fn خلية عصبية مغزلية ، pyn خلية عصبية كمثرية.

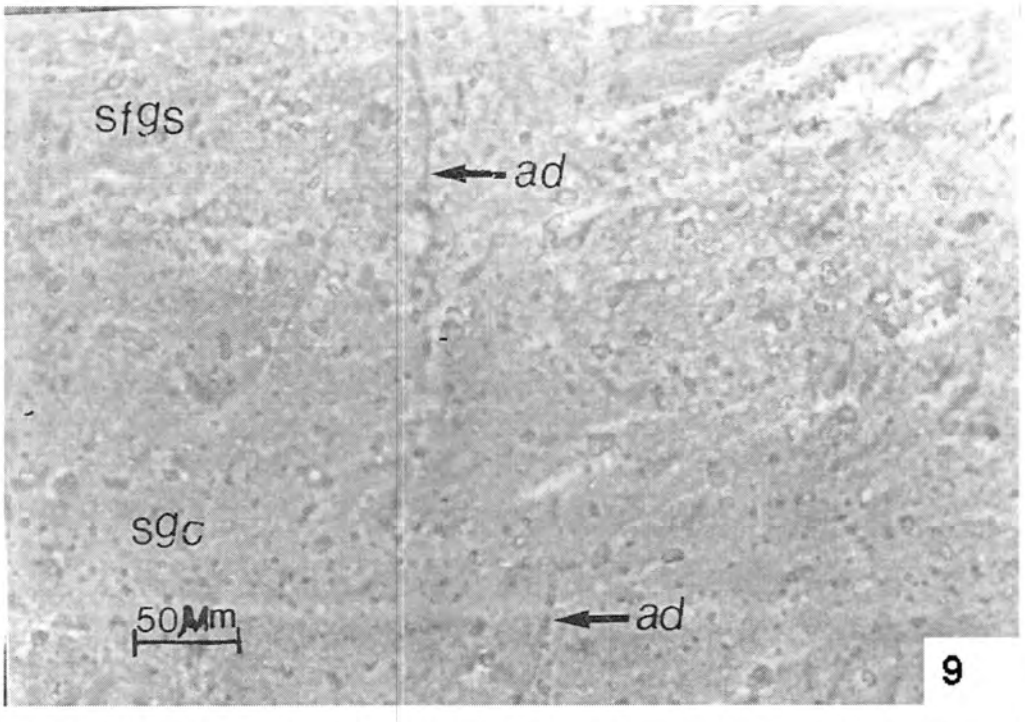

شكل – 9 : مقطع مستعرض يمر خلال الطبقة السنجابية المركزية يوضح التغصنات الصاعدة. ملون الكريسل فايوليت

النتائج والمناقشة

إن سقف الدماغ المتوسط أو السقف البصري هو تركيب ظهري بارز في الجهاز العصبي المركزي للفقريات اللاسلوية Anamniote vertebrates وهو مركز ضروري لمعالجة المعلومات الحسية الواردة ، ويعد من الناحية النسجية واحداً من أكثر المناطق تمايزاً في دماغ معظم الأسماك والبرمائيات مع وجود تنظيم صفائحي Laminated organization واضح لعناصرها الخلوية العصبية Neuronal elements (20).

أظهرت النتيجة الحالية إن السقف البصري لسمكة الحمري يتكون من ست طبقات رئيسة وهذا ما أشار أليه أيضا كلّ من (21) ، (22) ،(23) في سمكة*Acipenser transmontanus* وإن الطبقة الأولى هي الطبقة الحافية (SM) وبلغ سمكها 30-45 µm ،أما Laufer &Vanegas (24) فقد أشارا إلى إن سمكها بلغ 75 µm في سمكة *Eugerres plumieri* ، وذكر Schroeder &Vanegas (25) إن هذه الطبقة تحتل من ربع إلى ثلث السقف البصري في سمكتي *Bagrus* و *Ictalurus* بسبب صغر الطبقات التي تليها في هذين النوعين من الأسماك. في حين ذكر Schroeder *et al.*, (26) إن الطبقة الحافية (SM) تشغل ثلث السقف في السمكة السنجابية Squirrelfish. كذلك لوحظ إن هذه الطبقة تكون خالية تقريباً من الخلايا العصبية وتتركب نسجياً من ألياف عصبية لانخاعينية Unmmylinated fibers وهذا يتفق مع(25) عند دراستهما للدماغ في سمكتي *Bagrus* و *Ictalurus* . أما الطبقة الثانية من طبقات السقف البصري فهي الطبقة البصري(SO) وتتكون هذه الطبقة من جزأين، جزء سطحي Pars superficialis (SOs) ، وجزء عميق Pars profunda (SOp)، وهذا ما ذكرهReperant (27) أيضاً من خلال دراسته لدماغ سمكة *Polypterus senegalus*، إن سمك هذه الطبقة يتراوح 40-60 µm وتمثل الطبقة الرئيسية لألياف الشبكية الواردة Afferent retina fibers ، بينما أوضح Laufer &Vanegas (24) إن سمكها كان بحدود 50-100 µm في سمكة *Eugerres plumieri*، كما وأطلقا عليها طبقة المسلك البصري Optic tract layer حيث تتميز بوجود أعداد كبيرة من المحاوير المغمدة Mylinated axons. كذلك أوضح Schroeder &Vanegas (25) إن الطبقة البصرية (SO) والتي تمتلك ألياف سميكة وخلايا رفيعة نسبياً في سمكة *Ictalurus* ليس بالإمكان تميزها في سمكة *Bagrus* إذ تكون مطمورة في الطبقة التي

تليها وهي الطبقة الليفية السنجابية السطحية (SFGS). فالتغاير في طبقات السقف البصري غالباً ما يفسر على أساس التغاير في الأنواع وان أنماط بروزات سقف الشبكية Retinotactal أثبتت أنها قد تكون ذات مؤشرات مهمة في معرفة علاقة النشوء النوعي بين أنواع الأسماك الأخرى (28) حيث أوضحا ذلك من خلال دراستهما في ثلاث وثلاثين نوعاً مختلفاً من الأسماك شعاعيه الزعانف Ray finned fishes (Actinopterygii). إما الطبقة الثالثة فهي الطبقة الليفية السنجابية السطحية (SFGS) ، وقد بلغ سمكها 70-85 µm ، في حين بين Laufer &Vanegas (24) إن سمك هذه الطبقة في سمكة *Eugerres plumieri* كان بحدود 75-150 µm ، كما ذكر(25) Schroeder &Vanegas إن الطبقتين البصرية (SO) والليفية السنجابية السطحية (SFGS) تحتلان معاً مساحة اقل من سدس سمك السقف البصري في سمكتي *Bagrus* و *Ictalurus* . أشار Murray *et al.*, (22)إلى إن الطبقة الليفية السنجابية السطحية (SFGS) هي اسمك طبقة في السقف البصري لسمكة *Carassius auratus* . وإن الطبقة (SFGS) تتكون من ثلاث أشرطة أفقية Horizontal streaks ، وهذا يتفق مع (24). كما إن هذه الطبقة تعد من أكثر طبقات السقف عدداً في مكوناتها الخلوية وان الشكل الهرميPyramidal form هو الشكل البارز فيها لأجساد الخلايا العصبية ، أشار إلى ذلك أيضاً كلٌ من (24) و(26) .

كما أوضح Ghali *et al.*, (29) إن تكاثر الخلايا غير الاعتيادي في هذه الطبقة (SFGS) لا يترافق معه أية زيادة في خلايا الطبقات الأخرى وان النشوء المبكر في عدد الخلايا يعود إلى هجرة خلايا الدبق الصغري Microglia من مناطق أخرى من السقف البصري إلى هذه الطبقة ولا توجد هناك معلومات مقنعة تفسر هجرة هذه الخلايا إلى هذه الطبقة . وكذلك أوضح Roth *et al.*, (30) من خلال دراستهم في سقف الدماغ المتوسط في السلمندر Salamander إن الطبقات السطحية الثلاثة الأولى تسمى الطبقات السطحية للمسالك الصادرة للشبكية Superficial layers of retinal afferents أما الطبقتين الرابعة والخامسة فتسمى طبقات الألياف الواردة layers of efferents fibers . إما الطبقة الرابعة للسقف سمكة الحمري فهي الطبقة السنجابية المركزية(SGC) ، وتمثل اكبر طبقات السقف في هذه السمكة إذ يتراوح سمكها 80-100 µm، في حين اظهر Laufer &Vanegas (24) إن سمك هذه الطبقة بلغ 200 µm في سمكة *Eugerres plumieri* وعدها اسمك الطبقات أيضا. ولوحظ أيضا وجود شريط ليفي Fibrous streak كثيف جداً تمتد منه شبكه من البروزات الدقيقة Fine processes في الجزء

العلوي من هذه الطبقة مكونه الطبقة الظفيرية الداخلية Inner Plexiform Layer (IPL) وهذا يتفق مع كل من (25) و (26) و(31).وكذلك لوحظ ان الشكل المغزلي Fusiform shape هو الشكل المميز لأجساد خلايا هذه الطبقة فضلاً عن عدد من الخلايا الكمثرية الشكل Piriform shape وخلايا دبقية Glial cells صغيرة الحجم وهذا يتفق مع (25) و (26)تمتلك الخلايا الكبيرة في هذه الطبقة (SGC) اثنين من التغصنات القاعدية Basal dendrites والمتفرعة فقط للمنطقة الضيقة الواقعة قرب جسد الخلية إما تغصناتها القمية Apical dendrites فأنها تكون ممتدة إلى الطبقة الليفية السنجابية السطحية(SFGS)والطبقة البصرية(SO)(31). أما الطبقة الطبقة الالبومية المركزية (SAC) فهي الطبقة الخامسة لسقف سمكة الحمري وهي تشكل طبقة ضيقة يتراوح سمكها 25-40 µm وهذا يتفق مع (32) و(31) ، في حين أشارا Laufer &Vanegas (24) إن سمك هذه الطبقة كان بحدود 50-75 µm في سمكة *Eugerres plumieri* كذلك لوحظ إن هذه الطبقة تتكون من ألياف نخاعينية Mylinated fibersوهي تكون مسالك صادرة Efferenst pathways رئيسة خارجة من السقف البصري وهذا يتفق مع (32)و (33)ولوحظ أيضا من خلال النتائج إن هذه الطبقة (SAC) تمتلك نوعين من الخلايا العصبية هي خلايا عصبية كمثرية الشكل Pyriform shape صغيرة الحجم وخلايا متعددة الأقطاب Multipolar neurons كبيرة الحجم ، في حين أشار Vanegas *et al.*, (21) إن هذه الطبقة تمتلك نوعين من الخلايا العصبية ذات أجساد كبيرة الحجم هي خلايا كمثرية الشكل وخلايا متعددة الأقطاب. تمتلك الطبقات العميقة للسقف وهي الطبقة الالبومية المركزية (SAC)، والطبقة التي تليها على أجساد خلايا كبيرة الحجم Majority of cell bodies والتي ترسل تغصنات قمية Apical dendrites سميكة تمتد إلى الطبقات السطحية (20) . الفروع المحورية والتغصنية لخلايا هذه الطبقة تمتد إلى الطبقات السطحية ونهاياتها تتفرع تفرعات ثنائية Dichotomously لتصل إلى الطبقة الحافية (SM) (25). وذكر Sligar &Voneida (7) ان طبقات السقف البصري تكون مختزلة في سقف السمكة العمياء *Astyanax hubbsi* باستثناء الطبقة الالبومية المركزية (SAC) والطبقة التي تليها. إما الطبقة السادسة والأخيرة فهي الطبقة حول البطينية (SPV) وتشكل هذه الطبقة مساحة كبيرة من السقف يصل سمكها 75-90 µmوهذا يتفق مع (24) إذ بين إن سمك هذه الطبقة كان بحدود 75-100 µm في سمكة

Eugerres plumieri . وتظهر هذه الطبقة كطبقة خلوية كثيفة تظهر بلون داكن عند استخدام ملون نسل هذا ما أشار إليه أيضا (26)عند دراستهم في السمكة السنجابية Squirrlfish. وبين(25) إن الخلايا العصبية الموجودة في هذه الطبقة (SPV) هي خلايا كمثرية وخلايا كروية ذات حجم متوسط إضافة إلى عدد من الخلايا متعددة الأقطاب كبيرة. وأوضح (34) و(33) إن البطين البصري Optic ventricular يجاور الطبقة حول البطينية (SPV) من الأسفل حيث تكون هذه الطبقة متداخلة مع طبقة البطانة العصبية Ependymal layer ويظهر تحتها جزء من نسيج الصمام المخيخي Valvula cerbelli .

المصادر

1- الدهام ، نجم قمر، أسماك العراق والخليج العربي . الجزء الأول. مطبعة الإرشاد . بغداد. (1977)

2- Khalaf, K. T. The marine and freshwater fishes of Iraq. Ar-Rabitta press, Baghdad : 29 pp. (1961).

3- Camacho,C.S.; Msrin, O. and Gonzalez, A. Distribution and origin of the catecholaminergic innervation in the amphibian mesencephalic tectum. Vis. Neurosic., 19 : 321-333. (2002).

4- Kent, G. G. and Carr, R. K. Comparative anatomy of the vertebrates. 9th edn. MC Graw-Hill Higher Education, New York : 824 pp. (2001).

5- Groman, D. B. Histology of the Striped bass. Am. Fish. Soci., U.S.A. : 116 pp. (1982).

6- Yamamoto, N.; Yoshimoto, M.; Albert, J. S. Sawai, N. and Ito, H. Tectal fiber connections in a non-teleost Acttinopterygian fish, the *Sturgeon acipenser*. Brain Behav. Evol., 53 : 142-155. (1999).

7- Sligar, C. M. and Voneida, T. J. Tectal efferent in the Blind cave fish *Astyanax hubbsi*. J. Comp. Neur., 165: 107-124. (1976).

8- Nakagawa, H. and Matsumoto, N. Current density analysis of on / off channels in the frog optic tectum progress in Neurobiol., 16:1-44. (2000).

9- Halpern, M. Retinal projection in blind snakes. Science, 182 : 390 - 391. (1973).

10- حسين، أزهار رحيم. دراسة التركيب النسجي للسقف البصري Optic tectum في الزاحف وزغة (ابوبريص) نصفية الاصابع *Hemidactylus flaviviridis*. مجلة ابن الهيثم للعلوم الصرفة والتطبيقية . (23) 2 :13-25. (2010).

11- Romanoff, A. The avain embryo strauctural and functional development. McMacmillan Co., New York : 880 pp. (1960).

12- Hyde, P. S. and Knudsen, E. I. Topographic projection from the optic tectum to the auditory space mapin the inferior colliculus of the Barn Owl. J. Comp. Neur., 421 : 146-160. (2000).

13- الكناني، أحمد سلمان عبد الحسن، دراسة تكوينية للسقف البصري Optic Tectum في طائر السلوى *Coturnix coturnix japonica* . رسالة ماجستير ، كلية التربية (ابن الهيثم) ، جامعة بغداد: 75 ص. (2002).

14- Weichert, C. K. Anatomy of chordates, 4th edn. Mcgraw Hill Book Co., New York : 814 pp. (1970).

15- Gaillard, F. Nucleus isthmi, a satellite visual center of the optic tectum in amphiblans : anatomy physiology and behavioral function. Comp. Biochem. Physiol., 8 : 43- 78. (2001).

16- Olivier, E.; Porler, J. D. and May, P. J. Comparsion of the distribution and somatodendritic morphology of tectotectal neurons in the cat and monkey. Vis. Neurosci., 15 : 903-922. (1998).

17- Luna, L. G. Manual of histological staining methods of the forces institute of pathology, 3rd edn. Mc-Graw- Hill Book, New York : 258 pp. (1968).

18- Rodger, J.;Bartlett,C.A.;Beazley, L.D.and Sarah, A.D. Transient. up-regulation of the rostro caudal gradient of ephrin A2 in the tectum coincides with reestablishment of orderly projections during optic nerve regeneration in goldfish . Exp. Neur., 166 : 196-200. (2000)

19- Bancroft, J. D. and Stevens, A. Theory and practice of histology techniques. 2nd edn. Churchill. Livingston, London. 662 pp. (1982).

20- Nguyen, V.; Deschet, K.; Henrich, T.; Godet, E.; Joly, J.-S.; Wittbrodtt, J.; Chovrrout, D.and Bovrrat, F. Morphogenesis of the optic tectum In the medaka *(oryzias latipes):*a morphologyical and molecular study, With special emphasis on cell proliferation.J.Comp.Neur.,413:385-404. (1999).

21- Vanegas,H.;Laufer,M.and Amat, J. The optic tectum of a perciform teleost .1.General configuration and cytoarchitecture. J.Comp. Neur., 154 : 43-60. (1974).

22- Murray, M.; Sharma, S. and Edwards, M. A. Target regulation of synaptic number in the compressed retinotectal projection of Goldfish. J. Comp. Neur., 209: 374-385. (1982).

23- Ito, H.; Yoshimoto, M.; Albert, J. S.; Yamamoto,N. and Sawai,N. Retinal projections and retinal ganglion cell distribution patterns in a sturgeon (*Acipenser transmontanus*) a non-teleost Actinopterygian fish. Brain Behav. Evol., 53 : 127-141. (1999).

24- Laufer, M.and Vanegas, H. The optic tectum of aperciform teleost II. fine structure. J.Comp. Neur., 154 : 61-96. (1974a).

25- Schroeder, D.M. and Vanegas, H. Cytoarchitecture of the tectum mesencephali in two types of siluroid teleosts . J.Comp.Neur.,175 : 287-300. (1977).

26- Schroeder,D. M. ; Vanegas, H. and Ebbesson, S. O. E. Cytoarchitecture of the optic tectum of the Squirrelfish *Holocentrus*. J. Comp. Neur., 191 : 337-351. (1980).

27- Reperant,J.; Rio,J.P.;Miceli, D.; Amouzov, M.and Peyrichoux , J. The retinofugal pathways in the primitive African bony fish *polypterus senegalus* . Brain Res., 217: 225-243. (1981).

28- Von Bartheld, C. S. and Meyer, D. Comparative neurology of the optic tectum in ray-finned fishes : patterns of lamination formed by retinotectal projections. Brain Res., 420 : 277-288. (1987).

29- Ghali, R.P.;Herx, L.M.;Maa,A. and Levine, R. L. Mononuclear. cell proliferattion and hyperplasic during wallerian degeneration in the visual system of the Goldfish in the presence or absence of regenerating optic axons. Brain Res., 854 : 178-188. (2000).

30- Roth,G. ; Manteuffel, C. and Grunwald, W. Cytoarchitecture of the tectum mesencephali *salamanders* :a Golgi and HRP study. J.Comp. Neur., 291 : 27-42. (1990).

31- Yoshimoto, M.; Kikuchi, K; Yamamoto,N.; Somiya,H. and Ho, H. Sonic motor nucleus and its connections with octaval and lateral line nuclei of the medulla in a rockfish, *Sebastiscus marmoratus*. Brain behav. Evol., 54 : 183-204. (1999).

32- Ito, H. and Vanegas, H. Visual receptive thalamopetal neurons in the optic tectum of teleosts (Holocentridae). Brain Res., 290: 201-210. (1984).

33- Zottoli, S. J.; Rhodes, K. J.; Corrodi, J.G. and Mufson, E. J. Putative cholinergic projections from the nucleus isthmi and the Nucleus reticularis mesencephali to the optic tectum in the Goldfish (*Carassius auratus*). J. Comp. Neur., 273 : 385-398. (1988).

34- Harder, W. Anatomy of fishes E. Schweizerbartsche Verlag Chhandlung (Nageleu obermiller), Stuttgart : 612 pp. (1975).

التأثير السمي الخلوي للمستخلص الأثيلي الخام لأوراق نبات المعدنوس *Petroselinum cripum* في خط خلايا سرطان الحنجرة البشري Hep-2

[1]عباس عبد الله الجنابي، [2]شلال مراد حسين، [1]أفنان أسماعيل عبدالوهاب

[1]قسم العلوم التطبيقية/ الجامعة التكنولوجية

[2] المركز العراقي لبحوث السرطان والوراثة الطبية / الجامعة المستنصرية

تاريخ تقديم البحث : 2011/ 3/27 تاريخ قبول البحث : 2011/ 5/29

ABSTRACT

This study amid to investigate the effects of crude ethanolic extraction of *Petroselinum cripum* leaves on the proliferation of the cancer cell line Hep-2. The cytotoxicity of cancer cell line of concentration of (0.95, 1.9,3.8,7.7,15.5,31.25,62.5,125,250,500,1000,2000,3000,4000,6000,8000, 10000, 12000 and 16000)µg/ml showed there was no inhibition observedat concentration (0.95, 1.9, 3.8, 7.7, 15.5, 31.25 and 62.5)µg/ml. While at concentration of 250,500 and 1000 mg/ml the inhibition percentage was less than 50%.But at concentration of 2000 and 4000µg/ml the inhibition percentage was(63%,66%) respectively at while after 48hrs the concentration of (6000,8000,10000,12000,14000 and16000)µg/ml the inhibition percentage was more than70% at this study was found that the alcoholic extract hase toxic effect on cancer cell line ,on hep-2 70.242% of inhibition at 6000µg/ml and 75.778% of inhibition at16000µg/ml after 24hrs; inhibition percentage was 71.626% and77.093% at 6000µg/ml and 16000µg/ml respectively. Exposure and the percentage was 72.594% at concentration 6000 µg/ml to 77.136% at concentration16000 µg/ml after 72hrs . From this result we can concluded that this plant have a promising medicinal plant for effect on cancer,through out the toxic effects on cancer cell line .

الخلاصة

تم التحري عن التأثير السمي الخلوي للمستخلص الاثيلي الخام لأوراق نبات المعدنوس في خط خلايا سرطان الحنجرة البشري (Hep-2) ، أذ تم أخذ تراكيز مختلفة من المستخلص

(0.95، 1.9، 3.8، 7.7، 15.5، 31.5، 62.5، 125، 250، 500، 1000، 2000، 4000، 6000، 8000، 10000، 12000، 14000، 16000) مايكروغرام/مل ، فلوحظ عدم وجود تثبيط عند التراكيز (0.95، 1.9، 3.8، 7.7، 15.5، 31.25، 62.5، 125) مايكروغرام/مل اما التراكيز (1000,500,250)مايكروغرام/مل فكانت نسبة تثبيط نمو خلايا عندها اقل من 50 % وعند التركيزين (4000,2000) مايكروغرام/مل فكانت نسب التثبيط (63%,66%) على التوالي اما التراكيز (16000,14000,12000,10000,8000,6000)مايكروغرام/مل فكانت نسبة تثبيط نمو الخلايا عندها عالية تجاوزت 70% لذلك تم اعتماد هذه التراكيز والأخذ بها واختبار فعاليتها في القتل لفترات تعرض مختلفة هي 72,48,24 ساعة . توصلت الدراسة إلى وجود تأثير سمي قاتل للمستخلص الكحولي للنبات عند التراكيز الست المعتمدة أذ تراوحت نسب التثبيط 70.242 % عند التركيز 6000 مكغم/مل إلى 75.778 %عند التركيز 16000 مايكروغرام/مل عند فترة التعرض24 ساعة وكانت نسب التثبيط لخلايا الخط نفسه من71.626 % عند تركيز 6000مكغم/مل إلى 77.093% عند التركيز 16000 مكغم/مل عند فترة التعرض 48 ساعة وكانت النسب من72.594 %عند التركيز 6000 مايكوغرام/مل إلى 77.136 % عندالتركيز 16000 لفترة التعرض 72 ساعة . من هذه النتائج التي تم الحصول عليها يمكن الاستنتاج بان نبات المعدنوس يعد من أهم النباتات الطبية الواعدة ذات الدور الفعال في معالجة السرطان من خلال تأثيره التثبيطي والسمي القاتل في الخلايا السرطانية.

المقدمة

درس العلماء بصورة مستفيضة في بلدان مختلفة من العالم العديد من المستخلصات النباتية لتوضيح المكونات الكيميائية المؤثرة وراثيا، وتعد الدراسات المتعلقة بهذا الموضوع ذات طابع مهم في جوانب المعرفة العلمية والتطبيقية،أذ برزت في الآونة الاخيرة دراسات متخصصة بالنباتات الطبية بعد كشف النقاب عن مكانتها في الطب الحديث فأولت منظمة الصحة العالمية (WHO)أهمية كبيرة في توسيع استعمال الأدوية من المصادر النباتية بدلا من الادوية المصنعة كيميائيا[1] فكانت الدراسات التي قام بها العديد من الباحثين في المراكز البحثية والمتاحف المتخصصة,كشفت النقاب عن الأهمية الكبيرة لبعض المستخلصات النباتية واعطت للمهتمين

فرصاً تم من خلالها التعرف على الكثير من التراكيب الكيميائية ذات الفعالية الطبية[2]، فعلى سبيل المثال لا الحصر لوحظ للعديد من المستخلصات النباتية تأثير مضاد لبعض السرطانات لاحتوائها على مركبات تؤثر في آليات الانقسام الخلوي من خلال تأثيرها في تضاعف الحامض النووي الـ(DNA) اوأحد الانزيمات المهمة في التضاعف والتي تمنع تكوين الأنبيبات الدقيقة لخيوط مغزل انقسام الخلية كمادة الكولجيسين Colchicine المستخلصة من نبات *Colchicum cwtumnale* اذ تمنع بلمرة بروتين tubulin مما تؤدي الى توقف الكروموسومات في الطور الاستوائي وبالتالي تمنع أتمام عملية الأنقسام الخلوي [3]. كذلك الحال مع مادة Benzo phenanthridin وهي من القلويدات التي تعمل على تثبيط الأنقسامات المتعددة لبعض انواع خلايا الخطوط السرطانية للانسان والمقاومة للعقاقيرالطبية ودفعها الى الموت المبرمج Apoptosis [4].لذا عدت بعض المستخلصات النباتية الطبية كمضادات التسرطن Anti-carcinogens والسرطان Anti-cancer[5] . تزايدت اهمية النباتات الطبية عندما اتضح دورها في حماية المادة الوراثية من تأثير المطفرات البيئية وقابلية مكوناتها على تصحيح الآخطاء الوراثية التي تحدثها هذه الطفرات[6] . ونظرا الى ما تقدم اختير نبات المعدنوس *Petroselinum crispum* وهو نبات عشبي ثنائي الحول لهذه الدراسة.

المواد وطرائق العمل

الخط الخلوي السرطاني(Hep-2) Human epidermoid larynx carcinoma

استعمل هذا الخط عند التمريرة رقم (231) وهو خط خلايا سرطان الحنجره لرجل يبلغ من العمر 57 سنة [7 و8].ان هذا الخط تم تطبيعه للنمو على وسط RPMI-1640 المجهز بـ 10% من مصل العجل البقري في المركز العراقي لبحوث السرطان والوراثة الطبية، وعند تكون الطبقة الاحادية الكاملة (Confluent monolayer) تمت معاملة الخلايا بمحلول التربسين-فرسين وذلك لتهيئة المزرعة الثانوية Subculture .

تحضيرالوسط الزرعي للخط الخلوي السرطاني Preparation of medium of cancer cell line

تمت تهيئة الوسط الزرعي وفقاً [9] بخلط مكوناته مع بعضها البعض لتحضير l لتر منه , ومن ثم عقمت بأستعمال مرشح ذي ثقوب 0.22 مايكرون, ثم وزع الوسط الزرعي في قناني زجاجية

ذات غطاء محكم سعة 200 مل وحفظت في القناني بدرجة حرارة −20°م الى حين الأستعمال. تم الحصول على الخط السرطاني من المركز العراقي لبحوث السرطان والوراثة الطبية/ الجامعة المستنصرية . حيث تم أجراء الخطوات الخاصة بالزرع النسيجي تحت ظروف معقمة كالأتي :

1- أضيف2 مل من محلول التربسين/ فرنسين الى قنينة الزرع النسيجي بحجم 25سم^3 الحاوية على الخلايا بعد تفريقها من الوسط الزرعي القديم ثم حركت القنينة برفق وحضنت في الحاضنة بدرجة حرارة 37°م مدة 15 دقيقة لتفكيك الخلايا الملتصقة وكذلك خلخلة التصاقها بجدار القنينة للحصول قدر الأمكان على خلايا أحادية مفردة.

2- أضيفت الى القنينة الحاوية على الخلايا المتفككة ما يقارب15 مل من وسط نمو جديد (RPMI-1640) وتم تحريك القنينة جيداً وبعدها أفرغت محتويات القنينة الحاوية على الوسط الزرعي الجديد مع الخلايا الى قنينة أخرى جديدة بحيث يكون مستوى الوسط الزرعي مع الخلايا متساو بين القنينتين أي كل قنينة وضع فيها نفس الحجم تقريباً من الوسط الزرعي مع الخلايا وتسمى هذه العملية بالمزرعة الثانوية (Subculture) .

3- حضنت القناني بدرجة حرارة 37°م مدة يومين , بعد أن كتب عليها معلومات كاملة عن نوع الخلايا ونوع التمريرة الجديدة (New passage) وتم أجراء المزرعة الثانوية, وتمت متابعة القناني يوميا للتأكد من خلوها من أي تلوث وأن الخلايا بحالة جيدة وذلك بفحصها بواسطة المجهر المقلوب(Inverted microscope) وعندما يصبح النمو داخل القنينة جيداً فأن الخلايا تكون جاهزة للأستعمال.

أختبار سمية المستخلصات الخام لنبات المعدنوس على تكاثر الخطوط السرطانية

أذيب 0.1غم من المستخلص الايثانولي الخام للاوراق النباتية في 10 مل من المذيب [9 مل PBS+1 مل Dimethyl sulfoxid (DMSO)], ثم عقم المستخلصان بأستعمال مرشح ذي ثقوب 0.22 مايكرون وحضرت منه ستة تراكيز هي (6000، 8000، 10000، 12000، 14000، 16000) مايكروغرام/مليلتر , وتحت ظروف معقمة, أستعملت جميع التراكيز المحضرة مباشرة بعد إكمال عملية التحضيروحسب الخطوات التالية:

أ- جهز عالق الخلايا عن طريق معاملة الزرع النسيجي حجم 25 سم^3 بمحلول التربسين/فرسين بعد تفريغ الوسط الزرعي القديم وتحريك القنينة برفق, ثم حضنت في الحاضنة بدرجة حرارة 37°م مدة15 دقيقة, ثم أضيف له 20 مل وسط النمو ،أستعمل وسط النمو (RPMI 1640)، ثم تم مزج عالق الخلايا جيداً وتم نقل 0.2 مل بعد كل مزجة جديدة الى حفر طبق معايرة الزرع النسيجي ذي القعر المسطح Microtiter plate for tissue culture بأستعمال ماصة أوتوماتيكية دقيقة.

ب-ترك الطبق في الحاضنة بدرجة حرارة37°م لمدة 24 ساعة الى حين التصاق الخلايا في الحفرة, بعدها تم التخلص من الوسط الزرعي القديم في الحفرة وتم أضافة 0.2 مل من التراكيز المحضرة سابقا في كل حفرة وبواقع ثلاث مكررات لكل تركيز. تم عمل ثلاث مكررات للسيطرة(خلايا فقط) مضاف لها وسط زرعي خال من المصل Free media.

جـ- بعد مرور 24 ساعة أخرج الطبق من الحاضنة وأضيف إليه محلول صبغة البنفسج البلوري لجميع الحفر الحاوية على الخلايا بمقدار 0.2 مل لكل حفرة وكررت الخطوة نفسها بعد فترة حضن 48 و72ساعة.

د-أعيد الطبق مرة ثانية الى الحاضنة ليحضن مدة نصف ساعة ,وبعدها أخرج الطبق وأزيلت محتوياته وغسلت الخلايا بمحلول (PBS) الى حين زوال الصبغة الزائدة(البنفسج البلوري) أذ أن الخلايا الحية تأخذ الصبغة أما الميتة فلا تأخذها.

هـ- قرأت النتائج بأستعمال ELISA بطول موجي492 نانومتر.

و- تم حساب نسبة التثبيط لكل تركيز .

التحليل الأحصائي

حللت النتائج أحصائياً باتباع التصميم العشوائي الكامل Complete Randomized Design (CRD) ولمعرفة فيما أذا كانت الفروقات بين المعاملات معنوية أم لا , بأستعمال أختبار دنكن متعدد الحدود (Duncun multiple test) وبأستعمال البرنامج الأحصائي الجاهز SPSS [10].

النتائج والمناقشة

التأثير السمي للمستخلص الكحولي الخام لاوراق نبات المعدنوس في نمو خلايا الخط الخلوي السرطاني

تم اختبار قدرة المستخلص الكحولي لاوراق نبات المعدنوس على تثبيط نمو الخلايا السرطانية خارج جسم الكائن الحي وقد عوملت هذه الخطوط الخلوية بتراكيز مختلفة من المستخلص الكحولي بدءا من التركيز 0.095 مايكروغرام/مل الى التركيز 16000مايكروغرام/مل وقد تم اعتماد التراكيز الست الاعلى من 8000مايكروغرام/مل الى 16000مايكروغرام/مل لنسبة القتل العالية التي امتازت بها واهملت التراكيز القليلة وذلك لقابليتها الواطئة على القتل حيث تميزت التراكيز (من 0.095 الى 62.5)مايكروغرام/مل بانعدام قابليتها على التثبيط اما التراكيز (من 125الى 1000)مايكروغرام/مل فكانت لها نسب تثبيطية واطئة اقل من50% اما التركيزين(4000,2000)مايكروغرام/مل فكانت نسبة القتل63.1%,66.3% على التوالي لذلك ارتئينا اخذ التراكيز الاعلى من ذلك والتي كانت تمتاز بنسب قتل من 70% فما فوق لفعاليتها في القضاء على نسبه اكبر من الخلايا السرطانية ولثلاث فترات هي 72,48,24 ساعة واعتمد اختبار السمية الخلوية Cytotoxicity assay لتقويم تأثير تراكيز المستخلص في نمو الخلايا بدلالة النسبة المئوية لمعدل التثبيط IR%، والذي يستخرج من المعادلة الاتية :

$$\%IR = \frac{A-B}{A} X\ 100$$

حيث A تعني Control ، B تعني Test

عند معاملة الخط الخلوي السرطاني Hep-2 عند التمريرة (231) بتراكيز مختلفة من المستخلص الكحولي لاوراق النبات عند فترات التعرض الثلاث 72,48,24 ساعة وجد تأثير تثبيطي واضح في نمو الخلايا السرطانية وان نسبة التثبيط تزداد بزيادة التركيز وفترة التعرض.

المستخلص الكحولي لاوراق نبات المعدنوس

يتبين لنا من الجدول(1) ان لهذا المستخلص تأثيرا تثبيطيا كبيرا في نمو الخط الخلوي السرطاني Hep-2 للتراكيز الست المأخوذة وبفرق معنوي كبير عن مجموعة السيطرة وكانت اعلى نسبة للتثبيط عند فترة التعرض 24 ساعه هي 75.778% عند التركيز 16000مكغم/مل اما اعلى

نسبة للتثبيط عند فترة التعرض 48 ساعة فكانت 77.093% عند التركيز 16000مكغم/مل ايضا وكذلك بالنسبة لفترة التعرض 72ساعة اذ كانت اعلى نسبة للتثبيط هي 77.136% عند التركيز نفسه وكما هو مبين في الشكل (1) فأن نسبة التثبيط تزداد بزيادة التركيز وفترة التعرض وان التركيز16000مكغم/مل يتميز بأعلى نسبة قتل عند فترات التعرض الثلاث المختلفة وان اعلى نسبة للقتل هي عند هذا التركيز ولفترة تعرض 72ساعة وان الشكل(2) يوضح نسبة التثبيط الكبيرة لخلاياالخط السرطانيHep-2 وقلة عددها عند هذا التركيز وفترة التعرض مقارنة بخلايا الخط غير المعاملة بالمستخلص. ومن الواضح لنا ان نسبة القتل وتثبيط نمو الخلايا للخط الخلوي السرطاني Hep-2 تزداد بزيادة تركيز المستخلص وفترة التعرض رغم ان هذه الفروقات بين نسب التثبيط غير المعنوية عند مستوى المعنوية ($P<0.05$) ولكن هذا لاينفي وجود الزيادة في نسب التثبيط ولكن بمستويات قليلة ومتقاربة بزيادة التركيز وفترة التعرض ومن الجدول(1) يتبين لنا ان اعلى قيمة لمعامل الارتباط كانت عند 48ساعة حيث بلغت (0.919+) ثم الـ72ساعة حيث بلغت (0.914+) ثم الـ24ساعة حيث بلغت (0.913+) وهذا يؤكد ان للتراكيز المستخدمة قدرة تثبيطيه عالية جدا للخلايا السرطانيه للخط الخلوي Hep-2 مما يدل على اهمية المستخلص الفعالة وقدرتة العالية على تثبيط نمو خلايا الخط الخلوي السرطانيHep-2.

جدول -1: تأثير تراكيز مختلفة من المستخلص الكحولي الخام لاوراق نبات المعدنوس ولفترات التعرض الثلاث 72,48,24 ساعة للخط الخلوي السرطانيHep-2.

التركيز مكغم/مل	نسبة التثبيط ± الخطأ القياسي		
	24 ساعة	48 ساعة	72 ساعة
6000	2.94 ± 70.242	9.20 ± 71.626	10.22 ± 72.594
8000	4.66 ± 73.356	7.05 ± 74.74	14.52 ± 75.23
10000	1.85 ± 74.048	8.51 ± 75.086	6.99 ± 75.779
12000	3.31 ± 75.086	6.58 ± 76.124	9.80 ± 76.125
14000	2.66 ± 75.423	6.20 ± 76.47	5.81 ± 77.125
16000	7.49 ± 75.778	11.39 ± 77.093	13.33 ± 77.136

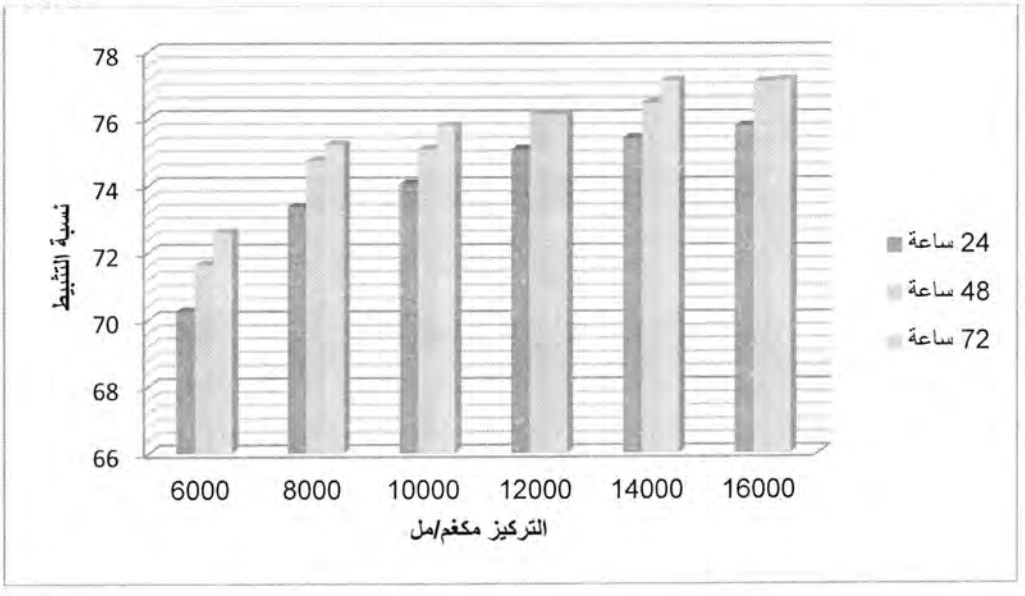

شكل -1: تأثير تراكيز مختلفة من المستخلص الكحولي الخام لاوراق نبات المعدنوس ولفترات التعرض الثلاث 72,48,24 ساعة للخط الخلوي السرطاني Hep-2 .

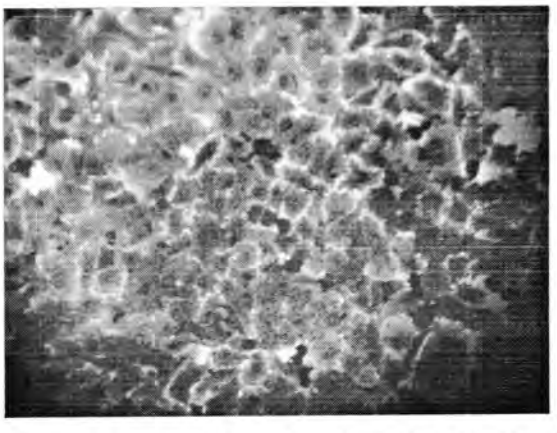

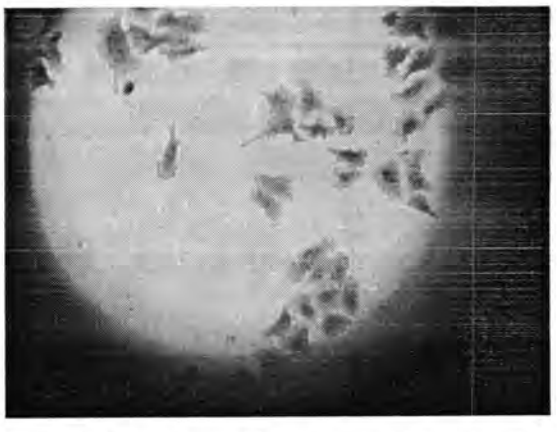

أ: الخط الخلوي السرطاني Hep-2 الذي يمثل تكون بشكل طبقة واحدة (×100).

ب: الخط الخلوي السرطاني Hep-2 المعامل بالمستخلص الكحولي لاوراق نبات المعدنوس عند التركيز 16000مكغم/مل وعند فترة تعرض 72 ساعة, يوضح الفراغات بين الخلايا وقلة عددها(×100).

شكل-2: يوضح المقارنة بين خلايا الخط الخلوي السرطاني Hep-2 غير المعاملة بالمستخلص والخلايا المعاملة بالمستخلص عند التركيز 16000 مكغم/مل ولفترة تعرض 72 ساعة (×100, Crystal violat).

ان النتائج التي توصلنا اليها في هذه الدراسة دعمت بما توصل اليه العديد من الباحثين حول ما تمتلكه المستخلصات النباتية من فعالية مضادة للخلايا السرطانية وان هذه الفعالية تعتمد بشكل اساس على التركيز المستعمل وفترة التعرض كما تعتمد على نوع المستخلص والمركبات الفعالة فيه ومدى حساسية الخلايا السرطانية لكل ذلك.وان النتائج التي تحصلنا عليها والتي اثبتت تأثير المستخلص الكحولي لنبات المعدنوس وقدرته على التثبيط العالي لنمو الخلايا السرطانية للخط Hep-2, والتي امتازت بزيادة نسبة التثبيط بزيادة التركيز وفترة التعرض حتى وان كانت بين التراكيز والفترات وهذا ما اشار له العديد من الباحثون في دراساتهم ومن هذه الدراسات ما قام به[11] على عشب السعد*Cyperus rotundusl* والذي اختبر قابليتة على تثبيط الخطوط الخلوية السرطانية AMN-3,RD,Hep-2 اذ استخدم ثلاث انواع من المستخلصات للنبات هي الهكساني والمائي والايثانولي وبثمان تراكيز مختلفة ولثلاث فترات تعرض72,48,24 ساعة وبشكل عام كانت النتائج تمتاز بزيادة نسبة التثبيط بزيادة التركيز وفترة التعرض مع وجود اختلافات في نسب التعرض بأختلاف التراكيز والمستخلصات المستخدمة كذلك هذا ما لاحظناه في دراسة[12] اذ قامت الباحثة بأستخدام ثلاث انواع من المستخلصات النباتية لنبات الكلغان *Silybum marianuml* وكانت المستخلصات (المائي الخام، الايثانولي الخام، الزيتي الخام) واستخدمت تراكيز مختلفة للمستخلص ودرست تأثيرها في الخطوط السرطانية RD,AMN-3,Hep-2 والخط الطبيعي REF ولاحظت الباحثة ان نسبة التثبيط للخلايا السرطانية للخطوط الخلوية الثلاث RD,AMN-3,Hep-2 تزداد بزيادة التركيز وفترة التعرض اما بالنسبة للخط الخلوي الطبيعي REF فأن النتائج لم تعطي نسب قتل معنوية مع مجموعة السيطرة والفروق قليلة وغير مهمة احصائيا. وقد وجدت[13] في دراستها على قشور نبات الرمان ان هناك نسب تثبيط لنمو الخلايا السرطانية للخطين الخلويين السرطانيين Hep-2,AMN-3 وان هذه النسب تزداد بزيادة التركيز وفترة التعرض حتى بلغت اعلى نسبة لتثبيط خلايا الخطين عند اعلى تركيز وهو700مكغم/مل ولفترة تعرض 72 ساعة وكانت النسبة (59.27%) للخط AMN-3 و (56.64%) للخط Hep-2 بينما في الخط الخلوي الطبيعي REF كانت نسب التثبيط عند التركيز 700مكغم/مل وبفترة تعرض 72ساعة هي(23%) والتي تعد قليلة بالنسبة لتثبيط الخلايا . كما لاحظت[14] امتلاك مستخلصات نبات الصفصاف فعالية تثبيط لسرطان الحنجرة البشري Hep-2 والـ AMN-3

ودراسة [13] عن تأثير اوراق المديد على الخطين الخلويين الـ Hep-2 والـ AMN-3 والخط الخلوي الطبيعي REF ودراسة[15] في دراسة تأثير المستخلصات النباتية لنبات التمر الزهدي لنمو سرطان Hep-2 والـAMN-3.وقد تعزى قدرة النباتات المختلفة على تثبيط مختلف الخطوط السرطانية الى وجود المركبات الكيميائية الزيتية الموجودة في تلك النباتات.حيث ان النباتات والاعشاب الطبية تمتلك العديد من المركبات ذات الفعاليات المختلفة ومن هذه الفعاليات هي الفعالية السمية المثبطة للخلايا السرطانية داخل جسم الكائن الحي او خارجه وان لهذه المركبات عدة اليات من شأنها ان تؤدي الى تثبيط قدرة الخلية السرطانية والحد من نموها وانتشارها وقتلها[16] .

ان نبات المعدنوس احد تلك النباتات الطبيعية التي تمتلك العديد من هذه المركبات الفعالة والمؤثرة في القتل وتثبيط الخلايا السرطانية ومن هذه المركبات القلويدات اذ ان لهذه المركبات اهمية في تثبيط نمو الخلايا السرطانية وهذا ما نلاحظة في القلويد **Isostry chnopentamino** الموجود في الشجرة الافريقية *Strychnos usambar ensis* اذ انه يحدث عملية الموت المبرمج للخطوط الخلوية لسرطان القولون Hct-116[17] .كما ان لقلويد Homohar ringtonine المعزول من جذور نبات *Cephalotauns herringtona* له دور في تثبيط الخلايا السرطانية من خلال تثبيط صنع البروتين والـ DNA [18] .كما ان نبات المعدنوس يحتوي على الفينولات المتعددة Polyphenols والتي تحتوي على مركبات الفلافونات Flavonoids التي تعمل بوصفها مركبات ضد عملية الاكسدة Antioxidant في تأثيرها على الخلايا السرطانية[19] وهذا ما اشار اليه[11] حيث نصت على ان المركبات الفينولية المتعددة ومن ضمنها الفلافونويد الموجود في عشب السعد لها دور كبير بأعتبارهاعوامل مضادة للاكسدة في فعاليتها التثبيطية للخطوط السرطانية (RD,AMN-Hep-2, 3) معتمدا في ذلك على التراكيز ونوع المستخلص، كما ان لهذه المركبات القدرة على احداث التأثير السمي على سرطان البروستات Vascular Endothelial Growth factor(VEGF) والذي يكون مسؤول عن تكوين الاوعيه الدمويه الجديده(Angiogensis) مما يعطي هذه المركبات دور اساسي في تثبيط وقتل الخلايا السرطانية، كما بين Elangovar واخرون[20] ان لمركبات الفلافونات تأثيرا تثبيطيا

على نمو خلايا الخط الخلوي السرطاني (Hep-2) وكذلك الخط الخلوي السرطاني(S-Sarcomy-L 80(L80 وذلك عن طريق ايقاف عملية تضاعف الـ DNA عند مرحلة S-phase خلال دورة حياة الخلية ومن الجدير بالذكر ان اهمية هذه المركبات في عملة تثبيط الخلايا السرطانية للخطوط الخلوية السرطانية المختلفة جاءت من قدرة هذه المركبات في التأثير على الاليه السرطانية من خلال تثبيط فعالية الجين Bcl-2[21] ونتيجة للخلل الحاصل في هذا الجين تدخل الخلية السرطانية مرحلة الموت المبرمج Apoptosis كما هو الحال في العديد من الخطوط الخلوية السرطانية لسرطان الدم البشري Human Leukemic cell Lines[22] ولكفاءة فعالية هذه المركبات فهناك العديد من الخطوط الخلوية السرطانية التي لها القدرة على تثبيطها مثل سرطان الثدي (Bc1) وسرطان القولون البشري(colo320)وسرطان الرحم البشري(CASKI) وسرطان البروستات البشري[23،24] .

كما ان للمركبات الفينولية المتعددة وخاصة تلك المضادة لعملية الاكسدة القدرة على تثبيط نمو الخلايا السرطانية والحد من انتشارها وذلك لامتلاكها القابلية في كسح Scavenger الجذور الحرة المتولدة عند تحول الخلايا من الطبيعية الى خلايا سرطانية [24].وان التربينات الموجودة في اوراق نبات المعدنوس والتي تمثل احد مركباته لها دور مؤثر والقدرة على تثبيط نمو خلايا سرطان المعدة من خلال قدرتها على خفض تصنيع الـ DNA وحث الخلايا على الموت المبرمج للخط الخلوي السرطاني Leukemia cell HL-601،وان لهذه المركبات اهمية بالغة في تثبيط والحد من انتشار خلايا الخط الخلوي السرطاني Human Myelogenous Leukemia وذلك من خلال ايقاف الدورة الخلوية عند طور G1 [25]. وقد لوحظ ان التأنينات Tanins الموجودة في اوراق النبات لها التأثير الواضح على الخلايا السرطانية للخط الخلوي السرطاني (HL-60) وذلك من خلال تجزئة شريط الـ(DNA) وحث الخلايا لنمو الموت المبرمج[26] .وتحتوي اوراق نبات المعدنوس ايضا على الصابونيات التي لها دور فعال في تثبيط الخلايا السرطانية وذلك من خلال ميكانيكيات متعددة وهذا ما لوحظ في نبات *Acacia victoria* حيث ان لها دور تثبيطي انتقائي في نمو الخطوط الخلوية السرطانية بواسطة توقف دورة الخلية في سرطان الثدي عند الانسان وكذلك تحدث الموت المبرمج للخلية في الخط الخلوي لسرطان الدم[27] وهذا ما لوحظ ايضا في العشبه الصينيه *Panax gensing* حيث انها استخدمت لعلاج السرطان بسبب قدرتها على تثبيط

السرطان في الحيوانات المختبرية[28] . يحتوي نبات المعدنوس ايضا على فيتامين -C- الذي يمتاز بأمتلاكة قدرة تثبيطية عالية للخلايا السرطانية من خلال فعاليتة المضادة للاكسدة Anti-oxidation اذ انه يكون سامًا للخلايا السرطانية من خلال عملية ازالة الجذور الحرة المتولدة بتكون الخلايا السرطانية[29] .من هذا كله يتوضح لنا اهمية نبات المعدنوس كنبات طبي فعال لقابليتة التثبيطية في تثبيط نمو الخلايا السرطانية اضافة الى اهميتة في معالجة امراض مختلفة اخرى.

المصادر

1- Islam, M. W. R; Radhakrishnan, X. M.; Liu, H. B. and AL-Naji, M. A. "Safety evaluation of *Zizyphus spinachristi* L. and *Teucrium stocksianum* biss.,used in traditional medicine in the Arabian Gulf", (1994).

2- عبد الوهاب، أفنان أسماعيل، "تأثير مستخلص الكحول الأثيلي الخام لبذور وأوراق نبات المعدنوس*Petroselinum crispum* في الفئران البيض وفي بعض الخطوط الخلوية السرطانية"، رسالة ماجستير، قسم العلوم التطبيقية/التقنيات الأحيائية، الجامعة التكنولوجية، (2010).

3- Usui,T.; Kondoh, M.; Cui, C-B., Mayami,T. and Osada,H. "Tryprostatin A,aspecific and novel inhibiton of microtubule" assembly.Biochem.J.,333:543-548. (1998).

4- Lopus, M. and Panda, D., "The enzophena thridine alkaloid sanguinarine perturbs micro-tubule assembly dynamic through tubulin binding", A possible mechanism for its antiproliferative activity .J.FEBSIO:2139-50. (2006).

5- Gurib-Fakim, A., "Medicinal plants.Tradition of yesterday and drugs tomorrow", Molecular Aspects of Medicine. (2005).

6- Manosroi, J.; Dhumtanoma, P. and Manosoi, A., "Anti-prolif.erative activity of essential oil extracted from Thai medicinal plants on KB and P388 cell lines.cancer", letters:1-7. (2005).

7- Toolan, H. W., "Transplantable human neoplasms maintained in cortisone treated laboratory animals:H-S.-1,Hep-1,Hep-2,Hep-3.Cancer", Res.,14:660-666. (1954).

8- Moore, A. E.; Sabachewesky, L. and Toolen, H.W., "Culture characteristics of four permanent lines of human cancer cells.Cancer" Res.,15:598-605. (1955).

9- Freshney,R. I., "Culture of animal cell:Amanual for basic technique", 4thed.Wileyliss, Ajohn wiley and Sons, Inc. Publication, New York. (2000).

10-العقيلي، صالح رشيد والشايب، محمد سامر، "استخدام البرنامج الاحصائي SPSS"، مطبوعات الجامعه، دار الشرق للطباعه، صفحه358. (1998).

11-الحلي، زيد عبد المنعم علي، "دراسة التأثير السمي والمضاد للأكسدة والمضاد لتكوين الاوعية الدموية الجديدة والحث على عملية الموت المبرمج للمستخلصات الخام والمنقاة جزئيا لعشب السعد.L *Cyperus rotundus* في مختلف الخطوط الخلوية السرطانية". اطروحة دكتوراه،معهد الهندسة الوراثية والتقنيات الأحيائية-جامعة بغداد. (2009).

12-سلمان، اسراء صكبان، "تأثير المستخلصات الخام لحبوب الكلغان *Silybum marianum* *L.* على الخطوط الخلوية السرطانية والطبيعية"، رسالة ماجستير، كلية العلوم للبنات-جامعة بغداد. (2008).

13- السعدي، اسيل ياسين كاظم، "تأثير المستخلص المائي الخام لقشور الرمان على خطوط الخلايا السرطانية النامية في الزجاج والفئران"، رسالة ماجستير، كلية العلوم-الجامعه المستنصرية. (2008).

14-الموسوي، ازهار جعفر، "دراسة تأثير المستخلصات الخام لنبات الصفصاف *Salix acmophylla* في نمو الخلايا الخلويه السرطانيه والخلايا اللمفاويه الطبيعيه للانسان خارج الجسم"، رسالة ماجستير، كلية التربيه-جامعة كربلاء. (2006).

15-الجريصي، ياسر حسن زيدان، "دراسة تأثير المستخلصات الخام لثمار ونوى الزهدي *Phoenix dactylifera* Cultivar Zahdi في تثبيط نمو بعض خطوط الخلايا السرطانيه في الزجاج وفي علاج سرطان الغدة اللبنيه المغروس في الفئران البيض". رسالة ماجستير. كلية العلوم-جامعة بغداد. (2007).

16- Mori, T.; Ohnishi ,M.; Komigama, M.; Tsutsui, A.; Yabnshita, H. and Okada, H., "Growth inhibitory effect of *Paradicsom paprika* in cancer cell lines". Oncology Reports, 9:807-810. (2002).

17- Frederich, M.; Bentires-Alj, M.; Tits, M.; Angenot, L.; Greiners, R.; Gielen, J.; Bours, V. and Merville, M. P., "Isostrychnopentamine an indolomonoter Penice alkaloid from *human Strychnos usambarensis* ,induces cell cycle arrest and apoptosis in human colon cancer cells", Journal of prarmacology and experimental therapeutics fast forward, 304(3):1103-1110. (2003).

18- Alexandrova, R.; Varadinova, T.; Velcheva, M.; Genova, P. and Sainova, I., "Cytotoxic effect of isoqyinoline alkaloids on tumor cell lines", Experimental pathology and parasitology, 4:8-14. (2000).

19- Lopez-Lazaro, M. ; Galvor, M.; Martin-Lorder, C. and Ayuso, M. J., "Cytotoxicity of flavonoids on Cancer cell Line. Structure-activity relation-ship". Med.chem., 1:82-114. (2001).

20- Elangovar,V.; Ramamrthy, N.;Balasubrama bian,S.;Sekar,N.and Govidsany, "Studies on the antiproliferative effect of some naturally occurring bioflavonoidal compounds against human carcinoma of larynt". (1994).

21- Caceres-Cortes, J.R.; Cantu-Graza,F.A.; Mendoza-Mata, M.T.; Charez-Gonzales ,M.A.Ramos-Mandujano,G. and Zambrano-Ramires , I.R., "Cytotoxic activity of Justica-Spicigera is inhibited by Bcl2 proto-oncoyenes and induces apoptosis in a cell cycle dependent fashion, phytothes". Res.,15:691-697. (2001).

22- Pellechia, M.I. and Reed,J.C., "Inhibition of anti-apoptosis BC1-2 family proteins by cancer chemoprevention and chemotherapy Curr". Pharm.DES.,10:1387-1398. (2004).

23- Lopez-Lazaro, M., "Flavonids as anticancer agents: structure–activity relation shaip study". Curr. Med. Chem., :691-714. (2002).

24- Forkmann, G. and Martens, S., "Metabolic engineering and applications of flavonoids", Curr.Opinion Biotech.,12:155-160. (2001).

25- Sadeghi, H. and Yazdanparst, R., "Antitumor Activity and cell cycle arrest of a new Diterpene Ester from *Daphne mucronata*". (2003).

26- Sakagami, H., "Effect of tannins on cancer cell lines". Anticancer Res. 15:2121-2128. (1995).

27- Hanausek, M.; Ganesh, P.; Walas Zek,; Arntzen, C. J.; Staga, T. J. and Gatterman, J. U., "Avicins, a family triterpenoid saponins from *Acacia victoriae* (Bentham), suppress H-ras mutations and aneuploidy in a murine skin carcinogenesis model", pro. Nat. Acdd. Sc. USA, 98:11557-11562. (2001).

28- Cogo, E. and Kevinlai, N. D., "Should ginseng be considered for cancer prevention Z. compl. And Alter". Med. 80:153-155. (2003).

29- Jacob, R.A., "The integrated antioxidant system". Nut. Res., 15:755-766. (1995).

تصنيع قطب البنزويت الانتقائي وأستخدامه في تعيين البنزوات كمادة حافظة

نبيل شوكت نصوري ، اسماء سوري محمد ، سلمى سهام جميل وخولة احمد عبد اللطيف
دائرة بحوث الكيمياء وفيزياء المواد، وزارة العلوم والتكنولوجيا، ص . ب .765 ، الجادرية، بغداد، العراق

تاريخ تقديم البحث : 2010/10/15 تاريخ قبول البحث : 2011/05/29

الخلاصة

تم تحضير أقطاب البنزويت والمتكونة من أغشية حاوية على معقدات البنزويت مع أملاح الامونيوم الرباعية وهي methyl-trioctyl ammonium benzoate (MTOA) و (THA) tetraheptyl ammonium benzoate وباستخدام المواد الملدنة tri-butyl phosphate (TBP) ، di- butyl phthalate (DBPH) و di- butyl phosphate(DBP). درست مواصفات هذه الأقطاب وشملت انحدار نيرنست , مدى التحسس , مدى التراكيز التي يعمل بها القطب ,تأثير pH والمواد المتداخلة . جميع الاقطاب المحضرة اعطت استجابة جيدة وكان الانحدار يتراوح من (60-57mV\decade) ومدى التحسس بحدود 10^{-4}M . اما الاقطاب المحضرة من مادة di- butyl phosphate لم تعطي أي استجابة لاحتمال عدم تآلف هذه المادة الملدنة مع معقدات البنزويت .

تراوحت قيم pH من 4.0-8.5 لكافة الأقطاب المحضرة كما ودرست التداخلات الحاصلة على هذه الأقطاب بوجود أيونات السترات , الاوكزالات , الخلات ، الكلوريد والنترات حيث كانت قيم معامل الانتقائية المقاسة قليلة بحدود 10^{-2}M لأيونات السترات , الاوكزالات , الخلات اما أيونات الكلوريد والنترات فكانت القيم بحدود 0.5M مما يدل عى تداخل هذين الأيونين مع أيون البنزويت.

عمر هذه الأقطاب كانت بحدود شهرين بعدها تبدأ المادة المعقدة بالنضوح من الغشاء الى المحلول الخارجي. كما وتم تعيين أيون البنزوات بواسطة طريقة الأضافات القياسية وكان الخطأ النسبي بحدود 2% لتراكيز 10^{-3}M لأيون البنزويت و 4% لتركيز(5.0×10^{-4} M) بنزويت كما وتم تعيين نقطة التعادل باستخدام طريقة كران .

ABSTRACT

Several benzoate selective electrodes were prepared based on membranes containing benzoate complexes; methyl tri-octyl ammonium benzoate (MTOA) and tetra-heptyl ammonium benzoate (THA) with plasticizers; tri-butyl phosphate (TBP), di-butyl phosphate (DBP) and di-butyl phthalate (DBPH). Electrode parameters were examined including, Nernest slope, detection limit, concentration range, effect of pH and interference. All electrodes gave good response with slopes of range 60 – 57 mV/ decade accept for electrodes based on plasticizer di- butyl phosphate gav poor response may be due to incompatibility of the plasticizer with benzoate complex. The pH values for the electrodes ranged from 4.0 to 8.5. The interference was studied in the presence of citrate, oxalate, acetate, nitrate and chloride ions on benzoate response. Selectivity coefficients were measured and the values around 0.01 for citrate, oxalate and acetate ions which indicates no interference on benzoate response accept for nitrate and chloride ions gave high selectivity around 0.5. The life time for the electrodes around 2 months after that time the complex start to leach from the membrane to the external solution. Standard addition method was used for quantitative determination of benzoate concentration in samples and found the relative errorare 2% and 4% for benzoate concentrations of 10^{-3} M and 5.0 x 10^{-4} M, respectively. As well as the potentiometric method was used for quantitative determination by using Gran plot method.

المقدمة

الأقطاب الأنتقائية الأيونية تعتبر من المتحسسات الجهدية تستخدم في المختبرات التحليلية، الصناعة، القياسات الفزيولوجية، التحاليل البيئية وفي التحاليل الدوائية. توسع استخدام الأقطاب الأنتقائية في مجال الأدوية لكون الطريقة دقيقة جدا وسريعة وسهلة التعيين.

قام نصوري وجماعته(1) بتحضير قطب promethazine HCl معتمدا على تكوين معقد مع phosphotungstic acid وبأستخدام عدة ملدناتز أستخدم القطب المعتمد على المادة الملدنة DBPH في تعيين الدواء في عدد من نماذج دوائية وكانت نسبة التعيين تتراوح بين 99.0 – 103% .

تم تحضير قطب للمادة الدوائية Atenolol والمعتمد ايضا على مادة phosphotungstic acid لتكوين المعقد من قبل نصوري وجماعته (2). تم تحضير الأقطاب بأستخدام عدة مواد

ملدنة ووجد بأن احسن قطب اعطى مواصفات جيدة يعتمد على المادة الملدنة DOPH حيث اعطى انحدار مقداره 55.9 mV/decade وأستخدم في تعيين Atenolol في نماذج دوائية مختلفة المنشأ. كما وتم تحضير اقطاب Ampicilline trihydrate مع عدة مواد ملدنة ووجد بأن احسن مواصفات للقطب هو بأستخدام المادة الملدنة TBP من قبل Al-Haidary وجماعته(3) وكان الأنحدار بحدود 58.0 mV/decade وحد تحسس بحدود 7.0×10^{-5} M مع دراسة الأنتقائية وتعيين الدواء في بعض العقاقير الطبية.

تعتبر مادة حامض البنزويك وبنزوات الصوديوم من المواد المهمة في الصناعة الدوائية وكمواد حافظة للأغذية ومواد التجميل . يستخدم حامض السالسيلك كمادة دوائية لعلاج التقرن وكذلك سالسيلات الصوديوم كمادة دوائية لعلاج الألتهاب وكمسكن (4) وهنالك طرق عديدة مختلفة لتعيين البنزوات منها الطريقة الجهدية حيث تعتمد على استخدام أقطاب البنزويت السائلة في التعيين.

قام العالم James وجماعته (5) بفحص وتحضير اقطاب التي تعتمد على املاح الاموئيوم الرباعية مثل Aliquat 336S حيث استخدمت هذه المادة مع البنزوات لتكوين المادة المعقدة مع اضافة 1-decanol كمادة ملدنة لتحضير أغشية اقطاب البنزويت من نوع (coated wire) بأستخدم البلاتين في القياس وكان الانحدار بحدود 53.0 mV/decade وحد التحسس بحدود $10^{-1} - 10^{-3}$ M.

قام الباحث Hara وجماعته (6) في تحضير قطب البنزويت الأنتقائي بأستخدام المادة tri-n-octylmethylammonium benzoate مع مادة o-dichlorobenzene و p-t-octyl phenol. الدراسة شملت تعيين معامل الأنتقائية وقيم pK_a للحوامض الكاربوكسيلية المؤثرة على القطب. :ما وتم تحضير قطب البنزويت المعتمد على المادة heptyl-4-trifluoroacetyl benzoate لتكوين المعقد من قبل Katsu and Hanada (7) واستخدم في تعيين فعالية cholinesterase في الدم. حساسية تعيين البنزويت بحدود (0.2 – 50 mM) وحد التحسس 10 µM. درس تأثير تراكيز البنزوات على استجابة قطب السالسليت الأنتقائي المحضر من قبل Al-Anni وجماعته (8) بأستخدام quaternary ammonium salts ووجد ان معامل الأنتقائية (log=-3.3)وهي قليلة جدا مما يدل عدم وجود اي تأثير على استجابة القطب.

في هذا البحث تم تحضير اقطاب البنزويت المتكون من املاح الأمونيوم الرباعية مع بعض المواد الملدنة وكان احسن الأقطاب المعتمدة على الملدن TBP و DBPH حيث كان الأنحدار مقارب الى نرنست 60.9 mV/decade و 58.8 mV/decade على التوالي ويمكن استخدام هذه الأقطاب في تعيين البنزوات في نماذج متعددة.

المواد وطرائق العمل

الاجهزة المستخدمة :

- جهاز قياس جهد القطب نوع Expandable Ion Analyzer Orion EA-940.
- مقياس الدالة الحامضية نوع pH– Meter M82 Radio Copenhagen .
- قطب الكالوميل المشبع SCE

المواد الكيماوية المستخدمة :

أملاح الامونيوم الرباعية وهي methyl-trioctyl ammonium benzoate, و tetraheptyl ammonium benzoate

والمواد الملدنة هي di- butyl phthalate, di- butyl phosphate, tri-butyl phosphate مجهزة من شركة BDH و Fluka AG بنقاوة عالية , المواد الاخرى المستعملة ذات نقاوة عالية جدا ومحاليلها حضرت في ماء مقطر اللأيوني .

طريقة العمل :

1- تحضير القطب : تم صنع القطب في المختبر حسب طريقة Craggs وجماعته (9) حيث يتكون القطب من جسم زجاجي وفي داخله قطب الفضة المغطى بكلوريد الفضة .

2- تحضير المادة الفعالة : 10 مل من 10% من ملح الامونيوم الرباعي استخلص بواسطة الكلوروفورم وتم تبادل ايون الكلورايد مع ايون البنزويت وذلك برج محلول ملح الامونيوم الرباعي مع (0.5-0.1 M) بنزوات الصوديوم ولمدة 30 دقيقة . تفصل الطبقة العضوية وتجفف بواسطة كبريتات الصوديوم للحصول على المعقد.

3- تحضير الغشاء : يمزج (0.04g) من المادة الفعالة مع (0.36g) من المادة الملدنة و (0.17g) من مسحوق PVC . اذيب المزيج في (6ml) من THF ويسكب داخل زجاجة مدورة قطرها (30-35 mm) ويترك لغرض التبخر للحصول على الغشاء.

4- منحني المعايرة : قيس جهد القطب الانتقائي في تراكيز مختلفة من ايونات البنزويت والتي تتراوح

من (1.0×10^{-6} M) الى(1.0×10^{-1}M) وترسم العلاقة بين جهد القطب وتركيز ايون البنزويت باستخدام ورق بياني نوع (Orion 7cycles Sime Logarithmic Paper).

5- معامل الانتقائية : استخدمت طريقة مزج المحاليل في تعيين معامل الانتقائية (10).

النتائج والمناقشة

حضرت الأقطاب المصنعة من الأغشية الحاوية على المادة المعقدة (MTOA- benzoate), (THA-benzoate)و المواد الملدنة tri-butyl phosphate و di-butyl phosphate درست المواصفات وشملت انحدار نيرنست , مدى التحسس , مدى التراكيز التي يتحسسها القطب ,تأثير pH , عمر القطب والتداخلات الحاصلة. الجدول (1) يبين مواصفات هذه الاقطاب .

الشكل (2) يبين منحني التدرج لأقطاب البنزويت المعتمدة على المادة الفعالة (MTOA- benzoate)

و المواد الملدنة DBPH, DBP, TBP حيث نلاحظ بان الاقطاب المعتمدة على الاغشية I, II اعطيا قيم انحدار نرنست وهي (60 mV\decade) و(57mV\decade) على التوالي .

القطب المعتمد على غشاء رقم III لم يعطي أي استجابة مما يدل على ان المادة الملدنة di-butyl phosphate غير مناسبة لصنع اقطاب البنزويت حيث ان هذه المادة الملدنة لاتتآلف مع المادة المعقدة (MTOA- benzoate) وانها تنفصل عنها وتنضح من الغشاء الى داخل المحلول اثناء اجراء القياس والارقام المحصورة بين الاقواس على المنحنيات تدل على الوقت اللازم للوصول الى حالة التوازن وتتراوح من 30 sec الى 4 min لغشاء رقم I و 30 sec الى 4 min لغشاء رقم II وبذلك يمكن استخدام هذه الأقطاب في تعيين ايون البنزويت في نماذج متنوعة.

فقد كان مدى التراكيز واسع ويتراوح من (10^{-1} M) الى(5.0×10^{-4}M) الى ومعامل الترابط بحدود واحد وكذلك pH تراوح بين 9-6 وعمر بحدود شهرين .

اما القطب المعتمد على غشاء رقم III اعطى استجابة ثابتة بكافة تراكيز البنزويت (10^{-6} M- 10^{-1}M) وكانت بحدود 40-50 mV مما يدل عدم صلاحية هذا القطب في تعيين البنزويت . من

خلال النتائج يستنتج بان احسن قطب للتعيين يعتمد على المادة الملدنة di- butyl phthalate والمادة الفعالة M TOA- benzoate (غشاء رقم II في جدول رقم1) .

كما تم تعيين مواصفات الأقطاب المعتمدة على اغشية متكونة من المادة الفعالة THA – benzoate (غشاء رقم V, IV) . المواصفات موضحة في جدول (1) حيث نلاحظ بان مدى تحسس هذه الاقطاب كانت احسن من الاقطاب المعتمدة على MTOA- benzoate وكانت (6.0×10^{-5} M) و (9.0×10^{-5} M) على التوالي للمواد الملدنة TBP, DBPH انحدار هذه الاقطاب كانت مطابقة لانحدار نرنست وتتراوح من (56.5mV/decade) الى (61.2mV/decade) .

درست التداخلات الحاصلة على استجابة اقطاب البنزويت المحضرة من قبل الايونات المتداخلة وهي الاوكزالات , الاستيت , السترييت , NO^{-3}, Cl- وتم تعيين معامل الانتقائية باستخدام طريقة مزج المحاليل .

نتائج معامل الانتقائية موضحة في الجدول (2).

تداخلات ايون الكلورايد والاستيت هي 0.3 ,0.5 على التوالي لغشاء رقم I وكانت اعلى بكثير من تداخلات ايوني السترييت والاوكزالات وكذلك لغشاء رقم II والاغشية الاخرى . اما ايون النترات فقد اثر تأثيرا كبيرا على استجابة الاقطاب وعدم حصول استقرارية للقطب وتذبذب عالي عند قياس جهد القطب . الشكل (3) يبين نموذج لتداخل ايون الاستيت على قطب البنزويت المتكون من غشاء حاوي على DBP, TOMA- benzoate كمادة ملدنة .تسلسل تداخل الايونات على النحو التالي :-

NO^{-3}> Cl^{-}> acetate > oxalate > citrate .

تم دراسة تأثير pH على استجابة اقطاب البنزويت المحضرة حيث استخدم تركيزين لايون البنزويت 10^{-2}M , 10^{-3}M في تعيين مدى pH وكانت قيم pH للمادة الملدنة TBP تراوحت بين 7-3 اما DBPH فان pH تراوحت من 6-9 والشكل (4) يبين تأثير pH على استجابة قطب البنزويت المتكون من المادة المعقدة ,trioctyl methyl ammonium benzoate والمادة الملدنة tri-butyl phosphate حيث ان الهبوط في جهد القطب عند pH الواطئة هي لتداخل ايونات الهيدروجين مع المعقد واحتمالية تفكك المعقد في الحامضية العالية .

استخدمت الطريقة المباشرة وطريقة الاضافات القياسية , طريقة متعدد الاضافات وطريقة رسم كران . نسبة الخطأ المقاس لهذه الطرق والاقطاب جميعها مثبتة في الجدول (3) .

تزداد نسبة الخطأ كلما قل تركيز ايون البنزويت بسبب ابتعاد منحني التدرج عن انحدار نرنست وتبتعد قيمة (r) عن الواحد . وهذا مؤشر مهم يحددنا في تعيين وتركيز ايون البنزويت في النماذج المقاسة

جدول -1 : مواصفات اقطاب البنزويت المحضرة

Memb. No.	Mediator	Slope mV/decade	Cone. Range/M	R	Detection limit /M	pH	Life time
I	Tri-butyl phosphate	60.9	10^{-1}-10^{-3}	0.9993	10^{-4}	3-7	1 month
II	Di- butyl phthalate	58.8	10^{-1}-5×10^{-4}	0.9997	10^{-4}	6-9	2 month
III	Di-butyl phosphate	*	*	*	*	*	*
IV	Di- butyl phthalate	58.4 56.5	10^{-1} -5×10^{-4} 10^{-1}- 10^{-4}	0.9995 0.9998	6×10^{-5}	4-7	2 month
V	Tri-butyl phosphate	57.0 61.2	10^{-1}-5×10^{-4}	0.9996 ≈1	9×10^{-5}	6-8.5	1 month

غشاء رقم I , II , III يعتمد على مادة MTOA- benzoate

غشاء رقم V, IV يعتمد على مادة THA- benzoate

* تعني عدم الاستجابة

جدول -2 : معامل الانتقائية للايونات المتداخلة مع قطب البنزويت

Interfering ion	Conc. of Interfering ion	Membrane No.			
		I	II	IV	V
citrate	$7\text{x}10^{-3}$ 10^{-2}	-	$4.6\text{ x}10^{-3}$ 4.1×10^{-3}	3.1×10^{-3} 3.3×10^{-3}	2.9 xl0-3 3×10^{-3}
oxalate	$7\text{x}10^{-3}$ 10^{-2}	1.4×10^{-2} 1.5×10^{-2}	2.3×10^{-2} 2.6×10^{-2}	1.6×10^{-2} 1.7×10^{-2}	2.1×10^{-2} 2×10^{-2}
acetate	$7\text{x}10^{-3}$ 10^{-2}	0.30 0.35	0.11 0.25	0.16 0.16	0.21 0.22
Cl^-	$7\text{x}10^{-3}$ 10^{-2}	0.50 0.55	0.90 1.00	0.32 0.33	0.65 0.66
NO^{-3}	$7\text{x}10^{-3}$ 10^{-2}	- -	- -	0.8 0.6	0.54 0.55

جدول -3 : نسبة الخطأ النسبي للطرق الجهدية الثلاث في تعيين البنزويت.

Memb.	Mediator	Cone. of	SA	MSA	Gran plot

No.		Benzoate/ M			
I	Tri-butyl phosphate	10^{-3}	3%	2%	5%
II	Di- butyl phthalate	10^{-3} 5×10^{-4}	2% 2%	5% 7%	5% 10%
IV	Di- butyl phthalate	10^{-3} 5×10^{-4}	1.6% 1.1%	1.1% 1.2%	1.2% 2%
V	Tri-butyl phosphate	10^{-3} 5×10^{-4}	2% 3.2%	2.4% 5%	1.2% 4%

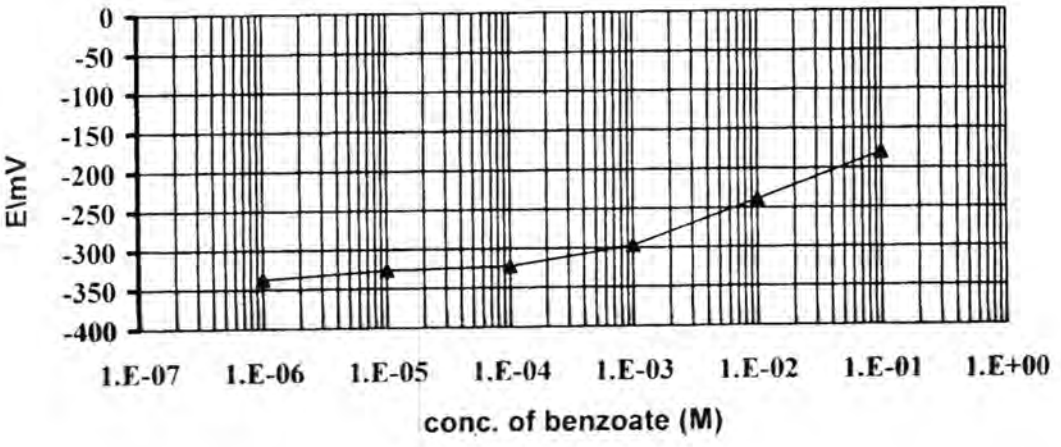

شكل -1 : منحني التدرج لقطب البنزويت باستخدام المادة الملدنة DBPH والمادة المعقدة MTOA- benzoate

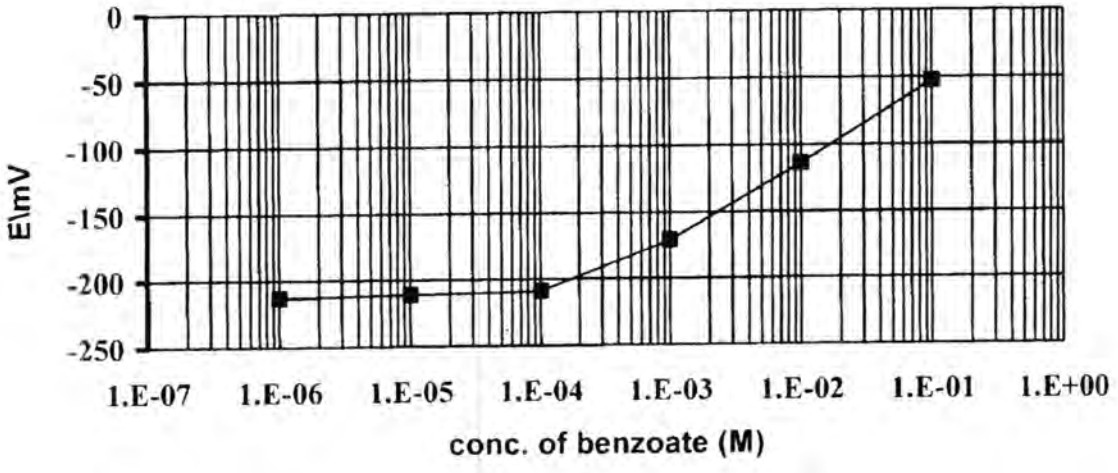

شكل -2 : منحني التدرج لقطب البنزويت باستخدام المادة الملدنة TBP والمادة المعقدة MTOA- benzoate

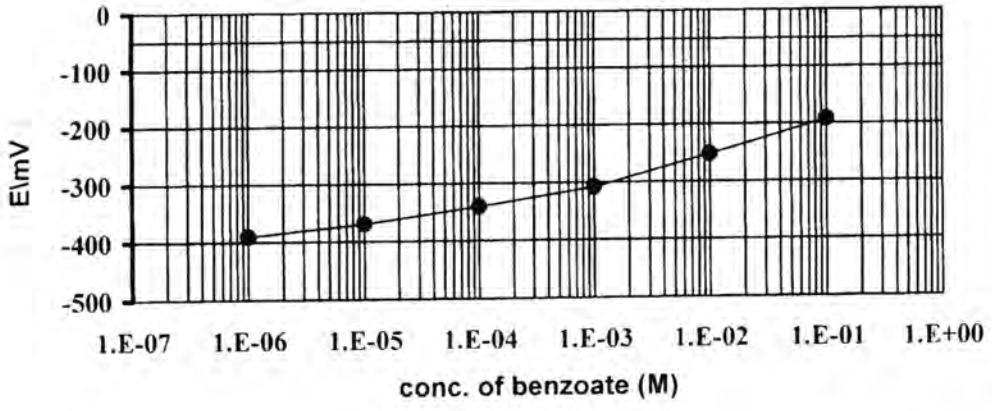

شكل -3 : منحني التدرج لقطب البنزويت باستخدام المادة الملدنة DBPH والمادة المعقدة THA- benzoate

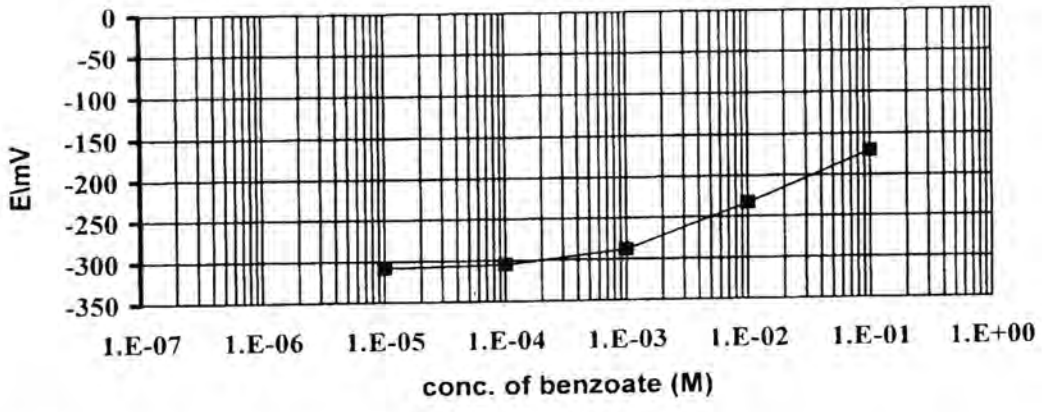

شكل -4 : منحني التدرج لقطب البنزويت باستخدام المادة الملدنة TBP والمادة المعقدة THA- benzoate

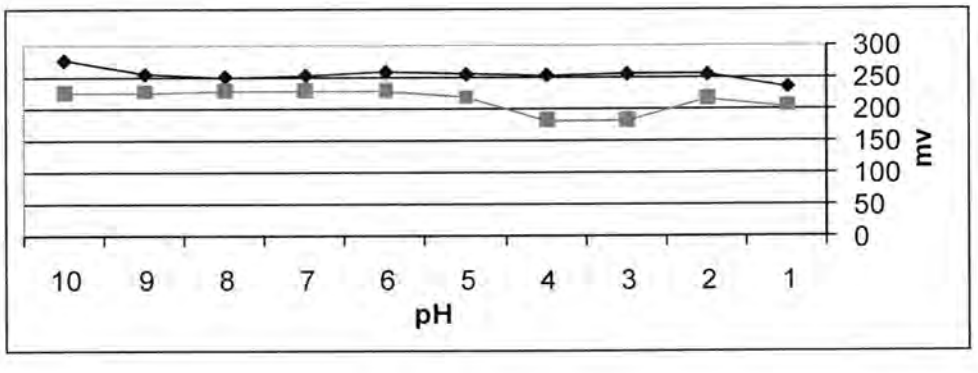

شكل -5 : تأثير pH على استجابة قطب البنزويت باستخدام المادة الملدنة DBPH والمادة المعقدة THA- benzoate

المصادر

1. Nassory N.S., Maki S.A. and Al-Phalahy B.A. "Preparation and Potentiometric Study of Promethazine Hydrochloride Selective Electrodes and Their Use in Determining Some Drugs" Turk. J. Chem.,Vol.32, No.5, 539-548 (2008).

2. Nassory N. S., Maki S.H. and Ali M.A. "Preparation and Characterization of an Atenolol Selective Electrode Based on a PVC Matrix Membrane" Turk. J. Chem., Vol.31, No. 1, 75-82 (2007).

3. Al-Haidary A.M., Nassory N.S. and Al-Saadi A.S.M. "Construction and Study Polymetric Membrane Selective Electrodes for Determination of Ampicillin Trihydrate" Ibn Al-Haitham J. for Pure and Applied Sciences, Vol.19, No.4A,101- 115 (2006).

4. The pharmaceutical codex, "Principle and Practical of Pharmaceutica" 21st ed., the Pharmaceutical Press, London (1994).

5. James H., Carmack G. and Freiser H. "Method of Manufacturing Ion-Selective Electrodes for Analyzing Selected Ions in Solution" Anal. Chem., Vol. 44, No.4, 856-857 (1972).

6. Hara H., Okazaki S. and Fujinaga T. "Enhancment of Selectivity of a Benzoate- Selective Liquid Membrane Electrode by Alkylphenol" Analytica Chimica Acta, Vol.121, No.12, 119-123 (1980).

7. Katsu T. and Hanada N., "Determination of Cholinesterase in Blood Serum Using a Benzoate-Selective Electrode Made With Heptyl-4-Trifluoroacetylbenzoate Neutral Carrier" Analytica Chimica Acta, Vol.321, No.5, 21-25 (1996).

8. Al-Anni S.S., Nassory N.S. and Al-Jubory M.E. "Salicylate-Selective Liquid Membrane Based on Quaternary Ammonium Salts in PVC Matrix Membrane" Iraqi J. of Chem. Vol. 26, No.3, 532-538 (2000).

9. Craggs A . Moody G.J. and Thomas J.D.R "PVC Matrix Membrane Ion- Selective Electrodes. Construction and Laboratory Experiments" J. Cem, Educ., Vol.51, No.8, 541- 544 (1974).

10. Moody G.J. and Thomas J.D.R "Selection Ion Sensitive Electrodes" Merrow Publishing Co., Watford (1971).

دراسة التغيرات الحاصلة في نسب تراكيز فيتامين (A,C,E) لمرضى السكر وعلاقتها بالعناصر النزرة (الخارصين والمغنيسيوم) والمالون ثنائي الالدهايد

جعفر هاشم* وجميل موسى** وكاظم خضير***

* وزارة العلوم والتكنولوجيا

**الجامعةالمستنصرية-كلية العلوم-قسم الكيمياء

**جامعة بغداد-كليةالعلوم للبنات

تاريخ تقديم البحث : 2011/ 3/30 تاريخ قبول البحث : 2011/ 5/29

ABSTRACT

This research study on the relationships between the trace elements and lipid peroxidation marker (MDA) for people with diabetes compared with healthy people. Samples were taken from the blood of patients (100) sample for different ages (6-69) years divided into: were patients

Group one: It includes diabetic patients type 1 of D.M. which the disease they have it for three years and more. Fifty patients, twenty five male and twenty five female.

Group two: It includes diabetic patients type 2 of D.M. which the disease they have it for five years and more. Fifty patients, twenty five male and twenty five female.

Group three (Control group): It includes Fifty presents. Twenty five male and twenty five female.

The trace element includes Zn, Mg by using Atomic Absorption Method. The results show decrement of the constriction level of trace elements (Zn,Mg) of the two groups of Diabetes Mellitus (type one, type two) in comparison with the control cases. In this study we attempted to shed light on the possible relationships between lipid peroxidation markers. Some serum antioxidants such as vitamin (A,C,E) were evaluated and were found to be lower compared to the control group. Different models were analyzed by a spectrum of Flame Atomic Absorption Atomic Absorption Spectrophotometry and HPLC.

الخلاصة

يهدف هذا البحث الى دراسة العلاقة بين بعض العناصر النزرة لمرضى السكري بنوعيه مع فيتامين (A,C,E) و(MDA) مقارنة مع الأشخاص الأصحاء. تم اخذ عينات من دم المرضى (100) عينة لأعمار مختلفة (9-69)سنة وتم تقسيم المرضى إلى :

المجموعة الأولى: وتشمل مرضى السكري النوع الأول المعتمدين على الأنسولين وكانت مدة المرض عندهم ثلاث سنوات وأكثر. وتشمل خمسون (50) مريضا، خمسة وعشرون (25) ذكرا ، وخمس وعشرون (25) انثى .

المجموعة الثانية: وتشمل مرضى السكري النوع الثاني غير المعتمدين على الأنسولين وكانت مدة المرض عندهم خمس سنوات وأكثر . وتشمل خمسون (50) مريضا ، خمسة وعشرون (25) ذكرا، وخمس وعشرون (25) انثى .

المجموعة الثالثة: شملت نماذج السيطرة متبرعين أصحاء ممتنعين عن الطعام لمدة (12) ساعة. وقد بلغ عدد المتبرعين الأصحاء خمسون شخصا (50) ، وهم خمسة وعشرون (25) ذكرا وخمس وعشرون (25) انثى وكانت أعمارهم تتراوح بين (9 –69) سنة .

وثبت من خلال البحث بان هناك نقص في العناصر النزرة (الخارصين. المغنيسيوم)

تم تحليل نماذج مختلفة بواسطة جهاز طيف الامتصاص الذري اللهبي Atomic Absorption Spectrophotometry . تم تقدير مستوى الأكسدة في مصل الدم بمقدار مايتكون من MDA إن المالون ثنائي الالدهايد هو من النواتج الثانوية للأكسدة الفوقية للدهون فان قياس هذه المادة يعطي انطباعا عن مستوى الأكسدة واستخدمت طريقة لونية تعتمد على التفاعل بين مركب حامض الثايو بار بتيورك والمالون ثنائي الالدهايد ليعطي مركبا لونيا اعلى امتصاصية له فيnm 532 . وتم قياس فيتامين(A,C,E) في مصل الدم بتقنية HPLC

المقدمة

يعد داء السكري(Diabetes Mellitus) من الأمراض الواسعة الانتشار ، إذ تلعب الوراثة وعوامل أخرى دورا كبيرا في ظهوره ، ومرض السكري هو مرض (ايضي) مزمن (MetabolicDisease) يتميز بزيادة مستوى السكر في الدم (Hyperglycemia) نتيجة لنقص نسبي أو كامل في الأنسولين الذي يفرز من خلايا البنكرياس من نوع بيتا (β) الموجودة في جزر

لانكرهانز (Islets of Langherhans)، إذ يؤدي هذا النقص الى نقص الموازنة في تمثيل الكاربوهيدرات والدهون والبروتينات [1] .

وهناك عوامل عديدة تساعد على ظهور الحالة المرضية مثل السمنة [2] ، والعامل الوراثي إذ يتفق العلماء بان للوراثة دورا مهما في الإصابة ، ويؤكد بعضهم على انه يعود الى عجز الدورة الدموية عن تغذية البنكرياس بصورة كافية [3]،او خلل في المناعة الذاتية والتوتر النفسي والمعاناة العصبية [3 , 4] ، اختلال التوازن الهرموني [5] ، والالتهابات الميكروبية [1] ، ويمكن أن تبدو الحالة المرضية كتأثير جانبي نتيجة الإصابة ببعض الأمراض المعروفة مثل أمراض الغدة النخامية (Pituitary gland) والدرقية (Thyroid) والغدة الكظرية(Adrenal gland) [5] وأمراض البنكرياس مثل الأورام كما أن التهابات البنكرياس لها تأثير في ظهور هذا المرض [6]. ويبدو أن لعمر المريض علاقة مباشرة في ظهور الحالة المرضية حيث كلما تقدم الإنسان في العمر كان احتمال الإصابة اكبر . كما أن بعض المصادر الحديثة تشير الى أن احتمالية إصابة الطفل بمرض السكري تصل الى (3%) إذا كان أحد الوالدين مصابا بالسكري وتصل النسبة إلى(10 %) إذا كان أحد الوالدين والطفل الأول مصابا وتصل النسبة الى (30 – 50 %) إذا كان كلا الوالدين من المصابين بداء السكري .

كذلك تبين من خلال الدراسات أن بعض النساء الحوامل يصبن بارتفاع السكر في الدم بالرغم من إنهن لم يسبق لهن الإصابة بمرض السكري قبل الحمل ، ويطلق على هذا النوع من مرض السكري بسكر الحمل (Gestational D.M) وهذا النوع من السكري يصيب حوالي(4%) من مجموع النساء الحوامل ، ويعزى سبب ارتفاع السكر لدى المرأة الحامل إلى بعض الهرمونات التي تغذي المشيمة للحفاظ على تغذية الجنين لذا ينصح الأطباء بعمل فحص السكر في الدم خلال فترة الحمل [7] . أما علاقة الجنس بظهور الحالة المرضية ، فيبدو أن الفتيان من الشباب اكثر عرضة للإصابة من الفتيات.

يعد داء السكري من اكثر الأمراض المزمنة انتشارا في العالم كما أن نسبته أخذت بالارتفاع حسب أخر تقارير منظمة الصحة العالمية (WHO) وجمعيات عالمية أخرى ، إذ يبلغ عدد المصابين بداء السكري حوالي (130) مليون شخص بالعالم وهذا الرقم سيتضاعف بحلول عام (2025) إذ يبلغ عدد المصابين بمرض السكري (300) مليون شخص مما يجعل مرض السكري من الأمراض الواسعة

الانتشار في العالم [8]. فيما اعلنت الجمعية العالمية لمرضى السكري أن عدد المصابين بمرض السكري حوالي (143) مليون شخص .

ويمكن تميز المرض مختبريا عن طريق قياس زيادة نسبة السكر في الدم (Hyperglycemia) وفي الإدرار (Glycouria)، وكذلك عمل تحليل الهيموغلوبين المسكر (HbA_{1c}) وهو هيموغلوبين متحد مع السكر موجود في كريات الدم الحمراء .إن مستوى السكر ضمن الحدود الطبيعية في الإنسان تتراوح بين (60 – 126)ملغم/ 100 مل من دم الإنسان ((FBS) (Fasting Blood Glucose [9].

المواد وطرائق العمل

تم الحصول على هذه النماذج من النوع الأول والثاني للمرض والذين تم تشخيصهم من قبل أطباء اختصاص في المركز الوطني لعلاج وبحوث السكري إذ بلغ عدد المرضى (100) مريضا.

وتم تقسيم المرضى إلى:

1 . المجموعة الأولى: وتشمل مرضى السكري النوع الأول المعتمدين على الأنسولين وكانت مدة المرض عندهم ثلاث سنوات وأكثر. وتشمل خمسون (50)مريضا، خمسة وعشرون (25) ذكرا ، وخمس وعشرون (25) انثى .

2 . المجموعة الثانية: وتشمل مرضى السكري النوع الثاني غير المعتمدين على الأنسولين وكانت مدة المرض عندهم خمس سنوات وأكثر . وتشمل خمسون (50) مريضا ، خمسة وعشرون ذكرا ، وخمس وعشرون (25) انثى .

3 . المجموعة الثالثة : شملت نماذج السيطرة من متبرعين أصحاء ممتنعين عن الطعام لمدة (12)ساعة تقريبا . وقد بلغ عدد المتبرعين الأصحاء خمسون شخصا (50) ، وهم خمسة وعشرون (25) ذكرا وخمس وعشرون (25) انثى وكانت أعمارهم تتراوح بين (9 – 67) سنة .

تقدير العناصر المعدنية في مصل الدم بوساطة جهاز الامتصاص الذري :

تقدير الخارصين (Zinc) [10].

تم تحضير تراكيز مختلفة من محلول كبريتات الخارصين ($ZnSO_4$) بأذابتها بالماء الأيوني . لعمل منحني قياسي لتركيز الخارصين .

يعامل مصل الدم بالماء الأيوني (0.2 ml of serum + 1.8 ml of D .W) للحصول على مصل دم رائق ونحسب معامل التخفيف. للحصول على التركيز الصحيح باستخدام مصباح خاص للخارصين بطول موجي (213.9nm) .

تقدير المغنيسيوم (Magnesium) . [11]

تم تحضير تراكيز مختلفة من محلول كبريتات المغنيسيوم ($MgSO_4$) باذابتها بالماء الأيوني لعمل منحي قياسي لتركيز المغنيسيوم .

تم معاملة مصل الدم بمحلول 1% من كلوريد اللنثانيوم (0.1 ml of serum + 4.9 ml of 1% Lanthanum chloride solution) للحصول على مصل دم رائق ونحسب معامل التخفيف للحصول على التركيز النهائي والصحيح للمغنيسيوم باستخدام مصباح خاص للمغنيسيوم بطول موجي (285.2nm) .

تقدير مستوى الأكسدة في مصل الدم بمقدار ما يتكون من الـMDA

إن المالون داي الديهايد هو من النواتج الثانوية للأكسدة الفوقية للدهون لذا فان قياس هذه المادة يعطي انطباعاً عن مستوى الأكسدة والطريقة المستخدمة هي طريقة لونيه تعتمد على التفاعل بين مركب حامض الثايوباربيوترك والمالون ثنائي الديهايد ليعطي مركباً لونياً أعلى امتصاص له في (532) نانومتر وقد استخدمت طريقة (Fong) لهذا الغرض(12) .

قياس فيتامين(A,C,E) في مصل الدم بتقنية HPLC

تستعمل في هذه الطريقة أعمدة صغيرة ذات أقطار بنحو (1–3) ملم تحتوي على ساند مؤلف من دقائق إحجامها بنحو (30) مايكرومتر يضغط محلول الاسترداد (Eluent) خلال العمود بمعدل جريان عالٍ (1–5) مل/دقيقة وعمليات الفصل بهذه الطريقة أسرع (100) مرة من طريقة كروموتغرافيا عمود السائل الاعتيادي. لذا وجدت الـ (HPLC) تطبيقات واسعة في تشخيص المركبات العضوية وفصلها على نطاق واسع.

لقياس كمية فيتامين (E) في مصل الدم استخدمت الطريقة المحورة من (Deleen heer) وكانت الطريقة المستخدم على النحو الآتي.

محلول مانع الأكسدة Antoxidant Solution

محلول مائي لكحول الايثانول بنسبة (1:9) ايثانول: ماء يحتوي على (10) غرام من حامض الاسكوربك، (0.1) غرام من البايروكالول للتر الواحد.

طريقة العمل: -

أخذ (0.1) مل من المصل واضيف له (2) مل من محلول مانع الأكسدة واستخلص المزيج مع محلول قياسي يحتوي على الفاتوكوفيرول المذاب في الهكسان وجفف المستخلص تحت تيار من النتروجين واعيدت إذابته في مزيج كلوروفورم: ميثانول بنسبة (1:2) (حجم: حجم) ثم يحقن (10) مايكرولتر في جهاز الـ (HPLC) فتظهر القمم باستخدام محلول الفصل غسلاً (elution) وهو خليط من (الميثانول: ماء) بنسبة (1:100) (حجم:حجم) بسرعة جريان (1.5) مل/دقيقة وباستخدام عمود نوع (ODS) C_{18} وقد قيست الامتصاصية على طول موجي (287) نانومتر فشخصت القيمة بمقارنتها مع مركب فيتامين (E) القياسي كماً ونوعاً.

أما فيتامين C فاستخدم الطور المتحرك بإذابة صوديوم اسيتيت و (EDTA) في الماء المقطر وبضبط pH عند 6 وثبت الطول ألموجي عند nm254 وباستخدام نفس العمود

كذلك فيتامين A استخدم الطور المتحرك (% 99) ميثانول (1%) ماء مقطر بطول موجيnm 330 وبنفس العمود (13).

النتائج والمناقشة

يبين الجدول (1) أن هناك انخفاضا في مستوى معدل تركيز الخارصين في مرضى داء السكري للمجاميع (2,1) مقارنة مع مجموعة السيطرة وهذا ما أكدته الأبحاث (14) إذ أظهرت النتائج انخفاضا في مستوى تركيز الخارصين في النوع الأول والثاني من داء السكري.

يعتبر عنصر الخارصين مهما جدا في الإنسان إذ انه عنصرا أساسيا لاكثر من (100) أنزيم معدني مثل الكحول ديهايدروجينيز(Alcohol dehydrogenase)

والحامض النووي(RNA) وبلمرة الحامض النووي (DNA) (15) والخارصين عنصر ضروري في نمو وانقسام الخلية وكذلك يدخل الخارصين كعنصر أساسي في عملية ايض الكولاجين (Collage Metabolism).وان نسبة إفراز الأنسولين استجابة الى حافز السكر يقل في حالة نقص عنصر الخارصين. ويمكن أن يعزى سبب انخفاض مستوى الخارصين في مصل الدم ربما الى زيادة كمية الإدرار التي تطرح في مرضى داء السكري بسبب زيادة مستوى الكلوكوز في مصل الدم وبالتالي يزداد الخارصين في الإدرار ، وكذلك عدم وجود انظمة بروتينية تحافظ على مستوى الخارصين في الجسم مثل السيروبلازمين لعنصر النحاس(16) .

يبين الجدول (2) أن معدل تركيز المغنيسيوم قد انخفض في مرضى السكري للمجاميع مقارنة مع مجموعة السيطرة يتفق هذا مع الأبحاث (17) إذ بينت النتائج انخفاض في مستوى تركيز المغنيسيوم للمرضى عند مقارنتهم بمجموعة السيطرة .

يعد المغنيسيوم من المعادن الأساسية في جسم الإنسان اذ أن النقص الحاد في عنصر المغنيسيوم يسبب ضعف العضلات(Muscle weakness) ، رعاش (Tremor) ، تهيج (Irritability) ، الهلوسة (Hallucinations) ، واحساسات غير طبيعية .

وجدت البحوث الحديثة أن (25 %) من مرضى داء السكري لديهم مستويات اقل من المغنيسيوم في الدم وقلة النشاط الإنزيمي الخاص بايض الكاربوهيدرات والذي يدخل فيه عنصر المغنيسيوم كأساسي .

أن نسبة الثلث من الكميات المأخوذة من المغنيسيوم عن طريق الفم تمتص بوساطة الأمعاء وان الكميات الزائدة من المغنيسيوم تطرح بصورة رئيسية عن طريق الكلى. أن مستويات المغنيسيوم في الدم تنظم بوساطة هرمونيين هما الأنسولين وهرمون والباراثايرود (Parathyroid hormone and Insulin) وإعطاء الأنسولين أو تحرره استجابة إلى أكل المواد السكرية أو النشوية يوضح دخول المغنيسيوم في عملية ايض الكلوكوز إذ انه تزداد كمية المغنيسيوم (18) .

يتحد المغنيسيوم (Mg) مع المركب (ATP) ليكون المعقد (Mg ATP) وهذا المعقد ينظم عمل الأنزيم (Protein kinase) وهو بدوره يدخل مباشرة في عملية ايض الكلوكوز الهرمونات الببتيدية .

انخفاض الفعاليات الإنزيمية لعدة طرائق ايضية يمكن أن تشاهد في مرضى داء السكري نتيجة لنقص الأنسولين والبحوث الأولية بينت وجود علاقة عكسية بين مستويات المغنيسيوم وكمية الكلوكوز في دم الإنسان الصائم في مرضى داء السكري المعالجين بوساطة الأنسولين.

وجد الباحث ديفلك ومجموعته(DeValk et al., 1998) في البحوث التي أجريت على مصل الدم للإنسان أن تأثير تزويد المرضى بالمغنيسيوم وبكميات تصل الى (10 mmol) يوميا لمدة ثلاثة اشهر على خمسين مريضا من النوع الثاني من داء السكري الذين يحتاجون الأنسولين تؤثر على عمل هرمون الأنسولين وضعف تام في العضلات مع اضطرابات أنزيمية(18). وأيضا فان كمية المغنيسيوم في بلازما الدم التي تطرح من خلال الإدرار تزداد مع ازدياد أعطاء المغنيسيوم عن طريق الفم .

يبين الجدول (3) أن هناك زيادة لمستوى المالون ثنائي الالدهايد (MDA) في مصل دم مجموعتي المرضى.

أن عملية الأكسدة الفوقية للدهون هي ظاهرة طبيعية تحدث بصورة مستمرة وبمعدلات قليلة عند جميع الأشخاص ومن نتائج هذه العملية هو أنتاج نواتج الديهايدية وحوامض شحميه حرة والمالون ثنائي الالدهايد MDA الذي تم قياسه في هذه الدراسة يعد كدليل كيموحيوي لعملية الأكسدة في الدهون(19) ، لقد أثبتت الدراسات بأن المرضى تحدث عندهم حالة زيادة في معدلات الايض مما يؤدي إلى إنتاج سريع للجذور الحرة فوقية للدهون وخاصة في بعض الأنسجة(20) .

يبين جدول (4) انخفاض في مستوى تركيز فيتامين (C) بالنسبة للمرضى مقارنة مع قيم السيطرة .

على الرغم من أن فيتامين (C) من الفيتامينات الذائبة في الماء فأهميته تأتي من ناحية الحفاظ على فيتامين (E) بشكله الفعال المختزل (21) كما وجد بعض الباحثين الذين درسوا التركيز والحالة التاكسدية للاسكوربيت أن قيمته اقل بكثير عند المرضى منه في الأصحاء لان معظم الاسكوربيت وجد على شكله المؤكسد .

أوضحت النتائج بان للفيتامينات A و C و E تأثيرات مختلفة في الجهازين المناعي والوراثي. وهذا يفسر في ضوء كون هذه الفيتامينات هي من مضادات الأكسدة (Anti-oxidants) (22) وان المؤكسدات (Oxidants) من العوامل المؤثرة في فعالية الجهاز المناعي وباتجاه تثبيط وظائفه(23).

تشير الدراسات بان فيتامين C يؤثر في معظم جوانب وظائف الجهاز المناعي، وان انخفاضه يؤثر في وظيفة هذه الخلايا (24). حيث اقترح بان هذا الفيتامين يوفر الحماية لدهون البلازما (Plasma lipids) ودهون الأغشية الخلوية (Membrane lipids) من فعل المؤكسدات من خلال ثلاث آليات:التداخل في بناء نيوكلوتيدات الخلية وبناء البروستوكلاندينات (Prostglandins) ويعزز إنتاج الحركيات الخلوية (Cytokines) (25). أن آاليات الأنفة الذكر تدخل ضمن المحصلة العامة لفعالية الجهاز المناعي وإذا كان فيتامين C مشمولا فيها فهذا يفسر النتائج الايجابية التي أشارت إليها الدراسة الحالية، لكن يبقى مجال البحث مفتوحا لدراسة الآلية أو الآليات التي من خلالها يعمل فيتامين C على تعزيز فعالية الجهاز المناعي.

يبين جدول(5) انخفاض في مستوى تركيز فيتامين (E) بالنسبة للمرضى مقارنة مع قيم السيطرة.

تؤكد أهميته في المحافظة على وظيفة الجهاز المناعي، وهو الأخر من مضادات الأكسدة (26). حيث وجد بأنه من مضادات الأكسدة الذائبة في دهون غشاء الخلية والذي قد يتأثر بالمؤكسدات (27). لقد تم التوصل لهذا الاستنتاج من خلال دراسات حالات نقص فيتامين E ، حيث وجد بأنها تتصاحب مع انخفاض في إنتاج الأضداد من الخلايا اللمفاوية (28) .

لذلك وجد علاقة عكسية مابين مستوى فيتامين E في الدم والإصابة بالبكتريا في الأشخاص المسنين، وان إعطائهم جرع من فيتامين E ساهم في تحسين فعالية الجهاز المناعي في القضاء على هذه الإصابات (29) إما آلية تأثير هذا الفيتامين في الجهاز المناعي، فقد اقترح بأنه يعمل على تثبيط احد عوامل الاستنساخ (Transcription factor) والمسمى NF-KB ، حيث انه يعد عاملا مؤثرا في إنتاج الخلايا لـ Interlukin-1 (30) .

يبين جدول (6) انخفاض في مستوى تركيز فيتامين (A) بالنسبة للمرضى مقارنة مع قيم السيطرة

فقد لوحظ فيتامين A بأنه يمتلك القابلية على التحفيز المناعي إلا أن الدراسات في هذا المجال كانت على الأشخاص المسنين والتي أوضحت بان فيتامين A يعمل على تعزيز فعالية الجهاز المناعي ومن خلال تأثيره في الخلايا اللمفاوية التائية المساعدة (CD4+ Cell) ومستلمات (Interlukin-2) على سطح الخلايا وكذلك الخلايا القاتلة الطبيعية Natural killer cells إضافة إلى ذلك فقد لوحظ علاقة ايجابية مابين مستوى فيتامين A في مجرى الدم وعدد خلايا وحيدة النوى (31). لقد تناولت العديد من الدراسات هذا الموضوع وتكاد تتفق مع بعضها البعض في مقدمة واحدة هي تعمل هذه الفيتامينات على حماية الكائن فقد تمت الإشارة فيها إلى إن الفيتامينات A و C و E هي من مضادات الأكسدة (32) .

والتي عادة ماتكون مستحثة بالملوثات البيئية التي يتعرض لها الإنسان خصوصا في العراق وعلى مدى العقدين الماضيين لذلك هل يمكن تحصين الإنسان بهذه الفيتامينات ضد الإصابة بالسرطان .

من دراسة نتائج البحث يمكن استنتاج الأتي:

1. أن النتائج قد أظهرت انخفاضا في مستوى تركيز المعادن الضئيلة الخارصين و المغنيسيوم و فيتامين (A,C,E) .

وزيادة لمستوى المالون ثنائي الالدهايد (MDA) في مصل دم مجاميع الدراسة الثلاثة في مرضى داء السكري بنوعيه الأول والثاني مقارنة بمجموعة السيطرة بينما مجاميع داء السكري الثلاثة مقارنة بمجموعة السيطرة.

جدول رقم –1 : معدلات تركيز الخارصين (Zn) في مصل الدم والانحراف المعياري له لكل من مجموعة السيطرة ومجاميع المرضى

Group	Mean ±S.D معدل الـ Zn (µg/dL)	T
Control	11. 14 ±3.89	
DM1	6.13 ±3.58	P < 0.0001
DM2	5.04 ±2.97	P < 0.0001

A : DM1 مرضى داء السكري من النوع الأول المعتمدين على الأنسولين .

B : DM2 مرضى داء السكري من النوع الثاني غير المعتمدين على الأنسولين

Control مجموعة السيطرة

(2) مستوى تركيز المغنيسيوم (Mg) في مصل الدم .

جدول –2 : معدلات تركيز المغنيسيوم في مصل الدم والانحراف المعياري له لكل من مجموعة السيطرة ومجاميع المرضى

Group	Mean ±S.D معدل الـMg (µg/dL)	T -test
Control	1.78 ±1.10	
DM1	0.73 ±0.48	P < 0.0001
DM2	0.85 ±0.49	P < 0.0001

A,B كما في جدول رقم (1)

جدول -3 : يوضح المعدل والانحراف المعياري لمستوى المالون ثنائي الالدهايد (MDA) في مصل دم مجموعة السيطرة ومجاميع المرضى

Group	Mean ±S.D MDA (نانومول/100مل)	T -test
Control	10.78 ± 0.48	
DM1	29.5 ± 4.8	P < 0.001
DM2	11.62 ± 0.98	P < 0.05

A,B كما في جدول رقم (1)

جدول -4 : يحدد معدل الانحراف القياسي والمعدل ومستوى الدلالة لتركيز فيتامين (C) في مصل دم مجموعة السيطرة ومجاميع المرضى

Group	Mean ±S.D (mg/dL) (Vit-C)	T -test
Control	1.98±0.98	
DM1	0.78± 0.42	P < 0.001
DM2	0.84± 0. 21	P < 0.001

A,B كما في جدول رقم (1)

جدول -5 : يحدد معدل الانحراف القياسي والمعدل ومستوى الدلالة لتركيز فيتامين (E) في مصل دم مجموعة السيطرة ومجاميع المرضى

Group	Mean ±S.D (mg/dL) (Vit-E)	T -test
Control	1.24+0.16	
DM1	0.91+1.40	P < 0.01
DM2	0.72+5.40	P < 0.001

A,B كما في جدول رقم (1)

جدول –6 : يحدد معدل الانحراف القياسي والمعدل ومستوى الدلالة لتركيز فيتامين (A) في مصل دم مجموعة السيطرة ومجاميع المرضى

Group	Mean ±S.D (mg/dL) (Vit-A)	T -test
Control	69.8±10.2	
DM1	40.4± 11.5	P < 0.01
DM2	31.25± 12.5	P < 0.001

A,B كما في جدول رقم (1)

المصادر

1- Selvin E, Steffes MW, Zhu H *et al* "Glycated hemoglobin, diabetes, and cardiovascular risk in nondiabetic adults". *N. Engl. J. Med.* **362** (9): 800–11 (2010).

2- Stewart WF, Ricci JA, Chee E, Hirsch AG, Brandenburg NA "Lost productive time and costs due to diabetes and diabetic neuropathic pain in the US workforce". *J. Occup. Environ. Med.* **49** (6): 672–9 (2007).

3- Davidson, M. B. Diagnosis and Classification of Diabetes Mellitus. In "Diabetes Mellitus Diagnosis and Treatment". 4th Edition. W. B. Saunders Company. P. 1 – 6(1998).

4- Belfiore, F. and Iannello, S. Etiological, Classification, Path physiology and Diagnosis. In "New Concepts in Diabetes and It's Treatment". Belfiore, F. and Mogensen,C. E. (Eds.). Karger Company.1– 6(2000) .

5- Cardell, B. S.. The Pancreas. In "Systemic Pathology". Symmers, W. St C. (Eds.). P. 1332(1978).

6- Willims, G. and Pickup, J. C. Diagnosis and Classification of Diabetes Mellitus. In "Hand Book of Diabetes". 1ed Edition. Blackwell Science Publication. P. 1 – 3(1992).

7- Hadden,D.V. Diabetes in Pregnancy: Past, Present and Future. In"Diabetes and Pregnancy an International Approach to Diagnosis and Management". Dornhorst,A. and Hadden,D.R.(Eds.) John Wiley &Son's Company. P. 3(1996).

8- درويش. علي بسام. "السكري يزيد من إمراض الأوعية الدموية". المجلة الطبية العربية. 1، 2- 5 (2002).

9- Edwards, G. R. Baird, J. D., Frier, B. M., Spephard, J. and Toft, A. D.. Endocrine and Metabolic disease. In "Davidson's Principles and Practice of Medicine". Edwards, C. R., Boucheir, I. A. and Chilvers, E. R. (Eds.). P. 724.

10- Jacques, V. and Rita, C. (1989). "Trace Element in Human Plasma or Serum". CRC Press. P. 37 – 135(1995).

11- Spelch,M., Bousquet, B. and Nicolas, G.. Clin. Chem. 26, 1462 – 1465(1980).

12- جعفر هاشم "دراسة تأثير التسمم بالرصاص على فيتأمينات الجسم والاكسدة الفوقية للدهون (2009) CSASC. Ar.v,vol(4) p79-84

13- حنان فاضل "دراسة تأثيرالتلوث بالزئبق على مضادات التأكسد لدى اطباء الاسنان" CSASC.Ar.v,vol(5)p363(2010)

14- Rohan , T. E.; Howe, G. R.; Friedenreich, C. M.; Jain, M. & Miller, A. B. Dietary fiber, vitamins A, C and E and risk of breast cancer: a cohort study, Cancer Causes and Control, 4 :29-37 (1993)

15- Watson, W. H.; Cai, J. & Jones, D. P Diet and apoptosis. Annual Reviews. org., 20 :485-505. (2000).

16- Lee, I. M. Antioxidant vitamins in the prevention of cancer. Proc. Assoc. Am. Physicians, 111 :10-15 (1999) .

17- Forman, D. and Vye, M.. Clin. Chem. 26, 145 – 147.

18- Maher, J. T. (1998). North India. J. AmColl. Nutr. 17, 564 – 570(1980).

19- Zagar, A. H., Bashir, M. I., Laway, B. A. and Wani, A. I.. EXP – Clin – Endocrinal – Diabetes. 108, 397 – 400 (2000).

20- Mure,K.& Rossman,T.G. Reduction of spontaneous mutagenesis in mismatch repair-deficient and proficient cells by dietary antioxidants. Mut. Res. Fund. and Mol. Mechanisms Mutagenesis, 480 :85-95 (2001) .

21- Rohan , T. E.; Howe, G. R.; Friedenreich, C. M.; Jain, M. & Miller, A. B. Dietary fiber, vitamins A, C and E and risk of breast cancer: a cohort study, Cancer Causes and Control, 4 :29-37 (1993) .

22- Watson, W. H.; Cai, J. & Jones, D. P. Diet and apoptosis. Annual Reviews. org., 20 :485-505 (2000) .

23- Lee, I. M. Antioxidant vitamins in the prevention of cancer. Proc. Assoc. Am. Physicians, 111 :10-15 (1999) .

24- Hughes, D. A. Dietary carotenoids and human immune function. Nutrition, 1 :823-827 (2001) .

25- Lyons, N. M.; Woods, J. A. & Obrien, N. M. Alfa–tocopherol but not gama–tocopherol inhibits 7-beta–hydroxy cholesterol induced apoptosis in human U937cell. Free Rad. Res., 5 :329-339 (2001) .

26- Bramley, P. M.; Elmadfa, I.; Kafatos, A.; Kelly, F. J.; Manios, Y.; Oxborough, H. E.; Schuch, W.; Sheehy, P. J. A. & Wgner, K. H. Vitamin E. J. Sci. Food Agric., 80 :913-938 (2000) .

27- Moller,P.&Loft,S Oxidative DNA damage in human white blood cells in dietary antioxidant intervention studies.Am.J.Clin.Nutr.76:303-310 (2000) .

28- Meydani, S. N. ; Meydani, M. & Blumberg, J. B. (1997) Vitamin E supplementation and in vivo immune response in healthy elderly subjects. JAMA, 277:1380-1386 (2002).

29- Asmis,R.& Jelk,J. Vitamin E supplementation of human macrophages prevents neither foam cell formation nor increased susceptibilityof foam cells to lysis by oxidized LDL.,Vasc.Biol.20:990-997 (2000) .

30- Hughes, D. A. Dietary antioxidants and human immune function. British nutrition foundation Nutrition Bulletin , 25 :35-41 (2000).

31- Kandarkar, S. V. & Sawant, S. S. The effect of vitamin C on the hamster cheek pouch treated with the water soluble carcinogen 4-nitroquinoline-1-oxide (4NQO). Oral Oncol. Eur.J. Cancer.,32B:230-237 (1996) .

32- Palozza, P. ; Serini, S. ; Torsello, A. ; Dinicuolo, F. ; Piccioni, E. ; Ubaldi, V. ; Pioli, C. ; Wolf, F. I. & Calviello, G. Beta-carotene regulates NF-Kappa-B-DNA-binding activity by a redox mechanism in human leukemia and colon adenocarcinoma cells. J. Nutr., 133: 381-388 (2003).

دراسة تأثير فيتامينات الجسم في دم مرضى التهاب المفاصل الرثوي

حنان فاضل عباس

وزارة العلوم والتكنولوجيا

تاريخ تقديم البحث : 2011/ 3/30 تاريخ قبول البحث : 2011/ 5/29

ABSTRACT

This study shed light on the damage caused by varieties of oxygen effective from free radicals and generating free radicals in patients with rheumatoid arthritis The study was included (50 patients)-grade inflammation of rheumatoid arthritis and (30) healthy volunteers as a control was measured by the rate of oxidation meta-fat as much as it formed of Malondialdehyde (MDA) it noticed an incresed in MDA level to (39.8nmol \ 100ml) for males (48.3nmol \ 100ml) in females as compared with the control group, (13.2 nmol \ 100ml) also a non-enzymatic defense systems such as vitamins (A, C, E) were measured by using the HPLC technique .The study showed a decreased in the concentration of vitamins for patients of both sexes as compared with the control group.

الخلاصة

اهتمت الدراسة بإلقاء الضوء على الضرر الذي تسببه أصناف الأوكسجين الفعال من الجذور الحرة والمولدة للجذور الحرة عند مرضى التهاب المفاصل الرثوى شملت الدراسة (50) مريضا مشخصا بالتهاب المفاصل الرثوي و (30) متطوعا من الأصحاء كمجموعة سيطرة تم قياس معدل الأكسدة الفوقية للدهون بمقدار ما يتكون من المالون داي الديهايد (MDA) وقد لوحظ الارتفاع الكبير في مستوى الـ (MDA) حيث بلغ (39.8nmol\100ml) للذكور (48.3nmol\100ml)عند الإناث مقارنة مع مجموعة السيطرة التي بلغ فيها مستوى أل (13.2nmol\100ml) (MDA) كذلك تم قياس بعض الأنظمة الدفاعية غير الإنزيمية مثل فيتامينات (A,C,E) باستخدام تقنية HPLC وأظهرت الدراسة النقص الحاصل في تركيز فيتامينات الجسم عند المرضى لكلا الجنسين مقارنة مع مجموعة السيطرة .

ان الهدف من هذه الدراسة هو

1- تسليط الضوء على مستويات الاكسدة الفوقية للدهون عن طريق قياس مستويات المالون داي الديهايد (MDA) في مصل دم مرضى التهاب المفاصل الرثوي ومقارنته بالاصحاء

2- تقدير مستويات بعض مضادات الاكسدة مثل (vitamins A, C, E) المهمة في حماية جسم الكائن الحي من الضرر التاكسدي

المقدمة

أن مرض التهاب المفاصل الرثوي RA من الامراض الالتهابيه المتسببه عن الجذور الحرة (1)و (2) وهو الذي تنظر الحالة فيه الى التلف او العجز الكلي للمفصل وهناك بعض الملامح قد تحدث منها تكوين عقد صغيرة روماتزمية ,التهاب شرياني ,اختلال عصبي ,التهاب الصلبة والتهاب التامور واعتلال الغدد اللمفاوية وضخامة الطحال (3) ان مرض التهاب المفاصل الرثوي من الامراض التي يمكن ان تصيب الانسان في جميع الاعمار وان المرض يمكن ان يصيب النساء اكثر من الرجال بنسبة (4) 1:3 أن أعلى احتمالية لحدوث المرض عند النساء في عمر 40-60 سنة . (5)

ومن الممكن أن يصيب أي مفصل زلالي الا ان مفاصل اليدين والقدمين هي التي تصاب في معظم الاحيان وتكون الاصابة في حالات كثيرة بصورة متناظرة على جانبي المفصل (6) وقد يتطور المرض ويصيب اكثر من مفصل واحد مثل المفصل الصدغي الفلكي . ومفصل العمود الفقري الرقبي مما تؤدي الاصابة الى تلف في العمود الفقري ومضاعفات عصبية . (7)

تبدو المفاصل في معظم المرضى في الدور الحاد والمبكر متورمه ومؤلمه ومتشنجه وتتطور الحالة خلال فترات زمنية قد تصل الى اسابيع او شهور مع الم حاد وتشنج وصعوبة في الحركة وبعض اعراض الالتهاب وتظهر بعض العقد الروماتزمية (8)تصاحبه في احيان كثيرة توعك شامل وتعب او فقر دم وقد تحدث نوبات مؤلمة وحادة ولفترة زمنية طويلة ولاسيما في الصباح وتزداد هذه النوبات مع شدة المرض وبغض النظر عن زمن الاصابة . (9)

هنالك أنواع متعددة من مضادات الاكسده التي تعمل كاسحات المركبات الاوكسجينية ROSاعتمادا على تركيبها ومن امثلتها حامض الاسكوربك فيتامين cالذي يعد اقدم مضادات الاكسده المعروفة ومن اشدها فعالية واقلها سمية .

ان فيتامين C (Ascorbic acid) قد قيست مستوياته في مرض التهاب المفاصل الرثوي RAووجد ان هناك انخفاضا معنويا في مستوياته في المفصل والسوائل المفصلية للمرضى وهذه عادة تتناسب عكسيا بزيادة قيم الاكسدة الفوقية للدهون وعلى الرغم من ان فيتامين (C)من الفيتامينات الذائبة في الماء فاهميته تاتي من ناحية الحفاظ على فيتامين (E) بشكله الفعال المختزل (10) كما وجد بعض الباحثين الذين درسوا التركيز والحالة التاكسدية للاسكور بيت ان قيمته اقل بكثير عند المرضى منه في الاصحاء لان معظم الاسكوربيت وجد على شكل مؤكسد(11).

أن فيتامين (E) من اهم مضادات الاكسدة بصورة عامة ومن اهمها في مرض ال RA

كونه من الفيتامينات الذائبة في الدهون وقد يكون الوحيد الذي يعمل في محيط لا قطبي والمتمثل بالطبقة الدهنية الثنائية في الاغشية الخلوية التي تكون الهدف الرئيسي للضرر الذي يسببه ال ROC)فلقد درس فيتامين (E) من ناحية تثبيطه للانزيمات المحللة للدهون A2 phosphose lipase (12) وكذلك من ناحية تثبيطه للاكسدة الفوقية للدهون على حيونات مختبرية . (13)

وعند قياس تركيز الالفا توكوفيرول في مصل دم مرضى التهاب المفاصل الرثوي وجد ان هناك انخفاضا كبيرا في مستوياته عنه في الاصحاء (14, 15)،واجرى باحثون اخرون تجاربهم على مرضى التهاب المفاصل الرثوي فوجدوا ان فيتامين (E) هو احد المصادر الطبيعية لمضادات الاكسدة الذائبة في الدهون وقد اثبتوا ذلك بالدراسات على المرضى من كلا الجنسين و خرجوا الى التوصية باعطاء فيتامين (E) تكون نحو عشرة اضعاف الحصة المسموح بها يوميا او لثلاث اسابيع فاكثر وقد اعطت هذه الدراسة نتائج مرضية ومن دون اي مضاعفات (16) كما درس الباحث(17) (1997),.miehie,w ميكانيكية عمل فيتامين (E) في مرضى التهاب المفاصل وادت الدراسة الى اعطاء فيتامين E))كعلاج وبحسب النتائج بالدراسة العشوائية فوجد ان فيتامين (E) يقلل من ال ROCويحسن من حالة المرضى ويقلل من الالم والالتهاب بنسبة تقارب العلاجات غير الستيرويدية التي تعطى كعلاج مضاد الى الالتهابات وبفعالية افضل كما قاس باحثون اخرون مستويات فيتامين (E) في كلا الجنسين من مرضى التهاب المفاصل الرثوي ووجد ان هناك نقصا قد يكون تاما في فيتامين (E) في مصل الدم لمرضى ال RA لكلا الجنسين . (18)

المواد وطرائق العمل

1- طريقة تقدير مستوى الاكسدة في مصل الدم تتم بقياس مقدار مايتكون من MDAالمالون ثنائي الالديهايد وهو من النواتج الثانوية للاكسدة الفوقية للدهون لذا فان قياس هذه المادة يعطي انطباعا عن مستوى الاكسدة واستخدمت طريقة لونية تعتمد على التفاعل بين مركب حامض الثايو بار بتيورك والمالون ثنائي الالديهايد ليعطي مركبا لونيا اعلى امتصاصية له في 532 نانومتر. (19)

2- قياس فيتامين (A,C,E) في مصل الدم بتقنية HPLC

تم قياس فيتامين Eباستخدام الطريقة المحوره من (Deleen heer) حيث تم تحضيرمحلول مانع الاكسدة والمحلول القياسي باستخدام طور متحرك (99%) ميثانول (1 %) ماء مقطر بطول موجي , nm287 نوع العمود C-18 (ODS) .

اما فيتامين C فقط استخدم الطور المتحرك باذابة صوديوم اسيتيت و (EDTA) في الماءالمقطر وبضبط pH عند 6 وثبت الطول الموجي عند nm254 وباستخدام نفس العمود كذلك فيتامين Aاستخدم الطور المتحرك (99%) ميثانول (1%)ماء مقطر بطول موجي nm 330 وبنفس العمود . (20)

النتائج والمناقشة

يبين لنا الجدول (1) إن هنالك زيادة في معدل مستويات الأكسدة الفوقية للدهون لمجاميع الدراسة مقارنة بمجموعة السيطرة .إذ استطاع الباحثون (21) تفسير ميكانيكية الزيادة في معدل الأكسدة الفوقية للدهون بسبب ارتفاع في مستويات الـ (ROS)وهي مولدات للجذور الحرة وسوف يحصل زيادة في التلف الحاصل في الخلايا ويسرع من عملية انتقال الإلكترونات والأكسدة الفوقية للدهون في الأنسجة البيولوجية داخل الخلية الحية .وإن هذه النتائج تتفق مع الباحث Tarazaوجماعته (22) (1997).

وعند زيادة هذه الأكسدة فان الجذور الحرة المتولدة والمتزايدة تؤدي إلى التلف الكثير للأغشية الخلوية والنهايات العصبية في الدماغ (23). أن عملية الأكسدة الفوقية للدهون هي ظاهرة طبيعية تحدث بصورة مستمرة وبمعدلات قليلة عند جميع الأشخاص ومن نتائج هذه العملية هو أنتاج نواتج الديهايدية وحوامض شحميه حرة والمالون ثنائي الالدهايد MDA الذي تم قياسه في هذه الدراسة يعد كدليل كيموحيوي لعملية الأكسدة في الدهون (24).

جدول –1: يوضح المعدل والانحراف المعياري لمستوى المالون ثنائي الالدهايد (MDA) في مصل دم مجاميع الدراسة الثلاثة

المجاميع	العدد	MDA (نانومول100/مل) Mean ±S.D	T
A	30	13.2±0.48	
B	50	39.8±5.25	P<0.001
C	50	48.3±0.85	P>0.05

A : مجموعة السيطرة من الأصحاء

B : مجموعة المرضى الذكور

C : مجموعة المرضى الإناث

يبين جدول (2) انخفاض في مستوى تركيز فيتامين (C) بالنسبة للمرضى مقارنة مع قيم السيطرة. على الرغم من أن فيتامين (C) من الفيتامينات الذائبة في الماء فأهميته تأتي من ناحية الحفاظ على فيتامين (E) بشكله الفعال المختزل (25) كما وجد بعض الباحثين (26)

الذين درسوا التركيز والحالة التاكسدية للاسكوربيت أن قيمته اقل بكثير عند المرضى منه في الأصحاء لان معظم للاسكوربيت وجد على شكل مؤكسد.

جدول -2: يحدد معدل الانحراف القياسي والمعدل ومستوى الدلالة لتركيز فيتامين (C) عند المجاميع الثلاثة .

المجاميع	العدد	Mean ±S.D (Vit-C) (mg/dL)	T
A	60	1.98±0.98	---
B	50	30.8±0.42	P<0.001
C	50	0. 0.91±0.21	P<0.001

A,B,C كما في جدول 1

أوضحت النتائج بان للفيتامينات A و C و E تأثيرات مختلفة في الجهازين المناعي والوراثي . وهذا يفسر في ضوء كون هذه الفيتامينات هي من مضادات الأكسدة (Anti-oxidants)(27) وان المؤكسدات (Oxidants)من العوامل المؤثرة في فعالية الجهاز المناعي وباتجاه تثبيط وظائفه .(28).

تشير الدراسات بان فيتامين C يؤثر في معظم جوانب وظائف الجهاز المناعي، وان انخفاضه يؤثر في وظيفة هذه الخلايا .(29)حيث اقترح بان هذا الفيتامين يوفر الحماية لدهون البلازما (Plasma lipids) ودهون الأغشية الخلوية (Membrane lipids) من فعل المؤكسدات من خلال ثلاث آليات :التداخل في بناء نيوكلوتيدات الخلية وبناء البروستوكلاندينات (Prostglandins) لطورالى دفوع السايتوكيتات ويعزز إنتاج البروتينات الخلوية (Cytokines) (30).أن آلاليات الأنفة الذكر تدخل ضمن المحصلة العامة لفعالية الجهاز المناعي وإذا كان فيتامين C مشمولا فيها فهذا يفسر النتائج الايجابية التي أشارت إليها الدراسة الحالية، لكن يبقى مجال البحث مفتوحا لدراسة الآلية أو الآليات التي من خلالها يعمل فيتامين C على تعزيز فعالية الجهاز المناعي .

يبين جدول (3)انخفاض في مستوى تركيز فيتامين (E) بالنسبة للمرضى مقارنة مع قيم السيطرة

جدول -3 : معدل الانحراف القياسي والمعدل ومستوى الدلالة لتركيز فيتامين (E) عند المجاميع الثلاثة.

المجاميع	العدد	Mean ±S.D (Vit-E) (mg/dL)	T
A	60	0.16 ± 1.24	---
B	50	1.40 ± 0.872	P<0.01
C	50	5.80 ± 0.751	P<0.001

A,B,C كما في جدول 1

تؤكد أهميته في المحافظة على وظيفة الجهاز المناعي، وهو الأخر من مضادات الأكسدة .(31) حيث وجد بأنه من مضادات الأكسدة الذائبة في دهون غشاء الخلية والذي قد يتأثر بالمؤكسدات(32). لقد تم التوصل لهذا الاستنتاج من خلال دراسات حالات نقص فيتامين E، حيث وجد بأنها تتصاحب مع انخفاض في إنتاج الأضداد من الخلايا اللمفاوية (33).

لذلك وجد علاقة عكسية مابين مستوى فيتامين Eفي الدم والإصابة بالبكتريا في الأشخاص المسنين، وان إعطائهم جرع من فيتامين Eساهم في تحسين فعالية الجهاز المناعي في القضاء على هذه الإصابات (34)إما آلية تأثير هذا الفيتامين في الجهاز المناعي، فقد اقترح بأنه يعمل على تثبيط احد عوامل الاستنساخ (Transcription factor)والمسمى NF-KB، حيث انه يعد عاملا مؤثرا في إنتاج الخلايا للـ Interlukin-1 (35) .

يبين جدول (4)انخفاض في مستوى تركيز فيتامين (A)بالنسبة للمرضى مقارنة مع قيم السيطرة

جدول -4: يحدد معدل الانحراف القياسي والمعدل ومستوى الدلالة لتركيز فيتامين (A) عند المجاميع الثلاثة.

المجاميع	العدد	Mean±S.D (Vit-A) (mg/dL)	T
A	60	69.8±10.2	---
B	50	44.6±11.8	P<0.01
C	50	35.50±15.3	P<0.001

A,B,C كما في جدول 1

فقد لوحظ فيتامين A بأنه يمتلك القابلية على التحفيز المناعي إلا أن الدراسات في هذا المجال كانت على الأشخاص المسنين والتي أوضحت بان فيتامين Aيعمل على تعزيز فعالية الجهاز المناعي ومن خلال تأثيره في الخلايا اللمفاوية التائية المساعدة (CD4+ Cell) ومستلمات (Interlukin-2) على سطح الخلايا وكذلك الخلايا القاتلة الطبيعية Natural killer cellsإضافة إلى ذلك فقد لوحظ علاقة ايجابية مابين مستوى فيتامين Aفي مجرى الدم وعدد خلايا وحيدة النوى .(36) والتي عادة ماتكون مستحثة بالملوثات البيئية التي يتعرض لها الإنسان خصوصا في العراق وعلى مدى العقدين الماضيين لذلك هل يمكن تحصين الإنسان بهذه الفيتامينات ضد الإصابة بالسرطان .لقد تناولت العديد من الدراسات هذا الموضوع وتكاد تتفق مع بعضها البعض في مقدمة واحدة هي كونه (37) تعمل هذه الفيتامينات على حماية الكائن فقد تمت الإشارة فيها إلى إن الفيتامينات Aو Cو E هي من مضادات الأكسدة .وعند العودة إلى فعالية الجهاز المناعي نجد إن خلايا الدم البيض لاسيما الخلايا البلعمية تسيطر على الإصابات الفيروسية والبكتيرية والطفيلية من خلال تحطيمها كيميائيا بعض المؤكسدات مثل NOو O_2و H_2O_2، أن هذه المؤكسدات تحمي الكائن الحي من الهلاك نتيجة الإصابة، إلا أنها يمكن أن تحدث ضرراً (Damage) للمادة الوراثية يتمثل بحصول طفرة وراثية (Genetic Mutation)، ويمكن أن تساهم هذه الطفرة)أو الطفرات (في عملية تسرطن الخلية، إلا أن وجود مضادات الأكسدة)مثل الفيتامينات (يساهم في منع ذلك (38)ان تولد وتكون ، وان هذه الجذور يمكن أن تتكون داخل الجسم بفعل المطفرات البيئية والتي لها القابلية على إحداث الضرر في (DNA)و (RNA) في الخلايا، كما تعمل أيضا على تثبيط بعض الإنزيمات من التفاعل مع الأحماض الأمينية .

وفي هذا الصدد افترضت آليات حياتية والتي تدعم بان الفيتامينات Aو Cو E يمكن أن تقلل من الطفرة الوراثية وبالتالي يمكن أن تقلل تسرطن الخلايا .حيث لوحظ بان فيتامين A يمنع الضرر في دنا الخلية المستحث بالجذور الحرة من خلال التداخل مع عملية ايض المطفرات الكيميائية إضافة إلى ذلك فان فيتامين A له تأثيرات مباشرة على نمو (Growth) وتمايز (Differentiation)الخلايا الظهارية ((Epithelial cells، وبالتالي فهو قد يعمل مضاد لمراحل التظفير الوراثي (Antagonist) أما في مجال التسرطن، فان الفيتامين يعمل على تعزيز الترابط الخلوي (Gap-junction communication)، وان مثل هذا التعزيز يقلل من التوسع الاستنسالي (Clonal expansion)وبالتالي يمنع التسرطن .(39).

أما فيتامين E، فهذا يمنع تكون المسرطنات (Carcinogens) مثل nitrosamines إضافة إلى قدرته في تعزيز المناعة الخلطية والخلوية وبالتالي يمكن أن يحطم الخلايا المتسرطنة ويشاركه في الفعل فيتامين Cوالذي يقوم باصطياد الجذور الحرة (Scavenge free

radicals). أن نتائج الدراسة الحالية تدعم ماتقدم خصوصا أذا ما آخذنا بنظر الاعتبار الفعل التازري لهذه الفيتامينات .

مما سبق نستنتج ما يأتي :

1- تكون الاكسدة الفوقية للدهون سببا في الامراض الالتهابية ولاسيما مرض التهاب المفاصل الرثوي .

2- ان مستوى الMDA) في مصل دم المرضى قد يكون مؤشرا الى المرض في مراحله المبكرة .

3- ان قياس بعض مستويات الاكسدة مثل فيتامينات (A, C, E) والنقص فيها قد يفسر التلف الحاصل في المفاصل.

ونوصي بما يلي :

1- تجربة اعطاء مرضى التهاب المفاصل الرثوي اطعمة غنية أو مدعمة بالفيتامينات وعنصر السيلينيوم , كذلك تناول الكمية الموصى بها من الاغذية الحاوية على الخارصين ون ثم اجراء التحاليل الخاصة بالمرضى لمعرفة مدى تحسن الحاله المرضية وقلة التشنجات الصباحية.

2- تحديد النسب المتناولة من الزيوت الحاوية على حوامض شحمية غير مشبعة عند مرضى التهاب المفاصل الرثوي.

المصادر

1- Aasetha J., Haugen, M., Forre,O. (1998) Analyst. 123(1): 3-6.

2- AL- Rawi, Z.S., AL-Azzawi, A.J., AL-Ajili. F.M., and AL- Wakil, R. Ann. Rheu. Dis. 37,73 (1978) .

3- Sliarnia, RJ. (I 983)Agents & Actions 13: 380—387.

4- Buchanan, W.W., & Dick,W.C. "Recent Advances in Rheumato1orv". Chrchill Living stone Inc (1981).

5- Mason, M.,& Currey, H.L.F. "An introduction to clinical rheumatology". 2'. ed., Pitman Medical (1975).

6- AL- Rawi, Z.S., AL-Azzawi, A.J., AL-Ajili. F.M., and AL- Wakil, R. Ann. Rheu. Dis. 37,73 (1978) .

7- Beeson,P.B & Mederrnott,W.M.D., "Text Book of Medicine" 30th

ed. W.B.Saunders Company Philadelphia - London Toronto. 1884-1885(1971).

8- Duthie, J. J. R. Ann. Rheum. Dis. 23, 193 (1964).

9- Hart, F.D. Br. Med.J.3: 131(1969) .

10- Rowley, D.A. (3ufleride, J.M.C, Blacke, D.R., Farr, M. & Ilalliwell, 13., (un Sd 66:691-695(1984).

11- Frel, B., Stocker, R. & Ames, B. N. Proc. Nati. Acad. Sci USA, 85, 9748(1988).

12- Douglas, Ch. E, Chan, A. C. & Choy, C.P.,: Biochim. Biophys. Acta 876,639-645(1986).

13- Hailer,S., Adam, P., Lemmcn, Ch. & Adam,0., Fat Sd. Technol. 10: 384-387(1993) .

14- Comstock, G.W., Burke, A.E., Hoffman, S.C., Helzlsouer, K.J., Bendich, A., Masi, A. T., Norkus, E. P., Malamet, R. L., & Gershwin, M.E., Ann- Rheum — Dis. 56 (5): 323-325(1997).

15- Hansen, G.V., Nielsen,L., Kluger,E.: Thysen, M., Emmertsen,H., _J Stengaard-Pedersen,K., Hansen.E.L., Unger, B., & Andersen, P.W. Scand. J., Rheumatol.: 25(5): 325-330 (1996) .

16- Edmonds, S. E., Winyard, P. G., Guo. R, Kidd, B., Langrish,M.P. Smith, A., Hansen, C., Ramm, S.,& Blake, D. R., Ann-RheumDis. 56(11):649-655(1997).

17- Miehie, W., Fortschr- Med. 20:115 (26): 39-42(1997).

18- Honkanen, V., Konttinen, Y. T., Sorsa, T., Hukkanen, M., Kemppinen, P., Santavirta, S. & Saari, H. J.Trace Elem. Electrolytes Health Dis 2:26] .(1991).

19- Chow,F. and Omaye,S. Lipids.]:837(1983).

20- Rose,R. and Nohiwold,DAnal. Biochem. 114:140-145.(1981).

21- Badger, A.M., Hanldler, J. A., Genell. C.A., Herzyk, D., gore, E., polsky, R., Webb, L. & bugelski, P.J., INT. J. Immuno. Pharmacol., 21:161(1999).

22- Taraza, C., Mohra, M., Vargolici, B., Dinu, V., Rom. J., Intern. Med., 35:89(1997).

23- Strubelt-O., Kremer- J, Tilse-A., Keogh- J, Pentz-R., Younes- M (1996) J. Toxicol – Environ-Health. Feb.23: 47(3): 267-83.

24- Nakai, A., Oya, A., Kobe, H.: J. Nippon Med Sch.; 67(6): 434-439, (2000).

25- Mure,K.&Rossman,T.G.Reduction of spontaneous mutagenesis in mismatch repair-deficient and proficient cells by dietary antioxidants. Mut. Res. Fund. and Mol. Mechanisms Mutagenesis, 480 :85-95(2001) .

26- Hughes, D. A. Dietary antioxidants and human immune function. British nutrition foundation Nutrition Bulletin , 25 :35-41(2000).

27- Rohan , T. E.; Howe, G. R.; Friedenreich, C. M.; Jain, M. & Miller, A. B. Dietary fiber, vitamins A, C and E and risk of breast cancer: a cohort study, Cancer Causes and Control, 4 :29-37(1993) .

28- Watson, W. H.; Cai, J. & Jones, D. P. Diet and apoptosis. Annual Reviews. org., 20 :485-505(2000) .

29- Lee, I. M. (1999) Antioxidant vitamins in the prevention of cancer. Proc. Assoc. Am. Physicians, 111 :10-15

30- Hughes, D. A. Dietary carotenoids and human immune function. Nutrition, 1 :823-827(2001) .

31- Lyons, N. M.; Woods, J. A. & Obrien, N. M. Alfa–tocopherol but not gama–tocopherol inhibits 7-beta–hydroxy cholesterol induced apoptosis in human U937cell. Free Rad. Res., 5 :329-339(2001) .

32- Bramley, P. M.; Elmadfa, I.; Kafatos, A.; Kelly, F. J.; Manios, Y.; Oxborough, H. E.; Schuch, W.; Sheehy, P. J. A. & Wgner, K. H. Vitamin E. J. Sci. Food Agric., 80 :913-938(2000) .

33- Moller, P. & Loft, S. Oxidative DNA damage in human white blood

cells in dietary antioxidant intervention studies. Am. J. Clin. Nutr. 76: 303-310(2002) .

34- محسن ,جعفر هاشم "دراسة تاثير التسمم بالرصاص على فيتامينات الجسم والاكسده الفوقيه للدهون. (2009) 97-91.p.4 ,vol.,CSASC Ar.v "

35- Asmis,R. & Jelk, J. Vitamin E supplementation of human macrophages prevents neither foam cell formation nor increased susceptibility of foam cells to lysis by oxidized LDL., Vasc. Biol. 20: 990-997(2000) .

36- Hughes, D. A. (2000) Dietary antioxidants and human immune function. **British nutrition foundation Nutrition Bulletin , 25 :35-41.**

37- محسن ,جعفر هاشم "الزيادة الحاصلة في الأكسدة الفوقية للدهون وعلاقتها بفيتامين أ والسيلينيوم نتيجة التلوث بالرصاص" International Journal for Sciences and Technology Vol.5, No. 1 pp.91-99(2010).

38- Mure, K. &Rossman,T. G. Reduction of spontaneous mutagenesis in mismatch repair-deficient and proficient cells by dietary antioxidants. Mut. Res. Fund. and Mol. Mechanisms Mutagenesis, 480 :85-95(2001).

39- Palozza, P.; Serini, S ; Torsello, A.; Dinicuolo, F.; Piccioni, E.; Ubaldi, V. ; Pioli, C. ;Wolf, F. I. & Calviello, G. Beta-carotene regulates NF-Kappa-B-DNA-binding activity by a redox mechanism in human leukemia and colon adenocarcinoma cells. J. Nutr., 133: 381-388(2003).

دراسة المكونات الكيميائية لمستخلصات جذور الراوند وتأثيرها على نمو بعض الاحياء الدقيقة

منال صادق حمودي

قسم الكيمياء / كلية العلوم

تاريخ تقديم البحث : 2011/ 4/18 تاريخ قبول البحث : 2011/ 5/29

ABSTRACT

This study included chemical constituents of aqueous and alcohol extracts of Rhubarb roots (**Rheum palmatum**), the aqueous extracts contains glycosides ,saponines, (a lot off in hot extract), phenolic compounds, flavonoids and tannins, no proteins was detected. Ethanolic extract have no saponines ,flavonoids , and proteins. It also examined inhibition ratio of S.GOT enzyme for the three types of Rhubarb root extracts showed(2.08 %),(3,38 %) ,and (4.47 %) for cold ,hot aqueus and alcoholic extracts respectively. The study included the influence extracts of Rhubarb root on different types of microorganisms, it was noted that the concentrations of (50,100) mg /ml have inhibition of intended microorganisms specifically ***Staphelocous aureus*** bacteria.

الخلاصة

تم في هذه الدراسة الكشف عن المجاميع الفعالة في المستخلصات المائية والكحولية لجذور نبات الراوند **Rheum palmatum** ، حيث احتوى المستخلص المائي الكلايكوسيدات و الصابونينات (المستخلص الساخن بكمية اكبر) و الفلافونيدات و المركبات الفينولية والتانينات وعدم احتواءه على البروتينات ، اما المستخلص الكحولي لم يحتوي على الصابونينات و الفلافونيدات و البروتينات ، وتم قياس نسبة التثبيط لانزيم S.(GOT) حيث كانت (2.08 %) للمستخلص المائي البارد و(3.38 %) للمستخلص الساخن و(4.47 %) للمستخلص الكحولي .

تم دراسة تأثير المستخلصات المائية والكحولية لجذورنبات الراوند على انواع مختلفة من الاحياء الدقيقة ، حيث لوحظ ان التركيز (100,50) ملغم / مل له تأثير على نمو الاحياء الدقيقة المستخدمة وتحديداً عند البكتريا Staphylococcus aureus .

المقدمة

الراوند الطبي (الكفي) يعرف علمياً بأسم **Rheum palmatum** والموطن الاصلي للنبات هو الصين وله عدة اصناف كالراوند الهندي R.tanguticum والراوند المخزني R.officinall، ولهما استخدامات طبية مماثلة للراوند الكفي، اما الراوند الذكر R.rhaponticum فيستخدم كمادة غذائية .(1).

والراوند نبتة عشبية معمرة من فصيلة polygonaceae لها اوراق راحية ومسننة يصل ارتفاعها ال مترين ونصف المتر ، عنق الورقة شحمي والازهار من نوع وحيدة الجنس تكون بشكل سنابل كثيفة بيضاء ، وله جذر سميك زاحف يتشعب الى عدة فروع و سيقانه مستديرة ومتشعبة ومجوفة .(1,2).

ان الجزء المستخدم من النبات هو الجذور الارضية وسيقان النبات واعناق الاوراق، تحتوي جذور الراوند الطبي على العديد من المركبات الفعالة كالكلايكوسيدات الانثراكوينونية بنسبة (3-5 %) و منها الرين (Rhein) وألوايمودين (Aloe-emodin) و الآيمودين (Emodin)، كما يحتوي على الفلافونيدات و اهمها الكاتيكين (Catechin) ، والكريسوفارمول (Chrysopharmol) والسينوسايد (Sennosides) وحامض الجاليك (Gallic acid) و حامض السنامنيك (Cinnaminic acid) و احماض فينولية و مواد عفصية (حامض التانيك 3-5 %) و كذلك فيتامين A ,B ,C و اوكزالات الكالسيوم ، ان الاهمية الدوائية لجذور الراوند تكمن في الآنثراكوينيونات (لها خصائص ملينة ومطهرة) ، فهي ملين قوي عند تناوله بجرعات كبيرة غير ان حامض التانيك يعاكس توازن المفعول الملين حيث يعمل ممسكاً عند تناوله بجرعات صغيرة . (1, 3) ، كما ان لمستخلصات الجذور تأثير فعال ضد البكتريا العنقودية الذهبية ، كما ثبت فعاليته كمضاد للالتهاب في عمله كواقي من الاصابة بالتهاب البنكرياس والاعتلال الكبدي (3,4).

وبينت الدراسة (5) ان المركبين الرين والوايمودين تعتبران كمضادات للسرطان، حيث يعملان على خفض امتصاص الكلوكوز من قبل الخلايا السرطانية مؤدياً الى حدوث خلل في العمليات الايضية الخلوية وبالتالي موت الخلية السرطانية . وكذلك اشارت الدراسة (6) الى ان

– البوتاسيوم في (500 مل) من محلول NaOH (0.2N) يضاف بعد ذلك (5 غم) من يوديد البوتاسيوم ويكمل الحجم الى لتر واحد بواسطة محلول NaOH (0.2N) } ، ان ظهور اللون البنفسجي يدل على وجود البروتينات . (10)

3-الكشف عن الصابونينات :

تم اخذ (5 مل) من المستخلص النباتي في انبوبة اختبار ورجه بشدة لمدة نصف دقيقة وعند ظهور رغوة كثيفة في الانبوبة دون اختفائها بعد مرور مدة تتراوح من (3-5 دقيقة) دل على وجود المواد الصابونية فيها .(10,11)

4-الكشف عن المركبات الفينولية :

وذلك بأذابة (1 غم) من كلوريد الحديديك في (100مل) ماء مقطر ,نأخذ (3 مل) من المستخلص النباتي واضيف له (2مل) من الكاشف ،ان ظهور اللون الاصفر المزرق يدل على وجود الفينولات . (10)

5-الكشف عن العفصيات :

وذلك بأضافة حجوم متساوية من المستخلص النباتي ومحلول (1 %) من كلوريد الحديديك ،ان ظهور اللون الازرق يدل على ايجابية الكشف . (10)

6-كشف عن الفلافونيدات :

تم بمزج حجوم متساوية من المستخلص النباتي والكاشف { يحضر بمزج حجوم متساوية من الايثانول بتركيز (50%) و KOH (50 %) }، ان ظهور اللون الاصفر يدل على وجود الفلافونيدات . (10,13,14)

دراسة الفعالية البايولوجية

تم دراسة الفعالية البايولوجية للمستخلص المائي (البارد والساخن) والكحولي لجذور نبات الراوند ،حيث تم تعقيم المحاليل اعلاه بجهاز المرشح اليدوي Millipore filter paper بأستخدام وسط Muller Hinton agar وثاقب فليني phelen porck بقطر (6 ملم) على البكتريا التالية :-

Klebsila sp . ، E. coli ، Staphylococcus aureus

وحظرت تراكيز مختلفة من المستخلصات الصلبة (100,50,10,1 ملغم / مل) ماء مقطر معقم (10,11)

دراسة تأثير المستخلص المائي (البارد و الساخن) والكحولي لجذور نبات الراوند على نشاط انزيم S.GOT :-

تم اضافة (1 مل) من المستخلص النباتي لجذور نبات الراوند الى المصل المأخوذ من اشخاص اصحاء واتبعت طريقة (Britman S. Frankel) المذكورة في Kit المجهز من قبل شركة (Biomaghreb) والمستخدم لقياس انزيم S.GOT ،حيث تم قياس نسبة التثبيط لكل عينة قبل وبعد اضافة المستخلص ، تم قياس المعقد الناتج عند طول موجي (505nm) .(15) وتم ايجاد النسبة المئوية للتثبيط كما يلي :-

$$\text{النسبة المئوية للتثبيط \%} = \frac{\text{الفعالية#بوجود#المثبط}}{\text{الفعالية#بدون#المثبط}} \times 100$$

النتائج والمناقشة

اثبتت الدراسة العملية للكشوفات الكيميائية النوعية للمستخلص المائي (البارد والساخن) لجذور نبات الراوند جدول (1) , ان الجذور تحتوي على مركبات فعالة من الكلايكوسيدات و صابونينات و مركبات فينولية والفلافونيدات و التانينات وعدم احتوائهما على البروتينات وهذا جاء مطابقاً لما قام به بعض الباحثين(3,4) ،اما المستخلص الكحولي فثبت احتوائه على الكلايكوسيدات والفينولات والتانينات وعدم احتوائه على الصابونينات والفلافونيدات والبروتينات .

تم قياس الآس الهيدروجيني (pH) لمستخلصات جذور نبات الراوند و اظهرت النتائج بأنها ذات وسط حامضي ،حيث كانت للمستخلص المائي البارد (pH =5.69) وللمستخلص المائي الساخن (pH =5.94) بسبب احتوائهما على الصابونينات والفينولات والفلافونيدات والتانينات بنسب متفاوتة و(pH =5.20) للمستخلص الكحولي بسبب احتوائه على الكلايكوسيدات والفينولات والتانينات بنسبة اعلى (مركبات عضوية).

اما النسبة المئوية لتثبيط انزيم S.GOT فكانت (2.08%) للمستخلص المائي البارد و(3.38%) للساخن و(4.47%) للمستخلص الكحولي ويعود سبب ذلك الى مكونات الفعالة للمستخلص حيث تعمل الانثراكوينونات (الراين و الايمودين) على التداخل في عملية نقل

الالكترون (Electron transport) مقللا بذلك من عمليات الاختزال في الخلية مخفضاً من انتاج الجذور الحرة (زيادة تأثير التثبيط) التي تعمل على زيادة فعالية انزيمات الكبد.(5,7)

وتم قياس تأثير المستخلصات المائية (البارد و الساخن) والكحولي على الفعالية المضادة للبكتريا (تثبيط النمو البكتيري) ، فقد اظهرت النتائج في الجدول (2) ، ان المستخلص المائي كانت له ادنى قيم تثبيطية مقارنة بالمستخلص المائي الساخن والكحولي ،حيث نلاحظ ان التركيز (1 ملغم / مل) لم يسجل اي تأثير تثبيطي لكل انواع البكتريا ،اما التركيز (10, 50 ملغم /مل) فكانت لهما مقاومة شديدة من قبل بكتريا (E. coli)،حيث لم يسجلا اي منطقة تثبيط لهما ،اما التركيز (100 ملغم / مل) فكانت له نسبة تثبيط جيدة للانواع البكتيرية الثلاثة تصل الى (6.2mm) في بكتريا (Staphylococcus aureus).

اما المستخلص المائي الساخن فقد سجل التركيز (1 ملغم / مل) نسبة تثبيطية واطئة (1- 1.2ملم) في البكتريا الثلاثة ، ارتفعت لتصل اقصاها الى (7.1mm) لبكتريا (Staphylococcus aureus)،عند التركيز (10ملغم/ مل) ، اما التركيز (50 ملغم / مل) فكانت نسبة تثبيطه جيدة وصلت ادناها الى (2.1mm) في بكتريا (E. coli) واعلاها (11 .5mm) لبكتريا (Staphylococcus aureus) ، اما التركيز (100 ملغم / مل) فكانت له قيم تثبيط عالية سجلت (16.3mm) عند البكتريا (Staphylococcus aureu) وادناها عند بكتريا (E. coli)، اما المستخلص الكحولي فلم يسجل التركيز (1 ملغم / مل) اي منطقة تثبيط للبكتريا الثلاثة مشابهاً بذلك المستخلص المائي البارد ، اما التركيز (10 ملغم / مل) فسجل قيم واطئة وصلت ادناها الى (1.0mm) عند البكتريا (E. coli) . اما التركيز (50ملغم / مل) كانت له قيم تثبيط جيدة وصلت الى (6.5mm) عند البكتريا(Staphylococcus aureu) اما التركيز (100 ملغم / مل) ايضاً سجل قيم تثبيط عليا عند البكتريا ذاتها وادناها عند البكتريا (.Klebsila sp) وصلت الى (4mm) .

يعود السبب في هذه الفعالية المضادة للبكتريا لآحتواء المستخلص المائي الساخن على الكلايكوسيدات والصابونينات والفينولات والفلافونيدات والتانينات (العفصيات)والتي يعد الكثير منها مضاد للبكتريا .فالتانينات تعمل على تثبيط الانزيمات والبروتينات الناقلة الموجودة في غشاء الخلية،وتكمن فعالية المركبات الفينولية على تغيير طبيعة بروتين الغشاء الخلوي خلال ارتباطها بالمواقع الفعالة للآنزيمات الخلوية (مجاميع الهيدروكسيل ستكون اواصر

هيدروجينية مع المواقع الفعالة), مما يثبط من التفاعلات الايضية الخلوية مؤثراً بذلك على نمو الكائن الحي وتكاثره (16).

مما سبق نستنتج ما يأتي :

1- احتواء المستخلص المائي لجذور نبات الراوند على مجموعة من المركبات الفعالة كالكلايكوسيدات والصابونينات والفينولات والفلافونيدات والتانينات وعدم احتوائها على البروتينات, اما المستخلص الكحولي فحتوى على الكلايكوسيدات والفلافونيدات والتانينات وكلا المستخلصين ذات وسط حامضي .

2- ان المستخلص المائي الساخن اكثر كفاء ة من المستخلص المائي البارد و الكحولي في تأثيره على النموالبكتيري عند التركيز (50و 100ملغم /مل).

3- ان جميع مستخلصات جذور نبات الراوند (المائي و الكحولي) صلية يعود السبب فيها الى خلوها من المواد الهلامية والاصماغ والشمع (1,2).

ونوصي بما يلي

1-عزل وتنقية وتشخيص المركبات الفعالة في جذور نبات الراوند لغرض استخدامها لعلاج او الوقاية من الكثير من الامراض كسرطان الجلد وخفض الكوليسترول .

2 -دراسة مكونات الآجزاء الاخرى للنبات وتأثيرها على النمو البكتيري ودورها في التطبيقات الطبية والعلاجية .

جدول -1 : المركبات الفعالة والاس الهيدروجيني (pH) للمستخلص المائي (البارد والساخن) والكحولي لجذور نبات الراوند

المركبات الفعالة	الكلايكوسيدات	الصابونينات	الفينولات	الفلافونيدات	التانينات	البروتينات	pH
المستخلص المائي البارد	+	+	+	+	+	_	5.69
المستخلص المائي الساخن	+	+	+	+	+	_	5.94
المستخلص الكحولي	+	_	+	_	+	_	5.20

(+) يدل على ايجابية الكشف (وجود المركب الفعال)

(-) يدل على سالبية الكشف

جدول –2 : تأثير المستخلص المائي (البارد و الساخن) والمستخلص الكحولي على النمو البكتيري

نوع البكتريا	نوع المستخلص	التثبيط عند التراكيز المستخدمة 1	10	50	100
Staphylococcus aureus	مائي بارد	لا توجد منطقة تثبيط	1,1 mm	3,1 mm	6,2 mm
	مائي ساخن	1,2 mm	7,1 mm	11,5 mm	16,3 mm
	كحولي	لا توجد منطقة تثبيط	2,5 mm	6,5 mm	12,5 mm
Escherichia coli	مائي بارد	لا توجد منطقة تثبيط	–	–	3,4 mm
	مائي ساخن	1,0 mm	2,3 mm	2,1 mm	4,0 Mm
	كحولي	لا توجد منطقة تثبيط	1,0 mm	2,2 mm	5,6 mm
Klebsila	مائي بارد	لا توجد منطقة تثبيط	–	2,1 mm	5,2 mm
	مائي ساخن	1,0 mm	5,5 mm	11,1 mm	13,1 mm
	كحولي	لا توجد منطقة تثبيط	1,1 mm	3,5 mm	4,0 mm

المصادر

1- شوفالييه،اندرو ،الطب البديل ،التداوي بالاعشاب والنباتات الطبية ، مترجم ، ص 124 .(2010)

2- Tyler, Varro E. Lynn R., james E. Robbers,: "Pharmacognosy", 9th ED. ,Lea & Febiger ,book co. Philadelphia ,p64 (1988) .

3- Cyong ,J. ,Anti-bacteroides fragilis substance from Rhubarb,J.Etnopharmacol May 19 (3):279.(1987)

4- Hu P.,tretmentof bacterial peritonitis with dachenggi decotion and Rhubarb in mic .Zhongguo Zhong Xi Yi jie ze zhi.jan.20 (1): 53-4.(2000)

5- Srinivas G, Babykutty S, Sathiadevan PP, Srinivas P. Molecular mechanism of emodin action: transition from laxative ingredient to an antitumor agent. Med Res Rev . 2007;27(5):591-608.

6- Goel V, Ooraikul B, Basu TK. Cholesterol lowering effects of rhubarb stalk fiber in hypercholesterolemic men. J Am Coll Nutr . 1997;16(6):600-604

7- Zhong hua shi yan he lin chuang bing Due Xue, Za Zhi. Jun, Inhibition effect of Rhubarb ethanol extract on herbs simplex virus infection in vivo.17 (2):169-73.(2003)

8- جلال كريم ، كريم ،دور المستخلص المائي للراوند Rheum ribes والزعتر Thymus في التثبيط التطفيري لعقار Gemcitabine والتأثير التسرطني لمادة 7,12-DMBA في ذكور الفئران البيض رسالة دكتوراه ، كلية التربية ابن الهيثم (2011).

9- Liu y, Yan f, Liu y. etal. Aqueous extract of Rhubarb stabilize vulnerable atherosclerotic plaques due depression of inflammation and lipid accumulation phytother Res; 22(7):935-942 (2008).

10- جاسم ،عبد القادر محمد نوري ،دراسة بعض مكونات نبات اليوكالبتوس وتاثير مستخلصاتها على نمو بعض الاحياء الدقيقة ،مجلة كلية العلوم ،16 (2) :62-71 (2005) .

11- كاظم باقر، رجاء ،وآخرون ،دراسة الفعالية البايولوجية للمستخلص المائي لقشور الرمان ،مجلة كلية التربية ، الجامعة المستنصرية ،5 (5):355-364 .(2010).

12- محمد، مصطفى طه ،دراسة مكونات بعض اوراق نبات عين البزون وتاثير مستخلصاتها على نمو الاحياء الدقيقة ،مجلة كلية العلوم المستنصرية ،18 (1):-28 (2007). 36

13- الدوركي ،سعاد يونس ،تاثير مستخلصات اوراق السدر والتبغ في نمو بعض الفطريات الجلدية والخمائر , رسالة ماجستير ،كلية العلوم ،الجامعة لمستنصرية ،(2003)

14- البياتي ،رضا ابراهيم ،الناصري ،نزار احمد ،السدح،منصور محسن ،دراسة مكونات المستخلص المائي لاوراق نبات القات ،مجلة علوم المستنصرية ،12 (4) :123-128 .(2001)

15- Determination of Amino Transferases (GOT-GPT) in sera, Britman S.Frankel S.,Am.J.Clin.path.,28,56(1957).

16- Plaza R., Chan, M. J., E.C. and Krieg N.R,:"Microbiology",5th Ed., McGraw –Hill book Co.,New York(1986).

دراسة طيفية عن تقدير تركيز ايونات الرصاص في مصل الدم للعاملين في معمل البطاريات

ختام جابر نبهان

الجامعة المستنصرية-كلية العلوم-قسم الكيمياء

تاريخ تقديم البحث : 4 /4/ 2011 تاريخ قبول البحث : 5/29 /2011

ABSTRACT

This study aims to evaluate lead and glucose level in serum of workers of (Batries – Factory Al – Wazyryai) . Twenty for the workers were included in this study and twenty out of the factory were taken as control group .serum lead , glucose level were significantly higher than control group . the study demonstrated positive and significant relation between Lead and glucose level in serum of workers.

الخلاصة

تهدف الدراسة لتقدير مستوى الرصاص والكلوكوز في مصل الدم في معمل البطاريات في الوزيريه . تضمنت الدراسة (20) من العاملين في معمل البطاريات و (20) شخص من خارج المعمل كمجموعة ضابطة . اظهرت الدراسات ان مستويات الرصاص و الكلوكوز في مصل الدم للعاملين قد ارتفع نسبيا مقارنة بالمجموعة الضابطة . كما اظهرت ان هناك علاقة ترابطية معنوية موجبة بين مستوى الرصاص ومستوى الكلوكوز في مصل دم العاملين .

المقدمة

ان الرصاص عنصر كيميائي ثقيل , وهو من اقدم الفلزات المعروفة في العالم وبالرغم من منافعه الكثيرة , فأنه قد يكون ضارا وتحدث الحالة المعروفة باسم (التسمسم الرصاصي) اذا دخلت كميات كبيرة من الرصاص للجسم(1), وتنتشر حالة التسمسم هذة بصورة رئيسية بين اولئك الذين يعملون في المصانع الكيميائية او في معمل التكرير حيث توجد كميات كبيرة من ابخرة الرصاص في الهواء(2)

ختام

يستخدم الرصاص اساسا" في مجال صناعة بطاريات التخزين الحامضية, الرصاصية, تحتوي هذه البطاريات على الرصاص النقي و مركبات الرصاص , وتوفر هذة البطاريات القدرة الازمة لتحريك الانظمة الكهربائية في الطائرات والسيارات وفي كثير من وسائل النقل الاخر (3). ويستخدم الرصاص في انتاج رابع اثيل الرصاص وهي مادة تضاف الى البنزين لتحسين اداء محركات السيارات, وكما يستخدم الرصاص في تغليف الكابلات الكهربائية , ويستخدم في تبطين المواسير والخزانات .

ان الكثافة العالية للرصاص تجعله حجابا واقيا جيدا ضد الاشعاع , لذا فان سبائك الرصاص تستخدم في تبطين جدران حجرات الاشعة السينية (X – Ray) في المستشفيات والمفاعلات النووية .

تكمن خطورة الرصاص في ميلة الى التراكم والتجمع في العظام حيث يقوم بطرد الكالسيوم مسببا فقر الدم لانة يقلل من عمر كريات الدم الحمراء , كما انه قد يؤدي الى ضرر دائمي في الدماغ مؤديا الى تشنجات قوية قد تؤدي لاحقا الى الموت(4) .

التسمم بالرصاص والمعروف (Colica Pictonum) او (مغص الرسام) هو حالة غير صحية سببها المستويات المتزايدة للتقدم المعدني الثقيل في الجسم , كما وان التسمم بالرصاص يحدث نتيجة التعرض للرصاص والتي تتضمن الهواء الملوث – الماء – التربة – الغذاء – ومنتجات استهلاكية , ان الرصاص سام للكثير من الاعضاء والانسجة ومنها القلب , العظام , الامعاء , الكلى , وانظمة منتجة وعصبية .

ان التعرض المهني هو طريقة شائعة للاصابة بتسمم الرصاص لدى البالغين , كما و يعتبر التسمم بالرصاص تهديدا لحياة الكثير من الاطفال والذي يأتي من خلال طلاء الجدران الحاوي على الرصاص والذي يوجد في العديد من المنازل وخاصة القديمة وايضا من خلال استخدام الانابيب , ويكون التسمم بالرصاص لدى الحوامل والاطفال الصغار سريعي التأثر بالرصاص بسبب عبور الرصاص للمشيمة بسهولة وقد يدخل مخ الجنين ومن ثم يتداخل مع التكوين الطبيعي وكذلك قد يخرج ذائبا في حليب الأم وزيادة مستواه تؤدي الى انخفاض الادراك العلمي , بطيء التعلم , صداع , فقر الدم , طيش وفي بعض الحالات يؤدي الى الموت (5) .

لقد اظهرت الدراسات الحديثة والتي قامت بها حملة السلامة باميركا على مستحضرات التجميل واثبتت الدراسات ان احمر الشفاه (الروج) الذي يستخدمة ملايين النساء يحتوي على

نسب عالية من الرصاص, وايضا للرصاص مشاكل على النساء من حيث زيادة مستواه حيث يؤدي الى الاجهاض وقلة الخصوبة وتغير الهرمونات واضطراب الدورة الشهرية وتأخر سن البلوغ , ومثلما يؤثر الرصاص على النساء فأنة ايضا يؤثر على الرجال حيث انة يؤدي الى العقم وافادت الدراسات المذكورة اعلاة ان زيادة الرصاص عند الرجال يلحق اضرارا بالنطف وان الكثير من الرجال الذين يتعرضون للرصاص هم الدهانين الذين يعملون بالطباعة بصورة خاصة, وان قدرة الرجال على الانجاب تقل بعد (6–12) شهرا وقد وجدوا ان نسب عالية من الرصاص في نطف الرجل ترتبط بتراجع القدرة على الاخصاب(6).

يدخل الرصاص جسم الانسان من خلال ابتلاع او تنفس المواد الملوثة والمشبعة به، ومن الممكن ان يحدث تأثير التسمم به سواء من التعرض لجرعة كبيرة لمرة واحدة او لجرعات صغيرة على مدار فترة طويلة من الزمن، يقوم الجسم بالتخلص من الرصاص احيانا عن طريق بعض الوظائف الحيوية مثل التبول او من خلال الخراج وكميات ضئيلة منه عن طريق التعرق, اما اذا لم يتخلص الجسم من الرصاص بهذه الوظائف الحيوية فانة سوف يؤدي الى المشاكل التي تم ذكرها سابقا(7).

ان الرصاص ليس لديه وظيفة محددة او معلومة تفيد جسم الانسان , لكن معدلاته كانت امنه وطبيعيه في الجسد البشري قبل التلوث والثورة الصناعية في الثمانينيات والتسعينيات حيث ان المعدلات كانت تقرب من الصفر(6).

لقد حدد المركز الاميركي للسيطرة ومنع الامراض(CDC) [Centers of Diseases Control] ومنظمة الصحة العالمية(WHO) [World Health Organization] ان مستوى الرصاص في الدم (0.05 mg /L) كمستوى مقبول(8) .

في دراسة للحسني لمصفى الدورة مدينة /بغداد وجد ان ارتفاع كبير لتركيز الرصاص عن الحد المسموح به لدى العاملين في المصفى وقد حددت المواصفة العراقية للتركيز المسموح بة (0.05 mg /L)كحد اقصى (9) . تمكن الباحثين حسن وزينب من قياس نسبة الرصاص في الدم للعاملين بمصفى الدورة واظهرت النتائج ان مستوى الرصاص تراوحت معدلاتها ما بين (42 – 10) PPm (10) .

ان النسبة اذ ا كانت اعلى من (14 mg/dl) تؤثر على نمو الخلايا , واذا كانت النسبة اعلى من(39mg /dl) تؤثر على تكوين هيموغلوبين والجهاز العصبي مسببة الارهاق

ختام

وفقدان الذاكرة وغيرها من المشاكل التي تم ذكرها , ومؤخرا اجريت دراسات بينت التاثيرات الصحية والضارة على الجهاز العصبي المركزي متضمنة ان يكون مستوى الرصاص في الدم اقل من(0.05 mg /L) مقترحين انة لا توجد نسبة ثابتة او واحدة يمكن اعتباراها طبيعية(11) .

توصل الباحث رضوان حسين من دراسة مستوى الرصاص لدى الاطفال و وجد ان غالبية اطفال الحضر (45.5 %)لديهم مستوى الرصاص في الدم(15 - 19 mg /L) وبمعدل (15.9) في حين (34.5 %) منهم لديهم مستوى اقل من(9 mg /dl) ومعدل(6.4), اما اطفال الريف فأن نصفهم 50 % كان لديهم مستوى اقل من(9 mg /dl) واما ال 50 % الباقية لديهم مستوى اقل من(15 - 44 mg /dl) ولايوجد لديهم احد بلغ مستوى الرصاص اعلى من(45 mg /dl) (12)

المواد وطرائق العمل

أ – جمع نماذج الدم :

تم سحب عينات الدم ل (20) من العاملين في معمل البطاريات في الوزيرية / محافظة بغداد تراوحت اعمار العاملين الذين سحب منهم الدم بين (30 - 65) سنة ولفترات عمل مختلفة تراوحت (7 - 39) سنة ولاقسام مختلفة من معمل البطاريات . سحبت (5 ml) من الدم الوريدي وكذلك تم سحب عينات الدم ل (20) شخص من خارج معمل البطاريات تراوحت اعمارهم (28 – 67) سنة وجميعهم من الذكور كمجموعة ضابطة في انابيب اختبار خالية من مانع التخثر , وضعت عينات الدم في جهاز الطرد المركزي Centerfuge في (3000 rpm) دورة بالدقيقة وذلك لفصل المصل , تم سحب المصل وخزنه في درجة حرارة (c° 20 -) لحين اجراء التحاليل .

ب– قياس نسبة تركيز الرصاص في مصل الدم :

تم اخذ (1 ml) من مصل الدم الذي سبق جمعه الى جهاز الامتصاص الذري الغير اللهبي Flameless Atomic Absorption وقيس تركيز الرصاص في شركة ابن سينا في الوزيرية.

ج- قياس نسبة السكر في مصل الدم :

تم في هذة الفقرة قياس نسبة السكر في مصل دم العاملين بواسطة الاكسدة الانزيمية بوجود (Glucose Oxidase) (14) , (13) وذلك في شركة ابن سينا في الوزيرية .

النتائج والمناقشة

من النتائج التي تم الحصول عليها والمبينة في الشكل رقم (1) وجدول رقم (1) ان مكان العمل يلعب دورا هاما في زيادة نسبة تركيز الرصاص حيث تبين النتائج ان العمال الذين يعملون في قسم التقطيع هم الشريحة الاكثر تعرضا للرصاص من الاقسام الاخرى (اللبخ – الشحن – التجميع) وهذا يدل على ان العمال الذين يعملون في قسم التقطيع هم الذين يتعرضون للرصاص وبشكل مباشر اكثر من غيرهم كونهم يستنشقون الرصاص المتطاير في جو العمل .

ان المجموعة الضابطة كان لها مستوى معدل تركيز الرصاص اقل وهذا موضح في الشكل رقم (1) والجدول رقم (1) , اما المجاميع العاملة في معمل البطاريات فقد كان لها معدل تركيز اعلى بقيمة معنّد بها احصائيا من المجموعة الضابطة معدلها (0.0199+ 0.03732) وكان $P<0.05$.

اما الشكل رقم (2) والجدول رقم (1) فيبين العلاقة بين مكان العمل ومستوى السكر في الدم حيث بينت النتائج انه كلما زادت نسبة تركيز الرصاص في الدم كلما زادت نسبة السكر في الدم وهذا ما موضح في الجدول رقم (1) والشكل رقم (1) يبين انه هناك علاقة بين مستوى السكر في الدم ومكان العمل للعاملين في معمل البطاريات حيث نلاحظ ان العاملين في قسم التقطيع والمتعرضين للرصاص اكثر من غيرهم تكون نسبة السكر في الدم لديهم اعلى من الاقسام الاخرى وهذا يدل على تكون نسبة السكر في الدم لديهم اعلى من الاقسام الاخرى وهذا يدل على ان هناك علاقة بين نسبة تركيز الرصاص في الدم ونسبة السكر في الدم اعلى بزيادة نسبة تركيز الرصاص , تزداد نسبة السكر في الدم على الاغلب اي العلاقة طردية , ومن الجدول رقم 1 نجد ان المجاميع العاملة في معمل البطاريات كان لها معدل تركيز اعلى بقيمة

ختام

معتد بها احصائيا من المجموعة الضابطة حيث كان معدل مستوى السكر للعاملين في المعمل (180.35+108.273) والمجموعة الضابطة معدلها (96.5+16.675) وكان $P<0.05$.

اما الشكل رقم 3 فيبين العلاقة بين نسبة تركيز الرصاص مع نسبة تركيز السكر حيث ظهرت لنا ان هناك علاقة طردية وهذا دليل على انه هناك علاقة مهمة بين مستوى السكر وتركيز الرصاص حيث انه كلما زادت نسبة تركيز الرصاص كلما زادت نسبة السكر ويعود السبب في ذلك الى ان : الرصاص يعتبر من العناصر الثقيلة والخطيرة لمعظم اعظاء الجسم واجهزته والتي تتعارض مع العمليات الايضية ووظائف الخلايا , كما انه يحدث تأثيرات مدمرة على مراكز تصنيع الدم والكلية وجهاز التكاثر والجهاز الهضمي , حيث ان زيادة نسبة تركيز الرصاص في الدم يؤدي الى خلل في افراز الانسولين او في طريقة عمل الانسولين في خلايا الكبد والخلايا المحيطة , خاصة الخلايا العضلية والخلايا الدهنية , او قد يكون خلل في خلايا الاستلام الخاصة بالانسولين مما يؤدي الى حصول مرض السكري(15), لذلك قامت بعض الدول بوضع نظام غذائي للذين يتعرضون للرصاص بنسبة اكثر من غيرهم

كما وضعت الية لاستخدام الرصاص والمخلوط مع الكازولين لتقليل تأثير الرصاص على الجسم ووظائفه الحيوية على اولئك الذين يعملون بالمهن والتي يدخل فيها الرصاص. كما ان هناك اقتراح اخر لارتفاع السكر عند المتعرضين للرصاص في المعامل والذي يعود الى ان ارتفاع نسبة تركيز الرصاص في الدم يعمل على انحفاض في وظيفة الكلى (اي حصول عطل في خلايا الكلى الذي يؤدي الى ارتفاع نسبة السكر في الدم) وهنا بدوره يؤدي الى اعطاء فرصة اكبر للاصابة بتليف الكلية (16) ان ارتفاع مستوى السكر في الدم يؤدي الى زيادة في مستوى الكالسيوم , وعند ذلك فأنه من المتوقع ان ينخفض مستوى امتصاص الرصاص ,لكن الرصاص القادم من المصادر الداخلية للجسم مثل العظام او من التعرض للتلوث البيئي , سيبقى في الدم وقد تكون ايضا هذه الحالة هي السبب في ارتفاع مستوى الرصاص(17).

من خلال ملاحظة الشكل رقم (4) تبين ان هناك علاقة موجبة $r = 0.01$ غير معتد بها احصائيا بين مستوى تركيز الرصاص في مصل دم العاملين في معمل البطاريات وفترة تعرضهم للرصاص ($P>0.05$)

هناك اجراءات وقائية يمكن من خلالها التقليل من خطورة الرصاص لدى العاملين بالمهن التي يدخل الرصاص فيها ومنها :-

- عدم تناول الطعام او الشراب في اماكن تواجد الرصاص .
- غسل الملابس الملوثة بالرصاص بعيدا عن الملابس الاخرى او يفضل ارسالها الى اماكن للتنظيف (خارجية) .
- الغذاء الصحي المتوازن , حيث ان التغذية السليمة تساعد على تجنب الاصابة بمعدلات الرصاص العالية التي تمتص في الدم ومن المصادر الغذائية التي تعادل تأثير الرصاص: (فيتامين (ج) – الحديد – الزنك – الكالسيوم – الفسفور) .

كما ان تكرار الوجبات الخفيفة والحرص على تناول الوجبات الرئيسية الثلاثة يساهم في تجنب الاصابة بتسمم الرصاص لان الرصاص من الصعب امتصاصه في المعدة الممتلئة (18) .

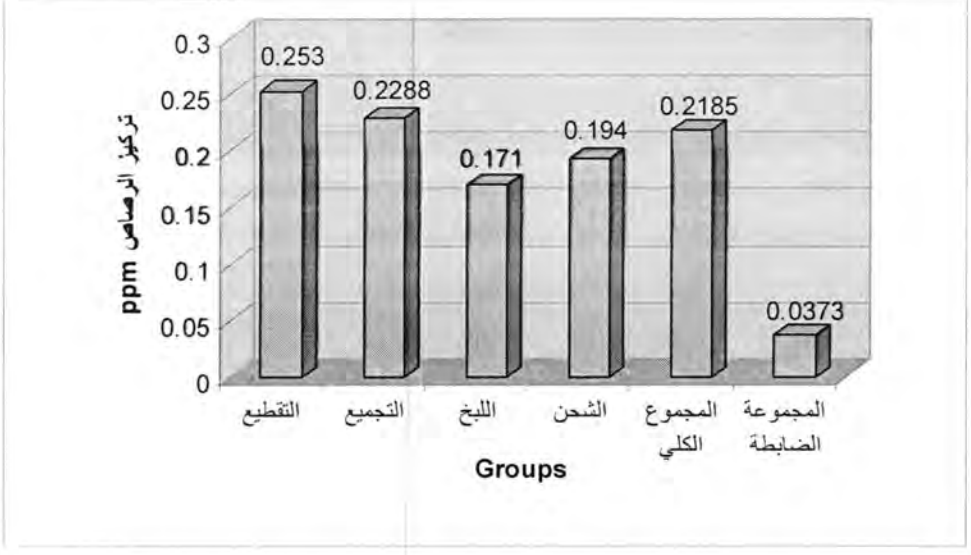

شكل –1: يبين العلاقة بين تراكيز الرصاص ومكان العمل

ختام

جدول -1: يبين معدل تركيز الرصاص و السكر والانحراف المعياري مع المجاميع للعاملين في المعمل والمجموعة الضابطة

المجموعات	العدد	معدل مستوى السكر ± الانحراف المعياري ملغم/100 مل	معدل تركيز الرصاص ± الانحراف المعياري ppm
التقطيع	7	112.106 ± 218.143	0.082 ± 0.253
التجميع	5	106.473 ± 129.6	0.102 ± 0.228
اللبخ	4	114.825 ± 191.5	0.048 ± 0.171
الشحن	4	112.976 ±166.5	0.032 ± 0.194
المجموع الكلي	20	108.273±180.35	0.0771± 0.2185
المجموعة الضابطة	20	16.675 ± 96.5	0.0199± 0.03732
T-test ,P valu(المجموع الكلي -المجموعة الضابطة)	20	2.265* , P < 0.05	7.272* , P < 0.05

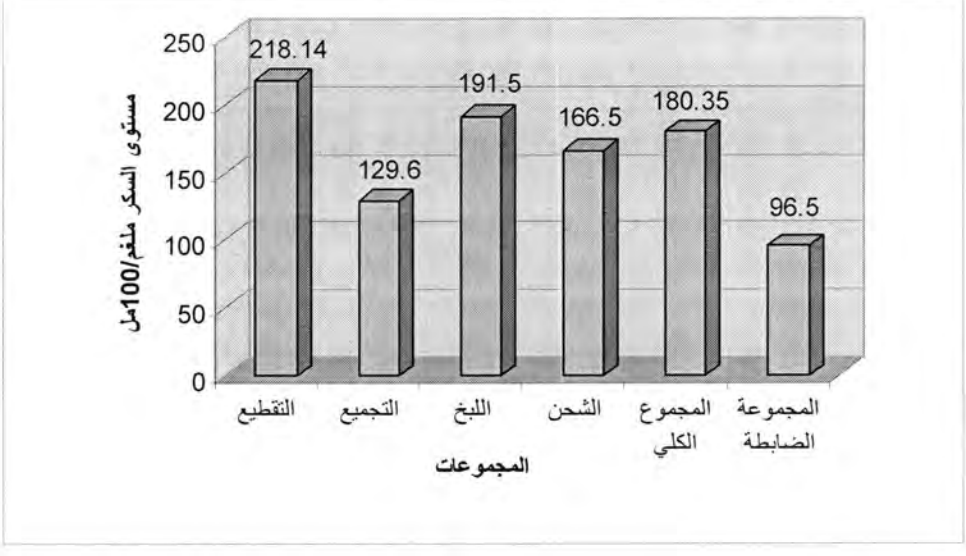

شكل -2: يوضح العلاقة بين مستوى السكر في الدم ومكان العمل

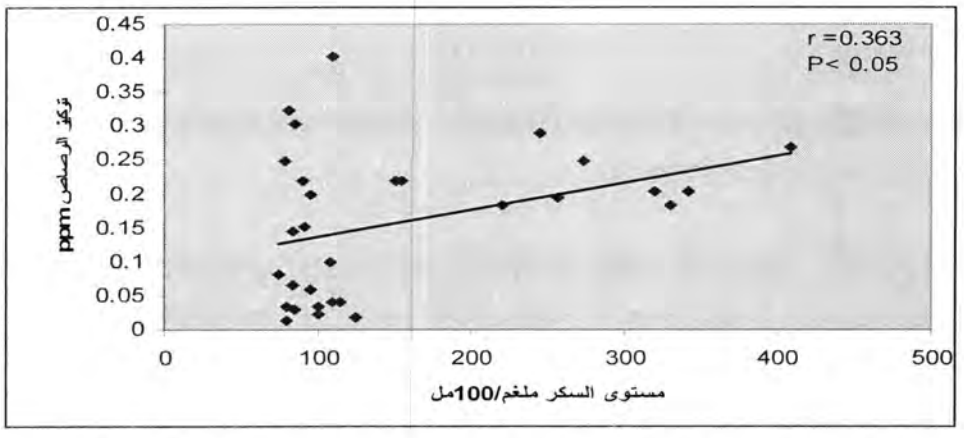

شكل – 3: يبين العلاقة بين نسبة تركيز الرصاص ونسبة تركيز السكر

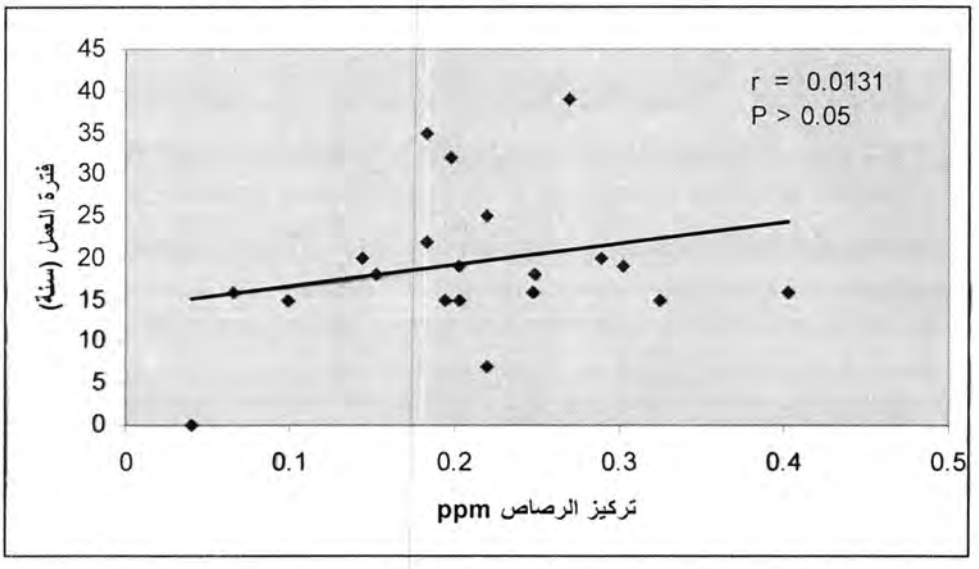

شكل – 4: يبين العلاقة بين تركيز الرصاص وفترة العمل

المصادر

1- Wood N. N. G and A-Earnchaw , "Chemistry of the Elements " 2nd ed ., Pergamen Press , (1998).

2- Ragen P. and Turner T., Working to Prevent head poisoning in air getting the head Out . JAAPA : official journal of the American Academy of physician Assistance 22(7) : 40 -5.PMID 19697571. (2009).

3- Casas J.S. and Sordo J. " Lead Chemistry Analytical Aspects , environmental Impact and Health effect " Santiago decompostelal . 1st edition . Elsevier . Puplucation . Santiago . (2006) .

4- Eichenberger, B. A, " Orgin and Nature of Selected Inorganic coustituents in National Water " Water Analysis (1) , Part (4) , Acadmic press,(1982).

5- Karri S., Saper K. and Kales R. B., "Lead encephalopathy due to traditional medicines ." 3 (1) :54-9 . PMID 18690981 (2008).

6- Guidotti T. and Ragain L., "Protecting children From Toxic Exposure : three strategies. "pediatric clinics of north America 54 (2) : 227 -35 , vii.doi : 1016/j.pcl.02.002. PMID 17448358 (2007).

7- Barbosa J. R., Tanu-Santos F., Gerlach J.E. and Parsons R. F., "Acritical Review of Bio markers used for monitoring human exposure to lead advantages , Limitations , and Fucture needs " . Environmental health perspectives 113 (12) : 1669-74 . PMID 16330345 . (2005).

8- Rogan W.J. and Wane . J.H. " Exposure to lead in children how is low enough ". the new England journal of Medicine , 348 : 1515 – 1516 . (2003).

9- الحسني، سعد ابراهيم. " المؤاشرات البيئية للمواد المترشحة في منظقة الدورة ." رسالة ماجستير , كلية العلوم , قسم علوم الارض , جامعة بغداد . (2003) .

10- Dahham Z.M and Hassan H.R , " Biochemical study on lead Effect upon oil Refinery workers . " A thesis from Baghdad University College of Science . (2010) .

11- Rossi K. E.," Low Level environmental head exposure a continuing challenge", The clinical bio chemists . Reviews / Australian Association of clinical Bio Chemists 29 (2) : 63 – 70 . PMID 18787644 . (2008).

12- الباحث : د.رضوان حسين ابراهيم , " تقويم مستوى الرصاص في دم الاطفال الضغار بمحافظة نينوى " . رسالة دكتوراه , كلية التمريض , جامعة بغداد , (2004)

13- Barhan D., Trinder P. Analyst 97 (1972).

14- Teuscher A., Richterich P., Schweiz Med . Wschr . 101 , 345 and 396 (1971) .

15- Babalola O. O, and AKinleye .A; "Status of the level of lead and Selected trace elements in diabetes mellitus patients in Abeokuta , Nigeria ." 1 (7), 127-131, December (2007).

16- Staessen J.A., Lauwerys R. R., Buchet J. P., Bulpitt C. J., and Rondia D . Imparment of renal function with increasing blood lead concentration in the general J.med > 327 (3) : 151 -156 (2000) .

17- Barbagello.M , Gupta .RK , Dominguez LJ and Resnick . LM , Cellular Ionic Alteration with age ; Relation to Hyper tention and Diabetes.J.Am Geriatr . SOC. 48: 1111-1116(2000).

18- HOTZ M., Kniepmann K., and K. John :"Occupational therapy in Padiatric Lead exposure prevention . "Am J OCCUP ther . Jan ; 52 (1) :53 – 9 .(1998).

ربط الصفيحة الدقيقة العيارية(صفيحة الألايزا) بالكلوبيولين المناعي نوع جي بالطريقة الكيمياوية

* رضا ابراهيم البياتي و **اكتفاء مزهر عبد الحسناوي و ***علي حيدر الساكني

*قسم الكيمياء – كلية العلوم –الجامعة المستنصرية

** وزارة العلوم والتكنولوجيا – بغداد – االعراق

*** قسم علوم الحياة– كلية العلوم–الجامعة المستنصرية

تاريخ تقديم البحث : 2011/ 3/30 تاريخ قبول البحث : 2011/ 5/29

ABSTRACT

In this research, the coating of microtiter plate by any protein, use of enzyme linked immunosorbent assay (ELISA) in order to prepare the kits of medical diagnostic for this technology, the coating to microtiter plate depending on the coating solution and used with protein (immunoglobulin G type) with factor to remove water (Ethyl (3,3-dimethyl amine proplene) carbodiimide- HCL (EDC)), which has given good results compared with the strip imported and the results showed no significant difference correlation coefficient r=0.99.

الخلاصة

في هذا البحث تم كشف سر المعرفة العلمي لربط أي بروتين على الصفيحة الدقيقة العيارية الخاصة بطريقة التحليل المناعي الانزيمي المتمثلة بتقانة الألايزا (ELISA) بهدف تحضير العدد الطبية التشخيصية لهذه التقانة المهمة ، اذ تم ربط الصفيحة بالاعتماد على محلول ربط(كاربونات – بيكاربونات الصوديوم) بقاعدية عالية (pH=9.6)، واستخدم مع البروتين (الكلوبيولين المناعي نوع جي) مادة عامل ازالة الماء (اثيل (3.3 ثنائي مثيل امين بروبيل) كاربون ثنائي الأمايد(EDC) (Ethyl (3,3-dimethyl amine proplene) carbodiimide- HCL التي أعطت نتائج جيدة بالمقارنة مع شريط مستورد وتبين من النتائج عدم وجود فرق معنوي بمعامل ارتباط r = 0.99 .

نقل تكنولوجيا تحضير العدد الطبية التشخيصية بتقانة الألايزا من خلال دراسة الظروف المثلى لهذه التقانة المهمة لتشخيص الامراض ، ويعد الربط على صفيحة الألايزا الخطوة الرئيسية لتحضير العدد التشخيصية بتقانة التحليل المناعي الانزيمي المتمثل بالألايزا (ELISA).

المقدمة

إن أساس التحليل المناعي الأنزيمي (EIA) يتألف من جزئين، التفاعل المناعي(Immunoreaction) وقياس الفعالية الأنزيمية (Enzyme activity) [1] . وتعتمد في عملها على السطح الصلد (Solid-phase) وبذلك فهي تشابه التحليل المناعي الفلورسيني والتحليل المناعي الإشعاعي.

وينقسم التحليل المناعي الأنزيمي إلى:-

- **تحليل مناعي أنزيمي متغاير** (Heterogeneous enzyme) مثل تقانة الأليزا (ELISA) . (1)
- **تحليل مناعي أنزيمي متشابه** (Homogeneous enzyme) مثل EMIT (1) .

وطريقة الأليزا (ELISA) أكثر خصوصية وحساسية للكشف عن العامل الرثياني من طرائق التلازن والتحليل المناعي الفلورسيني (2).

بدأت تقانة الأليزا عام 1971 من قبل (Engvall and Perlmann) [3] وتطورت التقانة عام 1981 لاسيما عند اكتشاف مرض الإيدز في فرنسا.

تعرف هذه التقانة الطبية (3) بأنها التقدير الكمي والنوعي لكميات قليلة جدا من المستضدات أو الأضداد في أطباق فيها فتحات دقيقة العيارية تسمى بالصفائح الدقيقة العيارية (Microtitre Plates) ويمكن الكشف عن (5) نانوغرام من المستضد أو الضد لكل مللتر من العينة بهذه التقانة (4).عند تحضير عدة (Kit) التحليل المناعي الأنزيمي للكشف عن العامل الرثياني (RF) يتم ربط الكلوبيولين المناعي (IgG) المنقى على سطح صلد منشط (به مجموعة فعالة)، ويعلم الضد (Anti-Human IgM) بالأنزيم (5) .

طريقة الأليزا هي نوع من أنواع التحليل المناعي الأنزيمي المتغاير (Heterogeneous) ولها أصناف حسب نوع التفاعلات (4) منها**التحاليل التنافسية (Competitive assays)** وبها أما

يعلم الضد أو المستضد بالانزيم، **التحاليل اللاتنافسية (Non-Competitive assays)** ووتعرف بطريقة الشطيرة (Sandwich) ، أو التحليل غير المباشر (Indirect) لقياس الأضداد والمستضدات.السطح الصلد عبارة عن مادة بلاستيكية (Plastic) تصنع من مواد عضوية متعددة الوحدات التركيبية (Polymer) مثل متعددة الستايرين (PS) ومتعدد البروبلين (PP) و كلوريد متعدد الفنايل (Poly vinyl chloride) وذات أشكال مختلفة، منها مايكون بشكل أنابيب اختبار (tubes)، كرات (beads) وصفائح دقيقة العيارية(Microtitre Plates)(4).

الصفائح الدقيقة العيارية تسمى بصفائح الأليزا (ELISA-Plates) وتختلف بأشكالها وعدد الحفر المكونة لها ، ويمتاز متعدد الستايرين (PS) بالربط الجيد للضد أو المستضد بوساطة الامتزاز الفعال (Passive adsorption) (6). يشمل الربط تفاعل بين السطح الصلد والكواشف المستخدمة في التحليل المناعي وتعتمد التفاعلات على عوامل منها: نسبة الانتشار، هندسة السطح، الوقت، التركيز، الوزن الجزيئي، درجة الحرارة وكيمياء السطح وكيمياء الكاشف (7). الربط أما أن يكون فيزياوياً أو كيمياوياً ، الربط الفيزياوي استقراريته قصيرة والربط الكيمياوي ذو استقرارية طويلة (8). الكواشف تكون محبة للماء (Hydrophilic) والسطح الصلد كارها للماء (Hydrophobic) وعلى هذا الأساس تنشط الصفائح بإضافة مجاميع فعالة لتقليل صفة اللاقطبية الموجودة على السطح وتسهيل الارتباط التساهمي (9).

تتكون الصفائح من 96 – حفرة (96-wells)، أو 8 حفر أو16 حفرة، وللحفرة أشكال مختلفة، منها المسطحة، المقعرة والتي لها شكل الحرف C، وتتنوع الصفائح حسب المجاميع الفعالة الموجودة على السطح، وجود المجاميع الفعالة على السطح قد يكون من خلال تحضير السطح نفسه أو باستخدام تفاعلات التشابك (10) . وجود مجاميع الأمين الفعالة على السطح الصلد تتخصص بالتفاعلات المناعية (4) . ويتم تنشيط الصفائح بوساطة الربط التساهمي (Covalent binding) بإضافة مجموعة الديهايد (-CHO) على الصفائح، وهو ربط كيميائي أطلق عليه (Chemobond) يمتاز بالاستقرارية القليلة التي تصل إلى أسبوعين كحد أقصى (11) .

يربط مصل الالبومين البقري (Bovine Serum albumin) على الصفيحة بتركيز2% (W/V) قبل إضافة الضد المراد ربطه على السطح في عمليات التنشيط (12)، ومن المواد الأخرى المستخدمة في تنشيط السطح مادة الكلوترالديهايد (Glutaraldehyde) (13). وبتفاعل متعدد

الستايرين (PS) مع (Anthraquinone 3-amine) وبوجود الأشعة فوق البنفسجية يمكن تنشيط السطح بإضافة مجاميع الأمين (14)، ومعاملة الجزيئة الحياتية (مثل الكلوبيولين المناعي IgG) بالحرارة التكتل (Aggregate) عند 60 درجة مئوية لمدة 30 دقيقة مع السطح الصلد (15).

يتبين من ذلك أن عملية الربط تعتمد على خاصية الامتزاز (Adsorbtion) (15). كامتزاز المستضدات الدهنية (Lipid antigens) مثل الكارديوليبين (Cardiolipin) على سطح متعدد الستايرين (PS) وبوجود مادة (Sodium deoxy cholate) (16)، ويتم ربط ضد هرمون الثايروكسين (Anti-T4) بتنشيط الضد بمادة المعروفة بعامل ازالة الماء (EDC)

(Ethyl (3,3-dimethyl amine proplene) carbodiimide- HCL)ويعامل السطح بمادة(octadecylamine) (17) .

وتنشط الصفائح باستعمال حوامض عضوية غير مشبعة مثل حامض الاكريلك (Acrylic acid) (18) أو حامض الكروتونك (Crotonic acid) بوجود أشعة كاما- Co60(19) ،وبسبب تسليط الأشعة على المتعدد (Polymer) تحدث تغيرات مفاجئة بخواصها نتيجة انشقاق أو انقسام أواصر السلسلة للمتعدد الرئيسة(20)، أو تشابك جزيئات المتعدد بعضها ببعض (Cross linking) ، ويتم الربط بطريقة الامتزاز ويربط الكلوبيولين المناعي نوع جي بأستخدام محلول دارىء ذو قاعدية عالية مثل محلول كاربونات –بيكاربونات الصوديوم (17).

المواد وطرائق العمل

صفيحة من نوع Maxisorp من شركة Nunc الدنماركية ،– اثيل (3.3 ثنائي مثيل امين بروبيل) كاربون ثنائي الأمايد(EDC) من شركة سكما ،(كاربونات الصوديوم الحامضية ، كاربونات الصوديوم ، فوسفات البوتاسيوم) من شركة BDH و الكلوبيولين المناعي نوع جي (IgG) تم فصله بمختبراتنا وهوعالي النقاوة .

تم ربط الكلوبيولين المناعي البشري (Human-IgG) باتباع طريقة بيرسون(Persson) وباستعمال مادة عامل إزالة الماء (EDC) (17).

واجريت الخطوات التالية:

1- حضر الكلوبيولين المناعي المنقى IgG بتركيز (100) مايكروغرام/ 1 مللتر من المحلول الدارئ الكاربونات – ثنائي الكاربونات (CBB) (Carbonate – Bicarbonate buffer) (0.05 مولاري ، PH =9.6) (حضر بإذابة (1.59) غرام من كاربونات الصوديوم (Na2CO3) و (2.93) غرام من بيكاربونات الصوديوم (Na2HCO3) ، (0.02) غرام من الثايومرسال في (800) مللتر من الماء اللاآيوني وعدل الأس الهايدروجيني إلى PH=9.6 ثم اكمل الحجم إلى لتر بالماء اللاأيوني).

وأضيف (100) مايكروليتر لكل حفرة من حفر الصفيحة وحضنت الصفيحة لمدة (24) ساعة وبدرجة حرارة (4) مئوية. واستخدم تركيز اخر (0.1مولاري بنفس الحامضية) (حضر باذابة الصوديوم (0.318)غرام من كاربونات الصوديوم مع (0.586) غرام من بيكاربونات الصوديوم واضيف (80) مللتر من الماء أللاأيوني وعدل الأس الهايدروجيني الى (PH=9.6) ثم اكمل الحجم الى (100) مللتر بالماء اللاأيوني)، واستخدم تركيز ثالث لمحلول الربط(0.2 مولاري, PH=9.6) حضر بمضاعفة الاوزان للتركيز المولاري 0.1 ، pH=9.6.

2- أضيف (100) مايكروليتر لكل حفرة من محلول EDC / IgGوتم بأضافة الكلوبيولين المناعي البشري IgG بتركيز (100 مايكروغرام / 1 مللتر محلول دارئ الفوسفات من مادة (3 ملي مولار ،PH=6.3) (تمت إذابة (0.0408) غرام من KH2PO4 في (80) مللتر من الماء اللاأيوني وعدل الأس الهايدروجيني إلى PH=6.3 وإكمل الحجم إلى (100) مللتر بالماء اللاآيوني) وأضيف (5) ملغرام من مادة EDC لكل (1) مللتر من المحلول . وحضنت الصفائح لمدة 24 ساعة في (4) درجات مئوية.

3- أهمل ما بداخل الحفر وغسلت بالماء اللاآيوني ثلاث مرات واحتفظ بها في الثلاجة لحين الاستعمال .

الأختبارات :

تم اختبار كفاءة الربط بتطبيق تقانة الاليزا حسب طريقة فولر (Voller) (16) وبالاعتماد على مقترن (Conjugate) المتمثل بـ (Goat Anti-Human-IgG-HRP) مستورد من شركة Biokit الأسبانية. أجريت المقارنة مع اشرطة (strips) من شركة (Biomat) الايطالية

ذات كفاءة ربط عالية (Hiegh binding)، وتمت دراسة كفاءة الربط على الصفيحة للحفر الموجودة فيها. اذ استخدمت محاليل من عدة -HCV لشركة Biokit الاسبانية.

اجريت مقارنة كفاءة الربط للكلوبيولين المناعي (IgG) البشري المنقى بتراكيز مختلفة (0.15, 0.6, 2.5, 10, 20, 40) مايكروغرام/مللتر وتمت الاذابة بمحلول الربط المتمثل بدارئ (الكاربونات– بيكاربونات) الصوديوم (CBB) وبتراكيز مختلفة (0.05،0.2،0.1)مولاري وكلها بنفس الاس الهيدروجيني PH=9.6 وكمايلي:-

1- اخذت صفيحة دقيقة العيارية واضيف 100 مايكروليتر لكل حفرة من كل تركيز (تم استعمال حفرتان لكل تركيز من الكلوبيولين المناعي واعيد لكل تركيز مولاري لمحلول الربط كاربونات –بيكاربونات الصوديومCBB).

2- تم تحضين الصفيحتان لمدة 24 ساعة في (4) درجات مئوية.

3- اضيف محلول IgG/EDC أضيف الكلوبيولين المناعي البشري IgG بتركيز (100 مايكروغرام / 1 مللتر لمحلول دارىء الفوسفات الحاوي على (EDC) والمذكور بالفقرة 2 من خطوات العمل . وكانت الاضافة بحجم 100 مايكروليتر لكل حفرة وحضنت لمدة 24 ساعة في (4) درجات مئوية.

4- غسلت الحفر ثلاث مرات بمحلول الغسل الخاص بالعدة المستوردة.

5- اضيف (100) مايكروليتر من المقترن (Goat - Anti. Human - IgG HRP) المستورد من شركة Biokit بتخفيف (1/50) بمحلول التخفيف الخاص بالعدة المستوردة وحضن لمدة ساعة في درجة حرارة الغرفة.

6- غسلت الحفر ثلاث مرات بمحلول الغسل (كما في الخطوة (4)).

7- اضيف (100) مايكروليتر من المادة الاساس (المحضرة بمحلول المادة الاساس الخاص بالعدة المستوردة) لكل حفرة وحضنت بالظلام لمدة (30) دقيقة وبدرجة حرارة الغرفة.

8- أضيف (100) مايكروليتر من محلول ايقاف التفاعل الخاص بالعدة المستوردة لكل حفرة.

9- تمت قراءة الكثافة الضوئية على طول موجي (492) نانوميتر باستخدام جهاز الاليزا (ELISA - Reader).

النتائج والمناقشة

دراسة تاثير تركيز محلول الربط ((CBB) **Carbonate – Bicarbonate buffer**)على الامتصاصية بتقانة الألايزا ،اجريت هذه الدراسة لتحديد التركيز الامثل لمحلول الربط واظهر التركيز (0.1مولاري) لمحلول الربط قراءات الكثافة الضوئية عالية مقارنة بالتركيزين الاخرين، وقد اشارت بعض البحوث (25) الى استخدام التركيز (0.1 مولاري) كتركيز امثل بمدة تحضين ثلاث ساعات بدرجة (37) درجة مئوية.والنتائج موضحة في جدول رقم (1).

جدول –1: التحليل الاحصائي باختبار (t-test) لمعدلات الكثافة الضوئية للتراكيز المختلفة لمحلول الربط كاربونات– ثنائي الكاربونات (CBB)

التركيز المولاري لمحلول الربط(CBB)	معدل الكثافة الضوئية $\overline{X}$	± الانحراف المعياري SD	الاحتمالية
0.05	1.86	0.011	0.05 > P
0.1	2.102	0.043	
0.2	0.79	0.031	

والنتائج الاحصائية تؤكد وجود فرق معنوي (significant) باختبار (t-test) عند (tow-tailed) من الجداول الاحصائية المعتمدة بالاحصاء الحياتي، بينت التراكيز المستخدمة لمحلول الربط من خلال النتائج وحسابات الاحصاء الحياتي المعتمدة لتفسير النتائج العلمية نجد ان تطبيق تقانة الألايزا وقياس الامتصاصية باستخدام المحلول الدارىء كاربونات –بيكاربونات الصوديوم عند التركيز المولاري 0.1 هي اعلى من التركيز المولاري 0.05 وهذه اعلى من التركيز المولاري 0.2 ممايدل على ان زيادة التركيز المولاري او نقصانه يؤثر سلبا على النتائج في تثبيت البروتين (الكلوبيولين المناعي نوع جيIgG)المرتبط الى الصفيحة الدقيقة العيارية . ومن الشكل (1) يتبين ان التركيز المولاري (0.1) هو التركيز الامثل لمحلول الربط كاربونات –بيكاربونات الصوديوم (CBB)

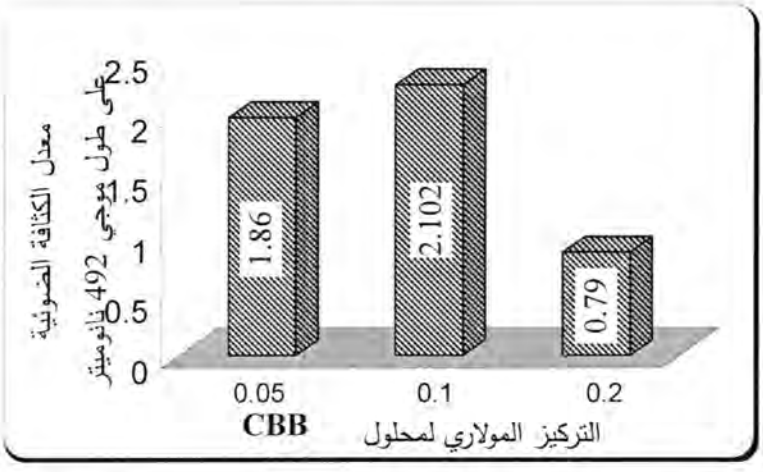

شكل-1: العلاقة بين التركيز المولاري لمحلول الربط والامتصاصية (الكثافة الضوئية) بتقانة الألايزا

والبحث أظهر نتائج جيدة بتطبيق تقانة الألايزا باستخدام مقترن (Conjugate) من عدة مستوردة، كانت الكثافة الضوئية عند طول موجي (492) نانوميتر بمعدل (1.516) باستخدام الشريط المستوردة والمرتبط بالحفر الكلوبيولين المناعي IgG.وبالمقارنة مع الصفيحة الدقيق العيارية والمصنوعة من متعدد الستايرين من نوع Maxisorp والتي ربطنا على سطح الحفر الكلوبيولين المناعي (IgG) البشري النقي كانت النتائج جيدة باختبار الألايزا مقارنتا مع المستورد. وبأستخدام تراكيز مختلفة من الكلوبيولين المناعي (IgG) النقي لتحديد افضل تركيز لعملية الربط، أجريت مقارنة لمعدلات الكثافة الضوئية للصفيحة التي ربط عليها الكلوبيولين والشريط المستورد واظهرت عدم وجود فرق معنوي (Not significant) بالتحليل الاحصائي باختبار (t-test) كما في الجدول (2). اذ تم ايجاد معامل الارتباط ($r = 0.99$) بأحصاء حياتي اعتمادا على جداول ثابته احصائيا وذلك يعني مقبولية الصفيحة المنشطة ومقاربة النتائج للشريط المستورد.

جدول -2 : يوضح معدلات الكثافة الضوئية للصفيحة المستخدمة والشريط المستورد لتراكيز مختلفة من الكلوبيولين المناعي IgG

تركيز الكلوبيولين المناعي IgG (مايكروغرام/ملتر)	معدلات القراءات للكثافة الضوئية $\overline{X}$ ± الانحراف المعياري

الشريط المستورد	الصفيحة المستخدمة	
0.006 ± 1.516	0.006 ± 1.492	40
0.005 ± 1.401	0.006 ± 1.398	20
0.008 ± 1.223	0.007 ± 1.187	10
0.005 ± 1.110	0.005 ± 0.106	2.5
0.009 ± 0.901	0.008 ± 0.863	0.6
0.007 ± 0.432	0.006 ± 0.319	0.15

المصادر

1- Ullman E.F And Maggio E.T, In "Enzyme Immunoassay", Ch.5, P. 105, Boca-Baton, Florida,(1980).

2- William N.Kelley ,M.D. and Shaun Ruddy,M.D,"Textbook of Rheumatology ",fifth Edition,Vol.1,chapter 16,p.241,(1997).

3- Hiroyuki Watanabe, Mitsuhiro Wakimasu and Koichi Kondo; A sensitive enzyme immunoassay for atrial natriuretic polypeptide ; J. of Immunol. Meth, 124, (25-28),(1989).

4- Farzana D. & Kai L. G. and Swee C. T.; Antibody immobilization on to polystyrene substrate-on-chip immunoassay for horse IgG based on fluorescence; Biomed Microdevices ,11:653–661,(2009).

5- L.A. Cantarero , J.E. Butler and J.W.Osborne ; The Adsrpative Characteristicsof proteins for polystyrene and their Significance in Solid –Phase Immunoassays; Analytical Biochemistry ,105,375-382,(1980).

6- Masahiro Sakaguchi ,Sakae Inouye and Shin-ichi Tamura ;Measurement of antigen –specific mouse IgE by a fluorometric reverse (IgE-capture)ELISA; J. of Immunol. Meth.;116,181-187. (1989).

7- A.Voller, A.Bartlett and D.E. Bidwell,Microplate enzyme immunoassay for the immunodiagnosis of virus infections ; J. of Clin. Patho. 31, 507-520, (1978).

8- Dhruvajyoti Roy, Ju-Won Kwak, Wan Joo Maeng, Hyungjun Kim, and Joon Won Park; Dendron-Modified Polystyrene Microtiter Plate: Surface Characterization with Picoforce AFM and Influence of Spacing between Immobilized Amyloid Beta Proteins; Langmuir 24, 14296-14305, (2008).

9- SIMONE VINCENZI, GIANNI ZOCCATELLI, FABIO PERBELLINI, CORRADO RIZZI;Quantitative Determination of Dietary Lectin Activities by Enzyme-Linked Immunosorbent Assay Using Specific Glycoproteins Immobilized on Microtiter Plates ; J. Agric. Food Chem, 50, 6266-6270 , (2002).

10- Francoise Megret ,Jean- Luc Guesdon and Joseph E.Alouf ;Solid Phase Enzyme Immunoassay of Pertussis Toxin Using Peroxidase or Biotin Labelled Antibodies; J. of Immunoassay ;8(1),43-71 ,(1987).

11- Heyun Shen, Junji Watanabeand Mitsuru Akashi,;Polyelectrolyte Multilayers-Modified Polystyrene Plate Improves Conventional Immunoassay: Full Covering of the Blocking Reagent ;Anal. Chem., 81, 6923–6928, 2009.

12- Robert J. Edwards, Alison M. Singleton, Alan R. Boobis and Donalds Davies; Cross-reaction of antibodies to coupling groups used in the production of anti-peptide antibodies ; J. of Immunol. Meth. ; 117,p. 215-220,(1989).

13- Mark Suter, A modified ELISA Technique for Anti-Hapter Antibodies; J. of Immunol. Meth; 53, 103-108,(1982).

14- Wilchee, M. and Bayer, E. A, In "Methods In Enzymology", 184, P.127, (1990).

15- LYN R. BRIGGS, CHRISTOPHER O. MILES and JOAN M. FITZGERALD ; Enzyme-Linked Immunosorbent Assay for the Detection of Yessotoxin and Its Analogues; J. Agric. Food Chem., 52, 5836-5842, (2004).

16- R.A.Thompson;"Techniques in Clinical Immunology ",oxford ,p.157 , (1981).

17- P.Tijssen, In "Laboratory Techniques In Biochemistry and Molecular Biology", Vol. 15, Printed in the Netherlands;(1985).

18- J.Frei, C., Heuck, P,G. Hill, M.M. El. Nageh, L. Pollor, W. Riesen and H. Lang, In "Production Of Basic Diaghnostic Laboratory Reagents", WHO Printed In Egypt.,(1995).

19- C. Michael Lederer and Virginia S. Shirley, In "Table Of Isotopes", 7th Ed., P. 177, Printed In The United States of America, (1978).

20- Farhatazis S. and Michael A.J. Rodgers, In "Radiation Chemistry", VCH-American, P. 468, (1987).

دراسة الظروف الخاصة بتقانة الاليزا

*حسين بديع جرجيس و **رضا ابراهيم البياتي و ***اكتفاء مزهر عبد

*و *** وزارة العلوم والتكنلوجيا

** قسم الكيمياء –كلية العلوم – الجامعة المستنصرية

تاريخ تقديم البحث : 2011/ 3/24 تاريخ قبول البحث : 2011/ 5/29

ABSTRACT

Pupose of study the Optimal Solutions Conditions which cancer and diagnostic medical kits in ELISA technique that depending on solvents with comparison study between same standard .Based on the associated link (Goat-Anti-Human-IgG-HRP). Study includin. the effect of incubation time during the coating ELISA fond significant difference (0.05>P) between the period of incubation(12 hours) time. The effect of temperature during the incubation time of the coating operation on the absorbance of the ELISA technology and proud tile the (4C°) given optional absorbent. The effect of concentration detergent with washing solution of ELISA the result explain no significant between (Tween-20) and (Triton X-100) for the Optical density and the optimal concentration for the addition detergent (0.05%) the increasing of the detergent concentration that decreasing of the ability of conceiting and the effect of (H2O2) concentration in ELISA showed the volume (50)µl for (5)ml of the substrate (citrate buffer 0.1M,pH=5.0) is optimal

الخلاصة

هدفت دراسة الظروف المثلى للمحاليل الخاصة بالعدد الطبية التشخيصية لتقانة الألايزا وقورنت مع بعض محاليل لعدة مستوردة (كمحاليل قياسية (Standards) اعتمدت الطريقة على ربط المقترن المسمى (Goat-Anti-Human-IgG-HRP). وتركزت الدراسة بمايلي : دراسة تاثير مدة التحضين اثناء الربط لتقانة الالايزا اذ تبين وجود فرق معنوي (0.05>P) بين مدة التحضين (12 ساعة) وفترات التحضين الاخرى، دراسة تاثير درجة الحرارة اثناء مدة التحضين لعملية الربط على الامتصاصية بتقانة الالايزا و تبين ان الدرجة الحرارية (4) درجات مئوية

اعطت امتصاصية جيدة،، دراسة تاثير نوع المنظفات وتراكيزها بمحلول الغسل في تقانة الالايزا أظهرت النتائج عدم وجود فرق معنوي (Not significant) بين المنظف Tween-20 والمنظف Triton x-100 لقراءات الكثافة الضوئية والتركيز الامثل للمنظف المضاف (0.05%) أما الزيادة في تركيز المنظف فانها تقلل من كفاءة الربط ، وبدراسة تاثير تركيز H_2O_2 بتقانة الالايزا اظهرت النتائج ان الحجم (50) مايكروليتر لكل (5) مللتر من محلول المادة الاساس (دارئ الستريت 0.1 مولاري ,pH=5.0) هو الأمثل.

المقدمة

بدأت تقانة الألايزا عام 1971 من قبل (Engvall and Perlmann) (1) وتطورت التقانة عام 1981 لاسيما عند اكتشاف مرض الإيدز في فرنسا.

تعرف هذه التقانة الطبية بأنها التقدير الكمي والنوعي لكميات قليلة جدا من المستضدات أو الأضداد في أطباق فيها فتحات دقيقة العيارية تسمى بالصفائح الدقيقة العيارية (Microtitre Plates) ويمكن الكشف عن (5) نانوغرام من المستضد أو الضد لكل مللتر من العينة بهذه التقانة (2).

استعملت تقانة الألايزا في العديد من العلوم الطبية لتشخيص الحالات المرضية فضلاً عن تحديد البروتينات كمياً ونوعياً وبتراكيزها الواطئة في الحالات المبكرة لأمراض علم الغدد الصماء Endocrinology بقياس تركيز الهورمونات وتقدير كميتها بالجسم يتم أستخدام تقانة الألايزا مثل: قياس هرمون HCG (Human Chorionic Gonadotrophin) (3) ، وهرمون LH (Luteinising Hormone) (4) ،وهرمون (Human Placental Lactogen) HPL (5).

وفي أدلة الكشف عن السرطان للتقصي عن بعض البروتينات كأدلة للكشف عن السرطان (6)، وفي علم الامراض المناعية وكمثال عليها تشخيص المعقدات المناعية الناتجة من الأضداد الذاتية مثل العامل الرثياني المسبب لألتهاب المفاصل (7).

تستعمل المنظفات في محاليل الغسل بتحليل الألايزا للتخلص من الكواشف غير المرتبطة مع السطح الصلد (8) وفي محاليل الغلق (blocking) ، والمنظفات جزيئات حاوية على جزء محب للماء (Hydrophilic) وجزء كاره للماء (Hydrophopic) وقد تكون المنظفات ايونية

مثل(SDS) أو لاأيونية مثل(Tween-20) (9) .وكل المنظفات تمنع مسك البروتينات إلى السطح الصلد في حالة استخدامها بمحاليل الربط (10) .

المواد وطرائق العمل

اجريت دراسة تاثير بعض العوامل المثبتة على معدل الكثافة الضوئية (الامتصاصية) بتقانة الألايزا، وتم الاعتماد على ربط المقترن المستورد (Goat-Anti-Human-IgG-HRP) بتخفيف 1/50 على الصفيحة الدقيقة العيارية لدراسة الظروف المثلى وتثبيت الامثل.

اولا: دراسة تأثير مدة التحضين اثناء الربط على الامتصاصية بتقانة الالايزا:-

حضر المقترن المستورد بتخفيف 1/50 بتركيز (0.1 مولاري) بمحلول الربط (كاربونات-بيكاربونات الصوديوم)، واضيف (100) مايكروليتر لكل حفرة (8-حفر) من كل صفيحة ولأربع صفائح دقيقة العيارية. وتم تحضين الصفائح في الثلاجة بأوقات مختلفة (12, 24, 48, 72) ساعة كل وقت من الأوقات المذكورة محددة بصفيحة من الصفائح الاربعة واكملت الطريقة بالخطوات التالية:

1- تم تحضين الصفيحة والشريط لمدة 24 ساعة في (4) درجات مئوية.
2- غسلت الحفر ثلاث مرات بمحلول الغسل الخاص بالعدة المستوردة.
3- اضيف (100) مايكروليتر من المقترن (Goat - Anti. Human - IgG HRP) المستورد من شركة Biokit بتخفيف (1/50) بمحلول التخفيف الخاص بالعدة المستوردة وحضن لمدة ساعة في درجة حرارة الغرفة.
4- غسلت الحفر ثلاث مرات بمحلول الغسل (كما في الخطوة (2)).
5- اضيف (100) مايكروليتر من المادة الاساس (المحضرة بمحلول المادة الاساس الخاص بالعدة المستوردة) لكل حفرة وحضنت بالظلام لمدة (30) دقيقة وبدرجة حرارة الغرفة.
6- أضيف (100) مايكروليتر من محلول ايقاف التفاعل الخاص بالعدة المستوردة لكل حفرة.
7- تمت قراءة الكثافة الضوئية على طول موجي (492) نانوميتر باستخدام جهاز الالايزا (ELISA - Reader).

ثانيا: دراسة تاثير درجة الحرارة اثناء مدة التحضين على الامتصاصية بتقانة الاليزا:

تمت اعادة الفقرة (اولا) باستخدام ثلاث صفائح منشطة باشعة كاما-CO^{60} وبعد الربط بدرجات حرارية مختلفة (4 ،37) درجة مئوية ودرجة حرارة المختبر (22) درجة مئوية وكل صفيحة من الصفائح الثلاثة حضنت بدرجة حرارية مختلفة. واكملت الطريقة بالفقرة (اولا) نفسها.

ثالثا: دراسة تاثير تركيز H_2O_2 بمحلول المادة الاساس على الامتصاصية بتقانة الاليزا:-

تم استخدام حجوم مختلفة من H_2O_2 بتركيز 6%.

تم اخذ صفيحة دقيقة العيارية وربط عليها المقترن (Conjugate) المستورد المحضر 1/50 بمحلول الربط (كاربونات-بيكاربونات الصوديوم), (0.1مولاري, pH=9.6) . (ولأربعة اعمدة بالصفيحة)، حضنت الصفيحة لمدة 24 ساعة في (4) درجات مئوية وبعدها غسلت حفر الصفيحة بمحلول الغسل الخاص بالعدة المستوردة ثلاث مرات،حضرت المادة الاساس (OPD) بمحلول دارئ الستريت (0.1 مولاري, pH=5.0) قبل الاستعمال مباشرة باذابة (4) ملغرام من مادة OPD في (5) مللتر من محلول المادة الاساس (دارئ الستريت) في انبوبة اختبار (حضرت اربعة انابيب اختبار) واضيف لكل انبوبة اختبار حجم مختلف من H_2O_2 تركيزه (6%) والحجوم المضافة (70, 50, 30, 10) مايكروليتر ،

تم استخدام عمود (8-حفر) لكل انبوبة اختبار المضاف لها حجم معين من H_2O_2وأضيف (100) مايكروليتر لكل حفرة،حضنت الصفيحة بالظلام مدة (30) دقيقة، اضيف (100) مايكروليتر لكل حفرة من محلول ايقاف التفاعل الخاص بالعدة المستوردة، تمت قراءة الكثافة الضوئية على طول موجي (492) نانوميتر بجهاز الاليزا (ELISA-Reader).

رابعا: دراسة تاثير تركيز المنظفات وانواعها:-

استخدم المنظف Tween-20 والمنظف Triton x-100 وحضر لكل منهما حجمان مختلفان.

تم تقسيم محلول الغسل الى اربعة اقسام واضيف المنظف كما يلي:-

1- الحجم (250) مللتر اضيف حجم (125) مايكرولتر من المنظف Tween-20 بنسبة مئوية (0.05%).

والحجم (250) مللتر ثاني اضيف حجم (250) مايكرولتر من المنظف Tween-20 بنسبة مئوية (0.1%).

وللحجمين الاخيرين اضيف المنظف TritonX-100 وبتراكيز Tween-20 نفسها.

2- تم اخذ صفيحة دقيقة العيارية واضيف المقترن المستورد المخفف 1/50 بحجم (100) مايكروليتر لكل حفرة وحضنت الصفيحة لمدة 24 ساعة في (4) درجات مئوية.

3- غسلت الحفر للعمود (1 ، 2) بمحلول الغسل الذي يحتوي على المنظف Tween-20 بتركيز 0.05% و 0.1% على التوالي وحضر العمود (3،4) الذي يحتوي على المنظف Triton X-100 بالتركيز (0.05% و 0.1%).

4- اضيف **(100)** مايكروليتر من المادة الاساس المحضرة مباشرة لكل حفرة وحضرت المادة الاساس **(OPD (0.4)** ملغرام +**(5)** مللتر من محلول المادة الاساس (دارئ الستريت) +**(50)** مايكروليتر من H_2O_2**)**.

5- حضنت الصفيحة مدة 30 دقيقة في درجة حرارة الغرفة.

6- اضيف (100) مايكروليتر لكل حفرة من محلول ايقاف التفاعل.

7- تم قياس الكثافة الضوئية على طول موجي (492) نانوميتر بجهاز الالايزا (ELISA-Reader).

النتائج والمناقشة

اولا: دراسة تأثير مدة التحضين اثناء الربط على الامتصاصية بتقانة الالايزا:-

اجريت هذه الدراسة لمعرفة مدة التحضين المثلى للربط وبينت النتائج ان المدة 24 ساعة هي المثلى واذا زادت مدة التحضين فانها تعطي امتصاصية مقاربة للمدة المثلى المحددة واختصاراً للوقت فان 24 ساعة كافية لحدوث عملية الربط لانها اعطت نتائج جيدة في هذه الدرجة.

وتبين وجود فرق معنوي (0.05>P) بين مدة التحضين (12 ساعة) وفترات التحضين الاخرى. ولايوجد فرق معنوي بين الأوقات الثلاثة الاخيرة، والشكل (1) يوضح العلاقة بين معدل الكثافة الضوئية ومدة التحضين لعملية الربط.

جدول -1: يبين التحليل الاحصائي باختبار (t-test) لفترات التحضين المختلفة لعملية الربط بتقانة الاليزا

ت	مدة التحضين (ساعة)	معدل الكثافة الضوئية $\overline{X}$	± الانحراف المعياري SD	الاحتمالية
1	12	0.988	0.021	0.05 > P
2	24	2.181	0.018	
3	48	2.169	0.07	
4	72	2.144	0.104	

ثانيا: دراسة تاثير درجة الحرارة اثناء مدة التحضين لعملية الربط على الامتصاصية بتقانة الاليزا:-

أظهرت اغلب الدراسات ان التحضين بدرجة (4) درجة مئوية هو الافضل, والنتائج التي تم الحصول عليها ايضا بينت ان الدرجة الحرارية (4) درجات مئوية اعطت امتصاصية جيدة، ودرجات الحرارة العالية تؤثر في الغالب على الجزيئات الحياتية المراد ربطها على السطح [12]. كما في الجدول (2).

جدول -2 : يوضح معدل الكثافة الضوئية لدرجات حرارية مختلفة اثناء مدة التحضين لعملية الربط بتقانة الاليزا

ت	درجة الحرارة (درجة مئوية)	معدل الكثافة الضوئية $\overline{X}$	± الانحراف المعياري SD	الاحتمالية
1	4	2.152	0.032	0.05 > P
2	22	1.815	0.023	
3	37	0.733	0.021	

يتبين من الجدول أعلاه وجود فرق معنوي (significant) والاحتمالية P<0.05 عند (Two - tailed)،

ثالثا: دراسة تاثير تركيز H_2O_2 بتقانة الالايزا:-

ان انزيم HRP يعمل بنظام بيروكسيد الهايدروجين H_2O_2 وبوجود المادة الاساس للانزيم يظهر التغير اللوني . واظهرت النتائج ان الحجم (50) مايكروليتر لكل (5) مللتر من محلول المادة الاساس (دارئ الستريت 0.1 مولاري ,pH=5.0).

وبوجود 4 ملغرام من المادة الاساس (OPD) هو الافضل لاعطاء امتصاصية جيدة بعد مدة تحضين 30 دقيقة في الظلام. والنتائج مبينة كما في الجدول (3)، اذ يتضح ان هناك فرقاً معنوياً P<0.05 والتي تم حسابها احصائيا من جداول معتمدة من احصائيات(t-test) وعند 95%، وبأخذ (70) مايكروليتر من H_2O_2 يوجد معدل كثافة ضوئية عالٍ الا ان الكفئ (Blank) عالٍ أيضاً اذ ظهرت الكثافة الضوئية (0.835) وتلك القراءة تسبب نسبة خطأ لذا يستبعد التركيز العالي لبيروكسيد الهيدروجين (H_2O_2) ويثبت الحجم (50) مايكروليتر كتركيز امثل، والشكل (3) يوضح تأثير H_2O_2 على معدلات الكثافة الضوئية لتقانة الالايزا.

جدول -3 : التحليل الاحصائي باستخدام اختبار (t-test) لمعدلات الكثافة الضوئية لحجوم مختلفة من H_2O_2 (6%)

حجم H_2O_2 (%6)(مايكروليتر)	معدل الكثافة الضوئية $\overline{X}$	معدل الكثافة الضوئية للكفئ (Blank)	± الانحراف المعياري SD	الاحتمالية
10	0.415	0.002	0.013	0.05 > P
30	0.945	0.013	0.014	
50	2.13	0.019	0.008	
70	2.981	0.835	0.0131	

رابعا: دراسة تاثير نوع المنظفات وتراكيزها بمحلول الغسل في تقانة الالايزا:-

بينت النتائج عدم وجود فرق معنوي (Not significant) بين المنظف Tween-20 والمنظف Triton x-100 لقراءات الكثافة الضوئية والتركيز الامثل للمنظف المضاف (0.05%) أما الزيادة في تركيز المنظف فانها تقلل من كفاءة الربط ، والنتائج مبينة في الجدول (4).

جدول -4: يبين التحليل الاحصائي باستخدام اختبار (t-test) لمعدل الكثافة الضوئية للمنظفات المستخدمة بتراكيز مختلفة

الاحتمالية	Triton x-100		Tween x-20		التركيز %
0.05 < P	± SD	$\overline{X}$	± SD	$\overline{X}$	
	0.06	2.154	0.056	2.136	0.05
	0.012	1.401	0.019	1.39	0.1

من النتائج المتقدمة اظهر اختبار (t-test) للتحليل الاحصائي للتراكيز 0.05% و 0.1% وجود فرق معنوي باحتمالية 0.05>P، ولايوجد فرق معنوي بين المنظفين،

المصادر

1- Hiroyuki Watanabe, Mitsuhiro Wakimasu and Koichi Kondo,A sensitive enzyme immunoassay for atrial natriuretic polypeptide J. of Immunol. Meth., 124, (25-28). (1989).

2- FENG-YIH YU, YUEH-HUI LIN, AND CHING-CHYUAN SU ; A Sensitive Enzyme-Linked Immunosorbent Assay for Detecting Carcinogenic Aristolochic Acid in Herbal Remedies ; J. Agric. Food Chem., 54, 2496-2501, (2006).

3- M.H. Boma and G. Bilkei ; Field experiences with early pregnancy diagnosis by progesterone-based ELISA in sows ;J.of Vetrinary Research,Vol.75,No.1,(2008).

4- J.A. Valares, J.A. Abecia, F. Forcada, Palac ın, L. Mata and P. Razquin; Development of a Simple Enzyme Immunoassay for the Determination of Ovine Luteinizing Hormone; Veterinary Research Communications, 31 ,427–436, (2007).

5- Tino J. Evariste Gafumbegete and Jan Gramberg ; Differential proteome analysis of tonsils from children with chronic tonsillitis or with hyperplasia reveals disease-associated protein expression differences ; Anal Bioanal Chem ,384: 1134–1144, (2006).

6- Shi-Rong H., Jia-Ming L., Tian-Long Y., Hai-Zhu L. and Jun-Li H.; Determination of Human Alpha-Fetoprotein (AFP) by Solid Substrate Room Temperature Phosphorescence Enzyme-Linked Immune Response Using Luminescent Nanoparticles ; Microchim Acta 152, 53–59 (2005).

7- Jonsson T.,Arnason JA and Valdimarsson H. ; Enzyme linkedimmunosorbent assay (ELISA)screening testfor detection of rheumatoid factor; Rheumatol Int ,6:199-201,(1986).

8- Andriej G. and Aleksandra L., Gearing and Thorpe, Coating of proteins to polystyrene ELISA plates in the presence of detergents, J. of Immunol. Meth. 106, 251-255, (1988).

9- Christopher R. Bird, Andrew J.H.,The use of Tween 20 alone as ablocking agent for immunoblotting can cause artefactual results J. of Immmunol. Meth., 106, 175-179. (1988).

10- Jhon J. Lagone and Helen Van Vunakis, In "Methods In Enzumology", Vol. 73, Part B. Academic Press, New York. (1981).

تقييم استخدام الطريقة الحركية في حساب السرعة الرأسية في العراق

سما خالد محمد

الجامعة المستنصرية-كلية العلوم-قسم علوم الجو

تاريخ تقديم البحث : 7 /4 /2011 تاريخ قبول البحث : 5/29 /2011

ABSTRACT

This study aims to calculate the vertical velocity of the air using the method of kinetic equation using continuity equation through the use of horizontal wind data for the surface layer of the atmosphere with its two components (U, V) and the calculation of the divergence using finite differences method by using Taylor theory. The data included the regions of Iraq and some parts of neighboring areas in the form of data grid extending from the longitude (37° 5 '- 49° E) and from the latitude (37° 5' - 27°N) and the distance between each two chosen points on the grid was (1.5°) and was for the first day of the months of January and July and for four times of observations (00, 06, 12, 18) UTC. Contour maps were drawn to the data obtained from the European site and the calculated in this study for the vertical velocity to determine the compatibility between them. It has been observed from these maps that there is a consensus in how the vertical velocity moves and not in the quantity (magnitude of speed) and this situation was more pronounced in the month of July compared to January. As for the effect of time monitoring the behavior of vertical velocity was compatibility between the behavior of velocities obtained from the ECMWF and considerably in all observations except the selected time of observation 06UTC where it was the consensus average. For the magnitude of the calculated vertical velocities have found results that this method involving ratios error in the calculation of the magnitude of vertical velocity, has been attributed to the fact that the calculated value of the velocity of the vertical at the level Pressure 1000 hPa very close to the surface of the earth (at a height of 100 m) and it is therefore very sensitive to errors in the boundary layer . Also, the equation used to calculate the vertical velocity in this study are subject to the conditions suit the fluid incompressible and non-homogeneous and this is not compatible with the air, which is the fluid compressible and homogeneous. In addition to the elliptical shape of the earth was a cause of error in calculating the distances between the meridians. Therefore, this

سما

method is somewhat succeeded in giving a description of the attitude of vertical velocity but was not successful in the calculation of the magnitude accurately. Therefore recommended to use other ways to calculate the magnitude of vertical velocity and compare it with what has been reached in this study.

الخلاصة

تهدف هذه الدراسة الى حساب السرعة الرأسية للهواء باستخدام الطريقة الحركية من خلال معادلة الاستمرارية باستخدام بيانات الرياح الافقية لطبقة الجو السطحية بمركبتيها (U,V) وحساب التباعد بطريقة الفروقات المركزية المحددة باستخدام نظرية تايلور . وشملت البيانات مناطق العراق وبعض اجزاء المناطق المجاورة على شكل شبكة معلومات تمتد من خط طول (37°5' – 49° E) ومن خط عرض (37°5' – 27° N) وكانت المسافة بين كل كل نقطتين مختاريتن على الشبكة هي 1.5° وكانت لليوم الاول من شهري كانون الثاني وتموزولاربع رصدات وهي (00,06,12,18)UTC . تم رسم خرائط كنتورية للبيانات المستحصلة من الموقع الاوربي والمحسوبة في هذه الدراسة للسرع الرأسية لمعرفة مدى التطابق بينهما. وقد لوحظ من تلك الخرائط ان هناك توافق في الكيفية التي تتحرك بها الرياح الرأسية وليس في الكمية (مقدار السرعة) وكانت هذه الحالة اكثر وضوحا في شهر تموز مقارنة بشهر كانون الثاني . اما بالنسبة لتاثير وقت الرصد على سلوك الرياح الرأسية فقد كان التوافق بين سلوك السرع المستحصلة من الموقع الاوربي والمحسوبة كبيرا في جميع الرصدات المختارة ما عدا وقت الرصد 06 UTC الذي كان فيه مدى التوافق متوسط . بالنسبة لمقدار السرع الرأسية التي تم حسابها فلقد تبين من النتائج ان هذه الطريقة تتضمن نسب خطأ في حساب مقدار السرعة الرأسية ، وقد تعزى الى كون القيمة المحسوبة للسرعة الرأسية عند المستوى الضغطي 1000 hPa قريبة جدا من سطح الارض (على ارتفاع 100 m) ولهذا فهي حساسة جدا للاخطاء الصغيرة في رياح الطبقة المحاددة . كما ان المعادلة المستخدمة لحساب السرعة الرأسية في هذه الدراسة تخضع لشروط تلائم المائع الغير قابل للانضغاط والغير متجانس وهذا لا يتوافق مع الهواء الذي يعد مائع قابل للانضغاط ومتجانس . اضافة الى ان شكل الارض البيضوي كان سببا في احداث نسبة خطأ في حساب المسافات بين خطوط الطول .

وعليه فان هذه الطريقة نجحت بشكل ما في اعطاء وصف لسلوك الرياح الرأسية ولكنها لم توفق في حساب مقدارها بشكل دقيق . لذا يوصى باستخدام طرق اخرى لحساب مقدار السرعة الرأسية ومقارنتها مع ما تم التوصل اليه في هذه الدراسة.

المقدمة

ان سرعة الرياح الرأسية ليست متغير مقاس في الانواء الجوية ، ويعد حسابها احدى اصعب المشكلات . وتمثل احد المركبات الثلاثية الابعاد لحركة الغلاف الجوي (1) . وقد يعزى سبب تكونها الى التسخين المباشر لطبقة الهواء القريبة من سطح الارض ، او التباعد او التقارب الافقي للرياح (divergence or convergence) عند كل المستويات الضغطية حيث انه لاتوجد امكانية لتراكم الهواء لدى تقاربه مما يؤدي الى صعوده نحو الاعلى ولا يكَون فراغا عند تباعده مما يؤدي الى نزوله الى الاسفل (2) ، او قد تنشأ بسبب تعرجات سطح الارض عند مستوى سطح البحر (مثل المناطق الجبلية) ، او بسبب احتكاك سطح الارض (مثل اليابسة والماء والغطاء النباتي والمناطق الصحراوية) وقد تنشأ بسبب تقدم الجبهة الهوائية الباردة (3) .

يعد حساب الرياح الرأسية مهم جدا نظرا لتأثيرها الكبير على الطقس اليومي ، فلها دور في تكون الغيوم والغبار حيث تحمل بخار الماء الى الاعلى فيتكاثف نتيجة التبريد الذاتي فيتحول الى قطيرات تتكون منها الغيوم والهطول اعتمادا على كمية الرطوبة . اما دورها في الغبار فالرياح الرأسية تعتبر المسبب الرئيسي له اذا توفرت العوامل الاخرى مثل تفكك التربة وجفافها وضعف الغطاء النباتي ، والرياح الرأسية لا تعمل على تصاعد الغبار وشدته فقط وانما تتحكم في فترة بقاءه في الجو ايضا (3) .

تقاس سرعة الرياح الرأسية في المحاور الكارتيزية (w) بوحدات (m/s) بينما في المحاور الضغطية (ω) والتي يتم فيها استبدال محور z بمحور الضغط p بوحدات ($hpa . hr^{-1}$) وتتراوح قيمتها بين (1-10)cm/s مع الاعتبار ان قيمتها تعتبر صفرا عند سطح الارض (2) .

يمكن الحصول على معلومات عن الرياح على ارتفاعات معينة باستخدام الراديوسوند الذي يحمل بواسطة بالون يرتفع عن سطح الارض (وهوجهاز مصمم لقياس الحرارة، الضغط والرطوبة). المعدات المثبتة على سطح الارض تتبع البالون وتقيس الزوايا الافقية والعمودية للبالون وارتفاعه عن سطح الارض . ومن هذه المعلومات يقوم جهاز الكومبيوتر بحساب وطباعة المقطع العمودي للرياح

سما

من سطح الارض وحتى اخر ارتفاع يصل اليه الجهاز (نموذجيا يصل الى الستراتوسفير قرب 30) km . وتسمى الرصدة المستحصلة من بالون الراديوسوند برصدة الراون سوند Rawinsonde observation .

اما في المناطق النائية في العالم والتي تقل فيها الرصدات الخاصة بطبقات الجو العليا ، فانه يمكن قياس سرعة الرياح واتجاهها عن طريق الاقمار الصناعية والى حد ما فان بيانات الرياح الاكثر موثوقية يمكن الحصول عليها من خلال الاقمار الثابتة Geostationary satellites والتي توضع فوق موضع معين . وبالنسبة الى هذا الموضع فان الاقمار الصناعية تظهر حركة السحب. اتجاه حركة السحب يشير الى اتجاه الرياح ، والمسافة الافقية التي تقطعها السحب خلال وقت معين تشير الى سرعة الرياح . مؤخرا ، تم توظيف رادار دوبلر Doppler radar للحصول على مقطع عمودي لسرعة الرياح واتجاهها فوق 16 km عن سطح الارض . ويسمى برصدة الرياح wind sounding . يبعث رادار دوبلر نبضات من الاشعة المايكروية والتي ترجع من الهدف ، ويعمل على مبدأ حركة الدوامات المضطربة والتي تتحرك مع الرياح والتي ينشأ عنها قيم غير قياسية للحرارة والرطوبة ، وهذه الدوامات تتحرك باتجاه او بعيدا عن هوائي الاستلام ، ان نبضات الرادار العائدة سيتغير ترددها ، ويمكن ترجمة الانحراف في التردد العائد من هذه الدوامات وتحويلها الى صورة عمودية لسرعة الرياح واتجاهها لعمود هواء بسمك 16km (4) .

هناك عدة طرق لحساب السرعة الرأسية نذكر منها (4) :

الطريقة الحركية kinematic method : وهي الطريقة الاسهل وتكون باستخدام التكامل لمعادلة الاستمرارية continuity equation باستخدام رصدات الرياح الافقية لمقياس كبير وحساب تصحيح التباعد divergence correction . وتعد قلة الرصدات وعدم الدقة في قياسات الرياح سببا في نشوء اخطاء كبيرة في حساب السرعة الرأسية .

الطريقة الاديباتيكية adiabatic method : والتي تعتمد على الطاقة الحرارية وهذه الطريقة غير حساسة كثيرا للاخطاء في قياسات الرياح . ويمكن حساب التغير الافقي للحرارة وتكون النتائج الى حد ما دقيقة باستخدام الرياح الجيوستروفيكية خصوصا في مناطق العروض الوسطى . ويمكن توظيف هذه الطريقة عند توفر بيانات الحرارة والارتفاع الجهدي ، ومع ذلك فان هذه الطريقة تتضمن

ميل الحرارة ولا يوصى باستخدامها لمنطقة واسعة الا اذا كانت الرصدات ليست متفاوتة زمنيا تفاوتا كبيرا .

طريقة الحركة اللولبية vorticity : وهي صيغة مبسطة لمعادلة الحركة اللولبية، ويهمل في هذه الطريقة كل من التغير العمودي للحركة اللولبية والالتوائية (twisting) ، اما الحركة اللولبية فيفترض ان تكون قيمتها صغيرة مقارنة بمؤشر كوريولس (coriolis parameter) عند التباعد. ويمكن حساب التغير الزمني والافقي للحركة اللولبية الجيوستروفيكية بدقة مما يؤدي الى ان حساب السرعة الرأسية باستخدام هذه الطريقة يكون اكثر مصداقية مقارنة بطريقة الطاقة الحركية.

استخدام معادلة الشبه جيوستروفيكية quasi-geostrophic omega: ويتم حساب السرعة الرأسية بشكل دقيق باستخدام القيم الآنية للارتفاع الجهدي. ولا تتطلب هذه الطريقة رصدات للرياح ولا تأخذ التغيرات الزمنية بنظر الاعتبار مما يجعلها الطريقة الاقوى بين الطرق المذكورة مسبقا .

هناك دراسات عديدة بحثت في امكانية حساب السرعة الراسية سواء باستخدام المعادلات المذكورة سابقا او باستخدام بيانات الرياح من خلال اجهزة كالراديوسوند والدروب سوند (Dropsonde). تناولت الابحاث التي قام بها معظم الباحثين في العراق الرياح الرأسية لمعرفة تأثيراتها السلبية على المناخ كالعواصف الغبارية او لايجاد تفسيرات لنشوء وانتهاء العواصف الترابية او لتوليد الطاقة الكهربائية عبر التوربينات (اي باستخدام طاقة الرياح) او لارتباطها بحالات الطقس الاخرى . ففي عام 1994 قام الجبوري بدراسة الحركة الراسية في العراق وربطها مع حالات الصحو والغيوم والامطار والغبار واستخدم الطريقة الحركية والطريقة العددية في حسابها وتوصل الى ان الطريقة الحركية تعطي نتائج غير مشجعة في التعبير عن الحالات الجوية مقارنة بالطريقة العددية (3). و في سنة 1997 قام Angevine بقياس السرعة الرأسية بواسطة UHF wind-profiling radars واظهرت دراسته وجود نسب خطأ في متوسط السرع الراسية المقاسة (5) . وفي سنة 2003 قام Jagannadha Rao وجماعته برصد متوسط السرعة الراسية وتغيراتها بواسطة الرادار الهندي المسمى mesosphere–stratosphere–troposphere (MST) عند محطة Gadanki وقاموا بعمل مقارنة بين رصدات الرادار والقيم المحسوبة بالطريقة الحركية والاديباتيكية مستخدمين بيانات الراديوسوند ، وكانت النتيجة ان اشارات الحركة الرأسية المحسوبة من الطريقة الحركية تتفق مع رصدات الرادار بالرغم من القيم تختلف باستثناء منطقة صغيرة تكون فيها السرع الرأسية متغيرة الاشارة من سالب الى موجب في الطبقة السفلى من التربوسفير خلال موسم

سما

الرياح الموسمية ، اما بالنسبة للطريقة الاديباتيكية فان السرع الراسية المحسوبة كانت صغيرة (6) . وفي سنة 2009 قام الباحث Junhong وجماعته بدراسة امكانية حساب السرعة الرأسية للهواء من سطح الارض وحتى الستراتوسفير باستخدام بيانات واسعة مستحصلة من الراديوسوند والدروب سوند dropsonde (هو جهاز استكشاف جوي تم استحداثه من قبل المركز الوطني للابحاث الجوية National Center for Atmospheric Research (NCAR) ، وصمم ليتم القاءه من طائرة على ارتفاع ما للحصول على قياسات اكثر دقة لتتبع ظروف العاصفة المدارية من خلال نزوله الى الارض (7)) . وهذه الدراسة ايدت هذه الطريقة في ان تستمد السرعة الرأسية من بيانات الراديوسوند والدروب سوند واظهرت قيمها . وبعمل مقارنة بين بيانات الراديوسوند ، الدروب سوند ، الطائرة و قيمة المقطع العمودي للرياح باستخدام الرادار اثبتت ان هذه الطريقة قادرة على وصف الحالات المرافقة للحركة الراسية القوية (الاكبر من 1 m/s) . اما السرع الرأسية تحت 5 km فوق سطح الارض تم قياسها بواسطة الراديوسوند . ومن خلال قيم السرع الراسية التي تم استنتاجها اظهرت هذه الدراسة معالم مثيرة للاهتمام لموجات الجاذبية gravity waves والاضطرابية turbulence (8) .

تهدف هذه الدراسة الى حساب السرعة الرأسية من خلال الطريقة الحركية kinematic method باستخدام معادلة الاستمرارية والتي تمثل الصيغة الرياضية لقانون حفظ الكتلة (conservation of mass) باستخدام بيانات الرياح الافقية لطبقة الجو السطحية بمركبتيها (U,V)وحساب التباعد بطريقة الفروقات المركزية المحددة باستخدام نظرية تايلور .

وباستخدام المعادلة المذكورة آنفا وباستخدام طريقة الفروقات المركزية المتناهية finite difference method تم ايجاد قيم تغير سرع المركبات الافقية بالنسبة للمسافة $\frac{\partial u}{\partial x}, \frac{\partial v}{\partial y}$

وبايجاد مجموعهما ثم ايجاد التكامل تم حساب قيمة السرعة الرأسية w .

الاسس النظرية لحساب السرعة الرأسية بالطريقة الحركية

ان قيم سرعة الرياح الرأسية صغيرة جدا مما يجعل قياسها امرا صعبا ، ولكن اذا ما توفرت بيانات عن السرع الافقية للرياح والتي تكون قيمها اعلى وطريقة قياسها اسهل سيكون بالامكان الاستدلال عن قيمها باستخدام معادلة الاستمرارية .

والصيغة الرياضية لهذه المعادلة كالأتي (9) :

$$\frac{1}{\rho}\frac{d\rho}{dt}+[\frac{\partial u}{\partial x}+\frac{\partial v}{\partial y}+\frac{\partial w}{\partial z}]=0 \quad \ldots\ldots(1)$$

في هذه الصيغة لم يتم افتراض ان المائع متجانس (homogeneous) وهذه الفرضية تعتبر مهمة بالنسبة لماء المحيط الذي يعتبر غير متجانس . واذا كان المائع غير قابل للانضغاط (incompressible) كما في حالة ماء البحر ، فأن $\frac{1}{\rho}\frac{d\rho}{dt}=0$ وستصبح معادلة الاستمرارية كألاتي(9) :

$$\frac{\partial u}{\partial x}+\frac{\partial v}{\partial y}+\frac{\partial w}{\partial z}=0 \quad \ldots\ldots(2)$$

وباعادة ترتيب الحدود في معادلة (2) فأن :

$$\frac{\partial w}{\partial z}=-(\frac{\partial u}{\partial x}+\frac{\partial v}{\partial y}) \quad \ldots\ldots(3)$$

اذا كانت الدالة (u) ومشتقتها (وهما دوال ل (x)) هي قيم محددة او متناهية فانه باستخدام نظرية تايلور Taylor Theorem فأن (10) :

$$u(x+h)=u(x)+hu'(x)+\frac{1}{2}h^2u''(x)+\frac{1}{6}h^3u'''(x)+.... \quad \ldots\ldots(5)$$

$$u(x-h)=u(x)-hu'(x)+\frac{1}{2}h^2u''(x)-\frac{1}{6}h^3u'''(x)+.... \quad \ldots\ldots(6)$$

وبجمع المعادلتين واهمال حدود المشتقات ماعدا المشتقات من الدرجة الاولى تم استنتاج المعادلة التالية :

$$u'(x)=(\frac{\partial u}{\partial x})\approx\frac{1}{2h}\{u(x+h)-u(x-h)\} \quad \ldots\ldots(7)$$

يجب ملاحظة ان h هنا تعني ∂x او ∂y . وهذه المعادلة تستخدم لحساب كل من $\frac{\partial u}{\partial x},\frac{\partial v}{\partial y}$ ، وبعد جمع الحدين المذكورين على ضوء معادلة الاستمرارية يمكن حساب $\frac{\partial w}{\partial z}$ ، ولاستخراج قيمة

سما

w على عمق معين h بالنسبة لسطح الارض (قيمة w على سطح الارض تساوي صفر) تعطى بالعلاقة التالية :

$$w_h = \int_0^{-h} dw = \int_0^{-h} \frac{\partial w}{\partial z} dz = -\int_0^{-h} \left[\frac{\partial u}{\partial x} + \frac{\partial v}{\partial y} \right] dz \qquad \ldots\ldots\ldots (8)$$

في هذه الدراسة تم احتساب قيمة w للهواء على ارتفاع معين من سطح الارض (وليس للماء تحت عمق معين) ، وبالتالي فان العلاقة اعلاه ستكون بالشكل التالي :

$$w_h = \int_{h1}^{h2} dw = \int_{h1}^{h2} \frac{\partial w}{\partial z} dz = -\int_{h1}^{h2} \left[\frac{\partial u}{\partial x} + \frac{\partial v}{\partial y} \right] dz \qquad \ldots\ldots\ldots (9)$$

حيث ان h1 يمثل القيمة الابتدائية للارتفاع ، h2 يمثل القيمة النهائية للارتفاع .

المواد وطرائق العمل

تم في هذه الدراسة اعتماد المعلومات الانوائية من موقع المركز الاوربي (European Centre For Medium-Range Weather Forcasts) وتضمنت المعلومات سرع الرياح الافقية لطبقة الجو السطحية بمركبتيها (U,V) على ارتفاع وبوحدات 10 m m/s (11) والسرع الرأسية لطبقات الجو العليا وتحديدا لمستوى (1000 hPa) اي على ارتفاع 100 m ولنفس الوحدات المذكورة آنفا (12) . وتجدر الاشارة هنا ان بيانات طبقات الجو العليا ليست مقاسة بشكل مباشر و انما بواسطة النماذج العددية numerical models وشملت المعلومات مناطق العراق وبعض اجزاء المناطق المجاورة على شكل شبكة معلومات grid تمتد من خط طول E (49° – 37°5') ولخط عرض تمتد من N (27° – 37°5') وكانت المسافة بين كل نقطتين مختاريتن على الشبكة هي (1.5°) وكانت لليوم الاول من شهري كانون الثاني وتموز ولاربع اوقات رصد وهي (00, 06, 12, 18) UT .

لايجاد قيمة h في المعادلة (7) والتي تمثل قيم (∂x و ∂y) فانه يجب حساب تلك المسافة على ارض الواقع بين نقاط الشبكة المختارة لخطوط الطول والممثلة ب ∂x وخطوط العرض الممثلة ب ∂y. ان درجات خطوط العرض متوازية ولهذا فان المسافة بين كل درجة تبقى غالبا

ثابتة، ولكن درجات خطوط الطول تكون الابعد عند خط الاستواء وتتقارب عند الاقطاب ولهذا فان المسافات بينها تتغاير بشكل كبير . كل درجة خط عرض تساوي تقريبا 111 km . والمدى يختلف بسبب شكل الارض الاهليلجي من 110.567 km عند خط الاستواء الى 111.699 km عند الاقطاب . اما بالنسبة لخطوط الطول فان درجة خط الطول تكون الاوسع عند خط الاستواء وتساوي 111.321 km ثم تتقلص الى الصفر عن الاقطاب (13) . ولكن يجب ان تكون المسافات بين جميع نقاط الشبكة المختارة متساوية لخطوط الطول حسبما تقتضي طريقة الفروقات المنتهية finite difference method ولهذا فانه تم ايجاد المسافة بين كل خطي طول عند خط عرض ثابت على اساس نقاط الشبكة المختارة وتم ايجاد المعدل لخطوط الطول والذي يساوي 139.6km لكل 1.5° اي ان المسافة تساوي 93.067 km لكل 1° . كما هوموضح في الجدول – 1 . هذا الجدول تم انشاؤه باستخدام صيغة haversine لحساب المسافات بين نقطتين على اساس كروية الارض (اهمال تأثير الشكل الاهليلجي) والذي يعتبر دقيق بشكل كافي لمعظم الاغراض ونسبة الخطأ المحسوبة على هذا الاساس تكون اكثر من 0.3 % (14) .

سما

جدول – 1 : يوضح المسافة الحقيقية المحسوبة بين خطوط الطول

									Longitude
Latitude		37.5-39.0	39.0-40.5	40.5-42.0	42.0-43.5	43.5 -45.0	45.0 – 46.5	46.5 - 48	48.0 – 49.5
	39.0	129.6	129.6	129.6	129.6	129.6	129.6	129.6	129.6
	37.5	132.3	132.3	132.3	132.3	132.3	132.3	132.3	132.3
	36.0	134.9	134.9	134.9	134.9	134.9	134.9	134.9	134.9
	34.5	137.5	137.5	137.5	137.5	137.5	137.5	137.5	137.5
	33.0	139.9	139.9	139.9	139.9	139.9	139.9	139.9	139.9
	31.5	142.2	142.2	142.2	142.2	142.2	142.2	142.2	142.2
	30.0	144.4	144.4	144.4	144.4	144.4	144.4	144.4	144.4
	28.5	146.6	146.6	146.6	146.6	146.6	146.6	146.6	146.6
	27.0	148.6	148.6	148.6	148.6	148.6	148.6	148.6	148.6
	Average	139.6	139.6	139.6	139.6	139.6	139.6	139.6	139.6

ولايجاد قيمة $\frac{\partial u}{\partial x}.\frac{\partial v}{\partial y}$ نستخدم طريقة الفروقات المتناهية وتحديدا الفروقات المركزية finite difference method وذلك لانها تعطي نتائج اكثر دقة مقارنة بالفروقات التقدمية forward والتراجعية backward . وتم استخدام بيانات السرع الافقية السطحية المقاسة على ارتفاع 10 m والمأخوذة من الموقع الاوربي (11) كجزء اول من العمل ، و تم استخدام بيانات السرع الرأسية العلوية للمستوى الضغطي 1000 hPa لعمل مقارنة بينها وبين القيم المحسوبة في هذه الدراسة (حيث يبلغ ارتفاع المستوى الضغطي 1000 hPa بحوالي 100 m (15)) والمأخوذة من نفس الموقع . واخيرا لحساب قيمة السرعة الرأسية vertical velocity للمستوى الضغطي 1000 hPa فانه تم ايجاد التكامل ل $\frac{\partial w}{\partial z}$ المحسوبة كما هوموضح في المعادلة (9) ولحدودالتكامل من 10 m الى 100 m وبوحدات m/s.

النتائج والمناقشة

لمعرفة ما تم التوصل اليه من نتائج في هذا البحث ، تم رسم البيانات المستحصلة من الموقع الاوربي والقيم المحسوبة من خلال هذه الدراسة للسرع الرأسية كخرائط كنتورية contour maps لمعرفة مدى التطابق بينهما، والاشكال التالية تتضمن تلك الخرائط لشهري كانون الثاني وتموز ولاربع رصدات .

لوحظ من تلك الخرائط ان هناك توافق في الكيفية التي تتحرك بها الرياح الرأسية وليس في الكمية (مقدار السرعة) وكانت هذه الحالة اكثر وضوحا في شهر تموز مقارنة بشهر كانون الثاني (كما في الاشكال (1.4b),(1.3b),(1.2b),((1.1b)) . ففي الشكل (1.1b) يبدو التماثل واضحا بالقرب من محطة السليمانية وتلعفر والذي يمثل شهر تموز اما في الشكل (1.1a) الذي يمثل شهر كانون الثاني فان التطابق يظهر واضحا ولكن مع ازاحة نحو اليمين مقارنة بقيم الموقع الاوربي ، ويظهر تطابق تام كما في الشكل (1.3a) بالقرب من محطة السليمانية لشهر كانون الثاني ايضا . وهذا ما وصل اليه Jagannadha Rao وجماعته في مقارنتهم بين القيم المحسوبة بالطريقة الحركية وقيم الرادار(6). اما بالنسبة لتاثير وقت الرصدعلى سلوك الرياح الرأسية فان التوافق بين سلوك السرع المأخوذة من الموقع الاوربي والمحسوبة كان كبيرا ولشهري كانون الثاني وتموزفي جميع

سما

الرصدات المختارة ما عدا وقت الرصد UTC 18الذي كان فيه مدى التوافق متوسط (كما في الشكل (1.4a)) .

بالنسبة لمقدار السرع الرأسية التي تم حسابها فلقد تبين من النتائج ان هذه الطريقة تتضمن نسب خطأ في حساب مقدار السرعة الرأسية وقد يرجع هذا الخطأ الى عدة اسباب منها : ان المسافات بين نقاط الشبكة المختارة كانت كبيرة نسبيا حيث كانت المسافة ثلاث درجات في حين لو كانت المسافة اقل ستكون النتائج اقل خطأ ولكن لتعذر الحصول على بيانات تكون المسافة بينها اقل تباعدا فانه تم اختيار المسافة المذكورة ، وهذا ما اثبته الجبوري سنة 1994 في دراسته لحساب السرعة الرأسية حيث توصل الى ان حساب الحركة الرأسية لكل منطقة من مناطق العراق افضل من حسابها لجميع مناطق القطر(3) . كما ان التقريبات المستخدمة في حساب المسافة الحقيقية بين نقاط الشبكة بسبب عدم وجود قيمة ثابتة للمسافات بين خطوط الطول ساهمت في وجود نسبة الخطأ. اضافة الى ان المعادلة المستخدمة في حساب السرعة الرأسية والممثلة بمعادلة رقم (3) التي تمثل معادلة الاستمرارية يفترض تطبيقها على المائع الغيرقابل للانضغاط incompressible كماء البحر ولكن الهواء قابل للانضغاط وتم اهمال هذه الصفة في هذه الدراسة . كما ان القيمة المحسوبة للسرعة الرأسية عند المستوى الضغطي 1000 hPa (اي على ارتفاع 100 m) قريبة جدا من سطح الارض ولهذا فهي حساسة جدا للاخطاء الصغيرة في رياح الطبقة المحاددة Boundary Layer واخيرا فان البيانات المأخوذة من الموقع الاوربي ECMWF هي ليست في الواقع مقاسة ولكنها متأتية من خلال النماذج العددية . ولهذا فانه عند عمل مقارنة بين القيم المقاسة والمحسوبة فان نتيجة المقارنة قد لا تكون متطابقة بالضرورة .

وعليه فان هذه الطريقة نجحت بشكل ما في اعطاء وصف لحالة الرياح الرأسية ولكنها لم توفق في حساب مقدارها بشكل دقيق . لذا يوصى باستخدام طرق اخرى لحساب مقدار السرعة الرأسية ومقارنتها مع ما تم التوصل اليه في هذه الدراسة .

مما سبق نستنتج :

1. وفق ما تبين من خلال هذه الدراسة يمكن استخدام الطريقة الحركية لاعطاء وصف للكيفية التي تتحرك بها الرياح الرأسية ولجميع اوقات الرصد بشكل عام . ويرجح استخدامها لمناطق جغرافية محددة وليست اقليمية للحصول على نتائج اكثر دقة .

2. تضمنت هذه الطريقة وجود تباين ملحوظ بين مقدار السرعة الرأسية المحسوبة ومصادر البيانات الاخرى ولهذا فان استخدامها لهذه الغاية ربما ينطوي على اخطاء كبيرة .

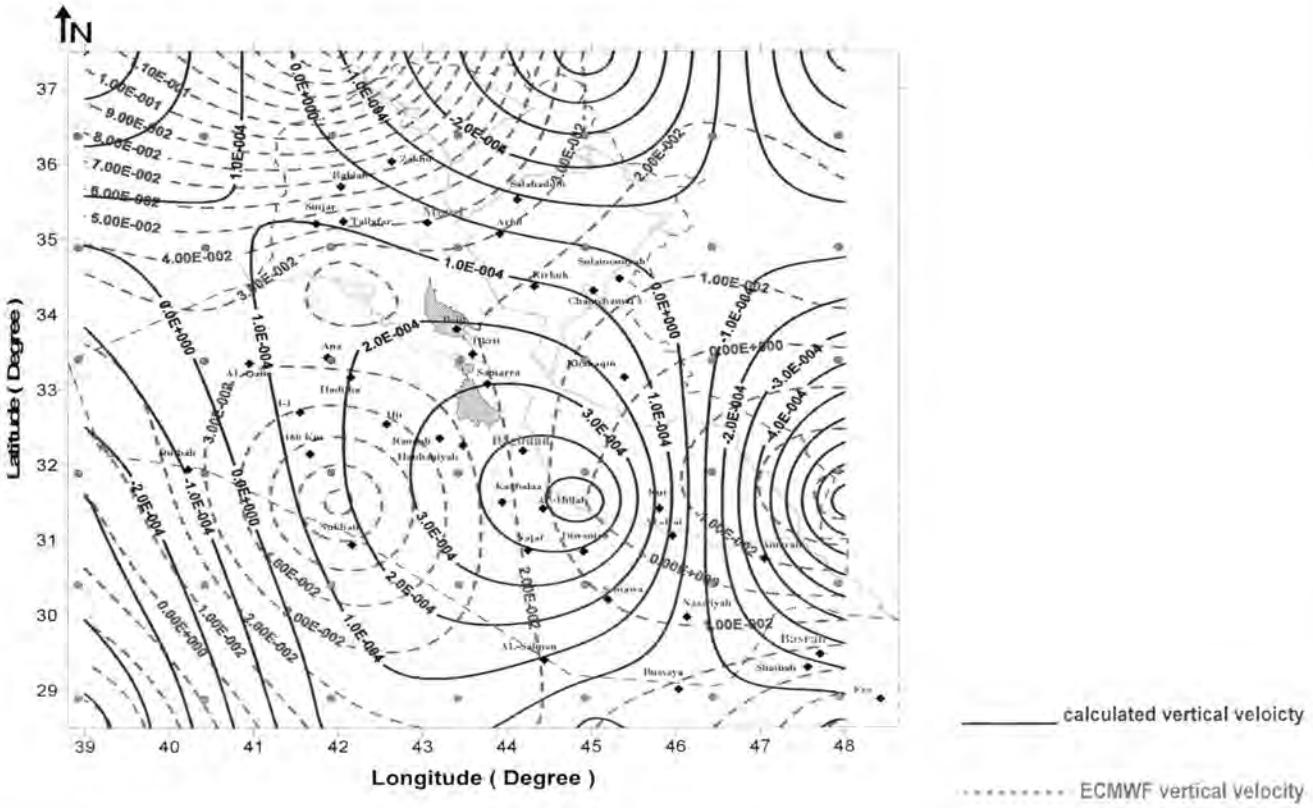

الشكل 1:- Vertical velocity at 00UTC on the 1st of January at 1000 hPa

سما

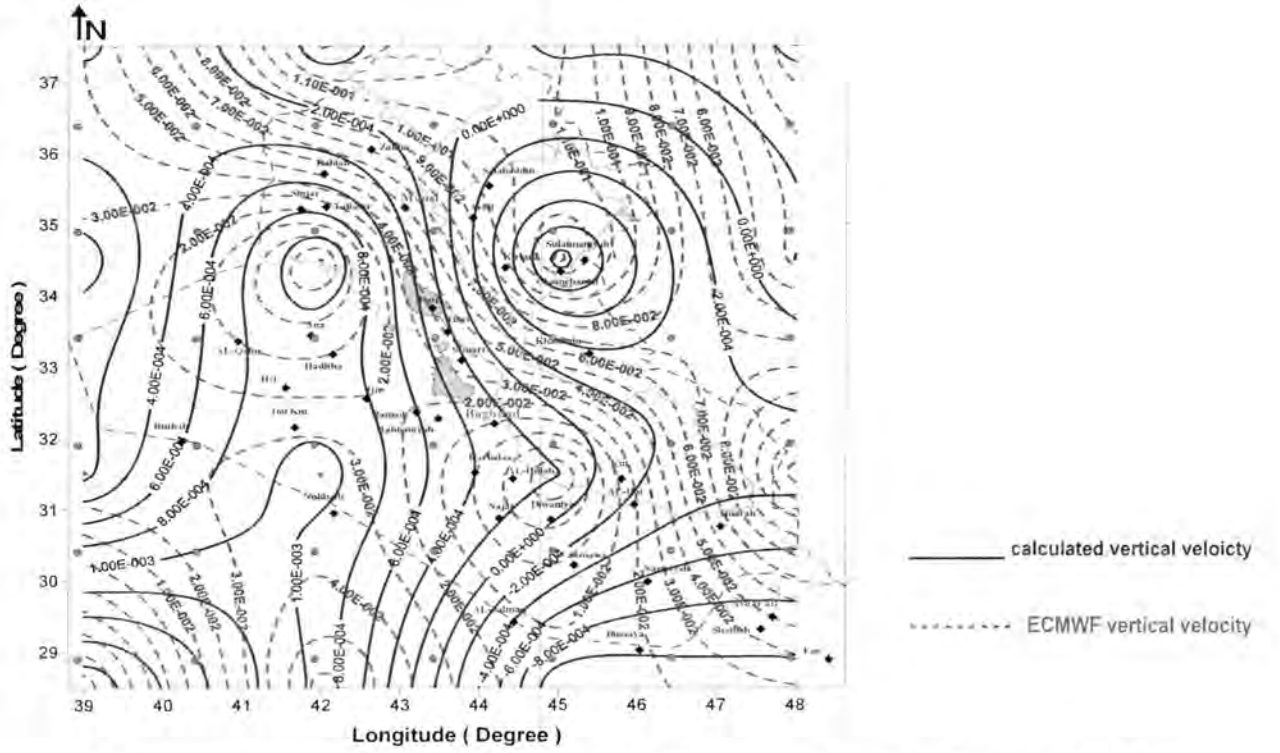

الشكل -2: Vertical velocity at 00 UTC on the 1st of july at 1000 hPa

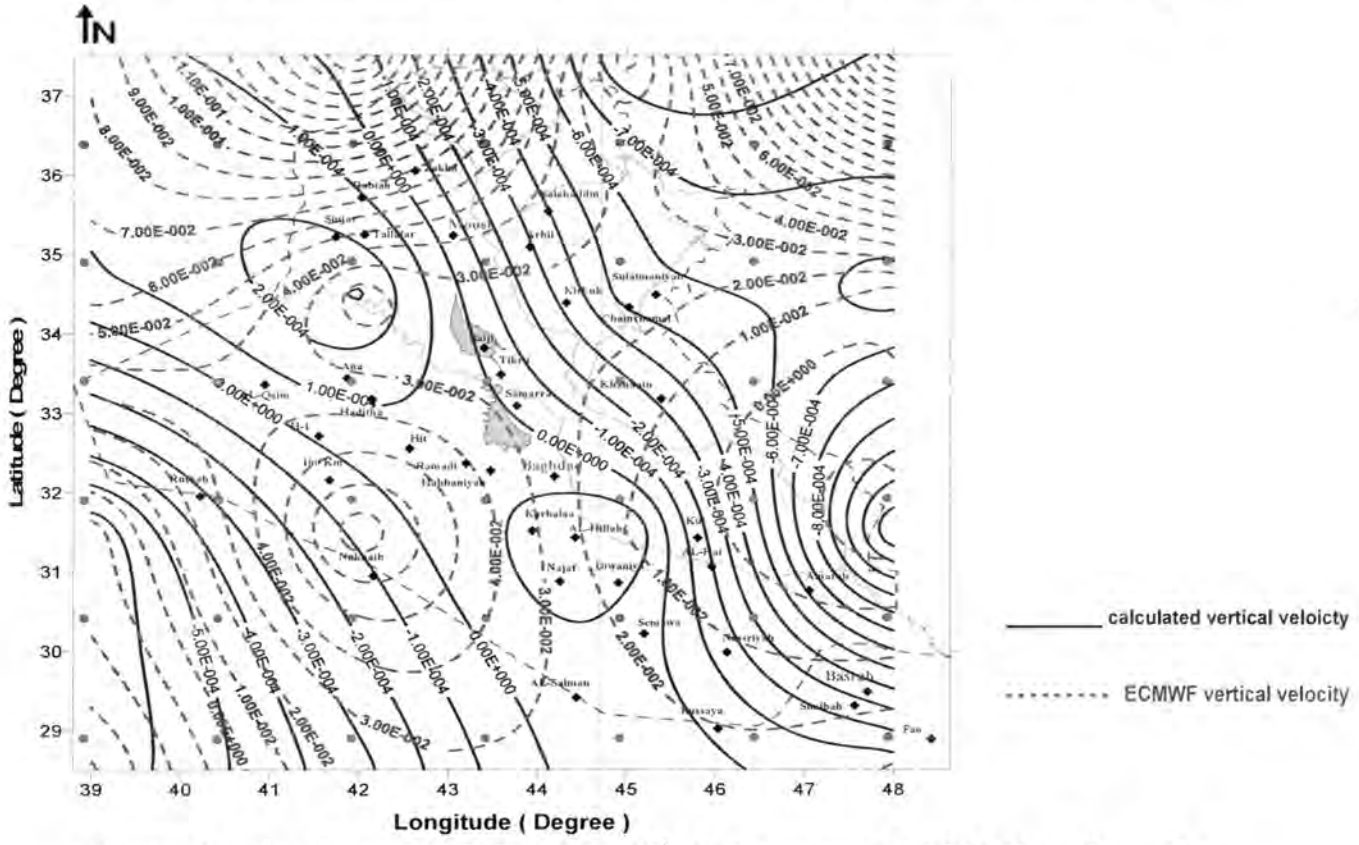

الشكل -3 : Vertical velocity at 06UTC on the 1st of January at 1000 hPa

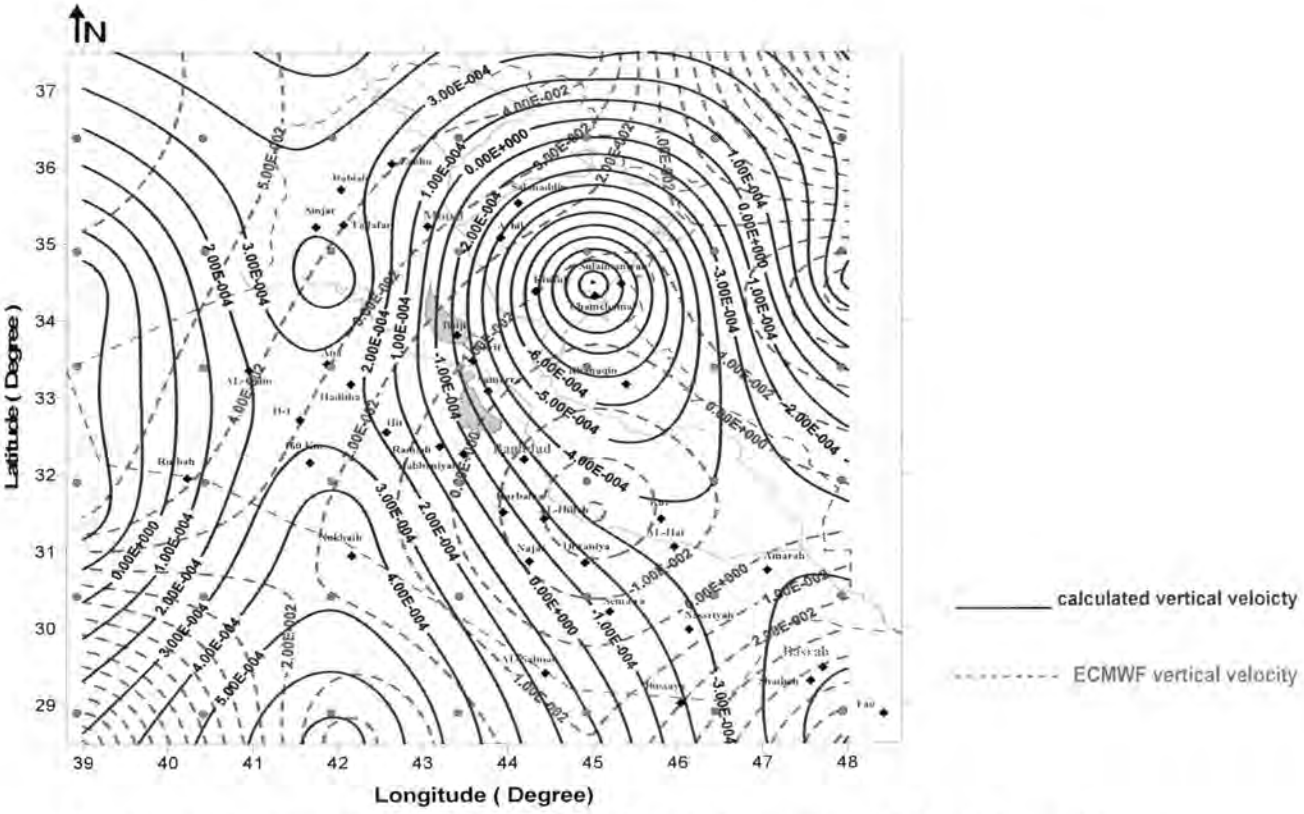

Vertical velocity at 06UTC on the 1st of july at 1000 hPa : 4- الشكل

سما

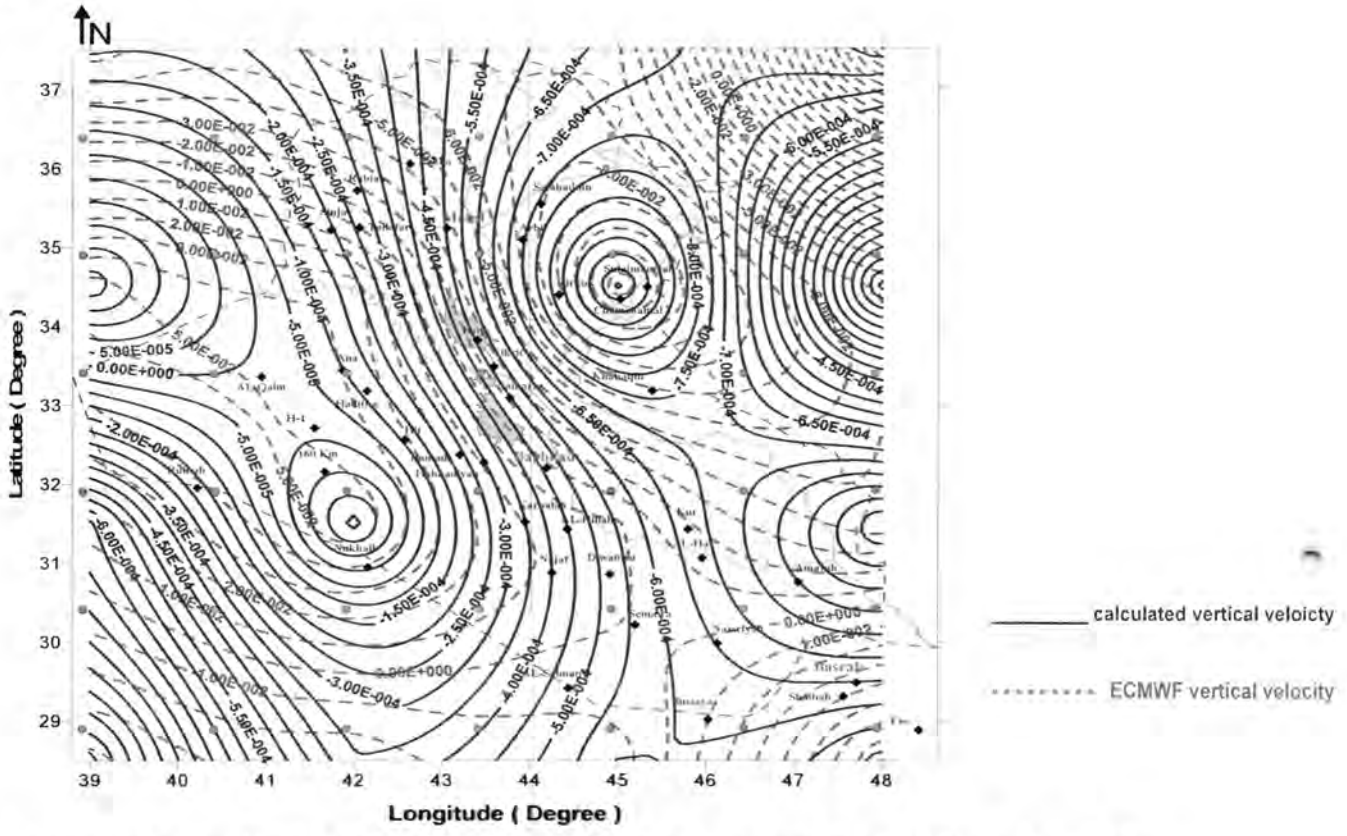

Vertical velocity at 12UTC on the 1st of January at 1000 hPa :5- الشكل

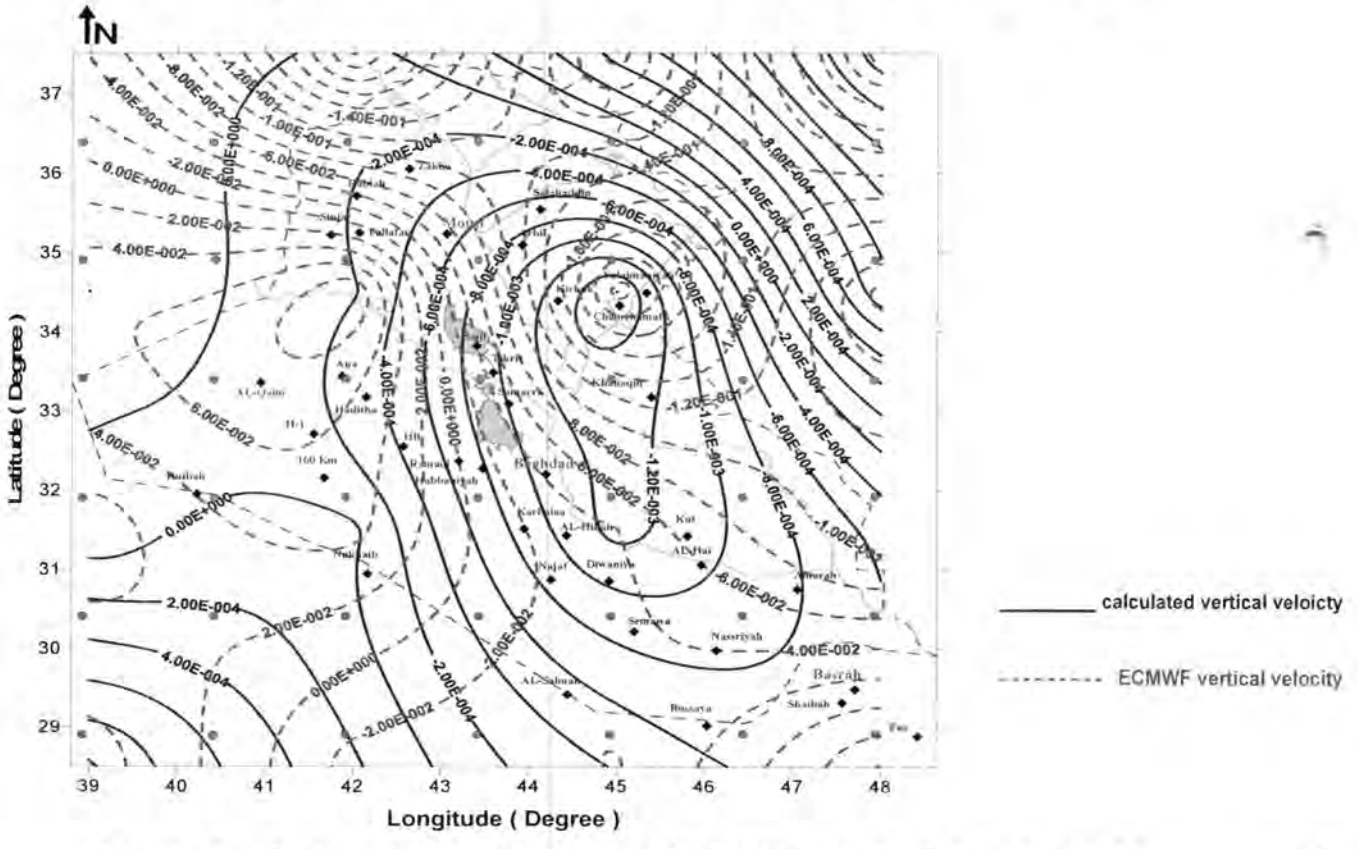

Vertical velocity at 12UTC on the 1st of july at 1000 hPa : 6- الشكل

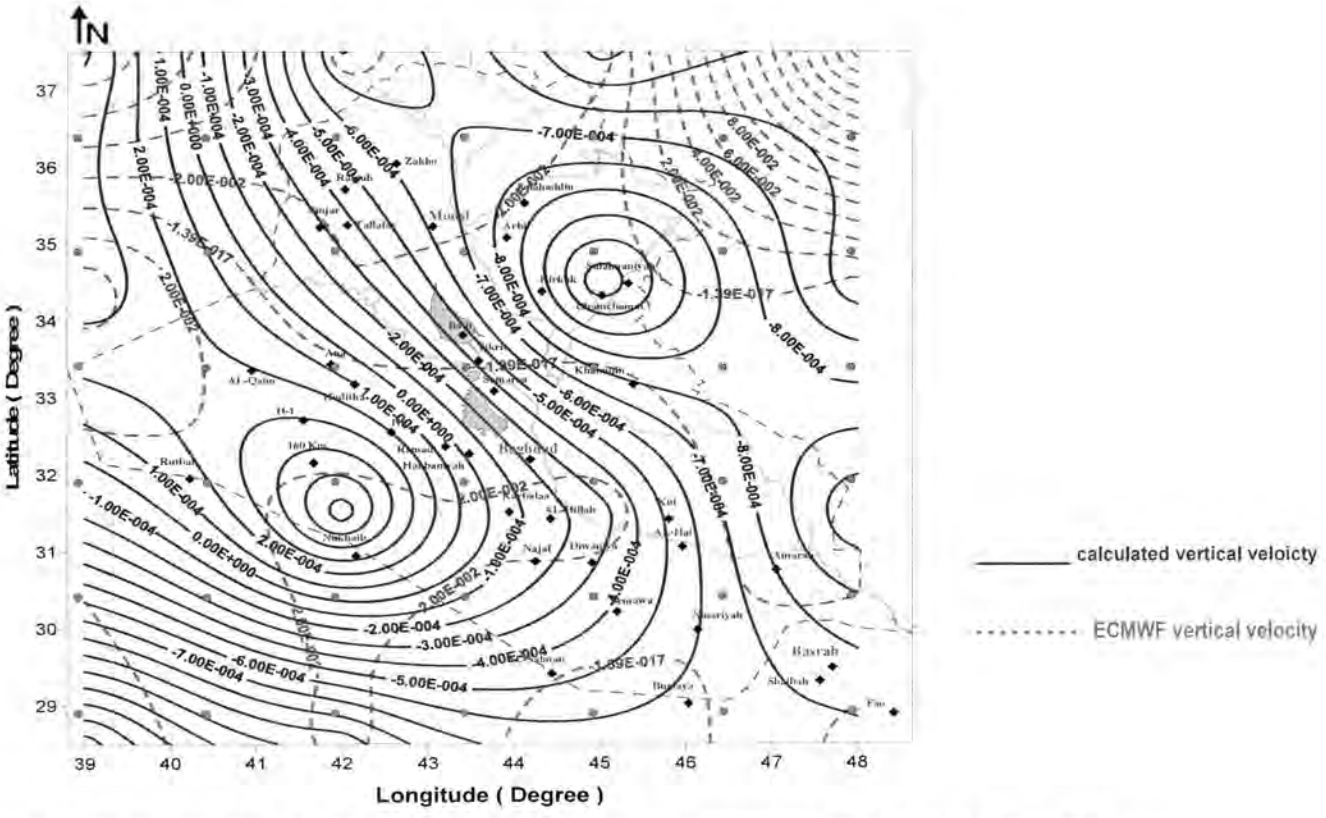

الشكل 7- : Vertical velocity at 18UTC on the 1st of january at 1000 hPa

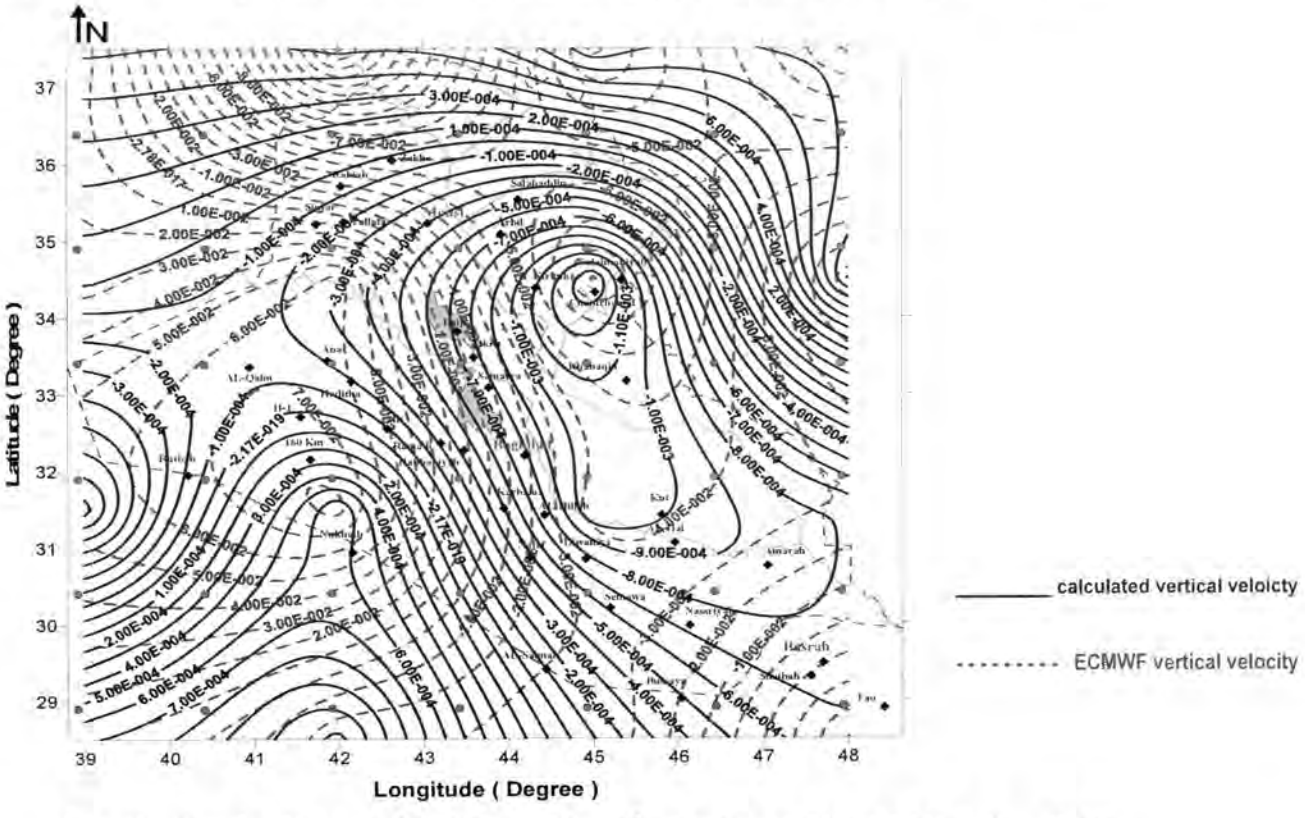

الشكل 8- : Vertical velocity at 18UTC on the 1st of july at 1000 hPa

سما

المصادر

1) Krishnamurti,T.N. , Bounoua,L. , " An Introduction To Numerical Weather Prediction Techniques",CRC Press, United State of America, 35,(1996).

2) الجبوري ، منعم حكيم ، سناء عباس ، " تجارب عملية في الرصد والتحليل والتنبؤ الجوي" ، مؤسسة مصر مرتضى للكتاب العراقي ، بغداد، الطبعة الاولى، ص 179، (2010) .

3) الجبوري ، منعم حكيم ،" دراسة حركة الرياح الرأسية وبعض تأثيراتها الانوائية في العراق" ، رسالة ماجستير، الجامعة المستنصرية , كلية العلوم , قسم الفيزياء . ص1، ص7-17، (1994) .

4) Ahrens,C.D., " Essential of Meteorology ,An Invitation To The Atmosphere" , Thomson Brooks /Cole , United State of America ,Fifth Edition ,163,(2008).

5) Angevine, W. M.," Errors in Mean Vertical Velocities Measured by Boundary Layer Wind Profilers", J. Atmos. Oceanic Technol., 14, Issue 3, 565–569,(1997) .

6) Jagannadha Rao, V. V. M., D. Narayana Rao, M. Venkat Ratnam, K. Mohan, S. Vijaya Bhaskar Rao," Mean Vertical Velocities Measured by Indian MST Radar and Comparison with Indirectly Computed Values", J. Appl. Meteor., 42, Issue 4, 541–552,(2003) .

7) National Research Council of the National Academies,"Strategic guidance for the National Science Foundation's support of the atmospheric sciences",National Academies Press, United State of America ,22,(2007).

8) Junhong,W. , Bian ,J. , Brown , W.O., Cole,H., Grubišić,V., Young,Y. ," Vertical Air Motion from T-REX Radiosonde and Dropsonde Data", *J. Atmos. Oceanic Technol.*, 26, Issue 5, 928–942,(2009).

9) Pond,S., Pickard,G.L.," Introductory Dynamical Oceanography" , Pergamon Press ,Great Britain, Second Edition, 19-23,(1983) .

10) Smith,G.D., " Numerical Solution of Partial Differential Equation" ,Oxford University Press,6, (1971).

11) European Centre for Medium-Range Weather Forecasts(ECMWF,The Centre), Era Interim , daily Fields, surface ,(2011), http://data-portal.ecmwf.int/data/d/interim_daily/levtype=sfc/%20%20surface

12) European Centre for Medium-Range Weather Forecasts(ECMWF,The Centre) Era Interim , daily Fields, pressure levels ,(2011). http://data-portal.ecmwf.int/data/d/interim_daily/%20%20surface=/levtype=pl/

13) Furstinger , N. , White , N., Korb , R.B., Weinberg , F., Miller , R.A., "Get Ready! for Social Studies: Geography", McGraw-Hill Professional , United State of America,23-24,(2002).

14) Sambells,J. , Purvis , M. , Lewis,A. , Turner,C. " Beginning Google maps applications with Rails and Ajax", Apress , United State of America ,269,(2007).

15) Unisys Weather Information Systems/Upper Air Data Details, (2011), http://www.weather.unisys.com/upper_air/details.php